

Third International Nonlinear Dynamics Conference

June 18-22, 2023



NODYCON 2023 BOOK OF ABSTRACTS

Edited by

The NODYCON 2023 Program Committee
Sapienza University of Rome

NODYCON 2023

THIRD INTERNATIONAL

NONLINEAR DYNAMICS CONFERENCE

Edited by

The NODYCON 2023 Program Committee

Department of Structural and Geotechnical Engineering

Sapienza University of Rome

Book of Abstracts of the Third International Nonlinear Dynamics Conference
Rome, June 18-22, 2023

Sponsors:

Sapienza University of Rome

Faculty of Civil and Industrial Engineering

Department of Structural and Geotechnical Engineering

Springer MTS Avio Thales Alenia Space Polytec

Under the Auspices of the City of Rome, Rome Technopole, Italian Ministry of Culture,
AIMETA, NODYS

FOREWORD

BY THE NODYCON 2023 CHAIR

Welcome to the Third International Nonlinear Dynamics Conference (NODYCON 2023)! NODYCON was first launched in 2019 as a way to continue the legacy of the renowned conference series initiated by Prof. Ali H. Nayfeh in 1986 at Virginia Tech, known as the Nonlinear Vibrations, Stability and Dynamics of Structures Conference. After Prof. Nayfeh's passing in 2017, who was also the founder of the Springer journal Nonlinear Dynamics in 1990, it was decided that a dedicated conference was needed to bring together the nonlinear dynamics community.

The inaugural NODYCON in 2019 served as a tribute to Prof. Nayfeh, recognizing his influential and inspiring scientific leadership in the field of nonlinear dynamics. Additionally, thanks to the generous support of Springer, the Ali H. Nayfeh Prizes were established in 2019 to recognize the best papers presented by graduate students and postdocs at the conference.

NODYCON 2023 holds significance for two reasons. Firstly, it marks the first hybrid post-pandemic conference of the NODYCON series. In 2021, due to the prevailing circumstances, NODYCON 2021, originally planned to be held in Rome, was transformed into a virtual online conference. Secondly, NODYCON 2023 will introduce the inaugural edition of the Ali H. Nayfeh Senior Award and the Early Career Award, which are supported by the NODYS Society.

In line with evolving paradigms, the call for papers for NODYCON 2023 attracted contributions that spanned traditional streams of nonlinear dynamics research while also highlighting the latest multi-disciplinary trends and developments in the field.

NODYCON 2023 received a remarkable response with 581 one-page abstracts submitted. Following rigorous reviews by external reviewers, the Program Committee, the Steering Committee, and the Advisory Committees, 486 abstracts were accepted for oral presentations and 28 abstracts were selected for presentation during the poster session. The diverse range of topics covered by these papers includes multi-scale dynamics, experimental dynamics, dynamics of structures, dynamics of adaptive and multifunctional metamaterial structures, reduced-order modeling, nonsmooth dynamics, nonlinear interactions, computational techniques, nonlinear system identification, dynamics of NEMS/MEMS/nanomaterials, multibody dynamics, fluid/structure interaction, the influence of nonlinearities on vibration control systems, nonlinear waves, ecosystem dynamics, social media dynamics, complexity in engineering, and network dynamics. These papers are organized into four major themes, which are also reflected in the technical sessions layout design:

Concepts and methods in nonlinear dynamics

Nonlinear dynamics of mechanical and structural systems

Nonlinear dynamics and control

Recent trends in nonlinear dynamics

We are pleased to announce that over 200 full papers have been submitted to Advances in Nonlinear Dynamics - Proceedings of the Third International Nonlinear Dynamics Conference (NODYCON 2023). The success of NODYCON 2023 hinges on the energy and enthusiasm of the researchers in

the field of nonlinear dynamics who have contributed high-quality papers on a wide array of topics. We would like to extend our special appreciation to the committee members of the Organizing, Steering, and International Advisory committees, whose names are listed below, as well as the external reviewers who have dedicated their valuable time and efforts to assess numerous papers.

We gratefully acknowledge the auspices of the City of Rome and its Mayor, the Italian Ministry of Culture, AIMETA (Italian Society of Theoretical and Applied Mechanics), NODYS (International Nonlinear Dynamics Society), and the sponsorship of Springer Science & Business Media, MTS, Avio, Thales Alenia Space, and Polytec.

We hope that you will have an unforgettable conference experience at NODYCON 2023!

Walter Lacarbonara
NODYCON 2023 Chair

June 2023

ORGANISING COMMITTEE

W. Lacarbonara (Sapienza University)

A. Luongo (University Of L'aquila)

G. Rega (Sapienza University)

F. Vestroni (Sapienza University)

M.J. Crowley (Sapienza University)

B. Carboni (Sapienza University)

L. Di Gregorio (Sapienza University)

G. Quaranta (Sapienza University)

P. K. Gourishetty (Sapienza University)

S. K. Guruva (Sapienza University)

V.Y. Janga (Sapienza University)

H. Joseph (Sapienza University)

STEERING COMMITTEE

E. Abdel-Rahman (University of Waterloo, Canada)

J. Awrejcewicz (Lodz University of Technology, Poland)

A. Bajaj (Purdue University, USA)

B. Balachandran (University of Maryland, USA)

M Cartmell (University of Strathclyde, UK)

L. Q. Chen (Shangai University, China)

M. Hajj (Stevens Institute of Technology, USA)

G. Haller (ETH, Switzerland)

K. R. Hedrih (Stevanović) (Mathematical Institute of Serbian Academy of Science and Arts, Belgrade and University of Niš, Serbia)

W. Lacarbonara (Sapienza University of Rome, Italy)

M. Leamy (Georgia Tech, USA)

S. Lenci (Polytechnic University of Marche, Italy)

C. H. Lamarque (ENTPE Lyon, France)

R. Leine (University of Stuttgart, Germany)
A. Metrikine (Delft University of Technology, Netherlands)
C. Nataraj (Villanova University, USA)
S. Natsiavas (University of Thessaloniki, Greece)
F. Pellicano (University of Modena, Italy)
F. Pfeiffer (Technische Universität München, Germany)
V. N. Pilipchuk (Wayne State University, USA)
G. Rega (Sapienza University of Rome, Italy)
S. Shaw (Florida Institute of Technology, USA)
C. Touzè (INSTA, France)
F. Verhulst (University of Utrecht, the Netherlands)
D. Wagg (University of Sheffield, UK)
J. Warminsky (Lublin University of Technology, Poland)
H. Yabuno (University of Tsukuba, Japan)

INTERNATIONAL ADVISORY COMMITTEE

K. Alhazza (Kuwait University, Kuwait)
M. A. Al Shudeifat (Khalifa University of Science, Technology and Research, UAE)
K. Asfar (University of Jordan, Jordan)
J. M. Balthazar (UNESP Bauru, Brazil)
M. Belhaq (University Hassan II, Morocco)
D. I. Caruntu (University of Texas - Rio Grande Valley, USA)
E. Chatzi (ETH, Switzerland)
A. Cunha (Rio de Janeiro State University, Brazil)
M. Daqaq (NYU Abu Dhabi, United Arab Emirates)
M. Defoort (Valenciennes University, France)
P. Eberhard (University of Stuttgart, Germany)
S. A. Emam (University of Sharjah, United Arab Emirates)
B. Feeny (Michigan State University, USA)
A. Fenili (Universidade Federal do ABC - UFABC, Brazil)

A. A. Frangi (Technical University of Milan, Italy)
O. Gottlieb (Technion Israel Institute of Technology, Israel)
P. Hagedorn (Technische Universität Darmstadt, Germany)
S. Kaczmarczyk (University of Northampton, UK)
T. Kalmar-Nagy (Technical University of Budapest, Hungary)
G. Kershen (University of Liège, Belgium)
C. K.Ahn (Korea University, Seoul, Korea)
I. Kovacic (University of Novi Sad, Serbia)
M. Lanzerotti (Virginia Tech, USA)
J. Ma (Lanzhou University of Technology, China)
P. Masarati (Technical University of Milan, Italy)
C. E. N. Mazzilli (Universidade de Sao Paulo, Brazil)
S. Nagarajaiah (Rice University, USA)
H. Nijmeijer (Eindhoven University of Technology, Netherlands)
J. H. Park (Yeungnam University, South Korea)
J. S. Pei (University of Oklahoma, USA)
G. Piccardo (University of Genova, Italy)
C.M.A. Pinto (Instituto Superior de Engenharia do Porto, Portugal)
J. Rhoads (Purdue University, USA)
L. Rosati (University of Naples "Federico II", Italy)
A. Shabana (University of Illinois at Chicago, USA)
A. Steindl (Technical University of Wien, Austria)
S. Theodossiades (Loughborough University, UK)
O. Thomas (Laboratoire d'Ingénierie des Systèmes Physiques et Numériques, France)
J. J. Thomsen (Technical University of Denmark, Denmark)
Z. Wang (Nanjing University of Aeronautics and Astronautics, China)
A. M. Wazwaz (Saint Xavier University, USA)
W. Zhang (Beijing University of Technology, China)

PROGRAM COMMITTEE

W. Lacarbonara (Sapienza University)
B. Carboni (Sapienza University)
M. Lepidi (University of Genoa)
G. Formica (University of Rome, RomaTre)
A. Pau (Sapienza University)
G. Quaranta (Sapienza University)
G. Ruta (Sapienza University)
Y. Shen (Sapienza University)
T. Shmatko (Sapienza University, Visiting Professor)
A. Arena (Sapienza University)
F. D'Annibale (University of L'Aquila)
M. Ferretti (University of L'Aquila)
D. Zulli (University of L'Aquila)
V. Settimi (Polytechnic University of Marche)

SPONSORS

SPRINGER NATURE

- GOLD -

Springer is a leading global scientific, technical, and medical portfolio, providing researchers in academia, scientific institutions, and corporate R&D departments with quality content through innovative information, products, and services. Springer has one of the strongest STM and HSS eBook collections and archives, as well as a comprehensive range of hybrid and open access journals. Springer is part of Springer Nature, a global publisher that serves and supports the research community. Springer Nature aims to advance discovery by publishing robust and insightful science, supporting the development of new areas of research, and making ideas and knowledge accessible around the world. As part of Springer Nature, Springer sits alongside other trusted brands like Nature Research, BMC, and Palgrave Macmillan.



- GOLD -

MTS Systems is a global supplier of test systems and industrial position sensors. The company provides test and measurement solutions to determine the performance and reliability of vehicles, aircraft, civil structures, biomedical materials and devices and raw materials. Examples of MTS products include: aerodynamics simulators, seismic simulators, load frames, hydraulic actuators and sensors. The company operates in two divisions: Test and Sensors. MTS test systems are designed to simulate the forces and motions that materials, products, and structures are expected to encounter. MTS Sensors are used by manufacturers of plastic injection molding machines, steel mills, fluid power, oil, and gas, medical, wood product processing equipment, mobile equipment and alternative energy. Sensors division products are also used to measure fluid displacement, such as liquid levels for customers in the process industries. With the acquisition of PCB Piezotronics Inc.

in 2016, MTS has increased Sensor products - microphones, vibration, pressure, force, torque, load, and strain sensors - and presence.



- GOLD -

Avio is a leading international group engaged in the construction and development of space launchers and solid and liquid propulsion systems for space travel. The experience and know-how built up over more than 50 years puts Avio at the cutting-edge of the space launcher sector, solid, liquid and cryogenic propulsion and tactical propulsion. Avio operates in Italy, France, and French Guyana with 5 facilities, employing approx. 1,200 highly qualified personnel, of which approx. 30% involved in research and development. Avio is a prime contractor for the Vega program and a sub-contractor for the Ariane program, both financed by the European Space Agency (“ESA”), placing Italy among the limited number of countries capable of producing a complete spacecraft.



- SILVER -

SPACE FOR LIFE, THALES ALENIA SPACE'S ASPIRATION!

A Joint Venture between Thales (67%) and Leonardo (33%), Thales Alenia Space is a global space manufacturer delivering, for more than 40 years, high-tech solutions for telecommunications, navigation, Earth Observation, environmental management, exploration, science, and orbital infrastructures. Thanks to our diversity of skills, talents and cultures, our customers (governments, institutions, space agencies, telecommunications operators), therefore have Space to Connect, Secure & Defend, Observe & Protect, Explore, Travel & Navigate. We also team up with Telespazio to form the Space Alliance, which offers a complete range of solutions including services. We are willing to have a win-win approach shared both with our partners and customers. The company recorded consolidated revenues of 2.2 billion euros in 2022 and has 8,500 employees. We operate in ten countries, with 17 facilities in Europe and an industrial plant in the United States. In Space, governments, institutions, and companies rely on Thales Alenia Space to design, operate and deliver satellite-based systems that help them position and connect anyone or anything, everywhere, help observe our planet, help optimize the use of our planet's – and our solar system's – resources.



- SILVER -

With over 400 employees worldwide, Polytec develops, produces, and distributes optical measurement systems for research and industry. The focus is on the technology areas of vibrometry, velocimetry, surface metrology, process analytics, machine vision and other optical technologies. Whether it's in space travel, architecture, medicine, nanotechnology, or mechanical engineering – Polytec expertise is always in demand across all industries. Laser vibrometry has proven its worth as an ideal tool for materials investigations – both for the measurement of structural dynamics and for the non-destructive detection and prevention of signs of fatigue. There is a wealth of applications in functional and long-term structural monitoring and in geological issues. Polytec manufactures a wide range of laser vibrometers that are the acknowledged gold-standard for non-contact vibration measurement. Laser Doppler vibrometers analyze samples of different size, from entire car bodies, large bridge parts over engines and actuators to micron-sized MEMS or delicate HDD components. Measuring the transfer functions, amplitudes and resonance frequencies in a non-intrusive way with the simple “point and shoot” method is the Single Point Vibrometer’s specialty. With the laser-based MPV-800 Multipoint Vibrometer, it is possible to carry out time-synchronous measurements with up to 48 channels and represent both frequency-dependent and time-dependent deflection shapes. The fiber-optic sensor heads are freely configurable and allow to perform flexible measurements – both parallel to a surface or arranged individually around the sample.

UNDER THE AUSPICES OF

ROMA



Rome is the capital city of Italy. With 2,860,009 residents in 1,285 km² (496.1 sq mi), Rome is the country's most populated city and the third most populous city in the European Union by population within city limits. The Metropolitan City of Rome, with a population of 4,355,725 residents, is the most populous metropolitan city in Italy. Rome is located in the central-western portion of the Italian Peninsula, within Lazio (Latium), along the shores of the Tiber. Vatican City (the smallest country in the world) is an independent country inside the city boundaries of Rome, the only existing example of a country within a city. Rome is often referred to as the City of Seven Hills due to its geographic location, and also as the "Eternal City". Rome is generally considered to be the "cradle of Western civilization and Christian culture", and the centre of the Catholic Church. Across a span of 28 centuries, Roman history has been influential on the modern world, especially in the history of the Catholic Church, and Roman law has influenced many modern law systems [from Wikipedia].



SAPIENZA
UNIVERSITÀ DI ROMA

The Sapienza University of Rome (Italian: Sapienza – Università di Roma), also called simply Sapienza or the University of Rome, and formally the Università degli Studi di Roma "La Sapienza", is a public research university located in Rome, Italy. It is one of the largest European universities by enrollments and one of the oldest in history, founded in 1303. The university is one of the most prestigious Italian universities, commonly ranking first in national rankings and in Southern Europe. In 2018, 2019, 2021 and 2022 it ranked first in the world for classics and ancient history. Since the 2011 reform, Sapienza University of Rome has eleven faculties and 65 departments. Today, Sapienza with 140,000 students and 8,000 among academic and technical and administrative staff, is the largest university in Italy. The university has significant research programmes in the fields of engineering, natural sciences, biomedical sciences, and humanities. It offers 10 Masters Programmes taught entirely in English.

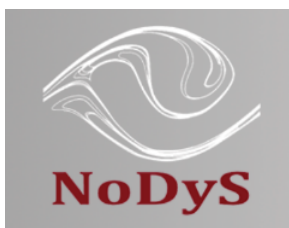


The Department of Structural and Geotechnical Engineering (DISG) has an illustrious history and a tradition of excellence in research, teaching, and activities towards the outside world, dating back to 1873. In scientific research there are three main areas: Mechanics of Solids and Structures, Structural Engineering and Geotechnical Engineering.

The Department's academic and research activities have achieved an international reputation for excellence in the areas of structural dynamics, seismic engineering, risk analysis, large-scale monitoring, the behaviour of complex structural and geotechnical systems, the design of structures, intelligent structures, the structural rehabilitation of historic and monumental buildings.



AIMETA (Italian Association of Theoretical and Applied Mechanics) brings together enthusiasts of mechanics in its various branches: theoretical, experimental, technical and applicative. Naturally everyone has a mentality suited to the direction in which his research and his teaching and professional activity are carried out, but for all the interest focuses on Mechanics, a very broad, multifaceted science in continuous development, "paradise of mathematical sciences", as said Leonardo, but also the foundation of all physical science.



NODYS (International Society of Nonlinear Dynamics) is a society established in 2018 to enable knowledge sharing and dissemination, international collaboration, and skills development in the field of nonlinear dynamics.



The Ministry of Culture (MIC) is a department of the Italian government. It is responsible for the protection of culture and entertainment and the preservation of artistic, cultural and landscape heritage. Founded in 1974 as the Ministry for Cultural and Environmental Heritage, over the years it has taken on different denominations.

NODYCON 2023 Awards

NODYCON 2023 will feature three types of awards.

- The Ali H. Nayfeh Prizes (1st, 2nd, and 3rd Prize), in honor of Nonlinear Dynamics's founding editor, the late Professor Ali H. Nayfeh, supported by Springer for the best papers presented by graduate students and postdocs at NODYCON 2023.
- The Ali Nayfeh Senior Award supported by the NODYS Society
- The Early Career Award supported by the NODYS Society.

The Award ceremony will be held during the Conference Banquet, June 21, 2023. The Ali H. Nayfeh prize for the first place is €500, for the second place €400, and for the third place €300.

The Awards committee for NODYCON 2023 includes:

- Prof. Matthew Cartmell, University of Strathclyde, UK
- Prof. Angelo Luongo, University of L'Aquila, Italy
- Prof. C. Nat Nataraj, Villanova University, USA.



Ali H. Nayfeh, Professor Emeritus of Nonlinear Dynamics
21 December 1933 – 27 March 2017

ALI H. NAYFEH PRIZES

The evaluation grid is based on the quality of the written paper using the criteria of novelty, achievement, and potential impact. The papers were submitted to the NODYCON 2023 Special Issue of Nonlinear Dynamics or to the NODYCON 2023 Springer Proceedings. The Ali H. Nayfeh Prizes selected for the 2023 edition are shown below.



First Prize: Dr. Rohit Chawla for the paper ‘Higher order transverse discontinuity mapping for hybrid dynamical systems’, co-authored with Aasifa Rounak and Vikram Pakrashi, University College Dublin, Ireland



Second Prize: Dr. Ahmed Barakat for the paper ‘Non-trivial solutions and their stability in a two-degree-of-freedom Mathieu-Duffing system’, co-authored with Eva Weig and Peter Hagedorn, Technical University of Munich, Germany;



Third Prize: Dr. Andrei Faragau for the paper ‘The interplay between the electro-magnetic and wave-induced instability mechanisms in the Hyperloop transportation system’, co-authored with Rui Wang, Andrei Metrikine, and Karel N. van Dalen, TU Delft, Netherlands.

ALI H. NAYFEH SENIOR AWARD & NODYS EARLY CAREER AWARD

The Nonlinear Dynamics Society (NODYS) solicited nominations for the inaugural Ali H. Nayfeh Senior Award and the Early Career Award.

The Senior Ali H. Nayfeh Award was established to recognize exceptional impact of research contributions and education of researchers and/or practitioners, and general leadership in advancing the field. The Senior Award is not an end-of-career award as it also aims to recognize mid-career individuals with a remarkable record of contributions. The inaugural 2023 edition attracted outstanding nominations which made the work of the Award Committee quite challenging.



Prof. Steven Shaw, Florida Institute of Technology,
USA

2023 SENIOR ALI H. NAYFEH AWARD

The NODYS Early Career Award is presented to an early-career recipient who demonstrates research excellence in the field of nonlinear dynamics. At the time of awarding, candidates must be under the age of 40 years, and be within 10 years of their terminal degree. The inaugural 2023 edition received strong nominations.



Dr. Pierpaolo Belardinelli, Polytechnic University of
Marche, Italy

2023 NODYS EARLY CAREER AWARD

Table of Contents

This Book of abstracts is organized into four major themes.

Concepts and methods in nonlinear dynamics

Nonlinear dynamics of mechanical and structural systems

Nonlinear dynamics and control

Recent trends in nonlinear dynamics

Within each theme, the abstracts are grouped into chapters which bear the same name of the conference technical sessions. By selecting the chapter name, the navigation tool will guide you to the chapter with the associated list of abstracts. Finally, by clicking on the abstract name, the one-page abstract will be displayed.

Concepts and methods in nonlinear dynamics	19
Fluid-structure interaction	19
Nonsmooth systems	22
Chaotic systems and uncertainty	25
Bifurcation and dynamic instability	27
Computational nonlinear dynamics	30
Nonlinear wave propagation	37
Multi body systems	38
Reduced-order models	40
Transient dynamics	42
Analytical techniques	43
 Mechanical and structural systems	 45
Mechanical systems and structures	45
Experimental dynamics	50
System identification and SHM	52
Aerospace structures	54
Constitutive and phenomenological models	55
Modal interactions and energy transfer	56
Rotating systems	57
Passive energy damping	58
 Nonlinear dynamics and control	 59
Nonlinear vibrations control	59
Sensors and actuators	62
Control of nonlinear systems	63
Networks synchronization	65
 New trends in nonlinear dynamics	 66
Vehicle dynamics	66
Energy harvesting	67
MEMS/NEMS	69
Fractional order system	71
Metamaterials	73
Biomechanics and small-scale robots (Organizer Prof. Y. Liu) . . .	74

Biological systems dynamics	77
Stochasticity and noise	78
Nonlinear phenomena in bio- and ecosystems dynamics	79

Concepts and methods in nonlinear dynamics

Fluid-structure interaction

- ← *Linear stability of thin liquid film flows over a uniformly heated slippery substrate under heat flux boundary condition*
Anandamoy Mukhopadhyay, Amar Gaonkar
- ← *Influence of Pulsating Internal flow on Marine Riser with Nonlinear Geometry*
Feras Alfossail, Shadid Nutaifat, Qasim Saleem, Americo Cunha Jr, Mohammad I. Younis
- ← *Vortex-induced forces and vibration of subsea structures in proximity to larger objects*
Henry Francis Annapeh, Victoria Kurushina
- ← *Vortex-induced loads on subsea pipelines due to marine biofouling*
Nikita Finogenov, Victoria Kurushina
- ← *A new Koopman-inspired approach to match flow field excitation with consequent structure responses for nonlinear fluid-structure interactions*
Cruz Y. Li, Zengshun Chen, Xisheng Lin, Tim K.T. Tse, Yunfei Fu
- ← *Use of chaotic invariants to identify regimes in circulating fluidized beds*
David de Almeida Fiorillo, Aline Souza De Paula, Geovany Borges
- ← *Aeroelastic limit cycle oscillations due to multi-element control surface with freeplay*
Larissa Drews Wayhs-Lopes, Douglas D. Bueno, Carlos E.S. Cesnik
- ← *The nonlinear phenomena in the unstable region of a single heated channel natural circulation loop with supercritical water*
Jin-Der Lee, Shao Wen Chen
- ← *The structural behaviour of 66kV submarine cable under sea waves and currents effect*
SungWoong Choi

- ← *Dynamics of curved cantilevered pipes conveying fluid*
 Mahdi Chehreghani, Ahmed Shaaban, Arun K. Misra, Michael P. Paidoussis
- ← *The remarkable role of hydrogen in conductors with copper and silver nanoparticles by mixed convection using viscosity Reynold's model*
 Syed Ibrar Hussain, Iftikhar Ahmad, Nida Yasmeen, Zulfiqar Umer
- ← *Reduced-order Model for the Hydrodynamics of an oscillating Surge Wave Energy Converter*
 Alaa Ahmed, Lisheng Yang, Muhammad R. Hajj, Raju Datla, Lei Zuo
- ← *Small In-plane Oscillations of a Slack Catenary by the Rayleigh-Ritz method*
 Bidhayak Goswami, Indrasis Chakraborty, Anindya Chatterjee
- ← *Vibrational Control: Mysterious Stabilization Mechanism in Bioinspired Flying Robots*
 Haithem Taha
- ← *Nonlinear stability of a thin viscoelastic film down a vertical wall: A numerical study*
 Akshay Desai, Souradip Chattopadhyay, Amar K. Gaonkar, Anadamoy Mukhopadhyay
- ← *Dynamics of piecewise linear oscillator coupled with wake oscillator*
 Parasuramuni Naga Vishnu, Jayaprakash K.R.
- ← *Investigation of Chaotic Flutter in a Wind Turbine Airfoil*
 Paul A. Meehan
- ← *Nonlinear Dynamics of Circular Cylindrical Shells Interacting with a Non-Newtonian Fluid*
 Francesco Pellicano, Antonio Zippo, Giovanni Iariccio
- ← *Nonlinear dynamics of imperfectly supported pipes conveying fluid*
 Mahdi Riazat, Mojtaba Kheiri

- ← *Closed-form solutions and conservation laws for a Korteweg-de Vries-like equation*
Chaudry Masood Khalique, Mduduzi Yolane Thabo Lephoko
- ← *Experimental Study of Nonreciprocal Acoustic Energy Transfer in an Asymmetric Nonlinear Vibro-Acoustic System*
Jiangming Jin, Jingxiao Huang, D. Michael Mcfarland, Alexander Vakakis, Lawrence Bergman, Huancai Lu
- ← *Semi-analytic solutions for the bending-bending-torsion coupled forced vibrations of a rotating wind turbine blade by means of Green's functions*
Xiang Zhao, Xu Jiang, Yinghui Li, Weidong Zhu
- ← *Effect of time-scale in the flow fluctuations on a sub-critical aeroelastic system*
Varun H S, Sunetra Sarkar

Nonsmooth systems

- ← *Investigation on Vibro-impacts of Electric Powertrain in Regenerative Braking Process*
Kun Liu, Wei Wu
- ← *Study the Bifurcations of a DoF Mechanical Impacting System*
Soumyajit Seth, Grzegorz Kudra, Grzegorz Wasilewski, Jan Awrejcewicz
- ← *Analysis and bifurcations of non-smooth Filippov predator prey system with harvesting*
Uganta Yadav, Sunita Gakkhar
- ← *Two-Dimensional Critical Dynamics of Kuramoto Model on Erdős-Rényi Random Graphs*
Hai Chen
- ← *Rheonomic frictional contacts for simulating drifting in conveyors and feeders*
Alessandro Tasora, Dario Fusai, Dario Mangoni
- ← *Entrainment in Self-Excited Filippov Systems*
Bipin Balaram, Jan Awrejcewicz
- ← *Vibration attenuation of dynamic systems using multiple motion constraints*
Wei Dai, Jian Yang
- ← *Modified Energy-based Time Variational Methods for Obtaining Periodic and Quasi-periodic Responses*
Aalokeparno Dhar, I. R. Praveen Krishna
- ← *Horizontal table vibration for parts-centering without feedback*
Dheeraj Varma Manthena, C. P. Vyasarayani, Anindya Chatterjee
- ← *A complete stability chart for the tippedisk*
Simon Sailer, Remco I. Leine

- ← *Harmonic expansion and nonsmooth dynamics in a circular contact region with combined slip-spin motion*
Mate Antali
- ← *Limit cycle bifurcations from infinity in relay systems*
Enrique Ponce, Emilio Freire, Javier Ros, Elisabet Vela
- ← *Maneuvering a Stick in Three-Dimensional Space Using Impulsive Forces*
Aakash Khandelwal, Nilay Kant, Ranjan Mukherjee
- ← *Quantized H_∞ Filtering for Discrete-Time Markovian-Jump T-S Fuzzy Systems with Time-Varying Delays via Event-Trigger Mechanism*
Soundararajan Ganesan, Ardak Kashkynbayev, Rakkiyappan Rajan
- ← *Three large amplitude limit cycles via Zero-Hopf bifurcation from infinity in D piecewise linear systems with symmetry.*
Javier Ros, Enrique Ponce, Emilio Freire
- ← *Existence of a uniform upper bound for the number of limit cycles of planar piecewise linear systems*
Victoriano Carmona, Fernando Fernández-Sánchez, Douglas D. Novaes
- ← *Stability and instability of a complex biodynamical discrete structure on a cantilever coupled to nonlinear springs*
Andjelka Hedrih, Katica Hedrih (Stevanović)
- ← *Ghost smooth and non-smooth bifurcations in vibro-impact pairs*
Daniil Yurchenko, Larissa Serdukova, Rachel Kuske, Christina Athanasouli
- ← *Semi-Implicit Integration and Data-Driven Model Order Reduction for Structures with Hysteresis*
Bidhayak Goswami, Anindya Chatterjee
- ← *Vibration-Induced Friction Force Modulation*
Enxhi Sulollari, Karel Van Dalen, Alessandro Cabbioi

← *Model reduction of a periodically forced slow-fast continuous piecewise linear system*

A. Yassine Karoui, Remco I. Leine

← *Time-dependent stability margin for autonomous, piece-wise, and discontinuous system*

Tomasz Burzyński, Piotr Brzeski, Przemysław Perlikowski

Chaotic systems and uncertainty

- ← *Relativistic chaotic scattering*
Jesús M. Seoane, Diego S. Fernández, Juan D. Bernal, Álvaro G. López,
Miguel A.F. Sanjuán

- ← *Multidimensional nonlinearity Time Series Forecasting Based on Multi-reservoir Echo State Network*
Jingyu Sun, Lixinag Li, Haipeng Peng, Shengyu Liu

- ← *Quasi-periodicity of temporarily constrained variable-length elastic pendulum*
Pawel Olejnik, Godiya Yakubu, Jan Awrejcewicz

- ← *Chaos Measure Dynamics and a Multifactor Model for Financial Markets*
Markus Vogl

- ← *Nonlinear and chaotic dynamics of a vibratory conveying system*
Simon Schiller, Wolfgang Steiner

- ← *The predictable chaos of rare events in complex systems*
Tommaso Alberti, Davide Faranda, Valerio Lucarini

- ← *Time-Periodic perturbation leading to chaos in a planar memristor oscillator having a Bogdanov-Takens bifurcation*
Marcelo Messias

- ← *Fixed-time adaptive neural tracking control for a helicopter-like twin rotor MIMO system*
Bacha Aymene, Chelihi Abdelghani, Chouki Sentouh

- ← *A new key generator based on an auto-switched hybrid chaotic system and its FPGA implementation*
Sid Hichem, Azzaz Mohamed Salah, Sadoudi Saïd

- ← *Investigation of chaos in the mechanistic turbulence model*
 Róbert Rochlitz, Bendegúz D. Bak
- ← *Structural reliability analysis based on the dynamic integrity of an attractor*
 Carlos E.N. Mazzilli, Guilherme R. Franzini
- ← *Stochastic basins of attraction for uncertain initial conditions*
 Kaio César Borges Benedetti, Stefano Lenci, Giuseppe Rega, Paulo Gonçalves
- ← *Chaotic dynamic induced by PI control in offshore oil production plants.*
 Nayher Andres Clavijo, Giovanni G. Gerevini, Fabio Cesar Diehl, José Carlos Pinto
- ← *Resource sensitive game*
 Der Chyan Bill Lin
- ← *Coexistence of hidden attractor and self-excited attractors on the plane*
 Eric Campos-Canton, Hector E. Gilardi-Velazquez, Guillermo Huerta-Cuellar
- ← *Compact Multiplier-less CORDIC-Based on FPGA Implementation of a Sine map for Chaotic Applications*
 Sara S. Abou Zeid, Hisham M. Elrefai, Wafaa S. Sayed, Lobna A. Said, Ahmed G. Radwan

Bifurcation and dynamic instability

- ← *A quantitative Birkhoff Normal Form for geometrically nonlinear hinged-hinged beams*
Laura Di Gregorio, Walter Lacarbonara
- ← *Nonlinear dynamic characteristics and four contact states of a spur gear pair considered tooth profile error and extended tooth contact*
Zhengfa Li, Zaigang Chen
- ← *Non-autonomous inverse Jacobi multipliers and periodic orbits of planar vector fields*
Isaac A. García, Susanna Maza
- ← *The integral of the cofactor as a characterization of centers*
Isaac A. García, Jaume Giné
- ← *Parametric resonance caused by mass imbalance on railway wheels*
Motoyoshi Shibata, Junta Umemoto, Hiroshi Yabuno
- ← *Dynamical analysis of spread of online misinformation and a delayed optimization technique*
Moumita Ghosh, Pritha Das
- ← *A parsimonious identification approach in the frequency-domain for experimental fractional systems of unknown order*
José Antunes, Philippe Piteau, Xavier Delaune, Romain Lagrange, Domenico Panunzio
- ← *Vibration suppression of a cable-stayed beam with external excitations by a nonlinear energy sink*
Houjun Kang, Yifei Wang, Yunyue Cong
- ← *A Comparative Study of Two Types of Bifurcation-Based Inertial MEMS Sensors*
Yasser S. Shama, Rana Abdelrahmana, Sasan Rahmanian, Samed Kocer, Eihab Abdel-Rahman
- ← *Dynamics of Purcell's three-link microswimmer model with actuated-elastic joints*
Gilad Ben-Zvi, Yizhar Or

- ← *Experimental and numerical analysis of a tube with clearance-induced impacts*
 Pau Becerra Zuniga, Sébastien Baguet, Benoit Prabel, Clément Grenat, Régis Dufour
- ← *Shear-torsional nonlinear galloping of base-isolated continuous beam*
 Simona Di Nino, Angelo Luongo
- ← *Nonlinear vibration of an inextensible rotating beam*
 Lokanna Hoskoti, Mahesh M. Sucheendran
- ← *Synchronization Based on Intermittent Sampling: PWL Multiscroll System*
 José Luis Echenausía Monroy, Jonatan Pena Ramirez
- ← *Properties of a two parameter logistic map with delay*
 Akshay Pal, Jayanta Bhattacharjee
- ← *Data-driven bifurcation analysis using a parameter-dependent trajectory*
 Jesús García Pérez, Amin Ghadami, Leonardo Sanches, Guilhem Michon, Bogdan I. Epureanu
- ← *Investigating the Stability of a Strongly Nonlinear Structure Through Shaker Dynamics in Fixed Frequency Sine Tests*
 Eric Robbins, Fernando Moreu
- ← *Hopf Bifurcation Analysis of the BVAM Model for Electrocardiogram*
 Ahsan Naseer, Imran Akhtar, Muhammad R. Hajj
- ← *Bistability in pressure relief valve dynamics*
 Fanni Kádár, Gabor Stepan
- ← *Mirroring of synchronization in multilayer configuration of Kuramoto oscillators*
 Dhrubajyoti Biswas, Sayan Gupta

- ← *The Complete Bifurcation Analysis of Buck Converter Under Current Mode Control*
 Aleksandrs Ipatovs, Dmitrijs Pikulins, Chukwuma Victor Iheanacho, Sergejs Tjukovs
- ← *The influence of the electro-magnetic levitation and its control strategy on the vertical stability of the Hyperloop transportation system*
 Andrei Fărăgău, Rui Wang, Andrei V. Metrikine, Karel N. Van Dalen
- ← *The influence of the frequency and velocity-dependent reaction force of the guideway on the vertical stability of the Hyperloop transportation system*
 Karel N. Van Dalen, Andrei B. Fărăgău, Andrei V. Metrikine
- ← *The effect of the mean wind force on the post-critical galloping response of shallow cables*
 Daniele Zulli, Angelo Luongo
- ← *How non-generic coincidences of local bifurcations can occur in fluid mechanics*
 Nan Deng, Laurette Tuckerman, Bernd R. Noack, Luc Pastur
- ← *On the influence of external damping on the dynamics of a generalized Beck's beam*
 Giovanni Migliaccio, Manuel Ferretti, Francesco D'Annibale
- ← *Fingered Stability Regions for Operator Splitting*
 Miklós Mincsovics, Tamás Kalmár-Nagy
- ← *Nonlinear dynamics and bifurcations of a planar undulating magnetic microswimmer*
 Jithu Paul, Yizhar Or, Oleg V. Gendelman

Computational nonlinear dynamics

- ← *Geometric Ito-Taylor Weak 3.0 integration scheme for dynamical systems on manifolds*
Ankush Gogoi, Satyam Panda, Budhaditya Hazra, Vikram Pakrashi
- ← *Numerical Calculation of Dynamics of Wiper Blade with Attack Angle*
Zihan Zhao, Hiroshi Yabuno
- ← *Modelling string vibrations with unilateral impacts in fretted musical instruments through the modal Udwadia-Kalaba approach*
Vincent Debut, José Antunes, Filipe Soares
- ← *A perturbation theory for the shape of central force orbits*
Ritapriya Pradhan, Tanushree Bhattacharya, Jayanta Bhattacharjee
- ← *On the Nonlinear Dynamics of In-contact Bodies subject to Stick-Slip and Wear Phenomena*
Arnaldo Casalotti, Francesco D'Annibale
- ← *Anomaly detection in nonlinear vibrational structures using variational auto-encoders*
Kiran Bacsa, Liu Wei, Eleni Chatzi (Poster)
- ← *Quasi projective synchronization of time varying delayed complex valued Cohen-Grossberg neural networks with mismatched parameters*
Sapna Baluni, Subir Das (Poster)
- ← *Parametric optimization of fold bifurcation points*
Adrien Mélot, Enora Denimal, Ludovic Renson
- ← *A Stochastic computational technique for the multi-Pantograph-delay systems through Trigonometric approximation (Poster)*
Iftikhar Ahmad, Siraj Ul Islam Ahmad, Hira Ilyas
- ← *Estimating seismic behavior of buckling-restrained braced frames using machine learning algorithms*
Benyamin Mohebi, Farzin Kazemi, Neda Asgarkhani

- ← *Modified Bouc-Wen model with damage and flexibility increase for the dynamic analysis of masonry walls*
Alessandra Paoloni, Domenico Liberatore, Daniela Addessi
- ← *An Algebraic Model for Hysteretic Responses exhibiting Cyclic Hardening and Softening Phenomena: Preliminary Results*
Raffaele Capuano, Nicolò Vaiana, Luciano Rosati
- ← *An improved variable-coefficient harmonic balance method for quasi-periodic solutions*
Junqing Wu, Jun Jiang, Ling Hong
- ← *A hybrid averaging and harmonic balance method for asymmetric systems*
Steven Shaw, Sahar Rosenberg, Oriel Shoshani
- ← *A general co-simulation approach based on a novel weak formulation at the interface*
Evangelos Koutras, Elias Paraskevopoulos, Sotirios Natsiavas
- ← *Abstract Dynamics: A Progressive Linearization of Nonlinear Dynamics*
Amir Shahhosseini, Kiran D'Souza
- ← *An Alternative Approach to Model Milling Dynamics*
Kaidong Chen, He Zhang, Nathan Van De Wouw, Emmanuel Detournay
- ← *Dynamic response of spatial beams with material softening and strain localization*
Sudhanva Kusuma Chandrashekhara, Dejan Zupan
- ← *Machine learning-based estimation of interstory drift distribution in reinforced concrete structures*
Benyamin Mohebi, Neda Asgarkhani, Farzin Kazemi, Natalia Lasowicz

- ← *Analysis of self-excited stick-slip vibrations in a model for creep groan using a combined Finite-Difference/Harmonic Balance approximation method*
 Jonas Kappauf, Simon Bäuerle, Hartmut Hetzler
- ← *Multi-scale uncertainty quantification of complex nonlinear dynamic structures with friction interfaces*
 Enora Denimal, Jie Yuan
- ← *Modeling Vortex-Induced Vibrations Displacement with Phenomena-Informed Neural Network*
 Mahmoud Ayyad, Muhammad R. Hajj, Arshad Mehmood, Imran Akhtar
- ← *Energy pumping of mechanical oscillators in an array configuration under impulse and parametric excitation*
 P Arjun, Vinod V
- ← *Quantum-Dot spin-VCSEL based Reservoir Computing for Hénon Attractor Reconstruction*
 Christos Tselios, Panagiotis Georgiou, Christina (Tanya) Politi, Dimitris Alexandropoulos
- ← *Optimizing Multilayer Perceptrons to Approximate Nonlinear Quaternion Functions*
 Arturo Buscarino, Luigi Fortuna, Gabriele Puglisi
- ← *On the velocity-based description in dynamic analysis of three-dimensional beams*
 Eva Zupan, Bojan Čas, Dejan Zupan
- ← *Iterative algorithm for dynamical integrity assessment of systems subject to time delay*
 Bence Szaksz, Giuseppe Habib
- ← *Phase space visualisation with non-variational chaos indicators*
 Jérôme Daquin, Carolina Charalambous

- ← *Unconditionally stable time stepping scheme for large deformation dynamics of elastic beams and shells*
Domenico Magisano, Leonardo Leonetti, Giovanni Garcea
- ← *Computing Periodic Responses of Geometrically Nonlinear Structures Modelled using Lie Group Formulations*
Amir Kamyar Bagheri, Valentin Sonneville, Ludovic Renson
- ← *Global Parametric Optimization for Structures with Nonlinear Joints in Vibration*
Quentin Ragueneau, Luc Laurent, Antoine Legay, Thomas Larroque, Romain Crambuer
- ← *Saddle-node bifurcation prediction from pre-bifurcation scenario*
Bálint Bodor, Giuseppe Habib
- ← *An extensive test campaign of a turbine bladed disk in the presence of mistuning and underplatform dampers, and numerical validation*
Giuseppe Battiato, Christian Maria Firrone, Valeria Pinto, Antonio Giuseppe D'Ettola
- ← *A FEA model generation method for irregular-shaped and nonhomogeneous structures*
Ming-Hsiao Lee
- ← *Robust topology optimization under non-probabilistic uncertainties*
Paolo Venini, Marco Pingaro
- ← *An insight on the parameter identification of a new hysteretic model addressing asymmetric responses*
Salvatore Sessa
- ← *Neuromorphic Computing Based on Physical Systems with Biologically Inspired Learning Rules*
D. Dane Quinn, Shaghayegh Rahimpour, Nikhil Bajaj, Aaron Batista, Carey Balaban

- ← *Mitigating vibration levels of mistuned cyclic structures by use of contact nonlinearities*
 Samuel Quaegebeur, Benjamin Chouvion, Fabrice Thouverez
- ← *New elemental damping model for nonlinear dynamic response*
 Chin-Long Lee
- ← *Active Learning for Probabilistic Machine Learning based modeling of Dynamical Systems*
 Tamil Arasan Bakthavatchalam, Selva Kumar Murugan, Murugesan Vadivel, Meiyazhagan Jaganathan, Gopinath Balu, Malaikannan Sankarashubbu
- ← *Experimental Analysis of a Nonlinear Piecewise Multi-Degrees of Freedom System*
 Cristiano Martinelli, Andrea Coraddu, Andrea Cammarano
- ← *Higher order transverse discontinuity mapping for hybrid dynamical systems*
 Rohit Chawla, Aasifa Rounak, Vikram Pakrashi
- ← *Energy transfer and dissipation in frictional systems with multiple contact interfaces*
 Cui Chao, Jian Yang, Marian Wiercigroch
- ← *Optimal projection in a Koopman-based sorting-free Hill method*
 Fabia Bayer, Remco Leine
- ← *An Equality-Based Formulation for Vibrating Systems with Two-Dimensional Friction*
 Mathias Legrand, Christophe Pierre
- ← *Allen–Cahn equation for multi-component crystal growth*
 Yunho Kim, Dongsun Lee
- ← *Operator Splitting in the Finite Element Analysis of Fokker-Planck Equations*
 Hangyu Fu, Lawrence Bergman, D. Michael McFarland, Xiangle Cheng, Huancai Lu

- ← *Self-supervised contrastive learning for chaotic time-series classification*
Salama Hassona, Wieslaw Marszalek
- ← *The Jerk Dynamics of Lorenz Model*
Jean-Marc Ginoux, Riccardo Meucci, Jaume Llibre, Julien Clinton Sprott
- ← *Spiral Bevel Gears nonlinear dynamics: chaotic response existence in multi degree of freedom systems*
Moslem Molaie Emamzadeh, Farhad S. Samani, Giovanni Iarriccio, Antonio Zippo, Francesco Pellicano
- ← *Response statistics of a conceptual two-dimensional airfoil in hypersonic flows with random perturbations*
Yong Xu, Weili Guo
- ← *Computation of the Wright function from its integral representation*
Dimitar Prodanov
- ← *NASA DART Mission: a preliminary mathematical dynamical model and its nonlinear circuit emulation*
Arturo Buscarino, Carlo Famoso, Luigi Fortuna, Giuseppe La Spina
- ← *Physics-constrained Deep learning of nonlinear normal modes of spatiotemporal fluid flow dynamics*
Abdolvahhab Rostamijavanani, Shanwu Li, Yongchao Yang
- ← *Numerical modeling and experimental validation of ballistic panel penetration*
Beata Jackowska-Zduniak
- ← *Finite element modelling of downhole rock breaking using a PDC bit*
Ahmed Al Shekaili, Yang Liu, Evangelos Papatheou
- ← *Mean-reverting schemes for solving the CIR model*
Samir Llamazares-Elias, Ángel Tocino
- ← *Implicit Milstein schemes: the preservation of properties when solving the CIR equation*
Ángel Tocino, Samir Llamazares-Elias

- ← *New formula of geometrically exact shell element undergoing large deformation and finite rotation*
Jielong Wang, Rongxin Feng, Shuai Zhang, Kang Jia
- ← *A Study on Damage to Lithium-ion Battery Separator using Nonlinear Finite Element Analysis*
Jun Lee, Hamin Lee, Cheonha Park, Chang-Wan Kim
- ← *Study of a double-zero bifurcation in a Lorenz-like system. Application to the analysis of the Lorenz system*
Antonio Algaba, Cinta Domínguez Moreno, Manuel Merino, Alejandro J. Rodríguez-Luis

Nonlinear wave propagation

- ← *Wave Propagation in Carbon Nanotube with Bilinear Foundation*
Biswajit Bharat, Jayaprakash K.R., Stefano Lenci
- ← *Self-adaptive wave propagation and synthetical vibration reduction of strongly nonlinear mechanical metamaterials*
Xin Fang, Peng Sheng, Chen Gong, Li Cheng
- ← *A vorticity wave packet breaking within a rapidly rotating vortex*
Philippe Caillol
- ← *Chirped optical solitons in fiber Bragg gratings with dispersive reflectivity*
Khalil Al-Ghafri, Mani Sankar
- ← *Doubly periodic solutions and breathers of the Hirota equation: Cascading mechanism and spectral analysis*
Huimin Yin, Qing Pan, K.W. Chow
- ← *Excitations of distorted magnetosonic lump waves by orbital charged space debris objects in ionospheric plasma*
Siba Prasad Acharya, Abhik Mukherjee, M. S. Janaki
- ← *Vacuum polarization energy in coupled-fermion ϕ^4 kink systems*
Danial Saadatmand, Herbert Weigel
- ← *Investigation of a nonlinear gradient elasticity model for the prediction of seismic waves*
Andrei B. Fărăgău, Marten Hollm, Leo Dostal, Andrei V. Metrikine, Karel N. Van Dalen
- ← *Fast numerical solution to nonlinear shallow water system*
Mikhail Lavrentiev, Andrey Marchuk, Konstantin Oblaukhov, Mikhail Shadrin
- ← *On the asymptotical description of solutions to the matrix modified Korteweg-de Vries equation*
Sandra Carillo, Cornelia Schiebold

- ← *Fast M-Component Direct and Inverse Nonlinear Fourier Transform*
Vishal Vaibhav
- ← *Nonlinear Lamb wave mixing in prestressed plates*
Meng Wang, Annamaria Pau
- ← *The nature and formation of rogue waves for nonlinear Schrödinger equation*
Stanko N. Nikolić, Najdan B. Aleksić, Omar A. Ashour, Milivoj R. Belić
- ← *Effect of nonzero temperature on the process of penetration of the potential barrier through the kink*
Jacek Gatlik, Tomasz Dobrowolski
- ← *Nonlinear distortion of high-intensity ultrasound holographic patterns*
Ahmed Sallam, Shima Shahab
- ← *On the existence and properties of solitary waves traveling in tensegrity-like lattices*
Julia De Castro Motta, Ada Amendola, Fernando Fraternali
- ← *Harmonic Scattering of Waves from Crossed-Thin-Rectangular Nonlinear Inclusions*
Pravinkumar Ghodake
- ← *Harmonic and superharmonic components in periodic waves propagating through mechanical metamaterials with inertia amplification*
Marco Lepidi, Valeria Settimi

Multi body systems

- ← *Real-time modeling of vehicle's longitudinal-vertical dynamics in ADAS applications*
Wei Dai, Yongjun Pan, Chuan Min
- ← *Algorithmic verification of Lyapunov stability for rigid multi-contact systems subject to impact and friction*
Péter Várkonyi
- ← *Nonholonomic dynamics of steer-free rotor-actuated Twistcar*
Zitao Yu, Jithu Paul, Yizhar Or
- ← *Application of Nonsmooth Dynamics to Rockfall Protection Ring Net Simulation*
Lisa Eberhardt, Remco I. Leine, Jonas Harsch, Simon R. Eugster, Perry Bartelt, Helene Lanter
- ← *A study on the dynamics of the flexible link mechanism with a spatial model of the translational joint with clearance*
Krzysztof Augustynek, Andrzej Urbaś, Jacek Stadnicki
- ← *Influence of the rope sling system on dynamics of a carried load*
Andrzej Urbaś, Krzysztof Augustynek, Jacek Stadnicki
- ← *Evaluation of Lie group Integration for Simulation of Rigid Body Systems*
Stefan Holzinger, Johannes Gerstmayr
- ← *Stability analysis for multibody systems subject to bilateral motion constraints*
Ioannis Ntinopoulos, Elias Paraskevopoulos, Sotirios Natsiavas
- ← *A reduced model for conical contact dedicated to flexible multi-body dynamics*
Matthieu Serre, Benoit Prabel, Habibou Maitournam
- ← *Recursive Inverse Dynamics of Flexible Multi-Body Systems based on Kane's Equations*
Pietro Pustina, Cosimo Della Santina, Alessandro De Luca

- ← *Stability Analysis of Large-Scale Multibody Problems using Lyapunov Exponents*
Pierangelo Masarati, Gianni Cassoni, Andrea Zanoni, Aykut Tamer
- ← *An Application of Bifurcation Analysis to Automotive Windscreen Wipers*
Bradley Graham, James Knowles, Georgios Mavros
- ← *Nonlinear effects in joints of multi-dimensional active absorbers for robotics*
Zbyněk Šika, Karel Kraus, Jan Krivošej

Reduced-order models

- ← *Delay-embedded modal analysis for spectral submanifold identification*
Joar Axås, George Haller

- ← *Fast computation and characterization of forced response surface of high-dimensional systems via spectral submanifolds and parameter continuation*
Mingwu Li, Shobhit Jain, George Haller

- ← *Developing sufficiently accurate reduced-order models using an efficient error assessment method*
Xiao Xiao, Thomas L. Hill, Simon A. Neild

- ← *Data-driven Nonlinear Normal Modal Identification and Reduced-order Modeling: A Physics-integrated Deep Learning Approach*
Shanwu Li, Yongchao Yang

- ← *A comparison of parametrizations of invariant manifolds for nonlinear model reduction*
Alexander Stoychev, Ulrich J. Römer

- ← *Embodied hydrodynamic sensing and estimation using Koopman modes*
Phanindra Tallapragada, Colin Rodwell

- ← *Computing Normal Forms of quadratic differential algebraic equations*
Alessandra Vizzaccaro, Aurelien Grolet, Marielle Debeurre, Olivier Thomas

- ← *Reduced-order model analysis of the pollutant dispersion on an urban street canyon*
Yunfei Fu, Xisheng Lin, Bingchao Zhang, Xinxin Feng, Chun-Ho Liu, Tim K.T. Tse, Cruz Y.T. Li

- ← *Using Machine Learning Models To Represent Isolated Nonlinearities Within Structural Systems*
D. Dane Quinn, David Najera-Flores, Anthony Garland, Konstantinos Vlachas, Eleni Chatzi, Michael Todd

- ← *Analysis of a data-driven planar drone model*
Dávid András Horváth, János Lelkes, Tamás Kalmár-Nagy

- ← *Multiple Equilibrium States in Large Array Resonators*
Chaitanya Borra, Nikhil Bajaj, Jeffrey Rhoads, D. Dane Quinn
- ← *Reduced-Order Models for Systems with Snap-Through*
Max De Bono, Simon A. Neild, Rainer Groh, Thomas L. Hill
- ← *A reduced-order modeling procedure to isolating energy- and evolution-wise dominant features of fluid-driven pollutant dispersion in a street canyon*
Yunfei Fu, Xisheng Lin, Mengyuan Chu, Fei Wang, Zhi Ning, Tim K.T. Tse, Cruz Y. Li
- ← *Substructural FRF based reduction technique for nonlinear systems*
Hossein Soleimani, Konstantinos Poullos, Jonas Brunskog, Niels Aage
- ← *Model Order Reduction of Nonlinear Thermal Systems using DEIM*
Gourav Kumbhojkar, Amar K. Gaonkar

Transient dynamics

- ← *Detection of Regime Changes in the Dynamics of Thermonuclear Plasmas for the Disruptions Prediction Improvement*
Teddy Craciunescu, Andrea Murari and JET Contributors
- ← *Safe Basins of Escape of a Weakly Damped Particle in a Truncated Quadratic Potential Well Under Harmonic Excitation*
Attila Genda, Alexander Fidlin, Oleg Gendelman
- ← *Locating transition behaviour in nonlinear signals*
Giovanna Zimatore, Giuseppe Orlando, Maria Chiara Gallotta, Cassandra Serantoni, Giuseppe Maulucci, Marco De Spirito
- ← *The transient charm of decay*
György Károlyi, Tamás Tél, Dániel Jánosi

Analytical techniques

- ← *Rolling a heavy ball on a revolving surface*
Katica R. (Stevanović) Hedrih
- ← *New results about compatibility conditions and solutions for a model of inerted gas in a vented fuel tank ullage*
José Luis Díaz Palencia, Julián Roa González
- ← *Regularity and spatially distributed solutions for interacting gases in complex domains*
José Luis Díaz Palencia, Julián Roa González
- ← *The blow-up method applied to monodromic singularities of the plane*
Brigita Ferčec, Jaume Giné
- ← *Nonlinear effects of the central body oblateness on the coplanar dynamics of solar sails*
Martin Lara, Elena Fantino, Roberto Flores
- ← *A study on an analytic optimization of variable pitch broaching*
Zsolt Iklodi, Zoltan Dombovari
- ← *Collinear point dynamics of a dumbbell satellite in fast rotation*
Martin Lara
- ← *Exact potentials in multivariate Langevin equations*
Tiemo Pederngana, Nicolas Noiray
- ← *Nonresonant averaging of an inhomogeneous nonlinear Mathieu equation*
Dhananjaykumar Tandel, Anindya Chatterjee, Atanu Mohanty
- ← *Fourier Analysis of a Duffing Equation with Delay*
Mark Walth, Richard Rand
- ← *Introduction to The Perpetual Mechanics Theory and Future Directions*
Fotios Georgiades

- ← *Analysis on nonlinear stiffness isolators revealing damping thresholds*
 Mu Qing Niu, Li-Qun Chen
- ← *Softening/hardening dynamics of nonlinear foundation beam with linear stiffening effect*
 Fangyan Lan, Tieding Guo, Wanzhi Qiao, Houjun Kang
- ← *Classification of the post-buckling solutions of a beam under large, but forceless, bending and torsion*
 Le Marrec Loïc, Lerbet Jean, Hariz Marwan
- ← *Sufficient conditions to exclude positive Lyapunov Exponents in the Thomas' system*
 Davide Martini, David Angeli, Giacomo Innocenti, Alberto Tesi
- ← *Modelisation of thermally induced jitter in a slender structure*
 Kathiravan Thangavel, Maurizio Parisse, Pier Marzocca
- ← *Resonant phase lags of an oscillator with polynomial stiffness*
 Martin Volvert, Gaëtan Kerschen

Mechanical and structural systems

Mechanical systems and structures

- ← *Improving rotor stability through direct piezoelectric effect*
Sérvio Haramura Bastos, Rui Vasconcellos
- ← *Numerical Simulation of a Bio-inspired, Bistable Plate System.*
Mrunal Bhalerao, Muhammad R. Hajj, Lei Zuo
- ← *Multiple Periodic Symmetric Limit Cycles of Two Coupled Sommerfeld Rotors*
Walter V. Wedig
- ← *Generating machine learning-based state maps from real-world friction-induced vibration data*
Charlotte Geier, Said Hamdi, Thierry Chancelier, Norbert Hoffmann, Merten Stender
- ← *A spring-mass mechanical system with moving edges having rich dynamical behaviour*
Jobin Josey, Balakrishnan Ashok
- ← *On the Statics and Torsional Dynamics of Coupled Kresling Origami Springs*
Ravindra Masana, Mohammed Daqaq
- ← *Higher order theories for the static and dynamic analysis of anisotropic shell structures*
Matteo Viscoti, Francesco Tornabene, Rossana Dimitri
- ← *Internal actuators and parametric oscillations in unconventional robotic locomotion*
Phanindra Tallapragada
- ← *Study of the effect of non-linear end supports on the unbalance response of the elastic shaft*
Jayanta Kumar Dutt, Krishanu Ganguly

- ← *Semi-Active Control Algorithm with Control-Structure Interaction for Magnetorheological Damper Used in Seismically-Excited Buildings*
Chia-Ming Chang, Chung-Chen Liu
- ← *Multiharmonic forced response analysis of a torsional vibration isolator using a nonlinear quasi-zero stiffness approach*
Sebastian Willeke, Michael Steidl, Norbert Reinsperger, Stephan Bohmeyer
- ← *Experimental Characterization and Numerical Modelling of Wire Rope Isolators*
Paolo Neri, Jeremiah Holzbauer
- ← *Unveiling bifurcation mechanisms of quasiperiodic partial rub oscillations in a piecewise smooth rotor-stator system*
Shan Fan, Ling Hong, Jun Jiang
- ← *Predicting limit cycle of modified Rayleigh differential equation*
Venkoba Shrikanth, Amar K. Gaonkar, Pramod Kumar Verma
- ← *Features of precession of a flexible rotor with a different number of elastic supports located with a clearance in the plane of rotation*
Anatoliy Azarov, Alexander Gouskov, Grigory Panovko
- ← *Nonlinear vibrations of a composite circular plate with a concentrated mass: effects of equilibrium configurations*
Ying Meng, Xiao Ye Mao, Hu Ding, Li-Qun Chen
- ← *Modelling Thermoelastic Damping in Nonlinear Plates with Internal Resonance*
Darshan Soni, Manoj Pandey, Anil K. Bajaj
- ← *An extensible double pendulum and multiple parametric resonances*
Shihabul Haque, Nilanjan Sasmal, Jayanta Bhattacharjee

- ← *Effect of magnet position in electro-magnetic transducer of middle ear implant*
 Rafal Rusinek, Krzysztof Kecik
- ← *Analysis of forced vibrations of the nonlinear elastic plate on a viscoelastic foundation subjected to hard excitation from harmonic load*
 Marina Shitikova, Anastasiya Krusser
- ← *Parameter Estimation for Linear Time-Varying (LTV) Uncertain System Using Physics-Informed Machine Learning*
 Junyeong Kim, Sejun Park, Ju H. Park, Sangmoon Lee
- ← *Space sunshade for global warming mitigation : dynamics and station keeping*
 B Shayak, Bala Balachandran
- ← *Mathematical Modelling of a Coefficient of Nonlinearity in Dynamics of Deep Groove Ball Bearing with Damage*
 Ivana Atanasovska, Dejan Momcilovic, Tatjana Lazovic
- ← *Flexible mechanisms as quasi-zero stiffness metamaterial resonators*
 Douglas Roca Santo, Leopoldo P.R. De Oliveira, Elke Deckers
- ← *An enhanced pathfollowing scheme for nonsmooth dynamics via improved computation of the monodromy matrix*
 Giovanni Formica, Franco Milicchio, Walter Lacarbonara
- ← *Dynamics of a damped variable mass system : Leaky balloon with string*
 Riddhika Mahalanabis, Balakrishnan Ashok
- ← *Recycled Smartdevices for Real-Time Monitoring of Civil Infrastructures*
 Arturo Buscarino, Carlo Famoso, Luigi Fortuna
- ← *Rocking Dynamics of Mud Motor Drilling using a Cosserat Rod Model*
 Meet Mehta, Ganesh R.

- ← *Origami Inspired Impact Energy Converter*
 Shadi Khazaaleh, Ahmed Dalaq, Mohammed Daqaq
- ← *Nonlinear dynamics of a visco-elastic beam under pulsating dead and follower forces*
 Francesco D'Annibale, Manuel Ferretti, Angelo Luongo
- ← *Pile installation via axial and torsional vibrations - the Gentle Driving of Piles method*
 Athanasios Tsetas, Apostolos Tsouvalas, Andrei Metrikine
- ← *Development and validation of an efficient model for bearing strain creep prediction*
 Hamid Ghorbani, Bart Blockmans, Wim Desmet
- ← *Solving the problem of nonlinear oscillations of a pendulum on a flexible stretchable thread.*
 Alexey Malashin
- ← *Nonlinear Modes of Jointed Structures with As-built Surface Topography*
 Robert Kuether, David Najera-Flores, Matthew Southwick
- ← *Digitally programmable piezoelectric metamaterials and nonlinear electromechanical structures with synthetic impedance circuits*
 Mustafa Alshaqqa, Obaidullah Alfahmi, Alper Erturk
- ← *Regular and complex behaviour in the pendulum system under a magnetic field*
 Yuliia Surhanova, Yuri Mikhlin
- ← *Resonance steady states and transient in some non-ideal systems*
 Yuri Mikhlin, Yana Lebedenko
- ← *Nonlinear Dynamics Analysis of Actuation Strategies of Clustered Tensegrity V-Expander Structures*
 Muhao Chen, Aguinaldo Fraddosio, Andrea Micheletti, Gaetano Pavone, Mario Daniele Piccioni, Robert E. Skelton

- ← *Subharmonic oscillations in PIIine ultrasonic motors*
Simon Kapelke
- ← *Nonlinear free vibration of functionally graded shallow shells with variable thickness resting on elastic foundations*
Tetyana Shmatko, Lidiya Kurpa, Jan Awrejcewicz
- ← *Free vibration analysis of functionally graded porous sandwich plates with a complex shape*
Tetyana Shmatko, Lidiya Kurpa, Walter Lacarbonara
- ← *Effect of Boundary Conditions on the Stability of a Viscoelastic Von Mises Truss*
Pritam Ghoshal, Qianyu Zhao, James Gibert, Anil Bajaj
- ← *An Origami Inspired Impact Energy Dissipator*
Ahmed Dalaq, Shadi Khazaaleh, Mohammed Daqaq
- ← *Accurate asymptotic description of nonlinear friction states for a detailed FEM model*
Salvador Rodríguez-Blanco, Javier González-Monge, Carlos Martel
- ← *Comparison between Pushover Methods for Seismic Analysis High-Rise RC Dual System Buildings*
Vinod Kumar Golla, Elena Oliver-Saiz, Francisco Lopez-Almansa (Poster)
- ← *Oscillations of a Nonlinear Beam in Contact with a Rigid Cylindrical Constraint*
Diptangshu Paul, Jayaprakash K R

Experimental dynamics

- ← *Numerical and experimental investigation of nonlinear dynamics of downhole drilling*
Ahmed Al Shekaili, Yang Liu, Evangelos Papatheou
- ← *A laboratory scale Foucault pendulum for the measurement of frame-dragging*
Matthew Cartmell, Edmondo A. Minisci
- ← *Effects of controller-induced dynamics on experimental bifurcation analysis*
Mark Blyth, Krasimira Tsaneva-Atanasova, Lucia Marucci, Ludovic Renson
- ← *Dynamic analysis of transmission line cables using nonlinear d frame element*
Nilson Barbieri, Gabriel De S. V. Barbieri, Renato Barbieri, Key Fonseca De Lima (Poster)
- ← *Rail-Structure-Interaction Parameters at Ballasted Viaduct in Rohtak - Gohana Elevated Stretch: Instrumentation, Measurements and Interpretation*
Nupur Saxena, Chandan Kumar, Pameer Arora, Samit Ray Chaudhuri
- ← *Tool Wear Supervising Applying Vibration Modal Analysis*
Piotr Wolszczak, Marcin Bednarz, Grzegorz Litak
- ← *Quasi-zero stiffness vibration isolator under vertical seismic loads*
Giovanni Iarriccio, Antonio Zippo, Moslem Molaie, Francesco Pellicano
- ← *A chain of real mechanical oscillators subjected to creep-slip friction and relatively high-frequency structural vibration*
Pawel Olejnik, Jan Awrejcewicz
- ← *Vibration analysis of electrical connector under different environments*
Rochdi El Abdi, F. Le Strat

- ← *An Electromagnetic Softening Spring: Experiment and Simulation*
 Maksymilian Bednarek, Bipin Balaram, Donat Lewandowski, Jan Awrejcewicz
- ← *Experimental Identification of Secondary Resonances using a Control-based Method*
 Tong Zhou, Gaëtan Kerschen
- ← *Analysis of Non-linear Vibrations Using DIC and the Smoothed Harmonics Method*
 Serena Occhipinti, Paolo Neri, Christian Maria Firrone, Daniele Botto
- ← *Rocking of rigid blocks on flexible foundations: modeling and experimental assessment*
 Pol D. Spanos, Alberto Di Matteo, Antonina Pirrotta
- ← *Experimental and numerical study of a magnetic pendulum*
 Peter Meijers, Panagiota Atzampou, Andrei Metrikine
- ← *Delayed acoustic self-feedback control of limit cycle oscillations in a turbulent combustor*
 Ankit Sahay, Abhishek Kushwaha, Samadhan A. Pawar, Midhun P. R., Jayesh M. Dhadphale, R. I. Sujith
- ← *Modeling turbulent thermoacoustic transitions using a mean-field synchronization approach*
 Samarjeet Singh, Amitesh Roy, Jayesh M. Dhadphale, Swetaprovo Chaudhuri, R. I. Sujith
- ← *Locomotion dynamics of an underactuated wheeled three-link robot*
 Leonid Rizyaev, Yizhar Or
- ← *A Platform for Data-Driven Nonlinear Dynamics and Mechatronics Education: A Student-Designed Spherical Magnetic Pendulum*
 James Oti, Anthony Migash, Ryan Mcdermott, Joseph Cornell, Nikhil Bajaj

System identification and SHM

- ← *Experimental design for corotating pinned spiral waves and synchronization*
Parvej Khan, Sumana Dutta (Poster)
- ← *Nonparametric identification for time-varying physical parameters and nonlinear restoring force based on UKF and Sage-Husa algorithm*
Ye Zhao, Bin Xu
- ← *Application of SINDy for the discovery of governing equations of a trapped particle in an acoustic radiation force field*
Mehdi Akbarzadeh, Sebastian Oberst, Shahrokh Sepehri Ahnema, Benjamin Halkon
- ← *Nonlinear system identification of a multi-story building with geometrical nonlinearity using a deterministic output-only-data approach*
Amirali Sadeqi, Dario Anastasio, Stefano Marchesiello
- ← *An investigation into model extrapolation and stability in nonlinear system identification*
Dario Anastasio, Stefano Marchesiello, Gianluca Gatti, Paulo J.P. Gonçalves, Alexander David Shaw, Micheal John Brennan
- ← *Machine learning-based dynamic method of rock characterisation for rotary-percussive drilling*
Kenneth Omokhagbo Afebu, Yang Liu, Evangelos Papatheou
- ← *An approach to monitor bolt faults in two-dimensional structures without reference*
Quankun Li, Qingzhou Zhao, Mingfu Liao, Xiaobo Lei
- ← *Physics-informed sparse identification of bistable nonlinear energy sink*
Qinghua Liu, Junyi Cao
- ← *Identification of non-linear model equations based on data-science approaches*
Simon Bäuerle, Timo Peter Baierl, Hartmut Hetzler
- ← *Neural network hyperparameter tuning for online model parameter updating using inverse mapping models*
Bas M. Kessels, Tom M.E. Janssen, Rob H.B. Fey, Nathan Van De Wouw

- ← *Reconstructing Nonlinear Backbone Curves from Smooth Coordinate Decomposition of Multivariate Impulse Response*
 Dalton Stein, David Chelidze
- ← *A Bayesian compressive sampling technique for determining the equations of motion of nonlinear structural systems*
 George D. Pasparakis, Vasileios Fragkoulis, Ioannis Kougioumtzoglou, Michael Beer
- ← *Physics Enhanced Sparse Identification of Nonlinear Oscillator with Coulomb Friction*
 Christos Lathourakis, Alice Cicirello
- ← *Experimental Characterization and Identification of the Shear Hysteretic Behavior of a Helical Wire Rope Isolator*
 Biagio Carboni, Nicolò Vaiana
- ← *A novel vibration response-based approach to monitor faults in bolted complex structures*
 Quankun Li, Qingzhou Zhao, Mingfu Liao, Xiaobo Lei
- ← *Data-driven delay identification with SINDy*
 Ákos Tamás Köpeczi-Bócz, Henrik Sykora, Dénes Tákacs
- ← *Model-based Unknown Input Estimation via Partially Observable Markov Decision Processes*
 Wei Liu, Zhilu Lai, Charikleia Stoura, Kiran Bacsá, Eleni Chatzi
- ← *Uncertainty Quantification in Parameter Estimation Using Physics-integrated Machine Learning*
 Zihan Liu, Amirhassan Abbasi, Prashant N. Kambali, C. Nataraj
- ← *Bayesian LSTM Neural Networks for Nonlinear System Identification*
 Thomas Simpson, Nikolaos Dervilis, Eleni Chatzi
- ← *Bifurcation scenarios in the hardware-in-the-loop experiments of highly interrupted milling processes*
 Rudolf R. Toth, Daniel Bachraty, Gabor Stepan

Aerospace structures

- ← *Control of orbital parameters of a dumbbell satellite using moving mass actuators*
Valery Pilipchuk, Steven Shaw, Nabil Chalhoub
- ← *Three-dimensional deployment of cable nets for active removal of space debris*
Paolo Fisicaro, Angelo Pasini, Paolo Sebastiano Valvo
- ← *Suspension nonlinear analysis and active vibration control of an aerospace structure*
Guoliang Ma, Liqun Chen
- ← *Control of orbital parameters of a dumbbell satellite using moving mass actuators*
Valery Pilipchuk, Steven Shaw, Nabil Chalhoub
- ← *Modal Testing of In Situ BAE TA Hawk Wing: Benchmark Dataset*
Matthew Bonney, David Wagg, Tim Rogers
- ← *Multi-layers radical morphing: shape transitions and vibration*
Ginevra Hausherr, Giulia Lanzara

Constitutive and phenomenological models

- ← *Stochastic delay modelling of landslide dynamics*
Srađ Kostić, Nebojša Vasović
- ← *A replacement model for nonlinear dynamics of electro-active liquid crystal coatings*
Anahita Amiri, Brandon Caasenbrood, Danqing Liu, Nathan Van De Wouw, Ines Lopez Arteaga
- ← *A new methodology for nonlinear analysis of magneto-rheological elastomers behavior under large amplitude oscillatory axial (LAOA) loadings*
Hossein Vatandoost, Ramin Sedaghati, Subhash Rakheja
- ← *Modeling Asymmetric Hysteresis: Continuous Development using Experimental Data*
Jin-Song Pei, Biagio Carboni, Walter Lacarbonara
- ← *Preliminary Results on the Simulation of Pressurized Sand Dampers by the Vaiana-Rosati Model*
Nicoló Vaiana, Luciano Rosati, Xenofon Palios, Nicos Makris
- ← *Differential Formulation of the Vaiana-Rosati Model*
Nicolò Vaiana, Luciano Rosati

Modal interactions and energy transfer

- ← *Inverted resonance capture cascade from low to high modal frequency*
Kevin Dekemele, Giuseppe Habib
- ← *Shape Optimization of Curved Mechanical Beams for Internal Resonance Enhancement*
Sahar Rosenberg, Oriel Shoshani
- ← *On the non-trivial solutions and their stability in a two-degree-of-freedom Mathieu-Duffing system*
Ahmed A. Barakat, Eva M. Weig, Peter Hagedorn
- ← *Nonlinear interactions of widely spaced modes*
Oriel Shoshani, Steven Shaw
- ← *A hysteretic vibration absorber for the mitigation of a flexible structure response*
Paolo Casini, Fabrizio Vestroni
- ← *On the role of wave resonances in the nonlinear dynamics of discrete systems*
Tiziana Comito, Miguel D. Bustamante
- ← *Nonresonant interactions between a linear system and a light double limit cycle oscillator*
Dhananjay kumar D. Tandel, Pankaj Wahi, Anindya Chatterjee
- ← *Koopman operator based Nonlinear Normal Modes for systems with internal resonance*
Rahul Das, Anil Bajaj, Sayan Gupta
- ← *Unsteady two-temperature heat transport in mass-in-mass chains*
Sergei D. Liazhkov, Vitaly A. Kuzkin
- ← *Introducing a Stack of Eccentric Rotors to Semantically Modify Non-linear Flexible Beam Continua*
Ioannis T. Georgiou

Rotating systems

- ← *A method for the analysis of the aeroelastic stability of slender wind turbines and its validation*
Chao Peng, Alessandro Tasora, Pin Lyu
- ← *Effect of Rub-Impact on Backward Whirl Excitation in a Cracked Rotor System*
Mohammad A. Al-Shudeifat, Rafath Abdul Nasar
- ← *Nonlinear dynamics of an accelerating rotor supported on self-acting air journal bearings*
Manas Ranjan Pattnayak, Jayanta Kumar Dutt, Raj Kumar Pandey
- ← *On the nonlinear dynamics of rotating hybrid nanocomposite blades with matrix crack*
Xu Ouyang, Krzysztof Kamil Żur, Hulun Guo
- ← *Parametric resonances due to torsional oscillations in a multi-degree of freedom driveline coupled by a series of universal joints*
Junaid Ali, Shveta Dhamankar, Evan Parshall, Gregory Shaver, Anil K. Bajaj, Keith Loiselle, Douglas Hansel
- ← *Transmission of rotation by a geometrically imperfect flexible shaft in a curved channel*
Yury Vetyukov
- ← *Nonlinear dynamics of asymmetric rotor subjected to rotor-stator contact*
Ali Fasihi, Grzegorz Kudra, Jan Awrejcewicz
- ← *Reduced order modeling of rotating structures featuring geometric non-linearity with the direct parametrisation of invariant manifolds method*
Adrien Martin, Andrea Opreni, Alessandra Vizzaccaro, Loïc Salles, Olivier Thomas, Attilio Frangi, Cyril Touzé

Passive energy damping

- ← *Enhanced performance of nonlinear energy sink under harmonic excitation using acoustic black hole effect*
Wang Tao, Ding Qian
- ← *Free balls in rotating or non-rotating tracks can mitigate rotor vibration*
Michael M. Selwanis, Mohammed M. Ibrahim, Mohamed S Khadr, Ahmed F. Nemnem
- ← *Approximate Analytical Investigation of the Variable Inertia Rotational Mechanism*
Nicholas Wierschem, Anika Sarkar
- ← *The optimum inerter-based isolation systems for dynamic response mitigation of multi-storey buildings*
Sudip Chowdhury, Arnab Banerjee, Sondipon Adhikari
- ← *Vibro-impact NES: Nonlinear mode approximation using the multiple scales method*
Balkis Youssef, Remco Leine
- ← *Vibration Damping in Fiber-Reinforced Bistable Composites with Magnetic Particles*
Alessandro Porrara, Giulia Lanzara
- ← *Magnetic Field and Ferrite Particles Interaction for Membranes with Augmented Shock- Absorption Capability*
Stefania Fontanella, Ginevra Hausherr, Shiela Meryl Cumayas, Antonio Loisi, Giulia Lanzara

Nonlinear dynamics and control

Nonlinear vibrations control

- ← *Variable Length Control of a Planar Pendulum with Time Averaged Constant Cable Length*
Harrish Joseph, Mary Lanzerotti, Walter Lacarbonara
- ← *Hoist Stabilization Design Method*
David Reineke, Duy Nguyen, Luyi Tang, Mary Lanzerotti, Walter Lacarbonara
- ← *Attenuating nonlinear effects of pendulum tuned mass damper by an isochronous spring*
Kai Xu, Xugang Hua, Walter Lacarbonara
- ← *Vibrational Resonance of a Driven Charged Bubble Oscillator*
Uchechukwu E. Vincent, O. Tosin Kolebaje, Benedicta E. Benyeogor, Peter V.E. McClintock
- ← *Nonlinear electroacoustic resonator at low excitation amplitudes: grazing incidence analysis*
Emanuele De Bono, Maxime Morell, Manuel Collet, Emmanuel Gourdon, Alireza Ture Savadkoohi, Claude-Henri Lamarque, Morvan Ouisse, Gaël Matten
- ← *A Nonlinear Piezoelectric Shunt Absorber with : Internal Resonance*
Zein Alabidin Shami, Cyril Touz, Christophe Giraud-Audine, Olivier Thomas
- ← *Damping and negative stiffness characteristics of an electromagnetic mechanism for vibration control*
Mehran Shahraeeni, Vladislav Sorokin, Brian Mace, Ashvin Thambyah, Sinniah Ilanko
- ← *Control of an acoustic mode by a digitally created Nonlinear Electroacoustic Absorber at low excitation levels: Analytical and Experimental results*
Maxime Morell, Manuel Collet, Emmanuel Gourdon, Alireza Ture Savadkoohi

- ← *Nonlinear control of friction-induced vibrations by using cascade architecture*
 Lyes Nechak, Pascal Morin
- ← *Nonlinear vibration control of a slightly curved beam with distributed piezoelectric patches*
 Jacek Przybylski
- ← *Seismic response control of a non-linear structure using magneto-rheological dampers*
 Mahdi Abdeddaim, Arnav Anuj Kasar, Salah Djerouni
- ← *Performance Improvement of Autoparametric Vibration Absorber by Eliminating the Viscous Damping and the Nonlinearity*
 Chao Zhang, Hiroshi Yabuno, Kenji Yasui
- ← *Vibration control with a magnetic tristable NES on a cantilever beam*
 Jun-Dong Fu, Shui Wan, Jiwei Shen, Kevin Dekemele
- ← *Nonlinear vibration isolators with spring damper inerter configured in linkage*
 Jian Yang, Baiyang Shi, Wei Dai
- ← *Numerical and experimental study of a pneumatic Nonlinear Energy Sink*
 Clément Raimond, Thomas Roncen, Thierry Jardin, Leonardo Sanches, Guilhem Michon
- ← *Exact dynamical solution of the Kuramoto-Sakaguchi Model for finite networks of identical oscillators*
 Antonio Mihara, Rene O. Medrano-T.
- ← *Frequency-Energy Analysis of Coupled Linear Oscillator with Unsymmetrical Nonlinear Energy Sink*
 Mohammad Al-Shudeifat
- ← *Preliminary numerical analysis of the Vibro-Impact Isolation systems under seismic excitations*
 Giuseppe Perna, Maurizio De Angelis, Ugo Andreaus

- ← *Time-delay vibration reduction control of tension leg in submerged floating tunnel*
 Jian Peng, Xiaowen Chen, Lianhua Wang, Stefano Lenci
- ← *An adaptive nonlinear hybrid vibration absorber*
 Louis Mesny, Sebastien Baguet, Simon Chesné
- ← *A 3D Structural Model for Nonlinear Dynamic Analyses of Rigid Blocks Supported by Wire Rope Isolators*
 Stefania Lo Feudo, Nicolò Vaiana
- ← *The enhanced nonlinear friction bearing isolators using negative stiffness inertial amplifiers*
 Sudip Chowdhury, Arnab Banerjee, Sondipon Adhikari
- ← *Long-stroke hydraulic damping device and verification of its vibration characteristics*
 Jingchao Guan, Xilu Zhao (Poster)
- ← *Effect of wear flat length on the global dynamics of rotary drilling*
 Kapil Kumar, Pankaj Wahi
- ← *Vibration control of lossless transmission lines with nonlinear terminators: a simplifying approach*
 Mohammad Amin Faghihi, Shabnam Tashakori, Ehsan Azadi Yazdi, Nathan Van De Wouw

Sensors and actuators

- ← *A method for measuring the mass of multiple substances simultaneously in viscous environments*

Zhang Mai, Hiroshi Yabuno, Yasuyuki Yamamoto, Sohei Matsumoto

- ← *Evaluating the Shape of a Nonlinear Deformed PVDF Wearable Pressure Sensors by Analyzing the Acoustic Travelling Wave Speed*

Masoud Naghdi, Haifeng Zhang

- ← *Sensing Sound with Electrospun Piezo Materials on a D-Printed Structure*

Krishna Chytanya Chinnam, Giulia Lanzara

- ← *Magneto-Dynamic Characterization of a Silicone Filament Embedded with Magnetic Composite Micro-Spheres*

Luis Pedro Viera Alexandrino, Alessandro Porrari, Giulia Lanzara

Control of nonlinear systems

- ← *Model-based and Model-free Control of a Parallel Manipulator with Flexible Links*
Maíra Martins da Silva, Fernanda Thaís Colombo
- ← *Super Twisting Sliding Mode Control with Accelerated Gradient Descent Method for Synchronous Reluctance Motor Control System*
Jun Moon, Hyunwoo Kim
- ← *Vibration Control of Time-Varying Nonlinear Systems*
Abdullah A. Alshaya
- ← *Assessment of Power Consumption Improvement in Position and Attitude Control of Spacecraft using Electromagnetic Force Assist*
Hector Gutierrez, Oceane Topenot, Solenne Lamaud
- ← *A Reference Governor for Constrained Control of a Multi Degree of Freedom Metamaterial*
Rick Schieni, Mehmet Simsek, Onur Bilgen, Laurent Burlion
- ← *Observer design for semi-linear stochastic partial differential equations*
Ragul Ravi, Ju H. Park, Mathiyalagan Kalidas
- ← *Active Vibration Suppression of Flexible Satellite With Appointed Time Convergence*
Danyu Li, Liang Zhang, Shijie Xu, Yuan Li, Naigang Cui
- ← *Control via Nonlinear Feedback Linearization with Machine Learning*
Hector Vargas Alvarez, Gianluca Fabiani, Nikolas Kazantzis, Constantinos Siettos, Ioannis G. Kevrekidis
- ← *Stabilization mechanism of limit cycle oscillation using control based continuation and phase locked loop*
Gourc Etienne, Vergez Christophe, Cochelin Bruno
- ← *Image-based aerial grasping of a moving target based on model predictive control*
Marjan Moghanipour, Afshin Banazadeh

- ← *Some comments on Nonlinear Dynamic behaviour and Control of a Duffing D oscillator*
 Jose M. Balthazar, Mauricio A. Ribeiro, Hilson Henrique Daum
- ← *Motion Control of a Pendulum via Magnetic Interaction*
 Panagiota Atzampou, Peter Meijers, Apostolos Tsouvalas, Andrei Metrikine
- ← *Koopman-Operator-Based Model Predict Control for Attitude Dynamics on $SO(3)$*
 Hongyu Chen, Ti Chen
- ← *On the stability of sampled-data systems with viscous damping and dry friction*
 Csaba Budai, Tamás Haba, Gábor Stépán
- ← *The Influence of a Non-Instantaneous Double Support Phase on the Efficiency of a HZD Controlled Bipedal Robot*
 Yinnan Luo, Ulrich J. Römer, Marten Zirkel, Lena Zentner, Alexander Fidlin
- ← *The migration of a Neural Network Observer training using the Deep Learning approach*
 Loukil Rania, Gazehe W.

Networks synchronization

- ← *Synchronization of Discrete-Time Fractional Complex Networks With Time Delays Via Event-Triggered Strategy*
Xiaolin Yuan, Guojian Ren, Yongguang Yu, Wei Chen
- ← *Anti-synchronization of Quaternion Valued Inertial Neural Networks with Unbounded Time Delays: Non-Separation Approach.*
Sunny Singh, Subir Das (Poster)
- ← *Explosive death transitions in a complex network of chaotic systems*
Samana Pranesh, Sayan Gupta (Poster)
- ← *Anomalies in Synchronization of Globally Coupled Mechanical Metronomes*
Omer Livneh, Oriel Shoshani
- ← *Embedding dimension of the dynamical manifold in the phase space as a measure of chimera states*
Olesia Dogonasheva, Boris Gutkin, Denis Zakharov
- ← *Synchronised States and Transients in Minimal Networks of Oscillators*
Andrea Elizabeth Biju, Sneha Srikanth, Krishna Manoj, Samadhan A. Pawar, R. I. Sujith
- ← *Bifurcations and Chimera States in Self-Excited Inertia Wheel Pendulum Arrays*
Gilad Yakir, Yuval Levi, Oded Gottlieb

New trends in nonlinear dynamics

Vehicle dynamics

- ← *Dynamic response of a geometrically nonlinear quarter car model with a MacPherson suspension travelling on a harmonic road profile*
Pankaj Wahi, Vaibhav Dhar Dwivedi
- ← *On the self-excited chatter vibration in motorcycles*
Alexander Schramm, Silvio Sorrentino, Alessandro De Felice
- ← *Investigation of the control characteristics for a driver-vehicle system with steering and throttle control*
Alois Steindl, Johannes Edelmann, Manfred Plöchl
- ← *Modelling and Simulation of the Nonlinear Vibrations of Axially Moving Long Slender Continua in Tall Host Structures*
Jakob Scheidl, Yury Vetyukov, Stefan Kaczmarczyk
- ← *Hybrid Autoregressive Neural Networks to predict forced nonlinear Vibrations*
Tobias Westmeier, Daniel Kreuter, Simon Bäuerle, Hartmut Hetzler
- ← *An Initial Bifurcation Analysis of an EV Pickup Truck*
Shaun Smith, Duc Nguyen, James Knowles, Mark Lowenberg, Sean Biggs
- ← *Reversing Along a Curved Path by an Autonomous Truck-Semitrailer Combination*
Levente Mihályi, Dénes Takács
- ← *The effects of road curvature on the stability of path-following of automated vehicles*
Illés Vörös, Dénes Takács
- ← *Stability control of two-wheeled trailers*
Hanna Zsafia Horvath, Adam Balint Feher, Denes Takacs
- ← *Analysis of nonlinear tire dynamics in high fidelity nonlinear Finite Element simulation*
Lukas Bürger, Frank Naets

Energy harvesting

- ← *Stochastic analysis of a bistable piezoelectric energy harvester with a matched electrical load*
Kailing Song, Michele Bonnin, Fabio Traversa, Fabrizio Bonani
- ← *Enhancing Aeroelastic Wind Energy Harvesting Using Quasi-Zero Stiffness*
Shun Chen, Liya Zhao
- ← *Numerical simulations of energy harvesting in a portal frame coupled with a nonlinear-energy sink*
Angelo M. Tusset, Alisson L. Agusti, Maria E. K. Fuziki, Giane G. Lenzi
- ← *An electromagnetic vibro-impact nonlinear energy sink for effective energy harvesting and vibration reduction of vortex induced vibrations*
Haiqin Li, Mengxin He, Ding Qian
- ← *Leveraging 2:1 Parametric Resonance in a Notional Wave Energy Harvester*
Giuseppe Giorgi
- ← *A broadband magnet-induced cantilever piezoelectric energy harvester coupled to nonlinear energy sink*
Jiwei Shen, Shui Wan, Jundong Fu, Kevin Dekemele
- ← *Experimental testing of a bi-stable point wave energy absorber under harmonic wave excitations*
Mohammad A. Khasawneh, Mohammed F. Daqaq
- ← *Self-tuning sliding mass electromagnetic energy harvester for dramatic frequency bandwidth enhancement*
Mohammad Bukhari, Oumar Barry
- ← *Escape from the potential well of bistable vibration energy harvesters using buckling level modifications*
Camille Saint-Martin, Adrien Morel, Ludovic Charleux, Emile Roux, Aya Benhemou, Quentin Demouron, Adrien Badel

- ← *Design and Optimization of Electromechanical Coupling in Electromagnetic Vibrational Harvester*
 Krzysztof Kecik, Ewelina Stezycka, Kateryna Lyubitska
- ← *Simultaneous passive suppression and energy harvesting from galloping using a bi-stable piezoelectric nonlinear vibration absorber*
 Guilherme Rosa Franzini, Vitor Schwenck Franco Maciel, Guilherme Jorge Vernizzi, Daniele Zulli
- ← *Probabilistic analysis of an asymmetric bistable energy harvester*
 João Pedro Norenberg, Americo Cunha Jr, Samuel Da Silva, Paulo Sergio Varoto
- ← *Effects of energy harvesting from a piezoelectric element attached to a propelling flexible tail*
 Hossam Alqaleiby, Mahmoud Ayyad, Muhammad R. Hajj, Lei Zuo

MEMS/NEMS

- ← *Reduced order modelling with Deep Learning methods of the steady-state response in MEMS*
Giorgio Gobat, Alessia Baronchelli, Attilio Frangi
- ← *Managing parametric frequency noise using nonlinearity in a High-Q micromechanical torsion pendulum*
Jon Pratt, Stephan Schlamminger, Aman R. Agrawal, Charles A. Condos
- ← *Mode Localization of Electrostatically Coupled Shallow MEMS Arches*
Hassen M. Ouakad, Ayman M. Alneamy
- ← *Nonlinear modeling of micro-cantilever beams*
Ayman Alneamy, Walter Lacarbonara, Eihab Abdel-Rahman
- ← *Differential Capacitance Gas Sensors*
Fehmi Najar, Mehdi Ghommam, Samed Kocer, Alaaeldin Elhady, Eihab Abdel-Rahman
- ← *How to Excite Anti-Symmetric Modes in a Symmetric MEMS?*
Sasan Rahmanian, Ayman Alneamy, Yasser S. Shama, Samed Kocer, Eihab M. Abdel-Rahman, Mustafa Yavuz
- ← *The response of nonlinear circular viscoelastic panels to electrodynamic excitation*
Anish Kumar, Oded Gottlieb
- ← *Multiple internal resonances and impacting dynamics of micromachined arch resonators*
Laura Ruzziconi, Rodrigo T. Rocha, Wen Zhao, Amal Z. Hajjaj, Mohammad I. Younis
- ← *Control of an electrostatically actuated micro portal frame with : internal resonance subjected to damping disturbances*
Wagner Barth Lenz, Rodrigo T. Rocha, Fahimullah Khan, Yousef Algoos, Mohammad I. Younis

- ← *Amplitude-Voltage Response of Superharmonic Resonance of Fourth Order of Electrostatically Actuated MEMS Cantilever Resonators*
 Dumitru I. Caruntu, Christopher I. Reyes
- ← *Vibration mitigation by two parametric anti-resonances in high-Q resonators: a preliminary case study*
 Miguel Ramírez Barrios, Fadi Dohnal
- ← *Detection of pull-in and periodic solutions of magMEMS model using Sturm's theorem*
 Piotr Skrzypacz, Bek Kabduali, Grant Ellis
- ← *Emergence of nonlinear damping in nanomechanical systems from thermal interactions*
 Ali Sarafraz, Farbod Alijani
- ← *A MEMS triple sensing scheme based on nonlinear coupled micromachined resonators*
 Zhengliang Fang, Stephanos Theodossiades, Amal Z. Hajjaj

Fractional order system

- ← *Fractional damping term in the Helmholtz and Duffing nonlinear oscillators*
Mattia Coccolo, Jesús M. Seoane, Miguel Ángel Sanjuán
- ← *Reliability Problem of a Fractional Stochastic Dynamical System Based on Stochastic Averaging Method and Deep Learning Algorithm*
Yu Guan, Li Wei, Dongmei Huang, Natasa Trisovic
- ← *Nonlinear vibration of small size beams on fractional visco-elastic foundation*
Nikola Nešić, Milan Cajić, Danilo Karličić, Julijana Simonović
- ← *On the Dynamics Analysis of Microresonator System with Fractional-order*
Tao Xi, Jin Xie, Zhaohui Liu
- ← *Generalized Fractional-Order Complex Logistic Map and Fractals on FPGA*
Sara M. Mohamed, Wafaa S. Sayed, Lobna A. Said, A. G. Radwan
- ← *Fractional-Order Extension and FPGA Verification of Chaotic Models for Several Diseases*
Sara M. Mohamed, Wafaa S. Sayed, Mohammad Adm, Lobna A. Said, A. G. Radwan (Poster)
- ← *Fractional control performance assessment of the nonlinear mechanical systems*
Patryk Chaber, Paweł D. Domański
- ← *Broadening the operational range of a fractionally damped piezoelectric energy harvester*
Stepa Paunović, Milan Cajić, Danilo Karličić
- ← *Fractal Response of a Nonlinear Packaging System*
Luis M. Palacios-Pineda, Óscar Martínez-Romero, Daniel Olvera-Trejo, Alex Elías-Zúñiga

- ← *State estimation of time-fractional reaction-diffusion SEIR model for COVID- with mobile sensors*
Fudong Ge, YangQuan Chen
- ← *Reliability of fractional-order hybrid energy harvesters under random excitations*
Ya-Hui Sun, Yong-Ge Yang, YangQuan Chen
- ← *Bird Like Trajectories in D Chaotic System Incorporated with Fractional Order, Memristor and Encryption*
Muhammad Ali Qureshi

Metamaterials

- ← *A Metamaterial Concept using the Hybrid Position Feedback Control Method and Bistable Structural Elements*
Mehmet Simsek, Rick Schieni, Laurent Burlion, Onur Bilgen
- ← *Nonlinear interactions in a nonlinear time-dependent chain*
Aurélie Labetoulle, Alireza Ture Savadkoohi, Emmanuel Gourdon, Lamarque Claude-Henri
- ← *Acoustic non-reciprocity in strongly nonlinear locally resonant lattices*
Mohammad Bukhari, Oumar Barry, Alexander Vakakis
- ← *Inverse Design of Periodic and Quasi-Periodic Nonlinear Mechanical Metamaterial*
Pravinkumar Ghodake
- ← *A Nonlinear Metamaterial Induced by Nonlinear Damping Effect with Inertia Amplifiers*
Bao Zhao, Xingbo Pu, Bart Van Damme, Andrea Bergamini, Eleni Chatzi, Andrea Colombi
- ← *Modal interactions in a non-linear mass-in-mass periodic chain*
Jean Flosi, Alireza Ture Savadkoohi, Lamarque Claude-Henri
- ← *Towards the Robust Optimal Design of Nonlinear Metamaterials*
Camila Da Silveira Zanin, Samy Missoum, Alireza Ture Savadkoohi, Sébastien Baguet, Régis Dufour
- ← *Topological Indices of Line Graph of Metal Organic Compound*
Muhammad Talha Farooq, Pawaton Kaemawichanurat (Poster)
- ← *Bandgap formation study of a geometrically nonlinear metamaterial*
Kyriakos Alexandros Chondrogiannis, Vasilis Dertimanis, Eleni Chatzi
- ← *Parametric resonance and extreme motions of a cantilever with a tip mass: an experimental-theoretical study*
Hamed Farokhi, Eetu Kohtanen, Alper Erturk

Biomechanics and small-scale robots (Organizer Prof. Y. Liu)

- ← *Multi-Objective Optimization Of a Vibro-Impact Capsule Moving In Small Intestine*
Jiapeng Zhu, Maolin Liao, ZhiQiang Zhu
- ← *AI assisted early bowel cancer detection using a self-propelled capsule robot*
Kenneth Omokhagbo Afebu, Jiyuan Tian, Evangelos Papatheou, Yang Liu, Shyam Prasad
- ← *Dynamics of a soft capsule robot self-propelling in the small intestine via finite element analysis*
Jiyuan Tian, Zepeng Wang, Yang Liu, Shyam Prasad
- ← *A nonlinear model for identifying human-exoskeleton coupling parameters in lower extremities*
Cheng Huang, Yao Yan
- ← *Dynamics of a vibro-impact self-propelled capsule encountering a bump in the small intestine*
Ruifeng Guo, Yao Yan
- ← *A Vibro-Impact Capsule Driven by its Inner GMM Exciter*
Zhi Li, Maolin Liao, Zhipeng Liu, Zexu Wang, Zhihang Feng
- ← *Shape Forming of a Soft Magnetic Microrobot Using Non-Homogeneous Magnetic Fields*
Kiana Abolfathi, Jose A. Rosales Medina, Hesam Khaksar, James H. Chandler, Klaus McDonald-Maier, Keyoumars Ashkan, Pietro Valdas-
tri, Ali Kafash Hoshidar
- ← *Wireless force sensing of a micro-robot penetrating a viscoelastic solid*
Moonkwang Jeong, Felix Fischer, Tian Qiu
- ← *Constrained Green's function for a beam with arbitrary spring and nonlinear spring foundation*
Xiang Zhao, Qi Wang, Weidong Zhu, Yinghui H. Li

- ← *Complex dynamics of a vibro-impacting capsule robot in contact with a circular fold*
 Shan Yin, Yao Yan, Joseph Páez Chávez, Yang Liu
- ← *Parameter identification of a vibro-impact capsule robot through optimisation*
 Shan Yin, Jiajia Zhang, Yang Liu
- ← *Rectilinear motion of a chain of interacting bodies in a viscous medium*
 Tatiana Figurina, Dmitri Knyazkov
- ← *The closed-loop controller optimization of a discontinuous capsule drive with the use of neural network in the uncertain frictional environment*
 Sandra Zarychta, Marek Balcerzak, Artur Dąbrowski, Andrzej Stefański
- ← *Comparison of feed-forward control strategies for hopping model with intrinsic muscle properties of different complexities*
 Dóra Patkó, Ambrus Zelei, Giuseppe Habib
- ← *Time-optimal control approximation for a discontinuous capsule drive*
 Marek Balcerzak, Sandra Zarychta, Artur Dąbrowski, Andrzej Stefański
- ← *Walking on an uneven terrain with a SLIP model based compliant biped*
 Saptarshi Jana, Abhishek Gupta
- ← *Dynamic modelling of a vibro-impact capsule robot self-propelling in the large intestine via finite element method*
 Zepeng Wang, Jiyuan Tian, Yang Liu, Shyam Prasad
- ← *Nonlinear transduction and dynamic buckling of dielectric elastomer actuators*
 Yi-Husan Hsiao, Yufen Chen
- ← *Numerical investigation of a piezoelectric wrinkled film-based vibration sensor for the vibro-impact capsule robot*
 Bo Wang, Haohao Bi, Yang Liu

- ← *Human balance during quiet stance with physiological and exoskeleton time delays*
Shahin Sharafi, Thomas K. Uchida
- ← *Characterisation of Miniaturised Soft Continuum Robots with Reinforced Chambers*
Jialei Shi, Wenlong Gaozhang, Helge A. Wurdemann
- ← *Microrobot control from individual to collective*
Kiana Abolfathi, Ali K. Hoshidar

Biological systems dynamics

- ← *Chemical Signalling and Pattern Formation in Schoener's Predator-Prey Model*
Purnedu Mishra, Dariusz Wrzosek
- ← *Synaptic scaling enables extreme selectivity in high-dimensional neurons*
Valeri A. Makarov, Sergey Lobov, Vasilisa Stepasyuk, Julia Makarova
- ← *Effects of rising sea surface temperature on the dynamics of coral-algal interactions*
Sasanka Shekhar Maity, Joydeb Bhattacharyya, Samares Pal
- ← *Hopf Bifurcation Analysis for a Delayed Nonlinear-SEIR Epidemic Model on Networks*
Madhab Barman, Nachiketa Mishra (Poster)
- ← *Multiscale Model of Cardiac Muscle Contraction using Langevin Dynamics and Biological Elastic Network Analysis*
Yasser Aboelkassem
- ← *Do strokes affect the brain's critical state? A theoretical perspective*
Jakub Janarek, Zbigniew Drogosz, Jacek Grela, Jeremi K. Ochab, Pawel Oswiecimka, Maciej A. Nowak, Dante R. Chialvo (Poster)
- ← *Non-linear dynamics of the temporomandibular joint disc*
Jerzy Margielewicz, Damian Gaska, Grzegorz Litak
- ← *Global dynamical analysis of age-structured population model*
Preeti Deolia, Anuraj Singh (Poster)

Stochasticity and noise

- ← *A novel alternative formalism of the Wiener path integral technique - circumventing the Markovian assumption for the system response process*
Ilias G. Mavromatis, Apostolos F. Psaros, Iannis A. Kougiumtzoglou
- ← *Diagrammatic perturbation theory for Stochastic nonlinear oscillators*
Akshay Pal, Jayanta kumar Bhattacharjee
- ← *Fuzzy Generalized Cell Mapping with Adaptive Interpolation (FGCM with AI) for Bifurcation Analysis of Nonlinear Systems with Fuzzy Uncertainties*
Ling Hong, Jun Jiang, Xiao-Ming Liu
- ← *Response statistics of a conceptual airfoil with consideration of extreme load conditions*
Qi Liu, Yong Xu
- ← *Modeling stick balancing with stochastic delay differential equations*
Gergő Fodor, Zoltán Kovács, Dániel Bachraty
- ← *Effect of an uncertain symmetry-breaking parameter on the global dynamics of the Duffing oscillator*
Kaio C.B. Benedetti, Paulo B. Gonçalves, Stefano Lenci, Giuseppe Rega

Nonlinear phenomena in bio- and ecosystems dynamics

- ← *Control policies for dengue: insights from a mathematical model*
Carla Pinto, Dumitru Baleanu, Amin Jajarmi
- ← *A data-driven uncertainty quantification framework for mechanistic epidemic models*
Americo Cunha Jr, David A.W. Barton, Thiago G. Ritto
- ← *Non-stationary dynamics in a complex marine biogeochemical model*
Guido Occhipinti, Cosimo Solidoro, Roberto Grimaudo, Davide Valenti, Paolo Lazzari
- ← *Resonance bifurcations in a discrete-time predator-prey system*
Anuraj Singh, Vijay Shankar Sharma (Poster)
- ← *An Overview on Time-frequency Effects of ECG Signals Using Synchroextracting Transform*
M. Varanis, S. Hemmati, M.C. Filipus, F.L. de Abreu, Jose M. Baltazar, C. Nataraj
- ← *Investigation of Parkinsonian tremor signals troughs nonlinear time series analysis*
Antonio Zippo, Francesco Pellicano, Giovanni Iariccio
- ← *Novel approaches and “similarity score” for the identification of active sites during patient-specific catheter ablation of atrial fibrillation*
Vasanth Ravikumar, Xiangzhen Kong, Henri Roukoz, Elena Tolkacheva

Stability of thin liquid film flows over a uniformly heated slippery substrate under Heat Flux boundary condition

Anandamoy Mukhopadhyay* and Amar Gaonkar*

* Department of Mathematics, Vivekananda Mahavidyalaya (The University of Burdwan), West Bengal 713103, India.

** Department of Mechanical, Materials and Aerospace Engineering, IIT Dharwad, Karnataka-580011, India.

Abstract. We investigate the stability of gravity-driven Newtonian, thin liquid film falling down a uniformly heated slippery inclined plane. The rigid inclined plane is not thermally insulated as considered by most authors ([1]- [3]) in their study. In real situation heat losses to the ambient air at the solid-air interface. Consequently, we have considered Heat Flux (HF)/mixed-type boundary condition as the thermal boundary condition on the rigid plate. This boundary condition involves the heat flux from the rigid plate to the surrounding liquid and the heat losses from the wall to the ambient air. Using long-wave expansion method we construct a highly nonlinear evolution equation in terms of the film thickness at any instant. Using normal mode approach the linear study reveals the onset of instability. Weakly nonlinear study demarcates the different stable/unstable zones and their variations with the variation of the wall film Biot number B_w and the slip length δ , associated with the heat losses at the solid-air interface and the slippery effects of the rigid substrate respectively. Finally, the numerical simulation of the evolution equation is performed using Crank-Nicolson scheme over a periodic domain. It confirms the results obtained by the linear and the weakly nonlinear study.

Introduction

Hydrodynamical stability of thin liquid film flows down a uniformly/non-uniformly heated vertical/inclined plane is a fascinating problem. Recently, few works ([1]- [3]) are published, where the rigid substrate is considered to be slippery, since in laboratory researchers are engaged to prepare hydrophobic/superhydrophobic surfaces to fulfill the demand of industry. Now the thermal boundary condition considered by the researchers ([1]- [3]), for the thin liquid film flow problem over a heated slippery substrate is of specified temperature (ST) boundary condition / Dirichlet condition, where the rigid substrate is assumed to be of thermally insulated and therefore no heat losses at the solid-air interface. In real situation there exists no such insulation that prevents heat loss to the ambient air. In the proposed model, our aim is to discuss the effect of slip length on the dynamics and the stability of thin liquid film flow, over a uniformly heated slippery substrate, under the HF boundary condition.

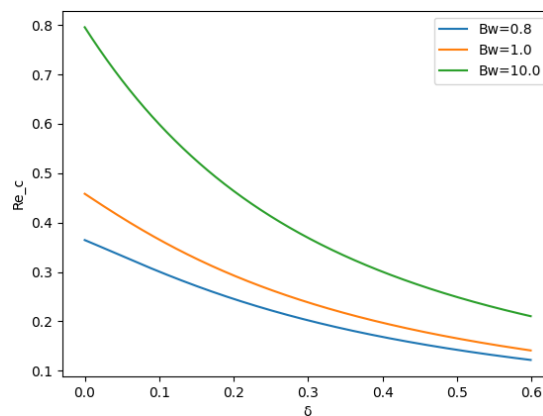


Figure : Variation of critical Reynold's number with the variation of slip length and for typical values of wall film Biot number $B_w = 0.8, 1.0, 10.0$.

Results and Discussions

As the wall film Biot number increases, the Re_c also increases. It confirms the stabilizing role of wall film Biot number B_w . Also, as the slip length δ increases, Re_c decreases. It shows the destabilizing role of the slip length, found by the linear stability analysis.

References

- [1] Samanta A. (2020) Non-modal stability analysis in viscous fluid flows with slippery walls. *Phys. Fluids* **32**:064105.
- [2] Chattopadhyay A., Desai A. S., Gaonkar A., Barua A. K. and Mukhopadhyay A. (2021) Weakly viscoelastic film on a slippery slope. *Phys. Fluids* **33**:112107.
- [3] Chattopadhyay A., Mukhopadhyay A. and Barua A. K. (2021) Thermocapillary instability on a film falling down a non-uniformly heated slippery incline. *Int.J. Non-linear Mech.* **133**:103718.

Influence of Pulsating Internal flow on Marine Riser with Nonlinear Geometry

Feras Alfosail^{*,**}, Shadid Nutaifat^{**}, Qasim Saleem^{**}, Americo Cunha Jr^{***} and
Mohammad I. Younis^{*}

^{*}King Abdullah University of Science and Technology, Thuwal 23955-9600, Saudi Arabia

^{**}Consulting Services Department, Saudi Aramco, Dhahran 31311, Saudi Arabia

^{***}Rio de Janeiro State University, UERJ

Abstract. In this work, we numerically explore the dynamics of inclined marine risers when it is subjected to pulsating internal fluid flow. The presence of geometric nonlinearities with static deflection makes the response of the inclined riser different from conventional top tension risers when subjected to pulsating internal flows. The riser model equation is solved via Galerkin method and validated using perturbation approaches for single mode. Then, we study the multi-modal dynamic response of the riser which reveals interesting and complex nonlinear interactions.

Introduction

Pulsating flow is a phenomenon that affects the oil and gas industries. It occurs due to abrupt perturbations and fluctuations in the internal fluid flow of the riser pipe which in return can affect and influence the vibrational motion of the structure. It occurs due to several reasons such as the nature of the multi-phase flow and sudden geometric changes [1]. Because the value of the excitation amplitude and frequency of fluctuation of the flow varies, the influence of the flow can be sever especially if the frequency of these flows are near structural resonances of the riser making them prone to failure by fatigue. On that basis, following the previous work in [2-3], the motion of the riser is analysed when it is subjected to internal flow fluctuations.

Results and Discussion

The inclined riser to be analyzed in this work is under mid-plane stretching and subjected to static deflection with pulsating internal fluid flow. The equation of the model is analyzed and solved to obtain dynamic response curves of the riser. Due to the squaring of the terms and flow of the internal fluid flow is unsteady, the excitation frequency is expected to occur at both Ω and 2Ω because of the nature of the parametric excitation. The dynamic response of the lowest three modes is depicted in Fig.1

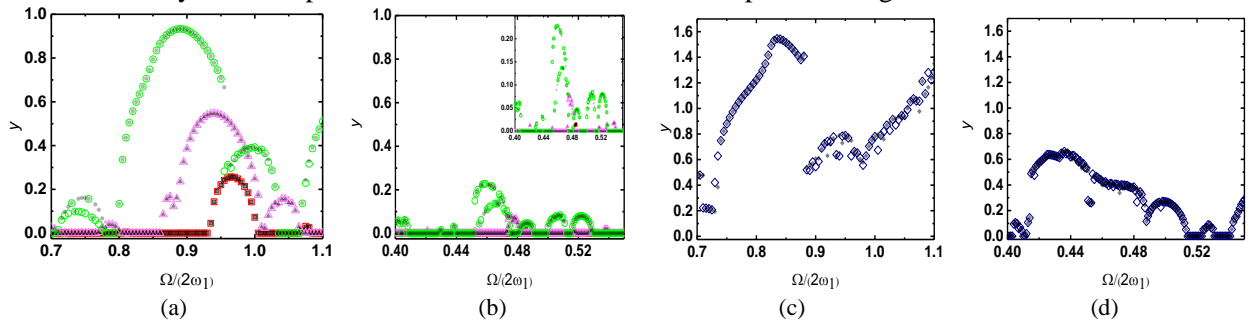


Figure 1: Frequency response curves around the first mode for $V = \sqrt{\sigma}$, $c_d = 0.416$ at $x=0.48$. (a,b) Backward Sweep (\square) $\gamma = 0.25$, (\triangle) $\gamma = 0.50$, (\circ) $\gamma = 0.75$. The inset is magnified of (b). (c,d) (\diamond) $\gamma = 1$. Filled shapes denotes forward sweep.

We observe, in Fig. 1, the frequency response curves for the lowest three modes of the riser. The influence of the different components that exists in the system is apparent as a result of the interaction. The softening nonlinearity effects due to the quadratic term is less apparent due to the competing effects between the first mode and contributions from other modes that exist in the response. This softening is observed very well in Fig. 1b in comparison to other cases around the secondary parametric resonance excited due to the squaring of the velocity term. In addition, the complexity of the interaction with other resonances in the response of the solution near Ω and 2Ω become more visible at higher fluctuating velocity as the solution demonstrate quasi-periodic leading to chaotic behavior. In addition, due to the nonlinear interaction, we observe the co-existence of solutions due to the presence of quadratic nonlinearities. As a result, the response of the riser reveals interesting complex and rich dynamic features.

References

- [1] Gedikli, E. D., and Dahl, J. M. (2017) Mode excitation hysteresis of a flexible cylinder undergoing vortex-induced vibrations. *J. Fluid. Struct.* **308-322**.
- [2] F. K. Alfosail, A. H. Nayfeh, and M. I. Younis. (2016) An analytic solution of the static problem of inclined risers conveying fluid. *Meccanica*, vol. **52**: **1175-1187**.
- [3] F. K. Alfosail, A. H. Nayfeh, and M. I. Younis. (2016) Natural frequencies and mode shapes of statically deformed inclined risers. *Int. J. of Nonlinear Mech.*

Vortex-induced forces and vibration of subsea structures in proximity to larger objects

Henry Francis Annapeh* and Victoria Kurushina*,**

*Laboratory of Vibration and Hydrodynamics Modelling, Industrial University of Tyumen, Tyumen, Russia, ORCID 0000-0003-1256-499X

**School of Engineering, Newcastle University, Newcastle upon Tyne, United Kingdom, ORCID 0000-0001-9294-5789

Abstract. Flow around three identical circular cylinders in statics and undergoing transversal vortex-induced vibration in close proximity to a subsea equipment is modelled using computational fluid dynamics. Simulation results include time histories of hydrodynamic coefficients, FFT data, pressure distribution, velocity fields, accompanied by the sensitivity analysis of the spacing among the structures and the flow profile.

Introduction

Analysis of the vortex-induced loads on structures in a group in a fixed position and experiencing vibration is essential to obtain correct fatigue estimates and ensure safe design of offshore systems. In the current work, a group of three subsea structures of a circular cross-section and arranged in tandem is modelled in statics and with one structure experiencing transversal oscillations. The circular structures are considered, first, standalone, and then placed in proximity to a larger piece of the subsea equipment, presented by a squared cylinder, as shown in Fig. 1. Three types of flow are investigated: uniform, linearly sheared current and the flow of a parabolic velocity profile. Proximity of structures, their hydrodynamic properties and flow features create complex wake interference effects, especially, when the lock-in and near-lock-in conditions are considered.

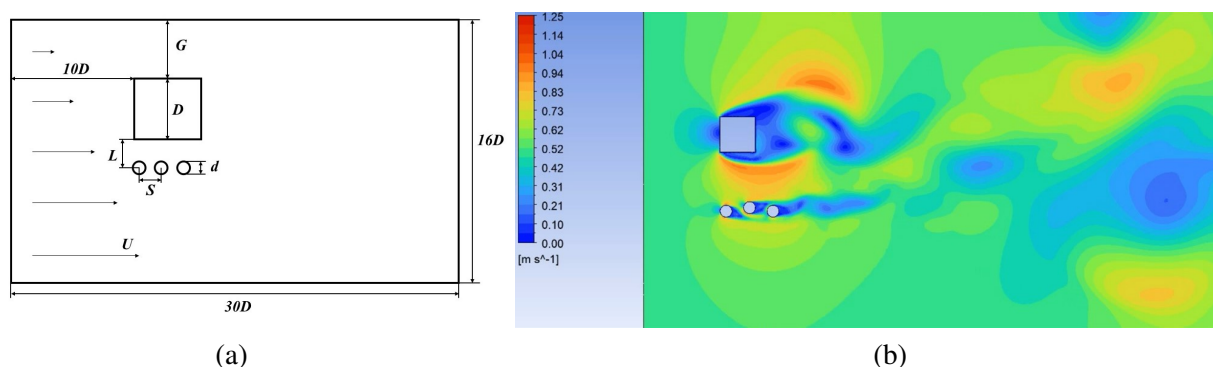


Figure 1: Group of identical subsea circular structures in proximity to an equipment under the linearly sheared flow: (a) general view on the computational domain; (b) velocity contour for the case of the moving middle structure.

Results and discussion

The computational fluid dynamics (CFD) method and the $k - \omega$ SST turbulence model is used in this study to investigate the vortex shedding process and vibration characteristics of the fluid-structure interaction. Simulations are performed with the ANSYS Fluent software, including the initial benchmarking of the numerical model with the published results for a submerged cylindrical object under the uniform flow conditions [1–3]. Changes are observed in the pressure and velocity fields, vortex formation process, frequency and amplitude of the hydrodynamics force components with respect to each structure, and displacement time histories for oscillating bodies. Several considered scenarios indicate variations in the flow field and load fluctuations related to the wake superposition from a larger subsea object and the group of smaller structures.

References

- [1] J. Franke and W. Frank. Large eddy simulation of the flow past a circular cylinder at $Re = 3900$. *J Wind Eng Ind Aerod*, 90(10):1191–1206, 2002.
- [2] S. Wornom, H. Ouvrard, M.V. Salvetti, B. Koobus, and A. Dervieux. Variational multiscale large-eddy simulations of the flow past a circular cylinder: Reynolds number effects. *Comput Fluids*, 47(1):44–50, 2011.
- [3] C. Norberg. Effects of Reynolds number and a low-intensity freestream turbulence on the flow around a circular cylinder. *Chalmers University, Goteborg, Sweden, Technological Publications*, 87(2):1–55, 1987.

Vortex-induced loads on subsea pipelines due to marine biofouling

Nikita Finogenov* and Victoria Kurushina*,**

*Laboratory of Vibration and Hydrodynamics Modelling, Industrial University of Tyumen, Tyumen, Russia

**School of Engineering, Newcastle University, Newcastle upon Tyne, United Kingdom, ORCID 0000-0001-9294-5789

Abstract. Marine biofouling is a major economic and technical concern worldwide for nearly all industries operating in water. The current work considers several geometrical configurations of the growing plants using the numerical computational fluid dynamics model to estimate the effect on the fluctuating fluid forces, pressure and vortex shedding patterns.

Introduction

The accumulation and growth of microorganisms, plants or small animals settling on subsea structures contributes to several aspects to be considered during the structural design of ship hulls, offshore platform supports, risers, jumpers, flowlines, subsea equipment, power cables, etc. Estimating the impact of marine biofouling represents a substantial modelling challenge for elements of both traditional oil and gas production systems and novel offshore energy harvesting systems. Biofouling expands the outer dimensions of subsea structures, increases its surface roughness, mass, changes the flow regime and resulting hydrodynamic loads from external currents and waves. Following the studies [1–3], the ongoing research attempts to identify the geometrical configurations leading to substantial alterations in the vortex shedding patterns and increase in the lift and drag forces using the computational fluid dynamics approach.

Results and discussion

The present work considers a circular cylinder in a fluid domain, where the structure with a partial coverage with fouling elements is subjected to a uniform flow, as shown in Fig. 1. The 2D numerical model is designed for the simplified cone-shaped fouling, equally-spaced over the downstream part of the structural circumference. The study considers several heights, widths and a different number of fouling elements and includes the mesh verification, simulations and analysis of hydrodynamic coefficients. The results obtained reveal maximum expected fluid forces, their dominant frequencies, vortex shedding patterns, changes to the velocity, pressure and vorticity fields.

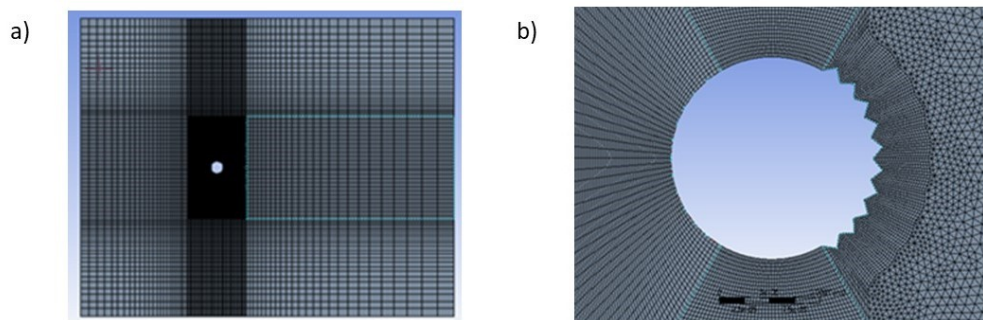


Figure 1: Numerical model for the flow over cylindrical structure with biofouling: a) general view on the mesh of the fluid domain; b) mesh around the structure with a simplified fouling model.

References

- [1] Zeinoddini M., Bakhtiari A., Ehteshami M., Seif, M.S. (2016) Towards an understanding of the marine fouling effects on VIV of circular cylinders: Response of cylinders with regular pyramidal roughness. *Appl Ocean Res* **59**:378-394.
- [2] Bakhtiari A., Zeinoddini M., Ashrafi-pour H., Tamimi V., Harandi M.M.A., Jadidi, P. (2020) The effects of marine fouling on the wake-induced vibration of tandem circular cylinders. *Ocean Eng* **216**:108093.
- [3] Ashrafi-pour H., Zeinoddini M., Tamimi V., Rashki M.R., Jadidi P. (2022) Two-degrees-of-freedom vortex-induced vibration of cylinders covered with hard marine fouling. *Int J Mech Sci* **233**:107624.

A new Koopman-inspired approach to match flow field excitation with consequent structure responses for nonlinear fluid-structure interactions

Cruz Y. Li^{1,2}, Zengshun Chen¹, Xisheng Lin², Tim K.T. Tse², and Yunfei Fu²

¹School of Civil Engineering, Chongqing University, Chongqing, China

²Dept. of Civil and Environmental Engr., The Hong Kong University of Science and Technology, Hong Kong SAR

Abstract. This work presents a novel method to form constitutive fluid-to-structure, excitation-to-response correspondences for insights into nonlinear fluid-structure interactions (FSI). It combines temporal orthogonality and phenomenological visualization, serving as a Koopman-inspired, POD-projected, and machine-learning-embedded method that can be seen as an advanced Discrete Fourier/Z-Transform. Successful implementation with a prism wake with homogenous and anisotropic turbulence attests to its capability to handle a broad spectrum of problems involving nonlinear and stochastic dynamics.

Introduction

One long-standing difficulty of fluid-structure interactions (FSI) is the inability to match a flow field excitation with consequent structure response(s). There is yet an effective method to perform the task because of FSI's multi-dimensional complexities, involving many research frontiers like fluid mechanics, structural dynamics, nonlinearity, dimensionality, turbulence, stochasticity and chaos, and so on.

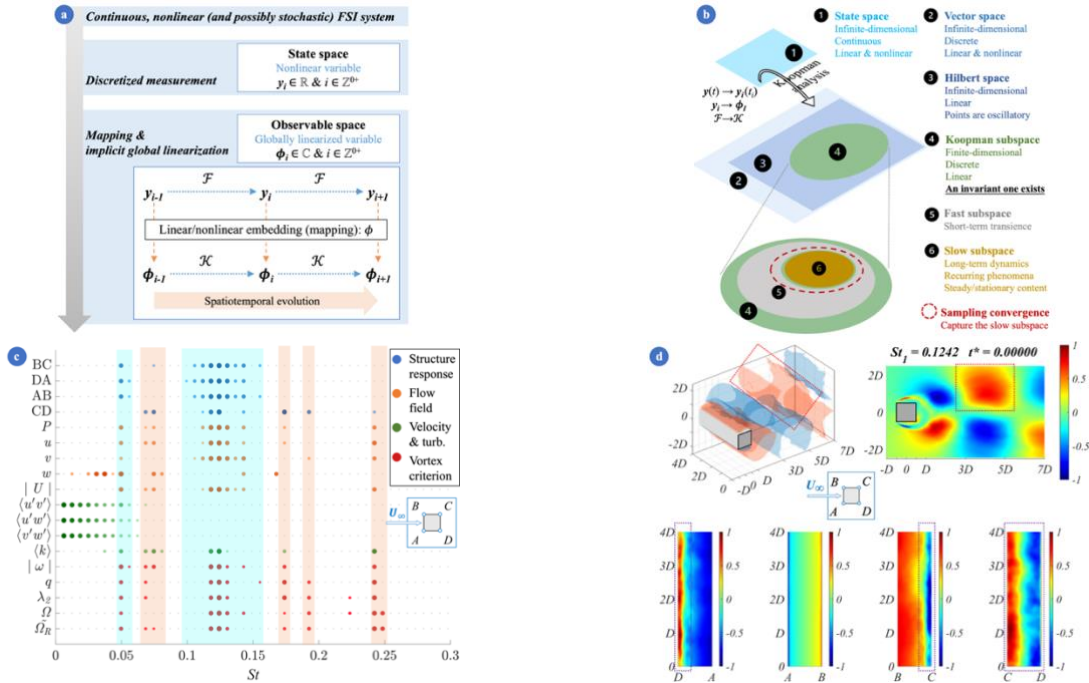


Figure 1: a) an overview of the Koopman theory; b) space transformations and mappings performed by Koopman algorithms; c) A demonstration of the multi-observable frequency-matching procedure to establish six dominant fluid-structure correspondences in the prism wake example; d) a snapshot of the dynamic Koopman mode showing the phenomenological content of matched flow field excitation and resultant structure surface pressures at $St = 0.1242$, the underlying mechanism is the formation of separation-induced asymmetric wall jets, shear-layer-triggered separation bubbles and reversed flows, reattachment as a result of excessive curvature and bubble enclosure, and eventual shedding of longitudinal substructure (i.e., rolls) as a part of a Karman vortex.

Results and discussion

Inspired by applied Koopmanism (Fig. 1a) [1], the authors developed and successfully actualized a data-driven approach to overcome the problem. The procedure begins with a series of space transformations and an implicit, globally optimal linearization, isolating orthogonal eigen tuples from spatiotemporally entangled raw measurements (Fig. 1b). Afterwards, the Koopman model distributes the dynamical content onto a discretized, sampling-independent Fourier spectrum, on which constitutive fluid-structure correspondence can be established by multi-observable frequency-matching (Fig. 1c). Finally, each fluid-structure pair can be visualized by the newly proposed dynamic Koopman mode, providing phenomenological information for full disclosures of underlying mechanisms (Fig. 1d). This method's data-driven nature means it can be applied to a broad spectrum of FSI cases, opening windows for new fluid mechanics insights. It also shows promise in control problems because each observed response can now be traced back to its excitation origin.

References

- [1] Budišić, M., Mohr, R., Mezić, I. (2012) Applied Koopmanism. *Chaos* **22**(4) 047510.

A parsimonious identification approach in the frequency-domain for experimental fractional systems of unknown order

Jose Antunes^{*}, Philippe Piteau^{**}, Xavier Delaune^{**}, Romain Lagrange^{**} and Domenico Panunzio^{**}

^{*}Center for Nuclear Sciences and Technologies, IST, Lisbon University, 2695-066 Bobadela, Portugal

^{**}Université Paris-Saclay, CEA, Service d'Études Mécaniques et Thermiques, F-91191 Gif-sur-Yvette, France

Abstract. When the order of experimental fractional systems is unknown, frequency domain identification is typically based on linear least-squares (L_2) methods, which often prove unsatisfactory. The main reason is that the solutions they provide are dense, often leading to a continuous of identified fractional differential orders, which obfuscate the very basic phenomena one wishes to highlight. In order to overcome such difficulty, the present work proposes the use of a L_1 based nonlinear identification approach, which naturally leads to parsimonious identified results. This method is successfully illustrated on a system transfer function with both integer and fractional differential terms.

Introduction

Fractional models are being increasingly used in many branches of physics and engineering [1]. In this work we deal with the identification of fractional models from experimental Frequency Response Functions (FRFs) in the frequency domain $H(i\omega)$, when the integro-differential equations discrete order(s) α_n are unknown:

$$Z(i\omega) = \frac{1}{H(i\omega)} = \frac{F(i\omega)}{X(i\omega)} = \sum_{n=1}^N c_n (i\omega)^{\alpha_n}$$

The linear identification procedure proposed by Hartley & Lorenzo [2] is straightforward to implement. The differential order continuum is discretized in the interval $[\alpha_{\min}, \alpha_{\max}]$ sampled at $\Delta\alpha$, so that $m=1, \dots, M$ differential order terms are identified. The FRFs $Z(i\omega_k) = 1/H(i\omega_k)$ are measured at $k=1, \dots, K$ frequencies. Then, the model is formulated in and solved by the Least Squares Deviation (LSD) method:

$$\begin{bmatrix} (i\omega_1)^{\alpha_1} & \dots & (i\omega_1)^{\alpha_M} \\ \vdots & \ddots & \vdots \\ (i\omega_K)^{\alpha_1} & \dots & (i\omega_K)^{\alpha_M} \end{bmatrix} \begin{Bmatrix} c_1 \\ \vdots \\ c_M \end{Bmatrix} = \begin{Bmatrix} Z(i\omega_1) \\ \vdots \\ Z(i\omega_K) \end{Bmatrix} \rightarrow \mathbf{M}\mathbf{c} = \mathbf{z} \rightarrow \mathbf{c}_{LSD} = \min \|\mathbf{M}\mathbf{c} - \mathbf{z}\|_{L_2} \rightarrow \mathbf{c}_{LSD} = \mathbf{M}^+ \mathbf{z} = (\mathbf{M}^T \mathbf{M})^{-1} \mathbf{M}^T \mathbf{z}$$

Results and discussion

Unfortunately, solutions provided by the LSD method are dense, producing a continuous of identified fractional differential orders as M increases, which is objectionable. In order to overcome this difficulty, we propose to replace the LSD by the Least Absolute Deviation (LAD) method, a nonlinear L_1 -based identification approach that is sparsity-promoting, leading to parsimonious results:

$$\mathbf{c}_{LAD} = \min \|\mathbf{M}\mathbf{c} - \mathbf{z}\|_{L_1}$$

We illustrate the identification results on the following test system, previously used by Hartley & Lorenzo [2]:

$$Z(\omega) = 1(i\omega)^2 + 1.4(i\omega)^{1.5} + 1(i\omega) + 1.4(i\omega)^{0.5} + 1$$

with three integer and two fractional derivatives. The range of integro-differential order hypothesized for identification is $\alpha \in [-1, 3]$, sampled at $\Delta\alpha = 0.1$, these conditions being highly stringent compared to [2]. The LAD identification is based on the Iterative Reweighted Least Squares (IRLS) algorithm [3], which can minimize any L_p norm. Figure 1 clearly demonstrates, not only the essential problem of the common LSD identification method, but also the significant improvements obtained when the sparsity-promoting LAD approach is used. Robustness of the identification results is currently being addressed.

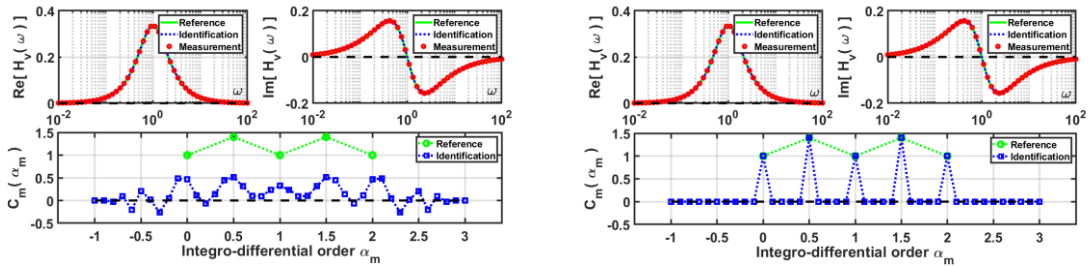


Figure 1: Left side - FRFs and derivative coefficients using common least-squares (L_2) identification; Right side - FRFs and derivative coefficients using nonlinear sparse (L_1) identification.

References

- [1] Machado J.A. et al. (2010) Some Applications of Fractional Calculus in Engineering. *Math. Probl. Engineering* **2010**/639801:1-34.
- [2] Hartley T.T., Lorenzo C.F. (2003) Fractional-Order System Identification Based on Continuous Order Distribution. *Signal Processing* **83**:2287-2300.
- [3] Björk A. (1996) Numerical Methods for Least Squares Problems. SIAM, Philadelphia.

Use of chaotic invariants to identify regimes in circulating fluidized beds

David de Almeida Fiorillo*, Aline Souza de Paula* and Geovany Borges**

*Department of Mechanical Engineering, University of Brasilia, 70910-900, Brazil

**Department of Electrical Engineering, University of Brasilia, 70910-900, Brazil

Abstract. This work addresses the fluidization regime identification from experimental time series of static pressure obtained along a cold fluidization column by means of chaotic invariants. The cold circulating fluidized bed FB plant is instrumented at three different points of the column for a spatiotemporal analysis. We propose a normalized chaos index based on the ratio of Kolmogorov entropy between different column positions, and a divergence parameter. The value of the divergence associated with the Hurst exponent (H) was able to identify all four fluidization regimes for all tested particles. The main contribution of this work is the proposal of a new spatiotemporal approach to identify fluidized bed regime based on chaotic invariants evaluated from static pressure time series.

Introduction

Circulating fluidized bed (CFB) gasifiers have great potential to convert large amounts of carbonaceous feedstocks (biomass, municipal and industrial solid waste) into fuel gas. In this conversion process, the inventory of solid mass is reduced, which hinders maintaining the desired fluidization regime. The regime identification is an essential task to control the process and ensure operational continuity. Important contributions to fluidization regimes characterization occurred when scientists showed the presence of chaos in time series of a gas-solid fluidized bed process [1]. Identifying the regime in a column fluidization is a nonlinear spatiotemporal problem. Some authors have attempted to identify local behaviour in CFB, but not the global fluidization regime of the column [2,3]. This work addresses the fluidization regime identification from experimental time series of static pressure obtained along a cold fluidization column by means of chaotic invariants.

Results and Discussion

The cold CFB plant is instrumented at the base (1), middle (3), and top (5) of the column for a spatiotemporal analysis. Three different particles – glass 355 μ m ID, sand 1.0mm ID, and sand 1.2mm ID – operating in four distinct regimes – expanded, bubbling, turbulent, and fast – are considered. We propose a normalized chaos index, IK_{ij} ($i, j = \{1, 3, 5\}$), based on the ratio of Kolmogorov entropy between different column positions, and a divergence $d = IK_{53} - IK_{13}$. The value of the divergence associated with the Hurst exponent (H) was able to identify all four fluidization regimes for all tested particles. Figure 1(a) shows the evolution of IK_{13} , IK_{53} and IK_{15} for the four analyzed regimes, while Figure 1(b) depicts Hurst exponent for different column positions and regimes for the sand particle 1.0mm. As main result, we learned that the expanded regime is associated with $d \approx 0$, $H_3 \approx H_5$ and $H_1 > 0.7$; the bubbling regime is related to $d \approx 0$ and $H_1 < 0.7$; the turbulent regime occurs when $0 < d < \max(d)$; while in fast regime d reaches its maximum value.

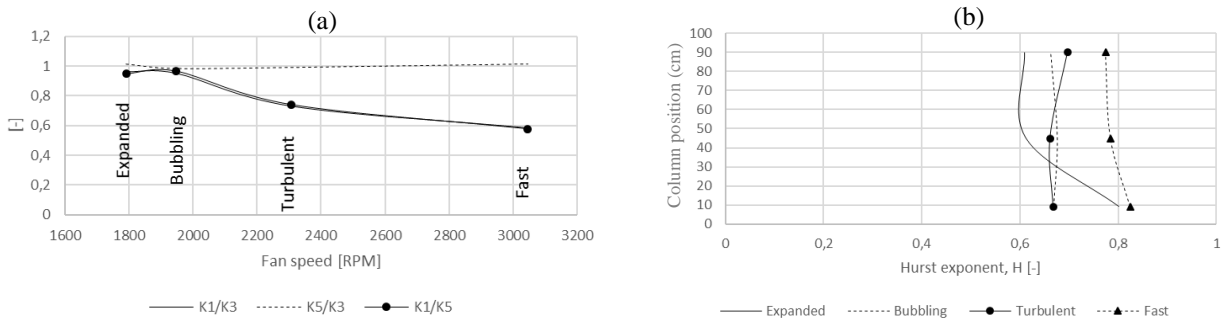


Figure 1: Results for sand 1.0mm: (a) Chaos indexes evolution in the different regimes; (b) Hurst exponent for different column positions and regimes.

References

- [1] van den Bleek, C. M., Schouten, J. C., Deterministic chaos: a new tool in fluidized bed design and operation. *The Chemical Engineering Journal and the Biochemical Engineering Journal*, 53: 75-37, 1993.
- [2] Letzel, H.M., Schouten, J.C., Krishna, R., van den Bleek, C.M., Characterization of regimes and regime transitions in bubble columns by chaos analysis of pressure signals. *Chemical Engineering Science*, 52: 4447-4459, 1997.
- [3] Marzocchella, A., Zijerveld, R. C., Schouten, J. C., van den Bleek, C. M., Chaotic Behavior of Gas-Solids Flow in the Riser of a Laboratory-Scale Circulating Fluidized Bed. *AIChE Journal*, 43(6):1458 – 1468, 1997.

Aeroelastic limit cycle oscillations due to multi-element control surface with freeplay

Larissa D. Wayhs-Lopes*, Douglas D. Bueno** and Carlos E. S. Cesnik ***

*Department of Mechanical Engineering and **Mathematics, São Paulo State University, Ilha Solteira, SP, Brazil

***Department of Aerospace Engineering, University of Michigan, Ann Arbor, MI, United States

*ORCID # 0000-0002-0706-2170, **ORCID # 0000-0002-1783-0524***ORCID # 0000-0002-5633-8815

Abstract. Single control surface (CS) freeplay has been well investigated in the aeroelastic field and several studies describe its effect on the limit cycle oscillations (LCO). Airworthiness regulations establish that this discontinuous non-linearity needs to be considered in both CS and trailing-edge tab, if the latter one exists. In this context, the present study introduces the effects of freeplay from both CS and tab on the LCO. The four degree-of-freedom typical section is considered, highlighting the main differences when compared with the freeplay of a single trailing-edge surface. The results show that higher amplitudes are identified for this configuration when compared to the classical case.

Introduction

Discontinuous nonlinearities as freeplay are commonly present in hinge connections. The piecewise linear torque of a hinge with freeplay (gap of amplitude 2δ in which the stiffness has no action) depends discontinuously on the rotation angle β , such that $T_\beta = k_\beta(\beta \pm \delta)$, if $|\beta| > \delta$ and $T_\beta = 0$, if $|\beta| < \delta$. Since this is a topic addressed by airworthiness regulations (MIL-A-8870C, by United States Military Standard; AC 23.629-1B and AC 25.629-1B by Federal Aviation Administration), the literature review for aeroelastic systems with freeplay is dense and one of the main effects observed is the appearance of LCO [1]. The effect of freeplay in a single control surface is largely studied [2], for example using the three degree-of-freedom (3-DOF) typical section based on Theodorsen's unsteady aerodynamics [3], even though the regulations highlight the need of considering the freeplay not only in the main control surfaces but also in the corresponding tabs. Mashhadani et al. [4] studied the airfoil typical section with an added fourth DOF, a tab attached to the trailing edge of the CS. The authors consider freeplay on the tab only. A recent work is found to examine freeplay in both leading and trailing control surfaces [5], showing how considering simultaneous freeplay in different CS is a new topic in the field. In this context, this work presents the effect of freeplay acting in both CS and tab for the LCO of the 4-DOF typical section (plunge, pitch, CS, and tab), employing the Hénon's technique for time marching.

Results and discussion

Figure 1 shows the bifurcation diagrams for the CS (left) and the tab (right) inversion points ($\dot{\beta} = 0$ and $\dot{\gamma} = 0$) for three scenarios regarding the freeplay inclusion: *i.* CS only, *ii.* tab only, and *iii.* both CS and tab. In general, the scenarios can be compared in terms of the flight speed where the LCO start, the maximum magnitude of the LCO, and their complexity, usually related to the amount of inversion points at certain speeds. Comparing the scenarios with CS freeplay (*i.* and *iii.*), the maximum CS magnitudes are of similar order whereas the maximum tab magnitudes are intensified by the presence of simultaneous CS element freeplay. Also, the scenario *i.* presents higher complexity around the freeplay boundary for CS motion. Comparing the scenarios with tab freeplay (*ii.* and *iii.*), the scenario *ii.* has more complex LCO in the range from $V/V_f = 0.24$ to $V/V_f = 0.56$ and the presence of multiple freeplay produces higher magnitudes, for both CS and tab motions. This latter conclusion is an important motivation to consider freeplay in various elements of a control surface.

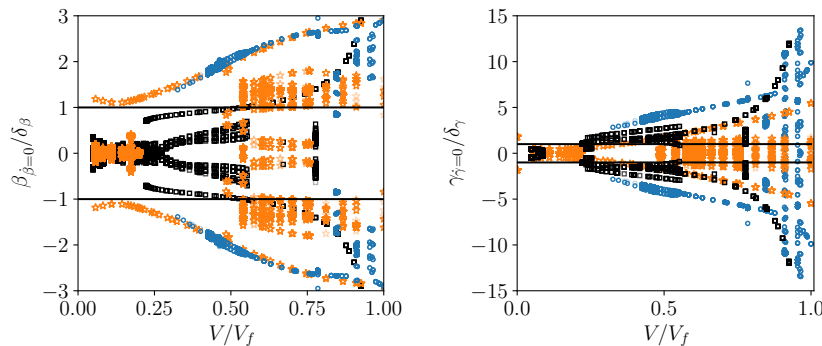


Figure 1: Bifurcation diagram for the control surface (left) and the tab (right) inversion points ($\dot{\beta} = 0$ and $\dot{\gamma} = 0$). Three scenarios of freeplay: *i.* (*) CS only, $\delta_\beta = 0.2$ deg; *ii.* (□) tab only, $\delta_\gamma = 0.4$ deg; *iii.* (o) both CS and tab, $\delta_\beta = 0.2$ deg and $\delta_\gamma = 0.4$ deg.

References

- [1] Dowell, E. H. and Edwards, J. and Strganac, T. (2003) Nonlinear Aeroelasticity. *J. Aircr.* **40**:857-874.
- [2] da Silva J.A.I., Marques F.D. (2022) Characterization of typical aeroelastic sections under combined structural concentrated nonlinearities. *J. Vib. Control* **28**:1739-1753.
- [3] Theodorsen, T. (1935) General Theory of Aerodynamic Instability and the Mechanism of Flutter. *NACA Rept. 496* **13**:374-387.
- [4] Al-Mashhadani W. J., Dowell E. H., Wasmi H. R., Al-Asadi A. A. (2017) Aeroelastic response and limit cycle oscillations for wing-flap-tab section with freeplay in tab. *J. Fluids Struct.* **68**:403-422.
- [5] Q. Yu and M. Damodaran, B.C. Khoo (2022) Nonlinear aeroelastic analysis of a multi-element airfoil with free play using continuation method. *J. Fluids Struct.* **109**:103482.

The nonlinear phenomena in the unstable region of a single heated channel natural circulation loop with supercritical water

Jin Der Lee* and Shao Wen Chen**

*Nuclear Science and Technology Development Center, National Tsing Hua University, Hsinchu, Taiwan, R.O.C.

**Institute of Nuclear Engineering and Science, National Tsing Hua University, Hsinchu, Taiwan, R.O.C.

Abstract. In this study, the nonlinear dynamic model of a supercritical natural circulation loop (NCL) is developed, and supercritical water is selected as the working fluid for analysis. Based on the design parameters of a next-generation supercritical water nuclear reactor, this study conducts nonlinear dynamic analysis of the system after the occurrence of instability. The results indicate that complex nonlinear phenomena could exist in the system, such as subcritical Hopf bifurcations, supercritical Hopf bifurcations and period doubling bifurcations. A distinct route from periodic oscillations to chaotic oscillations is identified through period doubling bifurcations. The analysis of fast Fourier spectral transform further confirms the existence of chaotic oscillation.

Introduction

The advanced applications with supercritical fluids are implemented in various aspects, e.g. the new type of thermal power plants and the next-generation nuclear power plants. The supercritical heated system is inherently a nonlinear system. Since the instabilities, especially density-wave instability, may deteriorate the operation and safety of a supercritical heated system, it is essential to clarify the nonlinear phenomena of them. However, the nonlinear dynamic models for supercritical heated systems are quite sparse in the literatures. Some subcritical system codes or CFD tools [1-2] were amended to investigate the nonlinear characteristics in the supercritical heated systems. At present, such large system codes are generally inappropriate for analyzing the nonlinear phenomena in detail due to their complexity and time-consuming. Therefore, the objective of this study is to develop a simple nonlinear dynamic model of a single heated channel NCL at a supercritical pressure, which can conduct nonlinear stability analysis for the system.

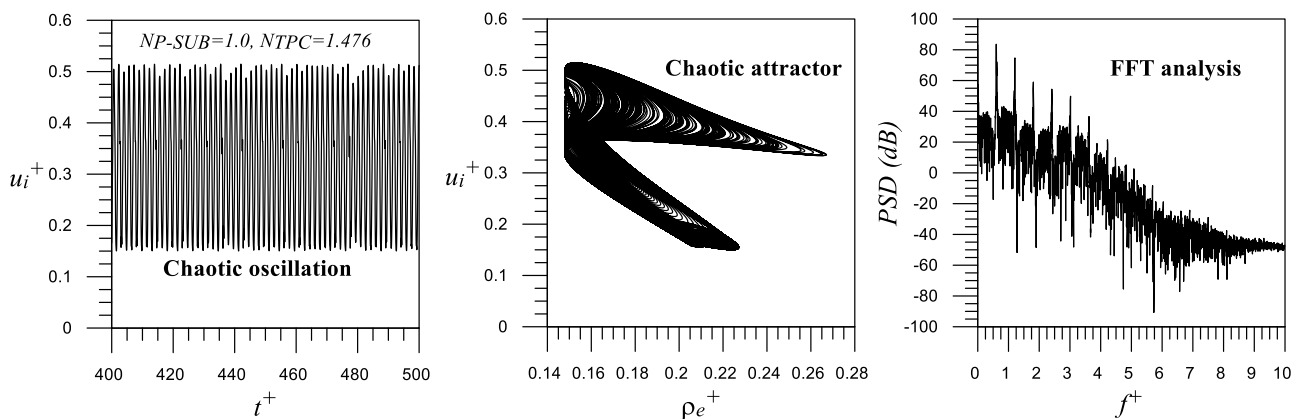


Figure 1: Chaotic oscillation, the corresponding attractor and Fast Fourier Transform (FFT) analysis.

Results and discussion

Employing three-region polynomial approximation [3], the nonlinear dynamic model of a supercritical heated channel NCL can be derived by the boundary condition: the summation of pressure drops through this closed NCL equals to zero. Through the nonlinear analysis, this study finds that outlet loss coefficient of the heated channel has a great influence on the nonlinear behaviors of the system. With a small outlet loss coefficient (i.e. $ke=1$), the nonlinear types in the unstable region are mainly subcritical Hopf bifurcation and supercritical Hopf bifurcation. If the system with a large outlet loss coefficient (i.e. $ke=8$), the complex nonlinear phenomena exist in the unstable region, particularly in the area of high inlet temperature. A route from limit cycle oscillations, periodic oscillations and eventually to chaotic oscillations (Fig. 1) is identified through period doubling bifurcations. The existence of chaotic oscillation is also verified through the analysis of fast Fourier spectral transform, as revealed in Fig. 1. It indeed illustrates an interesting chaotic attractor like butterfly wings.

References

- [1] Ambrosini W., Sharabi M. (2008) Dimensionless parameters in stability analysis of heated channels with fluids at supercritical pressure. *Nucl Eng Des* **238**: 1917-1929.
- [2] Ortega G'omez T., Class A., Lahey R.T., Schulenberg T. (2008) Stability analysis of a uniformly heated channel with supercritical water. *Nucl Eng Des* **238**: 1930-1939.
- [3] Lee J.D., Chen S.W., Pan C. (2019) Nonlinear dynamic analysis of parallel three uniformly heated channels with water at supercritical pressures. *Int J Heat Mass Tran* **129**: 903-919.

Dynamics of curved cantilevered pipes conveying fluid

Mahdi Chehrehgani*, Ahmed Shaaban*, Arun K. Misra* and Michael P. Païdoussis*

*Department of Mechanical Engineering, McGill University, QC, Canada, ORCID #

Abstract. The dynamics of curved cantilevered pipes conveying fluid was studied experimentally. Besides displaying a rich dynamical behaviour, interest in the subject arises mainly because in real-world applications, such as soft robots and solution mining, fluid-conveying pipes usually suffer geometric imperfections, often resulting in a curved pipe shape. A table-top-size apparatus consisting of a pressure vessel and a hanging straight or curved cantilevered pipe was utilized. Four different scenarios were investigated: (i) a straight pipe discharging water and submerged in air (pressure vessel filled with air), (ii) a curved pipe discharging water and submerged in air, (iii) a straight pipe aspirating water and submerged in water (pressure vessel filled with water), and (iv) a curved pipe aspirating water and submerged in water. It was found that curved cantilevered pipes conveying fluid exhibit interesting and extraordinary nonlinear fluid-structure interaction dynamics.

Introduction

The moderately simple fluid-elastic system of a pipe conveying fluid displays a rich dynamical behaviour and has become a *paradigm* in dynamics [1]. Even though the gyroscopic conservative system of a pipe with both ends supported cannot flutter [2] — despite the prediction of coupled-mode flutter by linear theory — cantilevered pipes become unstable via either a sub- or supercritical Hopf bifurcation into periodic motion [3]. Exploring the underlying Fluid-Structure Interaction (FSI) mechanisms of the dynamics of pipes conveying fluid, some studies in this topic are fundamental, rather than “application oriented” [4]. The interested reader is referred to [1,4] for a comprehensive review of the extensive studies on the subject. Compared to straight pipes, studies on initially curved pipes are limited — even though pipes commonly used in real-world applications usually suffer geometrical imperfections, including curvature. Additionally, works concerning curved pipes are mostly focused on pipes with supported extremities. The seminal work of Misra et al. [5,6], which compares the results of extensible or inextensible centreline theories, and that of Zhou et al. [7] investigates the dynamics of curved cantilevered pipes discharging fluid only theoretically. To the best of authors’ knowledge, there is no experimental study investigating the dynamics of cantilevered *curved* pipes discharging or aspirating fluid. Motivated by this lacuna, the purpose of this study is to explore experimentally the dynamics of initially curved fluid-discharging/aspirating cantilevered pipes, using the facility shown in Fig. 1.

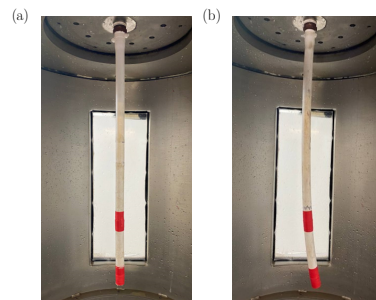


Figure 1: Photograph of (a) straight, and (b) curved cantilevered pipe used in the experiments.

Results and discussion

The flow velocity was increased to instability, and the motion of the pipe was tracked with a non-contacting high-speed camera system. The obtained time-series data from the recorded videos was processed to yield bifurcation diagrams, phase portraits, PDFs, PSDs, Lyapunov exponents, and position-triggered Poincaré maps. It was found that both discharging and aspirating curved pipes undergo a large flow-induced static deformation prior to the onset of an oscillatory instability about the static equilibrium position. Compared to straight pipes, the onset of flutter instability of their curved counterparts occurred at almost the same flow velocity. However, it may depend on the initial curved shape of the pipe, and this needs further investigation.

References

- [1] Païdoussis, M.P. (2022) Pipes conveying fluid: A fertile dynamics problem. *J. Fluids Struct.* **114**:103664.
- [2] Holmes, P.J. (1978) Pipes supported at both ends cannot flutter. *J. Appl. Mech.* **45**:619-622.
- [3] Bajaj, A.K., et al. (1980) Hopf bifurcation phenomena in tubes carrying a fluid. *SIAM J. on Appl. Math.* **39**(2):213-230.
- [4] Païdoussis, M.P. (2014) Fluid-Structure Interactions: Slender Structures and Axial Flow, 2nd edition, *Academic Press*.
- [5] Misra, A.K., et al. (1988) On the dynamics of curved pipes transporting fluid. Part I: inextensible theory. *J. Fluids Struct.* **2**:221-244.
- [6] Misra, A.K., et al. (1988) On the dynamics of curved pipes transporting fluid. Part II: extensible theory. *J. Fluids Struct.* **2**:245-261.
- [7] Zhou, K., et al. (2021) Static equilibrium configuration and nonlinear dynamics of slightly curved cantilevered pipe conveying fluid. *J. Sound Vib.* **490**:115711.

The remarkable role of hydrogen in conductors with copper and silver nanoparticles by mixed convection using viscosity Reynold’s model

Syed Ibrar Hussain^{1a}, Iftikhar Ahmad^{2b} and Nida Yasmeen^{2c}

¹Department of Mathematics and Computational Sciences, University of Palermo, Via archirafi 34, 90123 Palermo, Italy

²Department of Mathematics, University of Gujrat, Gujrat, 50700, Pakistan

^aSyedibrar.hussain@unipa.it, ^bdr.iftikhar@uog.edu.pk, ^c18091709-024@uog.edu.pk

Abstract. This article includes an analysis of the influence of mixed convection and variable viscosity under the effect of a transverse magnetic field on a stretching surface. Nano-fluid viscosity is supposed to be dependent on temperature. The effect of variable viscosity on the transversal magnetic field and hybrid convection can be seen by using Reynold’s model. The resulting nonlinear system of partial differential equations is transformed into a nonlinear system of first-order ordinary differential equations by the Lobatto IIIA approach, simplifying physical flow problems. Moreover, the impact of different parameters on temperature and velocity is shown graphically and tabulated results are also presented. The numerical findings obtained in this study are validated and very well in line with some previous literature findings. This research has helped to minimize the fluid flow and increases the fluid temperature and associated thermal boundary thickness by increasing the amount of Hartmann (parameter). In addition, the effect of the mixed convection and applied magnetic transverse fields are studied.

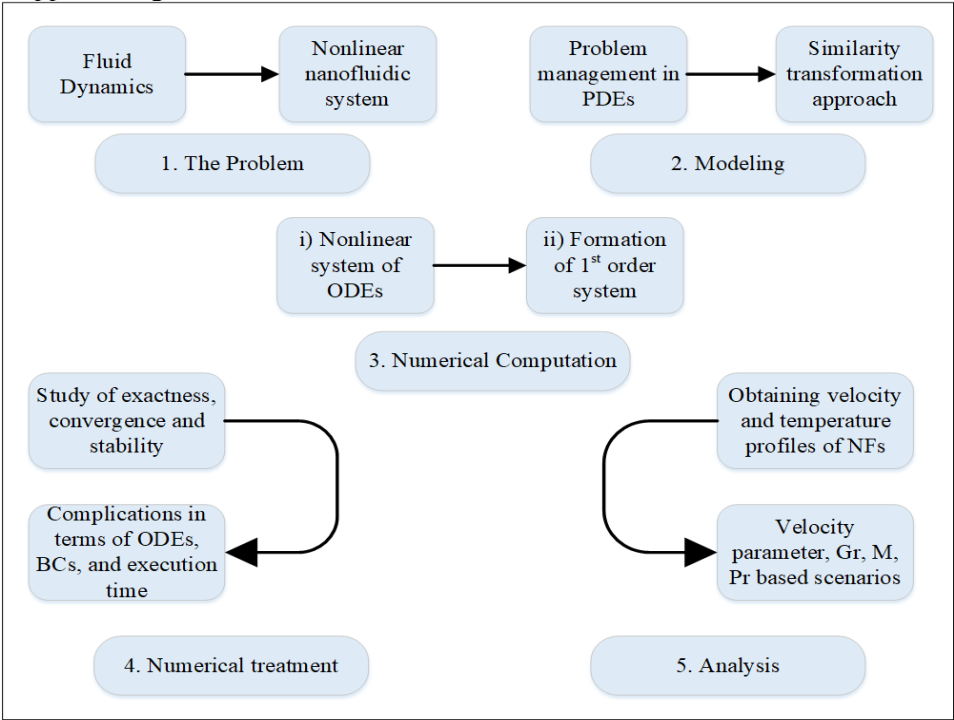


Figure 1: Graphical abstract of the proposed problem

Introduction

A numerical investigation by utilizing the novel numerical approach is implemented for the variable viscosity and mixed convection under the effect of a transverse magnetic field on a stretching surface. The numerical computation is performed, including the Exactness, convergence, and stability study. The numerical results are performed with various cases on velocity, parameter stretching ratio, GR, M, PR based scenarios and are presented in a tabular and graphical manner. A repeated scheme for the most effective solution of the implicit equation which is related to the and 6th order is the Runge-Kutta Lobatto IIIA method. The graphical abstract presented in figure 1 highlights the entire numerical process carried out in the proposed research. Lobatto IIIA method provide the most effective way for the quantitative solution of the non-linear stiff systems [1].

Results and discussion

This paper examines the influence of coupled temperature and convection-dependent viscosity on magnetic hydrodynamic Nanofluids (NFs) stagnation point movement towards a more expanding surface. Copper and silver nano-particles are considered in rigorous correlative research. Vogel's and reynold's models are used to investigate the influence of viscosity. In addition, the fluid flow is accelerated by the mixed convection. The base fluid's thermal conductivity is improved as the volumetric proportion of nanoparticles increases.

References

[1] Ahmad, I., Hussain, S.I., Raja, M.A.Z. and Shoaib, M., 2022. Transportation of Hybrid MoS2–SiO2, SiO2/EG Nanofluidic System Toward Radially Stretched Surface. *Arabian Journal for Science and Engineering*, pp.1-14.

Reduced-order model for hydrodynamic response of an oscillating surge wave energy converter

Alaa Ahmed*, Lisheng Yang**, Muhammad Hajj*, Raju Datla*, Lei Zuo**

*Department of Civil, Environmental and Ocean Engineering, Stevens Institute of Technology, Hoboken, NJ 07030

**Department of Naval Architecture and Marine Engineering University of Michigan, Ann Arbor, MI 48109

Abstract. Designing wave energy converters and testing them in ocean could be very expensive and complex, therefore requiring effective numerical modeling and simulations. The extensive cost of high-fidelity simulations can be inhibiting, especially in early stages of the design where different configurations need to be considered. Alternatively, a reduced-order model, based on representation of physical phenomena including added mass, radiation damping, and nonlinear unsteady hydrodynamics, can be used to optimize the geometry of the converter and in enhancing the control of the power takeoff. Here, we perform a systematic identification of representative terms for forces acting on an oscillating flap to develop a reduced-order model for its response in irregular waves.

Introduction

Because of its high density, wave power is considered as a renewable source that can support powering the grid, desalination power plants, remote communities, or coastal and deep ocean observation stations. One promising technology is the oscillating surge wave energy converter (OSWEC) [1], which consists of a flap hinged to the sea floor in shallow areas or to a submerged platform in deep waters. Using a power takeoff (PTO), energy is generated from its oscillating rotation under wave forcing. Simulating the hydrodynamic response can be carried out at multi-fidelity levels. High-fidelity simulations performed by solving the Navier-Stokes equations require extensive computing power and time. Medium fidelity simulations based on inviscid flow assumptions or linear wave theory require lesser time but remain expensive in the initial stages of the design iterations. On the other hand, a reduced-order model based on physical understanding and representation should yield a time-domain solution with an acceptable level of accuracy that can also be used in implementing PTO control. Difficulties in developing a time-domain model include accounting for the wave radiation and unsteady hydrodynamic forces and developing an evaluation of their relative magnitudes. In this paper, we will use validated free-decay and forced hydrodynamic numerical simulation to perform a systematic identification of the added mass, radiation damping and unsteady hydrodynamic forces. Particularly, a state-space model is used to replace the convolution term representing the radiation damping and a nonlinear term is used to represent the unsteady forces resulting from flow separation.

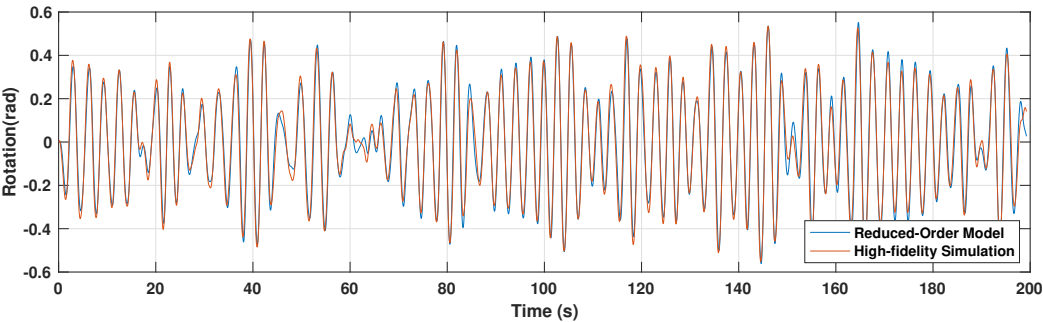


Figure 1: Comparison example of the OSWEC response under irregular wave excitation from high-fidelity and reduced-order model representations

Results and Discussion

Figure 1 shows a comparison between the results from developed reduced-order model and high-fidelity numerical simulations under irregular wave forcing. Based on RMS values, the error is less than 3% which indicates a high level of agreement. It is important to note that the computational time is reduced from 17 days for the high-fidelity simulation to only 13 minutes for the reduced-order model, which is significant when needing to determine potential power generated based on wave resources. In the full paper, we will stress the relative contributions and importance of the linear and nonlinear terms for different flap geometries. This characterization will be used to obtain approximate solutions for the hydrodynamic response and extended for implementation in the PTO control.

References

[1] Babarit, A., 2015. A database of capture width ratio of wave energy converters. *Renewable Energy*, 80, pp.610-628.

Small In-plane Oscillations of a Slack Catenary by the Rayleigh-Ritz method

Bidhayak Goswami*, Indrasis Chakraborty** and Anindya Chatterjee*

*Department of Mechanical Engineering, IIT Kanpur, India

**Lawrence Livermore National Laboratory, US Department of Energy

Abstract. We investigate small in-plane motions of a slack catenary using the Rayleigh-Ritz method. Using assumed modes and the Lagrangian approach, linearized equations with one holonomic constraint yield natural frequencies that match simple experiments. However, if the mode shapes thus obtained are themselves used as assumed modes, the approximation fails. A formulation that acknowledges *nonlinear* normal modes eliminates the constraint and gives the correct frequencies again. This problem offers interesting insights into approximations, constraints, and linearization.

Introduction

A *catenary* is an inextensible chain that hangs between two fixed ends. Its equilibrium shape is a hyperbolic cosine. Its in-plane oscillations have been studied by many authors before [1-5], using various approximations. The difficulty in directly using assumed modes in a Lagrangian formulation (i.e., the Rayleigh-Ritz method) is that the chain has a nonlinear pointwise inextensibility constraint involving spatial derivatives of the assumed modes. We cannot easily express the displacements of the chain in both horizontal and vertical directions using a complete basis of kinematically admissible functions. However, simple approximations are possible if we are willing to do numerical integration in space to obtain various coefficients within the Lagrangian.

We begin by approximating the vertical motion as $v(x, t) = \sum_{i=1}^N q_i(t) \phi_i(x)$, where the $\phi_i(x)$ are zero at the endpoints of the catenary. Pointwise inextensibility yields a series expansion for the spatial derivative of the horizontal displacement, i.e., $u_x(x, t)$. Integrating u_x from one endpoint gives a u that need not be zero at the other endpoint. This introduces a single scalar holonomic constraint on the q_i 's. Now implementing the Lagrangian formulation, we note that the potential energy in the Lagrangian is *linear* in the generalized coordinates and cannot cause oscillations. The Lagrange multiplier corresponding to the holonomic constraint plays that role. We obtain static equations that determine the Lagrange multiplier, and dynamic equations that use that multiplier value to yield natural frequencies and mode shapes as in Fig. (1).

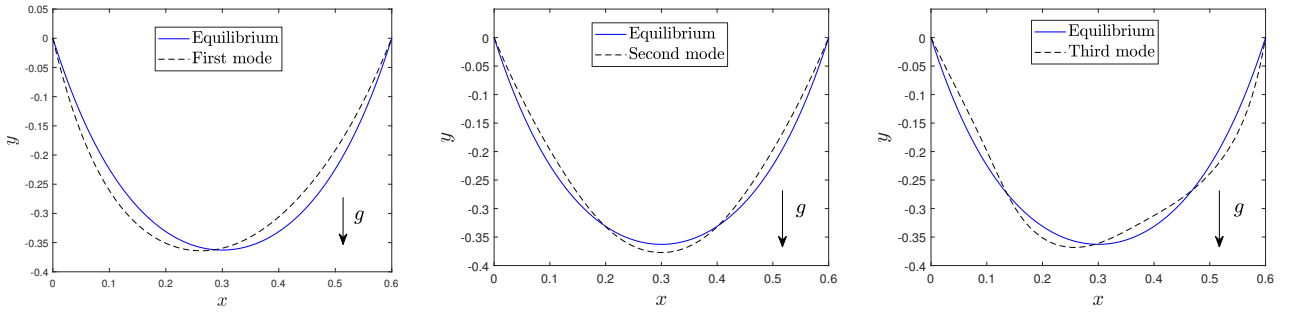


Figure 1: In-plane mode shapes of a slack catenary.

We now come to a puzzle. When the modes shapes determined above are reused in a fresh assumed modes calculation, the approach fails. First, the static equations used to find the Lagrange multiplier disappear; yet that multiplier value determines the natural frequencies. Second, the nonlinear constraint equation suggests that nonzero motion is impossible. Resolution lies in noting that the oscillations are along nonlinear normal modes. Deviations from the eigenspace must be allowed. Incorporating the deviation in a fresh assumed modes expansion and eliminating the holonomic constraint, we remove the Lagrange multiplier, introduce nonlinearity in the potential energy, and recover the correct natural frequencies and mode shapes.

Our study offers several interesting insights into Lagrangian mechanics. It also, for the first time to our knowledge, demonstrates use of the Rayleigh-Ritz method for this classical problem.

References

- [1] Routh, E. J., *Dynamics of a System of Rigid Bodies: Part II*, 6th edition, Dover Publications (1955). Originally published: 1860.
- [2] Saxon, D. S., and Cahn, A. S., Modes of vibration of a suspended chain, *The Quarterly Journal of Mechanics and Applied Mathematics*, 6(3): 273-285, (1953).
- [3] Ahmadi-Kashani, K., Vibration of hanging cables, *Computers and Structures*, 31(5): 699-715, (1989).
- [4] Rega, G., and Alaggio, R., Spatio-temporal dimensionality in the overall complex dynamics of an experimental cable/mass system, *International Journal of Solids and Structures*, 38(10-13): 2049-2068, (2001).
- [5] Rega, G., Nonlinear vibrations of suspended cables-Part I: Modeling and analysis, *Applied Mechanics Reviews*, 57(6): 443-478, (2004).

Vibrational Control: Mysterious Stabilization Mechanism in Bioinspired Flying Robots

Haitthem Taha*

*Department of Mechanical and Aerospace Engineering, University of California, Irvine, CA, USA

Abstract. Over the past two decades, there has been consensus among the biology and engineering communities that insects are unstable at hover. Here, we discuss a hidden passive stabilization mechanism that insects exploit through their natural wing oscillations: vibrational stabilization. This stabilization technique cannot be captured using the common averaging approach in literature. In contrast, it is discovered using a special type of calculus: the chronological calculus. This result is supported via experiments on a real hawkmoth subjected to pitch disturbance from hovering and also demonstrated on a flapping robot. This finding is particularly useful to biologists from one hand as the vibrational stabilization mechanism may also be exploited by many other creatures: Nature is teeming with oscillatory species. From the other hand, the obtained results will enable the engineering community to develop more optimal designs for bio-inspired flying robots by relaxing the stability requirements.

Introduction

Flapping flight dynamics may be represented by the exact same set of equations that govern the flight dynamics of conventional airplanes, which can be written in an abstract form as

$$\dot{\mathbf{x}}(t) = \mathbf{F}(\mathbf{x}, t) = \mathbf{f}(\mathbf{x}(t)) + \mathbf{g}_a(\mathbf{x}(t), \tau) \quad (1)$$

where the vector \mathbf{f} represents inertial and gravitational loads and the vector \mathbf{g}_a represents aerodynamic loads. A major distinction between flapping and conventional flight dynamics is that the former has a time-varying aerodynamic loads \mathbf{g}_a . Two symbols t and τ are used in Eq. (1) to denote the slow and fast time scales, respectively. The ratio between these two time scales is deceptively large; for the slowest flapping insect (the Hawkmoth), the ratio between the flapping frequency and the flight dynamics natural frequency is around 30 [1, 2], which naturally invokes averaging. That is, the aerodynamic loads oscillates with a too high frequency to affect the body. In other words, the body only feels the average values of the time-periodic aerodynamic loads. This assumption is found in most of flapping flight dynamics and control efforts.

Adopting the direct averaging assumption yields a nonlinear time-invariant (NLTI) system whose stability analysis is considerably easier than that of the nonlinear, time-periodic (NLTP) system (1). First of all, a periodic orbit representing equilibrium of the NLTP system (1) reduces to a fixed point (equilibrium point) of the NLTI system. Moreover, the averaging theorem guarantees exponential stability of a periodic orbit of the original NLTP (1) based on exponential stability of the corresponding fixed point of the NLTI system, provided that the flapping frequency is *high-enough*. Using this direct averaging approach, it has been known for a long time that insects are unstable at hover.

Results and discussion

Sarychev [3] developed higher-order averaging techniques for time-periodic systems, generalizing the classical averaging theorem to cases where the excitation frequency is not high-enough. In particular, Sarychev [3] introduced the notion of *complete averaging* for the nonlinear, time-periodic (NLTP) system as (1):

$$\dot{\bar{\mathbf{x}}}(t) = \epsilon \bar{\mathbf{F}}(\bar{\mathbf{x}}(t)) = \epsilon \mathbf{\Lambda}_1(\bar{\mathbf{x}}(t)) + \epsilon^2 \mathbf{\Lambda}_2(\bar{\mathbf{x}}(t)) + \dots, \quad (2)$$

where $\mathbf{\Lambda}_1(\mathbf{x}) = \frac{1}{T} \int_0^T \mathbf{F}(\mathbf{x}, t) dt$, and $\mathbf{\Lambda}_2(\mathbf{x}) = \frac{1}{2T} \int_0^T \left[\int_0^T \mathbf{F}(\mathbf{x}, \tau) d\tau, \mathbf{F}(\mathbf{x}, t) \right] dt$. That is, $\mathbf{\Lambda}_1$ simply represents the direct averaging contribution.

We used second-order averaging as discussed above to rigorously assess the flight dynamic stability of hovering insects. It is shown that the interaction between the periodic aerodynamic loads and the body motion induce stabilizing actions. In particular, it is found that $\mathbf{\Lambda}_2$ induces a pitch stiffness mechanism to the hovering flight dynamics, which is instrumental to static and dynamic stability of flying vehicles [4]. Therefore, the lack of pitch stiffness in $\mathbf{\Lambda}_1$ as predicted by direct averaging ultimately results in an unstable hovering flight dynamics of insects and FWMVs. However, the adopted higher-order averaging techniques revealed a vibrational stabilization mechanism in insect flight dynamics at hover that is similar to the Stephenson-Kapitza pendulum.

References

- [1] M. Sun, J. Wang, and Y. Xiong. Dynamic flight stability of hovering insects. *Acta Mechanica Sinica*, 23(3):231–246, 2007.
- [2] H. Taha, M. R. Hajj, and A. H. Nayfeh. On the longitudinal flight dynamics of hovering mavs/insects. *Journal of Guidance Control and Dynamics*, 37(3):970–978, 2014.
- [3] A. Sarychev. Stability criteria for time-periodic systems via high-order averaging techniques. In *Nonlinear Control in the Year 2000*, volume 2 of *Lecture Notes in Control and Information Sciences*, pages 365–377. Springer-Verlag, 2001.
- [4] R. C. Nelson. *Flight stability and automatic control*, volume 2. WCB/McGraw Hill New York, 1998.

Nonlinear stability of a thin viscoelastic film down a vertical wall: A numerical study

Akshay S Desai*, Souradip Chattopadhyay**, Amar K. Gaonkar* and Anadamoy Mukhopadhyay***

*Department of Mechanical, Materials and Aerospace Engineering, IIT Dharwad, Karnataka, India

**Department of Mathematics, North Carolina State University, NC, USA, ORCID 0000-0002-4418-6201

***Department of Mathematics, Vivekananda Mahavidyalaya, West Bengal, India, ORCID 0000-0001-8694-4720

Abstract. We numerically investigate the dynamics of a thin viscoelastic liquid flowing down a vertical wall, based on the earlier study of Cheng et al. (*J. Phys. D: Appl. Phys.*, vol. 33, 2000, 1674-1682). They discussed only the linear and weakly nonlinear stability analysis. However, nonlinear effects are more important when the amplitude of the disturbance is small but finite and therefore a nonlinear study is very much essential. We also identify how energy transfers from the basic state to the disturbance in this case.

Introduction

A vast body of thin film literature is devoted to the study of Newtonian films [1]. However, there are various fluids in practice which are non-Newtonian in nature. The viscoelastic fluid is a subclass of non-Newtonian fluids which exhibits features of both ideal fluids (viscosity) and solids (elasticity). Among numerous constitutive models of viscoelastic fluid, the most frequently applied in practical is Walter's B'' model as it has only one non-Newtonian parameter through which one can easily obtain a deeper insight of the behaviour of the viscoelasticity on the flow dynamics. The linear stability analysis of a viscoelastic liquid was first discussed by Gupta [2]. He considered a second-order fluid and observed that the viscoelastic parameter plays a destabilizing role on the primary instability. Cheng et al. [3] carried out the linear and weakly nonlinear stability analysis of the viscoelastic liquid flowing on a vertical wall. They found that the viscoelastic parameter has a destabilizing effect on the flow dynamics. In this study, we focus on the free surface evolution equation (37) of [3] to investigate the evolution of the film by numerical simulations. Nonlinear study provides us a first sight of the underlying nonlinear dynamics of the system and helps us to realize the mechanism which is responsible for the transfer of energy from the basic state to the disturbance.

We consider a thin viscoelastic liquid (Walter's B'' model) flow on a vertical wall. The interfacial surface of the film is $y = h(x, t)$, where h is the film thickness at any instant t . A highly nonlinear free surface equation $h_t + A(h)h_x + B(h)h_{xx} + C(h)h_{xxx} + D(h)h_x^2 + E(h)h_x h_{xx} = 0$ is obtained in [3], where the coefficients $A(h)$ to $E(h)$ are given in [3]. We consider that the initial condition is a simple harmonic disturbance superimposed on the interface as $h = 1 - 0.1 \cos(kx)$ in a periodic domain and approximate the spatial solution by a discrete Fourier series. The resulting system of nonlinear ODEs are solved by implicit Gear's method in time with relative error less than 10^{-6} . We also define an energy norm $\mathcal{E}_2 = (1/L) \int_0^L h^2 dx$ to investigate the energy transfer from the base state to the disturbances, where L is the computational domain.

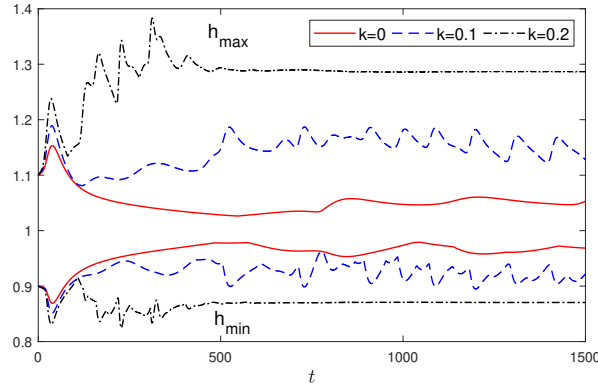


Figure 1: Maximum (h_{\max}) and minimum (h_{\min}) amplitude of surface wave instabilities for different viscoelastic parameter k with fixed $Re = 5$, $S = 12000$ and $\alpha = 0.1$

Results and discussion

1. Viscoelasticity promotes the oscillatory behaviour of the time-dependent wave forms.
2. The surface wave instability for a viscoelastic fluid is larger compared to the Newtonian film.
3. The growth rate of the energy norm is significantly influenced in presence of the viscoelasticity.

References

- [1] Kalliadasis S., Ruyer-Quil C., Scheid B., Velarde M.G. (2012) Falling Liquid Films. Springer.
- [2] Gupta A.K. (1967) Stability of a viscoelastic liquid film flowing down an inclined plane. *J. Fluid Mech* **28**:17-28.
- [3] Cheng P.J., Lai H.Y., Chen C.K. (2000) Stability analysis of thin viscoelastic liquid film flowing down on a vertical wall. *J. Phys. D: Appl. Phys.* **33**:1674-1682.

Dynamics of piecewise linear oscillator coupled with wake oscillator

P. Naga Vishnu* and K. R. Jayaprakash*

*Discipline of Mechanical Engineering, Indian Institute of Technology, Gandhinagar, Gujarat, India

Abstract. This study is concerned with the analysis of vortex induced oscillations of cylindrical beam with mode-1 crack. The cracked beam is modelled as a piecewise linear oscillator (PWL) coupled with the wake oscillator (Van der Pol (VdP) oscillator). Nonlinear normal modes (NNMs) of this coupled system and their stability are explored using method of averaging and PWL basis functions. The lock-in region (where NNMs cease to exist) is a function of the asymmetry parameter and behaviour of NNMs before and after lock-in are explored.

Introduction

PWL oscillatory models are used for mathematical modelling of several engineering problems like the dynamics of cracked beam [1] [2], mooring towers, suspension bridges etc. Analytical study of PWL oscillator poses challenges owing to their essentially nonlinear behaviour. The study of unforced single degree of freedom PWL oscillator is straight forward as its response can be obtained as a response in two linear regions and matched at the point of transition. However, the study of coupled PWL system poses the challenge of finding the exact transition point. Many researchers have considered both computational and analytical approaches in understanding the complex dynamics of single and two DOF PWL oscillators subjected to external and parametric excitation. Shaw et al. [3] have considered semi-analytical study of harmonically excited PWL oscillator exploring periodic solutions and their bifurcations. Anish et al. [4] studied the resonant response of symmetric, two-DOF PWL oscillator subjected to low-amplitude parametric excitation. In the present study the vortex induced oscillations of a cylindrical beam with mode-1 crack is studied. Due to mode-1 crack, the beam exhibits disparate effective stiffness depending on whether the crack is open or closed. When such a beam is subjected to flow-field, the flow-field couples with the beam and induces vortex induced oscillations which herein is modelled as PWL oscillator coupled with the wake oscillator [5] (VdP oscillator).

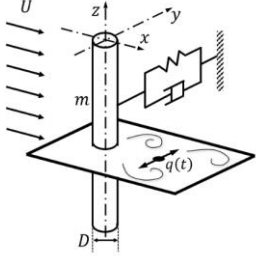


Figure 1: Cylinder in cross-flow (adapted from [5])

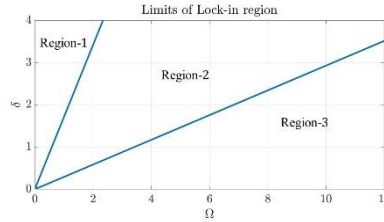


Figure 2: Lock-in region (Region-2) for $A = 12$, $M = 1/24$.

$$\ddot{y} + \varepsilon \lambda \dot{y} + k(y) - M \Omega^2 q = 0$$

$$\ddot{q} + \varepsilon \Omega (q^2 - 1) \dot{q} + \Omega^2 q - A \ddot{y} = 0$$

$$k(y) = \begin{cases} \delta^2 y, & y \geq 0 \\ y, & y < 0 \end{cases}$$

The fundamental mode of the cracked beam is considered for the analysis and is appropriately inertially coupled with the wake dynamics and the corresponding equation is shown above. Where y is the non-dimensional modal coordinate of the cylinder, q is the ratio of instantaneous and fluctuating lift coefficient, M is the non-dimensional effective mass and is a function of mass ratio, fluctuating lift and Strouhal number, A is the inertial coupling parameter, Ω is the non-dimensional shedding frequency, δ is the asymmetry parameter.

Results and discussion

We study the effect of asymmetry parameter on the dynamics of PWL oscillator coupled with wake oscillator. The lock-in region (Region-2) is observed to be a function of the asymmetry parameter for the unperturbed system. Interestingly, only in-phase NNMs are observed before (Region-1) lock-in and out-of-phase NNMs after (Region-3) lock-in. Since the analytical model is non-analytic due to the PWL function ($k(y)$), direct application of asymptotic methods is seldom possible. We consider method of averaging by invoking PWL basis functions [6] to explore the realization and stability of periodic solutions in the perturbed system.

References

- [1] Chati M., Rand R., Mukherjee S. (1997) Modal analysis of a cracked beam. *J. Sound and Vibration* **207**(2): 249-270.
- [2] Tandel V. (2021) Piecewise linear dynamics of a cracked beam, M.Tech Thesis, IIT Gandhinagar.
- [3] Shaw S. W., Holmes P. J. (1983) A periodically forced piecewise linear oscillator. *J. Sound and Vibration* **90**(1): 129-155.
- [4] Kumar A., Starosvetsky Y. (2021) Analysis of transition regions in the parametrically forced system of bi-linear oscillators: Resonant excitation in the neighbourhood of similar modes. *J. Sound and Vibration* **515**: 116435.
- [5] Facchinetti M. L., Langre E., Biotley F. (2004) Coupling of structure and wake oscillators in vortex-induced vibrations. *J. Fluids and Structures* **19** (3): 123-140.
- [6] Jayaprakash K. R., Tandel V., Starosvetsky Y. (2022) Dynamics of excited piecewise linear oscillators. *Nonlinear Dynamics* (under review).

Investigation of Chaotic Flutter in a Wind Turbine Airfoil

Paul A. Meehan *

* The University of Queensland, Brisbane, Australia

Abstract. The occurrence of chaotic motion in a fluttering airfoil is investigated using an efficient analytical predictive model. Flutter is an aeroelastic vibration instability of an elastic structure, such as an airfoil in a fluid, that results from an unstable interaction between the fluid and structural dynamics. Typical engineering applications of airfoils include aircraft wings and wind turbines. The structural equations of motion for the generalised two degree of freedom (pitch and plunge) coupled modes of an airfoil section are combined with unsteady aerodynamics, based on flutter derivatives and a continuous bilinear lift curve under damping and variable angle of attack. The mode coupling instability via dynamic divergence causes limit cycle behaviour via a Hopf bifurcation that breaks up into chaos characterised by period doubling behaviour after the critical flutter speed. Conditions under which chaotic instability occurs are identified and discussed for the case of a wind turbine section. The results provide insight into the occurrence and avoidance of airfoil flutter in aeroelastic structures like wind turbines.

Introduction

Flutter is an aeroelastic vibration phenomenon of an elastic structure in a fluid that results from an unstable interaction between the fluid and structural dynamics. Flutter vibrations occur typically above a lower critical speed and grow to an amplitude determined by the nonlinearities in the aerodynamics and/or structural dynamics. Flutter remains one of the most important issues for aircraft and structural engineering industries, motivating careful design to avoid fatigue failures such as in wind turbine blades. Theodorsen first provided a general theory for airfoil instability under unsteady aerodynamics [1]. Since then, an enormous amount of research on flutter modelling and prediction has occurred, as comprehensively reviewed in [2]. Essentially, the onset of binary flutter has been shown to be due to an unstable coupling of the pitching and plunging dynamics of a cross-section due to aerodynamics of the flow [1], [2]. Chaotic flutter has also been an intense area of research initiated from numerical identification in a two-degree of freedom airfoil with cubic nonlinearities eg [3]. Others have identified and investigated stall flutter chaos with aerodynamic, structural, kinematic and thermal nonlinearities eg [4]. Recently chaotic flutter was identified in an airfoil without the need for structural or thermal nonlinearity [5]. In this paper we extend these numerical and analytical investigations of chaotic flutter in an airfoil section to provide more efficient insight into its occurrence and avoidance in wind turbines.

Results and discussion

A reduced airfoil section model is modified and developed, that includes the dominant flutter mode coupled dynamics, unsteady flutter derivative aerodynamics and a bilinear lift model proposed and validated by [5]. The analytical methods for predicting the critical flutter onset speed, limit cycle amplitude and chaotic flutter for a wind turbine blade section are then described. The full nonlinear time domain model consisting of two autonomous coupled nonlinear second order systems, is numerically solved using the fourth and fifth order Runge–Kutta routine as part of DYNAMICS, written by Nusse and Yorke or the Radua method in MathCad 15.0 at a sampling rate of at least 20 times the flutter frequency. The nonlinear phenomena were investigated using the time history, phase space and bifurcation diagrams of Poincaré maps and Lyapunov Exponents. An example history showing chaotic instability is shown in *Figure. 1*.

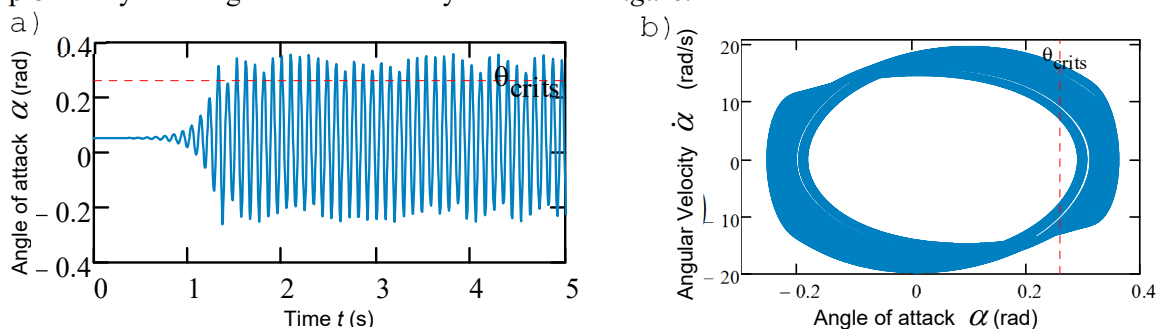


Figure. 1 a) Simulated time history and b) phase space of chaotic flutter in an airfoil section, stall angle θ_{crit}

The conditions under which chaotic instability under various initial section angle of attacks are investigated and identified in both a fundamental and wind turbine blade airfoil section in closed form to provide efficient analytical insight into the occurrence and avoidance of chaotic flutter.

References

- [1] Theodorsen, T. (1935) "General Theory of Aerodynamic Instability and the Mechanism of Flutter", NACA Report 496.
- [2] Dowell, EH et al (2021) A modern course in aeroelasticity, Solid Mechanics and its Applications, Vol 264, 6th Ed.
- [3] Zhao, L. C., & Yang, Z. C. (1990) Chaotic motions of an airfoil... J. of Sound and Vibration, 138(2), 245-254.
- [4] Tian, W. et al (2019) Nonlinear aeroelastic characteristics... Int. J. of Non-Linear Mechanics, 116, 123-139.
- [5] Meehan, P. A., Flutter prediction..., J. of Sound and Vibration. 535 (2022) 117117.

Nonlinear Dynamics of circular cylindrical shells interacting with a Non-Newtonian fluid

Francesco Pellicano*, Antonio Zippo* and Giovanni Iariccio**

* Università degli Studi di Modena e Reggio Emilia, Dip. di Ingegneria Enzo Ferrari, Centre InterMech - MO.RE.
Università degli Studi di Modena e Reggio Emilia, Dip. di Ingegneria Enzo Ferrari.

Abstract. This work is focused on nonlinear dynamics of a circular cylindrical shell interacting with a Non-Newtonian fluid (NN). The shell containing the fluid is harmonically excited from the base in order to investigate the complexity of the dynamic scenario. A dilatant NN fluid is considered, it is 60% corn-starch - 40% water mixture, commonly known as oobleck. The results show an extreme complexity of the dynamic scenario.

Introduction

The interaction of fluids with structures is of interest for several engineering fields such as bio-engineering or bio-mechanics but also in Medical Science. Several examples of Fluid Structure Interaction (FSI) problems can be found in Engineering: flutter (sub and supersonic), galloping, pipes instabilities, fully or partially filled tanks, heat exchangers. The human aorta is an important example of FSI with NN fluid (blood), which is highly viscous and non-Newtonian, the artery wall is hyper-elastic.

The interaction with fluids can cause several dynamic phenomena: static and dynamic instabilities; inertial effects with change of the natural frequencies and mode shapes; possible increment of damping.

The literature on FSI is mostly focused on inviscid or Newtonian fluids (compressible or incompressible). However, the Nature shows many examples of NN fluids interacting with solids and structures: blood, blood plasma, toothpaste, starch suspensions, corn starch, paint, melted butter, shampoo.

Results and discussion

In this study the nonlinear dynamics of a circular cylindrical shell, filled with NN fluid, see Figure 1, under seismic excitation is investigated. The system is harmonically excited from the base through an electrodynamic shaker in the neighbourhood of the resonance of the first axisymmetric mode. A dilatant fluid fills the shell, it is a mixture of 60% cornstarch and 40% water. The results show complex dynamics due to the coupling between the fluid and structure.

The dynamic scenario is carefully analyzed by means of time histories, spectra, phase portraits and Poincaré maps. The experiments show the onset of complex dynamics: subharmonic and quasiperiodic responses, Chaos.



Figure 1. Fluid filled shell

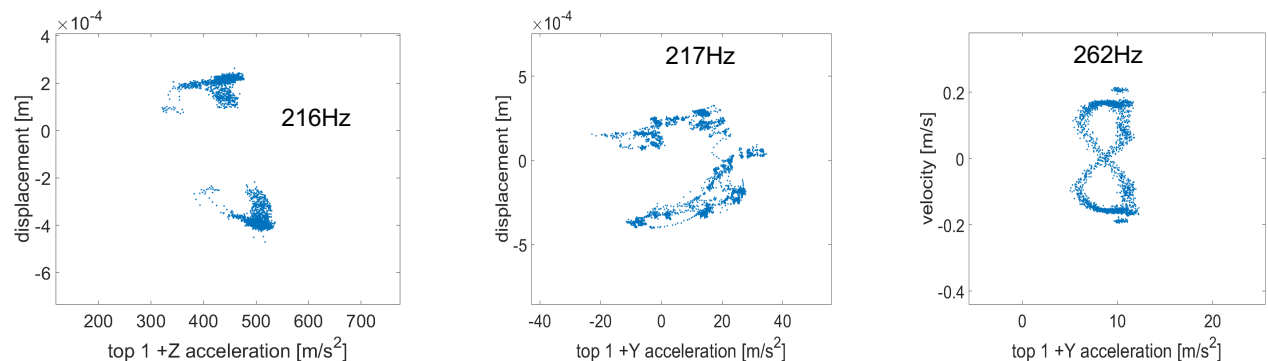


Figure 2. Poincaré maps.

References

- [1] Amabili M., Païdoussis M.P. (2003) Review of studies on geometrically nonlinear vibrations and dynamics of circular cylindrical shells and panels, with and without fluid–structure interaction, *Applied Mechanics Reviews* **56** 349–381.
- [2] Zippo A., Barbieri M., Iariccio G., and Pellicano, F. (2020) Nonlinear vibrations of circular cylindrical shells with thermal effects: an experimental study. *Nonlinear Dyn*; **99**: 373–391. DOI:10.1007/s11071-018-04753-1.
- [3] Pellicano, F. & Avramov, K.V. (2007) Linear and nonlinear dynamics of a circular cylindrical shell connected to a rigid disk, Comm. in Nonlin. Science and Numerical Simulation, **12**(4), 496-518 doi:10.1016/j.cnsns.2005.04.004.

Closed-form solutions and conservation laws for a Korteweg-de Vries-like equation

Chaudry Masood khalique*, and Mduduzi Yolane Thabo Lephoko

*International Institute for Symmetry Analysis and Mathematical Modelling, Department of Mathematical Sciences, North-West University, Mafikeng Campus, Private Bag X 2046, Mmabatho 2735, Republic of South Africa, ORCID # 0000-0002-1986-4859

Abstract. In this talk we study a second-order nonlinear Korteweg-de Vries-like (KdV-like) partial differential equation, which has several applications in various scientific fields. Firstly, we compute Lie point symmetries of the KdV-like equation. Thereafter the commutator table for the Lie point symmetries is generated, and we use Lie equations to produce one-parameter groups of transformations. Moreover, group-invariant solutions are obtained under each point symmetry. Furthermore, we use the conservation theorem due to Ibragimov to derive the conservation laws for the KdV-like equation.

Introduction

In [1] the authors introduced the new KdV-like equation

$$(D_{3,x}D_{3,t} + cD_{3,x}^2 + D_{3,x}^4) F \cdot F = 2F_{xt}F - 2F_tF_x + c(2F_{xx}F - 2F_x^2) + 6F_{xx}^2 = 0 \quad (1)$$

using the generalized bilinear derivative with the prime number $p = 3$. Three classes of different rational solutions were obtained using rational polynomial functions. Moreover, 2 and 3D plots of the rational solutions were presented in [1]. The authors of [2] studied the generalized bilinear differential equation of the KdV-like

$$(D_{3,x}D_{3,t} + D_{3,x}^4) f \cdot f = 2f_{xt}f - 2f_tf_x + 6f_{xx}^2 = 0 \quad (2)$$

and derived two classes of rational solutions to the resulting KdV-like equation. We note that when $c = 0$ in (1), we obtain equation (2). In this talk we study equation (2) from the symmetry standpoint.

Results and discussion

We start by constructing the Lie point symmetries of KdV-like equation (2) by using the Lie invariance criteria [3, 4]. This gives us four dimensional Lie algebra L_4 spanned by the four point symmetries. We then construct the commutator table for these four symmetries and on invoking Lie equations we obtain one-parameter groups of transformations. Thereafter, we perform symmetry reductions and derive group invariant solutions under each point symmetry. One such solution is the exponential function given as

$$u = e^{-\frac{1}{2}\varepsilon t^2}(C_1x + C_2), \quad (3)$$

where ε , C_1 and C_2 are constants. In order to understand the physical meaning of the obtained solutions we present two and three dimensional plots.

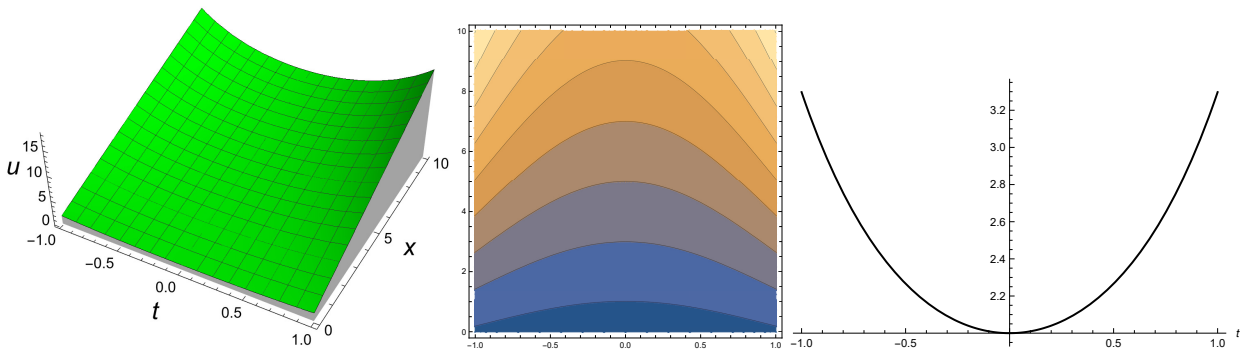


Figure 1: The dynamics of the group invariant solution (3) at $\varepsilon = C_1 = C_2 = 1$, furnishes a parabolic wave structure given in two and three dimensions. This wave structure has a significant application in electrical and electronics engineering. A parabolic antenna depicts an antenna that utilizes a curved surface parabolic reflector that has a cross-sectional shape. This parabola shape enables it to easily direct the radio waves. Besides, the most frequent used is a dish antenna or parabolic dish which has the shape of a dish. The main benefit of a parabolic antenna is the fact that it has high directivity [5].

In addition, the conserved quantities associated with the four symmetries are calculated using Ibragimov's theorem [6]. It is well known that the conserved quantities are very pertinent in physical sciences owing to their robust applications.

References

- [1] Liu J.G., Yang X.J., Wang J.J. (2022) A new perspective to discuss Korteweg-de Vries-like equation. *Phys. Lett. A* **451**:128429.
- [2] Zhang Yi, Ma, W. X. (2015) Rational solutions to a KdV-like equation. *Applied Mathematics and Computation* **256**:252-256.
- [3] Ovsiannikov L.V. (1982) Group Analysis of Differential Equations. Academic Press, New York.
- [4] Olver P.J. (1993) Applications of Lie Groups to Differential Equations. second ed., Springer-Verlag, Berlin.
- [5] <https://en.wikipedia.org/wiki/Parabolic-antenna>.
- [6] Ibragimov N.H. (2007) A new conservation theorem. *J. Math. Anal. Appl.* **333**:311-328.

Experimental Study of Nonreciprocal Acoustic Energy Transfer in an Asymmetric Nonlinear Vibro-Acoustic System

Jiangming Jin^{a,*}, Jingxiao Huang^a, D. Michael McFarland^a, Alexander F. Vakakis^c,
Lawrence A. Bergman^b, Huancai Lu^a

a. Sound and Vibration Laboratory, College of Mechanical Engineering, Zhejiang University of Technology, 18 Chaowang Road, Hangzhou 310014, China

b. Department of Aerospace Engineering, University of Illinois at Urbana-Champaign, 104 South Wright Street, Urbana, IL 61801, USA

c. Department of Mechanical Science and Engineering, University of Illinois at Urbana-Champaign, 1206 West Green Street, Urbana, IL 61801, USA

Abstract. An asymmetric and nonreciprocal vibro-acoustic system consists of a waveguide, three acoustic cavities with different sizes, and a strongly nonlinear membrane has been modelled, simulated, and experimentally demonstrated. The nonreciprocal transmission of acoustic energy in this prototype system is studied. Under forward excitation, internal resonance between the two nonlinear normal modes of the vibro-acoustic system occurs, and acoustic energy is efficiently and irreversibly transferred from the waveguide to the nonlinear membrane. However, under backward excitation, there is no internal resonance in the system. Consequently, the acoustic energy transfer of the system exhibits “giant nonreciprocity”, i.e., nearly unidirectional (preferential) transmission of acoustic energy. The theoretical model of the system is verified by experiment, and parametric analysis is also carried out. Wavelet analysis and energy spectra are employed to highlight the mechanism of nonreciprocal transfer of acoustic energy.

Introduction

A nonlinear acoustic system^[1] has a characteristic that its linear counterpart does not have, such as bifurcation or an energy-dependent resonant frequency, and so it can realize large nonreciprocal transmission of acoustic energy. Vakakis et al.^[2] designed a series of nonlinear mechanical systems to achieve nonreciprocal energy transfer based on the nonlinear energy sink mechanism. Cochelin et al.^[3] studied the phenomenon of targeted energy transfer in vibro-acoustic systems. However, there has been no quantitative, experimental study on asymmetric transmission of acoustic waves in those strongly nonlinear systems.

In this paper, a strongly nonlinear nonreciprocal vibro-acoustic system is constructed by adding a cavity on the opposite side of the membrane. The resulting system comprises a waveguide, three different size cavities, and a strongly nonlinear membrane. The two-degree-of-freedom model used to derive and simulate the governing equations of the system under forward and backward excitations were developed under the assumptions of a one-dimensional waveguide, von Karman shell theory, and low-frequency approximations for the acoustics in the cavities.

The nonreciprocal transfer of acoustic energy is realized by using different interaction mechanisms between nonlinear normal modes of the system under forward and backward excitations. The experimental results agreed well with the theoretical predictions, validating the discrete model and the system identification of its parameters; the discrete model could then be used with confidence to elucidate the governing nonlinear acoustics yielding nonreciprocity in the response of the system. The experimental and simulation data were further analyzed using wavelet analysis, energy spectra and other computational tools. The results reported herein contribute to practical designs of vibro-acoustic systems having the capacity of nonreciprocal, i.e., unidirectional, sound transmission.

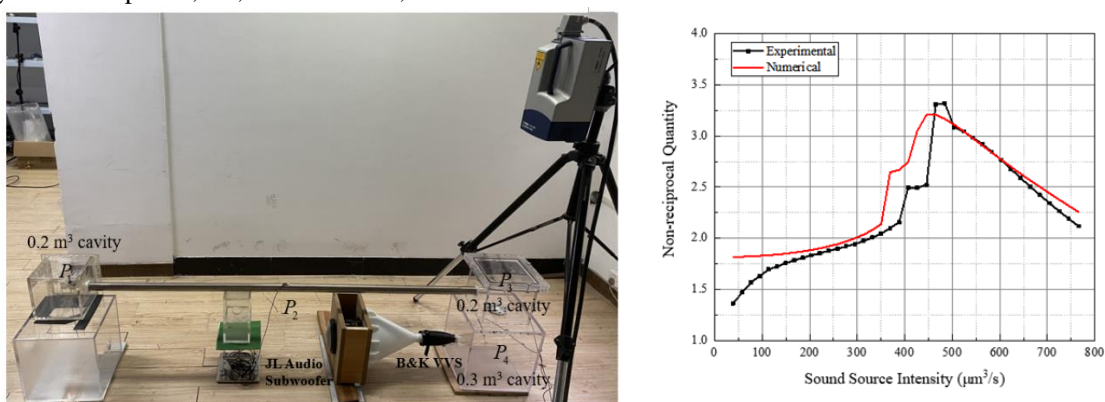


Figure 1: Nonreciprocal vibro-acoustic system (left) experimental set-up (right) comparison between experiment and simulation results of nonreciprocal measure.

References

- [1] Nassar H, Yousefzadeh B, Fleury R, Ruzzene M, Alù A, Daraio C, Norris A N, Huang G, Haberman M R. (2020). Nonreciprocity in acoustic and elastic materials. *Nature Reviews Materials* **5**:667-685.
- [2] JBunyan J, Moore K J, Mojahed A, Fronk M D, Leamy M, Tawfick S, Vakakis A F. (2018) Acoustic nonreciprocity in a lattice incorporating nonlinearity, asymmetry, and internal scale hierarchy: Experimental study. *Physical Review E* **97**: 52211
- [3] Bellet R, Cochelin B, Herzog P, Mattei P O. (2010) Experimental study of targeted energy transfer from an acoustic system to a nonlinear membrane absorber. *Journal of Sound and Vibration* **329**: 2768-2791.

Semi-analytic solutions for the bending-bending-torsion coupled forced vibrations of a rotating wind turbine blade by means of Green's functions

X. Zhao*, X. Jiang*, Y.H. Li **, W.D. Zhu***

*School of Civil Engineering and Architecture, Southwest Petroleum University, Chengdu, Sichuan, PR China

**School of Mechanics and Engineering, Southwest Jiaotong University, Chengdu, Sichuan, PR China

***Department of Mechanical Engineering, University of Maryland, Baltimore County, Baltimore, USA

Abstract. In recent years, wind power has received continuous attention as a renewable energy source in the context of carbon neutrality. A blade in wind turbine with an elongated structure are susceptible to damage due to aeroelastic instability. The basic solution of the system is derived by Laplace transformation and Green's function method, and then the system of second category of Fredholm integral equations about steady-state forced vibration of the blade can be derived according to the principle of superposition. The second type of Fredholm integral equation system is discretized numerically, and finally a semi-analytical solution of the coupled forced vibration of rotating wind turbine blades is obtained. By comparing the solution in this paper with the solution of the finite element method, the effectiveness of the solutions is verified. The results show that the inflow ratio at the hub has a great influence on the blade's flag displacement.

Introduction

Blades are the main force-bearing parts and the most vulnerable components, so studying the multi-modal coupling vibration of blades has practical engineering significance. Based on the finite element method, Park et al.^[1] studied the modal characteristics of rotating blades and proposed a calculation algorithm for solving the modal characteristics. Luczak et al.^[2] updated his finite element model through experimental data, and the new model obtained can effectively calculate the vibration characteristics of the blade. As an effective tool, various forced vibration problems are studied through Green's function. Zhao et al.^[3] studied the bend-torsional coupling forced vibration of the piezoelectric energy harvester, and derived the closed solution of the piezoelectric energy harvester subjected to the fluid vortex by the Green's function.

Although previous works have given some important results in engineering applications, most of the previous research methods are finite element method, and compared with analysis methods, the main disadvantage of finite element method is that parametric analysis is inconvenient and inaccurate. The Green's function of a linear vibration system represents the fundamental solution of the system, and through the principle of superposition, we can derive the solution of the system under arbitrary external loads.

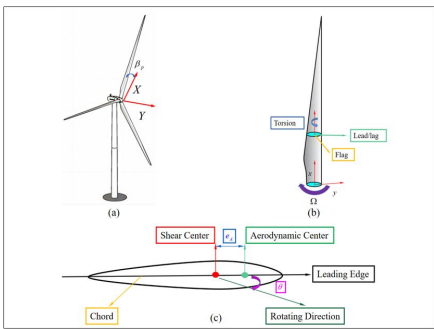


Figure 1: Schematic diagrams of (a) wind turbine, (b) blade and (c) blade section.

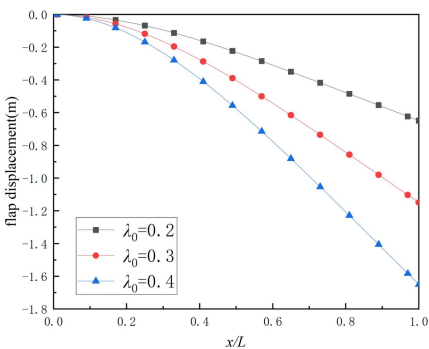


Figure 2: Effect of the inflow ratio at hub.

Results and discussion

Figure 1 shows the vibration of a rotating wind turbine blade in three directions (flap vibration, lead/lag vibration and torsional vibration) and a schematic diagram of the blade cross-section. In this paper, the semi-analytical solution of the coupled forced vibration of rotating wind turbine blades is obtained by using the Green function method, and some meaningful results are obtained.

It can be seen from Figure 2 that the inflow ratio size can change the flag displacement of blade, therefore, the inflow ratio at the hub is an important parameter to study the dynamic response of a rotating wind turbine blade.

References

- [1] J.H. Park, H.Y. Park, S.Y. Jeong, S.-I. Lee, Y.-H. Shin, J.-P. Park, (2010) Linear vibration analysis of rotating wind-turbine blade, *Curr Appl Phys* **10**: S332-S334.
- [2] M. Luczak, S. Manzato, B. Peeters, K. Branner, P. Berring, M. Kahsin, (2014) Updating Finite Element Model of a Wind Turbine Blade Section Using Experimental Modal Analysis Results, *Shock. Vib.* **2014**.
- [3] X. Zhao, W.D. Zhu, Y.H. Li, (2022) Closed-Form Solutions of Bending-Torsion Coupled Forced Vibrations of a Piezoelectric Energy Harvester Under a Fluid Vortex, *J Vib Acoust* **54**:204-211.

Effect of time-scale in the flow fluctuations on a sub-critical aeroelastic system

Varun H S*, Sunetra Sarkar*,**

*Department of Aerospace Engineering, Indian Institute of Technology Madras, Tamilnadu, India

**Complex Systems and Dynamics, Indian Institute of Technology Madras, Tamilnadu, India

Abstract. This study investigates the effect of time-scale in the flow fluctuations on a 2 DOF pitch-plunge aeroelastic system. The structure is supported by nonlinear soft springs and the fluid loads are evaluated using a semi-empirical model. The flow fluctuations are modelled as an OU process. It is seen that long time-scale noise advances the onset of intermittency but delays the onset of LCO when compared to short time-scale noise, presenting new design challenges.

Introduction

Stochastic noise has been known to play a major role in altering the dynamics of FSI systems[1, 2, 3]. They have been known to induce dynamical states like intermittency[2, 3] and change the jet-switching characteristics in the flow-field[1]. These studies show that the time-scales in the flow fluctuations are of utmost importance and hence, we investigate the effect of time-scale in the flow fluctuations on a sub-critical aeroelastic system. The structure is modelled as a 2 DOF pitch-plunge elastic system with nonlinear soft springs[4]. The fluid loads are calculated using the semi-empirical Wagner function[4]. The non-dimensional equations describing the aeroelastic system (with the flow fluctuations) take the form of an Ito SDE as given in Equation 1.

$$\begin{aligned} d\vec{X} &= f(\vec{X}, \tau; U) d\tau \\ dU &= \lambda(U_m - U) d\tau + \sigma dW \end{aligned} \quad (1)$$

where \vec{X} represents the system variables which include the auxillary variables needed to calculate the fluid load, τ the non-dimensional time, U the flow velocity. The flow fluctuations in U are modelled as an OU process [1] with mean U_m , time-scale parameter λ ($1/\lambda$ is the correlation time), W the Standard Wiener process and σ the noise intensity. Equation 1 is studied for two cases: $\lambda = 0.005$ (long time-scale); $\lambda = 0.5$ (short time-scale).

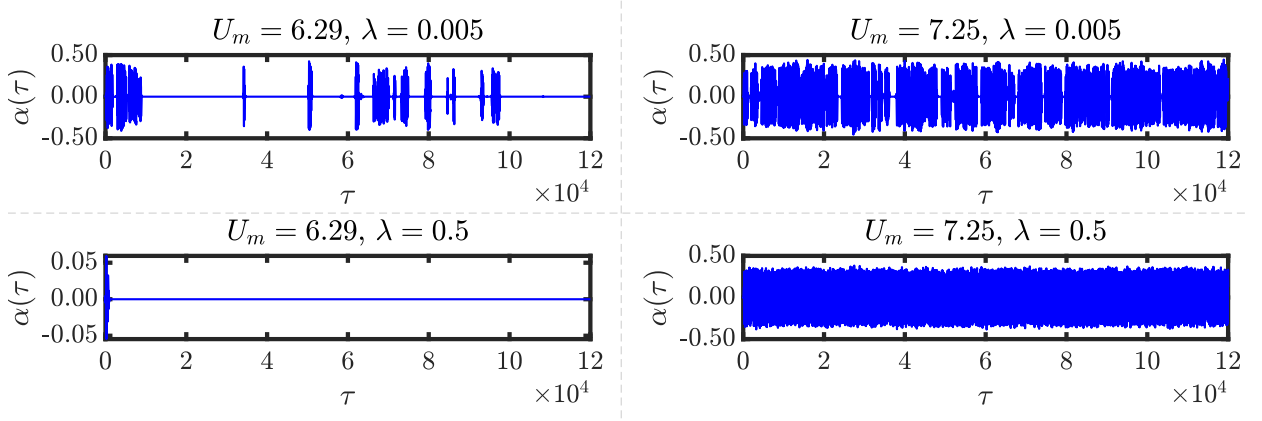


Figure 1: Pitch time series ($\alpha(\tau)$) for $U_m (= 6.29, 7.25)$ and $\lambda (= 0.005, 0.5)$

Results and Discussion

To study the effect of λ , the variance of the OU process in Equation 1 is taken as 1 ($\sigma^2/(2\lambda) = 1$). Figure 1 shows the pitch time series ($\alpha(\tau)$) for $U_m = 6.29, 7.25$. It is observed that for the initial conditions chosen (deterministically the system evolves to a LCO at $U = 6.29$), there is a delay in the onset of LCO as U_m is varied. The long time-scale case ($\lambda = 0.005$) has the system in a state of intermittency at $U_m = 6.29$, whereas at this U_m , the short time-scale case ($\lambda = 0.5$) evolves to the $\vec{0}$ state (Figure 1). However at $U_m = 7.25$, the $\lambda = 0.5$ case displays full-fledged LCO behaviour but intermittency persists in the $\lambda = 0.005$ case (Figure 1). Thus the long time-scale noise advances the onset of intermittency but delays the onset of full-fledged LCO when compared to the short-time scale noise. The time-scales of the input flow fluctuations affect the onset of different dynamical behaviour and hence is an important parameter for consideration during design.

References

- [1] Majumdar D., Bose C., Sarkar S. (2020) Effect of gusty inflow on the jet-switching characteristics of a plunging foil. *Phys. Fluids* **32**:117105 1-17.
- [2] Aswathy M. S., Sarkar S. (2019) Effect of stochastic parametric noise on vortex induced vibrations. *Int. J. Mech. Sci.* **153-154**:103-118.
- [3] Venkatramani J., Krishna S. K., Sarkar S., Gupta S. (2017) Physical mechanism of intermittency route to aeroelastic flutter. *J. Fluids Struct* **75**:9-26.
- [4] Lee B. H. K., Jiang L. Y., Wong Y. S. (1999) Flutter of an Airfoil with Cubic Restoring Force. *J. Fluids Struct* **13**:75-101.

Nonlinear dynamics of imperfectly supported pipes conveying fluid

Mahdi Riazat* and Mojtaba Kheiri*

*Fluid-Structure Interactions & Aeroelasticity Laboratory, Department of Mechanical, Industrial and Aerospace Engineering, Concordia University, QC, Canada

Abstract. We present numerical results from ongoing research on the nonlinear dynamics and stability of flexible pipes conveying fluid, imperfectly supported at the upstream end (i.e., inlet) and free at the other (i.e., exit). The three-dimensional (3-D) nonlinear equations of motion are developed using the extended Hamilton's principle, and the support imperfection is modelled as cubic stiffness terms. The support imperfection appears to alter the dynamics of the pipe in several ways, including critical flow velocities, amplitude of oscillations, and 2-D/3-D motion.

Introduction

Pipes conveying fluid are ubiquitous in engineering systems. Examples are brine strings used in solution mining and underground hydrocarbon storage, and seawater intake risers used in natural gas liquefaction. Flexible pipes conveying fluid with one end free exhibit quite complex and sometimes unexpected or counter-intuitive dynamical behaviour. Among those are 'destabilization by damping' and chaotic motion of cantilevered pipe with an end-mass [1]. Despite a large volume of studies on the dynamics of pipes conveying fluid, with few exceptions, all deal with perfectly supported systems, such as, cantilevered, pinned-pinned, and clamped-clamped pipes. Our research is motivated by the fact that in real-world systems, loose or imperfect supports may exist or occur (due to, e.g., manufacturing defects, installation errors, or wear), which might alter the dynamics and stability of the system. Kheiri et al. [2] developed a 2-D linear model to examine the effects of imperfect upstream (or inlet) support on the stability of pipes conveying fluid. The imperfectly-supported pipe was found to be generally less stable compared to the cantilevered (or perfectly-supported) pipe conveying fluid. Kheiri [3] developed a 2-D model to investigate the nonlinear dynamics of imperfectly-supported pipes conveying fluid. Large-amplitude motion of the authors' previous study.

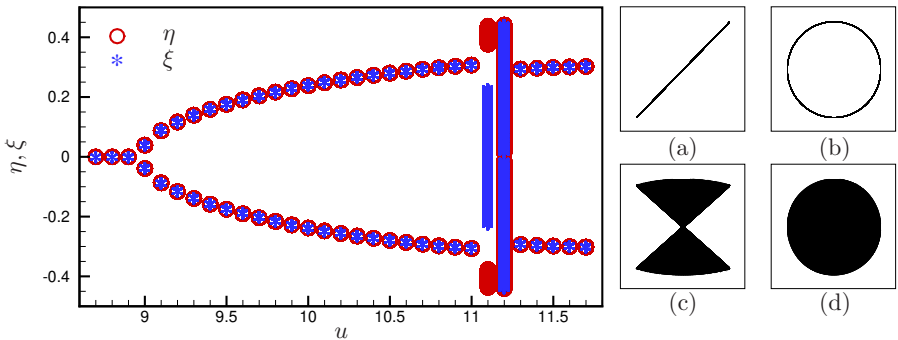


Figure 1: Bifurcation diagram showing the variation of the peak dimensionless displacement of a horizontal pipe conveying fluid as a function of the dimensionless internal flow velocity, u (mass ratio: $\beta = 0.45$, support imperfection: $\kappa = 30\eta' + 300\eta'^3$). The subplots show the trajectory of the free end of the pipe at (a) $u = 10.5$, (b) $u = 11.6$, (c) $u = 11.1$, and (d) $u = 11.2$.

Results and discussion

Figure 1 shows a typical bifurcation diagram for an imperfectly supported pipe conveying fluid. The pipe lies in the horizontal plane and the fluid-to-fluid+pipe mass ratio is $\beta = 0.45$. The variation of the peak dimensionless displacements in the y - and z -directions (represented by η and ξ , respectively) are shown as a function of the dimensionless flow velocity u . As seen, the system undergoes a Hopf bifurcation at $u \simeq 8.9$, leading to limit cycle oscillations. At $u \simeq 11.1$, quasi-periodic motion appears, which becomes periodic again at slightly higher flow velocities. At lower values of u motion is planar while it becomes 3-D at higher values of u , as evidenced by the subplots shown in the figure. Our numerical results show that a pipe with imperfect support may become unstable at a lower or higher flow velocity (depending on system parameters) compared to the perfectly supported pipe. Quasi-periodicity is often observed while periodic motion is the most prevalent form of motion. With symmetric support imperfection, both planar (at lower u) and 3-D (at higher u) motions are observed while with asymmetric imperfection planar motion is dominantly observed.

References

- [1] Païdoussis M. P. (2014) Fluid-Structure Interactions. Slender Structures and Axial Flow. Vol. 1, Academic Press, Amsterdam, NL.
- [2] Kheiri M., Païdoussis M. P., Costa Del Pozo G., Amabili M. (2014) Dynamics of a Pipe Conveying Fluid Flexibly Restrained at the Ends. *J. Fluids and Structures* **49**:360-385.
- [3] Kheiri M. (2020) Nonlinear Dynamics of Imperfectly-supported Pipes Conveying Fluid. *J. Fluids and Structures* **93**:102850.

The structural behaviour of 66 kV submarine cable under sea waves and currents effect

SungWoong Choi*

*Department of Mechanical System Engineering, Gyeongsang National University
(53064) 2, Tongyeonghaean-ro, Tongyeong-si, Gyeongsangnam-do, Republic of Korea

Abstract. Due to the energy changes, the submarine cross-linked three-core polyethylene power cable has been increasingly used, and its capacities had more than 66 kV. Due to the disadvantages using J-tube, new type of submarine was needed. Submarine cable system without using J-tube was consisted of three-core submarine cable and protective equipment. In the present study, the structural behaviour of 66 kV three-core submarine cable was investigated under various marine environment, mainly sea load of waves and currents effect.

Introduction

Due to the energy changes, the submarine cross-linked three-core polyethylene power cable has been increasingly used, and its capacities had more than 66 kV [1, 2]. The submarine cable is the hub connected to the land-based power grid, and the research on the submarine cable transmission technology is crucial to the better engineering applications [2]. Fixed type inner network submarine cables are installed with pre-installed on the substructure metal J-tube. In this type, submarine cables must be operated with the condition that they do not touch the seabed. Therefore, the work-space and environment is limited. In these trends, new type of submarine was needed without using J-tube. This type of submarine cable system without using J-tube was consisted of lots of protective equipment such as UP-pipe, bend restrictor, piggy back clamp, permanent clamp, and flexible protection tube. Among the protection equipment, permanent clamp and piggy back clamp was crucial components to the protection of submarine cable. In the present study, the structural behaviour of 66 kV three-core submarine cable was investigated under various marine environment, mainly sea load of waves and currents effect. The submarine cable was modelled with refined finite element model (FEM) using the commercial computational FEM software ANSYS (ANSYS, version 22). The numerical calculation of integration of the motion equations was conducted with the method of wave-structure interaction simulated by the numerical software ANSYS/AQWA.

Results and discussion

The previously investigated material properties of 66 kV three-core submarine cable and protective equipment of flexible protection tube was adopted. The sea load of waves and currents, and the distance between permanent clamp and piggy back clamp was considered with the previously examined environmental database. When the sea load of waves and currents was applied, the maximum total deformation was obtained in the middle of the piggy back clamps, and different values was shown with each applied load as shown in Fig. 1. The total deformation was ranged from 2.01 mm to 14.98 mm, and the stress values were ranged from 8.9 MPa to 54.43 MPa.

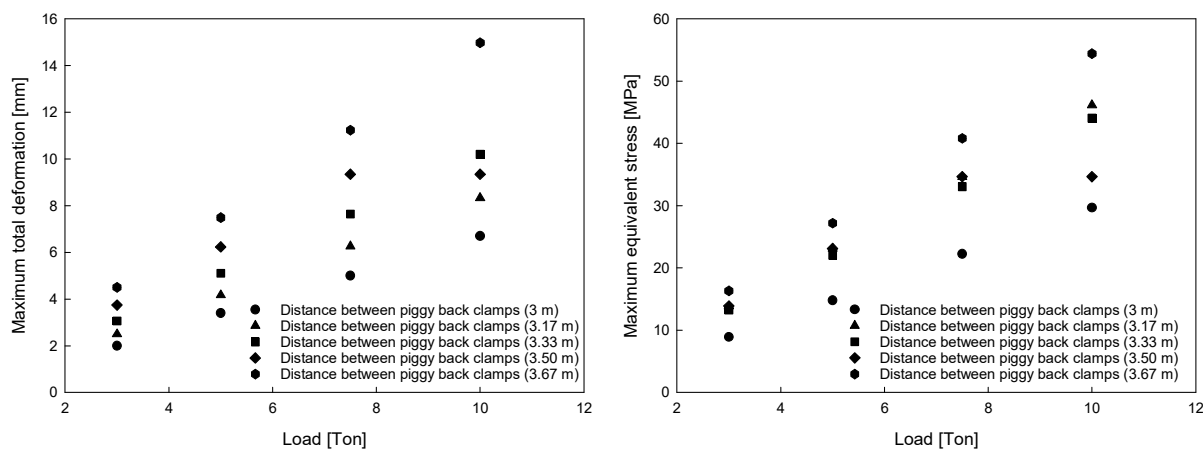


Figure 1: Total deformation and maximum equivalent stress of 66 kV three-core submarine cable.

References

- [1] Hammons, T. J. (2003). Power cables in the twenty-first century. *Electric power components and systems*, **31**: 967-994.
- [2] Zhang, Y., Chen, X., Zhang, H., Liu, J., Zhang, C., & Jiao, J. (2020). Analysis on the temperature field and the ampacity of XLPE submarine HV cable based on electro-thermal-flow Multiphysics coupling simulation. *Polymers*, **12**: 952.

A complete stability chart for the tippedisk

Simon Sailer and Remco I. Leine

Institute for Nonlinear Mechanics, University of Stuttgart, Germany
ORCID 0000-0002-1275-9634 and ORCID 0000-0001-9859-7519

Abstract. The tippedisk is a mathematical-mechanical archetype, showing a non-intuitive inversion behavior, if the disk is spun fast enough. By introducing a full 3D mechanical model and assuming set-valued force laws to account for normal and frictional contact forces, the dynamics of the tippedisk can be studied numerically. In addition, the model dimension can be reduced through model reduction techniques, yielding a lower dimensional model, being perfectly suited for closed form analysis of the qualitative dynamics. Previous work of the authors has shown that the bifurcation scenario contains a heteroclinic bifurcation, followed by a subcritical Hopf bifurcation. In this paper, we derive a complete stability chart that characterizes various bifurcation scenarios in closed form, which allows us to understand the qualitative dynamics of the tippedisk.

Introduction

The tippedisk forms a mathematical-mechanical archetype for friction induced instabilities that shows a counter intuitive inversion phenomenon when spun around an in-plane axis, cf. Fig. 1. As this inversion cannot be explained through energetic arguments, we have to employ to the whole field of nonlinear dynamics to study and understand the behavior of the system qualitatively. Since we aim to study the nonlinear behavior, we seek for closed form expressions that characterize the dynamics of the tippedisk. Due to the singularly perturbed structure of the system equations, tools and methods from singular perturbation and Melnikov theory are applied to derive conditions for the existence of heteroclinic orbits on a slow manifold [2, 3]. Asymptotic analysis is used to obtain closed form expressions.

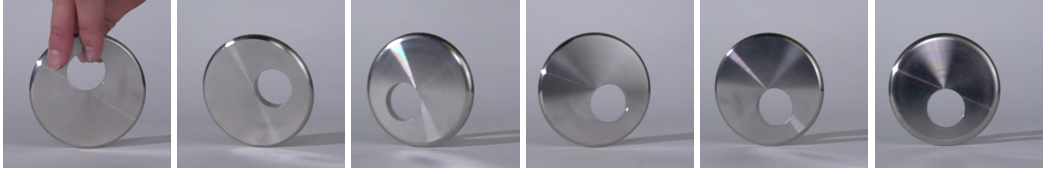


Figure 1: Stroboscopic sequence, showing the inversion phenomenon of the tippedisk.

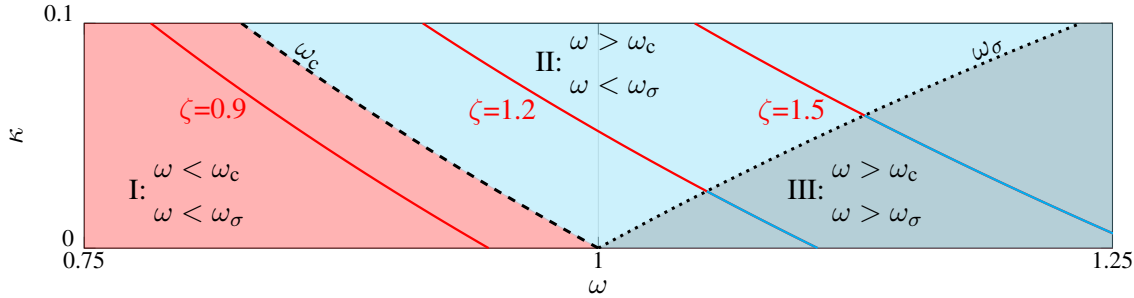


Figure 2: Stability chart: shows different bifurcation scenarios for variants of the tippedisk.

Results and Discussions

Combining the results of [1–3] and introducing dimensionless parameters and system equations, we will derive the complete stability chart Fig. 2 of the tippedisk. This diagram shows stability regions, characterizes Hopf bifurcations as sub- or supercritical, and allows for statements about the existence and asymptotic behavior of hereroclinic saddle connections. Furthermore, the consideration of fundamental dynamic properties provides a complete characterization of the qualitative dynamics of the tippedisk. Various stability regions imply different variants of the tippedisk with qualitatively distinct behavior, but all show the phenomenon of inversion. Validity of the presented analysis is shown by numerically computed bifurcation diagrams.

In summary, the presented analysis explains the inversion phenomenon of the tippedisk and provides a natural, intuitive interpretation of its qualitative behavior from the perspective of nonlinear dynamics.

References

- [1] Sailer S., Leine R.I. (2021) Model reduction of the tippedisk: a path to the full analysis. *Nonlinear Dyn.* **105**:1955-1975.
- [2] Sailer S., Leine R.I. (2021) Singularly perturbed dynamics of the tippedisk. *Proc. R. Soc. A* **477**:20210536.
- [3] Sailer S., Leine R.I. (2022) Heteroclinic bifurcation analysis of the tippedisk through the use of Melnikov theory. *ResearchSquare [Preprint]*, submitted to *Proc. R. Soc. A*, <https://www.researchsquare.com/article/rs-2320169/v1>

Investigation on Vibro-impacts of Electric Powertrain in Regenerative Braking Process

Kun Liu* and Wei Wu*

*National Key Laboratory of Vehicular Transmission, Beijing Institute of Technology, Beijing, P. R. China

Abstract. Due to gear backlashes of electric powertrain drivelines, vibro-impacts between gear teeth easily cause serious noise and vibration problems. To analyze the vibro-impacts of powertrain excited by regenerative braking, a dynamic model of an electric drive multistage gear system is established. In this model, the electromagnetic characteristics of the permanent magnet motor and the translational-rotational vibration of the gearbox are considered. The results show the relationship between the relative deformation of the gear teeth and the relative velocity. The phenomenon of multiple impacts and rebounds of the gear teeth in each impact is revealed. The transient impact force of bearing and multistage gear during impact are compared and analyzed. The research provides theoretical support for dynamic load study of the electric powertrain.

Introduction

Numerous studies on the vibro-impacts of automobile transmission have been performed. There is little research on the vibration phenomenon of electric powertrain in electric vehicles. The electric powertrain is an underdamped system because it omits the damping components. Therefore, the reversal of electromagnetic torque may lead to the gear vibro-impacts in the regenerative braking process. Study on the mechanism of vibro-impacts is essential to improve the drivability of the electric vehicle.

Baumann et al.[1] investigated the influence of several parameters on rattle noise level, e.g. backlash and helix angle. Brancati et al. [2] proposed a flywheel equipped with a torsional vibration damper. The device shows to be effective in mitigating the rattle phenomenon. Shi et al. [3] studied the effects of load, backlash and transmission error on vibro-impact properties. Xiang et al. [4] investigated the influence of supporting forces on vibro-impact. Dion et al. [5] developed a study of phenomena involving gear impacts with one loose gear inside an automotive gearbox.

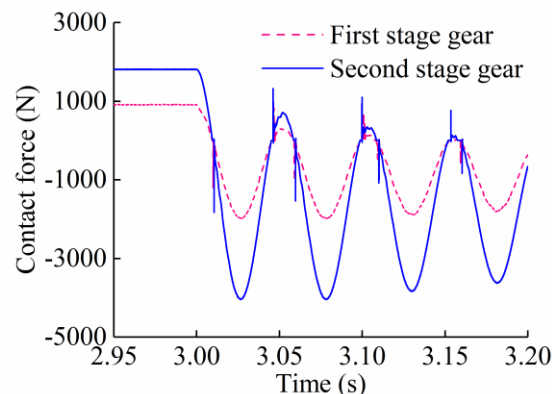


Fig. 1. Dynamic contact force of gear pair

Results and discussion

After the regenerative braking torque is applied, the low-order modal resonance is excited. Under the action of system damping, the vibration amplitude is gradually attenuated. When the teeth across the backlash, transient impact forces are generated. In the mesh state, a fluctuating mesh force is generated. The impact force of the second-stage gear pair is greater than that of the first-stage gear pair. It may be because the second-stage gear pair transmits a higher load. Both the impact force and the mesh force decrease gradually with time.

There is no transient impact force in the bearing. But after the regenerative braking torque is applied, the bearing force oscillates in a large range. The dynamic change of support force may affect the accurate calculation of the bearing remaining life.

References

- [1] Baumann, A., Bertsche, B. (2015) Experimental study on transmission rattle noise behavior with particular regard to lubricating oil. *J. Sound Vib* 341: 195-205.
- [2] Brancati, R., Rocca, E., Russo, R. (2019) Gear rattle reduction in an automotive driveline by the adoption of a flywheel with an innovative torsional vibration damper. *Proc. Inst. Mech Eng Pt K-J Multi-Body Dyn* 233(4): 777-791.
- [3] Shi, J.F., Gou, X.F., Zhu, L.Y. (2019) Modeling and analysis of a spur gear pair considering multi-state mesh with time-varying parameters and backlash. *Mech. Mach. Theory* 134: 582-603.
- [4] Shen, Y.H., Xiang, D., Wang, X., et al. (2018) A contact force model considering constant external forces for impact analysis in multibody dynamics. *Multibody Syst. Dyn* 44(4): 397-419.
- [5] Dion, J.L., Moyne, S.L., Chevallier, G., et al. (2009) Gear impacts and idle gear noise: experimental study and non-linear dynamic model. *Mech. Syst. Signal Pr* 23(8): 2608-2628.

Study the Bifurcations of a 2DoF Mechanical Impacting System

Soumyajit Seth*, Grzegorz Kudra*, Grzegorz Wasilewski*, and Jan Awrejcewicz *

*Department of Automation, Biomechanics, and Mechatronics, Lodz University of Technology, 1/15 Stefanowski Street (building A22), 90-924 Łódź, Poland, ORCID 0000-0003-3528-2020

Abstract. Impacting mechanical systems with suitable parameter settings exhibit a large amplitude chaotic oscillation close to the grazing with the impacting surface. The cause behind this uncertainty is the square root singularity and the occurrence of dangerous border collision bifurcation. In the case of one degree of freedom mechanical systems, it has already been shown that this phenomenon occurs under certain conditions. This paper proposes the same uncertainty of a two-degree freedom mechanical impacting system under specific requirements. This paper also shows that the phenomena earlier reported in the case of one degree of freedom mechanical systems (like narrow band chaos, finger-shaped attractor, etc.) also occur in the two degrees of freedom mechanical impacting system. We have numerically predicted the narrowband chaos ensues under specific parameter settings. We have also shown that the narrowband chaos can be avoided under some parameter settings. At last, we demonstrate the numerical predictions experimentally by constructing an equivalent electronic circuit of the mechanical rig.

Introduction

Various dynamical systems are observed in multiple areas of science and engineering, where impacts occur between the components of the systems. These systems exhibit a rich sort of dynamical phenomena, especially in the range of parameter values where grazing occurs. The phenomena include transitioning from one periodic attractor to another through the chaotic orbit at grazing, finger-shaped chaotic attractors at the bifurcation point in the Poincaré section, etc. These practical and engineering systems have been studied in detail for the last thirty years, especially on one degree of freedom mechanical impacting system under different configurations [1, 2]. The purpose of this work is to propose a forced two-degrees of freedom mechanical system with a compliant impact. Under some parameter settings, we have shown the onset of chaos in the bifurcation diagram when the amplitude of the externally applied periodic signal is varied. We also have shown that when there is a specific relation between the externally applied signal's frequency and the system's natural frequencies, the chaotic attractor can be avoided, as studied in one degree of freedom mechanical impacting system.

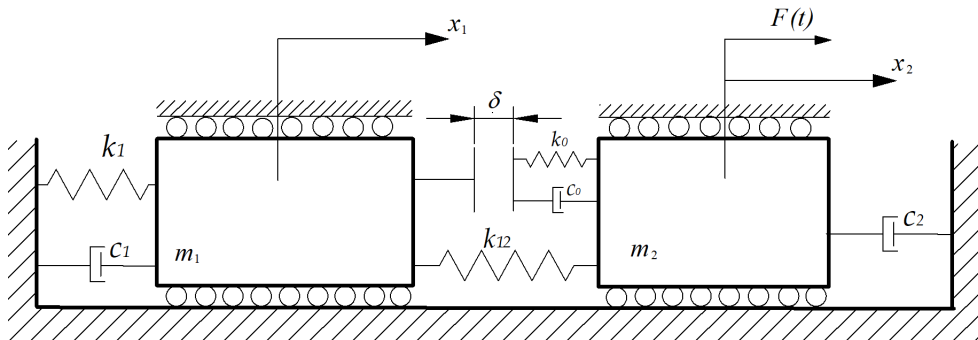


Figure 1: The schematic representation of a two-degree of freedom mechanical impacting system.

System description

A schematic diagram of a two-degree of freedom mechanical system under study is depicted in Fig. 1. It is a forced damped oscillator with a massless compliant obstacle that the mass m_1 can impact. The massless compliant obstacle is attached to another mass m_2 with a spring having spring constant k_o and a damper with the damping coefficient c_o . The mass m_1 is attached to a fixed support by a spring with spring constant k_1 and a damper c_1 . The mass m_2 is connected to the fixed support with a damper c_2 . The two masses m_1 and m_2 are connected with a spring having spring constant k_{12} . The forcing periodic function $F(t)$ is acted on the mass m_2 . Due to the application of the external forcing, the masses m_1 and m_2 started to oscillate from their equilibrium positions. x_1 and x_2 are the amount of displacements of the two masses m_1 and m_2 from their equilibrium positions, respectively. We have observed the dynamics of this system when the amplitude of $F(t)$ is changed.

References

- [1] Kundu S., Banerjee S., Ing J., Pavlovskaja E., Wiercigroch M. (2012) Singularities in soft-impacting systems. *Physica D: Nonlinear Phenomena* **241**: 553-565.
- [2] Seth S., Banerjee S. (2020) Electronic circuit equivalent of a mechanical impacting system. *Nonlinear Dynamics* **99**: 3113-3121.

Analysis and bifurcations of non-smooth Filippov predator prey system with harvesting

Uganta Yadav^{*}, Sunita Gakkhar^{*}

^{}Department of Mathematics, Indian Institute of Technology, Roorkee, India*

Abstract. In this study, it is assumed that harvesting is permitted only when the ratio of prey to predator is below a threshold value. The Filippov type dynamical system consisting of two smooth subsystems is investigated. The existence of harvesting factor within an interval dependent on biological parameters of the system would ensure the existence and stability of interior equilibrium state for the harvested system. The boundary that splits the two subsystems is classified into sliding and crossing region. It is also proved that there does not exist any escaping region on the boundary. Various equilibrium points such as boundary points, tangent points, pseudo-equilibrium points are found out for the boundary. The visibility condition for these tangent points are determined. Touching bifurcation and boundary bifurcation of the Filippov system is demonstrated numerically. The half saturation rate of predators plays a crucial role in determining whether the system to lie in specific sub-regions or is oscillating in between the two regions.

Introduction

In this study, the Filippov predator prey is formulated which balances the conflict between the exploitation and coexistence of both the species in the environment. When enough food (prey) is available to the predators, there is no hindrance in the coexistence of both the species. However, when the prey to predator availability is below a threshold value, the pressure on predators to survive increases. This pressure can either be decreased by providing additional food to the predators or by harvesting the predators. With the assumption that the predators are of economic interest. So, harvesting of predators is adopted as a control measure. It is assumed that harvesting is permitted only when the ratio of prey to predator is below a threshold value. Whenever the ratio is above this threshold value, harvesting is not allowed. The predator-prey system with the aim of controlling the predator population to level that conserve preys is considered. The hypothesis involved is that human need for harvesting increases with predator abundance and decreases with predators exiguous. This is also due to the fact that there is a threshold above which the financial damage is sufficient to justify the measure. From the analysis of this Filippov system it is concluded that the coexistence of the species is possible in two ways- either the existence of interior equilibrium states or the existence of limit cycle about the interior equilibrium state and the half saturation rate of predators plays a crucial role in determining this dynamical behaviour of the Filippov system.

Recently, application of Filippov systems has been extended to ecological models. Filippov epidemic model was discussed in [1, 2, 3]. Liu proposed a prey-dependent consumption model with impulsive control strategy [4]. The existence of a globally stable pest-eradication periodic solution when the impulsive period is less than some critical values is proved. The dynamics of a non-smooth predator prey system characterized by density-dependent intermittent refuge protection of the prey was studied by Bhattacharyya and Chattopadhyay [5]. When the level of apprehension of prey species is less than a threshold value, the existence of pair of pseudo equilibrium was established.

References

- [1] T. de Carvalho, R. Cristiano, L. F. Goncalves, D. J. Tonon, Global analysis of the dynamics of a mathematical model to intermittent HIV treatment, *Nonlinear Dynamics* 101 (1) (2020) 719–739.
- [2] H. Zhou, S. Tang, Bifurcation dynamics on the sliding vector field of a Filippov ecological system, *Applied Mathematics and Computation* 424 (2022) 127052.
- [3] Y. Xiao, S. Tang, J. Wu, Media impact switching surface during an infectious disease outbreak, *Scientific reports* 5 (1) (2015) 1–9.
- [4] B. Liu, L. Chen, Y. Zhang, The dynamics of a prey-dependent consumption model concerning impulsive control strategy, *Applied Mathematics and Computation* 169 (1) (2005) 305–320.
- [5] J. Bhattacharyya, J. Chattopadhyay, Non-smooth dynamics emerging from predator-driven discontinuous prey dispersal, *Nonlinear Dynamics* 106 (4) (2021) 3647–3668.

Critical Dynamics of Kuramoto Model on Erdős-Rényi Random Graphs

Hai Chen*

*Department of Physics, Zhejiang University, Hangzhou, China

Abstract. The Kuramoto model(KM) describes the dynamics and synchronization of coupled oscillators and has been intensively investigated in various physical and biological systems. In his original work, Kuramoto studied the fully connected oscillator system and determined its critical coupling strength K_c of phase transition from incoherent initial state to synchronized final state. The complexity of the model increases significantly when the system is on random graphs. In this work, we focus on the Kuramoto model under the Erdős-Rényi random graph topology and study its critical behaviors. Specifically, we demonstrate that statistically there exists an effective critical coupling K_{ec} which is the product of original coupling strength K and the graph link probability p on the two-dimensional critical curve. Under one-dimensional projection, the critical link probability p_c is inversely proportional to the coupling strength K and vice versa. We generate a large numerical data sample to simulate the KM on this topology and obtain well agreement between the semi-quantitative analysis and simulation result. These results provide insights on Kuramoto model's critical behavior on random graphs, and can be applied to determine real dynamical system's intrinsic properties and extended to other stochastic topologies.

Introduction

Synchronization of interacting elements is ubiquitous in nature, and has been widely investigated in many physical and biological systems, such as flashing fireflies, neurons in the brain, electric power grids and Josephson junction arrays[1]. Kuramoto introduced an analytically solvable model of coupled oscillators, and thus inspired extensive studies on phase synchronization research since the 1980s[2, 3]. In spite of its mature age, the theory of synchronization is still full of surprises, applications, and new features. The synchronization of coupled oscillators depends on many factors, such as the coupling strength, the network topology, the natural frequency distribution, interaction time delay, etc[4]. One of the key factors, the network topology, determines how interaction and information propagate among the elements. As the network topology's complexity increases, the evaluation of Kuramoto model's critical dynamics becomes very challenging[5]. The random graph model proposed by Paul Erdős and Alfred Rényi is simple yet elegant, and can be integrated into the Kuramoto model by connecting each pair of oscillators with a fixed link probability p . In spite of its limitations in simulating real-world networks that follow power-law degree distribution, it is the basis of many variations of random graph models, and has important applications in statistical physics(e.g., percolation theory[6]).

Summary

With statistical analysis and extensive numerical simulation, the critical dynamics of Kuramoto model on Erdős-Rényi random graph have been resolved in this work. We first show that under ER topology it is statistically equivalent to the traditional fully connected form, with effective coupling strength K_e reduced according to the link probability p . The two-dimensional critical curve of phase transition reveals the simple inverse proportional relations between link probability p and coupling strength K . This result agrees with the rigorous mathematical calculation by Chiba and Medvedev[7, 8]. Meanwhile this leads to possibility of probing a physical system's intrinsic coupling strength if it follows ER random graphs topology. On the basis of this work, it is possible to investigate the critical behaviors under more complex network topology, such as small-world and other stochastic graphs. We will also extend the topology studies with the presence of noise, time-delay, inertia, etc., to explore new features of Kuramoto model.

References

- [1] Pikovsky A., Rosenblum A., and Kurths J. (2001) Synchronization: A Universal Concept in Nonlinear Sciences. Cambridge Nonlinear Science Series. Cambridge University Press, Cambridge.
- [2] Kuramoto Y. (1984) Cooperative dynamics of oscillator community. *Prog. Theor. Phys., Suppl.*, **79**:223.
- [3] Acebrón J.A., Bonilla L.L., Vicente C.J.P., Ritort F., and Spigler R. (2005) The kuramoto model: A simple paradigm for synchronization phenomena. *Rev. Mod. Phys.*, **77**:137-185.
- [4] Strogatz S.H. (2000) From kuramoto to crawford: exploring the onset of synchronization in populations of coupled oscillators. *Phys. D: Nonlinear Phenom.*, **143**:1-20.
- [5] Arenas A., Díaz-Guilera A., Kurths J., Moreno Y. and Zhou C.S. (2008) Synchronization in complex networks. *Phys. Rep.*, **469**:93-153.
- [6] Schmeltzer C., Soriano J., Sokolov I.M., and Rüdiger S. (2014) Percolation of spatially constrained Erdős-Rényi networks with degree correlations. *Phys. Rev. E*, **89**: 012116.
- [7] Chiba H. and Medvedev G.S. (2019) The mean field analysis for the kuramoto model on graphs i. the mean field equation and transition point formulas. *Discrete Contin. Dyn. Syst.*, **39**:131-155.
- [8] Chiba H. and Medvedev G.S. (2019) The mean field analysis of the kuramoto model on graphs ii. asymptotic stability of the incoherent state, center manifold reduction, and bifurcations. *Discrete Contin. Dyn. Syst.*, **39**:3897-3921.

Rheonomic frictional contacts for simulating drifting in conveyors and feeders

Alessandro Tasora*, Dario Fusai** and Dario Mangoni***

* *Department of Engineering and Architecture, University of Parma, Italy, ORCID 0000-0002-2664-7895*

** *Department of Engineering and Architecture, University of Parma, Italy, ORCID 0000-0002-4287-3024*

*** *Department of Engineering and Architecture, University of Parma, Italy, ORCID 0000-0002-3256-2484*

Abstract. Within the context of non-smooth dynamics, we propose a new class of contact constraints that simulates the drifting of parts when in contact with conveyor belts, vibratory feeders or similar devices for transportation of parts. In the proposed formulation, contacts are handled as rigid contacts between parts and a stationary object, where a time-dependant term is added to the complementarity constraint in order to enforce the tangential motion of the parts. The needed parameters are quite simple, being limited to the friction coefficient and to a map of drifting speeds on the contact surface.

Introduction

Conveyor belts, vibratory feeders and similar devices are widely used in engineering applications, for example in the food industry, in granular material processing and in bulk material transportation. In general all these devices share a common issue when one needs to simulate them: the desired effect -namely, the drifting of parts over conveying surfaces- is a simple phenomena, yet the simulation requires complex models and/or short time steps (for instance the realistic simulation of a conveyor belt would require the simulation of large deformations of a rubber belt, etc.) To bypass the difficulty of modeling the transportation system, we propose a surrogate model based on non-smooth dynamics [1].

Method

In our approach, we use just static conveying surfaces, but at the same time the set-valued force laws for frictional contacts are extended to include a rheonomic term $\mathbf{C}_t = \{C_{t_u}, C_{t_v}\} \in \mathbb{R}^2$ where $(u, v, t) \mapsto \mathbf{C}_t$ is a user-defined function on the surface manifold, representing the required tangential drifting speed. Such speed map can be obtained from experiments, from numerical models or simply from analytical expressions: for example a linear conveyor belt of constant speed s would simply have $\mathbf{C}_t = \{s, 0\}$. Given a set \mathcal{G}_A of contact points, we express each contact law at the i -th contact point as a rheonomic cone complementarity:

$$\hat{\gamma}_i \in \Upsilon_{\mathcal{A},i} \perp \bar{\mathbf{u}}_i \in \Upsilon_{\mathcal{A},i}^*, \quad \forall i \in \{\mathcal{G}_A | \Phi_i = 0\} \quad (1)$$

where $\Upsilon_{\mathcal{A},i}$ is the second order Lorentz friction cone, $\Upsilon_{\mathcal{A},i}^*$ is its dual, Φ_i is the contact gap, $\hat{\gamma}_i$ is the reaction impulse, \mathbf{u}_i is the contact relative velocity, $\mathbf{v}_{\parallel,i}$ is the tangent velocity, μ_i is the friction coefficient, and

$$\bar{\mathbf{u}}_i = \left\{ \begin{array}{l} u_{n,i} + \mu_i \|\mathbf{v}_{\parallel,i}\| \\ u_{u,i} + C_{t_u}(u, v, t) \\ u_{v,i} + C_{t_v}(u, v, t) \end{array} \right\} \quad (2)$$

By doing this, we inherit the high performance and stability of the non-smooth formulation [2], at the same time allowing large time steps in the simulation of transportation phenomena. Other effects such as friction limits in sticking or sliding, or collision restitution, are preserved.

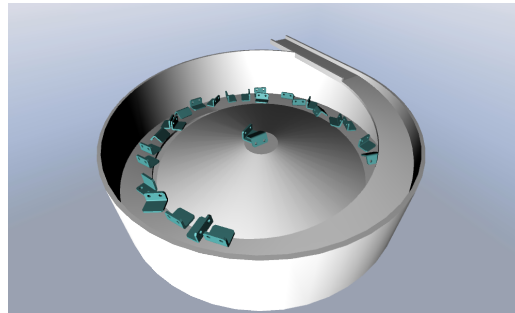


Figure 1: Simulation of a bowl feeder. The proposed method allows large time steps ($h = 0.01s$ in this case).

References

- [1] Acary, V., Brogliato, B. (2008) Numerical methods for nonsmooth dynamical systems: applications in mechanics and electronics. Springer, DE.
- [2] Tasora, A., Mangoni, D., Benatti, S., Garziera, R. (2021) Solving variational inequalities and cone complementarity problems in nonsmooth dynamics using the alternating direction method of multipliers. *Int J Numer Methods Eng* **122**:4093-4113.

Entrainment in Self-Excited Filippov Systems

Bipin Balaram*, Jan Awrejcewicz*

*Department of Automation, Biomechanics and Mechatronics, Łódź University of Technology, 90-924 Łódź, Poland.

Abstract. This work investigates entrainment in a self-excited discontinuous system of Filippov type. In terms of the Poincare winding numbers, the presence of $1:m$ and $n:m$ entrainment regions are reported. The existence of Devil's staircase is demonstrated numerically. It is shown that quasi-periodic orbits generate invariant polygons on the Poincare section, whose vertices function as natural condensation points for the generation of entrained m -periodic solutions.

Introduction

Entrainment in continuous, smooth systems has been studied extensively [1]. But, comparable emphasis does not seem to have been given for entrainment of discontinuous systems [2]. Here, we examine the mechanism of higher order entrainment in a 1 DoF self-excited Filippov system. The importance of invariant polygons in this context is emphasised.

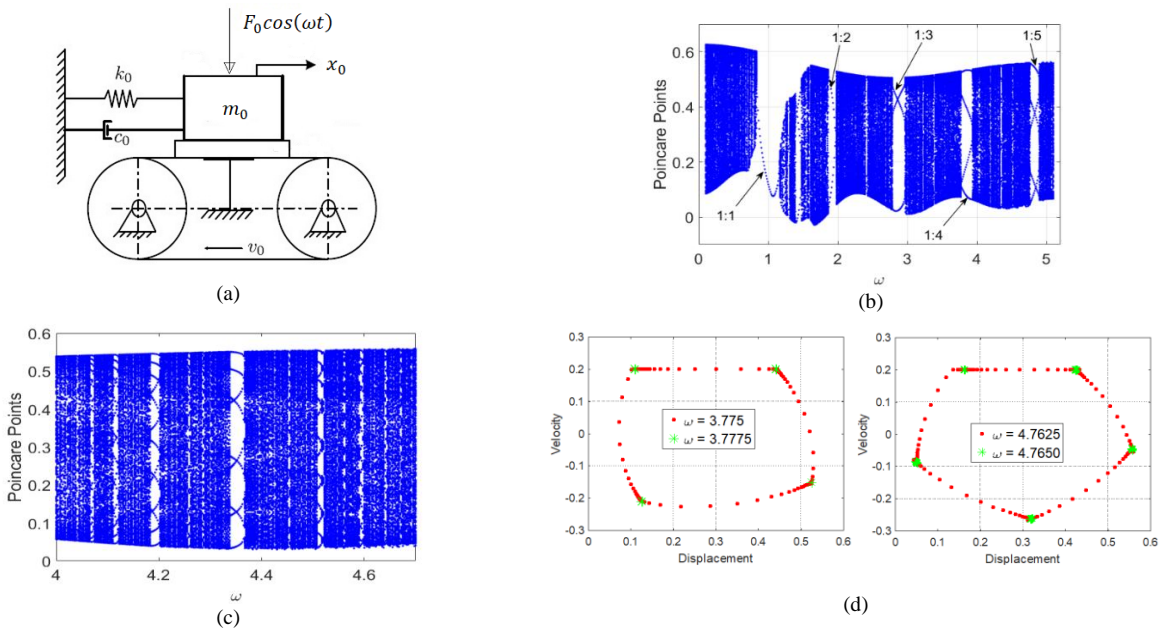


Figure 1: (a) 1 DoF Filippov model, (b) Bifurcation diagram, (c) Region between 1:4 and 1:5 windows, (d) Invariant polygons corresponding to quasi-periodic orbits and Poincare points of periodic orbits generated on their vertices.

Results and discussion

Fig. 1(a) shows the model with mass m_0 placed on a belt with uniform speed v_0 . k_0 and c_0 are stiffness and damping. x_0 is the horizontal displacement. Normal excitation $F_0 \cos(\omega t)$ is coupled to the horizontal motion through Stribeck frictional force between mass and the belt. The non-dimensional equation of motion can be written as $\ddot{x} + 2\zeta\dot{x} + x + (1 + F_N \cos(\omega t))(\mu_s \text{sgn}(\dot{x} - v_b) - k_1(\dot{x} - v_b) + k_3(\dot{x} - v_b)^3) = 0$.

Fig. 1(b) shows the bifurcation diagram with external frequency ω as parameter. In terms of the Poincare winding numbers [1], 1:1 and various $1:m$ entrainment regions are clearly observed. In Fig. 1(c) showing the enlarged view of the region between 1:4 and 1:5 entrainment windows, smaller windows of higher order $n:m$ entrainments are visible. This points towards the presence of Devil's staircase [1] in the model. Fig. 1(d) shows the transition from quasi-periodic to m -periodic orbits on the Poincare section. It is seen that the quasi-periodic orbits correspond to m -sided invariant polygons [3]. m -periodic entrained solutions are born by condensation of these polygons, with their vertices acting as natural places of condensation.

References

- [1] Balanov A., Janson N., Postnov D., Sosnovtseva O. (2009) Synchronization: From Simple to Complex. Springer-Verlag, Berlin.
- [2] Balaram B., Santhosh B., Awrejcewicz J. (2022) Frequency entrainment and suppression of stick-slip vibrations in a 3 DoF discontinuous disc brake model, *J. Sound Vibr.* **538**:117224.
- [3] Szalai R., Osinga H. M. (2008) Invariant polygons in systems with grazing-sliding. *Chaos* **18**:023121.

Vibration attenuation of dynamic systems using multiple motion constraints

Wei Dai*, Jian Yang**

*School of Naval Architecture and Ocean Engineering, Huazhong University of Science and Technology, Wuhan, China

**Faculty of Science and Engineering, University of Nottingham Ningbo China, Ningbo, China

Abstract. In this study, the dynamics and vibration transmission behavior of an impact oscillator with multiple motion constraints are investigated. The main sub-system is excited by an external harmonic force. A semi-analytical harmonic balance method and a time-marching method are used for the determination of system response. The effects of the constraint properties on the dynamic performance as well as the force transmission characteristics are examined.

Introduction

Contact nonlinearities exist in the operation of many dynamical systems, e.g., tooling machinery, drilling machines, roller bearings, meshing gears, etc [1]. The components may be engaged with each other during the motion. The contact interaction will change the physical properties of the assembly and will significantly influence the system performance [2]. The impact oscillators comprising constraint have been widely accepted as a representative model to study the nonlinear dynamic behaviour in the systems with clearance. In past research, the dynamics of impact oscillators were extensively investigated. However, very few studies were reported on the application of multiple constraints on the vibration attenuation design of dynamic systems, e.g., suppressing the vibration of propulsion shafting on board. This research investigates a multiple-degree-of-freedom impact oscillators considering multiple motion constraints. The equations of the motion of the system in a matrix form are

$$\begin{bmatrix} m_1 & 0 & 0 \\ 0 & m_2 & 0 \\ 0 & 0 & m_3 \end{bmatrix} \begin{Bmatrix} \ddot{x}_1 \\ \ddot{x}_2 \\ \ddot{x}_3 \end{Bmatrix} + \begin{bmatrix} c_1 + c_2 & -c_2 & 0 \\ -c_2 & c_2 + c_3 & -c_3 \\ 0 & -c_3 & c_4 + c_3 \end{bmatrix} \begin{Bmatrix} \dot{x}_1 \\ \dot{x}_2 \\ \dot{x}_3 \end{Bmatrix} + \begin{bmatrix} k_1 + k_2 & -k_2 & 0 \\ -k_2 & k_2 + k_3 & -k_3 \\ 0 & -k_3 & k_4 + k_3 \end{bmatrix} \begin{Bmatrix} x_1 \\ x_2 \\ x_3 \end{Bmatrix} + \begin{Bmatrix} f_1 \\ f_2 \\ f_3 \end{Bmatrix} = \begin{Bmatrix} f_0 e^{i\omega t} \\ 0 \\ 0 \end{Bmatrix}, \quad (1)$$

where f_1 , f_2 and f_3 denote the constraint forces act on the masses, respectively. The solutions of these equations can be determined by a harmonic balance approximation method and validated by the numerical integration method.

Results and discussions

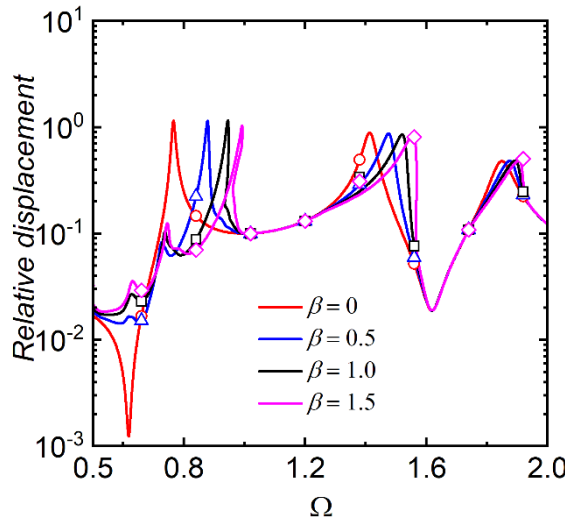


Figure 1: Relative displacement response between two subsystems.

Figure 1 show that the constraints can provide a hardening effect on the frequency response of the system. A higher constraint stiffness will further extend the transmissibility curves to the high frequencies, resulting in multiple solutions and super-harmonic components. This research facilitates further power flow analysis (PFA) on the vibration transmission and dissipation mechanism from the energy viewpoint. In this way, a deeper understanding of the vibration transmission behavior within the systems with clearance contact can be achieved, which will benefit the improvement of vibration attenuation designs for such systems.

References

- [1] Dai W., Yang J., Shi B. (2020) Vibration Transmission and Power Flow in Impact Oscillators with Linear and Nonlinear Constraints *Int J Mech Sci* **168**:105234.
- [2] Dai W., Yang J. (2021) Vibration transmission and energy flow of impact oscillators with nonlinear motion constraints created by diamond-shaped linkage mechanism *Int J Mech Sci* **194**:106212.

Modified Energy-based Time Variational Methods for Obtaining Periodic and Quasi-periodic Responses

Aalokeparno Dhar* and I.R. Praveen Krishna*

*Department of Aerospace Engineering, Indian Institute of Space Science and Technology, Thiruvananthapuram, Kerala, India

Abstract. Harmonic Balance Method (HBM) and Time Variational Method (TVM) are two semi-analytical methods that are used for solving periodically excited dynamical systems. Harmonic Balance Method is modified and extended in several works for solving free vibrations and systems with quasi-periodic responses. It is very important to study the homogeneous response to characterize the system with its features like natural frequencies and energy content. In this study, TVM is modified with the addition of energy equations for obtaining multi-frequency responses for multi-DOF autonomous systems, and these are applied to Duffing oscillator and 2-DOF pendulum system.

Introduction

Steady-state response of dynamical systems can be obtained using semi-analytical methods. Among these methods, Harmonic Balance Method[1] approximates the solution as a truncated Fourier series. Fourier series being periodic in nature, this method is an excellent tool used for obtaining limit cycles. This method is extended for multi-frequency excitation, called Multi Harmonic Balance Method (MHBM) and for homogeneous systems, called Harmonic Energy Balance Method (HEBM). One major drawback of these methods is its domain transformation method for the non-linear part of the system, which is a time-consuming process. Rook[2] introduced Time Variational Method, which skips the domain transformation step and solves the system in the time domain itself. Dhar and Krishna[3] extended this method similar to MHBM and obtained frequency-amplitude responses for quasi-periodically excited Duffing oscillator. In the beginning of this paper, the existing TVM and MTVM are described and applied to Duffing system. Cubic spline function is used as the basis function. The use of such a basis function requires modification in the concept of domain transformation in TVM, which is explained. In the following sections, the modified TVM is extended for computing periodic and quasi-periodic solutions for homogeneous systems named TVEM (Time Variational Energy based Method) and MTVEM (Multi Time Variational Energy based Method), respectively.

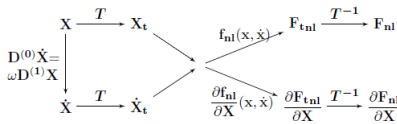


Figure 1: TVM modified with domain transformation

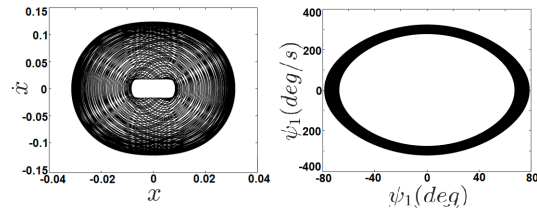


Figure 2: 2-DOF pendulum phase portraits x and ψ

Methodology and Result

TVM method is modified by introducing domain transformation shown in figure 1. The transformation T , being a linear map, is fast and does not produce any error in the process. This modified TVM is augmented with the Hamiltonian of the system forming TVEM. MTVM is modified using the Hamiltonian equation and the concept of energy split to obtain solutions at constant energy and different energy ratios in between the DOFs. TVEM and MTVEM are applied to the Duffing oscillator and pendulum system. Figure 2 shows result of the 2-DOF pendulum system (Translational DOF x and rotational DOF ψ) with total energy $E = 4$ and energy ratio of the first DOF $E_1/E = 0.12$ solved using MTVEM and validated with numerical integration and MHEBM.

References

- [1] M. S. Alam, Md. Abdur Razzak, Md. Alal Hosen, and Md. Riaz Parvez. (2016) The rapidly convergent solutions of strongly nonlinear oscillators. *Springerplus*, **5**:1258.
- [2] Todd Rook. An alternate method to the alternating time-frequency method.(2002) *Nonlinear Dyn.*, **27** :327–339.
- [3] Aalokeparno Dhar and I. R. Praveen Krishna.(2022) Semi-analytical approaches for solving duffing oscillator with multi-frequency excitation. In Walter Lacarbonara, Balakumar Balachandran, Michael J. Leamy, Jun Ma, J. A. Tenreiro Machado, and Gabor Stepan, editors, *Advances in Nonlinear Dynamics*, pages 609–621, Cham. Springer International Publishing.

Modified Energy-based Time Variational Methods for Obtaining Periodic and Quasi-periodic Responses

Aalokeparno Dhar* and I.R. Praveen Krishna*

*Department of Aerospace Engineering, Indian Institute of Space Science and Technology, Thiruvananthapuram, Kerala, India

Abstract. Harmonic Balance Method (HBM) and Time Variational Method (TVM) are two semi-analytical methods that are used for solving periodically excited dynamical systems. Harmonic Balance Method is modified and extended in several works for solving free vibrations and systems with quasi-periodic responses. It is very important to study the homogeneous response to characterize the system with its features like natural frequencies and energy content. In this study, TVM is modified with the addition of energy equations for obtaining multi-frequency responses for multi-DOF autonomous systems, and these are applied to Duffing oscillator and 2-DOF pendulum system.

Introduction

Steady-state response of dynamical systems can be obtained using semi-analytical methods. Among these methods, Harmonic Balance Method[1] approximates the solution as a truncated Fourier series. Fourier series being periodic in nature, this method is an excellent tool used for obtaining limit cycles. This method is extended for multi-frequency excitation, called Multi Harmonic Balance Method (MHBM) and for homogeneous systems, called Harmonic Energy Balance Method (HEBM). One major drawback of these methods is its domain transformation method for the non-linear part of the system, which is a time-consuming process. Rook[2] introduced Time Variational Method, which skips the domain transformation step and solves the system in the time domain itself. Dhar and Krishna[3] extended this method similar to MHBM and obtained frequency-amplitude responses for quasi-periodically excited Duffing oscillator. In the beginning of this paper, the existing TVM and MTVM are described and applied to Duffing system. Cubic spline function is used as the basis function. The use of such a basis function requires modification in the concept of domain transformation in TVM, which is explained. In the following sections, the modified TVM is extended for computing periodic and quasi-periodic solutions for homogeneous systems named TVEM (Time Variational Energy based Method) and MTVEM (Multi Time Variational Energy based Method), respectively.

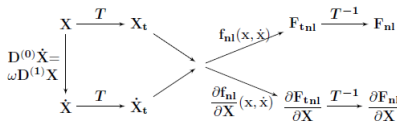


Figure 1: TVM modified with domain transformation

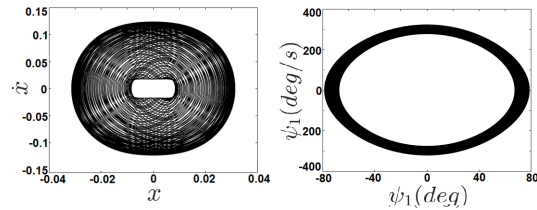


Figure 2: 2-DOF pendulum phase portraits x and ψ

Methodology and Result

TVM method is modified by introducing domain transformation shown in figure 1. The transformation T , being a linear map, is fast and does not produce any error in the process. This modified TVM is augmented with the Hamiltonian of the system forming TVEM. MTVM is modified using the Hamiltonian equation and the concept of energy split to obtain solutions at constant energy and different energy ratios in between the DOFs. TVEM and MTVEM are applied to the Duffing oscillator and pendulum system. Figure 2 shows result of the 2-DOF pendulum system (Translational DOF x and rotational DOF ψ) with total energy $E = 4$ and energy ratio of the first DOF $E_1/E = 0.12$ solved using MTVEM and validated with numerical integration and MHEBM.

References

- [1] M. S. Alam, Md. Abdur Razzak, Md. Alal Hosen, and Md. Riaz Parvez. (2016) The rapidly convergent solutions of strongly nonlinear oscillators. *Springerplus*, **5**:1258.
- [2] Todd Rook. An alternate method to the alternating time-frequency method.(2002) *Nonlinear Dyn.*, **27** :327–339.
- [3] Aalokeparno Dhar and I. R. Praveen Krishna.(2022) Semi-analytical approaches for solving duffing oscillator with multi-frequency excitation. In Walter Lacarbonara, Balakumar Balachandran, Michael J. Leamy, Jun Ma, J. A. Tenreiro Machado, and Gabor Stepan, editors, *Advances in Nonlinear Dynamics*, pages 609–621, Cham. Springer International Publishing.

Modified Energy-based Time Variational Methods for Obtaining Periodic and Quasi-periodic Responses

Aalokeparno Dhar* and I.R. Praveen Krishna*

*Department of Aerospace Engineering, Indian Institute of Space Science and Technology, Thiruvananthapuram, Kerala, India

Abstract. Harmonic Balance Method (HBM) and Time Variational Method (TVM) are two semi-analytical methods that are used for solving periodically excited dynamical systems. Harmonic Balance Method is modified and extended in several works for solving free vibrations and systems with quasi-periodic responses. It is very important to study the homogeneous response to characterize the system with its features like natural frequencies and energy content. In this study, TVM is modified with the addition of energy equations for obtaining multi-frequency responses for multi-DOF autonomous systems, and these are applied to Duffing oscillator and 2-DOF pendulum system.

Introduction

Steady-state response of dynamical systems can be obtained using semi-analytical methods. Among these methods, Harmonic Balance Method[1] approximates the solution as a truncated Fourier series. Fourier series being periodic in nature, this method is an excellent tool used for obtaining limit cycles. This method is extended for multi-frequency excitation, called Multi Harmonic Balance Method (MHBM) and for homogeneous systems, called Harmonic Energy Balance Method (HEBM). One major drawback of these methods is its domain transformation method for the non-linear part of the system, which is a time-consuming process. Rook[2] introduced Time Variational Method, which skips the domain transformation step and solves the system in the time domain itself. Dhar and Krishna[3] extended this method similar to MHBM and obtained frequency-amplitude responses for quasi-periodically excited Duffing oscillator. In the beginning of this paper, the existing TVM and MTVM are described and applied to Duffing system. Cubic spline function is used as the basis function. The use of such a basis function requires modification in the concept of domain transformation in TVM, which is explained. In the following sections, the modified TVM is extended for computing periodic and quasi-periodic solutions for homogeneous systems named TVEM (Time Variational Energy based Method) and MTVEM (Multi Time Variational Energy based Method), respectively.

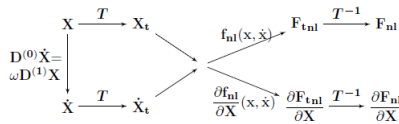


Figure 1: TVM modified with domain transformation

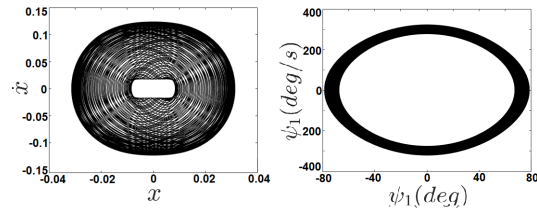


Figure 2: 2-DOF pendulum phase portraits x and ψ

Methodology and Result

TVM method is modified by introducing domain transformation shown in figure 1. The transformation T , being a linear map, is fast and does not produce any error in the process. This modified TVM is augmented with the Hamiltonian of the system forming TVEM. MTVM is modified using the Hamiltonian equation and the concept of energy split to obtain solutions at constant energy and different energy ratios in between the DOFs. TVEM and MTVEM are applied to the Duffing oscillator and pendulum system. Figure 2 shows result of the 2-DOF pendulum system (Translational DOF x and rotational DOF ψ) with total energy $E = 4$ and energy ratio of the first DOF $E_1/E = 0.12$ solved using MTVEM and validated with numerical integration and MHEBM.

References

- [1] M. S. Alam, Md. Abdur Razzak, Md. Alal Hosen, and Md. Riaz Parvez. (2016) The rapidly convergent solutions of strongly nonlinear oscillators. *Springerplus*, **5**:1258.
- [2] Todd Rook. An alternate method to the alternating time-frequency method.(2002) *Nonlinear Dyn.*, **27** :327–339.
- [3] Aalokeparno Dhar and I. R. Praveen Krishna.(2022) Semi-analytical approaches for solving duffing oscillator with multi-frequency excitation. In Walter Lacarbonara, Balakumar Balachandran, Michael J. Leamy, Jun Ma, J. A. Tenreiro Machado, and Gabor Stepan, editors, *Advances in Nonlinear Dynamics*, pages 609–621, Cham. Springer International Publishing.

Horizontal table vibration for parts-centering without feedback

Dheeraj Varma Manthena*, C. P. Vyasarayani* and Anindya Chatterjee **

*Mechanical and Aerospace Engineering, Indian Institute of Technology Hyderabad, Sangareddy, 502285, India

**Mechanical Engineering, Indian Institute of Technology Kanpur, 208016, India

Abstract. We study the slow average motions of a particle on a horizontally vibrating frictional table. The equations of motion have non-analytic nonlinearities. Numerical simulations show multiple time scales. The system is analyzed using the method of multiple scales (MMS). The slow-flow integrals are found using asymptotics, have logarithmic nonlinearities, are valid near the target location on the table, are easy to integrate numerically, and retain parametric excitation in slow time. The slow flow matches well with full numerical solutions. This is the first MMS analysis of a problem in this area that we are aware of.

Introduction

A point mass m under gravity g moves on a table with a coefficient of friction μ . The table kinematics is described by its instantaneous centre of rotation ($x_c(t) = R \cos(\Omega t)$, $y_c(t) = R \sin(\Omega t)$) and its angular velocity $\nu = H \cos(\omega t)$. This prescribed motion, for some parameter choices, generates a stable fixed point in space. This problem is of interest in robotics [1, 2] and is relevant to open-loop manipulation of part feeders in industry. We scale length and time by selecting $R = 1$ and $\omega = 1$. Further, letting $H = \epsilon A$, $\Omega = 1/2 + \epsilon \Delta$, and $\mu g = \epsilon^2 \alpha$, the equations of motion are:

$$\ddot{x} = \frac{-\epsilon^2 \alpha \left\{ \dot{x} + \epsilon A \cos(t) \left[y - \sin\left(\frac{t}{2} + \epsilon \Delta t\right) \right] \right\}}{\sqrt{\left\{ \dot{x} + \epsilon A \cos(t) \left[y - \sin\left(\frac{t}{2} + \epsilon \Delta t\right) \right] \right\}^2 + \left\{ \dot{y} - \epsilon A \cos(t) \left[x - \cos\left(\frac{t}{2} + \epsilon \Delta t\right) \right] \right\}^2}}, \quad (1)$$

$$\ddot{y} = \frac{-\epsilon^2 \alpha \left\{ \dot{y} - \epsilon A \cos(t) \left[x - \cos\left(\frac{t}{2} + \epsilon \Delta t\right) \right] \right\}}{\sqrt{\left\{ \dot{x} + \epsilon A \cos(t) \left[y - \sin\left(\frac{t}{2} + \epsilon \Delta t\right) \right] \right\}^2 + \left\{ \dot{y} - \epsilon A \cos(t) \left[x - \cos\left(\frac{t}{2} + \epsilon \Delta t\right) \right] \right\}^2}}. \quad (2)$$

Results and discussion

The method of multiple scales (MMS) works here. The corresponding slow flow equations can be obtained via asymptotic approximations for some integrals. These equations are

$$\frac{4\pi A}{\alpha} \zeta'' = [-C\eta' + S\zeta' + \zeta'] \ln(E) + [C\eta' - S\zeta' + \zeta'] \ln(F) - 4CA\eta + 4SA\zeta - G\zeta', \quad (3)$$

$$\frac{4\pi A}{\alpha} \eta'' = [-C\zeta' - S\eta' + \eta'] \ln(E) + [C\zeta' + S\eta' + \eta'] \ln(F) - 4CA\zeta - 4SA\eta - G\eta'. \quad (4)$$

In Eqs. 3-4, the superscript $'$ denotes a derivative with respect to T_1 . Further, $C = \cos(2\Delta T_1)$, $S = \sin(2\Delta T_1)$, $E = [\zeta'^2 - \eta'^2] S - 2\zeta'\eta'C + \eta'^2 + \zeta'^2$, $F = [\eta'^2 - \zeta'^2] S + 2\zeta'\eta'C + \eta'^2 + \zeta'^2$, and $G = 10 \ln(2) + 4 \ln(A) + 4$. In Fig. 1(a), full solutions for Eqs. 1-2 in the $x-y$ plane and for Eqs. 3-4 in the $\zeta-\eta$ plane are superimposed. The match is excellent. In Fig. 1(b), a comparison between y and η is shown. A zoomed-in portion of the same is shown in Fig. 1(c). The similar match for x and ζ is omitted to save space. We emphasize that fast oscillations of x and y are absent from ζ and η , though slow oscillations are retained. Those can be removed with unconventional calculations that we will present in another paper.

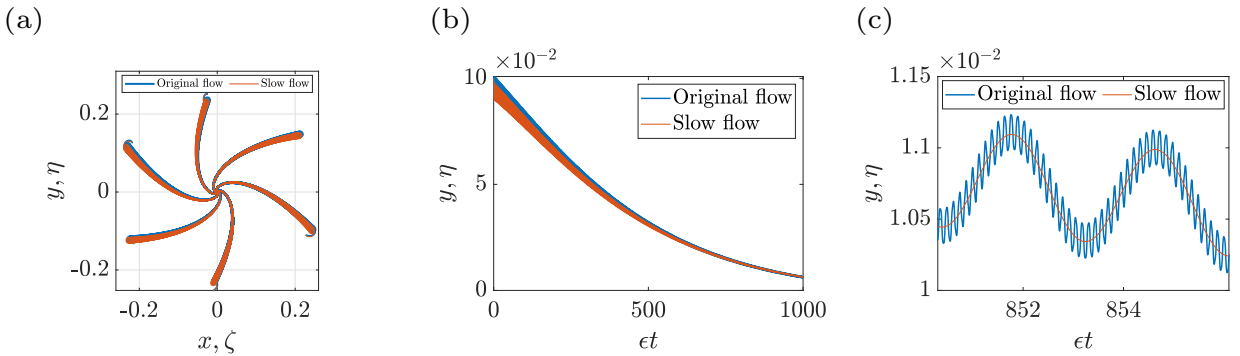


Figure 1: Comparison between solutions of Eqs. 1-2 and Eqs. 3-4: (a) x - y plane, (b) time response for $0 \leq \epsilon t \leq 1000$, and (c) time response for $850 \leq \epsilon t \leq 856$. These results were obtained with parameters $\alpha = 0.5$, $\epsilon = 0.01$, $A = 1$, $\Delta = 1.1$ and for near-zero-velocity initial conditions.

References

- [1] Reznik., D. S. (2000) The universal planar manipulator, PhD thesis, University of California, Berkeley.
- [2] Vose., T. H., Umbanhowar., P. and Lynch., K. M. (2009) Friction-induced lines of attraction and repulsion for parts sliding on an oscillated plate. *IEEE Transactions on Automation Science and Engineering* 6:685-699

Harmonic expansion and nonsmooth dynamics in a circular contact region with combined slip-spin motion

Mate Antali

Department of Applied Mechanics, Szechenyi Istvan University, Győr, Hungary

Abstract. We analyse a rigid body in planar motion while touching a rough plane at a finite-sized, circular contact area. By assuming Coulomb friction between the tangential and normal pressure distributions, the resultant forces and torques can be expressed formally with a nonsmooth dependence on the kinematic variables. In the literature, the exact form of the tangential forces is available for special pressure distributions expressed by transcendental functions; recently, an approximate linear model was introduced. Now, we present a nonlinear extension of the approximation, which can be used effectively to characterise slipping-sticking transitions between the bodies.

Introduction

Consider a rigid body touching a fixed, rough plane in a finite-sized circular contact area (see Fig. 1). Rigid body motion is assumed in the plane xy of the contact region. This motion is parametrized by the velocities u_x, u_y of the contact point and the angular velocity ω_z . The normal pressure distribution is assumed to be constant in time and to have the circular symmetric form $p(x, y) = \tilde{p}(\sqrt{x^2 + y^2})$. Consider permanent slipping, thus, $u_x = u_y = \omega_z = 0$ is excluded.

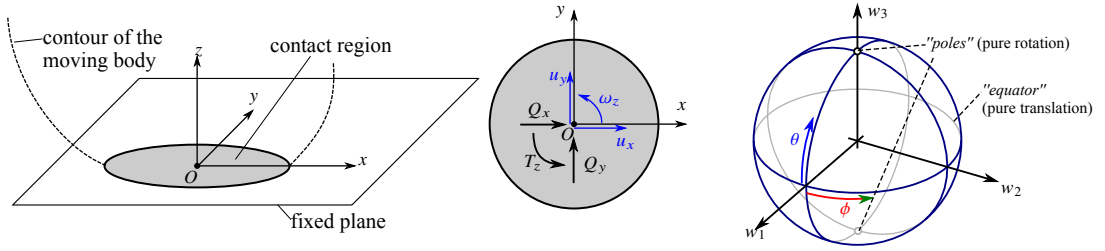


Figure 1: Left and middle panel: Kinematic and dynamic variables in the tangent plane of the circular contact area. Right panel: parametrizing the direction of slipping by the variable sets (w_1, w_2, w_3) and (θ, ϕ) .

Results and conclusion

According to [1], let us introduce the variables $(w_1, w_2, w_3) = (u_x, u_y, \rho\omega_z) / \sqrt{u_x^2 + u_y^2 + \rho^2\omega_z^2}$ to express the *direction* of the relative motion, where ρ is a scaling parameter. The variable set (w_1, w_2, w_3) lies in the unit sphere \mathbb{S}^3 as $w_1^2 + w_2^2 + w_3^2 = 1$. This unit sphere can also be parametrised by two angles θ and ϕ in the form $w_1 = \cos \theta \cos \phi$, $w_2 = \cos \theta \sin \phi$, $w_3 = \sin \theta$. Assume Coulomb friction model with a friction coefficient μ between the pressure distributions. Then, the resultant force system contains tangential forces Q_x, Q_y and the normal torque T_z (see Fig. 1). According to CITEE, the circular symmetric case leads to the form

$$\begin{aligned} Q_x &= -\mu P \frac{w_1}{\sqrt{w_1^2 + w_2^2}} \cdot Q_w(w_3) = -\mu P \cos \phi \cdot Q(\theta), \\ Q_y &= -\mu P \frac{w_2}{\sqrt{w_1^2 + w_2^2}} \cdot Q_w(w_3) = -\mu P \sin \phi \cdot Q(\theta), \\ T_z &= -\mu P \lambda \cdot T_w(w_3) = -\mu P \pi_{xy} \cdot T(\theta), \end{aligned}$$

where the normal force P and the coefficient λ are computed from \tilde{p} . The algebraic form of the functions Q_w, T_w, Q, T can be computed for constant [3] and parabolic [2] pressure distributions. In [1], the authors use the approximation $Q_w \approx \sqrt{1 - w_3^2}$ and $T_w = w_3$, which makes the above tangential forces and moment linear in w_3 and *harmonic* in θ , which lead to qualitative analysis of the nonsmooth dynamics. However, by this approximation, some bifurcations can be lost.

Now, we will expand the expressions by the truncated Fourier expansion of Q and T . We show that then, nonlinear terms appear in Q_w, T_w , and we can extend the nonsmooth dynamical analysis of [1] to find the bifurcations of fixed points on the sphere of $w_1^2 + w_2^2 + w_3^2 = 1$. The fixed points of this fast subsystem correspond to the limit directions where transitions are possible between slipping and sticking of the body. Our goal is to determine the combined slip-spin states just before sticking.

References

- [1] Antali M., Varkonyi P. L. (2022) The nonsmooth dynamics of combined slip and spin motion under dry friction. *Journal of Nonlinear Science* **32**(4) paper 58.
- [2] Leine R.I., Glocker C. (2003) A set-valued force law for spatial Coulomb-Contensou friction. *Eur. J. Mech. A* **22**(2): 193–216.
- [3] Magyari E., Weidman P.: (2020) Frictionally coupled sliding and spinning on an inclined plane. *Physica D: Nonlinear Phenomena* **413**: paper 132647.

Limit cycle bifurcations from infinity in relay systems

Enrique Ponce*, Emilio Freire*, Javier Ros*, and Elisabet Vela*

*Department of Applied Mathematics, E.T.S. Ingeniería, Universidad de Sevilla, SPAIN, ORCID #0000-0003-0467-5032

Abstract. Limit cycle bifurcations from infinity in 3D Relay systems, belonging to the class of three-dimensional symmetric discontinuous piecewise linear differential systems with two zones, are analyzed. A criticality parameter is found, whose sign determines the character of the bifurcation. When such non-degeneracy parameter vanishes, a higher co-dimension bifurcation takes place, giving rise to the emergence of a curve of saddle-node bifurcations of periodic orbits, which allows to determine parameter regions where two limit cycles coexist.

Introduction

The analysis of bifurcations from infinity helps to get a complete overview of the dynamical behaviour to be found in a given dynamical system. Limit cycle bifurcations from infinity has been considered in the past, see [1, 2, 3], but here we want to study the specific case of 3D relay systems, studying also its possible degeneration. Under generic hypothesis, there is no loss of generality in considering relay systems of the form

$$\dot{\mathbf{x}} = A\mathbf{x} - \mathbf{b} \operatorname{sign}(\mathbf{c}^\top \mathbf{x}), \quad A = \begin{pmatrix} t & -1 & 0 \\ m & 0 & -1 \\ d & 0 & 0 \end{pmatrix}, \quad \mathbf{b} = \begin{pmatrix} b_1 \\ b_2 \\ b_3 \end{pmatrix}, \quad \mathbf{c} = \begin{pmatrix} 1 \\ 0 \\ 0 \end{pmatrix}, \quad (1)$$

where $\mathbf{x} = (x, y, z)^\top \in \mathbb{R}^3$, the dot represents derivative with respect to the time τ , and coefficients t, m and d in matrix A are its linear invariants (trace, sum of principal minors and determinant).

Results and discussion

As a first step in the analysis, we present the extension of a previous result in [5] to discontinuous systems (1).

Theorem Consider system (1) under the assumption of complex eigenvalues for matrix A , that is there exist $\lambda, \sigma \in \mathbb{R}$ and $\omega > 0$ such that $t = 2\sigma + \lambda$, $m = 2\sigma\lambda + \sigma^2 + \omega^2$, $d = \lambda(\sigma^2 + \omega^2)$, and define the non-degeneracy parameter $\delta = b_3 - b_2\lambda - b_1\omega^2$. If $\delta \neq 0$, then, for $\sigma = 0$ the system undergoes a Hopf bifurcation from infinity, that is, one symmetric limit cycle of large amplitude appears for $\delta\sigma < 0$ and σ sufficiently small. Furthermore, when $\lambda \neq 0$, if $\delta > 0$ and $\lambda < 0$, then the bifurcating limit cycle for $\sigma < 0$ is orbitally asymptotically stable. Otherwise, if $\delta < 0$ or $\lambda > 0$ then the bifurcating limit cycle is unstable. In the case $\lambda = 0$, assuming $\delta = b_3 - b_1\omega^2 > 0$, a sufficient condition for the stability of the limit cycle that bifurcates for $\sigma < 0$ is $b_1 > 0$.

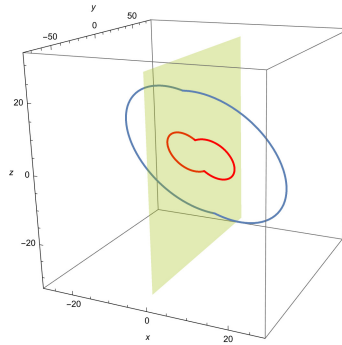


Figure 1: Coexistence of two limit cycles can be guaranteed through a degenerate bifurcation from infinity. Here, $\sigma = -0.01$, $\lambda = -1$, $\omega = 1$, $b_1 = -1$, $b_2 = 4$, and $b_3 = -4$, so that $\delta = 1 > 0$. The big limit cycle is stable, while the small one is unstable.

The case when the non-degeneracy parameter δ vanishes gives rise to a saddle-node bifurcation of periodic orbits and allows to justify the coexistence of two limit cycles, see Figure 1. The application of achieved results to systems in [4] will also be addressed, see [6] for more details.

References

- [1] Glover J. (1989) Hopf bifurcations at infinity, *Nonlinear Anal. Theory Methods Appl.* **13**:1393–1398.
- [2] He X. (1991) Hopf bifurcation at infinity with discontinuous nonlinearities, *J. Aust. Math. Soc. B* **33**:133–148.
- [3] Diamond P., Kuznetsov N., Rachinskii D. (2001) On the Hopf bifurcation in control systems with a bounded nonlinearity asymptotically homogeneous at infinity, *J. Differ. Equ.* **5**:1–26.
- [4] Di Bernardo M., Johansson K.H., Vasca F. (2001), Self-oscillations and sliding in relay feedback systems: symmetry and bifurcations, *Int. J. Bifurcat. Chaos* **11**:1121–1140.
- [5] Freire E., Ponce E., Ros J., Vela E., and Amador A. (2020), Hopf bifurcation at infinity in 3D symmetric piecewise linear systems. Application to a Bonhoeffer–van der Pol oscillator. *Nonlinear Anal. Real World Appl.* **54**:103112.
- [6] Freire E., Ponce E., Ros J., and Vela E. (2022), Hopf bifurcation at infinity in 3D Relay systems, *Physica D*, to appear.

Maneuvering a Stick in Three-Dimensional Space Using Impulsive Forces

Aakash Khandelwal*, Nilay Kant* and Ranjan Mukherjee *

*Michigan State University, East Lansing, MI 48823, USA

Abstract. The problem of maneuvering a stick in three-dimensional space using purely impulsive inputs is considered. A steady motion of the stick is one in which it is juggled between a sequence of configurations rotationally symmetric about the vertical axis; such a motion can be viewed as a periodic orbit. In particular, this work addresses the problem of transitioning from one steady orbit to another. The Impulse Controlled Poincaré Map approach is used to achieve the desired control objective. Simulation results verify the efficacy of the control design for several maneuvers.

Introduction

The robotic manipulation of objects without grasping, *i.e.* nonprehensile manipulation, represents an important class of problems [6, 7]. Juggling is a nonprehensile manipulation task whose dynamics are hybrid and non-smooth, comprised of impulsive dynamics due to contact with the actuator, and motion under gravity. The problem of juggling a stick, which is described by orientation in addition to position coordinates, is more challenging than that of juggling point masses [8, 1]. The dynamic model and control design for planar symmetric stick juggling has appeared in [3, 4]. The problem of juggling a stick in three-dimensions between a sequence of configurations rotationally symmetric about the vertical axis was considered in [5]. This work is extended here to treat the desired juggling motion as a function of time. The dynamics of the stick can be specified by five generalized coordinates, and three control inputs; the control action is purely impulsive and applied when the stick makes a fixed angle with respect to the vertical. The steady-state time of flight and the angle of precession about the vertical axis between consecutive rotationally symmetric configurations are treated as free variables. When they are chosen to be constant, they define a steady juggling motion. They may be varied slowly to transition from one steady juggling motion to another using the same control inputs - which is the focus of this work. The hybrid dynamics of stick juggling can be represented by a discrete-time Poincaré map. The map is conveniently expressed in a rotating reference frame (the reference frame of the juggler), and a steady juggling motion corresponds to a fixed point of this map. The Impulse Controlled Poincaré Map (ICPM) approach [2] can be used to achieve the control objective of stabilization of the fixed point of the map, and consequently the desired juggling motion. By treating the independently chosen steady-state values as time-varying, and recomputing the desired steady-state values and the control inputs at every intersection of the system trajectory with the Poincaré section, the ICPM approach can be applied to achieve the control objective of transitioning from one steady orbit to another.

Results and discussion

Simulations were carried out with the controller gains obtained using the LQR method. Three different maneuvers of the stick, wherein a transition from one steady juggling motion to another is observed, were considered. First, it was shown that the height of the orbit could be changed gradually as a function of time. The effect of an increase in the time of flight was considered next. Finally, the effect of simultaneous variation the angle of precession about the vertical axis and time of flight was considered. It was shown that the ICPM approach can be successfully applied to transition from one steady juggling motion to another. By choosing the free variables as slowly varying functions of time, a range of other maneuvers can be achieved. Future work will focus on experimental validation of steady-state stick juggling.

References

- [1] B. Brogliato and A. Z. Rio. On the control of complementary-slackness juggling mechanical systems. *IEEE Transactions on Automatic Control*, 45(2):235–246, 2000.
- [2] Nilay Kant and Ranjan Mukherjee. Orbital Stabilization of Underactuated Systems using Virtual Holonomic Constraints and Impulse Controlled Poincaré Maps. *Systems & Control Letters*, 146:104813, 2020.
- [3] Nilay Kant and Ranjan Mukherjee. Non-prehensile manipulation of a devil-stick: planar symmetric juggling using impulsive forces. *Nonlinear Dynamics*, 103(3):2409–2420, 2021.
- [4] Nilay Kant and Ranjan Mukherjee. Juggling a Devil-Stick: Hybrid Orbit Stabilization Using the Impulse Controlled Poincaré Map. *IEEE Control Systems Letters*, 6:1304–1309, 2022.
- [5] Aakash Khandelwal, Nilay Kant, and Ranjan Mukherjee. Nonprehensile manipulation of a stick using impulsive forces. *Nonlinear Dynamics*, 2022.
- [6] Kevin M. Lynch and Matthew T. Mason. Dynamic nonprehensile manipulation: Controllability, planning, and experiments. *The International Journal of Robotics Research*, 18(1):64–92, 1999.
- [7] Fabio Ruggiero, Vincenzo Lippiello, and Bruno Siciliano. Nonprehensile Dynamic Manipulation: A Survey. *IEEE Robotics and Automation Letters*, 3(3):1711–1718, 2018.
- [8] Arturo Zavala-Rio and Bernard Brogliato. On the Control of a One Degree-of-Freedom Juggling Robot. *Dynamics and Control*, 9(1):67–90, 1999.

Quantized H_∞ Filtering for Discrete-Time Markovian-Jump T-S Fuzzy Systems with Time-Varying Delays via Event-Trigger Mechanism

Soundararajan Ganesan*, Ardak Kashkynbayev* and Rakkiyappan Rajan**

*Department of Mathematics, Nazarbayev University, Nur-Sultan-010000, Kazakhstan.

**Department of Mathematics, Bharathiar University, Coimbatore-641046, India.

Abstract. The H_∞ filter design for delayed discrete-time Markovian-jump T-S fuzzy systems with quantized output measurement is the primary focus of this paper. To reach our notified goal, the event-trigger mechanism is designed so that the occupancy of the communication network resources is reduced. By manipulating the fuzzified Lyapunov-Krasovskii functional (LKF), sufficient conditions are derived by explicit expression of linear matrix inequalities (LMIs) which ensure the desired system is stochastically stable. Eventually, the proposed H_∞ filter design is validated by the implementation of the T-S fuzzy model of the tunnel diode circuit.

Introduction

The qualitative analysis of nonlinear systems is imperative so that the numerous practical systems show non-linearity when analyzing their dynamics. It is well known that T-S fuzzy models are capable of modelling nonlinear behaviour, by approximating any smooth nonlinear systems to any special accuracy within any compact set. Forever, it is quite common for network communication to have an information latching problem, which can be handled by extracting finite-state representations (modes) from Markovian-jump models. To be specific, discrete-time systems play a very vital role in digital signal analysis and processing. In place of it, the logarithmic quantizer is used to reduce the data-transmission rate in network communication. Additionally, energy consumption is reduced by the event-triggered transmission strategy and the lifetimes of the services are extended. On the other hand, the H_∞ filtering has been extensively studied to guarantee a bound of the worst-case estimation error where the statistics information on the disturbances is not required. Unfortunately, when it comes to the event-triggered scenario, the H_∞ filtering problem with quantization effects has not yet gained adequate research attention. Therefore, it is of significance to consider the event-triggered H_∞ filtering for nonlinear systems with quantization effects.

Results and discussion

In this paper, let us considered the following discrete-time T-S fuzzy Markovian-jump system:

IF θ_{1k} is M_{i1} and θ_{pk} is M_{ip} THEN $x(k+1) = A_{hr(k)}x(k) + A_{dhr(k)}x(k - \tau_r(k)) + B_{hr(k)}w(k)$ with the output measurement $y(k) = C_{hr(k)}x(k) + D_{hr(k)}v(k)$ and the estimated signal $z(k) = E_{hr(k)}x(k)$, where M_{ij} is a fuzzy set and θ_{jk} is the premise variable, $i \in \{1, 2, \dots, r\}$ and $j \in \{1, 2, \dots, p\}$, r is the number of IF-THEN rules; r, p are positive integers; $x(k) \in \mathbb{R}^n$ is the state; $v(k) \in \mathbb{R}^l$, $w(k) \in \mathbb{R}^n$ is the disturbance that belongs to $l_2[0, \infty)$; $A_{hr(k)}, B_{hr(k)}, C_{hr(k)}, D_{hr(k)}$, and $E_{hr(k)}$ are known matrices of appropriate dimensions; $\tau_r(k) \in [\tau_r^m(k), \tau_r^M(k)]$ is time-varying delay factor; The Markov-jump variable $\{r(k), k \in \mathbb{Z}_+\}$ is used to represent a mode of the subsystems. Further, the transmission instants sequence $\{k_s\}_{s \geq 0}$ with $k_0 = 0$ is generalized by the event-trigger instant $k_{s+1} = \min_{k > k_s} \{k / [y(k) - y(k_s)]^T \phi [y(k) - y(k_s)] \geq \sigma y^T(k_s) \phi y(k_s)\}$, where matrices $\phi > 0$ and $\sigma > 0$ are two event-triggered parameters to be designed properly.

From the input $\bar{y}(k)$, the filter has been estimated as

$$\hat{x}(k+1) = \hat{A}_{hr(k)}\hat{x}(k) + \hat{A}_{dhr(k)}\hat{x}(k - \tau_l(k)) + \hat{B}_{hr(k)}\bar{y}(k)$$

with estimation $\hat{z}(k) = \hat{E}_{hl}x(k)$, where $\hat{A}_{hl}, \hat{A}_{dhl}, \hat{B}_{hl}, \hat{C}_{hl}$ are filter parameters to be derived. The measured output is assumed to be quantized by the quantizer $q(y) = [q_1(y_1), q_2(y_2), \dots, q_l(y_l)]^T$. Based on filtering error analysis, we have estimated the error dynamics $\xi(k)$ and its stability has been confirmed by Theorem 1.

Theorem 1. For a given $\gamma > 0$, the filtering error system is stochastically stable, if there exists positive definite matrices $P_{hl}, P_{h+}, Q_1, Q_2, Q_3, R_1, R_2$, and M_1 , along with the scalar $\epsilon > 0$, for $h \in \rho, h^+ = (h_1(\theta(k+1)), h_2(\theta(k+1)), \dots, h_r(\theta(k+1))) \in \rho$ and $l \in \mathcal{S}$, which satisfies the LMI $[\phi_{nm}]_{5 \times 5} < 0$ such that $\phi_{11} = -P_{h+}, \phi_{13} = P_{h+}[\mathcal{A}_{ijl}, \mathcal{A}_{dijl}, 0, 0, 0, 0, 0, \mathcal{B}'_{ijl}, \mathcal{D}_{ijl}]$, $\phi_{14} = P_{h+}[\mathcal{B}_{ijl}, 0, 0, 0, 0, 0, 0, \mathcal{B}_{ijl}, \mathcal{B}_{ijl}]$, $\phi_{15} = [C_{ijl}^T, 0, 0, 0, 0, 0, 0, I, D_{ijl}^T]$, $\phi_{22} = -I$, $\phi_{23} = [\mathcal{E}_{ijl}, 0, 0, 0, 0, 0, 0, 0, 0]$, $\phi_{33} = [\phi_{33}^{ij}]_{9 \times 9}$, $\phi_{33}^{11} = -P_{hl} + Q_1 + Q_2 + Q_3 + \tau_l^2 R_1 + \tau_l^{m^2} R_2$, $\phi_{33}^{22} = -Q_3$, $\phi_{33}^{33} = -Q_1$, $\phi_{33}^{44} = -Q_2$, $\phi_{33}^{55} = -R_1$, $\phi_{33}^{66} = -M_1$, $\phi_{33}^{66} = -R_1$, $\phi_{33}^{77} = -R_2$, $\phi_{33}^{88} = -\phi(1 - \sigma)$, $\phi_{33}^{99} = -\gamma^2 I$, $\phi_{44} = -\epsilon I$, $\phi_{55} = -\epsilon I$, and the remaining terms ϕ_{nm} are zero.

References

- [1] Wang, W., Wen, Y., Sun, L., & Ma, K. (2022). H_∞ filter for discrete-time Takagi-Sugeno fuzzy systems with time-varying delays via a novel Wirtinger-based inequality. *Discrete Dynamics in Nature and Society*, 2022.
- [2] Zhang, T., Gao, J., & Li, J. (2018). Event-triggered H_∞ filtering for discrete-time Markov jump delayed neural networks with quantizations. *Systems Science & Control Engineering*, 6(3), 74-84.
- [3] Zheng, Q., Xu, S., & Zhang, Z. (2020). Nonfragile quantized H_∞ filtering for discrete-time switched T-S fuzzy systems with local nonlinear models. *IEEE Transactions on Fuzzy Systems*, 29(6), 1507-1517.

Three large amplitude limit cycles via Zero-Hopf bifurcation from infinity in 3D piecewise linear systems with symmetry.

Javier Ros*, Enrique Ponce* and Emilio Freire *

*Department of Applied Mathematics II, Universidad de Sevilla, Sevilla Spain, ORCID # 0000-0002-6396-1461

Abstract. The existence of the Zero-Hopf bifurcation from infinity is proven for a family of 3D piecewise linear systems with symmetry. Quantitative expressions are provided for the amplitude and period of the bifurcating large amplitude limit cycles living in two and three linearity zones. The simultaneous bifurcation of three limit cycles is shown. The theoretical results are applied to the Bonhöffer-van der Pol electronic oscillator.

Introduction

The zero-Hopf bifurcation for smooth systems has been widely analyzed, see for example [2], but this bifurcation has been rarely studied in piecewise linear differential systems, see [3], where the zero-Hopf bifurcation of a symmetric piecewise linear differential system with three zones in \mathbb{R}^3 was characterized obtaining the existence and stability of three periodic orbits bifurcating from the origin and two non trivial equilibria.

In the present work, the family of systems studied has the complex eigenvalues $\sigma(\varepsilon) \pm i\omega(\varepsilon)$, and the real one $\lambda(\varepsilon)$, and the non trivial equilibrium points tend to infinity when ε tends to zero, converting them in zero-Hopf equilibria. These zero-Hopf equilibria give place to a large amplitude bifurcating limit cycle, increasing the catalog of bifurcations at infinity in piecewise linear systems, see [1].

Main results

The piecewise linear differential system considered is written in the generalized Lienard's form defined by

$$\dot{\mathbf{x}} = \mathbf{F}(\mathbf{x}) = A_E \mathbf{x} + \mathbf{b} \text{sat}(x), \quad (1)$$

where $\mathbf{x} = (x, y, z)^\top \in \mathbb{R}^3$,

$$A_E = \begin{pmatrix} t_E & -1 & 0 \\ m_E & 0 & -1 \\ d_E & 0 & 0 \end{pmatrix} \quad \text{and} \quad \mathbf{b} = \begin{pmatrix} t_C - t_E \\ m_C - m_E \\ d_C - d_E \end{pmatrix}. \quad (2)$$

In order to analyze the zero-Hopf bifurcation at infinity, we will assume the linear matrix A_E of the external zones has eigenvalues $\lambda(\varepsilon)$, $\sigma(\varepsilon) \pm i\omega(\varepsilon)$, where,

$$\begin{aligned} \lambda(\varepsilon) &= \lambda_1 \varepsilon + \lambda_2 \varepsilon^2 + O(\varepsilon^3), \\ \sigma(\varepsilon) &= \sigma_1 \varepsilon + \sigma_2 \varepsilon^2 + O(\varepsilon^3), \\ \omega(\varepsilon) &= \omega_0 + \omega_1 \varepsilon + \omega_2 \varepsilon^2 + O(\varepsilon^3), \end{aligned}$$

with $\omega_0 > 0$. The main contribution is the following result.

Theorem Consider system (1)-(2) with the above eigenvalue configuration, with $\lambda_1 \neq 0$, $\sigma_1 \neq 0$, $d_C \neq 0$, $\omega_0 > 0$ and define the non-degeneracy parameter $\rho = d_C - \omega_0^2 t_C$. If $\rho \neq 0$, then, for $\varepsilon = 0$ the system undergoes a zero-Hopf bifurcation at infinity, that is, one symmetric limit cycle using the three zones of linearity appears for $\rho \sigma_1 \varepsilon > 0$ and ε sufficiently small. In particular, if $\rho < 0$ and $t_C < -\rho(\lambda_1 + \sigma_1)/(\sigma_1 \omega_0^2)$, then the limit cycle bifurcates for $\sigma_1 \varepsilon < 0$ and is orbitally asymptotically stable.

Furthermore, the period P of the periodic oscillation is an analytic function at 0, in the variable ε , and its series expansion is

$$P = \frac{2\pi}{\omega_0} + \frac{2\pi}{\omega_0} \left(\frac{\sigma_1 (\omega_0^2 - m_C)}{\rho} - \frac{\omega_1}{\omega_0} \right) \varepsilon + O(\varepsilon^2).$$

The amplitude of the bifurcating limit cycle has the following series expansion,

$$-y_0 = \frac{2\rho}{\pi \sigma_1 \omega_0 \varepsilon} + O(1).$$

References

- [1] Freire E., Ponce E., Ros J., Vela E., Amador A.F. (2020) Hopf bifurcation at infinity in 3D symmetric piecewise linear systems. Application to a Bonhöffer-van der Pol oscillator. *Nonlinear Anal. Real World Appl.* **54**: 103112.
- [2] Llibre J., Euzébio R. D. (2017) Zero-Hopf bifurcation in a Chua system. *Nonlinear Anal. Real World Appl.* **37**: 31–40.
- [3] Ponce E., Ros J., Vela E. (2013) Unfolding the fold-Hopf bifurcation in piecewise linear continuous differential systems with symmetry. *Physica D* **250**: 34–46.

Existence of a uniform upper bound for the number of limit cycles of planar piecewise linear systems

Victoriano Carmona*, **Fernando Fernández-Sánchez****, and Douglas D. Novaes***

* *Dpto. Matemática Aplicada & IMUS, Universidad de Sevilla, Spain, 0000-0002-2889-913X*

** *Dpto. Matemática Aplicada & IMUS, Universidad de Sevilla, Spain, 0000-0001-5774-6717*

*** *Dpto. de Matemática - IMECC, Universidade Estadual de Campinas (UNICAMP), Campinas, SP, Brazil, 0000-0002-9147-8442*

Abstract. This presentation is devoted to the open problem of the existence of a uniform upper bound for the maximum number of limit cycles of planar piecewise linear systems with two zones separated by a straight line. We give a positive answer to this question and establish that this number is less than 8.

Introduction

Roughly speaking, the second part of the 16th Hilbert's Problem consists in determining an upper bound for the maximum number of limit cycles of planar polynomial differential systems of degree n . This is one of the most important problems in the analysis of planar differential systems [5], and still remains unsolved even for $n = 2$, the simplest non trivial case.

Here, we consider a version for planar piecewise linear differential systems with two zones separated by a straight line,

$$\dot{\mathbf{x}} = \begin{cases} A_L \mathbf{x} + \mathbf{b}_L, & \text{if } x_1 \leq 0, \\ A_R \mathbf{x} + \mathbf{b}_R, & \text{if } x_1 \geq 0, \end{cases} \quad (1)$$

where $\mathbf{x} = (x_1, x_2) \in \mathbb{R}^2$, $A_{L,R} = (a_{ij}^{L,R})_{2 \times 2}$, and $\mathbf{b}_{L,R} = (b_1^{L,R}, b_2^{L,R}) \in \mathbb{R}^2$. For this kind of systems, a limit cycle is defined as an isolated crossing periodic solution.

One of the first works devoted to the study of a uniform upper bound for the maximum number of limit cycles of system (1) is authored by Lum and Chua [7]. There, they conjectured that, under the continuity hypothesis, system (1) had at most one limit cycle. This conjecture was proven in 1998 by Freire et al. [4]. In the literature, there are also partial results about upper bounds for other non-generic families of piecewise linear differential systems but, after more than 30 years since the Lum-Chua's conjecture [7] and hundreds of paper on this subject, the existence of a uniform upper bound for the maximum number of limit cycles that system (1) can have, still remains an open question.

Recently, after obtaining a new integral characterization for *Poincaré half-maps* [1], the authors have considered a new approach to the study of the periodic behavior of piecewise linear systems without the annoying case-by-case study usually needed in previous works. In [2], this approach has been used to give a new simple proof for the Lum-Chua's conjecture. Moreover, the same technique was used in [3] to prove that system (1) has at most one limit cycle when there are not sliding sets in the separation line.

Results and discussion

In this work, by using the integral characterization for Poincaré half-maps provided in [1] and some extensions of the Khovanskii's theory [6], it is proven that there exists a natural bound less than 8 for the number of limit cycles of system (1).

References

- [1] Carmona V., Fernández-Sánchez F. (2021) Integral characterization for Poincaré half-maps in planar linear systems. *J Differ Equations* **305**:319-346.
- [2] Carmona V., Fernández-Sánchez F, Novaes D. D. (2021) A new simple proof for Lum-Chua's conjecture. *Nonlinear Anal-Hybri* **40**:100992, 7.
- [3] Carmona V., Fernández-Sánchez F, Novaes D. D. (2022) Uniqueness and stability of limit cycles in planar piecewise linear differential systems without sliding region. arXiv:2207.14634.
- [4] Freire F., Ponce E., Rodrigo F., Torres F. (1998) Bifurcation Sets of Continuous Piecewise Linear Systems with Two Zones. *Int J Bifurcat Chaos* **8**(11):2073-2097.
- [5] Ilyashenko, Y. (2002) Centennial History of Hilbert's 16th Problem. *Bull Amer Math Soc* **39**(3):301-354.
- [6] Khovanskii A. G. (1991) *Fewnomials*. Translations of Mathematical Monographs 88. American Mathematical Society, Providence, RI.
- [7] Lum R., Chua L. O. (1991) Global properties of continuous piecewise linear vector fields. Part I: Simplest case in \mathbb{R}^2 . *Int J Circ Theor App* **19**(3):251-307.

Stability and instability of a complex biodynamical discrete structure on a cantilever coupled to nonlinear springs

Andjelka Hedrih^{*}, Katica (Stevanović) Hedrih^{*,}**

*Department of mechanics, Mathematical Institute of Serbian Academy of Sciences and Arts (MI SANU)

Belgrade, Serbia, ^{**} Faculty of Mechanical Engineering, University of Niš, Niš, Serbia

Abstract. To withstand the rigors of wind, rain, and their own weight, some young seedlings need assistance in the first year after planting at the permanent place in the form of single, double or triple staking methods. Using a previously developed model of complex discrete cantilever coupled with nonlinear spring we investigate the stability and instability of the complex structure regarding the number of nonlinear springs to which the structure is coupled. The geometric nonlinearity of the system is introduced by a spring with cubic nonlinear properties that oscillates in the horizontal plane. Stability of oscillations of these complex structures is important for proper stacking of young seedlings with different canopy shapes. First asymptotic approximations of nonlinear differential equations along amplitudes and phases of nonlinear modes of three-frequency oscillations of considered complex structure is derived. An analysis of interactions between nonlinear modes is done.

Introduction

It is of a great interest that staking of the young seedlings is done properly ensuring oscillations of the trunk that will stimulate the root growing and proper anchoring to the ground [1,2]. Stability of forced oscillations of double and triple staking methods is analysed using a modification of a previously developed model [3] of a young seedling staked with one stake. The purpose of the study is to analyse which canopy shapes are the most suitable for each particular staking method.

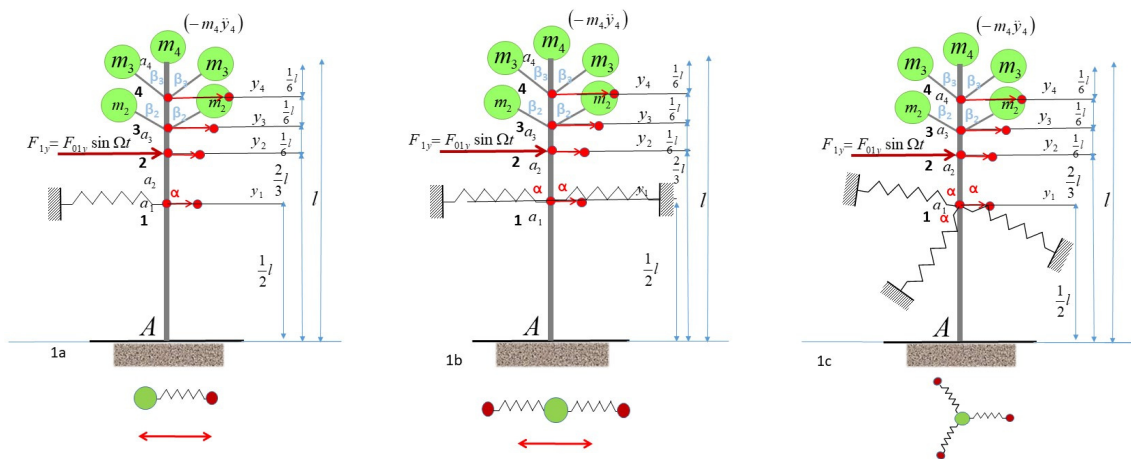


Figure 1: Complex discrete structure on a cantilever with: 1a. one spring with nonlinear properties 1b. two springs spring with nonlinear properties 1c. tree springs with nonlinear properties.

A young seedling staked with single, double or triple staking methods (Fig.1) is modelled as complex discrete biodynamical structure on a cantilever coupled with one/two/three nonlinear elastic springs at 2/3 of cantilever (tree stem) height. Springs with cubic nonlinear properties oscillate in the horizontal plane. Stability and instability of forced three-frequency nonlinear oscillations of these complex system under an external three-frequency force is analyzed.

Results and discussion

First asymptotic approximations of nonlinear differential equations along amplitudes and phases of nonlinear modes of three-frequency oscillations of considered complex discrete biodynamical structure are derived. An analysis of the interactions between nonlinear modes is done. Stability of structures on is analyzed by graphs of characteristic equations for different geometric parameters of the model.

References

- [1] Ramanujam L. A Nonlinear Model for Wind-Induced Oscillations of Trees. (2012). <http://scholarworks.umass.edu/theses/943/>.
- [2] Yongmin K., Harianto R., Daryl L. T.-T. (2020) Stability analysis of laterally loaded trees based on tree-root-soil interaction. *Urban Forestry & Urban Greening*. 49:126639
- [3] Hedrih (Stevanović) K., Hedrih A. (2022) Mathematical modelling of nonlinear oscillations of a biodynamical system in the form of a complex cantilever. *App. Math. Modell.* VSI: DSTA 2021, 112:110-135.

Ghost smooth and non-smooth bifurcations in vibro-impact pairs

Daniil Yurchenko^{*}, Larissa Serdukova^{**}, Rachel Kuske^{***} and Christina Athanassouli^{***}

^{*}ISVR, University of Southampton, UK

^{**}Department of Mathematics, University of Leicester, UK

^{***}School of Mathematics, Georgia Institute of Technology, USA

Abstract. This paper presents the recent work of the authors on analysis of smooth and non-smooth bifurcations and their interplay in a canonical model of an impact pair, subjected to a harmonic excitation. The map approach is used to treat the system analytically and the results of this study are presented.

Introduction

This paper presents the recent work of the authors on analysis of smooth and non-smooth bifurcations and their interplay in a canonical model of an impact pair, subjected to a harmonic excitation. The pair consists of a capsule in which a ball moves freely between impacts on either end of the capsule. The performed analysis is generic, but is also very relevant to a recently proposed energy harvesting system using dielectric elastomeric membranes with compliant electrodes, which are deformed at impacts changing their capacitance. While the sequences of bifurcations have been studied extensively in single degree of freedom impacting models, there are limited results for two degree of freedom impacting systems such as the impact pair. Using an exact analytical solution between the impacts and the stability analysis, we obtain sequences of period doubling and fold bifurcations together with grazing bifurcations [1]. Using this analysis, we identify the bifurcations on unstable or unphysical solutions branches, which we term ghost bifurcations.

Results and Discussion

Figure 1, to be discussed in detail at the presentation, presents two different types of bifurcations leading to transition from 1:1 to 2:1 and 3:1 periodic motion, where d is non-dimensional length of the capsule, G – the grazing bifurcations, PD – period doubling bifurcations and PD_G is the period doubling bifurcation which is terminated by grazing. Figure 1 left presents the transition through grazing, whereas Figure 1 right present grazing transition to 2:1 periodic motion through PD_G , whereas transition to 3:1 is occurred through grazing. The presentation addresses the mystery of why sometimes we observe grazing and sometimes PD transitions, and how the ghost bifurcations, not observed numerically or experimentally, can influence the birth or death of complex behaviours. The complete investigation of the interplay between ghost and observable grazing and PD bifurcations has been recently reported in [2] and this presentation is mainly based on this work. The effects of other system's parameters on the different bifurcation patterns are demonstrated.

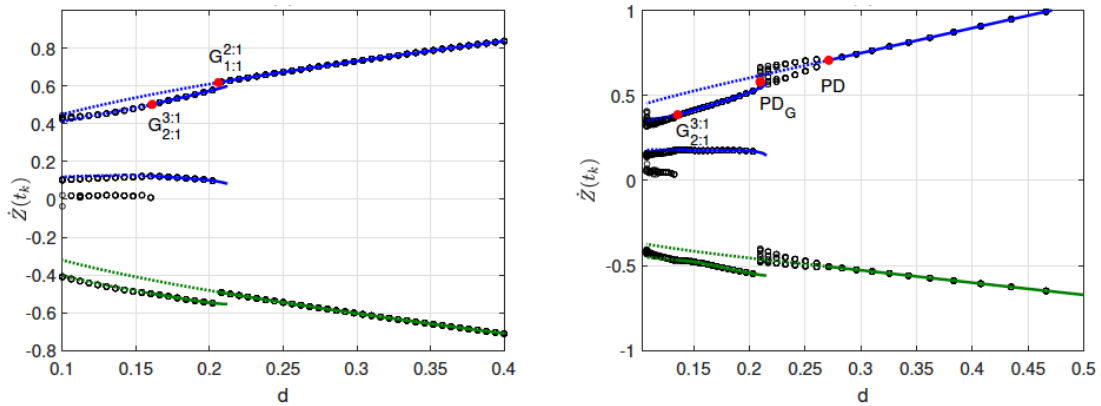


Figure 1: Bifurcation diagrams for the relative impact velocity. Black circles indicate results from attracting behavior obtained by numerical simulation of the full system (1)-(3). Solid (dotted) lines indicate stable (unstable or unphysical) analytical results for impact velocities \dot{Z}_k for 1:1 and 2:1 solutions. Blue (green) lines correspond to impacts on ∂B (∂T).

References

- [1] A. B. Nordmark. Non-periodic motion caused by grazing incidence in an impact oscillator. *Journal of Sound and Vibration*, 1991.
- [2] Larissa Serdukova, Rachel Kuske, Daniil Yurchenko. Fundamental competition of smooth and non-smooth bifurcations and their ghosts in vibro-impact pairs. *Nonlinear Dynamics*, 2023.

Semi-Implicit Integration and Data-Driven Model Order Reduction for Structures with Hysteresis

Bidhayak Goswami* and Anindya Chatterjee*
 *Department of Mechanical Engineering, IIT Kanpur, India

Abstract. Hysteresis models are popular for rate-independent structural damping. Hysteresis in material damping is distributed, nonlinear, and non-analytic. If incorporated in refined finite element (FE) models, numerical time integration is difficult. Generally, implicit integration methods show higher stability for stiff ODE systems arising in FE models. However, integrating the equations of hysteresis using implicit algorithms is difficult. Here we suggest a semi-implicit method where the structural part is treated implicitly and the hysteresis is treated explicitly. Results are very good: time steps can greatly exceed the smallest time period of the structure. Subsequently, we examine model order reduction. Structural modes can be projected directly as usual. Here we propose data driven model order reduction for the hysteretic damping part. The number of internal hysteretic states can be reduced by an order or magnitude with moderate accuracy.

Introduction

The Bouc-Wen model is a popular model for hysteresis. It needs a deformation-related variable that drives the hysteretic response. We formulate a finite element (FE) model of a beam with a lengthwise distributed hysteretic bending moment that is driven by the local curvature. The virtual work integral is estimated using hysteretic states (\mathbf{z}) that are monitored at Gauss points within each element. The governing equations are

$$\mathbf{M} \ddot{\mathbf{q}} + \mathbf{C} \dot{\mathbf{q}} + \mathbf{K} \mathbf{q} + \mathbf{A} \mathbf{z} = \mathbf{f}_0(t), \quad (1)$$

$$\dot{\mathbf{z}} = (\bar{\mathbf{A}} - \alpha \text{sign}(\dot{\chi} \circ \mathbf{z}) \circ |\mathbf{z}|^{n_h} - \beta |\mathbf{z}|^{n_h}) \circ \dot{\chi}, \quad (2)$$

where χ contains the beam curvatures at Gauss points, and the remaining symbols have their usual meanings from structural dynamics and Bouc-Wen hysteresis. The “ \circ ” operator denotes elementwise multiplication; also, the vector absolute value and exponentiation are elementwise as well.

In this paper we address numerical integration of the above FE model under high refinement (hundreds of elements). In our proposed semi-implicit scheme, the structural part is integrated implicitly adapting [1], and the hysteresis part is integrated explicitly while accounting for pointwise within-step rate reversals in the local curvature that drives the hysteretic response. For high n_h or low overall damping, numerical convergence is almost quadratic. For $0.5 < n_h < 1$ and somewhat larger damping, convergence is approximately linear. Next, we address modal projection in a refined FE model. Even after modal reduction, there remain very many hysteretic states to be integrated explicitly. Using initial simulation results we identify a subset of hysteretic states that can represent the overall hysteretic behavior. This leads to further model order reduction.

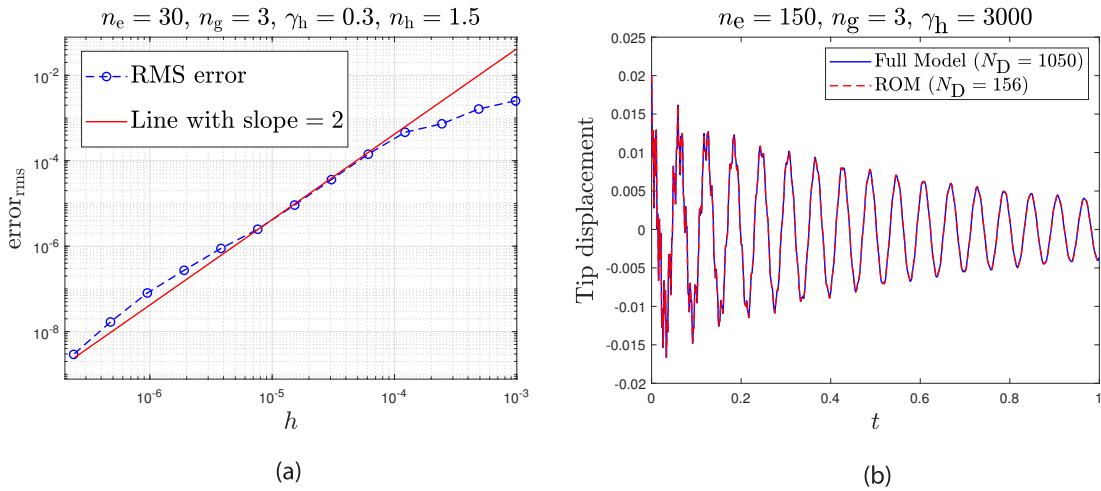


Figure 1: Accuracy of the algorithm and the reduced order model. γ_h is the damping strength, included within matrix \mathbf{A} of Eq. (1). In Fig. (1(a)), we see nearly quadratic convergence for $n_h = 1.5$ in an FE model with 30 elements and 3 hysteresis Gauss points in each element. Model order reduction results, starting from a 150 element model, can be seen in a tip displacement plot in Fig. (1(b)).

References

- [1] Piché, R., An L-stable Rosenbrock method for step-by-step time integration in structural dynamics. *Computer Methods in Applied Mechanics and Engineering*, 126(3-4): 343-354, (1995).
- [2] Bhattacharyya, S., and Cusumano, J. P., An energy closure criterion for model reduction of a kicked Euler–Bernoulli beam. *Journal of Vibration and Acoustics*, 143(4): 041001, (2021).

Vibration-induced friction force modulation

Enxhi Sulollari*, Karel van Dalen* and Alessandro Cabboi*

*Department of Engineering Structures, Faculty of Civil Engineering and Geosciences, TU Delft, the Netherlands

Abstract. Exploiting oscillatory forces is one of the most efficient ways to alter friction forces. Several studies on the influence of external vibrations on friction have been conducted investigating the effect of in- and out-of-plane oscillations. These studies consider loads of high-frequency, while a clear statement as to what is considered high-frequency is still missing. The common method of analysis for high-frequency is the method of direct separation of motion (MDMS). However, when studying the effect of a general sinusoidal excitation on friction using the MDMS, the analytical solutions become cumbersome or impossible to obtain. Therefore, this study aims to show that, for both linear and nonlinear systems, a general relation of the effect of excitation on friction, regardless of the frequency range, can be obtained by utilizing the frequency response curve.

Introduction

The fact that friction forces can be significantly reduced by applying vibrations has been known since at least the 1950s. For the first 2-3 decades, the evidence collected was mostly experimental. Friedman and Levesque [1], and later on Tolstoi [2] showed experimentally that friction is altered under the effect of vibration. However, all the results seemed to be strongly dependent on the characteristics of each test rig. Thus, no general law explaining the observed behaviour was identified. Since then, several experimental and theoretical studies have been conducted. Some of these theoretical studies include the research conducted by Thomsen [3] and Hoffmann [4], where the Method of Direct Separation of Motion was used. In all the existing works, however, the effect of the external load on friction has been studied with an emphasis on high-frequency harmonic loads, while a clear statement as to what is considered high-frequency is still missing.

Results and discussion

This study aims to show that a general relation, regardless of the frequency range, accounting for the induced effect of excitation on friction, can be easily obtained by utilizing the frequency response function of the linear dynamic system. Besides the study of linear systems, this work also presents the effect of excitation on friction for some nonlinear systems. To solve the case of a nonlinear system, the harmonic balance method will be used. The proposed method will be applied to a classical mass-spring-dashpot system on a moving belt. First, the Amontons-Coulomb friction law will be studied, considering the sliding regime only, for which the system becomes linear. For this system, the frequency response function, used then to obtain the effect of excitation on friction, can be easily found, Figure 1. For the nonlinear case, two problems will be studied. In the first one, a harmonically excited Duffing oscillator will be investigated, where the nonlinearity is present in the stiffness term. In the second problem, the Stribeck law will be considered, where the nonlinearity is present in the damping term. Stribeck law is characterized by a force-velocity curve with a negative slope at low velocities which corresponds to negative damping. Thus, self-excited oscillations might occur which further complicate the process of obtaining the frequency response function. Lastly, a link between the obtained results and the stick-slip analysis of a mass on the belt system will be presented.

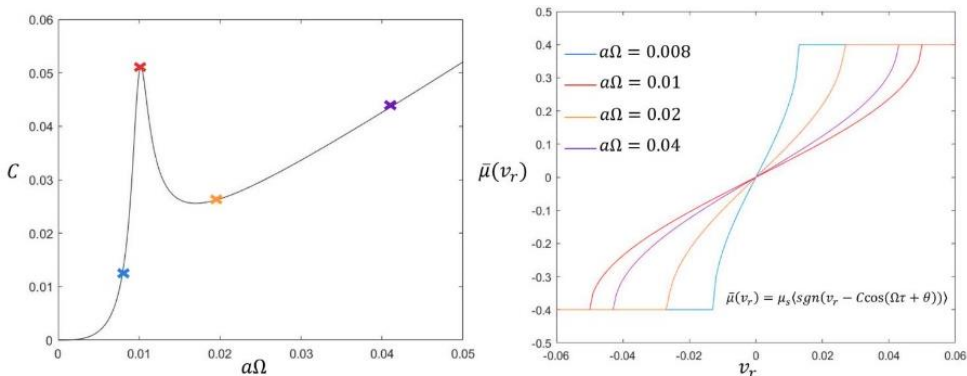


Figure 1: Frequency response function C vs excitation intensity $\alpha\Omega$ (left) and the corresponding effective friction $\bar{\mu}(v_r)$ vs relative velocity v_r (right) where α is the amplitude, Ω the frequency of excitation and θ a phase shift

References

- [1] Fridman H. D., Levesque P. (1959) Reduction of static friction by sonic vibrations. *J. Appl Phys* **30**(10):1572–1575.
- [2] Tolstoi D.M. (1976) Significance of the normal degree of freedom and natural normal vibrations in contact friction. *Wear* **10**(3):199–213.
- [3] Thomsen J. J. (1999) Using fast vibrations to quench friction-induced oscillations. *J. Sound Vib* **228**(5):1079–1102, 1999.
- [4] Hoffmann N., Wagner N., Gaul L. (2005) Quenching mode-coupling friction-induced instability using high-frequency dither. *J. Sound Vib* **279**(1):471–480.

Model reduction of a periodically forced slow-fast continuous piecewise linear system

A. Yassine Karoui and Remco I. Leine

*Institute for Nonlinear Mechanics, University of Stuttgart, Germany
ORCID 0000-0003-3350-5200 and ORCID 0000-0001-9859-7519*

Abstract. In this work, singular perturbation theory is exploited to obtain a reduced order model of a slow-fast piecewise linear 2-DOF oscillator subjected to harmonic excitation. The nonsmoothness of piecewise linear nature is studied in the case of bilinear damping as well as with bilinear stiffness characteristics. We propose a continuous matching of the locally invariant slow manifolds obtained in each subregion of the state space, which yields a 1-DOF reduced order model of the same nature as the full dynamics. The frequency response curves obtained from the full system and the reduced models show that the proposed reduction method can capture nonlinear behaviors such as super- and subharmonic resonances.

Introduction

Invariant manifolds play a major role in understanding the behavior of nonlinear dynamical systems. Among their properties, such manifolds can be used to obtain a reduced dynamics capturing the main features of the original system. The existing methods to find these manifolds often require smoothness properties of the system. A typical example is the theory of singular perturbations, where the reduction to a smooth slow manifold yields a reduced order model describing the slow dynamics of the original system. However, this theory cannot be applied on systems containing nonsmooth nonlinearities without suitable extension to take the nonsmoothness into account. A prominent class of nonsmooth systems consists in mechanical models with PWL nonlinearities, which may arise due to several effects such as damage or clearance [1]. In this work, the approach proposed in [2] for the use of singular perturbation theory on slow-fast PWL systems is extended from the autonomous configuration in \mathbb{R}^3 to nonautonomous two degrees of freedom slow-fast oscillators. Motivated by the quarter car model with bilinear damping characteristics [3], two examples of slow-fast PWL oscillators subjected to a harmonic excitation are used to illustrate the reduction in the case of bilinear damping and bilinear stiffness.

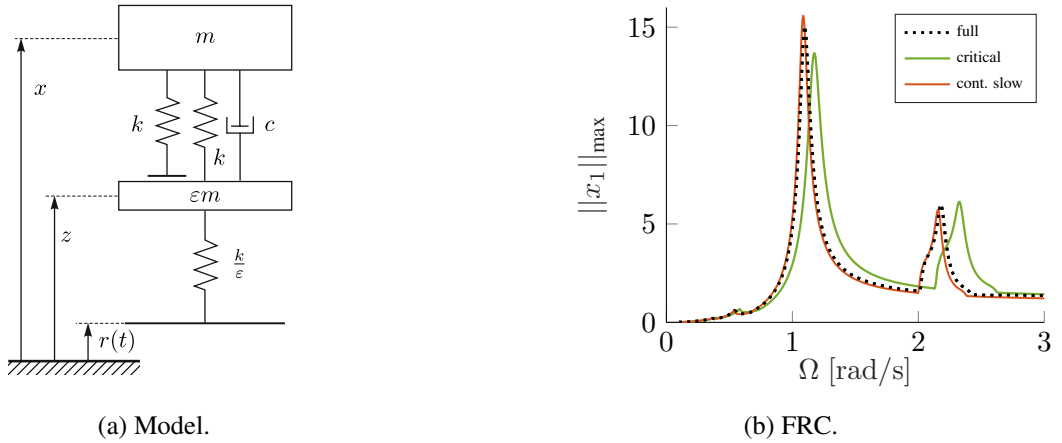


Figure 1: Model and frequency response curve of a 2-DOF slow-fast forced oscillator with PWL stiffness.

Results and discussion

In this contribution, a continuous matching of the locally invariant slow manifolds of a slow-fast forced system with piecewise linear nonlinearities is proposed. It was observed that the resulting reduced dynamics is able to approximate the behavior of the full system with high accuracy for a frequency range around the main harmonic. Due to the convergence property, the PWL system in the case of bilinear damping admits frequency-response curves (FRC) similar to a linear system, which were approximated with high fidelity by the proposed approach. For a similar PWL slow-fast oscillator with bilinear stiffness instead of damping, the system behavior becomes more complex due to the loss of the convergence property and the existence of nonlinear phenomena, such as super- and subharmonic resonances, becomes possible. These nonlinear resonances were accurately captured by the proposed reduction approach for the frequency range around the main resonance.

References

- [1] Butcher, E.: Clearance effects on bilinear normal mode frequencies. *Journal of Sound and Vibration* 224(2), 305–328 (1999)
- [2] Karoui, A.Y., Leine, R.I.: Analysis of a singularly perturbed continuous piecewise linear system. *Proceedings of the 10th European Nonlinear Dynamics Conference - ENOC (2022)*
- [3] Silveira, M., Wahi, P., Fernandes, J.: Effects of asymmetrical damping on a 2 DOF quarter-car model under harmonic excitation. *Communications in Nonlinear Science and Numerical Simulation* 43, 14–24 (2017)

Time-dependent stability margin for autonomous, piece-wise, and discontinuous system

Tomasz Burzyński*, Piotr Brzeski* and Przemysław Perlikowski*

*Division of Dynamics, Lodz University of Technology, Stefanowskiego 1/15, 90-924 Lodz, Poland

Abstract. In recent years, a variety of new metrics to analyze dynamical systems emerged. One of them is a metric called time-dependent stability margin, introduced for the first time in [1]. It is used for systems with coexisting stable attractors. The metric evaluates the stability of the system along the periodic orbit, indicating its reliability and resistance to perturbations. In this paper, the time-dependent stability margin is applied to investigate the real-world, discontinuous, and piece-wise mechanical system with impacts. Numerical results show that the periodic orbit vulnerability to perturbations is increased in close vicinity to the particular impact events. It may induce implications because after time impacts wear the system causing plastic deformation or backlash in the mechanisms. Consequently, it may lead to perturbation sufficient enough to change the attractor.

Introduction

Multi-stable systems are commonly known in mechanical engineering, mathematical biology, fluid dynamics, control engineering, and others. Over the years, a variety of techniques to analyze such systems were developed. Among others, we can distinguish basin stability metrics, basin entropy, survivability, and time-dependent stability margin.

The time-dependent stability margin [1] is a method designed to examine the stability of the system along the periodic orbit. In multi-stable mechanical systems due to coexisting attractors, we can experience a sudden change in dynamical response. The phenomena may be severe for the system as it can trigger undesired behavior. It can also be used to facilitate control over the system. The cost of control can be minimized by applying the impulse at the appropriate time when the stability margin of the current attractor is the smallest. Therefore, such analysis can provide significant advantages when a mechanical system and its control are designed.

In order to test the usefulness of the metric in real-world applications, we perform a time-dependent stability analysis of the novel-yoke-bell clapper system (Figure 1a) with variable geometry. The system is piece-wise due to the nature of excitation and discontinuous due to impacts between the bell and the clapper. The mathematical model of the system was experimentally validated in [2].

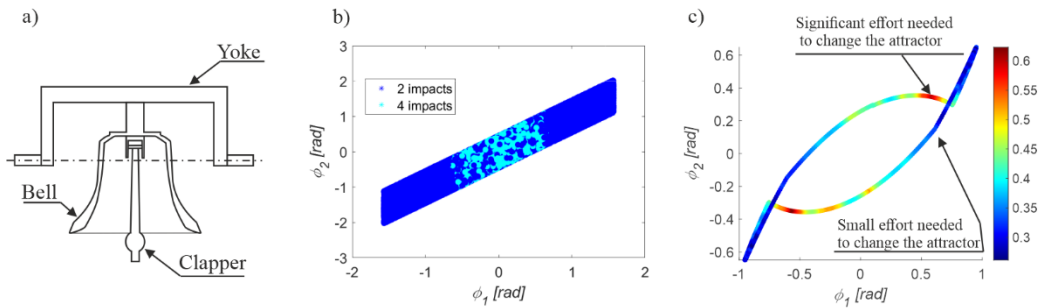


Figure 1: a) Schematic view of the considered system b) Basin of attraction c) Evolution of the stability margin along the attractor with four impacts per period of motion.

Results and discussion

Detailed information considering how the metric is calculated is described in [1]. Figure 1b shows two coexisting attractors (two and four impacts per one period of motion) in phase space, where ϕ_1 is the angular displacement of the bell and ϕ_2 is the angular displacement of the clapper. The stability margin along the attractor with four impacts per period of motion is presented in figure 1c. The metric indicates parts of the orbit that are the most prone to perturbations. In this case, it is in close vicinity to the first and third impact event. On the other hand, the safety margin is the biggest before the second and fourth impact.

After time, impacts wear the structure causing plastic deformation or backlash in the mechanism. As a consequence, the trajectory of the bell or the clapper may be changed and a disturbance may be introduced to the system possibly leading to a sudden change of attractor. This study shows the practical application of the novel tool for the analysis of multi-stable systems. It allows for further investigations considering the control of the system (by means of the desired transition between attractors) or optimization for robustness and safety.

References

- [1] Brzeski, P. et. al. (2018) Time dependent stability margin in multistable systems. *Chaos: An Interdisciplinary Journal of Nonlinear Science*. *Chaos* **28**: 093104.
- [2] Burzyński, T. et. al. (2022) Dynamics loading by swinging bells – Experimental and numerical investigation of the novel yoke-bell-clapper system with variable geometry. *Mechanical Systems and Signal Processing* **180**:109429.

Relativistic chaotic scattering

Jesús M Seoane*, Diego S Fernández*, Juan D Bernal*, Álvaro G López*, and Miguel AF Sanjuán*

*Nonlinear Dynamics, Chaos and Complex Systems Group. Departamento de Física. Universidad Rey Juan Carlos. Tulipán s/n, 28933 Móstoles, Madrid, Spain

Abstract. We analyze global properties of chaotic scattering such as the escape time distribution and the decay law of the Hénon-Heiles system in the context of special relativity. Our results show a scaling law between the exponent of the decay law and the β factor is uncovered where a quadratic fitting between them is found. Besides, we study on how time dilation occurs within the scattering region by measuring the time with a clock attached to the particle observing that the several events of time dilation that the particle undergoes exhibit sensitivity to the initial conditions. Finally, we apply these results in the scattering in three-body problem in relativistic regime.

Introduction

Chaotic scattering is a very relevant topic in nonlinear dynamics. Its applications are rooted in numerous fields of physics. There has been little research regarding the influence of the relativistic corrections in chaotic scattering problems. In particular, the global properties of the scattering system as, for example, the escape time distribution and the decay law of the particles, have not been much investigated as in the Newtonian case. Here, it is also studied some relevant characteristics of the exit basin topology of the relativistic Hénon-Heiles system: the uncertainty dimension, the Wada property, and the basin entropy. We also extend the previous results to systems where the gravitational interactions are not negligible once the relevance of the special relativity corrections in the context of chaotic scattering has been highlighted. For this purpose, a simple model which is related to the three-body problem, called the Sitnikov problem is used.

Results and discussion

Firstly, the results show that the average escape time decreases with increasing values of the relativistic factor β . The survival probability of the particles in the scattering region is also studied, uncovering an explicit scaling law between the exponent of the decay law and the β factor [1, 2]. On the other hand, we have used the post-Newtonian approximation for the relativistic Sitnikov problem. The influence of the gravitational radius λ of the primaries in the context of the chaotic scattering phenomena has been considered. Now, the metamorphosis of the KAM islands for which the escape regions change insofar λ increases is shown. Later, the unpredictability of the final state of the system when the gravitational radius changes is highlighted [3].

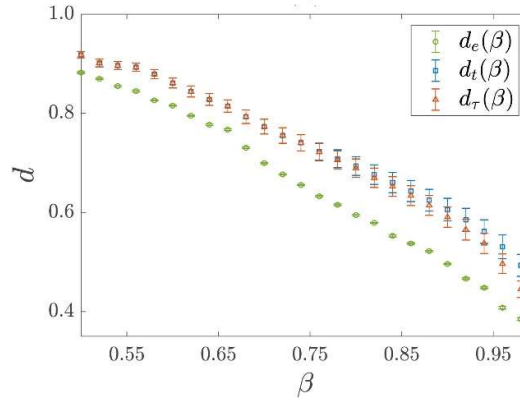


Figure 1: Fractal dimensions of the escape time functions for the cases of inertial (blue) and comoving (red) with the particle frames showing they are relativistic invariants. Green points denote the values of the fractal dimension according to exits.

Finally, in the study of the time dilation by measuring the time with a clock attached to the particle, we observe that the several events of time dilation that the particle undergoes exhibit sensitivity to the initial conditions. However, the structure of the singularities appearing in the escape time function remains invariant under coordinate transformations [4] as shown in Fig. 1 where the values of the fractal dimensions are depicted.

References

- [1] J. D. Bernal, J. M. Seoane, and M. A. F. Sanjuán. *Phys. Rev. E* **95**, 032205 (2017).
- [2] J. D. Bernal, J. M. Seoane, and M. A. F. Sanjuán. *Phys. Rev. E* **97** 042214 (2018).
- [3] J. D. Bernal, J. M. Seoane, J. C. Vallejo, L. Huang, and M. A. F. Sanjuán. *Phys. Rev. E* **102** 042204 (2020).
- [4] D. S. Fernández, A. G. López, J. M. Seoane, and M. A. F. Sanjuán. *Phys. Rev. E* **101**, 062212 (2020).

Multidimensional nonlinearity Time Series Forecasting Based on Multi-reservoir Echo State Network

Jingyu Sun^{1,2}, Lixinag Li^{* 1,2}, Haipeng Peng^{1,2} and Shengyu Liu¹

¹Information Security Center, State Key Laboratory of Networking and Switching Technology, Beijing University of Posts and Telecommunications, Beijing 100876, China #

²National Engineering Laboratory for Disaster Backup and Recovery, Beijing University of Posts and Telecommunications, Beijing 100876, China #

Abstract. Echo State Network(ESN) has a simple structure and can achieve excellent forecasting effect. In this paper, we will delve into the nonlinear prediction ability of echo state network, analyze the structure and principle of it, then propose a new multi-reservoir echo state network prediction model based on the output mode. Finally, the model is tested with different dimensions by Mackey-Glass and Lorenz chaotic systems. After verification, it is found that the proposed multi-reservoir echo state network can accurately predict longer.

Introduction

ESN has feedback connections between neurons and has rich dynamic properties, so it can store partial information and has the property of instant memory. It consists of three parts: input, hidden layer and output, and the most important and only trainable part of ESN is the output weight[2]. Among it, randomly and sparsely connected neurons make up the hidden layer of the ESN[1]. Thus, the input is represented by a high-dimensional, non-linear representation. The ESN improves the inherent shortcomings of the recurrent neural network, and has wide application in time series prediction, pattern recognition, image processing, signal processing and so on.

In recent years, ESN has been applied to various fields, among which series prediction is more widely used. Zhou et al. proposed an adaptive flow prediction method reservoir based on ESN[4]. Sun et al. used the ESN model to predict stock price[5]. Hu et al. proposed a modified optimization model of bagged ESN based on differential evolution algorithm to estimate energy consumption[6].

From above descriptions, it can be seen that the echo state network is used in sequence prediction in various fields. But researchers mostly focus on optimizing the single-layer echo state network, and use different optimization algorithms to achieve better prediction results. Generally speaking, the larger the number of nodes in the neural network, the more complex the system can be expressed. However, If the number of neurons in the only reservoir is increased, the network will be over-fitted. Therefore we found adding multiple reservoirs to the echo state network can increase network complexity while preventing overfitting. Inspired by this, we propose a Multi-reservoir echo state network(MESN) based on the fully connected output mode. Subsequently, the model is used to nonlinearity predict chaotic systems of different dimensions, through simulation and comparative experiments, to explore more significance of MESN.

Results and discussion

In this article, we constructed a new multi-reservoir echo state network to forecast multidimensional nonlinear time series. Besides, in order to avoid the disappearance of input, we add input to each reservoir by merging matrices. Then we use the complicated one-dimensional MackeyGlass.t17 and three-dimensional Lorenz chaotic system to conduct experiments respectively. The comprehensive results show that increasing the reservoir can increase the prediction effect to a certain extent, but it is not infinite.

Besides, no matter how much the number of layers and the reservoir are increased, the network runs very fast. Therefore, the ESN with multiple reservoir still has great advantages in structure and time. In addition to nonlinear time series prediction, ESN is also used in artificial intelligence, brain like computing and so on, it needs more and further research.

References

- [1] A. Duggento, M. Guerrisi, N. Toschi, (2021) Echo state network models for nonlinear granger causality, *Philosophical Transactions of the Royal Society A* 379 (2212): 20200256.
- [2] S. F. Stefenon, L. O. Seman, N. F. S. Neto, L. H. Meyer, A. Nied, K.-C. Yow, (2022) Echo state network applied for classification of medium voltage insulators, *International Journal of Electrical Power & Energy Systems* 134: 107336.
- [3] N. A. Silva, T. D. Ferreira, and A. Guerreiro, (2021) Reservoir computing with solitons, *New Journal of Physics*, 23 (2): 023013.
- [4] J. Zhou, H. Wang, F. Xiao, X. Yan, L. Sun, (2021) Network traffic prediction method based on echo state network with adaptive reservoir, *Software: Practice and Experience* 51 (11): 2238–2251.
- [5] G. Sun, J. Lin, C. Yang, X. Yin, Z. Li, P. Guo, J. Sun, X. Fan, B. Pan, (2021) Stock price forecasting: an echo state network approach, *Computer Systems Science and Engineering* 36 (3): 509–520.
- [6] H. Hu, L. Wang, L. Peng, Y.-R. Zeng, (2020) Effective energy consumption forecasting using enhanced bagged echo state network, *Energy* 193:116778.

Quasi-periodicity of temporarily constrained variable-length elastic pendulum

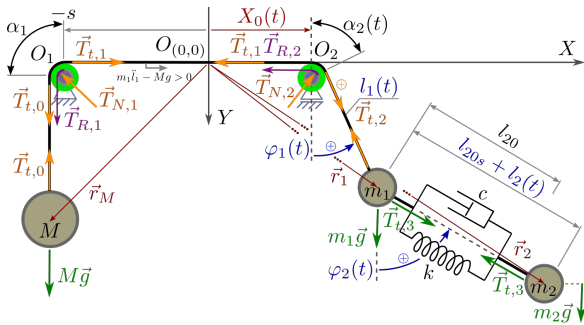
Paweł Olejnik*, Godiya Yakubu* and Jan Awrejcewicz *

*Department of Automation, Biomechanics and Mechatronics,
Faculty of Mechanical Engineering, Lodz University of Technology,
1/15 Stefanowski Str., 90-924 Lodz, Poland, ORCID 0000-0002-3310-0951

Abstract. In order to verify the very complex dynamics of temporarily constrained mechanical vibrations, a model of an elastic double pendulum of variable length with friction and a counterweight mass is introduced. The system has no physical restrictions in the form of stationary motion stops or even springs or dampers at the boundaries, constituting a dynamically unstable 4-DoF system with kinematic excitation. A series of numerical experiments based on the observation of time trajectories, bifurcation diagrams, Lyapunov exponents and the Kaplan-Yorke dimension have been computed. The bifurcation diagrams and parametric plots of the first Lyapunov exponent show that for some region of projection of Poincaré maps on a selected dimension, the system oscillates chaotically and mainly quasi-periodically in a very wide range of the control parameter of the bifurcation diagram.

Introduction

Mathematical model of the dynamical system shown in Fig. 1 is derived and simulated, where all forces and dimensions are indicated with respect to the origin O . It has two mechanisms of energy absorption: in the sliding friction with a temporary constraints at stick phases of the pulleys (green rings) and in the damper c .



Chaos Measure Dynamics and a Multifactor Model for Financial Markets

Markus Vogl*

**Executive Management, Markus Vogl {Business & Data Science}, Wiesbaden, Hesse, Germany*

Abstract. This paper applies rolling windows to generate time-varying data series of selected chaos measures (i.e. Hurst exponent, maximum Lyapunov exponent, Lyapunov sum and sample entropy). The series are analysed to elaborate on time-varying underlying data generating process (DGP) characteristics and dynamic chaos (in)stability of the original data. Furthermore, the denoted chaos measure series are combined into a multifactor model to propose an explicative rationale for the original data set's inherent factor composition. The rolling windows are applied to cascadic (level 12) Haar-wavelet filtered daily S&P500 logarithmic returns (2000-2020), which have been shown to consist of a mixture between (hyper)chaotic deterministic and stochastic chaos. The chaos measure series are analysed by a nonlinear analysis framework, which allows the extraction of the underlying characteristics of the empirical DGP of nonlinear time-series.

Introduction

This paper represents the finale of a larger research study, encompassing five publications. Initially, a mathematical literature review with citation network analysis about financial and risk modelling has been conducted (see [1]). It analyses over 800 mathematical models, states the non-existence of a “single-best” approach and proposes nonlinear models to perform better. Thereinafter, another literature review (~160k papers) about nonlinear dynamics and financial chaos has been deduced to elaborate on the reasons for nonlinear models to outperform (see [2]). During the course of the analysis, a 40-year-old debate in nonlinear dynamics and financial chaos has been rendered visible, namely, whether the empirical underlying DGP of a given time-series follows stochastic or chaotic dynamics and how these dynamics are safely quantifiable and distinguishable. Following these insights, a novel framework built upon the given literature has been created, allowing the save quantification of the empirical DGP of any nonlinear time-series (see [3,4]), simultaneously showing the denoised daily S&P500 logarithmic return series (2000-2020) to be a mixture of (hyper)chaotic versus stochastic dynamics, which drastically diminishes forecasting potentials (see [3]). Building on these insights, the bridge between these hyperchaotic dynamics, multifractals, momentum trading, efficient markets and scaling laws has been elucidated via rolling windows and time-varying Hurst exponents (see [4]). To provide more background, a dissipative chaotic system will deflate onto its own (strange) attractor, which, if intersected with Poincaré sections, results in fractal sets. Those fractal sets are described via scaling laws. Following Berghorn [5] states that financial data follows (multi)fractal scaling laws, namely, trend inducing mechanics, which in fact cause the momentum effect. Subsequently, due to the application of rolling windows to determine time-varying Hurst exponents, the total invalidity of the efficient market hypothesis and an explication for momentum crashes, namely, the vanishing of said (multi)fractal trends during crises periods, is shown [4]. Now, if the (rolling window) Hurst exponents interpreted as a fractal trending measure are valuable and are able to show structural instabilities of a chaotic system, other chaos measures, may potentially be also yielding explicative powers. Thus, the time-varying series via rolling windows of other chaos measures such as Lyapunov exponents are derived and analysed within this study.

Results and Discussion

The time-varying chaos measures under analysis each reveal complex underlying (non-chaotic) dynamics of their own, differing from the underlying original data. Following the nonlinear framework, each series can be quantified and the empirical DGPs properly specified. Moreover, dynamical breaks or shifts (i.e. chaos instabilities) between conservative and dissipative system characteristics during (financial) crises periods can be stated. A combination of these chaos measure series in a multifactor model yields notable explicable power in terms of the composition of the S&P500 return series stating a novel way of elucidating the underlying functioning of financial markets data and potential crisis predictability.

References

- [1] Vogl, M. (2021) Frontiers of Quantitative Financial Modelling: A Literature Review on the Evolution in Financial and Risk Modelling after the Financial Crisis (2008-2019) *Under Review. SSRN*, website https://papers.ssrn.com/sol3/papers.cfm?abstract_id=3764570.
- [2] Vogl, M. (2022) Controversy in financial chaos research and nonlinear dynamics: A short literature review. *Chaos Solit. Fractals* **162**:112444.
- [3] Vogl, M., Rötzel, P.G. (2022) Chaoticity versus stochasticity in financial markets: Are daily S&P 500 return dynamics chaotic? *Commun. Nonlinear Sci. Numer. Simul.* **108**:106218.
- [4] Vogl, M. (2022) Hurst Exponent Dynamics of S&P 500 Returns: Implications for Market Efficiency, Long Memory, Multifractality and Financial Crises Predictability by Application of a Nonlinear Dynamics Analysis Framework. *Under Review. SSRN*, website https://papers.ssrn.com/sol3/papers.cfm?abstract_id=3838850.
- [5] Berghorn, W. (2015) Trend momentum. *Quant. Finance* **15**(2):261-284.

Nonlinear and chaotic dynamics of a vibratory conveying system

Simon Schiller* and Wolfgang Steiner**

*Linz, Center of Mechatronics, Altenbergerstraße 69, 4040 Linz, Austria

**University of Applied Sciences Upper Austria, Stelzhamerstraße 23, 4600 Wels, Austria

Abstract. In this work a 2D model of a vibratory conveying system is presented. This simulation model allows to understand previously unexplained phenomena as multiple feeding velocities at the same operation point which were observed in practical measurements. The parameters which have an influence on this effect are studied and a method is developed how to predict and adjust the occurrence of multiple solutions. It is shown that this effect makes the calibration of the conveyor difficult in practice. Furthermore, it is proven that the system may show chaotic behavior in some configurations. These chaotic states in the simulation model are also shown with parameter studies and different methods are applied to predict the point at which the system becomes chaotic. Therefore, this work provides a deeper understanding of complex conveying processes using a simple simulation model.

Introduction

In modern conveying processes, the efficiency of conveyor systems is becoming increasingly important. This is caused by advancing customer requirements and enormous competitive pressure. Therefore, one has to understand the feeding process more and more deeply which is why a simplified simulation model is created. A main component of a simulation model of a feeding process is the contact model which is developed in [1]. For a detailed resolution of the contact process it is modeled as continuous process in contrast to the bouncing ball problem in [2]. Next, this vertical contact model is extended to horizontal direction which enables a representation of a feeding process. From the analysis in [2] it is known that the bouncing ball may show chaotic behavior. Therefore, this chaotic behavior [3] in vertical direction is coupled with the horizontal direction wherefore the 2D simulation model may show such chaotic behavior, too.

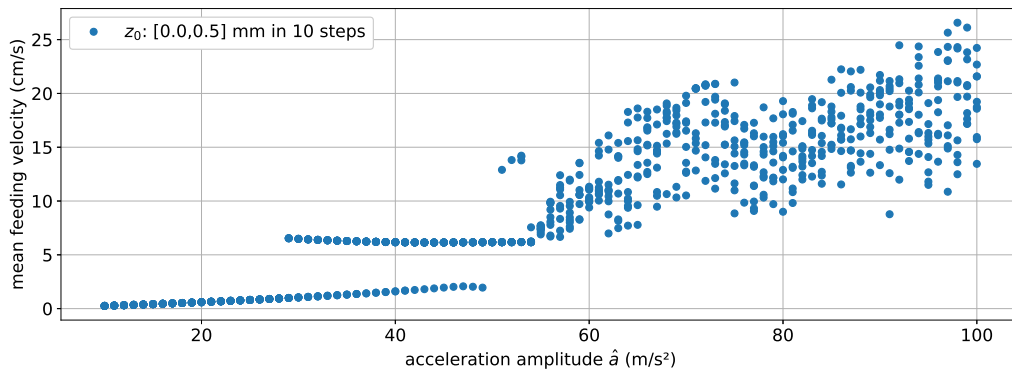


Figure 1: Multiple solutions of feeding velocity by varying initial conditions at certain operation points

Results and discussion

In Fig. 1 the results of the simulation of the conveying process are illustrated. The interesting variable is the mean feeding velocity in x-direction in a steady state motion. For different acceleration amplitudes of the conveyor, the initial position z_0 of the point mass is slightly varied. The results in Fig. 1 can be divided in 3 domains. In the first domain ($\hat{a} < 29 \text{ m/s}^2$), the mean feeding velocity is independent from the initial position z_0 . In the second domain between $\hat{a} = 29 \text{ m/s}^2$ and $\hat{a} = 50 \text{ m/s}^2$, two stationary motions depending on z_0 appear. Therefore, a critical initial position z_0 exists which is responsible for the respective stationary motion. In the third domain ($\hat{a} > 50 \text{ m/s}^2$), we observe a fully chaotic behavior with sensitive dependence on z_0 .

The chaotic behavior in the third domain is proven by computing Ljapunov exponent for continuous dynamical systems. A further method to visualize the chaotic behavior is to assess the curves in the phase space $\dot{x}(t)$ over $x(t)$. This shows non-closed contours if the system is in a chaotic state. Furthermore, the trajectories in the phase space are assessed with fractal dimensions which can be used as indicators for chaotic behavior, too. However, knowledge of the domains with multiple solutions and chaotic states can be used to adjust the conveyor. The verification of the statements may also be carried out in practice, which is part of future work.

References

- [1] M. Schoergenhummer, S. Schiller, D. Perchtold, and D. Six. A modeling and simulation approach for the design of linear feeding systems in industrial automation. *ACM International Conference Proceeding Series*, 2019.
- [2] J. Guckenheimer, P. Holmes, and M. Slemrod. *Nonlinear Oscillations, Dynamical Systems, and Bifurcations of Vector Fields*. Springer, New York, 1983.
- [3] R.W. Leven, B.P. Koch, and B. Pompe. *Chaos in dissipativen Systemen*. Springer, Vieweg+Teubner Verlag Wiesbaden, 1989.

The predictable chaos of rare events in complex systems

Tommaso Alberti*, Davide Faranda**, Valerio Lucarini***

*Istituto Nazionale di Geofisica e Vulcanologia, Rome, Italy, ORCID 0000-0001-6096-0220

**Laboratoire des Sciences du Climat et de l'Environnement, Gif-Sur-Yvette, France, ORCID 0000-0001-5001-5698

***University of Reading, Reading, United Kingdom, ORCID 0000-0001-9392-1471

Abstract. Many natural systems show emergent phenomena at different scales, leading to scaling regimes with signatures of chaos at large scales and an apparently random behavior at small scales. These features are usually investigated quantitatively by studying the properties of the underlying attractor. This multi-scale nature of natural systems makes it practically impossible to get a clear picture of the attracting set as it spans over a wide range of spatial scales and may even change in time due to non-stationary forcing. Here we present a review of some recent advancements in characterizing the number of degrees of freedom and the predictability horizon of complex systems showing non-hyperbolic chaos, randomness, state-dependent persistence and predictability. We compare classical approaches, based on Lyapunov exponents and correlation dimension, with novel frameworks based on combining adaptive decomposition methods with concepts from extreme value theory.

Introduction

Complex systems are made of different nonlinearly interacting intrinsic and extrinsic components resulting in various positive and negative feedbacks that can lead to the emergence of unpredictable temporal dynamics, or the ability of systems to spontaneously form temporal, spatial, or spatiotemporal patterns. Since 1960s complex systems have been studied in the framework of dissipative dynamical systems with the development of measures to quantify the topology of the state-space trajectories [1] and in revising some earlier concepts on their forecast horizon [2]. A one-parametric family of measures, the so-called generalized fractal dimensions, has been proposed based on a coarse-grained invariant measure linking the geometric properties of the state-space trajectories to the statistics of the dynamical scaling properties [3]. However, for systems exhibiting heterogeneous state-space structure or even non-stationarity, it would be useful to track the instantaneous number of degrees of freedoms, which are closely related to the predictability of the system and its associated recurrence characteristics [4]. The purpose of this study is to thoroughly extend an existing formalism of multi-scale measures [5] to characterize the instantaneous scale-dependent properties of complex systems by combining time series decomposition methods with concepts from extreme value theory that are related to the instantaneous number of degrees of freedom of the observed dynamics [6].

Results and discussion

Our results show that the newly introduced formalism, based on instantaneous scale-dependent dimensions, allows us to discern two properties that are inaccessible by previous global or scale-dependent analysis, namely the existence of different scale-dependent source processes (as the presence of noise or a dominant scale) and the structural stability of fixed points. Our study indicates that when considering different scales, the concept of a single universal attractor should be revised. Indeed, we have shown that a new structure of attractors, whose properties evolve in time, space and scale, is discovered by looking for fixed points and following their evolution from small to large scale and vice versa. Thus, the geometric structure of the attractor is gradually deformed and depends on the scale at which we are investigating the respective system. The main novelty introduced in this study is a powerful method to identify the existence of processes of different origin by looking at the spatial distribution of fractal dimensions across the full phase-space trajectories at different timescales. Our formalism also demonstrated the failure of the concept of universality of turbulent attractors since their properties depend on the scale we are focusing on. Given the changing nature of such attractors in time and scales we introduced the novel concept of *chameleon attractors* [7].

References

1. Grassberger P., Procaccia I. (1983) Characterization of strange attractors. *Phys. Rev. Lett.* **50**:346-349.
2. Kolmogorov A.N. (1959) Entropy per unit time as a metric invariant of automorphism. *Dok. Russ. Acad. Sci.* **124**:754-755.
3. Hentschel H.G.E., Procaccia I. (1983) The infinite number of generalized dimensions of fractals and strange attractors. *Physica D Nonlinear Phenomena* **8**:435-444.
4. Faranda D., Lucarini V., Turchetti G., Vaienti S. (2012) Generalized Extreme Value Distribution Parameters as Dynamical Indicators of Stability. *Int. J. Bif. Chaos* **22**:1250276.
5. Alberti T., Consolini G., Ditlevsen P.D., Donner R.V., Quattrocioni V. (2020) Multiscale measures of phase-space trajectories. *Chaos* **30**:123116.
6. Alberti T., Faranda D., Lucarini V., Donner R.V., Dubrulle B., Daviaud F. (2023) Scale dependence of fractal dimension in deterministic and stochastic Lorenz-63 systems. *Chaos* **33**:023144.
7. Alberti T., Daviaud F., Donner R.V., Dubrulle B., Faranda D., Lucarini V. (2023) Chameleon attractors in turbulent flows. *Chaos, Solitons & Fractals* **168**:113195.

Time-Periodic perturbation leading to chaos in a planar memristor oscillator having a Bogdanov-Takens bifurcation

Marcelo Messias

Departamento de Matemática e Computação, Universidade Estadual Paulista - UNESP, Pres. Prudente, SP, Brasil

Abstract. We consider a memristive circuit consisting of a locally-active current-controlled memristor, a compensation inductor and a bias resistor, which is modeled by a three-parameter two-dimensional system of ordinary differential equations. The system presents periodic oscillations, which arise at a Hopf bifurcation. We show that these oscillations evolve into a homoclinic orbit, in a Bogdanov-Takens bifurcation type scenario. By adding a small time-periodic excitation to the circuit, we obtain complex dynamical behavior, such as quasi-periodic and chaotic oscillations.

Introduction

The *memristor*, a nonlinear resistor with memory, is considered the fourth fundamental circuit element, besides resistor, capacitor and inductor. It was theoretically proposed in 1971 by Leon Chua [1] and its physical realization was possible only in 2007 [2]. Since then, the memristor attracts much interest from the academia and industry, due to its potential applications in several technological areas, like the construction of nonvolatile memories, logic operation circuits, artificial neural networks and chaotic oscillations [3]. Complex behavior arising in memristive systems can be generated by the locally-active characteristics of memristors [4]. At present, there are some researches on locally-active memristors and its interaction with other fundamental circuit elements [4, 5], but there is a lack of research on the mechanism creation of periodic and chaotic oscillations caused by them. We propose a new mechanism to obtain such a complex behaviors in memristive systems.

Results and discussion

We consider the periodic oscillator memristive circuit proposed in [5], consisting of three elements: a locally-active current-controlled memristor, a compensation inductor and a bias resistor. The circuit is modeled by the following system of ordinary differential equations

$$\dot{x} = 250[2x - x^2 - 2x^3 + x^4 + (5.4 - 2.8x)y], \quad \dot{y} = \frac{1}{L}[(S - y)R + 1.5(x - 0.5)y]. \quad (1)$$

where L , S and R are control parameters, x and y are state variables, which are proportional to the internal state of memristor and to the current in the circuit, respectively. The dynamics of system (1) was studied in [5], where the authors shown the occurrence of periodic oscillations, arising at a Hopf bifurcation, when the parameter L is varied. Then, they added a capacitor to the circuit, generating another state equation in system (1), in order to obtain a chaotic three-dimensional system [5]. In this work, we show that the periodic oscillations of system (1) tend to a homoclinic orbit, showing a Bogdanov-Takens bifurcation type scenario (see Fig. 1).

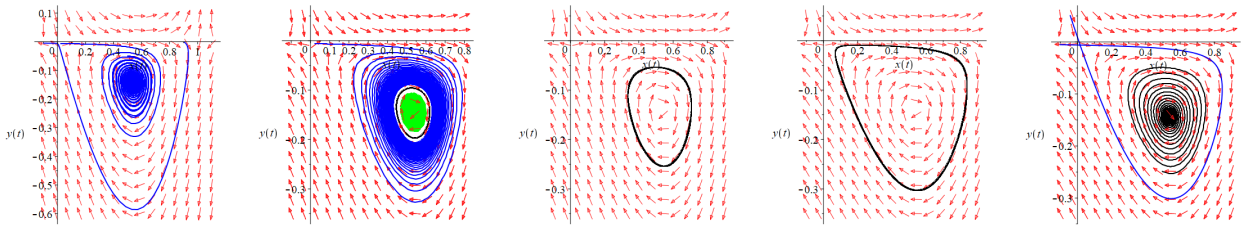


Figure 1: Bogdanov-Takens bifurcation scenario of the solutions of system (1) obtained varying the parameter L .

In order to obtain complex behavior, such as quasi-periodic, canards and chaotic oscillations, we add into system (1) a small external time-periodic excitation of the form $f(A, \omega, t) = A \cos(\omega t)$, obtaining a non-autonomous time-periodic system. With this procedure, we show that chaotic dynamics can be obtained in a memristive circuit with a locally-active memristor through the input of a periodic stimulus, instead of adding a new element to the circuit, which grows the dimension of the related differential system, as is often made in literature [5]. As far as we know, and also after a Google search, it is the first time that Bogdanov-Takens bifurcation and its time-periodic perturbation are considered in the study of memristive circuits and systems as a mechanism to generate complex dynamical behavior.

References

- [1] Chua L.O. (1971) Memristor: the missing circuit element. *IEEE Trans. Circuit Theory* **18**(5):507-519.
- [2] Strukov D.B, Snider G.S., Stewart D.R. and Williams R.S. (2008) The missing memristor found. *Nature* **453**:80-83.
- [3] Tetzlaff R. *Editor* (2014) Memristors and Memristive Systems. Springer New York.
- [4] Ascoli A., Slesazek S., Mähne H., Tetzlaff R. and Mikolajick T. (2014) Nonlinear dynamics of a locally-active memristor. *IEEE Trans. Circuits Syst. I* **62**:1165-1174.
- [5] Gu M., Wang G., Liu J., Liang Y., Dong Y. and Ying J. (2021) Dynamics of a bistable current-controlled locally-active memristor. *Int. J. Bifurcation and Chaos* **31**, 2130018 (20 pages).

Investigation of chaos in the mechanistic turbulence model

Róbert Rochlitz* and Bendegúz D. Bak*

*Department of Fluid Mechanics, Faculty of Mechanical Engineering, Budapest University of Technology and Economics, Budapest, Hungary

Abstract. In this work, the chaotic behaviour of the mechanistic turbulence model is examined for free vibrations and harmonic excitations. The multi-degree-of-freedom oscillator is investigated with different numbers of nonlinear springs, and the Lyapunov exponents of the system are calculated in order to determine whether it is chaotic.

Introduction

The mechanistic model of turbulence consists of a binary tree of spring connected masses, with dampers between its last two levels, as shown in Figure 1. The model with only linear springs was found to be capable of producing similar energy spectra to the Kolmogorov spectrum found in 3D homogeneous turbulence [1].

Using nonlinear springs at the bottom level provides a mechanism for targeted energy transfer [2], which efficiently dissipates the energy of the system [3]. A version of the model with nonlinear energy sinks at the last level exhibited a strong dependence on the initial conditions of the system [4]. However, this sensitive behaviour was not yet quantified with Lyapunov exponents, thus the chaoticness of the system was not determined.

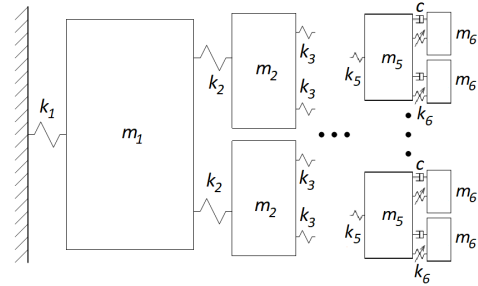


Figure 1: Mechanistic turbulence model with 6 levels

Results and discussion

The system is considered with different number of levels containing nonlinear springs, both with free vibrations and $A \cos(\omega t)$ harmonic forcing of the largest mass. Figure 2 shows the average energy fraction of the system for different ω values. It is expected that chaotic behaviour can be found in the regions where the energy of the last ($j = 6$) level is significant [5]. The Lyapunov exponents are numerically calculated using the method described by Argyris et al. [6], the sign of the largest exponent determines if the motion is chaotic. Preliminary results indicate that with harmonic excitation in the chaotic band, and one or two nonlinear levels, the largest Lyapunov exponent is $\lambda_1 \approx 0$, which means that the system is close to chaotic behaviour.

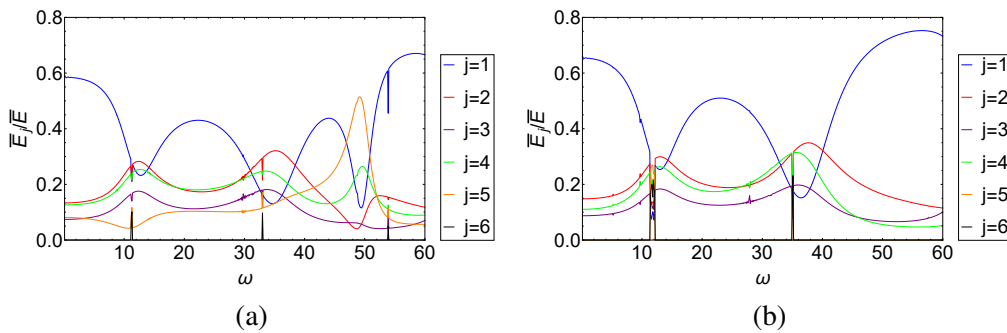


Figure 2: Average energy fraction of the system as a function of ω for (a) 1 nonlinear level, $A = 1$ and for (b) 2 nonlinear levels, $A = 15$

Acknowledgements

This work has been supported by the Hungarian National Research, Development and Innovation Fund under contract NKFI K 137726.

References

- [1] Kalmár-Nagy, T., Bak, B. D. (2019) An intriguing analogy of Kolmogorov's scaling law in a hierarchical mass-spring-damper model, *Nonlinear Dyn.* **95**, 3193–3203.
- [2] Vakakis, A. F., Gendelman, O. V., Bergman, L. A., McFarland, D. M., Kerschen, G., Lee, Y. S. (2008) Nonlinear Targeted Energy Transfer in Mechanical and Structural Systems, *Springer*.
- [3] Bak, B. D., and Kalmár-Nagy, T. (2019) Energy Cascade in a Nonlinear Mechanistic Model of Turbulence, *Tech. Mech.* **39**, 64–71.
- [4] Bak, B.D., Rochlitz, R., Kalmár-Nagy, T., Kristóf G. (2022) Mechanistic turbulence: Targeted energy transfer in a multi-degree-of-freedom nonlinear oscillator, *Conf. proc. of CMFF'22*, 362-369.
- [5] Chen, J. E., Theurich, T., Krack, M., Sapsis, T., Bergman, L. A., Vakakis, A. F. (2022) Intense cross-scale energy cascades resembling “mechanical turbulence” in harmonically driven strongly nonlinear hierarchical chains of oscillators, *Acta Mech.* **233**, 1289-1305.
- [6] Argyris, J.H., Friedrich, R., Haase, M., Faust, G. (2015) An exploration of dynamical systems and chaos: completely revised and enlarged, 2nd edition, *Springer*.

Structural reliability analysis based on the dynamic integrity of an attractor

Carlos E.N. Mazzilli* and Guilherme R. Franzini*

*Department of Structural and Geotechnical Engineering, Escola Politécnica, University of São Paulo, Brazil

Abstract. This paper addresses the reliability analysis of a dynamic system attractor, provided its dynamic integrity measure has been previously assessed in terms of a parameter for which the probability density function is known. The probability that the dynamic integrity measure should be equal or larger than a prescribed safe reference value, for the attractor to be considered “reliable”, is determined by a simple procedure. Application to an illustrative example is addressed. It is expected that such a simplified reliability analysis may be useful to improve current structural engineering design practices.

Introduction

Although the ideas discussed herewith may be applied to dynamical systems in general, the structural stability case is focused. The proposed concept of dynamic integrity [1,2] applied to buckling analysis has meaningfully improved the definition of a safe load. In fact, it is already well established that the threshold defined by the critical load of the so-called ‘perfect’ system (let’s call it Euler’s load) may be unsafe due to its potential imperfection sensitivity, resorting instead to a lower value (let’s call it Koiter’s load). Nevertheless, even this load may not be an adequate estimate of the safe load, since the associated attractor may have a small or even fractal basin of attraction, so that an even lower value (let’s call it Thompson’s load) should be considered for adequate engineering design. A dynamic integrity measure (e.g., *GIM*, *LIM* or *IF*) [1,2], to which we will generically refer to as *I*, seems to be a convenient way to define a safe design load, provided a minimum reference value (I_{ref}) is established. Yet, it is still missing in the state of the art of engineering practice a meaningful reliability measure, such as the probability that the dynamic integrity measure should be equal or larger than that prescribed safe reference value. This is what this paper intends to address.

Methodology

A methodology is proposed considering that the Dover Cliff profile [1] for the dynamic integrity measure *I* has been characterised as a function of a system control parameter *A* (for example, the load in a buckling analysis), according to $I(A)$, so that $\tan\alpha = -\frac{dI}{dA}$ is the local slope of the Dover Cliff profile. Supposing that the parameter *A* is a Gaussian random variable, with a standard deviation σ_A about the expected value \bar{A} , it is assumed that the output integrity measure will also be a Gaussian random variable with a local standard deviation $\sigma_I = \sigma_A \tan\alpha$ about the expected value \bar{I} . Hence, for every point (\bar{A}, \bar{I}) of the Dover Cliff profile, it can be defined the cut-off region for which the integrity measure complies with $I \geq I_{ref}$, provided $A \leq A_{ref}$, leading to the probability assigned for safety. For the sake of an illustration, this methodology is applied to the Dover Cliff profile of the archetypal model discussed in [3], with $I = GIM$ and $A = p$, in which $\tan\alpha \cong 2.5$ for the Thompson’s load $p_T \cong 0.245$ and $GIM_T \cong 0.100$, as shown in Fig.1. Assuming, for the sake of an example, a standard deviation $\sigma_A = 0.040$, the estimated output standard deviation would be $\sigma_I = 0.100$, leading to a probability of 31.73% for $GIM \geq GIM_T + \sigma_I = 0.200$ if $p \leq p_T + \sigma_A = 0.285$; a probability of 50% for $GIM \geq GIM_T = 0.100$ if $p \leq p_T = 0.245$; and a probability of 68.27% for $GIM \geq GIM_T - \sigma_I = 0.000$ if $p \leq p_T - \sigma_A = 0.205$. These results could be used to decide whether the choices of $GIM_T \cong 0.100$, and henceforth $p_T \cong 0.245$, were good enough for a safe engineering design.

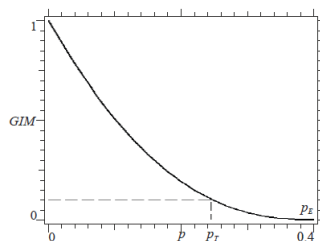


Figure 1: Dover Cliff profile extracted from Fig.8 of [3].

References

- [1] Soliman M.S., Thompson J.M.T. (1989) Integrity measures quantifying the erosion of smooth and fractal basins of attraction. *J. Sound Vibr.*, vol. 135, pp. 453-475.
- [2] Rega G., Lenci S. (2008) Dynamical integrity and control of nonlinear mechanical oscillators. *J. Vibr. Control*, vol. 14, pp. 159-179.
- [3] Lenci S., Rega G. (2011) Load carrying capacity of systems within a global safety perspective. Part I. Robustness of stable equilibria under imperfections. *Int. J. Non-Linear. Mech.*, vol. 46, pp. 1232-1239.

Stochastic basins of attraction for uncertain initial conditions

Kaio C. B. Benedetti*, Stefano Lenci**, Giuseppe Rega***, and Paulo B. Gonçalves*

*Department of Civil and Environmental Engineering, Pontifical Catholic University of Rio de Janeiro, Rio de Janeiro, Brazil

**Department of Civil and Building Engineering and Architecture, Polytechnic University of Marche, Ancona, Italy

***Department of Structural and Geotechnical Engineering, Sapienza University of Rome, Rome, Italy

Abstract. In this work the problem of stochastic basins of attraction for uncertain initial conditions and deterministic time evolution is addressed. It is shown how it is possible to determine the stochastic basins based on the sole knowledge of the deterministic basins of attraction, and the probability density function of the random initial conditions. The main results are illustrated with a paradigmatic example, the Helmholtz oscillator.

Introduction

The effects of uncertainties over global dynamic structures, such as attractors, basins, and manifolds, are difficult to address. Depending on the nondeterminism in the underlying dynamics, new definitions must be formulated, and the computational difficulty requires specialized algorithms [1]. Previous stochastic basin's definitions are adequate for parameter uncertainty and noise. Still, uncertain initial conditions had been only addressed through integrity measures [2], with the dynamics formulated deterministically.

To consider uncertain initial conditions in a probabilistic framework, it is assumed that the set of initial conditions \mathbf{x}_0 has a distribution $p(\mathbf{x}_0, \mathbf{x}, \sigma)$, where σ controls the uncertainty level and \mathbf{x} is a possible practical realization of the nominal initial condition \mathbf{x}_0 , and that the time evolution is deterministic. Let A be an attractor of the associated deterministic system, and B_A its deterministic basins of attraction. The stochastic basin of attraction is defined as the function $g_A(\mathbf{x}_0, \sigma) \in [0, 1]$ that gives the probability that \mathbf{x}_0 converge towards the attractor A . As an immediate consequence of this definition, we have that

$$g_A(\mathbf{x}_0, \sigma) = \int_{B_A} p(\mathbf{x}_0, \mathbf{x}, \sigma) d\mathbf{x}. \quad (1)$$

It is worth to note that this property allows the use of image filtering techniques. Assuming that $p(\mathbf{x}_0, \mathbf{x}, \sigma)$ is known, the computation starts from the determination of B_A through classical discretization methods (grid of starts, cell-mappings, Ulam method, ...), and then $g_A(\mathbf{x}_0, \sigma)$ is computed by (1) appositely discretized.

Results and discussion

Initially, the new basin definition is applied to the Helmholtz equation [3],

$$\ddot{x} + \delta \dot{x} + \alpha x + \beta x^2 = \lambda \sin(\omega t). \quad (2)$$

with initial conditions uniformly distributed over a cell square of dimension s (in pixels). The deterministic basin is obtained through a discretization of the phase-space window $x \in [-0.8; 1.8]$ and $\dot{x} \in [-1; 1]$ into 720×720 cells. Then, a box blur of pixel length s is applied. For increasing s levels, the results show a crescent fuzziness, initially concentrated in the basin boundaries and then spreading over the entire phase-space. Fractal boundaries are more susceptible to uncertainty, becoming fuzzy for lower s levels in comparison to robust regions. As expected, the fuzziness of the stochastic basins of attraction increases by increasing the uncertainty of initial conditions, and the “almost sure” basin $g_A(\mathbf{x}_0, \sigma) = 1$ rapidly shrinks.

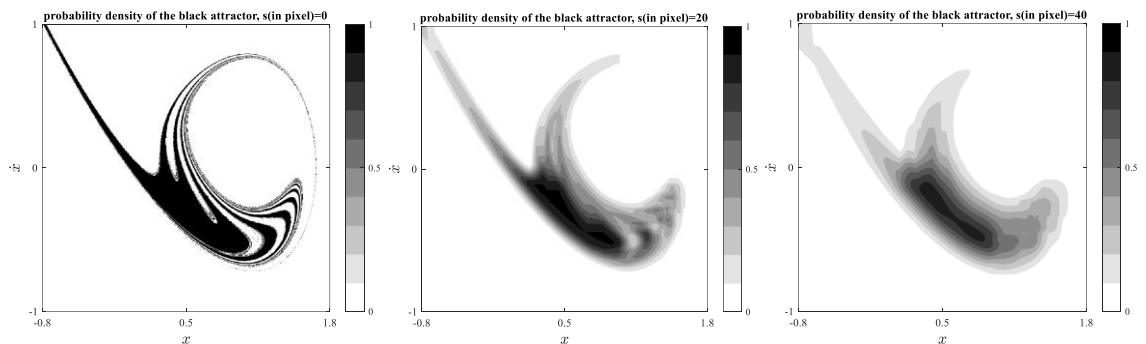


Figure 1: Stochastic basins of attraction for increasing stochastic spreadness s . Resonant attractor. $\alpha = -1$, $\lambda = 0.07$.

References

- [1] Benedetti, K.C.B., Gonçalves, P.B., Lenci, S., & Rega, G.: (2022) Global analysis of stochastic nonlinear dynamical systems. Part 1: adaptative phase-space discretization strategy. Submitt. to Nonlinear Dyn. <https://doi.org/10.21203/rs.3.rs-1781086/v1>
- [2] Lenci, S., & Rega, G. eds: (2019) Global Nonlinear Dynamics for Engineering Design and System Safety. Springer International Publishing, Cham
- [3] Rega, G., & Lenci, S.: (2005) Identifying, evaluating, and controlling dynamical integrity measures in non-linear mechanical oscillators. Nonlinear Anal. Theory, Methods Appl. 63, 902–914. <https://doi.org/10.1016/j.na.2005.01.084>

Chaotic dynamic induced by PI control in offshore oil production plants.

Nayher A. Clavijo*, Giovani G. Gerevini*, Fabio C. Diehl** and José Carlos Pinto*

*Programa de Engenharia Química/COPPE, Universidade Federal do Rio de Janeiro, Rio de Janeiro - RJ, Brazil, ORCID #0000-0002-1620-4265, #0000-0002-1163-029X, #0000-0003-2631-1811

** Centro de Pesquisas Leopoldo Americo Miguez de Mello—CENPES, PETROBRAS—Petróleo Brasileiro SA, Rio de Janeiro - RJ, Brazil, ORCID #0000-0002-7736-1395

Abstract. Several dynamic behaviors exhibited in a representative model of a Petrobras offshore oil production plant were studied, considering both, open-loop operation and closed-loop operation when using a feedback PI control scheme. The present work evaluated three different SISO control scenarios taking into account three controlled variables in order to determine the suppression effect of the oscillatory dynamic behavior raised due to the slugging flow phenomenon. It was observed that in the PI anti-slug control scheme when the pressure at the top of the riser was considered the controlled variable, the dynamics exhibited chaotic oscillations as a function of the PI tuning parameters. The chaotic behavior was characterized and it was determined the control scenarios and tuning conditions that favor the appearance or impression of complex dynamics behaviors.

Introduction

Frequently, floating facilities used for offshore oil and gas production consist of tubing-pipeline-riser systems. Despite this production technology being widely used, it has been observed these production systems are susceptible to exhibiting slugging, a common and undesirable multiphasic flow pattern phenomenon that causes periodic blockage of gas flow due to a large liquid slug accumulation through the riser and pipeline section. These slugging flow instabilities can generate harmful operating conditions leading to process safety losses, process production drop, and even plant shutdown [1].

Several approaches have been developed in order to avoid or remediate problems in pipeline-riser systems due to the slugging phenomenon, including automatic control strategies aimed to change the operating condition that favors the arise of the slugging flow. It is worth mentioning that the major part of slugging behaviors observed in industrial-scale processes and the corresponding phenomenological models described periodic oscillatory dynamics, and more complex dynamics have not been observed in these production scales [2].

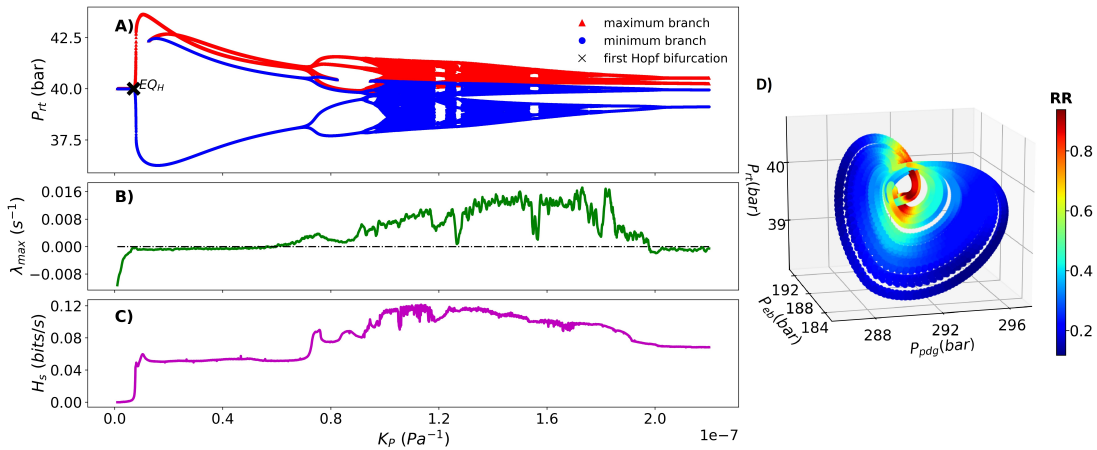


Figure 1: Chaotic behavior characterization induced due PI control action.

Results and discussion

The PI control scheme, applied to the upstream production system represented by the FOWM model [3] aimed to change or suppress the operational conditions that lead to slugging dynamics by manipulating the oil production valve opening. The PI controller suppression effect was measured as the capacity to shift the born location of the Hopf bifurcation to higher valve openings, i.e to higher production conditions. Fig1A shows the bifurcation diagram corresponding to the PI control scenario when the pressure at the top of the riser was the controlled variable. As one can see, the local extrema of the pressure oscillations describe the arising of chaotic behavior as a function of the PI tuning parameter K_p . Furthermore, the characterization of the chaotic behavior is determined by the largest Lyapunov exponent Fig(1B) and the Shannon entropy Fig(1C) criteria. In addition, Fig1D offers a qualitative characterization from a recurrence analysis.

References

- [1] Pedersen, S., Durdevic, P., Stampe, K., Yang, Z. (2016) *Int. J. Autom.* **13**:81-88.
- [2] Campos, M., Takahashi, T., Ashikawa, F., Simões, S., Stender, A., Meien, O. (2015) *IFAC-PapersOnLine* **48**:83-88.
- [3] Diehl, F., Anzai, T., Almeida, C., Von Meien, O., Neto, S., Rosa, V., Trierweiler, J. (2017) *Comput Chem Eng* **99**:304-313.

Resource Sensitive Game

Der Chyan Bill Lin*

*Department of Mechanical and Industrial Engineering, Toronto Metropolitan University, Toronto, Ontario, Canada

Abstract. The idea of resource sensitive game is proposed to address the evolutionary dynamics in multi-agent dynamical systems subjected to fluctuating resource. The co-evolution between a specifically define resource function and the players' payoff provides the key in our formulism. Numerical study based on the classical hawk-dove game is provided with momentum and contrarian hawkish player behaviours. Rich evolutionary dynamics with periodic and chaos is shown.

Introduction

Game theory provides the conceptual framework for studying multi-agent dynamical system with self-interest players [1]. The classical game models assume a constant player's payoff as well as an unlimited resource from which the payoffs are drawn. This is justifiable when the environment acts as a passive player who does not interact with the game. In an environment causing payoff variation, anomalous evolutionary stable states and sub-optimality in game dynamics were both reported [2]. The carbon metabolism in yeast cells provide a different scenario of an environment subjected to fluctuating resources, where 'cheater' strain yeast cells, coexisting with their cooperative counterparts in the population, can take a free ride with the glucose they need but never produce [3,4]. Gore et al. show that the underlying dynamics must necessarily exhibit hybrid characteristics of the prisoner-dilemma and hawk-dove games [3]. Indeed, from a predator-prey system to the so-called *tragedy of the commons* in general, the possibility of a more complex evolutionary dynamics has long been suggested when the players' objectives intertwined with the environment [4,5]. However, both the modelling of this player-resource interaction and its consequence in the evolutionary dynamics have not received sufficient attention in the past.

In this work, the idea of resource sensitive (RS) game is proposed. A time co-evolution of the players' payoff and the system resource is introduced to reveal the evolutionary complexity that is yet to be addressed by the existing game theory. We demonstrated the idea using the classical hawk-dove game with the payoff matrix

$$B = \begin{bmatrix} (b_n^h - c)/2 & b_n^h \\ 0 & b^d/2 \end{bmatrix}. \text{ Both momentum and contrarian hawkish behaviours are considered in the co-}$$

evolution with the system resource. The momentum player 'doubles down' in a rising resource environment whereas the contrarian acts in the opposite. The dynamical system of equations can be given by $x_{n+1} = x_n(b_n^h - (b_n^h + c)x_n/2)/A(n)$, $b_{n+1}^h = b_0^h + \epsilon[\tan^{-1}(\gamma\omega_n) + \pi/2]/\pi$, $\sigma_{n+1} = \sigma_n + d(b_n^h, c, b^d, \mu)x_n^2 + h(b_n^h, c, b^d, \mu)x_n + k(b_n^h, c, b^d, \mu)$, where x is the percentage of the hawkish population, $A(n)$, the averaged payoff, μ and ϵ , real constants in $[0,1]$, $\omega_n = (\sigma_n - \sigma_0)/\max(\sigma_1 - \sigma_0, \dots, \sigma_{n-1} - \sigma_0)$ and d, h, k are coefficients for the quadratic law of the resource σ_n . In addition to the classical evolutionary stable states, the RS hawk-dove game exhibits periodic and chaotic evolutions; see Fig. 1. The chaotic solution is particularly interesting in that a higher concentration of resource (wealth) in a smaller hawkish population is observed when the resource level rises, a sort of a rich-get-richer scenario.

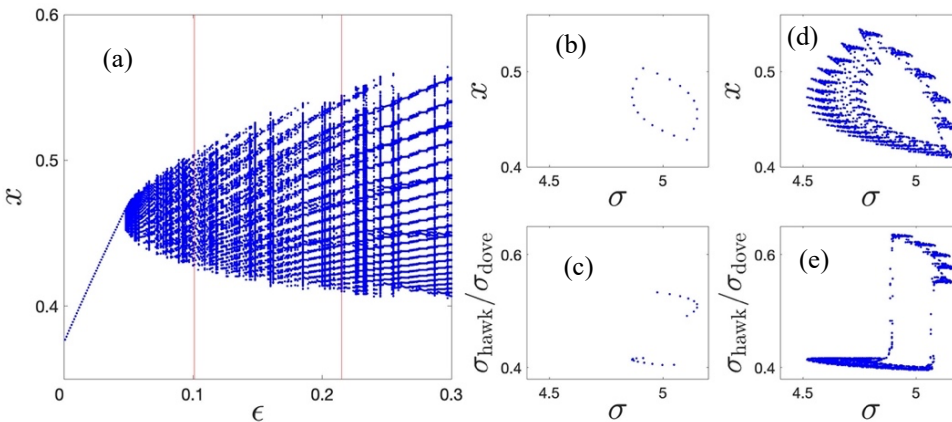


Fig. 1: Numerical simulation of the RS hawk-dove game with momentum hawk: (a) the hawk population x vs. ϵ . The x and hawkish-dovish wealth ratio, $\sigma_{\text{hawk}}/\sigma_{\text{dove}}$, vs. the resource level σ , respectively, in (b), (c), showing the periodic solution at $\epsilon = 0.101$, and (d), (e), showing the chaotic solution at $\epsilon = 0.215$. Simulation parameters: $\gamma = 900$, $\sigma_0 = 5$, $c = 1$, $b_0^h = 0.5$, $b^d = 0.7$, $\mu = 0.25$.

References

- [1] Parsons, S., Wooldridge, M (2002) *Autonomous Agents and Multi-Agent Systems* 5: 243–254.
- [2] Stollmeier, F., Nagler, J (2018) *Physical Review Letters* 120: 058101.
- [3] Gore J., Youk H., Van Oudenaarden A. (2009) *Nature*, 459, 253-256.
- [4] West, S.A., Griffin A.S., Gardner A., Diggle S.P (2006) *Nature Review, Microbiology* 4:597-607.
- [5] Gardner A., West S.A., Buckling A. (2004) *Nature* 430: 1024-1027.

Coexistence of hidden attractor and self-excited attractors on the plane

Eric Campos-Canton*, Hector E. Gilardi-Velazquez** and Guillermo Huerta-Cuellar***

*Division of Control and Dynamical Systems, Instituto Potosino de Investigacion Cientifica y Tecnologica, S.L.P., Mexico, ORCID 0000-0002-1098-1610, ** Facultad de Ingeniería, Universidad Panamericana, Aguascalientes, Mexico, ORCID 0000-0002-4978-4526, *** Dynamical Systems Laboratory, Centro Universitario de los Lagos, Universidad de Guadalajara, Jal., Mexico. ORCID 0000-0003-2956-104X.

Abstract. In this work, we introduce a class of continuous time planar systems that presents the coexistence of hidden and self-excited attractors. This class of planar systems is derived from three-dimensional piecewise linear (PWL) systems. Then, we present an approach to generate self-excited and hidden multiscroll attractors by defining a vector field on R^2 with an even number of equilibria.

Introduction

There are three classes of attractors, the first class is given by those classical attractors excited from unstable equilibria called *self-excited attractors* whose basin of attraction intersects at least a neighborhood of an equilibrium point, [1] and they are not difficult to find via numerical methods, and the second class is called *hidden attractors* whose basin of attraction does not contain neighborhoods of equilibria. The coexistence of a self-excited attractor and a hidden attractor was observed in the Chua's circuit and reported in [2]. The last class is generated by vector fields without equilibria called *non-self-excited attractors* [3]. Notice that a non-self-excited attractor is given by a system without equilibria, therefore satisfies the definition of hidden attractors. Multistability is the coexistence of two or more attractors, different scenarios of multistability have been reported in [4, 5]. Recently, a class of continuous time dynamical planar systems which was generated by means of the use of hysteresis and at least two unstable focus [6]. This class of systems shows stretching and folding behavior due to hysteresis.

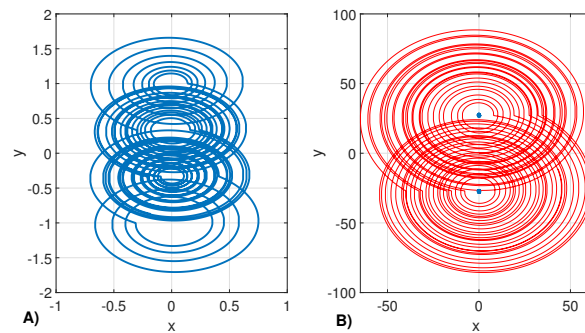


Figure 1: A) Four-scroll attractor. B) Coexistence of two self-excited attractors in blue and a hidden attractor in red.

Results and discussion

In the same spirit that [6], we derive a class of planar systems through a three-dimensional piecewise linear (PWL) systems that have two manifolds, one stable and the other unstable, to generate heteroclinic chaos. Then, we present an approach to generate self-excited and hidden multiscroll attractors by defining a vector field on R^2 with an even number of equilibria. The vector field is defined by affine linear systems such that each equilibrium point is a unstable focus point. So the space is partitioned in hyperbolic set. We start by generating a self-excited multiscroll attractor based on heteroclinic orbits. Interesting phenomena appear when the equilibria are separated by pairs, firstly, the system presents only one basin of attraction which is divided accordingly with the separation of the equilibria, and the coexistence of different self-excited double-scroll attractors arise. At a certain separation of equilibria, a hidden multiscroll attractors emerges, see figure 1.

References

- [1] Dudkowski, D., Jafari, S., Kapitaniak, T., Kuznetsov, N. V., Leonov, G. A. and Prasad, A. (2016) Hidden attractors in dynamical systems, *Physics Reports*, **637**: 1-50.
- [2] Leonov, G. A., Kuznetsov, N. V. and Vagitsev, V. (2011) Localization of hidden Chua's attractors, *Physics Letters A*, **375**: 2230-2233.
- [3] Escalante-Gonzalez, R. de J., Campos-Canton, E., and Nicol, M. (2017) Generation of multi-scroll attractors without equilibria via piecewise linear systems *Chaos: An Interdisciplinary Journal of Nonlinear Science* **27**: 053109.
- [4] Feudel, U. (2008) Complex dynamics in multistable systems, *International Journal of Bifurcation and Chaos* **18**: 1607-1626.
- [5] Anzo-Hernandez, A., Gilardi-Velazquez, H. E. and Campos-Canton, E. (2018) On multistability behavior of unstable dissipative systems, *Chaos: An Interdisciplinary Journal of Nonlinear Science*, **28**: 033613.
- [6] Campos, E. (2020) Derivation of a continuous time dynamic planar system with two unstable foci from a three-dimensional chaotic piecewise linear system, *Chaos: An Interdisciplinary Journal of Nonlinear Science* **30**: 053114.

Compact Multiplier-less CORDIC-Based on FPGA Implementation of a Sine map for Chaotic Applications

Sara S. Abou Zeid*, Hisham M. Elrefai*, Wafaa S. Sayed**, Lobna A. Said *
and Ahmed G. Radwan ***

**Nanoelectronics Integrated Systems Center (NISC), Nile University, Giza, Egypt*

***Engineering Mathematics and Physics Dept., Faculty of Engineering, Cairo University, Egypt*

****School of Engineering and Applied Sciences, Nile University, Giza, Egypt*

Abstract. This paper proposes a new modified sine chaotic map and implements both the conventional sine map and the proposed modified map on hardware. The proposed modified sine map exhibits continuous chaotic behavior against all values of the main system parameter. This is beneficial in pseudo-random number generation and encryption applications regarding system key design and ensuring chaotic behavior. The chaotic behavior of both maps is validated using time series, bifurcation diagrams, and maximum Lyapunov exponent. A reconfigurable CORDIC hardware block is used to compute the transcendental mathematical functions by employing shift-add and sub-operations. While the sin function is computed in circular rotation mode, the multiplication operation is computed in linear vectoring mode. The proposed hardware architecture is multiplier-less and, hence, it does not consume any DSPs. The sine and modified sine maps are realized on Xilinx Artix-7 FPGA board using Verilog HDL, yielding throughputs of 0.342 and 0.312 GBit/s, respectively.

Introduction

Many natural systems, such as fluid movement, rapid heartbeat, weather, and climate, exhibit chaotic behavior. Additionally, it happens on its own in some artificially constructed systems, such as the movement of people in the streets and the movement of air. Chaotic systems have vast importance which gives a focus to trying to implement them to aid in many applications such as encryption (Cryptography) which is mainly based on the unpredictability of the algorithm and output which requires a complex chaotic system to be reliable [1]. also, in [2] two image encryption applications are introduced based on the Sine map. Another use of the chaotic system is in the Robotics field which needs many cases and scenarios for the trial-and-error process to learn how to interact with many use cases [3]. Several research works in the literature presented chaotic maps with trigonometric nonlinearities, yet only a few of them implemented it on Hardware platforms. Zhongyun et al. implemented the Sine Chaotification Model (SCM) on FPGA. SCM increases the chaotic range and improves the dynamic complexity of the one-dimensional (1D) chaotic maps. In addition, it widens the parameters range corresponding to chaotic behavior making the maps more suitable for Pseudo-Random Number Generators [4]. Zhongyun et al. also implemented Sine Transform Based Chaotic System (STBCS), which combines the outputs of two chaotic maps on FPGA. STBCS results in new 1D maps with better complexity, range, and unpredictability [5]. The implementation of CORDIC for the sine function provides a significant improvement in the resource utilization of the FPGA, CORDIC only calculates the function using adders and shifters [6]. In this paper, the proposed solution focuses on implementing a modified sine map based on CORDIC for the design of Pseudo-Random Number Generators (PRNG) and encryption systems.

Results and discussion

The proposed designs for the modified sine map and sine map are interpreted in the hardware language Verilog HDL and are synthesized by using Xilinx Vivado targeting Xilinx Artix-7 FPGA board. The designs achieve a throughput of 0.342 and 0.312 Gbit/s for sin and modified sine maps, respectively. The number of LUTs used in the case of the sine map is 6459 and for the modified sine map is 6918. The proposed implementation uses the Reconfigurable multiplier-less CORDIC in [1] to calculate the sine function and the multiplication. As a result, the proposed architecture does not consume any DSPs. Also in [6] a summary of Reconfigurable CORDIC FPGA result.

References

- [1] Ismail, S. M., Said, L. A., Rezk, A. A., Radwan, A. G., Madian, A. H., Abu-Elyazeed, M. F., & Soliman, A. M. (2017). Generalized fractional logistic map encryption system based on FPGA. *AEU-International Journal of Electronics and Communications*, 80, 114-126.
- [2] S. K. Abd-El-Hafiz, A. G. Radwan, and S. H. AbdEl-Haleem, "Encryption applications of a generalized chaotic map," *Applied Mathematics & Information Sciences*, vol. 9, no. 6, p. 3215, 2015.
- [3] Zang X, Iqbal S, Zhu Y, Liu X, Zhao J. Applications of Chaotic Dynamics in Robotics. *International Journal of Advanced Robotic Systems*. 2016;13(2).
- [4] Z. Hua, B. Zhou and Y. Zhou, "Sine Chaotification Model for Enhancing Chaos and Its Hardware Implementation," in *IEEE Transactions on Industrial Electronics*, vol. 66, no. 2, pp. 1273-1284, Feb. 2019.
- [5] Z. Hua, B. Zhou and Y. Zhou, "Sine-Transform-Based Chaotic System With FPGA Implementation," in *IEEE Transactions on Industrial Electronics*, vol. 65, no. 3, pp. 2557-2566, March 2018.
- [6] NS. M. Mohamed, W. S. Sayed, A. G. Radwan and L. A. Said, "FPGA Implementation of Reconfigurable CORDIC Algorithm and a Memristive Chaotic System With Transcendental Nonlinearities," in *IEEE Transactions on Circuits and Systems I: Regular Papers*, vol. 69, no. 7, pp. 2885-2892, July 2022.

Fixed-time adaptive neural tracking control for a helicopter-like twin rotor MIMO system

Bacha Aymene*, Chelihi Abdelghani* and Chouki Sentouh **

*LMSE Laboratory, Department of Electrical Engineering, University of Biskra, Biskra, Algeria #

***LAMIH-UMR CNRS 8201, Department of Automatic Control, Hauts-de-France Polytechnic University, Valenciennes, France #*

Abstract. In this paper, a fixed-time adaptive neural control (FTANC) for a helicopter-like Twin Rotor MIMO System (TRMS) is presented. The proposed controller has been developed to achieve finite-time convergence of the system dynamics independently of the initial conditions. The control of the TRMS system is a challenging problem due to the significant non-linearities and the cross-coupling between the main and tail rotors. In this study, we proposed an adaptive radial basis function neural networks (RBFNNs) to estimate all unknown nonlinear functions and disturbances. The RBFNN is combined with backstepping technique to guarantee the trajectory tracking and the overall closed-loop stability. The effectiveness of the proposed control strategy is demonstrated through simulation tests in Matlab/Simulink software environment.

Introduction

The twin rotor MIMO system is an aerodynamic system similar to a helicopter flight. Its dynamic is highly nonlinear and unstable with a cross-coupled between the main and tail rotors. The TRMS has 2 DOF which can rotate in both vertical axes (yaw) and horizontal axes (pitch) [1]. So, it is a popular and challenging experimental platform for designing various control strategies. In the control literature, several controllers from linear to nonlinear and intelligent approaches have been developed to solve the TRMS stabilization problem and trajectory tracking, such as PID and LQR linear controllers, and feedback linearization, sliding mode and backstepping nonlinear control methods. In this paper, motivated by the control approach developed in [2], a fixed-time adaptive neural backstepping controller (FTANC) is designed to ensure both tracking performance and closed-loop stability of the TRMS system. The proposed controller can deal with the problems of parametric uncertainties, unknown nonlinear dynamic and disturbances. The convergence and stability of the fly system is ensured in finite time independently of the initial conditions.

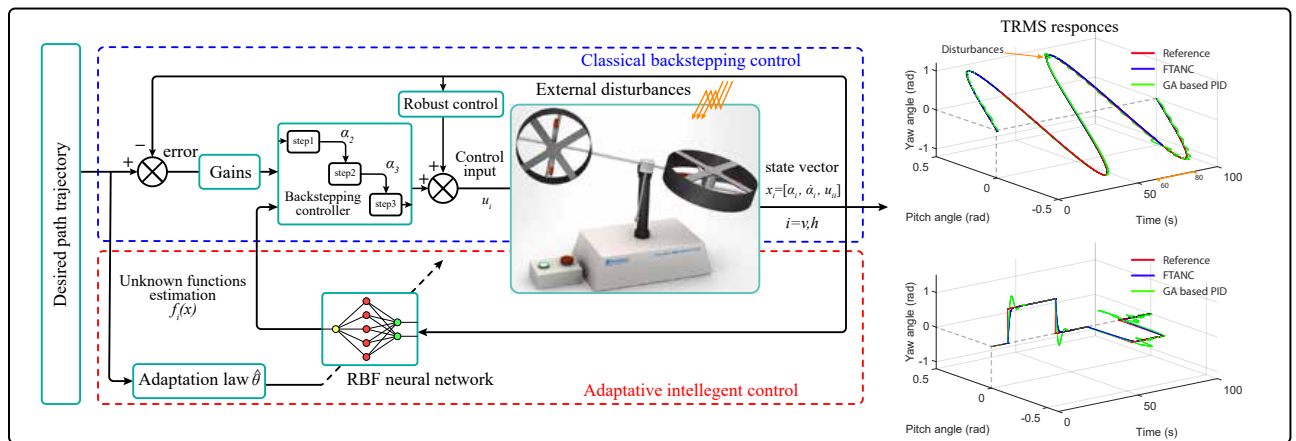


Figure 1: Block diagram of the proposed fixed-time adaptive neural control scheme for TRMS.

Fixed-time adaptive neural tracking control

In this approach, a radial basis function neural network (RBFNN) is combined with a backstepping control method to propose an intelligent adaptive control scheme for driving the TRMS. The RBFNN is introduced here to approximate all unknown nonlinear functions and disturbances, where the updating laws are derived using the rigorous Lyapunov proof. The proposed fixed-time controller has faster convergence and the upper bound of settling time can be estimated without any restriction on the initial conditions. The effectiveness and robustness of the proposed controller are demonstrated in a simulation environment. Our future research topics will aim to focus on the hardware implementation and the fault-tolerant control problem for the TRMS system.

References

- [1] Na, N. T. le, Huy, V. Q. (2021). Dynamic model of trms based on homogeneous transformation and euler-lagrange equation. *International Journal of Emerging Technology and Advanced Engineering*, 11(8). <https://doi.org/10.46338/IJETAE0821-01>
- [2] Ba, D., Li, Y. X., Tong, S. (2019). Fixed-time adaptive neural tracking control for a class of uncertain nonstrict nonlinear systems. *Neurocomputing*, 363, 273–280. <https://doi.org/10.1016/j.neucom.2019.06.063>

A new key generator based on an auto-switched hybrid chaotic system and its FPGA implementation

Sid Hichem^{*}, Azzaz Mohamed Salah^{*} and Sadoudi Saïd^{**}

^{*} Laboratoire Systèmes Electroniques et Numériques, EMP, Algiers, Algeria

^{**} Laboratoire Télécommunications, EMP, Algiers, Algeria

Abstract. In this paper a new key generator is presented, it is constructed by an auto-switched numerical resolution of multiple three dimensional continuous chaotic systems (Lorenz, Rössler, Chen) how excite a discrete chaotic system (Henon Map). The designed chaotic system provides complex chaotic attractors and can change its behaviors automatically via a chaotic switching-rule. The originality of the proposed architecture is that allows to solve the problem of the finite precision due to the digital implementation while provides a good compromise between high security, performance and hardware resources (low power and cost). Hardware digital implementation and FPGA circuit experimental results of this generator demonstrate that this promising technique can be applied in efficient embedded ciphering communication systems.

Introduction

Currently, several chaotic generators have been studied (Lorenz, Chen, Chua and Lü, etc) [1]. However, these main chaotic generators are easily identifiable by a simple visualization of their attractors that can be used in cryptosystems [2]. When chaotic systems are implemented or implanted in digital form, a dynamic degradation of the response occurs. More precisely, the dynamic properties of digital chaotic systems can become non-ideal. The most well-known problem is the existence of many chaotic short-length orbits, which can weaken the desired statistical properties of chaotic evolving digital data, resulting in degradation of the security of the encryption process [3]. In this context, it becomes important to mask or to develop mechanisms associated with these generators in order to increase the complexity of a cryptanalysis from an identification of the chaotic signals on one side and to solve the problem of precision during a digital implementation, on the other hand. In this work we will use the principle of chaos in order to propose, design and implement a new generator based chaos that better responds to the requirement of modern cryptography. The interest of our solution is to propose a complex chaotic system allowing an unidentifiable cipher key generator by an analysis of its attractors, while proposing optimized architecture and hardware implementation giving a very useful and attractive compromise between high speed, low area cost and secure data communications for embedded applications. Our proposed logic Register Transfer Level (RTL) architecture is based on pipelined numerical method to resolve several 3D chaotic differential equations characterizing some chaotic systems. In this work, we'll present, the modeling of the presented auto-switched system and its hardware architecture, the simulations results on Xsim of Vivado, the discussion of the hardware implementation results on Genesys 2 Kintex-7 Xilinx FPGA technology, performance evaluations, real-time measurements and the evaluation of the random dynamical behaviors of our new scheme through statistical tests in order to prove that the proposed hybrid generator exhibits truly random sequences suitable as cipher keys for the data encryption.

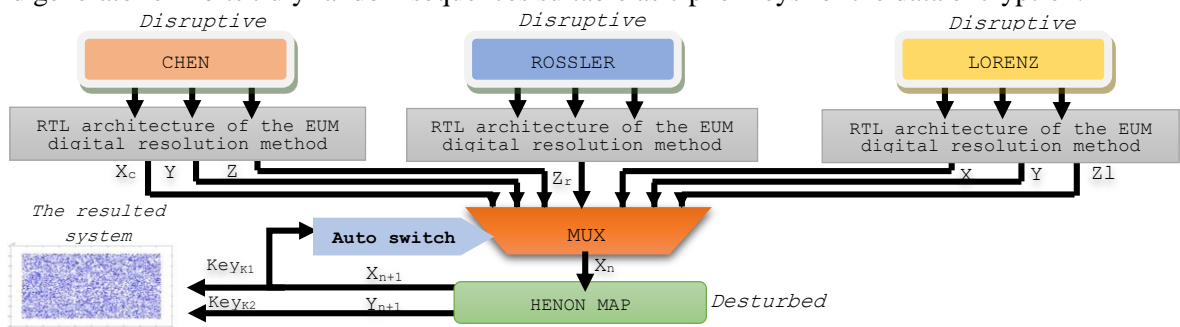


Figure 1: The perturbation technique adopted for the modeling of the proposed generator.

Results and discussion

The synthesis results after place, route and real time implementation show a low power consumption, a very low latency and low use of the resources of our FPGA card, all this is due to our working approach and the optimization of the codes developed. After visualization of the different signals of our generator, we observed the similarity between the simulation results and the real-time implementation results, which validates our hardware implementation approach. To quantify the random criterion of the keys generated, we performed a statistical analysis using the statistical test batteries of NIST, DIEHARD and ENT. We noticed that our results passed all the tests successfully. Consequently, we can say that the generated keys have a random character, so they are robust, and they are ready to be used in cryptosystems.

References

- [1] E. N. Lorenz (1963) Deterministic nonperiodic flow. *J. Atmos. Sci.* **130**:141-20.
- [2] M. S. Azzaz (2012) Implantation paramétrable d'un nouvel algorithme de cryptage symétrique basée Chaos par inclusion au sein d'une architecture reconfigurable de type FPGA. PhD thesis, Cotutelle de thèse EMPA. & U A. F.
- [3] G. Alvarez and S. Li (2006) Some basic cryptographic requirements for chaos-based cryptosystems. *Int. J. Bifurct. Chaos* **16**:2129-2151

A quantitative Birkhoff Normal Form for geometrically nonlinear hinged-hinged beams

L. Di Gregorio*, W. Lacarbonara*

*Dipartimento di Ingegneria Strutturale e Geotecnica, University of Rome La Sapienza, Rome, Italy

Abstract. The study of internal resonances of a system is crucial to investigate its stability. KAM (Kolmogorov Arnold Moser) theory is a powerful branch of perturbation theory born to face the small divisors (resonances) problem in hamiltonian dynamical systems. Its applicability to concrete physical problems is a well-known challenge because of the extreme smallness required for the perturbation parameter. Here we consider an undamped nonlinear hinged-hinged beam with stretching nonlinearity as an infinite dimensional hamiltonian system. We obtain analytically a quantitative Birkhoff Normal Form, via a nonlinear coordinate transformation that allows us to integrate the system up to a small reminder, providing a very precise description of small amplitude solutions over large time scales. The optimization of the involved estimates yields results obtained for realistic values of the physical quantities and of the perturbation parameter.

Introduction

We consider the dimensionless nonlinear beam equation with stretching nonlinearity

$$u_{tt} + u_{xxxx} - \left(m + \frac{1}{2\pi} \int_0^\pi u_x^2 dx \right) u_{xx} = 0, \quad (1)$$

for $t \in \mathbb{R}$ and $x \in [0, \pi]$, with the following hinged-hinged boundary conditions: $u(t, 0) = u(t, \pi) = u_{xx}(t, 0) = u_{xx}(t, \pi) = 0$. Here $\sqrt{I/A}u$ is the vertical displacement and $m = \frac{L^2 P}{\pi^2 EI}$ indicates the nondimensional axial force, where L, I, A, E, P are, respectively, the length of the beam, the moment of inertia, the cross-section area, the Young modulus, and the tensile axial force (possibly also negative entailing compressive force). Being conservative, Eq. (1) has a hamiltonian structure. Indeed, by letting $\omega_j^2 := j^4 + mj^2$ and $\phi_j(x) := \sqrt{2/\pi} \sin jx$, respectively, denote the eigenvalues and the eigenfunctions of the Sturm–Liouville operator $(\partial_{xxxx} - m\partial_{xx})$ on $[0, \pi]$, the Hamiltonian can be expressed as

$$H(\mathbf{p}, \mathbf{q}) = \sum_{j \geq 1} \omega_j I_j + \frac{1}{8\pi} \left(\sum_{j \geq 1} \frac{j^2}{\omega_j} q_j^2 \right)^2, \quad I_j := \frac{1}{2} (p_j^2 + q_j^2), \quad (2)$$

with $\mathbf{q} = (q_1, q_2, \dots)$, $\mathbf{p} = (p_1, p_2, \dots)$ spanning a suitable Hilbert space of sequences. Then, given a smooth solution $t \rightarrow (\mathbf{p}(t), \mathbf{q}(t))$ of Hamilton's equations, one finds that $u(t, x) := \sum_{j \geq 1} \frac{q_j(t)}{\sqrt{\omega_j}} \phi_j(x)$ is a solution of (1). If the linear frequencies ω_j are non-resonant, after a canonical change of variables close to the origin, the Hamiltonian is in BNF (Birkhoff Normal Form) up to some order $2d > 0$, namely $H = N(I) + R(\mathbf{p}, \mathbf{q})$, where $N(I) = \sum_{j \geq 1} \omega_j I_j + g(I)$ for some polynomial g of degree d in I and $R = O(|(\mathbf{p}, \mathbf{q})|^{2d+2})$. Since the nonlinear term \bar{N} is *integrable*, the BNF allows a precise description of the solutions with initial data $\epsilon := |\mathbf{p}(0)| + |\mathbf{q}(0)| \leq \epsilon_0$ up to times $|t| \leq T_0 \epsilon^{-2d}$, for suitably small ϵ_0 and T_0 . This immediately reads as a stability result for Eq. (1) with ϵ -small initial data $u(0, x)$ and $u_t(0, x)$. There are some results (see, e.g. [1]) on the BNF for the beam equation (with nonlinearities different from (1)) but with no physical applications. Indeed the typical problem in hamiltonian perturbation theory (especially for PDEs) is that the amplitude threshold, ϵ_0 here, is very small.

Results and discussion

For $m > -1$ we prove that the frequencies are non-resonant up to order 4, which, in general, corresponds to show that $\omega_i \pm \omega_j \pm \omega_k \pm \omega_\ell$ does not vanish for suitable combinations of positive integers i, j, k, ℓ and \pm signs. However, in the present case, due to the special form of the nonlinearity, the non-resonance condition reduces to $\omega_i - \omega_j \geq c > 0$ uniformly in $i > j \geq 1$. Then we can put the system in BNF up to order $2d = 4$. Moreover, for $0 < |m| < 1$ we are able to show that the frequencies are non-resonant up to order 6 (which reduces to $|\omega_i - \omega_j - \omega_k| \geq c > 0$ uniformly in $i > j \geq k \geq 1$), so that we can put the system in BNF up to order $2d = 6$. The main point here is that, *by optimizing the estimates, we are able to find realistic values for ϵ_0 and T_0* . For example for a steel beam of length $L = 2\text{m}$, height 0.02m , $P = -3.3\text{kN}$ and initial vertical displacement $2 \cdot 10^{-4}\text{m}$ (corresponding to $m = -0.5$, $\epsilon = 0.04$) we have stability time length of 60s (4300 oscillations). As far as we know, this is the first purely analytical result of this kind in hamiltonian perturbation theory for PDEs.

References

- [1] Geng J., You J.(2003) KAM tori of Hamiltonian perturbations of 1D linear beam equations, *J. Math. Anal. Appl.* **277**: 104-121.
- [2] Mook D., Nayfeh A. *Nonlinear oscillations*, Wiley Classic Library (1995).
- [3] Woinowsky-Krieger S.(1950) *The Effect of an Axial Force on the Vibration of Hinged Bars*, Journal of Applied Mechanics, 17, pp.83-102.

Nonlinear dynamic characteristics and four contact states of a spur gear pair considered tooth profile error and extended tooth contact

Zhengfa Li* and Zaigang Chen*

*State Key Laboratory of Traction Power, Southwest Jiaotong University, Chengdu, Sichuan, China

Abstract. The actual tooth profile of a spur gear will inevitably deviate from involute tooth profile due to the machining error, and so on. The nonlinear characteristics and contact state of the gear transmission system will be changed by tooth profile error, and the system stability will be affected accordingly. A dynamic model of spur gear pair is established by considering tooth profile error, extended tooth contact, and some time-varying parameters. Tooth profile error and extended tooth contact are directly involved in the calculation of the dynamic meshing force. Besides, the five Poincaré mapping sections Γ_i and corresponding triggers are established to capture the information on motion type, extended teeth contact, tooth disengagement, and tooth back contact of the system. Finally, the bifurcation characteristics and four contact states of the system are studied by using the established Poincaré mapping sections, bifurcation diagrams with multi-mapping sections and phase portraits.

Introduction

The system bifurcation, chaotic motion, and other nonlinear behavior in the gear transmission system will be induced due to tooth profile error [1, 2], and the system will also occur tooth disengagement and tooth back contact [3]. Meanwhile, the extended tooth contact caused by tooth profile error and tooth contact deformation will further complicate the nonlinear characteristics and contact state of the system [4, 5]. In the published literature, most scholars focused on the meshing excitations and nonlinear dynamics characteristics of the system considered tooth profile error [1-3], or the meshing excitations considered extended tooth contact [4, 5]. Tooth profile error and extended tooth contact are rarely considered simultaneously in the studies of nonlinear dynamic characteristics. The four contact states of the system, including tooth disengagement, back tooth contact, approaching tooth contact, and recessing tooth contact, were also not revealed. However, both the nonlinear characteristics and contact state of the system are critical to the transmission quality of the system.

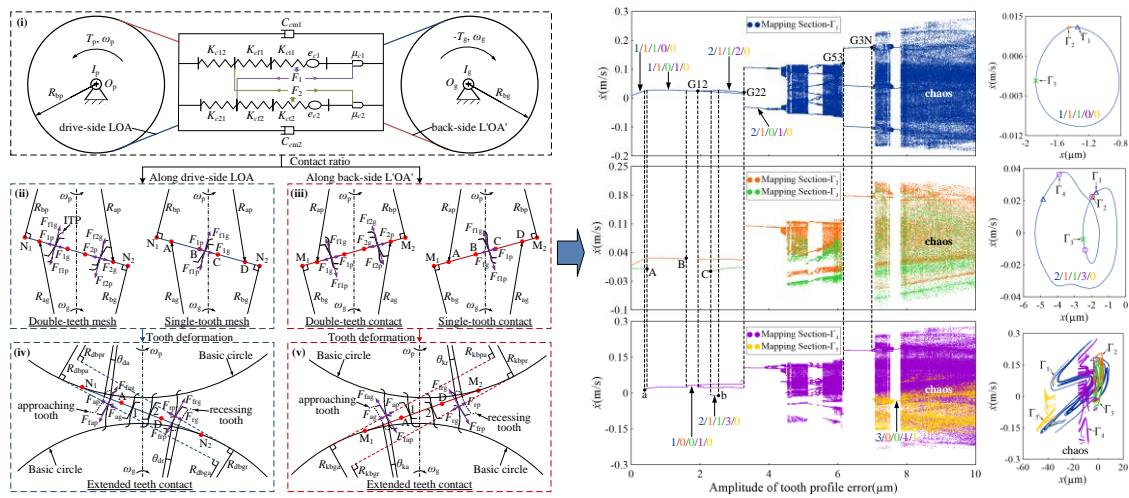


Figure 1: The dynamics model and calculation results.

Results and discussion

The established dynamics model and representative calculation results are shown in Fig. 1. The calculation results show that with the increase of the amplitude of tooth profile error, the system will go through the stable periodic motion, the alternation between periodic motion and chaotic motion, and unstable chaotic motion, as well as tooth disengagement and tooth back contact will also occur in turn. The contact of extended teeth is also changed because of system bifurcation, tooth disengagement, and tooth back contact.

References

- [1] Inalpolat M, Kahraman A. (2010) A dynamic model to predict modulation sidebands of a planetary gear set having manufacturing errors. *J. Sound Vib* **329**:371-393.
- [2] Chen Z G, Ning J Y, Wang K Y, et. al. (2021) An improved dynamic model of spur gear transmission considering coupling effect between gear neighboring teeth. *Nonlinear Dynam* **106**:339-357.
- [3] Li Z F, Chen Z G, Gou X F, et al. (2022) Study on safety characteristics of the spur gear pair considering time-varying backlash in the established multi-level safety domains. *Nonlinear Dynam* **109**:1297-1324.
- [4] Ma H, Pang X, Feng R J, et. al. (2015) Fault features analysis of cracked gear considering the effects of the extended tooth contact. *Eng Fail Ana* **48**:105-120.
- [5] Zhou C J, Chen S Y. (2014) Modeling and Calculation of Impact Friction Caused by Corner Contact in Gear Transmission. *Chin J Mech Eng-ne* **27**:958-964.

Non-autonomous inverse Jacobi multipliers and periodic orbits of planar vector fields

Isaac A. García* and Susanna Maza*

*Departament de Matemàtica, Universitat de Lleida, Spain

Abstract. We analyze the role that non-autonomous (and not necessarily periodic) inverse Jacobi multipliers have in the problem of the nonexistence, existence and localization as well as the hyperbolic nature of periodic orbits of planar vector fields. This work generalizes and extends previous results already appearing in the literature focusing in the autonomous or periodic case.

Introduction

We consider planar differential systems

$$\dot{x} = P(x, y), \quad \dot{y} = Q(x, y), \quad (1)$$

where P and Q are C^1 functions on the open set $U \subseteq \mathbb{R}^2$ and the dot denotes, as usual, derivatives with respect to the independent time variable t . We associate to system (1) the vector field $\bar{\mathcal{X}} = P(x, y)\partial_x + Q(x, y)\partial_y$ and state the precise definition of inverse Jacobi multiplier of system (1).

DEFINITION. A function $V : \mathbb{R} \times U \rightarrow \mathbb{R}$ is said to be an inverse Jacobi multiplier of system (1) if V is of class $C^1(\mathbb{R} \times U)$, it is not locally null and it satisfies the following linear first order partial differential equation:

$$\mathcal{X}(V) = V \operatorname{div}(\bar{\mathcal{X}}), \quad (2)$$

where $\mathcal{X} = \partial_t + \bar{\mathcal{X}}$ and the divergence of $\bar{\mathcal{X}}$ is $\operatorname{div}(\bar{\mathcal{X}}) = \partial_x P + \partial_y Q$.

We use the name autonomous inverse Jacobi multiplier V in case that $\partial_t V \equiv 0$ and periodic inverse Jacobi multiplier when there is $T > 0$ such that $V(T, x, y) = V(0, x, y)$ for all $(x, y) \in U$.

Results and discussion

Let $\Phi(t; (x, y)) \subset U$ be the flow associated to $\bar{\mathcal{X}}$ with $\Phi(0; (x, y)) = (x, y) \in U$. Given a T -periodic orbit Γ of $\bar{\mathcal{X}}$, we consider $\Sigma \subset \mathbb{R}^2$, a transversal section to the flow of $\bar{\mathcal{X}}$ with one endpoint $p_0 \in \Gamma$. We parameterize $\Sigma = \{(\bar{x}(s), \bar{y}(s)) \in U : 0 \leq s \ll 1\}$ such that $p_0 = (\bar{x}(0), \bar{y}(0))$. Let $\mathcal{P} : \Sigma \rightarrow \Sigma$ be the *Poincaré map* associated to Γ , that is, $\mathcal{P}(s) = \Phi(\tau(s); (\bar{x}(s), \bar{y}(s)))$ where τ is the first time return function which is the unique function such that $\tau(0) = T$, the period of Γ , and $\Phi(\tau(s); (\bar{x}(s), \bar{y}(s))) \in \Sigma$. Clearly $\mathcal{P}(0) = 0$ and the orbit Γ is hyperbolic if $\mathcal{P}'(0) \neq 1$ where the prime indicates derivative with respect to s .

Our main result is the forthcoming Theorem.

THEOREM. Assume that there exists a T -periodic orbit $\Gamma \subset U \subset \mathbb{R}^2$ of the C^1 -vector field $\bar{\mathcal{X}}$ defined in U and let $\mathcal{P} : \Sigma \rightarrow \Sigma$ be its Poincaré map associated to a transversal section $\Sigma \subset U$ parameterized by $0 \leq s \ll 1$ where $s = 0$ indicates the point $\Sigma \cap \Gamma$. Let $V(t, x, y)$ be an inverse Jacobi multiplier of $\bar{\mathcal{X}}$ defined in $\mathbb{R} \times U$. Then

$$V(T, x, y) = V(0, x, y) \mathcal{P}'(0) \quad (3)$$

for any point $(x, y) \in \Gamma$.

Some related references are given below.

References

- [1] Berrone L.R. and Giacomini H (2003), Inverse Jacobi multipliers, *Rend. Circ. Mat. Palermo* (2) **52**, 77–130.
- [2] Buică A. and García I.A. (2015), Inverse Jacobi multipliers and first integrals for nonautonomous differential systems, *Z. Angew. Math. Phys.* **66**, 573–585.

The integral of the cofactor as a characterization of centers

Isaac A. García* and Jaume Giné*

*Departament de Matemàtica, Universitat de Lleida, Spain, ORCID # 0000-0001-6982-9632

Abstract. In this work we deal with analytic families of real planar vector fields \mathcal{X}_λ having a monodromic singularity at the origin for any $\lambda \in \Lambda \subset \mathbb{R}^p$. There naturally appears the so-called center-focus problem which consists in describing the partition of Λ induced by the centers and the foci at the origin. We give a characterization of the centers (degenerated or not) in terms of a specific integral of the cofactor associated to a real invariant analytic curve which always exists.

Introduction

We consider families of real analytic planar differential systems

$$\dot{x} = P(x, y; \lambda), \quad \dot{y} = Q(x, y; \lambda), \quad (1)$$

with parameters $\lambda \in \mathbb{R}^p$ together with its associate family of vector fields $\mathcal{X}_\lambda = P(x, y; \lambda)\partial_x + Q(x, y; \lambda)\partial_y$. Throughout the work we restrict the family to the parameter space $\Lambda \subset \mathbb{R}^p$ so that the origin $(x, y) = (0, 0)$ is made sure to be a *monodromic singularity* of the whole family (1). That means that $P(0, 0; \lambda) = Q(0, 0; \lambda) = 0$ and the local orbits of \mathcal{X}_λ turn around the origin for any $\lambda \in \Lambda$. In this monodromic scenario, Ilyashenko [3] and Écalle [1] show independently that the origin only can be either a center or a focus since \mathcal{X}_λ is analytic. We recall that a *center* possesses a punctured neighborhood (period annulus) foliated by periodic orbits of \mathcal{X}_λ while in a neighborhood of the *focus* the orbits spiral around it.

Main results

We prove the following results.

THEOREM 1. *Let \mathcal{X} be real analytic planar vector field with coprime components and having a monodromic singular point at the origin. Then there exists a real analytic invariant curve $F(x, y) = 0$ of \mathcal{X} with $F(0, 0) = 0$ and F having an isolated zero in \mathbb{R}^2 at the origin.*

Let $(p, q) \in W(\mathbf{N}(\mathcal{X}))$ be two weights associated to the Newton diagram $\mathbf{N}(\mathcal{X})$ of \mathcal{X} and perform the *weighted polar blow-up* $(x, y) \mapsto (\rho, \varphi)$ given by $(x, y) = \phi(\rho, \varphi) = (\rho^p \cos \varphi, \rho^q \sin \varphi)$ transforming (1) into the polar vector field $\dot{\rho} = R(\varphi, \rho)$, $\dot{\varphi} = \Theta(\varphi, \rho)$ and consider the differential equation

$$\frac{d\rho}{d\varphi} = \mathcal{F}(\varphi, \rho) := \frac{R(\varphi, \rho)}{\Theta(\varphi, \rho)} \quad (2)$$

well defined in $C \setminus \Theta^{-1}(0)$ being the cylinder $C = \{(\theta, \rho) \in \mathbb{S}^1 \times \mathbb{R} : 0 \leq \rho \ll 1\}$ with $\mathbb{S}^1 = \mathbb{R}/(2\pi\mathbb{Z})$.

Let $F(x, y) = 0$ be a real invariant analytic curve of \mathcal{X} with cofactor K , that is, $\mathcal{X}(F) = KF$. In weighted polar coordinates this equation is transformed into $\hat{\mathcal{X}}(\hat{F}) = \hat{K}\hat{F}$ where $\hat{\mathcal{X}} = \partial_\varphi + \mathcal{F}(\varphi, \rho)\partial_\rho$, $\hat{F} = F \circ \phi$ and \hat{K} is the cofactor of the curve $\hat{F} = 0$.

Let $\rho(\varphi; \rho_0)$ be the solution of the Cauchy problem (2) with initial condition $\rho(0; \rho_0) = \rho_0 > 0$ and small, and $\gamma_{\rho_0} = \{(\varphi, \rho(\varphi; \rho_0)) : 0 \leq \varphi \leq 2\pi\} \subset C$ an arc of orbit of (2). We define $\int_{\gamma_{\rho_0}} \hat{K} = PV \int_0^{2\pi} \hat{K}(\varphi, \rho(\varphi; \rho_0)) d\varphi$, where PV stands for the Cauchy principal value.

THEOREM 2. *Let \mathcal{X} be a family of analytic planar vector fields having a monodromic singular point at the origin and K the cofactor associated to an analytic invariant curve. Then $\int_{\gamma_{\rho_0}} \hat{K}$ exists and moreover the origin is a center if and only if*

$$\int_{\hat{\gamma}_{\rho_0}} \hat{K} \equiv 0 \quad (3)$$

for any initial condition $\rho_0 > 0$ sufficiently small.

The talk is extracted from a preprint [2] still not submitted to any journal.

References

- [1] J. Écalle, Introduction aux fonctions analysables et preuve constructive de la conjecture de Dulac. Actualités Mathématiques. Hermann, Paris, 1992.
- [2] García I.A and Giné J. (2022) Stability of degenerate monodromic singularities by its complex separatrices. Preprint. University of Lleida.
- [3] Yu.S. Il'yashenko, Finiteness theorems for limit cycles. Translated from the Russian by H. H. McFaden. Translations of Mathematical Monographs, **94**. American Mathematical Society, Providence, RI, 1991.

Parametric resonance caused by mass imbalance on railway wheels

Motoyoshi Shibata*, Junta Umemoto** and Hiroshi Yabuno *

*Mechanical System Laboratory, University of Tsukuba, Tsukuba, Japan

**East Japan Railway Company, Tokyo, Japan

Abstract. This study investigates the effect of mass imbalance of the wheelset. By employing a 2-DOF mathematical model, it is theoretically shown that the effect produces parametric resonance and decreases the critical speed of the hunting motion. Also, the theoretically predicted phenomena are experimentally observed by using a simple apparatus.

Introduction

In recent years, the dynamics of railway vehicles has been actively studied to improve their performance for safety and comfort. To this end, it is essential to clarify the factors behind various phenomena occurring in railway vehicles. For example, when a rail vehicle wheelset exceeds a certain running speed, it swaies from side to side. This resonance is well known as hunting motion that is a self-excited oscillation by non-conservative contact forces acting between the wheel and the rail [1]. The effects of wheel and brake disc mass imbalance and rail surface roughness on the dynamics have also investigated. Szabo and Lorant [2] analyzed the linearized equations of motion of a railway vehicle by taking into account a time-varying coefficient excitation term expressing the imbalance in the governing equations. It is numerically shown that the critical speed for hunting motion decreases with increasing the imbalance. However, the characteristic of the instability phenomenon has not analytically or experimentally investigated. In this presentation, we clarify that theoretically and experimentally. Figure 1 shows a single railway wheelset with 2-DOF model considering the lateral and yaw motions y and ψ . The equations of motion for the lateral and yaw motions are expressed as [3]

$$M \frac{d^2 y}{dt^2} + \frac{2\kappa_{yy}}{v} \frac{dy}{dt} + (2k_y + \frac{2Q\gamma}{d_0})y - 2\kappa_{yy}\psi = 0, \quad (1)$$

$$I \frac{d^2 \psi}{dt^2} + \frac{2d_0^2 \kappa_{xx}}{v} \frac{d\psi}{dt} + \frac{2d_0 \kappa_{xx} \gamma}{r_0} y + 2k_x d_1^2 \psi = 0, \quad (2)$$

where γ is tread angle which is assumed large, t is the time, v is the running speed, M is the wheelset mass, I is the wheelset momoent of inertia around the z -axis, d_0 is the half-track gauge, d_1 is the distance between support springs, r_0 is the centered wheel rolling radius, k_x , k_y , κ_{xx} , κ_{yy} are the longitudinal and lateral stiffness and creep coefficients, respectively, and Q is the wheel load.

Results and discussion

In order to understand the effects of imbalance and the qualitative non-linear characteristics on the post destabilized states, we consider the periodic changes in wheel load and creep coefficients and introduce the third order non-linear restoring force in the lateral direction as a representative nonlinear force into Eqs. (1) and (2). Then, we theoretically analyze the nonlinear equations of motion by using a reduction method and the method of multiple scales. As a result, we obtain the variation of the critical speed depending on the magnitude of imbalance and the steady state amplitude in the state where the speed is above the critical one. Furthermore, the theoretically predicted phenomena were experimentally confirmed by using a roller rig and a wheelset device.

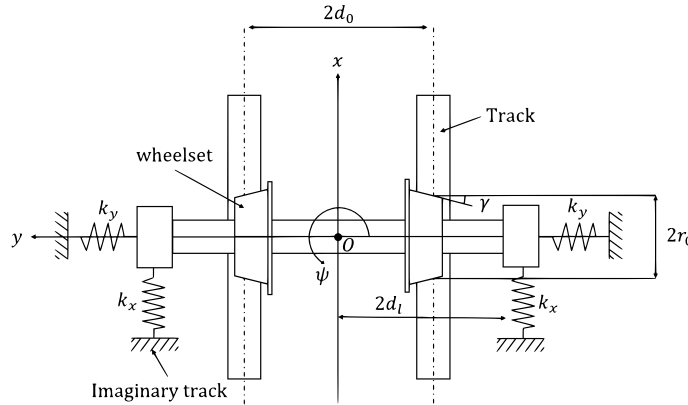


Figure 1: Two degree of freedom model of railway wheelset.

References

- [1] S. Iwnicki (2003) Simulation of wheel-rail contact forces, *Fatigue Fract. Eng. Mater. Struct.* **26**:887-900.
- [2] Z. Szabo, G. Lorant(2000) Parametric excitation of a single railway wheelset, *Veh. Syst. Dyn.* **33**:49-55.
- [3] K. Popp (1997) Parametric excitation of a wheelset, *ZAMM Z. angew. Math. Mech.* **77**:269-270.

Experimental and numerical analysis of a tube with clearance-induced impacts

Pau Becerra Zuniga^{a,b}, Sébastien Baguet^b, Benoit Prabel^{*}, Clément Grenat^c and Régis Dufour^b

^a Université Paris-Saclay, CEA, Service d'Études Mécaniques et Thermiques, 91191, Gif-sur-Yvette, France

^b Univ Lyon, INSA Lyon, CNRS, LaMCoS, UMR5259, 69621 Villeurbanne, France

^c Framatome, 92400 Courbevoie, France

Abstract. This contribution compares measurements and numerical calculations of the dynamics of a doubly clamped tube with clearance induced impacts. The response of the system is being measured at three points placed all along the tube. This measurements are then compared with the numerical results calculated with an algorithm that combines harmonic balance (HBM) and numerical pseudo arc length continuation (PAC).

Introduction

In pressurize water reactors, steam generators exchange the heat between primary and secondary circuit of the plant. Inside, a bundle of tightly packed U-shaped tubes (see Fig. 1) is used to move the hot primary coolant coming from the core. Meanwhile, an upwards stream develops outside the bundle as the secondary coolant interacts with the tubes. This configuration is reinforced with support plates all along the tubes to prevent them from large amplitude vibrations. While the presence of these supports serves its purpose, it also adds complexity when studying the vibration response of the U-tubes.

In this context, a comparison between the numerical and experimental results on a simplified example is presented : a double clamped tube in bending with a clearance placed in the middle point (as shown in Fig. 2) which will produce impacts in the tube when vibrating. The objective of this study is twofold : firstly, to bring to light the fact that even in the simplest examples (a tube with a single impact point), non linearity effects can be found (existence of multiple dynamic regimes) and therefore must be studied. And, secondly, to use a simple experiment to compare it with the numerical calculations carried out beforehand by the finite element software Cast3M [2], which permits testing a continuation algorithm currently in development. This algorithm uses harmonic balance and pseudo arc length continuation methods to predict the response of nonlinear mechanical systems and its development started within a previous thesis [1].

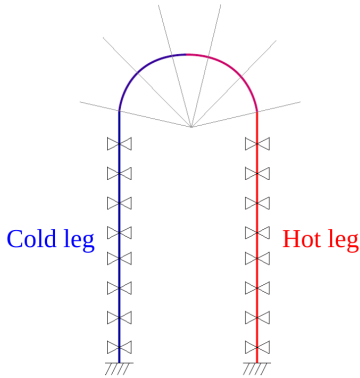


Figure 1: Single U-tube in Steam generator



Figure 2: Schematic representation of the experiment

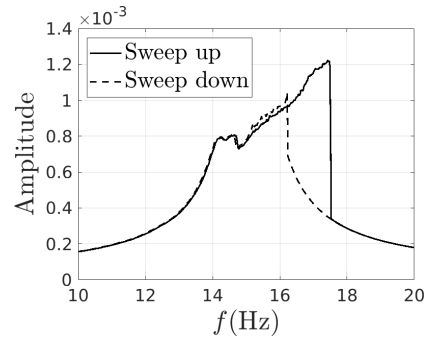
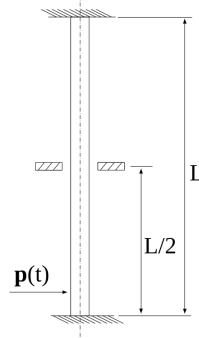


Figure 3: Frequency response at $2L/3$ height

Results and discussion

The experiment carried out consisted of a 2.6m long double clamped tube, with a symmetric central 1mm clearance and a shaker at the base (placed 0.3m from the base). This configuration allows us to change the position of the clearance in the tube section, being able to analyze the effect of the asymmetry on the system response. Accelerations have been measured in three different points placed all along the tube ($L/3$, $L/2$ and $2L/3$). In Fig. 3, it can be observed a frequency sweep up and down at the highest point of the tube. In this figure, a hysteresis effect on the amplitude of the response can be appreciated depending on the direction of the sweep. This phenomenon is characteristic from nonlinear mechanical systems, which gives birth to a range of frequencies where the system can vibrate with multiple amplitudes. Bifurcations due to symmetry breaking and sub-harmonic isolas will be studied both experimentally and numerically on this academic mock-up.

References

- [1] Alcorta Galvan, Roberto. (2021) Prediction of non-linear responses and bifurcations of impacting systems : Contribution to the understanding of steam generator vibrations. PhD thesis, Université de Lyon. <https://tel.archives-ouvertes.fr/tel-03406785/>
- [2] Cast3M, website <http://www-cast3m.cea.fr/>.

Shear-torsional nonlinear galloping of base-isolated continuous beams

Simona Di Nino^{*,**}, Angelo Luongo^{*,**}

^{*}International Center for Mathematics & Mechanics of Complex Systems, M&MoCS, University of L'Aquila, Monteluco di Roio (AQ), Italy

^{**}Department of Civil, Construction-Architectural and Environmental Engineering, University of L'Aquila, 67100 L'Aquila, Italy

Abstract. An equivalent one-dimensional visco-elastic beam model is proposed to study the aeroelastic behaviour of base-isolated tower buildings, subjected to a steady wind flow. The beam is internally constrained, so that it is capable to experience shear strains and torsion only. The system is constrained at the bottom end by a nonlinear visco-elastic device and free at the top end. The aeroelastic effects, responsible for self-excitation, are evaluated via the quasi-static theory, and the occurrence of Hopf bifurcation is detected. Critical and post-critical behaviour is analysed by applying a perturbation scheme. The influence of mechanical and aerodynamic coupling (between torsional and transversal vibrations) on the critical galloping conditions is investigated. Furthermore, the visco-elastic insulation system is calibrated to optimize the aeroelastic performances of the structure.

Introduction

Tall buildings are very sensitive to dynamic actions induced by wind, which causes a variety of instability phenomena. The aeroelastic analysis of multi-story buildings, when they are made of a sufficiently large number of floors, can be carried out by means of equivalent beam models, derived by suitable homogenization techniques (e.g., [1-3]). In particular, in [1] a shear-shear torsional beam model is formulated, by focusing the attention on the torsional and transversal coupling in galloping of fixed-free beams. In [2, 3], an insulation device is applied to the base of a planar (shear [2] or Euler-Bernoulli [3]) beam, to passively control galloping phenomena. Here, a continuous visco-elastic shear-torsional beam model, subjected to uniformly distributed steady wind flow, is formulated. A suitable visco-elastic device is interposed between the ground and the bottom of the beam, with the aim to mitigate the aeroelastic instability effects.

Model and results

An equivalent linear continuous shear-torsional beam model is used to describe the behavior of multi-story frame buildings. Aerodynamic forces and couples, distributed along the beam axis, are modeled in the framework of the quasi-steady theory. A passive control system is applied to the base of the beam, consisting of a viscoelastic device, made of a linear elastic spring and a nonlinear dashpot, assembled in parallel (Figure 1). Kinematics of the beam is assumed linear, and nonlinearities accounted for both in the aerodynamic forces and dashpot damping. Critical and post-critical behavior is analyzed by applying a perturbation scheme. In particular, the roto-translational galloping is investigated, with focus on the influence of the coupling between shear and torsion, according to the eccentricity between the torsional center and the centroid as well as the torsional-to-shear frequency ratio. Abrupt changes of the modal shape (torsional, translational or mixed) are observed when the torsional frequency is varied, together with a general increment of the critical wind velocity (when far from the resonant value). Finally, the parameters of the insulation system are properly calibrated to optimize the aeroelastic performances of the structure. The asymptotic results are validated via numerical time-integration of ordinary differential equations, derived via in-space finite differences.

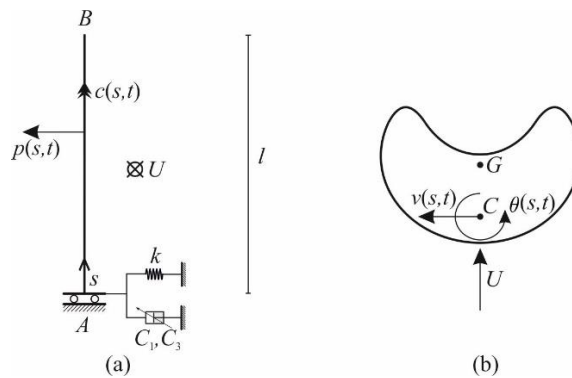


Figure 1: Base-isolated tall building under uniform steady wind flow: (a) beam model and external loading; (b) cross-section.

References

- [1] Piccardo G., Tubino F., Luongo A. (2015) A shear-shear torsional beam model for nonlinear aeroelastic analysis of tower buildings. *Z. Angew Math Phys* **66**: 1895–1913.
- [2] Di Nino S., Luongo A. (2020) Nonlinear aeroelastic behavior of a base-isolated beam under steady wind flow. *Int. J. Non-Linear Mech* **119**:103340.
- [3] Di Nino S., Luongo A. (2022) Nonlinear dynamics of a base-isolated beam under turbulent wind flow. *Nonlinear Dyn* **107**(2): 1529-1544.

Nonlinear vibration of an inextensible rotating beam

Lokanna Hoskoti* and Mahesh M. Sucheendran*

*Mechanical and Aerospace Engineering, Indian Institute of Technology Hyderabad, India - 502284

Abstract. An inextensible beam model is developed to study the nonlinear vibration of a rotating cantilever beam undergoing large deformation. General equations of motion governing the coupled axial-bending deformation are derived, and then inextensionality constraint is utilized to reduce two equations into one. The axial strain on the neutral fiber is decomposed into static and dynamic components and the extension due to the dynamic part is assumed to be zero. Nevertheless, the static strain, which is obtained from the solution of the steady-state axial displacement equation, is retained in the equation governing the planar motion of the beam. The method of multiple scales is adopted to derive the expression for frequency response and modulation equations for the first vibration mode. The results show that the first mode exhibits a hardening type of nonlinearity for lower rotation speeds and softens at higher rotational speeds.

Introduction

Rotating structures have many applications, such as wind turbines or helicopter blades, blades in gas turbine engines or turbo propeller blades in mechanical or aerospace engineering. Numerous authors have published papers on the dynamic analysis of a rotating blade idealized using simplified one-dimensional analytical models based on Euler-Bernoulli and Timoshenko beam theories with varying levels of complexity in geometry [1, 2]. A straight beam attached to a hub, rotating at an angular velocity, undergoing large deformation is considered in the present study. An inextensible model for a rotating beam under the harmonic excitation of frequency, ω , and magnitude, F , can be derived using the inextensionality constraint as [3]

Where, w and r are transverse displacement and hub radius nondimensionalized using the beam length. Ω is angular speed non-dimensionalised using the time, $t = \sqrt{\frac{\rho AL^4}{EI}}$

Results and discussion

The results are presented for the beam with slenderness ratio, $\sqrt{AL^2/I} = 693$, hub ratio, $r = 0.1$. The beam is made of homogeneous material with Young's modulus $E = 104$ GPa and density $\rho = 4400$ kg/m³ (order of magnitude of a Titanium alloy) [4]. The backbone curves of the fundamental mode of a rotating beam are plotted in Fig. 1. Each point in the backbone curve is the peak value of the frequency response curve at a given value of rotation speed and various magnitudes of excitation.

It is found that the rotation-induced nonlinearity significantly affects the beam's nonlinear dynamics.

There exists a critical rotation speed above which the nonlinearity of the first mode becomes softening, and it is hardening below.

References

- [1] Hodges D., Rutkowski M. (1981) Free-vibration analysis of rotating beams by a variable-order finite element method, *AIAA J.* **19**(11):1459-1466.
- [2] Yang J., Jiang L., Chen D., (2004) Dynamic modelling and control of a rotating Euler-Bernoulli beam, *J. Sound Vib.* **274**: 863-875.
- [3] González-Carbajal J., Rincón-Casado A., García-Vallejo D., Domínguez J., (2022) Nonlinear solutions for the steady state oscillations of a clamped-free rotating beam, *Eur. J. Mech. A/Solids.* **91** : 104413.
- [4] Thomas O., S  n  chal A., De   J.-F., (2016) Hardening/softening behavior and reduced order modeling of nonlinear vibrations of rotating cantilever beams, *Nonlinear Dyn.* **86**:1293-1318.

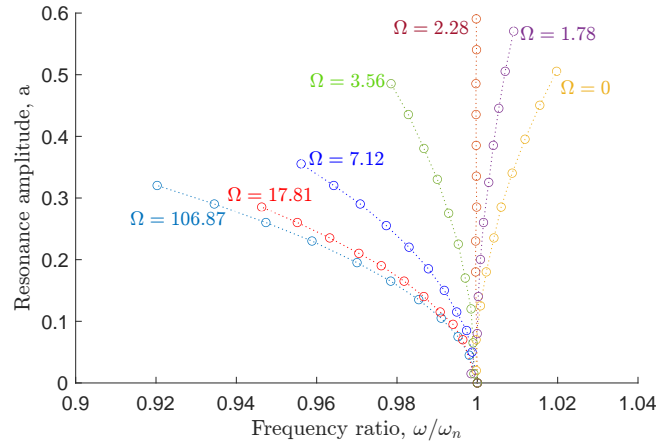


Figure 1: Backbone curves of the fundamental mode.

Synchronization based on intermittent sampling: PWL multiscroll system

José Luis Echenausía Monroy* and Jonatan Pena Ramirez*

*Applied Physics Division, Center for Scientific Research and Higher Education at Ensenada, CICESE. Carr. Ensenada-Tijuana 3918, Zona Playitas, Ensenada, 22860, B. C., Mexico,
ORCID: 0000-0001-5314-3935 (echenausia@cicese.mx), 0000-0001-8453-6694 (jperez@cicese.mx)

Abstract. This paper addresses the optimization of resources for the synchronization of chaotic multi-scrolls Piece-Wise Linear (PWL) systems. Considering intermittent coupling, where the system alternates between coupling and free oscillation, the ability of the system to maintain a synchronous state under the premise of data loss is analyzed. The results obtained represent favorable scenarios, in which the system is able to maintain synchrony with unidirectional coupling in the presence of a reduction in available samples of up to 90%.

Introduction

The literature contains work that uses synchronization techniques based on the fact that coupling is not always active in the system. For example, [1] shows that there are regions where a pair of chaotic oscillators should theoretically remain synchronous, but their response is temporarily interrupted, affecting the collective dynamical response. In [2], its consider a digital function that enables and disables coupling between systems. Recently, the study of systems based on the reduction of available information has gained the attention of the scientific community. The goal is to address two important issues: i) to make control techniques more efficient in creating algorithms and implementations that can have inactive states, and ii) to obtain much more robust systems [3], where the loss of information do not reduce the overall performance of the dynamic agent. This paper analyzes the ability of a unidirectional system based on two multi-scroll systems using a Piece Wise Linear (PWL) function as a nonlinearity to maintain complete synchronization, by periodically activating and deactivating the coupling. The synchronization errors between the systems are calculated and the periods of information loss are varied along with the strength of the coupling to find the optimal parameters at which the system converges to the desired state with the least amount of information possible.

Results and Discussion

The onset of complete synchronization in the coupled systems is studied by calculating the synchronization index S , which takes into account the synchronization error and the Pearson correlation between the state variables of the driving and driven systems, as in [4]. Using this method, it is possible to study the effects of creating larger intervals, in which the coupling strategy loses information versus the effects of increasing the coupling force. The obtained results show that there is a pair of parameters (number of samples and coupling force) for which the driven system is able to maintain complete synchronization even when the coupling strategy has lost more than 90% of the capable information. This important result shows that oscillatory systems based on PWL functions do not necessarily need to maintain constant communication between agents to oscillate in unison. Moreover, if this is translated into a communication scheme, the obtained results would allow significant communication loss, or abrupt interruption of the same due to the detection of a possible attack, while maintaining the synchronous state.

References

- [1] Gauthier, D. J., & Bienfang, J. C. (1996). Intermittent loss of synchronization in coupled chaotic oscillators: Toward a new criterion for high-quality synchronization. *Physical Review Letters* **77**(9) 1751.
- [2] Njougouo, T., Simo, G. R., Louodop, P., Fotsin, H., & Talla, P. K. (2020). Effects of intermittent coupling on synchronization. *Chaos, Solitons & Fractals* **139** 110082.
- [3] Modares, H., Kiumarsi, B., Lewis, F. L., Ferrese, F., & Davoudi, A. (2019). Resilient and robust synchronization of multiagent systems under attacks on sensors and actuators. *IEEE transactions on cybernetics* **50**(3) 1240-1250.
- [4] Echenausía-Monroy, J. L., Ontañón-García, L. J., & Ramirez, J. P. (2021). On Synchronization of Unidirectionally Coupled Multi-Scroll Systems: Dynamic vs Static Interconnections. *IFAC-PapersOnLine* **54**(17) 53-58.

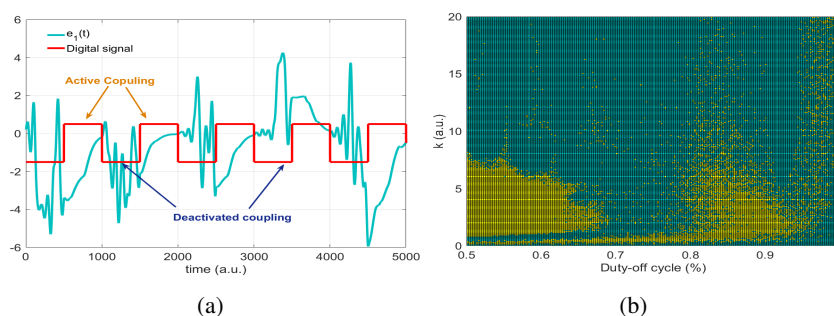


Figure 1: (a) Temporal behavior of the synchronization error of state x_1 and the activation function for the coupling between the systems. (b) Map of synchronization index obtained for $\alpha = 0.45$, #Samples=600, changing the duty-off cycle of the coupling. Yellow indicates synchronization.

Properties of a two parameter logistic map with delay

Akshay Pal*, Jayanta kumar Bhattacharjee *

*School of Physical Sciences, Indian Association for the Cultivation of Science, Jadavpur, Kolkata, India

Abstract. Logistic maps with delay (memory) have their origin in the effort [1] to discretize the integro-differential equations of non-equilibrium statistical mechanics. Buchner and Zebrowsky [2] studied it as a generic system. Their relevance in the field of economics has been established by Tarasova and Tarasov [3]. In this work , we point out that a class of infectious disease (eg. COVID-19) provide a source of a two parameter logistic map with delay. We analyze these maps to look at their fixed points, their stabilities and their transition to chaotic dynamics.

Introduction

We focus on a class of highly infectious disease where the infected person does not show any symptoms for the first few days. Such persons will be inadvertent spreaders of the disease for a number(τ) of days before they are quarantined. Following the differential equation approach [4], the rate of change of the number of infected people I_n on the n-th day will be proportional to $I_n - I_{n-\tau}$ and to the fraction of susceptible people which is $1 - I_n/N = 1 - X_n$. Assuming the total population N consists of only the infected and the uninfected but susceptible and a few of infected people are quarantined because of secondary factors we arrive at the model dynamics

$$X_{n+1} = \alpha X_n + \beta(X_n - X_{n-\tau})(1 - X_n) \quad (1)$$

This is our two parameter logistic map with delay. It has only one fixed point $X^* = 0$. The instability condition for $\tau = 1$ and $\tau = 2$ are given by:

$$\text{Instability region for } (\tau = 1) = \{(\alpha > 1) \cup (\beta > 1) \cup (\alpha + 2\beta + 1 < 0)\} \quad (2)$$

$$\text{Instability region for } (\tau = 2) = \{(\alpha > 1) \cup (\alpha < -1) \cup (2\beta^2 + \alpha\beta > 1)\} \quad (3)$$

Period doubling and onset of chaos with some variations is frequently seen when $\tau = 1$. For $\tau = 2$, we find extended period -3 regions. Alternating chaotic and periodic zones are common.

Results and Discussion

The thing to note in Fig 1.a ($\tau = 1$) is the complication following the onset of period 4. One sees the emergence of two chaotic bands and the re-emergence of the period 4 state and eventually the onset of chaos over an extended interval. In Fig 1.b ($\tau = 2$), the instability of the fixed point leads to a patterned response between two unstable fixed points characterized by avoided zones (white traces) and then the two unstable fixed points give way to a stable period three state which survives over an extended range of parameter space.

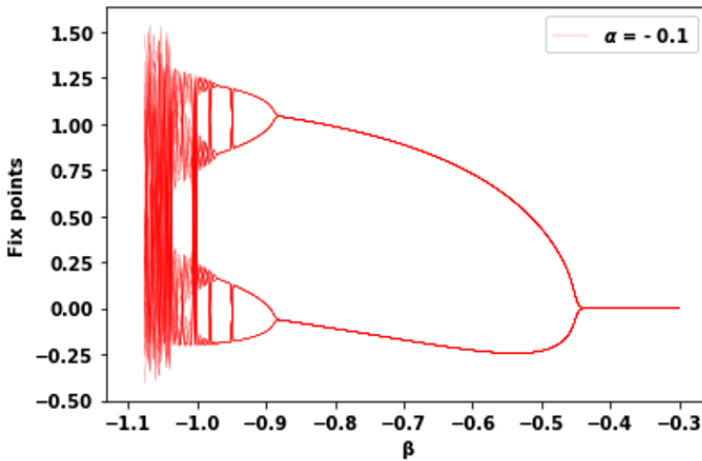


Fig 1.a: $\tau = 1, \alpha = -0.1$

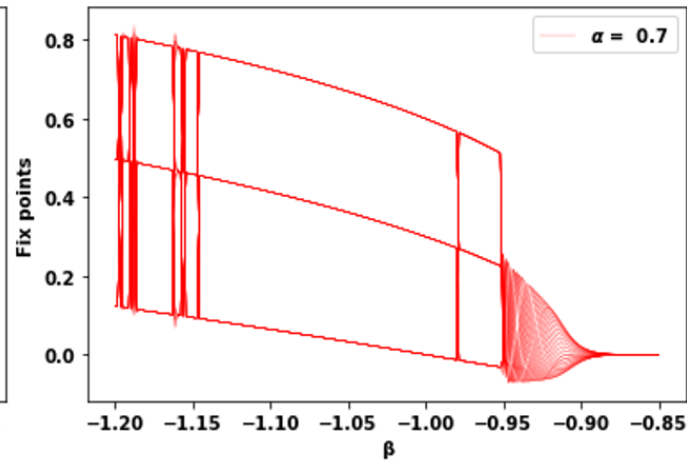


Fig 1.b: $\tau = 2, \alpha = 0.7$

References

- [1] A.Fulinski and A S Kleczkowski, Nonlinear Maps with Memory (1987) *Phys. Scr.* **35** 119
- [2] T.Buchner and J.J.Zebrowski, Logistic map with a delayed feedback (2000) *Phys Rev E* **63**, 016210
- [3] V.V.Tarasova and V.E.Tarasov, Logistic map with memory from economic model (2017) *Chaos, Solitons and Fractals* **955** 84
- [4] B Shayak and M M Sharma, A new approach to the dynamic modeling of an infectious disease (2021) *Math.Model.Nat.Phenom.* **16** 33
- [5] M.Kreck and E.Scholz, Bull, A Discrete Kermack–McKendrick Model Adapted to Covid-19 (2022) *Math.Bio.* **84**,44

Data-driven bifurcation analysis using a parameter-dependent trajectory

Jesús García Pérez^{*,**}, Amin Ghadami^{**}, Leonardo Sanches^{*}, Guilhem Michon^{*} and Bogdan I. Epureanu^{**}

^{*} *Department of Mechanics, Université de Toulouse, ICA, CNRS, ISAE-Supaéro, Toulouse, France*

^{**} *Department of Mechanical Engineering, University of Michigan, MI, USA*

Abstract. Identification of bifurcation diagrams in nonlinear systems is of great importance for resilient design and stability analysis of dynamical systems. Data-driven identification of bifurcation diagrams has a significant advantage for large dimensional and experimental systems where accurate system equations are not available. In this work, a novel forecasting approach to predict bifurcation diagrams in nonlinear systems is presented using a single trajectory of system dynamics before instabilities occur. Unlike previous techniques, the proposed method considers a varying bifurcation parameter during the same system recovery. This method is a hybrid approach that combines an asymptotic analysis provided by the method of multiple scales and a data-driven forecasting technique. Using the proposed approach allows stability analyses of nonlinear systems with limited access to experimental or surrogate data.

Introduction

Analyzing bifurcation diagrams is a significant challenge because the characterization of the post-bifurcation regime using traditional methods is a difficult task, particularly for large dimensional systems and structures. While time integration requires calibrated models and large computational costs, data-driven bifurcation analysis techniques appear as a potential alternative. In this context, Epureanu and Lim [1] proposed a technique to predict and construct bifurcation diagrams using measurements of system dynamics at several control parameters before instability occurs. This technique is based on the critical slowing down phenomenon (CSD) observed in nonlinear systems approaching certain types of instabilities including Hopf bifurcations. The forecasting technique has shown a significant advantage in predicting bifurcation diagrams such as large dimensional aeroelastic systems [2]. However, this method requires several recoveries at different constant flow speeds to predict the post-flutter dynamics. To overcome this limitation, we propose a hybrid forecasting method combining the bifurcation forecasting method and the method of multiple scales (MMS). The proposed forecasting approach uses the asymptotic analysis of the MMS to obtain a general normal form of the bifurcation for a system with general nonlinearities. The approximated normal form allows capturing the CSD as the bifurcation parameter varies during the system recovery. In consequence, the multiple recoveries requirement is leveraged.

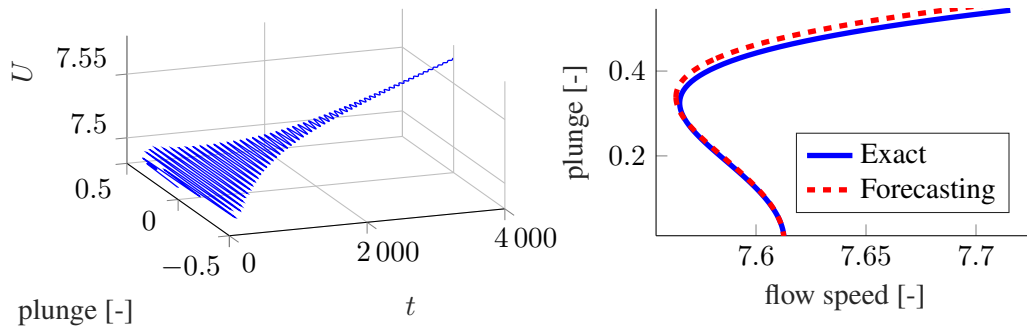


Figure 1: System recovery from perturbation with time varying flow speed (left) and exact and forecasted bifurcation diagram with one recovery forecasting for subcritical bifurcation (right)

Results and discussion

The proposed technique is applied to predict the bifurcation diagram of a typical pitch-plunge aeroelastic section exhibiting Hopf bifurcations. After applying a perturbation to the system, the flow speed is varied linearly from 97 to 99 % of the linear flutter speed to generate a trajectory. Figure 1 shows the single system recovery from perturbation (left) used to forecast the bifurcation diagram for the non-dimensional plunge (vertical displacement) for a subcritical Hopf bifurcation of the pitch-plunge airfoil (right). Results show that the approximated diagrams match the reference diagrams in both supercritical and subcritical cases despite the fact that only a single trajectory is used to predict and construct the diagrams. The proposed approach not only leverages the requirement of multiple measurements to forecast the bifurcation but also can provide early warnings of imminent instabilities as the flow speed is increased and the system is perturbed.

References

- [1] Lim, J., Epureanu, B. I. (2011) Forecasting a class of bifurcations: Theory and experiment. *J. Phys. Rev. E* **83**:016203.
- [2] Ghadami, A., Epureanu, B. I. (2018) Forecasting critical points and post-critical limit cycles in nonlinear oscillatory systems using pre-critical transient responses. *Int. J. Non-Linear Mech* **101**:46–156

Investigating the Stability of a Strongly Nonlinear Structure Through Shaker Dynamics in Fixed Frequency Sine Tests

E. Robbins¹, F. Moreu¹

¹Department of Civil, Construction, and Environmental Engineering, University of New Mexico, Albuquerque, NM 87131, USA

Abstract. Recent research has demonstrated developments to apply experimental continuation using the force dropout phenomena and fixed frequency voltage control sine tests to stabilize a nonlinear system through shaker dynamics. This approach has been demonstrated to stabilize the unstable response of a strongly nonlinear system near resonance. Recent fixed frequency voltage control tests on a strongly nonlinear system with a vibro-impact nonlinearity has revealed unexpected jumping behavior, like that seen during force controlled swept and stepped sine testing. In this research, the stabilizing effects of an electromechanical shaker coupled to a strongly nonlinear structure are investigated in fixed frequency voltage control tests using both numerical and experimental methods.

Introduction

Common experimental force control methods used for nonlinear dynamical testing such as stepped and swept sine testing often leads to imperfect quality in the control parameter and or bifurcations leading to the so-called jump-down or jump-up phenomena between stable solutions. Control algorithms such as control-based continuation [1] and phase-locked loop [2] have been used to control through the turning point bifurcations during nonlinear testing to measure the unstable branch which is of interest for model validation and calibration. Recent research has demonstrated the successful development of a sine testing method to obtain the unstable portion of the multivalued response curves of strongly nonlinear systems utilizing open-loop voltage control [3]. The purpose of this study is to investigate and identify the stabilizing parameters of an electromechanical shaker coupled to a nonlinear structure in numerical and experimental tests by utilizing the force drop-out phenomena in fixed frequency voltage control tests demonstrated in [3].

Results and Discussion

The numerical results suggested that there were various stabilizing parameters in the electromechanical shaker. However, the back electromotive force on the shaker produced by the relative velocity of the shaker body and armature was the one variable that strongly influenced the stabilizing effect of the shaker. The stabilizing effect from this parameter was also observed in experimental testing on a strongly nonlinear system suggesting there was strong corroboration between the numerical and experimental results. This study will help understand the stability of nonlinear systems that are coupled to electromechanical shakers.

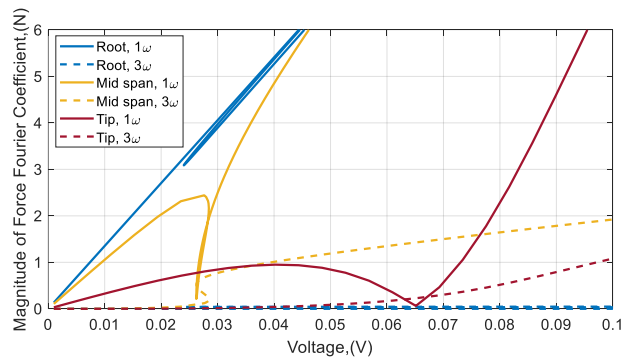


Figure 1. Parametric study revealing unstable and stable behaviors from different shaker drive points on a nonlinear beam

References

- [1] Bureau E., Schilder F., Santos I. F., Thomsen J. J., Starke J. (2013) Experimental bifurcation analysis of an impact oscillator—Tuning a non-invasive control scheme. *J. Sound and Vibration* **332**:5883-5897
- [2] Denis V., Jossic M., Giraud-Audine C., Chomette B., Renault A., Thomas O. (2018) Identification of nonlinear modes using phase-locked-loop experimental continuation and normal form. *Mechanical Systems and Signal Processing* **106**:430-452
- [3] Zhang G., Zang C., Friswell M. I., (2020) Measurement of multivalued response curves of a strongly nonlinear system by exploiting exciter dynamics. *Mechanical Systems and Signal Processing*, **140**:106474-106489

Hopf Bifurcation Analysis of the BVAM Model for Electrocardiogram

Ahsan Naseer *, Imran Akhtar* and Muhammad R. Hajj **

* College of Electrical and Mechanical Engineering (CEME), National University of Sciences and Technology (NUST) Islamabad

** Department of Civil, Environmental and Ocean Engineering, Davidson laboratory, Stevens Institute of Technology, 711 Hudson St, Hoboken, NJ 07030, USA

Abstract. Bio-electric activity of heart is modeled by the Barrio-Varea-Aragon-Maini (BVAM) Model. This model covers normal rhythm and several arrhythmia that lie in the chaotic region and exhibits several bifurcations, starting from a fixed-point bifurcation leading to chaotic region. Analytic solution of the BVAM model is developed in the local region to Hopf bifurcation. Center manifold reduction is applied to the governing equations to reduce the order of the system. The Method of Multiple scales is used on the center manifolds to develop normal form of the Hopf bifurcation for the center manifolds. These are then transformed back into original coordinates where the analytical solution is compared with the numerical solution.

Introduction

Heart disease is one of the leading causes of death in the world. Electrocardiograms (ECG) are time series signals used to inspect the activity of heart. There are various mathematical models that reproduce these ECG signals. A primitive model was developed by van der Pol [1] by coupling simple ordinary differential equations (ODE), which produces a signal that closely matches the sinus rhythm of ECG signal. Since then, several other models that capture normal sinus rhythm of the heart and arrhythmia [2] have been proposed. These ODEs are complex in nature and provide insight [3]. One such equation is the Barrio-Varea-Aragon-Maini (BVAM) model, which is obtained from generic reaction-diffusion system describing various patterns observed in biological and chemical systems [4, 5]. Recently this model was used for producing ECGs of normal sinus rhythm and arrhythmia [6].

In the present study, nonlinear analysis is performed on BVAM model that represents the bio-electric activity if the heart to identify bifurcation points. For one of the control parameters, Hopf bifurcation is determined and analytical solution is obtained using the Method of Multiple Scales. Normal forms of Hopf bifurcations are also determined which show the variation of amplitude against a single control parameter.

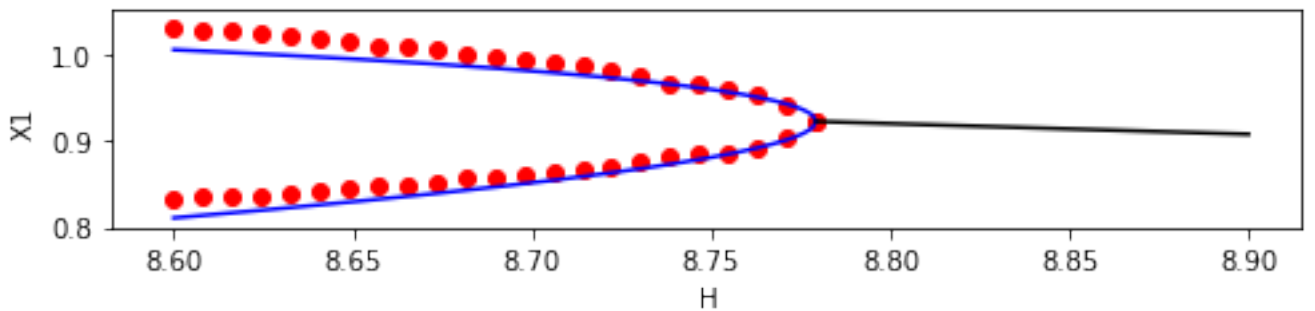


Figure 1: Amplitude Response Curve for one of the state variables x_1 against control parameter H , Stable Fixed Points [Black Solid line], Analytic Periodic Solution [Blue Solid line], Numerical Periodic Solution [Red dots]

Results and Discussion

We find two stable and one unstable fixed-points prior to Hopf bifurcation point. The two stable fixed-point solutions become unstable at Hopf bifurcation and a periodic solution emerges from the point of bifurcation for one of the state variables as shown in figure (1). Analytical solutions are obtained for these bifurcation points.

References

- [1] van der Pol et al. (1928) The heartbeat considered as a relaxation oscillation, and an electrical model of the heart. *Lond. Edinb. Dublin philos. mag. j. sci.* **6**:763-775.
- [2] Ryzhii et al. (2014) A heterogeneous coupled oscillator model for simulation of ECG signals. *Comput Methods Programs Biomed* **117**:40-49.
- [3] dos Santos et al. (2004) Rhythm synchronization and chaotic modulation of coupled Van der Pol oscillators in a model for the heartbeat. *Physica A Stat. Mech. Appl.* **338**:335-355.
- [4] Barrio et al. (1999) A two-dimensional numerical study of spatial pattern formation in interacting Turing systems. *Bull. Math. Biol.* **61**:483-505.
- [5] Woolley et al. (2010) Analysis of stationary droplets in a generic Turing reaction-diffusion system. *Phys. Rev. E* **82**:051929.
- [6] Quiroz-Juárez et al. (2019) Generation of ECG signals from a reaction-diffusion model spatially discretized. *Sci. Rep.* **9**:1-10.

Bistability in pressure relief valve dynamics

Fanni Kadar* and Gabor Stepan**

*, ** Department of Applied Mechanics, Budapest University of Technology and Economics, Budapest, Hungary,
* 0000-0001-8667-6914 #, ** 0000-0003-0309-2409 #

Abstract. The vibrations of pressure relief valves hinder the discharging process, thus, this phenomenon must be avoided. The vibrations emerge via Hopf bifurcations, which can be either super- or subcritical. The latter case involves bistable regions and hysteresis effect. The nonlinear analysis is essential for the exploration of the safe parameter zones. Bifurcation analysis is provided in a wide range of parameters comparing analytical, semi-analytical and numerical results.

Introduction

Direct spring operated pressure relief valves protect systems from unsafely high pressure. Despite the crucial safety role, harmful valve vibrations can emerge during operation leading to an insufficient discharge speed and noise. The dimensionless mathematical model of a valve connected to a vessel is already provided in the literature [1, 2] with the state variables y_1 , y_2 and y_3 (see Fig. 1 left):

$$\dot{y}_1 = y_2, \quad \dot{y}_2 = -2\zeta y_2 - (y_1 + \delta) + y_3, \quad \dot{y}_3 = \beta(q - y_1\sqrt{y_3}). \quad (1)$$

Hopf bifurcations were detected with either supercritical or subcritical characteristics, however, detailed analysis can not be found in the literature in view of the wide range of the parameter combinations. This work aims at revealing the safe parameter domains of system stiffness β , damping ratio ζ and dimensionless inlet flow rate q for fixed value of the set pressure δ . In order to guarantee the safe operation, not only the stability boundaries and the type of the Hopf bifurcations have to be determined but also the bistable solutions are to be indicated.

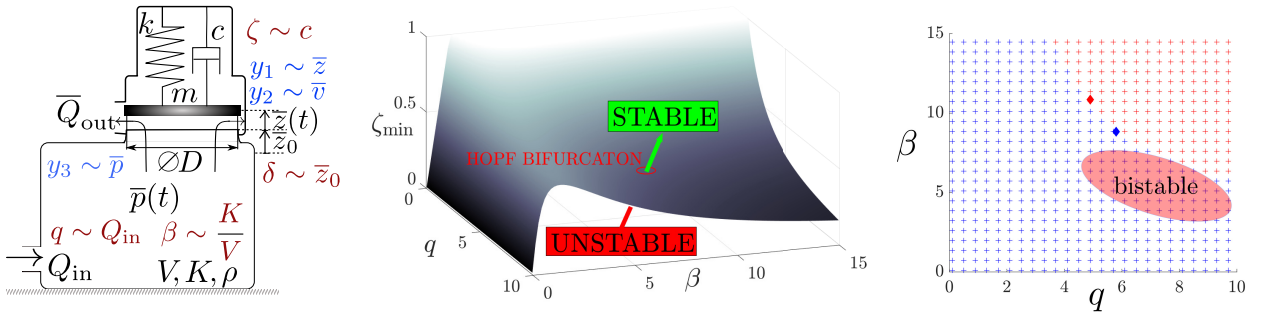


Figure 1: Mechanical model, dimensionless state variables and parameters (left), result of the linear stability analysis (middle), result of the nonlinear analysis (right)

Methods and results

As the result of the linear stability analysis, the Hopf bifurcation points define a surface in the parameter space (q, β, ζ) shown in Fig. 1 in the middle, where the stable parameter combinations are above the surface ($\zeta > \zeta_{min}$). Operation with $\zeta > \zeta_{min}$ still cannot prevent vibrations, because in case of the subcritical Hopf bifurcations, an unstable limit cycle surrounds the stable equilibrium restricting the extent of the basin of attraction. This phenomenon leads to bistable solutions that mean coexisting stable equilibrium and stable periodic orbit. In Fig. 1 on the right, a bifurcation type map is shown in the (q, β) plane for the bifurcation points at ζ_{min} by means of DDE Biftool. Blue crosses refer to the supercritical Hopf bifurcations and red crosses show the subcritical ones. The map was checked also analytically with the help of the Hopf bifurcation calculation including centre manifold reduction; this is illustrated by diamonds. Bifurcation diagrams were used to detect fold bifurcations in the limit cycle branches, which can create a globally subcritical characteristic even if the local characteristic is supercritical. The bifurcation diagrams were produced with continuation method, by analytical Hopf calculations, and from simulations by Runge-Kutta method. The location of these possible bistable solutions are also illustrated in the right panel of Fig. 1. In conclusion, the stable domains bounded by supercritical stability boundaries without folds are located in the domain of relatively small values of q and β , moreover the minimal damping ratio can be as high as an external damping is necessary for safe operation.

References

- [1] Hős C., Champneys A.R. (2012) Grazing bifurcations and chatter in a pressure relief valve model. *Physica D* **241**:2068-2076.
- [2] Kadar F., Hős C., Stepan G. (2022) Delayed oscillator model of pressure relief valves with outlet piping. *J Sound Vib.* **534**:117016.

Mirroring of synchronization in multilayer configuration of Kuramoto oscillators

Dhrubajyoti Biswas^{a,b} and Sayan Gupta^{b,c}

^aDepartment of Physics, Indian Institute of Technology Madras, Chennai, India 600036

^bThe Uncertainty Lab, Department of Applied Mechanics, Indian Institute of Technology Madras, Chennai, India 600036

^cComplex Systems and Dynamics Group, Indian Institute of Technology Madras, Chennai, India 600036

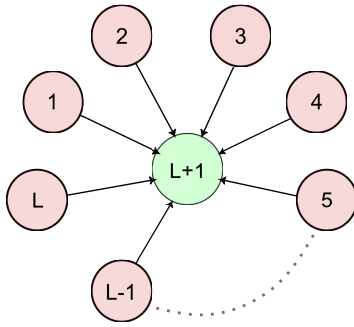
Abstract. In certain dynamical systems, a phenomena is observed where emergent dynamical behavior in one part of the system is seen to propagate into another part that is only weakly coupled to the first. This can be defined as *mirroring*. To model this, we propose a multilayer system of globally coupled Kuramoto oscillators with $(L+1)$ layers, with the first L layers being the master layers, all of which drive the $(L+1)^{\text{th}}$ layer, which is the slave layer. It implies that the dynamics of the $(L+1)^{\text{th}}$ layer is not only determined by it's own properties but also affected by each of the L master layers, which leads to the phenomena of mirroring. The properties of this model is investigated and results for mirroring in the slave layer is derived for different values of L as a function of other system parameters and verified using simulations.

Introduction

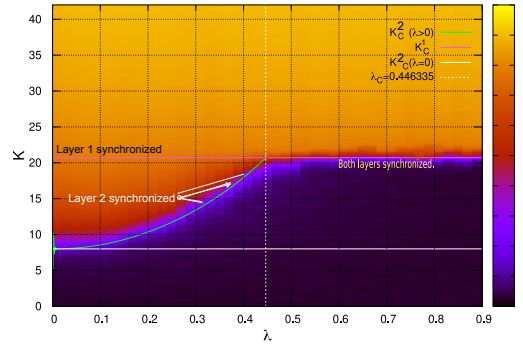
In this work, we investigate a multilayer network of globally coupled Kuramoto oscillators with $(L+1)$ equally populated layers. The layers from 1 to L represent the independent master layers, whereas the $(L+1)^{\text{th}}$ layer represents the slave layer (see Fig.(1a)). The dynamics of the slave layer depends not only on it's own properties but also on the unidirectional interlayer coupling that exists with all the master layers. Here, the focus is on “mirroring”, where dynamical phenomena (like synchronization) in the master layers is *mimicked* in the slave layer and we derive the conditions for it's occurrence. The dynamics of each master layer is governed by the globally coupled Kuramoto model [1], whereas the dynamics of the slave layer is described by

$$\dot{\phi}_i^{(L+1)} = \sum_k \lambda^{(k)} \left[\omega_i^{(k)} + \frac{K}{N} \sum_j \sin(\phi_j^{(k)} - \phi_i^{(k)}) \right] + \left(1 - \frac{1}{L} \sum_k \lambda^{(k)} \right) \left[\omega_i^{(L+1)} + \frac{K}{N} \sum_j \sin(\phi_j^{(L+1)} - \phi_i^{(L+1)}) \right]$$

for $i, j = 1, 2, \dots, N$ and $k = 1, 2, \dots, L$. Here, $\phi_i^{(l)}$ and $\omega_i^{(l)}$ denotes the phase and natural frequency respectively of the i^{th} oscillator in the l^{th} layer, $\lambda^{(l)}$ quantifies the contribution of the l^{th} master layer to the slave layer, K denotes the global coupling strength and N is the number of oscillators per layer.



(a) Topology (nodes \rightarrow layers)



(b) Variation of $r^{(2)}$ as a function of (K, λ)

Figure 1

Results and Discussions

Preliminary results are obtained for $L=1$ where we compute the synchronization order parameter [1] of the slave layer (say, $r^{(2)}$) as a function of both K and $\lambda=\lambda^{(1)}$ (see Fig.(1b), [2]) for a generalized Cauchy distribution of natural frequencies [3] with different shape and scale factors. A sharp boundary in the color map is observed, denoting the value of $K=K_C^{(2)}$ for which the slave layer transitions to partial synchronization. $K_C^{(2)}$ follows a non-linearly increasing function in the range of $\lambda \in (0, \lambda_C]$, the analytical expression [2] for which is plotted as a green solid line showing fair agreement with numerical simulations. For $\lambda > \lambda_C$, $K_C^{(2)}$ becomes constant at $K_C^{(2)}=K_C^{(1)}$, thus indicating mirroring. Generalization of these results for $L>1$ are currently in progress.

References

- [1] Juan A Acebrón, Luis L Bonilla, Conrad J Pérez Vicente, Félix Ritort, and Renato Spigler. The kuramoto model: A simple paradigm for synchronization phenomena. *Reviews of modern physics*, 77(1):137, 2005.
- [2] Dhrubajyoti Biswas and Sayan Gupta. Mirroring of synchronization in a bi-layer master–slave configuration of kuramoto oscillators. *Chaos: An Interdisciplinary Journal of Nonlinear Science*, 32(9):093148, 2022.
- [3] Per Sebastian Skardal. Low-dimensional dynamics of the kuramoto model with rational frequency distributions. *Phys. Rev. E*, 98:022207, Aug 2018.

Dynamical analysis of spread of online misinformation and a delayed optimization technique

Moumita Ghosh*, Pritha Das*

*Department of Mathematics, Indian Institute of Engineering Science and Technology, Shibpur, India, ORCID
<https://orcid.org/0000-0001-5859-3943#>

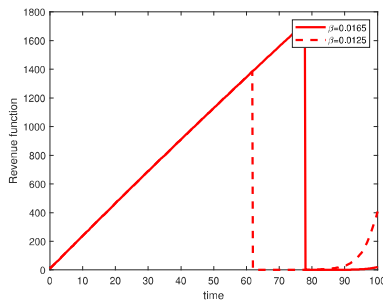
*Indian Institute of Engineering Science and Technology, Shibpur, India, #

Abstract. The Spread of online misinformation has momentous impact on people's daily life. Nowadays with advent of various social media platforms, the twisted news targeting the public opinion have started to disseminate significantly fast and in wide scale. Sometimes it really induces panic or influences mass perception [1, 2] that demands to study the dynamics of rumor spread [3, 4]. On the basis of attitudes of netizens toward misinformation, here we have proposed a delayed Susceptible-Exposed-Infected-Recovered (SEIR) model to study the dynamics of propagation of misinformation, considering four categories of netizens, namely, ignorant population (people, who are still uninformed of the misinformation), exposed population (who have encountered misinformation, believed it and pass it to lesser number of people), active spreaders (who create and deliberately spread misinformation on internet among large number of people having some vested personal or group interest), aware (people who are aware about the misinformation, do not spread and ask others not to spread). Here the delay is incorporated to signify that the online misinformation usually lacks credibility and it takes time to persuade netizens to believe it or circulate it to others. Next the critical value of the spread of misinformation (spreading threshold, \mathcal{R}_0) is derived, that gives the condition of prevalence of misinformation. With the help of \mathcal{R}_0 , we analyze the local stability dynamics for the corresponding non-delayed system. For the delayed system, the system bifurcates from its stable condition, when the time delay crosses a certain value. Also the streaming rate of misinformation destabilizes the system when it reaches its threshold value. To counter misinformation and inhibit its spreading process, an optimization technique with the help of mainstream media is formulated and solved by Pontryagin's maximum principle with constant delay. We use mainstream media as it easily reaches a large number of people and is efficient to control misinformation by promoting logical explanation behind it or broadcasting authentic news. Finally some numerical results are presented to validate our analytical findings.

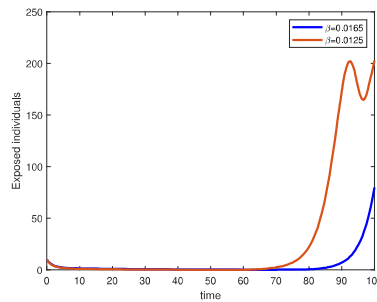
keywords: Online misinformation, Spreading threshold, delay, Hopf bifurcation, Optimal control

Results and discussions

To enhance the theoretical analysis some plots are simulated using MATLAB2018. The impact of some significant parameters with diverse impacts on \mathcal{R}_0 are discussed. We have also demonstrated how the bifurcation threshold value of spreading rate of misinformation changes with different delay values. And the following figures demonstrate impacts of control on our system. First figure presents the variation of cost function with slight change in β . One can see that, when the transmission rate increases a bit, the execution of control is



(a) Comparison of evolution of cost function with different values of β after application of control.



(b) Exposed population with higher value of β decreases to lower value after application of control.

also increased. But from the first figure, we see that the cost function corresponding to higher transmission rate is finally lesser than the cost function corresponding to lower transmission rate. Second figure shows the impacts of control on exposed population which depicts that the control is effective to control the rumor believers, the exposed individuals. Here control is effective only for exposed class, because control cannot stop deliberate (active) spreaders. We have proved that in case of an emergency caused by any sensitive misinformation, the control using mainstream media is efficient to inhibit the spreading rate and bring back the stability of the system with minimum cost.

References

- [1] Millman J. (2014) The Inevitable rise of Ebola conspiracy theories. *The Washington Post*.
- [2] Garrett R. K. (2019) Social media's contribution to political misperceptions in U.S. presidential elections. *PLoS ONE*.
- [3] Ghosh M., Das S. and Das P. (2021) Dynamics and control of delayed rumor propagation through social networks. *J. Appl Math Comput*.
- [4] Zhu L., Liu M., Li Y. (2019) The dynamics analysis of a rumor propagation model in online social networks. *Physica A* **520**:118-137.

A parsimonious identification approach in the frequency-domain for experimental fractional systems of unknown order

Jose Antunes^{*}, Philippe Piteau^{**}, Xavier Delaune^{**}, Romain Lagrange^{**} and Domenico Panunzio^{**}

^{*}Center for Nuclear Sciences and Technologies, IST, Lisbon University, 2695-066 Bobadela, Portugal

^{**}Université Paris-Saclay, CEA, Service d'Études Mécaniques et Thermiques, F-91191 Gif-sur-Yvette, France

Abstract. When the order of experimental fractional systems is unknown, frequency domain identification is typically based on linear least-squares (L_2) methods, which often prove unsatisfactory. The main reason is that the solutions they provide are dense, often leading to a continuous of identified fractional differential orders, which obfuscate the very basic phenomena one wishes to highlight. In order to overcome such difficulty, the present work proposes the use of a L_1 based nonlinear identification approach, which naturally leads to parsimonious identified results. This method is successfully illustrated on a system transfer function with both integer and fractional differential terms.

Introduction

Fractional models are being increasingly used in many branches of physics and engineering [1]. In this work we deal with the identification of fractional models from experimental Frequency Response Functions (FRFs) in the frequency domain $H(i\omega)$, when the integro-differential equations discrete order(s) α_n are unknown:

$$Z(i\omega) = \frac{1}{H(i\omega)} = \frac{F(i\omega)}{X(i\omega)} = \sum_{n=1}^N c_n (i\omega)^{\alpha_n}$$

The linear identification procedure proposed by Hartley & Lorenzo [2] is straightforward to implement. The differential order continuum is discretized in the interval $[\alpha_{\min}, \alpha_{\max}]$ sampled at $\Delta\alpha$, so that $m=1, \dots, M$ differential order terms are identified. The FRFs $Z(i\omega_k) = 1/H(i\omega_k)$ are measured at $k=1, \dots, K$ frequencies. Then, the model is formulated in and solved by the Least Squares Deviation (LSD) method:

$$\begin{bmatrix} (i\omega_1)^{\alpha_1} & \dots & (i\omega_1)^{\alpha_M} \\ \vdots & \ddots & \vdots \\ (i\omega_K)^{\alpha_1} & \dots & (i\omega_K)^{\alpha_M} \end{bmatrix} \begin{Bmatrix} c_1 \\ \vdots \\ c_M \end{Bmatrix} = \begin{Bmatrix} Z(i\omega_1) \\ \vdots \\ Z(i\omega_K) \end{Bmatrix} \rightarrow \mathbf{M}\mathbf{c} = \mathbf{z} \rightarrow \mathbf{c}_{LSD} = \min \|\mathbf{M}\mathbf{c} - \mathbf{z}\|_{L_2} \rightarrow \mathbf{c}_{LSD} = \mathbf{M}^+ \mathbf{z} = (\mathbf{M}^T \mathbf{M})^{-1} \mathbf{M}^T \mathbf{z}$$

Results and discussion

Unfortunately, solutions provided by the LSD method are dense, producing a continuous of identified fractional differential orders as M increases, which is objectionable. In order to overcome this difficulty, we propose to replace the LSD by the Least Absolute Deviation (LAD) method, a nonlinear L_1 -based identification approach that is sparsity-promoting, leading to parsimonious results:

$$\mathbf{c}_{LAD} = \min \|\mathbf{M}\mathbf{c} - \mathbf{z}\|_{L_1}$$

We illustrate the identification results on the following test system, previously used by Hartley & Lorenzo [2]:

$$Z(\omega) = 1(i\omega)^2 + 1.4(i\omega)^{1.5} + 1(i\omega) + 1.4(i\omega)^{0.5} + 1$$

with three integer and two fractional derivatives. The range of integro-differential order hypothesized for identification is $\alpha \in [-1, 3]$, sampled at $\Delta\alpha = 0.1$, these conditions being highly stringent compared to [2]. The LAD identification is based on the Iterative Reweighted Least Squares (IRLS) algorithm [3], which can minimize any L_p norm. Figure 1 clearly demonstrates, not only the essential problem of the common LSD identification method, but also the significant improvements obtained when the sparsity-promoting LAD approach is used. Robustness of the identification results is currently being addressed.

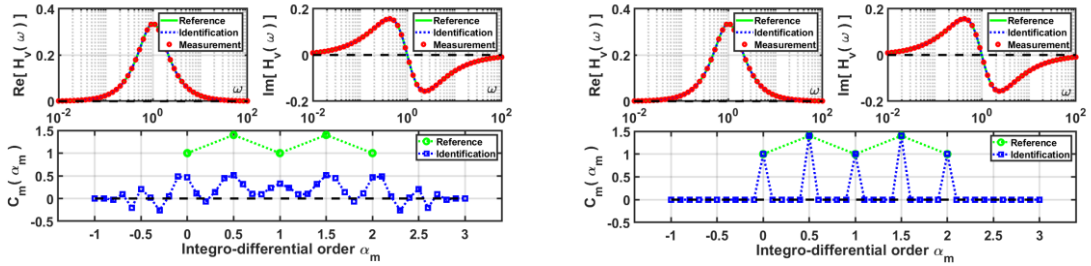


Figure 1: Left side - FRFs and derivative coefficients using common least-squares (L_2) identification; Right side - FRFs and derivative coefficients using nonlinear sparse (L_1) identification.

References

- [1] Machado J.A. et al. (2010) Some Applications of Fractional Calculus in Engineering. *Math. Probl. Engineering* **2010**/639801:1-34.
- [2] Hartley T.T., Lorenzo C.F. (2003) Fractional-Order System Identification Based on Continuous Order Distribution. *Signal Processing* **83**:2287-2300.
- [3] Björk A. (1996) Numerical Methods for Least Squares Problems. SIAM, Philadelphia.

Vibration suppression of a cable-stayed beam with external excitations by a nonlinear energy sink

Houjun Kang^{*}, Yifei Wang^{*} and Yunyue Cong^{*}

^{*} College of Civil Engineering and Architecture, Guangxi University, Nanning, China

Abstract. In this study, the influence of a nonlinear energy sink (NES) on the vibration of a cable-stayed beam structure under the excitation of external harmonic loads is studied. First, a theoretical model consisting of cable, beam and NES is established, as shown in Figure 1. By considering the interaction between the cable and the beam, the nonlinear dynamic equation of the cable-beam-NES coupled system is given. Then, the partial differential equations of the cable and beam are discretized into a set of ordinary differential equations using the Galerkin method. The incremental harmonic balance (IHB) method is used to solve the system of ordinary differential equations. Finally, the effect of the NES on the structural response of the cable-stayed beam is investigated. Meantime, the effect of the cable-beam coupling vibration on the vibration reduction effect of the NES attached to the cable was analyzed. The results show that the NES has a good suppression effect on the vibration of both the cable and the beam. In addition, the cable-beam coupling vibration reduces the vibration reduction effect of the NES attached to the cable.

Introduction

With the increase of the span of the cable-stayed bridge, the corresponding cable length becomes longer and longer, which makes the nonlinear problem of the cable-stayed bridge more prominent [1, 2]. At present, the commonly used vibration reduction measure is to add a damping device to the cable [3, 4]. However, although NES has been widely used in various engineering fields, there is no relevant research on the vibration control of cable-stayed beams by NES. In addition, the cable-beam coupling vibration of cable-stayed bridges is very easy to occur under the excitation of external loads. Does the cable-beam coupling vibration affect the vibration reduction effect of NES attached to the cable? This is a real-world engineering problem that is well worth studying.

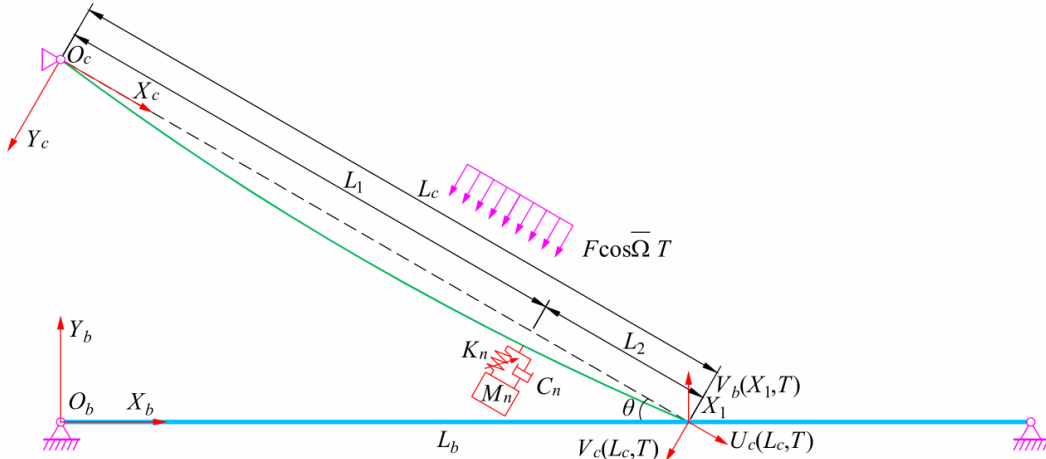


Figure 1: Coupled vibration model of cable-beam-NES

Results and discussion

The cable-beam coupling vibration has a great negative impact on the vibration reduction effect of NES. Moreover, the stronger the degree of cable-beam coupling vibration, the worse the vibration reduction effect of the NES on the cable. In the design phase of cable-stayed bridges, the effect of cable-beam coupling vibration on the vibration reduction of the cable should be considered.

The beam mainly has coupled vibration with the 1st mode of the cable. This is the main reason why the effect of cable-beam coupling vibration on the vibration reduction effect of the 1st mode of the cable with additional NES is greater than that of the 2nd and 3rd modes.

References

- [1] Rega G., Benedettini F. (1989) Planar non-linear oscillations of elastic cables under subharmonic resonance conditions. *J. SOUND VIB* **132**(3):367-381.
- [2] Wu Q., Takahashi K., Nakamura S. (2005) Formulae for frequencies and modes of in-plane vibrations of small-sag inclined cables. *J. SOUND VIB* **279**(3-5):1155-1169.
- [3] Cai C. S., Wu W. J., Araujo M. (2007) Cable vibration control with a TMD-MR damper system: Experimental exploration. *J. STRUCT ENG* **133**(5):629-637.
- [4] Su X. Y., Kang H. J., Guo T. D. (2022) Modelling and energy transfer in the coupled nonlinear response of a 1: 1 internally resonant cable system with a tuned mass damper. *MECH SYST SIGNAL PR* **162**:108058.

A Comparative Study of Two Types of Bifurcation-Based Inertial MEMS Sensors

Yasser S. Shama* ** ***, Rana Abdelrahmana* **, Sasan Rahmanian* **, Samed Kocer* **, and Eihab M. Abdel-Rahman* **

*Department of Systems Design Engineering, University of Waterloo, Waterloo, Ontario, Canada

**Waterloo Institute of Nanotechnology, University of Waterloo, Waterloo, Ontario, Canada

***Department of Mechanical Engineering, Benha Faculty of Engineering, Benha University, Benha, Egypt

Abstract. This paper compares the use of two types of bifurcations to implement MEMS inertial methane sensors, namely a cyclic-fold in the vicinity of the primary resonance and a primary Hopf in the vicinity of the subharmonic resonance of order one-half. We experimentally demonstrate a sensitivity enhancement, by more than 40%, for the latter over the former at the same operating conditions.

Introduction

Urban sprawl and industrial expansion are massive sources of pollution as they release large quantities of hazardous waste. Detecting and monitoring pollutants are essential in environmental management and control. Therefore, we need to deploy highly sensitive sensor arrays that can detect low concentrations of hazardous gases. MEMS gas sensors have been a leading technology in this field over the last two decades due to their small size, lightweight, low power consumption, and high functionality in real-time applications [1]. Researchers have lately pursued bifurcation-based sensing as a means to enhance the sensitivity and robustness of MEMS sensors by exploiting the sudden, typically large, jump in vibration amplitude experienced through bifurcations [1-3]. Here, we experimentally report an enhancement in the sensitivity of an out-of-plane electrostatic MEMS methane sensor in terms of both the amplitude of the detection signal and the shift in the location of bifurcation frequency subsequent to methane detection, comparing two different types of dynamic bifurcations under the same operating conditions.

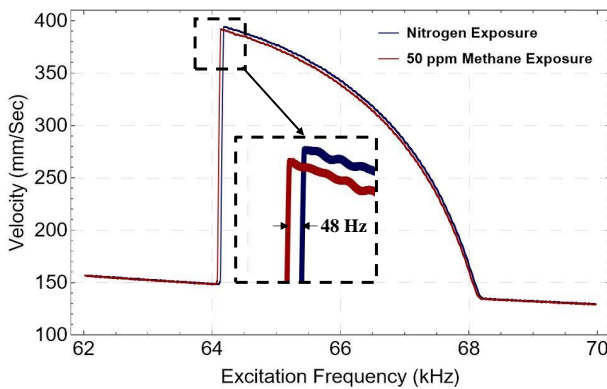


Figure 1: Subharmonic resonance before and after gas exposure

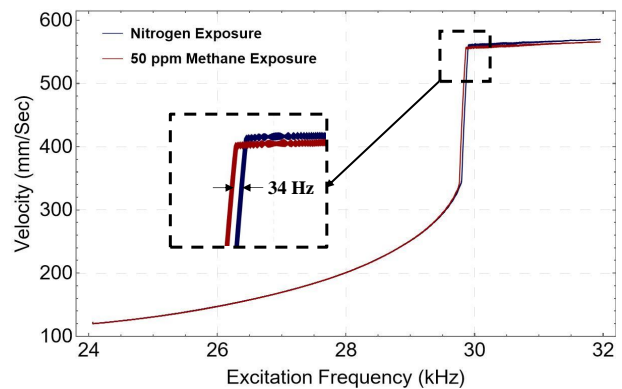


Figure 2: Primary resonance before and after gas exposure

Experimental setup and results

The MEMS sensor, a microplate supported by two cantilever beams, was fabricated in the PolyMUMPs process and functionalized with a potential polymer to detect methane. It was tested inside a test enclosure with an anti-reflective glass port for optical access. The sensor was electrostatically actuated with a biased AC signal using a function generator and a voltage amplifier. The velocity of the plate center was optically measured using a Laser Doppler Vibrometer (LDV) and digitized using a digital oscilloscope. The time domain data were post-processed using in-house software to obtain the frequency response. Figure 1 shows the sensor response in the vicinity of its subharmonic resonance of order one-half, and it shows that the frequency of the Hopf bifurcation at the left end of the non-trivial window dropped by 48 Hz upon exposure to a mixture of dry nitrogen and 50 ppm methane. Figure 2 shows the sensor response in the vicinity of the primary resonance, and it shows that the location of the cyclic-fold bifurcation at the end of the lower branch shifted by 34 Hz upon exposure to the same gas mixture. According to the obtained results, it appears that the Hopf bifurcation is more sensitive than the cyclic-fold bifurcation by more than 40%.

References

- [1] Al-Ghamdi M., Khater M., Stewart K., Alneamy A., Abdel-Rahman E. M., Penlidis A. (2018) Dynamic bifurcation MEMS gas sensors. *Journal of Micromechanics and Microengineering* **29**(1): 015005.
- [2] Younis M. I., Alsaleem F.(2009) Exploration of new concepts for mass detection in electrostatically-actuated structures based on nonlinear phenomena. *Journal of computational and nonlinear dynamics* **4**(2): 021010.
- [3] Meesala V. C., Hajj M. R., Abdel-Rahman E.(2020) Bifurcation-based MEMS mass sensors. *International Journal of Mechanical Sciences* **180**: 105705.

Dynamics of Purcell's three-link microswimmer model with actuated-elastic joints

Gilad Ben-Zvi and Yizhar Or

Faculty of Mechanical Engineering, Technion – Israel Institute of Technology

Abstract. Purcell's planar three-link microswimmer is a classic model of swimming at low-Reynolds-number fluid, inspired by motion of flagellated microorganisms. Many works analyzed this model, assuming that the two joint angles are directly prescribed in phase-shifted periodic inputs. In this work, we study a more realistic scenario by considering an extension of this model which accounts for joints' elasticity and mechanical actuation of periodic torques, so that the joint angles are dynamically evolving. Numerical analysis of the swimmer's dynamics reveals multiplicity of periodic solutions, depending on parameters of the inputs – frequency and amplitude of excitation, as well as joints' stiffness. We numerically study bifurcations, stability transitions, and symmetry breaking of the periodic solutions, demonstrating that this simple model displays rich nonlinear dynamic behavior with actuated-elastic joints.

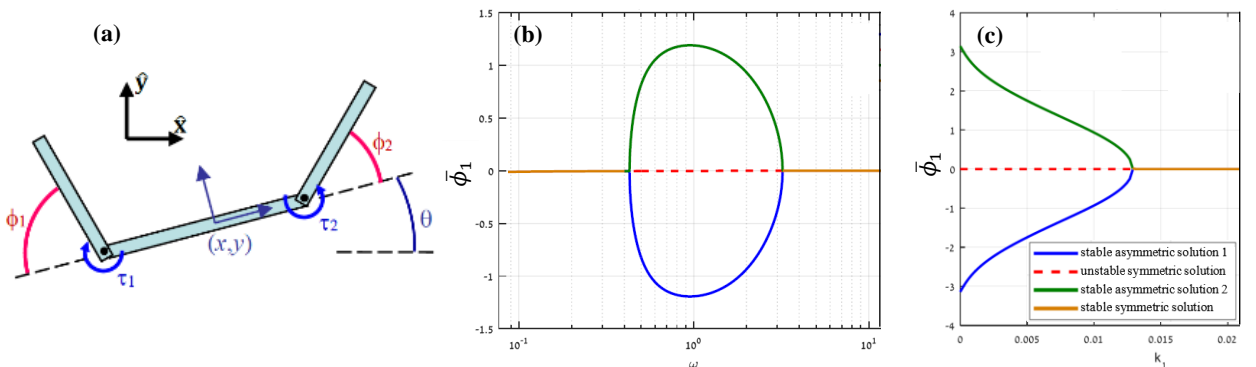
Introduction

Purcell's three-link microswimmer model has been introduced in [1]. The model consists of three rigid links connected by two joints whose angles ϕ_1, ϕ_2 are assumed to be controlled as phase-shifted time-periodic inputs. The dynamic equations of motion of Purcell's swimmer have been formulated in [2], assuming slender links under low-Reynolds-number hydrodynamics, and further analyzed in many other works. The work [3] introduced a modified model where one joint angle is periodically actuated as $\phi_1(t) = \varepsilon \sin(\omega t)$ while the other joint is *passive* and acted by a *torsion spring* with linear stiffness, so that the joint torque is $\tau_2 = -k\phi_2$. The work [3] considered the case of small amplitude $\varepsilon \ll 1$, where the only periodic solution of the system, which is orbitally stable, occurs with the passive joint angle $\phi_2(t)$ oscillating symmetrically about zero. Using asymptotic expansion, the swimmer's response as a function of the input frequency ω was studied in [3], showing existence of optimal frequency that maximizes the net displacement per cycle.

In this work, we consider an extension of this model in [3], with actuated-elastic joints, whose torques are given as $\tau_i = \varepsilon_i \sin(\omega t + \gamma_i) - k_i \phi_i$. This input can also be written in equivalent form of a local feedback law as $\tau_i = -k_i(\phi_i - \psi_i(t))$ where $\psi_i(t) = \tilde{\varepsilon}_i \sin(\omega t + \gamma_i)$ is a desired reference angle to be tracked.

Results and discussion

Using numerical integration of this dynamical system, we seek for T -periodic solutions where $T = 2\pi/\omega$, and analyze their orbital stability using Poincaré map and Floquet theory. Upon varying the actuation frequency ω and the stiffness ratio k_1/k_2 , we find pitchfork bifurcations where the symmetric periodic solution oscillating about mean values $\bar{\phi}_i = 0$ becomes unstable (dashed lines) and a pair of stable asymmetric solution branches evolve. The results demonstrate rich dynamic behavior of periodic solution multiplicity, which also enables steering the swimmer's path curvature by controlling its input frequency.



(a) Purcell's three link microswimmer model with actuated-elastic joints. Bifurcation diagrams of periodic solutions branches, the mean value of joint angle $\bar{\phi}_1$ as a function of varying parameter. Solid curves denote stable periodic solutions and dashed lines denote unstable ones. (b) Case of $0 < k_1 \gg k_2$, $\varepsilon_2 = 0$, varying frequency ω . (c) Case of fixed frequency ω and stiffness k_2 , and $\varepsilon_2 = 0$, varying stiffness k_1 .

References

- [1] Purcell, E. M. (1977). Life at low Reynolds number. *American Journal of Physics*, 45(1), 3-11.
- [2] Becker, L. E., Koehler, S. A., & Stone, H. A. (2003). On self-propulsion of micro-machines at low Reynolds number: Purcell's three-link swimmer. *Journal of Fluid Mechanics*, 490, 15-35.
- [3] Passov (Gutman), E., & Or, Y. (2012). Dynamics of Purcell's three-link microswimmer with a passive elastic tail. *The European Physical Journal E*, 35(8), 1-9.

Nonlinear dynamics and bifurcations of a planar undulating magnetic microswimmer

Jithu Paul*, Yizhar Or* and Oleg V. Gendelman*

* Faculty of Mechanical Engineering, Technion – Israel Institute of Technology, Technion City, Haifa 3200003, Israel

Abstract. A magnetically-actuated microswimmer model, motivated from biological microorganisms, which has two links representing a tail and a magnetized head is studied numerically and analytically. The links are connected by a passive elastic joint and the microswimmer is actuated by an external time-periodic magnetic field oscillating in plane. This simple system is very rich in dynamics and we identified that it may have co-existing periodic solutions, symmetric as well as asymmetric, and stability transitions with subcritical pitchfork bifurcations, induced by the system's parametric excitation.

Introduction

A leading concept for nano-swimmers actuation is using planar time-varying external magnetic field [1] which can be set to be $\mathbf{B}(t) = \gamma \hat{\mathbf{x}} + \beta \sin(\Omega \tau) \hat{\mathbf{y}}$ where $\beta, \gamma \geq 0$ are constants. A simple theoretical model for studying the planar locomotion of such swimmer is the two-link model proposed in [2], see Fig. 1. This model consists of two rigid links connected by a passive elastic joint represented as a torsion spring, and one of the links (the “head”) is magnetized along its longitudinal axis. The analysis in [2] focused on the case of small oscillations $\beta \ll \gamma$ and conducted asymptotic analysis of the motion in which the swimmer oscillates about and swims along $+\hat{\mathbf{x}}$ direction, which is a stable periodic solution. The analysis showed that there exist optimal actuation frequencies Ω for maximizing the mean speed or displacement per cycle. In this work, we revisit the two-link model in [2] and extend the analysis to cases of large oscillations $\beta > \gamma$ and even $\gamma = 0$, and study also the “backward” solution where the swimmer oscillates about and swims along $-\hat{\mathbf{x}}$ direction. While this swimmer’s orientation is statically unstable (for $\beta = 0, \gamma > 0$), we find that for $\beta \neq 0$, this gives a periodic solution, which undergoes stability transition and subcritical pitchfork bifurcation upon varying amplitude β and frequency Ω of the magnetic field’s input. We analyze the backward solution numerically as well as analytically using asymptotic expansion and harmonic balance. Under small-angle expansion, the system’s dynamics can be reduced to a nonlinear 2nd order differential equation with parametric excitation, which resembles the well-known Kapitza pendulum system [3]. Finally, we show optimization of the swimmer’s net motion with respect to both β and Ω .

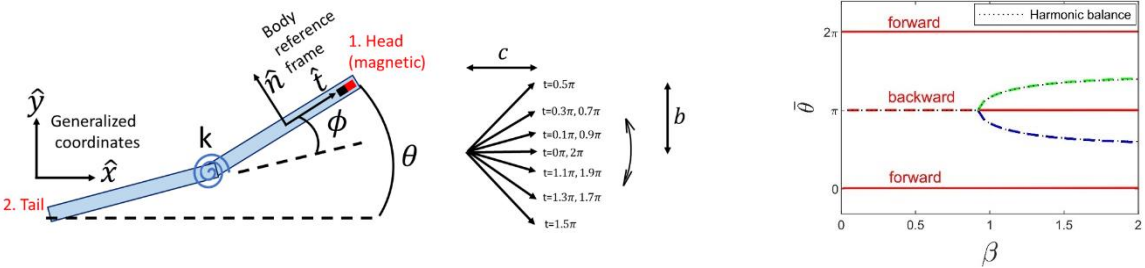


Figure 1: The model system and the bifurcation plot which comparing numerical (color lines) and analytical findings.

Results and Discussion

The dynamics of the microswimmer propulsion in the backward direction gives very interesting findings. In the forward direction, the motion is always stable, whereas in the backward direction ($\bar{\theta} = \pi$) the swimmer shows stability transition with subcritical pitchfork bifurcation, upon varying a single parameter out of β, γ, ω . The swimmer can go faster in the backward direction than the forward direction and nonzero net propulsion exists for the case $\gamma = 0$. The parameter γ can be tuned to obtain the optimum velocity or displacement in the stable region, which calls for the scope of an experimental validation and gives hint towards its engineering applications in the future. Again, γ is a very sensitive parameter in the system and the dynamics at $\gamma \rightarrow 0$ needs further investigation to get a full picture of the nonlinear dynamics in the domain. The numerical approach successfully calculated the stability, bifurcation and optimum values of the swimmer’s motion for the fixed point around $[\pi; 0]$, for different range of parameters. The harmonic balance approach, very well predicts the symmetric and asymmetric branches of the bifurcation, and the condition for stability transition.

References

- [1] R. Dreyfus, J. Baudry, M. L. Roper, M. Fermigier, H. A. Stone, and J. Bibette (2005) *Nature* **437**, 7060.
- [2] E. Gutman and Y. Or (2014) *Physical Review E* **90**, 01301.
- [3] Y. Harduf, D. Jin, Y. Or, and L. Zhang (2018) *Soft Robot.* **5**, 389; P. L. Kapitza.

The Complete Bifurcation Analysis of Buck Converter Under Current Mode Control

Aleksandrs Ipatovs*, Dmitrijs Pikulins*, Iheanacho Chukwuma Victor*, Sergejs Tjukovs

**Institute of Radioelectronics, Riga Technical University, Riga, Latvia*

Abstract. The paper is devoted to the complete bifurcation analysis of the nonlinear dynamics of one of the most widely used switching power supplies – buck converter under current mode control. The applied Method of Complete Bifurcation Groups allows the detection of all stable and unstable periodic modes of operation, showing the complicated structure of bifurcation patterns and their interaction with chaotic attractors. The research aims to identify the regions in the parameter space where the converter could operate as a source of robust chaotic oscillations.

Introduction

Chaotic dynamics of electronic circuits have raised great interest for several decades. The applications range from embedded chaos-based cryptosystems [1], intelligent sensing [2], and secure data transmission [3] to chaotic computing [4] and quantum chaos [5]. One of the most topical problems is the generation of chaotic oscillations. Different circuits have been proposed based on classical Chua or Rossler oscillators[6], digital implementation of chaotic maps [7], or production defects of commonly available operational amplifiers [8]. However, in all cases, there is a need for additional circuitry that does not guarantee the generation of robust chaos. In this research, we propose to utilize the properties of switching power converters, already present in most electronic equipment, to operate in chaotic modes. The main goal is to apply the Method of Complete Bifurcation Groups to the buck converter model to identify the regions of robust chaotic oscillations where no stable periodic orbits occur. This would allow the utilization of SPC as embedded sources of chaotic signals in a wide range of applications.

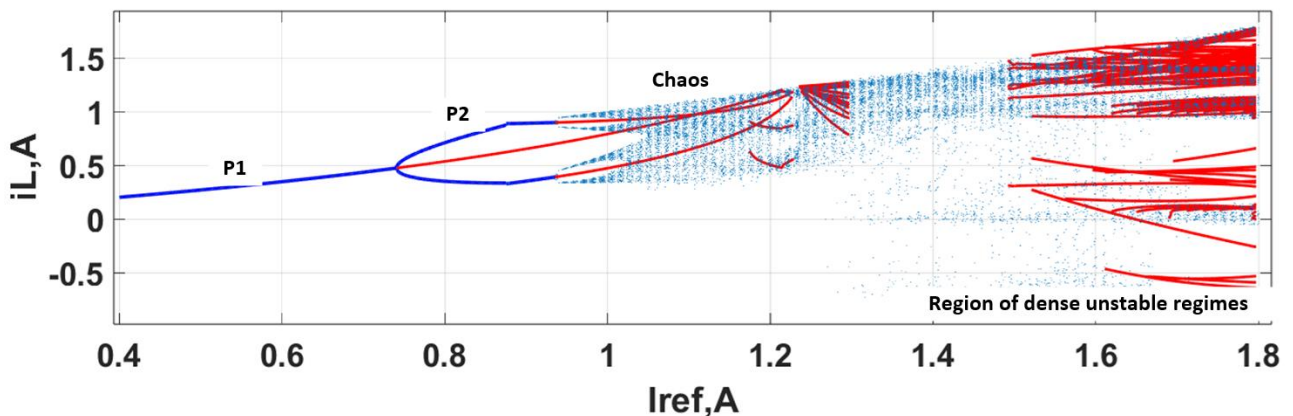


Figure 1: The complete bifurcation diagram of the buck converter under current mode control.

Acknowledgements

This work has been supported by the European Regional Development Fund within the Activity 1.1.1.2 "Post-doctoral Research Aid" of the Specific Aid Objective 1.1.1 "To increase the research and innovative capacity of scientific institutions of Latvia and the ability to attract external financing, investing in human resources and infrastructure" of the Operational Programme "Growth and Employment" (No.1.1.1.2/VIAA/4/20/651).

References

- [1] Alvarez, G. and Li, S., 2006. Some basic cryptographic requirements for chaos-based cryptosystems. *International journal of bifurcation and chaos*, 16(08), pp.2129-2151.
- [2] Karimov, T., Nepomuceno, E.G., Druzhina, O., Karimov, A. and Butusov, D., 2019. Chaotic oscillators as inductive sensors: Theory and practice. *Sensors*, 19(19), p.4314.
- [3] Kocamaz, U.E., Çiçek, S. and Uyaroglu, Y., 2018. Secure communication with chaos and electronic circuit design using passivity-based synchronization. *Journal of Circuits, Systems and Computers*, 27(04), p.1850057.
- [4] Ditto, W.L., Miliotis, A., Murali, K., Sinha, S. and Spano, M.L., 2010. Chaogates: Morphing logic gates that exploit dynamical patterns. *Chaos: An Interdisciplinary Journal of Nonlinear Science*, 20(3), p.037107.
- [5] Balasubramanian, V., Caputa, P., Magan, J.M. and Wu, Q., 2022. Quantum chaos and the complexity of spread of states. *Physical Review D*, 106(4), p.046007.
- [6] Malykh, S., Bakhanova, Y., Kazakov, A., Pusuluri, K. and Shilnikov, A., 2020. Homoclinic chaos in the Rössler model. *Chaos: An Interdisciplinary Journal of Nonlinear Science*, 30(11), p.113126.
- [7] Abdullah, H.A. and Abdullah, H.N., 2019. FPGA implementation of color image encryption using a new chaotic map. *Indonesian Journal of Electrical Engineering and Computer Science*, 13(1), pp.129-137.
- [8] Bucolo, M., Buscarino, A., Famoso, C., Fortuna, L. and Gagliano, S., 2021. Imperfections in integrated devices allow the emergence of unexpected strange attractors in electronic circuits. *IEEE Access*, 9, pp.29573-29583.

The influence of the electro-magnetic levitation and its control strategy on the vertical stability of the Hyperloop transportation system

Andrei B. Fărăgău*, Rui Wang*, Andrei V. Metrikine*, and Karel N. van Dalen*

*Department of Engineering Structures, Delft University of Technology, Delft, the Netherlands

Abstract. Hyperloop is an emerging transportation system that minimises the air resistance by having the vehicle travel inside a de-pressurised tube and eliminates the wheel-rail contact friction by using an electro-magnetic levitation system. Due to the very large target velocities, one of its challenges will be ensuring the system stability. This study aims to determine the velocity regimes in which the system is unstable, and, more specifically, is concerned with the influence of the electro-magnetic levitation and its control system on these velocity regimes. This study can help engineers designing the Hyperloop system avoid excessive vibrations that can lead to fatigue problems and, in extreme cases, to derailment.

Introduction

Hyperloop is a new emerging transportation system that is in the development stage. Its design minimises the air resistance by having the vehicle travel inside a de-pressurised tube (near vacuum) and eliminates the wheel-rail contact friction by using an electro-magnetic levitation (EMS) system, similar to the ones used by Maglev trains. By doing so, it can potentially reach much higher velocities than conventional railways, thus being a climate-friendly competitor to air transportation.

Some challenges faced by the Hyperloop system have already been identified and studied in the context of high-speed railways. However, the much larger target velocities will most likely lead to new challenges. One such a challenge is ensuring the stability of the system at large velocities. It is well known that the vibration of a vehicle travelling on an elastic guideway can become unstable when it exceeds a certain critical velocity [1, 2]. Consequently, knowing the unstable velocity regimes of the Hyperloop is of high importance for its design.

This study aims to determine the said unstable velocity regimes and focuses on the influence of the EMS and its control system on the instability velocity regimes. To this end, the Hyperloop system is modelled as an infinite beam continuously supported by a visco-elastic foundation subject to a moving mass (Fig. 1). The mass interacts with the guideway through a nonlinear electro-magnetic force governed by the EMS. A control strategy is necessary to ensure stability of the system even at quasi-static velocities. A basic control strategy (i.e., PD control) is used that includes a component proportional (P) to the air gap and one proportional to the derivative (D) of the air gap, in which the gains of each component are kept constant. Since the PD control can insert and extract energy from the system, its influence on the system's stability is currently unknown.

Preliminary results

If the control gains are appropriately chosen, instability occurs at very high velocities that are beyond the target ones, similar to high-speed railways. However, for some values that seem appropriate at low velocities can lead to a behaviour at large velocities which is very different to the mechanical counterpart (i.e., high-speed rail). For example, Fig. 1 shows that instability is onset slightly beyond the critical velocity, but stability is regained at even higher velocities. This seems to be a particularity of the present system since this is not observed in its mechanical counterpart. This study can help engineers designing the Hyperloop system avoid undesired excessive vibrations that can lead to fatigue problems and, in extreme cases, to derailment.

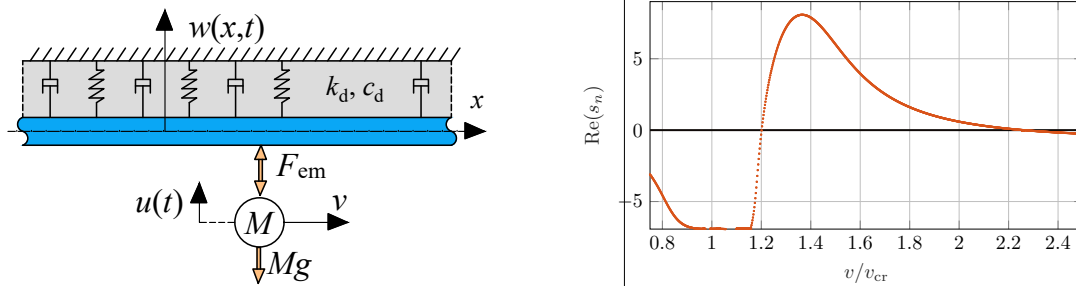


Figure 1: Schematics of the system (left panel) and eigenvalues of the linearised system versus relative velocity (right panel).

References

- [1] Denisov G. G., Kugusheva E. K., Novikov V. V. (1985) On the problem of the stability of one-dimensional unbounded elastic systems. *J. of App. Math. and Mech.* **49**:533-537.
- [2] Metrikine A. V. (1994) Unstable lateral oscillations of an object moving uniformly along an elastic guide as a result of an anomalous Doppler effect. *Acoustical Physics* **40**:85-89.

The influence of the frequency and velocity-dependent reaction force of the guideway on the vertical stability of the Hyperloop transportation system

Karel N. van Dalen*, Andrei B. Fărăgău*, and Andrei V. Metrikine*

*Department of Engineering Structures, Delft University of Technology, Delft, the Netherlands

Abstract. Hyperloop is an emerging transportation system that minimises the air resistance by having the vehicle travel inside a de-pressurised tube and eliminates the wheel-rail contact friction by using an electro-magnetic levitation system. This work studies the vertical stability of the Hyperloop system and its novelty lies in considering the frequency and velocity-dependent reaction force provided by the infinite elastic guideway. Furthermore, by also modelling the secondary suspension that connects the electro-magnetic levitation system to the vehicle, the effect of its additional damping on the vertical stability of the overall system is investigated. This study can help engineers designing the Hyperloop system avoid undesired excessive vibrations that can lead to fatigue problems and, in extreme cases, to derailment.

Introduction

Hyperloop is an emerging transportation system that is still in the development stage. Compared to high-speed railway, its envisioned design presents two major improvements. Firstly, air resistance experienced by the vehicle is minimized by having it travel inside a de-pressurised tube (near vacuum). Secondly, the wheel-rail contact friction is eliminated by using an electro-magnetic levitation system (EMS) similar to Maglev trains. These two major improvements lead to the vehicle potentially reaching much higher velocities than conventional or even high-speed railways. Together with the fact that it runs solely on electricity, the Hyperloop transportation system can become a climate-friendly competitor to air transportation.

One Hyperloop design has the vehicle suspended from top of the de-pressurised tube, with the nonlinear electro-magnetic force acting always in attraction while the gravitational force acts in opposite direction (Fig. 1). Following this design, the system is inherently unstable and requires a control strategy to ensure stability even at quasi-static velocities. In the current work, a basic control strategy (i.e., PD control) is used that includes a component proportional (P) to the air gap and one proportional to the time derivative (D) of the air gap.

This work aims to study the vertical stability of the Hyperloop system following the aforementioned design. While the stability of similar systems has been previously studied (e.g., [1]), the novelty of this work lies in considering the frequency and velocity-dependent reaction force provided by the infinite elastic guideway. Furthermore, by modelling also the secondary suspension that connects the EMS to the vehicle, the effect of its additional damping on the stability of the overall system can be investigated. The Hyperloop system is modelled as an infinite beam continuously supported by a visco-elastic foundation subject to a moving two degree-of-freedom oscillator (see Fig. 1).

Preliminary results

If the frequency-velocity reaction force of the guideway is not accounted for, the vehicle velocity has no influence on the system stability. Consequently, in previous studies, the feedback gains were determining the stability of the system for the whole velocity regime. This works shows that a stable system at small relative velocities can loose stability at large velocities. More interestingly, Fig. 1 shows that an unstable system at small relative velocities can gain stability at higher velocities. This study can help engineers designing the Hyperloop system avoid undesired excessive vibrations that can lead to fatigue problems and, in extreme cases, to derailment.

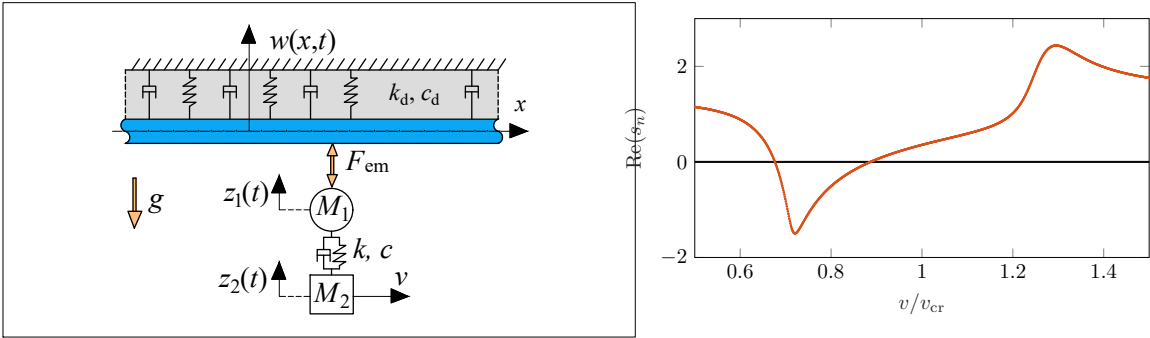


Figure 1: Schematics of the system (left panel) and eigenvalues of the linearised system versus relative velocity (right panel).

References

- [1] Wu H., Zeng X., Gao D., Lai J. (2021) Dynamic stability of an electromagnetic suspension maglev vehicle under steady aerodynamic load. *App. Math. Modelling* **97**:483-500.

The effect of the mean wind force on the post-critical galloping response of shallow cables

Daniele Zulli* and Angelo Luongo*

* Department of Civil, Construction-Architectural and Environmental Engineering, University of L'Aquila, Italy

Abstract. The post-critical aeroelastic behavior of horizontal, suspended, shallow cables is analyzed via a continuous model. Perturbation methods are used to obtain bifurcation equations ruling the essential behavior of the cable close to the galloping conditions. Discussion on the post-critical dynamical evolution is given, after numerical validation of the asymptotic outcomes.

Introduction

Cables are largely used structural elements and represent a strategic asset in many engineering applications. A general characterization of statics and dynamics of cables is found in [1], whereas their response to wind, especially in cold regions, i.e. where an ice accretion may break the typical axial-symmetry of the cross-sections, is usually evaluated within the Den Hartog formulation [2]. In-plane galloping analysis was performed on a continuous model in [3]. The motivation of this paper comes from previous analysis on the critical behavior of horizontal, suspended, shallow cables given in [4]. There, the in-plane and out-of-plane aerodynamic response of cables was analyzed via a continuous model, also accounting for an internal damping contribution which simulates a viscous-elastic constitutive material. In particular, the effect on the galloping conditions of the swing of the plane on which the cable lays was analyzed, giving rise to occurrence of symmetric or anti-symmetric critical modes, independently on the sag-to-span ratio of the cable, but only related to the initial attitude of the cross-section to the wind. Here, starting from the same model proposed in [4], the formulation is extended to analyze the post-critical behavior, making use of perturbation methods and comparing the outcomes with those given by numeric integration after the application of the finite difference method.

Results and discussion

Two different initial attitudes to wind of the iced cross-section of the cable are considered, namely case 1 and case 2, keeping fixed all the other geometrical and mechanical characteristic. In particular, in case 1 the cable is more prone to galloping than case 2. In correspondence, it is found that the critical mode, which is complex, is anti-symmetric for case 1 and symmetric for case 2 (see Fig. 1), it being strongly dependent on the equilibrium configuration reached by the cable in proximity of the galloping condition. This equilibrium configuration, which defines the fundamental path, is attained on a rotated plane on which the cable lays, whose rotation angle with respect to the vertical plane depends on the mean wind velocity. Starting from this occurrence, the post-critical analysis is performed via the Multiple Scale Method on the continuous model, providing the relevant bifurcation equation which allows one to describe the evolution of the shape and amplitude of vibration of the cable for larger velocities.

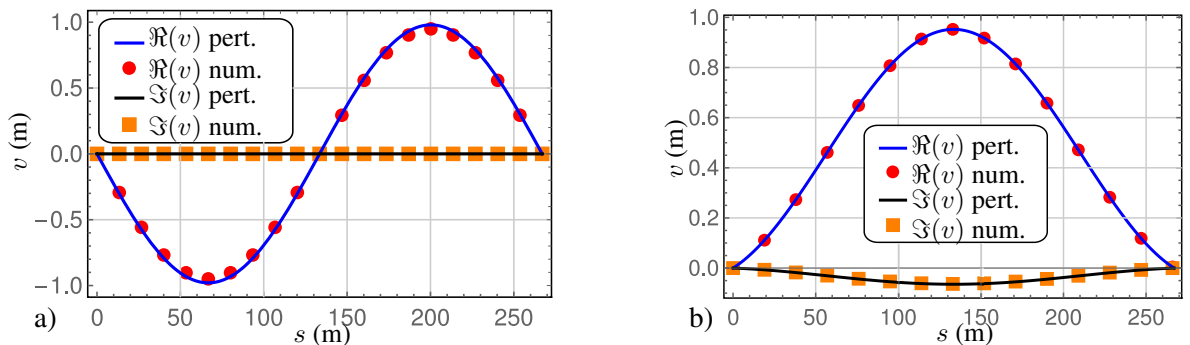


Figure 1: Critical mode of the cable for: a) case 1 ; b) case 2.

References

- [1] Irvine H. (1981) Cable Structures. MiT Press, Cambridge.
- [2] Den Hartog J. (1985) Mechanical Vibrations. Dover Publications, NY.
- [3] Ferretti M., Zulli D., Luongo A. (2019) A continuum approach to the nonlinear in-plane galloping of shallow flexible cables. *Adv Math Phys* **2019**:6865730.
- [4] Zulli D., Piccardo G., Luongo A. (2021) On the nonlinear effects of the mean wind force on the galloping onset in shallow cables. *Nonlinear Dyn* **103**:3127–3148.

How non-generic coincidences of local bifurcations can occur in fluid mechanics

N. Deng^{**}, L. Tuckerman^{***} and B.R. Noack^{**}, **Luc Pastur^{*}**

^{*}*Fluid Dynamics Department, ENSTA Paris – Institut Polytechnique de Paris, Palaiseau, France*
ORCID 0000-0003-0038-5898

^{**}*School of Mechanical Engineering and Automation, Harbin Institute of Technology (Shenzhen), Shenzhen, China*

^{***}*PMMH Lab, ESPCI Paris, PSL Research University Sorbonne Univ., Université de Paris, France*

Abstract. Generically, a local bifurcation only affects a single solution branch. Surprisingly, two supercritical pitchfork bifurcations, of the equilibrium and the periodic solutions, were observed to occur at nearly the same value of the Reynolds number in the “fluidic pinball” configuration. The mechanism of this non-generic coincidence is modelled and explained.

Introduction

It was recently discovered that in the “fluidic pinball” configuration, two supercritical pitchfork bifurcations are almost coincident at a value of the Reynolds number around 70, one affecting the steady solution of higher symmetry, the other a vortex shedding periodic regime in the wake of the three cylinders, as shown in Fig. 1 [1]. Generically, local bifurcations only affect single solution branches, e.g. either the steady solution or the periodic limit cycle, but not both simultaneously.

Results and discussion

We investigated the reasons for this unexpected coincidence. The two branches involved, although very different, share certain eigenvectors and eigenvalues which can explain the coincidence of the two bifurcations. The mechanisms involved in this non-generic coincidence, modelled and explained, suggests that non-generic coincident local bifurcations should be found in many other instances in fluid mechanics [1].

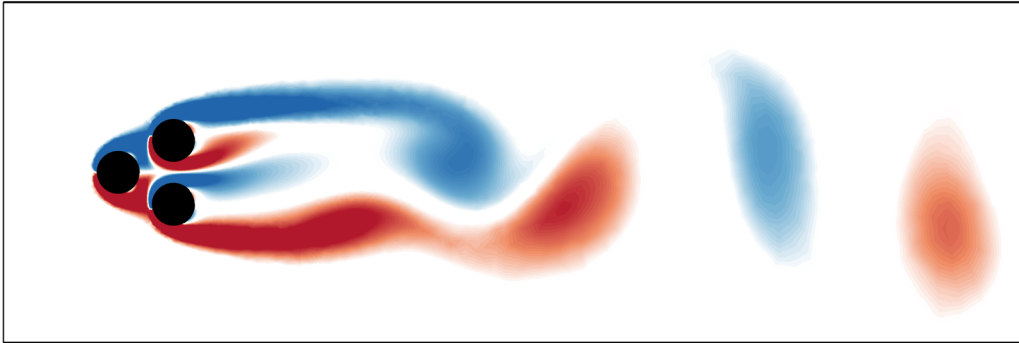


Figure 1: Snapshot of the vorticity field in a vortex shedding periodic regime of the fluidic pinball configuration at Reynolds 80. The three cylinders are mounted on the vertices of an equilateral triangle in a transverse flow coming from the left.

References

- [1] N. Deng, L.R. Pastur, L.S. Tuckerman, & B.R. Noack. Coinciding local bifurcations in the Navier-Stokes equations. *Europhysics Letters*, Vol. **135**(2), p. 24002, 2021.

On the influence of external damping on the dynamics of a generalized Beck's beam

Giovanni Migliaccio^{*}, Manuel Ferretti^{*} and Francesco D'Annibale^{*}

^{*}Department of Civil, Construction-Architectural and Environmental Engineering, University of L'Aquila, L'Aquila, Italy

Abstract. The influence of external damping on the dynamic behaviour of a generalized Beck's beam is discussed in this work. The cantilever beam is inextensible and shear-undeformable, it is subject to the action of distributed, linear and nonlinear external damping (modelling the interaction with the surrounding environment), and to follower and dead loads applied at the free tip. Hopf bifurcation conditions are detected after a stability analysis of the initial straight configuration. Subsequently, the integro-differential equations of motion of the system are studied via a multiple-scale approach to assess the influence of the external damping on the limit-cycle that may occur once the Hopf critical load is overcome.

Introduction

According to the Ziegler Paradox, the introduction of a positive, vanishing linear damping into a circulatory system can lower the Hopf bifurcation load [1]. The visco-elastic Beck's beam [2], namely a cantilever beam with distributed damping and a follower load at the free tip, is a paradigmatic example of a continuous system that is subject to such a paradox. Its linear behaviour has long been studied to increase the Hopf critical load and to improve the beam stability via external damping devices [3]. The nonlinear behaviour of beams of this kind with lumped devices at the free tip is addressed in [4] to investigate the system behaviour around the double-zero bifurcation. The influence of a distributed nonlinear hysteretic damping (of the internal type, due to material properties) on the post-critical scenario around the Hopf bifurcation is discussed in [5]. Here, we address the nonlinear dynamic behaviour of a generalized Beck's beam, which is subject to the action of distributed nonlinear external damping, plus follower and dead loads at the free end. The influence of the parameters associated with different nonlinear damping types are discussed. Assuming small nonlinearities, the bifurcation equation that governs the system dynamics around the Hopf bifurcation is studied. The semi-analytical results obtained in this way are compared with those derivable via numerical approaches. These latter are also employed to address the case of moderately large nonlinearities.

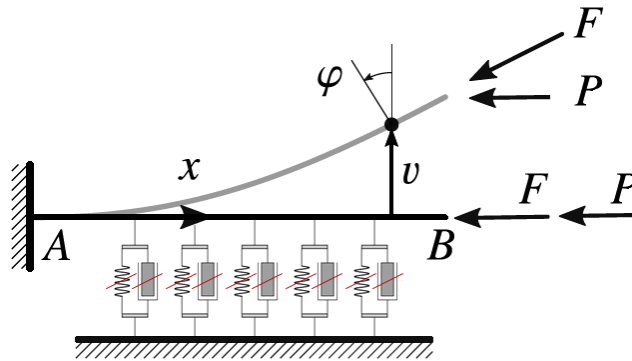


Figure 1: Schematic of the problem.

Results and discussion

The present study has shown that the constitutive characterization of the external damping can have a strong influence on the critical and post-critical behaviour of a generalized Beck's beam. In particular, the choice of the parameters associated with the nonlinear part of the damping is crucial and may induce beneficial or detrimental effects on the system nonlinear response. Comparisons with the results of purely numerical approaches confirm the theoretical findings obtained via the multiple-scale algorithm developed within this study, which turns out to be a reliable tool for nonlinear dynamic analyses. This work represents a first step towards a more reliable design of devices to control the detrimental effects of the nonlinear damping.

References

- [1] Bolotin V.V. (1963) Non conservative problems of the theory of elastic stability. Macmillan, NY.
- [2] Beck M. (1952) Die Knicklast des einseitig eingespannten, tangential gedrückten Stabes. *Z Angew Math Phys* **3**(3):225-228.
- [3] D'Annibale F., Ferretti M., Luongo A. (2016) Improving the linear stability of the Beck's beam by added dashpots. *Int J. Mech Sci* **110**:151-159.
- [4] Luongo A., Di Egidio A. (2005) Bifurcation equations through multiple-scales analysis for a continuous model of a planar beam. *Nonlin Dyn* **41**(1-3):171-190.
- [5] Luongo A., D'Annibale F. (2017) Nonlinear hysteretic damping effects on the post-critical behaviour of the visco-elastic Beck's beam. *Math Mech Solids* **22**(6):1347-1365.

Fingered Stability Regions for Operator Splitting

Miklós E. Mincsovcics, Tamás Kalmár-Nagy

Budapest University of Technology and Economics, Budapest, Hungary

Abstract. We compare the stability preserving properties of the Lie-Trotter, Strang-Marchuk, and symmetrically weighted sequential splitting by evaluating the trace and determinant of the split systems in terms the trace and determinant of the continuous system.

Introduction

Splitting methods are based on the decomposition of the underlying operator/matrix equation into a sum of simpler operators/matrices and solving a chain of these simpler problems. This method is used in various fields e.g. in fluid dynamics, for stiff systems which occur in combustion, air pollution, and reactive flow problems etc. A good exposition of splitting methods can be found in [1, 2].

The splitting literature is almost entirely dedicated to the investigation of convergence and its order of different splitting types. Our plan is different, we investigate the stability preserving properties.

Results

Consider the initial value problem

$$\begin{aligned} \dot{u}(t) &= Au(t), \\ u(0) &= u_0, \end{aligned}$$

with the decomposition

$$B + C = A.$$

This results in the iteration

$$\begin{cases} u_{n+1} = Su_n, \\ u_0 = u(0), \end{cases}$$

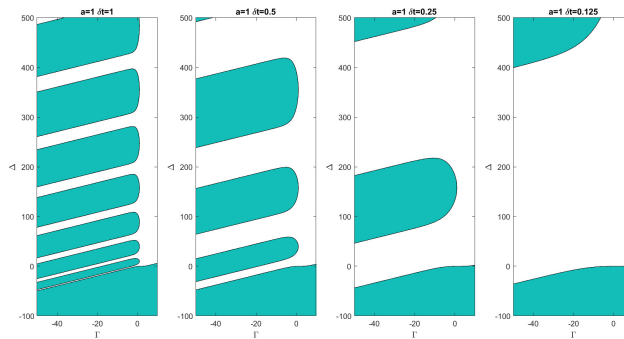
where for a fixed time-step δt the Lie-Trotter, Strang-Marchuk, and the symmetrically weighted sequential splitting methods result in the operators

$$S_{LT} = e^{B\delta t} e^{C\delta t}, \quad S_{SM} = e^{\frac{1}{2}B\delta t} e^{C\delta t} e^{\frac{1}{2}B\delta t}, \quad S_W = \frac{1}{2} \left(e^{B\delta t} e^{C\delta t} + e^{C\delta t} e^{B\delta t} \right).$$

We worked with the simplest setting - since the literature is almost absent about the stability preserving properties of the splitting methods - when the operator A is a matrix. We consider the “natural” decomposition

$$\mathbf{A} = \begin{pmatrix} a & b \\ c & d \end{pmatrix} = \mathbf{B} + \mathbf{C} = \begin{pmatrix} a & 0 \\ 0 & d \end{pmatrix} + \begin{pmatrix} 0 & b \\ c & 0 \end{pmatrix}.$$

In [3] we obtained that the stability regions of the split systems exhibit fingers (see Figure), i.e. the stability is not a monotonic property of the splitting timestep δt . We characterized the thickness of the stability fingers as well as the gap between them. Both the thickness and the size of gaps grow with decreasing splitting time step.



Acknowledgement

This work has been supported by the Hungarian National Research, Development and Innovation Fund under contract NKFI K 137726.

References

- [1] Faragó, István and Havasi, Ágnes, (2009), Operator splittings and their applications, *Nova Science Publ.*
- [2] McLachlan, Robert I and Quispel, G Reinout W, (2002), Splitting methods, *Acta Numerica*, vol.11, 341–434, Cambridge Univ. Press
- [3] Mincsovcics, M., & Kalmár-Nagy, T. (2022) Splitting headache: how well do splitting methods preserve stability? *International Journal of Nonlinear Mechanics*

Geometric Ito-Taylor Weak 3.0 integration scheme for dynamical systems on manifolds

Ankush Gogoi*, Satyam Panda**, Budhaditya Hazra** and Vikram Pakrashi *

*UCD Centre for Mechanics, School of Mechanical and Materials Engineering, University College Dublin, Dublin, Ireland

**Department of Civil Engineering, Indian Institute of Technology, Guwahati, Assam, India

Abstract. The understanding of the interaction of stochasticity and nonlinearity is a key aspect of modeling complex dynamical systems. The dynamics of physical systems with inherent uncertainties naturally evolve on a mathematical structure defined as a manifold. Towards this, the present work proposes a new higher order geometry preserving stochastic integration scheme based on Ito-Taylor expansion for stochastic dynamical systems evolving on the manifold. This study blends the concepts of Ito calculus and the theory of Lie groups. The preservation of the geometry of the manifold is ensured by exploiting the relation between Lie group and Lie algebra through the exponential map.

Introduction

Naturally occurring systems often have inherent randomness rendering their analysis difficult. Stochastic Differential Equations (SDEs) facilitate the accurate modeling of such dynamical systems. The application of SDEs for dynamical systems evolving on the Euclidean space is well established [1]. However, most of the physical systems evolve on manifolds, resulting in the analysis of such systems quite difficult since the dynamics is constrained by certain geometrical constraints [2]. Although several literature have developed integration schemes for dynamical systems on manifold, they are mostly centered around deterministic dynamics. Literature [2] developed a stochastic Magnus expansion based geometric Euler-Maruyama (g-EM) scheme for solving geometric SDEs. However, such lower order schemes are not suitable for solving nonlinear SDEs [1]. Towards this, a new higher order geometric stochastic integration scheme is developed for solving nonlinear geometric SDEs such that both stochasticity is taken into account as well as the geometry of the manifold is preserved. Consider a geometric SDE on the manifold as, $d\mathbf{X}(t) = \mathbf{A}(\mathbf{X}, t) \mathbf{X}(t) dt + \sum_{r=1}^d \mathbf{B}_r(\mathbf{X}, t) \mathbf{X}(t) dW_r(t)$, where, $\mathbf{X}(t)$ is the stochastic process and $dW_r(t)$ denotes the increments of Wiener process. Considering a stochastic Magnus expansion expansion [2], the solution is obtained as, $\mathbf{X}(t) = \exp(\Omega(t)) \mathbf{X}_0$, where, $\mathbf{X}(0) = \mathbf{X}_0$. $\Omega(t)$ is a matrix defined on the Lie algebra (space of skew-symmetric matrices) of the manifold such that an SDE corresponding to $\Omega(t)$ can be written as, $d\Omega(t) = \alpha(\mathbf{A}, \mathbf{B}_r) dt + \sum_{s=1}^d \beta_s(\mathbf{B}_r) dW_s(t)$ with $\Omega(0) = 0$. Since the Lie algebra is analogous to the Euclidean space, following the development in [1], the geometric Weak 3.0 mapping can be constructed for solving the aforementioned SDE on the Lie algebra.

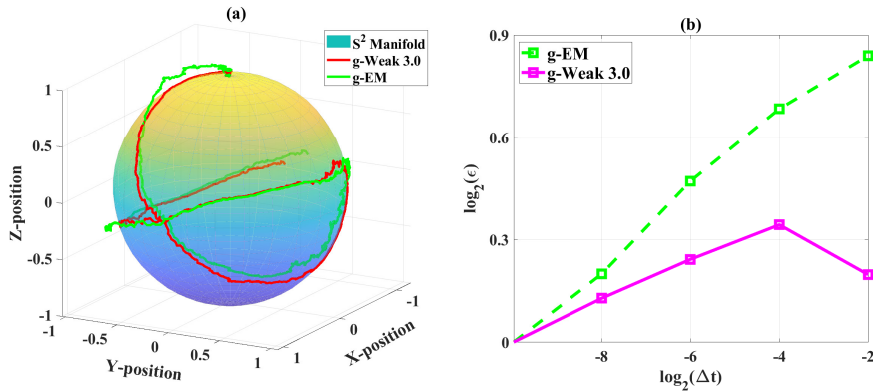


Figure 1: (a) Measure of geometry preservation, (b) Comparison of global error for stochastic Keplerian oscillator on S^2 .

Results and Discussions

Fig. 1(a) shows the response trajectory of the Keplerian oscillator on the sphere S^2 for a time step of $\Delta t = 0.01s$. It is clearly observed that the solution using non-geometric Weak 3.0 scheme [1] drifts away from the surface of the manifold, thus failing to preserve the geometry, whereas, the proposed geometric Weak 3.0 (g-Weak 3.0) scheme preserves the geometry for coarser time step. Fig. 1(b), shows that the global error for g-EM increases for coarser time step whereas, the global error corresponding to g-Weak 3.0 is significantly less, thus reducing the computational time. The global error is defined as, $\log_2(\max(E[X_{ref}]) - \max(E[X]))$.

References

- [1] Tripura T., Gogoi A., Hazra B. (2020) An Ito-Taylor weak 3.0 method for stochastic dynamics of nonlinear systems. *Appl. Math. Model.* **86** : 115-141.
- [2] Marjanovic G., Solo V. (2018) Numerical methods for stochastic differential equations in matrix lie groups made simple. *IEEE Trans. Autom. Control* **63** : 4035-4050.

Numerical Calculation of Dynamics of Wiper Blade with Attack Angle

Zihan Zhao* and Hiroshi Yabuno*

*Mechanical Systems Laboratory, University of Tsukuba, Tsukuba, Japan

Abstract. The automobile windshield is always made with a curvature. The oblique angle between the wiper blade and the windshield is called attack angle. Due to the attack angle, the wiper can easily jump up from the windshield while wiping, then the rainwater on the windshield is wiped off incompletely. In order to reduce this situation, it is important to clarify the dynamics of the wiper blade by taking into account the attack angle. In this study, the relationship between the attack angle and the jumping phenomenon is examined as follows. We introduce an analytical two-link model of the wiper blade that considers the exchange of dynamic and static friction between the windshield and the blade. Dynamic friction negatively related to the relative velocity of the motion, and static friction expressed by using a set-valued function that keeps the system in equilibrium. A simulation algorithm is established based on the equations of motion.

Introduction

The windshield of the automobile is generally made with a curvature to ensure excellent aerodynamic performance and aesthetics. An angle between the symmetry plane of the wiper blade and the normal vector of the windshield surface can be generated. Because the presence of the angle, which is called the attack angle, makes the wiper blade jump away from the windshield during wiping, it negatively affects the driving experience and poses a safety hazard. Therefore, it is essential to understand the dynamics of the wiper blade in consideration of the attack angle to avoid the jumping phenomenon. Lancioni et al. [1] conducted numerical analysis to elucidate how the attack angle affects the wiper blade to produce the jumping phenomenon. In addition to the slip state and stick state, the free flight state after jumping was analyzed. They found that a chattering of about 100 Hz was produced, indicating that this is a complex vibration that mixes the above three different states of motion. However, the wiper blade was only modeled with one link.

In this study, an analytical two-link model which takes into account the attack angle [2] is introduced. A numerical calculation program based on the equation of motion of this model is developed. The slip and stick states are distinguished by the difference of dynamic and static friction. Also, two states where the shoulder contacts to the head or not are considered. In the transitions between these different states, the transition times are exactly derived by the slack variable method [3]. Furthermore, in the state subject to the static friction, the Baumgarte's stabilization method [4] is employed in the numerical calculation program.

Results and discussion

This program can calculate the dynamics of the motion of wiper blade with attack angle in one round trip. Some numerical results depending on the attack angle are shown in Fig. 1. Figure 1(c) shows the changes in the angles of two links θ and ϕ with attack angles of 10 degrees. It can be confirmed that the angles becomes 0 at the same time during the wiping process, which means both links are perpendicular to the wiping surface, and at this time the calculation program stops because of the jumping phenomenon. However, as shown in Figs. 1(a) and 1(b), the jumping phenomenon does not occur where the attack angle is 0 and 5 degrees. It can be concluded that the two links of the wiper blade becoming perpendicular to the wiping surface during the wiping process is the reason of the jumping phenomenon.

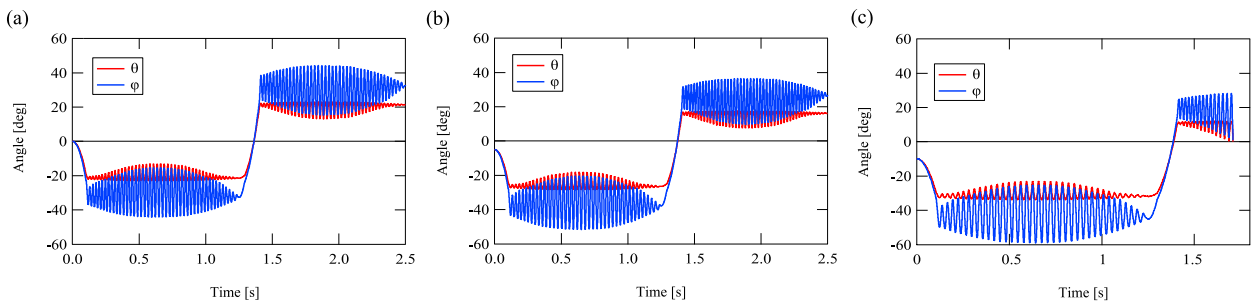


Figure 1: Numerical calculation results of the angles of the two links with different attack angles. (a) attack angle = 0°; (b) attack angle = 5°; (c) attack angle = 10°

References

- [1] Lancioni, G., Lenci, S., Galvanetto, U. (2016). Dynamics of windscreen wiper blades: Squeal noise, reversal noise and chattering. *Int. J. Non. Linear. Mech.* **80**:132-143.
- [2] Zhao, Z., Yabuno, H., Kamiyama, K. (2022). Dynamic Analysis of a Wiper Blade in Consideration of Attack Angle and Clarification of the Jumping Phenomenon. *Appl. Sci.* **12**:4112.
- [3] Turner, J. D. (2001) On the simulation of discontinuous functions. *Int. J. Appl. Mech.* **68**(5):751-757.
- [4] Baumgarte, J. (1972) Stabilization of constraints and integrals of motion in dynamical systems. *Comput. Methods in Appl. Mech. Eng.* **1**(1):1-16.

Modelling string vibrations with unilateral impacts in fretted musical instruments through the modal Udwadia-Kalaba approach

V. Debut^{*,***,*}, J. Antunes^{*,**} and F. Soares^{**}

^{*}Instituto de Etnomusicologia, Centro de Estudos em música e Dança – Universidade Nova de Lisboa, Lisboa, Portugal

^{**}Instituto Superior Técnico – Centro de Ciências e Tecnologias Nucleares, Lisboa, Portugal

^{***}Instituto Politécnico de Castelo Branco – Escola Superior de Artes Aplicadas, Castelo Branco, Portugal

Abstract. Following our previous work on the Udwadia-Kalaba (U-K) dynamical formulation as applied to musical instruments, we explore here the possibility of modeling the vibro-impact string motions in fretted instruments. The frets, distributed along the fingerboard, are modelled in terms of auxiliary oscillators intermittently coupled to the string allowing different types of contacts. Illustrative numerical simulations are presented by considering a fretted monochord.

Introduction

The nonlinear interaction of a vibrating string against an obstacle has recently called for a large body of research for simulation and sound synthesis of stringed musical instruments. For modelling contact, most of the methods presented so far adopt a penalty approach together with sophisticated discretization methods [1, 2, 3], or numerical techniques from nonsmooth contact dynamics [4]. Alternatively, the present authors demonstrated that reliable simulations of flexible systems involving point-constraints, either linear [6] or intermittent [7], can be carried out by using the Udwadia-Kalaba equation [8], which expresses the dynamics of the constrained system through a single dynamical matrix equation including constraints. Following our efforts in musical instrument simulation, this work places the focus on the implementation of the string nonlinear impact interactions with the multiple frets of a guitar within the modal U-K framework.

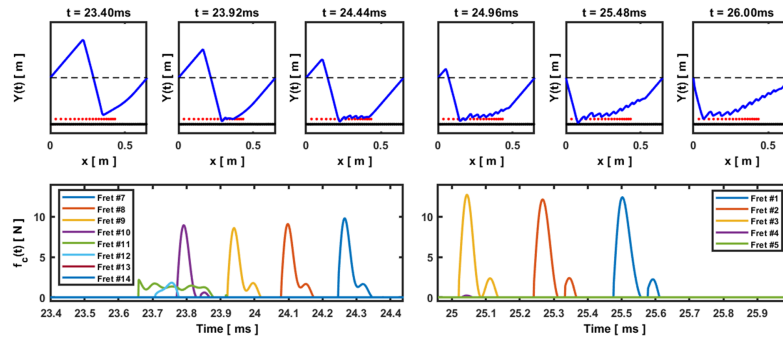


Figure 1: Computed snapshots of string motion against a set of 19-fret (distributed to allow chromatic playing) on a fingerboard together with the computed contact forces.

Results and discussion

The contact force is computed at each time step from the string modal motion and its calculation includes a condition of constraint release when the contact force changes from compression to traction. To deal with the spatial extent of the system, we keep track of the current contact configuration, and update the constraint matrix whenever a contact is detected or released. Because constraints are applied at the acceleration level, an accumulative drift can be observed in the computed motion and special care has been taken in the numerical integration by implementing the constraint violation elimination technique [9]. Figure 1 presents simulations results, where patterns in the contact force are highlighted, that seem quite realistic as are the resulting sounds.

References

- [1] Chatzioannou V., Van-walstijn M. (2015) Energy conserving schemes for the simulation of musical instrument contact dynamics. *J. Sound Vib.*, 339, 2015.
- [2] Issanchou C., Le Carrou J-L., Touzé C, Fabre B. and Doaré O. (2018) String/frets contacts in the electric bass sound: simulations and experiments. *Appl. Acoust.*, 129, 217-228.
- [3] Bilbao S., Torin A. (2014) Numerical simulation of string/barrier collisions: the fretboard. *DAFX 2014*.
- [4] Issanchou C., Acary V., Perignon F., Touzé C. and Le Carrou J-L. (2018) Nonsmooth contact dynamics for the numerical simulation of collisions in musical string instruments, *J. Acoust. Soc. Am.*, 143, 3195.
- [5] Issanchou C., Bilbao S., Le Carrou J-L., Touzé C, Fabre B. and Doaré O. (2017) A modal-based approach to the nonlinear vibration of strings against a unilateral obstacle: Simulations and experiments in the pointwise case. *J. Sound Vib.*, 393, 229-251.
- [6] Antunes J., Debut V. (2017) Dynamical computation of constrained flexible systems using a modal Udwadia-Kalaba formulation: Application to musical instruments. *J. Acoust. Soc. Am.*, 141, 764-778.
- [7] Antunes J., Debut V., Borsoi L., Delaune X., Piteau P. (2017) A modal Udwadia-Kalaba formulation for vibro-impact modelling of continuous flexible systems with intermittent contacts. *Procedia Eng.*, 199, 322-329.
- [8] Udwadia F.E., Kalaba R.E. (1992) A new perspective on constrained motion. *Proc. R. Soc. A*, 439, 407-410.
- [9] Yoon S., Howe R.M., Greenwood D.T. (1994) Geometric elimination of constraint violations in numerical simulation of Lagrangian equations. *J. Mech. Des.*, 116, 1058-1064

A perturbation theory for the shape of central force orbits

Ritapriya Pradhan*, Tanushree Bhattacharya* and Jayanta K. Bhattacharjee *

*School of Physical Sciences, Indian Association for the Cultivation of Science, Jadavpur, Kolkata 700032, INDIA

Abstract. The two body central force orbit can be solved exactly only for the gravitational and simple harmonic oscillator potentials. When one discusses nonlinear oscillators, the trajectory in space-time can be found by various kinds of perturbative techniques- one of the most prominent ones being the Lindstedt-Poincare perturbation theory. In this work we show that a Lindstedt-Poincare like perturbation theory can be set up for the shape of a general central force orbit by working round a circular orbit. One also gets an answer for spatial frequency by this process. The effectiveness of our technique is checked against numerical simulations.

Introduction

We consider the dynamics of a particle of mass ‘ m ’ moving in a central force field where the force is taken to be of the form $F = -m\lambda r^{-n}$, where n is any number such that bound orbits exist. The distance of the particle from the center of force is ‘ r ’ and ‘ λ ’ is the interaction strength. The conservation of the angular momentum (magnitude ‘ l ’ per unit mass) restricts the particle to a plane. In terms of the polar co-ordinates ‘ r ’ and ‘ θ ’, we have ($u = 1/r$)

$$\frac{d^2u}{d\theta^2} + u = \frac{\lambda}{l^2}u^{n-2} \quad (1)$$

Our perturbation theory is set up around the circular orbit characterized by $u_0 = (\frac{\lambda}{l^2})^{\frac{1}{3-n}}$. The energy of the orbit is $E_c = \frac{1}{2}l^2u_0^2\frac{n-3}{n-1}$. Appropriate modifications are necessary for $n = 1$. The deviation u_1 from the circular orbit defines the dimensionless quantity $X = \frac{u_1}{u_0}$. The variable X satisfies the dynamics

$$\frac{d^2X}{d\theta^2} + (3-n)X = \sum_{k=2}^{\infty} n^{-2}C_kX^k \quad (2)$$

The energy is expressed in terms of X as

$$\Delta E = E - E_c = \frac{1}{2}l^2u_0^2 \left[\left(\frac{dX}{d\theta} \right)^2 + 2X + X^2 - \frac{2}{n-1} \{ (1+X)^{n-1} - 1 \} \right] \quad (3)$$

We have thus reduced the orbit equation formally to an anharmonic oscillator equation with coordinate X and timelike variable θ . The order of perturbation theory is determined by how many powers of X is retained. In some ways this is another example of a traditional perturbation theory being used in an unexpected situation [1].

Results and Discussion

The orbit upto second order in ϵ is (initial conditions suitably chosen)

$$u = \left(\frac{\lambda}{l^2} \right)^{\frac{1}{3-n}} \left[1 - \epsilon^2 \frac{n-2}{4} + \epsilon \cos(\sqrt{3-n}\theta) + \epsilon^2 \frac{n-2}{12} \cos(2\sqrt{3-n}\theta) \right] \quad (4)$$

One gets a spatial frequency $\Omega = \sqrt{3-n}$ within this order. We get corrections to this as we go to higher order. Note, ϵ is the order of amplitude of X and hence is the perturbation parameter. Our results agree with the exact solutions for $n = 2$ and $n = -1$. The comparison between our perturbation theory result and the numerically obtained trajectory, spatial frequency is shown in Figure 1.

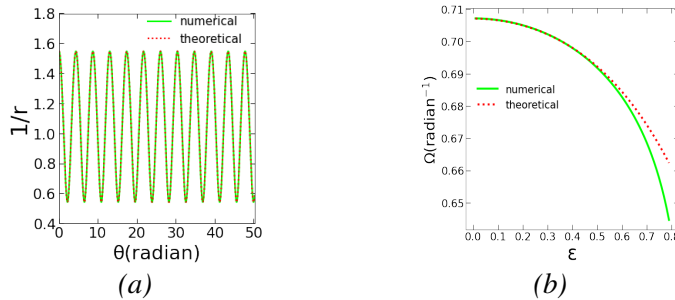


Figure 1: (a) Plot of $\frac{1}{r}$ as a function of θ for $n = 1$, $\epsilon = 0.5$, $u_0 = 1$ (b) Plot of Ω as a function of ϵ for $n = 2.5$

References

- [1] T Shah, R.Chattopadhyay, K.Vaidya, S.Chakraborty (2015) Conservative Perturbation Theory for Non Conservative Systems. *Phys Rev E* **92** 062927

On the Nonlinear Dynamics of In-contact Bodies subject to Stick-Slip and Wear Phenomena

Arnaldo Casalotti*, Francesco D'Annibale**

*Department of Architecture, University of Roma Tre, Italy, ORCID 0000-0002-9047-9523

**Department of Civil, Construction-Architectural and Environmental Engineering, University of L'Aquila, Italy, ORCID 0000-0002-6580-9586

Abstract. The dynamic behavior of a one degree-of-freedom oscillator, subject to stick-slip and wear phenomena at the contact interface with a rigid substrate, is investigated. The motion of the oscillator, induced by a harmonic excitation, is influenced by the tangential contact forces, exchanged with the rigid soil, which in turn depend on specific nonlinear constitutive models considered to account for stick-slip phenomena due to friction as well as wear due to abrasion. The nonlinear ordinary differential equations governing the problem are derived, whose solution is numerically obtained. In this context, the effect of the different interface models on the nonlinear dynamics is extensively analyzed and discussed.

Introduction

Detailed engineering design requires the study of specific mechanical behaviors: this is the case of in-contact bodies. In particular, it becomes a key aspect when interface phenomena such as friction and abrasion take place. In this context, it is thus necessary to formulate richer constitutive models that have to account for the in-time evolution of the interface [1, 2]. The description of stick-slip phenomena due to friction and wear due to abrasion, has been addressed in several studies. New interface models are derived in the general framework of the Thermodynamics of the irreversible processes and account for suitable internal variables of phenomenological type, grounding the formulation of the wear process in the context of Damage Mechanics [3]. Such models have been adopted in [4] to investigate the behavior of elastic bodies in tangential contact with a rigid substrate in discrete points, under quasi-static loading conditions. Motivations of this study rely on the fact that the contact modeling of complex interface behaviors has mostly been conducted in statics, and therefore further efforts can yet be conducted to investigate dynamic regimes, besides some examples can be found in e.g. [5, 6]. The nonlinear dynamic problem has been here addressed with reference to a rigid block, schematically represented in Fig. 1-a, subject to a harmonic load, whose motion gives rise to tangential stresses, evolving in time according to the nonlinear constitutive laws of [3] and sketched in Figs. 1-b,c, without and with wear, respectively.

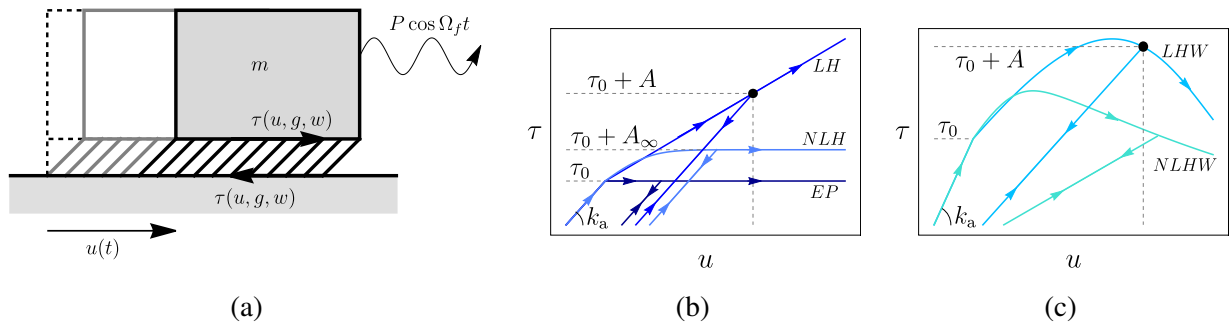


Figure 1: Oscillator in tangential contact: (a) structural scheme; (b) no-wear models; (c) wear models.

Results and Discussion

In the analyzed case, due to the nature of the constitutive equations, it is not possible to a priori know the steady-state response, since it strictly depends on the transient phase. Therefore, a numerical solution strategy is adopted to solve the nonlinear non-smooth ordinary differential equations. The frequency-response curves are the obtained to evaluate the system behavior under different excitation frequencies. Results show that the effect of the interface allows to dissipate the energy introduced by the excitation and the equivalent dissipation capacity strongly depend on the type of contact law.

References

- [1] Li, B., Li, P., Zhou, R., Feng, X. Q., Zhou, K. (2022) Contact mechanics in tribological and contact damage-related problems: A review, *Tribology International*, **171**, 107534.
- [2] Barber, J. R., Ciavarella, M. (2000) Contact mechanics, *Int. J. Solids Struct.*, **37**(1-2), 29-43.
- [3] D'Annibale, F. and Luongo, A. (2012) A damage constitutive model for sliding friction coupled to wear, *Continuum Mech. Thermodyn.*, **25**, 503-522.
- [4] D'Annibale, F., Casalotti, A., Luongo, A. (2021) Stick-slip and wear phenomena at the contact interface between an elastic beam and a rigid substrate, *Math. Mech. Solids*, **26**(6), 843-860, (2021).
- [5] Caughey, T. K. (1969) Sinusoidal excitation of a system with bilinear hysteresis, *J. Appl. Mech.*, **27**(4), 640-643.
- [6] Lacarbonara, W., Vestroni, F. (2003) Nonclassical responses of oscillators with hysteresis, *Nonlinear Dynam.*, **32**(3), 235-258.

Anomaly detection in nonlinear vibrational structures using variational auto-encoders

Kiran Bacsa^{*,**}, Wei Liu^{*,***} and Eleni Chatzi^{**}

^{*} Singapore-ETH Centre, Future Resilient Systems, Singapore, 138602, Singapore

^{**} ETH Zurich, Department of Civil, Environmental and Geomatic Engineering, Zurich, 8093, Switzerland

^{***} NUS, Department of Industrial Systems and Management, Singapore, 117576, Singapore

Abstract. We propose the use of a Variational Auto-encoder (VAE) with Long Short-Term Memory Neural Networks (LSTM) for the unsupervised learning of the dynamics of a nonlinear vibrational structure. We then show our model has learned the parameters of the structure by passing unit impulses through the encoder and decoder networks to obtain pseudo-impulse responses that mimic the true impulse responses of the structure. Our model is validated on a two-story shear frame with hysteric links to shown that our method generalises to nonlinear dynamics. Furthermore, we show that the inferred latent features can be used for auxiliary tasks, such as anomaly detection. In the case of the two-story shear frame, we introduce different types of structural damage through shifts in the elastic and hysteretic system properties. These damages prove easily identifiable when looking at the latent features learned by the VAE.

Introduction

Structural monitoring of engineered systems experiencing nonlinearities, e.g. geometric [1] or material [2], is non-trivial. While advances in Internet of Things (IoT) technologies have allowed for gathering of massive amounts of heterogeneous data, nonlinearity remains challenging to characterize, especially since most of the collected data is not labeled. This hardens the application of off-the-shelf machine learning tools, which rely on supervised learning paradigms. For accomplishing the task of anomaly detection on nonlinear systems, we here turn to unsupervised machine learning methods, such as VAEs to extract the intrinsic physical properties of a nonlinear structure.

From the latent representation learned in an unsupervised manner, we seek to solve two inverse problems: the recovery of the original excitation of the system and the geometry of the structure expressed in its modes. Once we have shown that our model has indeed encoded both these properties, we use the reduced features for discriminant tasks, such as anomaly detection. We validate the proposed scheme on a simulated two-story benchmark frame comprising multiple hysteric joints [3]. The bottom links are excited with a parameterized synthetic ground motion database [4]. Once the features are learned by the VAE, different types of anomalies are classified, which arise from structural damage.

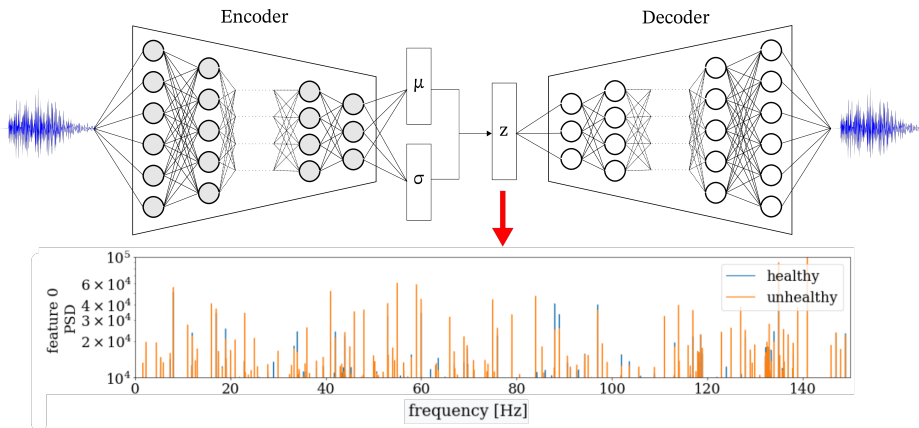


Figure 1: The autoencoder is trained to reconstruct the earthquake excitation acceleration histories of the system. Its latent features allow us to distinguish healthy from unhealthy structures.

Results and discussion

Once our model has been fully trained on the target dataset, we trigger the encoder and decoder networks to obtain pseudo-impulse responses of the VAE. The outputs under the trigger show close resemblance to the impulse response of the system. Future work will include the use of domain-adaptation techniques to reuse the features that were learned for real datasets, comprising too few samples to directly train a neural network.

References

- [1] Wenneker F. and Tiso P. (2014) A Substructuring Method for Geometrically Nonlinear Structures. *International Modal Analysis Conference*
- [2] Farhat C., Van der Zee K. G. and Gueuzaine P. (2004) Provably second-order time-accurate loosely-coupled solution algorithms for transient nonlinear computational aeroelasticity. *Computer Methods in Applied Mechanics and Engineering*
- [3] Vlachas K., Agathos K., Tatsis K. E., Brink A. R. and Chatzi E. (2021) Two-story frame with Bouc-Wen hysteretic links as a multi-degree of freedom nonlinear response simulator. *5th Workshop on Nonlinear System Identification Benchmarks*
- [4] Spiridonakos M. D. and Chatzi E. (2015) Metamodeling of dynamic nonlinear structural systems through polynomial chaos NARX models. *5th Workshop on Nonlinear System Identification Benchmarks*

Quasi projective synchronization of time varying delayed complex valued Cohen-Grossberg neural networks with mismatched parameters: Direct approach.

Sapna Baluni* and Subir Das*

*Department of Mathematical Sciences, Indian Institute of Technology (BHU), Varanasi (221005), India

Abstract. In this article the quasi-projective synchronization (QPS) of time-varying delayed complex-valued Cohen Grossberg Neural Networks (CGNNs) with mismatched parameters has been studied. As complete projective synchronization is impossible due to parameters' mismatches and projective coefficient, a drive has been taken to achieve quasi-projective synchronization of distinct complex-valued CGNNs. The purpose of this study is to find a criterion for quasi-projective synchronization of two non-identical CGNNs by constructing a suitable controller and by using direct method. The important contribution is to estimate the bound on the synchronization error. Some sufficient criteria for synchronization between master and response systems are also established. The efficiency of the proposed method is justified through numerical simulation applied to a specific example.

INTRODUCTION

So far numerous synchronization results have been developed such as anti-synchronization, complete synchronization, quasi-synchronization, projective synchronization, and multi-synchronization. Among the existing synchronization schemes, projective synchronization stands out as a significant feature of proportional synchronization of master and response systems. It can be used for the sake of fast communication like an extension of binary digits to M-nary digital communications [1]. The error during the implementation of practical synchronization does not always approach to zero with time, but fluctuate within a small range, which is called QPS [2]. This phenomenon is produced by several unavoidable factors, including non-identical parameters, projective coefficient, controller etc. In the research article [3], two real valued systems were formed separating the real and imaginary parts of complex valued functions and then with the help of these two real valued systems, criteria for stability and synchronization are obtained. The method of converting a complex system into real system not only increases the computational time but also complicates the theoretical analysis and complexity of the results. To avoid this problem it is better to discuss the synchronization problem of CVNNs by using the Direct method.

Results and discussion

A sufficient criterion is established for ensuring QPS between master and response systems with mismatched parameters. The upper bound of the synchronization error is estimated, as well as the connection between it and the controller parameter given in this article. Figs. 1 and 2 show QPS and quasi-synchronization between master and response systems with mismatched parameters, respectively. The article shows that the estimated upper bound depends on the projective coefficient k . As a result, the bound can be regulated by choosing the suitable controller parameter. The relevant evaluation is shown in the reference [1]. In [1], the projective coefficient k is a real positive constant, but in our case projective coefficient k is a complex number and there is no restriction on k . Hence, our conclusions are more generic. Also, Fig. 3 depicts the complete synchronization of two identical systems.

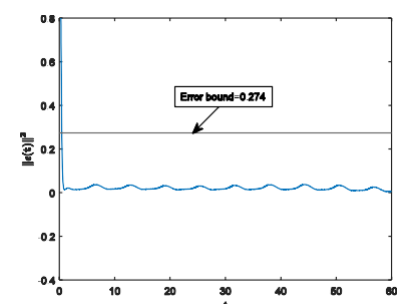


Fig. 1

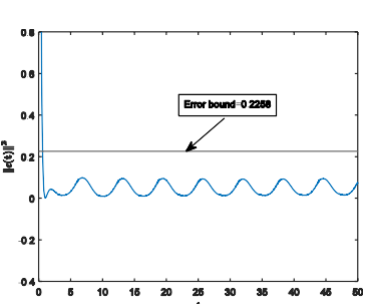


Fig. 2

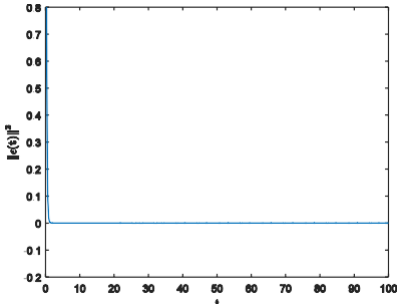


Fig. 3

References

[1] Guo, R., Lv, W., Zhang, Z., 2020. Quasi-projective synchronization of stochastic complex-valued neural networks with time-varying delay and mismatched parameters. *Neurocomputing* 415, 184–192

[2] Chee, C., Xu, D., 2006. Chaos-based m-ary digital communication technique using controlled projective synchronisation. *IEE Proceedings-Circuits, Devices and Systems* 153, 357–360.

[3] Chen, Q., Bin, H., Huang, Z., 2021. Synchronization of cvnns: A time-scale impulsive strategy. *IEEE Access* 9, 31762–31772.

Modified Bouc-Wen model with damage and flexibility increase for the dynamic analysis of masonry walls

Alessandra Paoloni*, Domenico Liberatore** and Daniela Addessi*

*Department of Structural and Geotechnical Engineering, Sapienza University of Rome, Rome, RM, Italy

**Department of History, Representation and Restoration of Architecture, Sapienza University of Rome, Rome, RM, Italy

Abstract. The purpose of the following study is to present a force-based macroelement for the static and dynamic analysis of the in-plane response of masonry panels. The nonlinear behaviour of masonry is described by a constitutive model based on the Bouc-Wen hysteretic formulation modified with the introduction of damage and flexibility increase by means of two scalar variables that regulate the rate and type of degradation. Damage is considered as a reduction of the hysteretic force, while flexibility increase is modelled through an enlargement of the elastic displacement, both depending on the dissipated energy. The aim is to give a more accurate representation of the strength and stiffness decay these walls undergo when subjected to cyclic loadings and to better represent the loading and unloading branches of the response curves. To investigate the effect of the degradation in the dynamic field, the behaviour of both a slender and a squat wall is analysed under harmonic excitations.

Introduction

A large part of the architectural heritage throughout the world is built using traditional materials. Among these, masonry is the most widely spread, and is still nowadays largely studied. Its fascinating and complex behaviour, due to the coupling bricks or blocks with mortar, together with the high uncertainty caused by the failure mechanisms occurring during cyclic and dynamic actions, has deserved the application of numerous formulations to reproduce its mechanical response. The Bouc-Wen hysteresis [1] has proved to be a reliable tool for the representation of the cyclic response of masonry, especially when modifications are introduced to account for the onset and propagation of damage [2,3].

The formulation already presented in [2] is here enhanced with the introduction of flexibility increase, depending on the dissipated energy and a scalar variable that regulates the rate of the stiffness degradation, for a more accurate description of the stiffness and strength decay observed in experimental tests.

The proposed macroelement, originally formulated in [3], uses the modified Bouc-Wen law to model the nonlinearity of masonry in a shear link and two lumped flexural hinges that are in series with an elastic beam element. Pinching and the high initial stiffness that characterize slender panels are also taken into account by the flexural hinges thanks to the introduction of a nonlinear elastic and an elastic negative device, respectively. Regarding the dynamic formulation, the lumped mass matrix and classical Rayleigh damping are implemented consistently with the equilibrated force-based approach adopted for the formulation of the macroelement.

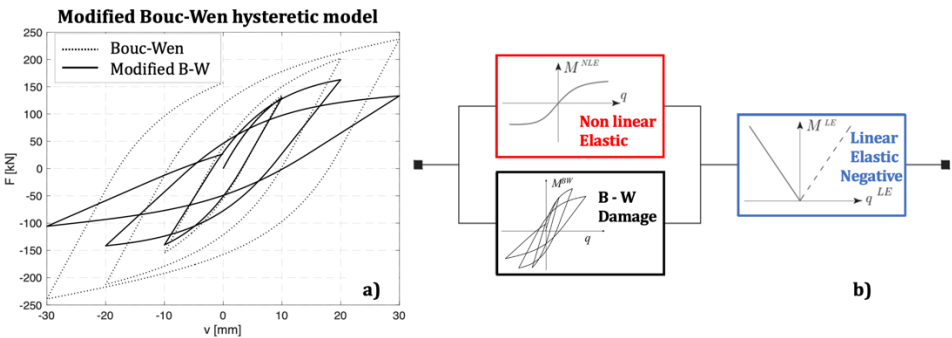


Figure 1: Modified Bouc-Wen model with damage and flexibility increase a); structure of the flexural hinge of the macroelement b).

Results and Discussion

Both the static and dynamic behaviour of masonry walls are investigated, considering two different geometric configurations, namely a slender and a squat panel. A good agreement of the static response compared to experimental results presented in literature is highlighted. Moreover, the impact of damage and damage with flexibility increase is investigated with respect to the classical Bouc-Wen model and the elastic case, with the aim of examining the performance of the model in the dynamic field, specially focusing on the influence of damage mechanisms on the dynamic characteristics of the structural response.

References

[1] R Bouc. A mathematical model for hysteresis. *Acta Acustica united with Acustica*, 24(1):16–25, 1971.
[2] Liberatore D., Addessi D. and Sangirardi M., (2019). An enriched Bouc-Wen model with damage. *European Journal of Mechanics/A Solids*, Vol. 77.
[3] Sangirardi M., Liberatore D., Addessi D., (2019). Equivalent frame modelling of masonry walls based on plasticity and damage. *International Journal of Architectural Heritage*, Vol. 13(7), pp. 1098–1109.

An Algebraic Model for Hysteretic Responses exhibiting Cyclic Hardening and Softening Phenomena: Preliminary Results

Raffaele Capuano*, Nicolò Vaiana* and Luciano Rosati *

*Department of Structures for Engineering and Architecture, University of Naples Federico II, Via Claudio 21, Napoli, 80125, Italy

Abstract. We provide closed-form expressions to evaluate the generalized work done by a generalized hysteretic force, simulated by using a recently formulated model denominated Algebraic Model. Such expressions are valid over a generic generalized displacement interval and are used to simulate the cyclic hardening and softening phenomena observed in many mechanical systems and materials. In addition, we also provide closed-form expressions for evaluating the work done by the generalized hysteretic force when a full cycle of generalized displacement is assigned.

Introduction

Modeling of cyclic hardening or softening phenomena affecting the hysteretic response of mechanical systems and materials needs to take into account several complex aspects; consequently, it is quite difficult to formulate a single model adopting few parameters. Over the years, many authors presented different models to reproduce such complex responses, as those characterized by cyclic degradation phenomena [1] and nonlinear kinematic hardening [2]. In this regard, we present an extension of the Algebraic Model (AM) described in [3] in order to accurately simulate cyclical hardening/softening phenomena. Such a model is computationally efficient, being based on closed-form expressions, and adopts parameters having a clear mechanical meaning.

Results and Discussion

Figure 1 shows the comparison between the analytical and experimental results obtained by using the proposed AM in two different cases. In particular, Figure 1a shows the results obtained by modeling the cyclic hardening hysteretic behavior exhibited by an annealed OFHC (oxygen free high conductivity) copper material when an axial sinusoidal strain is applied with a frequency of 0.008 Hz and an amplitude of 0.74. [4]. Moreover, Figure 1b illustrates the results obtained by modeling the cyclic softening hysteretic behavior exhibited by the Fujian standard sand when a transverse (shear) sinusoidal displacement is imposed with a frequency of 0.002 Hz, an amplitude of 10 mm, under the effect of a normal stress of 90 kPa [5].

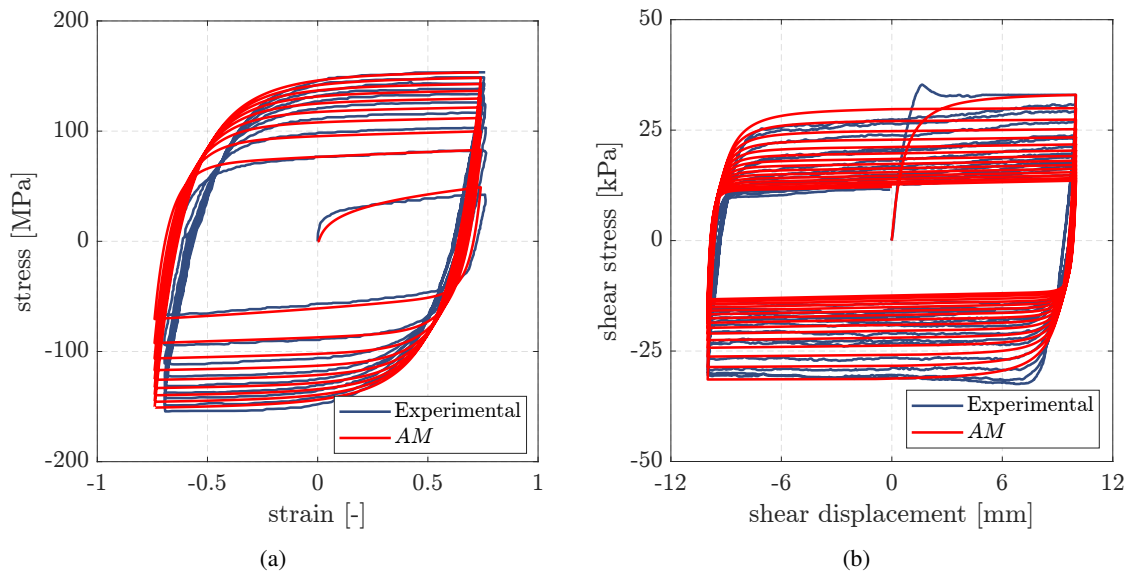


Figure 1: Comparisons of analytical and experimental results obtained for an annealed OFHC copper [4] (a) and a Fujian standard sand [5] (b) under cyclic loading.

References

- [1] Baber, T. T. and Noori, M. N. (1985). Random vibration of degrading, pinching systems. *J Eng Mech*, **111**(8):1010-1026.
- [2] Karavasilis, T. L., Krawala, S., and Hale, E. (2012). Hysteretic model for steel energy dissipation devices and evaluation of a minimal-damage seismic design approach for steel buildings. *J Constr Steel Res*, **70**:358-367.
- [3] Vaiana, N., Sessa, S., Marmo, F., and Rosati, L. (2019). An accurate and computationally efficient uniaxial phenomenological model for steel and fiber reinforced elastomeric bearings. *Compos Struct*, **211**:196-212.
- [4] Lamba, H. S., and Sidebottom, O. M. (1978). Cyclic plasticity for nonproportional paths: part 1—cyclic hardening, erasure of memory, and subsequent strain hardening experiments. ASME. *J Eng Mater Technol*, **100**(1):96-103.
- [5] Zhou, W., Wang, L., Guo, Z., Liu, J., and Rui, S. (2019). A novel t-z model to predict the pile responses under axial cyclic loadings. *Comput Geotech*, **112**:120-134.

An improved variable-coefficient harmonic balance method for quasi-periodic solutions

Junqing Wu^{*}, Jun Jiang^{*}, Ling Hong^{*}

^{*} State Key Laboratory for Strength and Vibration, Xi'an Jiaotong University, Xi'an, Shaanxi, China

Abstract. The variable-coefficient harmonic balance method (VCHBM) approximates quasi-periodic solutions by using a variable-coefficient Fourier series. In this work, VCHBM for tracking the quasi-periodic solutions with two irrational frequencies is improved from two aspects. First, a new formulation for alternating Frequency-Time method is proposed for VCHBM so that the time-consuming symbolic operations are avoided and the computation efficiency is enhanced. Secondly, a phase condition and a frequency condition are introduced into the arc-length continuation method to make VCHBM robust and effective. Numerical examples show the validity of the proposed improvements.

Introduction

Quasi-periodic responses widely exist in nonlinear dynamical systems, which arise under a quasi-periodic excitation or even under a single frequency excitation. Harmonic balance method (HBM) has been successfully applied to evaluate the periodic motions of nonlinear dynamical systems. Recently, multi-harmonic balance method (MHBM) [1] and variable-coefficient harmonic balance method (VCHBM) [2] are proposed as the extensions of HBM to quasi-periodic solutions. Since all the frequencies base are the prerequisite for MHBM, which is often unrealistic under a single frequency excitation. In comparison, VCHBM is relative robust in evaluating such a quasi-periodic response. However, the ways in implementing Alternating time-frequency method (AFT) and arc-length continuation (ALC) in VCHBM have flaws. Thus, improvements are proposed in order to make VCHBM more efficient and robust.

Results and discussion

For a non-autonomous nonlinear system with n -DOFs governed by the differential equations:

$$\mathbf{M}\ddot{\mathbf{x}}(t) + \mathbf{C}\dot{\mathbf{x}}(t) + \mathbf{K}\mathbf{x}(t) + \mathbf{f}_n(\mathbf{x}, \dot{\mathbf{x}}) - \mathbf{e}(\omega, t) = \mathbf{0}.$$

The quasi-periodic responses with two irrational frequencies are approximated by variable-coefficients harmonic balance method with a Fourier series $\mathbf{x}(\omega_1 t, \omega_2 t) = \mathbf{X}_0^0(\omega_2 t) + \sum_{j=1}^{H_{VC}} \mathbf{X}_{k_j^c}^c(\omega_2 t) \cos(k_j^c \omega_1 t) + \mathbf{X}_{k_j^s}^s(\omega_2 t) \sin(k_j^s \omega_1 t)$, where $\mathbf{X}(\omega_2 t) = \mathbf{Z}_0^0 + \sum_{i=1}^{H_{VC}} \mathbf{Z}_{k_i^c}^c \cos(k_i^c \omega_2 t) + \mathbf{Z}_{k_i^s}^s \sin(k_i^s \omega_2 t)$. By applying the harmonic balancing in term ω_1 and ω_2 sequentially, the differential equations are eventually transformed into the $nL_{VC}^1 L_{VC}^2$ -dimensional nonlinear algebraic equations in the frequency domain as $\mathbf{R}(\mathbf{Z}, \omega_1, \omega_2) = \mathbf{A}_{VC}(\omega_1, \omega_2)\mathbf{Z} + \mathbf{F}(\mathbf{Z}) - \mathbf{E}_{VC} = \mathbf{0}$ [2].

In order to enhance the efficiency of AFT in determining the Fourier coefficients of the nonlinear forces, a procedure of two-step DFT and two-step inverse-DFT are proposed as shown by Fig.1(a). Two transformation matrices Γ_{VC}^2 and Γ_{VC}^1 of DFT and their inverse of i -DFT are updated at each step of the iterations in order to avoid the time-consuming symbolic operations. In order to achieve a robust solution track of quasi-periodic responses with respect to a free parameter, after two steps of tangent prediction and orthogonal correction of ALC are briefly reviewed, two supplemented constraint conditions, namely frequency condition and phase condition, are introduced (see Fig.1b). Especially, the phase condition $\left[\left((\nabla_2 \otimes \mathbf{I}_{nL_1}) \mathbf{Z} \right)^T + \left((\nabla_2 \otimes \mathbf{I}_{nL_1})^2 \mathbf{Z} \right)^T (\nabla_2 \otimes \mathbf{I}_{nL_1}) \right] \Delta \mathbf{Z} = 0$ based on an alternate phase condition [3] guarantees a unique quasi-periodic solution with a fixed phase shift and makes VCHBM robust and effective.

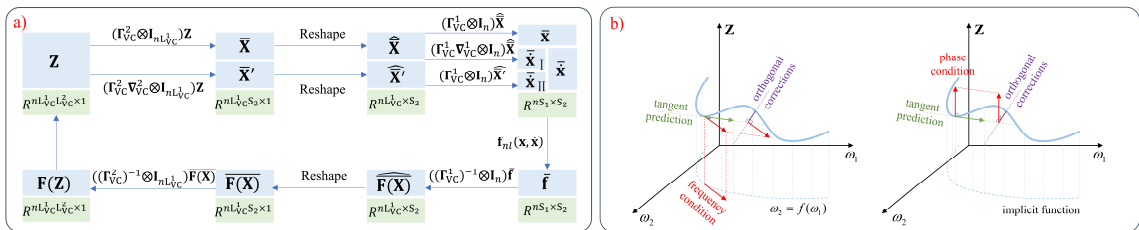


Figure 1: a) A segment after segment processing technique for AFT; b) A phase condition and a frequency condition for ALC

A SDOF Duffing oscillator system with a quasi-periodic excitation and a 2DOFs nonlinear energy sink (NES) system with a single frequency excitation are studied as examples to show the feasibility of the proposed new formulation for AFT and a more reasonable supplemented constraint condition for solution continuation.

References

- [1] Liao H., Zhao Q., Fang D. (2020) *Nonlinear Dyn.* **100**:1469-1496.
- [2] Zhou B., Thouverez F., Lenoir D. (2015) *Mech. Syst. Signal Process.*, **64-65**: 233-244.
- [3] Seydel R. (2009) *Practical Bifurcation and Stability Analysis*. Springer, NY.

A hybrid averaging and harmonic balance method for asymmetric systems

Steven W. Shaw*, Sahar Rosenberg** and Oriel Shoshani **

*Dept. of Mechanical and Civil Engineering, Florida Institute of Technology, FL, USA, ORCID #0000-0002-3874-4828

**Dept. of Mechanical Engineering, Ben Gurion University of the Negev, Israel

Abstract. We introduce a new technique that provides relatively simple approximations for the free and forced vibration response of weakly nonlinear systems, including those with asymmetric restoring forces. For free vibration, it captures the correct amplitude-frequency dependence, including cases of non-monotonicity. The method can also be used to determine the steady-state response of damped, harmonically driven vibrations, including stability results. The method is a blend of a first order perturbation calculation with higher order harmonic balance (HB), carried out by amplitude expansions. The HB aspect of the method captures information about higher harmonic overtones and the constant (DC) offset. General results are derived for an asymmetric system with up to quintic nonlinear stiffness terms. The results are validated using simulations. This approach will be useful for analyzing a variety of system models with polynomial nonlinearities.

Introduction

We consider weakly nonlinear vibration models with asymmetric restoring forces of the form

$$\ddot{x} + 2\Gamma\dot{x} + \omega_0^2x + \alpha_2x^2 + \alpha_3x^3 + \alpha_4x^4 + \alpha_5x^5 = F \cos(\omega t) \quad (1)$$

which arise in numerous applications. The structure of the steady state forced vibration response curves of such systems depends on the amplitude-frequency backbone curve obtained for free undamped ($F = 0, \Gamma = 0$) vibrations. These backbones can exhibit non-monotonic amplitude-frequency relationships. Accurate descriptions of such a backbone curve and of the forced response typically require tedious calculations, e.g., higher order perturbation methods (cf. [1]) or the use of action-angle coordinates (cf. [2]). In the present work we derive a method that is a combination of higher order HB and first order averaging to obtain accurate results for these systems with significantly less effort.

Results and Discussion

The solution process proceeds by assuming that the response is dominated by the fundamental harmonic with slowly varying amplitude a and phase ϕ . It is also assumed that the amplitudes and phases of the higher harmonics (HH) and the constant offset (DC) adiabatically track (a, ϕ) and have transients on a timescale that is neglected in the analysis. The HB method is applied using amplitude expansions, which provides closed form results for the DC and HH terms. These are then used in a standard first order averaging formulation to obtain the slow flow equations

$$\dot{a} = -\Gamma a - \frac{F}{2\omega_0} \sin \phi, \quad \dot{\phi} = \omega_0 - \omega + \frac{3\gamma_{\text{eff}}}{8\omega_0} a^2 + \frac{5\sigma_{\text{eff}}}{16\omega_0} a^4 - \frac{F}{2a\omega_0} \cos \phi,$$

where

$$\gamma_{\text{eff}} = \alpha_3 - \frac{10}{9} \left(\frac{\alpha_2}{\omega_0} \right)^2, \quad \sigma_{\text{eff}} = \alpha_5 - \frac{11}{12} \left(\frac{\alpha_2^2}{\omega_0^3} \right) + \frac{53\alpha_3}{20} \left(\frac{\alpha_2}{\omega_0^2} \right)^2 - \frac{14\alpha_2\alpha_4}{5\omega_0^2} + \frac{3}{80} \left(\frac{\alpha_3}{\omega_0} \right)^2.$$

It is important to note that these equations do not correctly capture the transient dynamics of (a, ϕ) , but accurately predict their steady state values and their stability.

The backbone curves are described by the $\dot{\phi}$ equation with $F = 0, \omega = \omega_0$. Sample response curves obtained from this method for a model with only quadratic and cubic nonlinearities are shown in the Figure (details will be provided in the presentation). The stable (unstable) branches of the response curves are denoted by solid (dashed) curves. The symbols \blacktriangleright and \blacktriangleleft indicate the fundamental harmonic amplitude of the steady-state obtained from simulations from sweep-up and sweep-down, respectively, obtained by time integration of Eq.(1) and computing the fundamental harmonic of the steady-state response. Note that the non-monotonicity feature of this system is not captured by standard second order perturbation methods, which provide only the γ_{eff} term [3]. The example demonstrates the ability of the method to capture non-monotonic behavior using a first order perturbation method. This method will be useful for describing the frequency response of asymmetric systems in terms of physical system parameters.

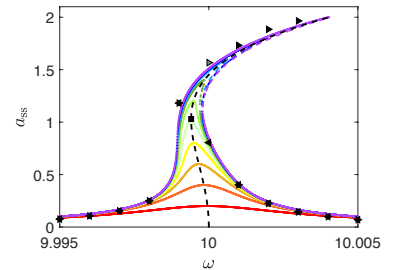


Figure 1: Sample response curves.

References

- [1] Wanzhi Qiao, Tieding Guo, Houjun Kang, and Yueyu Zhao, (2022) Softening–hardening transition in nonlinear structures with an initial curvature: a refined asymptotic analysis. *Nonlinear Dynam.* **107**:357–374.
- [2] N. J. Miller, S. W. Shaw, and M. I. Dykman (2021) Suppressing frequency fluctuations of self-sustained vibrations in underdamped nonlinear resonators. *Phys. Rev. Appl.* **15**:014024.
- [3] A. H. Nayfeh and D. T. Mook, (1995) *Nonlinear Oscillations*, Wiley Classics Library

A general co-simulation approach based on a novel weak formulation at the interface

Evangelos Koutras*, Elias Paraskevopoulos* and Sotirios Natsiavas*

*Department of Mechanical Engineering, Aristotle University, Thessaloniki, Greece

Abstract. Co-simulation methods are widely used to enable global simulation of a coupled system via composition of simulators. In this work, the focus is initially placed on a new scheme for the numerical integration of each subsystem, since the corresponding accuracy constitutes a keystone for the correct solution of a decomposed model. Subsequently, the new co-simulation techniques are presented. Specifically, a novel coupling strategy for satisfying the coupling conditions in their integral (weak) form, in the time domain, is proposed. This formulation constitutes a general framework for the generation of coupling condition schemes with varying accuracy and stability properties, based on the choice of basis and order of polynomials for the quantities involved. Finally, the methods presented are applied to a linear oscillator model and a couple of nonlinear pendulum models. Even though the models examined are relatively simple, the methods developed have general validity and can be applied for coupling arbitrary multibody or structural solvers.

Introduction

Co-simulation or solver coupling has already been utilized extensively in numerous engineering fields [1]. The core idea consists in a decomposition of the global mechanical model into two (or more) submodels. The different subsystems are connected by coupling variables, which are exchanged only at the macro-time (or communication) points. Among these points, the subsystems integrate their dynamics independently, using their own solver. Generally, the subsystems are coupled by physical force/torque laws (applied forces/torques) or by algebraic constraint equations (reaction forces/torques) [2]. Furthermore, co-simulation approaches are subdivided into explicit, implicit and semi-implicit methods. Finally, concerning the decomposition of the overall system into subsystems, three different possibilities are distinguished. Namely, force/force, force/displacement and displacement/displacement decomposition [2, 3].

Results and discussion

The new methods were initially applied to a linear oscillator model with two masses, constrained with a fixed joint, as depicted in Figure 1 (a). Then, nonlinear models of a single and a double pendulum were investigated with respect to the new numerical integration and co-simulation techniques, respectively. Within this study, the main emphasis is placed on verifying the accuracy of the schemes proposed. More specifically, a detailed analysis of the convergence and numerical error behavior is carried out in the aforementioned models. Typical results are presented in Figure 1 (b). Even though the models examined are relatively simple, the results obtained demonstrate the validity and accuracy of the new numerical integration and co-simulation techniques. Based on this, the new methods are currently extended and applied to complex structural and multibody dynamic systems.

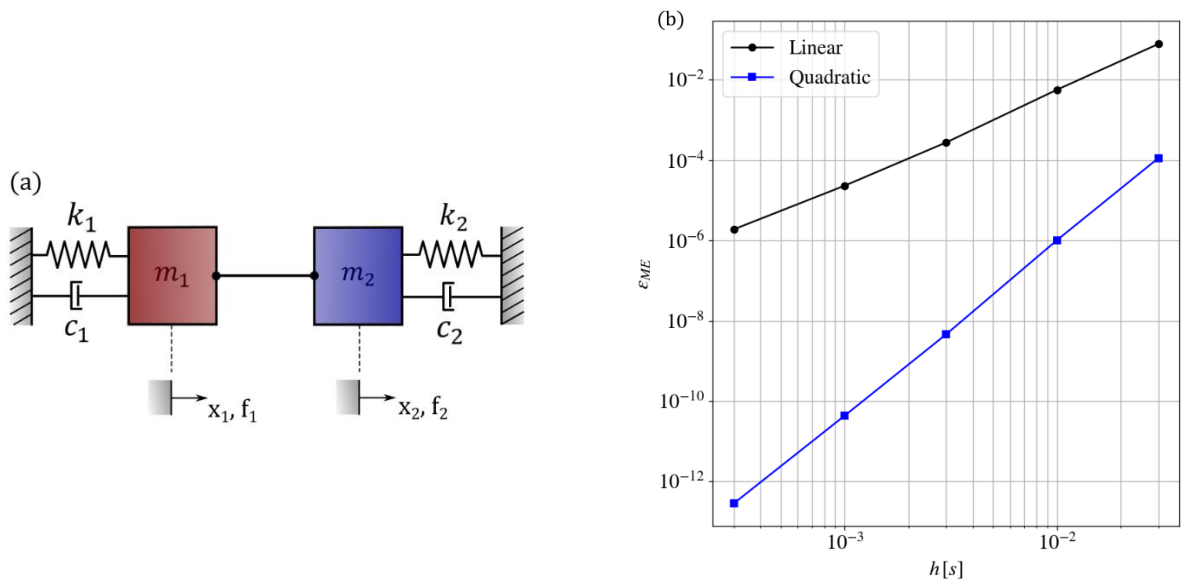


Figure 1: (a) A linear oscillator model and (b) typical numerical results for a nonlinear pendulum model

References

- [1] Gomes C., Thule C., Larsen P.G., Vangheluwe H. (2017) Co-simulation: State of the Art. *arXiv preprint* arXiv:1702.00686.
- [2] Schweizer B., Lu D. (2014) Semi-implicit Co-simulation Approach for Solver Coupling. *Arch. Appl. Mech.* **84**: 1739-1769.
- [3] Koutras E., Paraskevopoulos E., Natsiavas S. (2022) A Novel Co-simulation Approach for Mechanical Systems. *Multibody Syst. Dyn.* **55**: 83-102.

Abstract Dynamics: An alternative approach to local Lyapunov exponents in examining local unpredictability

Amir Shahhosseini* and Kiran D'Souza*

*Department of Mechanical and Aerospace Engineering, The Ohio State University, Columbus, Ohio 43235, USA

Abstract. This work proposes a computational approach that has its roots in the early ideas of local Lyapunov exponents, yet, it offers new perspectives toward analyzing these problems. The method of interest, namely abstract dynamics, is an indirect quantitative measure of the variations of the governing vector fields based on the principles of linear systems. The examples in this work, ranging from simple limit cycles to chaotic attractors, are indicative of the new interpretation that this new perspective can offer. The presented results can be exploited in the structure of algorithms (most prominently machine learning algorithms) that are designed to estimate the complex behavior of nonlinear systems, even chaotic attractors, within their horizon of predictability.

Introduction

An interesting idea in the analysis of nonlinear dynamics that stems from the case of linear systems is the notion of Lyapunov exponents. Lyapunov exponents are a measure of the exponential divergence of the trajectory from its original path upon experiencing an infinitesimal disturbance [1]. The Lyapunov exponents are characteristics of the attractor and determine the general expansion or attraction of the motion in the long run and are global properties that are independent of the trajectory if the dynamics is ergodic [2]. In sharp contrast, the idea of local Lyapunov exponents (LLEs) attempts to truncate the global approach of the Lyapunov exponents to the case of the divergence of infinitesimally perturbed trajectories in a finite (and mostly short-term) time interval. This idea is of significant importance when the short-term behavior of nonlinear dynamics is of interest. For many chaotic systems, such as the models of climate and economic dynamics, long-term prediction is proven to be impossible and frankly unnecessary but short-term predictions play a critical part [3].

The contribution of this work is the observation of patterns, and more specifically, dependencies in the eigenvalues of the Jacobian matrix when evaluated along the trajectory of the system. This observation stems from the fact that contrary to previous works, the time evolution of the eigenvalues is not the primary target but their relative behavior is examined. It is then observed that in nearly all the examples, there are areas, in the space of these eigenvalues, called the *abstract dynamics* space, where the eigenvalues vary linearly. Additionally, the one-to-one mappings of the eigenvalues to the trajectory of the state variables indicate an area-to-area mapping.

Results and Discussions

The results of this study indicate the existence of a level of order, although limited, in the response of certain chaotic systems that was not known before. The identification of this limited order can ease the local estimation process of chaotic attractors and may, in the most optimistic case, enable the obtainment of their analytical responses. Moreover, the results of this paper demonstrate the fading of the transient response of certain dynamical entities when the system is observed through this methodology. Inexorably, this can advance and simplify the identification process of numerous systems using raw numerical data. The scope of the applications are not limited to these two examples and more will be discussed in the full manuscript. Figure 1 demonstrates the abstract dynamics of the Lorenz attractor and it can be observed that the motion moves on a *cardinal line* for an extended period which has several implications.

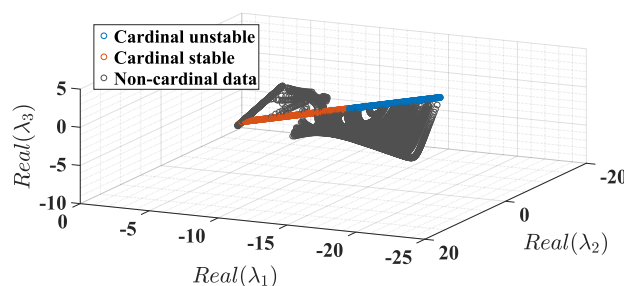


Figure 1: Abstract dynamics of the Lorenz attractor indicating a level of order in certain portions of the motion.

References

- [1] Parker, Thomas S and Chua, Leon (2012) Practical numerical algorithms for chaotic systems. *Springer Science & Business Media*
- [2] Vulpiani, Angelo and Cecconi, Fabio and Cencini, Massimo (2009) Chaos: from simple models to complex systems. *World Scientific*
- [3] Abarbanel, Henry DI and Brown, Reggie and Kennel, Matthew B (1991) Variation of Lyapunov exponents on a strange attractor. *Springer*

An Alternative Approach to Model Milling Dynamics

Kaidong Chen^{a,b}, He Zhang^a, Nathan van de Wouw^b and Emmanuel Detournay^a

^aDepartment of Civil, Environmental and Geo-Engineering, University of Minnesota, MN, USA

^bDepartment of Mechanical Engineering, Eindhoven University of Technology, Eindhoven, The Netherlands

Abstract. In models for the dynamics of the milling process, the characterization of the chip thickness plays a central role. In this abstract, we develop an alternative model for the computation of the chip thickness. The chip thickness is computed using (i) a surface function describing the evolution of the milled surface and (ii) the information about the shape of the workpiece. Combining a partial differential equation (PDE) governing the surface function with the ordinary differential equations (ODE) governing the tool dynamics, a mixed PDE-ODE model formulation is proposed to describe the milling process dynamics. Compared with the classical delay differential equation (DDE) formulation for milling dynamics, this novel formulation is more accurate because less assumptions have been made to compute the chip thickness. Case studies show that the two formulations generally agree well with each other. However, a sizable difference on predicted limit cycles, characterizing the periodic tool motion, occurs when the axial depth of cut is relatively large. This PDE-ODE formulation brings a novel perspective for analyzing milling processes as well as a means to assess the validity of models that based on DDE formulation.

Introduction

Dynamic models of the milling process can be classified into two classes [1]. Class I models only consider the movement of the tool and formulate the regenerative effect in terms of the current and specific previous positions of the tool. The majority of Class I models are formulated mathematically in terms of a delay differential equation (DDE) [2, 6]. In contrast, the Class II models simulate both the tool motion and the machined surface around the tool [1]; they provide a more direct way to compute the chip thickness. However, the published Class II models focus on the numerical discretization of the surface without an explicit mathematical framework, unlike the DDE formulation for Class I models. The aim of this work is to formulate the governing equations underpinning the Class II models. Inspired by the partial differential equation (PDE) approach [3, 4] recently developed to describe the evolution of the machined surface in the turning process, the authors formulated a PDE that governs the evolution of the machined surface in milling [5]. Here this PDE is combined with a system of ordinary differential equations (ODE) governing tool dynamics, thus resulting in a mathematical formulation of the Class II milling models.

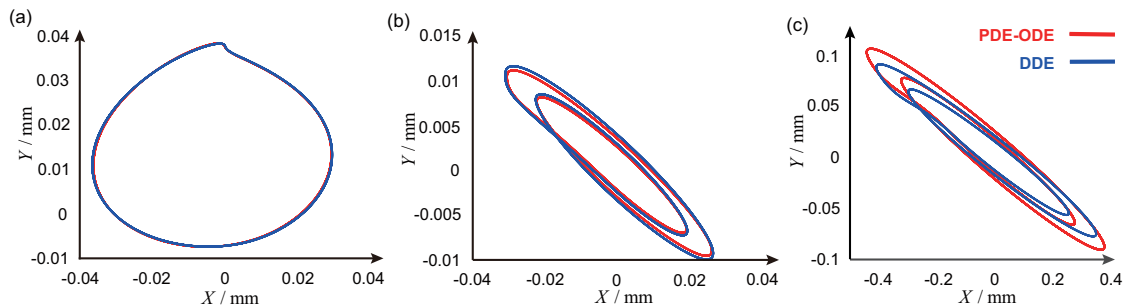


Figure 1: Limit cycles of tool center vibration: (a) radial immersion $a_e=100\%$, depth of cut $a_p=1$ mm, (b) $a_e=10\%$, $a_p=1$ mm, and (c) $a_e=5\%$, $a_p=20$ mm. Spindle speed 30000 rpm, feed rate 0.2 mm/tooth, details of the model parameters can be found in reference [6].

Results and discussion

Case studies have been carried out to compare the proposed PDE-ODE formulation and the classical DDE formulation on specific examples described in [6]. Fig.1 illustrates the limit cycles of tool vibration for three different cases. The two formulations agree with each other when the depth of cut is small. However, the limit cycle predicted by the PDE-ODE formulation is more accurate when the axial depth of cut is large, which is because the simplifications made in the DDE formulation is avoided in the PDE-ODE one. The proposed formulation serves as the mathematical foundation of the Class II models and brings a new perspective for analyzing the milling process.

References

- [1] Paris H., Peigne G., Mayer R. (2004) Surface Shape Prediction in High Speed Milling. *Int. J. Mach. Tools Manuf* **44**:1567-1576.
- [2] Szalai R., Stépán G., Hogan S.J. (2004) Global dynamics of low immersion high-speed milling. *Chaos* **14**:1069-1077.
- [3] Wahi P., Chatterjee A. (2008) Self-interrupted regenerative metal cutting in turning. *Int. J. Nonlin. Mech* **43**:111-123.
- [4] Liu X., Vljajic N., Long X., Meng G., Balachandran B. (2014) Multiple Regenerative Effects in Cutting Process and Nonlinear Oscillations. *Int. J. Dyn. Control* **2**:86-101.
- [5] Chen K., Zhang H., van de Wouw N., Detournay E. (2022) An Alternative Approach to Compute Chip Thickness in Milling. *J. Manuf. Sci. Eng* **144**:111006.
- [6] Faassen R.P.H., van de Wouw N., Nijmeijer H., Oosterling J.A.J. (2006) An Improved Tool Path Model Including Periodic Delay for Chatter Prediction in Milling. *J. Comput. Nonlinear Dyn* **2**:167-179.

Dynamic response of spatial beams with material softening and strain localization

Sudhanva Kusuma Chandrashekhara*, Dejan Zupan*

*Faculty of Civil and Geodetic Engineering, University of Ljubljana, Ljubljana, Slovenia

Abstract. Numerical modelling of mechanical response of slender and flexible structures characterized by initiation and propagation of damaged bands involving geometrical and material nonlinearities often results in instabilities. The adopted numerical solution methods become sensitive close to the critical points while investigating such responses. In the present work, we address the problem of strain localization and the dynamic behaviour of the beam-like structural elements at both pre- and post-critical load levels.

Introduction

In the analysis of slender flexible structures undergoing complex deformation, the precise prediction of the mechanical response in the post-critical regime poses a serious challenge for computational methods especially when describing the demanding phenomena such as softening within mathematical constitutive models. The present work focuses on the phenomenon of strain localization in beam-like structural elements which occurs when a material dependent critical condition is reached at some material point of the solid body that results in discontinuities in strain/displacement fields within a thin narrow band. The present work aims at the investigation of dynamic response of the structure undergoing softening at a localized cross-section using the novel energy preserving velocity-based finite element formulation by Zupan and Zupan [1] where typical problems associated with rotational degrees of freedom are completely avoided. The computational advantages of the formulation are preserved after the efficient detection of critical load level and the post-critical treatment of localized strains are implemented into the formulation.

Methodology

The system of governing equations for a three-dimensional Cosserat beam is a set of nonlinear partial differential equations which are as follows [1]:

$$\mathbf{n}' + \tilde{\mathbf{n}} = \rho A \dot{\mathbf{v}}, \quad (1)$$

$$\mathbf{M}' + \mathbf{K} \times \mathbf{M} + (\mathbf{\Gamma} - \mathbf{\Gamma}_0) \times \mathbf{N} + \hat{\mathbf{q}}^* \circ \tilde{\mathbf{m}} \circ \hat{\mathbf{q}} = \mathbf{\Omega} \times \mathbf{J}_\rho \mathbf{\Omega} + \mathbf{J}_\rho \dot{\mathbf{\Omega}}, \quad (2)$$

where prime(\prime) denotes the derivative with respect to x and dot ($\dot{\cdot}$) denotes the derivative with respect to time, $\tilde{\mathbf{n}}$ and $\tilde{\mathbf{m}}$ are the external distributed force and moment vectors per unit length, ρ is the mass density and \mathbf{J}_ρ is the mass moment of inertia of the cross section, \mathbf{N} and \mathbf{M} are the vectors of stress resultant force and moment respectively, \mathbf{v} and $\mathbf{\Omega}$ are the velocities and angular velocities, $\mathbf{\Gamma}$ and \mathbf{K} are the vectors of translational and rotational strains respectively. In the above equations, the quantities in the fixed basis are denoted in lower case notations and vice versa. The time discretization employed here is based on the midpoint rule while the spatial one is based on Galerkin finite element method. The primary unknowns are chosen to be the velocities and angular velocities due to their numerical advantages of additive-type update procedure and consistency of standard additive-type interpolations when expressed in appropriate reference frame. The proposed methodology performs well and gives accurate results for problems with strain softening.

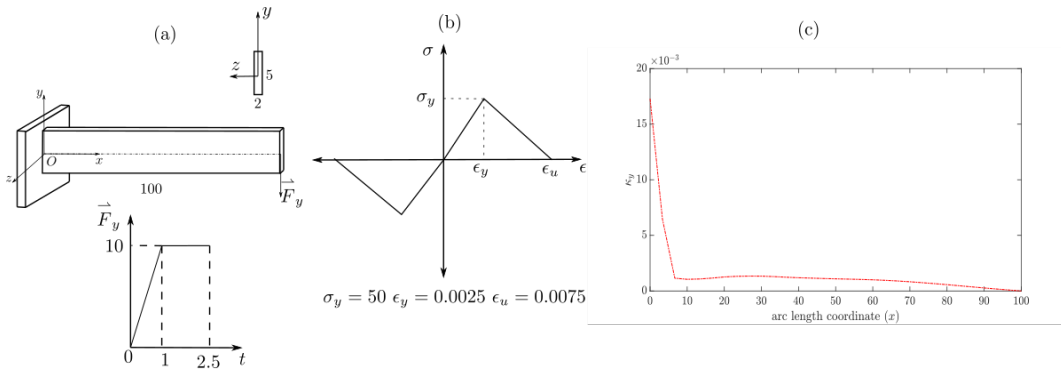


Figure 1: (a) Configuration of the cantilever beam, (b) stress-strain relationship, (c) variation of curvature along the length of the beam.

Figure 1 shows a simple cantilever made of bi-linear material with decreasing stresses after the critical value is reached. In the proposed example, the strains are localized at the clamped end while the obtained bending strain distribution is presented in figure 1(c) at time $t = 2.5$ s.

References

- [1] E. Zupan and D. Zupan, "On conservation of energy and kinematic compatibility in dynamics of nonlinear velocity-based three-dimensional beams", *Nonlinear Dynamics*, vol. 95, no. 2, pp. 1379-1394, 2018.

Analysis of self-excited stick-slip vibrations in a model for creep groan using a combined Finite-Difference/Harmonic Balance approximation method

Jonas Kappauf*, Simon Bäuerle* and Hartmut Hetzler*

**Engineering Dynamics Group, Department of Mechanical Engineering, University of Kassel, Germany*

Abstract. This contribution presents simulation results of stick-slip vibrations in a multi-degree-of-freedom model for disk brake creep groan. These self-excited periodic oscillations are approximated by a combined Finite-Difference/Harmonic Balance method (FD/HB). The method shows an increased efficiency compared to a pure FD or HB approach, especially for large-scale systems with localised non-linearities.

Introduction

Disc brake creep groan is caused by a negative slope of the friction coefficient as a function of the relative velocity within the brake pad/brake disk contact. The occurring non-linear limit cycles consist of sticking and sliding phases and are transmitted through the car chassis potentially leading to undesirable acoustic and structural vibrations. In the automotive industry, these creep groan vibrations thus cause high amounts of warranty cost and a subjective decrease in the level of quality perceived by the customer. Various analysis strategies can make a valuable contribution in avoiding these unwanted vibrations. In addition to measurements, a calculation-based detection of these limit cycles early in the development process of a brake system is therefore desirable.

Mechanical systems and approximation method

The mechanical/mathematical description of these systems is usually realised via finite element (FE) models. The non-linearities relevant here (non-linear bearing support and frictional contact forces) are limited to local areas. Therefore, a combined FD/HB method for approximating the periodic oscillations is proposed, which exploits the mathematical equation structure with the goal of reducing numerical cost.

Basically, this method separates the degrees of freedom (DoF) subjected to non-linearities – the so-called non-linear DoF – from those that have purely linear viscoelastic kinetic properties – the linear DoF. Then, the periodic motion of the linear DoF is expressed as a FOURIER series and approximated by Harmonic Balance, respectively. Due to the linearity of their equations of motion, an analytical expression of the linear DoF's motion in frequency domain results – being solely a function of the FOURIER coefficients of the non-linear DoF. The motion of these non-linear master DoF's is approximated by the Finite Difference method for boundary value problems. In summary, the resulting algebraic equation system is solely depending on the approximated values of the non-linear DoF and can be numerically solved by NEWTON-like schemes.

Discussion

As a test case for this approach to the analysis of brake creep groan, a mechanical model is investigated that exhibits essential properties of FE models. It comprises the brake pad-disc contact, essential chassis control arms and is motivated by experimental testing. The friction force is modelled by an exponentially decaying and regularised STRIBECK friction characteristic which causes self-excited vibrations. The resulting stick-slip limit cycles are approximated by the proposed FD/HB method for a variable resolution of the chassis control arms. This shows the increased efficiency of the method for a growing number of linear DoF in comparison to pure FD or HB methods. In addition, the vibrations are analysed regarding brake pressure and rotational speed. For this purpose, a predictor-corrector path continuation is utilized.

References

- [1] Huemer-Kals S., Kappauf J., Zacharczuk M., Hetzler H., Häslér K., Fischer P. (2022) Advancements on Bifurcation Behaviour and Operational Deflection Shapes of Disk Brake Creep Groan, *J. S. V.* vol. 534: e116978
- [2] Kappauf J., Bäuerle S., Hetzler H. (2022) A Combined FD-HB Approximation Method for Steady-State Vibrations in Large Dynamical Systems with Localised Nonlinearities. *Comp. Mech.* doi.org/10.1007/s00466-022-02225-3
- [3] Kappauf J., Hetzler H., Bäuerle S. (2022), A Hybrid Approximation Method for the analysis of periodic solutions of large-scale dynamical systems, *Proc. ISMA 2022*, tbp

Multiscale uncertainty quantification of complex nonlinear dynamic structures with friction interfaces

Enora Denimal*, Jie Yuan **

*University Gustave Eiffel, Inria, COSYS/SII, I4S, Campus de Beaulieu, Rennes, 35042, France #

**Aerospace Centre of Excellence, University of Strathclyde, Glasgow, G1 1XQ, UK#

Abstract. This work aims to investigate the interest in multi-scale uncertainty quantification for nonlinear dynamic systems with friction interfaces. Indeed, such structures experience uncertainties at different time and space scales due to the friction interface. The focus of this work is to quantify and link the uncertainties from friction interfaces at different scales to the nonlinear dynamic response of the structure. A multi-scale kriging approach is employed to propagate the uncertainty. An industrial test rig for dovetail joints will be used as a test case to demonstrate the proposed methodology.

Context

Large structural assemblies have many friction interfaces that are a major source of non-linearity and uncertainties and can have a significant impact on the dynamic response. Usually, friction interfaces are modelled with a flat surface using a macroscopic friction contact law that depends only on a few parameters. These parameters are usually obtained experimentally, showing a large variability leading to uncertain predictions of the overall dynamic response. Recent works indicate that the current macro-scale contact models are not sufficient to represent the physics at the friction interface and that micro-scale contact models must be taken into consideration. Previous UQ research in friction interfaces considered only macro-scale modelling and proved to be inaccurate in the prediction of the dynamic response due to the lack of consideration of micro-scale phenomena. Therefore, an efficient multi-scale modelling approach of the contact parameters and uncertainties is needed to simulate the micro-scale behaviour and to translate it at the macro-scale for the full nonlinear dynamic response.

Test case and results

The test case for this study is based on a fan blade root test rig setup [1] illustrated in Fig.1(a). The nonlinear normal modes (NNM) of the mechanical system are computed to obtain its nonlinear dynamic behaviour. A two scales numerical solver is used for this. The first scale computes the contact pressure and gap distribution at the different contact surfaces based on micro-scale considerations. The second computes the NNM of the system by considering the real contact pressure and gap distribution. In this work, a single micro-scale uncertain parameter is considered to demonstrate the approach, namely the central bump of the contact surface. The multi-scale approach proposed here, illustrated in Fig.1(b), consists of the creation of a first surrogate model to predict the contact pressure and gap distribution from the central bump, and a second surrogate model to predict the NNM from the contact pressure and gap distribution. From this, it is possible to get the distribution of the random contact pressure and the stochastic NNM of the system. Results show that such an approach allows getting deep insights into the system understanding.

Acknowledgement The authors acknowledge the support of RSE Saltire Facilitation Workshop Award (No.1865).

References

[1] Yuan, J., Salles, L., Schwingshackl, C. (2022). Effects of the geometry of friction interfaces on the nonlinear dynamics of jointed structure. In *Nonlinear Structures Systems, Volume 1* (pp. 67-74). Springer, Cham.

[2] Yuan, J., Fantetti A., Denimal E., Bhatnagar S., Pesaresi L., Schwingshackl C., Salles L. (2021) Propagation of friction parameter uncertainties in the nonlinear dynamic response of turbine blades with underplatform dampers *Mechanical Systems and Signal Processing* **156**: 107673.

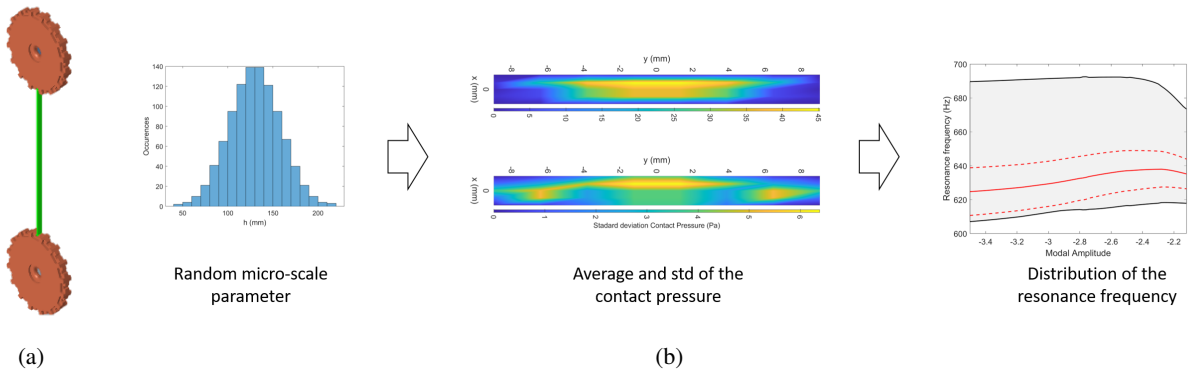


Figure 1: (a) FE model of the Dogbone rig (b) Multi-scale UQ process illustration

Modeling vortex-induced vibrations displacement with phenomena-informed neural network

Mahmoud Ayyad*, Muhammad R. Hajj*, Arshad Mehmood**, and Imran Akhtar ***

*Civil, Environmental and Ocean Engineering, Stevens Institute of Technology, Hoboken, NJ 07030, USA.

**Mechanical Engineering, University of Engineering and Technology, Peshawar, Pakistan.

***Mechanical Engineering, National University of Sciences and Technology, Islamabad, Pakistan

Abstract. Vortex-Induced Vibrations (VIV), as a phenomenon, can be modeled by a dynamical system (single equation) that includes a term that is negatively proportional to the velocity to account for the energy transfer from the flow to the structure, and another term that is proportional to an odd power of the velocity to yield limit cycle oscillations. We implement a data-driven system identification (discovery), referred to as Phenomena-Informed Neural Network, to identify the coefficients in the representative equation of these phenomena. The training data is obtained from direct numerical simulations of the Navier-Stokes equations. The representative equation can be effectively used to assess VIV control strategies.

Introduction

In the context of vortex-Induced Vibrations (VIV), energy transfer from the flow to the moving structure requires positive excitation represented by a negative damping term. Furthermore, limiting the amplitude of these vibrations requires a damping term proportional to a higher power of the velocity, e.g. cubic damping term [1]. As such, VIV oscillation amplitudes, Y , can be modeled or predicted by a phenomenological model such as the Rayleigh oscillator:

$$\ddot{Y} + C_1\dot{Y} + C_2Y + C_3\dot{Y}^3 = 0 \quad (1)$$

Hajj et al. [1] combined spectral analysis of data from direct numerical simulations of the Navier-Stokes equations with an approximate solution of equation (1) to identify C_1 , C_2 , and C_3 . Here, we implement a data-driven system identification (discovery) of equation (1), to be referred to as Phenomena-informed Neural Networks (PINN). The concept is to combine the phenomena-representing equation (1) with available data to train a Neural Network and identify C_1 , C_2 , and C_3 .

Results and Discussion

As schematically presented in figure 1a, the implemented Neural Network consists of four hidden layers with 30 nodes per layer. A total loss function, L_{total} , is used to update all the trainable parameters, i.e., weights, biases, and C_1 , C_2 , and C_3 . This loss function is the weighted sum of L_{data} , defined as the error between the predicted and simulated displacement values represented respectively by \hat{Y} and Y , and L_{DE} , defined as the error resulting from using \hat{Y} in equation (1). Based on an error threshold criterion, it took 264, 000 iterations to identify the trainable parameters. Figure 1b compares time series of numerically simulated and PINN-predicted oscillation amplitudes. The plot shows excellent agreement in the frequency and amplitude ($< 0.1\%$) of the two time series.

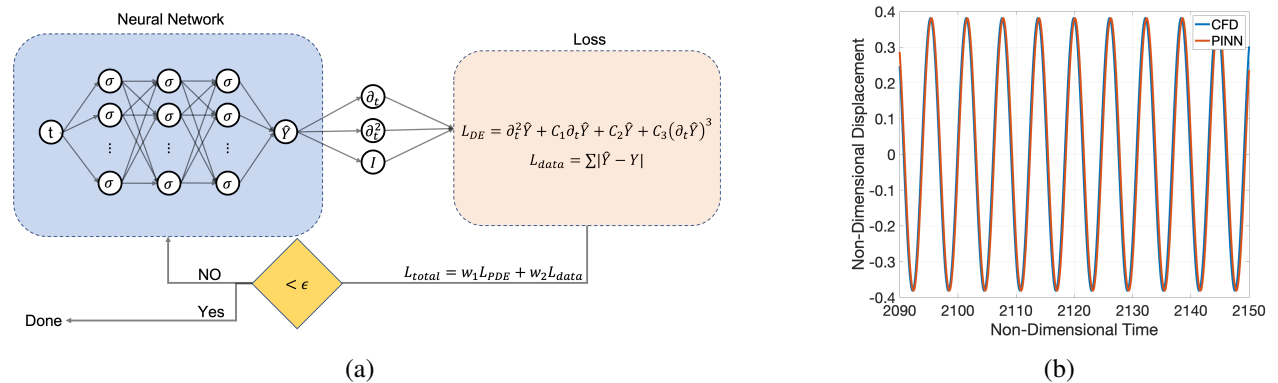


Figure 1: (a) PINN implementation, and (b) comparison of CFD- and PINN-generated time series of the VIV response. $Re=110$. Details of numerical simulations and conditions are provided in Hajj et al. [1].

References

- [1] Hajj M.R., Mehmood A., Akhtar I. (2021) Single-degree-of-freedom model of displacement in vortex-induced vibrations. *Nonlinear Dynamics* **103.2**:1305-1320.

Energy pumping of mechanical oscillators in an array configuration under impulse and parametric excitation.

P Arjun*, Vinod V*

*Department of Mechanical Engineering, Mar Baselios College of Engineering and Technology, APJAKTU, Thiruvananthapuram, KERALA, INDIA, ORCID:0000-0003-3897-3388 #

Abstract. The simplest form of a passive nonlinear sink in a vibrating system consists of two linear oscillators with a strong nonlinear attachment connected to one linear oscillator [1]. The energy pumping is unidirectional, i.e. absorbing vibrational energy from the linear to nonlinear oscillator. For better understanding of this energy pumping phenomenon we had considered a large number of oscillators in the form of array (chain) network. The main objective is to investigate the robustness of energy pumping towards the passive nonlinear sink at one end from the farthest oscillator in the other end of the chain. Furthermore, energy pumping in this large chain is investigated when subjected to parametric excitation in spring element instead of impulse excitation.

Introduction

In this paper, we present a model of ‘ N ’ oscillators with same linear natural frequency in a chain. In this chain, the first oscillator is having a strong nonlinear attachment (m_1) in its spring element which is presumed to act as a energy reservoir in the chain. The oscillators in the chain are arranged in such a way that the vibration energy under impulse excitation (F) from one end of the chain will have to traverse to the other end of the chain during the energy transfer. The computer simulations in MATLAB are done using Runge Kutta ode45 solver with time step of 10^{-3} used for integration and integration times of nearly 100 cycles.

Results and discussion

Energy transfer in a chain under impulse excitation

The results presented here are in a chain having $N = 10$. Here we initiate the analysis by giving an impulse (F) as initial velocity to an intermediate linear oscillator in the chain (m_5). For $F = 1.5$, no energy transfer occurs as major part of energy is stored in the excited oscillator. By increasing the initial energy level to say $F = 2.2$, there occurs an irreversible transfer of energy from m_5 to m_1 as in Figure.1(a). The reason behind this energy transfer is due to the internal resonance capture studied in [2]. An interesting point to be noted is even at $F = 2.2$ or any higher value, it is impossible to have such an energy pumping from the two ends of the chain i.e. m_{10} to m_1 . To analyse the energy pumping phenomenon from m_{10} , we give a slight frequency mismatch to m_1 in its linear natural frequency, We note that, in contrast to Figure.1(a), the energy pumping occurs from one end to other end of the chain as shown in Figure.1(b). This shows that a slight perturbation in frequency triggers the nonlinear energy transfer due to modal interaction. Also the energy pumping towards m_1 can be enhanced by bringing in self-oscillatory term in damping instead of spring cubic nonlinearity in the model.

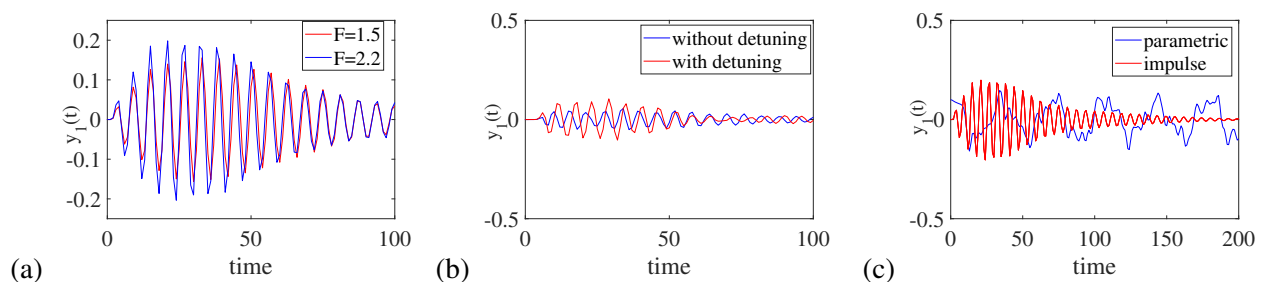


Figure 1: (a) Energy transfer towards m_1 at $F=2.2$ (b) Spatial spread of energy transfer from m_{10} via frequency detuning (c) Predominant energy pumping towards m_1 in a chain under parametric excitation.

Energy transfer in a chain under parametric excitation

Here also we consider the same $N = 10$ chain network. The parametric excitation $k_{pe} \cos \omega t$ is given to the stiffness term of m_5 and m_{10} as two separate simulation cases. In the first 200 seconds, no energy transfer occurs as the value of k_{pe} is kept zero. After 200 seconds the parametric stiffness excitation is turned on by increasing the value of k_{pe} to 0.2. This initiates the energy pumping from all oscillator nodes towards m_1 . Moreover the energy transfer due to this parametric resonance is more robust when compared with impulse excitation as in Figure.1(c). Frequency detuning in the nonlinear sink is not required here to pump energy from m_{10} to m_1 .

References

- [1] O. Gendelman, L. I. Manevitch, A. F. Vakakis, R. M'Closkey (2001) Energy Pumping in Nonlinear Mechanical Oscillators: Part I—Dynamics of the Underlying Hamiltonian Systems. *J. Applied Mechanics, ASME Trans.* **68**:34-41.
- [2] O. Gendelman, A. F. Vakakis (2001) Energy Pumping in Nonlinear Mechanical Oscillators: Part II—Resonance Capture. *J. Applied Mechanics, ASME Trans.* **68**:42-48.

Quantum-Dot spin-VCSEL based Reservoir Computing for Hénon Attractor Reconstruction

Christos Tselios*, Panagiotis Georgiou**, Christina (Tanya) Politi* and Dimitris Alexandropoulos**

*Department of Electrical and Computer Engineering, University of Peloponnese, Patra, Achaia, 22100, Greece

**Department of Materials Science, University of Patras, Rion, Achaia, 26504, Greece

Abstract. We introduce a Reservoir Computing setup where a QD VCSEL with optical spin injection and delayed optical feedback is used as reservoir. The proposed Reservoir Computing aims at ultrafast reconstruction of Hénon Attractor, benefiting from unique spin coupling between electrons and photons in spin-VCSELs leading to ultrafast dynamics. The speed achieved with QD spin-VCSEL based Reservoir Computing is 100 GSa/s, yielding a five-fold improvement compared to time series prediction processing speed of QW spin-VCSEL, while maintaining the error rate low.

Introduction

Spin-Vertical Cavity Surface Emitting Lasers (spin-VCSELs) for both gain materials, i.e. Quantum-Well (QW) and Quantum-Dot (QD), are undergoing increasing research effort for new paradigms in high-speed photon-enabled computing. Skontranis *et al.* have exploited two discrete wavebands and two polarization states of QD spin-VCSEL to enhance computational efficiency of signal equalization [1]. Harkhoe *et al.* have used polarization modulation in QW spin-VCSELs to improve the processing speed of a photonic Reservoir Computing (RC) for Santa Fe timeseries prediction task since the bandwidth in spin-VCSELs is only linked to the birefringence of the cavity [2]. The present contribution provides a link between spin-VCSEL's ultrafast dynamics and inherent advantages carried by QD laser technology. We perform another benchmark task to demonstrate the prediction of temporal signals. Hénon map has been established as a typical discrete-time dynamic system with chaotic behavior [3]. Our investigations reveal that information processing rate exceeds the one of QW spin-VCSEL [4].

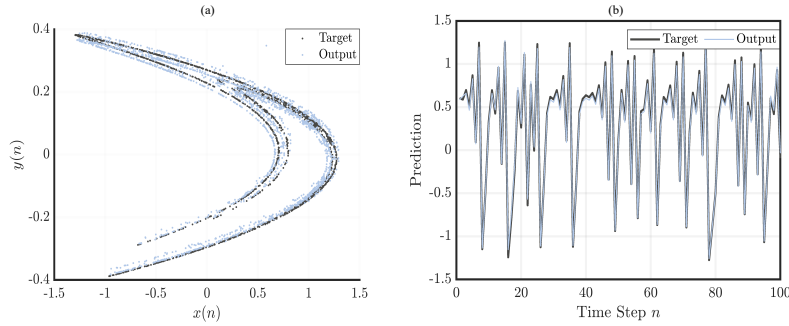


Figure 1: Performance illustration of (a) the Hénon Map reconstruction and (b) the time series prediction with $\alpha = 3$, $h = 1.1995$, $\eta = 3$, $\gamma_s = 200 \text{ ns}^{-1}$, $\gamma_p = 250 \text{ ns}^{-1}$, $\gamma_n = 1 \text{ ns}^{-1}$, $\gamma_0 = 400 \text{ ns}^{-1}$, $\gamma_a = -1.6 \text{ ns}^{-1}$, feedback strength $k_f = 30 \text{ ns}^{-1}$ and feedback delay time $\tau = 10 \text{ ps}$.

Results and discussion

We simulate the laser using the generalized spin-flip model for QD spin-VCSEL as described in [5] with additional terms for optical feedback. The data is inserted using the optical spin injection and is defined as $P(t) = I(t)M(t)$ during each time interval where $I(t)$ is the data to be trained/tested on and $M(t)$ is the mask. In our system we match feedback delay time τ_D to the mask length τ_M ($\tau_D = \tau_M = \tau$), leading to $N = \tau/\theta$, with θ the node-separation. A smaller θ can be tailored due to ultrafast dynamics in spin-VCSELs, allowing to store more neurons in a shorter delay line. For this task 2000 points are adopted for training while 2000 for testing, and the gauge of evaluation is the Normalized Mean Square Error (NMSE). For this benchmark we typically want the NMSE to be lower than 0.1. The use of $\theta = 0.5 \text{ ps}$ and $\tau = 10 \text{ ps}$ can improve information processing rate up to 100 GSa/s for efficient Hénon attractor reconstruction (see Figure 1) with relatively low NMSE (NMSE=0.052). Notably, QD-spin-VCSELs allow high-speed RC and with the employment of more energy and polarization states can provide an exciting platform for use in future photonic neuromorphic systems.

References

- [1] Skontranis M., Sarantoglou G., Bogris A. Mesaritakis C. (2022) Time-delayed reservoir computing based on a dual-waveband quantum-dot spin polarized vertical cavity surface-emitting laser. *Opt. Mater. Express* **12**:4047-4060.
- [2] Harkhoe K., Verschaffelt G., Van der Sande G. (2021) Neuro-Inspired Computing with Spin-VCSELs. *Applied Sciences* **11**:4232.
- [3] Hénon M. (2004) A Two-dimensional Mapping with a Strange Attractor. Springer, NY.
- [4] Yang Y. Zhou P., Mu P., Li N. (2021) Time-delayed reservoir computing based on an optically pumped spin VCSEL for high-speed processing. *Nonlinear Dyn* **107**:2619-2632.
- [5] Tselios C., Georgiou P., Politi C., Alexandropoulos D. (2022) Polarization Control of Quantum-Dot Spin-VCSELs. *physica status solidi (b)* **259**:2100532.

Optimizing Multilayer Perceptrons to Approximate Nonlinear Quaternion Functions

Arturo Buscarino^{**}, Luigi Fortuna^{**} and Gabriele Puglisi^{*}

^{*}*Dipartimento di Ingegneria Elettrica Elettronica e Informatica, University of Catania, Italy*

^{**}*IASI, Consiglio Nazionale delle Ricerche (CNR), Roma, Italy*

Abstract. In this contribution, a novel approach to optimize Multilayer Perceptron Artificial Neural Networks (MLP-ANN) devoted to approximate quaternion valued functions is presented. The approach is based on the definition of proper auxiliary networks devoted to predict the trends of the main network weights during the learning phase, thus reducing the number of epochs needed to reach a suitable abstraction level.

Introduction

In the last decade the use of artificial neural networks has received a growing interest in a wide variety of scientific fields. Our interest in this contribution focuses on multilayer perception based structures, able to deal with quaternion algebra. Quaternions have been introduced in order to generalize complex number properties to a three-dimensional space and have been used in a wide variety of practical applications, including the reformulation of Maxwell equations, the analysis of stresses in three-dimensional objects, and in digital filter design. Moreover, applications can be found also in robotics, due to the possibility of representing rotations in the three-dimensional space with quaternions instead of matrices. From the large variety of applications of quaternion algebra, the idea of developing a MLP-ANN structure able to deal directly with quaternions to approach these problems more efficiently has been discussed in [1]. In this contribution, we aim at optimizing the MLP-ANN structure for quaternions in order to improve the approximation of complex valued nonlinear functions and the efficiency of the learning algorithm. To this latter aim, we will focus on a recent implementation based on parallel computing of generic MLP-ANNs [2].

The main idea is to exploit the parallel computing capabilities of modern microprocessors in embedded devices to instantiate a set of auxiliary networks devoted to the prediction of the learning algorithm output, thus sensibly reducing the time to get a robust and efficient learning error. MLP-ANNs, in fact, are based on a learning phase during which inputs are presented to the network in order to favour its plasticity in the direction of abstracting the relationship among the inputs with the corresponding outputs. The variables of the problem are the so-called weights connecting the neurons of the ANN. The proposed approach introduces a series of auxiliary networks running in parallel with the main network, each devoted to predict the trend of the weights.

Results and discussion

Thanks to the parallel computing properties of current hardware and software technical solutions it is possible to reconsider algorithms and approaches presented in the literature before the diffusion of modern computers. This consideration led us to the implementation of the auxiliary networks paradigm to improve the efficiency of MLP-ANN for quaternion valued nonlinear functions.

A software improving the existing learning procedures for neural networks has been proposed and programmed through ANSI C language. It is possible to show practically the improvements, in terms of epochs needed to reach the convergence of the learning phase, by using datasets of different nature coming from technical high-precision circuits simulations, from highly complex experimental scenarios, such as nuclear fusion experimentations, and from planning of trajectory of robot manipulators. The adoption of auxiliary networks for the computing of the optimal weights increases remarkably the convergence velocity of a very simple kind of neural network, especially when the dimensions of the net in terms of layers and neurons are very high. In all the case studies taken into consideration, the desired approximation is reached with a reduced number of learning epochs in the order of 8000, as shown in Fig. 1.

References

- [1] Arena, P., Fortuna, L., Muscato, G., and Xibilia, M. G. (1997). Multilayer Perceptions to Approximate Functions Quaternion Valued. *Neural Networks*, 10(2), 335-342.
- [2] Bucolo, M., Buscarino, A., Fortuna, L., and Puglisi, G. (2022). Learning-on-learning approach for modeling. 48th Annual Conference of the IEEE Industrial Electronics Society, IECON 2022.

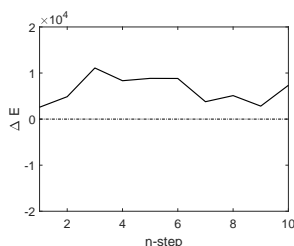


Figure 1: Experimental results: reduction in the number of learning epochs.

On the velocity-based description in dynamic analysis of three-dimensional beams

Eva Zupan*, Bojan Čas* and Dejan Zupan *

*Faculty of Civil and Geodetic Engineering, University of Ljubljana, Ljubljana, Slovenia

Abstract. In numerical formulations of three-dimensional beams the choice of primary interpolated variables is highly important for the efficiency and accuracy of the method. The crucial idea exploited in our approach is to employ velocity and angular velocity vectors in their suitable component descriptions to set the discrete computational model.

Introduction

Many computational challenges in dynamic modelling of frame-like structures are directly related to the properties of configuration space of three-dimensional beams which typically incorporates three-dimensional rotations. Since rotations form a non-commutative multiplicative group their computational treatment requires a special care. In contrast, the measures for their rate of change – the angular velocities are additive quantities when expressed with respect to the moving basis. The crucial idea is thus to employ velocities in fixed frame description and angular velocities in moving frame description as the primary unknowns of numerical model.

Kinematic compatibility

Another important property of continuous system, exploited in our work, is the direct relation between the strains and the velocities, called the *compatibility equations* [1]. In Cosserat rod theory the resultant strain measures at the centroid of each cross-section are directly introduced and expressed with kinematic variables by the first order differential equations

$$\mathbf{\Gamma} = \hat{\mathbf{q}}^* \circ \mathbf{r}' \circ \hat{\mathbf{q}} + \mathbf{\Gamma}_0, \quad \mathbf{K} = 2\hat{\mathbf{q}}^* \circ \hat{\mathbf{q}}', \quad (1)$$

where $\mathbf{\Gamma}$ and \mathbf{K} denote the translational and rotational strain, respectively, both expressed with respect to the local basis, while position vector \mathbf{r} and rotational quaternion $\hat{\mathbf{q}}$ are expressed in the fixed basis. It is important to observe that strains, velocities, and angular velocities are mutually dependent. Their direct relation is obtained by comparing mixed partial derivatives, which gives

$$\dot{\mathbf{\Gamma}} = \hat{\mathbf{q}}^* \circ \mathbf{v}' \circ \hat{\mathbf{q}} + (\mathbf{\Gamma} - \mathbf{\Gamma}_0) \times \mathbf{\Omega}, \quad \dot{\mathbf{K}} = \mathbf{\Omega}' + \mathbf{K} \times \mathbf{\Omega} \quad (2)$$

with \mathbf{v} denoting velocity and $\mathbf{\Omega}$ the angular velocity. In our approach we satisfy the kinematic compatibility equations (2) with the same accuracy as the governing equations. The discrete kinematic compatibility equations can be completely harmonized with the energy conservation demands, which results in robustness and long-term stability of the overall algorithm.

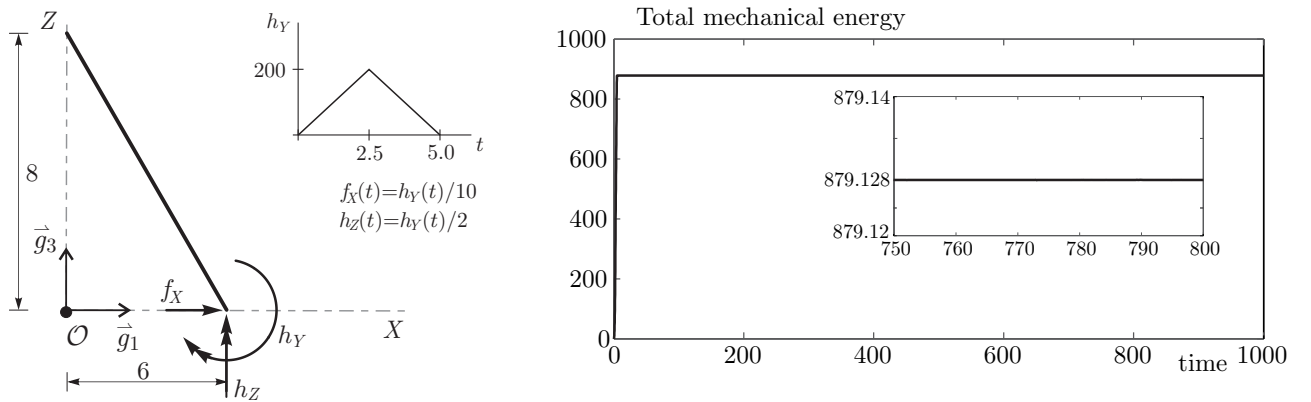


Figure 1: Free flight of a flexible beam: problem description (left) and total mechanical energy (right).

Figure 1 shows the performance of the present approach for the benchmark problem of flying flexible beam presented by Simo and Vu-Quoc [2] and characterized by very large displacements and rotations. The long-term stability and the energy preservation using our model can be observed.

References

- [1] Antman S. S. (2003) Invariant dissipative mechanisms for the spatial motion of rods suggested by artificial viscosity. *J. Elast.*, **70**(1-3):55–64.
- [2] Simo, J.C. , Vu-Quoc, L. (1988) On the dynamics in space of rods undergoing large motions - a geometrically exact approach, *Comput. Meth. Appl. Mech. Eng.* **66**(2), 125.

Iterative algorithm for dynamical integrity assessment of systems subject to time delay

Bence Szaksz*, Giuseppe Habib**

*,** Department of Applied Mechanics, MTA-BME Lendület “Momentum” Global Dynamics Research Group, Faculty of Mechanical Engineering, Budapest University of Technology and Economics, Budapest, Hungary

* ORCID: 0000-0003-1113-0698, ** ORCID: 0000-0003-3323-6901

Abstract. The robustness against external perturbations of the desired equilibrium of a dynamical system is an important measure, which can be described by the dynamical integrity. The current study provides an algorithm for determining the dynamical integrity of the equilibrium of systems subjected to time delay. The procedure looks for the local integrity measure, that is, the radius of the largest hypersphere centered in the equilibrium and entirely included within its basin of attraction. The algorithm overlooks possible fractal boundaries and provides a practically reasonable measure with relatively low computational cost.

Introduction

The stability of an equilibrium state is easy to determine; however, from a practical point of view, its dynamical integrity is also a relevant quantity, the efficient determination of which is still a challenging task. The proposed algorithm estimates the so-called local integrity measure (LIM) of the equilibrium state, that is, the radius of the largest hypersphere centered in the equilibrium and entirely included within its basin of attraction.

Results and discussion

An algorithm was developed to estimate the LIM of nonlinear ordinary differential equations in [1]. The present work extends it for the case of nonlinear delay differential equations (DDEs) with distinct time delay τ ; thus, an infinite dimensional state space should be investigated. The initial conditions of DDEs are functions of time leading to an infinite variety of initial functions with the same headpoint; therefore, the basin of attraction in the space of the physical coordinates can be defined only for specific types of initial conditions. The current work suggests to transform the equations into the space of the modal coordinates and use the free vibration of the undamped linear system as the initial function; however, the proposed algorithm works for other types of initial conditions as well. Another practical question is how to measure the distance in the space of coordinates with different dimensions, for which an energy-based distance definition is proposed.

A semi-discretization [2] based mapping is used to get the trajectories of the solutions corresponding to different initial conditions, which are categorized whether they are converging to the examined equilibrium or not. The diverging category is divided into three subcases: a) when the trajectory exits the predefined space boundary, b) when the trajectory converges to a new unknown solution, or c) when it converges to a periodic solution.

The classification of the trajectories is based on a cell subdivision of the phase space, similarly to the approach utilized in [1]. The difference is that, since the system's state is given by functions and not single points, trajectories are compared with each other as series of cells occupied by their points in the phase space; each series has a length equal to the largest time delay of the system.

The LIM is iteratively reduced if diverging solutions are found until a stopping criterion is met. To get efficient iterations, the simulations' initial conditions are chosen randomly and based on a bisection method. This enables the algorithm to quickly and accurately estimate the local integrity measure. The algorithm was successfully tested on a series of mathematical models, including a delayed Duffing oscillator (Fig. 1), a turning machining model and a delayed controlled inverted pendulum.

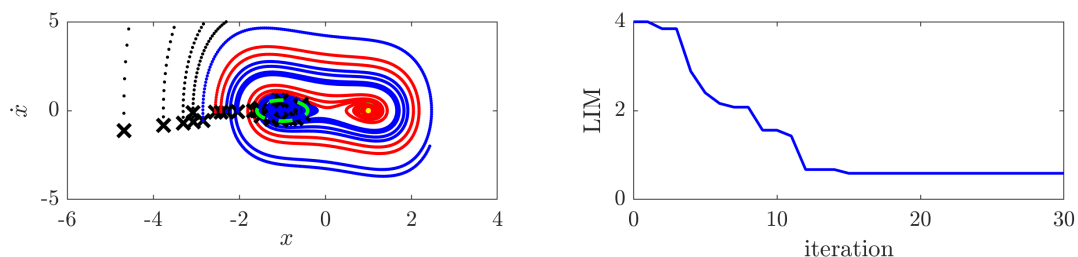


Figure 1: The results of the algorithm applied for the delayed Duffing oscillator $\ddot{x}(t) + 0.2\dot{x}(t) + x^3(t) = x(t-0.1)$. Left: trajectories in the state space; converging (blue) diverging (black and red); the green dashed circle indicates the estimated LIM. Right: The estimated LIM during the iteration.

References

- [1] Habib G. (2021) Dynamical integrity assessment of stable equilibria: a new rapid iterative procedure. *Nonlinear Dyn.* **106**(3): 2073-2096.
- [2] Insperger T., Stepan G (2011) Semi-discretization for time-delay systems: stability and engineering applications **178** Springer Science & Business Media

Phase space visualisation with non-variational chaos indicators

Jérôme Daquin*, Carolina Charalambous*

*Department of Mathematics (naXys), 61 Avenue de Bruxelles, Namur, 5000, Belgium

Abstract. This contribution reports on new global dynamics and non-variational tools able to discriminate between ordered and chaotic motions. The methods are based on geometrical properties of orbits (lengths and stretches), are free of variational equations and are valid for discrete and continuous models. We demonstrate the ability of the proposed indicators to portray Hamiltonian chaos in nearly-integrable settings, and reveal minute details of phase space of various systems in resonant configurations (possibly supporting resonant Arnold web).

Introduction

The problem of discriminating regular and chaotic orbits is of primary importance in several scientific and engineering fields. Over the years, a myriad of computational tools and diagnostics have been developed to achieve this task. These include variational methods relying on the concept of divergence of nearby orbits (*e.g.*, the Fast Lyapunov Indicator [1], the MEGNO index [2] or the SALI [3]), or frequential methods focusing on the spectrum (of some function) of the solution (*e.g.*, the popular frequency analysis method [4]). This contribution reports on easily implementable non-variational and non-frequential methods apt to discriminate chaotic orbits in continuous or discrete dynamical systems.

Results and discussion

Our methods are based on Lagrangian Descriptors [5] (hereafter, LDs), a mathematical and computational technique initially rooted in fluid dynamics, and on the so-called Maximum Eccentricity Method [6] (hereafter, MEM), steaming from the study of exoplanetary orbital systems. Both methods do not rely on variational equations, and exploit solely the knowledge of the orbit. The implementations are thus free of the tangent vector dynamics, and there is no need to quantify its growth over time. Using integrable or perturbed low dimensional dynamical systems (supporting possibly chaotic motions), we discuss properties of the LD and MEM metrics. In particular, by studying how they react on slices of initial conditions, we highlight their dynamical drivers (as exemplified in Fig. 1). The key-point in deriving our chaos indicators then relies on characterising the regularity of the LD and MEM metrics. We demonstrate that second-derivatives based indicators encapsulate sensitively the relevant dynamical information. Our indicators are benchmarked against classical and widely accepted chaos detection methods, and are applied to several models including the standard-map, fundamental models of resonances, symplectic mappings, 3 degrees-of-freedom Hamiltonian models supporting a dense web of resonances, and planetary systems in which diffusion occurs. Our results demonstrate relevance of the indicators for understanding phase space transport mediated by resonant and chaotic interactions, as omnipresent in celestial mechanics or astrodynamics.

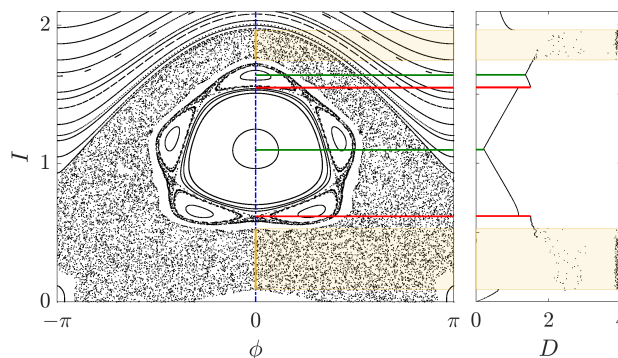


Figure 1: Poincaré map associated to a two-waves Hamiltonian and its associated diameter D metric computed over the line of initial condition $\phi = 0$. The D metric encapsulates relevant dynamical information on which it is possible to build a chaos indicator.

References

- [1] Froeschlé, CI and Gonczi, R and Lega, Elena. (1997) The fast Lyapunov indicator: a simple tool to detect weak chaos. Application to the structure of the main asteroidal belt. *P&SS* **45**:881-886.
- [2] Cincotta, P M and Giordano, CI Marcela and Simó, C. (2003) Phase space structure of multi-dimensional systems by means of the mean exponential growth factor of nearby orbits. *Phys. D: Nonlinear Phenom.* **182**:151-178.
- [3] Skokos, Ch and Antonopoulos, Ch and Bountis, TC and Vrahatis, MN (2004) Detecting order and chaos in Hamiltonian systems by the SALI method. *J. Phys. A: Math. Gen.* **37**:62-69.
- [4] Laskar, J (1993) Frequency analysis of a dynamical system. *CM&DA* **56**:191-196.
- [5] Mendoza, C and Mancho, Ana M. (2010) Hidden geometry of ocean flows. *PRL* **105**:038501.
- [6] Dvorak, R and Pilat-Lohinger, E and Schwarz, R and Freistetter, F. (2004) Extrasolar Trojan planets close to habitable zones. *A&A* **426**:37-40.

Unconditionally stable time stepping scheme for large deformation dynamics of elastic beams and shells

Domenico Magisano*, Leonardo Leonetti* and Giovanni Garcea*

*Dipartimento di Ingegneria Informatica, Modellistica, Elettronica e Sistemistica,
Università della Calabria 87036 Rende (Cosenza), Italy

domenico.magisano@unical.it, leonardo.leonetti@unical.it, giovanni.garcea@unical.it

Abstract. An implicit time-stepping scheme is proposed to achieve energy conservation and unconditional stability for elastic beams and shells undergoing large deformations. More generally, the method can be applied to all structural models, regardless of the nonlinearity in the relationship linking the strain to the kinematic degrees of freedom (displacements and rotations). In this respect, also nonlinear multi-body coupling laws can be included in penalty form by interpreting them as generalized strains. The time stepping scheme is a simple modification of the mid-point rule with the mean internal forces evaluated using the average value of the stress at the step end-points and an integral mean of the strain-displacement tangent operator over the step computed by time integration points.

Introduction

One-step implicit time integration methods such as Newmark's schemes lose the unconditional stability when used in large deformation problems [1], especially in long simulations. Simo and Tarnow proposed a simple method that guarantees unconditional stability by conserving the algorithmic energy in elastodynamics [1]. However, energy conservation is lost for other structural models where the relationship linking the strain to displacements and rotations is no longer quadratic. This work presents a numerical framework for long term dynamic simulations of elastic structures undergoing large deformations. The time-stepping scheme of Simo and Tarnow is generalized to achieve energy conservation for generally nonlinear strain measures and penalty coupling terms, like the nonlinear rotational one for thin shells [2]. The method is based on a particular integral mean of the internal forces over the step, that includes Simo and Tarnow's method as a reduced quadrature rule, and has unconditional stability.

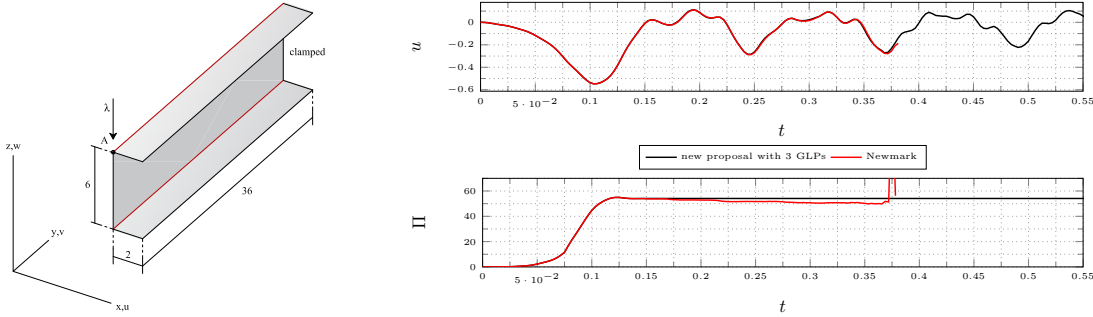


Figure 1: Newmark's trapezoidal rule fails due to the lack of energy conservation while the new proposal is unconditionally stable.

Results and discussion

Numerical results are reported for Reissner beams and assemblages of Kirchhoff-Love shells with smooth and non-smooth interfaces undergoing large deformations. Unconditional stability was proven in long simulations. Compared to the original Simo and Tarnow method, the new one does not conserve exactly the angular momentum. Interestingly, this last feature seems to be marginal in practical computations. Energy conservation assures stability. Conserving the angular momentum neither implies stability nor is synonym of higher accuracy. This is highlighted in the last test, where the momentum-conserving scheme needs a halved time step to get the same accuracy in displacements compared to our energy-conserving scheme. More details are available in [3], together with many other numerical examples. The method is also suitable for models with finite 3D rotations, by exploiting the pseudo-rotation vector.

References

- [1] Simo J.C., Tarnow N. (1992) The discrete energy-momentum method. Conserving algorithms for nonlinear elastodynamics. *Z. angew. Math. Phys.* **43**:757-792.
- [2] Leonetti L., Liguori F. S., Magisano D., Kiendl J., Reali A., Garcea G. (2020) A robust penalty coupling of non-matching isogeometric Kirchhoff-Love shell patches in large deformations. *Comput. Methods Appl. Mech. Eng.* **371**:113289.
- [3] Magisano D., Leonetti L., Garcea G. (2022) Unconditional stability in large deformation dynamic analysis of elastic structures with arbitrary nonlinear strain measure and multi-body coupling. *Comput. Methods Appl. Mech. Eng.* **393**: 114776.

Computing Periodic Responses of Geometrically Nonlinear Structures Modelled using Lie Group Formulations

A.K. Bagheri*, V. Sonnevile** and L. Renson*

*Department of Mechanical Engineering, Imperial College London, South Kensington, London, UK

**Chair of Applied Mechanics, Technical University of Munich, Garching, Germany

Abstract. This work presents a shooting algorithm to compute the periodic responses of geometrically nonlinear structures modelled using an $SE(3)$ Lie group beam formulation. The formulation is combined with a pseudo-arclength continuation method and used to compute the nonlinear normal modes (NNMs) of a doubly clamped beam. The efficiency of beam model is an advantage that can offset the computational cost of numerical continuation methods. Results are compared with a reference displacement-based FE model with von Kármán strains.

Introduction

New designs of mechanical structures are increasingly lighter and more flexible and exhibit geometric nonlinearities due to the presence of large displacements and rotations. A popular approach for modelling geometric nonlinearities is to use von Kármán finite element (FE) models, which assume Euler-Bernoulli bending and approximate the Green-Lagrange strain measures by including only the quadratic terms pertaining to the rotations. These methods are widely used for modelling both beams and plates and for creating reduced order models of such structures. However, due to its simplified and approximate treatment of strains and its linearised kinematics, von Kármán equations are not suitable for modelling large deformations. Geometrically exact beam theories can alternatively be used for such cases, however, the parametrisation of rotations can lead to FE discretisations which do not preserve strain invariance under rigid body motion [1]. Other beam models such as the intrinsic beam formulation deals with this issue by eliminating rotations and displacements from the equations of motion, however, they face additional difficulties in FE assembly and in imposing boundary conditions.

Beam formulations based on the Special Euclidean Lie Group $SE(3)$ circumvent these problems by coupling the rotations and positions and adopting a local frame approach. The invariance of the strains under rigid body motion comes naturally from this formulation. Moreover, shear locking is avoided thanks to a nonlinear interpolation formula based on the exponential map that couples the rotation and positions fields and governs the nonlinear configuration space [2]. In this work, the Lie group formulation is used to find unforced NNMs of geometrically nonlinear structures, where results are compared to that from a von Kármán beam model.

Results and Discussion

Results are shown for a straight clamped-clamped beam discretised with 30 elements where NNMs are calculated using the Lie group and von Kármán solvers. The frequency energy plot corresponding to the second NNM is seen in Figure 1. Two resonance tongues appear in the solution curve: the first starting approximately at 160 Hz and corresponding to a 3:1 interaction with mode 4, and the second starting approximately at 207 Hz and corresponding to a 5:1 interaction with mode 6. An additional interaction is captured by the Lie group solver along the first tongue corresponding to an internal resonance between modes 2 and 6, which is not found using the von Kármán solver. The effect of the discretisation on the accuracy of the results is shown in Figure 2, where the Lie group solver can capture the nonlinear dynamics with fewer beam elements, which is an added advantage over the von Kármán solver. Additional structures analysed are a cantilever and an L-shaped beam, where displacements and rotations are larger and the increased accuracy of the Lie group solver in capturing nonlinearities overcomes the limitations of the von Kármán model.

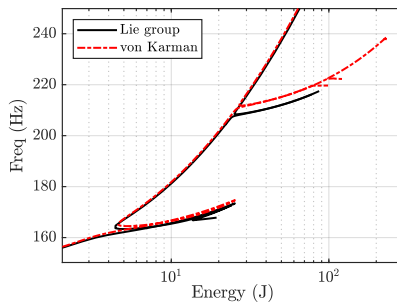


Figure 1: FEP of 2nd NNM of clamped-clamped beam

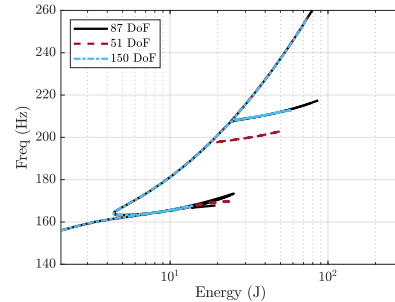


Figure 2: Effect of mesh size on NNM2

References

- [1] Jelenić, G., & Crisfield, M. A. (1999). Geometrically exact 3D beam theory: implementation of a strain-invariant finite element for statics and dynamics. *CMAA* **171**(1–2): 141–171.
- [2] Sonnevile, V., Cardona, A., & Brüls, O. (2014). Geometrically exact beam finite element formulated on the special Euclidean group $SE(3)$. *CMAA* **268**: 451–474.

Global Parametric Optimization for Structures with Nonlinear Joints in Vibration

Quentin Ragueneau^{*,**}, Luc Laurent^{*}, Antoine Legay^{*}, Thomas Larroque^{**}, Romain Crambuer^{**}

^{*}Laboratoire de Mécanique des Structures et des Systèmes Couplés, EA 3196, Cnam, HESAM Université, Paris, France

^{**}INGELIANCE Technologies, Centre de simulation numérique, Mérignac, France

Abstract. The optimal design of complex structures with nonlinear vibration is a significant concern for the industry. This work presents a numerical strategy relying on Bayesian Optimization for the parametric optimization of such structures with the aim of lowering the computational cost compared to classical global optimization algorithm. A specific focus is given on the mechanical solver for the resolution of the nonlinear dynamical problem using the Harmonic Balance Method combined with an Alternating Frequency/Time approach and a scheme for the numerical continuation of the solution path. This mechanical solver is then employed to build and enrich a Gaussian Process within a Bayesian Optimization procedure. The whole strategy is applied to the parametric optimization of a gantry crane.

Introduction

In the process of industrial structure design, numerical simulation combined with parametric optimization algorithms can provide the solution leading to the best performance. Complex assembled structures often include nonlinear phenomena at their joints (contact, friction, etc...) that this study aims at considering to get a more precise model and thus, a more optimal solution while performing a parametric optimization. However, the dynamical simulation of nonlinear models is computationally expensive, and the fulfillment of global optimization, which can require a very large number of computations, on such model could be impracticable in terms of computational time. Therefore, a specific strategy is proposed to make the parametric optimization of structures with nonlinear joints in vibration computationally reasonable. Taking advantage of the fact that only degrees of freedom at the interfaces are nonlinear, the first step consists in performing a Craig Bampton reduction [1]. Then, the solution based on the resulting reduced model is computed using the Harmonic Balance Method with an Alternating Frequency/Time approach [2]. It allows to find periodic solutions with reasonable accuracy avoiding the costly computation of possibly long transients. Numerical path continuation is also applied using a predictor-corrector method to follow the evolution of the solution with respect to the frequency and overcome potential turning points. The computational cost is still quite expensive, and the direct use of classical global optimization algorithm combined with this solver is not practicable especially since the problem includes numerous interfaces degrees of freedom. Therefore, a Bayesian Optimization [3] based on Gaussian Process [4] and an acquisition function is executed to achieve the global parametric optimization with a limited number of calls to the mechanical solver.

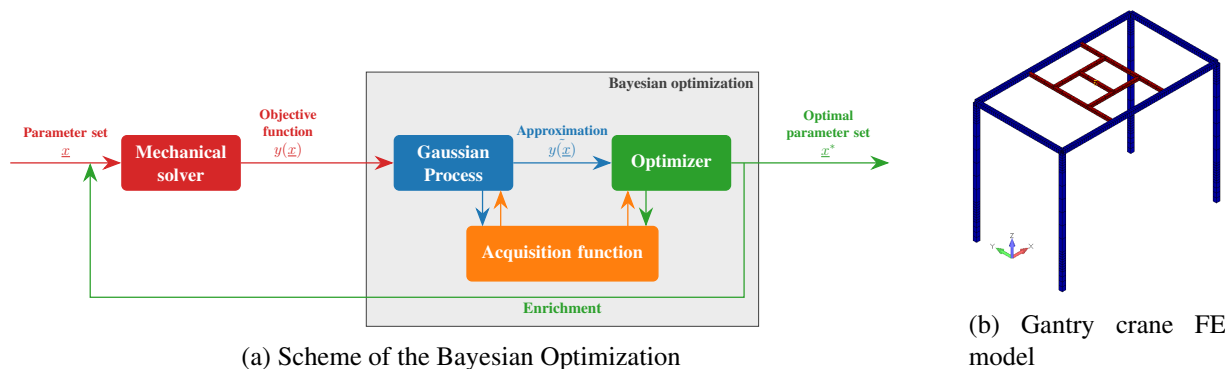


Figure 1: Parametric optimization of a gantry crane

Results and discussion

The strategy is applied to the parametric optimization of a gantry crane with localized contact. The mechanical solver proves to be reasonably efficient and able to handle the contact nonlinearity and especially to follow the turning points thanks to numerical continuation. The Bayesian Optimization allows to significantly reduce the number of simulations to perform compared to classical global optimization methods such as genetic algorithm.

References

- [1] Craig Jr R. R., Bampton M. (1968) Coupling of Substructures for Dynamic Analysis. *AIAA Journal* **6.7**:1313-1319.
- [2] Sarrouy E., Sinou J. (2011) Non-Linear Periodic and Quasi-Periodic Vibrations in Mechanical Systems - On the use of the Harmonic Balance Methods. *Adv. Acoust. Vib.*, IntechOpen. **Chap. 21**:419-434.
- [3] Frazier P. I. (2018) A Tutorial on Bayesian Optimization. *arXiv*. 1807.02811.
- [4] Rasmussen C. E., Williams C. K. I. (2006) *Gaussian Processes for Machine Learning*. The MIT Press.

Saddle-node bifurcation prediction from pre-bifurcation scenario

Balint Bodor and Giuseppe Habib

Department of Applied Mechanics, MTA-BME Lendület “Momentum” Global Dynamics Research Group, Faculty of Mechanical Engineering, Budapest University of Technology and Economics, Budapest, Hungary.

Abstract. A technique for the prediction of saddle-node bifurcation is developed. The technique is based on the energy decrement in the free vibration decay, which tends to zero in the vicinity of the bifurcation. This creates a deformation of the energy decrement profile recognizable also very far from the bifurcation, which enables one to estimate the existence and the position of a saddle-node bifurcation directly from the pre-bifurcation scenario in a safer environment from a dynamical integrity perspective. The developed technique is also implementable in experimental systems.

Introduction

Saddle-node bifurcations have the characteristic that the branch of periodic solutions leading to them exists only on one side of the bifurcation parameter. Accordingly, they might be unexpectedly encountered for variations of the bifurcation parameter [1]. A typical bifurcation scenario presenting this situation is illustrated in Fig. 1a. For $a < a_{SN}$, the only steady-state solution is an equilibrium point, which is globally stable. Conversely, for $a > a_{SN}$, the system has two additional steady-state periodic solutions, which undermine the dynamical integrity of the stable equilibrium. In this study, a technique for predicting the occurrence of saddle-node bifurcations, which does not require tracking branches of periodic solutions, is developed.

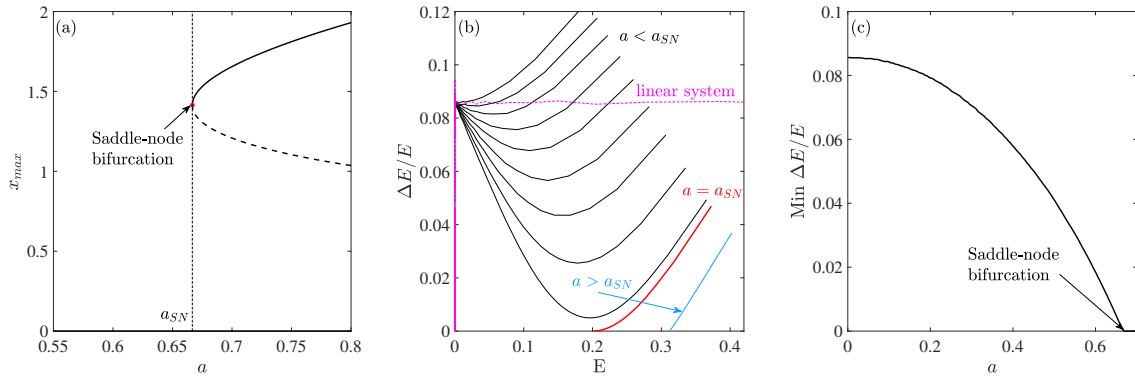


Figure 1: (a) Bifurcation scenario; (b) relative energy decrement per cycle; (c) locus of relative energy decrement minima leading. Results are obtained for the system $\ddot{x} + x + c_1\dot{x} - a\dot{x}^3 + \dot{x}^5 = 0$ [2].

Results and discussion

Let us consider the bifurcation diagram in Fig. 1. For $a < a_{SN}$, the equilibrium is globally stable. For any initial energy level, the energy monotonously decreases until zero. If the system were linear, the relative energy decrement per cycle would be constant. For $a > a_{SN}$, the energy decreases until zero within the basin of attraction of the stable equilibrium, while it can either decrease or increase within the basin of attraction of the stable periodic solution, until it converges to the periodic solution at an energy level different from zero. The saddle-node separates these two scenarios. To have a smooth transition between the two scenarios, it is necessary that, starting from $a < a_{SN}$, the relative energy decrement decreases as we approach the bifurcation and increases moving away from it, which means that the relative energy decrement presents a minimum in the vicinity of the bifurcation, which touches zero at the bifurcation. This conjecture is numerically verified for the considered system, as illustrated in Fig. 1b. The magenta line refers to the linearized system, the black line to the pre-bifurcation scenario and the blue to the post-bifurcation; they are separated by the red one, which touches the zero axes with a horizontal tangent. By picking the value of the minimum points and plotting them with respect to the bifurcation parameter a , we notice that a seeming parabola is obtained. This suggests that, by picking some minimum and performing a second-order interpolation, it is possible to estimate a_{SN} without having any information about the post-critical scenario. We remark that signs that the saddle-node exists are visible already very far from it. This result allows for detecting dangerous saddle-node bifurcations before they are encountered, even in real systems. In fact, the procedure uniquely requires time series of free vibration decays, obtainable numerically but also experimentally.

References

- [1] Strogatz S. H. (2018). Nonlinear dynamics and chaos: with applications to physics, biology, chemistry, and engineering. CRC press.
- [2] Habib G., Cirillo G.I., Kerschen G. (2018) Isolated resonances and nonlinear damping. *Nonlinear Dyn.* **93**:979-994.

An extensive test campaign of a turbine bladed disk in the presence of mistuning and underplatform dampers, and numerical validation

Giuseppe Battiato*, Christian M. Firrone*, Valeria Pinto* and Antonio Giuseppe D'Ettolè**

**Department of Mechanical and Aerospace Engineering, Politecnico di Torino, Torino, Italy*

***AvioAero, Rivalta di Torino, Torino, Italy*

Abstract. The design of lighter and highly loaded aircraft turbo-engines is driven by the need of improving their efficiency for a sustainable air propulsion. In this context, forced and self-excited vibrations in bladed disks must be mitigated to avoid HCF damage that jeopardizes the structural integrity of the whole engine. Current vibration prediction methods are not fully reliable due to complexities of the bladed disks design and nature of excitations. To improve the reliability of such methods, it is necessary to (i) investigate key problems like mistuning and nonlinear friction damping, and (ii) to validate design methodologies. In this paper, the results of a test campaign to study the effect of mistuning and of underplatform dampers are presented and discussed. The data collected have been used to validate an in-house numerical code. The code exploits an efficient reduction method for large finite element (FE) models of mistuned bladed disks.

Introduction

The design of aircraft turbo-engines is driven by the need of improving their efficiency for a sustainable air propulsion. This leads to a lighter design of blades, vanes and seals, that are usually prone to vibrations. In working conditions, both forced and self-excited vibrations must be mitigated to avoid high cycle fatigue (HCF) failure. To improve the reliability of the current vibration prediction methods, several European projects have been launched (i) to investigate the effects of mistuning and nonlinear friction damping, and (ii) to improve the design practices. Several efforts in the testing and numerical prediction of mechanical vibrations in turbine bladed disks have been made in the ARIAS European project [1]. In this paper, the test campaign performed at the GE Avio testing laboratory, on the ARIAS bladed disk test case are presented and discussed. The bladed disk has been tested in the tuned and the intentionally mistuned configurations, either in the presence or not of underplatform dampers (UD). The blades response has been measured and processed by Blade Tip-Timing system. The data collected in the test campaign have been used to validate a numerical code developed for the prediction on the nonlinear forced response (FR) of mistuned bladed disks in the presence of UD. To avoid the high computational costs associated to the solution of nonlinear FR, the code exploits the reduction method for large finite element (FE) models of mistuned bladed disks presented in [2].

Results and discussion

The test campaign has been performed on a turbine bladed disk having 144 blades. Each blade has a real aerodynamic airfoil with a tip able to accommodate the permanent magnets for the mechanical excitation, a balancing mass and a mistuning mass. The latter is installed depending on the disk configuration to test, i.e. either mistuned or tuned, with or without mistuning masses respectively. The tested mistuned configuration follows the alternate pattern 0-1, where the 0 and 1 denote the blades without and with mistuning mass. The bladed disk has been tested in vacuum conditions for the excitation of either synchronous or asynchronous vibrations. The numerical validation has been performed on the reduced order models (ROM) of the tuned and mistuned bladed disk, that have been created by using the reduction method presented in [2]. The reduction process has led to two ROMs having approximatively the 0.007% of the degrees-of-freedom (dofs) of the full FE model. For both ROMs the same set of master dofs have been retained: the accessory dofs for the force application and the response monitoring, and the dofs at the blades' platform for the contact forces prediction due to the relative motion between the blades and the UD. The force amplitude used in the numerical simulation has been tuned using as a reference the averaged experimental data obtained in the absence of UD. The modal damping has been set equal to the one identified from the experimental FR. As expected, the numerical FR for the modes of interest (i.e. flap and torsional) show good agreement with the experimental ones, in terms of vibration amplitude and Q-factor, while a deviation less of the 10% has been found for natural frequency. This is due to uncertainty associated to the contact areas and stiffness associated to the actual coupling between blades and disk, that has not been deeply investigated. The same excitations have been used to excite the ROMs in the presence of UD. In most of the examined cases, the numerical vibration amplitude at resonance as well as the Q-factor fall in the range of uncertainty resulting from the analysis of the experimental data, denoted by a mean value and a standard deviation.

References

- [1] <https://www.arias-project.eu/>
- [2] Pinto, V., Battiato, G. and Firrone, C.M., 2022. A Reduction Technique for the Calculation of the Forced Response of Bladed Disks in Presence of Contact Mistuning At Blade Root Joints. *Journal of Engineering for Gas Turbines and Power*. <https://doi.org/10.1115/1.4055722>

A FEA model generation method for irregular-shaped and nonhomogeneous structures

Ming-Hsiao Lee*

**National Center for High-performance Computing, Hsinchu, Taiwan*

Abstract. This study proposes a FEA model generation method to handle biomedical objects which are highly irregular-shaped and nonhomogeneous, i.e., highly nonlinear structures. The method is based on the sectioned medical scanning data, e.g., CT scan, which has included bone density data, to generate analysis models according to the irregular shapes and randomly distributed bone densities, so that the analysis models can match the irregular shapes and randomly-distributed stiffness of the real bones. Using these more realistic models to simulate the dynamic characteristics, such as natural frequencies, of the objects, better results can be obtained.

Introduction

The finite element method, although widely being used in various fields, has difficulty to model some special applications in which extremely irregular shapes and uneven distribution of materials are treated, such as the cases in biomedical engineering, where the objects to be treated are extremely irregular-shaped, and the materials are completely nonhomogeneous in nature. For example, the bone shape of the human body is extremely irregular and varies from person to person, so it becomes very difficult to generate the geometry models with traditional CAD systems. Moreover, the bone density which affects the stiffness [1] is randomly nonhomogeneous, even the bone densities of the same person are different at different portions and vary over time. This situation makes it very difficult to generate the analysis models with traditional pre-processing systems. Such problems, if they are analysed in the traditional finite element modelling, most of the time adopt the assumption that the material is homogeneous. In this approach, the real stiffness of the bones cannot be accurately modelled, so do the natural frequencies, which are important during certain medical operations. This study proposes a model generation method which is based on the sectioned medical scanning data, e.g., Computerized Tomography (CT scan), which includes bone density data, to generate analysis models according to the irregular shapes and randomly distributed bone densities, so that the analysis models can match the irregular shapes and randomly-distributed stiffness of the real bones. With these realistic models, better results can be achieved. For example, for a bone of the same person, the bone stiffness changes over time can also be effectively simulated to evaluate the effects of the age or therapy. The dynamic characteristics of the objects can also be accurately obtained, such as natural frequencies.

Results

The case shown in Fig. 1 is a certain person’s mandible. Originally, it was found too weak because of the loss of bone density due to aging. After the therapy, the bone density is increased and improved. Although the mandible shape of the same person is still the same, the bone density distribution has changed. With the proposed modelling method, two FEA models which have the same shapes but with different bone density distribution were generated and used to simulation to evaluate the stiffness and natural frequencies of the same mandible at different time. If the stiffness is weakened, the natural frequencies decrease, so it may encounter the resonance problem during using electric ultrasonic toothbrushes and tooth drills. The results can tell the improvement of the therapy as thrown in Fig. 2. The natural frequencies also increase as well.

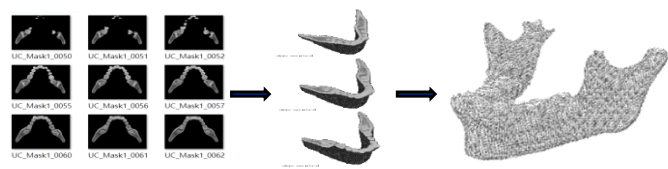


Figure 1: FEA model based on CT scan data and include the bone density data

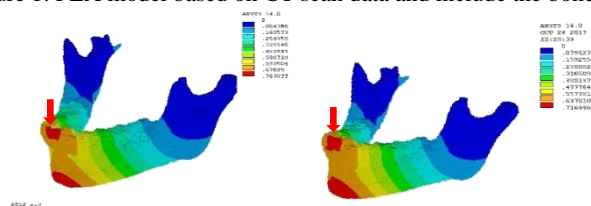


Figure 2: The results of the ‘before’ model (left) and ‘after’ model (right), the stiffness is increased after therapy

References

[1] Kostas, T. et al (2005): Dose reduction in maxillofacial imaging using low dose Cone Beam CT. European Journal of Radiology, Vol. 56, pp.413–417

Robust topology optimization under non-probabilistic uncertainties

Paolo Venini* and Marco Pingaro**

*Department of Civil Engineering and Architecture, University of Pavia, Pavia, Italy, 0000-0002-0023-1197#

**Department of Structural and Geotechnical Engineering, Sapienza University of Rome, Rome, Italy, 0000-0002-7037-8661#

Abstract. A novel approach to static and dynamic topology optimization has recently been proposed by the authors that aims to minimize a proper norm of the input/output transfer matrix, say \mathbf{G} . The key ingredient is the Singular Value Decomposition (SVD) that is useful with respect to engineering point of view.

Introduction

This work presents a topology optimization approach that is innovative with respect to two distinct matters. First of all the proposed formulation is capable to handle static and dynamic topology optimization with virtually no modifications. Secondly, the approach is inherently a multi-input multi-output one, i.e. multiple objectives can be pursued in the presence of multiple loads. The method is based on the input-output mapping that is inherently algebraic in the static case and becomes such in the dynamic case thanks to the adoption of a frequency-domain framework. The Singular Value Decomposition (SVD) [1] of the resulting transfer function, say \mathbf{G} , represents then the core of the proposed approach. Singular Value Decomposition is useful with respect to two different matters:

- norms used as goal functions may be uniquely defined in terms of the singular values of \mathbf{G} . The sensitivity analysis may therefore be given a compact and clear format that was shown to work properly in statics as well as in dynamics [2];
- from an engineering point of view, any singular value is shown to be the gain (blow-up factor) of the associated input-output channel in which the system is decomposed. Singular values are therefore the inherent quantities that should enter any structural optimization formulation.

Results and discussion

That said, the goals of this paper are the following ones:

- Load (and possibly material) uncertainties are added to the structural model to be designed and a formulation is proposed that is capable to handle such uncertainties and drive the procedure toward a robust optimal design within a worst-case scenario approach (see Fig. 1);
- toward a fully geometrically non-linear analysis, a preliminary approach is derived that allows to derive optimal topology with respect to buckling using a sequence of linearised problems, each of which is of the same type as the one introduced above.

Numerical examples concerning static and dynamic problems are presented.

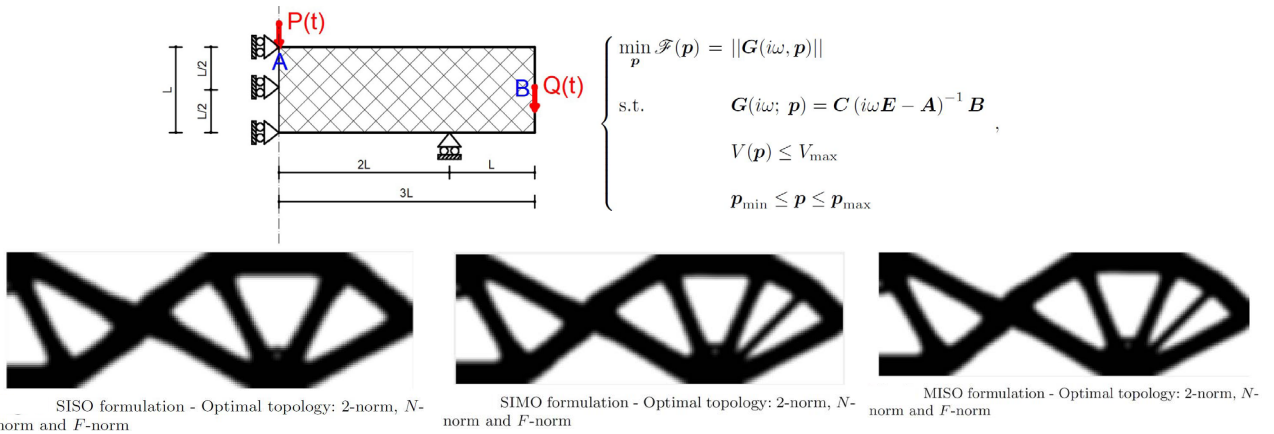


Figure 1: Example of optimization in elastostatic condition: SISO - single load case and standard compliance minimization (left), SIMO - single load case and minimization of the compliance vector norm (center), MISO - two load cases and standard compliance minimization (right)

References

- [1] K. Strang 2019 Linear Algebra and Learning from Data. Cambridge Press, Wellesley, Wellesley.
- [2] Venini, P., Pingaro, M. (2023) Static and dynamic topology optimization: an innovative unifying approach. *Structural and Multi-disciplinary Optimization* (accepted).

An insight on the parameter identification of a new hysteretic model addressing asymmetric responses

Salvatore Sessa*

*Department of Structures for Engineering and Architecture, University of Naples Federico II, Napoli, Italy,
ORCID 0000-0003-3209-5051

Abstract. It is presented an investigation concerning an inverse identification algorithm for the experimental characterization of the constitutive parameters relevant to a recently developed constitutive model addressing asymmetric hysteresis.

Introduction

Within the context of nonlinear analysis of structures exhibiting hysteretic phenomena, generalized classes of new phenomenological material models have been recently proposed [1] and extended to asymmetric [2] smooth hysteresis loops with hardening and softening behavior, thus permitting the analytical computation of uniaxial responses.

The hysteretic model

Compared to constitutive models having similar behaviours, classes proposed in [1] and [2] turn out to be significantly more efficient since they do not present any differential relationship and, hence, the need to invoke iterative procedures. Nevertheless, due to their phenomenological nature, these models are characterized by sets of constitutive parameters that need to be calibrated by matching experimental evidences, a task of particular complexity for the asymmetric model presented in [2].

The identification procedure

The identification procedure is based on the definition of least-square residuals between the theoretical and experimental responses that are minimized by simplex- and gradient-based optimization algorithms. In particular, due to the occurrence of hardening and softening phenomena, three different residuals must be defined in order to match a given experimental response both in terms of amplitude, stiffness, and transition between the tensile and compressive regions.

Moreover, in order to ensure a robust convergence, and especially to formulate a standard identification protocol, the procedure includes pre-processing phases in which suitable first-trials of the parameter sets, to be used by subsequent minimization procedures, are esteemed.

Numerical applications, as well as a comparison with the Generalized Bouc-Wen material [4], prove the robustness of the presented strategies as well as the capabilities of such phenomenological models within the context of seismic analysis of nonlinear structures and vibration isolation.

Funding and acknowledgments

The present research was supported by the University of Naples Federico II and the *Compagnia di San Paolo*, which are gratefully acknowledged by the author, as part of the Research Project *MuRA*, FRA grants, CUP E69C21000250005.

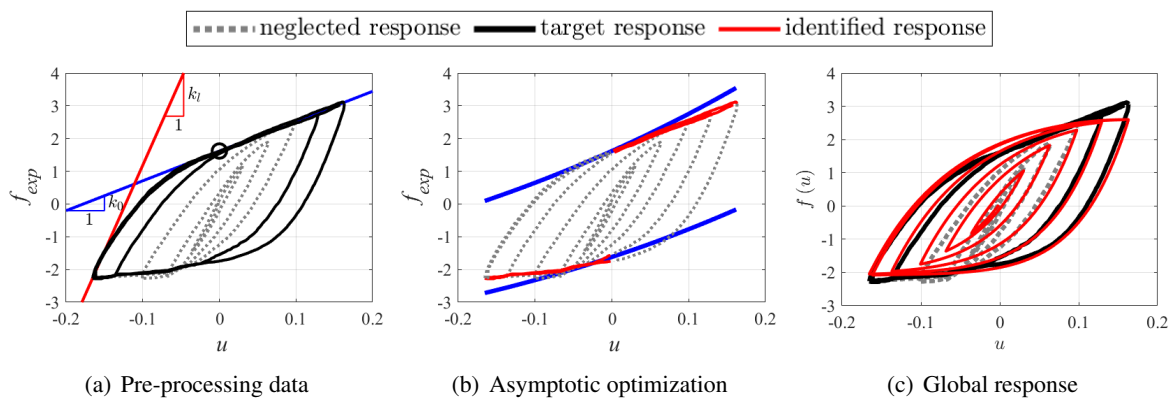


Figure 1: Pre processing data, asymptotic and global response optimization.

References

- [1] Vaiana N., Sessa S., Marmo F., Rosati L. (2018) A class of uniaxial phenomenological models for simulating hysteretic phenomena in rate-independent mechanical systems and materials. *Nonlinear Dynam.* **93**(3):1647-1669.
- [2] Vaiana N., Sessa S., Rosati L. (2021) A generalized class of uniaxial rate-independent models for simulating asymmetric mechanical hysteresis phenomena. *Mech. Syst. Signal Pr.* **146**:106984.
- [3] Vaiana N., Sessa S., Marmo F., Rosati L. (2019) An accurate and computationally efficient uniaxial phenomenological model for steel and fiber reinforced elastomeric bearings. *Compos. Struct.* **211**:196-212.
- [4] Song J., Der Kiureghian A. (2006) Generalized Bouc-Wen model for highly asymmetric hysteresis. *J. Eng. Mech.* **132**(6):610-618.

Neuromorphic Computing Based on Physical Systems with Biologically Inspired Learning Rules

D. Dane Quinn¹, Shaghayegh Rahimpour², Nikhil Bajaj², Aaron Batista², Carey Balaban²

¹The University of Akron, Akron OH, USA; ²University of Pittsburgh, Pittsburgh PA, USA

Abstract. This work considers an application in neuromorphic computing, whereby physical components are employed to undertake computing applications, inspired by the human brain and nervous system. The present system is based on a coupled network of FitzHugh-Nagumo oscillators, with each oscillator characterized by a temporal spiking response based on the inputs from those oscillators to which it is coupled. With a biologically inspired learning rule, the coupling between oscillators is modified so that the output oscillators fire a specified times. This work explores the application of different forms of coupling as well as different learning rules based in part on spike timing dependent plasticity, the mechanisms believed to underlie how the human brain learns.

Introduction

A system of N FitzHugh-Nagumo oscillators is described by the equations of motion

$$\dot{v}_i = v_i - \frac{v_i^3}{3} - w_i + \sum_{j=1}^N f_{ij}, \quad \tau \dot{w}_i = v_i + a - b w_i, \quad i = 1, \dots, N, \quad (1)$$

where f_{ij} represents a coupling between oscillator i and oscillator j . Note that this is a simplified version of the Hodgkin-Huxley model of a spiking neuron and also is a generalization of a van der Pol circuit. In this neuromorphic computing application the network is trained so that individual output oscillators fire at specific predetermined times [1]. For example, in a motor control application such firing could relate to the timing of different actuators acting in a large-scale system. The coupling between oscillators is assumed to accumulate voltage, so that an oscillator i fires only when the input voltage, represented by $\sum_j f_{ij}$ reaches a sufficient voltage level.

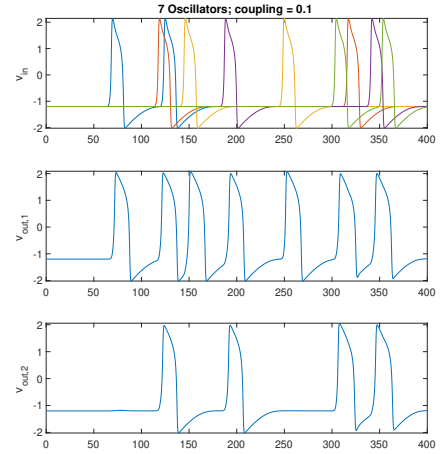
Results and Discussion

The performance goal is based on a specified output spike timing, while learning is implemented based on spike timing dependent plasticity [2], commonly described as “neurons that fire together wire together” and assumed to underlying changes in the architecture of the human brain.

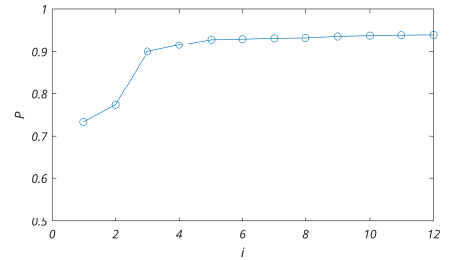
In Figure 1a, an example response of a network with $N = 7$ oscillators is shown. In this system, 5 oscillators are excited and serve as inputs, so that each oscillator fires twice during the time interval shown. Each input oscillator is then coupled to each of the 2 output oscillators. Note that the firing of these output oscillators is determined by the response of the input layer. Based on a biologically inspired learning rule, the network coupling is altered dependent on the overall performance of the system, so that as the system learns the actual timing of the output neurons approaches the target values, as illustrated in Figure 1b.

References

- [1] Hoppensteadt F.C., Izhikevich E.M. (2001) Synchronization of MEMS resonators and mechanical neuro-computing. *IEEE Transactions on Circuits and Systems* **48**(2):133–138.
- [2] Frémaux N., Sprekeler H., Gerstner W. (2010) Development/plasticity/repair functional requirements for reward-modulated spike-timing-dependent plasticity. *The Journal of Neuroscience* **30**(40):13326–13337.



(a) Output spike train



(b) Timing performance

Figure 1: Network of FitzHugh-Nagumo oscillators; 5 input oscillators, 2 output oscillators

Mitigating vibration levels of mistuned cyclic structures by use of contact nonlinearities

Samuel Quaegebeur*, Benjamin Chouvion** and Fabrice Thouverez *

*Ecole Centrale de Lyon, LTDS UMR 5513, 69130 Ecully, France

**Centre de recherche de l'école de l'air, Ecole de l'air et de l'espace, 13661, Salon-de-Provence

Abstract. In cyclic systems, manufacture tolerances and possible wear of the structure lead to small random variations (also called random mistuning) of the nominal (tuned) cyclic-symmetric mechanical system. Most of the time, these imperfections result in systems with vibration levels higher than the tuned one, and are thus detrimental. Friction nonlinearities are used in the nominal design as a damping mechanism to dissipate the vibrational energy. The aim of this paper is to show that they can also mitigate the negative influence of random mistuning. This result is achieved through statistical studies on a high-fidelity nonlinear finite-element model of a bladed-disk. In order to restrain the numerical cost of deterministic simulations, state-of-the-art nonlinear reduction methodologies are employed.

Introduction

Computing the vibrational displacement of a structure is of the utmost importance to design the system and predict its potential failure. Although numerical tools are accurate in a deterministic way, manufacture tolerances and possible wear of the structure create discrepancies between the simulations and the real-life system. These slight differences may severely impact the expected system dynamics.

For linear systems, researchers have developed reduced-order model (ROM) to decrease significantly the size of the system while keeping an accurate prediction of its dynamics. Applying these ROMs with an accelerated Monte-Carlo method, Castanier et al. have been able to quantify the amplification factor (AF) of a bladed-disk FE model [1].

The purpose of this work is to apply a recent nonlinear ROM [2] to study the impact of mistuning on a high-fidelity FE model (approximately 700,000 degrees of freedom) of a bladed-disk with contact nonlinearities. This original contribution focuses on computing the nonlinear AF of a randomly mistuned bladed-disk for different types of harmonic excitation. A particular attention is paid to the level of energy in the structure because, unlike in the linear case, it strongly impacts the AF.

Results and discussion

While linear mistuned systems can exhibit a vibration level 120% higher than the nominal system (see black curve in Figure 1a), this value can be decreased to 30% in the presence of a nonlinearity strong enough. Similar behaviour is observed for another kind of harmonic force exciting different dynamics of the system (see Figure 1b). Such a result is of the utmost importance for turbomachines engineers and will facilitate the future design of engines.

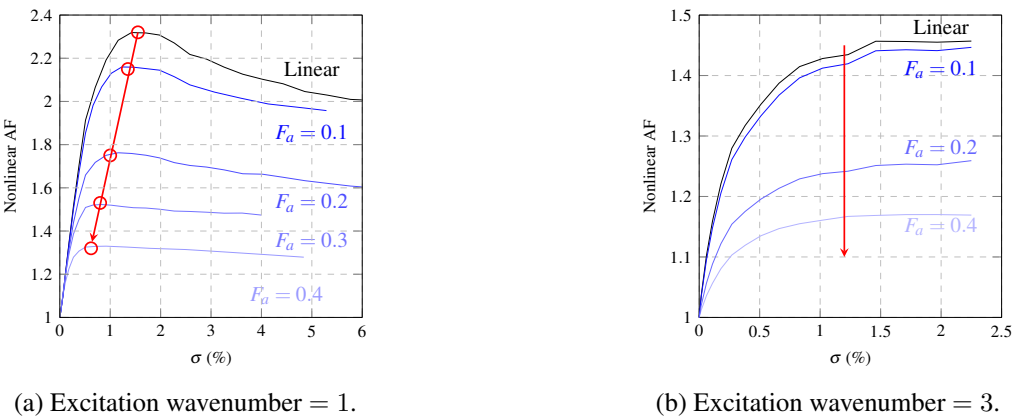


Figure 1: Parametric study conducted for different levels of nonlinearity (F_a) and mistuning (σ). The curves illustrate the AF below which 95% of the maximum amplitudes of vibration are situated.

Contact nonlinearities act as a damping mechanism and have the beneficial effect of reducing the level of vibration and thus extending the lifespan of mechanical systems. Our study shows another beneficial feature, namely that contact linearities also tend to mitigate the detrimental effect of mistuning.

References

- [1] Castanier, M. P. and Pierre, C. (2006) Modeling and analysis of mistuned bladed disk vibration : status and emerging directions. *J. Propuls. Power* **22**: 384-396
- [2] Quaegebeur, S., Chouvion, B., Thouverez, F. (2021) Nonlinear cyclic reduction for the analysis of mistuned cyclic systems. *J. Sound Vib* **499**: 116002

Effect of wear flat length on the global dynamics of rotary drilling

Kapil Kumar and Pankaj Wahi

Department of Mechanical Engineering, Indian Institute of Technology Kanpur, India

Abstract. The regenerative effect developed by the variable thickness of cut in rotary drill system yields self-excited vibrations. These vibrations are the main cause of excessive wear on the tool edge. This cause a wear flat to develop behind the cutting edge. Interaction between the wear flat and rock surface results in a normal force and frictional torque which can effect the overall dynamics of the drill system. We have included a wear flat in the bit-rock interaction model and have considered a lumped parameter model with two degrees of freedom for this analysis. Numerical simulations have been done to analyze the effect of wear flat length which shows the linear stability of the system is not affected by the wear flat length for steady-state conditions. However, the global dynamic behavior of the drilling system varied with the wear-flat length. Here we have studied the effect of various parameters such as coefficient of friction, wear-flat length and damping ratio on the system dynamics.

Introduction

Rotary drilling systems are used to drill deep borewells which are used in exploration and extraction of tract fossil fuels. It consists of a rotary table, a series of hollow pipes (drill-string), a drill collar, and a drill bit. Self-excited vibrations resulting from the regenerative forces are often manifested as bit-bounce and stick-slip vibrations. Gupta and Wahi [1, 2, 3] have studied the effect of various parameters on the stability of the system assuming a sharp edge cutter. A linear stability analysis has been studied by Zhang and Detournay [4] wherein they consider a multi-dimensional model with a wear flat length. However, the global dynamics of drill systems with worn tools have not been studied yet to the best of our knowledge. This model incorporated the various case of normal reaction force acting on the cutter. A simplified rotary drill system with two degrees of freedom is considered; one is in the axial and the other in the torsional direction. The forces and torque between the tool and the rock surface can be considered as reported in [5]. When the normal reaction force is fully mobilized with the surface, the equation of motion in the non-dimensional form of the lumped parameter model is

$$\begin{aligned}\ddot{x}(\tau) + 2\zeta\beta\dot{x}(\tau) + \beta^2x(\tau) = \\ n\psi\delta_0 - n\psi\delta(\tau)H(\omega_0 + \dot{\theta}(\tau))H(\delta(\tau)) + \Lambda_1l(1 - H(v_0 + \dot{x}(\tau))H(\delta(\tau))), \\ \ddot{\theta}(\tau) + 2\kappa\dot{\theta}(\tau) + \theta(\tau) = \\ n\delta_0 - n\delta(\tau)H(\omega_0 + \dot{\theta}(\tau))H(\delta(\tau)) + \Lambda_2l\left(1 - H(v_0 + \dot{x}(\tau))H(\delta(\tau))\text{sgn}(\omega_0 + \dot{\theta}(\tau))\right),\end{aligned}\quad (1)$$

where n is the number of cutters, β is the ratio of axial and torsional frequency, ζ and κ are the axial and torsional damping coefficient, δ_0 is the steady thickness of cut, ω_0 is the non-dimensional angular velocity of the rotary table, τ is the non-dimensional time scale, l is the non-dimensional wear flat length, Λ_1 and Λ_2 are non-dimensional constants. The instantaneous thickness of the cut is modelled as reported in [1] where the cut surface function L is defined between two simultaneous cutters. The function L is governed by the partial differential equation (PDE) reported in [1] with the appropriate boundary condition. These coupled ODE and PDE can be converted into a finite set of first-order system of ODEs with a reduced Galerkin approximation method. Now we have done the numerical analysis to study the effect of parameters on the system.

Results and discussion

We have first considered that the normal reaction force is fully mobilized, i.e., the normal reaction at the wear flat is constant irrespective of the depth of cut and the numerical simulation has been done. It is found that the linear stability analysis of the steady drilling state has not been affected due to the wear-flat on cutters in the non-dimensional parameter space. However, the fully mobilized assumption leads to chattering phenomenon at the inception of the bit-bounce vibrations, i.e., when the cutter is about to leave the rock surface ($\dot{x} + v \leq 0$). Hence, we have incorporated the case when the normal reaction force is linearly varied with the depth of cut before the reaction force is fully mobilized. This leads to a gradual reduction in the normal force when contact is about to be lost and suppresses the chattering behavior. Details of these will be presented at the conference.

References

- [1] Gupta S. K., Wahi P. (2016) Global axial–torsional dynamics during rotary drilling. *J. Sound Vib.* **375**:332-352.
- [2] Gupta S. K., Wahi P. (2018) Bifurcations in the axial–torsional state-dependent delay model of rotary drilling. *Int. J. Non Linear Mech.* **99**:13-30.
- [3] Gupta S. K., Wahi P. (2018) Criticality of bifurcation in the tuned axial–torsional rotary drilling model. *Nonlinear Dyn.* **91**:113-130.
- [4] Zhang H., Detournay E. (2022) A high-dimensional model to study the self-excited oscillations of rotary drilling systems. *Commun. Nonlinear Sci. Numer. Simul.* **112**:106549.
- [5] Detournay E., Richard T., Shepherd M. (2008) Drilling response of drag bits: theory and experiment. *Int. J. Rock Mech. Min. Sci.* **45**:1347-1360.

Active Learning for Probabilistic Machine Learning based modeling of Dynamical Systems

Tamil Arasan*, Selva Kumar*, Murugesan*, Meiyazhagan*, Gopinath* and Malaikannan*
* Saama AI lab, Chennai, India

Abstract. Machine learning models have shown a significant impact in modeling physical simulations. While machine learning has many benefits, one major drawback is the need for a large amount of data. We explore active learning as a remedy for addressing this issue. In our work, we studied the dynamics of two different dynamical systems, modeled their behavior using the Active Learning (AL)-enabled Gaussian Process (GP), and compared it with the vanilla GP. We demonstrate that AL-enabled GP shows superior performance with a lesser number of data points. AL can query for salient samples given a larger dataset to achieve orders of magnitude better Mean Square Error (MSE). In particular, for some instances, we were able to cut down the required samples by $\frac{1}{3}^{rd}$ and reduce the error rate by more than 10 orders of magnitude.

Introduction

Scientific Computing has begun adopting data-driven techniques such as Probabilistic Machine learning, Deep Learning, and more to accurately model physical phenomena using dispersed, noisy observations from coarse-grained grid-based simulations. In particular, Machine Learning models based on neural networks are data-hungry, and their performance is directly affected by the quality and quantity of the data. Moreover, the supervised machine learning models demand labeled data, which for scientific experiments, is expensive to gather in large quantities. This issue can be tackled using Active Learning, a special case of supervised learning. In this work, we used Active Learning to train the Gaussian Process to model different Nonlinear Dynamical systems, namely, Nonlinear Schrödinger (NLS) equation and Gross-Pitaevskii equation (GPE).

Method

Active Learning is selecting data in an iterative fashion to improve model performance by maximizing information acquisition with limited training samples. AL adds a certain cleverness on which samples to choose to improve the model's accuracy. In this method, the model is initially trained with a small subset of the data, and then a query strategy is used to acquire more useful samples from the dataset. Our work aims to sample more points in the steep regions and fewer points in the smooth regions i.e to bring good fitting in the entire parameter space of the wave function. The query strategy searches for the samples using their confidence of the model for the samples, i.e samples with the highest variance are selected for training the Gaussian Process [1] in the next iteration.

Following our earlier work [2], we have experimented with modeling the ground state wave function of One and Two Component GPE for using an active learning framework. We train Gaussian Process (GP) models with and without Active learning method enabled. We use modAL python package for running the experiments. We compare GP without Active learning (GP) and GP with Active Learning enabled (GP_AL) based two metrics, **(i) Number of samples required to achieve same error rate and (ii) Error rate for same number of samples.** For GP, we use 500 samples for training, whereas for GP_AL, we start the training with 50 samples and let the query strategy figure out the next samples. We let the training proceed until the error rate of GP_AL reaches up to GP for a fair comparison. We also compare GP_AL and GP by letting GP_AL consume the same number of samples as GP and compare the error rate of both. We observe a multi-fold decrease in the error rate of GP with active learning enabled for the same number of samples. To pronounce the versatility of our work, we experimented with the same setting for the case of NLSE, and it reduced the data requirement by 10% of the original data.

Conclusion

In this work, we propose a novel approach to exploit the Active Learning framework for training machine learning models like GP for modeling dynamical systems. We compared models trained with and without Active Learning. We observed that the Active Learning method could successfully query for salient samples to achieve the same error rate with a far smaller subset of the data. When feature space is complex, Active Learning achieves orders of magnitude better error rate for the same amount of data. Future direction will explore how to incorporate the Active Learning method into the data generation and gathering process for Physical Simulations.

References

- [1] MacKay, D. The humble gaussian distribution (2006). <https://www.seas.harvard.edu/courses/cs281/papers/mackay-2006.pdf>
- [2] Bakthavatchalam, T. A., Ramamoorthy, S., Sankarasubbu, M., Ramaswamy, R., & Sethuraman, V. (2021). Bayesian Optimization of Bose-Einstein Condensates. Scientific Reports, 11(1), 1-9. <https://doi.org/10.1038/s41598-021-84336-0>

Experimental Analysis of a Nonlinear Piecewise Multi-Degrees of Freedom System

Cristiano Martinelli*, Andrea Coraddu** and Andrea Cammarano[†]

* Department of Naval Architecture, Ocean & Marine Engineering, University of Strathclyde, U.K.

** Department of Maritime and Transport Technology, Delft University of Technology, The Netherlands

[†] James Watt School of Engineering, University of Glasgow, U.K.

Abstract. The growing industrial demand for lightweight and low-carbon emission systems is eroding the safety factors adopted in the linear design of vehicles and structures. This exposes the ultimately nonlinear nature of mechanical systems, creating the need for a better understanding of their nonlinear behaviour. In this context, we have experimentally investigated the dynamic behaviour of a nonlinear two-degree-of-freedom mechanical system with piecewise stiffness characteristics. The system is clamped at both ends and one constraint is directly excited by a shaker. The system allows the adjustment of non-contact gaps and stiffness of the piecewise characteristic and provides a valuable resource for the validation and verification of numerical studies in this field. The experimental results show the very rich dynamics of the system, revealing the presence of quasi-periodic, chaos, and multi-periodic responses as well as branches of bifurcating stable solutions.

Introduction

The need for high-performance and lightweight mechanical structures is revealing the intrinsic nonlinear nature of mechanical systems [1, 2, 3]. Between them, piecewise-smooth dynamical systems represent a particular class of systems which find practical applications in the study of mechanical oscillators and aeroelastic systems with free-play gaps, linear-capsule and impact drilling systems, the description of aerodynamics forces, foldable wings for low carbon emission aircraft, mechanical gear systems, non-linear energy harvesters, and non-linear vibration suppression systems. Nevertheless, in the literature, only a few experimental studies account for nonlinear Multi-Degrees of Freedom (MDOF) mechanical systems with piecewise characteristics, and most of them are dedicated to structures with free ends, like nonlinear energy sinks [4]. Moreover, the large majority of these studies provide only a limited amount of data, generally referring only to a single feature, e.g. a single orbit, and neglecting the rich dynamics content of these systems. Thus, in this paper, we propose a detailed experimental analysis of the dynamics of a nonlinear MDOF piecewise system, focusing attention on the nonlinear transfer functions and system attractors.

Results and discussion

The experimental test rig is constituted of masses, supports, and stoppers with adjustable positions, and the analysis is carried out at different excitation amplitudes and frequencies to highlight the details of its dynamics. The experimental results show the presence of quasi-periodic, chaotic, and multi-period responses which can co-exist at the same excitation frequency, as shown in Figure 1.

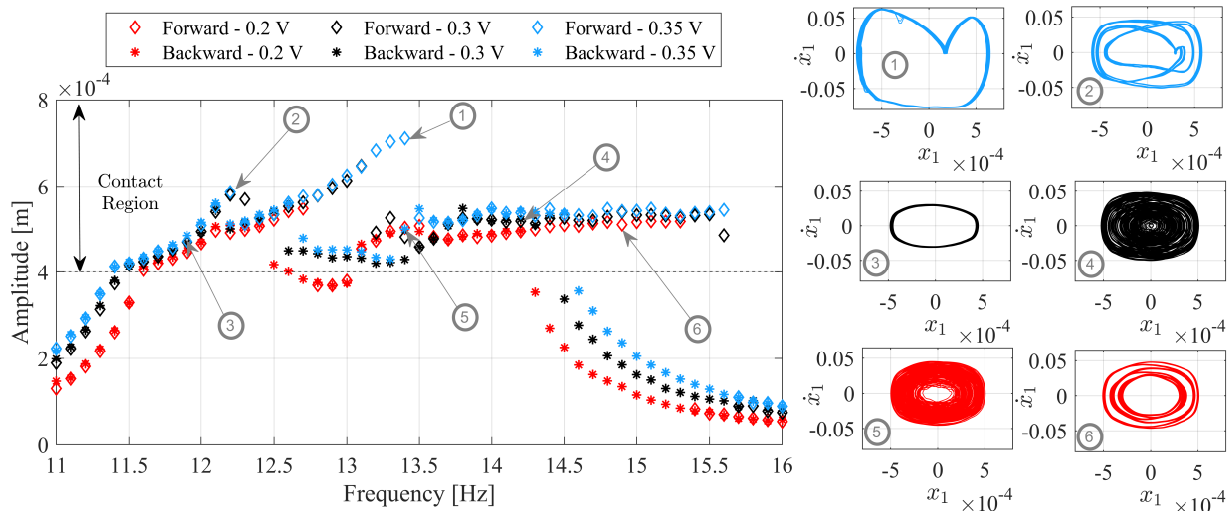


Figure 1: Experimental nonlinear transfer functions between the input sinusoidal voltage applied on the shaker and the impacting mass displacement for forward/backward frequency sweeps (left) and some associated orbits (right).

References

- [1] Wagg D., Neild S. (2015), *Nonlinear Vibration with Control*, Springer Cham, Switzerland.
- [2] Noël J. P., Kerschen G. (2017) Nonlinear system identification in structural dynamics: 10 more years of progress. *Mech. Systems and Signal Proc.* **83**: 2-35.
- [3] Kerschen G., Worden K. , Vakakis A., Golinval J.C. (2006) Past, present and future of nonlinear system identification in structural dynamics. *Mech. Systems and Signal Proc.* **20** : 505-592.
- [4] Geng X.F., Ding H. (2022) Two-modal resonance control with an encapsulated nonlinear energy sink. *J. Sound Vib.* **520**: 116667.

Higher order transverse discontinuity mapping for hybrid dynamical systems

Rohit Chawla, Aasifa Rounak and Vikram Pakrashi

UCD Centre for Mechanics, Dynamical Systems and Risk Laboratory, School of Mechanical and Materials Engineering, University College Dublin, Dublin, Ireland.

SFI MaREI Centre, UCD Energy Institute, University College Dublin, Dublin, Ireland.

Abstract. This work presents a higher order correction to the transverse discontinuity mapping(TDM) for accurate prediction of trajectories for piecewise-smooth(PWS) hybrid systems where degree of smoothness(DoS) is zero. To demonstrate this, a PWS system representing the simplest case of fluid-structure interaction(FSI) where the structure undergoes vortex induced vibrations(VIV) in a uniform flow is studied. Nonsmoothness manifests when a barrier is encountered obstructing the structure's motion. Investigation of this PWS FSI system show discontinuity induced bifurcations(DIBs) and chaos. The derived higher order TDM is implemented to perform a stability analysis and corresponds well with the bifurcation results. A comparison of the higher order corrections with the first order TDM shows significant improvements. The necessity of a higher order TDM to accurately predict the outcomes of a PWS impacting system is highlighted.

Introduction

PWS systems exhibit behaviours like DIBs (grazing, sliding, chattering), period adding cascades, coexistence of multiple attractors, quasi-periodicity and chaos [1]. To estimate stability of the linearized states, the behaviour of infinitesimally perturbed trajectories, during a border collision, is examined. Two nearby trajectories interact with the barrier at different instants of time, δ_i s. With the predicted flight times, the perturbed paths are mapped using TDM; only valid for transversal interactions with the boundary. Therefore, it is essential to accurately predict δ_i s, since the TDM is a function of δ_i s and the separation between the trajectories. In general for impacting systems, the $\mathcal{O}(1)$ terms of $\delta(t)$ are not a function of the system parameters. Thus, neglecting higher order terms causes incorrect prediction of the dynamics. Moreover, for some parameters showing chaotic trajectories, the perturbed paths exponentially diverge as the system evolves. For such cases, the $\mathcal{O}(1)$ terms of δ_i s might lead to inaccurate estimates of the state. Here, the time difference, δ_i s and subsequently the TDM for the PWS FSI system are derived while retaining the $\mathcal{O}(2)$ terms. To demonstrate the applicability, a 4-D FSI system comprising of a structural (harmonic) oscillator ($y(t)$), undergoing VIV transverse to the cross-flow, is assessed [2]. Here, the lift force is modelled as a Van der Pol oscillator. Non-smoothness is introduced by placing a barrier in the vicinity of the structure. The structure, upon interaction with the barrier, undergoes an instantaneous reversal of velocity defined by a restitutive law with coefficient of restitution $r = 0.8$.

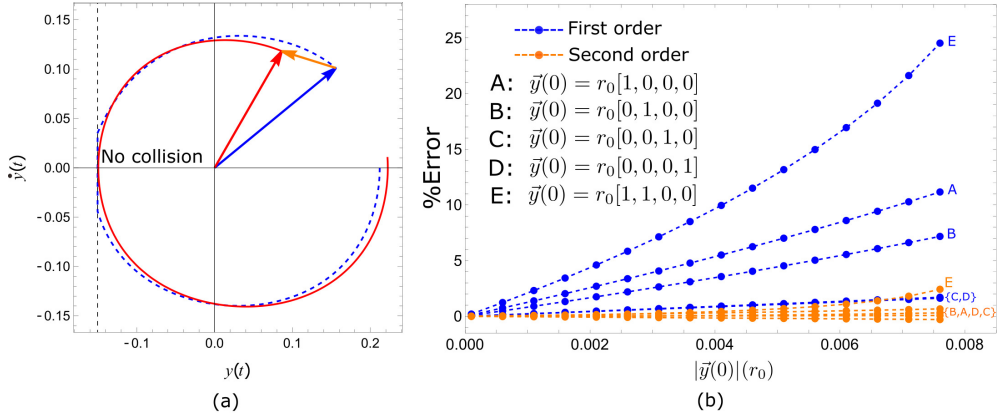


Figure 1: (a) Perturbed trajectory (in red) with initial norm of 0.01 units showing no border collision (b) % Error in δ using $\mathcal{O}(1)$ and $\mathcal{O}(2)$ with initial perturbations \tilde{y} lying on 4-D hyper-sphere labelled A to E normalized as r_0 , shown in x axis.

Results and discussions

A comparison of % error in δ_i s using $\mathcal{O}(2)$ [3] over $\mathcal{O}(1)$ reveals a significant improvement, see Fig. 1(b). The $\mathcal{O}(2)$ terms of δ_i s and TDM indicate that some trajectories might miss the discontinuity boundary, see Fig. 1(a). This is contradictory to the predictions using $\mathcal{O}(1)$ and the saltation matrix, which states that an impact will occur, that leads to an incorrect prediction of the perturbed trajectories. Direct numerical simulations reveal that the $\mathcal{O}(2)$ accurately predicts the behaviour of these trajectories near the border.

References

- [1] Bernardo, M., Budd, C., Champneys, A.R. and Kowalczyk, P., (2008) Piecewise-smooth dynamical systems: theory and applications. *Springer Science & Business Media*, (Vol. 163).
- [2] Facchinetti, M.L., De Langre, E. and Biolley, F., (2004) Coupling of structure and wake oscillators in vortex-induced vibrations. *Journal of Fluids and structures*, **19**(2), pp.123-140.
- [3] Chawla, R., Rounak, A. and Pakrashi, V., (2022) Stability analysis of hybrid systems with higher order transverse discontinuity mapping. *arXiv preprint arXiv:2203.13222*.

Energy transfer and dissipation in frictional systems with multiple contact interfaces

Cui Chao*, Jian Yang* and Marian Wiercigroch**

*Faculty of Science and Engineering, University of Nottingham Ningbo China, Ningbo 315100, PR China

**Centre for Applied Dynamics Research, University of Aberdeen, Aberdeen AB24 3UE, Scotland, UK

Abstract. The vibration energy transmission and dissipation characteristics of a system with multiple frictional contacts modelled by Coulomb friction are investigated. The internal vibration transmission between masses and energy dissipation is studied quantitatively using the power flow analysis approach. The harmonic balance (HB) method with alternating frequency time (AFT) scheme and direct numerical integrations are used to obtain the dynamic responses and power flow variables. Results show that the level of vibrational dissipation within frictional system depends substantially on the interfacial contact properties and thus is tailorable by changing friction coefficients. Complex nonlinear dynamic phenomena of the system arising from frictional contacts are revealed and the primary energy dissipation source of the frictional system is identified. The findings are expected to some insights into the vibration suppression design for frictional systems.

Introduction

An in-depth understanding of effects of the friction on vibrating systems is vital to achieve designs of superior dynamic performance. The strong non-smooth nonlinearity resulted from the contact frictional interface brings about challenges in the design and analysis of frictional structures. While work has been reported from the complex dynamic responses, such as stick-slip responses, associated with frictional systems, more work is needed to achieve enhanced dynamic design in terms of vibration suppression performance. The vibration power flow analysis approach offers a promising tool to reveal new nonlinear phenomena of systems with friction by taking a new viewpoint of vibration energy transfer and dissipation [1]. In this paper, a system with multiple frictional contacts as shown in Fig. 1(a) is studied taking into consideration of various frictional contact roughness. The vibration power flow analysis based on HB-AFT is carried out, with the time-averaged energy transfer between subsystems and dissipation at the contacts defined and evaluated.

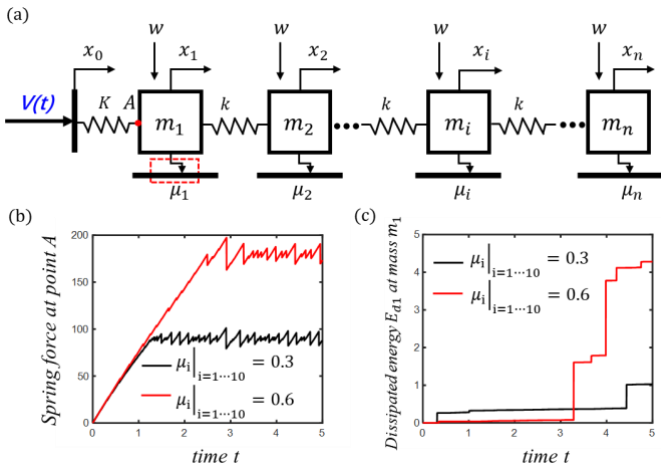


Figure 1: (a) 10-DOF system with various friction contact between masses and the ground; (b) time histories of spring force at point A (i.e., the tangential force); (c) accumulated dissipated energy by friction at m_1 .

Results and discussion

Figure 1(a) shows a 10-DOF system with prescribed velocity $v(t)$ at its left-hand-side end and parameters set as stiffness $K = 0.8$ MN/m, normal force $w = 30$ N, $m_i|_{i=1 \dots 10} = 1.2$ g, and $k = 25$ MN/m. For Fig. 1(b) and (c), v is set constant at 0.1 mm/s while other values can also be considered. The time histories of the spring force at point A, namely the tangential load, are obtained and shown in Fig. 1(b). The accumulated energy dissipation by friction at the interface of m_1 is depicted in Fig. 1(c). By varying the friction coefficient μ_i , it is evident that both the maximum spring force at point A (i.e., the tangential load) and the accumulated dissipated energy by the friction at m_1 can be modified. The results show that the dynamic response, energy dissipation and transfer can be achieved by tailor-designing the frictional contacts.

Reference

[1] Dai W., Yang J., & Wiercigroch M. (2022) Vibration energy flow transmission in systems with Coulomb friction. *Int. J Mech Sci*, **214**:106932.

Optimal projection in a Koopman-based sorting-free Hill method

Fabia Bayer, Remco I. Leine

Institute for Nonlinear Mechanics, University of Stuttgart, Germany
ORCID 0000-0002-2038-3374 and ORCID 0000-0001-9859-7519

Abstract. In this work, the performance of a novel method to determine the stability of periodic solutions based on the Hill matrix is examined. Using the Koopman framework, the linear time-periodic perturbed dynamics around a periodic solution can be approximated by a linear autonomous system of higher order, whose system matrix is the well-known Hill matrix. The monodromy matrix can hence be approximated by the Hill matrix, using only a matrix exponential and a projection. This projection is not uniquely determined, and various ways to obtain a suitable projection are discussed in this paper. The numerical efficiency of the novel method is illustrated for the vertically excited multiple pendulum.

Introduction

The numerical characterization of periodic solutions and their stability in nonlinear systems is a task of great interest in engineering application. One common approach to find these periodic solutions is the Harmonic Balance method (HBM). The HBM itself does not give stability information, however the Hill matrix \mathbf{H} can be found and constructed easily. As its eigenvalues approximate the Floquet exponents, this can be used as a stability criterion. However, in a so-called *sorting* process, only a nontrivial subset of these eigenvalues must be considered for correct assertion of stability. This is an ongoing area of research [1, 2].

Recently, the authors proposed a Koopman-based stability method [3]. For the perturbed dynamics \mathbf{y} , the dynamics of the Koopman basis $\Psi(\mathbf{y}, t) = [N_{\mathbf{u}}i\omega t, \dots, -N_{\mathbf{u}}i\omega t]^T \otimes \mathbf{y}$ are approximated by

$$\dot{\Psi} \approx \dot{\mathbf{z}} = \mathbf{H}\mathbf{z}$$

$$\mathbf{y}(t) = \mathbf{C}(t)\Psi(t) \approx \mathbf{C}(t)\mathbf{z}(t) = \mathbf{C}(t)e^{\mathbf{H}t}\mathbf{W}\mathbf{y}_0,$$

yielding $\mathbf{C}(T)e^{\mathbf{H}T}\mathbf{W}$ as an approximation of the monodromy matrix Φ_T . Its n eigenvalues, the Floquet multipliers, carry the stability information. The projection \mathbf{C} from the linear autonomous Koopman lift to the monodromy matrix is not unique and influences the accuracy of the determined Floquet multipliers.

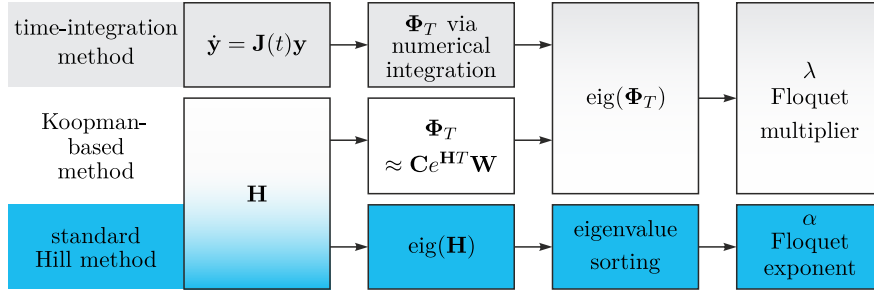


Figure 1: Flowchart comparing the three general stability approaches for periodic solutions.



Results and discussion

Application of the above method to a vertically excited multiple pendulum as a generalization of the Mathieu equation shows that the choice of the projection matrix \mathbf{C} in the presented method greatly influences accuracy and convergence speed. If \mathbf{C} is chosen to be constant and picking the middle rows of Ψ , convergence to the correct Floquet multipliers is observed. The convergence rate can, however, be improved by other choices. In particular, evaluation of the approximated perturbed dynamics over one period using an integral or a low number of time samples yields a projection matrix that improves this convergence rate. However, both these techniques can exhibit numerical issues. If the maximum considered frequency $N_{\mathbf{u}}$ is large, the quadratic program needed for the integral approach tends to stall due to a numerically semidefinite or even indefinite cost matrix. Numerical rank loss can also occur while solving a linear equation system of time samples, again preventing the ideal \mathbf{C} from being found. However, this rank loss can be circumvented by using more or differently spaced time instants. For the multiple pendulum, structure in these optimal solutions can be used to explicitly specify a \mathbf{C} matrix for larger but similar systems, circumventing these numerical problems.

References

- [1] Zhou J., Hagiwara T., Araki, M. (2004) Spectral characteristics and eigenvalues computation of the harmonic state operators in continuous-time periodic systems. *Systems & Control Letters* **53**(2): 141–155
- [2] Lazarus, A., Thomas, O. (2010) A harmonic-based method for computing the stability of periodic solutions of dynamical systems. *Comptes Rendus Mécanique* **338**(9): 510–517
- [3] Bayer, F., Leine, R.I. (2022) Sorting-free Hill-based stability analysis of periodic solutions through Koopman analysis. *Research-Square [Preprint]*, submitted to *Nonlinear Dynamics*, <https://www.researchsquare.com/article/rs-2183060/v1>

An Equality-Based Formulation for Vibrating Systems with Two-Dimensional Friction

 Mathias Legrand* and  Christophe Pierre**

*Department of Mechanical Engineering, McGill University, Québec, Canada

**Department of Mechanical Engineering, Stevens Institute of Technology, New Jersey, USA

Abstract. A new compact and efficient formulation is presented for the construction of periodic solutions of vibrating systems with two-dimensional dry friction occurrences. Rather than relying on penalization or regularization, the approach is based on an exact formulation of the non-smooth governing equations as equalities, and periodic solutions are sought in a weighted residual sense via a Ritz-Galerkin projection. To increase efficiency, the Jacobian of the friction forces is calculated in a piecewise linear fashion. The implementation is straightforward, as it relies on basic integral quadrature schemes and existing nonlinear solvers, and does not suffer from typical limitations or hypotheses. The theory is applied to a system with two-dimensional friction contact, demonstrating its simplicity and effectiveness.

Introduction

Non-smooth nonlinearities due to unilateral contact and dry friction are ubiquitous in structural engineering systems. Turbomachinery rotors are a prime example of industrial systems that are subject to intermittent contact and feature dry friction dampers to mitigate adverse vibrations. While predicting the dynamic response of non-smooth systems is of great importance and has been the subject of much research over the years, their equations of motion can be remarkably challenging to solve, because Signorini unilateral contact and Coulomb friction conditions are inequalities. Existing methods commonly rely on the penalization of the friction force by introducing a finite stiffness or on the smoothing of the contact force [1]. Frequency-domain formulations require the calculation of the contact conditions in the time domain at each iteration of the nonlinear solver via an FFT [2], while time-domain methods mandate advanced time-stepping or event-driven schemes [3].

Results and discussion

Here the fundamental approach introduced in [4] is extended to systems with two-dimensional frictional occurrences. The key idea is to express the equations governing the non-smooth friction terms as *equalities* rather than inequalities. This enables the construction of periodic solutions in a weighted residual sense, by (i) expanding all unknowns of the problem in terms of an appropriate truncated basis of periodic functions (here the Fourier basis), (ii) projecting the equations of motion, which feature only equalities, onto the Fourier basis functions, and (iii) solving iteratively the resulting system of time-independent nonlinear equations.

The integrals generated by the projection procedure are computed numerically using a classical quadrature scheme such as a Riemann sum, and the resulting nonlinear equations are solved using a non-smooth Newton or hybrid Powell solver. A key advantage is that no penalization or regularization hypothesis is made. Also, there is no need for an FFT-based alternating frequency-time procedure to calculate the Coulomb conditions in the time domain [1] or for artificially introducing dissipation to construct the periodic solutions [2]. A typical periodic response at the friction point is depicted in Figure 1, which shows that the sticking and slipping phases of the motion are captured.

Two major advances are presented. First, the Jacobian is expressed in an exact, piecewise linear fashion instead of being computed numerically in the nonlinear solver, making computations significantly more efficient and accelerating convergence. Second, the formulation is applied to a two-dimensional frictional surface, as opposed to a line. Friction conditions are written as two coupled equalities (as opposed to a single equality for a contact line), which are solved for in a weak sense using the Ritz-Galerkin projection. Results show that the formulation is remarkably simpler and more powerful than existing methods. In particular, the direction of sliding motion on the contact surface becomes an unknown of the problem, alleviating the need for cumbersome hypotheses and procedures required by current methods regarding the sliding direction.

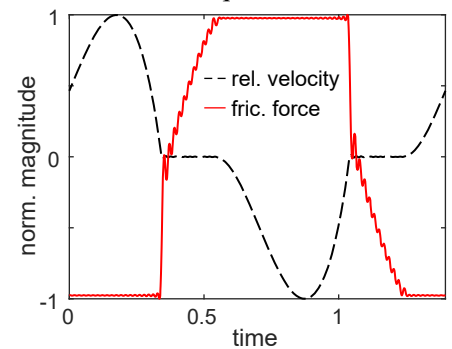


Figure 1: Periodic solution with sticking (velocity = 0) and slipping (force = ± 1).

References

- [1] Cameron T.M., Griffin J.H. (1989) An Alternating Frequency/Time Domain Method for Calculating the Steady-State Response of Nonlinear Dynamic Systems. *J. Appl. Mech.* **56**(1):149-154.
- [2] Nacivet S., Pierre C., Thouverez F., Jézéquel L. (2003) A Dynamic Lagrangian Frequency-Time Method for the Vibration of Dry-Friction-Damped Systems. *J. Sound Vib.* **265**:201-219.
- [3] Acary V., Brogliato B. (2008) Numerical Methods for Nonsmooth Dynamical Systems: Applications in Mechanics and Electronics. Springer, Berlin.
- [4] Legrand M., Pierre C. (2022) Compact Weighted Residual Formulation for Periodic Solutions of Systems Undergoing Unilateral Contact and Frictional Occurrences. 10th European Nonlinear Dynamics Conference, Lyon, 17-22 July 2022.

Allen–Cahn equation for multi-component crystal growth

Yunho Kim* and Dongsun Lee **

*Department of Mathematical Sciences, Ulsan National Institute of Science and Technology, Ulsan, South Korea,
ORCID # 0000-0003-2679-0090

**Department of Mathematical Education, Incheon National University, Incheon, South Korea,
ORCID # 0000-0003-2367-0659

Abstract. We propose a multi-component Allen–Cahn equation for crystal growth. There are quite a few models for crystal growth in the literature. In particular, there are phase-field models inspired by the Allen–Cahn equation for a single crystal. We would like to extend such phase-field models for single crystals to multiple crystals. Under the k -fold symmetry, growth of multiple crystals is well modeled and simulated by our method. In particular, the merging phenomenon of nearby crystals is captured in our simulations.

Introduction

The Allen–Cahn equation introduced by Allen and Cahn [1],

$$u_t = \epsilon \Delta u + \frac{1}{\epsilon} W'(u),$$

is a well-known phase separation model with a double well potential $W(u) := \frac{(1-u^2)^2}{4}$. This is also interpreted as a gradient flow of the Ginzburg–Landau energy functional $E(u) := \frac{\epsilon}{2} \int_{\Omega} |\nabla u(\mathbf{x})|^2 d\mathbf{x} + \frac{1}{\epsilon} \int_{\Omega} W(u(\mathbf{x})) d\mathbf{x}$. When modeling multiple components, we use a phase variable $\phi = \phi_A + \phi_B$. Under the k -fold symmetry, we use the k -fold symmetric interfacial energy $\epsilon(\phi) = \epsilon_0(1 + \epsilon_k \cos(k\phi))$.

Results and Discussion

The model we propose is

$$\begin{aligned} \epsilon^2(\phi) \frac{\partial \phi}{\partial t} &= \nabla \cdot (\epsilon^2(\phi) \nabla \phi) - \left[\frac{2\phi - 1}{2} + \lambda u \frac{\phi(\phi - 1)}{4} \right] \phi(\phi - 1) + \text{div}(F(\phi)) + \beta(\phi), \\ \frac{\partial u}{\partial t} &= D \Delta u + \frac{1}{2} \frac{\partial \phi}{\partial t}, \end{aligned}$$

where $F(\phi) = \left(|\nabla \phi|^2 \epsilon(\phi) \frac{\partial \epsilon(\phi)}{\partial \phi_x}, |\nabla \phi|^2 \epsilon(\phi) \frac{\partial \epsilon(\phi)}{\partial \phi_y} \right)$ and $\beta(\phi)$ is defined by

$$\begin{aligned} \beta(\phi) &:= -\frac{1}{2} \left[2\epsilon(\phi_A) \nabla \epsilon(\phi_A) \cdot \nabla \phi_A - W'(\phi_A) - 4\lambda u W(\phi_A) + \text{div}(F(\phi_A)) \right. \\ &\quad \left. + 2\epsilon(\phi_B) \nabla \epsilon(\phi_B) \cdot \nabla \phi_B - W'(\phi_B) - 4\lambda u W(\phi_B) + \text{div}(F(\phi_B)) \right]. \end{aligned}$$

Below are two simulation results. Unlike other models, our phase-field model can simulate the merging phenomenon of nearby crystals.



(a) Left: ϕ_A , Middle: ϕ_B , Right: $\phi = \phi_A + \phi_B$

(b) Crowded crystals with three phases

Figure 1: (a) 6-fold case, (b) 8-fold case

We will also present more numerical simulations and discuss comparison results.

References

- [1] Allen S.M., Cahn J.W. (1979) A microscopic theory for antiphase boundary motion and its application to antiphase domain coarsening. *Acta Metall* **27**:1085-1095.
- [2] S.M. Wise, C. Wang, J.S. Lowengrub, An energy-stable and convergent finite-difference scheme for the phase-field crystal equation, *SIAM J. Numer. Anal.* **47**(3) (2009) 2269–2288.
- [3] D.S. Lee, J.S. Kim, Comparison study of the conservative Allen–Cahn and the Cahn–Hilliard equations, *Math. Comput. Simulat.* **119**(6) (2016) 35–56.

Operator Splitting in the Finite Element Analysis of Fokker-Planck Equations

Hangyu Fu*, Lawrence A. Bergman**, D. Michael McFarland*, Xiangle Cheng*, and Huancai Lu*

*College of Mechanical Engineering, Zhejiang University of Technology, Hangzhou, China

**Aerospace Engineering Department, University of Illinois at Urbana-Champaign, Urbana, Illinois, USA

Abstract. The Fokker-Planck equation governing the probability density function (pdf) of a mechanical system can be readily discretized in state space using finite element analysis. However, even low-dimensional systems, such as a single-degree-of-freedom Duffing oscillator with two states, lead to matrix equations of large dimension, and these systems of equations grow rapidly as the number of states increases. If multiple parameter values or initial conditions are to be considered, computation of the nonstationary response by standard integration techniques rapidly becomes impractical. We examine here the use of operator splitting, where the finite element matrices are formulated separately for the convection and diffusion terms in the FP equation, leading to a time marching scheme based on the resulting state transition matrices. It is found that the pdf can be computed much more efficiently using this approach than with, for example, an adaptive Runge-Kutta algorithm.

Introduction

The nonstationary probability density function (pdf) of a mechanical system is governed by the Fokker-Planck (FP) equation, a partial differential equation (PDE) which is readily obtained from a state-variable representation of the original equation of motion. This PDE can be discretized in state space using, for example, a Galerkin finite element formulation, resulting in an equation of the form $\mathbf{M}\dot{\mathbf{p}}(t) + \mathbf{K}\mathbf{p}(t) = \mathbf{0}$, subject to the initial conditions $\mathbf{p}(0) = \mathbf{p}_0$. It is typically found that 100 elements are needed in each dimension of the state space to obtain a stable, accurate solution, resulting in approximately 10,000 degrees of freedom in the discrete problem. The problem size grows exponentially with the number of states in the system, and calculations for 2-degree-of-freedom (DOF) systems with four states (two displacements and two velocities) generally remain impractical in most applications (such as in design, where repeated solutions are required).

We have applied operator splitting to this problem by separating the convection and diffusion terms in the FP equation and discretizing them separately to produce two matrices, \mathbf{K}_1 and \mathbf{K}_2 , whose sum replaces \mathbf{K} in the equation above. These are found to be much better conditioned than the original matrix; as a result, a state transition matrix (STM) can be computed for each of them. These are used to advance the solution by fixed time steps, using either a composite STM or a more accurate (Strang splitting [1]) algorithm.

Results and discussion

Preliminary results obtained with this approach are very promising. As an example, we consider the single-DOF Duffing oscillator with negative linear stiffness studied by Spencer and Bergman [2]. Figure 1 compares a cross section of the stationary pdf to the exact solution, and shows the numerical solution for the pdf at a point computed with and without splitting. In this example, running on an x86 (notebook) processor, computation of the response for 4 linearized natural periods using an adaptive Runge-Kutta algorithm required 548.8 minutes; with operator splitting, this was reduced to 4.6 minutes.

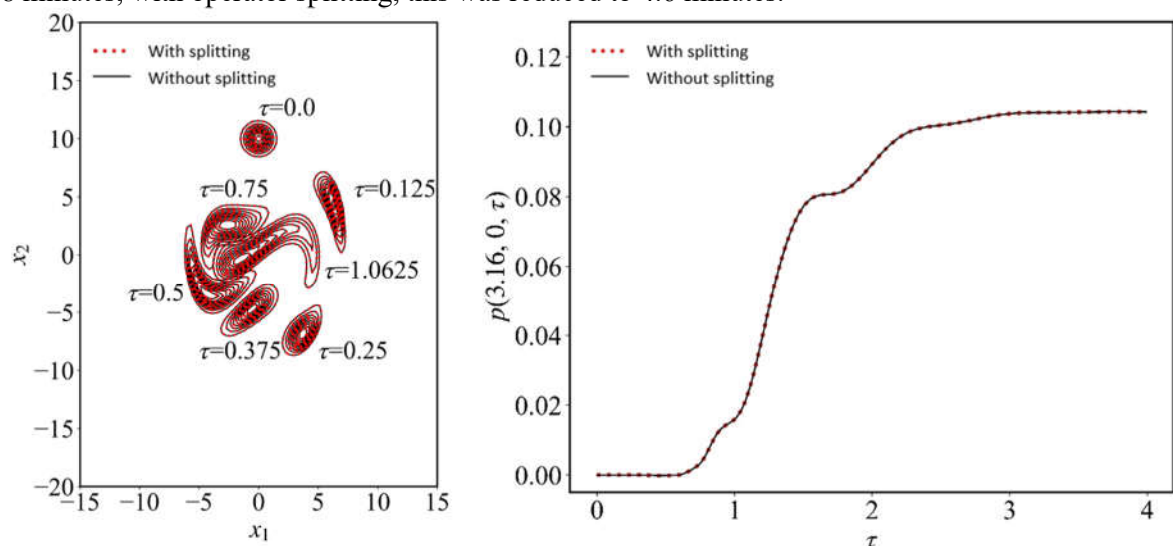


Figure 1: Results for the Duffing oscillator: (left) superimposed contour plots of the nonstationary pdf at selected times; (right) growth over time of the pdf at the location of a local maximum stationary value.

References

- [1] McLachlan R. I. and Quispel G. R. W. (2002) Splitting Methods. *Acta Numerica* **11**:341–434.
- [2] Spencer B. F. and Bergman L. A. (1993) On the Numerical Solution of the Fokker-Planck Equation for Nonlinear Stochastic Systems. *Nonlinear Dynamics* **4**(4):357–372.

Self-supervised contrastive learning for chaotic time-series classification

Salama Hassona* and Wieslaw Marszalek**

*Department of Computer Science, Opole University of Technology, Opole, Poland, ORCID 0000-0003-1074-5420

**Department of Computer Science, Opole University of Technology, Opole, Poland, ORCID 0000-0001-6087-0567

Abstract. We apply a self-supervised contrastive learning approach to reconstruct a two-parameter bifurcation diagrams of the chaotic nonlinear dynamical systems. By using only 1% of the dataset labels we can reconstruct the diagrams with the accuracy of about 92%. Furthermore, the method does not require a prior knowledge of the system or the labeling of the whole nonlinear time-series dataset, which makes it as useful as other statistical methods, for example, the surrogate data ones, 0-1 test for chaos, and others. We use the transformed Temporal and Contextual Contrasting (TS-TCC) framework and apply the residual components and scaling as our data augmentation techniques to train the TS-TCC framework. We test our approach against the regular TS-TCC model and the supervised approach, obtaining very promising results.

Introduction

It is often crucial to compute bifurcation diagrams in order to assess the stability and effects of multiple parameters on the overall dynamical properties of nonlinear systems. The case of one-parameter bifurcation diagrams is fairly easy to deal with, but it is more difficult (due to computational requirements) to do so when two or more parameters change at once. Many studies have been published in recent years suggesting employing various machine learning techniques to handle such multi-parameter cases, for example, the Extreme Learning Machines, Time Series Forests with Entropy, LKCNN and LSTM networks, and others. Although those models perform well on the training datasets, they have two major drawbacks: firstly, they need a large amount of labeled data and, secondly, they tend to overfit while tested on the new datasets as shown in [1, 2]. These drawbacks lead us to **the main objective of this work**, which is improving the generalization abilities of the machine learning models in order to make them applicable in the real problems with decreased amount of the labeled data needed to achieve satisfactory results. We achieved that by applying the Temporal and Contextual Contrasting (TS-TCC) framework [3], using the residual components, and scaling as the data augmentation techniques to train the TS-TCC framework.

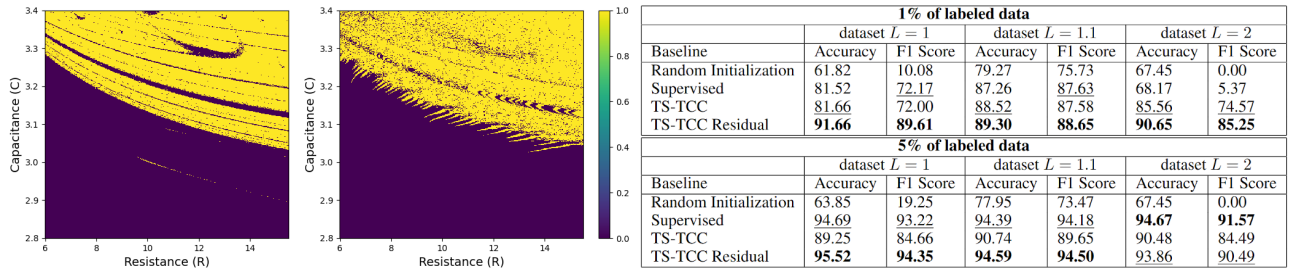


Figure 1: From left: two-parameter bifurcation diagram generated using the method (similar to Poincaré section) described in [4]; reconstructed two-parameter bifurcation diagram with the TS-TCC Residual Framework using 1% of labeled data; tables with the results, using 1% and 5% of labeled data for three sets of $R \times C \times L$ parameters: (a) $(6, 15.5) \times (2.8, 3.4) \times 1$, (b) $(6, 15.5) \times (2.8, 3.4) \times 1.1$, and (c) $(20, 29.5) \times (2.2, 2.8) \times 2$. The best results are in bold, and the second best are underlined.

Results and discussion

The results of the TS-TCC and TS-TCC Residual frameworks are presented in Figure 1. We obtained very high-performance metrics for both TS-TCC networks trained on only 1% and 5% of labeled data for all three sets of parameters. The TS-TCC Residual achieved around 89–91% accuracy trained on 1% of labeled data, while the TS-TCC achieved accuracy between 81–88%. The results clearly show that training the TS-TCC framework on residual components for the nonlinear chaotic arc RLC circuit is much more stable and less impacted by the parameter changes. Similar conclusions can be made for the training on 5% of labeled data. The reconstructed diagram shown in Figure 1 gives fairly good approximation of the original diagram. We conclude that (1) the TS-TCC framework trained on the residual components of the considered signals achieves better accuracy than the original TS-TCC framework; (2) taking only a handful of labeled data, the self-supervised methods perform very well and are more useful than the supervised machine learning methods for oscillatory time-series classification; (3) by improving the accuracy of the TS-TCC framework, we can obtain the general method for multi-parameter bifurcation diagrams generation, that can compete with the currently used statistical methods.

References

- [1] Boullé N., Dallas V., Nakatsukasa Y., Samaddar D. (2020) *Physica D: Nonl. Phenomena*, 403:132261, doi:10.1016/j.physd.2019.132261.
- [2] Hassona S., Marszalek W., Sadecki J. (2021) *Applied Soft Computing*, 113, doi:10.1016/j.asoc.2021.107874.
- [3] Eldele E. et al. (2021) *Proc. Thirtieth Int. Joint Conf. on Artificial Intelligence*, 2352-2359, doi:10.24963/ijcai.2021/324.
- [4] Marszalek W., Sadecki J. (2019) *IEEE Trans. Circuits & Systems II: Exp. Briefs*, 66:687-691, doi:10.1109/TCSII.2018.2871063.

The Jerk Dynamics of Lorenz Model

Jean-Marc Ginoux¹, Riccardo Meucci², Jaume Llibre³ and Julien Clinton Sprott⁴

¹Aix Marseille Univ, Université de Toulon, CNRS, CPT, Marseille, France, ginoux@univ-tln.fr,

²National Institute of Optics - CNR, Florence, Italy,

³Departament de Matemàtiques, Universitat Autònoma de Barcelona, 08193 Bellaterra, Barcelona, Spain,

⁴University of Wisconsin 1150 University Avenue Madison, WI 53706-1390 USA.

Abstract. The Lorenz model is widely considered as the first dynamical system exhibiting a chaotic attractor the shape of which is the famous butterfly. This similarity led Lorenz to name the *sensitivity to initial conditions* inherent to such chaotic systems, the *butterfly effect* making its model a paradigm of chaos. Nearly thirty years ago, Stefan J. Linz presented in a very interesting paper an “exact transformation” enabling to obtain the jerk form of the Lorenz model and a nonlinear transformation “simplifying its jerky dynamics”. Unfortunately, the third order nonlinear differential equation he finally obtained precluded any mathematical analysis and made difficult numerical investigations since it contained exponential functions. In this work, we provide in the simplest way the jerk form of the Lorenz model. Then, a stability analysis of the jerk dynamics of Lorenz model prove that fixed points and their stability, eigenvalues, Lyapunov Characteristics Exponents and of course attractor shape are the exactly the same as those of Lorenz original model.

Introduction

At the very beginning of the sixties, Edward Norton Lorenz (1917-2008), a meteorologist from the famous M.I.T. (Massachusetts Institute of Technology) succeeded in establishing a model for atmospheric convection comprising only three variables. The solution of this weather forecasting model that Lorenz [4] plotted in a three-dimensional phase space is compelled to evolve on a chaotic attractor which resembles the wings of a butterfly. It is probably this form that prompted Lorenz to call the “sensitivity to initial conditions” (described by the French mathematician Henri Poincaré as early as 1908 in his philosophical writings *Science and Method* [5]) the “butterfly effect”. During these last two decades, the seminal works of Gottlieb [2] and Sprott [7, 8, 9, 10, 11, 12, 13] have triggered out an increasing interest in the study of chaotic oscillators based on jerk equations, that is, oscillators which can be completely described by third-order ordinary differential equations of the form $\ddot{x} = f(\ddot{x}, \dot{x}, x)$. In 1997, Stephan J. Linz [3] proposed in a very interesting paper an “exact transformation” enabling to obtain the jerk form of the Lorenz model and a nonlinear transformation “simplifying its jerky dynamics”. Unfortunately, the third order nonlinear differential equation he finally obtained precluded any mathematical analysis and made difficult numerical investigations since it contained exponential functions. Let’s notice that the jerk form in x of the Lorenz model that we will provide below is exactly the same as those obtained by Linz but presented in a different way. In 2014, Buscarino *et al.* [1] used *linear combinations* of the three nonlinear ordinary differential equations modeling the Chua’s circuit to deduce its jerk forms in x and z . Recently, Xu and Cao [14] proposed to use the so-called *controllable canonical form* to provide all the jerk forms dynamics of Chua’s circuit. In this paper, following the method of *linear combinations* proposed by Buscarino *et al.* [1], we provide the jerk form in x of Lorenz model. Thus, by making a comparison of fixed points and their stability, eigenvalues, Lyapunov Characteristic Exponents and attractor shapes between the original three-order Lorenz model and its first jerk form in x we demonstrate the topological equivalence of both systems.

References

- [1] Buscarino, A., Fortuna, L. and Frasca, M. (2014) The Jerk Dynamics of Chua’s Circuit, *Int. J. Bifurcation Chaos*, 24(06), 1450085.
- [2] Gottlieb, H. P. W. (1996) Question 38. What is the simplest jerk function that gives chaos? *Amer. J. Phys.*, 64, 525.
- [3] Linz, S. J. (1997) Nonlinear dynamical models and jerky motion, *American Journal of Physics*, 65, 523-526
- [4] Lorenz, E. N. (1963) Deterministic Nonperiodic Flow, *Journal of Atmospheric Sciences*, 20(7), 130-141.
- [5] Poincaré, H. (1914) *Science and Method*, Thomas Nelson & Sons, London, Edinburgh, Dublin & New York (Translated from the first French edition: Science et Méthode, Ernest Flammarion, Paris, 1908).
- [6] Sprott, J. C. (1994) Some simple chaotic flows, *Phys. Rev. E* 50(2), R647-R650.
- [7] Sprott, J. C. (1997) Some simple chaotic jerk functions, *Am. J. Phys.* 65(6), 535-543.
- [8] Sprott, J. C. (2000a) A new class of chaotic circuits, *Phys. Lett. A*, 266, 19-23.
- [9] Sprott, J. C. (2000b) Simple chaotic systems and circuits, *Am. J. Phys.* 68(8), 758-763.
- [10] Sprott, J. C. (2003) *Chaos and Time-Series Analysis*, Oxford University Press.
- [11] Sprott, J. C. (2009) Simplifications of the Lorenz Attractor, *Nonlinear Dynamics, Psychology, and Life Sciences*, 13(3), 271-278.
- [12] Sprott, J. C. (2010) *Elegant Chaos: Algebraically Simple Chaotic Flows*, World Scientific, Singapore.
- [13] Sprott, J. C. (2011) A new chaotic jerk circuit, *IEEE Trans. Circ. Syst.-II: Exp. Briefs*, 58, 240-243.
- [14] Xu, W. and Cao, N. (2020) Jerk forms dynamics of a Chua’s family and their new unified circuit implementation, *IET Circuits Devices Syst.* 15, 755-771.

Spiral Bevel Gears nonlinear dynamics: chaotic response existence in multi degree of freedom systems

Moslem Molaie*, Farhad S. Samani**, Giovanni Iariccio*, Antonio Zippo*, Francesco Pellicano*

* Department of Engineering “Enzo Ferrari”, University of Modena and Reggio Emilia, Modena, Italy.

** Department of Mechanical Engineering, Shahid Bahonar University of Kerman, Kerman, Iran.

Abstract. The present study investigates the dynamic behavior of the spiral bevel gears (SBGs) by developing two degrees of freedom dynamic model (2 DOF) to four degrees of freedom (4 DOF) which involves the rotational shaft stiffness. The governing equations of motion are derived based on a nonlinear time-varying model. The nonlinearity and time dependency emanate from the backlash and contact ratio of the pinion and the gear, respectively. Depending on the working conditions, it could be happened that the system experience a backside contact which is an undesirable phenomenon in gear systems. A comparison between two systems, i.e., 2 DOF and 4 DOF, is done to understand what kind of phenomena are neglected by decreasing the DOF. The root mean square (RMS) diagrams and bifurcation diagrams are employed to analyze the vibration response of the system. The interesting point is that the simplification in dynamic model could lead to a different dynamic response respect to the reality.

Introduction

Bevel gears are using for the power transmission systems with limited space. Without bevel gears, the drive motors, gearboxes, and driven equipment may locate on the linear position, consequently the total space of the driving equipment is vast. For high-speed gearboxes using spiral bevel gears (SBGs) instead straight bevel gears is essential due to the high level of vibration magnitude. Bevel gears are applicable in different engineering fields, e.g., aerospace, terrestrial vehicles, and in heavy industries whenever it is required to transmit a high load between nonparallel shafts [1]. In Ref. [2], Samani et al. investigated nonlinear vibration of the SBG with a novel tooth surface modification. However, they showed that the considered higher-order transmission error method is not able to decrease the vibration level for the considered frequency ratios. The effectiveness of squeeze film dampers for passive vibration control of SBGs is evaluated by Chen et al., [3]. Figure 1 represented the dynamic model, which is used for simulation. The translational degrees of freedom for both, driver and driven gears are constrained in all directions as well as the rotations. the gears can only rotate around their axes. By considering the shaft rotational stiffness, the dynamic model becomes 4 DOF, i.e., two rotational DOF for the pinion and the gear, and two degrees of freedom for the load and the motor. The nonlinear differential equations with time-varying mesh stiffness are solved via numerical integration based on an adaptive step-size implicit Runge-Kutta scheme.

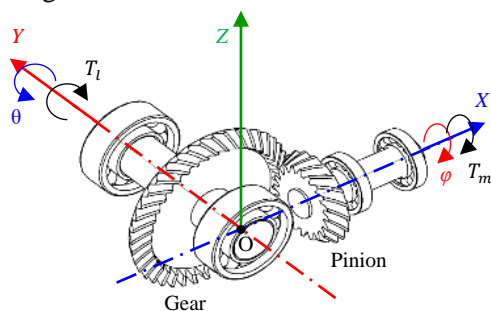


Figure 1: The dynamic model of a gear system with rotational degrees of freedom.

Results and discussion

The systems, regardless of the number of DOF experienced three types of contact: drive-side contact, separation tooth, and undesirable backside contact. By comparing the response of the dynamic models with 2-DOF and 4-DOF, the dynamic behavior of the system altered. The vibration amplitude, RMS, considering 2-DOF is higher than the system with 4-DOF at primary and super-harmonic frequency ratios. Besides, the maximum magnitude of vibration happens during backside contact. Vice versa, close to the primary resonance, the 4-DOF system represented chaotic response, while 2-DOF presents 4T harmonic response. At $\omega_m/\omega_n = 0.46$, the 2-DOF system presents chaotic response for a narrow range of frequency while it is eliminated in 4-DOF system.

References

- [1] Molaie, M., Samani, F.S., Zippo, A., Pellicano, F.: Spiral Bevel Gears: nonlinear dynamic model based on accurate static stiffness evaluation. *Journal of Sound and Vibration* 544, 117395 (2023).
- [2] Samani, F.S., Molaie, M., Pellicano, F.: Nonlinear vibration of the spiral bevel gear with a novel tooth surface modification method. *Meccanica* 54(7), 1071-1081 (2019).
- [3] Chen, W., Chen, S., Hu, Z., Tang, J., Li, H.: Dynamic analysis of a bevel gear system equipped with finite length squeeze film dampers for passive vibration control. *Mechanism and Machine Theory* 147, 103779 (2020).

Response statistics of a conceptual two-dimensional airfoil in hypersonic flows with random perturbations

Yong Xu^{*,**} and Weili Guo^{*}

^{*}School of Mathematics and Statistics, Northwestern Polytechnical University, Xi'an 710072, China

^{**}MIIT Key Laboratory of Dynamics and Control of Complex Systems, Northwestern Polytechnical University, Xi'an 710072, China

Abstract. We investigate a conceptual pitch-plunge airfoil in hypersonic flows, considering the effects of irregular fluctuations and external random load modeled as a Gaussian white noise. The dynamical responses of the airfoil model especially the bifurcation behaviors are studied via the harmonic balance method. Subsequently, the effects of stochasticity on the hypersonic airfoil system are explored in the regimes of subcritical and supercritical Hopf bifurcations depending on the system parameters. Several interesting phenomena, in particular, intermittency and stochastic transition between the low-amplitude oscillation state and the undesirable high-amplitude oscillation state are triggered under random perturbations. This work will provide new insights into the safety and reliability design of hypersonic aircraft.

Introduction

Hypersonic airfoils generally refer to the ones at Mach number greater than five and the aerodynamic loads are greater. The existence of nonlinearities makes the airfoil system undergo Hopf bifurcation [1,2]. Moreover, the flight environment of aircraft is quite complex, which contains many stochastic factors including irregular fluctuations and external random load [3-5]. However, there is less research on the stochastic dynamics of airfoil models in hypersonic flow. The influences of stochastic disturbance on the hypersonic airfoils are not sufficiently studied. We study the stochastic response of a conceptual two-dimensional airfoil excited by irregular fluctuations in the flow and external random load modeled as a Gaussian white noise.

Results and Discussion

The dimensionless coupled motion equations with the external random load are established as

$$\begin{aligned} \xi'' + x_\alpha \alpha'' + 2\zeta_\xi \frac{\varpi}{U} \xi' + \left(\frac{\varpi}{U}\right)^2 G(\xi) &= O_{EA}, \\ \frac{x_\alpha}{r_\alpha^2} \xi'' + \alpha'' + 2\zeta_\alpha \frac{1}{U} \alpha' + \frac{1}{U^2} M(\alpha) &= P_{EA} + \eta(t), \end{aligned}$$

in which ξ and α denotes the dimensionless plunge and pitch degrees of freedom, ϖ is the intrinsic frequency ratio, r_α is the radius of gyration about the elastic axis, ζ_ξ, ζ_α are the damping coefficients of the plunge and pitch degrees of freedom, and O_{EA}, P_{EA} are the dimensionless aerodynamical coefficients. The external random load $\eta(\tau)$ satisfies $E[\eta(t)] = 0, E[\eta(t)\eta(t+\tau)] = D\delta(\tau)$, where D is the noise intensity. The irregular fluctuations in the flow can be written as $U(t) = U_m + \phi(t)$, where U_m is the average flow velocity and $\phi(t)$ is the fluctuating component with zero mean. The obtained results are shown in Fig.1. Bistable behaviors are observed and the effects of the system parameters are discussed. Under the random loads, stochastic transitions

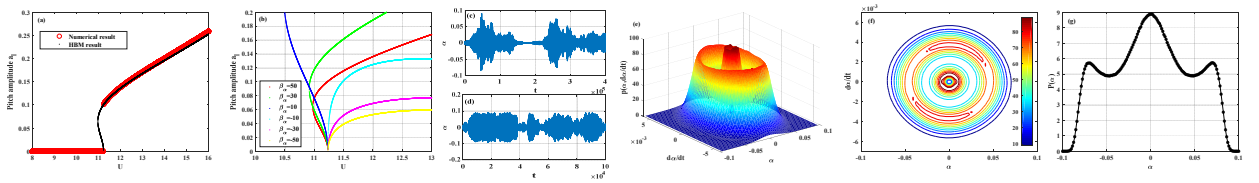


Figure 1: Response statistics of the conceptual airfoil systems. (a) Pitch amplitude versus the flow velocity U ; (b) The subcritical and supercritical region with different β_α ; (c) Time history of pitch motion in supercritical region with $U_m = 13.88$; (d) Time history of pitch motion in subcritical region with $D = 1 \times 10^{-10}$; (e,f) Steady-state joint probability density function and countours with $U_m = 13.95$; (g) Steady-state marginal probability density function with $D = 1 \times 10^{-10}$.

References

- [1] Liu Q., Xu Y., Li Y. G., Kurths J., Liu X. C. (2021) Fixed-interval smoothing of an aeroelastic airfoil model with cubic or free-play nonlinearity in incompressible flow. *Acta Mech. Sin* **37**:1168-1182.
- [2] Liu Q., Xu Y., Kurths J., Liu X. C. (2022) Complex nonlinear dynamics and vibration suppression of conceptual airfoil models: A state-of-the-art overview. *Chaos* **32**:062101.
- [3] Liu Q., Xu Y., Kurths J. (2020) Bistability and stochastic jumps in an airfoil system with viscoelastic material property and random fluctuations. *Commun. Nonlinear Sci. Numer. Simul* **84**:105184.
- [4] Ma J. Z., Liu Q., Xu Y., Kurths J. (2022) Early warning of noise-induced catastrophic high-amplitude oscillations in an airfoil model. *Chaos* **32**:033119.
- [5] Ma J. Z., Xu Y., Li Y. G., Tian R. L., Kurths J. (2019) Predicting noise-induced critical transitions in bistable systems. *Chaos* **29**:081102.

Computation of the Wright function from its integral representation

Dimitar Prodanov*

*EHS, IMEC, 3001 Leuven, Belgium (e-mail: dimitar.prodanov@imec.be)

MMSDP, ICT, Bulgarian Academy of Sciences, 1431 Sofia, Bulgaria, ORCID 0000-0001-8694-0535

Abstract. The contribution presents a novel computational technique for the Wright function using numerical quadratures.

Introduction

The Wright function, introduced by E.M. Wright, is a special mathematical function originally defined by the infinite series:

$$W(a, b|z) := \sum_{k=0}^{\infty} \frac{z^k}{k! \Gamma(ak + b)}, \quad z, b \in \mathbb{C}, \quad a > -1$$

The Wright function provides a unified treatment of several classes of special functions, notably the Bessel functions, the error function erf , the Airy function Ai , and the Whittaker function [1]. It is also related to the derivatives of the Gaussian $\exp(-x^2/2)$ and the Airy functions. The Wright function arises in the theory of the space-time fractional diffusion equation with the temporal Caputo derivative. Therefore, methods of its computation can be of general interest. Previous studies [2] treated only the case $|b| \leq 1$.

Results and Discussion

The present contribution removes this restriction and strives for full generality of the computational technique, which covers many applications, such as, for example, the computation of the Prabhakar and Mittag-Leffler functions. This is achieved by the use of the complex integral representation of the function along the Hankel contour encircling the negative real semi-axis:

$$W(a, b|z) = \frac{1}{2\pi i} \int_{Ha^-} \frac{e^{\xi+z\xi^{-a}}}{\xi^b} d\xi$$

using the method of stationary phase. The algorithm is implemented as a standalone library using the double-exponential (DE) quadrature integration technique [3] in the Java programming language and can be downloaded from <https://github.com/dprodanov/dspquad>. A reference Maxima implementation was developed both for QUADPACK [4] and for DE libraries. Function plots are presented in Fig. 1 (left – negative $|a| < 1$, right – $a = 1$).

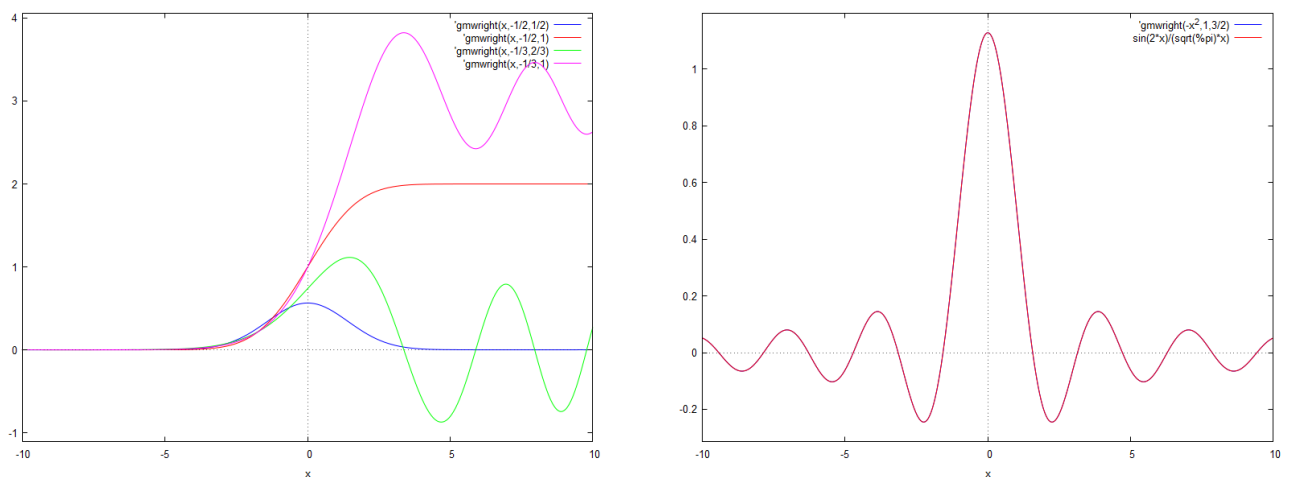


Figure 1: Wright function plots

References

- [1] Gorenflo, R., Luchko, Yu., Mainardi, F. (1999) Analytical properties and applications of the Wright function. *Fract. Calc. Appl. Anal.* 2(4), 383–414
- [2] Luchko, Y. (2008) Algorithms for evaluation of the Wright function for the real arguments' values, *Fract. Calc. Appl. Anal.*, 11, 57 – 75
- [3] Takahasi, H. and M. Mori (1974) Double exponential formulas for numerical integration, *Pub. RIMS Kyoto Univ.* 9, 721 – 741
- [4] Piessens, Robert; de Doncker-Kapenga, Elise; Überhuber, Christoph W.; Kahaner, David (1983). *QUADPACK: A subroutine package for automatic integration.* Springer-Verlag. ISBN 978-3-540-12553-2.

NASA DART Mission: a preliminary mathematical dynamical model and its nonlinear circuit emulation

Arturo Buscarino^{*,**}, Carlo Famoso^{*}, **Luigi Fortuna**^{*,**}, and Giuseppe La Spina^{*}

^{*}*Dipartimento di Ingegneria Elettrica Elettronica e Informatica, University of Catania, Italy*

^{**}*IASI, Consiglio Nazionale delle Ricerche (CNR), Roma, Italy*

Abstract. On the last September 22nd, 2022 a NASA Spacecraft try to deflect the orbit of the asteroid Dimorphos orbiting around Didymos. The orbit of Dimorphos had been shortned of about 32 minutes with respect to the original one. In this communication, it is proposed a simple mathematical model that allows to emulate the DART mission behavior.

Introduction

The problem is approached referring to the Kepler two-bodies problem. That leads to a set of six differential equations model in the state-space representation. The model is highly nonlinear and the condition that emulates the experiment is approached by varying the initial condition of the small mass asteroid during its dynamical behavior. The numerical problem has been approached both by using the Eulero methods and the classical 5th order Runge Kutta algorithm [1]. Moreover, it is in progress the realization of an analog electronic circuit emulator of the system that allows to realize faster and qualitative more efficient experiments.

Results and discussion

The obtained results derived by a trial and error procedure leading to suitable results compared with the experimental trajectory given from NASA [2].

The preliminary study is addressed to stimulate the interest of researchers in approaching the deflection of asteroids as a trajectory control problem and to work on the model of the coupled asteroids in order to have a reliable simulation platform also including hybrid configurations with both digital and analog computational units.

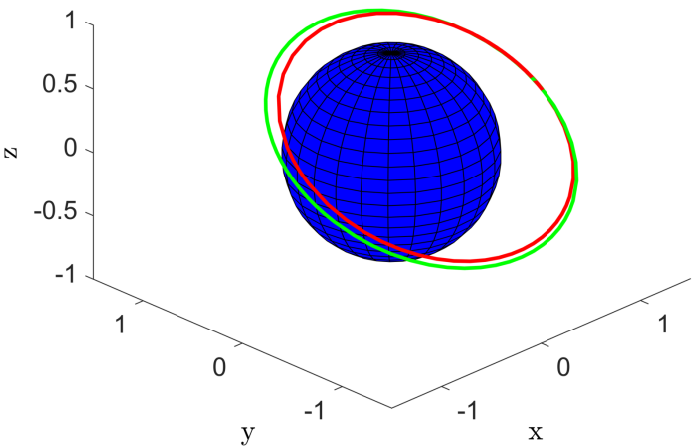


Figure 1: Experimental results of modeling DART mission: original trajectory (green curve), controlled trajectory (red curve).

References

[1] Curtis, H. (2013). Orbital mechanics for engineering students. Butterworth-Heinemann.
[2] <https://www.nasa.gov/press-release/nasa-confirms-dart-mission-impact-changed-asteroid-s-motion-in-space> (accessed on November 25th, 2022)

Physics-constrained Deep learning of nonlinear normal modes of spatiotemporal fluid flow dynamics

Abdolvahhab Rostamijavanani*, Shanwu Li* and Yongchao Yang*

*Department of Mechanical Engineering – Engineering Mechanics, Michigan Technological University, Houghton, MI, USA

Abstract. This study presents a physics-constrained deep learning method for identifying and visualizing the invariant nonlinear normal modes (NNMs), which contain the spatiotemporal dynamics of fluid flow potentially exhibiting strong nonlinearity. To develop the nonlinear modal transformation, NNM-CNN-AE integrates a multi-temporal-step dynamics prediction block with a convolutional autoencoder constrained by NNM physics (NNM-CNN-AE). In addition, we simultaneously learn the NNMs containing the spatiotemporal dynamics of the flow fields, reduced-order reconstruction and predict long-term flow fields.

Introduction

In this study, we present a physics-constrained deep learning method to discover and visualize from data the invariant nonlinear normal modes (NNMs) which contain the spatiotemporal dynamics of the fluid flow potentially containing strong nonlinearity. Specifically, we develop a NNM-physics-constrained convolutional autoencoder (NNM-CNN-AE) integrated with a multi-temporal-step dynamics prediction block to learn the nonlinear modal transformation, the NNMs containing the spatiotemporal dynamics of the flow, and reduced-order reconstruction and long-time future-state prediction of the flow fields, simultaneously. In test cases, we apply the developed method to analyze different flow regimes past a cylinder, including laminar flows with Low Reynolds Number (LRN) in transient and steady states ($R_D=100$) and High Reynolds Number (HRN) flow ($R_D=1000$), respectively. The results indicate that the identified NNMs are able to reveal the nonlinear spatiotemporal dynamics of these flows, and the NNMs-based reduced-order modeling consistently achieves better accuracy with orders of magnitudes smaller errors in construction and prediction of the nonlinear velocity and vorticity fields, compared to the linear proper orthogonal decomposition (POD) method and the Koopman-constrained-CNN-AE using the same number or dimension of modes. We perform an analysis of the modal energy distribution of NNMs and find that compared to POD modes, the few fundamental NNMs capture a very high level of total energy of the flow, which is advantageous for reduced-order modeling and representation of the complex flows.

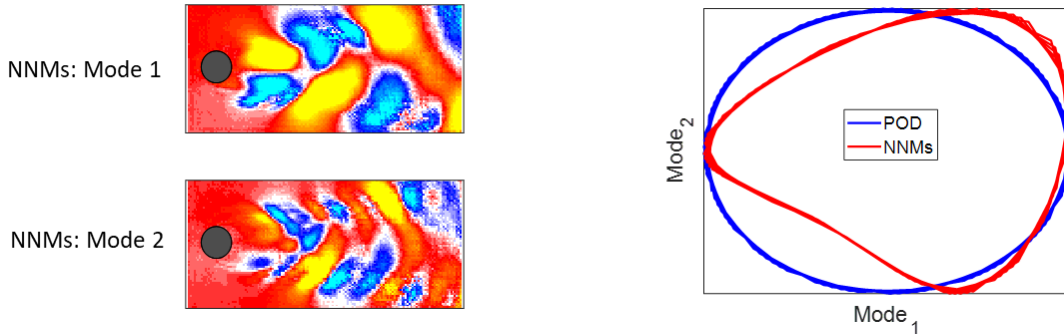


Figure 1: NNMs modes of streamwise velocity field over a cylinder and corresponding phase portraits of NNMs and POD modes

Results and discussion

Figure. 1 illustrates the identified NNMs spatial modes of a flow over a cylinder in laminar regime (streamwise velocity) and the phase portrait of NNMs modal coordinates and corresponding POD coordinates. The identified NNMs have distorted spatial patterns, capturing the nonlinear nature of the flow. This is also can be seen in the phase portrait of the trajectory of the first and second modes of POD and NNMs, where the NNMs curve is more distorted (nonlinear) while the trajectory plot of POD modes is circular. These results suggest the identified NNMs are able to reveal the nonlinear physics behind the flow in the laminar regime better compared to the linear method POD. These nonlinear spatiotemporal features captured by NNMs are also beneficial to the reduced-order reconstruction and prediction of the flow field potentially containing nonlinearity.

References

- [1] Lusch, Bethany, J. Nathan Kutz, and Steven L. Brunton. "Deep learning for universal linear embeddings of nonlinear dynamics." *Nature communications* 9, no. 1 (2018): 1-10.
- [2] Murata, Takaaki, Kai Fukami, and Koji Fukagata. "Nonlinear mode decomposition with convolutional neural networks for fluid dynamics." *Journal of Fluid Mechanics* 882 (2020).

Numerical modeling and experimental validation of ballistic panel penetration

Beata Jackowska-Zduniak*

*Institute of Information Technology, Warsaw University of Life Sciences, Str. Nowoursynowska 159, building 34, 02-776 Warsaw, Poland

ORCID 0000-0001-9332-9275

Abstract. In the paper, the model of a protective panel ensuring the 3rd level of ballistic protection according to STANAG standards was proposed. Adequacy of proposed approach to the problem was tested on the example of a selected type of armor-piercing projectile 7.62x54R B32. The scope of paper included preparation of numerical models formulated using axi-symmetric and three-dimensional descriptions. Built models were validated and verified using experimental results. Conducted multi-variant numerical analyzes show that the developed numerical model satisfyingly corresponds to the real course of the perforation process for assumed experimental conditions. At the model validation stage, an error in determining the residual velocity of the projectile in the range of 0.8-2% was obtained. As a result of verification, the final result of simulation was obtained in accordance to experimental observation.

Introduction

The tasks that Armed Forces around the world are currently facing define the minimum requirements for a ballistic panel necessary to protect light combat vehicles involved (STANAG 4569 normative documents - protection levels for logistic crews and light armored vehicles). The challenge faced by people designing such a protective panels is to minimize the threat to combat vehicles in result of fire from small-caliber weapons with the use of 7.62x54R B32 armor-piercing projectile. Protective elements should be characterized by low weight, due to the dynamic characteristics of the vehicle, and a sufficiently high ability to absorb impact energy. The research included i.a. features of the system of protection against the effects of a small arms projectile, such as the modular structure of the armor. Such construction of the ballistic panel allows easy assembly and quick replacement of the armor part, if the protective plate is partially damaged. Computer modeling methods have been an important tool in the research process for years. Popularity of computer simulations is related to the fact that they are an intermediate link between theoretical analytical considerations and experimental research. The review of the literature shows that in numerical models a simplified description of the phenomenon of perforation/penetration is used, and the projectiles used do not meet the standards of a specific threat level. Experimental verification of the obtained results is also often not carried out.

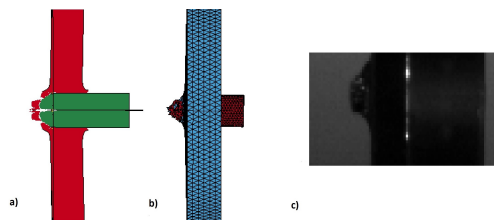


Figure 1: Comparison of the disc perforation at the same moment of time for the numerical model (a) 2D, (b) 3D and (c) experiment.

Result and discussion

The model validation and verification stage showed a satisfactory level of correctness of obtained modeling results. The maximum error due to the residual velocity of the projectile reached 2% for the validation variant of the axisymmetric model and 0.8% for the three-dimensional model. For verification variants, both 2D and 3D, obtained from the simulation, the residual velocity was 0 m/s, the same as in the experiment. It is worth noting that the way of cracking and fragmentation of ceramic tiles and the presence of a cork in the axial symmetric variant for the ARMOXA disc is consistent with experimental observations. On the other hand, it was not possible to obtain a cork for the 3D variant, which is related to the selection of failure parameters for the Johnson-Cook model. As mentioned earlier, this model is not able to reproduce all the physical behavior of the material, similarly to the cracking of the cork in the axisymmetric model. The visual consistency of the final form of shield destruction with the results obtained on the basis of the simulation is visible in Figure 1. The obtained results prove: correct adoption of the basic assumptions of the model, properly performed spatial discretization of models, proper selection of constitutive models of materials with appropriate material data, acceptable method of describing damage / damage and material erosion.

References

- [1] Scazzosi R., Giglio M., Manes A. (2021) Experimental and Numerical Investigation on the Perforation Resistance of Double-Layered Metal Shield under High-Velocity Impact of Armor-Piercing Projectiles. *Materials* **14**(626).
- [2] Dey S., Clausen A. H., Børvik T. (2006) A preliminary study on the perforation resistance of high-strength steel plates in *EURODYMAT - 8th International Conference on Mechanical and Physical Behaviour of Materials under Dynamic Loading*.

Finite element modelling of downhole rock breaking using a PDC bit

Ahmed Al Shekaili*, Yang Liu* and Evangelos Papatheou*

*Engineering Department, University of Exeter, North Park Road, Exeter, UK, EX4 4QF

Abstract. The demand of improving drilling productively and reducing the cost of drilling process significantly depends on the efficiency of drilling tools and the understanding of drilling behaviours. The drillstring, which is one of these main tools during the drilling operation, used to drill a hole by transmitting the required torque and drilling fluid to the drill-bit. Due to the tough destructive nature of the drilling process, the drillstring always exposed to various unwanted vibrations that turns the drill-bit to a severe wear and failure along with the other accessories. These vibrations diminish the drillstring life due to its nonlinear occurrence as an excessive axial, lateral and torsional mode. This work provides adequate understanding to the nonlinear drillstring dynamics to predict the premature vibrations and study drilling parameters using a finite element (FE) model that was validated experimentally using a laboratory drilling rig. Riedel Hiermaier Thoma material (RHT) model was adopted in which a series of experiments tests were conducted to identify its parameters. Our numerical results present a strong correlation with the experimental results for analysing the nonlinear dynamics to characterise the effect of drillstring impact and friction with the surrounding states and performing a parametric study to predict the effects of weight on bit and rotary speed on the rate of penetration.

Introduction

The nonlinear dynamics caused by the drillstring, which is a long sequence of connected drill-pipes with other additional equipment are very complicated issue in oilwell drilling. These dynamics are subjected to various nonlinear axial, lateral and torsional vibrations due to the shocks between the drill-bit and rock formation and impacts between the drillstring with the borehole [1]. Therefore, this work aims to investigate the nonlinear drillstring dynamics caused during drilling prospecting to enhance the rate of penetration and non-productive time as well as to avoid the unexpected economic consequences. This study will provide a significant foundation to analyse the nonlinear dynamics and optimise drilling parameters using both experimental and numerical methods (see Fig. 1). The effectiveness of the numerical model is essentially achieved by the employed material model as shown in Fig. 1(c). RHT model was taken into account to formulate the drilling model along with the damage model in both initially vertical wells and then developed to involve horizontal wells [2], see Fig. 1(d). Limited studies were conducted to study the effect of drillstring dynamics during rock breaking with the RHT model in rotary drilling [3]. It is significant to study the drillstring to estimate drilling nonlinearities and optimise drilling parameters for a better production performance.

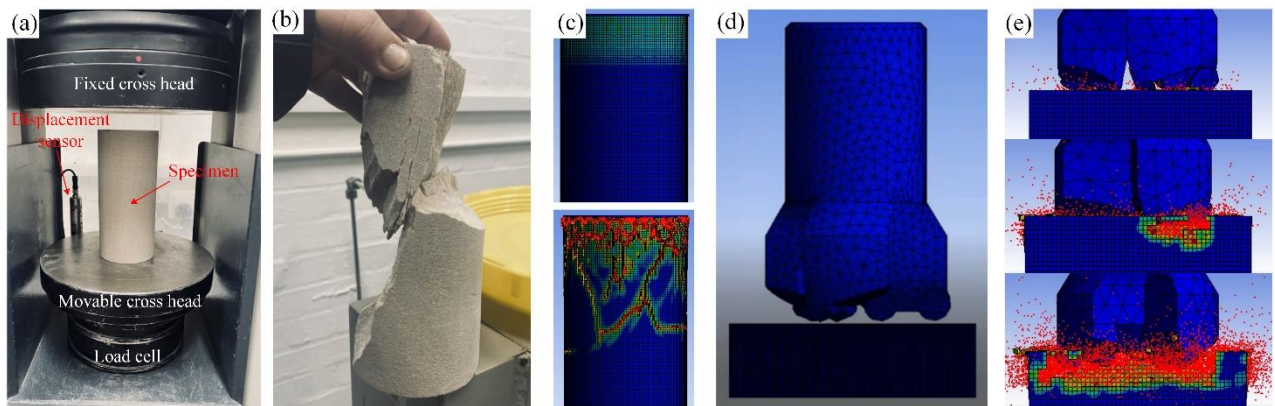


Figure 1: (a) Compressive test and (b) failure; (c) Compressive failure, (d) drilling model and (e) rock breaking via FE modelling.

Results and Discussion

The RHT model was initially verified from various compressive and tensile tests to obtain its parameters for the elastic limit, failure and damage surface that eventually validated with the FE model. The model was convenient to analyse the rock breaking behaviour and consequently relate the drilling performance with the experimental drilling rig results. For instance, at speed 15 rpm, force and torque on bit shows a good agreement for both FE and experimental results as presented in Fig. 1(e). The identified drilling parameters can help to predict drillstring dynamics, so providing timely mitigation methods for undesired instabilities.

References

- [1] Spanos P. D., Chevallier A. M., Politis N. P., Payne M. L. (2003) Oil and gas well drilling: a vibrations perspective. *Shock Vibr. Dig.* **35**:85-103.
- [2] Grunwald C., Schaufelberger B., Stolz A., Riedel W., Borrvall T. (2017) A general concrete model in hydrocodes: verification and validation of the Riedel–Hiermaier–Thoma model in LS-Dyna. *Int. J. Prot. Struct.* **8**:58-85.
- [3] Xi Y., Wang W., Fan L., Zha C., Li J., Liu G. (2022) Experimental and numerical investigations on rock-breaking mechanism of rotary percussion drilling with a single PDC Cutter. *J. Pet. Sci. Eng.* **208**:109227.

Mean-reverting schemes for solving the CIR model

Samir Llamazares-Elias* and Ángel Tocino**

* Departamento de Matemáticas, Universidad de Salamanca, Spain, ORCID # 0000-0001-9219-6749

** Departamento de Matemáticas, Universidad de Salamanca, Spain, ORCID # 0000-0002-7910-1570

Abstract. A family of methods for the numerical solution of the CIR model reproducing the mean-reversion property of the exact solution is presented. The convergence of the methods in the strong and weak senses is established. In addition, a method that captures exactly the first and second long-term moments of the CIR process is found.

Introduction

The Cox-Ingersoll-Ross (CIR) model describes the interest rate as the solution to the nonlinear equation

$$dX(t) = \alpha(\theta - X(t))dt + \sigma\sqrt{X(t)}dW_t \quad (1)$$

where W_t is a standard Wiener process and $\alpha, \theta, \sigma \in \mathbb{R}^+$. The solution is mean reverting: In fact, the long term first and second moments of the CIR process are given by:

$$\lim_{t \rightarrow \infty} \mathbb{E}[X(t)] = \theta, \quad \lim_{t \rightarrow \infty} \text{Var}(X(t)) = \frac{\sigma^2 \theta}{2\alpha}.$$

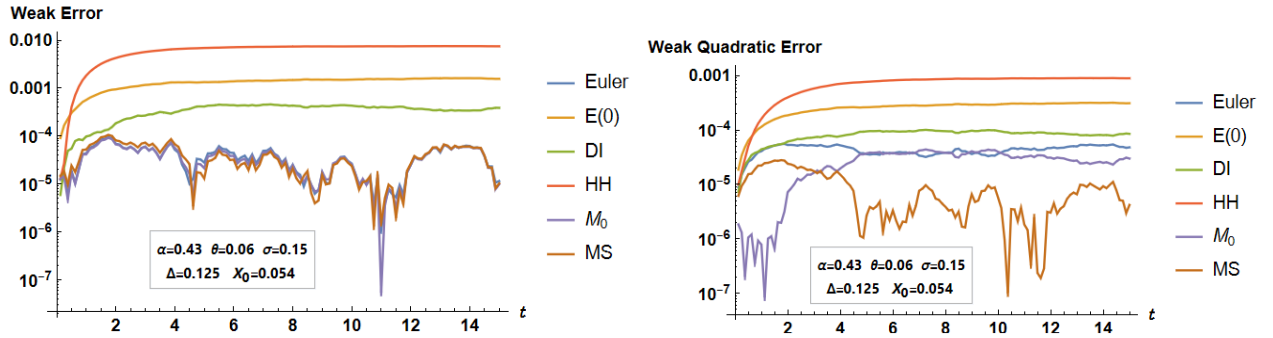
Numerical methods specially designed to solve the CIR equation have been proposed in the literature [1, 2, 3, 4]. A desirable property of any numerical method for solving an SDE is the preservation of qualitative properties of the exact solution [5]. In this sense, our goal is to propose schemes that applied to the CIR problem give numerical solutions that preserve the first and the second long-term moments.

Results and discussion

To solve numerically the equation (1), as a modification of a method presented in [1], we propose the schemes

$$X_{n+1} := \left(\left(1 - \frac{\alpha}{2} \Delta + K_{\Delta} \Delta^2 \right) \sqrt{X_n} + \frac{\sigma}{2} \Delta W_n + S_{\Delta} \Delta \Delta W_n \right)^2 + \left(\alpha \theta - \frac{\sigma^2}{4} \right) \Delta$$

where $K_{\Delta} = \mathcal{O}(\Delta^0)$, $S_{\Delta} = \mathcal{O}(\Delta^0)$. We prove that these schemes converge to the exact solution in the strong and weak senses. Later we give sufficient conditions to obtain numerical solutions that inherit the mean-reverting property. Numerical experiments confirm our findings, as can be seen in the following figure where our proposed methods, M_0 and MS, preserve the first and the first two moments respectively.



References

- [1] Alfonsi A. (2005) On the discretization schemes for the CIR (and Bessel squared) processes. *Monte Carlo Methods Appl.* **11**:355-384.
- [2] Deelstra G., Delbaen F (1998) Convergence of discretized stochastic (interest rate) processes with stochastic drift term. *Appl. Stochastic Models Data Anal.* **14**:77-84.
- [3] Dereich S., Neuenkirch A., Szpruch L. (2012) An Euler-type method for the strong approximation of the Cox-Ingersoll-Ross process. *Proc. R. Soc. Lond. Ser. A* **468**:1105-1115.
- [4] Hefter M., Herzwurm A. (2018) Strong convergence rates for Cox-Ingersoll-Ross processes—full parameter range. *J. Math. Anal. Appl.* **459**:1079-1101.
- [5] Higham D., Mao X. (2005) Convergence of Monte Carlo simulations involving the mean-reverting square root process. *Journal of Computational Finance.* **8**(3), 35-61.

Implicit Milstein schemes: properties preservation when solving the CIR equation

Angel Tocino* and Samir Llamazares-Elias**

* Departamento de Matemáticas, Universidad de Salamanca, Spain, ORCID # 0000-0001-9219-6749

** Departamento de Matemáticas, Universidad de Salamanca, Spain, ORCID # 0000-0002-7910-1570

Abstract. In this work, the stochastic θ -Milstein method is used to numerically solve the CIR equation. Then, an analysis is conducted on the preservation of the CIR processes properties by the numerical solution, namely, its positivity and its reversion to the long-term mean.

Introduction

The Cox-Ingersoll-Ross (CIR) model describes the interest rate as the solution to the nonlinear equation

$$dX(t) = \alpha(\mu - X(t))dt + \sigma\sqrt{X(t)}dW_t \quad (1)$$

where W_t is a standard Wiener process and $\alpha, \mu, \sigma \in \mathbb{R}^+$. Although the diffusion coefficient does not fulfill the Lipschitz condition, specific results showing the existence and uniqueness of the strong solution can be found in the literature [9]. We are interested in two properties of the exact solution:

- (P) Positivity: If $2\alpha\mu > \sigma^2$, the solution remains positive if it starts positive: $X_t > 0$ for $t \in \mathbb{R}^+$ if $X_0 > 0$.
(MR) Mean reversion: The long term mean coincides with the parameter μ : $\lim_{t \rightarrow \infty} \mathbb{E}[X(t)] = \mu$.

Numerical methods specially designed to solve the CIR equation have been proposed in the literature [1, 2, 3, 4]. A desirable property of any numerical method for solving an SDE is the preservation of qualitative properties of the exact solution [5]. Our goal is to propose schemes that, applied to the CIR problem, give numerical solutions that preserve properties (P) and (MR).

Results and discussion

We prove that the numerical solution given by the stochastic θ -Milstein methods

$$X_{n+1} = X_n + \alpha(\mu - X_n)\Delta(1 - \theta) + \alpha(\mu - X_{n+1})\Delta\theta + \sigma\sqrt{X_n}\Delta W_n + \frac{\sigma^2}{4}(\Delta W_n^2 - \Delta),$$

with $\theta \geq 1$ to solve the CIR equation (1), preserve the positivity of the exact solution, as well as, without any additional restriction on the step size Δ , the long-term mean of the exact solution. These theoretical results are illustrated on the left and right pictures respectively of Figure 1.

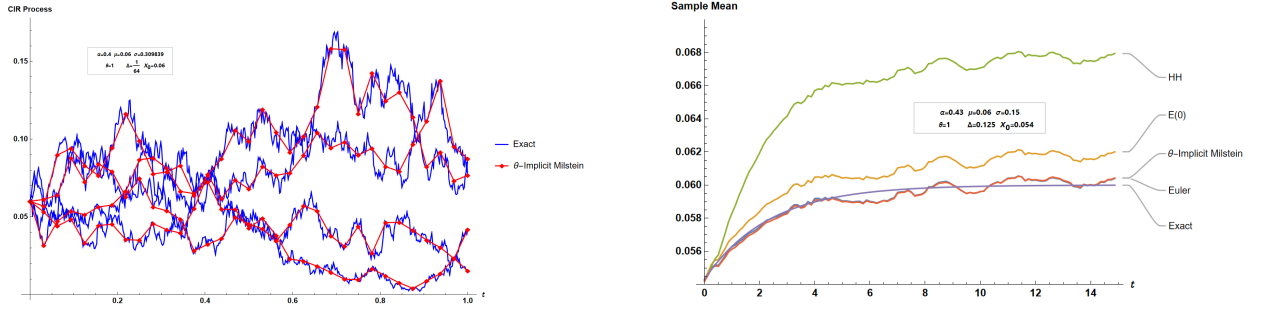


Figure 1: Left: Four trajectories of the exact solution and the corresponding numerical approximations with the fully implicit ($\theta = 1$) Milstein method. Right: Evolution of first moment of the exact solution and the numerical approximations with Euler, θ -Milstein together with the methods proposed in [1] and [4].

References

- [1] Alfonsi A. (2005) On the discretization schemes for the CIR (and Bessel squared) processes. *Monte Carlo Methods Appl.* **11**:355-384.
- [2] Deelstra G., Delbaen F (1998) Convergence of discretized stochastic (interest rate) processes with stochastic drift term. *Appl. Stochastic Models Data Anal.* **14**:77-84.
- [3] Dereich S., Neuenkirch A., Szpruch L. (2012) An Euler-type method for the strong approximation of the Cox-Ingersoll-Ross process. *Proc. R. Soc. Lond. Ser. A* **468**:1105-1115.
- [4] Hefter M., Herzwurm A. (2018) Strong convergence rates for Cox-Ingersoll-Ross processes—full parameter range. *J. Math. Anal. Appl.* **459**:1079-1101.
- [5] Higham D., Mao X. (2005) Convergence of Monte Carlo simulations involving the mean-reverting square root process. *Journal of Computational Finance.* **8**(3), 35-61.
- [6] Higham, D. (2000) A-stability and stochastic mean-square stability. *BIT* **40**:404-409.
- [7] Kloeden P., Platen E., (1992) Stochastic Differential Equations. Springer, Heidelberg.
- [8] Llamazares-Elias, S., Tocino, A. Mean-reverting schemes for solving the CIR model, *Submitted*.
- [9] Yamada Y., Watanabe S. (1971) On the uniqueness of solutions of stochastic differential equations. *J. Math. Kyoto Univ.* **11**:155-167.

New formula of geometrically exact shell element undergoing large deformation and finite rotation

Jielong Wang*, Rongxin Feng*, Shuai Zhang* and Kang Jia *

*No.401B Office Building 102, Future Science and Tech. Park, Changping Dist., Beijing, 102211, P.R. China

Abstract. The paper develops two new geometrically exact shell elements that allow large deformation and finite rotation. Both of them are based on the Reissner-Mindlin shell theory, where the shell is considered as a surface with oriented directors. Accordingly, two different descriptions for rotational fields of oriented directors are given. The first description takes advantage of two rotational variables of the pseudo-rotation vector, and the second one employs two spherical coordinates to avoid the vectorial parameterizations of rotation tensor. With the application of Mixed Interpolation of Tensorial Components (MITC), these shells are shear-locking free, feature second-order accuracy and contain nine nodes. Each node has five degrees of freedom, three for translations and two for rotations. Finally, numerical simulations show these new shell elements have the ability of dealing with large deformations and finite rotations with high efficiency and good accuracy.

Introduction

The computational shell theory was studied over the past decades, and various shell elements have been developed for the linear and nonlinear analysis. Up till now, many researchers are still devoted to modeling the nonlinearities in computational shell theory, such as large deformations, buckling and post-buckling etc. When measuring shear strains through the thickness, the Reissner-Mindlin shell elements [1] are necessary. This type of elements uses rotational degrees of freedom to describe the rotations of the fiber, resulting in shell elements with five or six degrees of freedom per node. It has been pointed out [2] that these rotational degrees of freedom are frequently the source of convergence difficulties in implicit structural analyses. This paper presents two different approaches to describe the arbitrary rotations of the fiber by using the pseudo-rotation vector and the spherical coordinates of the fiber, respectively. Unlike the classical approach that treats the rotations of fiber as general rotations of rigid body in space, this paper points out for the first time that finite rotation of the fiber is completely different from finite rotation of the rigid body described by using the rotation tensor. The fiber can be mathematically viewed as a unit vector containing two independent parameters, such that its rotation can be described by the pseudo-rotation vectors with two components in an incremental analysis, then determines the orientation of local Cartesian basis. It affords powerful theoretical background for the formula of fiber displacement in Hughes doubly curved shells[3]. The second description utilizes the spherical coordinates of fiber with unit length. Its orientation can be determined by the rest two of spherical coordinates.

Results and Discussion

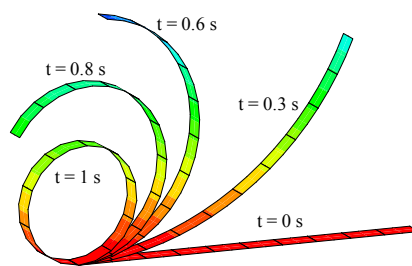


Figure 1: Deformed configurations for a cantilever beam under pure moment.

Figure 1 shows the ability of the new shell elements to predict large deformation. A cantilevered beam meshed into 10 shell elements is deformed into a pure circle when the torque applied to the end of the beam increase from zero to the critical value. In summary, the innovations of this paper include: 1) Two new geometrically exact shell elements with simplified formula are developed to model the relatively thin structures with large deformations and arbitrary motions, efficiently. 2) The Green-Lagrange strain tensor is modified to include only the approximations of higher-order terms, ensuring that the shell element can efficiently describe the geometrical nonlinearities. 3) It points out for the first time that finite rotation of the fiber is completely different from finite rotation of the rigid body described by using the rotation tensor.

References

- [1] Benson D. J. Bazilevs Y. Hsu M. C. Hughes T. J. R. (2010) Isogeometric shell analysis: The Reissner-Mindlin shell. *COMPUT METHOD APPL M*, **199**: 276-289.
- [2] Benson D.J. Bazilevs Y. Hsu M.C. Hughes T. J. R. (2011) A large deformation, rotation-free, isogeometric shell. *COMPUT METHOD APPL M*, **200**: 1367-1378.
- [3] Hughes T.J.R. (1992) The Finite Element Method: linear static and dynamic finite element analysis. Prentice Hall, Inc., Englewood Cliffs, New-Jersey

A Study on Damage to Lithium-Ion Battery Separator using Nonlinear Finite Element Analysis

Jun Lee*, Hamin Lee*, Cheonha Park** and Chang-wan Kim**

*Graduate School of Mechanical Engineering, Konkuk University, Seoul, Republic of Korea

**School of Mechanical Engineering, Seoul, Republic of Korea

Abstract. In this study, a nonlinear mechanical detailed layer (NDL) model was developed to predict the mechanical nonlinear behavior of lithium-ion battery cells and the nonlinearity of internal short circuits due to separator damage. The load-displacement curve, the moment and location of internal short circuit, and the type of separator breakage were compared with the experimental results by simulating indentation test of lithium-ion battery with three spherical indenters, and the nonlinear mechanical behavior and separator breakage mechanism were accurately predicted.

Introduction

Due to the recent increase in electric vehicles in accordance with environmental regulations, cases of thermal runaway and capacity degradation of lithium-ion batteries due to mechanical loads are increasing. Accordingly, there is a trend to utilize mechanism analysis using numerical analysis techniques. However, the numerical analysis model used in previous studies has limitations in that it cannot accurately calculate the mechanical response that causes thermal runaway and capacity loss by using a homogenized model that only considers linear features. In this study, a nonlinear mechanical detailed layer (NDL) model was developed to predict the mechanical nonlinear behavior of lithium-ion battery cells and the nonlinearity of internal short circuits due to separator damage. The NDL model reflected the material nonlinearity and anisotropy of the positive electrode, negative electrode, separator, and current collector, as well as the number and thickness of each layer, identical to those of the actual battery.

Result and discussion

The load-displacement curve, the moment and location of internal short circuit, and the type of separator breakage were compared with the test results of Sahraei et al. [1] and Chung et al. [2] by simulating indentation test of lithium-ion battery with three spherical indenters. The analysis results showed that as the diameter of the spherical indenter increased, the peak value of the reaction force increased, and the indentation depth at which the internal short circuit occurred also increased, and the mechanical deformation and separator breakage mechanism were accurately predicted.

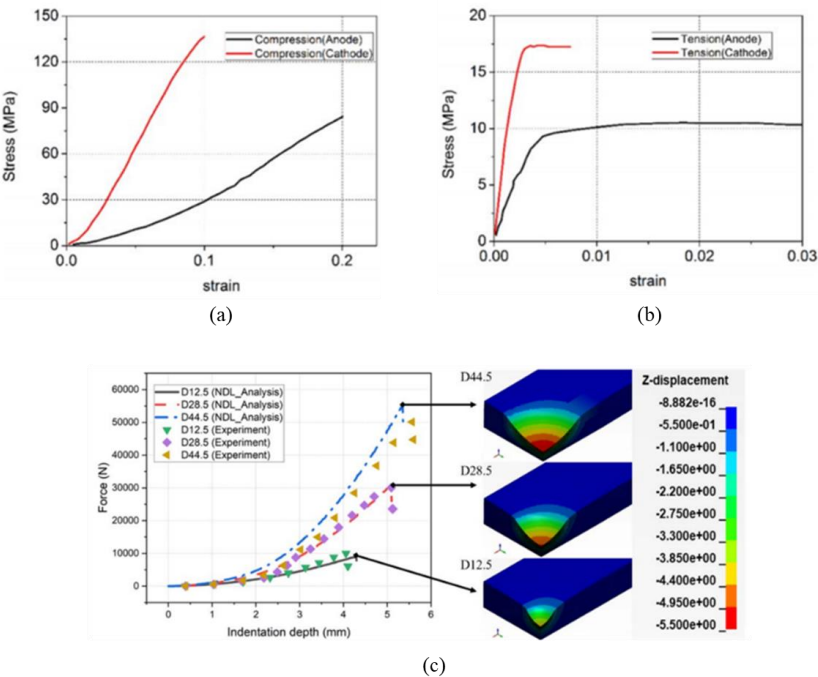


Figure 1: Nonlinear stress-strain curve of anode and cathode of (a) compression and (b) tension and (c) nonlinear load-displacement responses for three different diameter indentation tests

References

- [1] G. Kermani and E.Sahraei (2017) *Energies*,**10** ,1730.
- [2] S. H. Chung, T. Tancogne-Dejea, J. Zhu, H. Luo, and T. Wierzbicki (2018) *J.Power Sources*, **389**, 148

Study of a double-zero bifurcation in a Lorenz-like system. Application to the analysis of the Lorenz system

A. Algaba*, M.C. Domínguez-Moreno*, M. Merino* and A.J. Rodríguez-Luis**

*Departamento de Ciencias Integradas, Centro de Estudios Avanzados en Física, Matemática y Computación, Universidad de Huelva, Spain.

**Departamento de Matemática Aplicada II, E.T.S. Ingeniería, Universidad de Sevilla, Spain

Abstract. In this work we consider a Lorenz-like system and study the double-zero bifurcation it exhibits. The local study of the double-zero bifurcation provides partial results that are extended by means of numerical continuation methods. Specifically, a curve of heteroclinic orbits is detected. The degeneracies exhibited by this global connection guarantee the presence of a very rich dynamical behavior. Finally, the results obtained allows to explain the origin of the curves of homoclinic and heteroclinic connections related to the T-point-Hopf bifurcation exhibited by Lorenz system.

Introduction

We consider the system

$$\dot{x} = \sigma(y - x), \quad \dot{y} = \rho x - y - xz, \quad \dot{z} = -bz + xy + Dz^2, \quad (1)$$

where $D \in \mathbb{R}$, so that the Lorenz system

$$\dot{x} = \sigma(y - x), \quad \dot{y} = \rho x - y - xz, \quad \dot{z} = -bz + xy, \quad (2)$$

is embedded in (1) when $D = 0$. System (1) is also invariant under the change $(x, y, z) \rightarrow (-x, -y, z)$.

The origin E_1 of system (1) exhibits a double-zero bifurcation [1] (a double-zero eigenvalue with geometric multiplicity two), for $\rho = 1, b = 0, \sigma \neq -1, D \neq 0$, in which a second equilibrium $E_2 = (0, 0, b/D)$ is also involved. Our theoretical analysis demonstrate the existence of transcritical, pitchfork and Hopf bifurcations of equilibria as well as a heteroclinic cycle between E_1 and E_2 . Moreover, a degenerate double-zero bifurcation occurs when $\sigma = 1/3$.

Results and discussion

By means of numerical continuation methods, the local results can be extended and applied to the study of (1) when $D \neq 0$ (see Figs. 1(a)-(c)). In this way we find several degeneracies in the heteroclinic connections that lead to complex dynamical behavior (some of them are even of codimension three). For instance, in the vicinity of one of these degenerate heteroclinic cycles we conjecture the existence of an infinite sequence of bifurcation curves of various types that emanate from the corresponding point in the parameter plane: saddle-nodes of asymmetric and symmetric periodic orbits, period-doublings of the asymmetric periodic orbits, symmetry-breakings of the symmetric periodic orbits, homoclinic connections of the origin..., which implies the existence of diverse types of attractors in a neighborhood of the origin. On the other hand, when we decrease the value of D until reaching $D = 0$, our study allows to see how the global connections related to the double-zero bifurcation of system (1) give an explanation of the origin of the curves of homoclinic and heteroclinic connections related to the T-point-Hopf bifurcation exhibited by Lorenz system (see Fig. 1(d)) [2, 3].

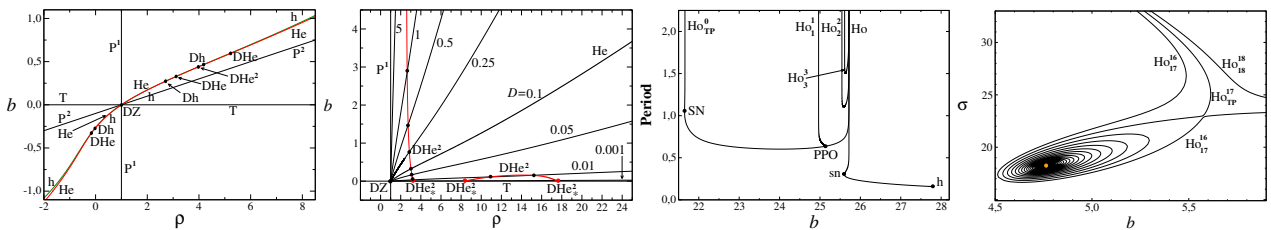


Figure 1: (a) Partial bifurcation set for $\sigma = 3, D = 0.1$. (b) Curves of nondegenerate heteroclinic cycles related to the double-zero degeneracy for several values of D . (c) Bifurcation diagram of periodic orbits related to several homoclinic connections, for $\rho = 50, D = 0.21, \sigma = 100$. (d) Curves of homoclinic connections related to a T-point heteroclinic loop when $\rho = 50, D = 0$ (Lorenz system).

References

- [1] A. Algaba, M.C. Domínguez-Moreno, M. Merino, A.J. Rodríguez-Luis, Double-zero degeneracy and heteroclinic cycles in a perturbation of the Lorenz system, Commun. Nonlinear Sci. Numer. Simul. 111 (2022) 106482.
- [2] P. Glendinning, C. Sparrow, T-points: a codimension two heteroclinic bifurcation. J. Stat. Phys. 43 (1986) 479–488.
- [3] A. Algaba, F. Fernández-Sánchez, M. Merino, A.J. Rodríguez-Luis, Analysis of the T-point-Hopf bifurcation in the Lorenz system. Commun. Nonlinear Sci. Numer. Simul. 22 (2015) 676–691.

Parametric optimization of fold bifurcation points

Adrien Mélot*, Enora Denimal* and Ludovic Renson **

*Univ. Gustave Eiffel, Inria, COSYS-SII, I4S, Campus Beaulieu, 35042 Rennes, France

**Vibration University Technology Centre, Department of Mechanical Engineering, Imperial College London

Abstract. The aim of this work is to optimize the parameters of a mechanical system in order to force fold bifurcation points to appear at targeted frequencies. To this end, an original harmonic balance-based optimization procedure is developed. Functions similar to those employed during bifurcation tracking analyses are used to characterize fold bifurcations in the objective function. The proposed approach is illustrated on a Duffing oscillator with cubic nonlinearity.

Introduction

The ever-increasing demand for lighter structures and more efficient systems requires that the effects of nonlinearities be evaluated at the design stage. One of the most notable characteristic that sets apart nonlinear systems from their linear counterparts is bifurcation phenomena. When a parameter is varied, e.g. the forcing frequency, a bifurcation may occur, resulting in qualitatively different responses such as quasi-periodic or chaotic oscillations. Bifurcation analysis, which aims at predicting and studying such phenomena is a thriving research field. Recent research investigated the computation of the stability of periodic solutions [1] or the parametric analysis of bifurcation points [2, 3, 4]. However, very few studies [5] attempted optimizing the structural parameters of a mechanical system for it to exhibit bifurcations at desired locations and never in the context of nonlinear vibrations. In this work, we develop a computational optimization framework based on the harmonic balance method (HBM), which is widely used in the nonlinear mechanical vibration community. The formulation of the objective function for the optimization strategy relies on a bifurcation measure formulated via a bordering technique and Hill stability analysis and allows one to simultaneously handle multiple bifurcation without two being matched to the same target location.

Results and discussion

The proposed methodology is applied to a Duffing oscillator with hardening cubic nonlinearity. The initial forced response curve shown in Figure 1 (left) exhibits 8 bifurcations: 6 folds and 2 branch points. Two target locations for the fold bifurcations are defined as $\Omega_{tar,1} = 2$ and $\Omega_{tar,2} = 2.5$ rad/s and the optimization is carried out with respect to the damping coefficient. Figure 1 (right) shows the forced response curve computed with the optimized value of the damping coefficient. It is clear that the fold bifurcations located on the primary resonance match with the imposed target locations. One can also note that only two folds are present as the objective function is defined such that the minimum is reached when the number of detected bifurcations match the number of targeted locations [6]. These results are promising and give confidence for application on industrial test cases.

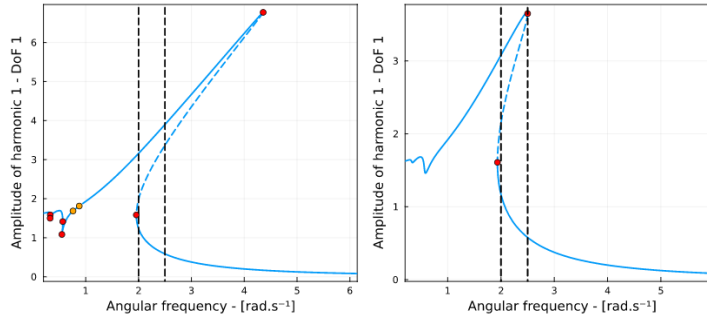


Figure 1: Forced response curve of the Duffing oscillator before (left) and after (right) optimization of the damping coefficient. Target locations $\Omega_{tar,1} = 2$ and $\Omega_{tar,2} = 2.5$ rad/s (vertical black dashed lines). Fold bifurcations and branch points represented by red and orange circle markers, respectively.

References

- [1] Lazarus A., Thomas O. (2010) A harmonic-based method for computing the stability of periodic solutions of dynamical systems. *C. R. Méc.* **338**:510–517
- [2] Detroux T., Renson L., Masset L., Kerschen G. (2015) The harmonic balance method for bifurcation analysis of large-scale nonlinear mechanical systems. *Comput. Methods Appl. Mech. Eng.* **296**:18–38
- [3] Xie L., Baguet S., Prabel B., Dufour R. (2017) Bifurcation tracking by Harmonic Balance Method for performance tuning of nonlinear dynamical systems. *Mech. Syst. Signal Process.* **88**:445–461
- [4] Mélot A., Rigaud E., Perret-Liaudet J. (2022) Bifurcation tracking of geared systems with parameter-dependent internal excitation. *Nonlinear Dyn.* **107**:413–431
- [5] Boullé N., Farrell P. E., Paganini A. (2022) Control of bifurcation structures using shape optimization. *SIAM J. Sci. Comput.* **44**:A57–A76
- [6] Szep G., Dalchau N., Csikasz-Nagy A. (2021) Parameter inference with bifurcation diagrams. Preprint

A Stochastic computational technique for the multi-Pantograph-delay systems through Trigonometric approximation

Iftikhar Ahmad*, Siraj-ul-Islam Ahmad* and Hira Ilyas **

*Department of Mathematics, University of Gujrat, Gujrat, Pakistan, ORCID #0000-0002-8051-8111

* Department of Physics, COMSATS University Islamabad, Pakistan.

Abstract. A stochastic mathematically designed technique with logarithmic and trigonometric transformation function have been implemented for numerical treatment of multi-Pantograph differential systems. Several local optimization solvers including Interior Point, Active set, Genetic Algorithms and Sequential Quadratic Programming have been used to calculate multi-Pantograph model. Numerical experiments showed that obtained solutions through proposed scheme are better in accuracy than results presented in the literature for well-known analytical techniques, including Variational Iterative Method, Differential Transform Method and Homotopy Methods. Moreover, on the basis of several independent runs comprehensive statistical measures have been presented to endorse the validity, accuracy and reliability of the proposed scheme.

Introduction

Pantograph delay differential equations (PDDE) are characterized as functional differential equations with delays. Ockenden and Taylor [1] originated pantograph equation on collection of electric current through pantograph head of an electric locomotive. These equation are characterized by the existence of a linear functional argument. Pantograph equations have important role in explaining many differential phenomena, such as economy, probability theory, astrophysics, electrodynamics, non linear dynamic system, control theory, number theory, quantum mechanics, biological sciences and many industrial applications. Various methods have been implemented or used for solution of such equations worldwide, including recently developed methods such as Variational Iterative Method (VIM), Adomian Decomposition Method (ADM), and Differential Transform Method (DTM), etc. For detailed review the interested reader can see the articles by Yüzbaşıa and Sezer [3], Muroya et al. [4] and Li and Lua [5]. The most general form of pantograph equation [2] having with variable coefficients is given as

$$y^{(m)}(x) + \sum_{j=0}^n \sum_{k=0}^{m-1} y^{(k)}(\beta_{jk} + \alpha_{jk}x) p_{jk}(x) + g(y) = f(x); \quad 0 \leq x \leq b < \infty$$

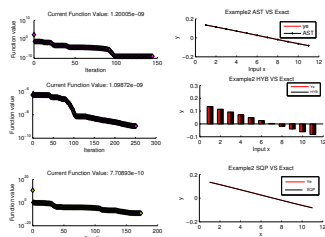


Figure 1: The results obtained through SQP, AST and HYB comparison with reference solution

Results and discussion

The developed stochastic techniques using new activation function in optimization process is executed through local and global solvers for three different problems, which provide acceptable solutions for the Pantograph-delay problems as shown in Fig.1. The proposed stochastic numerical scheme applied on pantograph delay equations to find approximate solutions matching with reference solutions with a short time management. The proposed numerical optimization solvers can easily handle the pantograph-delay equations without any restrictions and constraints on the parameters, and are promising methods for delay equations. The proposed mathematical models are having simplicity of concept, comfort of implementation, and broader applicability.

References

- [1] J.R. Ockendon and A.B. Tayler, The dynamics of a current collection system for an electric locomotive, Proc. Roy.Soc. London Ser. A 322 (1971) 447-468.
- [2] S. Yuzbas and M. Sezer, An exponential approximation for solutions of generalized pantograph-delay differential equations, Applied Mathematical Modelling, (2013).
- [3] Şuayip Yüzbaşıa, Mehmet Sezerb, "An exponential approximation for solutions of generalized pantograph-delay differential equations", Applied Mathematical Modelling, 37 9160-9173
- [4] Y. Muroya, E. Ishiwata and H. Brunner, On the attainable order of collocation methods for pantograph integro-differential equations, J. Comput. Appl. Math., 152 (2003) 347-366.
- [5] M. Liu and D. Li, Properties of analytic solution and numerically solution of multi-pantograph equation, Appl. Math. Comput, 155 (2004) 853-871.

Estimating seismic behavior of buckling-restrained braced frames using machine learning algorithms

Benyamin Mohebi*, Farzin Kazemi** and Neda Asgarkhani**

*Faculty of Engineering and Technology, Imam Khomeini International University, Qazvin, Iran.

Email: mohebi@eng.ikiu.ac.ir

**Faculty of Civil and Environmental Engineering, Gdansk University of Technology, ul. Narutowicza 11/12, 80-233 Gdansk, Poland

Abstract. Over the last few decades, there has been a growing interest in exploring the seismic behaviour of Buckling-Restrained Braced Frames (BRBFs) as passive device for dissipating seismic energy. Machine Learning (ML) methods of Decision Forest (DF), Artificial Neural Networks (ANNs), Gradient Boosting Machines (GBM) and LightGBM were used to predict the seismic response of two-, to twelve-story BRBFs located in soil D. The partial dependence-based features selection method is proposed to increase the capability of methods for estimation of seismic response of BRBFs subjected to far-fault ground motions. The results showed that the GBM and DF methods with accuracy of 97% and 95%, respectively, can be used to predict the seismic response of BRBFs. Therefore, applying the proposed methods can facilitate the response prediction procedures and help designers, while decreases the total computational efforts.

Introduction

Buckling-Restrained Braced Frames (BRBFs) are used in the construction of buildings to provide lateral stability during earthquakes. The seismic response of BRBFs is of critical importance, as it affects the overall structural integrity of the building and the safety of the occupants [1]. One way to study the seismic behaviour of BRBFs is through Machine Learning (ML) methods. Decision Forest (DF) method and Artificial Neural Networks (ANNs) are two popular methods that have been used in this field. In the context of BRBFs, the DF method can be used to analyse the various parameters that affect the seismic response of the structure [2] and [3]. Another ML algorithm that has gained popularity in recent years is Gradient Boosting Machines (GBM). The GBM is a type of ML algorithm that uses decision trees to build an ensemble of models that work together to improve prediction accuracy [4]. LightGBM is a recent addition to the family of GBM algorithm. It is a fast, distributed and high-performance machine learning algorithm that is designed to handle large amounts of data [5].

Result and discussion

In this study, the seismic lateral responses of two-, to twelve-story BRBFs have been studied extensively using the proposed ML methods such as the DF, ANNs, GBM and LightGBM, which were improved by partial dependence-based features selection method. The proposed method can decrease the time of computational efforts in a big training dataset, while it can improve the ability of the ML methods for prediction of seismic responses with lowest achievable input features. This can improve the capability of the method for those of existing BRBFs without possibility of preparing the features of ML-based prediction model. Figure 1 presents the scatter plots of train and test data points related to the interstory drift ratio of the 4-story BRBF using improved ANNs algorithm.

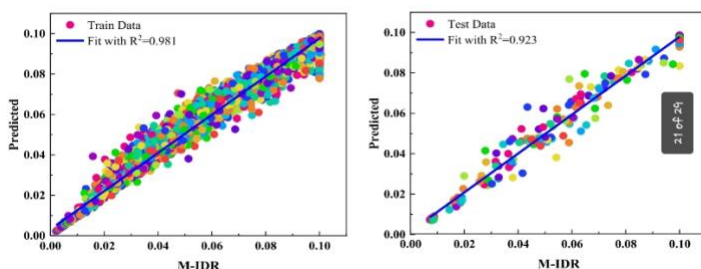


Figure 1. Scatter plots of train and test data points related to the interstory drift ratio of the 4-story BRBF using improved ANNs method.

References

- [1] Kazemi F, Jankowski R. Seismic performance evaluation of steel buckling-restrained braced frames including SMA materials. *J Constr Steel Res.* 2023; 201: 107750.
- [2] Kiani J, Camp C, Pezeshk S. On the application of machine learning techniques to derive seismic fragility curves. *Comput Struct.* 2019; 218:108–22.
- [3] Nguyen NV, Nguyen HD, Dao ND. Machine learning models for predicting maximum displacement of triple pendulum isolation systems. *Structures.* 2022; 36:404–15.
- [4] Oh BK, Glisic B, Park SW, Park HS. Neural network-based seismic response prediction model for building structures using artificial earthquakes. *J Sound Vib.* 2020; 468: 115109.
- [5] Luo H, Paal SG. Artificial intelligence-enhanced seismic response prediction of reinforced concrete frames. *Adv Eng Inform.* 2022; 52: 101568

Machine learning-based estimation of interstory drift distribution in reinforced concrete structures

Benyamin Mohebi*, Neda Asgarkhani**, Farzin Kazemi** and Natalia Lasowicz**

*Faculty of Engineering and Technology, Imam Khomeini International University, Qazvin, Iran.

Email: mohebi@eng.ikiu.ac.ir

**Faculty of Civil and Environmental Engineering, Gdansk University of Technology, ul. Narutowicza 11/12, 80-233 Gdansk, Poland

Abstract. Nowadays, due to cost beneficial of Reinforced Concrete (RC) structures compared to steel structures, there is a growing interest for designing and improving the knowledge on the behaviour of this type of structures. This research overcomes the difficulty of estimation of Interstory Drift Distribution (IDD) in RC structures using Machine Learning (ML) algorithms of Artificial Neural Networks (ANNs), Extra Trees Regressor (ETR), Gradient Boosting Machines (GBM) and LightGBM. The aim of this research is to provide a general prediction model to estimate the IDD with the highest accuracy for using the behaviour assessment of existing or newly designed RC structures. The results of analysis showed that the ETR algorithm can accurately predict the IDD of two-, to ten-story RC structures and provide a plot curve of actual and predicted values of IDD with accuracy of 98.34%, while other improved ML methods have acceptable results.

Introduction

Exploring the lateral behavior of the Reinforced Concrete (RC) structures can improve the knowledge of civil engineers regarding the designing and performance of RC buildings. Therefore, it is on the interest of the engineers to have a prediction model for estimating the performance level [1] and seismic failure probability of the RC buildings [2]. The GBM (Gradient Boosting Machine) and LightGBM are both ML algorithms that belong to the family of gradient boosting algorithms. They are both used for supervised learning tasks, such as classification and regression. The main difference between them is in the way they handle large datasets. LightGBM uses a novel algorithm to achieve faster training and better accuracy on large datasets. Studies showed that using these methods can improve the accuracy of prediction leading to faster training and better scalability [3]. In addition, Artificial Neural Networks (ANNs) and Extra Trees Regressor (ETR) have the ability to learn complex non-linear relationships between inputs and outputs [4]. They are commonly used for supervised learning tasks and have also been used in civil engineering for tasks such as structural health monitoring, earthquake prediction, and structural design optimization [5].

Result and discussion

In this study, a ML-based model was developed for predicting the distribution of seismic response of RC structures. The methods of ETR and LightGBM were selected as the best methods to predict the peak IDD of RC structures. For this purpose, the seismic lateral responses of two-, to ten-story RC structures have been studied extensively using the proposed ML methods such as the ETR, ANNs, GBM, and LightGBM. The proposed method can decrease the time of computational efforts while provide a general prediction model for estimating the Interstory Drift Distribution (IDD) in RC structures with accuracy more than 98.34%. Figure 1 presents the IDD of the 6-, and 8-story RC structures using improved ETR algorithm with the highest accuracy.

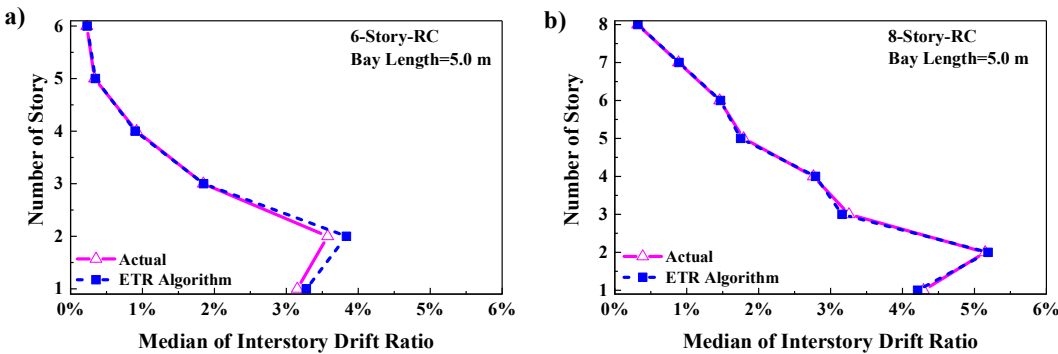


Figure 1. Distribution of the interstory drift ratio of the 6-, and 8-story RC structures using improved ETR algorithm.

References

[1] Kazemi, F., Asgarkhani, N., and Jankowski, R.: Machine learning-based seismic response and performance assessment of reinforced concrete buildings. Archives of Civil and Mechanical Engineering, 23(2), 94, (2023).
[2] Kazemi, F., Asgarkhani, N., and Jankowski, R.: Machine learning-based seismic fragility and seismic vulnerability assessment of reinforced concrete structures. Soil Dynamics and Earthquake Engineering, 166, 107761, (2023).
[3] Kiani J, Camp C, Pezeshk S. On the application of machine learning techniques to derive seismic fragility curves. Comput Struct. 2019; 218:108–22.
[4] Oh BK, Glisic B, Park SW, Park HS. Neural network-based seismic response prediction model for building structures using artificial earthquakes. J Sound Vib. 2020; 468: 115109.
[5] Luo H, Paal SG. Artificial intelligence-enhanced seismic response prediction of reinforced concrete frames. Adv Eng Inform. 2022; 52: 101568.

Doubly periodic solutions and breathers of the Hirota equation: Cascading mechanism and spectral analysis

H. M. Yin*, Q. Pan* and K. W. Chow*

**Department of Mechanical Engineering, the University of Hong Kong, Pokfulam, Hong Kong*

Abstract. We take the Hirota equation which is a further modification of the nonlinear Schrödinger equation with additional terms that are responsible for third-order dispersion and a correction to the cubic nonlinearity. ‘No-phase-shift’ and ‘phase-shifted’ doubly periodic solutions for Hirota equation are obtained by theta and elliptic functions. Cubic dispersion preserves numerical robustness, since slightly disturbed exact solutions as initial states still evolve to the analytical configurations. A plane wave with a cosine wave perturbation will trigger repeated occurrence of breathers, i.e., a manifestation of the Fermi-Pasta-Ulam-Tsingou recurrence. At the formation time of the breathers, the profiles of the numerical breathers agree well with the exact doubly periodic solutions. The spectra are studied analytically and computationally, which provide the motivation for introducing ‘cascading mechanism’. This mechanism elucidates the dynamics leading to the first formation of breathers.

Introduction

The nonlinear Schrödinger equation is a widely applicable model in elucidating the evolution of wave systems in many physical disciplines, e.g. fluid mechanics and optics [1, 2]. Breathers are pulsating modes, and rogue waves are surprisingly large displacements from a tranquil background. These modes are closely related to the modulation instability of plane waves. This instability arises from the interplay of dispersion and nonlinearity, and will lead to growth of small amplitude disturbances. Typically, these breathers decay after attaining maximum displacement. On reaching sufficiently small amplitude, nonlinear effect is triggered again, leading to the occurrence of breathers for the second time [3]. This cycle is repeated, and is taken as one manifestation of the Fermi-Pasta-Ulam-Tsingou recurrence (FPUT) in classical physics. Our objective is to extend this type of FPUT analysis to higher order members of the Schrödinger family of evolution equations.

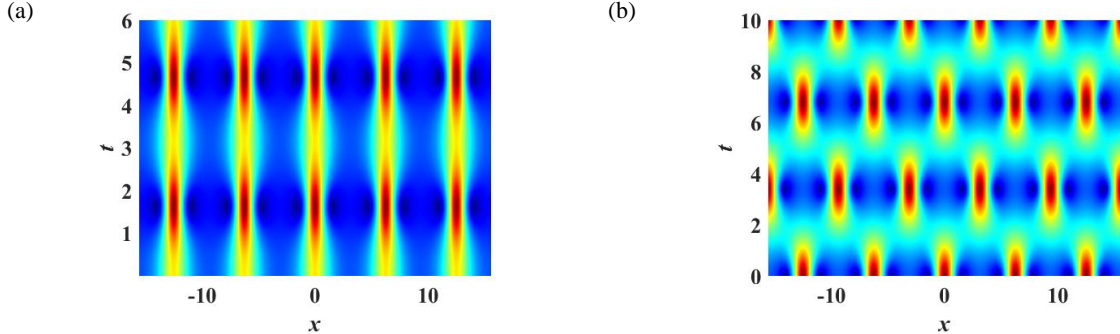


Figure 1 (a) ‘No-phase-shift’ and (b) ‘phase-shifted’ doubly periodic solutions

Results and Discussion

The properties and dynamics of breathers and doubly periodic solutions of the Hirota equation are studied. Doubly periodic solutions are established by utilizing the bilinear derivatives of theta functions. Theoretically, we expect modes similar to the Kuznetsov-Ma and Akhmediev breathers will result by long wave limit. Instead, we give a quick derivation in terms of a Darboux transformation and concentrate on the cascading mechanism and spectral analysis. The cascading mechanism can elucidate the first formation of a breather. More precisely, higher order harmonics exponentially small initially can nevertheless be amplified at a higher rate. Eventually, all these modes attain roughly the same magnitude at one instant of time (or one spatial location in the optical fiber setting), which signifies the first occurrence of a breather. We substantiate these assertions with a spectral analysis.

References

- [1] Craik, A. D. D. (1985) Wave Interactions and Fluid Flows. Cambridge University Press, New York.
- [2] Kivshar, Y. S., Agrawal, G. (2003) Optical Solitons: From Fibers to Photonic Crystals. Academic Press, San Diego.
- [3] Chin, S.A., Ashour, O.A., Belić, M.R. (2015) Anatomy of the Akhmediev breather: Cascading instability, first formation time, and Fermi-Pasta-Ulam recurrence. *Phys. Rev. E* **92**: 063202.

Excitations of distorted magnetosonic lump waves by orbital charged space debris objects in ionospheric plasma

Siba Prasad Acharya^{*1}, Abhik Mukherjee^{**} and M. S. Janaki^{*}

^{*} Plasma Physics Division, Saha Institute of Nuclear Physics, HBNI, Kolkata, West Bengal, India, ORCID

¹0000 – 0002 – 3090 – 8621

^{**} Tsung-Dao Lee institute, Shanghai Jiao Tong University, Shanghai, China

Abstract. We consider the forced Kadomtsev-Petviashvili I (KPI) equation derived in a recent work on magnetosonic waves excited by space debris objects of Acharya et al. [Adv. Space Res. 69, 4045-4057 (2022)] for further analysis in this work. For first time, we have derived a special exact distorted lump wave solution of the forced KPI equation for a specific localized form of the forcing function. The reason for choosing such a typical forcing function has been discussed in detail in the context of orbital motions of charged space debris objects in ionospheric plasma. Such exotic magnetosonic lump wave structures showing characteristic distortions resulted by orbital charged space debris objects can have potential implications in their indirect detection methods.

Introduction

The excitations of nonlinear magnetosonic waves by orbital motions of charged space debris objects have been recently investigated in inertial magnetohydrodynamics (MHD) framework by Acharya et al. [1]. These magnetosonic waves are found to be governed by a forced Kadomtsev-Petviashvili (KP) equation where the forcing function interprets effects of charged space debris objects functioning as current density sources. In particular, nonlinear evolution of slow magnetosonic waves in entire parameter space and fast magnetosonic waves in a large region of parameter space has been shown to be governed by a forced KPI equation. Similarly, forced KPII equation governs dynamics in the remaining small region of parameter space for fast magnetosonic waves [1]. One important point in this context is that lump wave solutions showing bending features or distortions for the forced KPI equation have not been analysed in [1, 2, 3]. But such exotic magnetosonic wave structures can be of potential importance in designing indirect detection systems for space debris objects. Inspired by this fact, we have derived a special exact pinned distorted lump wave solution of the forced KPI equation in this work for a specific localized form of the forcing function for first time. The reason for choosing such a peculiar forcing function has been discussed in context of orbital space debris objects using [4, 5].

Results and discussions

The most important result of the special exact pinned distorted magnetosonic lump wave solution is that its characteristic distortions have been modelled in our work with an arbitrary function satisfying a set of appropriate localization conditions. The effects of orbital charged space debris objects are incorporated in our model using these localization conditions which specify the forcing function in the forced KPI equation. One significant advantage of our work is that different types of distortions in lump waves consistent with practical observations can be formulated with appropriate values of the arbitrary function. A typical distorted lump wave solution for an appropriate value of the arbitrary function has been shown in Figure 1.

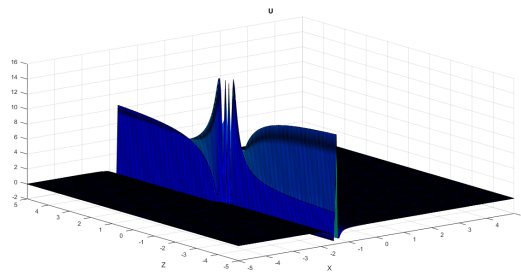


Figure 1: Distorted magnetosonic lump wave excited by a space debris object.

References

- [1] Acharya S. P., Mukherjee A., Janaki M. S. (2022) Charged space debris induced nonlinear magnetosonic waves using inertial magnetohydrodynamics. *Adv. Space Res.* **69**:4045-4057.
- [2] Acharya S. P., Mukherjee A., Janaki M. S. (2021) Accelerated magnetosonic lump wave solutions by orbiting charged space debris. *Nonlinear Dyn.* **105**:671-689.
- [3] Acharya S. P., Mukherjee A., Janaki M. S. (2021) Bending of pinned dust-ion acoustic solitary waves in presence of charged space debris. *Phys. Rev. E* **104**:014214.
- [4] Sen A., Tiwari S., Mishra S., Kaw P. (2015) Nonlinear wave excitations by orbiting charged space debris objects. *Adv. Space Res.* **56**: 429-435.
- [5] Truitt A. S., Hartzell C. M. (2021) Three-dimensional Kadomtsev-Petviashvili damped forced ion acoustic solitary waves from orbital debris. *J. Spacecrafts Rockets* **58**:3.

Fast M-Component Direct and Inverse Nonlinear Fourier Transform

Vishal Vaibhav

Indian Institute of Technology Delhi, New Delhi, India, ORCID 0000-0002-4800-0590

Abstract. In this work, I demonstrate how to develop low-complexity algorithms for direct/inverse M-component nonlinear Fourier Transform (NFT) using exponential integrators.

Introduction

A nonlinear generalization of the conventional Fourier transform, referred to as *nonlinear Fourier transform* (NFT), can be achieved via the M -component Zakharov-Shabat (ZS) scattering problem which can be stated as follows [1, 2]: Let $M = \nu + 1$. For any complex-valued signal $\mathbf{q} \in \mathbb{C}^{\nu \times 1}$ ($\mathbf{r} = -\mathbf{q}^*$) and for $\zeta \in \mathbb{R}$, let $u \in \mathbb{C}^{(\nu+1) \times J}$ with

$$u_t = -i\zeta\sigma u + U(t)u \quad \text{where } \sigma = \begin{pmatrix} 1 & \mathbf{0}_\nu^\top \\ \mathbf{0}_\nu & -I_{\nu \times \nu} \end{pmatrix} \text{ and } U = \begin{pmatrix} 0 & \mathbf{q}^\top \\ \mathbf{r} & 0_{\nu \times \nu} \end{pmatrix}, \quad (1)$$

$\mathbf{0}_\nu \in \mathbb{R}^{\nu \times 1}$ and $0_{\nu \times \nu} \in \mathbb{R}^{\nu \times \nu}$ have all entries zero and $I_{\nu \times \nu} \in \mathbb{R}^{\nu \times \nu}$ is the identity matrix. Here ‘ ζ ’ is referred to as the *spectral parameter* and $U(t)$ is interpreted as the *scattering potential*. The solution of the ZS scattering problem consists in finding the so-called *scattering coefficients* as a function of the spectral parameter ζ . A schematic of the transform is presented in Fig 1.

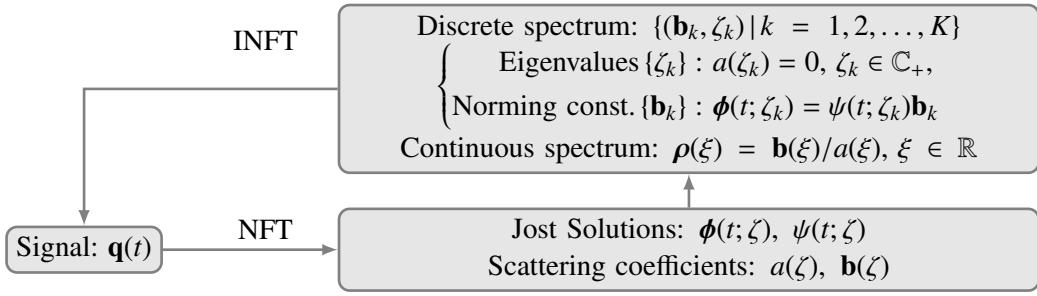


Figure 1: The figure shows a schematic of the nonlinear Fourier transform (NFT) and the inverse NFT (INFT).

The ZS scattering problem is an extremely powerful tool in studying nonlinear phenomena in nature, specially the class of initial value problems that are integrable via inverse scattering transforms. Our motivation to consider this problem stems from the recent surge of interest in NFTs for optical fiber communication (OFC) at higher signal powers. It turns out that encoding/decoding information using direct/inverse NFT can potentially mitigate the nonlinear cross-talk at higher signal powers in OFC which seem to limit the capacity of the current system. Let us note that this is the most general version of NFT which allows for larger degrees of freedom to be exploited: (a) polarization degrees of freedom (which corresponds to $M = 3$) (b) multiple fiber modes (which corresponds to $M > 2$) [3].

The Algorithm

The case $M = 2$ [1] was treated by the author in two papers [5, 4] where algorithms for NFT/INFT with complexity $O(NK + N \log^2 N)$ and order of convergence $O(N^{-2})$ was presented (K : number of eigenvalues, N : number of samples of the signal). For the direct NFT, the determination of eigenvalues is not included in the complexity estimate. In this work, we extend these results to $M > 2$ using exponential integrators of order 2. The discrete system thus obtained happens to have the so-called *layer-peeling* property which plays a key role in the development of the new algorithms. Further, the transfer matrices have the familiar polynomial structure which makes it amenable to FFT-based fast polynomial multiplication. The mathematical details will be presented in a full-length paper.

References

- [1] M. J. Ablowitz, D. J. Kaup, A. C. Newell, and H. Segur, “The inverse scattering transform - Fourier analysis for nonlinear problems,” *Stud. Appl. Math.*, vol. 53, no. 4, pp. 249–315, 1974.
- [2] Ablowitz, M., Prinari, B., and Trubatch, A. (2003). Matrix nonlinear Schrödinger equation (MNLS). In Discrete and Continuous Nonlinear Schrödinger Systems (London Mathematical Society Lecture Note Series, pp. 90–129). Cambridge: Cambridge University Press.
- [3] Turitsyn *et al.*, “Nonlinear Fourier transform for optical data processing and transmission: advances and perspectives,” *Optica*, vol. 4, no. 3, pp. 307–322, 2017.
- [4] V. Vaibhav, “Fast inverse nonlinear Fourier transformation,” *Phys. Rev. E*, vol. 98, p. 013304, 2018.
- [5] V. Vaibhav, “Fast inverse nonlinear Fourier transformation using exponential one-step methods: Darboux transformation,” *Phys. Rev. E*, vol. 96, p. 063302, 2017.

Nonlinear Lamb wave mixing in prestressed plates

Meng Wang*, Annamaria Pau**

*Dept. Astronautical, Electrical and Energy Eng., Sapienza Univ. of Rome, Rome, Italy, ORCID # 0000-0003-2946-0185

**Dept. Structural and Geotechnical Eng., Sapienza Univ. of Rome, Rome, Italy, ORCID # 0000-0002-4946-0302

Abstract. We address the nonlinear wave propagation in a homogeneous and isotropic prestressed elastic plate, accounting for material and geometric nonlinearities. Two internally-resonant Lamb wave modes of different frequencies (ω_1 and ω_2) are allowed to mix within the material, which generates a third type of harmonic waves at frequencies ($\omega_1 \pm \omega_2$). In this study, we investigate the time and space evolution of the resonant higher harmonics for the one-way resonant mixing of waves using a finite element model. We employ also multiple-scale methods to verify some phenomena emerging from the numerical analysis. The influence of prestress on the wave mixing resonance conditions is elucidated by observing the material nonlinear parameter, which proved to be quite effective in the detection of a change in the state of stress.

Introduction

Among the various nonlinear ultrasonic NDE techniques, the method of second harmonic generation (SHG) takes advantage of the spatially cumulative nature of the second harmonic generated by a propagating wave. Various studies have been conducted using the method of SHG to quantitatively evaluate fatigue and creep damage in the early stages [1, 2]. When two waves propagate in a nonlinear medium, their interaction generates a third wave, called mixed wave. If these two primary waves satisfy certain resonance conditions, the mixed wave is also a propagating wave, and its maximum amplitude is proportional to the size of the mixing zone and to the distance travelled. We have in this case a wave triplet. It happens that two identical propagating longitudinal waves and their resonant second harmonic are such a triplet [3]. The generation of the second harmonic is simply the resonant mixing of two identical propagating longitudinal waves, or self-mixing. In the technique called one-way mixing, two primary waves propagating in the same direction are employed. Here, we conduct numerical finite-element simulations to investigate the spatial variation of higher harmonics and mixed waves generated in the one-way mixing, and elucidate the dependence of these amplitudes on the initial prestress. Multiple-scales analytical techniques are also used to motivate some unexpected numerical results.

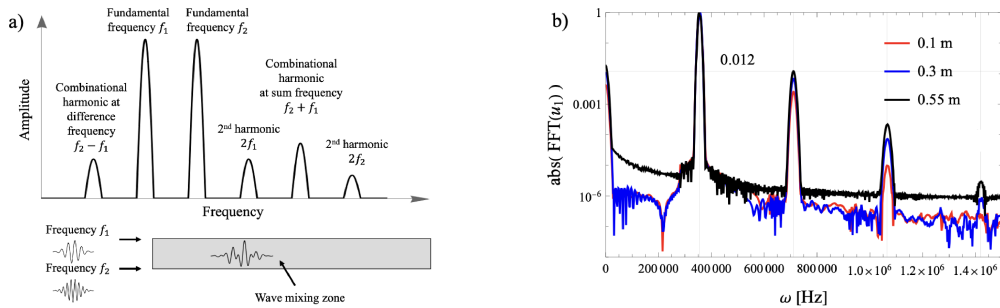


Figure 1: (a) Schematic diagram of frequency spectrum for ultrasonic guided wave mixing, and wave mixing zone in plate. (b) Normalized spectrum of S1-S2 Lamb wave modes at different distances from the excitation boundary in resonance condition.[4]

Results and discussion

The problem considered concerns the propagation of waves in a prestressed Aluminum plate. The finite-element model employed is a second-order plane-strain approximation accounting for material and geometric nonlinearities, considering different states of prestress. It is shown that, for internally-resonant S1 and S2 modes, the nonlinear parameter increases with propagation distance and when the initial stress increases. Besides the well-known internal resonance S1-S2, other resonances due to reciprocal interaction and mixing of these two waves at integer multiples of the primary frequency can be observed. In fact, multiple higher resonance conditions exist, though these higher resonances were not reported in the literature, because their occurrence cannot be predicted by the classical two-scales perturbation analysis. Here, their existence is demonstrated and their characteristics are outlined resorting to the method of multiple scales. The one-way mixing involving different combinations of resonant frequencies is investigated, in view of their potential application to the sensing of the state of stress.

References

- [1] Sun, M., Qu, J. (2020) Analytical and numerical investigations of one-way mixing of Lamb waves in a thin plate. *Ultrasonics* **108**: 106180.
- [2] Hughes, J.M., Kotousov, A., Ng, C.T. (2022) Wave mixing with the fundamental mode of edge waves for evaluation of material nonlinearities. *J. Sound Vib* **527**:116855.
- [3] Jones G.L., Kobett, D.R. (1963) Interaction of elastic waves in an isotropic solid. *J. Acoust. Soc. Am* **35**:5.
- [4] Wang, M., Pau, A. (2023) Stress monitoring of plates by means of nonlinear guided waves. *10th Eur. Workshop Struct. Health Monit* **270**:212-220.

The nature and formation of rogue waves for nonlinear Schrödinger equation

Stanko N. Nikolić^{*,**}, Najdan B. Aleksić^{*,**}, Omar A. Ashour^{***}, and Milivoj R. Belić^{*}

^{*}Division of Arts and Sciences, Texas A&M University at Qatar, P.O. Box 23874 Doha, Qatar

^{**}Institute of Physics Belgrade, University of Belgrade, Pregrevica 118, 11080 Belgrade, Serbia

^{***}Department of Physics, University of California, Berkeley CA 94720, USA

Abstract

We discuss the nature of rogue waves (RW), their ingrained instability and dynamic generation in systems governed by the standard cubic nonlinear Schrödinger equation (NLSE). We also discuss the spatiotemporal pattern of high intensity peaks in the form of multi-elliptic RW clusters.

Introduction

Rogue waves are high-intensity nonlinear waves that suddenly appear and disappear without a trace in oceans and optics. They can be build up using Darboux transformation (DT) scheme from trivial, so called zero seed NLSE solution, using Lax pair formalism and recursive relations. The idea is to construct fundamental NLSE solution of various orders, known as Akhmediev breathers, analytically from DT. We can extract initial conditions from analytical solutions and generate high intensity peaks (rogue waves) dynamically.

Results and discussion

We analyze the method of mode pruning for suppressing the modulation instability of RWs and to produce stable Talbot carpets by RWs (figure 1) that are recurrent images of light waves. We focus on cases when rogue waves appear as numerical artefacts, due to an inadequate numerical treatment of modulation instability. We further display how statistical analysis based on different numerical procedures can lead to misleading conclusions on the rogue waves nature [1].

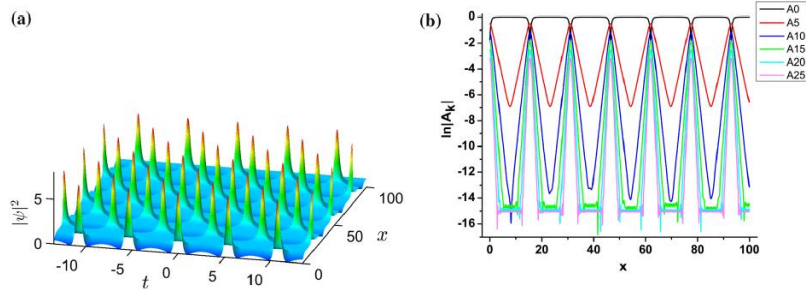


Figure 1: Double-periodic numerical solutions made of the first-order NLSE breathers, using the pruning procedure in the fast Fourier transform: (a) five breathers in the box with the pruning, (b) its spectrum.

The next research topic is the formation of rogue waves. We analyze the various spatiotemporal patterns of RWs which may have the form of multi-elliptic clusters (figure 2). Such structures may be obtained on uniform and elliptic dnoidal backgrounds using the DT scheme. We solve the eigenvalue problem of the Lax pair of order n in which the first m evolution shifts are equal, nonzero, and eigenvalue dependent, while all eigenvalues' imaginary parts are close to one. We show that an Akhmediev breather of order $n - 2m$ appears at the origin and can be considered as central rogue wave. We show that the high-intensity narrow peak, with the complex intensity distribution in its vicinity, is enclosed by m ellipses consisting of the first-order Akhmediev breathers. The number of maxima on each ellipse is determined by its index and solution order [2].

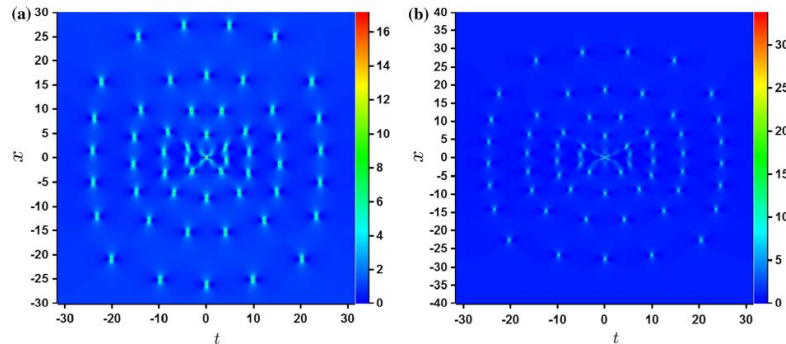


Figure 2: 2D color plots of rogue wave clusters on the uniform background having four ellipses ($m = 4$) around $n - 2m$ order rogue wave, formed at the origin $(0,0)$ of the (x,t) plane. The orders of Darboux transformation and the Akhmediev breather representing the high-intensity central peak are: (a) $n = 10$ with the second-order rogue wave, and (b) $n = 11$ with the third-order rogue wave.

References

- [1] Belić M.R., Nikolić S.N., Ashour O.A., Aleksić N.B. (2022) On different aspects of the optical rogue waves nature. *Nonlinear Dynamics* **108**:1655-1670.
- [2] Nikolić S.N., Alwashahi S., Ashour O.A., Chin S.A., Aleksić N.B., Belić M.R. (2022) Multi-elliptic rogue wave clusters of the nonlinear Schrödinger equation on different backgrounds. *Nonlinear Dynamics* **108**:479-490.

Effect of nonzero temperature on the process of penetration of the potential barrier through the kink

Jacek Gatlik* and Tomasz Dobrowolski*

**Doctoral School, Pedagogical University of Krakow, Kraków, Poland, ORCID 0000-0001-8678-7251*

***Pedagogical University of Krakow, Kraków, Poland, ORCID 0000-0001-7034-4229*

Abstract. The research focuses on studying the effect of thermal noise on the motion of a kink in a curved region of the Josephson junction. Results of simulations relying on the full field model were compared with the analytical formula proposed on the basis of the Foker-Planck equation. The obtained results show that for temperatures above 1 Kelvin the proposed analytical formula has very good agreement with the solutions of the full field model.

Introduction

In 1962 the British physicist B. Josephson presented a model describing the tunnelling of Cooper pairs between two superconductors separated by a thin insulator layer. Currently, a system composed of two superconductors separated by a thin insulator layer is called a Josephson junction. In the description of the Josephson junction the equation (sine-Gordon) appears which also has soliton solutions including the so-called fluxon defined as the soliton carrying the magnetic flux quantum.

The current research is concentrated on the impact of thermal noise on kink motion through the curved region of the long Josephson junction. We considered the kink motion in the modified sine-Gordon model with the position dependent dispersive term

$$\partial_t^2 \phi + \alpha \partial_t \phi - \partial_x (\mathcal{F}(x) \partial_x \phi) + \sin \phi = -\Gamma \quad (1)$$

where the function $\mathcal{F}(x)$ contains information about the curvature of the junction. In the equation α represents the dissipation in the system caused by quasiparticle current and Γ represents the bias current. The physical motivation for the description of curvature effects in the framework of this model has been detailed in the article [1]. Based on perturbation theory applied to the sine-Gordon equation with the perturbations from bias current (which describes the effects of non-zero temperature of the system), damping and the curved structure, a model for the kink velocity was derived. This approach, uses a method not previously applied to the sine-Gordon model, based on the projection of kink energy onto the dynamical equation of motion and was presented in detail in the article [1]. The probability distribution of the kink velocity was found on the base of the derived Fokker-Planck equation. The analytical results were compared with the simulations based on the full field model. Due to potential applications in normal and high-temperature superconductors, the comparison was made from zero to $T = 50K$, $T = 20K$, and $T = 5K$.

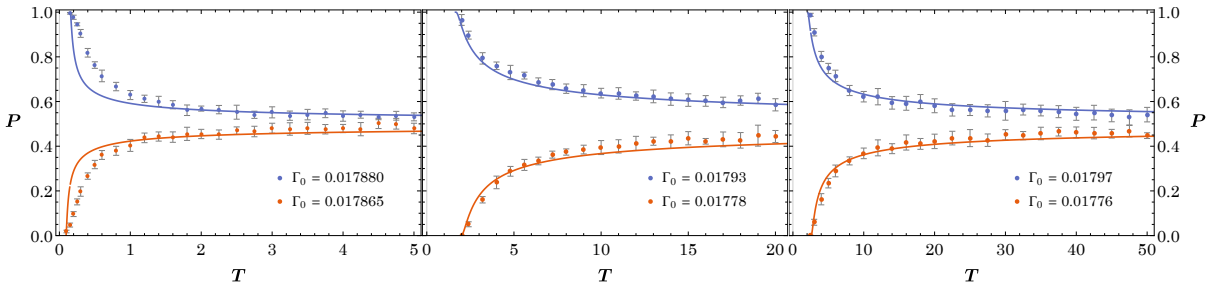


Figure 1: The probability of transition of the fluxon obtained from the field model compared in the various interval of T with the analytical formula. The blue line and points correspond to the bias current exceeding its threshold value and the red to the bias current below its threshold value.

Results and discussion

The agreement of the proposed model with the results from the full field model solutions is very good in the temperature range from $1K$ to $50K$. For temperatures below $1K$ a relativistic effect on the width of the kink was included in the analysis, but despite this, in the temperature range from $0K$ to $1K$ the model shows only partial agreement. The most likely reason for the discrepancy of the presented model with the results of the full model for temperatures below $1K$ is the presence of resonance windows, which were detected in the studied system.

References

- [1] Gatlik J., Dobrowolski T. (2021) Modeling kink dynamics in the sine-Gordon model with position dependent dispersive term. *Physica D* **428**:133061.
- [2] Gatlik J., Dobrowolski T. (2022) The impact of thermal noise on kink propagation through a heterogeneous system. arXiv:0706.1234 [nlin.PS].

Nonlinear distortion of high-intensity ultrasound holographic patterns

Ahmed Sallam* and Shima Shahab*

Mechanical Engineering Department, Virginia Tech, VA, USA

*ORCID 000-0002-2103-5443

** ORCID 000-0003-1970-5345

Abstract. High-intensity focused ultrasound (HIFU) is an emerging non-invasive therapeutic technology that has the potential to treat a wide range of medical disorders. By precisely focusing the ultrasonic energy, HIFU can heat up, destroy, or change target tissue. Acoustic holograms have been introduced as a novel and cost-effective method for creating elaborate and highly precise ultrasound fields. In HIFU, the linearity assumptions are no longer valid and will result in significant errors in the predicted sound field. The pseudospectral method was used to perform homogeneous three-dimensional nonlinear acoustic simulations. It will be shown that the nonlinear distortion leads to significant effects on the spatial distribution of the ultrasound field. The peak positive pressure and heat deposition become highly localized. While nonlinear effects flatten the peak negative pressure distribution with minimal and are shown to be vital for correctly estimating cavitation zones.

Introduction

Acoustic holograms are used for constructing elaborate focused ultrasound (FU) fields. By storing the phase information of the desired wavefront using a 3D-printed thickness map, the desired complex acoustic pressure field can be constructed by a single acoustic source. As the acoustic intensity increases, nonlinear effects become prominent leading to distorted and asymmetric waveforms. Studies that highlight the interaction of complex physics between the constructed holographic sound field and nonlinearities are absent. Here, the pseudospectral method is used to perform three-dimensional nonlinear acoustic simulations to investigate the evolution of modulated ultrasound field produced by an acoustic hologram as the acoustic intensity increases. The numerical model solves a set of coupled partial differential equations equivalent to a generalized Westervelt equation. The spatial pattern of the peak positive pressure, peak negative pressure, intensity, heat deposition, and cavitation zones were studied for a range of source pressure levels.

Results and discussion

The simulations were initiated with a linear sound field using a source pressure amplitude of $P_0 = 0.1$ MPa. The source amplitude was then increased to $P_0 = 1.8$ MPa to study the effects of rising nonlinearities on the sound field. As a result, the sinusoidal shape is distorted to a steeper waveform as the wave propagates further. Harmonics at integer multiples of the fundamental frequency are generated as a result of waveform distortion. Furthermore, diffraction effects cause a relative phase shift in the harmonics with respect to the fundamental component, resulting in an asymmetric waveform and a discrepancy between the peak positive pressure and the peak negative pressure as shown in figure 1. The peak positive pressure and heat deposition

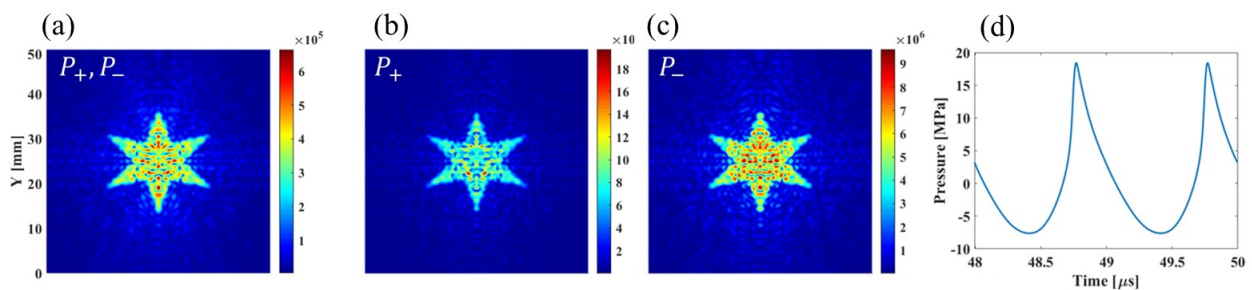


Figure 1: The distributions of linear amplitude [Pa] (a) at the target plane for a source pressure of $P_0 = 0.1$ MPa. Positive pressure [Pa] (b), negative pressure [Pa] (c) distributions at the target plane for a $P_0 = 1.8$ MPa source pressure and time waveform of the maximum positive pressure point (d).

become highly localized. Harmonic generation causes the heat deposition distribution to become extremely confined, with a nonuniformity index of 700%. While nonlinear effects flatten the peak negative pressure distribution and are shown to be vital for correctly estimating cavitation zones. Linear propagation predicts larger cavitation zones due to the higher gain of the linear negative pressure. Our findings guide the informed use of acoustic holograms in high-intensity focused ultrasound (HIFU). We also envision that this investigation would encourage the inclusion of nonlinear effects in the realm of computer-generated holography, allowing for the creation of specific HIFU fields to improve the efficacy and precision of therapeutic procedures.

References

- [1] Pierce, Allan D (2019) Acoustics: an introduction to its physical principles and applications.
- [2] Duck, Francis A and Baker, Andrew Charles and Starritt, Hazel C (2020) Ultrasound in medicine.

On the existence and properties of solitary waves traveling in tensegrity-like lattices

Julia de Castro Motta*, Ada Amendola* and Fernando Fraternali*

*Department of Civil Engineering, University of Salerno, Fisciano (SA), 84084, Italy

Abstract. Mass-spring chains equipped with tensegrity prisms that feature a locking-type response support the propagation of compression solitary waves under impulsive loading. We carry on an analytical study, analysing the existence and properties of solitary pulses travelling on tensegrity-like lattices, which exhibits an interaction potential similar to that of tensegrity prisms, but easier to handle analytically. Previous literature results were compared to the ones found in this study, revealing a good qualitative matching between the responses of tensegrity and tensegrity-like mass-spring chains. We show that the solitary pulses traveling in such systems tend to assume a peakon-like profile as the wave speed reaches a limit value v_{lim} , which produces the locking of the chain.

Introduction

It is known that 1D mass-spring chains equipped with tensegrity prisms that feature a locking-type response under compression loading (Fig.1(a)) support the propagation of compression solitary waves under impulsive loading [1-3]. This work presents an analytic study on the existence and properties of solitary waves on tensegrity-like lattices. These lattices are formed by a mass-spring chain, in which the nonlinear springs exhibit a tensegrity-like response. The interaction potential of the tensegrity-like lattices is similar to that of tensegrity prisms chains with locking-type response, but more manageable from the analytic point of view. Using Weierstrass theory of one-dimensional Lagrangian systems, it is possible to implicit derive the shape of the pulses traveling through tensegrity-like lattices.

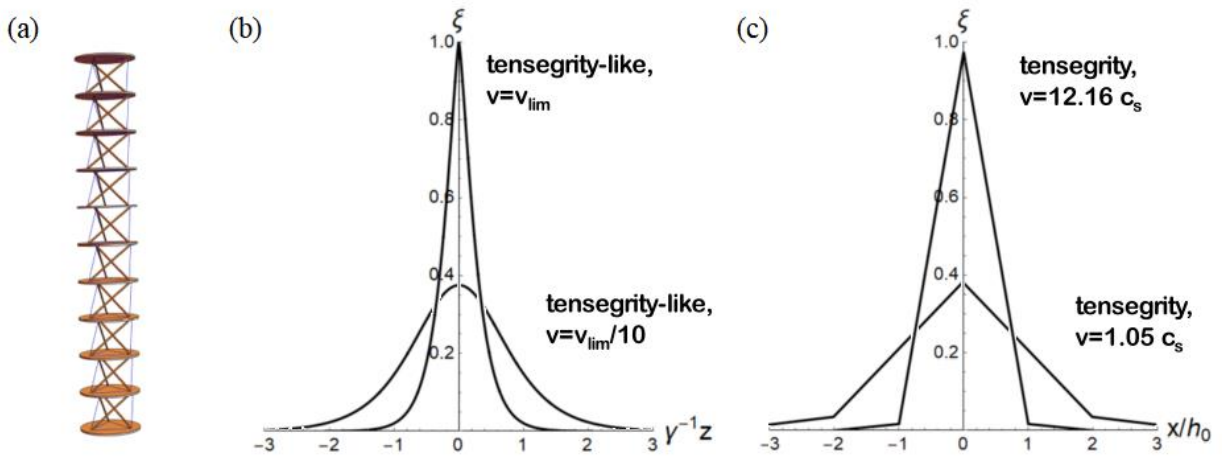


Figure 1: (a) Tensegrity mass-spring chain. (b) Wave profiles for different wave speeds: analytical results of the tensegrity-like lattices. (c) Wave profiles for different wave speeds: obtained numerically for tensegrity chains in [1].

Results and discussion

We show that the solitary pulses traveling in such systems exist. Moreover, we show that their shapes depend on the wave speed and tend to assume a peakon-like profile as the wave speed reaches a limit value v_{lim} , which produces the locking of the chain (Fig.1(b)). A comparative analysis with previous literature results was carried on (Fig.1(c)) revealing a good qualitative matching between the responses of tensegrity and tensegrity-like mass-spring chains, as both exhibit the localization behaviour as the wave speed is increased. This behavior can be applied on the design of mechanical metamaterials with wave-focusing capabilities, as well as new actuators/sensors for damage detection by the generation of stress waves. Furthermore, the stability of the solitary wave solutions obtained in this work can be investigated.

References

- [1] F. Fraternali, L. Senatore, C. Daraio, (2012) Solitary waves on tensegrity lattices. *J. Mech. Phys. Solids* **60** 1137-1144.
- [2] F. Fraternali, G. Carpentieri, A. Amendola, R.E. Skelton, V.F. Nesterenko, (2014) Multi- scale tunability of solitary wave dynamics in tensegrity metamaterials. *Appl. Phys. Lett.* **105** 201903.
- [3] A. Micheletti, G. Ruscica, F. Fraternali, (2019) On the compact wave dynamics of tensegrity beams in multiple dimensions. *Nonlinear Dyn.* **98** 2737-2753.

Harmonic Scattering of Waves from Crossed-Thin-Rectangular Nonlinear Inclusions

Pravinkumar Ghodake

Department of Mechanical Engineering, Indian Institute of Technology Bombay, Mumbai, India

Abstract. Nonlinear wave manipulations, like the presence and absence of higher harmonics and mode conversions due to harmonic scattering of nonlinear waves from uniquely proposed nonlinear inclusions, are demonstrated in this study using the finite element method due to the limitations of theoretical techniques. The sensitivity of the parameters that control the shape and distribution of nonlinear inclusions is explored to capture possible overall nonlinear effects due to complex harmonic scattering and interference of scattered waves. The exchange of harmonic energies between harmonically scattered longitudinal and transverse waves from multiple nonlinear inclusions is demonstrated. This study will help researchers to design nonlinear metamaterials to control nonlinear waves, as harmonic scattering manipulates nonlinear waves effectively.

Introduction

Interaction of monochromatic (f) longitudinal waves with the local single nonlinear inclusion modeled as quadratic and cubic nonlinear material results in harmonic scattering of the nonlinear waves; the theoretical solution is obtained by Kube (2017) using Green's functions [1]. Harmonically scattered waves show the presence of longitudinal and transverse waves and their higher harmonics ($2f$, $3f$) over the 360° scattered angles. This understanding is used to quantify highly local early-stage damages using a nonlinear ultrasonic technique [1]. As the number of nonlinear local damages increases, the complexity of multiple interactions of harmonically scattered waves increases, and theoretical techniques fall short of studying such problems. The finite element method is used in this study to understand the complex behavior of harmonically scattered nonlinear waves from multiple nonlinear inclusions of complex shapes. Considering the direction and mode dependency of harmonically scattered waves, a unique shape of nonlinear inclusion is proposed, as shown in Figure 1a, to explore the possibilities of nonlinear wave manipulations. Nonlinear inclusions are modeled as the Murnaghan hyperelastic material. There is no impedance mismatch between the matrix material and the embedded nonlinear inclusions.

Results and Discussion

The interaction of the monochromatic ($f = 2 \text{ MHz}$) longitudinal wave with the proposed shape of nonlinear inclusions shows the generation of higher harmonics ($2f$ & $3f$), as seen in Figure 2a. The harmonic responses of the received waves at transducer T_2 show that with an increase in the number of embedded nonlinear inclusions, the amplitude of higher harmonics decreases (Figure 1b) when $\theta = 45^\circ$.

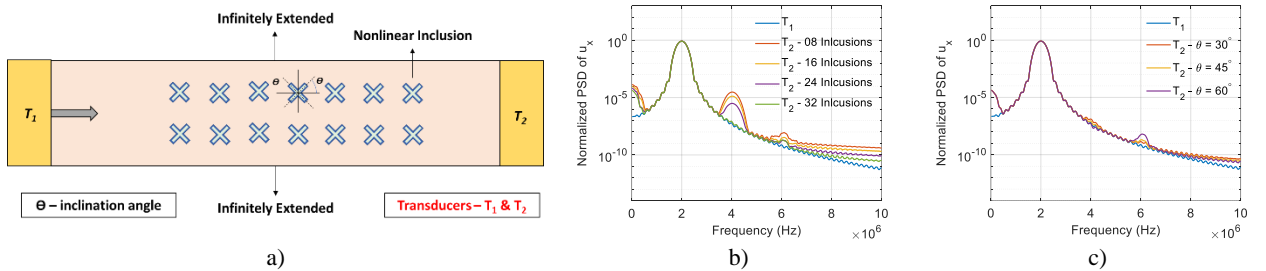


Figure 1: (a) Schematics of wave propagation in linear material embedded with nonlinear inclusions; frequency responses of the waves due to harmonic scattering (b) with an increase in the number of nonlinear inclusions by keeping $\theta = 45^\circ$ (c) with respect to the change in inclination angle of the crossed thin rectangles by keeping 32 nonlinear inclusions in the domain (T_1 – Input Transducer, T_2 – Receiving Transducer).

As the number of periodically spaced nonlinear inclusions reaches 32 (Figure 1b), 2^{nd} ($2f$) and 3^{rd} ($3f$) harmonics along with the static term ($0f$) go away despite the presence of such a high number of nonlinear inclusions, and this can be referred as an elastically invisible set of nonlinear inclusions. Due to multiple complex phenomena like harmonic scattering, mode conversion, and trapping of harmonically scattered waves in the linear regions because of interference, higher harmonics get canceled as they reach the receiving end. The change in inclination angle (θ) affects the amplitude of the 3^{rd} harmonics greatly, but it's nearly insensitive towards amplitudes of 2^{nd} harmonics (Figure 1c). Results clearly show that we can manipulate nonlinear waves by tuning parameters related to embedded nonlinear inclusions. These computational studies will motivate researchers to design novel nonlinear metamaterials.

References

- [1] Kube C. M. (2017) Scattering of Harmonic Waves from a Nonlinear Elastic Inclusion. J. Acoust. Soc. Am., 141(6):4756–4767.

Harmonic and superharmonic components in periodic waves propagating through mechanical metamaterials with inertia amplification

Marco Lepidi*, Valeria Settimi**

*DICCA - Dept of Civil, Chemical and Environmental Engineering, University of Genova, Italy

**DICEA - Dept of Civil and Building Engineering, and Architecture, Polytechnic University of Marche, Ancona, Italy

Abstract. In the nonlinear dynamics of periodic microstructured systems, the amplitude-dependent dispersion properties of mechanical metamaterials are attracting increasing interest. The paper investigates the free harmonic and superharmonic response of a non-dissipative one-dimensional waveguide with pantographic mass amplification. The effects of the quadratic and cubic inertia nonlinearities on the dispersion curve are analyzed. A perturbation strategy based on the Fourier series decomposition is adopted to determine the superharmonic amplitudes of the propagating periodic waves.

Introduction

The dispersion properties of microstructured periodic waveguides are a scientific topic of major interest in nonlinear dynamics. Particularly, the long-dating tradition of research studies concerning the propagation of nonlinear elastic waves in oscillator chains and other periodic structures [1, 2] is being catalyzed by the recent extraordinary development of microstructured materials and mechanical metamaterials [3]. Specifically, a pressing technological demand is boosting the innovation in the emerging field of architected passive media. In order to broaden the existing range of achievable functionalities, the periodic cell of mechanical metamaterials is often enriched with auxiliary flexible microstructures inducing relevant linear and nonlinear dynamic phenomena, like local resonances, controlled instabilities, gyroscopic couplings, inertia amplifications [4, 5].

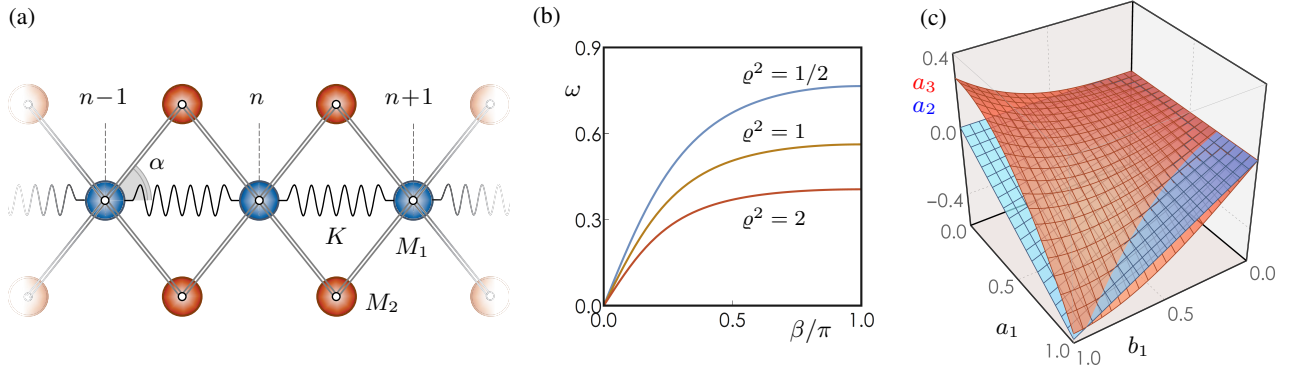


Figure 1: Mechanical metamaterial: (a) periodic atomic chain, (b) linear dispersion curves, (c) superharmonic amplitudes.

Results and discussion

A minimal physical system featured by a periodic pantographic mechanism of inertial amplification can be realized by an infinite one-dimensional non-dissipative chain of interconnected massive atoms (Figure 1a). In the periodic pantographic mechanism, two point masses (*primary blue atoms*) are elastically coupled to each other and rigidly connected to a pair of auxiliary point masses (*secondary red atoms*). The free undamped dynamics of the atomic chain is governed by a second-order differential (in time) difference (in space) equation with quadratic and cubic inertia nonlinearities. Attention is paid to the free propagation of harmonically periodic waves. To this purpose, the solution of the governing equation is expressed in a time-space Fourier series involving harmonic (ω) and superharmonic ($2\omega, 3\omega$) time components. Considering first the range of small oscillations, the amplitudes of the Fourier components are ordered in power series of a small perturbation parameter. Solving the resulting perturbation equations allows the parametric assessment of (i) the linear dispersion curve at the lowest order, exhibiting a marked dispersive behavior (Figure 1b), (ii) the nonlinear amplitude-dependent dispersion curve and (iii) the superharmonic amplitudes at the higher orders (Figure 1c).

References

- [1] Vakakis, A.F., King, M.E. (1995). Nonlinear wave transmission in a monocoupled elastic periodic system. *J. Acoust. Soc. Am.* **98**(3): 1534-1546.
- [2] Romeo F., Rega G. (2006). Wave propagation properties in oscillatory chains with cubic nonlinearities via nonlinear map approach. *Chaos Solitons Fractals* **27**(3): 606-617.
- [3] Hussein, M.I., Leamy, M.J., Ruzzene, M. (2014). Dynamics of phononic materials and structures: Historical origins, recent progress, and future outlook. *Appl. Mech. Rev.* **66**(4): 040802.
- [4] Settimi, V., Lepidi, M., Bacigalupo, A. (2021). Nonlinear dispersion properties of one-dimensional mechanical metamaterials with inertia amplification. *Int. J. Mech. Sci.* **201**: 106461.
- [5] Settimi, V., Lepidi, M., Bacigalupo, A. (2023). Analytical spectral design of mechanical metamaterials with inertia amplification. *Eng. Struct.* **274**: 115054.

Wave Propagation in Carbon Nanotube with Bilinear Foundation

B. Bharat *, K. R. Jayaprakash ** and S. Lenci ***

*Department of Mechanical Engineering, IIT Kharagpur, Kharagpur, West Bengal, India

**Discipline of Mechanical Engineering, IIT Gandhinagar, Gandhinagar, Gujarat, India

***Dipartimento di Ingegneria Civile, Edile e Architettura, Università Politecnica delle Marche, Ancona, Italy

Abstract The propagation of harmonic wave in an infinite, single walled carbon nanotube (SWCNT) supported on a bilinear elastic foundation is investigated. The SWCNT is modelled as a Euler Bernoulli beam incorporating nonlocal effects invoking using Eringen's stress gradient theory. The foundation stiffness is considered to be disparate in tension and compression, resulting in piecewise linear (PWL) foundation stiffness in the system. Two independent solutions corresponding to the mutually exclusive configurations are considered and impose the matching boundary conditions at the interface. We explore the effect of nonlocality on the realization and stability of traveling wave solutions in such a medium.

Introduction

In recent years, there has been increased interest in carbon nanotubes, their synthesis and mechanics owing to their exceptional mechanical and electrical properties [1]. To name a few, they are being investigated extensively for potential applications as sensors, fibres embedded into matrices, tunable oscillators etc. These studies have modelled these nanoscale systems using atomistic and continuum models. In this study we consider continuum elastic models of SWCNTs. As a result of their ability to undergo large, reversible deformations without developing lattice defects, SWCNTs are assumed to be elastic. There have been extensive studies of SWCNT dynamics using one-dimensional reduced order models such as Euler Bernoulli beam [2], Timoshenko beam and Sanders-Koiter thin shell theory. The nonlocal character of these small-scale systems is incorporated using the stress and strain gradient theory [3]. The SWCNTs are often supported on substrates with nonlinear stiffness and one class of such substrates is an essentially nonlinear PWL stiffness. The effect of PWL stiffness on the propagation characteristics of beams and strings has been studied by Lenci et al. [4]. However, the effect of PWL foundation on wave propagation in SWCNTs with nonlocal effects hasn't been considered previously and is the subject of this study.

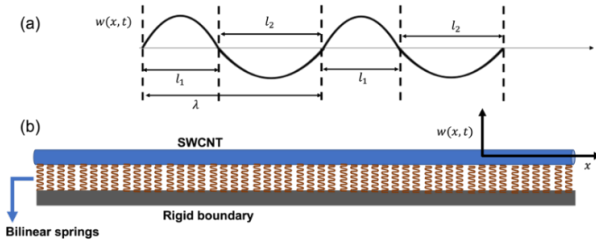


Figure 1: (a) Schematic of one dimensional SWCNT, (b) SWCNT supported on PWL spring

$$\rho_0 A w_{tt} + EI w_{4x} - \rho_0 A e_0^2 a^2 w_{ttxx} + k(w)w = 0 \quad (1)$$

$$k(w) = \begin{cases} k_1 & \forall w \geq 0 \\ k_2 & \forall w < 0 \end{cases}$$

The equation of motion (Eq. 1) of a SWCNT modelled as a Euler-Bernoulli beam of effective density ρ_0 , Young's modulus E supported on PWL foundation (refer Fig. 1) is shown above. We have incorporated the nonlocal parameter e_0 and a is the atomistic characteristic length [4]. The SWCNT is supported on a substrate with PWL stiffness $k(w)$. A single wave consisting of non-identical half wavelengths l_1 and l_2 as shown in Fig. 1(a) is considered. The essential and non-essential boundary conditions at the interface between the configurations $w \geq 0$ and $w < 0$ are matched and additionally, the wave speed for the two configurations is set equal so that the wave propagates without distortion. The resulting set of equations is numerically solved to obtain the half wavelengths, frequency and the constants of integration.

Results

A numerical analysis provides multiple solutions, whereas there are very few physically possible solutions satisfying the conditions. These solutions are numerically continued to explore their evolution as nonlocal and the asymmetry parameter are varied. As a result, stress gradient theory (nonlocality) increases the inertia effect, leading to a reduction in wave speed when compared to the regular beam equation. Asymptotic analysis is performed with the nonlocal parameter as a small parameter and its effect on the realization of periodic solutions and their stability.

References

- [1] Schodek S., Daniel L., Ferreira P., Ashby M. F. (2009) Nanomaterials, Nanotechnologies and Design: An Introduction for Engineers and Architects. Butterworth-Heinemann, Oxford
- [2] Huang K., Cai X., Wang M. (2020) Bernoulli-Euler beam theory of single-walled carbon nanotubes based on nonlinear stress-strain relationship. *Materials Research Express* **7**(12): 125003.
- [3] Gopalakrishnan S. (2016) Wave Propagation in Materials and Structures. CRC Press, Boca Raton
- [4] Demeio L., Lenci S. (2022) Periodic traveling waves in a taut cable on a bilinear elastic substrate. *Applied Mathematical Modeling* **110**: 603-627

Vacuum polarization energy in coupled-fermion ϕ^4 kink systems

Danial Saadatmand* ** and Herbert Weigel *

* *Institute for Theoretical Physics, Physics Department, Stellenbosch University, Matieland 7602, South Africa*

** *National Institute for Theoretical and Computational Sciences (NITheCS), South Africa*

Abstract. We study the quantum effects of kink solitons coupled to a bound fermion. In particular, we compute the fermion vacuum polarization energy that represents the renormalized Dirac sea contribution to the total energy.

Introduction

Boson field theory models in one time and one space dimensions ($D = 1 + 1$) wherein spontaneous symmetry breaking produces discrete, degenerate vacua are almost certain to contain (static) soliton solutions which are characterized by localized energy densities. The field equation for such a soliton is equivalent to minimizing the classical energy, E_{cl} . The leading, one-loop quantum correction to E_{cl} is the renormalized sum of the shifts of the zero point energies of the quantum fluctuations. These shifts reflect the polarization of the vacuum induced by the soliton and thus this quantum correction is frequently called the vacuum polarization energy E_{VPE} . Then $E_{\text{cl}} + E_{\text{VPE}}$ is next-to-leading in the semi-classical expansion.

In Refs.[1, 2] new soliton configurations were constructed by coupling the boson to a single fermion bound state and minimizing the quasi-classical energy which is the sum of E_{cl} and this bound state energy E . We have revisited [3] that construction for two reasons. First, in Refs.[1, 2] the Dirac sea contribution was omitted. But in any legitimate expansion scheme this contribution is of the same order as the one from the single level. Second, solutions with the single fermion occupying a negative energy level were also constructed. There is no physical interpretation of such a configuration without the Dirac sea. We therefore consider the fermion part of E_{VPE} which is the renormalized Dirac sea contribution to the energy.

In $D = 1 + 1$ the scalar field Φ is dimensionless while the fermion spinor Ψ has canonical energy dimension $\frac{1}{2}$. To make the Yukawa coupling constant g dimensionless we write the Lagrangian as

$$\mathcal{L} = \frac{1}{2} \partial_\mu \Phi \partial^\mu \Phi - \frac{\lambda}{4} \left(\Phi^2 - \frac{M^2}{2\lambda} \right)^2 + i \bar{\Psi} \not{\partial} \Psi - g \sqrt{\frac{\lambda}{2}} \bar{\Psi} \Phi \Psi. \quad (1)$$

Results and discussion

In all numerical simulations we set the scale by choosing $M = 2$ and eventually vary λ . We have reproduced the kink solitons reported in Ref.[1] who only considered $M^2 = 2\lambda$. In addition we have constructed solutions deviating from this particular case for different values of the Yukawa coupling constant g . Note that $M = 2$ causes g to be the mass of a non-interacting fermion since $\langle \Phi \rangle^2 = \frac{M^2}{2\lambda}$.

With the fermion coupling, the boson soliton profile is a distorted kink but it maintains to be odd under spatial reflection so that there are two parity channels of the fermion spinors. With this separation (the fermion part of) E_{VPE} can straightforwardly be computed using spectral methods [4]. Then the fermion contribution to the total energy has two components: $E + E_{\text{VPE}}$. In all cases considered we found that E_{VPE} adds positively. It is substantial and may even outweigh the energy gain from binding the single level so that $E + E_{\text{VPE}} \gtrsim g$. This suggests that a consistent treatment of the Dirac sea destabilizes the solutions from Ref.[1]; certainly this is the case when the single level is chosen to be a higher energy excited bound state.

We have also explored the parameter dependence of various energy components (classical, fermion and boson quantum corrections). From this we conjecture that the model is consistent only when $M^2 \gg \lambda$ and that significant binding of the fermions requires $g \sim \frac{M^2}{\lambda} \gg 1$. In that regime the solitons from Ref.[1] may be legitimate solutions.

References

- [1] Klimashonok V. Perapechka I. and Shnir Y. (2019) Fermions on kinks revisited. *Phys. Rev. D* **100**: 105003.
- [2] Gani V. A. Gorina A. Perapechka I. and Shnir Y. (2022) Remarks on sine-Gordon kink-fermion system: localized modes and scattering. *Eur. Phys. J. C* **82**: 757.
- [3] Saadatmand D. and Weigel H. (2022) Excited fermions on kinks and the Dirac sea. [arXiv:2212.02790 [hep-th]].
- [4] Graham N. Quandt M. and Weigel H. (2009) Spectral Methods in Quantum Field Theory. *Lect. Notes Phys.* **777**: 1.

Investigation of a nonlinear gradient elasticity model for the prediction of seismic waves

Andrei B. Fărăgău*, Marten Hollm**, Leo Dostal**, Andrei V. Metrikine*, and Karel N. van Dalen*

*Department of Engineering Structures, Delft University of Technology, Delft, the Netherlands

**Institute of Mechanics and Ocean Engineering, Hamburg University of Technology, Hamburg, Germany

Abstract. A novel nonlinear gradient elasticity model for predictions of the seismic waves has been proposed by the authors in previous works, where higher-order gradient terms are introduced to capture the effect of small-scale soil heterogeneity/micro-structure. Here, several characteristics of the proposed model are investigated in depth. More specifically, the behaviour of the system is investigated for initial conditions that induce different levels of nonlinearity. Results show that when the initial conditions induce a high nonlinearity in the system, the response can exhibit peculiar shapes. Furthermore, the nonlinear system predicts a non-zero plateau trailing behind as the initial shape propagates away. It is shown that the higher the initial nonlinearity, the more pronounced the plateau. These findings offer insight into the characteristics of the proposed nonlinear gradient elasticity model.

Introduction

The prediction of the so-called seismic site response (i.e., the response of the top soil layers induced by seismic waves) is important for designing structures in earthquakes prone areas. For seismic loads that induce large soil strains, accounting for the nonlinear behaviour of the soil can be of importance for accurate predictions. In a previous authors' work [1], a nonlinear gradient elasticity model was proposed for predicting the seismic site response. The nonlinear constitutive behaviour of the soil is governed by the hyperbolic soil model, in which the (secant) shear modulus G is dependent on the shear strain γ through a non-polynomial relation, as follows

$$G(\gamma) = \frac{G_0}{1 + (|\gamma|/\gamma_{\text{ref}})^\beta}, \quad (1)$$

where G_0 is the small-strain shear modulus and γ_{ref} and β are material constants. Furthermore, the classical wave equation was extended to a nonlinear gradient elasticity model to capture the effects of small-scale heterogeneity/micro-structure. The same model is used in this work too, in which a Gaussian pulse is imposed as an initial condition and the solution is determined using a novel finite difference scheme (see Ref. [1]). This work investigates the behaviour of the proposed model for different levels of initial nonlinearity. Namely, γ_{ref} is varied such that the initial nonlinearity induced by the initial conditions varies. This study offers insight into the characteristics of the proposed nonlinear gradient elasticity model.

Preliminary results

Compared to the classical continuum, higher-order gradient terms are introduced into the equation of motion, which lead to dispersive effects [2] prohibiting the formation of un-physical jumps in the response. Fig. 1 shows that the higher the induced nonlinearity, the more skewed the response; for extremely high nonlinearity, the response exhibits peculiar shapes (see right panel). Furthermore, the higher the nonlinearity, the more pronounced the plateau trailing behind the bulk of the propagating shape. The in-depth investigation of the proposed model's characteristics can be helpful when using it to accurately predict the seismic site response.

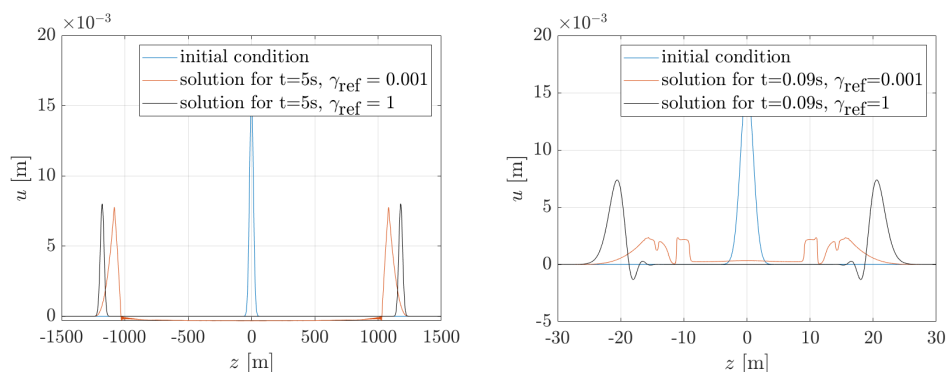


Figure 1: Displacement fields for varying levels of initial nonlinearity: quasi-linear ($\gamma_{\text{ref}} = 1$), mild nonlinearity ($\gamma_{\text{ref}} = 0.001$, left panel) leading to $G(\gamma_{\text{max}}) = 0.6G_0$, and extreme nonlinearity ($\gamma_{\text{ref}} = 0.001$, right panel) leading to $G(\gamma_{\text{max}}) = 0.1G_0$. The initial pulse is much thinner in the right panel causing a higher nonlinearity.

References

- [1] Dostal L., Hollm M., Metrikine A.V., Tsouvalas A., van Dalen K.N. (2022) Localized stationary seismic waves predicted using a nonlinear gradient elasticity model. *Nonlinear Dyn* **107**:1107-1125.
- [2] Metrikine A. (2006) On causality of the gradient elasticity models. *J. Sound Vib.* **297**:727-742.

Fast numerical solution to nonlinear shallow water system

Mikhail Lavrentiev*, Andrey Marchuk**, Konstantin Oblaukhov* and Mikhail Shadrin*

*Institute of Automation and Electrometry SB RAS, Novosibirsk, Russia

**Institute of Computational Mathematics & Math Geophysics SB RAS, Novosibirsk, Russia

Abstract. The paper presents a fast numerical solution to nonlinear shallow water system with the use of an ordinary personal computer. It should help with the timely evaluation of tsunami wave potential threats at a particular part of the coast. High performance is achieved by using hardware acceleration which is a specialized Calculator, based on the Field Programmable Gates Array (FPGA) microchip. Precision of the obtained numerical solutions was proved by comparing it to the available existing solutions. The achieved performance makes it possible to calculate the wave parameters along the coast within a minute, provided that the initial sea surface displacement at tsunami source is given. In case of a strong seismic event offshore Japan, it takes nearly 20 minutes for tsunami wave to reach the nearest coast. The proposed approach can provide tsunami warning centres with the decision support information about evacuation measure before the wave reaches the coast.

Introduction

After the Great Tohoku Earthquake of March 11, 2011 offshore Japan, it became clear that tsunami warning systems could be significantly improved. For the local tsunami, it takes nearly 20 min to propagate from the source to the nearest coast. Modern software packages, such as: MOST (Method of Splitting Tsunamis, NOAA Pacific Marine Environmental Laboratory, Seattle, WA USA) [1] and TUNAMI-N1/TUNAMI-N2 (Tohoku University, Japan) [2], provide high accuracy simulation of the tsunami wave generation, propagation, and inundation. However, they cannot deliver the needed analysis in a few minutes even when relying on the supercomputer processing. It should be also noted that disaster events, such as the one of March 11, 2011, may lead to power shutdowns. At the same time, in order to evaluate possible negative tsunami wave implications (including infrastructure destruction and loss of human life), one does not need to know the exact wave amplitude at a particular populated coastal area or industrial site.

So, the desired tsunami warning system must: (1) work very fast (within several minutes), (2) be independent of power supply (in case of emergency) and (3) provide a realistic approximation of tsunami wave height (10% accuracy or slightly higher would be acceptable). All these requirements could be achieved by using an ordinary modern personal computer with the specialized co-processor – the FPGA based Calculator, proposed and tested in [3].

Results and Discussion

A parallel version of the McCormack finite-difference scheme (which has the second order approximation) was implemented on the FPGA platform. It takes only 38.4 sec to simulate 1-hour (7,200 time steps) wave propagation for the digital bathymetry grid of 2401x2401 nodes. Geographically small changes in tsunami source position (given in Fig. 1, left) result in valuable changes in the wave maximal heights distribution.

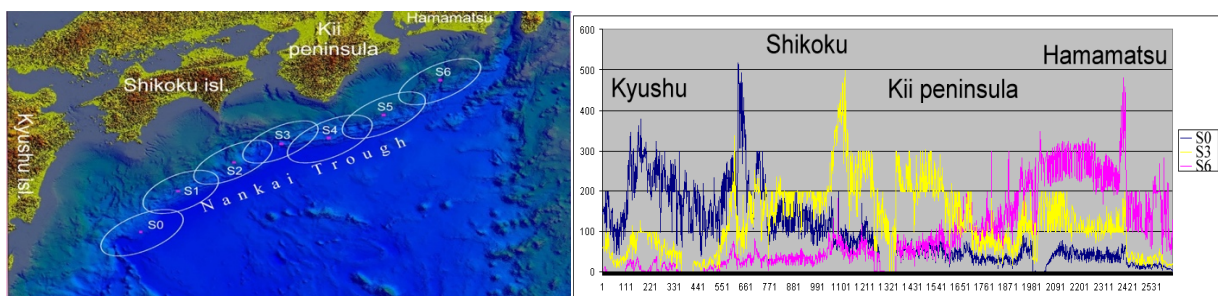


Figure 1. Digital bathymetry, water area southwest of Japan. Ellipses S0-S6 show positions of model tsunami sources (left). Distribution of tsunami wave maximal heights along the coast. Blue line = S0 model source, yellow line = S3 source, pink line = S6 source (right).

Using the hardware acceleration (FPGA-based Calculator), it is possible to determine “safe” and “dangerous” locations along the coast within a few minutes calculating wave propagation over the several hundred kilometers wide water area. It is expected that in a few years tsunami warning systems will be able to save human lives and reduce economic loss even in cases of strong offshore earthquakes.

References

- [1] Gica E., Spillane M., Titov V., Chamberlin C., Newman J. (2008) Development of the forecast propagation database for NOAA’s short-term inundation forecast for tsunamis (SIFT). NOAA Technical Memorandum, 2008.
- [2] Yalciner A.C., Alpar B., Altinok Y., Ozbay I., Imamura F. (2002) Tsunamis in the Sea of Marmara: Historical Documents for the Past, Models for Future. *Marine Geology* **190**:445-463.
- [3] Lavrentiev M.M., Lysakov K.F., Marchuk An.G., Oblaukhov K.K., Shadrin M.Yu. Hardware/Software Solution for Low Power Evaluation of Tsunami Danger (2022) *J. Low Power Electronics&Appl* **12**:1-16.

On the asymptotical description of solutions to the matrix modified Korteweg-de Vries equation

Sandra Carillo^{*,**} and Cornelia Schiebold^{***}

^{*}Dipartimento di “Scienze di Base e Applicate per l’Ingegneria” LA SAPIENZA - Università di Roma, Rome, Italy

^{**}I.N.F.N. - Sezione Roma1, Gr. IV - Mathematical Methods in NonLinear Physics (MMNLP), Rome, Italy

^{***}Department of Science Education and Mathematics Mid Sweden University, Sundsvall, Sweden

Abstract. Noncommutative integrable systems extend classical soliton equations like the Korteweg-de Vries or the Nonlinear Schrödinger equation to the level of equations in (at least) matrix-valued functions. Characteristic properties - like nonlinear superposition - reemerge, but usually in more complicated form, which requires deeper investigation. The results represent a further development of the study in [3] and [4] which answers to the question to understand the asymptotical behaviour of special cases of matrix solutions of the mKdV equation.

Introduction

The equations under investigation is the matrix mKdV equation: $V_t = V_{xxx} + 3\{V^2, V_x\}$, where capital case is used to denote that the unknown are, in general, operators and, hence, non commutativity property is assumed. In the present investigation the attention is focussed on the case when V , is represented by a 2×2 matrix. Motivated by explicit solutions given in [4] with striking interaction behaviour, the aim of the present work is to contribute to a better understanding of 2-soliton solutions to the matrix modified Korteweg-de Vries (mKdV) equation by providing an explicit asymptotic analysis for solutions with regular spectral matrices (in the sense of [10]). The main tool is a parameter-dependent formula for the N-soliton solutions to the matrix modified Korteweg-de Vries equation given in [7] (see also [3] for an explicit proof). An asymptotic description of the 2-soliton solutions (for the $d \times d$ -matrix mKdV) in the case that the spectral matrices are invertible. An example is provided in the two pictures where the soliton behaviour emerges.

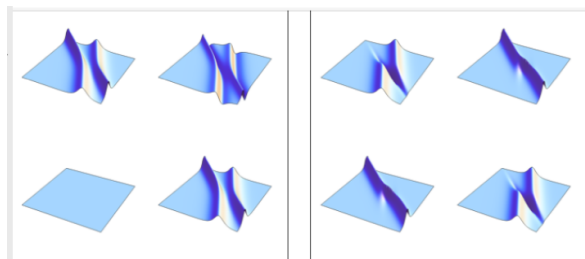


FIGURE 1. The solutions in Example 1 are depicted for $-10 \leq x \leq 10$ and $-5 \leq t \leq 5$ with plot range between $-\sqrt{2}$ and $\sqrt{2}$, the solution in a) to the left, the solution in b) to the right.

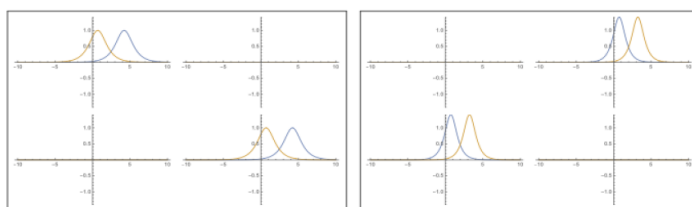


FIGURE 2. The solution from Example 1 a) is plotted for $t = -20$ (the brown curve) and $t = 20$ (the blue curve). The plot to the left is plotted in the frame $(x-t, t)$, the plot to the right in $(x-2t, t)$, both for $-10 \leq x \leq 10$ with plot range between $-\sqrt{2}$ and $\sqrt{2}$.

As a result, we obtain - precisely as in the scalar case - that the collision is elastic and only results in a phase-shift. This is in contrast to interactions involving a non-invertible spectral matrix, which may in addition lead to a change of the asymptotic appearance of the interacting waves.

References

- [1] S. Carillo, *KdV-type equations linked via Bäcklund transformations: remarks and perspectives*, Applied Numerical Mathematics, **141** (2019) pp. 81-90.
- [2] S. Carillo, M. Lo Schiavo, E. Porten, C. Schiebold, *A novel noncommutative KdV-type equation, its recursion operator, and solitons*, J. Math. Phys., **59**, (4), (2018), 14 pp.
- [3] S. Carillo, M. Lo Schiavo, C. Schiebold, *Matrix soliton solutions of the modified Korteweg-de Vries equation*, NODYCON 2019 Springer Proceedings, B. Balachandran, J. Ma, W. Lacarbonara, G. Quaranta, J. Machado, G. Stepan, Ed.s, (2020), 75-83.
- [4] S. Carillo, C. Schiebold, *Construction of soliton solutions of the matrix modified Korteweg-de Vries equation*, NODYCON 2021 Springer Proceedings, B. Balachandran, J. Ma, W. Lacarbonara, G. Quaranta, J. Machado, G. Stepan, Ed.s, (2020), 75-83.
- [5] S. Carillo, M. Lo Schiavo, C. Schiebold, *Bäcklund Transformations and Non Abelian Nonlinear Evolution Equations: a novel Bäcklund chart*, SIGMA, **12** (2016), 087, 17 pages, doi:10.3842/SIGMA.2016.087.
- [6] S. Carillo, M. Lo Schiavo, C. Schiebold, *Abelian versus non-Abelian Bäcklund Charts: some remarks*, Evolution Equations and Control Theory, **8** (1), (2019), 43-55.
- [7] S. Carillo, M. Lo Schiavo, C. Schiebold, *N-soliton matrix mKdV solutions: a step towards their classification*, preprint.
- [8] S. Carillo, C. Schiebold, *Non-commutative KdV and mKdV hierarchies via recursion methods*, J. Math. Phys. **50** (2009), 073510.
- [9] S. Carillo, C. Schiebold, *Matrix Korteweg-de Vries and modified Korteweg-de Vries hierarchies: Non-commutative soliton solutions*, J. Math. Phys. **52** (2011), 053507.
- [10] V.M. Goncharenko, *Multisoliton solutions of the matrix KdV equation*, Theor. Math. Phys. **126**, (2001).
- [11] C. Rogers, W.K. Schief, *Bäcklund and Darboux Transformations: Geometry and Modern Applications in Soliton Theory*, Cambridge University Press, Cambridge, 2002.

Self-adaptive wave propagation and synthetical vibration reduction of strongly nonlinear mechanical metamaterials

Xin Fang*, Peng Sheng*, Chen Gong** and Li Cheng**

*National University of Defense Technology, Changsha, Hunan, China; E-mail: xinfangdr@sina.com

**Department of Mechanical Engineering, Hong Kong Polytechnic University, Hung Hom, Kowloon, Hong Kong, China

Abstract. We find and demonstrate that the band structure or bandgap inside a nonlinear metamaterial self-adapts to propagation space and time, which breaks the understanding indicated by Bloch theorem. Moreover, we realized the synthetical vibration reduction (low-frequency, broadband, light-weight, highly efficient, and strong environmental suitability) desired in most engineering applications.

Introduction

Nonlinear acoustic/elastic metamaterials (NAMs) refer to mechanical metamaterials possess strongly nonlinear dynamic effects that trigger many peculiar behaviors. Their unusual properties for controlling elastic wave are attracting rising attention. Many new unusual properties remain unveiled. Moreover, strongly nonlinear metamaterials can present ultralow and ultrabroad band attenuation of vibration and sound radiation. However, it is very challenging to conceive a vibration control measure that simultaneously possess the capability of low-frequency, broadband, light-weight, highly efficient, and strong environmental suitability. Such synthetical vibration reduction is highly desired in most engineering applications such as the aircraft, spacecraft and high-speed trains need.

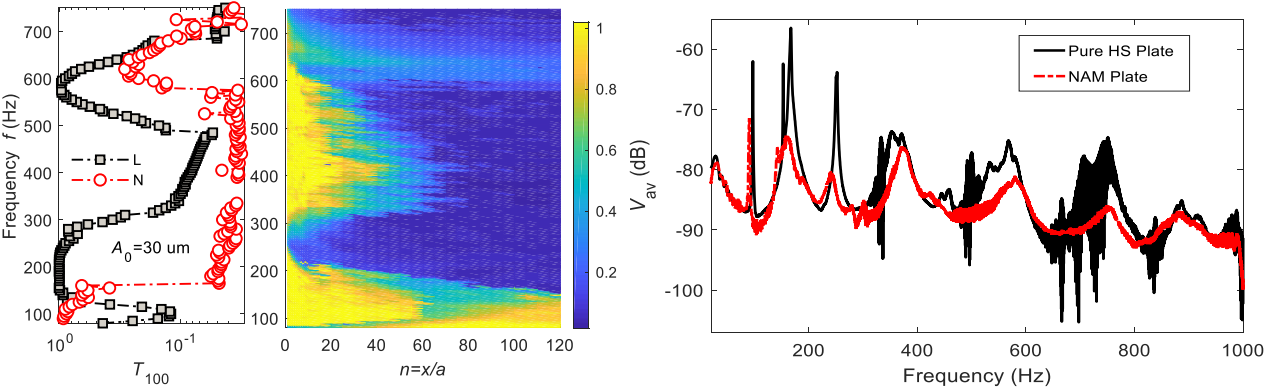


Figure 1: Self-adaptive wave propagation and synthetical vibration reduction effects

Results and discussion

This paper reports two aspects of the latest progress on nonlinear metamaterials: (1) Band degeneration and self-adaptive propagation. Bandgap and band properties play important roles in wave manipulation of metamaterials. We find that the strongly nonlinear metamaterials present particular band degeneration and bifurcation, accompanied with the wave mode transfer in their unit cells. More importantly, we find and demonstrate that the band structure or bandgap inside a nonlinear metamaterial self-adapts to propagation space and time, which breaks the understanding indicated by Bloch theorem. The self-adaptivity is a general physical property for different nonlinear metamaterials. (2) Synthetical unusual vibration reduction. We systematically investigate the vibration and sound radiation of strongly nonlinear elastic metamaterial plates or beams. We find that the double-ultra effect is sensitive to the bridging coupling between nonlinear local resonances, but is non-sensitive to the attached mass, indicating an exceptional way to achieve “light-weight”. Furthermore, we optimize the vibration reduction of metamaterial beams, stiffened plate and sandwich honeycomb plate. Our experiments demonstrate that the nonlinear metamaterial design can reduce the vibration in 0~1000 Hz of stiff structures by 10-20 dB with only 6%~20% attached mass. The synthetical unusual vibration reduction is achieved. All these indicate the significant application prospect of strongly nonlinear metamaterials.

References

- [1] Fang X., Wen J., Bonello B., Yin J., Yu D. (2017) Ultra-low and ultra-broad-band nonlinear acoustic metamaterial. *Nature Commu.* 8: 1288
- [2] Fang, X., Wen, J., Benisty H., Yu, D. (2020) Ultrabroad acoustical limiting in nonlinear metamaterials due to the adaptive-broadening bandgap effect. *Phys. Rev. B* 101, 104304
- [3] Sheng P., Fang X., Dai L., Yu D., Wen J. (2023) Synthetical vibration reduction of the nonlinear acoustic metamaterial honeycomb sandwich plate. *Mech. Syst. Signal Pr.* 185: 109774

A vorticity wave packet breaking within a rapidly rotating vortex

Philippe Caillol

Department of Fundamental Sciences, Exact Science Center (CCE),
University of Bio-Bio ORCID # 0000-0002-6548-2595, Chile

Abstract. This study considers the interaction between a free vorticity wave packet and a rapidly rotating vortex in the slowly-evolving regime, a long time after the initial, unsteady, and strong interaction. The interaction starts when the amplitude modulated neutral mode enters resonance with the vortex on a spiraling critical surface, where the phase angular speed is equal to the rotation frequency. The singularity in the modal equation on this asymmetric surface strongly modifies the flow in its neighborhood, the three-dimensional (3D) helical critical layer, the region where the wave/vortex interaction occurs. Through matched asymptotic expansions, we find an analytical solution of the leading-order motion equations inside the 3D critical layer (CL). The system of the coupled evolution equations of the wave amplitude and the low-order CL-induced mean flow on the critical radius has been derived in the quasi-steady regime. The main outcome is that the wave packet/vortex interaction leads to a fast vorticity wave breaking.

Introduction

Though the motion in intense atmospheric vortices such as tropical cyclones can be considered highly axisymmetric above the surface boundary layer, observation often shows asymmetric features. The latter are generated, for instance, by the environmental wind shear, the beta effect, turbulent stress at the sea surface, and moist convection. Through a radiating wave-induced axisymmetric adjustment, these asymmetries are believed to play a significant role in the intensification of these vortices [1]. Latent heat release, for example, creates asymmetric potential vorticity (PV) anomalies that outward propagate in the form of PV waves; their breaking was recently related to the inner spiral rainbands. Observation and numerical simulations indeed show that inner spiral bands mainly exhibit vorticity wave characteristics [2].

Understanding the dynamics of these spiral bands and their contribution to the vortex evolution can greatly help improving the prediction of violently rotating vortex intensity. Wave activity analysis in numerical hurricane-like vortex models shows that vortices only interact with vorticity waves and that the related modes are continuous, that is, admit a CL singularity. This study therefore wishes to improve the understanding of the nonlinear dynamics of continuous vorticity modes embedded in rapidly rotating vortices. In particular, it examines the complex dynamical coupling between a vorticity wave packet and the azimuthally averaged 3D wind through the nonlinear CL theory in the quasi-stationary state assumption. In the previous analytical studies dealing with 2D or 3D, nonlinear and singular wave packets, the induced mean flow was however omitted, which was a stringent mistake.

Results and discussion

This interaction generates a vertically sheared 3D mean flow of higher amplitude than the wave packet. The chosen envelope regime assumes the formation of a mean radial velocity of the same order as the wave packet amplitude, deviating the streamlines in a spiral way with respect to the rotational wind. The critical layer pattern, strongly deformed by the mean radial velocity, loses its symmetries with respect to the azimuthal and radial directions [3]. The knowledge of the wave amplitude, the leading-order mean axial and azimuthal velocity, and axial vorticity evolutions at the critical radius can be simply determined from three first-order differential equations. Numerical simulations of the first-order mean flow truncated system show that the wave packet and vortex kinetic energies slightly grow inside the envelope before the breaking onset in most of the cases, whereas the vortex was intensifying at the expense of the wave packet in the previous and unsteady interaction. The vertical wind shear has the highest effect on the wave/mean flow interaction. When the shear is moderate, it enhances intensification but when it is very large, it prohibits it in both the unsteady and slowly evolving stages [4]. Including the second-order mean flow in this system could, however, avoid the breaking and would permit the interaction to generate an asymptotic constant-speed travelling coherent vortical structure.

References

- [1] Montgomery M. T., Kallenbach R. J. (1997) A theory for vortex Rossby-waves and its application to spiral bands and intensity changes in hurricanes. *Q. J. R. Meteorol. Soc.* **123**:435-465.
- [2] Chen Y., Brunet G., Yau M. K. (2003) Spiral bands in a simulated hurricane. Part II: Wave activity diagnostics. *J. Atmos. Sci.* **60**:1239-1256.
- [3] Caillol P. (2022) A vorticity wave packet breaking within a rapidly rotating vortex. Part I: The critical layer flow. *Stud. Appl. Math.* **148**:825-864.
- [4] Caillol P. (2022) A vorticity wave packet breaking within a rapidly rotating vortex. Part II: Wave/ mean flow interaction. *Stud. Appl. Math.* **148**:865-917.

Chirped optical solitons in fiber Bragg gratings with dispersive reflectivity

Khalil S. Al-Ghafri* and Mani Sankar*

*University of Technology and Applied Sciences, P.O. Box 14, Ibri 516, Oman

Abstract. The present work investigates the chirped optical solitons in a medium of fiber Bragg gratings (BGs) with dispersive reflectivity. BGs is considered here with polynomial law of nonlinear refractive index. The model of coupled nonlinear Schrödinger equations is analyzed and reduced to an integrable form under specific conditions. The results are obtained with the aid of soliton ansatz technique. Different structures of wave solutions including W-shaped, bright, dark, kink and anti-kink solitons are retrieved and their behaviors are presented so as to enhance the applications of fiber BGs.

Introduction

The data transmission through optical fiber for intercontinental distances is based on soliton propagation that arises due to delicate balance between chromatic dispersion (CD) and fiber nonlinearity. However, the CD may have low count that leads to limit the transmission distances. Thus, Bragg gratings (BGs) is found to be one of the effective techniques to tackle this problem by introducing induced dispersion to compensate for low CD and subsequently ensure the existence of soliton transmission. In literatures, many studies have been carried out using the technology of fiber BGs to investigate chirped and chirp-free optical solitons with different forms of nonlinearity, see [1–4]. The current study mainly discusses the dimensionless form of the coupled nonlinear Schrödinger equations in fiber BGs having polynomial law of nonlinearity given by [4]

$$iq_t + a_1 r_{xx} + (b_1 |q|^2 + c_1 |r|^2)q + (d_1 |q|^4 + f_1 |q|^2 |r|^2 + g_1 |r|^4)q + (l_1 |q|^6 + m_1 |q|^4 |r|^2 + n_1 |q|^2 |r|^4 + p_1 |r|^6)q + i h_1 q_x + k_1 r = 0, \quad (1)$$

$$ir_t + a_2 q_{xx} + (b_2 |r|^2 + c_2 |q|^2)r + (d_2 |r|^4 + f_2 |r|^2 |q|^2 + g_2 |q|^4)r + (l_2 |r|^6 + m_2 |r|^4 |q|^2 + n_2 |r|^2 |q|^4 + p_2 |q|^6)r + i h_2 r_x + k_2 q = 0, \quad (2)$$

where the functions $q(x, t)$ and $r(x, t)$ stand for forward and backward propagating waves, respectively, whereas a_j for $j = 1, 2$ represent the coefficients of dispersive reflectivity. In the coupled equations above, b_j indicate the coefficients of self-phase modulation (SPM) and c_j denote the cross-phase modulation (XPM) for cubic nonlinearity portion. For quintic nonlinear part, d_1 are the coefficients of SPM while f_j and g_j are the coefficients of XPM. Regarding septic nonlinearity, l_j are the coefficients of SPM while m_j, n_j and p_j are the coefficients of XPM. Finally, h_j accounts for inter-modal dispersion and k_j define detuning parameters. All of the coefficients are real valued constants and $i = \sqrt{-1}$.

The objective of the present study is to investigate chirped optical solitons in fiber BGs. The system of equations (1) and (2) is handled with the help of traveling wave transformation and then some specific conditions are assumed to ensure an integrable form for the coupled system. The generated traveling wave reduction is effectively solved by means of soliton ansatz method which yields various forms of chirped optical solitons.

Results and discussion

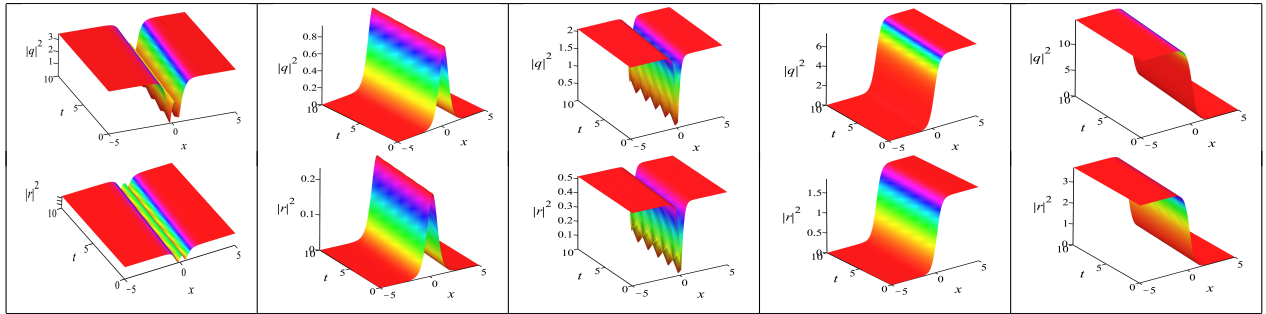


Figure 1: The profile of W-shaped, bright, dark, kink and anti-kink solitons.

The derived wave solutions for the model of the coupled NLSE (1) and (2) describe distinct chirped solitons having nonlinear phase functions in terms of the reciprocal of amplitude function which are entirely different from the previous studies in the literature. The obtained optical solitons include several forms such as W-shaped, bright, dark, kink and anti-kink solitons. These new results obtained here are expected to contribute in improving the experimental studies and engineering applications related to fiber BGs.

References

- [1] Biswas A., Ekici M., Sonmezoglu A., Belic M.R. (2019) *Optik* **185**:50.
- [2] Zayed E., Alngar M., Biswas A., Ekici M., Alzahrani A., Belic M. (2020) *J. Commun. Technol. Electron.* **65**:1267.
- [3] Yildirim Y., Biswas A., Khan S., Guggilla P., Alzahrani A.K., Belic M.R. (2021) *Optik* **237**:166684.
- [4] Zayed E.M., Alngar M.E., Biswas A., Ekici M., Triki H., Alzahrani A.K., Belic M.R. (2020) *Optik* **204**:164096.

Real-time modelling of vehicle's longitudinal-vertical dynamics in ADAS applications

Wei Dai*, Yongjun Pan* and Chuan Min*

*College of Mechanical and Vehicle Engineering, Chongqing University, Chongqing 400044, China

Abstract. We develop an efficient vehicle multibody model for longitudinal-vertical dynamics used in ADAS applications. The dynamic properties of the chassis, suspensions, and tires are considered and modelled, which results in accurate vehicle dynamics and states. This vehicle system is modelled using a semi-recursive multibody dynamics formulation, the vehicle kinematics and dynamics are obtained accurately via the system tree-topology. In addition, a fork-arm removal technique is proposed to reduce the number of bodies, relative coordinates, and loop-closure constrained equations. Finally, the dynamic simulations of the vehicle are performed on the bumpy and slope roads. The numerical results are compared with the reference data both in accuracy and efficiency. The comparative results verify the effectiveness of the proposed vehicle model.

Introduction

In recent years, several advanced driver assistance systems (ADAS) have been studied in terms of ride comfort, transportation safety, and efficiency. These ADAS applications require accurate and efficient vehicle models to acquire vehicle states and dynamic responses that can be used for intelligent control. In addition, vehicle multibody models must run robustly and in real-time on hardware with limited memory. For this reason, it is crucial to develop efficient multibody modelling techniques for autonomous vehicles.

Modelling of Vehicle Coupling Dynamics

The longitudinal-vertical dynamics of an autonomous vehicle is modelled using an efficient semi-recursive multibody method. This 7-DOF vehicle model based on the sophisticated 14-DOF model is created to reduce the size and complexity of the vehicle system for greater efficiency and its motion equations can be written as

$$\mathbf{R}_z^T \mathbf{R}_d^T \mathbf{M}^\Sigma \mathbf{R}_d \mathbf{R}_z \ddot{\mathbf{z}}^i = \mathbf{R}_z^T \mathbf{R}_d^T \left(\mathbf{Q}^\Sigma - \mathbf{T}^T \bar{\mathbf{M}} \frac{d(\mathbf{T} \mathbf{R}_d \mathbf{R}_z)}{dt} \dot{\mathbf{z}}^i \right) \quad (1)$$

where \mathbf{T} is the path matrix. \mathbf{R}_d and \mathbf{R}_z respectively represent the first and second velocity transformation matrices; $\bar{\mathbf{M}}$ are the inertia matrices of the whole system. \mathbf{Q}^Σ represents the accumulated external forces of the vehicle system; $\ddot{\mathbf{z}}^i$ and $\dot{\mathbf{z}}^i$ are the set of independent relative accelerations and velocities respectively. In addition, a fork-arm removal technique is proposed. The fork-arm in the MacPherson independent suspension is viewed as the combination of two rigid rods. By using the rod-removal technique to remove those equivalent rigid rods, the fork-arm is represented by two equations with constant-length constraints.

Results in Accuracy and Efficiency

The dynamic simulations of the 7-DOF vehicle multibody model on both bumpy and sloping roads are conducted. A 14-DOF vehicle multibody model and the proposed vehicle model are compared in terms of their solution accuracy and efficiency. Their results of X- and Z-axis displacement and velocity, as well as pitch angle and rate are nearly identical when the vehicle traverses the bumpy road or the sloping road. And the CPU time for a dynamic simulation on bumpy and sloping roads is 4.806 s and 4.790 s, respectively. The respective efficiencies increased by 35.37% and 35.14% in comparison to the 14-DOF vehicle model. The dynamic simulations on bumpy and sloping roads verify the effectiveness of the proposed vehicle model and the efficiency of the simulation calculations.

References

- [1] Jiménez, F.; Naranjo, J.E.; Anaya, J.J.; García, F.; Ponz, A.; Armingol, J.M. Advanced driver assistance system for road environments to improve safety and efficiency. *Transp. Res. Procedia* 2016, 14, 2245–2254.
- [2] Pan, Y.; Callejo, A.; Bueno, J.L.; Wehage, R.A.; García de Jalón, J. Efficient and accurate modeling of rigid rods. *Multibody Syst. Dyn.* 2017, 40, 23–42.
- [3] Mahalingam, I.; Padmanabhan, C. A novel alternate multibody model for the longitudinal and ride dynamics of a tracked vehicle. *Veh. Syst. Dyn.* 2021, 59, 433–457.
- [4] García de Jalón, J.; Álvarez, E.; de Ribera, F.; Rodríguez, I.; Funes, F. A Fast and Simple Semi-Recursive Formulation for Multi-Rigid-Body Systems. In *Advances in Computational Multibody Systems*; Ambrósio, J., Ed.; Computational Methods in Applied Sciences; Springer: Dordrecht, The Netherlands, 2005; Volume 2, Chapter 1, pp. 1–23.
- [5] García de Jalón, J.; Bayo, E. *Kinematic and Dynamic Simulation of Multibody Systems: The Real Time Challenge*; Springer-Verlag: New York, NY, USA, 1994.

An Application of Bifurcation Analysis to Automotive Windscreen Wipers

Bradley Graham*, James Knowles* and Georgios Mavros *

*Department of Aeronautical and Automotive Engineering, Loughborough University, UK

Abstract. In this work we study the effects of automotive windscreen wiper design variables on the dynamics. To do this we utilise a lumped parameter model and numerical bifurcation analysis to determine operational regions of instability. This is achieved through an iterative two continuation calculation to produce surfaces of both the Hopf and Saddle node bifurcations. The continuation results agree well with known bounds of stable wiper operation.

Introduction

Whilst the purpose of windscreen wipers is well-defined, the non-linear contact and sliding mechanisms which govern the operation are complex. However, unlike almost every other aspect of vehicle development, empirical data is relied upon as oppose to predictive models to inform design decisions. This reliance on empirical data places constraints of questionable necessity on design criteria, the result of which can restrict both the vehicle designers and wash-wipe engineers producing the optimum product. This work presents an analysis of the impact that a selection of wiper design criteria has on the dynamic stability of a windscreen wiper system.

Approach

We consider a contact distribution that is calculated by finite element analysis at the park position of a commercially available screen. A mathematical expression for the distribution is subsequently derived to allow for precise manipulation of contact distribution shaping. In order to study the impact that a selection of wiper design criteria has on the dynamic stability of the system, a reduced complexity mechanical model is established. The contact distribution along with a continuously differentiable Stribeck curve which features six constants and the angular velocity of the wiper blade is used to capture the transient friction characteristics[1]. Bifurcation analysis is then applied to determine Hopf bifurcations, the subsequent periodic orbits and associated saddle node bifurcations.

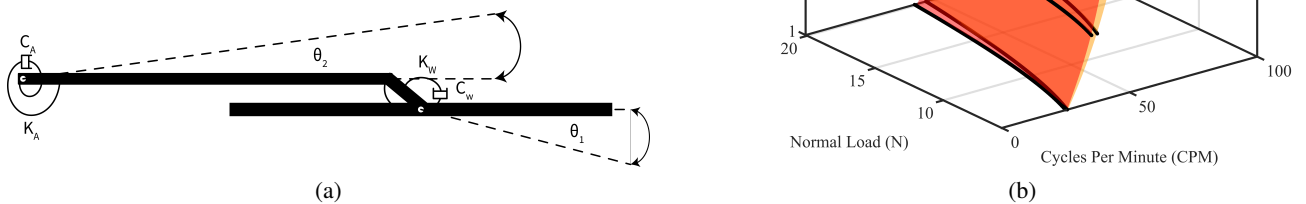


Figure 1: (a) Reduced Complexity Lump Parameter Model of an Automotive Wiper, (b) Three Parameter Continuation Diagram tracing the Hopf and Saddle Node Bifurcations

Figure 1a shows a schematic of the wiper system used throughout the study. Figure 1b shows a three parameter continuation diagram tracing the Hopf (red surface) and Saddle node (amber surface) bifurcations. The results are interpolated using three parameters to construct a surface of bifurcations. Such a surface can be used to determine optimum regions of operation for wiper blades. The results of our work agree well with known operational regions of automotive wiper blades.

Conclusions

The non-linear complexities and current reliance on empirical data associated to windscreen wipers necessitate the development of models and analyses such as presented above. The work presented shows calculated regions of instability associated to the manipulation of windscreen wiper design parameters. These results can be used by vehicle designers and wash-wipe engineers to efficiently study the impact of design decisions on the stable areas of operation of automotive windscreen wipers. Thus providing valuable insight into the relationship between vehicle design and wipe quality.

References

- [1] Makkar C., Dixon W. E., Sawyer W. G., Hu G. (2005) A New Continuously Differentiable Friction Model for Control Systems Design *IEEE/ASME International Conference on Advanced Intelligent Mechatronics*. Monterey, CA, USA, 24-28 July 2005

Evaluation of Lie group Integration for Simulation of Rigid Body Systems

Stefan Holzinger and Johannes Gerstmayr

Department of Mechatronics, University of Innsbruck, Innsbruck, Austria

Abstract. As commonly known, direct time integration of the kinematic equations of rigid bodies modeled with three rotation parameters is impossible in the general case due to singular points. Common workarounds are Euler parameters, either with unorthodox normalization or by switching to differential algebraic equations. More recent approaches use Lie group integration methods, as they allow a singularity-free integration of spatial rotations. So far, however, few studies have addressed whether Lie group integration methods are more accurate and efficient compared to formulations based on Euler parameters or Euler angles, which could be a crucial aspect for the decision to extend an existing multibody code with Lie group integration methods. In this paper, we compare several explicit and implicit Lie group integration methods in terms of accuracy and computational efficiency with formulations based on Euler parameters and Euler angles using several non-linear, typical rigid body systems.

Introduction

Rigid bodies are commonly used to model complex mechanical systems. As rigid bodies have six degrees of freedom, it is obvious to use three parameters to model translations and three to model rotations. Modelling spatial rotations with three rotation parameters (RP) is problematic, as there is no singularity-free representation of spatial rotations with three RP. Formulations based on three RP apply for example reparameterization strategies [1], while state of the art formulations use Euler parameters (unit quaternions) as RP to avoid singularities [2]. More recent approaches use Lie group integration methods [3], as they not only enable a representation of spatial rotations in a setting that is free of singularities, they also allow to use three RP for modelling multibody systems [4] and exhibit favorable properties for the simulation of multibody systems. However, Lie group integration methods are inherently coordinate-free, which makes them incompatible with multibody simulation codes that are based on RP. Apart from the aspect of extensibility of an existing multibody code with Lie group integration methods, the objective of this paper is to determine, whether Lie group integration methods are more accurate and efficient compared to conventional approaches. So far, few studies have addressed the latter question, despite the fact that its answer could be crucial for the decision to extend an existing multibody code with Lie group integration methods. Therefore, in this paper, the accuracy and computational efficiency of explicit and implicit Lie group integration methods is compared to Euler angle and Euler parameter based formulations using several non-linear rigid body systems.

Results and Discussion

It is found, that explicit Lie group integration methods outperform formulations based on RP in terms of accuracy and computational efficiency in most of the considered rigid body systems. Especially for systems with high rotational speeds, explicit Lie group integration methods turn out to be more accurate than a formulation based on Euler angles while the computational efficiency is almost the same, as exemplarily shown in Fig. 1.

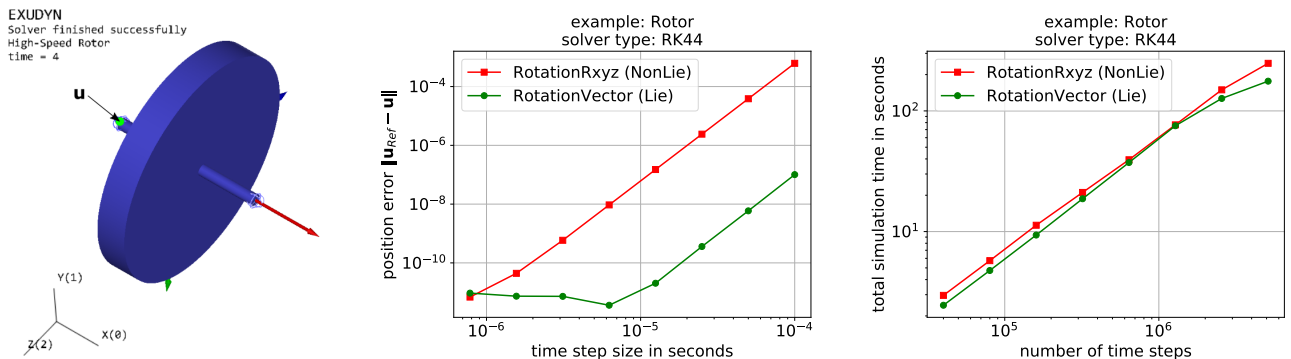


Figure 1: *Left:* Schematic representation of a flexibly mounted rotor rotating at 30000 rpm; *Center:* Convergence of the position error of the point u located at the rotor at the position of the left support; *Right:* Total simulation time; The abbreviation 'RotationRxyz (NonLie)' marks a formulation based on Euler angles and 'RotationVector (Lie)' marks a Lie group integration method which uses the rotation vector to model spatial rotations, cf. [4]. Both methods, use an explicit 4th-order Runge-Kutta method for time integration.

References

- [1] Singla P., Mortari D., Junkins J. L. (2005) How to avoid singularity when using Euler angles? *Advances in the Astronautical Sciences* **119**:1409-1426.
- [2] Shabana A.A. (2010) Computational Dynamics. Wiley.
- [3] Brüls O., Cardona A., Arnold M. (2012) Lie group generalized- α time integration of constrained flexible multibody systems. *Mechanism and Machine Theory* **48**:121-137.
- [4] Holzinger S., Gerstmayr J. (2021) Time integration of rigid bodies modelled with three rotation parameters. *Multibody System Dynamics* **53**:345-378.

Stability analysis for multibody systems subject to bilateral motion constraints

Ioannis Ntinopoulos*, Elias Paraskevopoulos* and Sotirios Natsiavas*

*Department of Mechanical Engineering, Aristotle University, Thessaloniki, Greece

Abstract. A stability analysis is performed for a class of mechanical systems, with multiple bodies subject to equality motion constraints. This analysis is based on an appropriate set of equations of motion, which are expressed in terms of the original coordinates as a system of strongly nonlinear second order ordinary differential equations. The results clarify certain critical issues associated with classical numerical methodologies, like constraint violation and gradual drift from the exact response.

Introduction

Dynamics of multibody mechanical systems involving motion constraints remains a challenging problem in several technical areas of large importance, like automotive, railway, marine and aerospace structures. Usually, the equations of motion of such systems are presented as a set of differential-algebraic equations (DAEs) of high index. Since the treatment of these equations is a delicate task [1], much research effort has been devoted to the subject. Essentially, all the previous efforts are based on application of index reduction or coordinate partitioning techniques. In contrast, the equations of motion employed in the present work are a coupled set of second order nonlinear ordinary differential equations (ODEs) [2]. This is achieved by combining some fundamental concepts of Analytical Dynamics and Differential Geometry [3]. These advantages are exploited in the present work, where a stability analysis is performed based on this new set of equations of motion. This analysis is also essential for investigating the stability of various numerical integration schemes applied to the numerical discretization of the equations of motion. In contrast to previous studies on the subject, all the eigenvalues of the linearized system are bounded and are given a specific physical meaning.

Results and discussion

The class of mechanical systems examined is subject to k motion constraints with general form

$$A(q)\underline{v} = \underline{0}, \quad (1)$$

where \underline{q} and \underline{v} represent the n generalized coordinates and velocities of the system, respectively and A is a known $k \times n$ matrix. Then, by adopting the classical Analytical Dynamics framework [3], the equations of motion are derived as a set of $n + k$ second order ODEs for the $n + k$ unknowns \underline{q} and $\underline{\lambda}$, where $\underline{\lambda}$ are the Lagrange multipliers. For stability analysis, appropriate linearization leads to an eigenvalue problem with form

$$\begin{bmatrix} K - \omega^2 M & -A^T (\bar{K} - \omega^2 \bar{M}) \\ -(\bar{K} - \omega^2 \bar{M}) A & 0 \end{bmatrix} \begin{pmatrix} \underline{\hat{q}} \\ \underline{\hat{\lambda}} \end{pmatrix} = \underline{0}, \quad (2)$$

where the diagonal matrices \bar{M} , \bar{C} and \bar{K} are fully determined by the motion constraints [2,3]. This problem is shown to possess $m = n - k$ simple eigenvalues, coinciding with those obtained after eliminating the motion constraints, plus a set of k double eigenvalues (with geometric multiplicity 1), related to the constraints. The results shed light on certain critical issues, like the constraint violation and the gradual drift from the exact response associated with classical numerical methods. Some typical results are presented in Fig. 1.

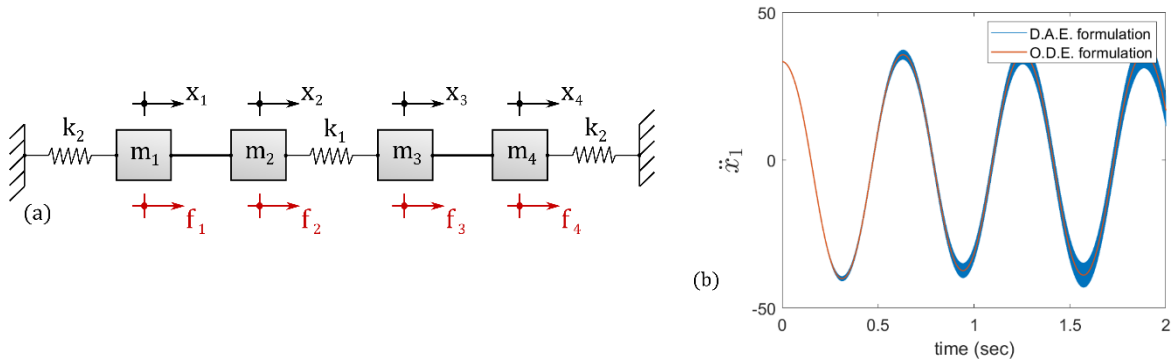


Figure 1: (a) An oscillator model and (b) numerical results (for acceleration \ddot{x}_1) verifying the instability of the DAE model.

References

- [1] Geradin, M., Cardona, A. (2001) Flexible Multibody Dynamics. John Wiley & Sons, NY.
- [2] Potosakis, N., Paraskevopoulos, E., Natsiavas, S. (2020) Application of an Augmented Lagrangian Approach to Multibody Systems with Equality Motion Constraints. *Nonlinear Dyn.* **99**:753–776.
- [3] Natsiavas, S., Passas, P., Paraskevopoulos, E. (2022) Nonlinear Dynamics of Constrained Multibody Systems based on a Natural ODE Formulation. *Nonlinear Dyn.* (accepted).

A reduced model for conical contact dedicated to flexible multi-body dynamics

Matthieu Serre*, Benoit Prabel* and Habibou Maitournam**

*Université Paris-Saclay, CEA, Service d'Etudes Mécaniques et Thermiques, 91191, Gif-sur-Yvette, France #

**IMSIA, ENSTA Paris, EDF, CEA, Institut Polytechnique de Paris, 91762, Palaiseau Cedex, France #

Abstract. An efficient time integration scheme for flexible multi-body dynamics with frictional impacts dedicated to finite element simulations is presented. Considering bulky compact components the linear theory of elastodynamics may be applied and two separate explicit Newmark integration schemes coupled only by non-linear forces are used for elastic vibration and rigid body dynamics respectively. After a brief study focused on conservation properties, a dedicated rigid-body integration scheme is selected. To avoid contact detection and classical mesh to mesh computation a parametric study based on static computations is performed to express the reaction forces as analytical functions of few positional arguments. The penalty method is applied and combined with the Coulomb law to modelize impacts between the two colliding bodies. The results are then illustrated on a use case with configuration dependent contact geometry. Finally the global model aims at interpreting experiments on such configurations.

Introduction

Wear is inherent to a large variety of industrial mechanisms including components of water pressurized reactors. Under the action of the cooling fluid two neighboring components may vibrate and collide. In time repeated frictional chocs induce mutual wear and thus a modification of the contact profile between the two bodies. The present paper focuses on a numerical strategy to simulate about 100 s of structural dynamic with constant contact geometry. Coupling with contact evolution due to wear is considered at a higher time scale. Our case study concerns slender bodies modeled as Timochenko beams yet bulky enough to work in the framework of the Linear Theory of Elastodynamics [4]. As a result elastic vibrations and rigid-body motion remain coupled only by non-linear forces. After a brief study on rigid-body dedicated integration schemes (Fig:1.(a)), an explicit Newmark algorithm [1] is implemented. A survey over a large panel of rigid-body integration schemes has been performed in [3]. For efficiency sake a simple contact model combining the penalty method and the Coulomb law is preferred to avoid impulses. For the most complex contact zones, a parametric study based on static calculus is performed to come up with an analytical formulation of reaction forces (Fig:1.(c)). This allows to dodge time-onerous detection algorithms and mesh to mesh calculation.

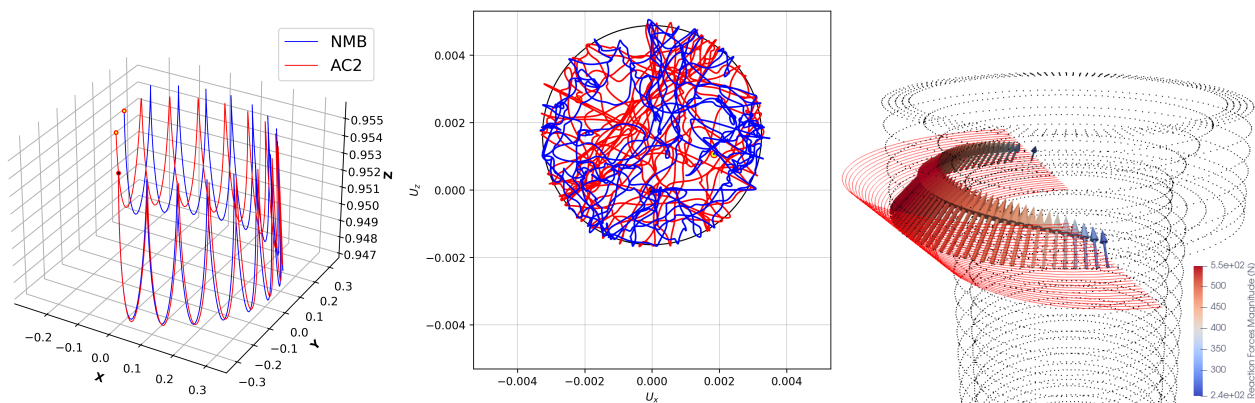


Figure 1.(a): Symmetrical top: center of mass trajectory for the NMB [2] & AC2 [1] integration schemes

Figure 1.(b): Neutral fiber trajectories on a beam cross section

Figure 1.(c): Reaction forces for a circle-cone contact

Results and discussion

Figure 1. gives a general overview of some of the results obtained with the dynamic model including accurate trajectories and reaction forces on any chosen point (Fig:1.(b)). It is noteworthy that while a simple beam model is used it is still able to keep track of the frictional solicitations on a local scale. The results are validated through comparison with macroscopic experimental observations. The upcoming work will focus on local wear computation using the tangential energy dissipated during collisions.

References

- [1] J. C. Simo, K. K. Wong (1991) Unconditionally stable algorithms for rigid body dynamics that exactly preserve energy and momentum. *J. Num. Methods* **31**:19-52.
- [2] P. Krysl, L. Endres (2005) Explicit Newmark/Verlet algorithm for time integration of the rotational dynamics of rigid bodies. *J. Num. Methods* **62**:2154-2177.
- [3] G. Ortolan, A. Saccon (2012) A numerical test of long-time stability for rigid body integrators. *J. Num. Methods* **90**:390-402.
- [4] A. A. Shabana (2013) Dynamics of Multibody Systems. Cambridge University Press, NY, pp. 226-227.

Recursive inverse dynamics of flexible multi-body systems based on Kane's equations

Pietro Pustina*, Cosimo Della Santina**,** and Alessandro De Luca *

*Department of Computer, Control and Management Engineering, Sapienza University of Rome, Rome, ITA

**Department of Cognitive Robotics, Delft University of Technology, Delft, NL

***Institute of Robotics and Mechatronics, German Aerospace Center (DLR), Oberpfaffenhofen, GER

Abstract. Controlling flexible multi-body systems requires for real-time implementation efficient algorithms that solve the inverse dynamics, an overlooked problem until recently. In this work, we leverage Kane's equations to obtain an inverse dynamics procedure with linear complexity in the number of bodies. The method is simple and coordinate-free because it is independent of the particular coordinates adopted for discretization and inter-body connections. Furthermore, it applies to bodies with lumped and distributed mass and accounts for the changes in the inertial parameters of the system.

Introduction

Flexible multi-body systems model many processes of practical interest, such as lightweight manipulators, helicopter rotors, and spacecraft. Model-based controllers for these systems are designed upon finite-dimensional descriptions of the dynamics obtained by discretization of the strains. In this way, a finite number of generalized coordinates defines the system configuration. The equations of motion become those of a second-order constrained mechanical system, making the control problem tractable. However, such controllers implicitly rely on efficient inverse dynamics (ID) formulations for real-time implementation. Despite all the effort devoted to solving the forward dynamics, the ID problem has captured far less attention [2]. In the last few years, the soft robotics [4] community manifested a new interest in the topic [3, 5, 6]. Fig. 1 shows a soft robot prototype.



Figure 1: A pneumatic soft robot consisting of three segments. Each segment can bend in any direction by inflating its four air chambers.

Results and discussion

We exploit Kane's equations to derive an ID procedure for a system of N flexible bodies with a tree topology and a fixed base. These equations, which have been extensively used for modeling flexible systems [1] yield a formulation with an inherent recurrent structure and allow removing nonworking constraint forces. As opposed to [2], the approach does not assume that the body motion can be separated as the sum of a rigid and a deformable contribution. Indeed, this hypothesis is invalid for models obtained from piecewise constant or functional discretizations of the strain fields, which are techniques commonly adopted to formulate control-oriented models of continuum soft robots. In particular, [3] generalizes the RNE algorithm for a geometric model of soft-rigid multi-body systems. Instead, [5] presents a novel formulation of Cosserat beams where the strains are reduced through a functional space representation. Despite being elegant and concise, these approaches require the reader to be familiar with the tools of geometric mechanics and depend on the technique used to discretize the strains. In [6], the authors overcome these limitations by applying the Newton-Euler equations on a lumped mass model of flexible systems. The method is simple but relies on rigid body equations. Consequently, it does not entirely describe the dynamics. Our approach is tractable and independent of the kinematic description of the deformations. Furthermore, each body can have lumped or distributed mass, and it can be connected to its predecessor in the chain by any joint or an hinge. Differently from [6], the resulting equations account for the changes in the inertial parameters of the system. The algorithm also applies to systems with rigid bodies.

References

- [1] Banerjee A. K., Dickens J. M. (1990). Dynamics of an arbitrary flexible body in large rotation and translation. *J. of Guidance, Control, and Dynamics* **13**(2):221–227.
- [2] Boyer F., Khalil W. (1998). An efficient calculation of flexible manipulator inverse dynamics. *Int. J. of Robotics Research* **17**(3):282–293.
- [3] Renda F., Seneviratne L. (2018). A geometric and unified approach for modeling soft-rigid multi-body systems with lumped and distributed degrees of freedom. *2018 IEEE Int. Conf. on Robotics and Automation (ICRA)*, pp. 1567–1574.
- [4] Della Santina C., Catalano M. G., Bicchi A. (2020) Soft robots. In: *Encyclopedia of Robotics*. Springer, Berlin, pp. 1–15.
- [5] Boyer F., Lebastard V., Candelier F., Renda F. (2020). Dynamics of continuum and soft robots: A strain parameterization based approach. *IEEE Transactions on Robotics* **37**(3):847–863.
- [6] Jensen S. W., Johnson C. C., Lindberg A. M., Killpack M. D. (2022). Tractable and Intuitive Dynamic Model for Soft Robots via the Recursive Newton-Euler Algorithm. *2022 IEEE Int. Conf. on Soft Robotics (RoboSoft)*, pp. 416–422.

Stability Analysis of Large-Scale Multibody Problems using Lyapunov Exponents

Pierangelo Masarati*, Gianni Cassoni*, Andrea Zanoni* and Aykut Tamer**

*Department of Aerospace Science and Technology, Politecnico di Milano, Italy

***Imperial College London, United Kingdom*

Abstract. Lyapunov Characteristic Exponents are stability indicators of solutions to nonlinear problems. However, their estimation can be very demanding, in terms of both complexity of implementation and sheer computational cost, limiting their applicability to large-scale multibody dynamics problems. This paper addresses the effective use of Jacobian-less methods to estimate Lyapunov Exponents from large-scale multibody problems.

Introduction

Lyapunov Characteristic Exponents (LCE) or, in short, Lyapunov Exponents (LE), represent the spectrum of the Cauchy problem $\dot{\mathbf{x}} = \mathbf{f}(\mathbf{x}, t)$, $\mathbf{x}(t_0) = \mathbf{x}_0$. Considering a solution $\mathbf{x}(t)$, they are defined as

$$\lambda_i = \lim_{t \rightarrow +\infty} \frac{1}{t} \log \|_i \mathbf{x}(t)\|$$

where ${}_i\mathbf{x}(t)$ is the solution of the linear, time-variant (LTV) problem ${}_i\dot{\mathbf{x}} = \mathbf{f}_{/\mathbf{x}}(\mathbf{x}(t), t){}_i\mathbf{x}$, ${}_i\mathbf{x}(t_0) = {}_i\mathbf{x}_0$. As many LCEs as the size of the problem's state exist; however, estimating all of them is critical, as in theory independent values of ${}_i\mathbf{x}_0$ should be selected, such that each of them evolves along an independent direction. Numerically, even the faintest perturbation of each ${}_i\mathbf{x}_0$ with a contribution in the state subspace direction resulting in the largest λ_i , the maximum LCE (MLCE), would make all the limits converge to the MLCE itself. Numerical methods have been devised to overcome this issue; among them, the continuous QR and SVD methods, and the discrete QR method are the most effective. However, these methods require the Jacobian matrix of the problem, $\mathbf{f}_{/\mathbf{x}}(\mathbf{x}(t), t)$, evaluated along the reference trajectory $\mathbf{x}(t)$, and can hardly be formulated for problems described by Differential-Algebraic Equations (DAE), as is the case of the most popular multibody formulations. In this paper, we propose to use Jacobian-less methods to estimate LCEs of large-scale multibody dynamics problems directly from the time histories that result from the solution of the original Cauchy problem. One such method is proposed in [1].

Results

Complex multibody dynamics problems often occur in rotorcraft aeromechanics. Owing to the large linear and angular motion a helicopter rotor is subjected to, the kinematic complexity and variety of arrangements existing (and foreseen) for rotor hubs, and the highly nonlinear constitutive properties of several components, like lead-lag dampers, multibody dynamics is ideal for their analysis. Typical analyses may result in (nearly) time-periodic solutions; for this reason, a typical approach to stability analysis of periodic orbits is the Floquet-Lyapunov method; however, it may be convenient to devise a method that does not require the computation of a periodic orbit, or even its mere existence. LCEs are ideal, in this case, as stability analysis can progress along with the numerical integration of the problem.

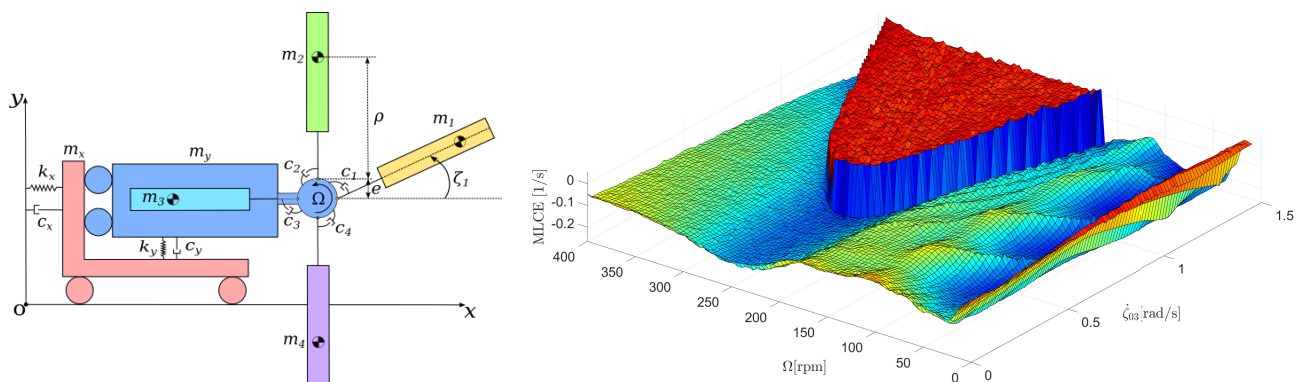


Figure 1: Left: rotor/support model; right: sensitivity of MLCE to amplitude of initial perturbation.

In Fig. 1 we present a sketch of a popular rotorcraft ground resonance model and the MLCE estimated using the method proposed in [1] as a function of the rotor angular velocity, Ω , and the amplitude of the initial perturbation of the angular velocity of a blade. The method will be assessed by comparing results with equivalent ones, when possible, and its application to more complex problems will be illustrated.

References

- [1] Rosenstein M. T., Collins J. J., De Luca C. J. (1993) A practical method for calculating largest Lyapunov exponents from small data sets. *Physica D: Nonlinear Phenomena*. **65**(1-2):117-134 doi:10.1016/0167-2789(93)90009-P

Influence of the rope sling system on dynamics of a carried load

Andrzej Urbaś, Krzysztof Augustynek and Jacek Stadnicki

*Department of Mechanical Engineering Fundamentals, University of Bielsko-Biala, Bielsko-Biala, Poland

Abstract. The dynamics analysis of the mobile crane carrying a load hung on different rope sling systems is presented in the paper. The considered mobile crane is modelled in the form of a tree structure of a main kinematic chain with auxiliary subchains. The carried load is modelled in two variants as a cylinder hung on one, three and four ropes sling system; and as a box is hung on one, two and four ropes sling system. Numerical results of the crane cycle input movement simulations for these models are compared with the simulation results of the model in which the load is modelled as a lumped mass hanged on a single rope.

Introduction

In most publications referring to dynamics of cranes, a load is treated as a lumped mass hung on a single rope. This simplification causes inaccuracy in determining the trajectory and energy of the load after finishing a cycle of crane input movement, which are important due to the precision of load positioning [1-4].

The model of the crane used in the dynamics analysis is presented in Fig. 1. The proposed model consists of: crane suspension subsystem b , supporting structure c_m (i.e. rotary column, two boom sections and telescopic boom section) and two load lifting subsystems $c_{a,\alpha} |_{\alpha \in \{1,2\}}$ (i.e. hydraulic cylinders). The carried load is modelled as cylinder l_c and box l_b , which can be hung on $r_\alpha |_{\alpha \in \{1,2,3,4\}}$ rope sling systems.

The crane input movement cycle is divided into five phases, i.e. load lowering ($f^{(d_3)}$), crane rotation ($t^{(d_1)}$), load telescoping ($f^{(d_4)}$), load lifting ($f^{(d_2)}$) and load swinging.

The dynamics equations are formulated using the joint coordinates, homogeneous transformation matrices and the Lagrange equations of the second order.

The proper simulations have been carried out and the results have been compared with the results obtained for lumped mass l_m on the graph of the kinetic energy integral mean value (Figs 2 and 3).

The contribution of this work is to point out that the application of a mathematical model of a crane with a load in the form of a lumped mass may not reflect the real dynamics of a crane.

It is worth adding that the value of the kinetic energy of the load after input movement cycle finishing is often assumed as a criterion in optimisation tasks.

References

- [1] Kacalak W., Budniak Z., Majewski M. (2018) Stability assessment as a criterion of stabilization of the movement trajectory of mobile crane working elements. *Int. J. Appl. Mech. Eng.* **23**:65-77.
- [2] Cekus D., Kwiatoń P. (2021) Method of determining the effective surface area of a rigid body under wind disturbances. *Arch. Appl. Mech.* **91**:1-14.
- [3] Gao T., Huang J., Singhose W. (2022) Eccentric-load dynamics and oscillation control of industrial cranes transporting heterogeneous loads. *Mech. Mach. Theory* **172**:104800.
- [4] Urbaś A., Augustynek K., Stadnicki J. (2022) Kinetic Energy-Based Indicators to Compare Different Load Models of a Mobile Crane. *Materials* **15**:8156, <https://doi.org/10.3390/ma15228156>.

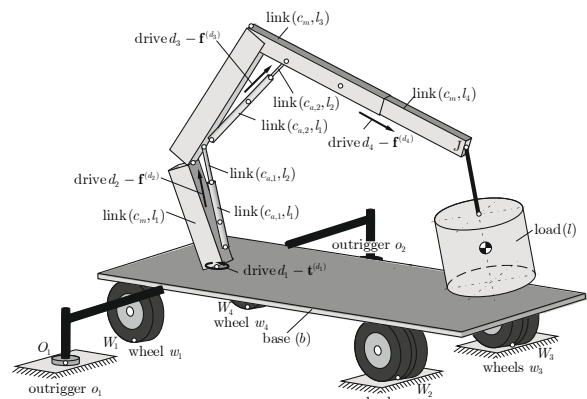


Figure 1: Model of the crane

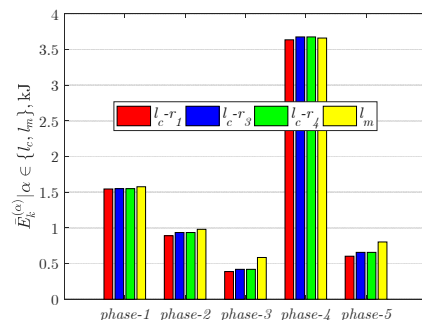


Figure 2: Kinetic energy integral mean value of the cylinder and the lumped mass in phases of input movement

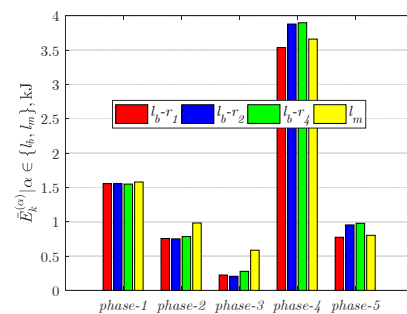


Figure 3: Kinetic energy integral mean value of the box and the lumped mass in phases of input movement

Nonlinear effects in joints of multi-dimensional active absorbers for robotics

Zbyněk Šika*, Karel Kraus* and Jan Krivošej*

*Faculty of Mechanical Engineering, Czech Technical University in Prague, Praha, Czech Republic

Abstract. Different imperfections and various nonlinear friction regimes in joints of mechatronic systems substantially deteriorate their behaviour. This also largely applies to multi-dimensional active vibration absorbers with actuators and sensors in feedback control laws. High functional accuracy is often required for the active absorbers, leading to conflicting demands on the design and thus to the necessity of advanced elimination and/or compensation of these unwanted nonlinearities. The research ranges from the optimization of absorber design, through friction compensation based on an adaptive model or an advanced observer, to modifications of absorber control strategies. Some of investigated elimination methods are experimentally tested on a demonstrator of a controlled planar vibration absorber with three degrees of freedom.

Introduction

Industrial serial robots are typically able to cover large workspace, but their mechanical properties don't allow combining high accuracy and high dynamic of operations. The same is valid also for new very light robot concepts. Widely spread usage of robots, even for tasks such as drilling [1], leads to high demands to accuracy and speed. The absolute measurement of the end-effector for fast position feedback as well as usage of inbuilt robot motors for vibration suppression is often problematic. The authors of the paper are therefore dealing with an alternative concept of using compact active multi-dimensional absorbers for robots [2]. Reducing the vibrations of the robots by means of active absorbers can be realized with the help of built-in and local sensors only. In addition, active absorbers allow the adaptation to variable dynamic properties of the robot. There are many control laws that can be used, one of them is the so-called delayed resonator concept [3].

Results and discussion

The operation of any real controlled mechanism is strongly influenced by imperfections and passive effects in the kinematic joints. Research and ways to compensate these nonlinearities are very current, for example, the use of LuGre models [4] and their combinations with advanced observers [5] can be mentioned. High demands are placed on the exact function of active absorbers for the given purposes in robotics, which leads to the need to solve the problem of imperfections of real kinematic joints. An experimental demonstrator was assembled for this purpose (Figure 1) including six AVM60-25 voice-coil actuators, linear ball bearings, built-in encoders and precise revolute/spherical joints. The first phase of the research consisted in the identification of variantly formulated nonlinear passive resistances effects models (LuGre, neural network based and others) during different motion regimes of the 3 DOF absorber demonstrator. Adaptation of the parameters took place using the parallel simulation of the mechanism model in the control system of the actuators. During these identifications, the repeatability of the results and the degree of uncertainty of the obtained models were also determined. The second phase investigated the integration of some obtained nonlinear models to the control laws specific for active vibration suppression. Generalization of computed-torque type methods and their combination with active vibration control strategies was the main goal of these experiments. The current results of both of these research phases will be presented, including open questions for further investigation.

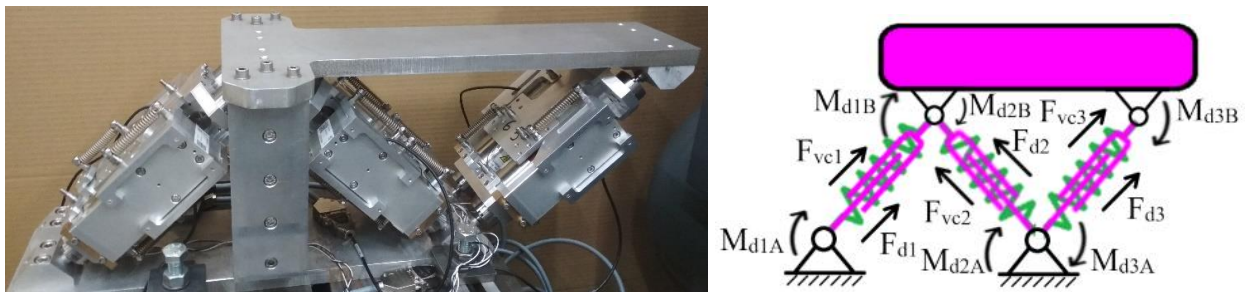


Figure 1: Demonstrator of an active planar 3 DOF vibration absorber and scheme of its mechanical model.

References

- [1] Olsson T. et al. (2010) Cost-efficient Drilling Using Industrial Robots with High-bandwidth Force Feedback *Robot. Comput.-Integr. Manuf.* **26**(1):24-38.
- [2] Kraus K. et al. (2020) Mechatronic Robot Arm with Active Vibration Absorbers *J. Vib. Control* **26**(13-14):1145-1156.
- [3] Šika Z., Vyhliďal T., Neusser Z. (2021) Two-dimensional Delayed Resonator for Entire Vibration Absorption *J. Sound Vibr.* **500**:116010.
- [4] Huang S., Liang W. (2019) Intelligent Friction Compensation *IEEE-ASME Trans. Mechatron.* **24**(4):1763-1774.
- [5] Sancak K.V., Bayraktaroglu Z. Y. (2021) Observer-based Friction Compensation in Heavy-duty Parallel Robot *J. Mech. Sci. Technol.* **35**(8):3693-3704.

Algorithmic verification of Lyapunov stability for rigid multi-contact systems subject to impact and friction

Péter L. Várkonyi

Department of Mechanics, Materials, and Structures, Budapest University of Technology and Economics, Budapest, Hungary, ORCID: 0000-0002-2220-0295.

Abstract. Quasi-static object manipulation, grasping, and robotic locomotion tasks require tests of local stability of equilibria involved in the motion plan in order to avoid unpredictable failure. Standard stability tests are not available due to the non-smoothness and discontinuity of rigid body dynamics under unilateral contact and dry friction. In the present work, a recently published algorithmic stability test using semi-definite programming and Lyapunov's direct method is extended. Tailor-made generalizations of Lyapunov's direct method are proposed. The applicability of the extended stability test to multi-contact systems is demonstrated for the first time. As a case study, sufficient stability conditions of a planar rigid body resting on a slope with 2 point contacts are found numerically.

Background

The dynamics of rigid objects and multibody systems under unilateral contact, friction and impact is rich, and only partially understood. Stability analysis of equilibria is particularly challenging. At the same time, verifying the stability of an equilibrium state is essential for many applications like object manipulation, grasping, and robotic locomotion. Lyapunov's direct method is based on constructing a function over state space, which is decreasing along trajectories of the dynamics and has a local minimum point at the equilibrium state under investigation. However the theory does not include a general recipe on how to construct such a function.

It has been pointed out recently [1] that verification of Lyapunov stability by construction of a Lyapunov function can be formulated as an optimization problem over sums-of-squares polynomials, for which efficient numerical algorithms are available. Several examples of Lyapunov stability certificates were presented by [1], but none of those involved multiple contacts.

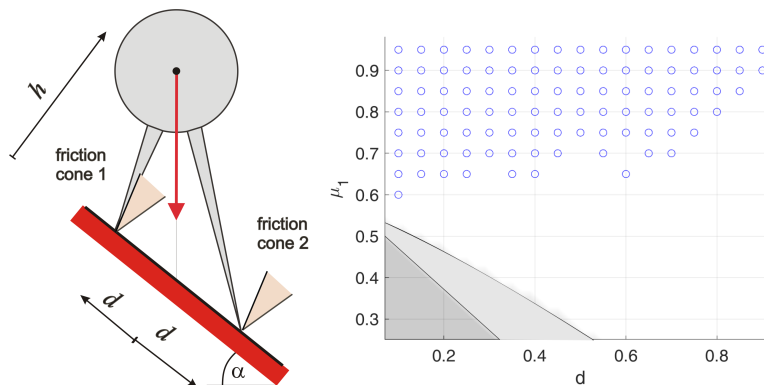


Figure 1: Left: a rigid body on a slope of angle α with 2 point contacts subject to gravity load. The center of the circle is the center of mass, and the radius of gyration of the object is chosen as length unit. Coulomb friction with coefficient μ_i is assumed at both contact points. Right: illustration of the algorithmic stability test for slope angle $\alpha = 30^\circ$; $h = 1$; $\mu_2 = 1$; and inelastic impacts. Background colors show regions of model parameters d , μ_1 where the system is provably unstable (dark grey); unstable according to numerical simulation (light grey) or stable according to numerical simulation (white). Empty circles mark points where the proposed stability test successfully verified stability.

Extensions of Lyapunov's direct method and application to multi-contact equilibria

The verification techniques of [1] were applied by the author to the problem of a planar rigid body with two point contacts on a slope (Fig. 1). Since the original version of the method failed to verify stability in all cases, two extensions of Lyapunov's direct method were proposed. The first one allows the use of piecewise smooth Lyapunov functions constructed as the maximum of several polynomials. The second extension allows Lyapunov functions, which may temporarily increase along trajectories.

The generalized stability test was applied to the same problem. In the case of perfectly inelastic impacts, semi-analytic conditions of stability are available in the literature. In the case of partially elastic impacts, the analytic, exact conditions of stability are not available, but stability can be predicted based on systematic numerical simulations. In both cases, the proposed method could verify stability for many values of model parameters (Fig. 1). To the best knowledge of the author, the proposed method is the first algorithmic Lyapunov stability test successfully applied to multi-contact equilibria.

References

- [1] Posa M., Tobenkin M., Tedrake R. (2015) Stability analysis and control of rigid-body systems with impacts and friction. *IEEE Transactions on Automatic Control* **61**: 1423-1437.

Nonholonomic dynamics of steer-free rotor-actuated Twistcar

Zitao Yu*, Jithu Paul*, and Yizhar Or**

*Faculty of Mechanical Engineering, Technion – Israel Institute of Technology

Abstract. Underactuated wheeled vehicles are commonly studied as nonholonomic systems with periodic actuation. Two classical examples inspired by riding toys are the Snakeboard and the Twistcar, which were analyzed using planar models. In this work, we present a new model – the steer-free rotor-actuated Twistcar, which combines the characteristics of these two models, and differs from them by having one passive shape variable, and by the added dissipation due to wheels' rolling resistance. Using numerical analysis, we show that the system exhibits multiplicity of periodic solutions. Varying parameters such as actuation frequency and structural length ratio lead to bifurcations, stability transitions, and symmetry breaking of these periodic solutions. We will also present ongoing research progress on experimental demonstration in a robotic prototype, as well as asymptotic analysis of a simplified approximation of the system.

Introduction

The dynamics of underactuated wheeled vehicles governed by nonholonomic constraints have been an extensively researched topic for decades. One of the classic examples is the *Snakeboard* [1], which is actuated by controlling the wheels' heading angles and an oscillating rotor attached to the body. Choosing different gaits of periodic inputs enables steering the Snakeboard along desired paths [1]. Another example is the *Twistcar* [2], in which the joint connecting the body and steering link is periodically actuated, either by prescribing the steering angle or the mechanical torque. Asymptotic analysis of the Twistcar revealed abundant nonlinear phenomena in its dynamics, such as movement direction reversal depending on the vehicle's structure [2]. In both works, all shape variables are actuated, and the body motion shows growing oscillations superposed on the unboundedly growing mean value.

In this work, we introduce the combined model *Steer-free Rotor-actuated Twistcar*, see Fig. 1. It has a single actuation of an oscillating inertial rotor angle $\psi(t)$ relative to the body, while the steering joint angle is *passive*, and evolves dynamically. In addition, we consider viscous dissipation caused by the wheels' rolling resistance, and possibly damping of the passive steering joint. This results in existence of periodic solutions of the system, in which the dissipated mechanical energy per cycle is balanced by the energy input of the actuation.

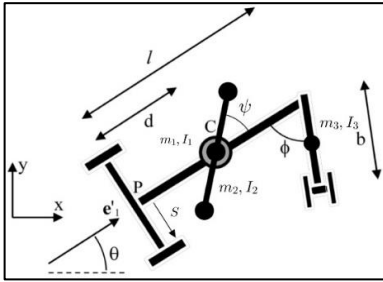


Figure 1: Model of the steer-free rotor-actuated Twistcar

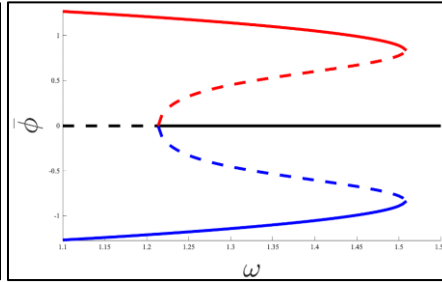


Figure 2: Periodic solution branches – mean steering angle $\bar{\phi}$ as a function of the actuation frequency ω .

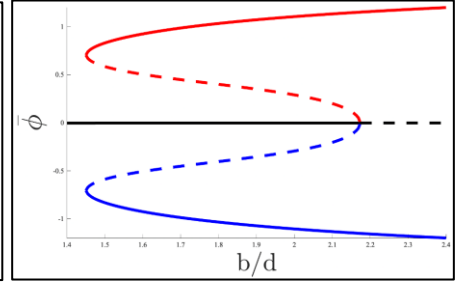


Figure 3: Periodic solution branches – mean steering angle $\bar{\phi}$ as a function of structural length ratio b/d

Results and discussion

Invariance properties of the vehicle's dynamics enable some reduction of the system's dimensionality, and numerical integration is utilized for seeking periodic solutions and analyzing their orbital stability via the evaluation of Floquet multipliers. We find multiplicity of periodic solutions, some are stable (i.e. convergent from nearby perturbed initial states) while others are unstable (i.e. divergent). Continuously varying a single parameter of the system while tracking all branches of periodic solutions reveals interesting bifurcations and stability transitions. Fig. 2 and Fig. 3 show solution branches of the mean value of the passive joint angle $\bar{\phi}$ as a function of the actuation frequency (Fig. 2) and structural length ratio b/d (Fig. 3). The solid curves denote stable periodic solutions whereas the dashed curves denote unstable ones. One can see that the symmetric periodic solution $\bar{\phi} = 0$, having zero net body rotation, changes from unstable to stable through a subcritical pitchfork bifurcation where a pair of unstable asymmetric branches evolve. Another critical transition is folded (saddle-node) bifurcation where the unstable asymmetric solution branches fold back into stable asymmetric branches. Remarkably, this implies that for some regions of the parameters (ω or b/d), the only stable periodic solution is symmetric, while in another region the only stable solutions are pair of asymmetric ones, and in an intermediate region the systems exhibit multi-stability of symmetric and asymmetric solutions. Finally, we plan to present ongoing research progress on experimental demonstration in a robotic prototype, as well as asymptotic analysis of a simplified approximation of the system, in the spirit of [2].

References

- [1] Ostrowski, J., Lewis, A., Murray, R., & Burdick, J. (1994, May). Nonholonomic mechanics and locomotion: the snakeboard example. In *Proceedings of the 1994 IEEE International Conference on Robotics and Automation* (pp. 2391-2397). IEEE.
- [2] Chakon, O., & Or, Y. (2017). Analysis of underactuated dynamic locomotion systems using perturbation expansion: the twistcar toy example. *Journal of Nonlinear Science*, 27(4), 1215-1234.

Application of Nonsmooth Dynamics to Rockfall Protection Ring Net Simulation

Lisa Eberhardt*, Remco I. Leine*, Jonas Harsch*, Simon R. Eugster*,
Perry Bartelt** and Helene Lanter***

*Institute for Nonlinear Mechanics, University of Stuttgart, Germany,

ORCID 0000-0002-9857-7080, 0000-0001-9859-7519, 0000-0003-1065-2216 and 0000-0002-4562-1287,

**WSL Institute for Snow and Avalanche Research SLF, Davos, Switzerland

***Gebrugg AG, Romanshorn, Switzerland, ORCID 0000-0002-3852-7401

Abstract. The simulation of rockfall protection ring nets with rocks of arbitrary convex shape poses a challenging task. One major aspect hereby is the formulation of the net-rock interaction. We approach this problem by using nonsmooth contact dynamics with hard unilateral constraints, as this allows our model to describe impacts as well as frictional contact. The net is modeled as a discrete multibody system using a finite number of material points. To take into account the influence of rock shape, the rock is modeled as rigid body with the shape of an arbitrary convex polytope. For each material point a frictional contact law with the rock model is formulated.

Introduction

In alpine regions large rocks, often significantly heavier than one ton, pose a great threat for humans and infrastructure if they become loose and fall downwards. One possibility to prevent damage is the use of rockfall protection ring nets which are able to capture rocks with a kinetic energy up to 11 000 kJ. The extremely high impact forces, which such a net has to endure, necessitate extensive testing in the terrain or on test sites. Due to practical reasons, only a limited number of tests under very specific conditions can be conducted. Numerical simulations are used to obtain insight for more general test cases. The state-of-the-art in rockfall net simulation uses purely spherical rock shapes and neglect friction.

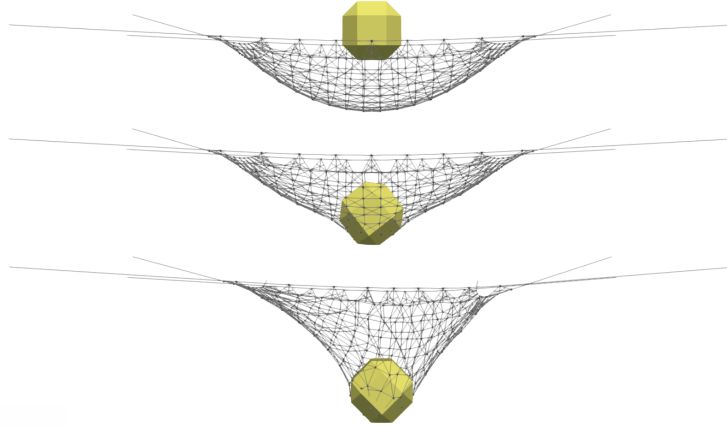


Figure 1: Snapshots of simulation result with rotating $EOTA_{111}$ norm block as rock model.

Simulation with set-valued frictional contact laws

The approach taken here models the rock as an arbitrary convex polytope and uses the nonsmooth contact dynamics method to take set-valued frictional contact laws into account. The discrete net model of [1] is employed for the net itself, whereas hard unilateral contact with Coulomb friction is added between rock and net. For numerical simulations, we used Moreau's timestepping scheme [2], which directly discretizes the measure differential inclusion

$$\begin{aligned} Mdu - h(q, u)dt &= W(q)dP \\ &+ \text{normal cone inclusions for } dP, \end{aligned}$$

capturing the system dynamics. Special attention is paid to the efficient calculation of contact distances between the rings of the net and the rock. Current research focuses on incorporation of cables in the model to accommodate for the sliding of the rings over the cables, which causes the so-called curtain effect.

References

- [1] A. Volkwein, *Numerische Simulation von flexiblen Steinschlagschutzsystemen*. PhD thesis, ETH Zurich, Zürich, 2004. Diss., Technische Wissenschaften, Eidgenössische Technische Hochschule ETH Zürich, Nr. 15641, 2004.
- [2] R. Leine and N. Wouw, van de, eds., *Stability and convergence of mechanical systems with unilateral constraints*. Lecture Notes in Applied and Computational Mechanics, Germany: Springer, 2008.

A study on the dynamics of the flexible link mechanism with a spatial model of the translational joint with clearance

Krzysztof Augustynek, Andrzej Urbaś, and Jacek Stadnicki

**Department of Mechanical Engineering Fundamentals, University of Bielsko-Biala, Bielsko-Biala, Poland*

Abstract. The paper presents the dynamics model of the RPSUP mechanism with a clearance in a translational joint. The spatial model of the clearance in the translational joint is proposed. In this model, inner surface of the slider is discretized into rectangular zones in which the contact between the slider and guide is detected. For each zone, three scenarios of the contact are possible: point, line, and surface contact. In numerical simulations interactions between the flexible coupler and the clearance in the translational joint will be studied and compared.

Introduction

The fifth class kinematic pairs (revolute and translational joints) are among the most popular types of joints in mechanisms. The possibility of modelling non-linear effects in these joints, such as friction or clearance, is very important from the point of view of the dynamics of the system [1–4]. There are many works in the literature devoted to both planar and spatial models of clearance in revolute joints [3]. The situation is different in the case of translational joints with clearance, where only a small number of papers deal with spatial models of clearance [1, 2]. In these models, some number of conditions are formulated to describe special cases of the position of the slider with respect to the guide.

This paper proposes an approach in which the internal surfaces of the slider are discretized into rectangular contact zones, where the contact between the slider and the guide can be analysed (Fig. 1). Depending on the number of nodes in contact and the depth of penetration, three cases of contact are considered: *point*, *linear* and *surface*. The normal contact force in node $(i, j)_p$ is calculated using the following formula [1]

$$\|\mathbf{f}_n^{(i,j)_p}\| = K^{(i,j)_p} \left(\delta_m^{(i,j)_p} \right)^{1.5} + C^{(i,j)_p} \dot{\delta}_m^{(i,j)_p},$$

where the generalized stiffness and damping $K^{(i,j)_p}$, $C^{(i,j)_p}$ depend on the type of contact (point, linear, surface), and $\delta_m^{(i,j)_p}$ is an average penetration depth in node $(i, j)_p$. The tangent force due to friction is modelled using the LuGre friction model.

The proposed model of the clearance will be analysed for the spatial RPSUP mechanism with the flexible coupler. The coupler is discretized using the Rigid Finite Element Method. The dynamics equations of motion are derived using the Lagrange equations of the second kind. Homogeneous transformation matrices and joint coordinates are applied in the derivations process. In numerical simulations, the influence of link flexibility and clearance in the translational joint on the dynamics response of the mechanism will be studied.

References

- [1] Wu X., Sun Y., Wang Y., Chen Y. (2020) Dynamic analysis of the double crank mechanism with a 3D translational clearance joint employing a variable stiffness contact force model. *Nonlinear Dyn.* **99**:1937–1958.
- [2] Qian M., Qin Z., Yan S., Zhang L. (2020) A comprehensive method for the contact detection of a translational clearance joint and dynamic response after its application in a crank-slider mechanism. *Mechanism and Machine Theory.* **145**:103717.
- [3] Erkaya S., Doğan S., Şefkathioğlu E. (2016) Analysis of the joint clearance effects on a compliant spatial mechanism. *Mechanism and Machine Theory.* **104**: 255–273.
- [4] Zheng X., Li J., Wang Q., Liao Q. (2019) A methodology for modeling and simulating frictional translational clearance joint in multibody systems including a flexible slider part. *Mechanism and Machine Theory.* **142**:103603.

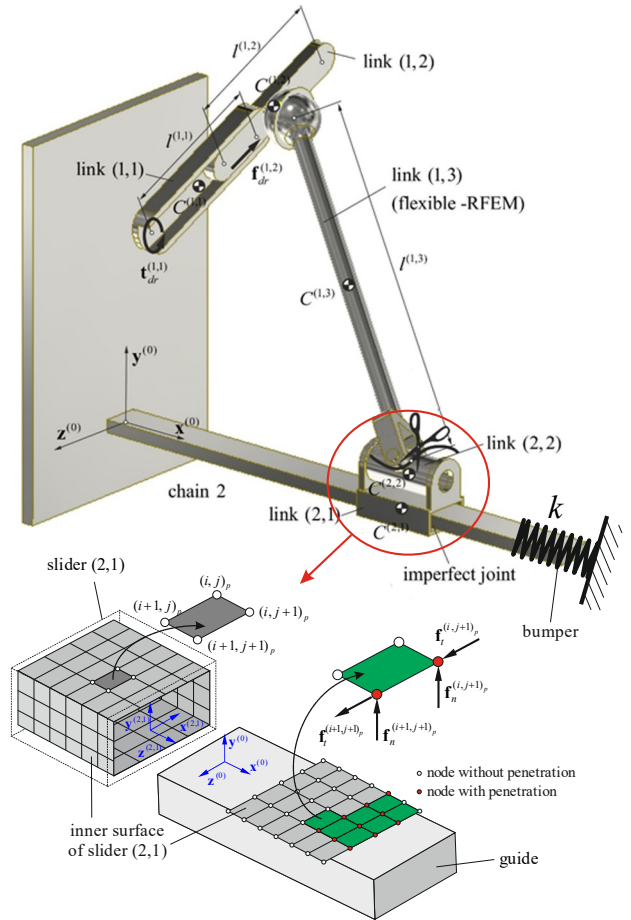


Figure 1: Model of RPSUP mechanism with the clearance in slider (2,1)

Delay-embedded modal analysis for spectral submanifold identification

Joar Axás* and George Haller*

*Department of Mechanical and Process Engineering, ETH Zürich, Switzerland

Abstract. We show that in a delay-embedded space, the linearized dynamics at a fixed point can be computed solely from the eigenvalues of the full linearized system independent of its eigenvectors. This observation provides guidelines for choosing the delay embedding parameters. It also implies that the tangent space of a delay-embedded spectral submanifold (SSM) is fully determined by the spectrum of the corresponding eigenspace. Thus, we can facilitate the identification of SSMs from data by prescribing their tangent spaces based on eigenvalue estimates. Applying this procedure to data from tank sloshing experiments, we identify a 6D SSM and correctly predict the system’s multimodal decay.

Introduction

In data-driven model identification, delay embedding is routinely used. Examples of model reduction methods based on delay embedding include eDMD [1], HAVOK [2], and false nearest neighbors [3]. Another approach where delay embedding has been employed is data-driven model reduction to SSMs [4, 5]. Takens’ embedding theorem states that delay-embedding a signal from a generic observable function on the full phase space at least $2d + 1$ times recovers d -dimensional invariant objects. In practice however, their identification crucially depends on choosing the timelag and embedding dimension properly. Improved understanding of how invariant objects are reconstructed in observable spaces can thus aid model order reduction methods significantly.

Results and discussion

We show that on a delay-embedded SSM, the linear part of the dynamics is fully determined by the eigenvalues of its spectral subspace. Therefore, when the eigenvalues of interest are known, we can facilitate computation of a delay-embedded SSM by prescribing the tangent space, even if the observable function and the SSM in the full phase space are unknown. We apply this method to data from sloshing experiments, where a tank partially filled with water is mounted on a moving platform horizontally excited by a motor, and the surface profile of the fluid is recorded (Figure 1a) [4]. As the forcing amplitude increases, more sloshing modes are activated.

4

B. Bäuerlein and K. Avila

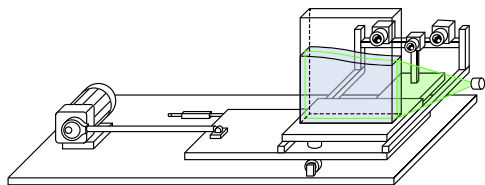


FIGURE 2. Sketch of the experiment. A motor (a) drives an eccentric disk which converts the rotary motion of the motor into a quasi-harmonic horizontal oscillation of the platform. A positioning sensor (c) directly records the motion of the platform on which the tank (d), two high-speed cameras (e) and an USB-camera (f) are mounted. For the PIV measurements a light sheet (g) is provided by a laser passing through a cylinder lens (implied) and a slit (h).

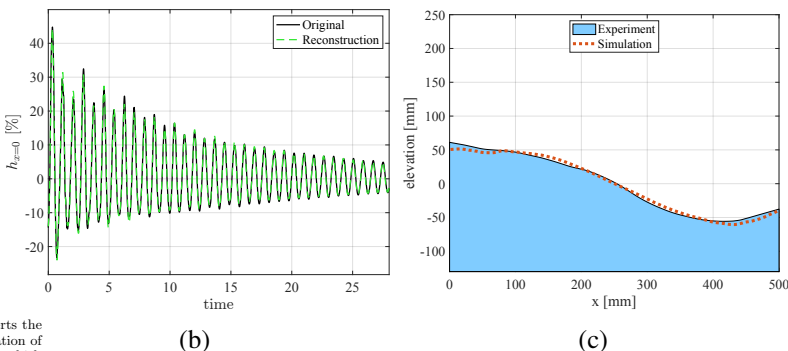


Figure 3. (a) Experimental setup for tank sloshing. (b) Measurement and 6D SSM prediction of the leftmost point on the surface profile. (c) SSM prediction of full surface profile.

dynamics. We find that neither the exact substrate shape, nor the frequency spectrum are useful to determine the nonlinear resonance maxima. The key indicator is the phase-lag between driving and response. We systematically investigate the role of initial conditions. While previous work successfully captured the dynamics of the first mode with a 2D SSM [4, 5], here, we model the multimodal decay on a 6D SSM. The key technology allowing this enhancement is the enforcement of the tangent space in our SSM reconstruction, based on the theoretically known first three eigenfrequencies. Figure 1b shows good agreement between the experimental surface profile elevation at the tank wall and the delay-embedded SSM reduced prediction. Furthermore, our 6D reduced model accurately predicts the full surface profile decay in Figure 1c. Finally, our theory on delay-embedded modal analysis provides insight into optimal parameter choice applicable to any model reduction method.

2. Methods

Our experiments were performed in a rectangular container subjected to harmonic horizontal excitation. A schematic of the experimental setup is shown in figure 2. The tank (width $w = 500$ mm, depth $l = 50$ mm) is partially filled with water. The tank is mounted on a moving platform horizontally excited by a motor (a) drives an eccentric disk which converts the rotary motion of the motor into a quasi-harmonic horizontal oscillation of the platform. A positioning sensor (c) directly records the motion of the platform on which the tank (d), two high-speed cameras (e) and an USB-camera (f) are mounted. For the PIV measurements a light sheet (g) is provided by a laser passing through a cylinder lens (implied) and a slit (h).

- [1] Williams M.O., Kevrekidis I.G., Rowley C.W. (2015) A Data-Driven Approximation of the Koopman Operator: Extending Dynamic Mode Decomposition. *Nonlinear Dyn.* 9, 1307–1346.
- [2] Brunton S., Brunton B.W., Proctor J., Kutz J.N. (2017) Chaos as an intermittently forced linear system. *Nat. Commun.* 8(1), 1–10.
- [3] Abarbanel H.D.I., Kennel M.B. (1993) Local false nearest neighbors and dynamical dimensions from observed chaotic data. *Phys. Rev. E* 47:3057–3068.
- [4] Cenedese M., Axás J., Bäuerlein B., Avila K., Haller G. (2022) Data-driven modeling and prediction of non-linearizable dynamics via spectral submanifolds. *Nat. Commun.* 13(1), 1–10.
- [5] Axás J., Cenedese M., Haller G. (2022) Fast data-driven model reduction for nonlinear dynamical systems. *Nonlinear Dyn. In production.*

A study on the dynamics of the flexible link mechanism with a spatial model of the translational joint with clearance

Krzysztof Augustynek, Andrzej Urbaś, and Jacek Stadnicki

**Department of Mechanical Engineering Fundamentals, University of Bielsko-Biala, Bielsko-Biala, Poland*

Abstract. The paper presents the dynamics model of the RPSUP mechanism with a clearance in a translational joint. The spatial model of the clearance in the translational joint is proposed. In this model, inner surface of the slider is discretized into rectangular zones in which the contact between the slider and guide is detected. For each zone, three scenarios of the contact are possible: point, line, and surface contact. In numerical simulations interactions between the flexible coupler and the clearance in the translational joint will be studied and compared.

Introduction

The fifth class kinematic pairs (revolute and translational joints) are among the most popular types of joints in mechanisms. The possibility of modelling non-linear effects in these joints, such as friction or clearance, is very important from the point of view of the dynamics of the system [1–4]. There are many works in the literature devoted to both planar and spatial models of clearance in revolute joints [3]. The situation is different in the case of translational joints with clearance, where only a small number of papers deal with spatial models of clearance [1, 2]. In these models, some number of conditions are formulated to describe special cases of the position of the slider with respect to the guide.

This paper proposes an approach in which the internal surfaces of the slider are discretized into rectangular contact zones, where the contact between the slider and the guide can be analysed (Fig. 1). Depending on the number of nodes in contact and the depth of penetration, three cases of contact are considered: *point*, *linear* and *surface*. The normal contact force in node $(i, j)_p$ is calculated using the following formula [1]

$$\|\mathbf{f}_n^{(i,j)_p}\| = K^{(i,j)_p} \left(\delta_m^{(i,j)_p} \right)^{1.5} + C^{(i,j)_p} \dot{\delta}_m^{(i,j)_p},$$

where the generalized stiffness and damping $K^{(i,j)_p}$, $C^{(i,j)_p}$ depend on the type of contact (point, linear, surface), and $\delta_m^{(i,j)_p}$ is an average penetration depth in node $(i, j)_p$. The tangent force due to friction is modelled using the LuGre friction model.

The proposed model of the clearance will be analysed for the spatial RPSUP mechanism with the flexible coupler. The coupler is discretized using the Rigid Finite Element Method. The dynamics equations of motion are derived using the Lagrange equations of the second kind. Homogeneous transformation matrices and joint coordinates are applied in the derivations process. In numerical simulations, the influence of link flexibility and clearance in the translational joint on the dynamics response of the mechanism will be studied.

References

- [1] Wu X., Sun Y., Wang Y., Chen Y. (2020) Dynamic analysis of the double crank mechanism with a 3D translational clearance joint employing a variable stiffness contact force model. *Nonlinear Dyn.* **99**:1937–1958.
- [2] Qian M., Qin Z., Yan S., Zhang L. (2020) A comprehensive method for the contact detection of a translational clearance joint and dynamic response after its application in a crank-slider mechanism. *Mechanism and Machine Theory.* **145**:103717.
- [3] Erkaya S., Doğan S., Şefkathioğlu E. (2016) Analysis of the joint clearance effects on a compliant spatial mechanism. *Mechanism and Machine Theory.* **104**: 255–273.
- [4] Zheng X., Li J., Wang Q., Liao Q. (2019) A methodology for modeling and simulating frictional translational clearance joint in multibody systems including a flexible slider part. *Mechanism and Machine Theory.* **142**:103603.

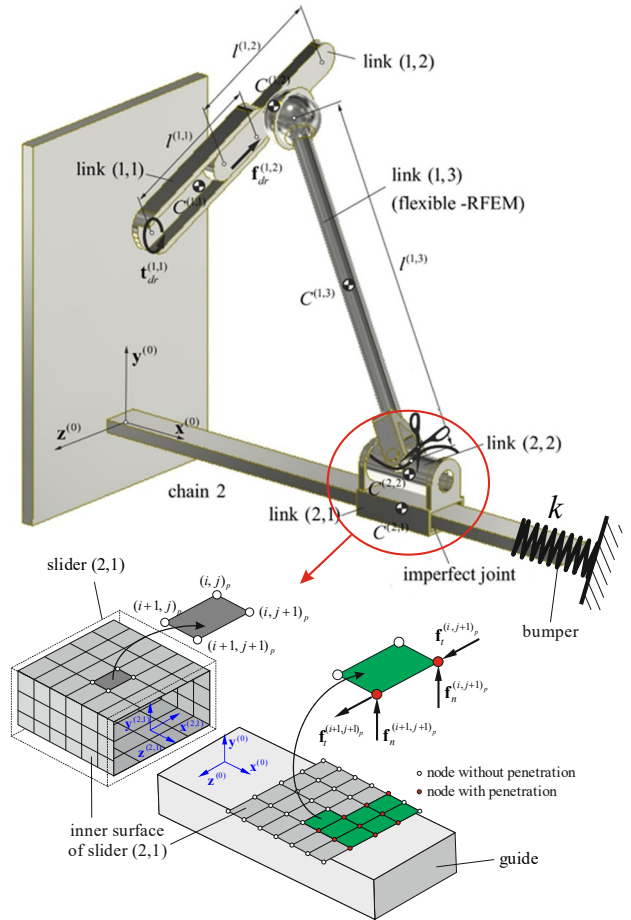


Figure 1: Model of RPSUP mechanism with the clearance in slider (2,1)

Fast computation and characterization of forced response surface of high-dimensional mechanical systems via spectral submanifolds and parameter continuation

Mingwu Li*, Shobhit Jain* and George Haller *

*Institute for Mechanical Systems, ETH Zürich, Switzerland

Abstract. Forced response curves (FRCs) have been widely used to characterize the nonlinear dynamics of mechanical systems subject to periodic excitations. Forced response surfaces (FRSs), which depict the nonlinear forced response over a range of excitation amplitudes, however, have been rarely computed in the literature. FRSs remove the need for a case-by-case computation of FRCs over a sample of excitation amplitudes and automatically uncover any isolas in the forced response, that are otherwise hard to predict. Here, we construct spectral submanifold-based reduced-order models (ROMs) of high-dimensional mechanical systems and equip these ROMs with multidimensional manifold continuation of fixed points to efficiently extract FRSs. By solving optimization problems on these ROMs, we also show how to extract the ridges and valleys in an FRS, which delineate the main physical features of the forced response. We demonstrate fast and effective FRS computation using the proposed approach over finite-element models of structural systems.

Introduction

We consider a periodically forced nonlinear mechanical system with forcing frequency Ω and forcing amplitude ϵ . Let \mathcal{A} be the amplitude of the periodic orbit. The frequency response surface (FRS) is a two-dimensional manifold in the space $(\Omega, \epsilon, \mathcal{A})$ that is foliated by the FRCs. Ridges and valleys in the surface present the skeleton of the response surface. In addition, the projection of them onto the plane (Ω, \mathcal{A}) gives the *damped backbone curve*. The ridges and valleys are obtained as a collection of local extrema of the one-parameter family of FRCs under variation in ϵ . Since covering a two-dimensional manifold is much more demanding than that of a one-dimensional manifold, one can use ridges and valleys to characterize the main features of the FRS without computing it. However, locating these ridges and valleys are still computationally challenging for high-dimensional problems.

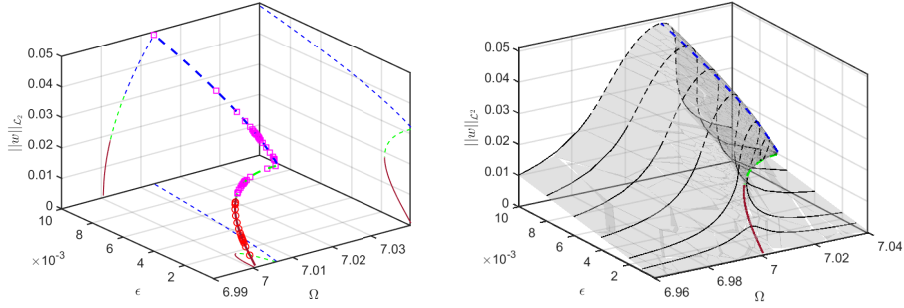


Figure 1: Left: Ridges and valleys obtained from SSM-based ROM(lines) and the full system via collocation (markers). Right: FRS and its the ridges and valleys obtained via the SSM-based ROM along with sampled FRCs obtained from the full system via collocation.

Results and discussion

We remove this bottleneck using reduced-order models (ROMs) on spectral submanifolds (SSMs) [1]. Specifically, we reformulate the periodic orbits of the full system as fixed points of their low-dimensional ROMs on SSMs computed via SSMTTool [2]. We then use multidimensional manifold continuation [3] of these fixed points to compute the FRS of the full system. Furthermore, we use a successive continuation [4] to locate the ridges and valleys directly with the computation of only one forced response curve.

We apply the proposed method to a cantilever beam with a nonlinear support. This system is discretized with 50 DOFs. As seen in Fig. 1, the results from SSM predictions match well with that of collocation methods. Here, the complete FRS is obtained in less than half an hour via the SSM reduction, while the 6 sampled FRCs are obtained in nearly 6 hours using a collocation method on the full system. Furthermore, generating the ridges and valleys via the SSM reduction took 31 seconds whereas that using a collocation scheme on the full system took 1.5 days. Note that the isolas are uncovered automatically via this FRS computation, as shown in Fig. 1.

References

- [1] Haller G., Ponsioen S. (2016) Nonlinear normal modes and spectral submanifolds: existence, uniqueness and use in model reduction. *Nonlinear Dyn.* **86**(3):1493–1534.
- [2] Jain, S., Thurnher, T., Li, M., Haller, G.: SSMTTool 2.2: Computation of invariant manifolds & their reduced dynamics in high-dimensional mechanics problems. <https://doi.org/10.5281/zenodo.4614201>.
- [3] Dankowicz, H., Wang, Y., Schilder, F., Henderson, M. E. (2020). Multidimensional manifold continuation for adaptive boundary-value problems. *J. Comput. Nonlinear Dyn.*, **15**(5), 051002.
- [4] Li, M., Dankowicz, H. (2018). Staged construction of adjoints for constrained optimization of integro-differential boundary-value problems. *SIAM J. Appl. Dyn. Syst.*, **17**(2), 1117-1151.

Developing sufficiently accurate reduced-order models using an efficient error assessment method

Xiao Xiao*, Thomas L. Hill* and Simon A. Neild *

*Department of Mechanical Engineering, University of Bristol, Bristol, UK

Abstract. Before utilizing a reduced-order model (ROM) of a complex finite element model, the ROM's accuracy should be checked and, if the accuracy is not satisfactory, the ROM must be developed further. This work proposes an efficient error assessment approach to evaluate the ROM's accuracy, which does not require additional data points from the finite element model. Furthermore, a strategy of updating the load cases to aid improvement in accuracy is highlighted. Finally, a 7th-order ROM's construction procedure is used as an example to illustrate the proposed method.

Introduction

The ICE method can generate the ROM of the finite element (FE) model with geometric nonlinearity by capturing the FE model's static force relationship accurately. This method uses a series of static load cases, F_{r0} , and the corresponding static modal displacement, r_0 , to estimate the ROM's parameters via the fitting procedures, and the ROM's accuracy is strongly dependent on the fitting results[1]. Generally, the fitting results can be evaluated by comparing the nonlinear stiffness force between the ROM and the FE model, but the later requires the calculation of additional data points in the FE software. The purpose of this study is to propose an approximate error formula to evaluate the ROM's accuracy efficiently without additional FE executions and then use this error formula to guide where additional data points are needed to improve the accuracy. Specifically, we propose comparing the ROM's accuracy with a higher-order (in terms of power of polynomial used) ROM which might be viewed as an approximation to the full order FE code[2]. In this approach, the approximate error for evaluating the n^{th} -order ROM's accuracy can be written as,

$$\hat{\varepsilon}_n(r) = \frac{\|f_n(r) - f_{n+2}(r)\|}{\max\|f_{n+2}(r)\|} \quad (1)$$

where the r is the modal displacement in the ROM, the $f_n(r)$ and $f_{n+2}(r)$ are the stiffness forces in the n^{th} and $(n + 2)^{\text{th}}$ -order ROM, respectively. The Eq.(1) is computationally efficient, as it does not require extra static FE analysis. This error formula can then also be used to govern where an additional data point is needed should the ROM's accuracy be insufficient.

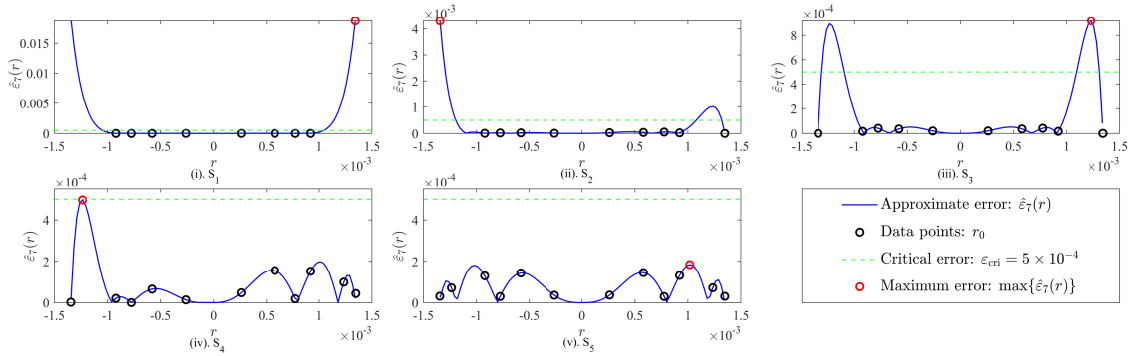


Figure 1: The ROM's construction and evaluation

Results and discussion

Figure 1 depicts a 7th-order ROM's construction procedures. As the initial load distribution S_1 is given, the next load cases can be determined from the Eq.(1). Specifically, the point related to the maximum error, $\max\{\hat{\varepsilon}_n(r)\}$, under the S_i will be extracted and the next load case will be calculated by substituting the coordinate of this point into ROM's nonlinear stiffness force. Then, the load distribution will be updated to S_{i+1} by adding this new load case in S_i , and ROM will be constructed and evaluated again based on the S_{i+1} until the $\max\{\hat{\varepsilon}_n(r)\}$ smaller than ε_{cri} . Meanwhile, it can be observed that every new load case can decrease the fitting error continuously, which indicates the new load case provided by the proposed method is reasonable. From the results, it suggests that the approximate error formula can not only evaluate the fitting error efficiently but can efficiently guide the load case selection, which can keep the total times of static analysis small.

References

- [1] Park K., Allen M.S. (2021) Quasi-static modal analysis for reduced order modeling of geometrically nonlinear structures. *J. Sound Vib.* **502**:116076.
- [2] Nicolaidou E., Melanthuru V.R., Hill T.L., Neild S.A. (2020) Accounting for quasi-static coupling in nonlinear dynamic reduced-order models. *J. Comput. Nonlinear Dynam.* **15**(7):071002.

Multiple Equilibrium States in Large Array Resonators

Chaitanya Borra¹, Nikhil Bajaj², Jeffrey F. Rhoads³, D. Dane Quinn^{1*}

¹The University of Akron, Akron OH, USA; ²University of Pittsburgh, Pittsburgh PA, USA; ³Purdue University, West Lafayette IN, USA

Abstract. This work considers the response of a globally coupled array of oscillators, each with cubic nonlinear stiffness, in the presence of global reactive and dissipative coupling. Based on the continuum formulation for this system first presented in C. Borra et al (Journal of Sound and Vibration, 393:232–239, 2017), the individual resonators are excited to sufficient amplitude to allow for multiple coexisting equilibrium distributions. The method of multiple scales is then applied to the system to describe evolution equations for the amplitude and phase of each resonator, and the equilibrium structure of the system is studied as the reactive and dissipative coupling parameters are varied. For specific families of the equilibrium distributions two-parameter bifurcation sheets can be constructed., and these sheets are connected as individual resonators transition between different branches for the corresponding individual resonators.

Introduction

The equations of motion for a discrete system of coupled resonators [1] can be written as

$$m_i \ddot{z}_i + c_i \dot{z}_i + k_{1,i} z_i + k_{3,i} z_i^3 - \frac{\tilde{\alpha}}{N} \sum_{j=1}^N \dot{z}_j - \frac{\tilde{\beta}}{N} \sum_{j=1}^N z_j = \tilde{f}(t), \quad (1)$$

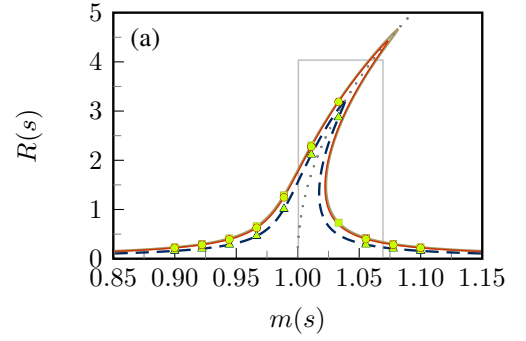
where each individual resonator in the N -element array is characterized by the index i and has an associated displacement z_i . The parameters $\tilde{\alpha}$ and $\tilde{\beta}$ characterize the magnitude of the dissipative and reactive global coupling respectively, and finally each resonator is subject to an external time-dependent excitation represented by $\tilde{f}(t)$. This system is analyzed using the method of multiple scales applied in a continuum limit of the population, first introduced in Borra et al. [2].

Results and Discussion

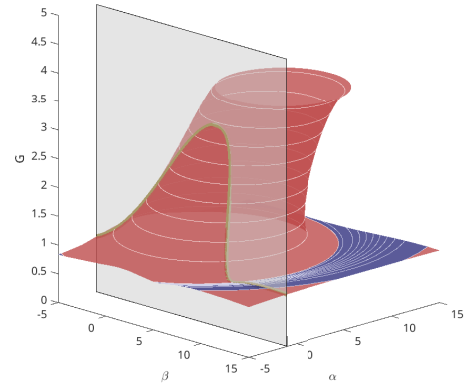
As illustrated in Figure 1a, for given values of the coupling parameters $(\tilde{\alpha}, \tilde{\beta})$, coexisting stationary distributions of the population of resonators exist. In the figure three distinct equilibrium populations are shown for $N = 10$ resonators, each with given mass detuning. Further, distinct two-parameter bifurcation sets can be obtained for specific population characteristics as the coupling varies, an example of which is shown in Figure 1b. The resulting families of bifurcation sets can be pieced together to then understand the overall bifurcation structure of the system.

References

- [1] Sabater A.B., Hunkler A. G., Rhoads J.F. (2014) A single-input, single-output electromagnetically-transduced microresonator array. *Journal of Micromechanics and Microengineering*, 24:65005
- [2] Borra C., Pyles C.S., Wetherton B.A., Quinn D.D., Rhoads J.R. (2017) The dynamics of large-scale arrays of coupled resonators. *Journal of Sound and Vibration*, 392:232–239, 2017.



(a) Coexisting equilibrium distributions, $N = 10$; each distribution is indicated by a different line and marker style (most notable at $i = 7$).



(b) Bifurcation Sheet

Figure 1: Equilibrium Structure

*quinn@uakron.edu

Reduced-Order Models for Systems with Snap-Through

Max de Bono, Simon A. Neild, Rainer Groh, Thomas L. Hill

School of Civil, Aerospace and Mechanical Engineering, University of Bristol, Bristol, BS8 1TR, UK

Abstract. Traditionally, Reduced-Order Models (ROMs) have been unable to capture the highly nonlinear dynamics of snap-through systems. In the case of morphing aeroelastic structures, the computational cost of optimising multi-stable systems is a major bottleneck in the design process, and accurate ROMs would be a significant step in overcoming this. This work investigates the application of a technique to generate ROMs that can capture large in-plane displacements and demonstrates its applicability to snap-through.

Introduction

Snap-through is an important failure mode in many thin-walled or easily buckled structures [1] and is also used as a mechanism for effectively introducing multi-stability into morphing structures, including next-generation turbine blades and aerofoils [2]. Accounting for snap-through in design requires accurately capturing its dynamics. This is typically highly computationally expensive due to the strong nonlinearity of the phenomenon. Snap-through systems can experience significant in-plane displacements which, traditionally, have been challenging to capture in indirect ROMs. However, with the development of the *Implicit Condensation and Expansion with Inertial Compensation* (ICE-IC) method, the effect of in-plane kinetic energy can be efficiently captured without expanding the reduction basis of the ROM [3]. This work investigates the applicability of this method to snap-through systems.

Results and Discussions

The ICE-IC method is used to compute ROMs for a two DoF, single mass oscillator with significant in-plane kinetic energy and a FE modelled, pinned-pinned, pre-compressed beam. The ROM accurately predicts the backbone curve for the 2 DoF system, which is a marked improvement compared to when the coupled kinetic energy is neglected (see Panel (a) of Figure 1). The dynamics of the FE beam is also well predicted for simple single-mode snap-through, as shown in Panel (b) of Figure 1. However, for increased generality, the reduction basis needs to include at least two unstable modes which results in a far more complex static data set. Further work is required to demonstrate that the dynamics would be well captured by such a ROM.

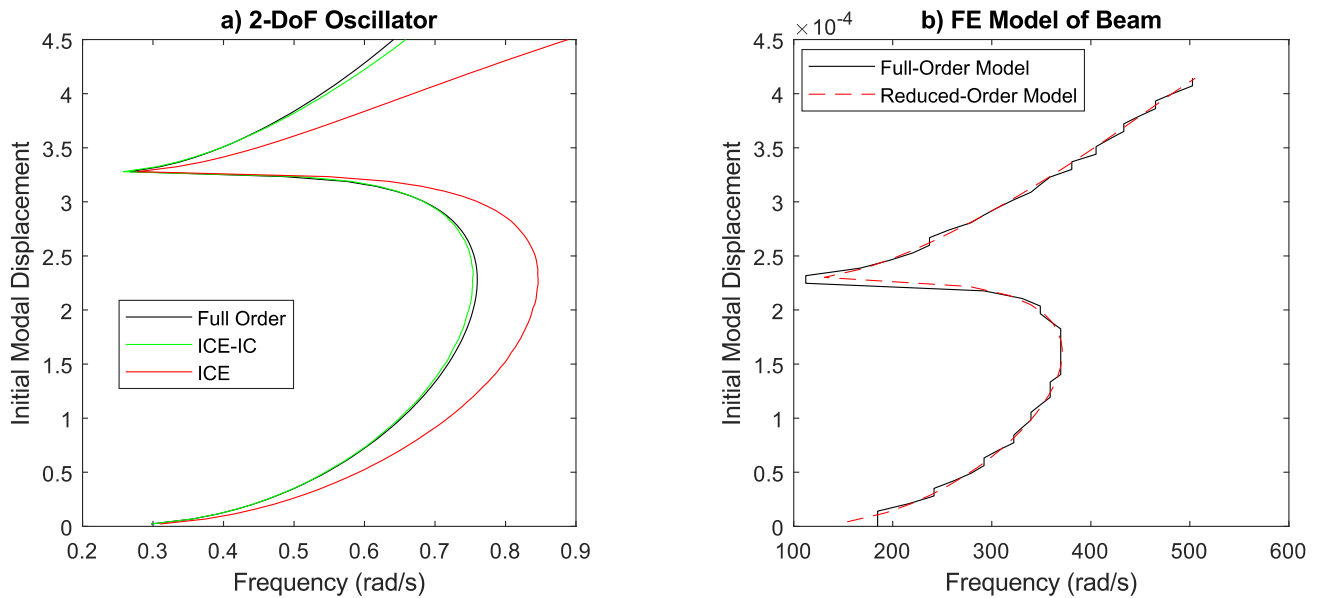


Figure 1: Frequency of the free response for a given initial modal displacement for (a) the 2 DoF system and (b) the FE beam. The full model and ICE-IC ROM are shown in both and the ICE only ROM is given as a point of comparison in the 2 DoF system.

References

- [1] Ghaboussi, J., Healey, T. J., & Pecknold, D. A. (1985) Snap-Through and Bifurcation in a Simple Structure. *J. Eng Mech* **111**(7):909–922
- [2] Schultz, M. (2008) A Concept for Airfoil-Like Active Bistable Twisting Structures. *J. Intell Mater Syst Struct* **19**(2):157–169.
- [3] Nicolaidou, E., Hill, T. L., & Neild, S. A. (2020) Indirect Reduced-Order Modelling: Using Nonlinear Manifolds to Conserve Kinetic Energy. *Proc. R. Soc. A* **476**(2243)

A reduced-order modeling procedure to isolating energy- and evolution-wise dominant features of fluid-driven pollutant dispersion in a street canyon

Yunfei Fu^a, Xisheng Lin^a, Mengyuan Chu^b, Fei Wang^c, Zhi Ning^b, K.T. Tse^a and Cruz Y. Li^{a,d}

^aDepartment of Civil and Environmental Engineering, The Hong Kong University of Science and Technology, Clear Water Bay, Kowloon, Hong Kong

^bDivision of Environment and Sustainability, The Hong Kong University of Science and Technology, Clear Water Bay, Kowloon, Hong Kong

^cDepartment of Civil and Environmental Engineering, The Hong Kong Polytechnic University, Hung Hom, Kowloon, Hong Kong

^dDepartment of Civil Engineering, Chongqing University, Chongqing, China

Abstract. This paper develops a reduced-order modeling procedure, namely an adjoint Proper Orthogonal Decomposition (POD)-Dynamic Mode Decomposition (DMD) analysis, to isolate the energy and evolution-wise dominant features of fluid-driven pollutant dispersion in a street canyon. Based on large-eddy simulation (LES) results of a generic street canyon, this systematic procedure identified three types of flow field modes according to energetic and dynamic significance, providing useful guidance for pollutant dispersion phenomenon analysis.

Introduction

Among the present Reduced-order models (ROMs), Proper Orthogonal Decomposition (POD) is one popular scheme that has been widely employed to investigate pollutant dispersion and wake dynamics around buildings and moving vehicles [1]. The limitations of POD lie in its modes mixed in frequency components and its neglecting some low-energy modes that impose significant dynamical effects on the flow field. The former leads to difficulty identifying flow patterns corresponding to each dominant frequency. The latter leads to poor low-dimensional reconstruction models, even when the majority of energy in a dataset has been captured [2]. DMD is another purely data-driven ROM introduced by Schmid [3], in which each mode contains a unique frequency, providing great convenience in identifying specific dynamic features. However, DMD is weak in determining the highly physically relevant modes due to lacking an approach to ranking eigenvalue significance.

Due to the two schemes' limitations, this paper develops an adjoint POD-DMD analysis procedure to isolate dominant features of fluid-driven pollutant dispersion in a street canyon from the perspectives of both energetic and dynamic significance. The dominant flow field structure patterns and their contribution to pollutant dispersion are identified and summarized.

Results and Discussion

In this paper, the adjoint POD-DMD procedure contains four steps. Firstly, conduct POD and DMD, respectively, to the raw flow field data. Secondly, based on the dominant frequencies of the high-energy POD mode, identify three types of DMD modes according to energy contribution and dynamical effects. Thirdly, conduct superposition to DMD modes within a type to identify the key features, as shown in **Fig. 1**. Finally, corresponds the dominant flow patterns to possible pollutant dispersion phenomenon.

Results show that energetically & dynamically significant modes (**Fig. 1a**) show the mainstream and the main vortex structures occurring near the stagnation point, the separating point, and the fluid reattachment area. Energetically significant & dynamically insignificant modes (**Fig. 1b**) represent where the turbulent kinetic energy is the largest, leading to periodically sudden pollutants increase near the building roofs and the wake region. Energetically insignificant & dynamically significant modes (**Fig. 1c**) show the reversed flow structures occurring near the stagnation point, inside the street canyon, and in the wake region, leading to slow but continuous pollutant increase near the upstream building roof and the windward wall.

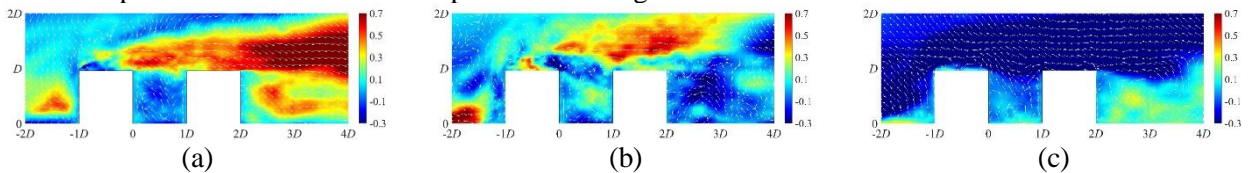


Fig. 1 Normalized velocity vectors of (a) energetically & dynamically significant modes (b) energetically significant & dynamically insignificant modes (c) energetically insignificant & dynamically significant modes

References

- [1] F. Wang, C. H. Liu, J. Xie (2021) Wake dynamics and pollutant dispersion behind a light-duty lorry. *Physics of Fluids* **33**(9):095-127.
- [2] C. W. Rowley, S. T. M. Dawson (2017) Model Reduction for Flow Analysis and Control. *Annu Rev Fluid Mech* **49**(1):387-417.
- [3] P. J. Schmid (2010) Dynamic mode decomposition of numerical and experimental data. *J. Fluid Mech* **656**:5-28.

Substructural FRF based reduction technique for nonlinear systems

Hossein Soleimani^{*,**}, Konstantinos Poullos^{*,**}, Jonas Brunskog^{***} and Niels Aage^{*,**}

^{*}*Solid Mechanics, Department of Civil and Mechanical Engineering, Technical University of Denmark, 2800 Kgs. Lyngby, Denmark*

^{**}*Centre for Acoustic-Mechanical Micro Systems (CAMM), Technical University of Denmark, 2800 Kgs. Lyngby, Denmark*

^{***}*Acoustic Technology, Department of Electrical Engineering, Technical University of Denmark, 2800 Kgs. Lyngby, Denmark*

Abstract. Prediction of the forced response of coupled structures in contact may become computationally expensive due to the nonlinearity in the system. However, the dominant nonlinearity in the coupled structure is localized at the contact interface which gives the opportunity to solve the nonlinear equations only for connection degrees of freedom (DOF) instead of whole structure. In this paper, a new reduction technique for dynamic analysis of nonlinear coupled structure in frequency domain, is presented. The method reduces the number of nonlinear equations to the half of the number of connection DOFs in the coupled structure. Notably, model order substructuring techniques such as fixed, free and mixed interface methods reduce the system to N nonlinear equations, where N is the total number of connection DOFs plus the number of modes included in each substructure. The performance of the method is examined through a case study, and it is shown that the method reduces the computational cost.

Introduction

Most devices contain components that are assembled together for a specific function. Assembling in some applications is inevitable because each component has different material and domain of performance, such as hearing aids which consist of electrical, acoustic and mechanical component. Accurate prediction of dynamic response of coupled structures requires detailed finite element model of each component and nonlinear modeling of the connections which makes it computationally expensive. Despite using high performance computers, developing physics based reduction techniques is necessary to reduce the computational cost.

Component mode synthesis (CMS) methods are one of the well known techniques to reduce the size of the system. These methods can be categorized to fixed interface [1], free interface [2] and mixed interface [3] methods. In all of these methods the system will reduce to the number of connection degrees of freedom plus number of modes included in each substructure. Increasing accuracy of the solution comes with increasing the number of included mode shapes which gives rise to the number of nonlinear equation that should be solved. In this paper we present an approach in which we separate the governing equation of the substructures in frequency domain and using receptance matrix of the each substructure, a close form nonlinear equation is derived as:

$$\mathbf{x}_{rel} = \mathbf{H}_{be}^I \mathbf{f}_e^I - \mathbf{H}_{be}^{II} \mathbf{f}_e^{II} + (\mathbf{H}_{bb}^I + \mathbf{H}_{bb}^{II}) \mathbf{c}(\mathbf{x}_{rel}) \quad (1)$$

where \mathbf{x}_{rel} is the relative displacement vector at the joint and $\mathbf{c}(\mathbf{x}_{rel})$ is the vector of Fourier coefficient of nonlinearity and \mathbf{H}^j is receptance matrix of substructure $j = I, II$ and indices b and e refer to connection and excitation DOFs, respectively. After solving Eq. 1 using the Newton–Raphson method along with arc-length continuation, the internal force at connection can be calculated. Note that the method does not require the full receptance matrix of the substructure. For calculating the displacements at specific degrees of freedom (m), It is only required to calculate or measure the receptance matrix of the substructures at corresponding degrees of freedom (m), connection and excitation DOFs in the system.

Results and discussion

To investigate the performance of the method, a case study has been considered and the results show that the proposed reduction technique decreases the computational cost comparing to the notable Component Mode Synthesis (CMS) methods, due to excluding the modal amplitudes and halving the connection degrees of freedom in nonlinear equations. Another advantage of the method is that the receptance matrix can be measured or calculated and increasing the number of mode shapes for calculating the receptance matrix, will not affect the number of nonlinear equations in the system. It also gives the opportunity to computed the receptance matrix by expansion based methods such as SOAR [4] and Krylov subspace [5] without any effect on the number of nonlinear equations.

References

- [1] Craig Jr R.R., Bampton M. (1968) Coupling of Substructures for Dynamic Analyses. *AIAA J* **6**:1313-1319.
- [2] Rubin S. (1975) Improved Component-Mode Representation for Structural Dynamic Analysis. *AIAA J* **13**:995-1006.
- [3] Voormeeren S., Valk P., Rixen D. (2010) A General Mixed Boundary Model Reduction Method for Component Mode Synthesis. *IOP Conf. Ser.: Mater. Sci. Eng.* **10**:012116.
- [4] Bai Z., Su Y. (2005) SOAR: A Second-Order Arnoldi Method for the Solution of the Quadratic Eigenvalue Problem. *SIAM J. Matrix Anal. Appl.* **26**:640-659.
- [5] Bai Z. (2002) Krylov Subspace Techniques for Reduced-Order Modeling of Large-Scale Dynamical Systems. *Appl Numer Math* **43**:9-44.

Model Order Reduction of Nonlinear Thermal Systems using DEIM

Gourav Kumbhojkar*, Amar Gaonkar*

*Department of Mechanical, Materials and Aerospace Engineering, Indian Institute of Technology Dharwad,
Karnataka, India

Abstract. A Proper orthogonal decomposition and hyper-reduction-based model order reduction method (MOR) is employed to obtain the computationally efficient solution of nonlinear thermal systems in one- and two-dimensional domains. Material nonlinearity, as well as nonlinearity due to boundary conditions, are considered. The hyper-reduction approach based on POD and Discrete Empirical Interpolation Method (DEIM) is used to solve the nonlinear system and compare the computational performance with the full finite element model.

Introduction

The finite element discretization of nonlinear partial differential equations leads to large scale nonlinear ordinary differential equations. The solution of these equations in time is computationally challenging. To obtain the computationally efficient solutions, model order reduction techniques are employed. The projection-based Proper orthogonal decomposition methods [1] are popularly used for model order reduction of nonlinear systems. However, to obtain the nonlinear matrices in lower dimensional subspace one has to first compute these matrices in the original dimensional space and then do the reduction which adds extra computations. To tackle this issue hyper-reduction methods such as Discrete Empirical Interpolation Method (DEIM), Energy-conserving Sampling and Weighing method (ECSW), etc. are proposed [2].

In this work we employ the POD-DEIM based MOR method to solve nonlinear heat transfer problems in one dimension and two dimensions. We consider the material nonlinearity and nonlinearity due to boundary conditions. The governing equations of the 2D system in the consideration is given in Eq. (1),

$$\frac{\partial}{\partial x} \left(\kappa(T) \frac{\partial T}{\partial x} \right) + \frac{\partial}{\partial y} \left(\kappa(T) \frac{\partial T}{\partial y} \right) = \rho C_p(T) \frac{\partial T}{\partial t} \quad (1)$$

The resulting system of nonlinear first order ODEs after FE discretization is given in Eq. (2),

$$\mathbf{C}(\mathbf{T})\dot{\mathbf{T}} + \mathbf{K}(\mathbf{T})\mathbf{T} = \mathbf{f} \quad (2)$$

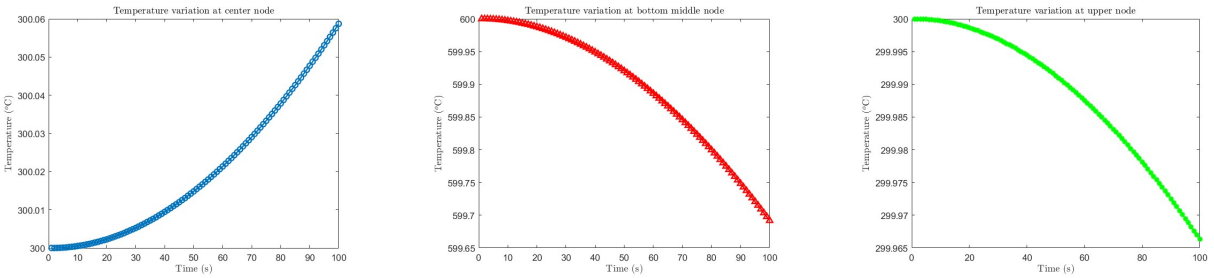
where, $\mathbf{K}(\mathbf{T})$ and $\mathbf{C}(\mathbf{T})$ are the nonlinear conductivity and capacitance matrices, respectively. Let Φ be matrix consisting of POD modes for the problem under consideration. The reduced order model obtained by the POD method is given by,

$$\mathbf{C}_r(\mathbf{T})\dot{\mathbf{T}} + \mathbf{K}_r(\mathbf{T})\mathbf{T} = \mathbf{f}_r \quad (3)$$

where, $\mathbf{C}_r = \Phi^T \mathbf{C} \Phi$, $\mathbf{K}_r = \Phi^T \mathbf{K} \Phi$ and $\mathbf{f}_r = \Phi^T \mathbf{f}$ are the reduced matrices. The computational complexity of Eq. (3) is further reduced by implementing DEIM algorithm.

Results and Discussions

We carry out the numerical experiment of 1D and 2D heat transfer problem with temperature dependent thermal conductivity and heat capacity. We consider Dirichlet and convection boundary conditions. In both one- and two-dimensional systems, DEIM gives more than 20 times faster computation compared to the full order model and 8 times speedup with respect to POD-based model, while maintaining accuracy of around 99%. Following are temperature variations at a few selected nodes:



References

- [1] Benner, P., Gugercin, S. and Willcox, K. A survey of projection-based model reduction methods for parametric dynamical systems. SIAM review. 57(4), 483-531 (2015).
- [2] Chaturantabut, S. and Sorensen, D. C. Nonlinear model reduction via discrete empirical interpolation. SIAM Journal on Scientific Computing. 32 (5), 2737-2764 (2010).

Reduced-order model analysis of the pollutant dispersion on an urban street canyon

Yunfei Fu*, Xisheng Lin*, Bingchao Zhang*, Xinxin Feng**, Chun-Ho Liu**, K.T. Tse* and Cruz Y.Li*,***

*Department of Civil and Environmental Engineering, The Hong Kong University of Science and Technology, Clear Water Bay, Kowloon, Hong Kong.

**Department of Mechanical Engineering, The University of Hong Kong, Pokfulam Road, Hong Kong

***Department of Civil Engineering, Chongqing University, Chongqing, China

Abstract: Pollutant dispersion within street canyons is one of the most challenging topics today. The complex flow patterns, along with turbulence effects, can be regarded as a multi-dimensional non-linear system with a huge amount of information. This paper applies spectral proper orthogonal decomposition (SPOD), one of the cutting-edge reduced-order modeling (ROM) techniques, to capture the main features of the complex non-linear phenomena and save the computational resources for data processing. The relationship between flow structures and pollutant concentration field is illustrated via SPOD cospectra, while the turbulence-induced pollutant removal mechanism is demonstrated via SPOD modes. The results show that both external large-scale coherent structures at the canyon roof level, and waves caused by the canyon vortex play a crucial role in pollutant removal within the street canyon.

Introduction

As a basic unit of urban canopy elements, the street canyon model is widely investigated to understand the interactions between the urban canopy and the atmosphere. In the current study, an idealized street canyon is modeled via computational fluid dynamics (CFD). The model is composed of two parallel buildings with width (streamwise- z) \times height (spanwise- y) \times length (crosswind- x) $= H \times H \times 10H$, with the width of the street between the two buildings set as H . The air pollutant sulfur hexafluoride (SF6) is emitted from four line sources situated at the bottom of the model. The flow field and pollutant concentration field are simulated by Large-Eddy Simulation (LES) method (See figure 1).

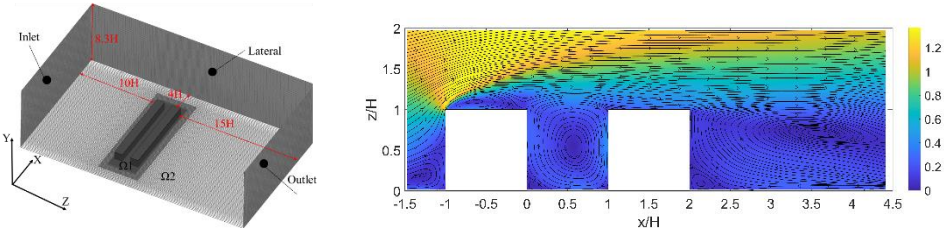


Figure 1: Schematic of the street canyon model and the mean velocity field

Results and Discussion

Compared to obtaining complete information of the system, ROM techniques can help to extract the main spatial-spectral features and dynamic properties from a complex flow field in the street canyon. This paper applies SPOD as a post-processing technique to determine the relationship between turbulent motion and pollutant removal. SPOD is a kind of cutting-edge ROM method, which has the advantages of both traditional POD (proper orthogonal decomposition) and DMD (dynamic mode decomposition)[1]. SPOD modes capture the external large-scale coherent structures and those waves caused by the canyon vortex at building roof (see figure 2). The SPOD cospectra are defined to elucidate the spatial-temporal variation of the phase relationship between the velocity components and concentrations (see figure 3). Mode f4 and f5 represent the large vortex structure in the canyon, those intermittent oblique stripes agree well with the vertical velocity distribution. Mode f1 and f2 represent the large-scale coherent structures, while f3 appears to fall between these two groups of modes. All the modes demonstrate that both external large-scale coherent structures at the canyon roof level, and waves caused by the canyon vortex play a crucial role in pollutant removal within the street canyon.

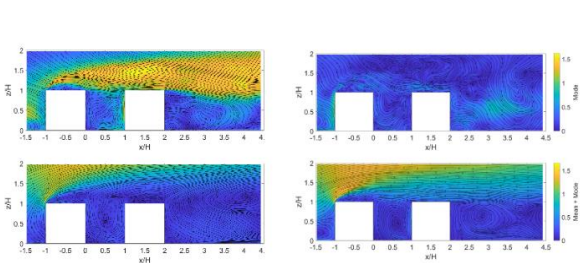


Figure 2: SPOD modes with the real and imaginary parts of the eigenfunction

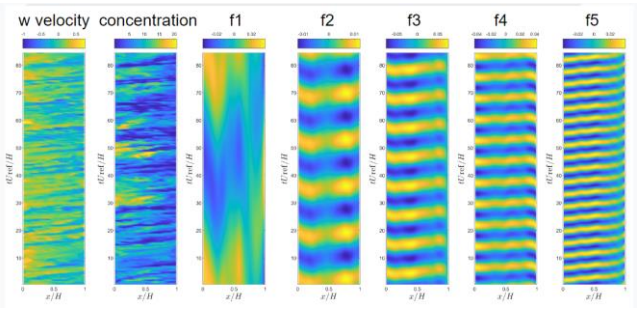


Figure 3: SPOD cospectra for vertical velocity components and concentrations.

References

[1] A. Towne, O.T. Schmidt, T. Colonius, Spectral proper orthogonal decomposition and its relationship to dynamic mode decomposition and resolvent analysis, *J. Fluid Mech.* 847 (2018) 821–867, <https://doi.org/10.1017/jfm.2018.283>.

Using Machine Learning Models To Represent Isolated Nonlinearities Within Structural Systems

D. Dane Quinn^{1*}, David Najera-Flores^{2,3}, Anthony Garland⁴, Vlachas Konstantinos⁵, Eleni Chatzi⁵, and Michael Todd³

¹The University of Akron, Akron, OH USA; ²ATA Engineering, San Diego, CA USA; ³University of California San Diego, La Jolla, CA USA; ⁴Sandia National Laboratories,[†] Albuquerque, NM, USA; ⁵ETH Zürich, Zürich, Switzerland

Abstract. In a structural system with an isolated nonlinear region, a neural network is trained to predict the effect of the nonlinearities within the region on the remaining structure. Based on a novel order-reduction formulation developed previously, these predicted forces are incorporated within an associated ideal system to predict the response of the overall structural system, thus replacing the detailed description of the isolated region and providing a computationally efficient model of the nonlinear system.

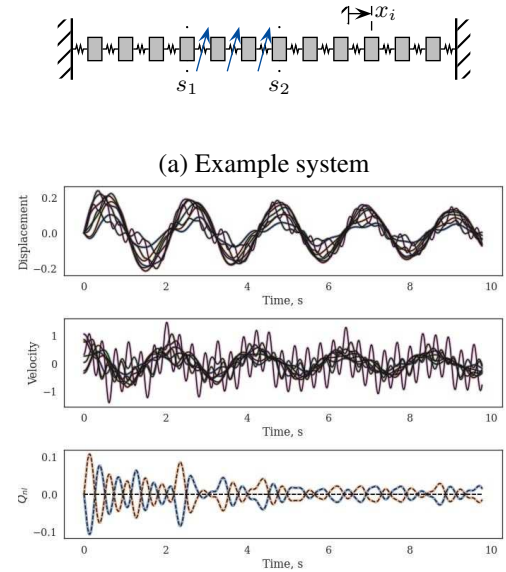
Introduction

Techniques in machine learning, including neural networks, open the possibility of describing the response of engineering systems where the underlying physics is either unknown or too complicated to accurately resolve in a computationally efficient simulation. The present work seeks to employ predictions from a neural network to represent the nonlinearities in an isolated region of a larger structural system, so that the neural network essentially serves as a constitutive model for the nonlinearities. A novel order-reduction approach developed previously by Quinn and Brink [1] is used to introduce the effect of the nonlinearities on the underlying ideal linear system, which are then captured by the application of the neural network. This approach is illustrated with a example structural system where the nonlinearities are assumed to arise from cubic stiffness and damping, as well as state-dependent damping so that the isolated region contains internal hysteretic variables.

Results and Discussion

The system is assumed to be decomposed into a region \mathcal{C}_1 that is linear, coupled to a region \mathcal{C}_2 containing the nonlinearities in the structure. In the order-reduction method the effects of the nonlinearities are captured by an internal force vector \mathbf{Q} that only reflects the influence of the nonlinearities within the isolated region \mathcal{C}_2 on the external linear region \mathcal{C}_1 . This force is then determined from a model capturing the nonlinear response, but localized to the isolated region. As a result, the response of the linear region is determined only by the internal force vector.

This approach is illustrated on a chain of oscillators, representing the discretization of a rod undergoing longitudinal deformations, as illustrated in Figure 1a. The nonlinearities are localized within the region $s \in (s_1, s_2)$, while the remainder of the rod is linear. A Multilayer Perceptron is used to identify the internal force \mathbf{Q} that acts at the boundaries of the isolated region, arising from the nonlinearities. After training, this predicted internal force is used within an ODE solver to determine the response subject to initial conditions and external forcing. The training takes place with a single specific realization of initial conditions and excitation. However, this is sufficient to provide accurate predictions when the system is subject to a variety of initial conditions and excitations, as illustrated in Figure 1b.



(b) System response with an excitation distinct from the training excitation.

Figure 1: Isolated Nonlinearities

References

- [1] Quinn D.D., Brink A.R. (2021) Global system reduction order modeling for localized feature inclusion. *Journal of Vibration and Acoustics*, 143:041006, 2021.

*quinn@uakron.edu

[†]Sandia National Laboratories is a multimission laboratory managed and operated by National Technology and Engineering Solutions of Sandia, LLC, a wholly owned subsidiary of Honeywell International, Inc., for the U.S. Department of Energy's National Nuclear Security Administration under contract DE-NA0003525. This paper describes objective technical results and analysis. Any subjective views or opinions that might be expressed in the paper do not necessarily represent the views of the U.S. Department of Energy or the United States Government.

Analysis of a data-driven planar drone model

Dávid András Horváth*, János Lelkes**, Tamás Kalmár-Nagy***

Department of Fluid Mechanics, Faculty of Mechanical Engineering, Budapest University of Technology and Economics, HUN, ORCID:0000-0002-3534-0457, 0000-0002-6205-4923**, 0000-0003-1374-2620*** #*

Abstract. The main aim of this paper is a new data-driven aerodynamical model for multi-rotor drones and helicopters. The training dataset was created by validated CFD simulations utilizing the virtual blade model. A regression algorithm was used to develop the data-driven model, resulting in a simple model in a short amount of time. Using the data-driven model, the generated forces and moments by the rotating blades can be modeled with high accuracy when the motion state of the structure is known. The result of the paper is a nonlinear drone model whose control algorithm can consider the nonlinear aerodynamical effects. With the help of this model, the maneuverability and precision of drones can be increased in the future.

Introduction

Unmanned aerial vehicles or drones are increasingly common for various tasks, as they have some distinct advantages over conventional aircraft. One of these is that they are much more agile than their traditional counterparts, which stems from the fact that they are much smaller, and human limits do not have to be considered [1]. One popular type of drone is the quadcopter with four rotors, where control is achieved by varying the rpm of the individual rotors only. However, these drones are inherently unstable and exhibit strongly nonlinear, coupled, and underactuated dynamics. For this reason, an accurate aerodynamic model is important to design control algorithms [2].

In this study, the lift of a single propeller was computed using CFD simulations for several different flight conditions. The virtual blade model [3] was applied to reduce the computational cost. From the results of the simulation, an aerodynamic model was built for the lift of a propeller which takes into account the velocity and the angular velocity. This model was applied to a planar quadcopter model [4] and it was compared with a simpler aerodynamic model which only considers the angular velocity.

Results and discussion

To compare the two models, an identical PD controller was used and identical trajectories were prescribed. In most of the cases involving smooth trajectories, the main difference between the models is the resulting angular velocities of the rotors. However, in some cases, especially when the prescribed trajectory is discontinuous, there can also be significant differences in the resulting trajectories. An example is shown in Figure 1, the model based on the CFD simulations is shown in blue, the simpler model by dashed green, and the prescribed trajectory in dotted red.

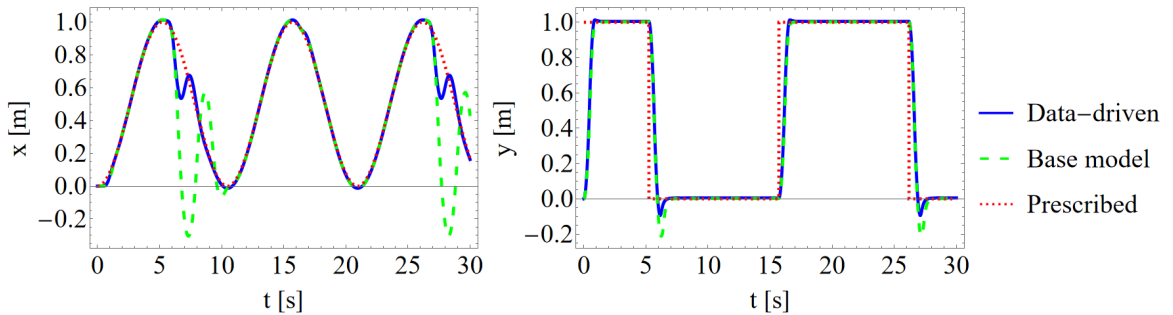


Figure 1: The resulting horizontal and vertical displacements for the two models compared with the prescribed trajectory.

From Figure 1 it can be observed that in the vertical direction, the trajectory is followed more accurately than in the horizontal direction. In the horizontal direction, the trajectory that results from using the base model deviates significantly from the prescribed trajectory.

The result of this investigation is a nonlinear drone model whose control algorithm considers the nonlinear aerodynamical effects. With the help of this model, the maneuverability and accuracy of drones can be increased in the future.

References

- [1] S. Gupte, P. I. T. Mohandas, and J. M. Conrad, A survey of quadrotor unmanned aerial vehicles, in 2012 Proceedings of IEEE Southeastcon, pp. 1-6, IEEE, 2012.
- [2] X. Zhang, X. Li, K. Wang, and Y. Lu, A survey of modelling and identification of quadrotor robot, in Abstract and Applied Analysis, vol. 2014, Hindawi, 2014.
- [3] S. Wahono, Development of virtual blade model for modelling helicopter rotor downwash in openfoam, tech. rep., Aerospace Division, Defence Science and Technology Organisation, 2013.
- [4] P. Venkatesh, S. Vadhvana, and V. Jain, Analysis and control of a planar quadrotor, arXiv preprint arXiv:2106.15134, 2021

Data-driven Nonlinear Normal Modal Identification and Reduced-order Modeling: A Physics-integrated Deep Learning Approach

Shanwu Li* and Yongchao Yang*

*Department of Mechanical Engineering – Engineering Mechanics, Michigan Technological University, Houghton, MI, USA

Abstract. Identifying the characteristic coordinates or modes of nonlinear dynamical systems is critical for understanding, analysis, and reduced-order modeling of the underlying complex dynamics. While normal modal transformation exactly characterizes any linear systems, there exists no such a general mathematical framework for nonlinear dynamical systems. Nonlinear normal modes (NNMs) are natural generalization of the normal modal transformation for nonlinear systems; however, existing research for identifying NNMs has relied on theoretical derivation or numerical computation from the closed-form equation of the system, which is usually unknown. We present a data-driven method with physics-integrated deep learning for identifying NNMs and reconstructing the NNM-spanned reduced-order models of unknown nonlinear dynamical systems using response data only. We leverage the modeling capacity of deep neural networks with integration of physics knowledge about nonlinear dynamics to identify the forward and inverse nonlinear modal transformations and the associated modal dynamics evolution. We discuss the performance and applicability of the method on different nonlinear systems with comparisons with existing methods.

Introduction

Dynamical systems generally exhibit complex nonlinear phenomena, such as frequency-energy dependence and modal interaction. Their accurate modeling and representation typically require high-dimensional models, resulting in great difficulties in analysis and computations. Reduced-order modeling (ROM) aims to alleviate such modeling and computation challenges by identifying reduced-order models (ROMs) that accurately capture the dynamics embedded in the original high-dimensional space. While the proper orthogonal decomposition (POD) method has been successfully applied in ROMs with the advantage of computational efficiency thanks to its simplicity, its linear nature reduces its performance when handling intrinsically nonlinear dynamical systems. Nonlinear normal modes (NNMs), defined as invariant manifolds [1] in the state space, are natural bases that span a nonlinear subspace with clear physical interpretations. Furthermore, the generalized invariance property of NNMs allows finding the lowest-dimensional subspaces that capture the nonlinear dynamics. We present our recent study on developing a physics-integrated deep learning approach to discover ROM from measurement data only; it simultaneously identifies the NNMs-spanned subspace with a hierarchical order and the associated nonlinear modal dynamics. Specifically, our approach consists of 1) a hierarchical autoencoder that identifies the nonlinear modal transformation function of NNM with a hierarchical order which indicates the relative contribution of each NNM to the observed responses; and 2) a dynamics-coder that identifies the evolution function of the NNM coordinates.

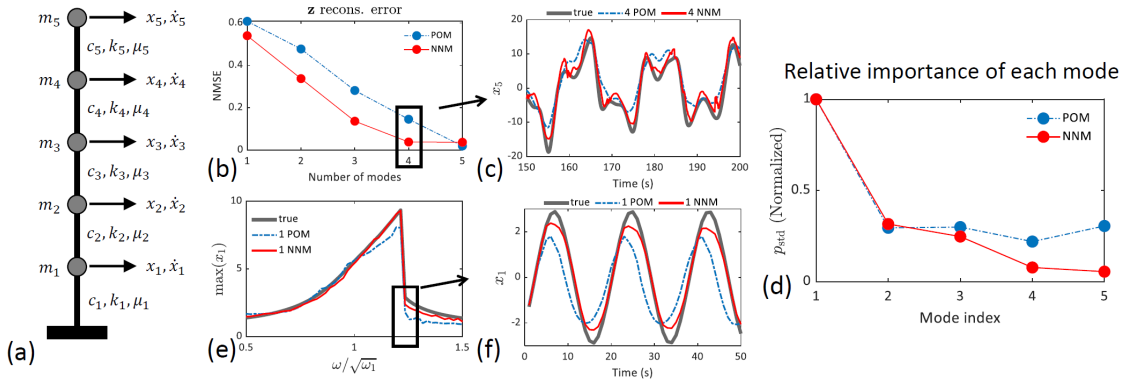


Figure 1: Numerical experiments on a nonlinear shear-type 5DOF system and the identification results.

Results and discussion

Reconstructions using identified NNM coordinates have smaller error than that by POD mode (POM) coordinates. Same conclusion can be drawn from the predicted time histories of states by 4-order ROMs based on POMs and NNMs. The oscillation amplitudes of transformed response that reveal relative importance of each identified mode for the observed response are shown in (d). For forced nonlinear systems, it is seen in (e) that the NNM-based ROM identified by our approach shows higher accuracy than POM-based ROM, especially in the vicinity of bifurcation frequency where the nonlinearity of the system is prominent.

References

- [1] Shaw, S. W., and Pierre, C. 1993. Normal Modes for Non-Linear Vibratory Systems. *Journal of Sound and Vibration*, 164(1):85–124.

A comparison of parametrizations of invariant manifolds for nonlinear model reduction

Alexander Stoychev* and Ulrich J. Römer**

*Institute of Engineering Mechanics, Karlsruhe Institute of Technology, GERMANY, ORCID #0000-0001-8996-6327

**Institute of Engineering Mechanics, Karlsruhe Institute of Technology, GERMANY, ORCID #0000-0002-6393-6063

Abstract. A comparison of three different parametrization styles for the approximation of invariant manifolds is performed for eight different dynamical systems. The impact of the parametrization style on finite order approximations is investigated by comparison to exact solutions. A modified parametrization style is shown to yield superior results for two example systems thus motivating further research into the development of better parametrizations in the future.

Introduction

The approximation of invariant manifolds is a popular approach for reduced order modeling of nonlinear dynamical systems. Stable and sufficiently attractive (slow) invariant manifolds represent the system's behavior of interest since solution trajectories of the full system that start close to such a manifold converge towards it and may be approximated by the solution trajectory on the invariant manifold. For a given (smooth) dynamical system, invariant manifolds in a neighborhood of a solution such as a fixed point can be approximated numerically by the parametrization method [1, 2]. An ansatz of multivariate polynomials for the invariant manifold and the reduced dynamics thereon yields a sequence of systems of linear equations to determine the unknown coefficients that can be solved recursively starting at the lowest order [3, 4]. However, this procedure gives fewer equations than unknowns which means that there is some methodological ambiguity that needs to be resolved. Depending on what additional conditions are introduced to resolve this ambiguity, this approach gives a certain parametrization—e. g. the graph style parametrization (GSP) or the normal form parametrization (NFP). Different parametrization yield better or worse approximations, depending on the specific dynamic system that they are applied to. Although a posteriori error analysis is possible [5], it is difficult to choose the best parametrization a priori. To illustrate the impact of the parametrization choice and motivate further research into the development of further parametrizations, we apply GSP, NFP and NFP for systems with (near) resonances to a series of benchmark problems that are designed to favor one parametrization style [6].

Results and discussion

Approximations of invariant manifolds and the reduced dynamics thereon are calculated for eight dynamical systems. Exact solution of the invariant manifolds that we want to approximate numerically with all three parametrization styles are known for seven of those systems; the eighth system is a finite element model taken from the literature. Except for the last system, the dynamics of the full systems and their exact invariant manifold are given by multivariate polynomials of order 3 or less. However, most parametrization styles are not able to recover these low dimensional expressions, instead giving infinite series approximations with limited convergence ranges. We present some unexpected results such as one case where a parametrization is able to recover not just the exact invariant manifold, but also another solution, namely a limit cycle on this manifold. Lastly, we show a heuristically modified parametrization gives a superior approximation for the invariant manifold and the reduced dynamics thereon than GSP or NFP at the same order for the eighth system we considered.

The presented study illustrates that the inherent ambiguity, if resolved sub-optimally, gives rise to bad approximations with small convergence ranges. Future developments and improvements of the parametrization method should take this into account. The presented systems may serve as a possible benchmark for any such developments, since their invariant manifolds and solution behavior are known exactly.

References

- [1] Cabré, P., Fontich, E., de la Llave, R. (2003) The Parametrization Method for Invariant Manifolds I: Manifolds Associated to Non-resonant Subspaces. *Indiana Univ. Math. J.* **52**(2):283-328.
- [2] Haro, Á. et al. (2016) *The Parameterization Method for Invariant Manifolds*. Springer, Cham.
- [3] Jain, S., Haller, G. (2021) How to compute invariant manifolds and their reduced dynamics in high-dimensional finite element models. *Nonlinear Dyn.* **107**:1417–1450.
- [4] Vizzaccaro, A. et al. (2022) High order direct parametrisation of invariant manifolds for model order reduction of finite element structures: application to large amplitude vibrations and uncovering of a folding point. *Nonlinear Dyn.* **110**(4):776-82.
- [5] Breden, M. et al. (2016) Computation of maximal local (un)stable manifold patches by the parameterization method. *Indagationes Mathematicae* **27**(1):340–367.
- [6] Stoychev, A., Römer, U.J. (2022) Failing Parametrizations: What can go Wrong when Approximating Spectral Submanifolds. Submitted to *Nonlinear Dyn.*

Embodied hydrodynamic sensing and estimation using Koopman modes

Phanindra Tallapragada* and Colin Rodwell

*Department of Mechanical Engineering, Clemson University, SC, USA, ORCID #

Abstract. The ability to sense flows and estimate some features in the near field is very important for underwater robot. Many species of fish can accomplish such sensing even when they are blinded using their lateral line or kinematics of fins. The complexity and high (infinite) dimensionality of fluid flows around a swimmer require new methods for such flow sensing. Recent advances on Koopman operator of a dynamical system combined with machine learning offers a new way to extract useful information of the flow based on pressure or kinematic measurements from a swimmer's body. We present experimental and computational results of a trailing hydrofoil sensing and estimating the wake Strouhal number and the distance of an upstream body using on board measurements.

Introduction

Objects moving in water or stationary objects in streams create a vortex wake. An underwater robot encountering the wake created by another body experiences disturbance forces and moments. These disturbances can be associated with the disturbance velocity field and the bodies creating them. Essentially the vortex wakes encode information about the objects and the flow conditions. Underwater robots that often function with constrained sensing capabilities can benefit from extracting this information from vortex wakes. We consider the problem of the estimation of the spatial location of an up stream obstacle or oscillating body in a flow past a pitching hydrofoil and a the reconstruction of the near body flow. It is assumed that pressure on the surface of the hydrofoil can be measured at fixed locations on the body along with the pitch angular velocity of the hydrofoil. Using time series pressure measurements on the surface of the hydrofoil and the angular velocity of the hydrofoil, a Koopman operator can be constructed that propagates the snapshots of data forward in time. The modes from a spectral decomposition of this operator then extracts important features from the measurements and can be the inputs for machine learning to estimate features of the flows and obstacles.

Results and Discussion

Model reduction and reconstruction of reduced order models in such complex dynamical systems where only limited data on observables is available can be possible via the framework of the Koopman operator, a topic that has attracted much attention in recent years [1, 2]. We proposed a framework (see fig. 1) for sensing flows using measurements from a body immersed in the fluid in [3]. In numerical simulations of flow past an upstream body, pressure is measured on the surface of a downstream pitching hydrofoil along with its pitch angular velocity. Denoting the observables as $g(t) = [P_1(t), \dots, P_N(t), \Omega(t)]^T$ where $P_i(t)$ denotes the pressure on the foil at location i at time t and $\Omega(t)$ denotes the foil angular velocity similarly at time t , the Koopman operator \mathcal{K} is a linear operator $\mathcal{K} : L^2 \mapsto L^2$ and propagates the observables forward in time $\mathcal{K}_T g(t) = g(t + T)$. The eigenvalues and eigenvectors (or the singular values and singular vectors) of this operator extract features of the measurements. These feature vectors are then used as an input to deep networks to estimate the obstacle distance [3]. The results however go beyond the estimation of the distance to the obstacle as in [3], but instead show that reconstruction of the flow in subdomain containing the trailing body is possible from the Koopman modes obtained from observables from the hydrofoil. These results are a significant addition to the literature on Koopman modes and flow reconstruction since measurements are obtained from the body alone and not the fluid domain and thus have relevance to autonomous robots.

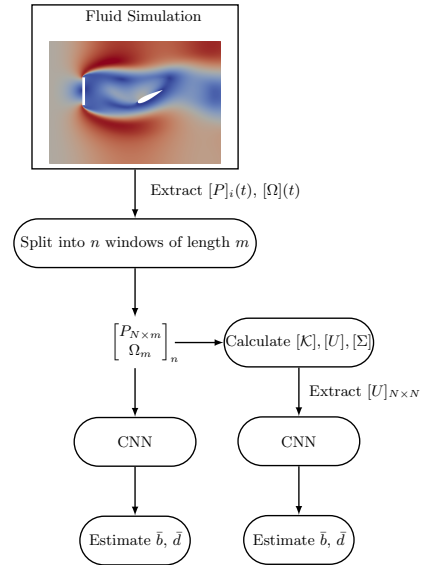


Figure 1: A Koopman operator is constructed using pressure measurements from the surface of the trailing body. The modes of this operator are used to train a deep network to estimate the obstacle distance.

References

- [1] E. M. Bollt Q. Li, F. Deitrich and I. G. Kevrekidis (2017) Extended dynamic mode decomposition with dictionary learning: A data-driven adaptive spectral decomposition of the koopman operator. *CHAOS*, **27**:103111.
- [2] S. Otto and C. Rowley (2019) Linearly recurrent autoencoder networks for learning dynamics. *SIAM Journal on Applied Dynamical Systems*, **18**(1):558–593.
- [3] C. Rodwell and P. Tallapragada (2022) Embodied hydrodynamic sensing and estimation using Koopman modes in an underwater environment. *Proceedings of the American Control Conference*:1632-1637.

Computing Normal Forms of quadratic differential algebraic equations

Alessandra Vizzacarro^{**}, Aurelien Grolet^{*}, Marielle Debeurre^{*}, Olivier Thomas^{*}

^{*}Arts et Métiers, Lille, France

^{**}University of Bristol, Bristol, UK

Abstract. In this paper, we present a general way of computing reduced normal form of nonlinear dynamic systems. The proposed method relies on a so-called quadratic recast in order to transform the dynamical equations into a quadratic DAE and then compute a reduced normal form of the DAE. We present an elegant (and easy to implement) method to write and solve the homological equation, that relies on linear algebra in the vector space of (finite degree) multivariate polynomials. An example is considered to illustrate the results of the method. This constitutes a general way of computing normal form that is aimed to be implemented into the MANLAB package.

Introduction

We consider computation of reduced order models of nonlinear dynamic system using the normal form theory [1, 2, 3]. Usually, the normal form method is presented by considering a system with only polynomial nonlinearity (or a Taylor expansion of the nonlinearity). To increase the generality of the normal form, we propose to consider that the initial dynamic system is under the form of a *DAE with quadratic nonlinearity only*. This is the same hypothesis, as is the MANLAB package, which allows for the application of the Asymptotic Numeric Method on a wide variety of systems [4]. Although this seem restrictive, it can be shown that most nonlinear systems can be written under this form, provided that one includes enough auxiliary variables in the so called quadratic recast [4].

Results and discussion

We consider the quadratic DAE: $A\dot{y} = Ly + Q(y, y)$, where y is the vector of unknowns containing N generalized positions, N generalized velocities and M auxiliary variables (Lagrange multipliers from mechanical constraints or auxiliary variables arising from the quadratic recast). A is the mass matrix (of size $2N + M$, possibly singular), L is a linear operator (matrix of size $2N + M$) and Q a quadratic operator. For the normal form computation, we are searching for: (i) a change of coordinates $y = W(z)$ where $z \in \mathbb{C}^n$ is a set of (complex) normal variables with n elements (n even, and usually $n \ll 2N$), and (ii) a (reduced) dynamic function $f(z) \in \mathbb{C}^n$ for the normal variables, such that: $\dot{z} = f(z)$. Substituting the expression for the normal dynamics and the change of variable into the original DAE leads to the following homological equation: $A(\nabla_z W)f = LW(z) + Q(W(z), W(z))$. Both the change of coordinates and the reduced dynamics are considered to be (multivariate) polynomials of given degree d so that they can be written as: $W(z) = \sum W_i z^{\alpha_i}$, $W_i \in \mathbb{C}^{2N+M}$ and $f(z) = \sum f_i z^{\alpha_i}$, $f_i \in \mathbb{C}^n$. The computation of the normal form then reduces in finding the vectors of coefficients W_i and f_i for each monomial z^{α_i} up to degree d . This is realized by balancing the coefficients of each monomial z^{α_i} in the homological equation. At first order, the equations are associated to the linear monomials and can be solved using the linear eigen-modes of the system. At higher orders, one has to solve an equation of the form: $(A\sigma_i(f) - L)W_i + A \sum_{k=1}^n Y_k f_{i,r} = R_i(W)$. The idea is to have a reduced dynamic under its simplest form, so most of the coefficients of f should be zero. However, when $(A\sigma_i(f) - L)$ is singular one needs to include terms associated to resonant modes in the reduced dynamics. The strategy is sequential: the system is solved for each monomial of a given degree, and then the operation is repeated iteratively for the monomials of the next degree until the maximum degree d has been reach. Finally, several examples will be considered (Fig.1).

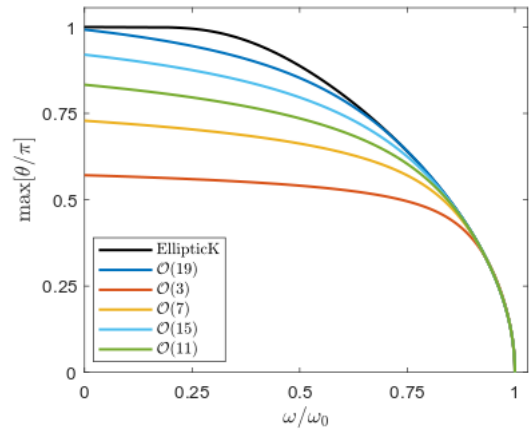


Figure 1: Backbone curve for the pendulum obtained with the normal form of the quadratic DAE at several order.

References

- [1] Vizzacarro A., Opreni A., Salles L., Frangi A., Touzé C. (2022) High order direct parametrisation of invariant manifolds for model order reduction of finite element structures: application to large amplitude vibrations and uncovering of a folding point. *Nonlin Dyn* **110**:525-571.
- [2] Jain S., Haller G. (2022) How to compute invariant manifolds and their reduced dynamics in high-dimensional finite-element models. *Nonlin Dyn* **107**:1417-1450.
- [3] Guillot L., Cochelin B., Vergez C. (2019) A generic and efficient Taylor series-based continuation method using a quadratic recast of smooth nonlinear systems. *Int J Numer Methods Eng* **119**:261-280.

Detection of Regime Changes in the Dynamics of Thermonuclear Plasmas for the Disruptions Prediction Improvement

Teddy Craciunescu^{*,***} Andrea Murari^{**,***} and JET Contributors¹

^{*} National Institute for Laser, Plasma and Radiation Physics, Bucharest-Magurele, Romania

^{**} Consorzio RFX (CNR, ENEA, INFN, Università di Padova, Acciaierie Venete SpA), Padova, Italy

^{***} EUROfusion Consortium, JET, Culham Science Centre, Abingdon, UK

Abstract. A series of time series analysis methods is deployed to determine when the plasma dynamics of the tokamak configuration varies, indicating the onset of drifts towards a form of collapse called disruption. The analysis of a representative set of plasma discharges shows that the information for disruptions prediction is available in the diagnostic signals 300 ms before the beginning of the collapse, a time interval which allows mitigation actions.

Introduction

In particular circumstances, nonlinear systems can collapse suddenly and abruptly. Anomalous detection is therefore an important task. Unfortunately, many phenomena occurring in complex systems out of equilibrium, such as disruptions in tokamak thermonuclear plasmas, cannot be modelled from first principles in real time compatible form and therefore data driven, machine learning techniques are often deployed. A typical issue, for training these tools, is the choice of the most adequate examples. Determining the intervals, in which the anomalous behaviours manifest themselves, is consequently a challenging but essential objective.

Results and discussion

A series of methods is deployed to determine when the plasma dynamics of the tokamak configuration varies, indicating the onset of drifts towards a form of collapse called disruption. The techniques rely on changes in various quantities derived from the time series of the main signals: from the embedding dimensions [1] to recurrence plots measures for assessing the similarity of the evolution of different time series [2-3] and to indicators of transition to a chaotic regime [3]. The methods, being mathematically completely independent, provide quite robust indications about the intervals, in which the various signals manifest a pre-disruptive behaviour.

The analysis of several discharges in different experiments reveals that the first signs of an approaching disruption are present in the plasma current and locked mode amplitude signals about 300 ms before the beginning of the collapse. Earlier warning or alarms, launched by predictors using the signals considered in the present work, should therefore be considered false alarms. However, 300 ms are a comfortable time interval to undertake mitigation actions. The techniques presented should therefore allow building a significantly more reliable training sets for the predictors already providing quite satisfactory performance.

Unfortunately, most of the analysis techniques deployed are quite demanding in terms of computational resources. The only fast one is the 0-1 chaos test. On usual computers, the routine, provided by the *DynamicalSystems.jl* software package [5], written in Julia language, runs in about 1.2 ms, already compatible with real time applications (on JET the cycle time of the real time network is 2 ms). All the other methods require from about 500 ms to 1 second to run. The potential of acceleration measures and implementation using GPUs will be a matter of future investigations.

With regard to the plasma dynamics, very interesting new information has emerged. The signal processing techniques has revealed that the plasma evolution leading to disruptions typically consists of two phases. First the dynamics becomes more chaotic or at least less coherent, for a couple of hundreds of ms. Then, in the interval closer to the beginning of the collapse, the signal become again more coherent and less chaotic. This behaviour should be further investigated also because it shows analogies with other anomalous events namely the onset of epilepsy.

References

- [1] Kennel, M., Brown, R., Abarbanel, H. (1992) Determining embedding dimension for phase-space reconstruction using a geometrical construction. *Phys. Rev. A* **45**:3403–3411
- [2] Eroglu, D., Marwan, N., Stebich, M., Kurths, J. (2018) Multiplex recurrence networks. *Phys. Rev. E* **97**: 012312.
- [3] Lacasa, L., Nicosia, V., Latora, V (2015) Network structure of multivariate time series. *Sci. Rep.* **5**:15508.
- [4] Gottwald, G. A. Melbourne, I. (2004) A new test for chaos in deterministic systems. *Proc. Roy. Soc. A*, **460**:603–611.
- [5] Datseris, G. (2018) DynamicalSystems.jl: A Julia software library for chaos and nonlinear dynamics. *J. Open Source Softw.* **3**:598.

¹ See the author list of ‘Overview of JET results for optimising ITER operation’ by J. Mailloux et al 2022 Nucl. Fusion 62 042026

Safe Basins of Escape of a Weakly Damped Particle From a Truncated Quadratic Potential Well Under Harmonic Excitation

Attila Genda^{*}, Alexander Fidlin^{*} and Oleg Gendelman^{**}

^{*}*Institute of Engineering Mechanics, Karlsruhe Institute of Technology, Karlsruhe, Germany*

^{**}*Mechanical Engineering, Technion – Israel Institute of Technology, Haifa, Israel*

Abstract. The safe basins (SB) of escape of a weakly damped particle from a symmetrically truncated quadratic potential well under harmonic excitation are investigated. It is assumed that the excitation frequency is in the vicinity of the resonant frequency of the potential well. An analytic approach to determine the size and the location of the non-escaping set in the plane of the initial conditions (IC) depending on several model parameters is introduced.

Introduction

Escape from a potential well is a classic problem arising in numerous fields of engineering [1] and natural sciences [2]. Escape can be caused by different types of excitation starting with the appropriate initial conditions via harmonic excitation [2] to stochastic noise [1] and impact loading. Safe basins of escape describe the set of initial conditions for which the particle does not escape from the well under a certain parameter combination [3]. The determination and understanding of the parameters' impact on the SB is of great engineering importance contributing to the design of robust systems and applications. *Karmi et al.* succeeded to derive a conservation law for forced escape with the use of action angle variables and averaging for a quadratic-quartic potential truncated at different energy levels [4], the fully analytic treatment of the SB, however, is rarely possible due to the complexity of the problem. In the following, one of the exceptional cases is presented, escape of a weakly damped particle from a truncated quadratic potential well under harmonic excitation.

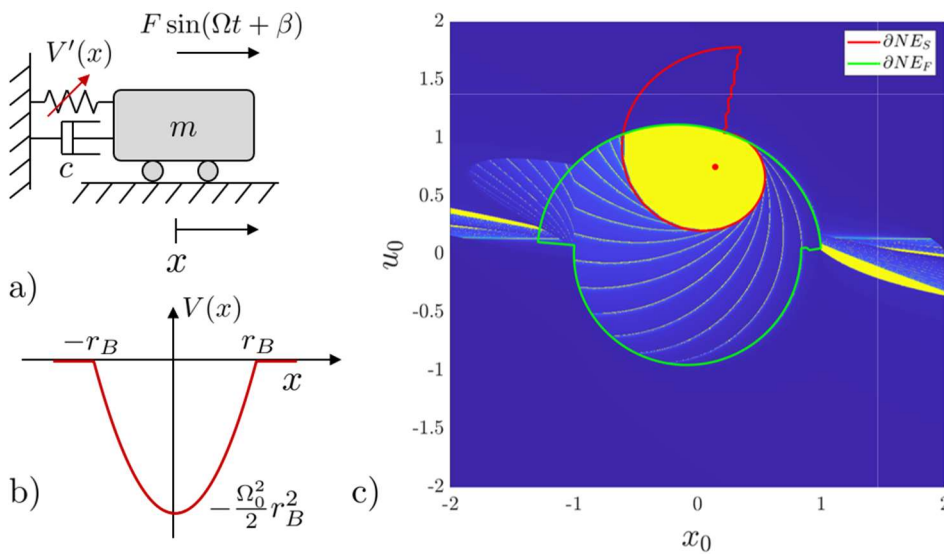


Figure 1: a) The scheme of the problem; b) the truncated quadratic potential; c) comparison of the safe basins of escape obtained numerically (yellow regions) and analytically (red and green lines referring to different escape scenarios) for some parameter setting.

Results and discussion

The solution of the equation of motion of the system shown in Fig. 1a-1b. can be obtained analytically as long as the particle is inside the well. In the analytic approach escape is identified once the particle reaches the potential boundary. It is possible to determine the envelope of the beat-like oscillating solution which leads to inequalities in polar coordinates describing the set of non-escaping coordinates in the IC plane. Two escape mechanism are identified, slow and fast escape determining together the SB (c.f. Fig. 1c). The essential properties of the SB can be described by using only two parameters. The analytic approach also explains why and how the erosion of the SB becomes more sudden if the damping coefficient is increased.

Funded by the Deutsche Forschungsgemeinschaft (DFG, German Research Foundation) – Project number: 508244284.

References

- [1] Orlando D., Goncalves P., Lenci S., Rega G. (2017) Influence of the mechanics of escape on the instability of von Mises truss and its control. *Procedia Eng.* **199**: 778–783.
- [2] Virgin L. N., Plaut R.H., Cheng C.C. (1992) Prediction of escape from a potential well under harmonic excitation. *Int. J. Non. Linear. Mech.* **27**(3): 357–365.
- [3] Rega G., Lenci S. (2008). Dynamical Integrity and Control of Nonlinear Mechanical Oscillators. *J. Vib. Control.* **14**:159-179.
- [4] Karmi G., Kravets P., Gendelman O. (2021) Analytic exploration of safe basins in a benchmark problem of forced escape. *Nonlinear Dyn.* **106**:1573–1589.

Locating transition behaviour in nonlinear signals

Giovanna Zimatore^{1,2}, Giuseppe Orlando³, Maria Chiara Gallotta⁴, Alessandro Giuliani⁵, Cassandra Serantoni^{6,7}, Giuseppe Maulucci^{6,7} and Marco De Spirito^{6,7}

¹Department of Theoretical and Applied Sciences, eCampus University, Novedrate (CO), Italy; ²IMM-CNR, Bologna, Italy; ³Department of Economics and Finance, Università degli Studi di Bari "A. Moro", Bari, Italy; ⁴Department of Physiology and Pharmacology "Vittorio Erspamer", Sapienza University, Rome, Italy; ⁵Istituto Superiore di Sanità, Rome, Italy; ⁶Fondazione Policlinico Universitario A. Gemelli IRCCS, Rome,; ⁷Università Cattolica del Sacro Cuore, Rome, Italy

Abstract. In this paper we compare results obtained in the nonlinear Recurrence Quantification Analysis (RQA) of time series of different dynamic systems (i.e. i) financial time series [1-2], ii) heart rate (HR) time series [3-5] and iii) acoustic emissions [6])

The RQA is fully unconstrained by stationarity limitations, does not require lengthy data streams, and is focused on quantifying the correlation structure of the investigated dynamics. These factors make this analysis method well-suited for locating transitions in signals.

Introduction

A crisis or a critical transition of systems is oftentimes preceded by a substantial increase in both internal correlation and variance. This appears across a wide range of environments spanning from physiology to ecology and finance [7].

Results and discussion

In this work, we show that, in three very different contexts of application, RQA approach drives potentially valuable results. i) Orlando and Zimatore (2018)[1], confirm that RQA may be used for detecting structural changes of a given time series as well as for its characterization and that recurrence plots (RPs) may furnish insights when comparing real-world economic data with simulations used to model financial crises and Black Swans [2]; ii) in physiology, RQA is commonly used to characterize the complexity of HR time series, when, during physical activity, the nonlinear analysis of HR time series is monitored [3] and is a valid alternative to assess metabolic thresholds [4-5]. The implication is that an automated determination method can be implemented to evaluate fitness levels as well as for planning and monitoring training; iii) Acoustic emissions (AE) recorded from crustal rocks by piezoelectric sensors [6] are also a field of application of RQA. Since these emissions occur a few days before major seismic events, the percent of determinism derived from RQA on AE decreases. This suggests the applicability of RQA as an earthquake precursor detection method. However, it is necessary to observe that the coupling of the cardio-respiratory system, where the autonomic nervous system (ASN) modulation can be considered a sort of active feedback mechanism, is more similar to the control of economic fluctuation when exogenous shocks occurred; on the contrary, the self-organization of many interacting components as tectonic plates and faults that contribute to the geocomplexity it is mainly an internal mechanism of the system [8]. In all three systems the accuracy of the location of the transition depends on the sampling time of the time series and on the width of the epoch chosen for the analysis.

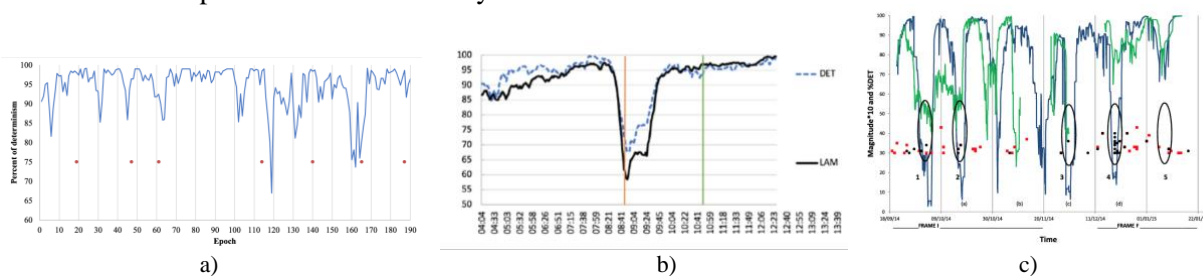


Figure 1: Percent of determinism by epoch-by-epoch RQA calculated from a) financial time series and crisis (dots)[1]; b) heart rate time series during incremental physical exercise [6]; c) acoustic emission time series acquired in Orchi (blue line) and Savoia (green line) stations and seismic events (squares and dots) [7]).

References

- [1] Orlando G., et al. (2018) Recurrence quantification analysis of business cycles. *Chaos Solit.* **110**: 82-94.
- [2] Orlando G., et al. (2020) Business Cycle Modeling Between Financial Crises and Black Swans: Ornstein-Uhlenbeck Stochastic Process versus Kaldor Deterministic Chaotic Model. *Chaos* **30**(8): 083129
- [3] Serantoni C., et al. (2022) Unsupervised Clustering of Heartbeat Dynamics Allows for Real Time and Personalized Improvement in Cardiovascular Fitness. *Sensors* **22**(11): 3974.
- [4] Zimatore G., et al. (2021) Recurrence quantification analysis of heart rate variability to detect both ventilatory thresholds. *PLoS ONE* **16**(10): e0249504.
- [5] Zimatore G., et al. (2022) Detecting metabolic thresholds from nonlinear analysis of heart rate time series. A review. *Int. J. Environ. Res. Public Health.* **19**(19): 12719
- [6] Zimatore G., et al. (2017) The remarkable coherence between two Italian far away recording stations points to a role of acoustic emissions from crustal rocks for earthquake analysis. *Chaos* **27** (4), 043101
- [7] Gorbán A.N., et al. (2010) Correlations, risk and crisis: From psychology to finance. *Physica A* **389**(16): 3193–3217.
- [8] Chelidze T., et al. (2015) Dynamical patterns in seismology. *Recurrence Quantification Analysis*. Springer, Cham.

The transient charm of decay

György Károlyi*, Tamás Tél** and Dániel János**

*Institute of Nuclear Techniques, Budapest University of Technology and Economics, Hungary,
ORCID # 0000-0002-1021-9554

**Department of Theoretical Physics, Eötvös University, Budapest, Hungary

Abstract. Undriven dissipative systems are investigated to find the best way to characterize the chaotic decay towards a simple resting state. Traditional tools developed in regard to transient chaos are based on the presence of an infinity of unstable orbits, however, these are not present in undriven dissipative systems. We show that, instead of the recently proposed instantaneous, snapshot view of these systems, they must be observed at equal energy levels to find when the boundary between basins of attraction change from fractal to smooth.

Introduction

In undriven dissipative systems all motion decays since dissipation continually decreases the available mechanical energy. Chaotic motion can only show up transiently. Traditional transient chaos is, however, caused by the presence of an infinity of unstable orbits. In the lack of these, chaos in undriven dissipative systems is of another type: it is termed doubly transient chaos as the strength of transient chaos is diminishing in time, and ceases asymptotically [1]. To characterize the behavior of such systems, the snapshot view has been suggested [2, 3], but it does not lead to a clear characterization of e.g. the fractality of the boundary between the basins of attraction. We suggest that a view based on equal energy levels might be a better choice.

Results and discussion

A clear view of the dynamics of purely dissipative systems is provided by identifying KAM tori or chaotic regions of the dissipation-free case, and following their time evolution in the dissipative dynamics. The tori often smoothly deform first, but later they become disintegrated and dissolve in a kind of shrinking chaos. We show that using an equal energy level view instead of the usual snapshot view preserves the tori structure. Various dynamical measures can be utilized for the characterization of this process and they illustrate that the strength of chaos is first diminishing, and after a while disappears, the motion enters the phase of ultimate stopping. Meanwhile, with the decrease of the energy, the boundary between basins of attraction become gradually simpler, from fractal to smooth. However, to find a clear fractal property, basins of attraction must be observed at equal energy levels.

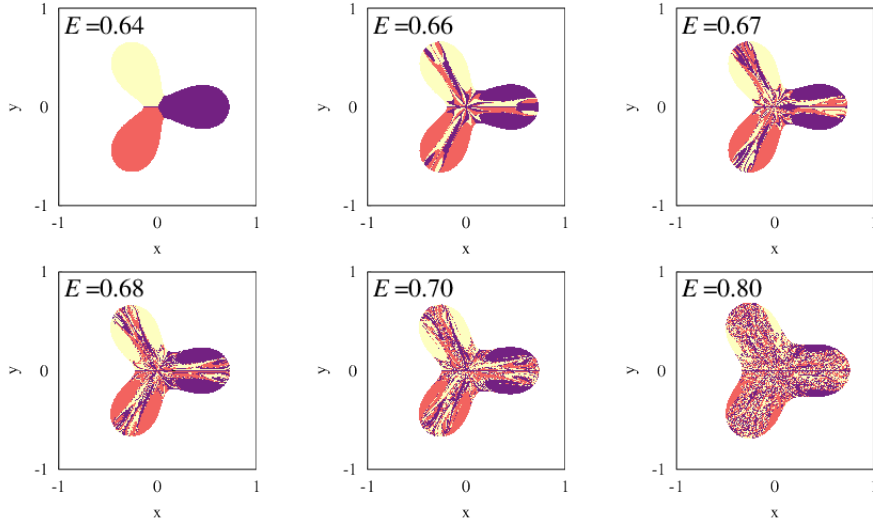


Figure 1: Basin boundary for the magnetic pendulum at equal energy levels.

References

- [1] A.E. Motter, M. Gruiz, Gy. Károlyi, T. Tél (2013): Doubly transient chaos: Generic form of chaos in autonomous dissipative systems. *Physical Review Letters* **111**: 194101.
- [2] Gy. Károlyi, T. Tél (2021): New features of doubly transient chaos: complexity of decay. *Journal of Physics: Complexity* **2**: 035001.
- [3] D. János, Gy. Károlyi, T. Tél: Climate change in mechanical systems: the snapshot view of parallel dynamical evolutions. *Nonlinear dynamics* **106**: 2781-2805.

The transient charm of decay

György Károlyi*, Tamás Tél** and Dániel János**

*Institute of Nuclear Techniques, Budapest University of Technology and Economics, Hungary,
ORCID # 0000-0002-1021-9554

**Department of Theoretical Physics, Eötvös University, Budapest, Hungary

Abstract. Undriven dissipative systems are investigated to find the best way to characterize the chaotic decay towards a simple resting state. Traditional tools developed in regard to transient chaos are based on the presence of an infinity of unstable orbits, however, these are not present in undriven dissipative systems. We show that, instead of the recently proposed instantaneous, snapshot view of these systems, they must be observed at equal energy levels to find when the boundary between basins of attraction change from fractal to smooth.

Introduction

In undriven dissipative systems all motion decays since dissipation continually decreases the available mechanical energy. Chaotic motion can only show up transiently. Traditional transient chaos is, however, caused by the presence of an infinity of unstable orbits. In the lack of these, chaos in undriven dissipative systems is of another type: it is termed doubly transient chaos as the strength of transient chaos is diminishing in time, and ceases asymptotically [1]. To characterize the behavior of such systems, the snapshot view has been suggested [2, 3], but it does not lead to a clear characterization of e.g. the fractality of the boundary between the basins of attraction. We suggest that a view based on equal energy levels might be a better choice.

Results and discussion

A clear view of the dynamics of purely dissipative systems is provided by identifying KAM tori or chaotic regions of the dissipation-free case, and following their time evolution in the dissipative dynamics. The tori often smoothly deform first, but later they become disintegrated and dissolve in a kind of shrinking chaos. We show that using an equal energy level view instead of the usual snapshot view preserves the tori structure. Various dynamical measures can be utilized for the characterization of this process and they illustrate that the strength of chaos is first diminishing, and after a while disappears, the motion enters the phase of ultimate stopping. Meanwhile, with the decrease of the energy, the boundary between basins of attraction become gradually simpler, from fractal to smooth. However, to find a clear fractal property, basins of attraction must be observed at equal energy levels.

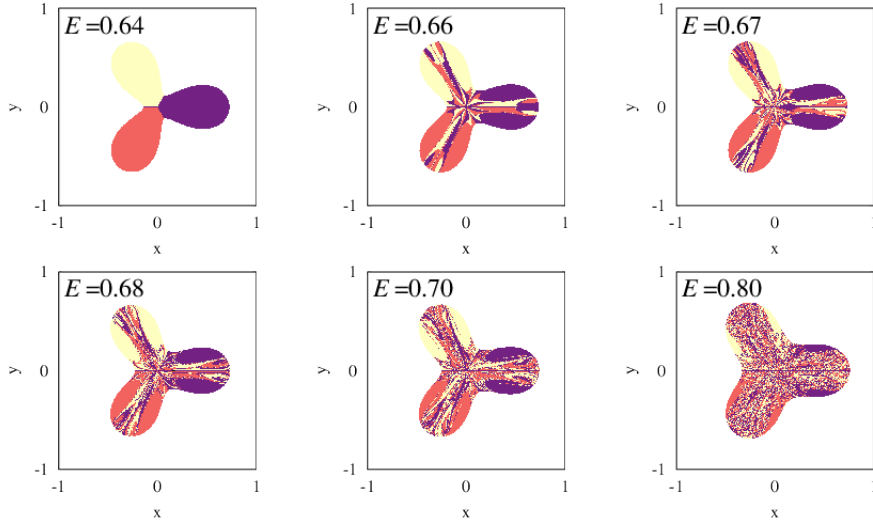


Figure 1: Basin boundary for the magnetic pendulum at equal energy levels.

References

- [1] A.E. Motter, M. Gruiz, Gy. Károlyi, T. Tél (2013): Doubly transient chaos: Generic form of chaos in autonomous dissipative systems. *Physical Review Letters* **111**: 194101.
- [2] Gy. Károlyi, T. Tél (2021): New features of doubly transient chaos: complexity of decay. *Journal of Physics: Complexity* **2**: 035001.
- [3] D. János, Gy. Károlyi, T. Tél: Climate change in mechanical systems: the snapshot view of parallel dynamical evolutions. *Nonlinear dynamics* **106**: 2781-2805.

New results about compatibility conditions and solutions for a model of inerted gas in a vented fuel tank ullage

José Luis Díaz Palencia* and Julián Roa González*

*Department of Mathematics and Education. Universidad a Distancia de Madrid.

Abstract. The fire safety concerns are of paramount relevance in fuel tank designs. One of the most extended solutions to decrease the fuel tank flammability is the inerting system, that has been extensively used in aircraft fuel tanks. The intention is to provide new results about the compatibility conditions in vented fuel tanks, to ensure that the forced convection does not detrimentally impact the formation of an inerted ullage. In addition, we provide some new solutions that complement the existing literature together with a validation based on data from a real flight test.

Introduction

A Boeing 747-131 owned by Trans World Airlines crashed on July, 1996 over the Atlantic Ocean. One of the design solutions proposed, to avoid similar accidents, consisted on the removal of the oxygen and the replacement by nitrogen in the fuel tank ullage [1]. This solution, known as Inerting System, is currently well implemented in civil and military aircrafts. In [2], a model is constructed with a mass balance. In [3], the authors analyze a PDE to describe the concentration of fuel vapors. In [4], the three main physical ideas related with the gases interaction were introduced: diffusion, reaction and forced convection. At the moment of such a model proposal, it was not clear what conditions are required so that the forced convection, in vented fuel tanks, does not lead to impact the effective diffusive mechanisms of the inerted gas to reach all the tank zones.

Results and discussions

The proposed model for the interaction between oxygen (Θ) and nitrogen (N) is ([4]):

$$N_t = \Delta N + a \cdot \nabla N - \Theta^n(N - r); \Theta_t = \Delta \Theta + a \cdot \nabla \Theta - N^m \Theta; N_0(x), \Theta_0(x) \in L^1_{loc}(\mathbb{R}^3) \cap L^\infty(\mathbb{R}^3),$$

where $r \geq \max_{x \in \mathbb{R}^3} \{N_0(x)\}$, a is the vented convection vector and $n, m \in (0, 1)$ two calibrated constants. Given the solution $(N, \Theta) \in C^{2+\gamma, 1+\gamma/2}(\mathbb{R}^3 \times (0, T))$, $\gamma > 0$ with $\Theta_t \leq 0$ and $N_t \geq 0$, two new compatibility conditions, involving the initial distributions, are shown to ensure that the reaction and diffusive terms predominate over the vented convection: $\int_{\mathbb{R}^3} N_0^m \geq |a| \Theta_0$, $\Theta_0^n \geq 2a \cdot \nabla N_0$. Based on the data obtained from [4], the new compatibility conditions are indeed met. The air is formed of 80% of nitrogen ($N_0 = 0.8$) and 20% of oxygen ($\Theta_0 = 0.2$). Then $\nabla N_0 = 0$, such that: $\Theta_0^n \geq 2a \cdot \nabla N_0 = 0$. Note that $\Theta_0^n = 0.2^{0.586} = 0.389$ (refer to [4] for the value of n). The second compatibility condition is achieved as $0.389 > 0$. Considering the first compatibility condition: $\int_{tank} N_0^m dV = 0.80^{0.025} V_{tank} = 0.80^{0.025} \cdot 1.5 \cdot 6 \cdot 6.5 = 58.17$. The volume of the tank is the typical for a Boeing 747 (see again [4] for further details). We have $|a| \Theta_0 = 0.0125 \cdot 0.2 = 0.0025$ (for the value of $|a|$ refer to [4]). Then: $\int_{tank} N_0^m dV > |a| \Theta_0$. We should notice that the compatibility conditions are met. In addition, the following new flat solutions have been obtained: $N(t) = \|N(x, 0)\|_p + \theta t$ and $\Theta(t) = \|\Theta(x, 0)\|_p - \frac{1}{\theta(m+1)}(\|N(x, 0)\|_r + \theta t)^{m+1}$, where θ is the minimum level of oxygen concentration (usually $\theta \sim 0.05$, see [2]) and $p > 0$, typically $p = 1$ for a finite mass distribution. The solutions are obtained for a discrete time set of amplitude: $T = \frac{(\|\Theta(x, 0)\|_r - \theta^{1/n})^{\frac{1}{m+1}} - (\theta^{1/n})^{\frac{1}{m+1}}}{\theta}$.

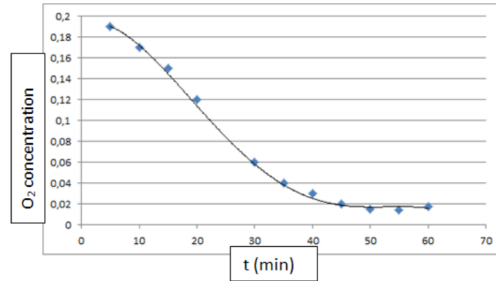


Figure 1: The black line represents the oxygen concentration evolution in steps of amplitude T .

References

- [1] Bahrami, A. (2008) Fuel Tank Ignition Source Prevention Guidelines. FAA Advisory Circular.
- [2] The National Transportation Safety Board. (2000) In-flight Breakup Trans World Airlines Flight 800. NTSB, NY.
- [3] Ghadirian, E., Brown, J. and Wahiduzzaman, S. (2019) A quasy-steady diffusion based model for design and analysis of fuel tank evaporate emissions. SAE.
- [4] Palencia, J.L.D. (2021) Travelling Waves Approach in a Parabolic Coupled System for Modelling the Behaviour of Substances in a Fuel Tank. *Appl. Sci.*, **11**, 5846.

Regularity and spatially distributed solutions for interacting gases in complex domains

José Luis Díaz Palencia* and Julián Roa González*

*Department of Mathematics and Education. Universidad a Distancia de Madrid.

Abstract. Modeling the interaction of gases in complex geometries is typically a hard work due to the difficulty in predicting what kind of interaction is relevant given by diffusion, advection or reactive/absorptive mechanisms. This is particularly important in mixtures of gases, where the interaction can lead to an explosive condition. For instance in the fuel tanks. Our intention is to introduce a model for the interaction between oxygen and nitrogen, develop new regularity conditions and obtain flat solutions together with spatially distributed ones.

Introduction

The interaction between gases can be described based on diffusion, advection and reaction/absorption. In the presented work, we are concerned with the possibility of having an explosive mixture of gases leading to hazardous consequences (see the Boeing 747-131 that crashed over the Atlantic Ocean in 1996). The aerospace authorities claimed for a solution making an inerted atmosphere introducing nitrogen in the fuel tank (see [1] and the models [2] and [3]). The model in [3] was solved by the travelling waves, but no results were provided about the regularity of solutions or other kinds of solution: flat solutions and spatially distributed.

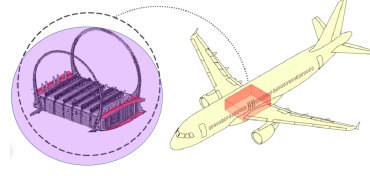


Figure 1: A320 Centre Wing Box. The purple sphere has a radius of $6.249m$. The volume $|x| \leq 6.249m$ was obtained as a result (see the next section) and covers the center tank. The oxygen concentration is at a safe level $\Theta = 0.0258$ at any location within the volume.

Results and discussions

The model to describe the interaction between the nitrogen (N) and the oxygen (Θ), is ([3]): $N_t = \rho \Delta N + a \cdot \nabla N + \Theta^n$; $\Theta_t = \sigma \Delta \Theta + a \cdot \nabla \Theta - N^m$; $\Theta_0(x), N_0(x) \in L^\infty(\mathbb{R}^3) \cap L^1_{loc}(\mathbb{R}^3)$, ρ and σ are the gases diffusivities, a refers to the vector of vented convection and $n, m \in (0, 1)$ are two constants to be calibrated with a real scenario. Given the parabolicity of the involved operator, and considering positive initial distributions in the domain, it holds that $(N, \Theta) \in C^{2+\varepsilon, 1+\varepsilon/2}((0, T) \times \mathbb{R}^3)$, $\varepsilon > 0$, together with $\Theta_t \leq 0$ and $N_t \geq 0$. The study of regular and flat solutions follows from a change of variable and the comparison with previously known results. Indeed making: $N(x, t) = N(\eta(x, t), t)$, $\Theta(x, t) = V(\eta(x, t), t)$, $\eta = x + at$, the system is converted into a problem whose dynamics acts in the advection vector and has the form: $N_t = \Delta_\eta N + \Theta^n$, $\Theta_t = \Delta_\eta \Theta - N^m \leq \Delta_\eta \Theta + N^m$. This last problem has been shown to be regular in [4] leading to conclude that the solutions to our problem are sufficiently regular and do not exhibit blow up in $(0, T)$. Based on this, it is possible to obtain two flat bounding solutions given by the reaction/absorption terms: $\hat{N}(t) = At^{\frac{1+n}{1-mn}}$, $A^{1-mn} = \frac{(1-mn)^{1+n}}{(n+1)(m+1)^n}$, $\hat{\Theta}(t) = Bt^{\frac{1+m}{1-mn}}$, $B = \frac{A^m(1-mn)}{1+m}$. In the search of spatially distributed solutions we make use of selfsimilar profiles of solutions. This approach is valid in the case of slow advection (this is the case as $a = 0.0125 m/min$, see [3]) so that the selfsimilar scaled symmetry is not much impacted. The solution for the oxygen is:

$$\Theta(x, t) = \Theta_0(x) - A_\Theta \int_{\mathbb{R}^3} (|x - r|)^{\frac{1+m}{1-mn}-2} B_\Theta(t) e^{-\frac{|r|^2}{4t}} dr, \quad (1)$$

where $A_N = \frac{1}{2\Gamma(2\alpha_N+1)}$, $A_\Theta = \frac{1}{2\Gamma(2\alpha_\Theta-1)}$, Γ is the Gamma function. $B_N(t) = t^{-\alpha_N}$, $B_\Theta(t) = t^{1-\alpha_\Theta}$ with $\alpha_N = \frac{1}{2} \frac{2-(n-1)m}{1-mn}$, $\alpha_\Theta = \frac{1}{2} \frac{1+m}{1-mn}$. For particular values in n, m refer to [3]. According to the data in [1] for a single filter working, at $t = 60 min$, the level of oxygen concentration is $\Theta = 0.0258$. According to the solution in the expression (1), it holds that: $0.0258 \geq 0.2 - A_\Theta |x|^{\frac{1+m}{1-mn}-2} B_\Theta(t = 60 min) e^{-\frac{|r|^2}{4 \cdot 60} V_T}$. A solution for this last expression is $|x| \leq 6.249m$ (see the Figure 1).

References

- [1] Bahrami, A. (2008) Fuel Tank Ignition Source Prevention Guidelines. FAA Advisory Circular.
- [2] The National Transportation Safety Board. (2000) In-flight Breakup Trans World Airlines Flight 800. NTSB, NY.
- [3] Palencia, J.L.D. (2021) Travelling Waves Approach in a Parabolic Coupled System for Modelling the Behaviour of Substances in a Fuel Tank. *Appl. Sci.*, **11**, 5846.
- [4] Escobedo, M. and Herrero, M. (1991) A uniqueness result for a semilinear reaction-diffusion system. *Proc. Amer. Math. Soc.*, **112**, 175-185.

The blow-up method applied to monodromic singularities of the plane

Brigita Ferčec*, Jaume Giné**

* Faculty of Energy Technology, University of Maribor, Hočevarjev trg 1, 8270 Krško, Slovenia,

*Center for Applied Mathematics and Theoretical Physics, University of Maribor,
Mladinska 3, SI-2000 Maribor, Slovenia, ORCID # 0000-0003-0990-2775

**Departament de Matemàtica, Universitat de Lleida, Av. Jaume II, 69. 25001 Lleida, Catalonia, Spain,
ORCID # 0000-0001-7109-2553

Abstract. The blow-up method proved its effectiveness to characterize the integrability of the resonant saddles giving the necessary conditions to have formal integrability and the sufficiency doing the resolution of the associated recurrence differential equation using induction. In this work we apply the blow-up method to monodromic singularities in order to solve the center-focus problem. The case of nondegenerate monodromic singularities is straightforward since any real nondegenerate monodromy singularity can be embedded into a complex system with a resonant saddle. Here we apply the method to nilpotent and degenerate monodromic singularities solving the center problem when the center conditions are algebraic.

Introduction

A monodromic nondegenerate singular point placed at the origin of a differential system on \mathbb{R}^2 takes the form

$$\dot{u} = v + P(u, v), \quad \dot{v} = -u + Q(u, v), \quad (1)$$

where $P(u, v)$ and $Q(u, v)$ are real analytic functions without constant and linear terms. Such singular point is a center, if and only if, the system has a first integral of the form $\Phi(u, v) = u^2 + v^2 + \sum_{k+l \geq 3} \phi_{kl} u^k v^l$, analytically defined around it. Therefore the center-focus problem reduces to prove the existence of such analytic first integral. We can complexify system (1) defining the complex variable $x = u + iv$ and system (1) is transformed to the equation $\dot{x} = ix + R(x, \bar{x})$. Considering its complex conjugate equation and defining $y := \bar{x}$ as a new variable and \bar{R} as a new function we obtain the complex system $\dot{x} = x + G(x, y)$, $\dot{y} = -y + H(x, y)$ after the time scaling $idt = dT$. The above power series becomes now $\Psi(x, y) = xy + \sum_{i+j \geq 2} \psi_{ij} x^i y^j$, satisfying $\dot{\Psi} = \sum_{i=1} v_{2i+1} (xy)^{2i+2}$, where v_{2i+1} are polynomials in the parameters of the system. We note that if all the polynomials v_{2i+1} vanish then the power series $\Psi(x, y)$ becomes a first integral of the system. The singular point at the origin is now a $1 : -1$ resonant saddle singular point and the values v_{2i+1} are the *saddle constants*, see [2, 3]. The $1 : -1$ resonant saddle singular point is generalized into the $p : -q$ resonant saddle singular point which placed at the origin the differential system is the form $\dot{x} = px + F_1(x, y)$, $\dot{y} = -qy + F_2(x, y)$, where F_1 and F_2 are analytic functions without constant and linear terms with $p, q \in \mathbb{Z}$ and $p, q > 0$, see [1, 3] and references therein. In this case a $p : -q$ resonant saddle singular point is called a resonant center, if and only if, there exists a meromorphic first integral $\Psi = x^q y^p + \sum_{i+j \geq p+q} \psi_{ij} x^i y^j$ around it.

Results and discussion

The blow-up method to detect formal integrability works performing the blow-up $(x, y) \rightarrow (x, z) = (x, y/x)$, So that the origin is replaced by the line $x = 0$, which contains two singular points that correspond to the separatrices, and study if one of these two resonant saddle points is orbitally analytically linearizable. Finally to prove the sufficiency of the original system we can apply the following result.

Theorem 1 Assume that we have proved that system in variables (x, z) has a formal first integral $\tilde{\mathcal{H}}(x, z)$ then if the function $\tilde{H} = \tilde{\mathcal{H}}(x, y/x)$ is well-defined at the origin of system in the variables (x, y) then it is analytic integrable around it.

Summarizing we study the connected singular points at infinity and if they are formally integrable and the first integral can be extended up to the origin then the origin is also formally integrable. Here we apply the method to nilpotent and degenerate monodromic singularities in order to solve the center-focus problem. For degenerate monodromic singularities there is no method to approach the center-focus problem. The method shows that the formal integrability of the points at infinity is intimately linked with the center problem at the origin even though the center at the origin be non formally integrable. The method determine center conditions for monodromic singularities which are algebraically solvable. We solve several non trivial examples.

References

- [1] Dulac H. (1908) Détermination et intégration d'une certaine classe d'équations différentielles ayant pour point singulier un centre, *Bull. Sci. Math. Sér. (2)* **32**: 230–252.
- [2] Ferčec B., Giné J. (2019) Blow-up method to compute necessary conditions of integrability for planar differential systems, *Appl. Math. Comput.* **358**: 16–24.
- [3] Romanovski, V.G., Shafer D.S. (2009) The Center and Cyclicity Problems: A Computational Algebra Approach, Birkhäuser, Boston.

Nonlinear effects of the central body oblateness on the coplanar dynamics of solar sails

Martin Lara^{***}, Elena Fantino^{**}, and Roberto Flores^{***,*}

^{***}SCoTIC – University of La Rioja, Logroño, Spain, ORCID 0000-0001-6754-916X

^{**}Aerospace Engineering Department, Khalifa University, Abu Dhabi, UAE, ORCID 0000-0001-7633-8567

^{*}Centre Internacional de Mètodes Numèrics en Enginyeria (CIMNE), Barcelona, Spain, ORCID 0000-0001-6027-9515

Abstract. The nonlinearities introduced by the coupling of solar radiation pressure and oblateness perturbations are known to yield radical changes in the long-term dynamics of solar sails. After a reduction process in which short-period terms are removed by perturbation theory, we arrive to a time-dependent two degrees of freedom Hamiltonian depending on one physical and one dynamical parameter. While the reduced model is non-integrable in general, coplanar orbits constitute an integrable invariant manifold. We discuss the qualitative features of the coplanar dynamics, and find three regions of the parameters space characterized by the existence of different regimes of the reduced flow.

Introduction

The dynamics of natural and artificial bodies in the solar system is dominated by the Keplerian attraction of either the sun or a different natural solar system body. However, nonlinear perturbations introduced by different effects, like the non-centralities of the gravitational potential of the main attracting body or solar radiation pressure (SRP), may accumulate with time thus introducing notable changes with respect to the Keplerian dynamics. For objects with high area-to-mass ratio, SRP is an important effect that is fundamental in the description, for instance, of the dust dynamics in planetary rings. But it can be used too as an endless propellant for artificial satellites powered by solar sails. The effects of SRP alone are well known and had been thoroughly discussed [1]. However, the description of the coupled effect of the central body oblateness and SRP perturbations, while repeatedly reported in the literature [2, 3], to our knowledge is still incomplete.

Results and discussion

We make an additional effort in describing the nonlinear dynamics under coupled SRP and oblateness perturbations. More precisely, we focus on the coplanar manifold, in which the orbits of the sun and the massless body lie on the equatorial plane of the central body. Results are summarized in Fig. 1, where plot (b) shows three regions in the parameters plane separated by two curves that are computed analytically. The reduced flow is represented by eccentricity vector diagrams (plots (a) and (c) of Fig. 1), which are constructed as contour plots of the long-term Hamiltonian. In the region above the red line we only find a single fixed point corresponding to an elliptic orbit with the periapsis frozen at 180° , on average, where two different kinds of flow are possible (plot (a)). Namely, elliptic orbits with *oscillating* periapsis exist between the fixed point and the dashed contour through the origin, otherwise the periapsis of the orbits *rotates* traveling 360° . A saddle-node bifurcation happens when crossing the red curve in the parameters plane, and below it we find three fixed points. Two additional regions of orbits with oscillating and rotating periapsis are now possible, which are determined by the contour corresponding to the energy of the fixed point of the hyperbolic type. However, in the region between the red bifurcation line and the dashed curve in plot (b), the contour of the hyperbolic fixed point embraces the one of the circular orbits, making only three different kinds of flow possible.

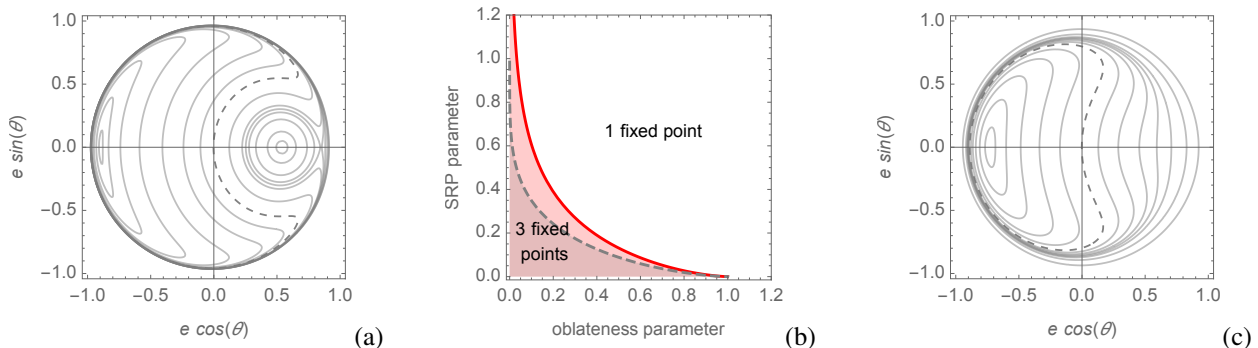


Figure 1: Qualitative dynamics of the coplanar orbits in the parameters SRP-oblateness space. θ is the periapsis-sun direction angle. In addition, we obtained the infinitesimal contact transformation that removes the short-period terms from the original Hamiltonian, in this way providing the needed mathematical support to the usual averaging assumptions used in the computation of the long-term dynamics.

References

- [1] Deprit A. (1984) Dynamics of orbiting dust under radiation pressure. In: Berger A. (ed) *The big bang and Georges Lemaître*. Springer, Dordrecht, 151-180.
- [2] Krivov A.V., Getino J. (1977) Orbital evolution of high-altitude balloon satellites. *A&A* **318**:308-314
- [3] Alessi E.M., Colombo C., Rossi, A. (2019) Phase space description of the dynamics due to the coupled effect of the planetary oblateness and the solar radiation pressure perturbations *Celest Mech Dyn Astron*, **131**:43

A study on an analytic optimization of variable pitch broaching

Zsolt Iklodi* and Zoltan Dombovari *

*MTA-BME Lendület Machine Tool Vibration Research Group, Department of Applied Mechanics, Budapest University of Technology and Economics, Budapest H-1521, Hungary

Abstract. An analytic technique for the optimization of tooth distances in variable pitch broaching is presented, by solving the vaguely equivalent variable pitch milling problem using zeroth order approximation of the anyway periodic coefficients of arising parametric excitation. To achieve the highest possible material removal rate on the prescribed cutting speed range of the workpiece material, the phase of the regenerative delayed terms is tuned to cancel the undesirable self-excited (chatter) vibrations of the broaching tool, based on the vibration (chatter) frequencies obtained from the analysis of Hopf-bifurcations type stability loss of the cutting operation.

Introduction

As a multiple stage subtractive manufacturing process, broaching is subject to the same regenerative effects as other conventional machining techniques such as milling or turning, and thus prone to the self-excited vibrations, also known as chatter [1]. Avoiding these harmful vibrations is crucial for fulfilling the generally high surface quality and integrity requirements of such high precision operations. However, scientific research on the dynamic stability analysis of broaching is remarkably scarce. Most studies concerning broaching focus on process monitoring or cutting edge geometry optimization, employing empirical and finite element techniques [2]. This study is motivated by two main goals. First, conducting a stability analysis of broaching operations through the formulation of a simplified mechanical model, which is presented on Figure 1.(a), and second, optimizing the tooth distribution of broaching tools, to achieve the highest possible material removal rates on a given cutting speed, while guaranteeing chatter free operation.

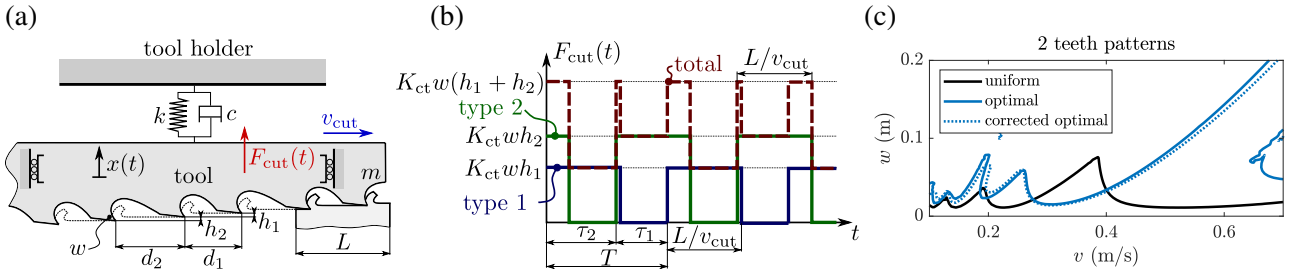


Figure 1: Panel (a): one degree of freedom mechanical model of variable pitch broaching. Panel (b): periodic forcing in variable pitch broaching with a two-teeth repeating pattern. Panel (c): stability map of broaching with uniform pitch and with phase optimized two-teeth repeating pattern.

Results and discussion

Even though broaching is generally regarded as a time limited operation, through transient simulations, it has been shown, that optimizing the tool geometry based on stability analysis of periodic orbits of infinitely long broaching operations can produce favourable and reliable results. After formulating a zeroth order approximation the periodic cutting force terms illustrated on Figure 1.(b), the optimization of tooth distances in infinitely long variable pitch broaching becomes equivalent with the optimization of pitch angles in variable pitch milling. Consequently, the optimization process followed the same steps that were employed in [3], by tuning the phase delay of regenerative terms to completely cancel out self excited vibrations on a given chatter frequency, which can be calculated either analytically for uniform, or numerically for variable pitch cases. The result of this optimization technique for two teeth repeating patterns is demonstrated on the stability map shown on Figure 1.(c). Here several cutting speed ranges can be found where the acquired variable pitch broaching tool provides higher resistance to chatter, an enables machining with higher material removal rates.

Acknowledgement

This project has received funding from the European Union's Horizon 2020 Research and Innovation Programme under grant agreement No. 958357, and it is an initiative of the FoF Public Private Partnership.

References

- [1] Axinte D. (2007) An experimental analysis of damped coupled vibrations in broaching. *International Journal of Machine Tools and Manufacture* **47**:2182-2188.
- [2] Arrazola, P. J., Rech, J., M'saoubi, R., & Axinte, D. (2020) Broaching: Cutting tools and machine tools for manufacturing high quality features in components. *CIRP Annals* **69**:554-577.
- [3] Budak, E. (2003) An analytical design method for milling cutters with nonconstant pitch to increase stability, part I: theory. *J. Manuf. Sci. Eng.*, **125**:29-34.

Collinear point dynamics of a dumbbell satellite in fast rotation

Martin Lara*

*SCoTIC – University of La Rioja, Logroño, Spain, ORCID 0000-0001-6754-916X

Abstract. For technically feasible tether lengths, the dynamics of fast rotating tethered satellites at the collinear points is reduced to an integrable problem depending on two parameters, one related with the tether's length and the other with the size of the orbit. The reduced dynamics maps orbits of the tether's center of mass onto points on the sphere, and shows how the tether length plays the role of a control parameter that can be used to mimic the relevant features of libration point orbits using orbits of a much smaller size than those spawned by the natural dynamics.

Introduction

The perturbed dynamics of dumbbell satellites in fast rotation with light tether of small dimensions, is formally analogous to the oblateness perturbation of a central attractor [1], whose modifications on the mass point dynamics are well known. Because of that, dumbbell satellites applications to mitigate orbital instabilities due to either the irregular nature of the Selenopotential or third-body perturbations have been proposed in which the length of the tether can be used as a control mechanism that, for instance, mitigates the strong instabilities affecting libration point (LP) orbits [2, 3]. The computation of LP orbits can be approached analytically when the nonlinearities remain at the level of a perturbation of the saddle \times center \times center dynamics stemming from the collinear points. Then, the integrals of the linearized dynamics can be extended to the whole problem by perturbation methods. Application of this technique to the Hill problem showed that the slow dynamics emerging from a LP can be reduced to an integrable problem whose phase space is the sphere [4]. Fixed points of the reduced flow on the sphere match periodic orbits of the Lyapunov, halo, and bridge-family types —the latter pertaining to the family that links planar and vertical Lyapunov orbits with a two-lane bridge of periodic orbits. Good approximations to these characteristic orbits can be obtained from high orders of the analytical perturbation solution without having to resort to the usual numerical continuation procedures.

Results and discussion

We apply the same analytical techniques to the dumbbell satellite model, and obtain a very simple one-degree-of-freedom Hamiltonian depending on two parameter. Depicting the intersection of different levels of this energy-type surface with the sphere is computationally inexpensive and provides an immediate insight on the dumbbell satellite LP orbits dynamics. The global description of the dumbbell satellite's slow dynamics about the LP is then obtained in the form of an atlas: Each sheet of the atlas corresponds to a point in the parameters plane, for which the phase space is given by the trajectories on the sphere (see Fig. 1 for reference). In this way we easily check how the dumbbell satellite in fast rotation modifies the classical LP orbits. In particular, it is shown how halo orbits can be twisted and narrowed about the vertical direction by increasing the tether's length, to the extent of making the halo to collapse into a vertical Lyapunov orbit, which in this way recovers stability, or how halo orbits can be additionally generated in regions in which the natural dynamics alone would prevent them to exist. Therefore, the use of a dumbbell satellite may provide interesting alternatives for mission orbit design.

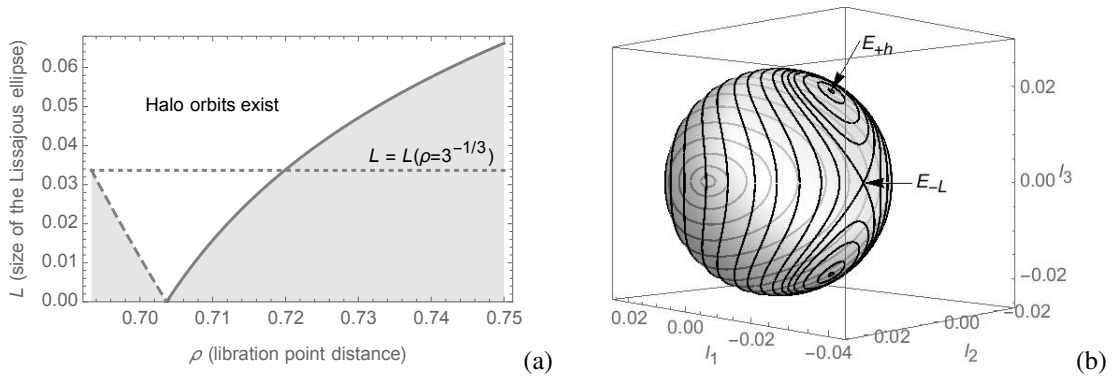


Figure 1: Sketch of the parameters plane (a), and sample flow in the light region where halo orbits exist (b).

References

- [1] Peláez J., Lara, M. (2009) Dynamics of fast-rotating tethered satellites. *Publ. Real Acad. Ciencias Zaragoza* **32**:75-83
- [2] Lara M., Peláez J., Bombardelli C., Lucas F.R., Sanjurjo-Rivo M., Curreli D., Lorenzini E.C., Scheeres D.J. (2011) Dynamic Stabilization of L_2 Periodic Orbits Using Attitude-Orbit Coupling Effects. In: *Proc. 22th International Symposium on Space Flight Dynamics*, São José dos Campos, Brazil, February 28 - March 4, 2011
- [3] Lara M., Peláez J., Urrutxua, H. (2020) Modifying the atlas of low lunar orbits using inert tethers. *Acta Astronautica* **79**:52-60
- [4] Lara M. (2017) A Hopf variables view on the libration points dynamics. *Celest. Mech. Dyn. Astron.* **129**:285-306

Exact potentials in multivariate Langevin equations

Tiemo Pedergrana*, Nicolas Noiray*

* CAPS Laboratory, Department of Mechanical and Process Engineering, ETH Zürich, Sonneggstrasse 3, 8092 Zürich, Switzerland

Abstract. Systems governed by a multivariate Langevin equation featuring an exact potential exhibit straightforward dynamics but are often difficult to recognize because, after a general coordinate change, the gradient flow becomes obscured by the Jacobian matrix of the mapping. In this work, a detailed analysis of the transformation properties of Langevin equations under general nonlinear mappings is presented. We show how to identify systems with exact potentials by understanding their differential-geometric properties. To demonstrate the power of our method, we use it to derive exact potentials for broadly studied models of nonlinear deterministic and stochastic oscillations. In selected examples, we visualize the potentials to illustrate how our method enables new analytical descriptions of the classic phenomena of beating, synchronization and symmetry breaking. Our results imply a broad class of exactly solvable stochastic models which can be self-consistently defined from given deterministic gradient systems.

Introduction

In stochastic dynamical systems featuring exact potentials driven by white noise, the evolution of a n -dimensional set of variables $x = (x_1, \dots, x_n)^T: \mathbb{R} \rightarrow \mathbb{R}^n$ over time $t \in \mathbb{R}$ is governed by following the Langevin equation:

$$\dot{x} = -\nabla \mathcal{V}(x, t) + \Xi. \quad (1)$$

In Eq. (1), $\dot{(\cdot)}$ is the time derivative, ∇ is the gradient operator, $\mathcal{V}: \mathbb{R}^n \rightarrow \mathbb{R}$ is the potential, $\mathcal{F}_i = -\nabla_i \mathcal{V}(x, t)$ is the i th component of the restoring force \mathcal{F} and the vector $\Xi = (\xi_1, \dots, \xi_n)^T: \mathbb{R} \rightarrow \mathbb{R}^n$ contains uncorrelated white noise sources ξ_i , $i = 1, \dots, n$ of equal intensity Γ . The individual entries ξ_i of Ξ are assumed to be delta-correlated: $\langle \xi_i \xi_{i, \tau} \rangle = \Gamma \delta(\tau)$, where $\langle \cdot \rangle$ is the expected value operator, $(\cdot)_{, \tau}$ denotes a positive time shift by τ and δ is the Dirac delta function. In particular, we are concerned with identifying the presence of an underlying exact potential in general noise-driven systems taking the form

$$\dot{x} = \mathcal{F}(x, t) + \mathcal{B}(x) \Xi, \quad (2)$$

where \mathcal{F} is a vector- and \mathcal{B} a n -by- n tensor field. With the knowledge of \mathcal{F} , one can easily deduce if an exact potential \mathcal{V} exists for x by checking the following necessary and sufficient conditions: $\nabla_i \mathcal{F}_j = \nabla_j \mathcal{F}_i$ for all i and $j \neq i$. However, if these conditions are not fulfilled, this does not preclude the existence of an exact potential governing the original variables that were transformed into x via a certain nonlinear mapping. We therefore argue that, instead of applying the above conditions, Eq. (2) should be compared to a Langevin equation with potential *after* a coordinate change defined by an arbitrary nonlinear mapping $x = f(y)$, see Fig. 1. Below, we give a brief summary of our main results.

Results

Assuming purely additive noise in the equations governing the underlying potential system which transforms objectively under local rotations and reflections, the resulting transformed Langevin equation with potential reads, after redefining $y \rightarrow x$,

$$\dot{x} = -g^{-1}(x) \nabla \tilde{\mathcal{V}}(x, t) + h^{-1}(x) \Xi, \quad (3)$$

where the Jacobian of f , $J(x) = \nabla f(x)$, was assumed to be nonsingular (invertible) with polar decomposition $J = Qh$, $Q = Q^{-T}$ is orthogonal, $g = h^T h$ is the positive definite metric tensor, $(\cdot)^T$ is the transpose, h is a positive definite matrix and $\tilde{\mathcal{V}}(x, t) = \mathcal{V}(f(x), t)$ is the transformed potential.

In this work, we derive necessary and sufficient conditions for the existence of an exact potential in a noise-driven system given by Eq. (2). Our results imply a self-consistent way of modeling noise in given deterministic gradient flows $\dot{x} = -\nabla \mathcal{V}(x, t)$, and the resulting models are exactly solvable if the potential is stationary.

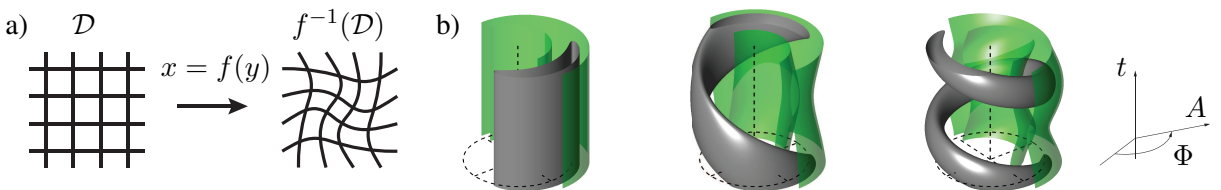


Figure 1: a) Transformation of a domain \mathcal{D} under a general nonlinear mapping f . b) Time-dependent potential of a forced Van der Pol oscillator for different parameter values. A is the amplitude, φ is the phase, $\Phi = \varphi - \Delta t$ is the reduced phase and Δ is the detuning.

References

- [1] Risken H. (1984) The Fokker-Planck Equation. Springer, Berlin Heidelberg.
- [2] Gardiner C.W. (1985) Handbook of stochastic methods. Springer, Berlin Heidelberg.

Nonresonant averaging of an inhomogeneous nonlinear Mathieu equation

D. D. Tandel*, Anindya Chatterjee* and Atanu K. Mohanty**

* Mechanical Engineering, Indian Institute of Technology Kanpur, India

** Instrumentation and Applied Physics, Indian Institute of Science Bangalore, India

Abstract. An ion in a Paul trap obeys the Mathieu equation. An added DC dipolar field in a quadrupole ion trap adds a constant and a small quadratic term to the governing equation. We examine the resulting dynamics with light damping using second-order averaging. For the unperturbed equation, i.e., the linear inhomogeneous Mathieu equation, we use Fourier series instead of Mathieu functions. We do not focus on specific resonances and consider general nonresonant conditions. Slow flows, obtained after manipulating rather long Fourier series expansions, offer a very good match with the full equation. Phase portraits of the slow flow show that a basic periodic solution, found separately using harmonic balance, is generally stable. Practical trap operation involves parameter values where the perturbation approximation struggles a bit, but still works. Satisfactory insights into trap operation are obtained.

Introduction

Traditional ion trap mass spectrometers have two endcaps and a ring electrode. When the endcaps are grounded and AC excitation is given to the ring electrode, axial motions obey the Mathieu equation. An added dipolar DC excitation across the endcaps is used for collision induced dissociation, or breaking large ions into smaller fragments. An early treatment of such excitation was given by Plass [1] using Mathieu functions and a constant added term. Here we use a simpler basic solution and include a small quadratic term that is actually present under DC excitation. In particular, we study

$$\zeta'' + \varepsilon^2 \eta \zeta' - 2q \cos(2\xi) \zeta = \mu (1 + \varepsilon \zeta^2), \quad (1)$$

where the prime (') denotes differentiation with respect to nondimensional time ξ ; and where ζ , η , q and μ are nondimensional and represent ion displacement, damping, AC quadrupole and DC dipolar excitations, respectively. Earlier, Abraham and Chatterjee [2] used harmonic balance in averaging to study a weakly nonlinear homogeneous Mathieu equation near resonances. Here we allow an inhomogeneous term and general q .

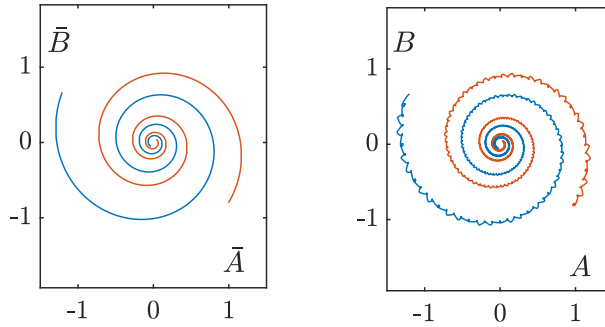


Figure 1: Comparison of phase portraits obtained from Eq. (1): slow flow (left) and full numerics (right).

Results and discussion

We first consider a general solution $\zeta = A\phi_1(\xi) + B\phi_2(\xi) + \chi(\xi)$ of a linear Mathieu equation with a constant right hand side. We approximate ϕ_1 , ϕ_2 and χ using several terms in harmonic balance approximations. We also numerically approximate q as a simple function of β , which is left as a free parameter. Second order averaging yields slow flow equations for the amplitudes $\bar{A}(\xi)$ and $\bar{B}(\xi)$, which agree well with full solutions of Eq. (1) (Fig. 1). The coefficients in the slow flow show stability of the origin in the averaged phase portrait, indicating stability of χ for general β . This stability result for the general nonresonant case, the nature and size of χ , as well as some simple further approximations for χ itself, can be useful for practical operations of the trap under dipolar excitation.

References

- [1] Plass W.R. (2000) Theory of dipolar dc excitation and dc tomography in the rf quadrupole ion trap. *Int. J. Mass Spectrom.* **202**:175-197.
- [2] Abraham G.T., Chatterjee A. (2003) Approximate asymptotics for a nonlinear Mathieu equation using harmonic balance based averaging. *Nonlinear Dyn.* **31**:347-365.

Analysis on nonlinear stiffness isolators revealing damping thresholds

Mu-Qing Niu* and Li-Qun Chen*

*School of Science, Harbin Institute of Technology, Shenzhen, Guangdong, China

Abstract. An analytical method is proposed to predict all the possible frequency responses of vibration isolators with nonlinear stiffness under different damping. The amplitude-frequency response relation is derived from a harmonic balance method as an algebraic equation. The whole damping region is divided into large damping, medium damping and small damping sub-regions according to the root conditions of the equation. The damping thresholds are obtained, and the frequency response in each sub-region is predicted. Nonlinear phenomena of full-band isolation, bounded response and unbounded response are revealed, and the sufficient and necessary condition for each case is presented. Simulations are performed on nonlinear isolators with cubic stiffness, fifth-order stiffness, and arctangent stiffness, respectively. The damping thresholds and typical frequency responses at each damping sub-region are demonstrated, and the results are verified by the numerical integration based on Runge-Kutta method.

Introduction

For a nonlinear stiffness isolator, the vibration equation can be transformed into an algebraic equation based on the harmonic balance method. In most existing researches, responding amplitudes are solved from the algebraic equation for a given excitation frequency, and the analysis is based on the root condition. The multivalued amplitudes correspond to the jump phenomenon [1]. However, the method is unsuitable for isolators with high-order stiffness due to the difficulty in solving high-order equations, and the analysis is usually restricted to a limited damping region for simplification. The algebraic equation is a quartic equation of the frequency regardless of the stiffness order. It shows promise in proposing a general analysis method for nonlinear stiffness isolators based on the frequency root condition. All the possible frequency responses are expected to be predicted covering the whole damping region. In addition, the multivalued frequencies endow the frequency responses with different features, and new nonlinear phenomena can be exhibited.

Results and discussion

An analytical method is proposed for the isolator with a symmetric nonlinear restoring force. The whole damping region is divided into large damping, medium damping and small damping sub-regions corresponding to single-root, intersecting multi-root and non-intersecting multi-root conditions of the frequency, respectively. The multivalued amplitudes are analysed through the derivatives of the frequency solutions, and the damping thresholds for jump phenomena are obtained. The frequency response in each damping sub-region can be predicted. A single-valued frequency is possible to exhibit a full-band isolation indicating the transmissibility smaller than 1 at all frequencies. Multivalued frequencies at all amplitudes lead to an unbounded response indicating an infinite amplitude. The solvability condition results in a bounded response indicating a limited amplitude regardless of the damping. The sufficient and necessary condition for each phenomenon is presented. The flow chart of the proposed method is shown in Figure 1. Simulations are performed on isolators with cubic stiffness, fifth-order stiffness, and arctangent stiffness, respectively. The damping thresholds of the cubic stiffness isolator are shown in Figure 2, and typical frequency responses in each damping sub-region are demonstrated in Figure 3. A further study incorporated with analytical and numerical methods is performed to reveal the characteristics of the unbounded response.

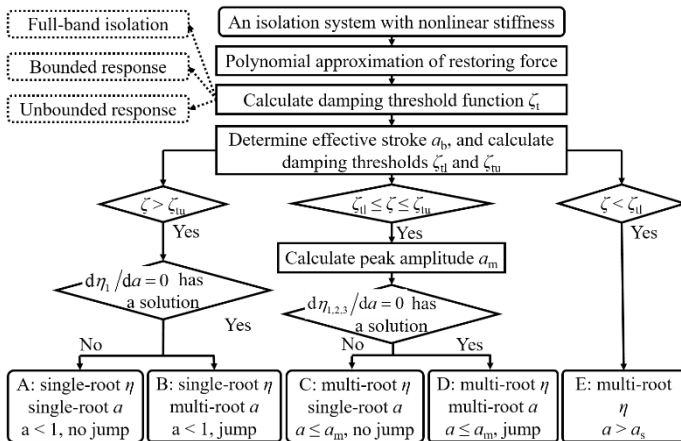


Figure 1: Flow chart of the analysis procedure

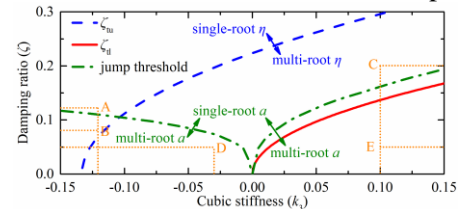


Figure 2: Damping thresholds of cubic stiffness isolator

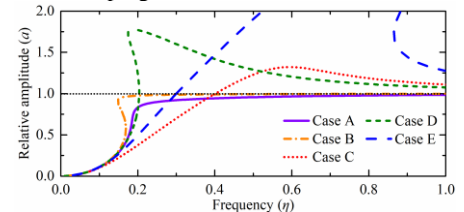


Figure 3: Frequency responses of cubic stiffness isolator

References

- [1] Nayfeh A. H., Mook D. T. (1995) Nonlinear Oscillations. Wiley-VCH, Weinheim.

Softening/hardening dynamics of nonlinear foundation beam with linear stiffening effect

Fangyan Lan^{*}, Tieding Guo^{*}, Wanzhi Qiao^{**} and Houjun Kang^{*}

^{*}College of Civil and Architecture Engineering, Guangxi University, Nanning, China

^{**}College of Civil Engineering, Hunan University, Changsha, China

Abstract. Softening/hardening dynamics of a nonlinear foundation beam is asymptotically studied by focusing on its linear stiffening effect. A softening-hardening transition phenomenon is predicted when varying linear stiffness, and in particular, in the vicinity of transition, it is found that standard third-order perturbation analysis fails and a refined high-order (quintic) one is theoretically required to capture essential nonlinear behaviours. Further, a softening-hardening transition inclination concept is defined which turns out to play a key role for the close-to transition nonlinear dynamics.

Introduction

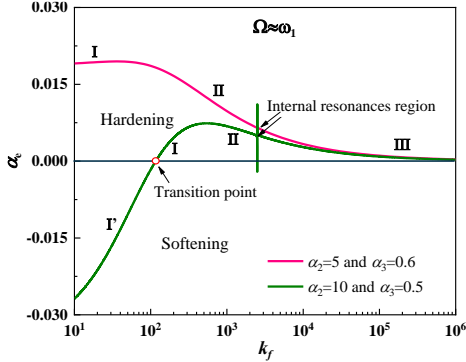
A nonlinear foundation beam is of great interests in both theoretical and application aspects [1], with two competing mechanisms involved, which leads to a typical softening-hardening transition phenomena [2]. We focus on linear stiffening effect on softening/hardening dynamics of nonlinear foundation beam governed by

$$\ddot{w} + w^{(4)} + k_f w + \varepsilon \alpha_2 w^2 + \varepsilon^2 \alpha_3 w^3 + 2\mu \dot{w} = F(x) \cos(\Omega t) \quad (1)$$

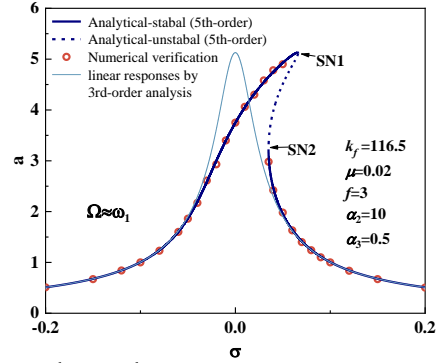
where w is displacement, and k_f , α_2 , α_3 are linear, quadratic, and cubic stiffness, respectively, with μ being damping and $F(x)\cos(\Omega t)$ being external excitation. ε is a small parameter.

Results and discussion

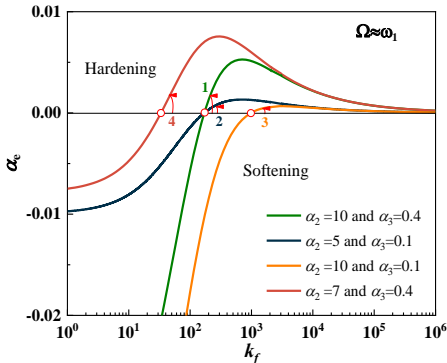
Considering $\Omega = \omega_n + \varepsilon^2 \sigma$ and employing a standard 3rd-order perturbation, one can derive a modulation equation with an effective nonlinear coefficient $\alpha_e(k_f, \alpha_2, \alpha_3)$ [1, 2]. α_e dominates the softening/hardening dynamics. Variation of α_e with respect to the linear stiffness k_f is presented in Fig.1 (a). At a critical linear stiffness, $\alpha_e \rightarrow 0$, the standard perturbation fails and a high-order one is required as illustrated in Fig.1(b). However, for small transition inclination, standard third-order perturbation analysis at transition turns more reliable as presented in Fig.1 (c) and (d).



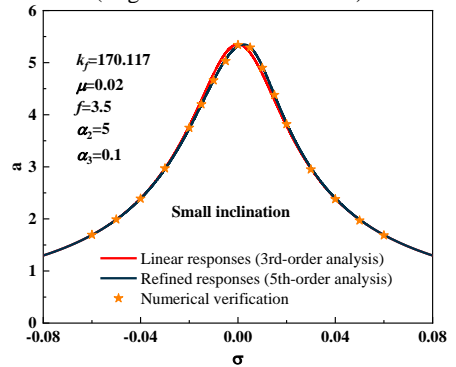
(a) effective nonlinear coefficient α_e vs. linear stiffness k_f



(b) 5th- vs. 3rd-order perturbation at transition (large transition inclination)



(c) α_e vs. k_f with different transition inclinations



(d) 5th- vs. 3rd-order perturbation at transition (small transition inclination)

Figure 1 Linear stiffening effect on softening/hardening dynamics of nonlinear foundation beam

References

- [1] Lacarbonara W. (1997) A theoretical and experimental investigation of nonlinear vibrations of buckled beams, Ph.D thesis, Virginia Polytechnic Institute and State University
- [2] Lan F., Guo T., Qiao W., and Kang H (2022), An asymptotic study of softening/hardening dynamics of nonlinear foundation beam with a linear stiffening effect, to be submitted

Classification of the post-buckling static and dynamic solutions of a beam under large, but forceless, bending and torsion

Loïc Le Marrec*, Jean Lerbet** and Marwan Hariz ***

*Univ Rennes, CNRS, IRMAR - UMR 6625, F-35000 Rennes, France

**Université Paris-Saclay, CNRS, Univ Evry, Laboratoire de Mathématiques et Modélisation d'Evry, 91037, Evry-Courcouronnes, France

***CESI, 93 Bd de la Seine, 92000 Nanterre

Abstract. The present work proposes a full classification of solutions for beam subjected to bending and torsion at both ends. The formulation is geometrically exact for large three-dimensional transformations, without hypothesis on thickness, slenderness or material. The study is based on analytical and explicit solutions on Kirchhoff rod. This leads on both quantitative and qualitative observation that could be exploited for a large domain of applications. These observations concern both the static transformation and super-imposed dynamical perturbations.

Introduction

In this study, we are interested in analytical expressions concerning large transformations of a straight beam. No force acts along the beam or as boundary condition. Moment is imposed only at the boundaries. The hypotheses are the following: the beam is elastic, homogenous and has linear constitutive relation. It is shown that under these hypotheses, Timoshenko, Euler-Bernoulli and Kirchhoff beam models lead to the same equilibrium equations. Static solutions are first presented and dynamic behavior super-imposed on these configurations are investigated.

General problem under these hypotheses is presented in a dimensionless form. Geometry and material of the beam are described thanks to three non-dimensional parameters: a slenderness-ratio and two effective rigidities. Bending and torsional moments are encoded by two non-dimensional parameters: the first one is related to the whole energy stored by the structure, the second one is related to the type of moments (according to a predominant torsion or bending). A particular attention is given to the domain of variation of each dimensionless parameter, in order to take into account non-symmetric cross-section, thin cross-section and large type of solicitations.

For the static problem, it is shown that two invariants – that depend on the two parameters related to moments and energy density – govern the problem. These invariants are similar to the invariants encountered for finite rotation of a rigid body with the only difference regarding the variables (space in place of time) and the applications between these two different approaches. Accordingly, four regimes arise that depend on the two effective rigidities. Solutions were found in an analytical way, in terms of Jacobian elliptic functions. A detailed discussion is made regarding the role of the control parameters.

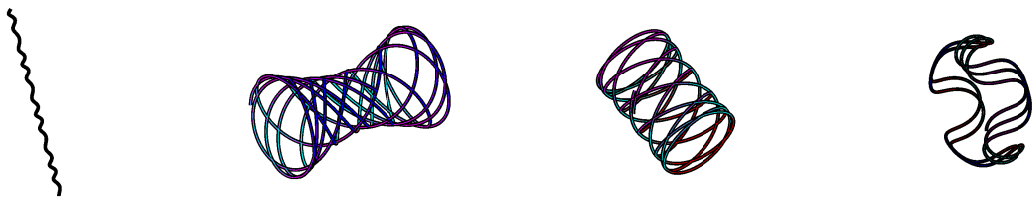


Figure 1: The four regimes of deformation of the beam

Discussion

It is shown that according to the regimes, the beam could roll up in a finite domain whatever its length. The size of such finite domain could be defined in an analytical way. According to relation between the non-dimensional parameters, this process, leads to periodic or only pseudo-periodic patterns.

In a second time, dynamical equations governing the presence of super-imposed infinitesimal perturbations is given thanks to the methodology used in [2]. It is the occasion to present the partial coupling of this problem and the various characteristics of the mass and rigidity matrices, involved for such problem. These matrices are space dependent and allow the determination of a stability criteria which is highly dependent on the four regimes encountered in the static configuration. Numerical simulations will follow this presentation.

References

- [1] Hariz M., Le Marrec L., Lerbet J. (2021) Explicit analysis of large transformation of a Timoshenko beam: post-buckling solution, bifurcation, and catastrophes. *Acta Mechanica* **232**(9), 3565-3589.
- [2] Le Marrec L., Lerbet J., Rakotomanana L. R. (2018) Vibration of a Timoshenko beam supporting arbitrary large pre-deformation. *Acta Mechanica* **229**(1), 109-132.

Sufficient conditions to exclude positive Lyapunov Exponents in the Thomas' system

Daive Martini**, David Angeli*,**, Giacomo Innocenti** and Alberto Tesi**

*Department of Electrical and Electronic Engineering, Imperial College London, London, SW7 2AZ, UK

**Department of Information Engineering, University of Florence, FI, IT

Abstract. Sufficient conditions to rule out the presence of attractors with positive Lyapunov exponents in the Thomas' system are formulated via the 2-additive compound of the Jacobian. It will be shown how the problem can be solved both analytically and by using Linear Matrix Inequalities.

Introduction

Ruling out the possibility of chaotic or oscillatory behaviors in dynamical systems has been widely studied and many techniques have been proposed (see, e.g., [1]). A Jacobian-based technique was introduced by Muldowney in the seminal paper [2], in which the author formulates conditions on the matrix norm of the 2-additive compound of the Jacobian to exclude the existence of nonconstant periodic solutions. Subsequently, the results in [2] has been extended in [3] to rule out periodic and almost periodic solutions. In the same spirit, in [4] it is shown how conditions on the 2-additive compound of the Jacobian can be also exploited to rule out attractors with positive Lyapunov exponents from a known invariant set \mathcal{E} and how the problem can be traced back to a LMI problem of the form

$$D(P(x)) = \left(\frac{\partial f^{(2)}}{\partial x}(x) \right)^T P(x) + P(x) \left(\frac{\partial f^{(2)}}{\partial x}(x) \right) + \dot{P}(x) \leq 0 \quad \forall x \in \mathcal{E}, \quad (1)$$

where $P(x)$ is a properly designed matrix. In this work, we analyze the stability properties of solutions of the Thomas' system applying the results presented in [4].

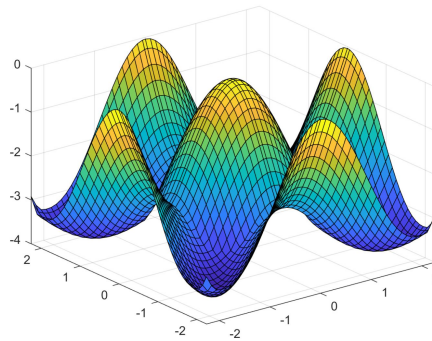


Figure 1: Determinant of $D(P(x))$ within the invariant set \mathcal{R} .

Results and discussion

One of the most investigated system in chemical reaction, ecology and evolution is the Thomas' system [5]. It is known that the Thomas' system has a convex and compact invariant set $\mathcal{R} = \{x \in \mathbb{R}^3 : b|x|_\infty \leq 1\}$, where $x = (x_1, x_2, x_3)^T$ is the state vector and b is a positive parameter. Inside the invariant set, the system displays a rich dynamical behavior due to the various bifurcations that occur as b varies in $(0, 1]$. The aim is to find the minimum value b_m of b such that problem (1) can be solved by using the technique in [4]. The value of $b_m = 0.443$ can be obtained both analytically or numerically by solving a LMI problem tuned on only four points of \mathcal{R} , which implies that no attractors with positive Lyapunov exponents exist for $b \geq 0.443$. This is confirmed by Figure 1 which reports the function

$$\max_{x_3: (x_1, x_2, x_3) \in \mathcal{R}} \det(D(P(x)))$$

inside the projection of the box \mathcal{R} with respect to the x_3 axis for $b = b_m$, thus showing that the determinant is negative.

References

- [1] Sastry S. (2013) Nonlinear systems: analysis, stability, and control. *Springer Science & Business Media* **10**.
- [2] Muldowney J. S. (1990) Compound matrices and ordinary differential equations. *The Rocky Mountain Journal of Mathematics* 857–872.
- [3] Angeli D., Al-Radhawi M. A., Sontag E. D (2021) A Robust Lyapunov Criterion for Nonoscillatory Behaviors in Biological Interaction Networks. *IEEE Transactions on Automatic Control* **67**(7):3305–3320.
- [4] Martini D., Angeli D., Innocenti G., Tesi A. (2022) Ruling out Positive Lyapunov Exponents by using the Jacobian's Second Additive Compound Matrix. *IEEE Control Systems Letters*.
- [5] Sprott J. C., Chlouverakis K. E. (2007) Labyrinth chaos. *International Journal of Bifurcation and Chaos* **17**(6):2097–2108.

Modelisation of Thermally Induced Jitter in an Orbiting Slender Structure

Kathiravan Thangavel¹, Maurizio Parisse², Pier Marzocca³

¹Graduate student, School of Aerospace Engineering, Sapienza University of Rome, Via Salaria, 875, 00138, Rome, Italy.

²Professor, School of Aerospace Engineering, Sapienza University of Rome, Via Salaria, 875, 00138, Rome, Italy.

³Director, Sir Lawrence Wackett Aerospace Research Centre, RMIT University, Victoria 3001 Australia.

Abstract. Thermomechanical interactions aboard spacecraft interesting field of research and study. Since Bruno Boley's 1954 publication, numerous authors have contributed, if not with a multidisciplinary perspective. The Alouette 1 anomaly in 1962 signalled the start of a long succession of unexpected events due to mechanical and thermal interaction. This study uses a simple model to illustrate the basic mechanism behind thermal shock-induced elastic vibrations. This occurs when a spacecraft's flexible appendage is previously shadowed by its main body after an attitude manoeuvre [Ulysses, 1990] or during the transitions shadow-Sun and vice-versa. A thin structure was used to compare thermal and mechanical characteristic times and realise the strong coupling. The accurate thermal analysis offers a time-dependent thermal bending moment that acts as a boundary condition in the subsequent modal analysis of the structural element, triggering elastic transverse vibrations.

Introduction

Since the 1960s, thermally induced vibration has turned out to be a breakdown in spacecraft with flexible appendages. Space beams, such as spacecraft booms, solar arrays etc., could go through thermally induced vibration owing to abrupt temperature changes on night-day and day-night alterations in orbit, as shown in Figure 1. The flexible appendages of spacecraft, such as antennae and solar arrays, are exposed to a sudden solar heat flux during the orbital eclipse transition. Boley [1] predicted the thermally induced vibration of thin beams for the first time. Boley indicated that this problem involves transient heat conduction and structural dynamics. To avoid this type of failure, extensive research was conducted to design the spacecraft components properly. Authors [2-4] researched thermally induced solar panel dynamics, including an analysis of satellite attitude dynamics caused by thermally induced structural motions, an assessment of material degradation effects, and a laboratory investigation of a satellite solar panel's thermal-structural performance. Analytical and experimental results show thermal bending deformations with acceleration transients that have characteristic thermal snap disturbance histories in response to rapid changes in heating. According to the research, thermal snap disturbances in solar panels are caused by temperature differences that vary at a non-constant rate throughout the panel's thickness.

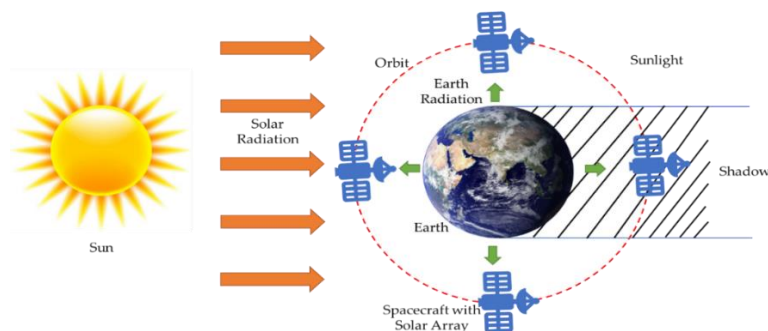


Figure 1: Satellite thermal environment in orbit.

Results and Discussion

This research work aims to analytically analyse more about the thermally induced vibration caused by solar heating. To investigate thermally induced vibrations, a novel method is proposed. The proposed analytical method allows the designer to analyse a thermally induced problem effectively with retaining the nonlinearity in the model. The research presents a new design guideline for analysing the thermal jitter of a thin spacecraft structure, which is a common occurrence in space engineering. A simplified modelisation provides a step-by-step procedure for studying and analysing the phenomenon of thermal jitter.

References

- [1] Boley BA, "Thermally induced vibrations of beams," J. Aeronaut. Sci., vol. 3, no. 2, pp. 179–181, 1956.
- [2] E. A. Thornton, Thermal Structures for Aerospace Applications. AIAA Education Series, 2012.
- [3] J. D. Johnston and E. A. Thornton, "Thermally Induced Dynamics of Satellite Solar Panels," *J. Spacecraft. Rockets*, 2008.
- [4] Xu, Qiuyi & Li, Shu & Wang, Li & Dong, Apeng & Meng, and Yang. (2019). Thermomechanical Coupling Analysis and Optimisation of Metallic Thermal Protection System. *Shock and Vibration*. 2019. 1-14. 10.1155/2019/1890237.

Resonant phase lags of an oscillator with polynomial stiffness

Martin Volvert, Gaëtan Kerschen

Space Structures and Systems Laboratory, Department of Aerospace and Mechanical Engineering, University of Liège, Liège, Belgium

Abstract. Nonlinear systems can exhibit complex behaviours, such as secondary resonances, which are sometimes overlooked in the industry. This work aims at giving a first analytical insight on the behaviour of those secondary resonances and especially their resonant phase lags, nonnecessarily equal to $\pi/2$, using a first-order averaging technique. These phase lags can be later used for experimental nonlinear modal analysis techniques such as phase-locked loop.

Introduction

First- and higher-order averaging technique is commonly used to describe analytically the behaviour of weakly nonlinear systems [1, 2]. However, the analysis is generally made for Duffing and Helmholtz oscillators, respectively. The present work extends the existing studies to an oscillator with arbitrary polynomial stiffness:

$$\ddot{x}(t) + 2\zeta\omega_0\dot{x}(t) + \omega_0^2x(t) + \sum_{d=2}^{\infty} \alpha_d x^d(t) = \gamma \sin \omega t \quad (1)$$

Results and discussion

First, for the primary resonance, assuming small damping ζ , nonlinear coefficients α_d and forcing γ , and writing the solution as $x(t) = A \sin(\omega t - \phi)$. The governing equations show that nonlinearities with even powers do not participate to the motion, and that the phase lag ϕ_a at amplitude resonance is, at first-order: $\tan \phi_a = \frac{\omega_a}{\zeta\omega_0}$, where ω_a is the amplitude resonance frequency. ϕ_a is close to $\frac{\pi}{2}$ since the damping is small. $\phi_p = \frac{\pi}{2}$ is thus defined as the phase lag at phase resonance.

Second, secondary resonances can be studied by assuming small damping and nonlinear coefficients, but strong forcing. The solution can then be expressed as $x(t) = \Gamma \sin \omega t + A_k \sin(k\omega t - \phi_k)$ for $k : 1$ superharmonic resonances and $x(t) = \Gamma \sin \omega t + A_\nu \sin(\frac{\omega}{\nu} t - \phi_\nu)$ for $1 : \nu$ subharmonic resonances. The governing equations show that nonlinearities with odd (even) powers only generate odd (even) secondary resonances, *i.e.*, when k and ν are odd (even), and for which amplitude resonance occurs close to $\phi_p = \frac{\pi}{2}$ ($\phi_p = 0$), defined as the phase lag at phase resonance for odd (even) secondary resonances.

Higher-order averaging can be used to show that nonlinearities with odd (even) powers do generate even (odd) secondary resonances. For example, even secondary resonances can be found for a Duffing oscillator and the associated phase lag at phase resonance is $\frac{3\pi}{4\nu}$ [3].

These results are illustrated on a 3 : 1 superharmonic (Fig. 1a) and a 1 : 3 subharmonic (Fig. 1b) where amplitude and phase resonances are shown for an oscillator whose nonlinear term is $\alpha_7 x^7(t)$. Both amplitude and phase resonances occur almost simultaneously for each type of secondary resonance.

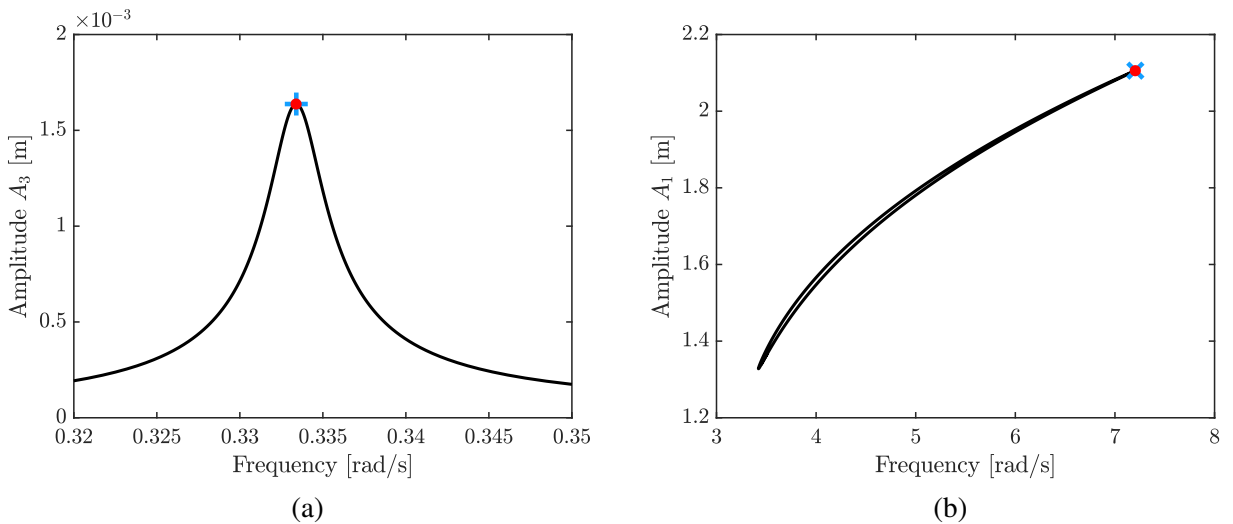


Figure 1: Evolution of the amplitudes A_3 and A_1 around the 3:1 and 1:3 superharmonic and subharmonic resonances (black), phase (red) and amplitudes (blue) resonances

References

- [1] Nayfeh A. H. (1973) Perturbation methods., John Wiley & Sons, New York.
- [2] Yagasaki K. (1998) Higher-order averaging and ultra-subharmonics in forced oscillators, *J. Sound Vib.* **210**:529–553.
- [3] Volvert M., Kerschen G. (2022) Resonant phase lags of a Duffing oscillator, *Int J Non Linear Mech* **146**:104150

Introduction to The Perpetual Mechanics Theory and Future Directions

Fotios Georgiades

*Independent Researcher, Athens, Greece. ORCID-ID:0000-0002-2784-6976

Abstract. The perpetual point's definition applied in the dynamic analysis of mechanical systems leads that they can be associated with manifolds defining rigid body motions. Herein, through 4 examples the dynamics prescribed by a formalism developed around the perpetual manifolds is shown. The characteristics of the dynamic analysis, in terms of mechanics are examined. As a summary, for the first time the following are prescribed explicitly: particle-wave motion, zero internal forces, no energy loss, perpetual machines of third kind. Therefore, the developed formalism can be claimed that forms the basis of The Perpetual Mechanics Theory. Possible future research directions are discussed too.

Introduction

Perpetual points (PPs) in mathematics have been defined in [1] and their application in examining the dynamics of linear unforced mechanical systems (MS) leads that they are comprising manifolds defining rigid body motions [2]. Further, using the PPs definition the perpetual mechanical systems (PMSs) are defined as the unforced MS that admits perpetual manifolds of rigid body motions (RBMs). In [3] a theorem defines the correlation of the “external forces” (herein is used) applied to a PMS resulting RBMs and leads that the PMS can have free or embedded configuration. In Fig. (1a) these two configurations of PMS (4 in total) with the force's functions, are shown. The free PMSs (with index $i=f$) arise by setting zero the c_x and the k_x . One free PMS is nonlinear with $k=1 \text{ N/m}^3$ (index $j=NL$), and the other with zero k is having only linear internal forces ($j=L$). The two embedded PMSs ($i=e$) arise by setting $c_x=0.016 \text{ N}\cdot\text{s/m}$ and $k_x=1 \text{ N/m}$, for nonzero k ($j=NL$), and zero k ($j=L$). Using equal Initial Conditions (ICs) in numerical integrations lead to the displacements that Fig. 1b is depicting, whereas the PMSs on each configuration has the same RBM.

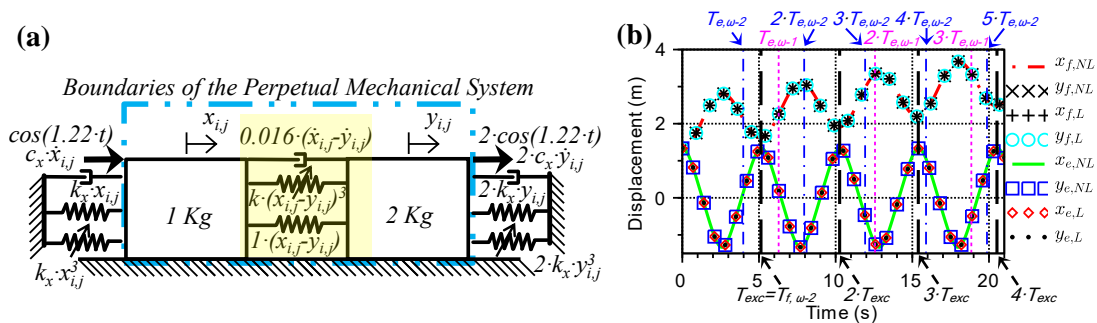


Figure 1: (a) The 4 configurations (different i,j) of the mechanical systems, with their associated forces. (b) The displacements of the 4 mechanical systems with the same to all masses ICs (1.3328999 m, 0.0560637 m/s).

Results and discussion

As a summary so far, with a specific mathematical method the displacements associated with RBM have been prescribed and shown. The examination Fig. 1 in terms of mechanics leads to certain conclusions: a) in Fig. (1b) the RBM of the embedded PMS ($x_{e,L}$, $x_{e,NL}$) is particle-standing wave motion, that has been designed using this formalism [4] (steady state with numerically defined IC.s), and of the free PMS ($x_{f,L}$, $x_{f,NL}$) is a particle-longitudinal wave motion [3]; b) the systems with linear internal forces and those with nonlinear internal forces have the same motion; c) in the yellow highlighted area of Fig. (1a), all the individual forces in RBM are zero [5], d) there is no internal degradation/energy storage, e) there is no internal energy loss [5], f) the PMS when earn energy behave as a perpetual machines of 3rd kind [5]. The a-f conclusions, explicitly prescribed through theorems and corollaries partially forming the formalism leading to new design [4], so arguably can be claimed that all the relevant articles e.g., [2-5] form the basis of ‘The Perpetual Mechanics Theory’. Future research directions can be considered in Mathematics e.g., for other types of systems, in Physics e.g., about the 2nd Law of thermodynamics, and in Engineering e.g., for new designs.

References

- [1] Prasad A. (2015) Existence of perpetual points in nonlinear dynamical systems and its applications. *Int. J. Bif. Chaos* **25**: 1530005.
- [2] Georgiades F. (2021) Perpetual points in natural dissipative with viscous damping mechanical systems: A theorem and a remark. *Proc. of IMechE: Part-C J. of Mech. Eng. Sci.* **235**:4526-4534.
- [3] Georgiades F. (2021) Augmented Perpetual Manifolds and Perpetual Mechanical Systems-Part I: Definitions, Theorem and Corollary for Triggering Perpetual Manifolds, Application in Reduced Order Modeling and Particle-Wave Motion of Flexible Mechanical Systems. *ASME J. Comput. Nonlinear Dyn.* **16**:071005.
- [4] Georgiades, F., 2022, Exact Augmented Perpetual Manifolds Define Specifications for the Steady States of Similar Rigid Body Modes, A Corollary for Nonautonomous Systems, *International Journal of Structural Stability and Dynamics*, 22 (15): 2250167.
- [5] Georgiades F. (2022) Augmented perpetual manifolds and perpetual mechanical systems-part II: Theorem for dissipative mechanical systems behaving as perpetual machines of third kind. *Nonlinear Dyn.* **108**:789-825.

Fourier Analysis of a Duffing Equation With Delay

Mark Walth, Richard Rand

Department of Mathematics, Cornell University, Ithaca NY, USA

Abstract. We investigate the Duffing-like equation with delay $\ddot{x} + cx(t - T) + x^3 = 0$, where $T > 0$ delay and c is a parameter. In [1], the authors used the method of harmonic balance to discover that this equation displays a remarkable singularity: when T becomes positive, there is a bifurcation in which infinitely many limit cycles with large amplitudes and high frequencies are born. In this work, we extend the techniques used in [1], revealing more complicated dynamics in the delayed Duffing equation. Using a higher order harmonic balance approach allows us to detect the existence of previously unnoticed limit cycles, as well to predict what we have termed a *period splitting bifurcation*.

Introduction

The equation

$$\frac{d^2x}{dt^2} + cx(t - T) + x^3 = 0 \quad (1)$$

has a number of remarkable properties. Here, c is a parameter, and $T \geq 0$ is a delay. In [4], the authors proved that the origin is linearly unstable for all $T > 0$. Later, in [1], the authors predicted that for all $T > 0$, there exist an infinite number of stable limit cycles with very high frequency and large amplitudes. The amplitudes of the limit cycles were determined by using the method of harmonic balance, using the ansatz $x(t) = A \cos(\omega t)$. In subsequent work, including [2] and [3], the authors were able to rigorously prove that the equation supports infinitely many periodic solutions. In particular, in [2, 3], Sah, Fiedler, et. al. were able to find a class of exact solutions by “lifting” certain solutions of the non-delayed Duffing equation to the delay case. We refer the reader to [2] for a more thorough history of progress in understanding this equation.

Results and Discussion

In this work, we investigate equation solutions of (1) using a higher order harmonic balance method, in which we approximate $x(t)$ with a truncated Fourier series of higher order. This extends the results found in [1], allowing us to detect previously unnoticed limit cycles. Our main result is that we are able to predict a qualitative change in the geometry of the limit cycles as T increases, in what we have chosen to term a *period splitting bifurcation*. This bifurcation is characterized by the periodic motion transitioning from oscillating at a single dominant frequency to suddenly oscillating with two component frequencies. See Figure 1 for an illustration. We wish to emphasize how a single computational technique detects such a variety of behaviors of solutions.

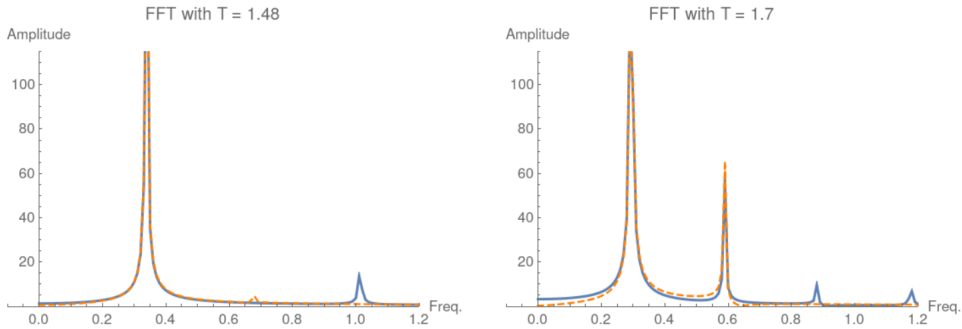


Figure 1: Fast Fourier Transform just before bifurcation (left) and just after (right). Orange dashed is curve predicted by harmonic balance, blue solid is result of numerical integration.

References

- [1] M. Davidow, B. Shayak, and R. Rand, “Analysis of a remarkable singularity in a nonlinear DDE,” *Nonlinear Dynamics*, vol. 90, Oct. 2017, doi: 10.1007/s11071-017-3663-2.
- [2] S. M. Sah, B. Fiedler, B. Shayak, and R. Rand, “Unbounded sequences of stable limit cycles in the delayed Duffing equation: an exact analysis,” *Nonlinear Dynamics*, vol. 103, Jan. 2021, doi: 10.1007/s11071-020-06012-8.
- [3] B. Fiedler, A. López Nieto, R. H. Rand, S. M. Sah, I. Schneider, and B. de Wolff, “Coexistence of infinitely many large, stable, rapidly oscillating periodic solutions in time-delayed Duffing oscillators,” *Journal of Differential Equations*, vol. 268, no. 10, pp. 5969–5995, May 2020, doi: 10.1016/j.jde.2019.11.015.
- [4] Bhatt, S.J., Hsu, C.S.: Stability criteria for second-order dynamical systems with time lag. *J. Appl. Mech.* 33(1), 113–118 (1966).

Improving rotor stability through direct piezoelectric effect

Sérvio Haramura Bastos* and Rui Vasconcellos*

* Sao Paulo state University (UNESP), Faculty of Engineering of São João da Boa Vista

Abstract. The aeroelastic instability known as whirl-flutter becomes very relevant to development of the next generation of propeller-driven aircraft, influencing specially the design of wings, nacelle and rotor. Although this instability is classically treated as linear, all aeronautical structures may present a certain level of nonlinearity that can be predicted in the project or can arise during operational life, affecting the aircraft's performance and reliability directly. Thus, the development of techniques to increase stability margins in the presence of some type of nonlinearity becomes important in the current aeronautical scenario. So, the present research sought the application of piezoelectris passively, together with a structural cubic hardening nonlinearity in the mounting of a rotor system. Possible results includes extension of useful speed range and limited amplitude oscillations after the instability speed, with direct influence of piezoelectric effects in amplitude reduction.

Introduction

The optimal relationship between performance and safety in aircraft is fundamental when aeroelastic solutions are sought. Although nonlinearities are neglected in several problems, the system's behavior may be highly affected when they arise in aeronautical structures leading to dangerous situation. Corrective solutions to mitigate undesirable nonlinear effects and understanding how they affect system's behavior becomes important [1]. In addition, apparently overcome problems arise in the present due to modern air mobility. The whirl-flutter, which is characterized as a divergent elliptic precession movement that occurs in the rotor due to non-stationary forces and moments [2], can be harmful and influence the design of the new generation of propeller aircraft, and therefore, needs special attention.

Although, techniques to control this instability are explored, the piezoelectric investigation to this propose and energy harvesting remains underinvestigated, specially when structural nonlinearities are considered.

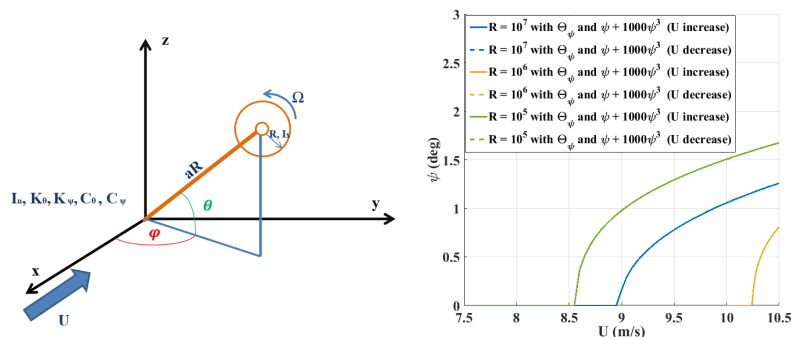


Figure 1: (a) At the left, rotor-nacelle system representation submitted to whirl-flutter. (b) At the right, yaw response for different load resistances.

Results and Discussion

In order to observe nonlinear-piezo-aeroelastic model's behavior submitted to whirl-flutter, a two degree-of-freedom rotor-nacelle model, considering a quasi-stationary aerodynamics [3], shown in Fig. 1a, was modified including both piezoelectric approach described by [4] and the structural hardening nonlinearity. Preliminary results have shown that the nonlinearity in the yaw degree of freedom provides a limit cycle oscillation (LCO) in the post-flutter regime. The presence of an *unimorph* configuration piezoelectric in yaw postponed the critical speed, meaning that the Hopf bifurcation occurred at different speeds with a subcritical behavior depending on the load resistance, as depict Fig. 1b. In the final paper, both configurations, *unimorph* and *bimorph* will be considered in pitch and yaw degrees of freedom.

Acknowledgments

This research was financed in part by the the Coordenação de Aperfeiçoamento de Pessoal de Nível Superior – Brasil (CAPES) – Finance Code 001 and by Grant 2021/09276-5, São Paulo Research Foundation (FAPESP).

References

- [1] Abdelkefi, A., Vasconcellos, R., Marques, F. D., Hajj, M. R. (2012) Bifurcation analysis of an aeroelastic system with concentrated nonlinearities. *Nonlinear Dyn* **69**:57-70.
- [2] Čečrdle J. (2017) Aeroelastic Stability of Turboprop Aircraft: Whirl Flutter. Flight Physics–Models, Techniques and Technologies, Ed.: Konstantin Volkov, InTech Publications, Rijeka, Croatia, 1, 139-158.
- [3] Mair, C., Rezgui, D., Titurus, B. (2018) Nonlinear stability analysis of whirl flutter in a rotor-nacelle system. *Nonlinear Dyn* **94**(3):2013–2032.
- [4] Erturk A., Inman, D. J. (2008) A distributed parameter electromechanical model for cantilevered piezoelectric energy harvesters. *J Vib Acoust* **130**(4):041002-1.

Numerical Simulation of a Bio-inspired, Bistable Plate System.

Mrunal Bhalerao*, Muhammad Hajj** and Lei Zuo***

*Department of Mechanical Engineering, Virginia Tech, Blacksburg, VA, USA

**Department of Civil, Environment and Ocean Engineering, Stevens Institute of Technology, Hoboken, NJ, USA

***Department of Naval Architecture and Marine Engineering, University of Michigan, Ann Arbor, MI, USA

Abstract. In this paper, the authors aim to numerically simulate the experimentally observed dynamic and static behaviour of a bi-directionally curved, buckled, plate-based bistable system inspired from the Venus flytrap. This system consists of a thin rectangular plate with a slot along its centre line thus creating two sub-plates. Displacement constraints placed on the free, cantilevered edges of the sub-plates cause the bending and twisting of the plate thus giving rise to bi-directional curvature and the buckling bistability. It has been seen experimentally that this system shows a unique hysteretic behaviour during the snap through phenomena. The Poisson-Kirchhoff classical thin plate theory has been used to explain this unique hysteric behaviour. Initially, the parameters governing the snap-through have been identified and studied. A static analysis has been performed to formulate the stiffness of the system followed by a dynamic analysis by assuming a sinusoidal force input.

Introduction

The usefulness of bistable systems in broadband energy harvesting has already been proved [1]. Several methods have been used to create bistable systems [1]. Recently, Qian et al [2] developed a plate-based bistable system inspired from the leaf blades of the Venus flytrap. Although several plate-based bistable systems have already been rigorously studied [3], this is a novel bistable system which requires no external bistability inducing mechanisms, moreover the unique bending and twisting observed due to the end displacement constraints have not been studied numerically as per the knowledge of the authors.

Building on to the existing self-contained bistable system in [3], the authors have proposed a modified version of this system as shown in Fig.1(d) to improve repeatability and reduce variability. The sheet metal plate is given a lateral in-plane displacement as indicated in Fig.1(a) while clamping, this induces bi-directional curves (Fig.1(b) and Fig.1(c)) in the plate, thus causing the bistability. The stiffness curve of the system has been determined experimentally by giving small incremental displacements at point P (Fig.1(d)) in the transverse direction and measuring the opposing force exerted by the system at each displacement as shown in Fig.1(e). Using the Poisson-Kirchhoff's classical thin plate theory, the unique stiffness curve of the bistable system obtained experimentally has been explained. Using the developed numerical model, the response of the system for an external sinusoidal forcing function has been determined.

Results and Discussion

Apart from the snap-through mechanism observed in conventional bistable systems, it has been observed that under quasistatic conditions the path followed by the system from stable state A to B is not the same as that taken by the system from stable state B to A. The authors have attempted to explain this hysteretic behaviour, numerically. Fig.1(f) shows stiffness curve of the bistable system.

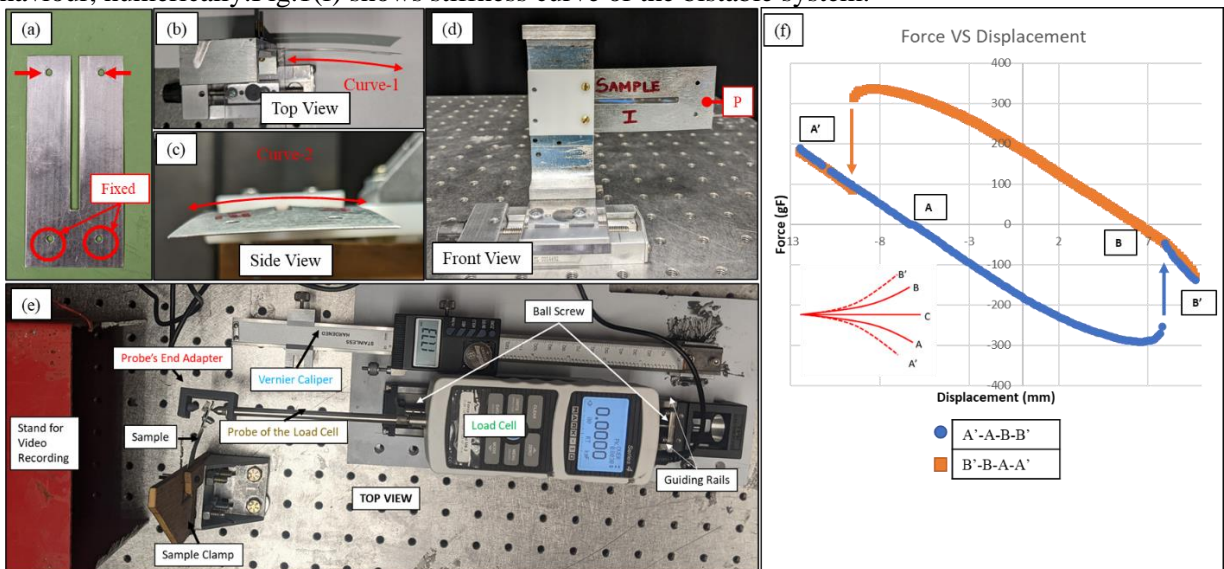


Figure 1: (a) Sheet metal plate (b) Top view of the bistable system. (c) Side view of the bistable system. (d) Front view of the bistable system. (e) Experimental Apparatus. (f) Force VS Displacement curve

References

- [1] R L Harne and K W Wang (2013) A Review of the Recent Research on Vibration Energy Harvesting via Bistable Systems. Smart Mater. Struct. 22 023001.
- [2] F. Qian, M. R. Hajj, and L. Zuo (2020) Bio-inspired bi-stable piezoelectric harvester for broadband vibration energy harvesting, Energy Conversion and Management, Volume 222, 113174.
- [3] A. F. Arrieta, P. Hagedorn, A. Erturk, and D. J. Inman (2010) A Piezoelectric Bistable Plate for Nonlinear Broadband Energy Harvesting, Appl. Phys. Lett. 97, 104102.

Multiple Periodic Symmetric Limit Cycles of Two Coupled Sommerfeld Rotors

Walter V. Wedig*

*KIT Karlsruher Institut für Technologie, Karlsruhe, Germany

Abstract. The paper extends the Sommerfeld rotor to two unbalanced, rigidly coupled, elastically supported rotors which rotate in a synchronous operation with the same rotation speed, when both driving moments are equal. For equal moments with opposite signs, there is an asynchronous operation with the same limit cycle in the phase plane of displacement and velocity of the horizontal rotor vibrations. New forms of symmetric limit cycles are calculated when the applied driving moments are unequal. For high-speed rotations, driving moments are applied near the ratios 1:1, 1:3 and 1:4 in order to derive symmetric forms of single, triple or quadruple periodic limit cycles, respectively. For the special case that the rotations of both rotors are rigidly coupled, a new speed moment characteristic is calculated by means of time-free Fourier solutions.

Introduction to Sommerfeld rotors

The Sommerfeld rotor [1] is extended to two unbalanced viscos-elastically supported rotors shown in Figure 1. The application of same driving moments m_1 and m_2 to both rotors leads to vibrations of rotor displacement ξ and velocity ζ described by the one-periodic limit cycle shown in Figure 2. The rotation speeds of both rotors are investigated by means of the mean values $E(v)$, $E(\eta)$ and the fluctuating parts Δv , $\Delta \eta$, respectively.

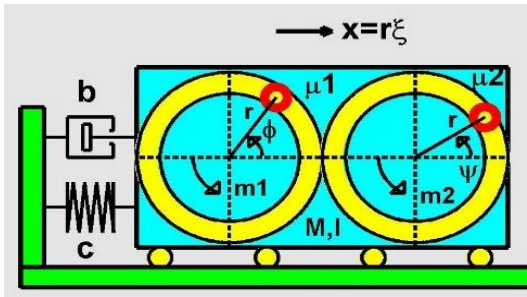


Figure 1: Airplane wing model with two rotors

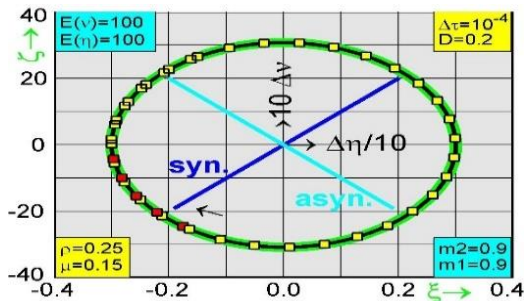


Figure 2: Limit cycle of displacement and speed

New results are derived when both rotations are operated, independently. Figure 3 shows the triple periodic, double symmetric limit cycle when the ratio of the driving moments is near 1:3. In Figure 4, a quadruple limit cycle is calculated where sharp cycle lines are extended to limit flows because $E(v)/E(\eta)$ differs from 1/4.

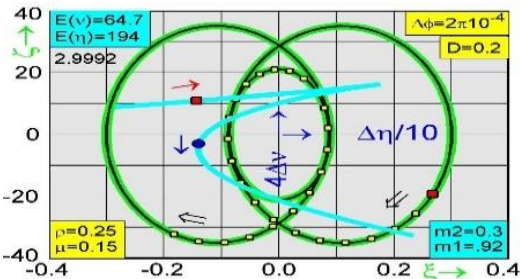


Fig. 3: Triple periodic symmetric limit cycle

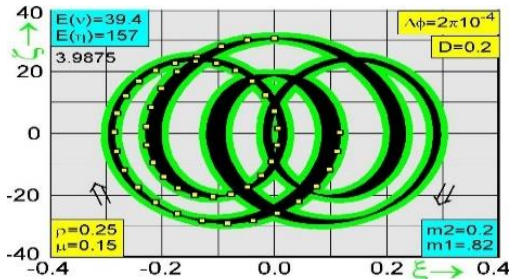


Fig 4: Quadruple periodic limit cycle flow

Limit cycles of time-free rotor equations

The paper introduces orthogonal equations of motion [2] into rotor dynamics where time is substituted by angle [3]. This avoids almost periodic solutions. Stability can be investigated by means of the Floquet theory. Approximated solutions are calculated by means of Fourier expansions. In case that both rotations are coupled, the paper derives a new speed moment characteristic which corrects the classical version by means of the moment of inertia of the unbalanced mass related to the mass moment of inertia of the entire rotor.

References

[1] Sommerfeld A. (1902): Beiträge zum dynamischen Ausbau der Festigkeitslehre, Zeitschrift des Vereins Deutscher Ingenieure, Vol. 46, pp. 391–394 (in German).

[2] Wedig W.V. (2022): Multiple Sommerfeld Effects in Vehicle Dynamics. In Lacorbonara, W., Balachandra, B, Lamey, M.J., Ma,J., Machado, J.A.T. Stepan, G. (eds) Advances in Nonlinear Dynamics, Proceedings of the Second International Nonlinear Dynamics Conference, Vol 2, pp.538-550.

[3] Wedig W.V. (2021): Speed Oscillations of a Vehicle Rolling on a Wavy Road. In Special Issue "Performance and Safety Enhancement Strategies in Vehicle Dynamics and Ground Contact", *Appl. Sci.*,11(21) . *Sci.*,11(21) .

Generating machine learning-based state maps from real-world friction-induced vibration data

Charlotte Geier*, Said Hamdi**, Thierry Chancelier**, Norbert Hoffmann*,***, Merten Stender*

*Dynamics Group, Hamburg University of Technology, Hamburg, Germany; **Hitachi Astemo France S.A.S., Drancy, France; *** Imperial College London, Department of Mechanical Engineering, London, UK

Abstract. Understanding the rich bifurcation behavior of friction-excited mechanical structures such as brake systems remains a challenge in engineering today. Currently, a complete bifurcation map that represents the system state over a large bifurcation parameter range cannot be obtained from physics-based models or experimental data alone. This work presents a machine-learning based method for obtaining bifurcation maps of the entire parameter space in a purely data-driven fashion. A machine learning model is built to predict the system’s dynamical state from experimental data, picking up hidden bifurcation mechanisms. This model is then exploited to assess the system state for a wide range of synthetic, physics-conform data, yielding a complete map of the bifurcation parameter space. Results suggest that the method can detect hidden dimensions and parameters driving the bifurcation which were inaccessible previously.

Introduction

Friction-induced vibrations represent a major challenge in mechanical engineering structures, such as brake systems, clutches, drill-strings, and others. Under specific loading conditions, the dynamical systems undergo bifurcations that will feed frictional energy into the structure, thereby exciting unwanted and potential vibrations. Today, the complete bifurcation parameter map cannot be obtained from either physics-based models or directly from experimental data [1, 2]. While the former is limited due to modeling assumptions and parameter uncertainties, the amount of available measurement data is inherently sparse. Recently, it has been shown that machine learning-based approaches can yield digital twins for friction-induced dynamical systems [3]. These data-based models are a powerful tool for the prediction of system stability. This work proposes a purely data-driven approach to generating bifurcation maps from real-world measurement data of a friction brake system.

Results and Discussion

A machine learning model is trained to predict the brake system state using external load data obtained from a brake system undergoing commercial vibration testing. After training and validation, the digital twin of the brake system has picked up the complex parametric relations and hidden mechanisms which drive the systems dynamics. As the load parameter space is sampled only sparsely by experiments, the digital twin can be used to predict behavior in the remaining space, thereby drawing complete bifurcation maps, see Figure 1. To do so, a physics-conform data augmentation is installed to generate synthetic measurement data for all requested load parameter combinations. Thereby, a full bifurcation map is generated even though the original measurement space was only sparsely sampled. Validation of those maps is achieved using the experimental data at hand.

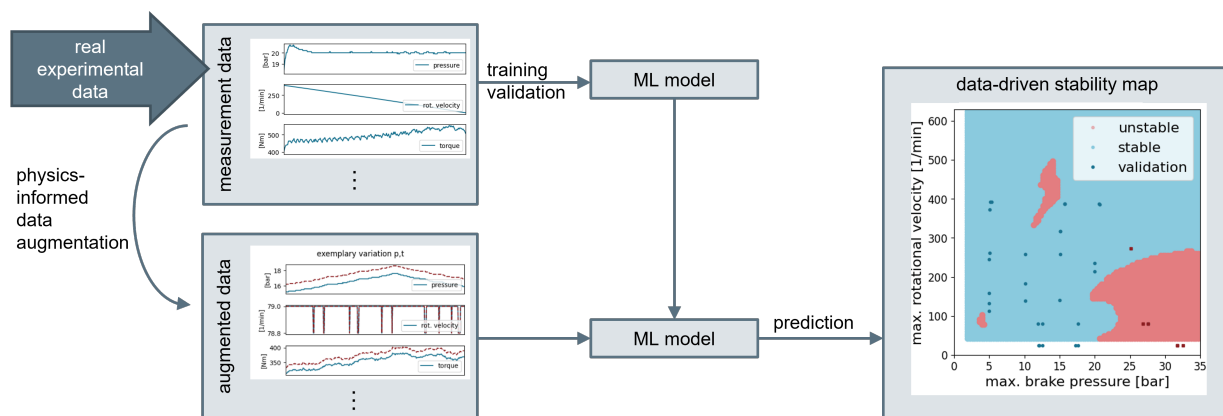


Figure 1: Generation of a data-based bifurcation map from measurement data of real-world data of a brake system.

Results indicate that this method yields consistent results. The complex bifurcation pattern of a real-world brake system is revealed, i.e. hidden mechanisms and driving (bifurcation) parameters that were previously impossible to grasp. Machine learning bifurcation maps can therefore be a powerful tool for the understanding of complex dynamical systems.

References

- [1] Massi F. et al. (2007) Brake squeal: Linear and nonlinear numerical approaches. *Mech Syst and Signal Process* **21**:2374-2393.
- [2] Hochlenert D. (2009) Nonlinear stability analysis of a disk brake model. *Nonlinear Dynamics* **58**:63-73.
- [3] Stender M. et al. (2021) Deep learning for brake squeal: brake noise detection, characterization and prediction. *Mech Syst and Signal Process* **149**:107181.

A spring-mass mechanical system with moving edges having rich dynamical behaviour

Jobin Josey^{*1} and Balakrishnan Ashok^{*2}

^{*}Centre for Complex Systems & Soft Matter Physics, International Institute of Information Technology Bangalore (IIITB), 26/C Hosur Road, Electronics City, Bengaluru 560100, India.

Abstract. We report some of our theoretical results on the behaviour of a mass suspended between two springs and oscillating in a plane with movable suspension points. Our investigations of the system consider the case of springs which are Hookean, as well as when they show nonlinear behaviour, with spring softening and hardening. The effect of external forcing has also been considered, as also the effect of damping in the system. An intensive study of the system has been conducted yielding diverse dynamical regimes, spanning from regular oscillations to chaotic behaviour. The change in stability of the system has been investigated, and the bifurcation mechanisms involved, studied. This study has important applications in various physical systems, ranging from biological systems to mechanical structures in everyday life.

Introduction

The system under study consists of two springs affixed symmetrically to a mass in between them, with the other end of each spring kept fixed to edges that also have a degree of freedom in the same plane. Such mechanical systems are very useful to understand the physical and structural response of other complicated mechanical structures as well as in nature, such as in living systems, including muscle behaviour. Earlier work on such systems include that by Whineray [1], and Arnold and Case [2], who investigates the case of a mass fixed between two springs (a rubber band), but with fixed points of suspension and which are Hookean in nature, the system reduces to a Duffing oscillator under the approximations made therein [2]. Our system is more complicated, and we consider the case of linear and nonlinear springs separately, as also the case where the points of suspension are free to move along an axis in the plane, which has not been treated before in the literature. The form of the nonlinear spring constants is partially motivated by previous work that showed the interaction between carbon nanotubes quantified by the interaction energy obtained through quantum mechanical calculations could be mimicked classically by nonlinear springs [3]. Both forced and free vibrations of the constrained springs are considered, with and without damping, and the equations of motions are solved numerically. The stability of the system is studied intensively, and oscillatory and chaotic regimes are identified. Bifurcation diagrams, Poincare sections, and the largest Lyapunov exponents are calculated.

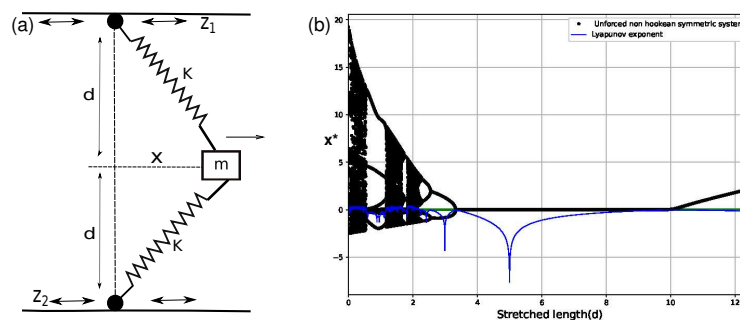


Figure 1: (a) The system, (b) Bifurcation diagram of position x^* plotted against stretched length d , also showing the corresponding largest Lyapunov exponent.

Results and discussion

We observe a rich range of dynamics in this deceptively simple system. Regular, oscillatory behaviour is observed, as also quasi-periodic and chaotic regimes. The system has a complex dynamical structure that varies dramatically depending upon the system parameters. The system also behaves distinctly depending upon whether the springs are compressed or elongated with reference to their relaxed lengths. An investigation of the parameter space considering the displacement of the suspension points as parameters reveals a rich portrait of interweaved chaotic and periodic regimes, which change drastically depending upon the value of the relaxed length and the introduction of even very small damping. The stability diagrams of the system with Hookean and non-Hookean springs show some unexpected structures and very distinct appearances. Further details are reported elsewhere [4].

References

- [1] Whineray, S. (1991) A cube-law air track oscillator. *Eur. J. Phys* **12**:90-95.
- [2] Arnold, Thomas W. and Case, William (1982) Nonlinear effects in a simple mechanical system. *American Journal of Physics* **50**:220-224.
- [3] Mishra, B. K. and Ashok, B. (2018) Coaxial Carbon Nanotubes: from Springs to Ratchet Wheels and Nanobearings. *Mater. Res. Express* **5**:075023.
- [4] Josey, J. and Ashok, B. (2022) Complex dynamics of a spring-mass mechanical system. (under submission).

Semi-Active Control Algorithm with Control-Structure Interaction for Magnetorheological Damper Used in Seismically-Excited Buildings

Chia-Ming Chang* and Chung-Chen Liu*

*Department of Civil Engineering, National Taiwan University, Taipei, Taiwan

Abstract. High control performance is achievable for active control if the interaction between the active control devices and structure is considered. For semi-active control, the dynamics of these dampers (e.g., magnetorheological dampers, MR dampers) should be included in the control design. This study aims to develop and experimentally verify a semi-active control algorithm that accounts for the MR damper-structure interaction in the designed controller. Moreover, this control algorithm can directly calculate the required input voltage (or current) to MR damper(s) at each time step and avoid the two-step approach that computes the required control force first and then converts the force into the input voltage. This study also conducts a series of numerical and hybrid simulations to verify the proposed method. As seen in the results, the proposed semi-active method in this study can reduce structural responses and produce more reactive input commands under seismic excitation.

Introduction

Semi-active control has been considered to be capable of achieving similar control performance to active control. However, most semi-active control strategies using magnetorheological (MR) dampers didn't account for the control-structure interaction, which has been proved to be more effective in active control applications [1]. Therefore, this study proposes a new semi-active control method that considers the interaction between MR dampers and structures. In this study, the time-variant control-structure system is realized by the first-order approximation of the state-space approach, while the MR damper is included in the state-space representation by a bilinear force-velocity relationship (i.e., bi-viscous model) per the input voltage [2]. Thus, the additional input to the structure-control system is the input voltage (or current) to the dampers. The instant optimal control command (i.e., input voltage) can be determined by the linear quadratic regulator (LQR) algorithm [3]; meanwhile, the state of the structure-control system can be estimated by the Kalman filter, as shown in Figure 1. An example of a single degree-of-freedom structure with an MR damper is provided. In addition, an experimental study is carried out to verify the proposed semi-active control method through hybrid simulation.

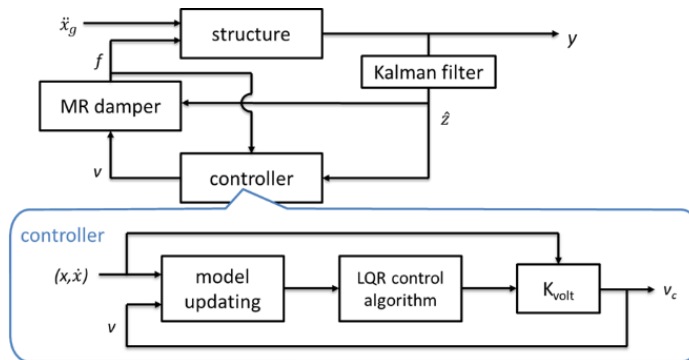


Figure 1: Semi-active control implementation for the proposed control method.

Results and discussion

This study successfully developed and implemented a semi-active control method that considered the control-structure interaction for MR dampers. In the numerical results, the proposed control method achieved similar performance to the clipped-optimal method; still, the input voltage history was more realistic and coherent with seismic excitation. As found in the experimental results, the proposed method was more adaptive than the clipped-optimal method against different levels of earthquakes. This adaptiveness needed less power to drive MR dampers and resulted in better performance for seismic protection of buildings. Moreover, higher energy dissipation was also found in the proposed method.

References

- [1] Chang C. M., Spencer Jr B. F. (2010) Active base isolation of buildings subjected to seismic excitations. *EARTHQ ENG STRUCT D*, **39**(13), 1493-1512.
- [2] Loh C. H., Chang, C. M. (2006) Vibration control assessment of ASCE benchmark model of cable-stayed bridge. *STRUCT CONTROL HLTH*, **13**(4), 825-848.
- [3] Yang J. N., Li Z., Liu S. C. (1992) Stable controllers for instantaneous optimal control. *J ENG MECH-ASCE*, **118**(8), 1612-1630.

Multiharmonic forced response analysis of a torsional vibration isolator using a nonlinear quasi-zero stiffness approach

Sebastian Willeke, Michael Steidl, Norbert Reinsperger, and Stephan Bohmeyer

Hasse & Wrede GmbH, Technology & Innovation department, Georg-Knorr-Straße 4, 12681 Berlin, Germany

Abstract. The forced response of a nonlinear coupling element featuring an angular displacement range with quasi-zero stiffness (QZS) is studied numerically by means of multiharmonic simulations. The paper focuses on the development of an iterative simulation procedure for the prediction of torsional vibration isolation. It is based on the multiharmonic balance method and an alternating frequency time domain approach in combination with a numerical continuation of the sought solution branch using a predictor-corrector scheme. The simulation procedure is validated against time domain solutions for a single degree of freedom oscillator. A parametric study regarding the excitation torque amplitude, the amount of damping, the degree of isolation as well as the static offset from the nominal operating point is conducted. Finally, the procedure is applied to the torsional vibration analysis of a generic internal combustion engine. The results indicate a potential reduction of torsional drive train vibrations by up to 93 % using the QZS isolation principle.

Introduction

Various engineering applications comprise drivetrains which consist of rotating shafts transmitting the driving torque from a powering unit. Torsional vibrations due to torque fluctuations may result in undesired noise emission or lead to severe damage of the drivetrain's components. Besides established countermeasures like damped vibration absorbers, a passive isolation concept using a nonlinear coupling element with quasi-zero stiffness (QZS) is proposed, see Fig. 1. By connecting a linear coupling element with a positive rotational stiffness ($k_{lin} = \text{const.} > 0$) in parallel to a nonlinear coupling element ($k_{nl} = k_{nl}(\varphi)$) with a rotational negative stiffness (RoNeSt), a QZS region is obtained at a static angular displacement φ_{stat} . By this means, the QZS coupling maintains its main purpose, i.e. the transmission of a static torque T_{stat} , and, in addition, provides an optimal vibration isolation due to a negligible dynamic coupling stiffness at its nominal operating point.

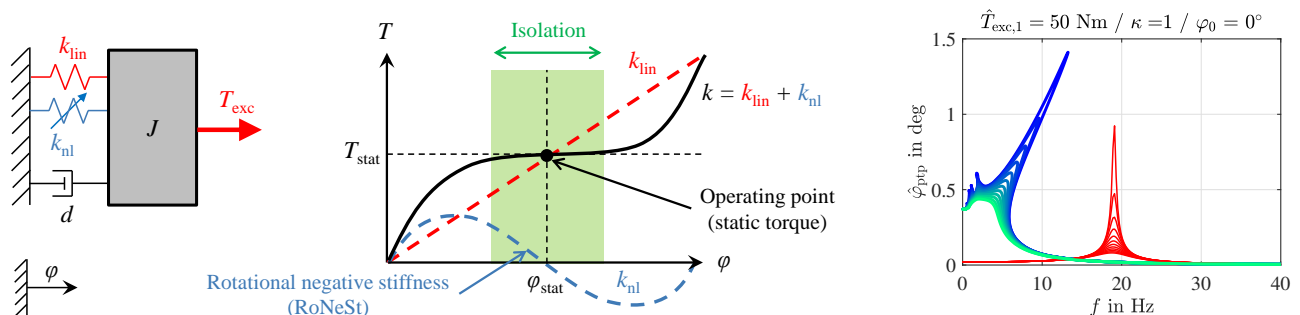


Figure 1: Torsional quasi-zero stiffness isolator (left) and nonlinear forced response for various damping levels (right)

Numerical forced response analyses of QZS isolators indicate a significant reduction of vibrations over a wide frequency range. They are, however, often limited to the fundamental vibration harmonic and neglect higher-order terms. Therefore, this paper presents a simulation procedure based on the multiharmonic balance method which employs an alternating frequency time domain approach in combination with a pseudo-arclength continuation method using a predictor-corrector scheme, see [1, 2].

Results and discussion

A comparison of the simulation outcome with time domain results shows that the procedure is able to accurately predict the isolator's multiharmonic response including unstable regions of the solution branch. Furthermore, it benefits from a reduced computational cost compared to the corresponding steady-state time domain simulations. A parametric study reveals a strong nonlinear response behavior for increased displacement amplitudes. Despite a variation of the excitation torque amplitude, the response reduction due to the torsional vibration isolation is maintained, but the response mitigation strongly depends on the degree of isolation. The latter is used to define a static stability limit. The consideration of a mismatch between the static operation point and the isolator's nominal conditions deteriorates its torsional vibration isolation capabilities. Finally, the exemplary application of the simulation procedure for the torsional vibration analysis of an internal combustion engine reveals a significant potential to reduce drivetrain vibrations by up to 93 % using torsional vibration isolation.

References

- [1] Cardona, A., Coune, T., Lerusse, A., Geradin, M. (1994): A multiharmonic method for non-linear vibration analysis. *Int. J. Numer. Meth. Eng.* **37**(9), 1593-1608.
- [2] Seydel, R. (2009): Practical Bifurcation and Stability Analysis. Springer.

Experimental Characterization and Numerical Modelling of Wire Rope Isolators

Paolo Neri*, Jeremiah Holzbauer**

*Department of Civil and Industrial Engineering, University of Pisa, Pisa, Italy

**Fermi National Accelerator Laboratory, Batavia, Illinois, USA

Abstract. The following paper presents a systematic procedure to achieve the experimental characterization of wire rope isolators. Additionally, an innovative development of the Bouc-Wen model is proposed to improve the fitting between experimental and numerical data. The proposed model is then validated through independent sinusoidal and random vibration tests to demonstrate the capabilities of the model in describing the physical non-linear phenomena, such as hysteresis cycles.

Introduction

Wire rope isolators (WRI) are non-linear devices which are commonly used to isolate vibration both during transportation and operation of machineries [1]. Their hysteretic behaviour produces a relevant damping factor, which guarantees a good isolation performance without the need of further dampers. Nevertheless, the conventional linear spring-damper model is not able to describe the actual component behaviour, so that it cannot be used at design stage. Additionally, mechanical properties provided by the manufacturers are generally partial, ambiguous, not rigorous and limited to equivalent stiffness and damping coefficients. These parameters are generally good to predict the quasi-static behaviour of the spring, such as the deflection under the applied weight. Nevertheless, they are not suitable to predict the vibrating behaviour, to describe the hysteresis cycles and to predict the actual filtering capabilities. Thus, more complex models are needed [2]. In this paper, a systematic procedure to experimentally characterize the component behaviour is proposed. The so-called Bouc-Wen non-linear model [3] was considered as reference for this hysteresis problem, and further developed to improve the matching between numerical and experimental results.

Results and discussion

The proposed enhanced Bouc-Wen model is based on nine constant parameters, which must be determined by fitting experimental data of the studied WRI. To this extent, experimental testing was performed along the three main directions of the component, namely principal, longitudinal and transversal. The force-displacement curve of the component, under different loading conditions, was measured by using sensorized hydraulic pistons (i.e. tensile testing machine and customizable hydraulic test-bench). As an example, Figure 1 shows the main results after model fitting, with reference to the principal direction. The blue curves are referred to experimental data, while the green curves are referred to the numerical predicted data. Figure 1(a) shows the results obtained during the static test, which was used to fit the model parameters. The curves prove a really good match in the whole tested region and, thus, the potentiality of the proposed model in representing the physical phenomenon. Figure 1(b) and (c) show the results of independent validation tests, whose data were not used during the parameter optimization process. Figure 1(b) refers to purely sinusoidal loading at 10 Hz (under compression preload) while Figure 1(c) refers to random load (in the range 1-30 Hz). As can be seen, the curves are properly overlapped. This demonstrates that the developed model and the proposed fitting procedure can predict the non-linear behaviour of the studied WRI, properly describing the hysteresis cycles.

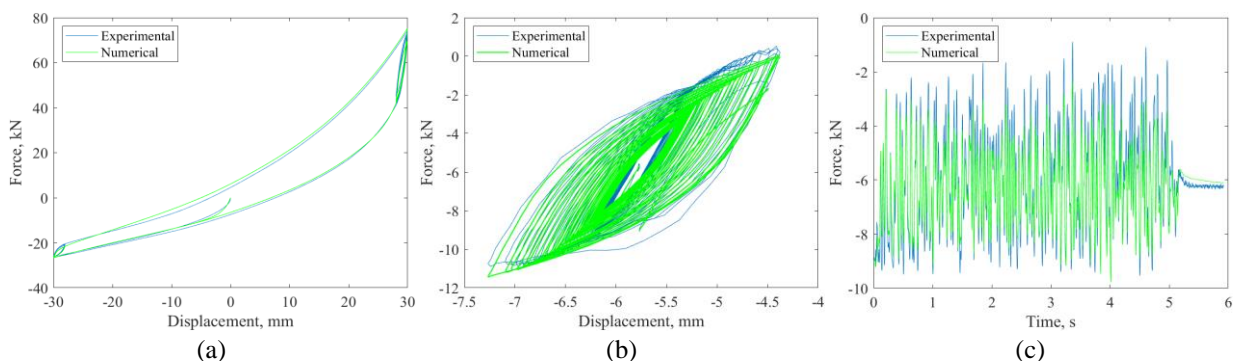


Figure 1: Comparison between experimental and numerical data: (a) static optimization test, (b) sinusoidal test and (c) random test.

References

- [1] Balaji, P.S. et Al. (2015), Wire rope isolators for vibration isolation of equipment and structures—A review, *IOP Conf Ser-Mat Sci*, **78**:1-10
- [2] Balaji P. et Al. (2016), An analytical study on the static vertical stiffness of wire rope isolators, *Mech. Sci. Technol*, **30**:287-295.
- [3] Wang H.X. et Al. (2015), Experimental investigations on the dynamic behaviour of o-type wire-cable vibration isolators. *Shock Vib*, **2015**:1-12.

Unveiling bifurcation mechanisms of quasiperiodic partial rub oscillations in a piecewise smooth rotor-stator system

Shan Fan*, Ling Hong* and Jun Jiang*

* State Key Laboratory for Strength and Vibration, Xi'an Jiaotong University, Xi'an, Shaanxi, P.R. China

Abstract. An approach combining the methods of multi-grid Point Mapping under Cell Reference (mPMUCR) and Stagger-and-step is first developed in order to efficiently determine both attractors and unstable saddle-type invariant sets in high-dimensional nonlinear dynamical systems. Then, the mechanism behind catastrophic bifurcations of the quasiperiodic partial rub oscillations in a piecewise smooth rotor-stator system are unveiled from the point view of global analysis.

Introduction

Rotary machinery is an important facility widely used in various fields, while Rotor-stator rubbing is a key issue affecting the mechanical efficiency and reliability of the rotor machinery. Many contact- and friction-related dynamical phenomena in rotor-stator rubbing systems are summarized recently in [1] and [2]. Quasiperiodic partial rub oscillations are an important type of non-smooth responses in the rotor-stator rubbing systems. Although, the bifurcation into the quasiperiodic partial rub oscillations may be determined in some cases, for instance, through Hopf bifurcation of the synchronous full annular rub motions for the emergence of the quasiperiodic partial rub oscillation in [3]. The bifurcations around emergence and disappearance of the quasiperiodic partial rub oscillations in the range of small contact friction but high rotating speeds are not well understood until now, due to the difficulty in capturing unstable invariant tori.

For global analysis of general nonlinear dynamical systems, numerical methods are the only workable tools. mPMUCR [4] is developed to take the advantages of methods in point scale and cell scale to efficiently capture attractors in point scale but unstable invariant sets as cell coverings in high-dimensional state space. In order to improve the resolution of the rough cell coverings of unstable invariant sets, Stagger-and-step method, which is devised to find chaotic saddles (chaotic transient) efficiently in dynamical systems [5], is also employed. The rough cell coverings of unstable invariant sets provide useful and targeted initial points for the Stagger-and-step method so that a fine depiction of multiple torus saddles can be also efficiently and accurately determined, which is shown in Figure 1 (a) and (b).

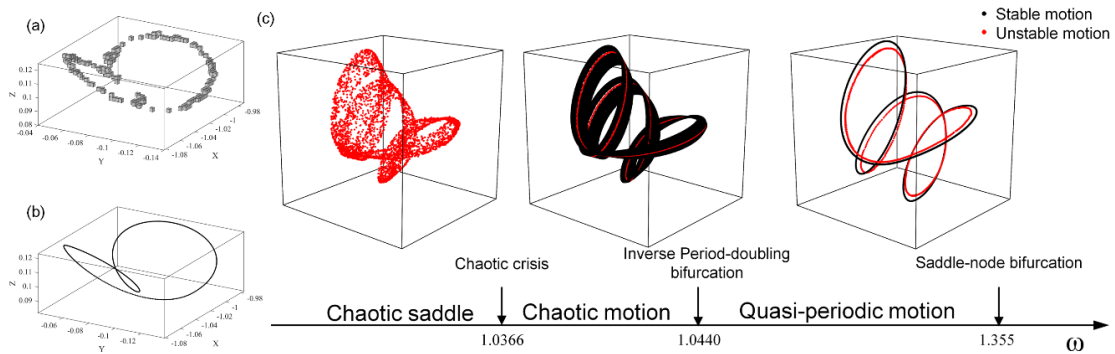


Figure 1: (a) Cell coverings of a torus saddle by mPMUCR in a three dimensional projection of Poincare section. (b) The torus saddle in point scale by Stagger-and-step method with the initial points from mPMUCR. (c) Sketch of the bifurcation process of aperiodic rubbing oscillations in a three dimensional projection of Poincare section.

Blue-sky catastrophic bifurcations in the quasiperiodic partial rub oscillations

Using the proposed computational methods, the bifurcations behind emergence and disappearance of the quasiperiodic partial rub oscillations in a piecewise smooth rotor-stator rubbing system are uncovered. It is found that the quasiperiodic partial rub oscillations emerges through an inverse doubling of torus from a chaotic attractor, which is produced from a chaotic saddle after chaotic crisis. The quasiperiodic partial rub oscillation disappears through a collision between the stable and the unstable tori in Figure 1(c).

References

- [1] Jacquet-Richardet, G, et al. (2013) Rotor to stator contacts in turbomachines. Review and application. *Mech. Syst. Signal Proc* **40**:401–420.
- [2] Prabith, K., et al. (2020) The numerical modeling of rotor–stator rubbing in rotating machinery: a comprehensive review. *Nonlinear Dyn.* **101**:1317–1363.
- [3] Jiang, J. et al. (2001) Stability analysis of sliding whirl in a nonlinear Jeffcott rotor with cross-coupling stiffness coefficients. *Nonlinear Dyn* **24**:269–283.
- [4] Jiang, J. et al. (1998) An iterative method of point mapping under cell reference for the global analysis: theory and a multiscale reference technique *Nonlinear Dyn* **15**, 103–114.
- [5] Sweet, D. (2001) Stagger-and-step method: Detecting and computing chaotic saddles in higher dimensions *Phys. Rev. Lett.* **86**, 2261

Predicting limit cycle of modified Rayleigh differential equation

V. Shrikanth*, Amar K. Gaonkar* and Pramod Kumar Verma*

*Department of Mechanical, Materials and Aerospace Engineering,
Indian Institute of Technology Dharwad, India, ORCID 0000-0001-9820-173X

Abstract. The Rayleigh differential equation is used to model the oscillations of a clarinet reed. Surprisingly, the same equation with a small modification can be used to model Coulomb friction. This modification can accurately model weakly nonlinear friction systems. The Rayleigh equation having cubic nonlinearity in velocity gives rise to an unstable limit cycle. In this work, an analytical expression is proposed to predict the said limit cycle, which holds good even for strong nonlinearity. The analytical expression is a third order polynomial in α , which is the damping constant.

Introduction

The general equation of motion of a dry friction oscillator in its nondimensionalized form is $z'' + \beta \text{sgn}(z') + z = \tilde{f}(\tau)$. By the method of harmonic balancing [1] and assuming the system to have a periodic motion [2], the signum function can be approximated to the third harmonic to express the equation of motion as

$$z'' + \alpha (z' - (2/3)(z')^3) + z = \Gamma \cos \Omega \tau \quad (1)$$

where α is damping constant, Γ is the forcing amplitude and Ω is the frequency, all nondimensional parameters. The ranges are $0 < \alpha < 1$, $0 < \Gamma < 1$ and $\Omega \in \mathbb{R}^+$. Eq.(1) is the modified Rayleigh equation.

Results and Discussion

The state space description of the Eq.(1) under autonomous condition is given by

$$\dot{u} = v \quad \text{and} \quad \dot{v} = -u - \alpha v (1 - (2/3)v^2) \quad (2)$$

where $u = z$ and $v = z'$. The derivatives in Eq.(2) are with respect to τ . There is only one equilibrium/fixed point at $(u^*, v^*) \equiv (0, 0)$ found at the intersection of the two nullclines $\dot{u} = 0$ and $\dot{v} = 0$. Existence of limit

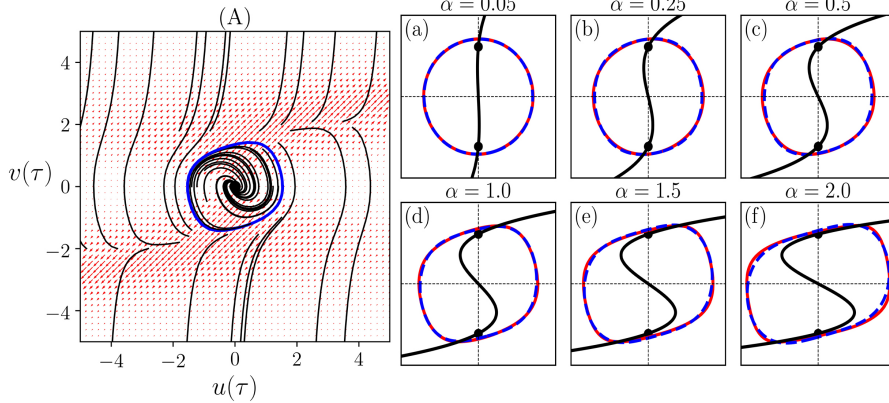


Figure 1: (A) Phase trajectories and flow field for the Eq.(1) without any external forcing. The autonomous system has an unstable limit cycle represented by the blue coloured line. (a)–(f) Comparison of numerical and analytical limit cycles and nullcline $\dot{v} = 0$ for varying values of α

cycle [3], approximate limit cycle [4] and Hopf bifurcation [5], from a state of no motion at all to a state of self-oscillations at a fixed amplitude. An analytical equation to express the limit cycle(s) can be derived to encompass the cases presented in Fig. 1(a)–(f). The equation should reduce to a circle when $\alpha \rightarrow 0$ as shown in Fig. 1(a), while the same equation should be able to represent the limit cycle shown in Fig. 1(f). The equation for the limit cycle is as follows:

$$u^2 (\alpha u^2 + 1) + \gamma v^2 - \delta uv = \chi \quad (3)$$

where $\gamma \equiv \gamma(\alpha)$, $\delta \equiv \delta(\alpha)$ and $\chi \equiv \chi(\alpha)$. The ordinates of the limit cycle(s) is always greater than \tilde{v} and approaches \tilde{v} when $\alpha \gg 1$. In order to accommodate the rotation of the limit cycle which is evident in Fig. 1(d)–(f), the coordinates u and v can be replaced by $\bar{u} = u \cos \varphi + v \sin \varphi$ and $\bar{v} = v \cos \varphi - u \sin \varphi$ with $\varphi \equiv \varphi(\alpha)$. The variation of the parameters in Eq.(3) as a function of the damping term α can be expressed as $\gamma = 1.871\alpha^3 - 1.014\alpha^2 + 2.573\alpha + 0.914$. Similarly, the variation of δ with α is $\delta = 0.462\alpha^3 - 0.469\alpha^2 + 0.966\alpha - 0.052$. The variation of φ against α is $\varphi = -0.0065\alpha^2 + 0.0374\alpha + 0.1301$. Dependence of χ on α is $\chi = 2.685\alpha^3 - 0.958\alpha^2 + 3.891\alpha + 1.946$.

References

- [1] Dominic Jordan and Peter Smith. *Nonlinear ordinary differential equations*. OUP Oxford, 2007.
- [2] Ali H Nayfeh and Dean T Mook. *Nonlinear oscillations*. John Wiley & Sons, 2008.
- [3] Miguel A López and Raquel Martínez. A note on the generalized rayleigh equation: limit cycles and stability. *J Math Chem*, 51(4):1164–1169, 2013.
- [4] MR Akbari, DD Ganji, A Majidian, and AR Ahmadi. Solving nonlinear differential equations of vanderpol, rayleigh and duffing by AGM. *Front. Mech. Eng.*, 9(2):177–190, 2014.
- [5] Lior Ben Arosh, MC Cross, and Ron Lifshitz. Quantum limit cycles and the rayleigh and van der pol oscillators. *Phys. Rev. Res.*, 3(1):013130, 2021.

Features of precession of a flexible rotor with a different number of elastic supports located with a clearance in the plane of rotation

Anatoly Azarov^{*}, Alexander Gouskov^{*} and Grigory Panovko^{**}

^{*}*Bauman Moscow State University, Moscow, Russia*

^{**}*Mechanical Engineering Research Institute, Moscow, Russia*

Abstract. A design model of a rotary system in the form of a cantilevered flexible shaft with a massive disk at the free end is considered. In the plane of rotation of the disk, point elastically damped supports are discretely located with a clearance, stabilizing the vibrations of the rotor in the supercritical zone. The influence of a different number of supports on the evolution of the rotor precession in the supercritical zone after the Poincare-Andronov-Hopf bifurcation is investigated. The effect of the clearance and friction at the contact of the disk with the supports on the precessional movement of the rotor is analyzed.

Introduction

The supercritical behavior of a rotor system in the form of a cantilevered fixed flexible shaft with an unbalanced disk at the free end is investigated (Figure 1). To stabilize the amplitudes of transverse vibrations of the rotor in the plane of rotation of the disk, point viscoelastic supports are discretely installed with a radial clearance [1]. Three options for the placement of supports are considered: one support, two supports – on opposite sides of the disk, three supports at an angle of $2\pi/3$ relative to each other. The distributed mass of the rotor shaft and the internal friction of the material are taken into account according to the Voigt elastic-viscous body model. With normal contact of the rotor with the support, normal (elastic) forces in the support and tangential forces (dry friction) arise.

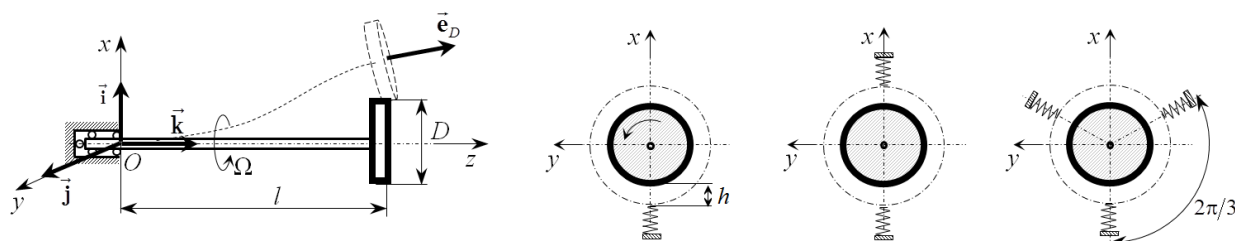


Figure 1: Design scheme.

Differential equations describing transverse radial and angular oscillations of the rotor during its rotation are obtained, taking into account gyroscopic moments from the disk and circulation forces caused by internal friction. For subsequent discretization and construction of a finite element model of the rotor, the solution is obtained using the Green function for the Bernoulli-Euler rod. A generalizing definition of the rotor precession index is introduced, which makes it possible to calculate the frequency and direction of precession from information about transverse vibrations of the rotor in two mutually perpendicular directions. For all the cases under consideration, the evolution of precession and the spectral composition of precession motion oscillations after the Poincare-Andronov-Hopf bifurcation are analyzed [2, 3].

Results and discussion

The main attention in the work is paid to determining the type of precession of the rotor without calculating its full spectrum, which makes it possible to directly determine precession in the case of nonlinear interaction with additional supports. For the case of a single support, it is established that, depending on the eccentricity of the disk and the supercritical velocity, both periodic modes and non-periodic rotor oscillations can occur. In the case of two supports, a backward whirling of the rotor occurs. In the case of three supports, a stable backward whirling (close to synchronous) is maintained at a certain level of rotor imbalance. The greatest amplitude of oscillations of the angular velocity of the precession of the rotor occurs at the whirling frequency multiplied by the number of viscoelastic supports installed with an initial clearance.

Acknowledgement. The work was carried out with the financial support of the RSF grant (<https://rscf.ru/en/project/21-19-00183/>).

References

- [1] Lahriri S., Weber H., Santos I., Hartmann H. (2012) Rotor–stator contact dynamics using a non-ideal drive. *J. Sound Vibr* **331**(20):4518–4536
- [2] Ding Q., Cooper J., Leung A.Y. (2002) Hopf bifurcation analysis of a rotor/seal system. *J. Sound Vibr* **252**(5): 817-833.
- [3] Karpenko E.V., Pavlovskaja E.E., Wiercigroch M. (2003) Bifurcation analysis of a preloaded Jeffcott rotor. *Chaos Solit Fract* **15** (2):407-416

Nonlinear vibrations of a composite circular plate with a concentrated mass: effects of equilibrium configurations

Ying Meng*, Xiao-Ye Mao*, Hu Ding* and Li-Qun Chen*

*Shanghai Institute of Applied Mathematics and Mechanics, School of Mechanics and Engineering Science, Shanghai University, Shanghai, 200444, China

Abstract. Nonlinear vibrations of a composite circular plate with a concentrated mass are investigated with the focus on the effects of curved equilibrium configurations caused by weights. A mathematical model is derived from the generalized Hamiltonian principle considering the weights. The Galerkin method is applied to determine equilibrium configurations and the results are validated by the finite element method. The fundamental frequency and the steady-state responses are respectively calculated in free vibrations and harmonically forced vibrations. The results demonstrate that the weights have more significant effects on the curved equilibrium configurations for the larger substrate radius, the larger concentrated mass, and the smaller upper and lower radii. The account for the weights increases the fundamental natural frequency, and the relative difference increases with the increasing weights. The account for the weights increases the resonant amplitude, and the absolute difference increases with the increasing weights.

Introduction

Circular plates with concentrated masses have been used in different industries. They are often exposed to severe dynamic loading resulting to large vibrations. Thus, it is significant to investigate nonlinear vibrations of circular plates with concentrated masses. Currently, nonlinear vibrations of circular plates with masses have been studied by Huang [1], Li et al. [2], Yuan et al. [3], and other scientists. When a circular plate with concentrated masses vibrates nonlinearly, the weight affects the equilibrium configuration, and the changing configuration in turn affects vibration frequencies and shapes. Several investigations have demonstrated the crucial role of weights. Chen et al. [4] investigated the effects of the weight of the nonlinear energy sink (NES) on structural vibrations. They found that the weights should be accounted for when the primary structure is excited by small excitations or coupled with large NES masses. However, the effects of the weights on nonlinear vibrations of circular plates with masses are rare in the literature. This is the motivation here.

Results and discussion

The generalized Hamiltonian principle is applied to obtain the governing equation with boundary conditions. Equilibrium configurations and a discretization model for vibrations around the configurations are derived from the Galerkin method. The model can be used to determine the fundamental frequency and the steady-state responses. The investigation yields the following findings: (1) The account of the weights introduces additional linear and quadratic terms to the governing equation and weakens the hardened nonlinearity. (2) The static equilibrium configuration increases with the increasing concentrated mass, substrate radius and the decreasing upper and lower radii. (3) In free vibrations, the curved equilibrium configuration caused by the weights increases the fundamental natural frequency, and the relative difference increases with the increasing curved equilibrium configuration. (4) In harmonically forced vibrations, the curved equilibrium configuration increases the resonant amplitude, and the absolute difference increases with the increase of the curved equilibrium configuration.

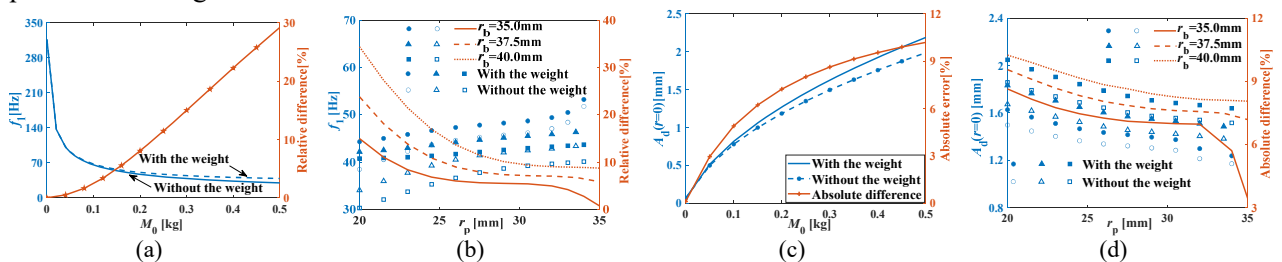


Figure 1: Natural frequencies and resonant amplitudes for varying parameters: (a-b) variation of natural frequencies and the relative difference with the concentrated mass, the substrate radius, and the upper and lower radii; (c-d) variation of resonant amplitudes and the absolute difference with the concentrated mass, the substrate radius, and the upper and lower radii.

References

- [1] Huang S. (1998) Non-linear vibration of a hinged orthotropic circular plate with a concentric rigid mass. *J. Sound Vib* **214**(5): 873-883.
- [2] Li S. R., Zhou Y. H., Song X. (2002) Non-linear vibration and thermal buckling of an orthotropic annular plate with a centric rigid mass. *J. Sound Vib* **251**(1): 141-152.
- [3] Yuan T. C., Yang J., Chen L. Q. (2017) Nonlinear characteristic of a circular composite plate energy harvester: experiments and simulations. *Nonlinear Dyn* **90**(4): 2495-2506.
- [4] Chen L. Q., Li X., Lu, Z. Q., et al. (2019) Dynamic effects of weights on vibration reduction by a nonlinear energy sink moving vertically. *J. Sound Vib* **451**: 99-119

Modelling Thermoelastic Damping in Nonlinear Plates with Internal Resonance

Darshan Soni*, Manoj Pandey** and Anil K. Bajaj*

*School of Mechanical Engineering, Purdue University, IN, USA

**Department of Mechanical Engineering, Indian Institute of Technology Madras, TN, India

Abstract. We use a nonlinear, reduced-order, coupled thermo-elastic model, derived from von Kármán plate equations to study the resonant response of simply supported thin rectangular plates under free and forced vibrations and understand the experimentally observed behaviour, specifically the change in temperature. The model is studied using Galerkin approximation, harmonic balance and numerical continuation techniques. Multimode response for plates is considered for non-resonant excitation as well as near 1:1 resonance between the second and third eigenmodes of the system, with harmonic forcing close to a natural frequency. Internal resonance and associated coupled-mode dynamics is observed, with noticeable decrease in modal amplitudes and some increase in plate natural frequencies due to thermo-elastic coupling.

Introduction

Experimental study of nonlinear vibration of 3D printed rectangular plates [1], fabricated using nonlinear materials, show significant increase in temperature due to continuous motion, suggesting strong coupling between mechanical motion and thermal response of the system. A thermo-mechanical constitutive model for thin plates, based on the Berger's approximation of von Kármán plate theory and energy equations [2], is used to study the vibration response of these under free and forced vibration conditions. A reduced set of coupled nonlinear ODE's for the evolution of transverse displacement $w(x, y, t)$ as well as temperature variables, the in plane stress ($N^T(x, y, t)$) and bending moment ($M^T(x, y, t)$), is obtained by the Galerkin projection of coupled thermal-structural PDEs onto the free vibration modes of the S-S-S plate [3]. One-mode and two-mode spatial approximations are considered. For example, for the one-mode approximation, letting $w = w_1(t) \sin\left(\frac{\pi x}{a}\right) \sin\left(\frac{\pi y}{b}\right)$, $M^T = m_1(t) \sin\left(\frac{\pi x}{a}\right) \sin\left(\frac{\pi y}{b}\right)$ and $N^T = n_1(t) \sin\left(\frac{\pi x}{a}\right) \sin\left(\frac{\pi y}{b}\right)$ gives the following set of coupled nonlinear ODEs:

$$\ddot{w}_1(t) + 0.05\dot{w}_1(t) + w_1(t) + 0.334w_1^3(t) - 0.067m_1(t) - 0.0014 w_1(t)n_1(t) = F\cos(\Omega t) \quad (1)$$

$$\ddot{n}_1(t) + 0.002\dot{n}_1(t) + 7 \times 10^{-4}T_\infty + 0.0994w_1(t)\dot{w}_1(t) = 0 \quad (2)$$

$$\ddot{m}_1(t) + 0.337\dot{m}_1(t) + 1.18w_1(t) = 0 \quad (3)$$

Nonlinear coupling is seen in the above, only for the w_1 and n_1 equations. These equations are studied using direct numerical integration, through the harmonic balance method and by using pseudo arc-length based continuation schemes. They are also compared to finite element based results.

Results and Discussion

Single-mode approximation of the system shows significant damping being introduced by the thermo-elastic coupling, which affects both the amplitude and frequency of the system. Multimode response is studied for the case of a plate with 1:1 relation between the second and third eigenmode frequencies, achieved through a precisely chosen aspect ratio of 1.633 for the plate [3]. Internal resonance is observed, resulting in activation of both modes while the external force is orthogonal to one of the modes. The coupling of thermal response again results in decrease in the amplitude, while increasing the resonant frequency. There is a corresponding increase in the temperature shown in Figure 1 at the midpoint of the plate. Thermal coupling also leads to an increase in the frequency range corresponding to the coupled mode.

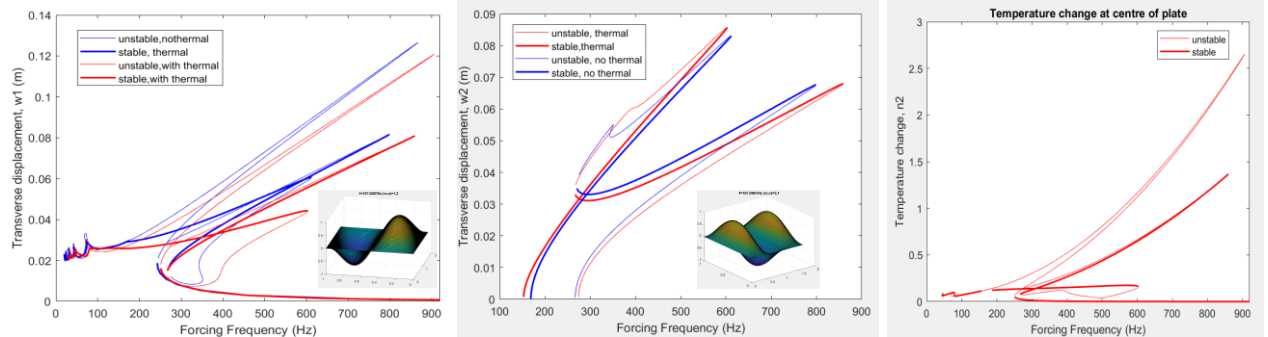


Figure 1. Multiple solution branches and bifurcations for: a) Mode 2 and b) Mode 3 transverse response for the two-mode model with 1:1 resonance; c) Temperature variation at the plate midpoint. Thick/thin lines corresponds to stable/unstable solutions respectively.

References

- [1] Bilal, N., Tripathi, A., & Bajaj, A.K. (2020). On experiments in harmonically excited cantilever plates with 1:2 internal resonance. *Nonlinear Dyn* 100, 15–32.
- [2] Saetta, E., & Rega, G. (2014). Unified 2D continuous and reduced order modeling of thermomechanically coupled laminated plate for nonlinear vibrations. *Meccanica* 49(8), 1723–1749.
- [3] Chang, S. I., Bajaj, A.K., & Krousgrill, C.M. (1993). Non-Linear vibrations and chaos in harmonically excited rectangular plates with one-to-one internal resonance. *Nonlinear Dyn* 4, 433–460.

An extensible double pendulum and multiple parametric resonances

Shihabul Haque*, Nilanjan Sasmal* and Jayanta K. Bhattacharjee*

*School of Physical Sciences, Indian Association for the Cultivation of Science, Jadavpur, Kolkata 700032, INDIA

Abstract. We consider a double pendulum where the lower pendulum is an elastic one. This is a system with three natural frequencies and we find that the responses of a hard spring and a soft spring are very different with the resonance at the beat frequency being of special interest.

Introduction

Our system is a double pendulum with masses m_1 and m_2 having lengths l_1 and l_2 respectively. The lower pendulum (m_2 , l_2) is elastic and has a spring constant k . The Lagrangian of the system can be written in terms of the angular displacements, θ_1 and θ_2 , made with the vertical and the extension of the lower mass m_2 with respect to its equilibrium position, r . We focus on the quadratic linearity (first deviation from normal mode dynamics). The dynamics is then governed by,

$$\begin{aligned} M l_1^2 \ddot{\theta}_1 + M g l_1 \theta_1 + m_2 l_1 (l_2 + r) \ddot{\theta}_2 + 2 m_2 l_1 \dot{r} \dot{\theta}_2 + k l_1 (\theta_1 - \theta_2) r &= 0 \\ (l_2 + r) \ddot{\theta}_2 + l_1 \ddot{\theta}_1 + 2 \dot{r} \dot{\theta}_2 + g \theta_2 &= 0 \\ \ddot{r} + \omega_0^2 r &= l_1 (\theta_1 - \theta_2) \dot{\theta}_1 + l_1 \dot{\theta}_1^2 + l_2 \dot{\theta}_2^2 + \frac{g}{2} \theta_2^2 \end{aligned}$$

Here, $M = m_1 + m_2$. The normal mode frequencies are Ω_1 , Ω_2 for the two angular modes and ω_0 for the extension mode. We can read off the existence of four parametric resonance conditions as,

$$\omega_0 = 2\Omega_1, 2\Omega_2, \Omega_1 \pm \Omega_2$$

In each case one can construct a six dimensional dynamical system following the standard procedure [1]. We show here the results for the resonance in the beat mode, $\omega_0 = \Omega_1 - \Omega_2$, and $\omega_0 = 2\Omega_2$.

Results and Discussion

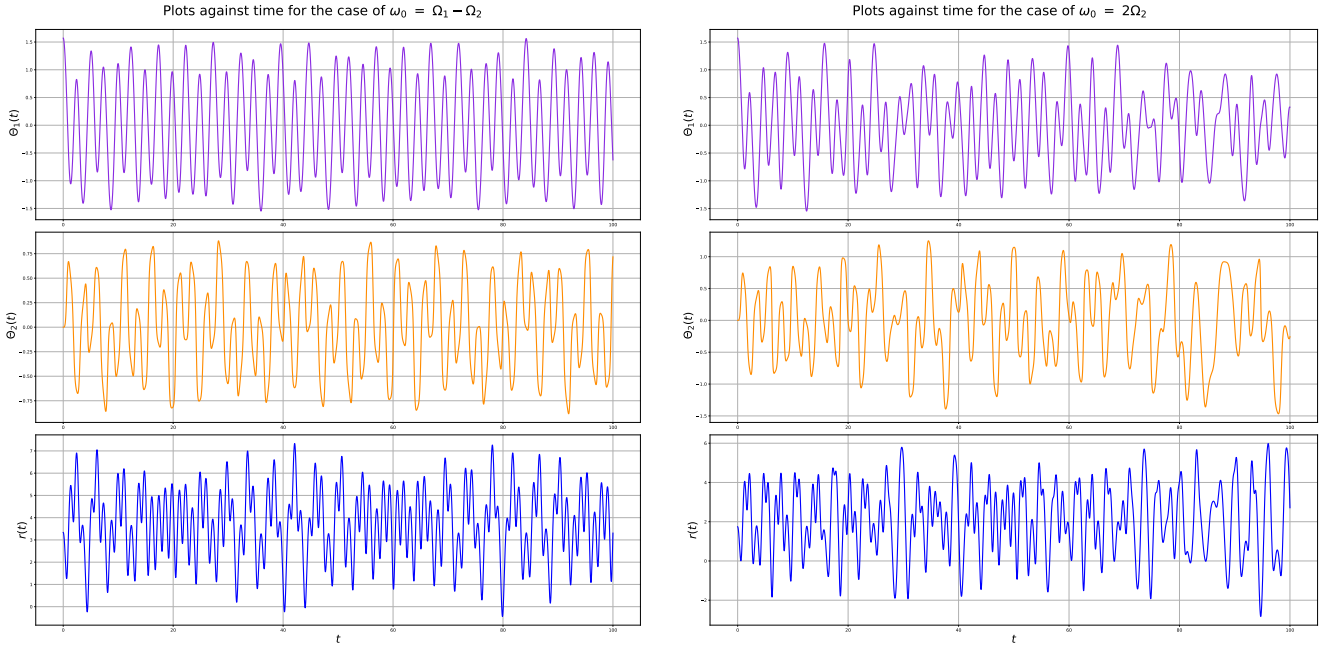


Fig: Time variation of the 3 modes for 2 different resonance conditions. The values taken for the plots are: $m_1 = 5.6$ kg; $m_2 = 5$ kg; $l_1 = 3$ m; $l_2 = 3.4$ m. The spring constant is about 14.69 N/m for the beat frequency and 28.1 N/m for the other.

We find 4 distinct parametric resonances at $\omega_0 = 2\Omega_1, 2\Omega_2, \Omega_1 \pm \Omega_2$. Of these, 2 are plotted above. The beat frequency resonance shows a marked periodicity in the variation of the first 2 modes which is particularly striking and suggests a distinct response compared to other values of the frequencies. Further work is being done to determine an approximate analytical description of the amplitude variation of the 3 modes under resonance.

References

- [1] Lai H. M. (1984) On the recurrence phenomenon of a resonant spring pendulum. *Am. J. Phys.* **52**:219-223.
- [2] Jia, Y., Du, S., & Seshia, A. A. (2016) Twenty-Eight Orders of Parametric Resonance in a Microelectromechanical Device for Multi-band Vibration Energy Harvesting. *Sci. Rep* **6** 30167. <https://doi.org/10.1038/srep30167>

Effect of magnet position in electro-magnetic transducer of middle ear implant

Rafal Rusinek*, Krzysztof Kecik*

*Lublin University of Technology, Nadbystrzycka 36, Lublin, 20-618, Poland

Abstract. The paper is devoted to modelling and numerical analysis of the middle ear with an implantable middle ear hearing device. The main focus is put on electromechanical coupling between the biomechanical subsystem of the middle ear and electrical subsystem of the implant. The electromechanical coupling describes the interaction between electrical and mechanical systems, and it is defined as nonlinear dependence of magnet position relative to the coil's transducer centre. This is a novel approach, that generates new resonances, instabilities, subharmonic and also chaotic stapes vibrations depending on a voltage excitation. Finally, the stapes motion from numerical simulations stimulated by the floating mass transducer is compared to experimental results performed on the human temporal bones. The findings of this research can be used practically to develop a better construction of a floating mass transducer.

Introduction

Sound transfer through the human ear is disturbed very often because of clinically significant hearing deficits [1]. If a hearing loss is mild or moderate, it can be improved by conventional hearing aids (non-invasive, not requiring surgery) that consists of a microphone to pick up sound, amplifier circuitry that makes the sound louder and a miniature loudspeaker to deliver the amplified sound into the ear canal. However, patients with moderately severe or severe hearing loss have to be equipped with more technologically advanced devices, such as implantable middle ear hearing devices (IMEHDs) that is analysed here.

Results and discussion

The model of the IME presented in [2] is now modified and improved in order to fulfil the purpose of this study. First of all, it is assumed according to the physical system construction, that the coil is fixed to the can of the FMT (the improvement of the previous model). Moreover, the EC is presented as nonlinear dependence of the magnet position related to the coil (the modification of the previous model). The new model of IME with the schematic view of the middle ear is shown in Fig.1. Magnet shift (position relative to the coil) is important for

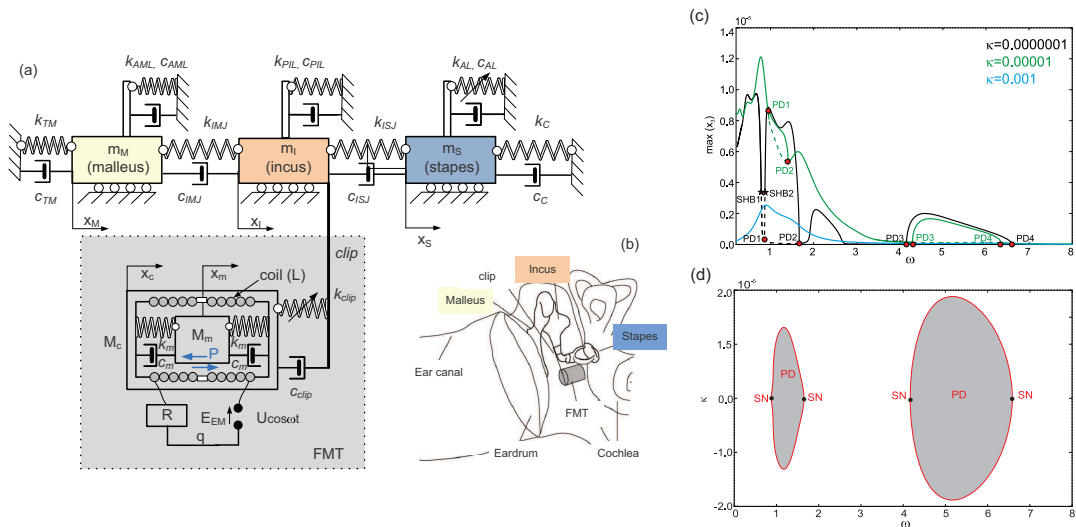


Figure 1: Electromechanical model of the implanted middle ear (a) with resonance curves obtained for different magnet shift κ (b) and regions of subharmonic motion (c).

stapes vibration as presented in Fig. 1b and c because it change the resonance curve, that is amplitudes and resonance peaks (Fig. 1b). Moreover, improper magnet position can cause subharmonic stapes vibrations. That is harmful from medical (practical) point of view.

References

- [1] Haynes D. S., Young J. A., Wanna G. B., Glasscock M. E. (2009) Middle ear implantable hearing devices: An overview, Trends in Amplification.
- [2] Rusinek R., Kecik K. (2021) Effect of linear electromechanical coupling in nonlinear implanted human middle ear. *Mechanical Systems and Signal Processing* **151**:107391.

Analysis of forced vibrations of the nonlinear elastic plate on a viscoelastic foundation subjected to hard excitation from harmonic load

Marina V. Shitikova^{1,2} and Anastasiya I. Krusser¹

¹Research Centre on Dynamics of Solids and Structures, Voronezh State Technical University, Voronezh, Russia

²National Research Moscow State University of Civil Engineering, Moscow, Russia

Abstract. In the present paper, the dynamic response of a nonlinear Kirchhoff-Love plate resting on a viscoelastic foundation in a viscoelastic medium, damping features of which are described by the Kelvin-Voigt fractional derivative model is studied for the case of forced vibrations excited by harmonic load. The damping properties of the viscoelastic Fuss-Winkler-type foundation are described by the fractional derivative standard linear solid model. Supposing that only two natural modes of vibrations strongly coupled by the internal resonance 1:1 are excited, the generalized method of multiple time scales in conjunction with the expansion of the fractional derivative in terms of a small parameter has been utilized for solving nonlinear governing equations of motion. Assuming the amplitude of external load to be hard, resolving equations are obtained for determining nonlinear amplitudes and phases for various types of external resonances that may occur in systems with cubic nonlinearities.

Introduction

The problem of vibrations of a plate on a viscoelastic foundation has many engineering applications, and therefore is of great interest to many researchers. In order to describe the viscoelastic behavior of Fuss-Winkler-type or Pasternak-type foundations, different models of viscoelasticity have been suggested during the last few decades [1,2]. Apart from the well-known models for viscoelastic materials, such as Kelvin-Voigt, Maxwell or standard linear solid models, one may refer to their fractional derivative generalizations [3], which are becoming increasingly widespread nowadays.

Previous analysis of the free damped vibrations of an nonlinear elastic plate on a viscoelastic foundation has shown [4], that the one-to-one internal resonance could occur in such a mechanical system when the natural frequencies of two coupled modes are close to each other. This problem was generalized for the case of force-driven vibrations of the plate subjected to moving harmonic load in conditions of combination of internal and external resonances [5].

Professor Naife in his monographs [6,7] showed that when analyzing the response to an external harmonic load, four cases should be distinguished depending on whether the excitation is “soft” or “hard”, resonant or nonresonant [6,7]. It was also demonstrated that in addition to primary resonance in systems with cubic nonlinearities secondary resonances could occur under the hard excitation, namely, superharmonic resonance and subharmonic resonance [6].

Results and Discussion

The main purpose of the present research is to study the effect of hard excitation from harmonic load on the forced nonlinear vibrations of a von Karman elastic plate resting on a viscoelastic Fuss-Winkler-type foundation, the damping features of which are described by the fractional derivative standard linear solid model. The generalized method of multiple time scales in conjunction with the expansion of the fractional derivative in terms of a small parameter has been utilized for solving nonlinear equations of motion for the case when amplitude of applied force is large value. The governing equations are obtained and solved numerically for determining of nonlinear amplitudes and phases for the cases when internal resonance one-to-one is accompanied by the superharmonic or subharmonic resonances excited in nonlinear plate. The effect of nonresonant hard excitation on the amplitude and frequency of undamped and damped vibrations of the plate is shown, which depends on the amplitude of applied force. The resulting sets of equations for all types of excited resonances allows one to control also the damping properties of the surrounding medium and the foundation by changing the fractional parameters from zero to unit.

References

- [1] Younesian D. (2019) Elastic and viscoelastic foundations: a review on linear and nonlinear vibration modeling and applications. *Nonlinear Dyn* **97**: 853–895.
- [2] Rossikhin Yu.A., Shitikova M.V. (2010) Application of fractional calculus for dynamic problems of solid mechanics: Novel trends and recent results. *Appl. Mech. Rev* **63**:010801.
- [3] Shitikova, M.V., Krusser, A.I. (2022) Models of viscoelastic materials: a review on historical development and formulation. Springer, Cham.
- [4] Shitikova, M.V., Krusser, A.I. (2020) Nonlinear vibrations of an elastic plate on a viscoelastic foundation modeled by the fractional derivative standard linear solid model. *EASD Procedia EUROdyn*: 355-368.
- [5] Shitikova, M.V., Krusser, A.I. (2021): Force driven vibrations of nonlinear plates on a viscoelastic Winkler foundation under the harmonic moving load. *International Journal for Computational Civil and Structural Engineering* **17**(4): 161–180.
- [6] Nayfeh, A.H., Mook, D.T. (1995) *Nonlinear Oscillations*. Wiley, New York.
- [7] Nayfeh, A.H. (1973) *Perturbation Methods*. Wiley, New York.

Human balance during quiet stance with physiological and exoskeleton time delays

Shahin Sharafi* and Thomas K. Uchida*

*Department of Mechanical Engineering, University of Ottawa, Ottawa, Ontario, Canada

Abstract. Human balance is studied using an inverted pendulum model, considering the effect of time delays in the muscle reflex controller and the controller of an exoskeleton. The model includes two motors at the ankle joint whose torques represent the moments generated by all plantarflexor and dorsiflexor muscles. These “muscle-like” motors obey a proportional–derivative (PD) reflex control law where the states are subject to physiological feedback delays. The exoskeleton applies torques to the ankle joint, also obeying a PD control law but with a different time delay. The stability of this system is analyzed using Galerkin projection to convert the governing neutral delay differential equation (NDDE) into a system of ordinary differential equations (ODEs); the eigenvalues of the ODE system are then computed. Stability charts demonstrate the ability of the exoskeleton to stabilize an inherently unstable biological system.

Introduction

Falling is the leading cause of injury in elderly individuals. A deeper understanding of human balance will enable the development of exoskeletons that can predict and prevent falls. Human balance has been studied using experimental techniques, but experiments are limited by the time and cost of collecting data. Many simulation-based studies of human balance during quiet stance employ a single inverted pendulum model, which has an upright equilibrium point that is inherently unstable. Ahsan et al. [1] studied inverted pendulum models of unassisted human balance, and found that proportional–derivative–acceleration (PDA) feedback generally results in larger stability margins than PD control. In this work, we investigate the stability of human balance during quiet stance when assisted by an exoskeleton at the ankle, where a PD control law is assumed for both the biological reflex controller (gains K_{pb} and K_{db}) and the exoskeleton controller (gains K_{pe} and K_{de}), and they are assumed to have different time delays (200 ms and 100 ms, respectively). Active muscle torque is assumed to depend on the angle and angular velocity of the ankle joint [2]. To study the stability of the governing NDDE, we convert it into a system of partial differential equations, then use the Galerkin approximation method to obtain a system of first-order ODEs whose behaviour approximates that of the original NDDE system. In the Galerkin method, we impose the boundary conditions using the Lagrange multiplier approach [3].

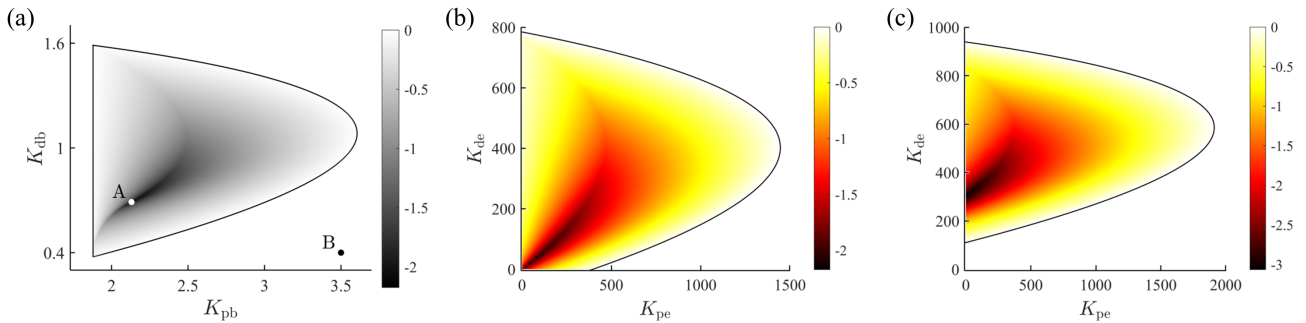


Figure 1: Stability charts of the human stance model (a) without an exoskeleton, (b) with an exoskeleton at point A ($K_{pb} = 2.13$, $K_{db} = 0.69$), and (c) with an exoskeleton at point B ($K_{pb} = 3.5$, $K_{db} = 0.4$). Colour bars indicate the location of the rightmost eigenvalue; black solid lines are the analytical stability boundaries.

Results and Discussion

The stability chart of the unassisted system is shown in Fig. 1(a), obtained using the Galerkin method and validated against the stability boundary computed analytically [4]. Point A denotes the pair of biological controller gains resulting in the most stable system; point B is one example of an inherently unstable biological system. As shown in Fig. 1(b), the stability of the system at point A can be improved by the exoskeleton, though not substantially. Note that the system is inherently stable at point A (i.e., for $K_{pe} = K_{de} = 0$). As shown in Fig. 1(c), the inherently unstable system at point B can be stabilized with the assistance of the exoskeleton. This simulation framework can be used to study the stability of human balance with exoskeleton assistance, considering a range of gains and time delays of the muscle reflex controller and exoskeleton controller.

References

- [1] Ahsan Z., Uchida T.K., Subudhi A., Vyasarayani C.P. (2016) Stability of human balance with reflex delays using Galerkin approximations. *J Comput Nonlinear Dyn* **11**:041009.
- [2] Ashby B.M., Delp S.L. (2006) Optimal control simulations reveal mechanisms by which arm movement improves standing long jump performance. *J Biomech* **39**:1726–1734.
- [3] Vyasarayani C.P. (2013) Galerkin approximations for neutral delay differential equations. *J Comput Nonlinear Dyn* **8**:021014.
- [4] Insperger T., Milton J., Stépán G. (2013) Acceleration feedback improves balancing against reflex delay. *J R Soc Interface* **10**:20120763.

Space sunshade for global warming mitigation : dynamics and station keeping

B. Shayak* and B. Balachandran*

*Department of Mechanical Engineering, University of Maryland, College Park, Maryland, USA

Abstract. A steady rise in worldwide temperature has prompted investigations into different approaches to combat global warming. Geoengineering, or manipulation of Earth's climate from external to it, has been considered as a climate mitigation strategy since the 1980s [1,2]. Here, space-based solar shades are used to reduce the amount of sunlight received on Earth. Different solar shades are considered, and the associated dynamics and efficacy are examined.

Introduction

The most popular solar shading concept is a shade mounted at L1, the Lagrange point between the Earth and the Sun, at 1.5 million km from the Earth. L1 is a saddle point with motions along the Earth-Sun direction being unstable and along the normal direction being stable. The instability results in the need for station keeping manoeuvres, with actuations Δv averaging about 1-2 m/s per annum [3]. A second alternative is a shade in a geosynchronous orbit. Luni-solar perturbations adversely affect the position of derelict satellites in this orbit [4], amounting to a station keeping requirement of about $\Delta v = 45$ m/s per annum. Nevertheless, the orbit proximity may offset the increased station keeping requirements and simplify the travel logistics.

Results and Discussion

For a solar shade of large surface area and a low mass, the solar radiation pressure is significant. This force has the same $1/r^2$ dependence as Sun's gravitational pull, but this is directed away from the Sun and normal to the shade. In a recent work [5], it has been proposed to use radiation pressure for long-distance navigation of a sunshade. Here, the potentially stabilizing effects of a variable-area shade will be examined. The equation of motion of the shade in the rotating Earth-Sun reference frame is

$$m\ddot{\mathbf{r}} = -\frac{GM_e m}{|\mathbf{r} - \mathbf{r}_e|^3}(\mathbf{r} - \mathbf{r}_e) - \frac{GM_s m}{|\mathbf{r} - \mathbf{r}_s|^3}(\mathbf{r} - \mathbf{r}_s) + \frac{kA}{|\mathbf{r} - \mathbf{r}_s|^2} \hat{\mathbf{x}} + m\omega^2 \mathbf{r} - 2m\boldsymbol{\omega} \times \dot{\mathbf{r}} \quad (1)$$

where \mathbf{r} denotes the position of the shade from the origin at the Sun-Earth center of mass, x is the direction from Sun to Earth, M_e , \mathbf{r}_e , M_s and \mathbf{r}_s are the masses and position vectors of the Earth and Sun from this origin, $\boldsymbol{\omega}$ is the rotation rate of the non-inertial frame, and G the gravitational constant. The extra term is the third one, which arises from the radiation pressure; it is proportional to the area A of the sunshade and a constant k . For shade with extensible panels, long-term bounded trajectories may be devised which maintain position by deploying and retracting the panels. An L1 sunshade provides nearly uniform cooling over the entire Earth, as shown in Fig. 1L, while a geosynchronous shade has the potential for significant local cooling and negligible cooling across the entire Earth (see Fig. 1R, for a shade at a radius of 20 km).

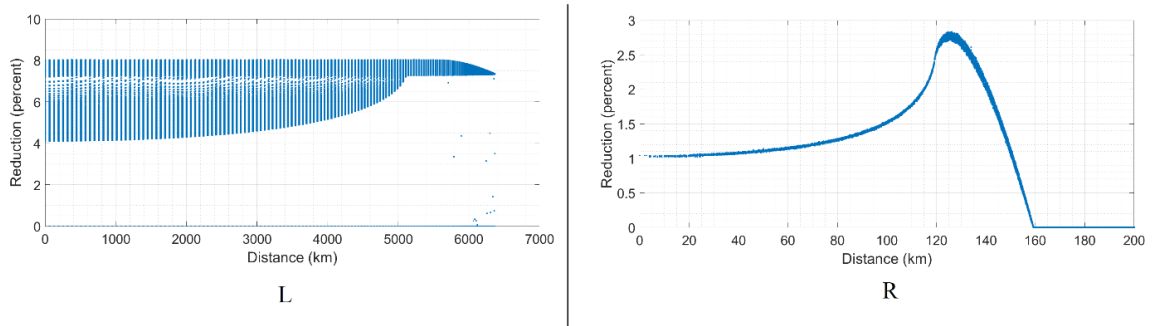


Figure 1 : Solar radiation percentage reduction at points on the Earth's surface as a function of radial distance from the Earth's location directly in front of the shade. In the panel L, the situation for a shade of radius 2000 km mounted at L1 is shown. The overall reduction is 6.6 percent across the entire Earth. There are multiple reductions for each distance due to different angles of depression and azimuth.

It is hoped that for an extended object such as a sunshade, opposing destabilizing tendencies may be harnessed to achieve a net reduction in station-keeping requirements. Further details will be presented at the conference.

References

- [1] Early J. (1989) Space based solar shield to offset greenhouse effect. *J. Brit. Interplanetary Soc.* **42**:567-569.
- [2] Angel R. (2006) Feasibility of cooling the earth with a cloud of small spacecraft near the inner Lagrange point L1. *PNAS* **103**:17184-17189.
- [3] Roberts C. E. (2002) The SOHO Mission L1 halo orbit recovery from the attitude control anomalies of 1998. *Libration Point Orbits and Applications Conf.*
- [4] Anderson P. V. et. al. (2015) Operational considerations of geo debris synchronization dynamics. *66th International Astronautical Congress* **A6,7,3**:27478.
- [5] Fuglesang C. and Miciano M. G. H. (2021) Realistic sunshade system at L1 for global temperature control. *Acta Astronautica* **186**:269-279.

Mathematical Modelling of a Coefficient of Nonlinearity in Dynamics of Deep Groove Ball Bearing with Damage

Ivana D. Atanasovska*, Dejan B. Momcilovic** and Tatjana M. Lazovic***

*Mathematical Institute of the Serbian Academy of Sciences and Arts, Belgrade, Serbia

**Institute for testing of materials-IMS Institute, Belgrade, Serbia

***Belgrade University, Faculty of Mechanical Engineering, Belgrade, Serbia

Abstract. The presented research is a part of widely research of the nonlinear dynamic behaviour of rolling bearings, which are the parts of all rotating assemblies and machinery. In accordance with the state-of-the-art requirements for the advanced mechanical design and industrial digitalization, the large experiments and research are performed and the new mathematical model of the dynamic behaviour of rolling bearings with damages is developed. The results obtained for a particular type of deep groove ball bearings are presented, and the possible further research and implementation of the obtained model in digitalized self-monitoring systems is discussed.

Introduction

The existing demands for light weight design of mechanical elements in correlations with the demands for increasing reliability and machinery digitalization, lead to the requirements for developing new methods and mathematical models for permanent monitoring and maintenance of the crucial machinery parts. The rolling bearings monitoring is mandatory in all rotating assemblies and machinery in the framework of digitized production, and required precise predefined mathematical relations and models for programming the self-monitoring digitalized systems.

The main postulates of the theory of nonlinear dynamics [1, 2] are used in the presented research in order to develop the mathematical model for efficient prediction of behaviour of deep groove ball bearings with defects. The particular type of single-row deep groove ball bearing 6206 is chosen, and large set of experimental testing of samples with pre-manufactured damages on the inner and outer raceway is performed [3].

Results and discussion

For developing a mathematical model of a damaged single-row rolling bearings, the differential equation of motion is derived as a special case of a general nonlinear oscillator [2] with strong cubic nonlinearity [1]. For radial rolling bearings, this matrix form of the equation of nonlinear dynamics could be reduced to a one-degree-of-freedom system [4] given as:

$$m_{red}\ddot{y} + C_r\dot{y} + K_r y + qy^3 = F$$

The nonlinear part of this equation, represented by the coefficient of nonlinearity q , depicts how existing damage influences the rolling bearing vibrations. For a particular radial rolling bearing type, an expression for the coefficient q is obtained by an iterative procedure based on the experimental measurements of the bearing vibration response [3], and defined to be dimensionally consistent with the presented equation of motion. The coefficient of nonlinearity depends on the damage dimension, local contact deformation and external load distribution among rolling elements. Based on an empirical iterative procedure, the following formula is proposed for the conical-shaped damages on the inner raceway of the 6206 ball bearings:

$q = \left(\frac{d_d}{d_0}\right)^3 \frac{F_\delta}{\delta^3}$, Fig.1, where: d_d – is the diameter of the damage on a contact surface; d_0 – is the average diameter of the damage for a particular rolling bearing type obtained by the producer; F_δ – is a load distributed on the most loaded rolling element, obtained by Finite Element Analysis and δ – is a local deformation on the most loaded rolling element in contact with the damaged raceway surface, obtained by Finite Element Analysis performed for a particular case of the rolling bearing type, as well as for a particular type and dimensions of the modelled damage.

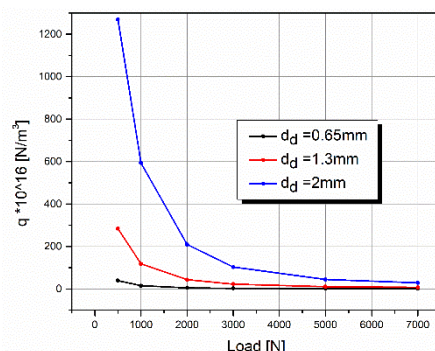


Figure 1: Nonlinearity coefficient variation

References

- [1] Cveticanin L. (2012) Ninety years of Duffings equation. *Theor appl mech, SI: Addr Mech*, **40**(S1): 49-63. doi: 10.2298/TAM12S149C
- [2] Kovacic I. and Gatti G. (2020) Helmholtz, Duffing and Helmholtz-Duffing Oscillators: Exact Steady-State Solutions. *IUTAM Bookseries 37 - IUTAM Symp ENOLIDES*, pp.167-177. doi: 10.1007/978-3-030-23692-2_15
- [3] Soldat N., Mitrovic R., Atanasovska I., Tomović R. (2020) A methodology for analyzing radial ball bearing vibrations. *Trans FAMENA*, **44**(1): 13-28, doi:10.21278/TOF.44102
- [4] Atanasovska I., Soldat N., Patil S., Mitrovic R., Tomovic R. (2022) Damage Factor Calculation for Condition Monitoring of Rolling Bearings. *Arab J Scie Eng*, online first articles, doi: 10.1007/s13369-022-07126-4

Flexible mechanisms as quasi-zero stiffness metamaterial resonators

Douglas Roca Santo*, Leopoldo P.R. de Oliveira*, Elke Deckers**, *

*Department of Mechanical Engineering, São Carlos School of Engineering - University of São Paulo, Brazil, ORCID #0000-0003-0038-2777, #0000-0001-7023-7431

** KU Leuven, Campus Diepenbeek, Dept. of Mechanical Engineering, Wetenschapspark 27, 3590 Diepenbeek, Belgium
*DMMS Core lab, Flanders Make, Belgium, ORCID #0000-0003-3462-5343

Abstract. There is an ever-increasing interest in resonant metamaterials (RMM), as they promote vibration attenuation in small packaging. In linear RMMs, the bandwidth and depth of the attenuation are linked to the resonator mass, which results in significant added mass. In this context, nonlinear RMMs can provide interesting dynamic properties that result in frequency band broadening or more efficient energy absorption with different excitation levels. Properties include resonance frequency shifts and quasi-zero stiffness, which can provide better isolation and more efficient attenuation to the host structure. This work investigates the design and experimental validation of nonlinear resonators based on flexible mechanism topologies. The use of flexible elements tackles the dissipation mechanisms which inhibit the desired nonlinear phenomena in conventional linkage systems. The additive-manufactured resonators are tested under various static and dynamic conditions, with the aid of a Digital Image Correlation (DIC) system, to validate the design procedure.

Introduction

Vibration attenuation can be achieved via periodicity, which results in highly attenuated waves via an effect similar to band rejection [1], often referred to as *bandgaps*. Resonant metamaterials promote similar vibration attenuation with smaller packaging [2]. However, the frequency band and depth of the attenuation are directly linked to the resonator mass in linear metamaterials, which can result in significant added mass.

Results and Discussion

By leveraging nonlinear elements to provide frequency band broadening or more efficient energy absorption, we investigate the parametric design and physical realisation of quasi-zero stiffness resonant elements. Such nonlinear systems can provide resonance frequency shifts, resulting in better isolation and more efficient attenuation to the host structure [3, 4]. The proposed design can be seen in Fig. 1. The concept starts with a support structure and a flexible beam, to which a concentrated mass will be added at the centre. Both structures are additive-manufactured in ABS and work under prestress: The lateral poles are manufactured in the inverse shape of a tip-loaded cantilever, such that when assembled, they will be approximately straight up (Fig. 1b), while the flexible beam is designed to work on its post-buckling state [5]. When perceiving base excitation at low levels, the device behaves like a linear tuned mass damper (TMD) in either of its bi-stable positions. However, when the load is increased for certain frequency regions, the system undergoes its quasi-zero stiffness region and, eventually, flips between the stable poles.

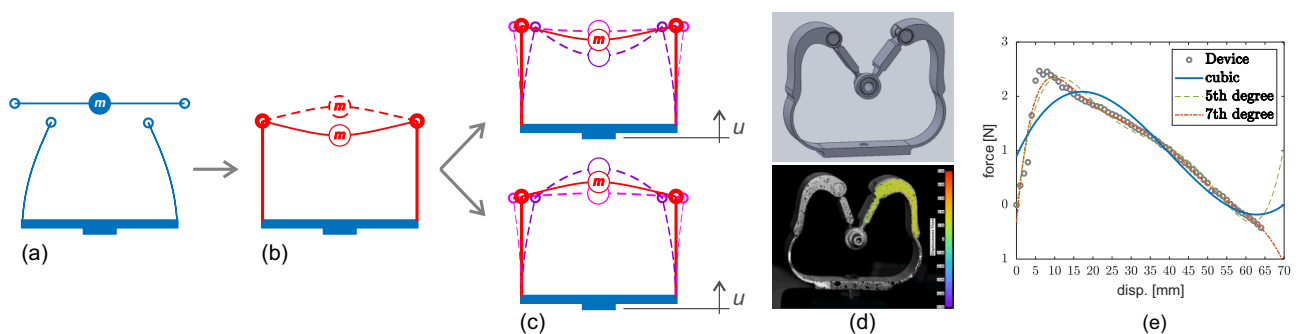


Figure 1: Bistable flexible mechanism: (a) unloaded parts, (b) prestressed assembly, (c) vibration around equilibria, (d) CAD concept and DIC measurements and (e) experimental nonlinear stiffness and curve fits.

Figure 1(d) shows the additive manufactured resonators model and DIC image processing, while (e) shows the experimental nonlinear stiffness achieved with such a design. Preliminary results [3] indicate that using such nonlinear resonators can increase the bandwidth of local resonance-type bandgaps.

References

- [1] Brillouin, L. (1953) *Wave propagation in periodic structures: electric filters and crystal lattices*, Dover Publications, 2nd Ed.
- [2] Pires, F.A., Wandel, M., Thomas, C., Deckers, E., Desmet, W., Claeys, C. (2022) Improve sound transmission loss of an aircraft's lining panel by the use of locally resonant metamaterials, ISMA-USD, Leuven, Belgium. 11pp.
- [3] Santo, D.R., Oliveira, L.P.R., Gonçalves, P.J.P. (2022) On the dynamic behavior of mono-coupled continuous structures attached to nonlinear resonators, ISMA-USD, Leuven, Belgium. 11pp.
- [4] Gatti, G., Shaw, A.D., Gonçalves, P.J.P., Brennan, M.J. (2022) On the detailed design of a quasi-zero stiffness device to assist in the realisation of a translational Lanchester damper. *Mech Syst Signal Process* **164** 108258.
- [5] Emam S., Lacarbonara, W. (2022) A review on buckling and postbuckling of thin elastic beams *Europ J of Mechanics/A Solids* **92** 104449

An enhanced pathfollowing scheme for nonsmooth dynamics via improved computation of the monodromy matrix

Giovanni Formica*, Franco Milicchio** and Walter Lacarbonara***

* Department of Architecture, Roma Tre University, Italy, ORCID #0000-0002-6410-8083

** Department of Engineering, Roma Tre University, Italy, ORCID #0000-0002-4875-4894

*** Department of Structural and Geotechnical Engineering, Sapienza University of Rome, Italy, ORCID #0000-0002-8780-281X

Abstract. One of the key features of pathfollowing schemes for non-autonomous nonlinear dynamical systems is the computation of the Jacobian of the Poincaré map (*i.e.*, the *monodromy matrix*), which, being employed as iteration matrix, governs both the accuracy and robustness of the whole numerical strategy. In the context of nonsmooth nonlinear dynamic systems, this matrix can only be computed via numerical differentiation, which leads to subtractive cancellation errors. By means of a wide numerical campaign for meaningful multi-DOFs systems, we discuss strategies to reduce such errors via an enhanced pathfollowing scheme, recently proposed by the authors.

Introduction

Exploring manifolds of solutions of nonlinear dynamical problems with enhanced continuation algorithms is attracting high scientific and technological interest, especially when handling both accurately and efficiently large-scale engineering systems [1]. We focus on pseudo-arclength continuation approaches searching numerically for the fixed points of a Poincaré map \mathbf{P} of nonlinear dynamical systems along the curve of the corresponding periodic solutions. The cornerstone of such approaches when facing nonsmooth dynamical systems (*e.g.*, systems with hysteresis and discontinuities of various kinds) is the construction of the Jacobian matrix involving the computation of the monodromy matrix \mathbf{H} . The central difference scheme used to compute \mathbf{H} leads to cumulative errors, which turn out to be the combination of the errors introduced by using the small finite-difference coefficient with the errors affecting the time integration to obtain \mathbf{P} . Here we present an upgrade of the pseudo-arclength numerical strategy proposed in [2], and developed in a C++ software library (freely available at <https://zenodo.org/record/7245478>). The strategy works with an acceleration procedure, based on a Krylov subspace loop, nested in a modified Newton-Raphson scheme using \mathbf{H} as iteration matrix.

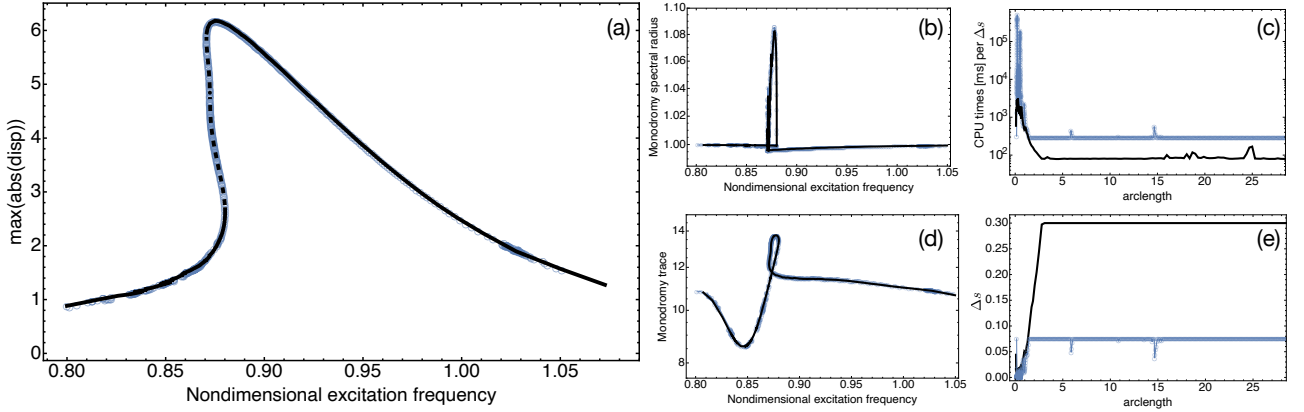


Figure 1: (a) frequency response curves and (b, d) monodromy invariants (spectral radius and trace, respectively) for hysteretic 10-dof system; (c) CPU times per arclength step-size Δs and (e) Δs along the arclength of the solution path (SP solid line, CD dotted circles).

Results and discussion

The proposed numerical scheme works as a Runge-Kutta single-pass (SP) method, where a numerical differentiation computed by L nczos integration is directly employed within the time step integration yielding the monodromy matrix. This makes the small finite-difference coefficient act on a time-discretization error which is one-order-of-magnitude greater than the time-discretization error affecting the integration of the perturbed Poincar  map as in standard central difference (CD) schemes. We here report the results concerning a 10-dof system (30-dim state problem) featuring hysteretic nonlinear springs and linear dashpots which connect masses in a parallel arrangement. We compare the performance of the strategy using the CD scheme with that employing the proposed SP scheme. The latter proves to be not only more accurate but also more robust than the former, leading to a faster convergence. Figure 1(e) shows how the SP scheme allows to achieve convergence employing an arclength step size Δs of the solution path 4 times larger than the standard CD scheme, and the CPU time per Δs in SP is about 3.5 lower than the CPU time required by CD, see Figure 1(c).

References

- [1] Ahsan Z., Dankowicz H., Li M., Sieber J. (2022) *Nonlinear Dyn* **107**:3181–3243.
- [2] Formica G., Milicchio F., Lacarbonara W. (2022) *Int J Non-Linear Mech* **145**:104116.

Dynamics of a damped variable mass system : Leaky balloon with string

Riddhika Mahalanabis^{*1} and Balakrishnan Ashok^{*2}

^{*}Centre for Complex Systems & Soft Matter Physics, International Institute of Information Technology Bangalore (IIITB), 26/C Hosur Road, Electronics City, Bengaluru 560100, India. ¹ ORCID #0000-0002-3586-7881, ² ORCID #0000-0002-6378-0150

Abstract. In this work we explore the dynamics of a variable mass system in the form of a leaky balloon with an attached string. Both the interaction of the string with an underlying surface, as well as the variable mass of the balloon itself, contribute to the non-constant mass of the system, which can be treated as a toy model for several other complicated variable mass systems. Our results show that despite being very simple, this system shows a plethora of interesting behaviour that can have important implications for real-world systems such as in stents and in targeted drug delivery.

Introduction

The dynamics of a balloon moving along one direction is non-trivial due to a string attached to it, and by its changing mass due to escape of the gas it contains, two distinct contributions that make for some interesting behaviour. This is a classic example of a variable mass system. We also account for damping effects on the system and investigate its behaviour under forcing. Such a system can act as a model system for various real-world phenomena. In an earlier treatment of a balloon with a string floating in air but without any gas leaking from it, Yariv *et al.* have described the interesting oscillatory motion that it displays, while also drawing an analogy to that of a piston in a fluid [1]. A few other variable mass systems considered in the literature include those by Denny [2], Bartkowiak and collaborators [3] who investigate a variable mass pendulum, Digilov and Reiner's investigations of a damped, variable mass, spring-pendulum [4], and the several detailed investigations of van Horssen and collaborators of variable mass oscillators (for instance [5]).

Results and Discussion

We present some of the results of our theoretical investigations (both analytical and numerical) of the behaviour of a variable mass balloon-string system near and far from its critical points. We observe how different mass-loss mechanisms and damping methods affect the system. Oscillations in the system die out faster for viscous damping than for quadratic damping. Scaling analysis of the system tells us that although viscous damping can be neglected for certain system parameters, quadratic damping cannot and significantly influences system behaviour. We also discuss how the importance of some system parameters compare to that of the system's dimensions and can be the dominating factor. In addition to Digilov's conclusion that the rate of mass loss significantly affects the system's behaviour, we find that the mechanism of mass loss is also crucial and results in pronounced differences in the leaky balloon system's approach to equilibrium. It is seen that the system retains its robustness even in the presence of external forcing and slowly moves towards a stable attractor, where the rate of attaining the equilibrium state is strongly dependent on the type of damping it experiences. We further try to understand how the ratio of time-scales of balloon oscillation to that of the applied periodic force affects the system. Further details are presented elsewhere [6].

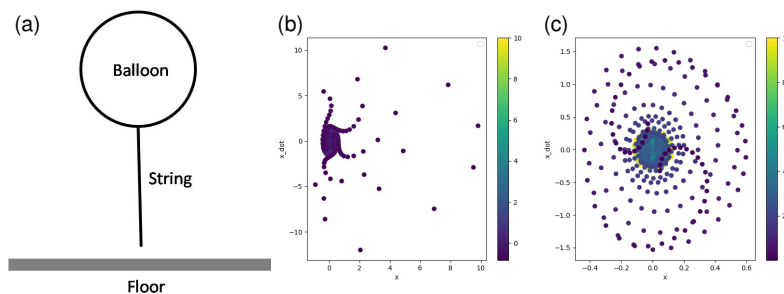


Figure 1: (a) The system, (b) Velocity vs. displacement for leaky balloon, mass-loss indicated by the colour, (c) Details of (b).

References

- [1] Yariv, A., Scheuer, J., Crosignani, B., & Di Porto, P. (2007) The case of the oscillating party balloon: A simple toy experiment requiring a not-so-simple interpretation. *Am. J. Phys.* **75**:696-700.
- [2] Denny, M. (2021) Balloon and chain: an instructive variable mass system. *Eur. J. Phys.* **42**:025013.
- [3] Bartkowiak, T., Grabski, J. K., & Kołodziej, J. A. (2016) Numerical and experimental investigations of the dynamics of a variable mass pendulum. *Proc. IMechE. Part C: J. Mechanical Engineering Science* **230**: 2124-2132.
- [4] Digilov, R. M., Reiner, M., & Weizman, Z. (2005) Damping in a variable mass on a spring pendulum. *Am. J. Phys.* **73**:901-905.
- [5] van Horssen, W. T., Abramian, A. K., Hartono. (2006) On the free vibrations of an oscillator with a periodically time-varying mass. *Journal of Sound and Vibration* **298**:1166-1172.
- [6] Mahalanabis, R. and Ashok, B. (2022) Dynamics of a variable mass system. (under submission).

Recycled Smartdevices for Real-Time Monitoring of Civil Infrastructures

Arturo Buscarino**, Carlo Famoso* and Luigi Fortuna **

*Dipartimento di Ingegneria Elettrica Elettronica e Informatica, University of Catania, Italy

**IASI, Consiglio Nazionale delle Ricerche (CNR), Roma, Italy

Abstract. This contribution summarizes some preliminary results obtained in the development of a platform based on recycle smartdevices to monitor the vibrations of buildings and infrastructure. The platform, designed within the framework of a project funded by the Italian Ministry of Economic Development, exploits the accelerometer, the other sensors and communication boards included in smartdevices which have reached their end-of-life. The idea is to realize a fully autonomous setup capable of acquiring information provided by the different sensors, store the datasets in a cloud server which can be accessed either during the monitoring phase or the post-processing phase, and perform locally a real-time nonlinear analysis to extract features leading to alarms.

Introduction

Essentially two types of monitoring are implemented, i.e. static monitoring, performed regularly in medium-long intervals and useful for the observation of quasi-static phenomena, and dynamic monitoring, providing continuously the information, with measurements performed at medium-short intervals, according to the phenomenon to be observed (seismic or windy episode). In this contribution, we outline a low-cost and green strategy to the realization of a reliable building monitoring based on unused smartdevices which are capable to provide the needed information with high reliability and with time constants and resolution comparable with a daily monitoring activity.

In the normal context of private or low-complexity buildings, a small number of monitoring station is required. In order to contain the costs of the platform, we referred to an extremely widespread technology, such as that present in smartdevices which, even if they contains properly working and reliable sensors, have completed for software compliance their life cycle. According to reliable estimates, about 350,000 smartphones are thrown away every day, and of these the vast majority are still functional and offer sensors, connectivity and the ability to process information on site [1].

Results and discussion

If properly placed in a site of the building, monitoring stations based on reused smartdevices allow to determine the acceleration to which that certain point of the structure is subjected. The most common accelerometers in smartphones are capacitive, equipped with Micro Electro-Mechanical Systems (MEMS) sensors. In some operating conditions, these accelerometers are more efficient in measuring constant accelerations linked to quasi-static phenomena than piezoelectric accelerometers. The post-processing of the raw data provided allows for the extrapolation of indirect information that helps to create a complete and comprehensive picture of the environment being monitored: speed, inclination, subsidence.

The prototype developed during the project is reported in Fig. 1(a). It consists in a box hosting a recycled smartphone and a battery which can be recharged by using solar panels.

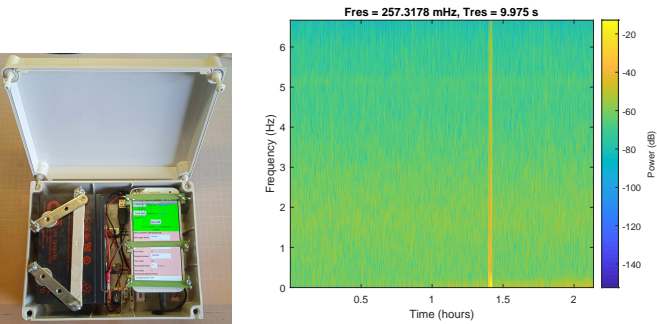


Figure 1: Experimental results: (a) Prototype of the monitoring box; (b) nonlinear spectrogram showing the onset of oscillations. Preliminary measurements have been acquired considering two locations within a building: near one of the main piles and near the external walls of a room located in the upper floors. A nonlinear frequency analysis allowed to identify the onset of oscillations, as shown in Fig. 1(b) even considering a low accuracy in the sensor quantization, which are originally designed for sensing larger vibrations. This validates the system and allows for planning the next steps in the road-map which includes the monitoring of an old church bell tower.

References

[1] Bucolo, M., Buscarino, A., Famoso, C., Fortuna, L., and Gagliano, S. (2020). Automation of the Leonardo da Vinci machines. *Machines*, 8(3), 53.

Pile installation via axial and torsional vibrations - the Gentle Driving of Piles method

Athanasios Tsetas*, Apostolos Tsouvalas* and Andrei V. Metrikine*

*Faculty of Civil Engineering and Geosciences, Delft University of Technology
Stevinweg 1, 2628 CN Delft, The Netherlands

Abstract. This paper presents the study of a new pile installation technique that combines axial and torsional excitation, namely the Gentle Driving of Piles (GDP) method. Both numerical modelling and field tests are employed to analyse the mechanics of the GDP method. Furthermore, a three-dimensional numerical model for the analysis of the pile installation process is presented, comprised by a thin cylindrical shell (pile), a linear elastic layered half-space (soil) and a history-dependent frictional interface. The overall problem is formulated in a mixed time-frequency form and solved via an efficient approach based on the Harmonic Balance Method. The model predictions are compared against field data and the experimental findings are further analysed in order to shed light into the complex pile-soil behaviour during installation.

Introduction

Presently, over 80% of the offshore wind turbines in Europe are founded on monopiles, which are commonly installed by impact hammering. However, this method generates significant underwater noise emissions, harmful to marine life. To this end, environmentally friendly alternatives are investigated for monopile installation, such as vibratory methods. Axial vibratory pile driving is used onshore for decades, with advantageous features such as high installation speed and low axial pile loading. However, its use in the offshore industry is limited, due to the lack of field data and knowledge gaps related to the complex pile-soil behaviour. To further the potential of vibration-based methods, the Gentle Driving of Piles (GDP) has been proposed by TU Delft [1]. The GDP method is based on simultaneous application of low-frequency axial and high-frequency torsional excitation and aims to improve installation performance and reduce underwater noise emissions.

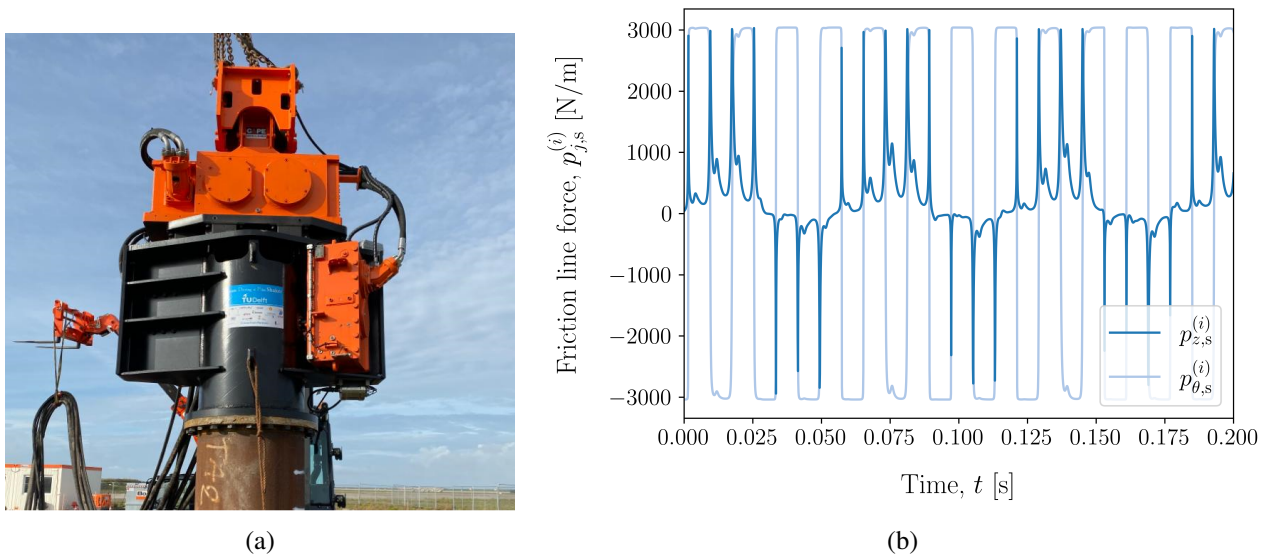


Figure 1: (a) The GDP shaker connected to a test pile and (b) axial and circumferential friction forces at the pile-soil interface during pile installation.

Results and discussion

Medium-scale field tests have been performed at Maasvlakte II site, at the port of Rotterdam, in which different installation methods were studied, with a focus on the GDP method. Based on these experiments, the proof of concept of the method was achieved and a set of field data were obtained to further analyse the installation tests. Furthermore, a new numerical model has been developed for the analysis of pile installation via the GDP method. A comparison of the numerical results with the field tests showcases the predictive capabilities of the developed model. The field observations are discussed on the basis of the newly developed model and the driving mechanisms are uncovered. Conclusively, the redirection of the friction force vector is identified as the main mechanism that enhances the installation performance by the introduction of high-frequency torsion.

References

- [1] Metrikine, A. V., Tsouvalas, A., Segeren, M. L. A., Elkadi, A. S. K., Tehrani, F. S., Gómez, S. S., Atkinson, R., Pisanò, F., Kementzetzidis, E., Tsetas, A., Molenkamp, T., van Beek, K. and de Vries, P. [2020], Gdp: A new technology for gentle driving of (mono)piles, in 'Proceedings of the 4th International Symposium on Frontiers in Offshore Geotechnics, Austin, TX, USA, 16–19 August 2020'.

Development and validation of an efficient model for bearing strain creep prediction

Hamid Ghorbani^{1,2}, Bart Blockmans^{1,2} and Wim Desmet^{1,2}

¹*Department of Mechanical Engineering, Division LMSD, KU Leuven, Belgium*

²*Flanders Make, Core Lab Dynamics of Mechanical and Mechatronic Systems*

Abstract. This contribution presents a novel reduced-order modelling approach for the efficient simulation and prediction of outer ring strain creep in ball bearings. The approach combines an analytical modelling of the rolling element interactions with reduced-order finite element modelling of the outer ring and housing. A parametric model-order reduction technique specifically tailored for bearing creep prediction is applied to reduce the computational complexity of the model and allows rapid yet accurate assessment of multiple design iterations. The accuracy of the model reduction technique and overall modelling methodology is validated with numerical simulations and experimental measurements.

Introduction

Rolling element bearings in modern drivetrains are subjected to high and dynamic loadings. To prevent early bearing failures, predictive tools are used in the early design phase to identify and avoid detrimental loading conditions in the final design. A particularly challenging failure mechanism to predict is outer ring strain creep. This phenomenon occurs when the induced shear stresses at the outer surface of the outer ring locally overcome the static friction force between the outer ring and the housing it is assembled in, causing the outer ring to rotate and eventually wear out the housing bore. Outer ring strain creep has been successfully modelled using the Finite Element (FE) method by various researchers [1,2], with planet bearing creep in wind turbine gearboxes receiving considerable attention in the last years [3]. However, these modelling approaches rely on commercial FE software combined with high-performance computing clusters, and are thus not suited for repeated design iterations. In this presentation, the main challenges in developing an accurate yet efficient numerical tool for the prediction of bearing strain creep are discussed. These challenges relate to the high number of Degrees of Freedom (DOFs) in the FE representation of the outer ring and bearing housing (see Fig. 1), the relatively long simulated times needed to draw conclusions on bearing creep severity and velocity, and the accurate computation of stick-slip friction forces throughout the large convex-concave contact area between the bearing and the housing.

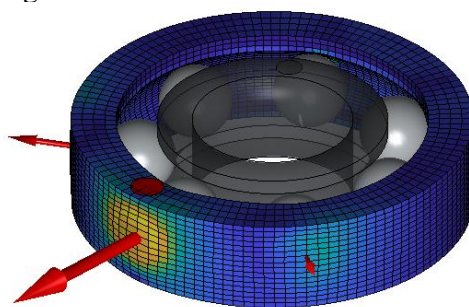


Figure 1: Hybrid reduced-order bearing model used to predict outer ring strain creep velocity.

Results and discussion

As strain creep is dominated by frictional contact between the deformed outer surface of the bearing's outer ring and the inner bore of the housing, FE discretization is applied only to the outer ring of the bearing, with internal contact interactions being modelled by an analytical lumped-parameter method based on Hertzian contact theory (see Fig. 1). In order to reduce the number of DOFs, a configuration-dependent model-order reduction scheme is applied that is based on a small set of a priori static contact analyses. In order to further increase computational efficiency in dynamic analysis, a separation is made between dynamic and quasi-static DOFs. Finally, frictional contact forces in the interface between outer ring and housing are computed based on a continuous friction model that differentiates between regions of (elastic) stick and (constant or elastic) slip. In doing so, bearing creep predictions in agreement with full-order model simulations and experimental measurements are obtained in a matter of seconds-minutes, rather than hours-days.

References

- [1] Maiwald, A., & Leidich, E. (2013). FE simulations of irreversible relative movements (creeping) in rolling bearing seats—influential parameters and remedies. In *Proceedings of the World Congress on Engineering and Computer Science* (Vol. 2).
- [2] Schiemann, T., Pörsch, S., Leidich, E., & Sauer, B. (2018). Intermediate layer as measure against rolling bearing creep. *Wind Energy*, 21(6), 426-440.
- [3] Gnauert, J., Schlüter, F., Jacobs, G., Bosse, D., & Witter, S. (2021). Simulative investigation of ring creep on a planetary bearing of a wind turbine gearbox. *Forschung im Ingenieurwesen*, 85(2), 219-227.

Solving the problem of nonlinear oscillations of a pendulum on a flexible stretchable thread

Alexey Malashin^{*}, Arkadiy Ostromogilskiy^{*}

^{*}Faculty of Mechanics and Mathematic, Lomonosov Moscow State University, Moscow, Russia

Abstract. The paper considers the problem of oscillation of a pendulum on a flexible, stretchable thread. The equations of motion are nonlinear partial differential equations. A new method is proposed for solution. The influence of longitudinal and transverse vibrations of the thread is investigated. The transfer of energy from the longitudinal vibrations of the load to the transverse vibrations of the thread is revealed.

Introduction

Interest in a similar problem arose due to the fact that a nonlinear oscillatory process with several degrees of freedom occurs in vibrations of a pendulum on a stretchable thread. There are works on the vibrations of a pendulum with a spring. The solutions in non-resonance case and asymptotic solutions in resonance were obtained that show there are transfer of energy between vertical and horizontal vibrations. At resonance frequencies ratio regarding horizontal and vertical directions were found to be equal to 1:2. In the paper we discuss the case when longitudinal and transverse vibrations occur in the thread. The equations describing the motion of a pendulum on a flexible elastic thread are nonlinear partial differential equations.

Results and discussion

The analysis of the incoming dimensionless parameters shows that there are several characteristic times in the system under consideration — the period of oscillation of the pendulum, the time of propagation of longitudinal waves along the thread, as well as the time of propagation of transverse waves. A new asymptotic method is proposed for constructing an analytical solution that takes into account both fast and slow movements when the application of a small parameter leads to a change in the type of partial differential equation. Solutions of the system of equations are obtained. The influence of natural oscillations of a spring pendulum on longitudinal and transverse vibrations of the thread is investigated. A numerical solution of this nonlinear system of equations is also obtained and compared with an analytical solution. It is shown that a pendulum system on a flexible elastic thread is characterized by a motion characteristic of a swinging spring when the following conditions are occurred: a small ratio of the mass of the thread to the mass of the load, no tension drop to zero and no initial nonlinear disturbances. In the first approximation, frequency corrections to the oscillations of a swinging spring are found, which arise if wave processes in the thread are taken into account. It is obtained that the lower the tension, the greater the amplitude of the transverse vibrations of the thread. In particular, the drop in tension leads to instability of oscillations along one axis. The transfer of energy from the longitudinal vibrations of the load to the transverse vibrations of the thread is revealed. In the numerical experiments carried out, it was possible to record a significant increase in the amplitude of the transverse deviations of the thread. It is analytically shown that the parametric resonance between the natural oscillations of the pendulum and the longitudinal-transverse oscillations of the thread differs from the classical one (described by the Mathieu equation), since the frequencies of these oscillations have a different order. The influence of natural oscillations of a spring pendulum on transverse vibrations of a thread at non-resonance and resonance is shown in Fig. 1.

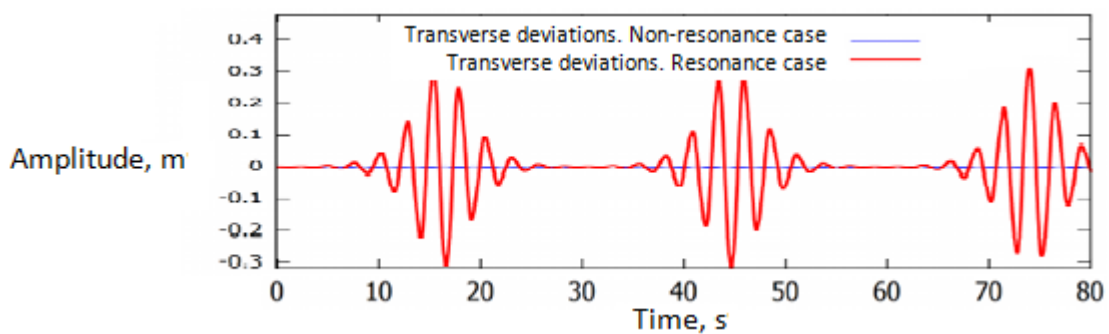


Figure 1: Amplitude of transverse vibrations of the tread of a pendulum with stretchable thread.

References

- [1] Nayfeh A.H. (1973) Perturbation Methods. N. Y.: Wiley.
- [2] Awrejcewicz J., Petrov A.G. (2008) Nonlinear oscillations of an elastic two-degrees-of freedom pendulum. *Nonlinear Dynamics*. V. 53. № 1-2.
- [3] Petrov A.G. (2006) Nonlinear vibrations of a swinging spring at resonance. *Mechanics of Solids*. V. 41. № 5.

Nonlinear Modes of Jointed Structures with As-built Surface Topography

R.J. Kuether*, D.A. Najera-Flores**, and M. Southwick***

*Sandia National Laboratories, Albuquerque, NM, USA

**ATA Engineering Inc., San Diego, CA, USA

***Sandia National Laboratories, Livermore, CA, USA

Abstract. Structures with bolted joints produce large variability in nonlinear dynamic behavior, making it challenging to accurately capture even with high-fidelity models. Several parameters contribute to the observed variation, including preload, alignment, and material properties, among others. This study explores the influence of surface topography on the nonlinear phase resonant modes of a mechanical system. Small variations in as-built surface geometry can influence the contact stress distributions within the preloaded bolted joint. Contact stress distribution and gaps provide the initial conditions for time-varying contact conditions during its dynamic response and influence how the surfaces separate and slip over time. This work develops a parameterized model of a bolted structure to investigate the sensitivity of the nonlinear phase resonant modes as a function of surface profile variation to better characterize the dominant sources of variability observed in bolted assemblies.

Introduction

Surface topography plays an important role in science and engineering and is known to influence wear, friction, and contact stress within bolted joints [1]. Surface texture is influenced by the manufacturing and machining process, so it is important to characterize and define the surfaces for the intended application. It has been hypothesized that the largest wavelengths in the surface geometry within a bolted joint interface most strongly influence the global time-varying contact stress distribution within the mechanical interface of the bolted joint. The purpose of this study is to parametrically model the surface topography and predict the preloaded equilibrium state and the nonlinear phase resonant modes [2] of the preloaded assembly.

Results and discussion

An example of a milled surface is shown in Figure 1, where the cumulative topography is plotted in the top row. The spatial wavelengths can be filtered into different components, namely form, waviness, and roughness, going from largest to smallest wavelength (or feature size). These surface profiles are mapped onto the discretized surface of a finite element model to predict their sensitivity to quantities of interest such as contact stress distribution, nonlinear energy dissipation, and nonlinear natural frequencies. This study will help understand the surface profile length scales that cause the structure’s nonlinear behavior to deviate from those with a nominally flat surface topography.

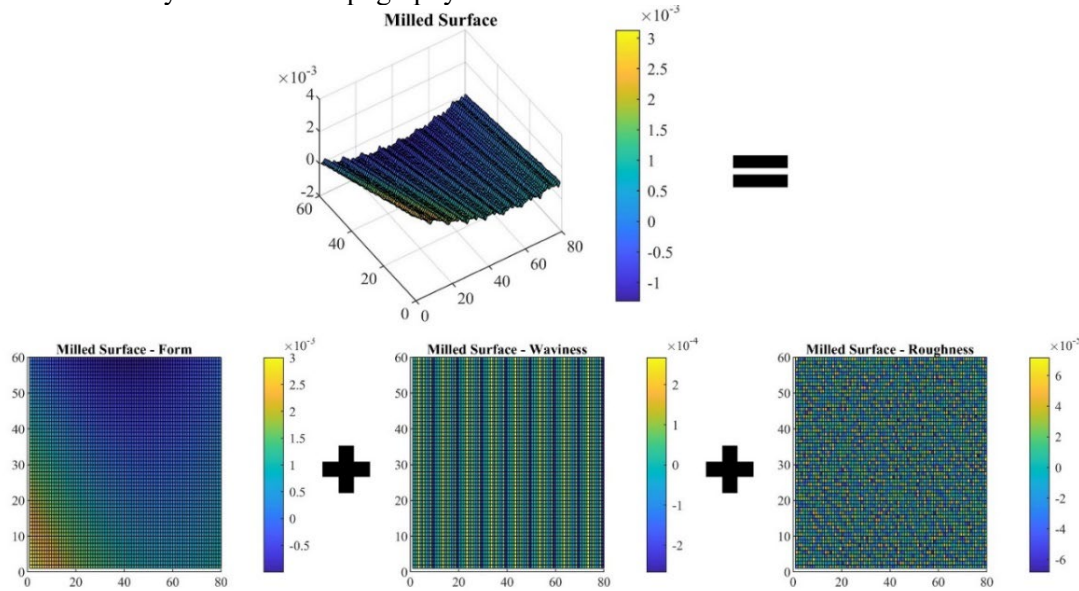


Figure 1: Machined surface filtered into separate form, waviness, and roughness wavelengths.

References

- [1] Wall M., Allen M.S., Kuether R.J. (2022) Observations of modal coupling due to bolted joints in an experimental benchmark structure. *Mechanical Systems and Signal Processing* 162:107968.
- [2] Volvert M., Kerschen G. Phase resonance nonlinear modes of mechanical systems. *Journal of Sound and Vibration* 511:116355.

Acknowledgments This paper describes objective technical results and analysis. Any subjective views or opinions that might be expressed in the paper do not necessarily represent the views of the U.S. Department of Energy or the United States Government. Supported by the Laboratory Directed Research and Development program at Sandia National Laboratories, a multimission laboratory managed and operated by National Technology and Engineering Solutions of Sandia LLC, a wholly owned subsidiary of Honeywell International Inc. for the U.S. Department of Energy’s National Nuclear Security Administration under contract DE-NA0003525. SAND2022-13567 A.

Digitally programmable piezoelectric metamaterials and nonlinear electromechanical structures with synthetic impedance circuits

Mustafa Alshaqqa*, Obaidullah Alfahmi*, and Alper Erturk*

*George W. Woodruff School of Mechanical Engineering, Georgia Institute of Technology, Atlanta, GA, USA

Abstract. We summarize our efforts on using synthetic impedance circuits in two domains: digitally programmable (1) piezoelectric metamaterials with spatially and spatiotemporally varying properties, and (2) nonlinear piezoelectric structures enabled through Duffing-type shunts. In the first domain, we demonstrate the capabilities in this new class of metamaterials using spatially varying inductive shunts for rainbow trapping and spatiotemporal modulation of inductive shunts for reciprocity breaking, via experiments and numerical simulations. In the second part, we extend the synthetic impedance shunts to nonlinear Duffing type hardening/softening inductance and present experimental results and harmonic balance simulations to show exceptional tunability from hardening to softening Duffing dynamics with the same single structure.

Introduction

Tunability and reprogramming are not straightforward in typical mechanical (elastic/acoustic) metamaterials and metastructures. We explore possibilities to this end using synthetic impedance shunts. In another research domain, it is well known that nonlinearities can be exploited in vibration attenuation and isolation. Researchers have recently explored nonlinear mechanical attachments in metastructures [1,2]. Here, we explore synthetic impedance circuits for piezoelectric structures to enable nonlinear attachments that are digitally programmable.

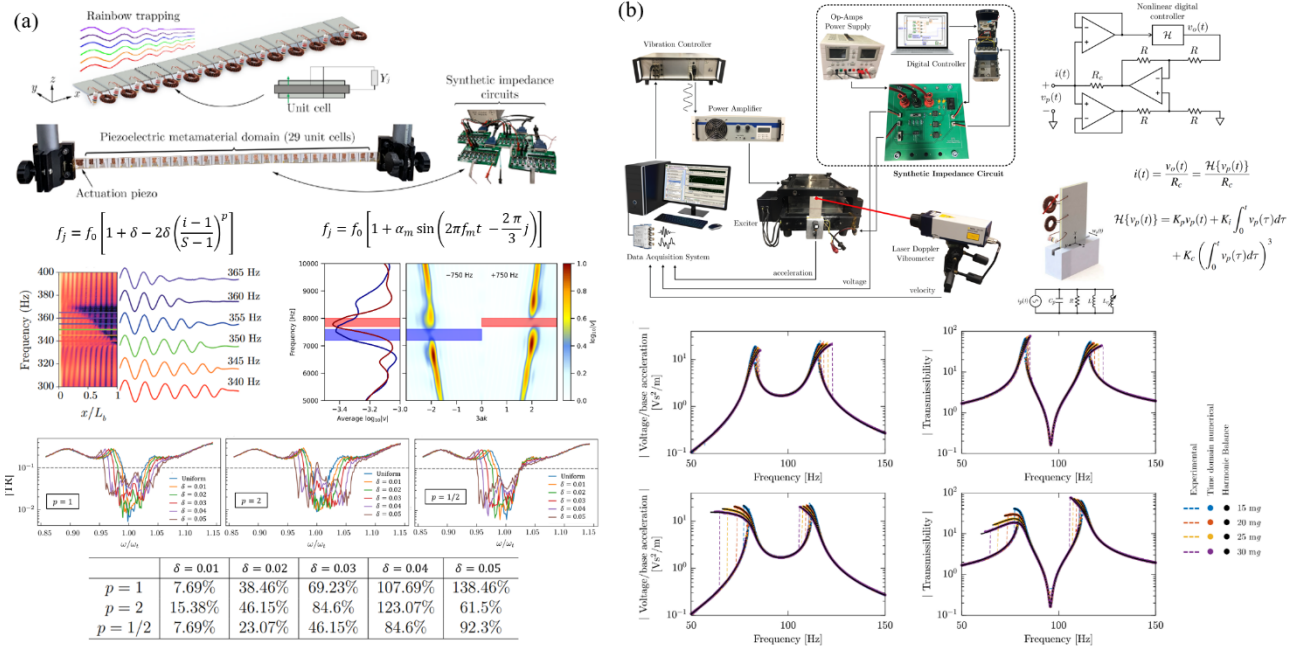


Figure 1: Synthetic impedance-based programmable piezoelectric metamaterials and nonlinear electromechanical structures: (a) Examples of rainbow trapping and nonreciprocal wave propagation by spatially and spatiotemporally programming the inductive shunts, along with results of bandgap enhancement in the rainbow case. (b) Duffing-type hardening and softening inductive synthetic circuit connected to a cantilevered piezoelectric structure under base excitation.

Results

Through digital programming of inductive shunts, we have demonstrated concepts spanning from the rainbow trapping phenomenon and bandgap enhancement by means of that (via various profiles of inductive shunt frequencies from fractional to quadratic) [3] to tunable nonreciprocal wave propagation (Fig. 1a). We have also established Duffing type digitally-controlled nonlinear shunts [4] to implement (Fig. 1b) in metastructures.

References

- [1] Casalotti, A., El-Borgi, S., and Lacarbonara, W., 2018, "Metamaterial Beam with Embedded Nonlinear Vibration Absorbers," *International Journal of Non-Linear Mechanics*, **98**, pp. 32-42.
- [2] Xia, Y., Ruzzene, M., and Erturk, A., 2020, "Bistable Attachments for Wideband Nonlinear Vibration Attenuation in a Metamaterial Beam," *Nonlinear Dynamics*, **102**, pp. 1285-1296.
- [3] Alshaqqa, M., Sugino, C., and Erturk, A., 2022, "Programmable Rainbow Trapping and Bandgap Enhancement via Spatial Group Velocity Tailoring in Elastic Metamaterials," *Physical Review Applied*, **17**, L021003.
- [4] Alfahmi, O., Sugino, C., and Erturk, A., 2022, "Duffing-type Digitally Programmable Nonlinear Synthetic Inductance for Piezoelectric Structures," *Smart Materials and Structures*, **31**, 095044.

Regular and complex behaviour in the pendulum system under a magnetic field.

Yuliia E. Surhanova* and Yuri V. Mikhlin*

*Department of Applied Mathematics, National Technical University "Kharkiv Polytechnic Institute", Kharkiv, Ukraine

Abstract. Dynamics of two coupled pendulums under a magnetic field are considered by taking into account a dissipation in the system. Inertial components of the pendulums are essentially different, and a ratio of masses is chosen as a small parameter. Padé approximants is used for the magnetic forces approximation. The method of multiple scales is used to construct nonlinear normal modes (NNMs), one of them is a localized one. An appearance of the complex behaviour when the system parameters change is investigated.

Introduction

The system containing two pendulums under the influence of electromagnetic force is studied in a few papers [1,2]. Here we consider a such dissipated system of two pendulums under a magnetic field when the inertial characteristics of these pendulums are essentially different. To describe the system dynamics, first of all, the nonlinear normal modes (NNMs) [3,4], one of them is a localized one, are constructed by the multiple scales method. The used Padé approximants demonstrate a good correspondence of the magnetic forces analytical presentation with experimental results presented in [1,2].

Equations of motion of the system under consideration concerning the pendulum angles are the following:

$$\begin{cases} \varepsilon I \ddot{\varphi}_1 = \varepsilon M_{mag_1} + \varepsilon M_{D1}(\varphi_1, \varphi_2) + \varepsilon M^{(g)}(\varphi_1) + M^{(k)}(\varphi_1, \varphi_2), \\ I \ddot{\varphi}_2 = \varepsilon M_{mag_2} + \varepsilon M_{D2}(\varphi_1, \varphi_2) + M^{(g)}(\varphi_2) + M^{(k)}(\varphi_1, \varphi_2). \end{cases} \quad (1)$$

Here I is the moment of inertia, $M_{mag_{1,2}}$ represent magnetic forces, $M_{D1,2}$ are damping moments, $M_{D1} = -C_1 - C_e(\varphi_1 - \varphi_2)$, $C_1\dot{\varphi}_1$ and $C_2\dot{\varphi}_2$ are moments of resistance to viscous air, $C_e(\dot{\varphi}_1 - \dot{\varphi}_2)$ и $C_e(\dot{\varphi}_2 - \dot{\varphi}_1)$ are damping moments created by the elastic element, $M^{(g)}, M^{(k)}$ are returning moments of gravity and elastic forces, respectively, $M^{(g)} = -mgs \sin \varphi_{1,2}$, $M^{(k)} = -k_l(\varphi_1 - \varphi_2)$, $r = mgs$, instead of the sine function, we use the shortened Taylor series, $\sin(\varphi) \cong \varphi - \frac{\varepsilon}{6} \cdot \varphi^3$, s is a distance between the pendulum center of mass and the axis of rotation, m is the biggest pendulum mass, ε is a small parameter characterizing the ratio of two pendulums masses, k_l is the binding elastic element stiffness.

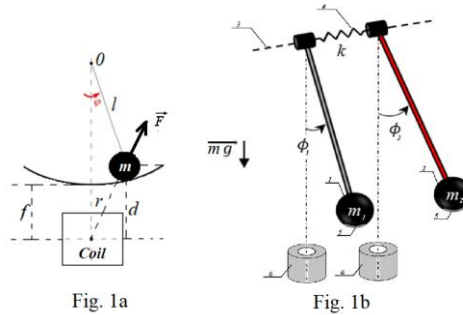


Figure 1: Schemes of the single particle and the magnetic force interaction (Fig.1a) and of the coupled pendulums system (Fig.1b).

Results and Discussion

The multiple scales method is used. In zero approximation, the relation $\varphi_{10} = \varphi_{20}$ is obtained for the coupled (in-phase) vibration mode, and the relation $\varphi_{20} = 0$ is obtained for the localized vibration mode. Numerical simulations show a good exactness of the obtained analytical solution for relatively small values of the parameter ε . With increasing the parameter ε there is a gradual transition from the localized vibration mode to the out-of-phase one. Numerical simulation, including calculation of the frequency spectrum, and analysis of this NNMs stability under change of the system parameters and initial angles, permits to reveal of regular behavior in the shape of NNM, as well irregular behavior, preferably for small values of the initial angles of the pendulums, and for relatively small values of the parameters k_l and s .

References

- [1] Wijata A., Polczyński K., Awrejcewicz J. (2021) Theoretical and numerical analysis of regular one-side oscillations in a single pendulum system driven by a magnetic field. *Mech Syst Signal Process* **150**:107229.
- [2] Polczyński K., Wijata A., Awrejcewicz J., Wasilewski G. (2019) Numerical and experimental study of dynamics of two pendulums under a magnetic field. *P I MECH ENG I-J SYS* **233**:441–453.
- [3] Mikhlin Yu.V., Avramov K.V. (2010) Nonlinear normal modes for vibrating mechanical systems. Review of theoretical developments. *Appl Mech Rev* **63** (6):060802.
- [4] Avramov K.V., Mikhlin Yu.V. (2013) Review of applications of nonlinear normal modes for vibrating mechanical systems. *Appl Mech Rev* **65** (2):020801.

Resonance steady states and transient in some non-ideal systems

Yuri V. Mikhlin* and Yana O. Lebedenko*

*Department of Applied Mathematics, National Technical University "Kharkiv Polytechnic Institute", Kharkiv, Ukraine

Abstract. We study a resonance behavior of two system with a limited power-supply (or non-ideal systems, NIS). Namely, the NIS having the pendulum as absorber, and the NIS presented the portal frame are considered. The multiple scales method is used to describe such systems dynamics near the resonance 1:1. Transient in these NIS is successfully constructed using the rational Padé approximations. Tending of the transient to the resonance steady state with increase of time is shown.

Introduction

The systems with limited power supply (or non-ideal systems, NIS) are characterized by interaction of the source of energy and elastic sub-system which is under action of the source. For NIS the external applied excitation depends on the excited elastic sub-system dynamics. The most interesting effect appearing in non-ideal systems is the Sommerfeld effect [1], when the large amplitude resonance regime is appeared, and the big part of the system energy passes from the energy source such vibrations. Resonance dynamics of the systems with limited power supply is first analytically described by V.Kononenko [2]. Then different aspects of the NIS dynamics are investigations in numerous papers (see, in particular, an overview [3] and a book [4]). We analyze here a resonance dynamics of two 3-DOF non-ideal systems (Fig.1), namely, the system having the pendulum as absorber, and the system describing dynamics of the portal frame having the shaft supported by two bearings where two steel wires have essentially nonlinear characteristics. Both steady state resonance regimes and transient are constructed in such systems.

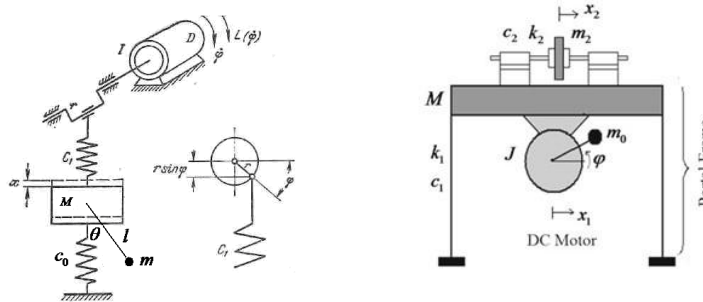


Figure. 1. Two models under consideration

Results and discussion

Dynamics of the system resonance behavior is described by the multiple scales method, where the small parameter characterizes a smallness of the absorber masses with respect to the masses of the system elastic part, a smallness of vibration components in variability in time of the motor rotation angle velocity with respect to the main constant component, a smallness of dissipation. Small nonlinearity in elastic forces is also taken into account. A steady state is constructed. Then a transient in the system is successfully constructed by Padé approximants containing exponents. Numerical simulation demonstrates both the good accuracy of the constructed steady state, as well an approach of the obtained transient to the resonance steady state with increasing time. It is also shown that the essential reduction of the resonance vibration amplitudes can be obtained by choose of the system parameters.

References

- [1] Sommerfeld A. (1902) Beiträge zum dynamischen ausbau der festigkeitslehe. *Phys. Z.* 166-186.
- [2] Kononenko V.O. (1969) *Vibrating Systems with Limited Power Supply*. Illife Books, London.
- [3] Balthazar J.M. et al. (2018) An overviewon the appearance of the Sommerfeld effect and saturation phenomenon in non-ideal vibrating systems (NIS) in macro and mems scales. *Nonlinear Dynamics* **93**(1): 19–40.
- [4] Cveticanin L., Zukovic M., Balthazar J.M. (2018) *Dynamics of Mechanical Systems with Non-Ideal Excitation*. Springer, Cham.
- [5] Baker G.A., Graves-Morris P. (1981) *Padé Approximants*. Addison-Wesley, London.

Nonlinear Dynamics Analysis of Actuation Strategies of Clustered Tensegrity V-Expander Structures

Muhao Chen*, Aguinardo Fraddosio**, Andrea Micheletti***, Gaetano Pavone**, Mario Daniele Piccioni** and Robert E. Skelton*

*Department of Aerospace Engineering, Texas A&M University, TX, USA (M. Chen ORCID # 0000-0003-1812-6835)

**Polytechnic University of Bari, Bari, Italy

***University of Rome Tor Vergata, Rome, Italy

Abstract. This work focuses on the dynamic analysis of cable-actuation processes of clustered tensegrity V-Expander modular structures. We present the study of energy-efficient cable actuation strategies for clustered tensegrity V-Expander towers subjected to shape changes in extension, flexure, shear, and torsion. First, based on the Lagrangian method and FEM approach, the equations governing the statics and dynamics of clustered tensegrities are given. After that, we analyze the nonlinear static and dynamic behavior during morphing processes realized with different actuation speeds. Then, the actuation efficiency of each particular choice of actuating cable is evaluated and discussed. The approaches developed here have general validity and can be used to design other types of cable-driven tensegrity structures.

Introduction

V-Expanders are lightweight [1], deployable, and easy to assemble tensegrity modules [2]. The topology of a V-Expander tower assembled by two or more elementary cells is shown in Figure 1. A clustered string is a group of individual cables combined into one continuous string that runs over pulleys or through loops at the nodes [3]. We present the study of an energy-efficient cable-actuation strategy for clustered V-Expander tensegrity structures subject to different shape changes based on the nonlinear clustered tensegrity dynamics and statics. Based on the Lagrangian method and FEM approach, the equilibrium equations of statics and dynamics for clustered tensegrity structures are given. Then, the cable-actuation process is realized by choosing suitable sets of cables as active and passive elements among the whole set of cables. The length of the active cables decreases during actuation, while passive cables adjust their length accordingly following the motion of the structure. Five shape-change types are considered: stretching, shrinking, flexure, shear, and torsion, as shown in Figure 2. We analyze the nonlinear static and dynamic behaviors during the morphing process with different actuation speeds. The actuation efficiency of each particular choice of active and passive cables is also discussed. The approaches developed in this paper can also be used to design and analyze other types of deployable cable-driven tensegrity structures.

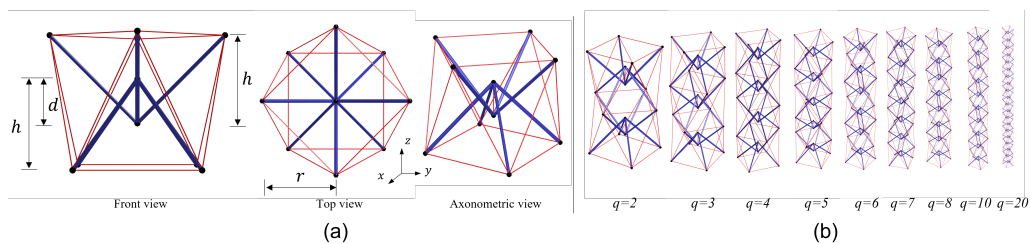


Figure 1: The V-Expander tensegrity: (a) the front, top, and axonometric views of one V-Expander cell, (b) the V-Expander column with different complexities. The thick blue lines are bars, and the thin red lines are cables.

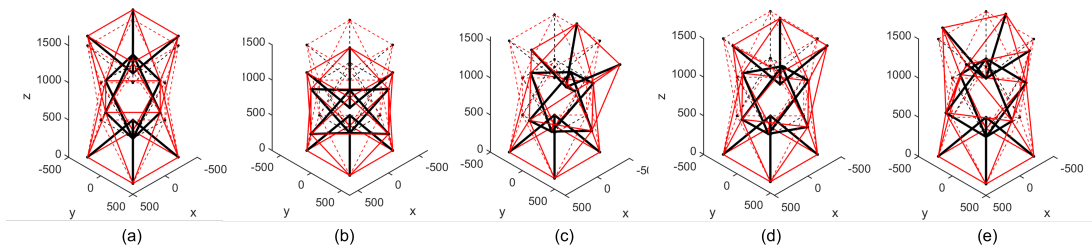


Figure 2: The energy-efficient cable-actuation strategy for the five shapes changes: (a) stretching, (b) shrinking, (c) flexure, (d) shear, (e) torsion. The solid and dotted lines represent the mode shapes and the initial configuration, respectively.

References

- [1] Fraddosio, A., Marzano, S., Pavone, G., Piccioni, M.D., 2017. Morphology and self-stress design of V-expander tensegrity cells. *Compos. B. Eng.* **115**:102–116.
- [2] Fraddosio, A., Pavone, G., Piccioni, M.D., 2019. Minimal mass and self-stress analysis for innovative V-expander tensegrity cells. *Compos. Struct.* **209**:754–774
- [3] Ma, S., Chen, M. and Skelton, R.E., 2022. Dynamics and control of clustered tensegrity systems. *Eng. Struct.* **264**:p.114391.

Subharmonic oscillations in PILine[®] ultrasonic motors

Simon Kapelke*

*Physik Instrumente (PI) GmbH & Co. KG, Karlsruhe, Germany

Abstract. PILine[®] ultrasonic motors belong to the group of standing wave ultrasonic motors and use certain eigenmodes of a piezoelectric actuator to generate motion. The motion of the actuator is transmitted to a moving slider by means of friction using a coupling element, which performs a high-frequency oblique or elliptical motion. Within this contribution, a typical noise phenomenon related to operation of standing wave ultrasonic motors is investigated by means of experimental observations and a model-based analysis of vibro-impact dynamics caused by the nonlinear interaction between coupling element and slider. After introducing the basic driving principle of standing wave ultrasonic motors and an appropriate model reduction, numerical parameter studies are carried out for the normal motion of the piezoelectric actuator. Depending on the chosen parameters, the results show significant subharmonic oscillations, which are in good agreement with the corresponding experimental observations.

Introduction

Although being commonly used in many different applications, ultrasonic motors can be very sensitive with respect to certain driving conditions, in particular when they are operated under open-loop conditions. Depending on the specific application, several undesired noise phenomena related to the operation of ultrasonic motors are known from literature, which are typically handled by using advanced driving or control techniques (e.g. [1]). However, improved understanding of the relevant dynamic processes is required in order to efficiently develop new ultrasonic motor and corresponding control structures.

Model-based investigations on ultrasonic motors are mostly carried out regarding their mechanical performance and neglecting the dynamics of the piezoelectric actuator (e.g. [2]). On the other hand, only few publications are known accounting for the nonlinear interaction between coupling element and slider as a possible mechanism for the onset of low-frequency vibrations (e.g. [3]). Within this contribution, subharmonic oscillations due to vibro-impact dynamics of the ultrasonic motor are discussed using experimental and model-based approaches.

Results and discussion

Under certain open-loop driving conditions, the PILine[®] experimental set-up under investigation generates a squealing noise although being operated in the ultrasonic frequency range. In order to investigate the corresponding dynamics, the normal motion of the piezoelectric actuator is measured using a *Polytec VibroFlex Xtra* laser vibrometer. The results contain significant vibrations below the ultrasonic excitation frequency f_e , which can be identified as subharmonic oscillations with base frequency $f_b = \frac{1}{n}f_e$.

For a corresponding model-based analysis, a simple model for the normal actuator motion y is given by

$$m\ddot{y} + d\dot{y} + c_A y + N = 0, \quad N = \begin{cases} c_P(y + a \sin \omega_e t - h), & \text{contact} \\ 0, & \text{separation} \end{cases} \quad (1)$$

Herein, m is the mass of the piezoelectric actuator, d and c_A are damping and stiffness properties of the normal actuator suspension and N is the normal contact force, which is determined using the local contact stiffness c_P . a and $\omega_e = 2\pi f_e$ are the excitation amplitude and angular frequency, respectively, and h corresponds to the location of the slider.

Over a wide range of parameters, the corresponding numerical results show decaying oscillations with a non-trivial frequency. Using an averaging approach to separate the slow system dynamics from the fast excitation, this non-trivial frequency can be identified as the natural frequency of an averaged system for the slow system dynamics. Herein, the non-smooth contact characteristics are replaced by an average normal contact force subjected to a smoothing effect due to the high-frequency excitation of the piezoelectric actuator. This kind of system behavior is considered as regular floating type operation of standing wave ultrasonic motors.

However, the numerical results also contain stable low-frequency solutions for certain parameters, which can be identified as subharmonic oscillations and show good qualitative agreement with the corresponding experimental results. In this case, the actuator performs a bouncing type normal motion, such that longer separation phases occur in contrast to the desired purely high-frequency motion. This behavior may cause the previously described undesired noise as well as reduced dynamics and performance of the ultrasonic motor.

References

- [1] B. Delibas and B. Koc, "A method to realize low velocity movability and eliminate friction induced noise in piezoelectric ultrasonic motors", *IEEE/ASME Transactions on Mechatronics*, vol. 25, pp. 2677–2687, 2020.
- [2] M.-S. Tsai, C.-H. Lee, and S.-H. Hwang, "Dynamic modeling and analysis of a bimodal ultrasonic motor", *IEEE Transactions on Ultrasonics, Ferroelectrics, and Frequency Control*, vol. 50, no. 3, pp. 245–256, 2003.
- [3] W. Wurpts and J. Twiefel, "Analysis of ultrasonic vibro-impact systems with equivalent circuits and the harmonic balance method", *Sensors and Actuators A: Physical*, vol. 200, pp. 114–122, 2013.

Nonlinear free vibration of functionally graded shallow shells with variable thickness resting on elastic foundations

Kurpa Lidiya*, Shmatko Tetyana**, Awrejcewicz Jan***, Timchenko Galina*

*Department of Applied Mathematics, National Polytechnic University "KhPI", Kharkov, Ukraine

**Department of Higher Mathematics, National Polytechnic University "KhPI", Kharkov, Ukraine

***Department of Automation, Biomechanical and Mechatronics, Lodz University of Technology, Lodz, Poland

Abstract. Geometrically nonlinear free vibration of the shallow shells of an arbitrary shape of the plan with variable thickness is studied. The shell is fabricated from functionally graded materials (FGM) and supported by elastic foundation. The refined shear deformation theory of the first order (FSDT) is used to obtain the theoretical formulation of the problem. Simple power law is applied to calculate the effective characteristics of the FGM in the thickness direction. Variation of the thickness of the shallow shells is carried out according to the given law: it can be linear, parabolic or another law. Elastic foundation is described by Pasternak's model. The proposed approach is based on application of the R-functions theory, variational Ritz's method, and procedure by Bubnov-Galerkin.

Introduction

From the analysis of the available literature, it can be concluded that there is a small number of publications in which the question of linear vibrations of the FGM shells with variable thickness, resting on an elastic foundation [1, 2], is studied. And there are practically no works on nonlinear vibrations of shallow shells of variable thickness, with complex shape in the plan. The present study focuses on these questions. The system of nonlinear equations of motion for FGM shallow shells is received using FSDT and Hamilton's principle. It is assumed that a plan form of the shell can be complex. Power law is used to calculate the effective material properties. Influence of the foundation is considered through relation $p_0 = K_w w - K_p \nabla^2 w$ [1].

Results and discussion

Proposed method is based on approach developed by authors earlier [3], which uses the R-functions theory [4] essentially. Validation of the suggested method and created software is made by comparison of the calculated results with known ones. New results for shallow shells with square and complex shape of the plan were obtained. For example, backbone curves for clamped (CL) and simply supported (SS) FGM (Al/Al₂O₃) square cylindrical shells ($a/R_x = 0.2, a/R_y = 0$) with parabolic [2] $h(x, y) = h_0 \left(1 - \alpha \left(x/a\right)^2\right)$ ($\alpha = 0.5$) and constant thickness ($\alpha = 0$) are presented in Fig 1, 2. Behaviour of the nonlinear frequencies is shown in Fig.3.

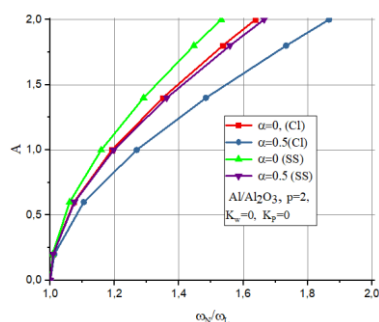


Figure 1: Backbone curves of cylindrical shell ($K_w=0, K_p=0$)

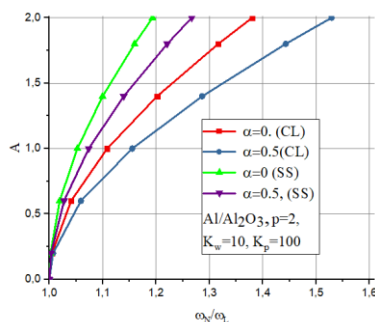


Figure 2: Backbone curves of cylindrical shell ($K_w=10, K_p=100$)

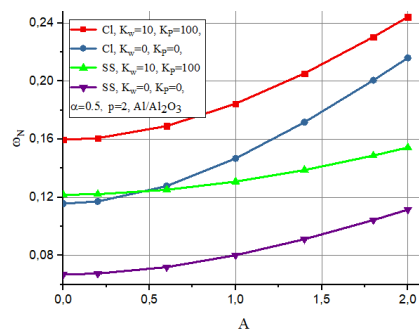


Figure 3: Nonlinear frequencies of cylindrical shell

As expected, the greatest increase in nonlinear frequencies is observed for clamped shells. Decreasing the parameter α increases the thickness of the shell and, consequently, increases the value of the frequencies.

References

- [1] Shen H-S, Wang H. (2014) Nonlinear vibration of shear deformable FGM cylindrical panels resting on elastic foundations in thermal environments. *J. Composites: Part B* **60**: 167-177.
- [2] Kumar V., Singh S.J., Saran V.H., Harsha S.P. (2022) Vibration response of shear deformable functionally graded material plate with parabolic variable thickness. *IOP Conf. Series: Mater. Sci. Eng.* **1248** 012069 doi:10.1088/1757-899X/1248/1/012069.
- [3] Kurpa L., Shmatko T., Timchenko G. (2021) Nonlinear dynamic analysis of FGM sandwich shallow shells with variable thickness of layers. *Nonlinear Mechanics of Complex Structures*, Advanced Structured Materials, H. Altenbach et al. (eds.), **157**: 57-74.
- [4] Rvachev V.L. (1982) The R-functions theory and its applications. Kiev: Nauk. Dumka (in Russian).

Free vibration analysis of functionally graded porous sandwich plates with a complex shape

Shmatko Tetyana*, Kurpa Lidiya**, Lacarbonara Walter***

*Department of Higher Mathematics, National Polytechnic University "KhPI", Kharkiv, Ukraine

**Department of Applied Mathematics, National Polytechnic University "KhPI", Kharkiv, Ukraine

***Department of Structural and Geotechnical Engineering, Sapienza University of Rome, Italy

Abstract. Free vibration analysis of geometrically nonlinear FGM sandwich porous plates of different shape and boundary conditions are studied. The face layers are composed of FGM (mixture of metal and ceramics) and the isotropic core is made of ceramics. The employed mathematical model is framed in the context of the first order shear deformation theory (FSDT). The power-law model is applied to determine the effective material properties of the structure. The R-functions theory combined with variational Ritz's method are used to carry out the free vibration analysis of porous sandwich plates. The natural frequencies of porous FGM sandwich plates are studied upon variation of the porosity to appreciate the underlying frequency linear shifts. New results for plates of complex shape with a hole are reported. The effects of the porosity volume fraction, the porosity models, the type of FGM, the layout of layers, boundary conditions on the linear and nonlinear frequencies are investigated.

Introduction

Functionally graded materials are new types of composite materials that have been extensively applied in many manufacturing processes in the last decades. These materials made of alloys of metal and ceramics do not typically suffer the stress discontinuity that is observed in multi-layered composites. Use of the FG sandwich structures allows to solve some mechanical problems since the gradual variation of material properties is attained at the interfaces between the core and face layers. Porosities and micro-voids are technical challenges rising out of the manufacturing process which lead to a reduced mechanical performance of FGM. That is why this issue has motivated wealth of theoretical and practical studies [1]. In this paper FSDT is used to investigate linear and geometrically nonlinear vibrations of porous FGM sandwich plates endowed with different shapes and boundary conditions.

Results and discussion

The proposed method consists of three steps. The linear vibration problem is solved in the first step. To solve this problem the R-functions theory [2] combined with the Ritz method are employed in a distinctively new approach. The main advantage of the R-functions theory is the possibility of constructing admissible functions in analytical form practically for an arbitrary domain. The eigenvalues and eigenfunctions found in analytical form are employed in the second step. Solution of the auxiliary inhomogeneous task of elasticity problem allows to reduce the initial system of PDEs to the following nonlinear second order ODE:

$$\ddot{y}_1(t) + \omega_L^2 y_1(t) + y_1^2(t)\beta + y_1^3(t)\gamma = 0. \tag{1}$$

The solution of equation (1) is carried out in the third step, both numerically via the 4th order Runge-Kutta integration method and analytically by the method of multiple scales. The values of the coefficients in equation (1) are obtained in analytical form as integrals above given domain [2]. Figure 1 demonstrates effect of the porosity on frequency (linear and nonlinear) for Al/Al₂O₃ sandwich plate with different layout of layers.

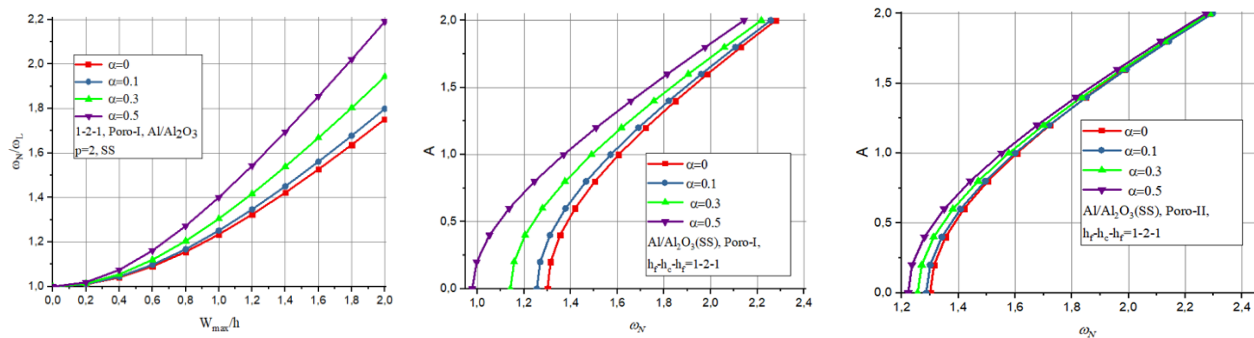


Figure 1: Linear and nonlinear frequencies of Al/Al₂O₃ sandwich plate with different layout of layers and type of porosity α

References

- [1] Daikh A.A., Zencour A.M. (2019) Free vibration and buckling of porous power-law and sigmoid functionally graded sandwich plates using a simple higher-order shear deformation theory. *Mater/Res/Express* 6 115707.
- [2] Awrejcewicz J., Kurpa L., Shmatko T. (2018) Linear and nonlinear free vibration analysis of laminated functionally graded shallow shells with complex plan form and different boundary conditions. *J. Non-linear Mechanics*. **107**: 161-169.

Effect of Boundary Conditions on the Stability of a Viscoelastic Von Mises Truss

Pritam Ghoshal*, Qianyu Zhao*, James Gibert* and Anil K. Bajaj *

*Ray W.Herrick Laboratories, School of Mechanical Engineering, Purdue University, IN, USA

Abstract. This research aims to analyze the stability of bi-stable dome-shaped structures represented as a lumped parameter viscoelastic Von Mises Truss under different boundary conditions. Traditionally, the stability of these lumped parameter systems has been studied under pin-pinned boundary conditions. However, a closer investigation of the deformation of the dome reveals that the contact between the dome and the surface is not fixed. Instead, it slides outwards as the dome is indented. This phenomenon raises the question of whether the stability will alter if the boundary conditions are altered. With this motivation, we explore two alternate boundary conditions: 1) symmetric and 2) asymmetric. We demonstrate how relaxing or constraining the contact surface leads to change in the bifurcation point. This work allows us to gain some fundamental insights in modeling and controlling the spatiotemporal behavior of biological and engineering structures.

Introduction

The study of viscoelastic domes has mainly been limited to either experiments or finite element simulations. Recently, Gomez et al. [1] studied the stability and dynamics of a viscoelastic dome represented as a lumped parameter Von Mises truss. They analyzed the dynamics in the pseudo-bistable region using the method of multiple scales and derived an analytical expression for the snapping time. Liu et al. [2] used a similar lumped parameter system to study the effect of dimple-shaped imperfections on the stability of viscoelastic domes. However, most treatments of these systems using lumped parameter models consider pin-pinned boundary conditions and do not take into account the sliding of the dome as it is indented. If the dome were to be connected to another structure, then the manner in which the joint between the dome and the structure is implemented would dictate the boundary conditions of the dome. This motivates us to explore alternate boundary conditions. Here we study two alternate boundary conditions: 1) where both the pin joints in the conventional system are replaced by sliders (Figure 1(a)), and 2) an asymmetric boundary condition, where only one of the pin joints is replaced with a slider. We also study how friction at the sliders influences the stability of the system.

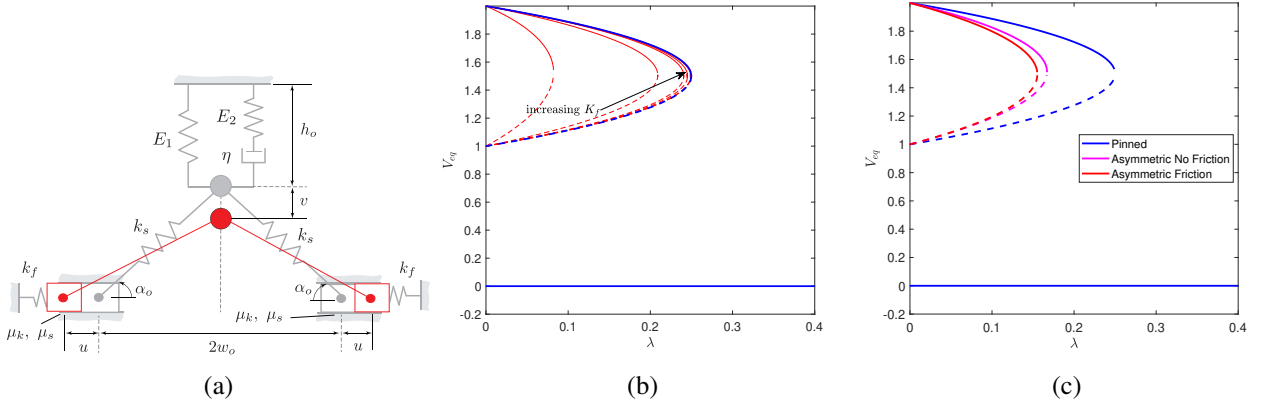


Figure 1: (a) Schematic of Von Mises Truss in undeformed or natural configuration (gray) and deformed configuration (red), (b) Equilibrium points (V_{eq}) of system in (a), plotted against the bifurcation parameter (λ), i.e. the relative stiffness between the viscoelastic element and the truss's central springs, for various horizontal spring stiffness (K_f), and (c) Bifurcation diagram for the system with asymmetric boundary condition, with and without friction, compared against the conventional system with pin-pinned boundary condition. Solid lines indicate stable equilibrium points. Dashed lines indicate unstable equilibrium points.

Results and Discussion

The parameter value at bifurcation (λ_b) varies non-linearly with the horizontal spring stiffness (K_f). With increase in horizontal spring stiffness, the equilibrium points converge to those of the conventional system as shown in Figure 1(b). The influence of the asymmetric boundary condition on the equilibrium points of the truss is shown in Figure 1(c). We find that when the boundary conditions are relaxed, the bifurcation occurs at a lower parameter value. Friction at the sliders also causes the system to bifurcate at a lower parameter value.

References

- [1] Gomez M., Moulton D.E., Vella D. (2019) Dynamics of viscoelastic snap-through. *J. Mechanics and Physics of Solids* **124**:781-813.
- [2] Liu T., Chen Y., Liu L., Liu Y., Leng J., Jin L. (2021) Effect of imperfections on pseudo-bistability of viscoelastic domes. *Extreme Mechanics Letters* **49**:101477.

An Origami Inspired Impact Energy Dissipator

Ahmed S. Dalaq*, Shadi Khazaaleh* and Mohammed F. Daqaq *

*Engineering Division, New York University Abu Dhabi (NYUAD), Saadiyat Island, UAE

Abstract. A bio-inspired Origami pattern known as the Kresling pattern can make a versatile spring that is capable of exhibiting linear, nonlinear, and bistable behavior. One of the most notable yet often overlooked attributes of this Kresling Origami spring (KOS) is its kinematics that intrinsically couples the translation and rotational degrees of freedom. We employ this attribute in the design of an energy dissipating column that transmits incident energy (loads and impacts) into rotational motion at the base of the column, that is then dissipated by dry friction. The amount of energy dissipation can be tuned by adjusting the geometric design parameters of the KOS, the friction coefficient at the base, and/or the stroke distance.

Introduction

Countless architectures emerge in nature as a result of evolutionary processes occurring at several length scales. In the entima of Hawk moths (*Acherontia atropos* [1]), lies an intricate corrugation-like architecture that is related to an Origami pattern known as the Kresling pattern. Among the many different applications inspired by this unique pattern, engineers have proposed its utilization as a nonlinear tunable spring for niche applications including locomotion, switching, vibration isolation, and impact absorption [2,3]. One key yet often overlooked attribute of a Kresling spring is its unique kinematics which intrinsically couples translational and rotational motions by a process of folding at the interfaces between the panels forming the spring [2]. Combining this attribute with recent advances in computational modeling [1] and fabrication [3] permits designing compact devices for energy capture and transfer that were, otherwise, made of bulky cams, gears, springs and traditional mechanical elements. Herein, we exploit this translation-rotational coupling to design origami-inspired impact absorbing columns made of a stack of Kresling springs, particularly intended to convert incident pulse loads or displacements into in-plane rotation. The rotational energy is then dissipated through dry-friction pads mounted at the base of the column (Fig. 1a). We develop analytical and computational models to capture the response of the proposed impact absorber and tune its behaviour to maximize energy dissipation as function of *i*) the number of stacked Kresling units in the column, *ii*) the individual geometric properties of the unit, and *iii*) the geometry and size of the base. An optimum design is then fabricated and tested for assessment of its intended function and performance.

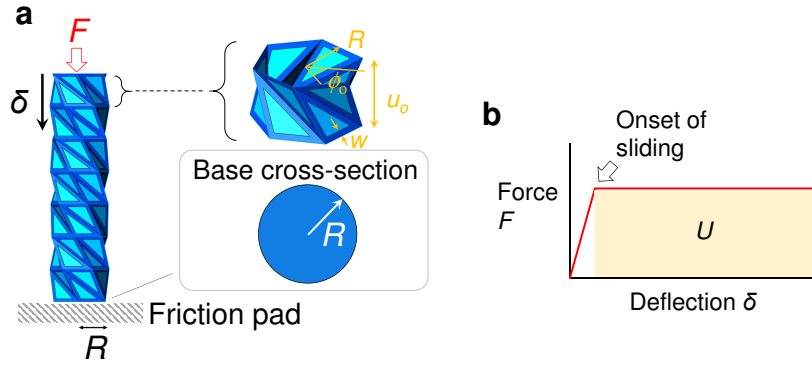


Figure 1: (a) Origami based column; (b) typical force-deflection curve as a response to incident loads.

A short note on the mechanical response

The response of a Kresling based column made of N units depends on the geometric parameters of the Kresling unit, namely, radius R , relative angle ϕ_o , height u_o , flexible frame width w , and panel thickness t . Those parameters (u_o/R , ϕ_o , w/t) define the mechanical response prior to the onset of sliding. After the onset of sliding, the friction coefficient between the friction pad and the base solely dictates the ensuing force-deflection response, provided that the developed shear forces at the base maintain sliding friction during which energy U is dissipated (shaded region in Fig. 1b). The dissipated energy scales with the number of unit cells; i.e. ($U \propto N$).

References

- [1] Kresling B. (2020) The Fifth Fold: Complex Symmetries in Kresling-origami Patterns. *J. Symmetry: Culture and Science* **31**:403-416.
- [2] Dalaq A. S., Daqaq M. F. (2022) Experimentally-validated computational modeling and characterization of the quasi-static behavior of functional 3D-printed origami-inspired springs. *J. Materials Design* **16**:110541.
- [3] Khazaaleh S., Masana R., Daqaq M. F. (2022) Combining advanced 3D printing technologies with origami principles: A new paradigm for the design of functional, durable, and scalable springs. *J. Composites Part B: Engineering* **236**:109811.

Accurate asymptotic description of nonlinear friction states for a detailed FEM model

Salvador Rodríguez-Blanco*, Javier González-Monge* and Carlos Martel *

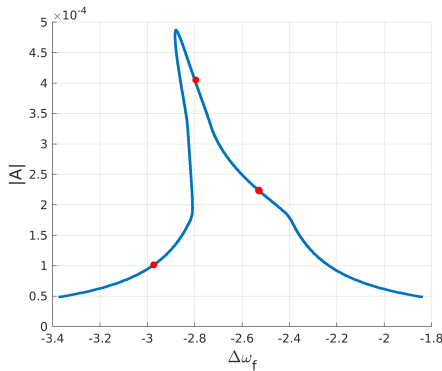
*Department of Applied Mathematics to Aerospace Engineering, Universidad Politécnica de Madrid, Madrid, Spain

Abstract. This work presents a novel asymptotic method that drastically reduces the computational effort to determine the dynamical behaviour of cantilever slender structures with nonlinear friction at the attachment. The resulting resonance curve for these structures, despite of being frequently computed using a high fidelity finite element model, looks very similar to that from a one dimensional nonlinear oscillator. Therefore, using asymptotic techniques we derive an equivalent one dimensional nonlinear model that captures the physics of the problem in the time scale of interest. The computation of the nonlinear resonance curve with this asymptotic model is reduced to the evaluation of a simple analytical expression, and it shows a very good agreement with full nonlinear FEM simulations.

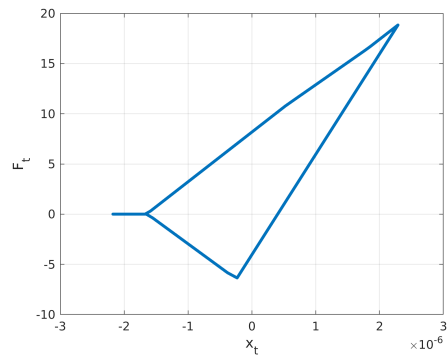
Introduction

The accurate computation of the dynamical response of a bladed-disk system usually requires finite element models with millions of degrees of freedom. Each sector presents nonlinear friction effects at the contact interfaces, which are crucial to correctly determine the response of the system but only affect a very small subset of degrees of freedom [1]. These effects produce the dissipation that saturates the vibration amplitude of the system produced by an instability (flutter) or by external excitation close to a resonant frequency (forced response). Since nonlinear friction is small, the system is numerically stiff, and the integration over a large number of elastic cycles is required for the system to converge. However, even when using a highly detailed FEM model, the resonance curve for a cantilever blade with nonlinear friction effects at its root looks similar to that of a one dimensional nonlinear oscillator.

The most commonly used reduction techniques rely on the restriction of the motion of the structure to a finite set of modes (e.g., Craig-Bampton [2]). Nevertheless, the approach in this work is quite different, and it is based in asymptotic perturbative techniques that have already been successfully applied to mass-spring models [3]. Using the fact that nonlinear friction is a small effect, we separate the system into two time scales: a fast one, which corresponds to the oscillations with the elastic frequency of the blade; and a slow modulation, where the effect of nonlinear friction at the contact interfaces is relevant. This method is suited for slender structures with nonlinear friction effects at the attachment, like cantilever blades in a turbomachinery bladed-disk.



(a) Resonance curve computed using the asymptotic model. The red dots are full order model solutions.



(b) Friction cycle of one of the contacts with stick-slip transitions and gap-contact states.

Results and discussion

The complete FEM equations of a detailed structure is reduced to an equivalent one dimensional nonlinear equation. In particular, we apply these techniques to the forced response of a simplified blade like model with a stick-slip friction law and contact-gap configurations (see Fig. 1b). The resonance curve computed from the asymptotically reduced one dimensional equation is shown in Fig. 1a, which just requires the evaluation of an analytical expression. The model is able to capture highly nonlinear effects and shows a very good agreement with the full model, which requires several hours to converge each point in the resonance curve in Fig. 1a.

References

- [1] Petrov, E. P. and Ewins, D. J., "State-of-the-art dynamic analysis for non-linear gas turbine structures" (2004) *Proceedings of the Institution of Mechanical Engineers, Part G: Journal of Aerospace Engineering*, Vol. 218, No. 3, pp. 199-211, <https://doi.org/10.1243/0954410041872906>.
- [2] Craig, R. R. and Bampton, M. C. C., "Coupling of substructures for dynamic analyses" (1968) *AIAA Journal* Vol. 6, No. 7, pp. 1313-1319, <https://doi.org/10.2514/3.4741>.
- [3] Martel, C. and Corral, R. "Asymptotic Description of Maximum Mistuning Amplification of Bladed Disk Forced Response" (2009) *J Eng Gas Turb Power*, Vol. 131, <https://doi.org/10.1115/1.2968868>.

Comparison between Pushover Methods for Seismic Analysis High-Rise RC Dual System Buildings

Vinod Kumar Golla*, Elena Oliver-Saiz* and Francisco López-Almansa*

*Architecture Technology Department, Universitat Politècnica de Catalunya – BarcelonaTech, Barcelona, Spain.

Abstract. Seismic design of RC high-rise buildings is commonly performed with simplified pushover strategies. The conventional pushover methods have added great acceptance and have become a standard tool for seismic assessment in many codes. However, for high-rise buildings, the high-mode effect is so substantial that the conventional method does not estimate the seismic demand fairly. Therefore, several modal and adaptive pushover methods have been proposed. This paper aims to compare nine representative Non-linear Static Procedures (NSP) with Nonlinear Time-History Analyses (NLTHA) for high-rise RC dual system buildings and propose modifications oriented to improve their use in this type of structure. In seismic design, dual systems are commonly used to resist the lateral load, being composed of shear walls and frames, these are convenient because of the possibility of controlling the drift at both top and bottom stories, their high structural redundancy, and several architectural advantages.

Introduction

According to previous studies [1] the conventional nonlinear static procedures [2] are somehow unable to consider the higher mode effects. To overcome these limitations and deficiencies, numerous multi-mode pushover analysis methods have been developed: Modal Pushover Analysis [3], N2 [4], Consecutive Modal Pushover Analysis [5], Adaptive Pushover Analysis [6], and Spectrum-based Pushover Analysis [7], among others. Previous studies [2-4,6] have shown that the applicability of such methods, which are preliminarily developed for frame structures, is not guaranteed for other structural configurations. However, only few studies have investigated the accuracy and applicability of pushover analysis in the quick seismic demand calculation of shear wall and wall-frame structures [6]. Furthermore, most of these multi-mode pushover methods cannot efficiently estimate the seismic demands of frame structures with sufficient accuracy. Hence there is still a need for developing an accurate and efficient method for predicting the seismic demand of high-rise dual system buildings. In the current study, four prototype dual system 30 and 45-storey buildings (B30A, B30B, B45A, B45B), are designed for the site location of Delhi; they are modelled in OpenSees software.

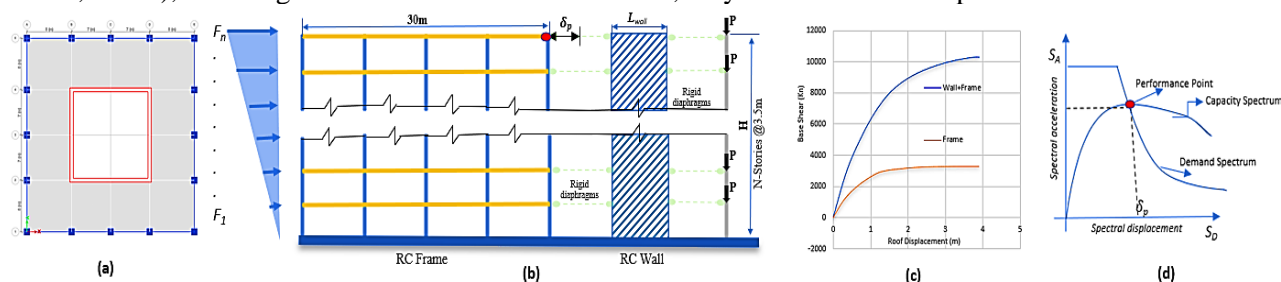


Fig. **a.** Plan layout of the prototype buildings, **b.** 2D Dual wall-frame system on the right of the RC wall, the leaning column is shown, **c.** Pushover curve for the B45A prototype building, **d.** Determination of a performance point.

Results and discussion

This paper presents a numerical study about the reliability of pushover analyses (conventional, modal, and adaptive) for high-rise RC dual system buildings. The study consists of comparing the results of four 30 and 45-storey representative prototype dual system buildings with nonlinear dynamic analyses for several representative seismic records. Although Modal Pushover and Adaptive Pushover methods perform better than the conventional pushover methods, there are still some concerns regarding high-rise dual system buildings.

References

- [1] Krawinkler H, Seneviratna GDPK. 1998. Pros and cons of a pushover analysis of seismic performance evaluation. *Engineering Structures*. **20**(4-6):452-464.
- [2] FEMA 356. 2000. Prestandard and Commentary for the Seismic Rehabilitation of Buildings. *Federal Emergency Management Agency*.
- [3] Chopra AK, Goel RK. 2002. A modal pushover analysis procedure for estimating seismic demands for buildings. *Earthquake Engineering & Structural Dynamics*. **31**(3):561-582.
- [4] Fajfar P, Gasperic P. 1996. The N2 method for seismic damage analysis of RC buildings. *Earthquake Engineering & Structural Dynamics*. **25**:31-46.
- [5] Poursha M, Khoshnoudian F, Moghadam AS. 2009. A consecutive modal pushover procedure for estimating the seismic demands of tall buildings. *Engineering Structures*. **31**(2):91-599.
- [6] Papanikolaou V, Elnashai AS. 2005. Evaluation of conventional and adaptive pushover analysis. I: Methodology. II: Comparative results. *Journal of Earthquake Engineering*. **9**(6).
- [7] Yang L, Kuang JS. 2017. Spectrum-based pushover analysis for estimating seismic demand of tall buildings. *Bulletin of Earthquake Engineering*. **15**:4193-214.
- [8] IS 1893. 2016. Criteria for Earthquake Resistant Design of Structures. *Bureau of Indian Standards*.

Oscillations of a Nonlinear Beam in Contact with a Rigid Cylindrical Constraint

Diptangshu Paul* and K. R. Jayaprakash*

* Discipline of Mechanical Engineering, Indian Institute of Technology Gandhinagar, Gujarat, India

Abstract. In this work we consider the free oscillations of a fixed-free nonlinear Euler Bernoulli beam in contact with a rigid cylindrical constraint. In addition to the geometric nonlinearity due to deformation, the unilateral constraint introduces nonlinearity due to change in effective beam length as it deforms. We explore the existence of nonlinear normal modes (NNMs) and their dynamics in this dynamical system invoking the Galerkin method, method of averaging and FE methods.

Introduction

Energy dependent frequency of oscillations of a pendulum is well known. Owing to Huygens (1656) ingenuity of varying the effective length of string as it wraps/unwraps around (cycloidal) foundation, the oscillations were rendered isochronous. In the late twentieth century, researchers started investigating the dynamics of flexures as they wrap/unwrap around obstacles. Fung et al. [1] considered Euler-Bernoulli beam with rigid cylindrical foundation on one side and investigated the effect of the resulting nonlinear transversality condition. Crespo da Silva et al. [2] developed a nonlinear Euler-Bernoulli beam model with inextensibility constraint and explored the free and forced nonlinear oscillations and the resonances thereof. In the current study we consider the nonlinear beam [2,3] coming into contact with a unilateral cylindrical constraint (Fig. 1).

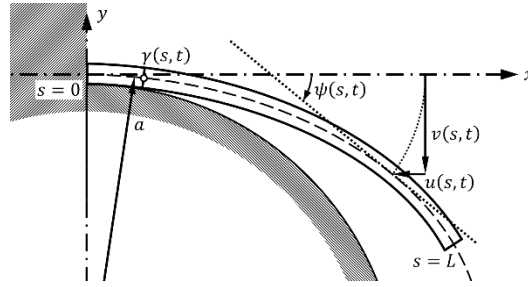


Figure 1: Kinematics of the nonlinear beam.

Discussions

To study the conservative dynamics of the beam, we use the principle of noncontemporaneous variation resulting in the governing equation Eq. (1), where notations and symbols have usual meaning. In this study we consider point-wise inextensibility of the beam and introduce Lagrange multiplier to incorporate the corresponding constraint. Considering a fixed-free boundary condition, the beam wraps around the cylinder such that u and v conform to the constraint $(s + u)^2 + (a + v)^2 = a^2$ over the region $0 \leq s \leq \gamma(t)$. The axial force in the beam over this domain is constant and is equal to $F = -EI v_{sss}(\gamma(t)) v_s(\gamma(t))$. However, the axial force (Eq. (2)) in the subsequent domain $\gamma^+(t) < s \leq L$ is time varying such that the force at the free end is zero. In essence, such a varying axial force is required to maintain the overall inextensibility of the beam.

$$\rho A v_{tt} + EI v_{sss} + EI \{v_s(v_s v_{ss})\}_s + \frac{\rho A}{2} \left\{ v_s \int_L^s \left(\int_0^s v_s^2 ds \right)_{tt} ds \right\}_s = 0 \quad (1)$$

$$F = -EI v_{sss} v_s - \frac{\rho A}{2} \int_L^s \left(\int_0^s v_s^2 ds \right)_{tt} ds \quad (2)$$

The transversality condition to be satisfied at the last point of contact ($\gamma(t)$) corresponds to the difference between a combination of v_{sss} and its lower derivatives before and after this point of contact. Owing to the complexity of the problem, our analytical study considers a combination of Galerkin method, method of averaging and finite element methods to explore the existence of nonlinear normal modes [4,5] and their stability thereof.

References

- [1] Fung R. F., Chen C. C. (1997) Free and Forced Vibration of a Cantilever Beam Contacting with a Rigid Cylindrical Foundation. *J. Sound Vib.* **202**(2):165-185.
- [2] Crispo da Silva M. R. M., Glynn C.C. (1978) Nonlinear Flexural-Flexural-Torsional Dynamics of Inextensional Beams. II. Forced Motions. *J. Struct. Mech.* **6**(4):449-461.
- [3] Nayfeh A. H., Pai P. F. (2004) Linear and Nonlinear Structural Mechanics. Wiley-VCH, Weinheim.
- [4] Nayfeh A. H., Chin C., Nayfeh S. A. (1995) Nonlinear Normal Modes of a Cantilever Beam. *J. Vib. Acoust.* **117**(4):477-481.
- [5] Vakakis A. F., Manevitch L. I., Mikhlin Y. V., Pilipchuk V. N., Zevin A. A. (1996) Normal Modes and Localization in Nonlinear Systems. John Wiley, NY.

Origami Inspired Impact Energy Converter

Shadi Khazaaleh^{1,2}, Ahmed S. Dalaq¹ and Mohammed F. Daqaq^{1,2}

¹Engineering Division, New York University Abu Dhabi (NYUAD), Saadiyat Island, UAE

²Department of Mechanical and Aerospace Engineering, Tandon School of Engineering, NYU, Brooklyn, NY, USA

Abstract. Springs made by employing the Kresling origami pattern have various unique characteristics that can be tailored by simply tuning their geometrical design parameters. One of these characteristics is the ability of these springs to behave as a simple coupling mechanism that transforms translational motion into rotational motion and vice versa. We exploit this coupling feature to design a structure that can effectively convert the energy incident by an axial load into a rotational energy which can be harnessed through a rotary energy harvester consisting of a magnetic mass inside an induction coil.

Introduction

Over the past few years, origami has inspired the design and fabrication of various structures and materials with unique mechanical characteristics that are useful in many engineering applications. Specifically, the Kresling pattern is a class of non-rigid origami patterns which is used for building springs having several favourable attributes, such as tunable stiffness, multistability, translation-rotation motion coupling, and quasi-zero-stiffness (QZS) to name a few [1, 2]. In this work, we utilize the translation-rotation coupling feature of the Kresling origami springs (KOS) for applications in energy conversion and harvesting. In particular, the special kinematics of the KOS transforms translational motions applied at one end into rotational motions at the other end. The rotational energy can then be exploited by attaching an energy conversion mechanism, such as a harvester, at the base. The amount of energy that is harnessed is proportional to the change in magnetic flux, which, in turn, is proportional to the angular velocity of the magnet rotation inside the coil. Figure 1a shows a schematic of the proposed harvester. To study the dynamic behaviour of the KOS under loading across the design space defined by its main design parameters, we build a computational model, based on finite element methods (FEM) [3], using COMSOL Multiphysics. Simulations are carried out to find the optimum design that maximizes angular velocity and energy conversion efficiency. The results are validated by experimental measurements using an Instron universal testing machine (UTM) and an in-house built impact testing setup. Tested samples are fabricated by multimaterial 3D printing using a polyjet printer (Stratasys J750). Finally, the optimum performing design is used to construct the harvester, and energy conversion is demonstrated experimentally by attaching a magnetic mass and an induction coil at the base.

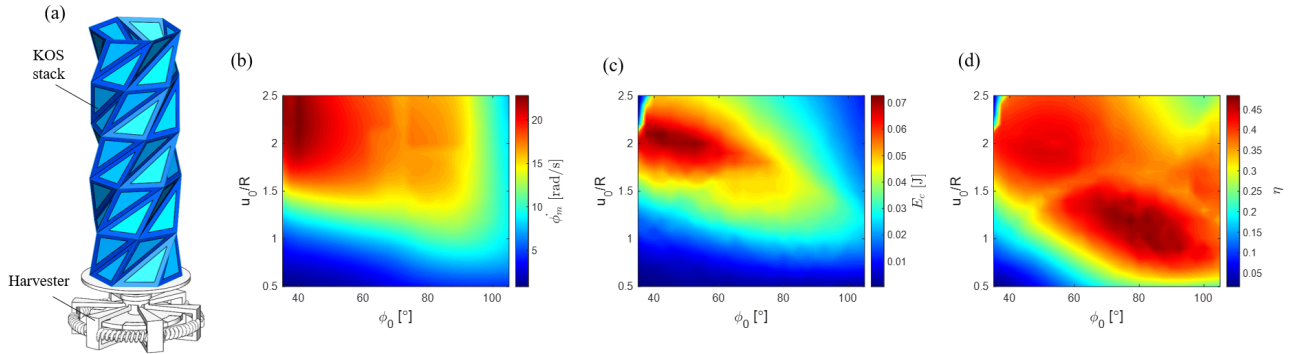


Figure 1: (a) Schematic of KOS stack with energy harvester, and simulation results showing contour maps of (b) peak angular velocity, (c) converted energy, and (d) conversion efficiency.

Results and Discussion

Simulation results shown in figures 1b-1d depict contour maps of the peak angular velocity, $\dot{\phi}_m$, converted energy, E_c , and conversion efficiency, η , across the design space. We fabricated and tested several designs scattered throughout the design space, and compared their behaviour with the simulations, which showed good agreement.

References

- [1] Kresling B. (2020) The Fifth Fold: Complex Symmetries in Kresling-origami Patterns. *J. Symmetry: Culture and Science* **31**:403-416.
- [2] Khazaaleh S., Masana R., Daqaq M. F. (2022) Combining advanced 3D printing technologies with origami principles: A new paradigm for the design of functional, durable, and scalable springs. *J. Composites Part B: Engineering* **236**:109811.
- [3] Dalaq A. S., Daqaq M. F. (2022) Experimentally-validated computational modeling and characterization of the quasi-static behavior of functional 3D-printed origami-inspired springs. *J. Materials & Design* **16**:110541.

Nonlinear dynamics of a visco-elastic beam under pulsating dead and follower forces

Francesco D'Annibale*, Manuel Ferretti* and Angelo Luongo*

*Department of Civil, Construction-Architectural and Environmental Engineering, University of L'Aquila, L'Aquila, Italy

Abstract. The effects of the interaction between pulsating dead and follower forces on the linear and nonlinear behaviours of a cantilever visco-elastic beam are discussed in this research work. The beam is modelled as an inextensible and shear-undeformable one-dimensional polar continuum, that is loaded at the free end by both periodically varying in time dead and follower forces. Linear and nonlinear stability analyses of the trivial rectilinear configuration are performed via asymptotic and numerical methods. The effects of the combined load actions on the critical response, i.e. on the stability threshold, and on the post-critical behaviour, i.e. on the limit-cycle amplitude, are detected and discussed.

Introduction

The dynamic stability and the nonlinear analysis of structures under the action of pulsating loads, and follower forces, has been the object of several studies in the literature [1,2]. Due to these actions, different dynamic interesting phenomena may arise, also including: simple and circulatory Hopf bifurcations [2-4], damping destabilization paradox [2], double-zero bifurcation [5], parametric excitation inducing instability [1], super- and sub-critical limit-cycles, hard loss of stability and quasi-periodic motion.

However, although all these kind behaviours have been in-depth analysed when a single action, dead or follower, is applied, periodically varying in time or constant, less attention has been devoted to the interaction phenomena, on both the linear and nonlinear fields, occurring when these kinds of actions are simultaneously applied.

This research line is framed in previously mentioned context, and aims to shed the light on the above discussed interaction phenomena, by analysing the linear and nonlinear dynamics of a clamped visco-elastic Beck's beam (sketched in Fig. 1), loaded by two type forces: i) a dead load, whose intensity is periodically varying in time; ii) a follower force, keeping its direction tangent to the axis line, whose intensity consists of a constant plus a periodically varying part. The analysis is carried out through asymptotic and numerical approaches, grounded Multiple Scale Method and Finite Difference Method, respectively.

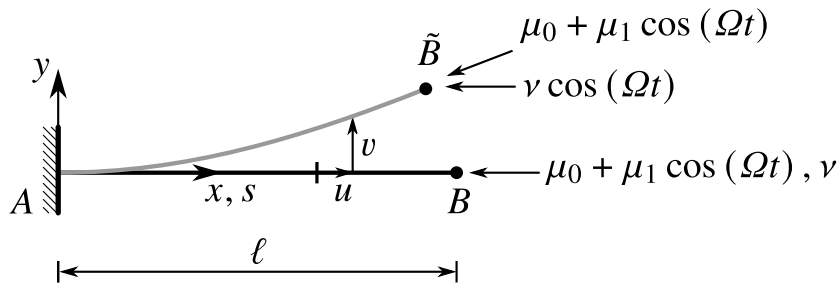


Figure 1: Clamped beam under the action of pulsating dead and follower forces.

Results and discussion

The main results of this work can be summarized in: (i) the asymptotic and numerical detection of the stability charts and (ii) of the bifurcation equations, governing the dynamics around the simple Hopf bifurcation; (iii) the analysis of the limit-cycle amplitude, arising in the post-critical regime. The effects of the interaction between dead and follower parametric excitations have been discussed both in the linear and nonlinear field, thus finding safe and dangerous loading conditions, with respect to the overall dynamic behaviours.

A good agreement between the asymptotic results and the numerical solutions has been detected, thus entailing that the developed multiple-scale algorithm is an effective tool in analysing the linear and nonlinear behaviours.

References

- [1] Bolotin V.V. (1964) The dynamic stability of elastic systems. Holden-Day, SF.
- [2] Bolotin V.V. (1963) Nonconservative problems of the theory of elastic stability. Macmillan, NY.
- [3] Beck M. (1952) Die Knicklast des einseitig eingespannten, tangential gedrückten Stabes. *Z Angew Math Phys* **3**(3):225-228.
- [4] Luongo A., D'Annibale F. (2017) Nonlinear hysteretic damping effects on the post-critical behaviour of the visco-elastic Beck's beam. *Math Mech Solids* **22**(6):1347-1365.
- [5] Luongo A., D'Annibale F. (2013) Double zero bifurcation of non-linear viscoelastic beams under conservative and non-conservative loads. *Int. J. Nonlin Mech* **55**:128-139.

Rocking Dynamics of Mud Motor Drilling using a Cosserat Rod Model

Meet A. Mehta*, and R. Ganesh*

*Department of Mechanical Engineering, Indian Institute of Technology Bombay, Mumbai 400076, India

Abstract. “Rocking the pipe” is employed as a technique to reduce static friction while drilling oil wells with a mud motor. In this work, we investigate the dynamics of pipe rocking in the presence of drillpipe-wellbore clearance using Cosserat rod theory. The numerical results for a single frequency rocking input at the surface show that the system behavior is inherently nonlinear: the downhole section undergoes coupled rotational and lateral motion due to frictional contact interaction, and their characteristics are dependent on the frequency and amplitude of the rocking input. These results demonstrate that “rocking the pipe” can result in excitation of lateral vibrations in the downhole tool, which needs to be taken in to account while designing optimal rocking regimes to ensure smooth drilling.

Introduction

Directional drilling for oil wells can be accomplished by slide drilling, wherein a mud motor which converts hydraulic power to mechanical torque is used as the power source. A drawback of slide drilling is its low efficiency, due to drag losses as a result of axial sliding along the wellbore. One possible solution is to “rock the pipe” at the surface, so that a portion of the drillpipe remains in dynamic contact with the wellbore thereby reducing friction. However, this rocking motion must be designed carefully and not transmitted to the bit, as that can lead to loss of directional control. Many researchers have explored optimal rocking regimes in slide drilling, using empirical studies based on measured field data [1], as well as linear models that consider the axial and torsional dynamics of the drillpipe [2]. However, the nonlinearity associated with the drillstring-wellbore contact is seldom considered. While the Kirchhoff rod model [3] is the most prominent method to incorporate the nonlinear contact dynamics, we consider the Cosserat rod model in our study, in order to leverage existing computational packages available for simulating the dynamics of Cosserat rods [4]. To model drillstring dynamics, we developed an algorithm to account for cylindrical contact in the software, and the salient results obtained for a sinusoidal rocking input are shown in Fig. 1.

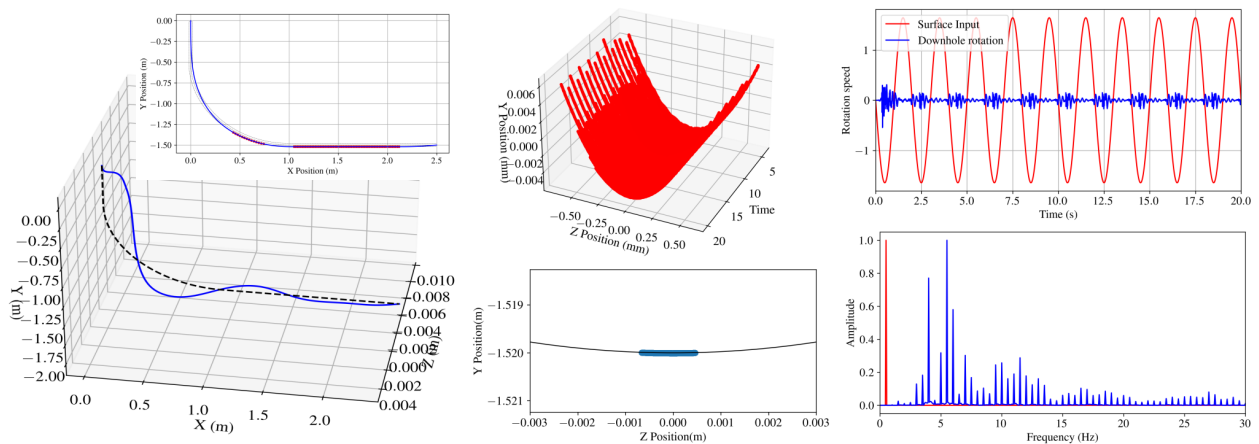


Figure 1: Dynamics of drillpipe in a curved wellbore with clearance, subjected to a rocking input at the surface. The leftmost plot shows the deformation at the end of the simulation, and the inset shows the region of the drillpipe in contact with the wellbore (as highlighted (in red) in the inset figure, which shows the planar projection of the deformed shape). The middle plots show the time history of motion of the cross-section of the drillstring in the horizontal section. The rightmost plots compare the amplitude and frequency of the rotation speed at the surface and downhole for the rocking input.

Results and Discussion

The leftmost plot in Fig. 1 shows that the static deformation of the drillpipe in a curved wellbore with clearance is non-planar, with only a part of the drillpipe being in contact with the wellbore (as highlighted (in red) in the inset figure, which shows the planar projection of the deformed shape). A consequence of this contact interaction is that the lateral and torsional modes of deformation are now coupled, and the drillpipe in the horizontal section rolls on the surface of the wellbore (as shown in the middle plots of Fig. 1). For a single low-frequency rocking input at the surface, the downhole rotation speed is observed to consist of many frequency components, with the dominant component being much higher than the input frequency (rightmost plots of Fig. 1). Further numerical simulations show that the dominant frequency component is dependent on the wellbore configuration, as well as the surface input parameters. These results demonstrate the need to consider the nonlinear dynamics of contact interaction while designing optimal pipe rocking regimes for slide drilling.

References

- [1] Steven Duplantis (2016). Slide drilling with a twist. Oilfield Review, 28 (2), pp. 50-56. [\[Link\]](#)
- [2] Ian Rostagno (2019). Friction reduction optimization for extended reach and horizontal wells. MS Dissertation, UT Austin. [\[Link\]](#)
- [3] Alexandre Huynen et al. (2014). Eulerian formulation of the torque and drag problem. Third International Colloquium on Nonlinear Dynamics and Control of Deep Drilling Systems. [\[Link\]](#)
- [4] Arman Tekinalp et al. (2022) PyElastica: A computational framework for Cosserat rod assemblies. GitHub [\[Link\]](#).

On the Statics and Torsional Dynamics of Coupled Kresling Origami Springs

Ravindra Masana and Mohammed Daqaq

Engineering Division, New York University Abu Dhabi, UAE.

Abstract. Often the ancient Japanese art form Origami has inspired engineers to develop functional engineering systems. We are particularly interested in Kresling pattern origami and developed functional Kresling Origami Springs (KOS). In this work we theoretically and experimentally study the coupled KOSs and the varied characteristics that entail under torsional loads. It is demonstrated that by varying the total height of the coupled KOS the torsional stiffness can be readily tuned. The preliminary analysis under dynamic loading exhibited interesting complex dynamics.

Introduction

In recent times, origami has emerged from being just an art to a platform for building functional engineering systems with versatile characteristics. There are various patterns of origami that have been studied in the literature for engineering applications and one such pattern that has garnered significant attention is Kresling pattern origami. With its high load bearing capacity, tunability, programmability and unique deployment characteristics it inspired the design of flexible antennas, selectively collapsible structures, robot manipulators and crawling and peristaltic robots. However, the traditional origami materials often employed introduce inevitable uncertainties and limit the functionality with low fatigue life. Overcoming these challenges, using multi-phase materials functional and durable Kresling Origami Springs (KOS) with mono-stable, bi-stable potential and Quasi-Zero Stiffness (QZS) characteristics are developed [1]. Using the 3D printed KOS, we intend to study the rich dynamics of these structures which for the most part have been limited to theoretical studies. Towards that goal in this work, we experimentally study and analyse the coupling in the longitudinal and rotational degrees of freedom of the KOS. With that understanding we developed Kresling Origami Spring Pair (KOSP) with two KOSs of opposite chirality connected together as shown in Fig.1(a). The KOSP is pre-compressed to a certain height, u_T , at which height as the pure rotation is prescribed at one end, the intermediate plane rotates and translates between the two fixed ends in the process compressing one constitutive KOS while expanding the another by an equal amount. As the direction of rotation is reversed the expansion and compression happens in the opposite KOSs as shown in Fig 1(b). The measured torque is the net effective restoring torque of the individual KOSs to the deformation.

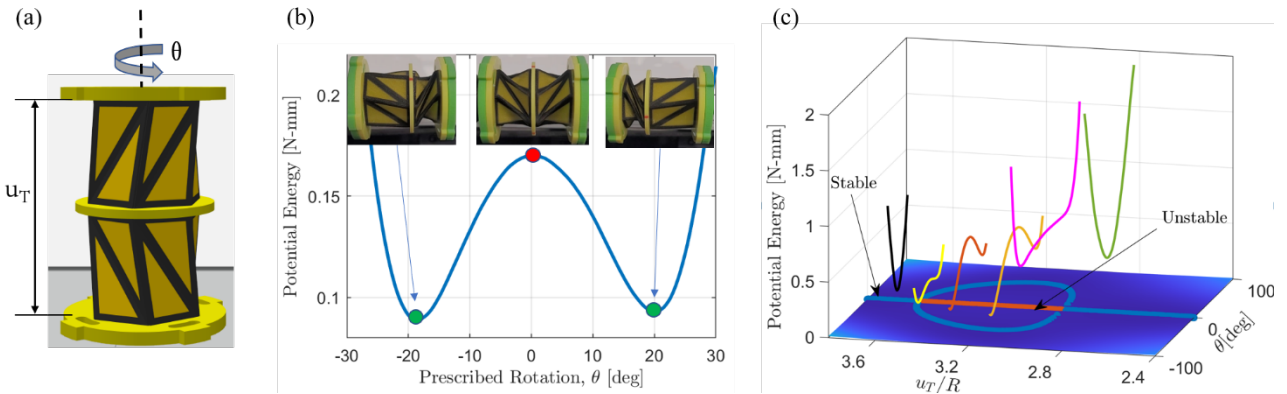


Figure 1: (a) Schematic of the Kresling Origami Spring Pair (KOSP); (b) Calculated potential energy from experimentally measured torque, in-figures show form of the KOSP at stable and unstable equilibria; (c) Potential energy tuning with pre-compression of KOSP (experimental), surface plot shows analytical prediction using truss model [2].

Figure 1 (c), shows potential energy tuning of the KOSP with the pre-compressed height, starting at left the KOSP is monostable and as the KOSP is compressed, it undergoes super critical pitchfork bifurcation and the KOSP becomes bi-stable in torsion. On further compression at about $u_T/R \sim 2.8$ the KOSP becomes a QZS spring and on further compression the KOSP becomes monostable again. We find that with careful selection of design parameters interesting characteristics such as multi-stability and asymmetricity can also be realized. Based on our initial observation the varied static characteristics of the KOSP entail very interesting complex dynamic responses that can be manipulated for torsional vibration isolation, torsional wave guiding etc.

References

- [1] S. Khazaaleh, R. Masana, M. F. Daqaq, Combining advanced 3D printing technologies with origami principles: A new paradigm for the design of functional, durable, and scalable springs, *Composite Part B*. 236,109811 (2022).
- [2] R. Masana, M. F. Daqaq, Equilibria and bifurcations of a foldable paper-based spring inspired by kresling-pattern origami, *Phys. Rev. E*100,063001 (2019).

Higher order theories for the static and dynamic analysis of anisotropic shell structures

Matteo Viscoti*, Francesco Tornabene* and Rossana Dimitri*

*Department of Innovation Engineering, Università del Salento, Lecce, 73100, Italy

Abstract. In this contribution we present a generalized approach for the static and dynamic analysis of doubly curved shell structures laminated with generally anisotropic materials. Based on Higher Order Shear Deformation Theories (HSDTs), the three-dimensional static and the dynamic response of structures of very complex shapes is detected using a two-dimensional approach. The fundamental equations are obtained from the Hamiltonian Principle, and they are numerically solved by the Generalized Differential Quadrature (GDQ) method. The accuracy of the methodology is pointed out in some validating examples. Then, parametric investigations are performed on many laminated shells of different materials and shapes.

Theoretical aspects and numerical strategies

New advances in several engineering fields require alternative approaches for the numerical modelling of innovative materials and structures of very complex shapes. In this context, the geometric description is a key factor for an efficient prediction of the structural response. Referring to the evaluation of the unknown field variable, Higher Order Shear Deformation Theories (HSDTs) [1] are used with a generalized formulation so that the three-dimensional response of doubly-curved structures laminated with generally anisotropic materials is predicted with a reduced computational effort (Figure 1). The present continuum-based model is based on an efficient homogenization of the constitutive material, taking into account all the possible coupling and stretching effects that occur in very complicated lamination schemes. Furthermore, an effective strategy for the assessment of surface and point loads is presented [2]. As far as the solution of the problem is concerned, the GDQ method is adopted to solve the fundamental equations directly in the strong form using a very little number of degrees of freedom [3]. Once the two-dimensional solution is derived, an efficient post-processing technique leads to an accurate prediction of the three-dimensional response of the structure even though the proposed formulation provides a two-dimensional solution of the problem under investigation.

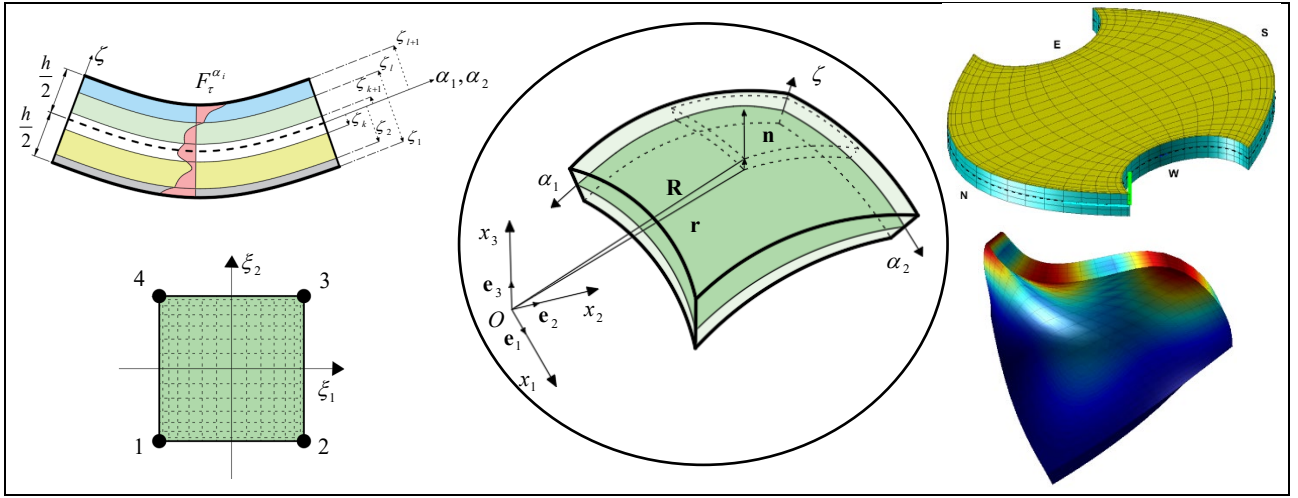


Figure 1: Two-dimensional GDQ modeling of laminated anisotropic doubly-curved shell structures.

Numerical examples and parametric investigations

The accuracy of the present higher order model is verified in a series of validating examples performed on structures of different shapes and materials, where the numerical results are compared to those coming from refined three-dimensional Finite Element models. Structures of different shapes and materials are studied, taking into account in the lamination scheme, among others, honeycomb cells, Functionally Graded Materials (FGMs) and Carbon Nanotubes (CNTs) [3]. Furthermore, the effect of a general variation of the constituent material is considered, as well as the presence of porosity. Finally, systematic parametric investigations are carried out in order to show the sensitivity of the geometry and the materials used.

References

- [1] Tornabene, F., Viscoti, M., Dimitri, R. (2022). Higher order theories for the free vibration analysis of laminated anisotropic doubly-curved shells of arbitrary geometry with general boundary conditions. *Compos. Struct.* **297**:115740.
- [2] Tornabene, F., Viscoti, M., Dimitri, R. (2023). Static Analysis of Anisotropic Doubly-Curved Shell Subjected to Concentrated Loads Employing Higher Order Layer-Wise Theories. *Comput. Model. Eng. Sci.* **134**:1393-1468.
- [3] Tornabene F., Baccocchi M. (2018) Anisotropic doubly-curved shells. Esculapio, Bologna.

Internal actuators and parametric oscillations in unconventional robotic locomotion

Phanindra Tallapragada*

*Department of Mechanical Engineering, Clemson University, SC, USA, ORCID #

Abstract. Unconventional means of actuation and modes of locomotion in robot can be achieved via the periodic motion of internal degrees of freedom. Such internal actuation when coupled with other mechanics can produce motion in a variety of physical settings, from fast fish-like swimming motion in water or terrestrial motion when coupled with nonholonomic constraints to fast motion of soft robots. The talk will present results on the nonlinear dynamics of such motion.

Introduction

Mobility in robots is usually achieved by a few common means; with a few exceptions these are wheels or legs in ground robots, propellers in flying robots, articulated tails or fins and propellers in swimming robots. However less explored is the means by which internal actuators or degrees of freedom, that do not directly interact with the environment, produce locomotion. Periodic motion of an internal body such as a rotor can produce a variety of gaits. This is demonstrated in four different settings. In the first, periodic oscillations of an internal rotor inside a nonholonomic system, a Chaplygin sleigh, leads to limit cycles in a velocity space and a serpentine motion of the Chaplygin sleigh [1]. When the body has an additional passive tail, these limit cycles can undergo bifurcations resulting in different gaits [2]. In the second example the oscillations of a rotor inside a Joukowski foil submerged in water creates a reverse Karman wake and leads to fish-like motion [1]. In the third example, high frequency internal vibrations enable a small body with bristles to propel itself due to stick-slip motion or climb pipes and navigate a pipe network. In the last example, oscillations of an internal rotor enables a body to jump. While the mechanics of the four examples differ, the common theme is that of the motion of internal degrees of freedom.

Results and Discussion

The findings from the first two examples, is that fish-like swimming can be modeled as a nonholonomic system subjected to periodic excitation. Building on the work in [1] and [2], it is shown that the propulsion speed has a complex dependence on the frequency-amplitude of the excitation. Further more the periodic excitation, which leads to periodic yaw motion of the body submerged in water, then couple parametrically to the roll oscillations of the body. It can be shown that the swimming body becomes roll unstable for some frequency-amplitude yaw oscillations, in a manner that is similar to that of the Mathieu oscillator, suggesting trade-offs in speed-agility vs stability for underwater robots. More interestingly the addition of passive appendages on a fish-like robot not only confers the ability to achieve different gaits, but also allows embodied sensing of hydrodynamic wakes based purely on the kinematics of the passive tail. In the third example a body with bristles containing a vibrational motor propels itself due to the slip motion enabled by parametric resonant oscillations. In [3] it was shown that such a system can be modeled by a Mathieu oscillator with slip dynamics. In more recent work it is demonstrated that for a soft robot with a vibrational motor, which can be modeled by a Hill's equation, parametric oscillations when in an unstable regime enable the soft robot to navigate a pipe network or climb pipes. In the last example, fast internal motion of a rotor inside a soft or a rigid body produces jumping motion. The four examples demonstrate the versatility of motion that is possible through internal actuators.

References

- [1] B. Pollard, V. Fedonyuk and P. Tallapragada (2019) Swimming on limit cycles with nonholonomic constraints. *Nonlinear Dynamics* **97**:2453–2468.
- [2] C. Rodwell and P. Tallapragada (2022) Induced and tunable multistability due to nonholonomic constraints. *Nonlinear Dynamics* **108**(3):2115-2126.
- [3] P. Tallapragada and C. Gandra (2021) A mobile Mathieu oscillator model for vibrational locomotion of a bristlebot. *Journal of Mechanisms and Robotics* **13**(5):054501.

Study of the effect of non-linear end supports on the unbalance response of the elastic shaft

Jayanta Kumar Dutt* and Krishanu Ganguly*

*Department of Mechanical Engineering, Indian Institute of Technology Delhi, India – 110016

Abstract. Nonlinearities in modelling the dynamic behaviour of systems are often neglected for simplicity, however, accurate prediction of response and the issue of stability, especially in the cases of low tolerance on response, justifies the nonlinear dynamic model of a system. This study focuses on the analytical prediction of the unbalanced response of a Jeffcott rotor with rolling element bearings at ends supported on viscoelastic supports, and the role of support damping on the nonlinear dynamic behaviour, particularly the undesirable jump phenomenon of the rotor. Deformation-dependent stiffness of rolling element bearings makes the system of equations nonlinear. A detailed study with non-dimensional parameters is attempted to find optimum damping for minimizing the response.

Introduction

Considering the bearings at the ends of the rotor-shaft to have linear stiffness characteristic generally mean that the stiffness of the bearings does not depend on the deformation of the journal. However, it has been shown that the ball and roller bearings possess non-linear stiffness characteristic i.e. the stiffness of these bearings vary with the deformation of the rolling element [1]. The effect of these non-linear bearing stiffness characteristics on the unbalance response of the rotor in a rotor shaft system supported on viscoelastic supports has been studied.

Results and discussion

Figure 1 (left) shows the system schematically. As the excitation is sinusoidal in nature due to the unbalance in the rotor, the stiffness of the viscoelastic support is complex in nature. The deformation dependent stiffness of both ball and roller bearings has been found out in [1]. It is seen that the stiffness of the ball bearing is proportional to the square root of the deflection of the rolling element, whereas for a roller bearing the stiffness is proportional to the deflection of the rolling elements raised to the exponent 1/9.

The method of solution is identical to that given in [2] where the authors have calculated the unbalance response of a rotor shaft system on nonlinear bearings and have not considered any support mass.

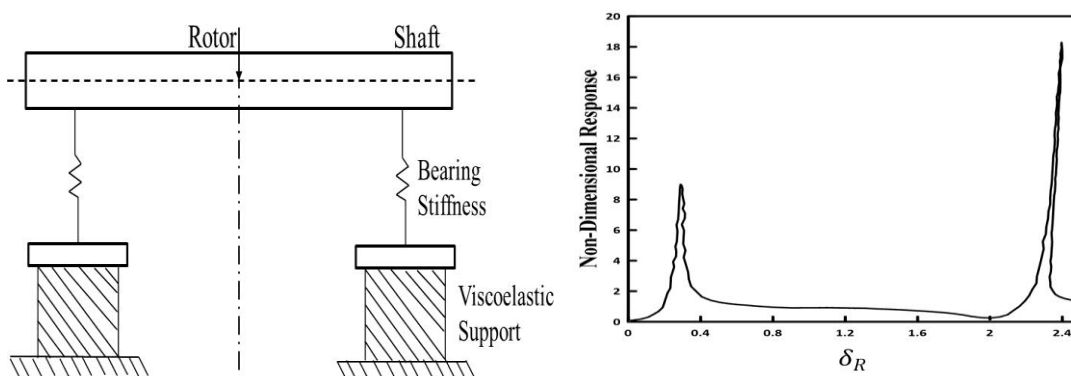


Figure 1: System configuration (left) and unbalance nonlinear response (right)

A detailed parametric analysis of the unbalance response amplitude of the rotor shown in Figure 1 (right) has been done to find out the effect of each parameter on the response. One parameter has been chosen each time and its value has been varied keeping the value of the other parameters unchanged. A jump phenomenon is observed visible mainly in the second peak of the unbalance response plot which is a typical characteristic of the system having non-linear element.

References

- [1] Harris T. A., Mindel M. H. (1973) Rolling element bearing dynamics. *Wear* **23(3)**:311-337.
- [2] Genta G., A. Repaci, (1987) Circular whirling and Unbalance Response of Nonlinear Rotors. *Proceedings of the ASME Conference on Mechanical Vibration and Noise, Boston, Massachusetts, Rotating Machinery Dynamics* **2**:441-448.

A chain of real mechanical oscillators subjected to creep-slip friction and relatively high-frequency structural vibration

Paweł Olejnik* and Jan Awrejcewicz*

*Department of Automation, Biomechanics and Mechatronics,
Faculty of Mechanical Engineering, Lodz University of Technology,
1/15 Stefanowski Str., 90-924 Lodz, Poland, ORCID 0000-0002-3310-0951

Abstract. In this work, a real mechatronic system of coupled inertia oscillating under the action of relatively high-frequency structural vibrations as well as its mathematical description is presented. A vibration exciter is incorporated into the model system in the form of an imbalanced rotor, simulating the presence of real structural vibration. As such kind of unavoidable excitation can be detected in any real machine's functioning, the very small amplitude and relatively fast forcing is proved to cause a significant change in frictional response of the observed real creep-slip motion.

Introduction

In the design, a structural vibration analysis of specific areas of the machine is often undertaken. The discussed problems of dynamics are often caused by dry and viscous friction or a rotating imbalance occurring, among others, in driving and braking systems, stabilizing platforms, miscellaneous turbine and pump solutions, etc. The most common factor in these different types of vibration is that the structure responds with some repetitive dynamical behavior that affects its physical properties, accurateness of positioning and other. The considered system of mechanical oscillators can be modeled using the physical representation shown in Fig. 1.

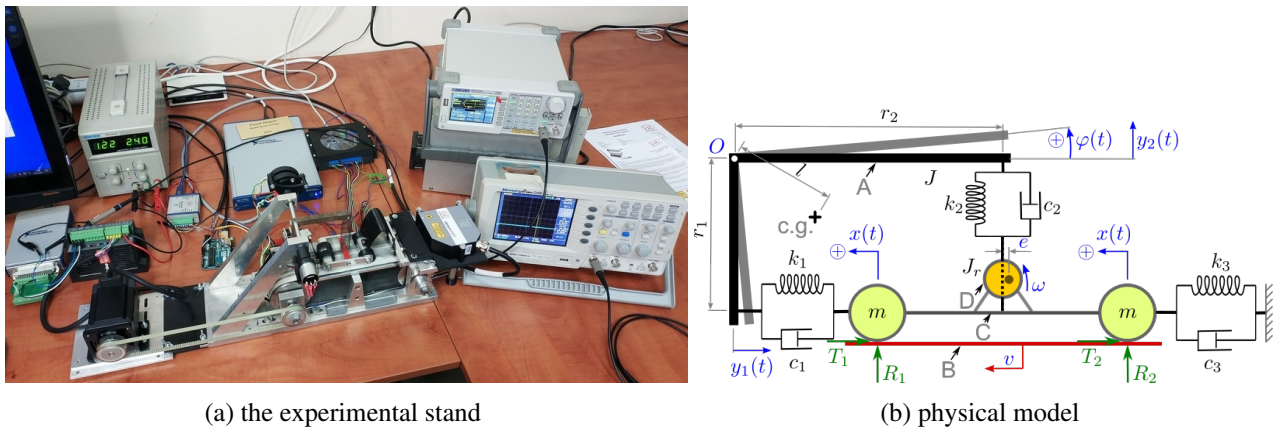


Figure 1: A real chain of three coupled oscillators (against y_1 , y_2 , ω) with friction J – m – J_r (a) and its physical model (b): A – stiff pendulum body of mass moment of inertia J , B – horizontally moving soft base, C – stiff beam in a contact at R_1 and R_2 with the base B, coupling the two oscillators J – m , D – imbalanced rotor mounted on C, elasticity: k_1 , k_2 , k_3 ; structural damping: c_1 , c_2 , c_3 of the spring elements and friction forces T_i .

Taking into consideration the three coupled inertia shown in the configuration from Fig. 1, i.e., the pendulum body (A), the frictional oscillator (C) and the imbalanced rotor (D), we begin the analysis from the derivation of mass moment of inertia of the pendulum rotating about its center of gravity.

Results and discussion

Various phenomena caused by high-frequency vibration of the sliding body's structure and occurring in the considered system consisting of coupled rotating elements with the non-ideal source of energy pumped to the considered structure have been reported. The imbalance of the rotor mass m_r (D) on the slider's body (C), as shown in Fig. 1b plays a significant role in the formation and disappearance of self-excited vibration in the structure. In work [1] such a system was considered, where the imbalanced rotor's function was delivered by a direct-current induction motor, mounted in the center of the sliding body. Our experimental observations go beyond the above by presenting real time trajectories at the presence and absence of the additional pump of vibration energy to the system being a reason of intermittent stick-slip behavior.

Funding: This research was funded by Narodowe Centrum Nauki grant number 2019/35/B/ST8/00980 Poland.

References

- [1] Vinícius Piccirillo, Thiago Gilberto Prado, Angelo Marcelo Tusset, and José Manoel Balthazar (2020) Dynamic integrity analysis on a non-ideal oscillator. *J. MESA*, **11**:541–547.

Vibration analysis of electrical connector under different environments

R. El Abdi* and F. Le Strat**

*Univ. Rennes- CNRS, Institut de Physique de Rennes. UMR 6251, F-35000 Rennes, FRANCE

**Entreprise Renault, DEA-TCM. 78084 Guyancourt, FRANCE

Abstract. An electrical automotive connector was composed of a female part and a male part subject to the vibrations of the vehicle, which could cause relative movements between these two parts. A relative movement of the contact zone between these two parts can lead to an irreversible mechanical degradation and an electrical perturbation by the formation of a third-body layer at the contact zone. Our study was about the dynamic measurement of electrical behavior of metallic connectors under imposed alternate movement with sinusoidal form.

Introduction

In the automotive fields, the vehicle vibrations induce movement on hundreds of connectors, which were located near the engine, inside the seat and at many other zones. The engine vibrations could induce a displacement between the male and female part i.e. the pin and the clip (Fig.1) and could generate an electrical failure due to the well-known fretting-corrosion phenomenon. A relative displacement of 5 μm was enough to produce remains at the interface between the pin and the clip and set an intermittent failure at the interface. This phenomenon represents 60 % of electrical failure within a car. Electrical contacts were made of a substrate of copper alloy plated with a thin protective layer of non-noble metals. Tin was usually used as a protective layer of the substrate in order to combine a good conductivity, good reliability and a low cost. A pure tin was malleable and reacts with the oxygen to give hard and brittle remains, which cause high surface damages. The substrate could be reach and it generates copper oxide remains at the contact surface leading to an irreversible degradation, which avoids a good current conduction [1-2].

Results and discussion

The aim of this work was to give further information to understand the oxygen influence on the current conduction of a tin-plated contact and oxidized remains. An experimental bench was used to introduce an inert gas at the interface of a tin-plated connector in order to avoid the formation of insulating remains due to the oxygen of the air. The nitrogen gas was chosen during the tests; it was chemically inert for the tin and the copper and it represents 79 % of the atmosphere. Samples were typical terminals of connector. The bench was composed of a piezo-electric actuator, which provides a controlled movement between the clip and the pin (Fig.1). A generator provides a stable current through the interface and the measurements of contact voltage were performed with a voltmeter and a scope for a real-time analysis. The bench was mounted on an anti-vibration table in order to avoid external vibrations. The imposed alternate movement has a sinusoidal form. The displacement of different parts of the used connector decreases when frequency increases (Fig.2). A resonance frequency was observed at 205 Hz for the pin, the clip and the clip holder. The displacements of the clip and the clip holder (inserted into the sample holder) are 1.5 μm greater than the actuator displacement. This result indicates the fixing of the clip and the clip holder to the sample holder needs to be examined. The study will also shows the importance of the environment, the amplitude and the frequency.

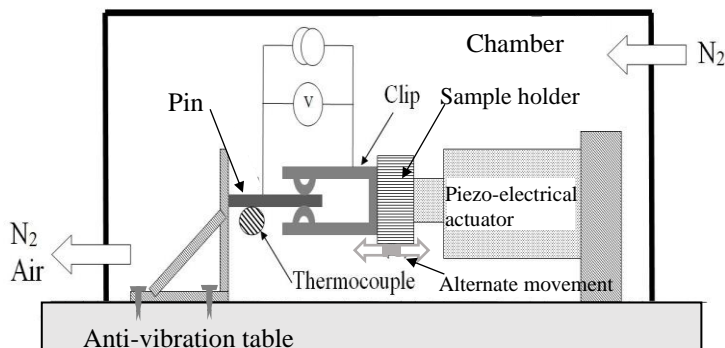


Figure 1: Schematization of vibration setup: Controlled movement supplied by piezo-electrical actuator

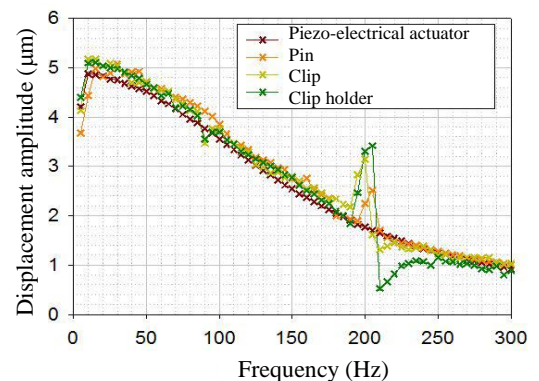


Figure 2: Displacement versus vibration frequency

References

- [1] Chen C., Flowers G.T., Bozack M. and Suhling J. (2009) Modeling and analysis of a connector system for prediction of vibration-induced fretting degradation. *IEEE Holm Conference on Electrical Contacts* 129-135.
- [2] Labbe J., El Abdi R., Carvou E., Le Strat F. and Plouzeau C. (2014) Vibration induced at contact point of tighten-up connector system. *IEEE Holm Conference on Electrical Contacts* 200-204.

An Electromagnetic Softening Spring: Experiment and Simulation

Maksymilian Bednarek*, Bipin Balam*, Donat Lewandowski*, Jan Awrejcewicz*

*Department of Automation, Biomechanics and Mechatronics, Lodz University of Technology, Lodz, Poland.

Abstract. We present a simple, low-cost design of a nonlinear softening stiffness mechanism using electro-magnetic forces. An algebraic form for the stiffness force is obtained and close agreement between experimental and numerical time responses is illustrated.

Introduction

Applied scientists have started utilising nonlinearity to improve system performance, rather than considering it a menace to be avoided. Nonlinear stiffness mechanisms have found wide applications in various areas recently [1]. This has increased the need for new ways of fabricating nonlinear components. We present a simple, low-cost, electro-mechanical design of a nonlinear softening stiffness. It has the further advantage that variations to the stiffness curve can be brought about easily. Fig. 1(a) shows the experimental setup. It consists of a mass (1), supported on two aerostatic supports (2), and fitted with a magnet (3) and a helical spring (4). The magnet moves through an electro-magnetic coil (5) as the mass oscillates. A harmonic exciter (6) is mounted on the mass. Softening nonlinearity is generated by the force between the magnet and the electromagnetic coil when a current is passed through it.

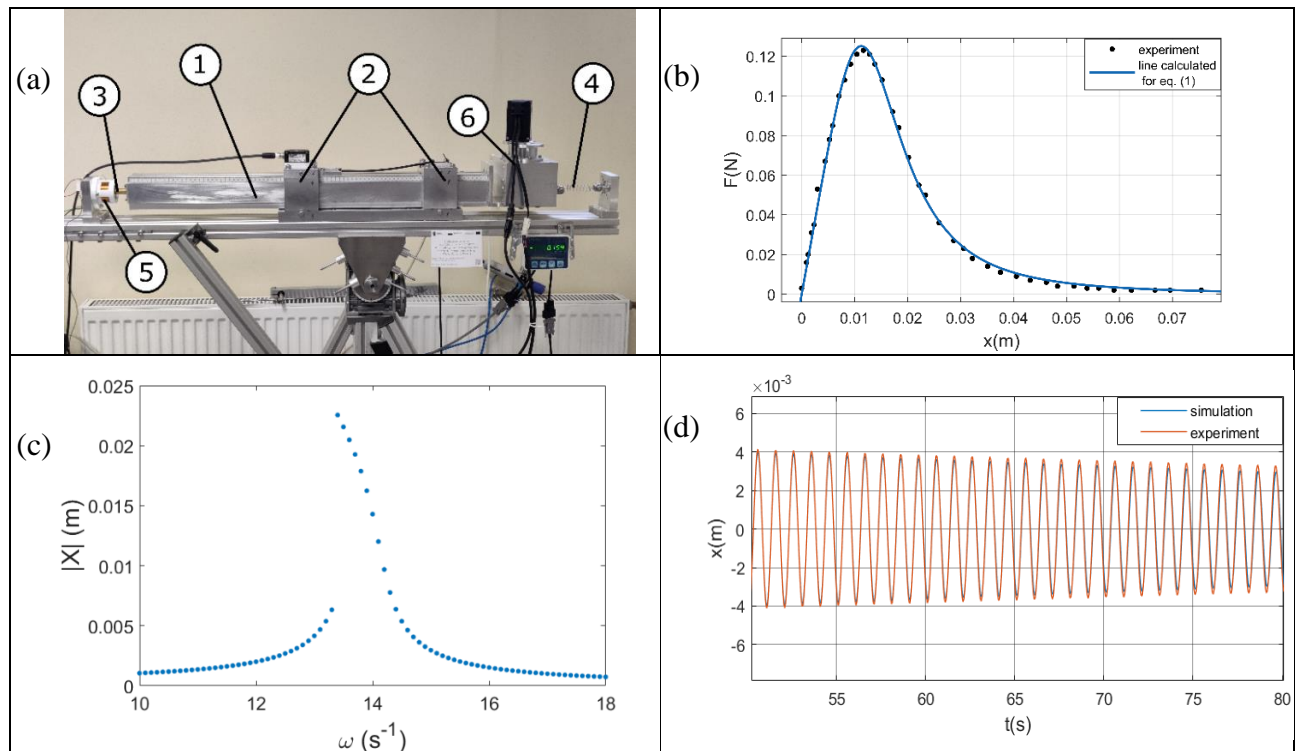


Figure 1: (a) The experimental setup, (b) Force – Displacement curve, (c) Frequency response curve, (d) Time response plot.

Results and discussion

Fig. 1(b) shows the force-displacement characteristic of the system without helical spring and the exciter. The experimental points are very closely approximated by the force function $F(x) = Ip \left(\frac{x/q}{1 + (x/q)^4} \right)$ [2], where I is the current in coil and p and q are constant for a given coil-magnet pair. The numerically obtained frequency response curve with the above $F(x)$, shown in Fig. 1(c), clearly shows the softening character of the stiffness. Fig. 1(d) shows the close agreement between the experimental time response and the one obtained by numerically solving the governing equation of the system with above softening stiffness $F(x)$.

References

- [1] D. J. Wagg, L. Virgin (Eds.), Exploiting Nonlinear Behavior in Structural Dynamics, Springer-Verlag GmbH Wien, 2012.
- [2] M. Bednarek, D. Lewandowski, J. Awrejcewicz, Determining magnetic and electromagnetic springs forces and their usage damping vibrations, in: Advances in Nonlinear Dynamics, NODYCON Conference Proceedings Series, Springer, 2022.

Identification of Secondary Resonances using a Control-based Method

T. Zhou* and G. Kerschen*

*Department of Aerospace and Mechanical Engineering, University of Liege, B-4000 Liege, Belgium

Abstract. Recently, advanced experimental measurement techniques such as phase-locked-loop feedback control and control-based continuation have been developed, mainly for identifying primary resonances. The objective of the present study is to characterize secondary resonances by taking advantage of adaptive digital filters, a powerful tool that can be incorporated as a building block in the control loop. Adaptive filters allow the experimenter to perform online Fourier decomposition so that the Fourier coefficients of the harmonic components of interest can be estimated at each time instant. The phase properties of secondary resonances are then exploited for the identification of the associated frequency response and backbone curves. It is demonstrated that the phase resonances of odd and even superharmonic resonances of a nonlinear structure can be effectively targeted. The designed testing scheme is found to stabilize the unstable orbits and circumvent the problems induced by bifurcations.

Introduction

Control-based vibration testing methods have shown promise in identifying folded and unstable responses of nonlinear systems. These methods can provide more insights into the dynamics as compared to the conventional testing approaches (i.e., without the use of a controller). Most existing studies focus on the characterization of primary resonances of mechanical systems, which can feature different types of nonlinearity [1, 2]. However, multi-harmonic responses can be activated with a harmonic excitation, which, in turn, can trigger the excitation of secondary resonances such as superharmonic and subharmonic resonances.

The objective of this study is to develop a control-based testing scheme which can characterize secondary resonances. To this end, we resort to phase-locked loops (PLLs) coupled to adaptive digital filters, which allow the experimenter to perform online Fourier decomposition. The periodic response is fitted with a truncated Fourier series $x(t) = \sum_{n=1}^N \hat{x}_n \sin(n\Omega t + \phi_n)$, where ϕ_n is the phase lag of n -th harmonic. PLL feedback control is first implemented to identify the frequency response curves of the secondary resonance of interest, by exploiting the monotonous evolution of the phase lag between the harmonic of interest and the forcing. PLL can also track backbone curves based on the phase resonance criterion in [3]. The frequency of the harmonic excitation $f(t) = \hat{f} \sin(\int_0^t \Omega(\tau) d\tau)$ acting on the structure is determined by a PI controller, with $\Omega(t) = \Omega_0 + K_P(\Phi_{\text{ref}} - \Phi_n(t)) + K_I \int_0^t (\Phi_{\text{ref}} - \Phi_n(\tau)) d\tau$. Here, Φ_{ref} is the assigned reference phase.

Results and discussion

The algorithm is first tested on a Duffing oscillator, $\ddot{x} + 0.001\dot{x} + x + x^3 = f$, in a virtual experiment. As shown in Figure 1, there is a good agreement between the results computed by the harmonic balance method and PLL testing. The responses exhibiting bifurcations can be effectively tackled by adjusting Φ_{ref} , thanks to the use of the adaptive filter and feedback control. The backbone curves of the 3:1 and 2:1 resonances are obtained by setting Φ_{ref} to be $-\pi/2$ and $-3\pi/4$, respectively. The phase resonance criterion can predict both resonance frequencies and amplitudes accurately.

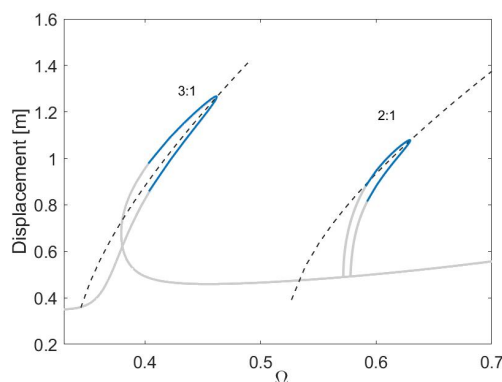


Figure 1: Frequency response curves (blue) and backbone curves (black) of 3:1 and 2:1 resonances identified by PLL for $\hat{f} = 0.4$ N. The reference solution is provided by the harmonic balance method (grey).

References

- [1] Peter S., Leine R. I. (2017) Excitation power quantities in phase resonance testing of nonlinear systems with phase-locked-loop excitation. *Mech. Syst. Signal Process.* **96**:139-158.
- [2] Abeloos G. et al. (2022) A consistency analysis of phase-locked-loop testing and control-based continuation for a geometrically nonlinear frictional system. *Mech. Syst. Signal Process.* **170**:108820.
- [3] Volvert M., Kerschen G. (2021) Phase resonance nonlinear modes of mechanical systems. *J. Sound Vib.* **511**:116355.

Analysis of Non-linear Vibrations Using DIC and the Smoothed Harmonics Method

Serena Occhipinti*, Paolo Neri**, Christian Maria Firrone* and Daniele Botto*

*Department of Mechanical and Aerospace Engineering, Politecnico di Torino, Torino, Italy

**Department of Civil and Industrial Engineering, Università di Pisa, Pisa, Italy

Abstract. This work focuses on the development of a methodology to extend the down-sampling method to the study of the dynamic behavior of components when non-linear phenomena must be considered. The proposed method is general but in this work it was applied together with a full-field measurement using the Digital Image Correlation. The proposed approach overcomes the cameras low frame rate limitation in case of steady state periodic oscillations by making use of a new sub-sampling technique, named *Smoothed Harmonics Method*. This method allows an accurate reconstruction of the under-sampled signal. The method was applied to a beam with non linear stiffness loaded with harmonic excitation.

Introduction

Non-contact full-field measurement techniques have gained a predominant role since they overcome the main limitations of single point contact techniques: i.e. added mass effect, data transmission for rotating machines and difficulties on describing complex and high-frequency deformed shapes. In this scenario, the development of 3D full-field measurements techniques based on Digital Image Correlation (DIC) are gaining the interest of researchers. The work presented in [1] shows promising results in applying full-field DIC measurements to non-linear phenomena by exploiting high-speed imaging devices. Nevertheless, a high-speed stereo camera system can be unaffordable for most research centres and, moreover, highest frame rates can be achieved only reducing the image resolution, which results in sensitivity loss for small displacements. Many alternative approaches were then developed in literature to overcome this issue by using high-resolution low-speed cameras to measure high-frequency linear vibrations. In particular, [2] extended the applicability of the down-sampling approach to band-limited signals. Nevertheless, the feasibility of this approach in the case of non-linear phenomena was not proven yet. Therefore, the objective of this work is to develop a methodology for using the standard high-resolution, low-speed cameras, to study high-frequency nonlinear phenomena. Accordingly, a new down-sampling method denoted to as *Smoothed Harmonics Method* (SHM) was developed and applied to reconstruct the non-linear response of a beam.

Results and Discussion

SHM can detect the amplitude and phase of a given harmonic contribution of an aliased signal. SHM allows the signal in the time domain to be accurately reconstructed when the frequencies of its main harmonics are known. This method was applied to the analysis of the non-linear response of a beam with a clamped end and an unilateral contact at the other end. Due to the non-linearity of the system both superharmonics and subharmonics components of the excitation frequency are present in the response. This behavior has been explained with a qualitative numerical model and accurately measured with a high resolution high speed laser vibrometer on a reference point of the beam. In particular, the response was found in the range of 10–70 Hz with a frequency of the excitation force of 20 Hz. The sampling frequency of the cameras was set to 9.9 Hz. Figure 1 shows the comparison between the reconstructed signal, DIC+SHM, and the laser signal at the reference point. The comparison shows a good agreement between the high-resolution measured signal and the DIC+SHM results. This result demonstrates the feasibility of the proposed methodology.

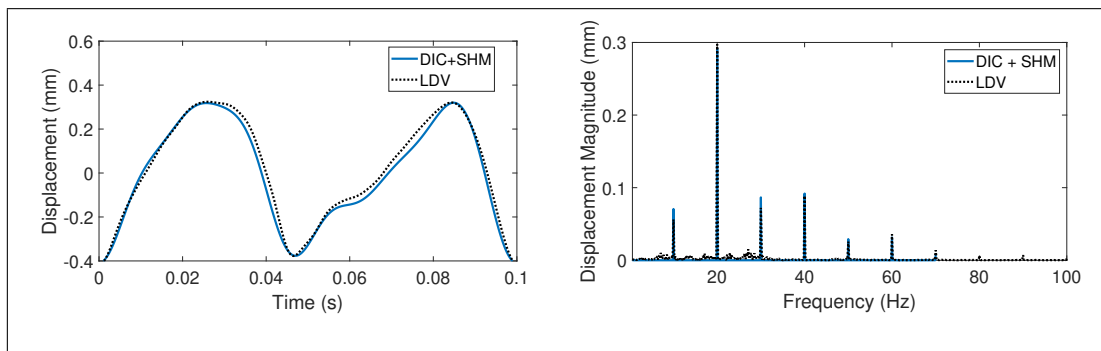


Figure 1: Time and frequency domain comparison between the reconstructed signal, DIC+SHM, and the Laser Doppler Vibrometer (LDV) signal measured at a reference point.

References

- [1] Chabrier R., Sadoulet-Reboul E., Chevallier G., Foltête E., Jeannin T. (2021) Full-field measurements with Digital Image Correlation for vibro-impact characterisation. *Mech Syst Signal Pr* **156**:107658.
- [2] Neri P. (2022) Frequency-band down-sampled stereo-DIC: Beyond the limitation of single frequency excitation. *Mech Syst Signal Pr* **172**:108980.

Rocking of rigid blocks on flexible foundations: modeling and experimental assessment

Pol D. Spanos*, Alberto Di Matteo** and Antonina Pirrotta**

*Department of Mechanical Engineering and Materials Science, Rice University, Houston, USA

**Department of Engineering, University of Palermo, Palermo, Italy

Abstract. In this paper harmonic rocking responses of a rigid block subjected to foundation shaking is examined. Several foundation models are considered comprising the classical rigid one, as well as linear and nonlinear flexible foundation models which account for the possibility of uplifting in the case of strong excitation. An identification procedure of the appropriate model parameters is developed based on the associated steady state response amplitude determined through an averaging procedure in case of harmonic base excitation. The analytical study is supplemented by experimental tests for several marble-block geometries on both rigid and flexible foundations. Numerical vis-à-vis experimental data are presented, assessing the accuracy of the different models in capturing certain salient features of the phenomenon even for quite soft foundation materials.

Introduction

The behaviour of block-like structures allowed to rock due to base excitation has been a longstanding problem of technical interest and still attracts the attention of a significant number of researchers. Several alternative analytical models have been proposed, among which the Housner model (HM), and the Winkler foundation model (WFM) are primarily used. The first deals with the motion of a rigid block rocking about its base corners on a rigid foundation [1]. The second deals with the motion of a rigid block rocking and bouncing on a flexible foundation of distributed linear springs and dashpots (Winkler foundation) [2].

Recently, to further study the complex behaviour which may arise during the rocking motion of rigid blocks on flexible foundations, additional aspects of the problem have been captured by an enhanced nonlinear model for the base-foundation interaction. In this regard, the Hunt-Crossley's nonlinear impact force model commonly used in the literature to represent the nonlinear nature of impact and contact phenomena has been adopted. Thus, the foundation is treated as a bed of continuously distributed tensionless springs in parallel with nonlinear dampers, with stiffness coefficient k and damping coefficient λ , respectively [3].

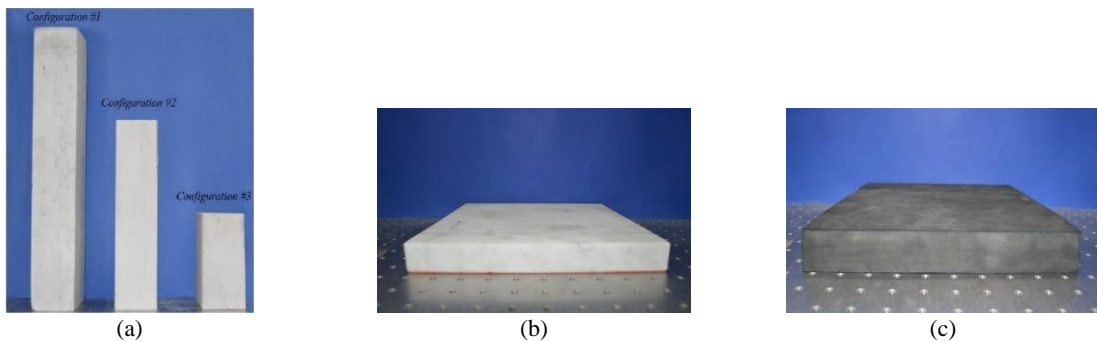


Figure 3: Blocks and base foundation: (a) Marble block configurations; (b) Rigid base (marble material); (c) Soft base (Aerstop CN20 material).

Results and discussion

The rocking phenomenon has been extensively studied. However, most of the previous studies have been analytical in nature. Further, many experiments on rocking blocks have considered the behavior of rigid blocks on rigid foundations, while the problem of rigid blocks on flexible foundation has less been investigated [3]. In this regard, in this paper an approximate analytical method has been developed for studying the rocking responses in case of harmonic base excitations. Specifically, a combination of static condensation and the method averaging has been employed to derive the rocking response amplitude for harmonic excitations. These results have been then used to derive a novel identification procedure for the model parameters. Further, an extensive experimental study has been conducted in the Laboratory of Experimental Dynamics at the University of Palermo, Italy. In this context, and due to their obvious relevance for historical monuments, tests are presented for several marble-block geometries on both rigid (marble) and flexible foundations (Fig. 1). The results have shown the reliability of the proposed identification procedure and the accuracy of the considered models in the various situations and configurations.

References

- [1] Housner G.W. (1963) The behavior of inverted pendulum structures during earthquakes. *Bull. Seismol. Soc. Amer* **53**:403-417.
- [2] Koh A.S., Spanos P.D., Roesset J.M. (1986) Harmonic rocking of rigid block on flexible foundation. *J. Eng. Mech.* **112**:1165-1180.
- [3] Spanos P.D., Di Matteo A., Pirrotta A., Di Paola M. (2017) Rocking of rigid block on nonlinear flexible foundation. *Int. J. Non-linear Mech.* **94**:362-374.

Experimental and numerical study of a magnetic pendulum

Peter Meijers*, Panagiota Atzampou* and Andrei Metrikine*
*Delft University of Technology, Faculty of Civil Engineering and Geosciences,
Stevinweg 1, 2628CN Delft, the Netherlands

Abstract. An experiment has been performed on a magnetic pendulum, which interacts with an electromagnet. The free non-linear vibrations of the pendulum-magnet system are studied to identify and analyse the system's characteristics. Due to the presence of the electromagnet, a modulation of the pendulum's natural frequency is observed. A mathematical model is formulated that is able to reproduce the experimental results.

Introduction

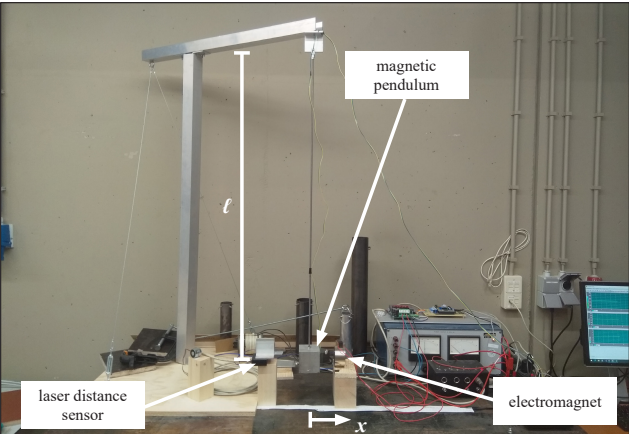
Increasing demand for energy from renewable resources has led to a spectacular increase in the number of offshore wind turbines planned to be installed [1]. Installation using floating vessels is critical to meet the demand, as such allows for faster installation in deeper water. Undesired motion of the payload caused by vessel motions is one of the limiting factors for operations. Current methods to reduce the motion of the payload are based on tugger line systems [2, 3], which can only apply a pulling force. Ideally, the load can be pushed and pulled to improve the control. Therefore, an alternative system is investigated here, which is based on magnetic interaction of the payload and an magnetic actuator.

Experimental setup

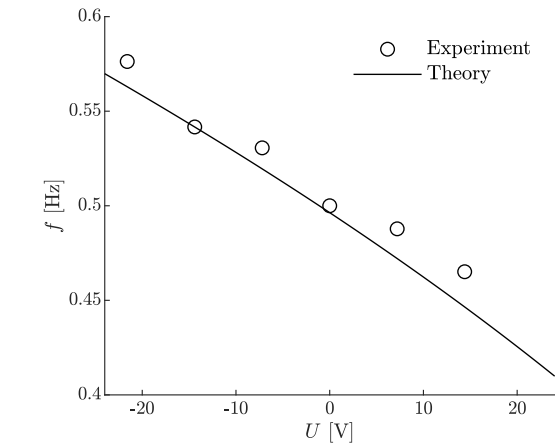
For a proof of concept, an experimental setup has been designed and built (Figure 1a), which consists of a pendulum with an aluminium mass to which a permanent magnet is attached at its side. The pendulum can be excited by an electromagnet, which is on the same axis as the poles of the permanent magnet. To register the motion of the suspended mass, a laser distance sensor is employed. To characterise the system and to calibrate a model for the distance-dependent magnetic interaction, the free vibrations of the pendulum in the presence of the electromagnet are analysed.

Results and discussion

When no voltage is supplied to the electromagnet, the natural frequency of the pendulum is $f = 0.49$ Hz and its equilibrium is $x = 0$ m. For different constant supplied voltages, the data shows that the equilibrium point shifts away from $x = 0$ m and that the fundamental frequency of free vibrations is modulated due to the action of the magnet (Figure 1b). The experimental data is in good correspondence with results from the numerical model of the system. Using the model, it is shown that the observed modulation results from the non-linear nature of the magnetic interaction between the two magnets.



(a) Setup of the magnetic pendulum.



(b) Modulation of the pendulum's natural frequency with varying voltage of the electromagnet.

References

[1] WindEurope. Offshore Wind in Europe. Key trends and statistics 2019. Technical report, WindEurope, 2020.
[2] Zhengru Ren, Zhiyu Jiang, Zhen Gao, and Roger Skjetne. Active tugger line force control for single blade installation. *Wind Energy*, 21(12):1344–1358, 2018.
[3] Zhiyu Jiang. Installation of offshore wind turbines: A technical review. *Renewable and Sustainable Energy Reviews*, 139:110576, 2021.

Delayed acoustic self-feedback control of limit cycle oscillations in a turbulent combustor

Ankit Sahay*, Abhishek Kushwaha*, Samadhan A. Pawar*, Midhun P. R.*, Jayesh M. Dhadphale* and R. I. Sujith*

*Department of Aerospace Engineering, Indian Institute of Technology Madras, Chennai, India

Abstract. We use delayed acoustic self-feedback to suppress limit cycle oscillations (LCO) in a turbulent combustor during thermoacoustic instability (TAI). The acoustic field of the combustor is coupled to itself through a single coupling tube attached at the antinode position of the acoustic standing wave. As the length of the coupling tube is increased, the amplitude and dominant frequency of the acoustic pressure fluctuations (p') gradually decrease toward the state of maximum suppression of the LCO. Correspondingly, the p' signal changes from LCO to low amplitude aperiodic oscillations via intermittency. The temporal synchrony between the global heat release rate (HRR) and p' fluctuations changes from synchronized periodicity to desynchronized aperiodicity through intermittent synchronization. At optimum parameters, this method suppresses the large amplitude LCO by disrupting the feedback loop between acoustic, hydrodynamic, and HRR fluctuations present in the combustor during TAI.

Introduction

Time-delayed feedback has been used to stabilize unstable periodic orbits in various dynamical systems such as lasers and neural networks [1]. Recent research has demonstrated that delayed acoustic self-feedback using a connecting tube suppresses limit cycle oscillations in several laminar systems, such as acoustic pipelines [2] and Rijke tubes [3]. A Hopf bifurcation causes a laminar system, such as a Rijke tube, to lose stability and become unstable [4]. In contrast, turbulent thermoacoustic systems are complex systems in which large amplitude limit cycle oscillations arise due to closed-loop interaction between hydrodynamic, acoustic, and heat release rate fluctuations. Such large amplitude self-sustained limit cycle oscillations in combustion systems can lead to performance loss and structural damage to components of gas turbines and rocket engines. In this study, we show that delayed acoustic self-feedback disrupts this complex interactions between the flame, the flow, and the acoustic field of the turbulent combustor, thus mitigating the limit cycle oscillations.

Results and Discussions

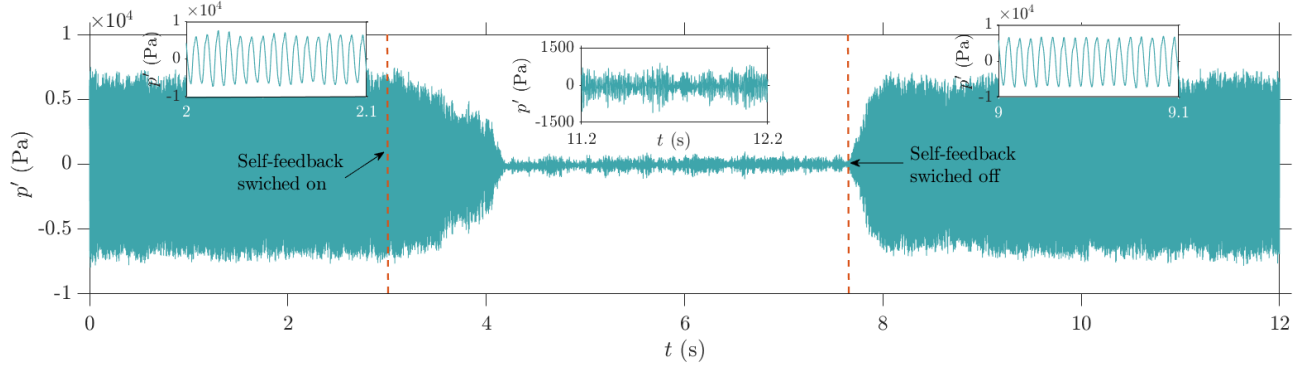


Figure 1: Acoustic pressure time series p' indicating the influence of delayed acoustic self-feedback on the amplitude of limit cycle oscillations. The magnified sections illustrate the dynamics of p' during different stages of delayed acoustic self-feedback.

As we approach the state of maximum suppression, the dynamics of acoustic pressure fluctuations changes from limit cycle oscillations to low-amplitude aperiodic oscillations via intermittency. In addition, the coupled behaviour between acoustic pressure and heat release rate oscillations changes from phase synchronisation to desynchronization via intermittent synchronisation. Furthermore, the coherent zones of acoustic power production observed in the spatial field of the combustor during the state of thermoacoustic instabilities entirely disintegrate during the state of maximum suppression. The magnitude of acoustic pressure fluctuations during the suppression state is comparable to that observed during the stable operation state of the combustor

References

- [1] Hövel, P., Dahlem, M., Dahms, T., Hiller, G., Schöll, E. (2009) Time-delayed feedback control of delay-coupled neurosystems and lasers *IFAC Proceedings* **42.7**:235-240.
- [2] Lato, T., Mohany, A. and Hassan, M. (2019) A passive damping device for suppressing acoustic pressure pulsations: The infinity tube *J. Acoust. Soc.* **146**:4534-4544.
- [3] Srikanth, S., Sahay, A., Pawar, S. A., Manoj, K. and Sujith, R. I. (2022) Self-coupling: an effective method to mitigate thermoacoustic instability *Nonlinear Dyn.* **196**.
- [4] Etikyal, S. and Sujith, R. I. (2017) Change of criticality in a prototypical thermoacoustic system *Chaos* **27**:023106.

Modeling turbulent thermoacoustic transitions using a mean-field synchronization approach

Samarjeet Singh*, Amitesh Roy*, Jayesh M. Dhadphale*, Swetaprovo Chaudhuri** and R. I. Sujith*

*Department of Aerospace Engineering, Indian Institute of Technology Madras, Chennai, India

**Institute for Aerospace Studies, University of Toronto, Ontario, Canada

Abstract. We develop a mean-field synchronization model where the heat release rate fluctuation within the confinement is modeled as an ensemble of phase oscillators evolving under the influence of acoustic pressure oscillations. The model captures the continuous and abrupt transition to thermoacoustic instability observed in disparate combustor configurations. Most importantly, the model captures spatiotemporal synchronization and pattern formation, which underlies the observed transition. The model encapsulates states of spatiotemporal desynchronization, chimeras, and global phase synchronization very well. The generality of the model highlights the possibility of extending the present model to predict limit cycle transitions in other fluid dynamical systems beyond thermoacoustics.

Introduction

Thermoacoustic instability in gas turbine combustors has disastrous consequences and presents a significant challenge in developing next-generation aircraft and power generation engines [1]. These instabilities develop through spatiotemporal synchronization of pressure and heat release rate fluctuations, resulting in self-sustained oscillations [2]. The instability is notoriously difficult to predict and control, and can have disastrous consequences such as severe damage to the engine components and even mission failures [3]. Therefore, the motivation of the present model comes from the observation that the transition to the state of thermoacoustic instability is associated with the emergence of global phase synchronization of the acoustic pressure and heat release rate fluctuations [2, 4]. In this study, we consider the flame response as an ensemble of phase oscillators restricted to evolve at a collective rhythm under the influence of acoustics. We derive the limit cycle solution using the method of averaging and estimate the amplitude and phase of the limit cycle oscillations for the thermoacoustic mean-field model. We demonstrate the applicability of the model in capturing both continuous and abrupt transitions to limit cycle oscillations. We show that the model is able to describe disparate transitions based on the underlying synchronization characteristic. We depict that the continuous and abrupt transitions to the limit cycle oscillations are associated with second-order and first-order synchronization transitions, respectively.

Results and Discussions

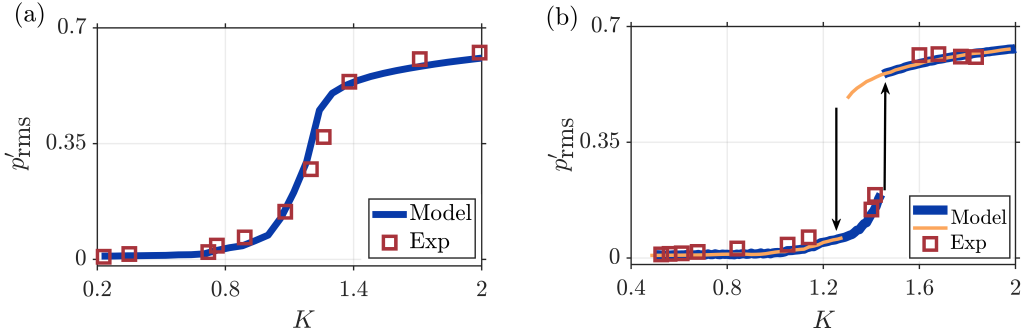


Figure 1: The bifurcation plot depicts the variation of normalized p'_{rms} as a function of coupling strength (K) in different combustors. Figure 1 shows the comparison of the bifurcation diagram obtained from the model (—) and experiments (□). In figure 1a, we show a continuous, sigmoid-type transition to the state of thermoacoustic instability through intermittency observed in the bluff-body dump combustor when the control parameter (K) is varied. In contrast, figure 1b exhibits an abrupt transition to the state of high-amplitude thermoacoustic instability through intermittency and low-amplitude thermoacoustic instability observed in the swirl-stabilized dump combustor. Importantly, the model has the ability to capture the states of spatial desynchronization, chimera, and synchronization underlying these transitions (not shown here). Therefore, we believe the model emerges as a powerful tool capturing the synchronization characteristics underlying different transitions by taking frequency distribution from an experimentally measured heat release rate spectrum as the only input.

References

- [1] Sujith R. I. & Pawar S. A. (2021) Thermoacoustic Instability: A Complex Systems Perspective. Springer Nature.
- [2] Mondal S., Unni V. R. & Sujith R. I. (2017) Onset of thermoacoustic instability in turbulent combustors: an emergence of synchronized periodicity through formation of chimera-like states. *J. Fluid Mech.* **811**, 659.
- [3] Juniper M. P. & Sujith R. I. (2018) Sensitivity and nonlinearity of thermoacoustic oscillations. *Annu. Rev. Fluid Mech.* **50**, 661.
- [4] Hashimoto T., Shibuya H., Gotoda H., Ohmichi, Y. & Matsuyama, S. (2019) Spatiotemporal dynamics and early detection of thermoacoustic combustion instability in a model rocket combustor. *Phys. Rev. E* **99**, 032208.

Locomotion dynamics of an underactuated wheeled three-link robot

Leonid Rizyaev, Yizhar Or

Faculty of Mechanical Engineering, Technion – Israel Institute of Technology, Haifa, Israel

Abstract – The wheeled three-link snake robot is a well-known example of an underactuated system modelled using nonholonomic constraints, preventing lateral slippage of the wheels. A kinematically controlled version assumes that both joint angles are directly prescribed as phase-shifted periodic input. In another version of the robot, only one joint is periodically actuated while the second joint is passively governed by a visco-elastic torsion spring. In our work, we constructed the two versions of the wheeled robot and conducted motion experiments under different actuation inputs. Analysis of the motion tracking measurements revealed significant amount of lateral slippage, in contrast to the standard nonholonomic models. Therefore, we proposed modified dynamic models which include wheels' lateral slippage and viscous friction forces, as well as rolling resistance. After parameter fitting, these dynamic models reach good agreement with the motion measurements, including effects of input's frequency on the mean speed and net displacement per period. This illustrates the importance of incorporating slippage and friction into the system's model.

Introduction

Underactuated multi-link robot locomotion has been addressed in many literature studies. One of the most classic examples is the wheeled three-link snake robot, composed of three rigid links supported by wheels and connected by rotary joints. Ideally, the wheels are assumed to resist lateral slippage, which induces non-holonomic constraints on the robot's motion [1]. These types of systems are called underactuated since their locomotion is generated by changing the shape, rather than directly controlling the body variables. A later work [2] studied the dynamics of the kinematically controlled snake robot near its singular symmetric states where $\phi_1 = \phi_2$. Regarding the semi-passive actuation, the work [3] focused on analysing the vehicle's dynamics with a single actuated joint, while the other joint is passive, governed by visco-elastic torsion spring, applying torque as $\tau_1 = -k\phi_1 - c\dot{\phi}_1$. Our work extends the previous studies both theoretically and experimentally. We analyzed the motion of the three-wheel snake (Fig. 1a) in both shape-actuated and semi-passive configurations. We conducted motion tracking measurements of our robotic prototype in both configurations, measuring the influence of input frequency on the motion, both in asymmetric input gaits, and symmetric ones that cross singular configurations.

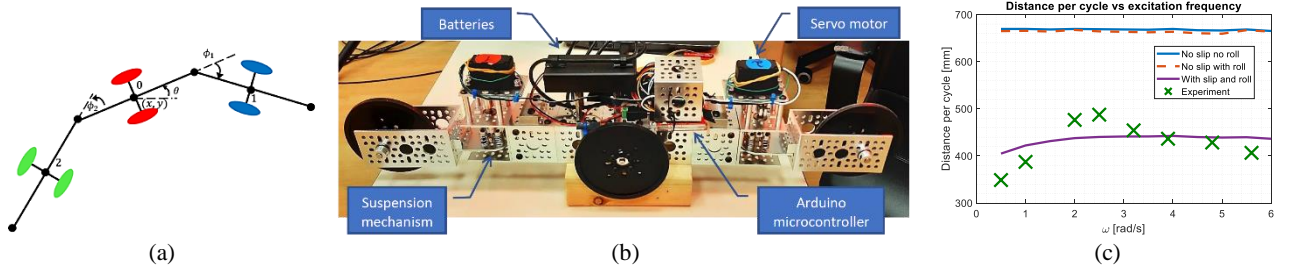


Figure 1: (a) The three-link robot model. (b) Our three-link robot with kinematic actuation at both joints. (c) Comparison with simulation results of different models with and without roll/slip dissipation for the of the kinematically-actuated robot.

Results and core findings

Motion measurements for the shape-actuated configuration show significant influence of actuation frequency on the mean speed and displacement (Fig. 1c), which cannot be explained by the kinematic equation of nonholonomic constraints based on no-slip conditions $v_i^\perp = 0$. This effect is caused by non-negligible lateral slippage of the wheels, due to inertial effects, as well as nearing singularities. To account for slippage, and to avoid non-smoothness and numerical sensitivity incurred by Coulomb-type friction [2], we incorporated linear viscous damping friction forces, as $f_i = -c_s v_i^\perp$ for each axle. In addition, rolling resistance of the wheels is also represented as linear damping $f_j^\parallel = -c_r v_j^\parallel$ for each wheel. After calibration of the roll/slip damping coefficients, we obtained good quantitative agreement with the experimental results (Fig. 1c). For the semi-passive configuration, the model predicts dependence on actuation frequency, even with no-slip constraints, and the effect of slip dissipation is increased for symmetric actuation which passes near singular states.

References

- [1] Shammas, E. A., Choset, H., & Rizzi, A. A. (2007). Geometric motion planning analysis for two classes of underactuated mechanical systems. *The International Journal of Robotics Research*, 26(10), 1043-1073.
- [2] T. Yona and Y. Or, "The wheeled three-link snake model: singularities in nonholonomic constraints and stick-slip hybrid dynamics induced by Coulomb friction," *Nonlinear Dynamics*, vol. 95, no. 3, pp. 2307-2324, 2019.
- [3] T. Dear, S. D. Kelly, M. Travers, and H. Choset, "Locomotive analysis of a single-input three-link snake robot," 2016 IEEE 55th Conf. Decis. Control. CDC 2016, no. Cdc, pp. 7542-7547, 2016.

Bifurcation scenarios in the hardware-in-the-loop experiments of highly interrupted milling processes

Rudolf R. Toth*, Daniel Bachrathy* and Gabor Stepan*

*Department of Applied Mechanics, Budapest University of Technology and Economics, Budapest, Hungary

Abstract. Hardware-in-the-loop (HIL) measurements of highly interrupted milling processes were conducted. A real spindle was used with a dummy tool on which the cutting forces were emulated with contactless sensors and actuators. During the experiments, Hopf- and period-doubling bifurcations were identified. The results of these measurements were compared with a 1 degree of freedom (DoF) delayed oscillator model. While the two show good agreement in the stability charts and the types of bifurcations observed, they also draw attention to the relevance of run-out compensation.

Introduction

The main limiting factor of efficiency and productivity in machining operations is the occurrence of regenerative vibrations (called chatter), which can increase wear on machine tools and produce intolerable machined surface quality. One approach to limit these harmful vibrations is the design of milling tools with irregular geometry [1]. The manufacturing of these tools themselves is a complex process making their design and prototyping expensive and time-consuming. The HIL environment allows for the emulation of cutting forces related to any tool geometry and material property without a need for prototyping. It has previously been shown that our HIL system is capable of reproducing the Hopf-bifurcation related vibrations in turning processes [2]. In the measurement presented here, a highly-interrupted down-milling process is investigated with a simple straight edge three-tooth ($Z = 3$) milling tool with 10% radial immersion. The oscillations of the dummy tool were measured at different axial depths of cut and spindle speeds. The emulated forces are updated at a frequency of 100 kHz using a low inductance coil. This high frequency is necessary to describe the sudden changes related to the virtual milling tool entering and leaving the material. The regenerative effects are emulated using a laser-based sensor, while the ferrite dummy tool is held by a real spindle (Fig. 1 panel a)) [2].

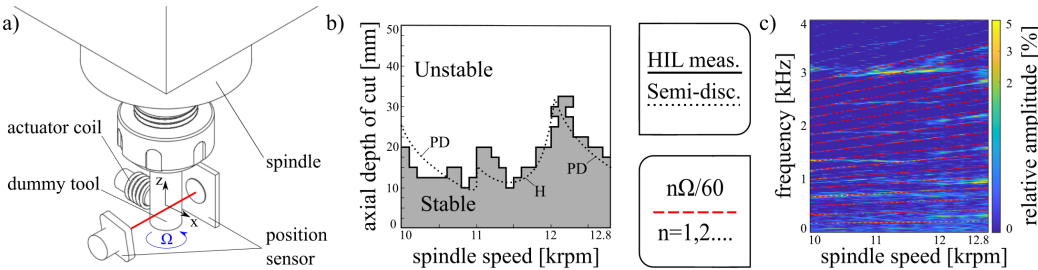


Figure 1: Panel a) Components of HIL system. Panel b) Stability charts. Panel c) Frequency content.

Results and discussion

The stability of the milling process was determined by the amplitude of the resulting vibrations at each parameter combination (Fig. 1 panel b)). This is compared to a stability map produced with the semi-discretization method applied to the corresponding 1 DoF mechanical model [3], which predicts the existence of three lobes in the actual spindle speed region. This calculation also describes the bifurcations related to the loss of stability, which is period-doubling for the lobes on the left and the right, and Hopf-bifurcation for the lobe in the middle. The stability regions show good agreement of the calculations and the measurements. For the identification of the bifurcations, the frequency content of the measured oscillations was used (Fig. 1 panel c)). In the region of the middle lobe, the dominant frequency is close to the natural frequency of the dummy tool with no linear dependence on the spindle speed Ω , which is in accordance with the Hopf-bifurcation. The right-side lobe shows the period-doubling frequencies, which are linearly dependent on the spindle speed and are harmonics of the half tooth-pass frequency. The results of this measurement show, that this HIL system is capable of emulating real milling processes by capturing the period-doubling bifurcations unique to milling processes besides the Hopf-bifurcations shown in previous turning experiments. The deviation between theory and experiment at the left-side lobe draw the attention to the relevance of run-out compensation in the HIL system.

References

- [1] Stepan G., Hajdu D., Iglesias A., Takacs D., Dombovari Z. (2018) Ultimate capability of variable pitch milling cutters. *CIRP Ann.-Manuf.Technol.* **67**:373-376.
- [2] Beri B., Miklos A., Takacs D., Stepan G. (2020) Nonlinearities of hardware-in-the-loop environment affecting turning process emulation. *Int. J. Mach. Tools Manuf.* **157**: Article 103611.
- [3] Insperger T., Mann B.P., Stepan G., Bayly P.V. (2003) Stability of up-milling and down-milling, part 1: alternative analytical methods. *Int. J. Mach. Tools Manuf.* **43**:25-34.

A Platform for Data-Driven Nonlinear Dynamics and Mechatronics Education: A Student-Designed Spherical Magnetic Pendulum

James Oti*, Anthony Migash*, Ryan McDermott*, Joseph Cornell*, and Nikhil Bajaj*

*Department of Mechanical Engineering and Materials Science, University of Pittsburgh, Pittsburgh, PA, USA

Abstract. The spherical magnetic pendulum is a classic experiment that is relatively straightforward to construct and allows for improved intuitive understanding of nonlinear systems, chaos, as well as understanding the tools that are used to explore such systems, such as basins of attraction. In this work, we consider the design of a prototype spherical magnetic pendulum that exhibits chaotic behavior. The eventual goal is to produce a public display that allows laypersons to interact with an instrumented apparatus and contribute to an experimentally generated map of the system’s basins of attraction. Another goal of the project is to serve as an opportunity to introduce the participating students to mechatronic instrumentation techniques for dynamic systems. The collected trajectory data is aggregated, for use in coursework topics in data-driven nonlinear dynamics, including recursive neural networks and variants, physics-informed neural networks, and system identification.

Introduction

The spherical magnetic pendulum is a classic experiment, often seen as a common desktop toy, with a magnetic “bob” at the end of the pendulum and magnets on the base. It demonstrates the extreme sensitivity to initial conditions characteristic of chaotic nonlinear systems [1], [2]. Prior experimental efforts used simple data collection approaches to use this system as a teaching tool [3] but had relatively noisy trajectory tracking (results were admirable given the low cost of implementation). In this work, a capstone student team was assembled, and assigned budgetary and performance constraints to create a prototype, instrumented spherical pendulum towards creating a demonstration of chaotic behavior that would be suitable for interaction with the public. A second goal was to generate data for use in coursework for methods in data-driven nonlinear dynamics. The public display and coursework uses both require smooth, accurate trajectory measurement beyond that provided by prior work.

Results and Discussion

The design team had significant freedom in their approach and used local resources for laser cutting and 3D printing to produce a pendulum system appropriately sized for interaction with human users (Figure 1(a)). A hinge design translates motion to individual paddles isolated the two angular coordinates, and the motion of the paddles is tracked at 2 kHz by Avago ADNS-9800 High-Performance LaserStream Sensors, used in computer mice. The apparatus consists of a Raspberry Pi Model 400 computer connected to a monitor, running custom scripts programmed in Python, and connects to an Arduino Mega microcontroller responsible for communicating with the sensors. The mouse sensors combined with the paddles allow for tracking accuracy of better than 0.5 mm. To prevent long-term drift due to the trajectory integration approach, a periodic self-calibration system was implemented based on beam-break sensors attached to the paddles. Figure 1(b) gives a representative measured trajectory, from start by a human releasing the pendulum from an arbitrary initial condition to the pendulum finally stopping at one of the magnets. The data generated by the system is aggregated and will be made available publicly for use in coursework in data-driven nonlinear dynamics, for topics such as recursive neural networks, physics-informed neural networks, and system identification (examples of such coursework will be presented). The coursework will have been applied in a Machine Learning for Dynamic Systems and Control course in the Spring of 2023. Future efforts will involve students developing alternative designs and means for measurement and improving the real-time visualization of the pendulum motion towards a final public display piece.

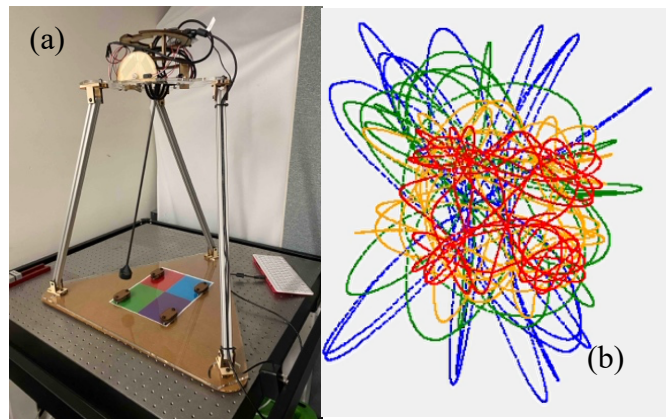


Figure 1): (a) The student-designed spherical magnetic pendulum, and (b) representative measured trajectory (the color varies with time along the trajectory for visualization).

References

- [1] J. R. Claycomb and J. H. Valentine, “The butterfly effect for physics laboratories,” *Phys. Educ.*, vol. 50, no. 2, p. 170, Feb. 2015.
- [2] S. D’Alessio, “The magnetic pendulum and weather,” *Phys. Educ.*, vol. 55, no. 6, p. 063002, Nov. 2020.
- [3] L. M. Ramos, C. R. N. Reis, L. B. Calheiro, and A. M. B. Goncalves, “Use of Arduino to observe the chaotic movement of a magnetic pendulum,” *Phys. Educ.*, vol. 56, no. 1, p. 015013, Dec. 2020.

Effects of controller-induced dynamics on experimental bifurcation analysis

Mark Blyth*, Krasimira Tsaneva-Atanasova**, Lucia Marucci* and Ludovic Renson***

**Department of Engineering Mathematics, University of Bristol, Bristol, UK*

***Hub for Quantitative Modelling in Healthcare, University of Exeter, Exeter, UK*

****Department of Mechanical Engineering, Imperial College London, London, UK*

Abstract. Control-based continuation (CBC) is an experimental method that uses feedback control to probe the dynamics of a physical system. CBC relies on finding control targets that render the control system non-invasive, recovering the naturally occurring system behaviours without modifying their geometry or location. Here, we highlight a case where a CBC experiment fails due to the controller inducing spurious, invasive dynamics in the system. A limit cycle in a slow-fast system is controlled successfully, however the controller causes it to collapse through a canard explosion in the prediction step of a continuation. We propose strategies to overcome this issue, and use it as a case-study to highlight how control strategies and residual invasiveness can impact the results of an experimental bifurcation analysis.

Introduction

A feedback controller is noninvasive if it stabilises a control target $x^*(t)$, and the associated control action $u(x^*, x, t) \equiv 0$. Controllers can nevertheless exert a nonzero control action when pushing a system onto a target, so that unstable responses become stabilised and directly observable [1]. Zero control action guarantees that observed features are intrinsic to the system, as the controller will not modify the dynamics. In practise however, small invasiveness is to be expected, for example from feedback delays in a controller, or through intentional perturbations and random errors when solving for noninvasive targets. For some control schemes, this invasiveness can cause the controller to modify the system dynamics in unwanted ways. Continuity suggests that small invasive errors in x^* lead to small control actions $u(x^*, x, t)$, and hence small errors between intrinsic and observed system responses. Here we propose a counterexample, where a small error in a control target causes the controller to induce a catastrophic error in the system response. Our example arises in the CBC of relaxation oscillations. Large-amplitude oscillations in a slow-fast system can rapidly collapse through a canard explosion. Due to the autonomous nature of our chosen control law, a canard explosion is able to happen in the prediction step of a continuation, causing CBC to fail.

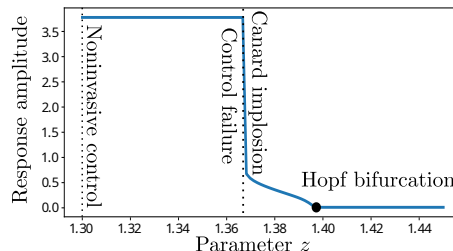


Figure 1: Angle-encoded controller [3] causes the dynamics of interest to collapse through a canard explosion as z is increased.

Results

We consider as a case study the Fitzhugh-Nagumo model [2]. An autonomous control scheme is constructed using the method of angle-encoding [3]. This proceeds by embedding time-dependent observations $x(t)$ in a reconstructed limit cycle, and calculating the angle ϕ of an embedded state relative to a reference direction and origin. Proportional control is applied with errors defined between measurements $x(\phi)$ and an angle-indexed control target $x^*(\phi)$, to phase-lock control targets to system responses. This control strategy acts as a phase constraint, producing a locally unique oscillatory solution to the noninvasive equations, and avoids the need to compute an oscillatory period. The control scheme is initialised with a noninvasive control target from open-loop data, then system bifurcation parameter z is increased without changing the control target, to emulate natural parameter continuation. As illustrated in Fig. 1, the controlled limit cycle collapses through a canard explosion, destroying the dynamics of interest. This happens due to a combination of the slow-fast dynamics, and the autonomous control scheme. Natural parameter continuation modifies the system parameter in a prediction step, whereas pseudo-arclength continuation also changes the control target; this causes the canard explosion to happen sooner. We use observations about the control law to justify how this issue can be avoided, by moving the angle-defining polar origin. More generally, we emphasise that care must be taken to ensure that CBC experiments remain within a parameter range for which intrinsic dynamics can be observed, and that this parameter range may be small.

References

- [1] Sieber, J. and Krauskopf, B., 2008. Control-based bifurcation analysis for experiments. *Nonlinear Dyn.*, 51(3), pp.365-377.
- [2] FitzHugh, R., 1961. Impulses and physiological states in theoretical models of nerve membrane. *Biophys. J.*, 1(6), pp.445-466.
- [3] Blyth, M., Tsaneva-Atanasova, K., Marucci, L. and Renson, L., 2022. Numerical methods for control-based continuation of relaxation oscillations. *arXiv preprint arXiv:2209.10210*.

Dynamic analysis of transmission line cables using nonlinear 3d frame element

Nilson Barbieri^{*,**}, Gabriel de Sant'Anna Vitor Barbieri^{*}, Renato Barbieri^{***} and Key Fonseca de Lima^{*}

^{*}Department of Mechanical Engineering, Pontifícia Universidade Católica do Paraná, Curitiba, Brasil

^{**}Department of Mechanical Engineering, Universidade Tecnológica Federal do Paraná, Curitiba, Brasil

^{***}Centro de Ciências Tecnológicas, Universidade do Estado de Santa Catarina, Joinville, Brasil

Abstract.

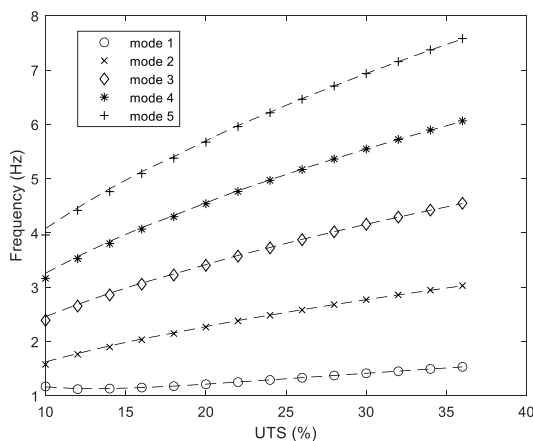
The 3D frame finite element is used in this work to investigate the nonlinear dynamic behavior of electrical transmission line cables. The elastic stiffness matrices (small displacements) and the geometric stiffness matrix (large displacements) are obtained through Timoshenko's beam theory. The mathematical model is validated by comparing numerical and experimental natural frequencies. The experimental modal behavior is obtained using three different cables with approximate lengths of 54m. The experimental data are obtained through accelerometers arranged along half of the sample and the system is excited using an impact hammer. The same mathematical model is used to validate the torsional behavior by adjusting the angle of twist. In this case, another test bench was used, varying the position of a lever. Excitation was obtained by manually moving the lever clockwise and counterclockwise.

Introduction

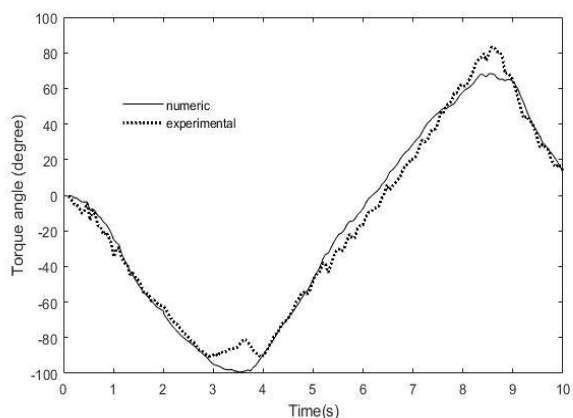
The mathematical model is obtained using the 3d non-linear frame element. The used element has 2 nodes and 12 degrees of freedom (Timoshenko 3d beam element). The stiffness matrix is composed of two parts: elastic stiffness matrix (small displacements) and geometric stiffness matrix (large displacements). The differential equation of motion has the following form [1]:

$$\mathbf{M}\ddot{\mathbf{u}}(t) + \mathbf{K}_E\mathbf{u}(t) + \mathbf{K}_G(\mathbf{u})\mathbf{u}(t) = \mathbf{f}(t)$$

where: \mathbf{M} is the mass matrix; \mathbf{K}_E and $\mathbf{K}_G(\mathbf{u})$ are the elastic and geometric stiffness matrices; $\mathbf{f}(t)$ is the external excitation vector; $\ddot{\mathbf{u}}, \mathbf{u}$ are the acceleration and displacement vectors. Figure 1(a) shows the experimental data (symbols) and numeric values (dashed lines) for the variation of the first five natural frequencies in relation to the variation of the percentage of the ultimate tensile strength (mechanical load). Figure 1(b) shows the experimental (symbol) and adjusted numeric (dotted line) of the torque angle [2].



(a)



(b)

Figure 1: Variation of natural frequencies (a) e torque angle (b).

It is noted that the adjustments of natural frequencies and torque angle had good agreement between numerical and experimental values.

References

- [1] Chandrupatla T. R., Belegundu A. D. (2002) *Introduction to finite elements in engineering*. Prentice Hall, Upper Saddle River, New Jersey.
- [2] McConnell K.G., Zemke W.P. (1982) A Model to Predict the Coupled Axial Torsion Properties of ACSR Electrical Conductors. *Experimental Mechanics* 237-244.

Rail-Structure-Interaction Parameters at Ballasted Viaduct in Rohtak - Gohana Elevated Stretch: Instrumentation, Measurements and Interpretation

Nupur Saxena*, Chandan Kumar*, Pameer Arora** and Samit Ray-Chaudhuri*

*Department of Civil Engineering, Indian Institute of Technology, Kanpur, UP, India

**Northern Railways, Delhi, India

Abstract. This work deals with India's first elevated multi-span (about a kilometer long) Bridge along the Rohtak-Gohana stretch having Continuous Welded Rail (CWR) with a ballasted deck. The work focuses on instrumentation involving various sensors for real-time measurement of responses for evaluation of the effects due to rail-structure-interaction (RSI). For this study, three spans were selected with varying attributes such as stiffness, span length, height of piers and type of deck. Parameters such as total relative displacement of the rail with respect to the deck, vertical displacement of the deck at the ends, and horizontal support reaction generated at the supports under normal train running conditions, were recorded using data acquisition system for a period of several days. The results of this work show that, while the limits prescribed in the codes are reasonable, further research is needed to better understand the interaction effects.

Introduction

CWR are long-length jointed rail tracks formed by welding many short rails together to form several kilometers long rails. Owing to their long lengths and the resistance offered by ballast and rail fasteners, such rails cannot expand or contract freely in the central portion. A bridge deck is however able to move to some extent due to thermal and traffic loads while the CWRs over on the bridge are usually restrained. This leads to relative displacement between the rail and the bridge, which in turn induces additional stresses in the rail. Also, an extra horizontal support reaction is developed due to this phenomenon. Relative displacement of rail with respect to the bridge is an important parameter as it causes RSI effects. If these parameters exceed the permissible limits, then the track's safety may get hampered due to the loosening of ballast. The increase in tensile and compressive stresses beyond the permissible value could lead to fractures and buckling issues in the rail. Therefore, it is immensely vital to ensure that these parameters are within the prescribed limits as mentioned by UIC 774-3R and RDSO (Indian Railways) codes. Simoes et al. observed that stiffness of the abutment and foundation greatly influences the axial forces in the track. Somaschini et.al. concluded that the high-order resonances up to 30 Hz between the deck and the passing train local vibration modes possess a major influence on the extreme acceleration. In general, the overall RSI effects are of nonlinear nature primarily owing to ballast and rail fastening mechanism, which are difficult to model in absence of actual measurement data. Measured data are thus not only useful for checking the adequacy of the code provisions but also to update analytical model for further predictions.



Figure 1: Continuous Welded rail track at Rohtak.

Results and Discussion

The result of this work shows that the absolute horizontal displacement of the deck, relative longitudinal displacement of rail with respect to the deck under tractive/braking forces, and the bending effects due to vertical loads are reasonable considering the code prescribed limit. However, further research is needed to better understand the interaction effects. It is also found that the span under the tallest piers has the greatest relative displacement and mid-span displacement. Also, it can be observed that a higher horizontal support reaction is generated on the abutment side, which can be related to larger stiffness on the abutment side.

References

- [1] UIC (2001) UIC 774-3R: Track/bridge Interaction - Recommendations for calculations, FRA.
- [2] RDSO (2015) -BS 114-2: Guidelines for carrying out rail-structure interaction studies on metro systems, IND.
- [3] RDSO (2016) BS- 106-R: Guidelines for instrumentation of bridges, IND.
- [4] Simões R., Calçada R., Delgado R. (2008) Track-bridge interaction in railway lines: Application to the study of the bridge over the River Moros. Track-Bridge Interaction on High-Speed Railways. CRC Press, LDN.
- [5] Somaschini C., Matsuoka K., Collina A. (2017) Experimental analysis of a composite bridge under high-speed train passages. *Procedia Eng.* **199**:3071-3076.

TOOL WEAR SUPERVISING APPLYING VIBRATION MODAL ANALYSIS

Piotr Wolszczak*, Marcin Bednarz** and Grzegorz Litak*

* Lublin University of Technology, Faculty of Mechanical Engineering, Department of Automation, Lublin, Poland

** Zamość Academy, Zamość, Poland,

Abstract. Application of modal analysis of tool vibration signal during cutting allows the separation of components caused by phenomena associated with the drive system and components generated in the cutting zone. However, the interpretation of these results is difficult. The article presents ways of using modal analysis in relation to signals observed during drilling or milling. The tool vibration signal was recorded using vibroacoustic sensors and then subjected to empirical decomposition. An additional frequency analysis of the extracted component signals was carried out in order to identify their sources and select the components generated in the cutting zone. In this way, vibrations related to the spindle speed and the number of tool blades were filtered out. Comparing the results of the physical experiment with the results of numerical simulations, it was possible to distinguish the components related to the deflection of the tool shank and the work of the blades. The applied method is illustrated by examples of comparisons of the operation of tools with changed geometry, the influence of machining parameters and the monitoring of the initial lapping phase of the blades. The presented method of optimizing machining parameters is especially important when machining difficult-to-machine materials.

Introduction

One of the ways of wear of cutting tools is chipping and chipping of the edges of the cutting blades. They are formed as a result of the action of cutting forces on the rake surface [1, 2]. Self-excited vibrations are generated during the detachment of the material layer. Accumulating vibrations contribute to chipping of the blades by changing the nature and increasing the value of the cutting forces, which remain undispersed, and by material fatigue. In the case of carbide materials, the method of initial lapping of the tools can be significant for the further usefulness of the tool. In the workshop, initial wear is observed by the machine operator's hearing and by visual inspection of the tools and machined surface after the first few passes. Instruments used so far in laboratory tests are used more and more often in workshop conditions [3]. Manufacturers of cutting tools use electronic devices to determine the operating characteristics of their products and to select the optimal operating parameters [4].

Results and discussion

Vibration sensors connected to the registration, processing and visualization system are used to measure the forces generated in the cutting zone. In the case of rotating tools, the sensors are placed on machine components or material. Based on the values of the recorded accelerations, it is concluded about the variability of the forces acting on the tool. The use of such a form of monitoring involves the need to develop a measurement method and measurement procedures in order to avoid various types of systematic errors, e.g. related to changing the location of sensors.

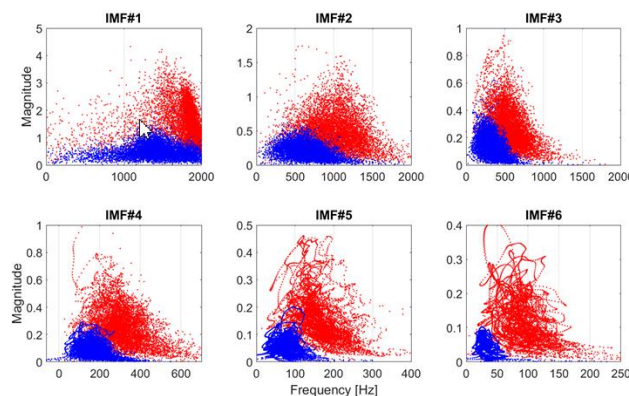


Figure 1: Example results of dependences amplitude and frequency modes of decomposition empirical Hilbert-Huang sample runs of the tool type “Hi-Feed” in the course of: red - cutting operation, and blue - tool linear movement [5].

References

- [1] Sarhan A. et al. (2001) Interrelationships between cutting force variation and tool wear in end-milling. *Journal of Materials Processing Technology* **109**: 229-235.
- [2] Choudhury S.K., Rath S. (2000) In-process tool wear estimation in milling using cutting force model. *Journal of Materials Processing Technology* **99**: 113-119.
- [3] Dimla E. i Dimla Snr. (2000) Sensor signals for tool-wear monitoring in metal cutting operations—a review of methods. *International Journal of Machine Tools and Manufacture*. **40**: 1073-1098.
- [4] Ghani J.A., et al. (2011) Monitoring online cutting tool wear using low-cost technique and user-friendly GUI. *Wear*. **271**: 2619-2624.
- [5] Wolszczak P., Litak G., Łygas K. (2017) Monitoring of cutting conditions with the empirical mode decomposition. *Adv. Sci. Technol. Res. J.* **11**:96-103.

Quasi-zero stiffness vibration isolator under vertical seismic loads

Giovanni Iarriccio, Antonio Zippo, Moslem Molaie and Francesco Pellicano

Department of Engineering, University of Modena and Reggio Emilia, Modena, IT

Abstract. An experimental study on the vibration of a payload isolated through a quasi-zero stiffness (QZS) isolator subject to vertical ground motion is presented. QZS isolators exploit kinematic nonlinearities to enhance the vibration attenuation of a linear mass-spring system. In this paper, stepped-sine tests have been performed to identify the system parameters and determine the isolator transmissibility. The parameter identification has been carried out by fitting a phenomenological model to the experimental data. The QZS isolator transmissibility exhibits a natural frequency reduction, and the system effectively suppresses the ground harmonic vibration about the fundamental frequency of the mass-spring isolator. A non-negligible presence of dry friction has been observed, leading to the stick-slip phenomenon, and affecting the suspension activation at low frequencies. Then, the suspension response under different realistic earthquake signals is presented and critically discussed.

Introduction and Results overview

Every year, more than one million seismic events and a large number of fatalities challenge the human population [1]. The development of new building technologies, and early warning and prevention systems can make the difference in countering the disastrous effects of an earthquake. In this framework, exploiting the inherent nonlinearities inside the system could represent a way to develop a new class of high-performance devices for preventing buildings from disastrous damages during seismic events.

The proposed mechanism consists of a tripod made by a translating mass m resting on a vertical spring of stiffness k_v , three oscillating rods of length l connected to the mass and to three horizontal springs of stiffness k_h , and a base plate [2]. The oscillating mass is constrained by three linear sliders to translate over a vertical guide, and loose tolerances have been considered to reduce the over constrain, see Figure 1(a).

Considering the Christchurch earthquake as the shaker base input, the experimental results shown that QZS mechanism improves the vibration suppression guaranteed by the respective linear mass-spring system and successfully isolates the payload from the ground motion, providing acceleration peak reduction of 85.95 % and 80.87 % in terms of RMS, see Figure 1(b).

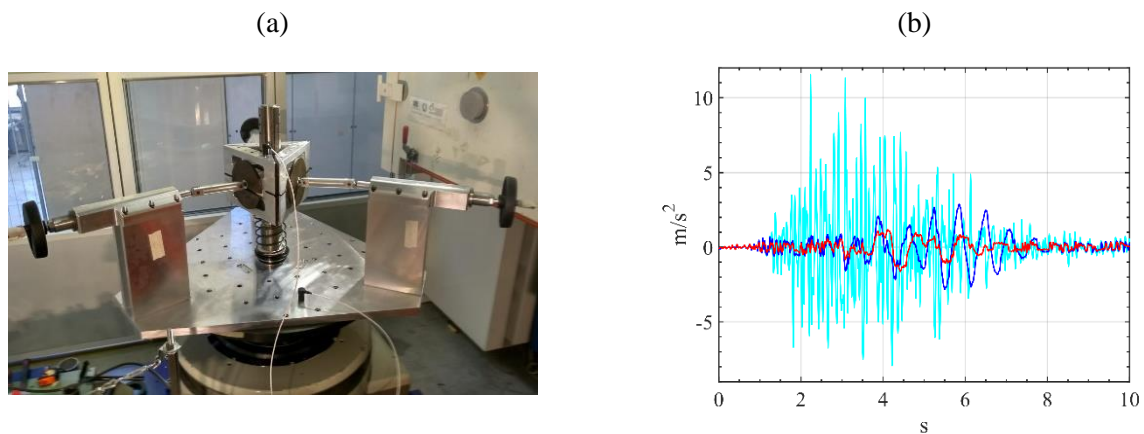


Figure 1: (a) Quasi-zero stiffness isolator and, (b) system response to Christchurch earthquakes. (— ground acceleration, — linear suspension, and — QZS isolator)

References

- [1] Doocy, S., Daniels, A., Packer, C., Dick, A., and Kirsch, T. D., (2013), The Human Impact of Earthquakes: A Historical Review of Events 1980-2009 and Systematic Literature Review., PLoS Curr., 5.
- [2] Iarriccio, G., Molaie, M., Zippo, A., Pellicano, F. Experiments on a Quasi-zero Stiffness Suspension for Passive Vibration Control (2022) Mechanisms and Machine Science, 122 MMS, pp. 306-312. DOI: 10.1007/978-3-031-10776-4_36

Experimental design for corotating pinned spiral waves and synchronization

Parvej Khan* and Sumana Dutta*

**Department of Chemistry, Indian Institute of Technology Guwahati, Assam, India*

Abstract. The synchronization phenomena and the mutual coordination is very common in nature. It is widely spread from human brain to menstrual cycle of two friends to network of fireflies. Oscillators in biology do synchronize. Here in this study, we examine the synchronization phenomena in a chemical system with Belousov-Zhabotinsky reaction. We used pinned spiral rotors for our experiments, because Pinning obstacles are considered as scar tissue in our heart. We designed our experiment in such a way where the directions of all the rotors are same. We found a change of synchronization states with time.

Introduction

Self-organization and pattern formation is very ubiquitous in nature. Patterns are seen in animal coats to spiral galaxy. Spiral and scroll waves formation occurs in our brain, heart etc. Formation of spiral waves in our heart is often dangerous and can even lead to death through cardiac arrhythmias. So, it is necessary to study the behaviour or the dynamics of the spiral waves for better understanding our cardiac wave patterns.

Study on the control of the dynamics is carried out using various gradients like thermal, electric field or using cross field. Synchronization study in experimental system with BZ reaction is one of the recent kinds of study of these excitable waves. Recent study on interaction of multiple spirals shows the wave-length and core-separation dependency of spirals leads to different kind of interaction like attraction, repulsion. Steinbock and others numerically show the synchronization phenomena of pinned rotors depends on wavelength and the separation of the two rotors. Rotational synchronization in phase and frequency of counterrotating pinned spirals are also shown in simulation as well as in experiments with BZ reaction where the diameters of the obstacles were different. Here in this manuscript, we study the synchronization behaviour of pinned spiral waves moving in same direction. As scar tissue can be compared with the heterogeneous obstacle, so we need to study the dynamics when these spiral waves gets attached to this obstacle.

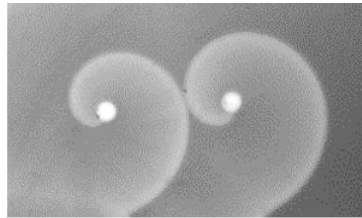


Figure 1: Two corotating pinned spirals.

Results and discussion

We studied about the synchronization phenomena of two corotating spirals pinned to heterogeneity. We carried out our experiments with BZ reaction system, we also did some simulations with Barkley reaction-diffusion model. We observed the synchronization pattern changes with time with compared to beginning.

References

- [1]] H. Kalita, P. Khan, and S. Dutta, Rotational synchronization of pinned spiral waves, *Physical Review E* **106**:034201(2022).

Numerical and experimental investigation of nonlinear dynamics of downhole drilling

Ahmed Al Shekaili*, Yang Liu* and Evangelos Papatheou*

*Engineering Department, University of Exeter, North Park Road, Exeter, UK, EX4 4QF

Abstract. Drilling operation is essentially achieved and determined with the help of the drillstring which is composed of various accessories that are joined together to deliver the necessary torque from the rotary table to the drill-bit. The drillstring is normally exposed to different nonlinear dynamics that occur an axial, lateral and torsional base excitations, which consequently lead to fail under forms of bit-bouncing, whirling and stick-slip phenomena. This work aims to study the nonlinear dynamics caused by the interactions of drillstring with borehole, contacts of drill-bit with rock formation, instability of the drillstring and variation of the drilling influencing parameters. The characteristic behaviours of the drillstring were analysed by using a constructed experimental rig and were compared with a mathematical model. The experimental rig was able to simulate those undesired nonlinear phenomena which can draw a wider understanding into their mitigation methods.

Introduction

The drillstring, which is one of the main mediators to transmit the required torque from the surface to a drill-bit, has been remarkably responsible to produce necessary strength to drill rock formation during drilling operation along with an axial force. The operation of rock drilling encounters several undesired dynamic vibrations such as coupled or uncoupled axial, lateral and torsional modes that occur predominantly due to the difference of drillstring slenderness ratio between its diameter and length [1]. These nonlinear phenomena are significant causes for precocious issues of drillstring components and drilling performance when they are exposed to severe intermittent contacts of drillstring with borehole and intricate interactions of drill-bit with rock. They turn the drilling fulfilment to a catastrophic failure due to tool wear and damage which consequently increase the drilling non-productive time and cost [2]. This study provides a significant technical support to understand and analyse the nonlinear drillstring by experimentally optimising drilling parameters as shown in Fig.1 (a) and predicting its vibrations. An extensive work was conducted to model the nonlinear dynamics of drilling in different theoretical approaches while inadequate works have been conducted experimentally as a fully coupled vibration in both vertical and horizontal drillstring [3]. The present work is intended to extend by involving a flexible drillstring to analyse the influence of slenderness ratio using different types of rocks.

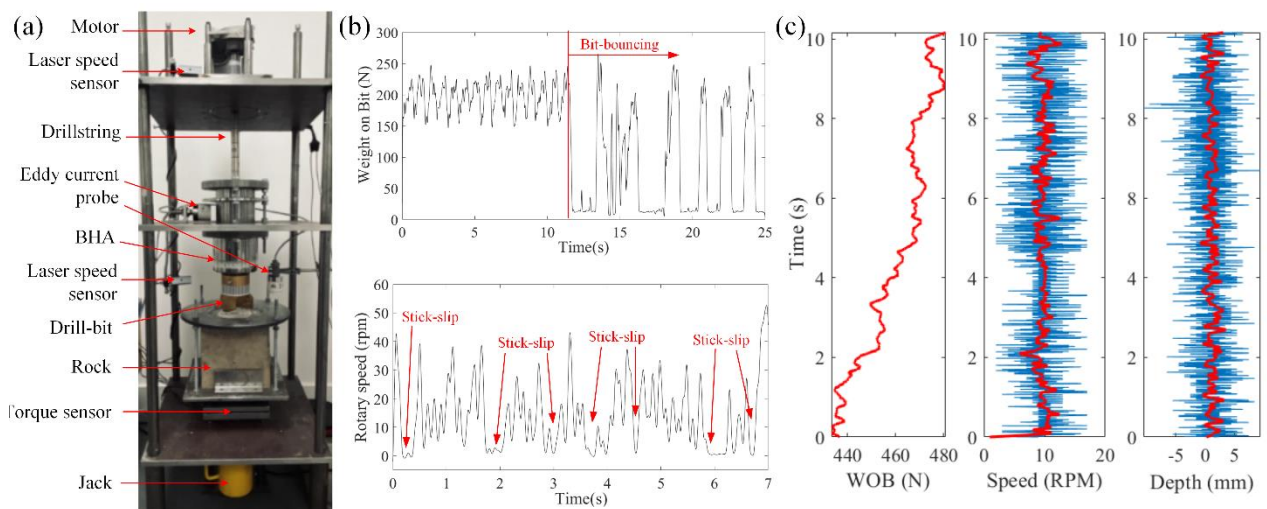


Fig. 1: (a) Experimental rig, (b) drillstring dynamic phenomena: bit-bouncing and stick-slip, and (c) drilling performance: time histories of weight-on-bit (WOB), rotary speed and rate of penetration (ROP) during a drilling process.

Results and Discussion

Experimental results shown in Fig. 1(b) reveal the complex behaviours excited during the drilling operation, such as stick-slip and bit-bouncing, in which a particular intention is paid to understand the various influencing factors that limit safe drilling, see Fig. 1(c). Experimental results present a good agreement with the proposed numerical model to visualise the nonlinear dynamics of the experimental drilling rig. The severity of lateral and torsional vibrations increases significantly within high impact and frictions of rotary speed and weight on bit compared to the axial vibrations.

References

- [1] Tucker W. R., Wang C. (1999) An integrated model for drill-string dynamics. *J. Sound Vib.* **224**:123-165.
- [2] Kapitaniak M., Vaziri V., Pérez Chávez J., Nandakumar N., Wiercigroch M. (2015) Unveiling complexity of drill-string vibrations: Experiments and modelling. *Int. J. Mech. Sci.* **101-102**:324-337.
- [3] Lian Z., Zhang Q., Lin T., Wang F. (2015) Experimental and numerical study of drill string dynamics in gas drilling of Horizontal Wells. *J. Nat. Gas Eng.* **27**:1412-1420.

A laboratory scale Foucault pendulum for the measurement of frame-dragging

Matthew P. Cartmell* and Edmondo A. Minisci*

*Department of Mechanical and Aerospace Engineering, University of Strathclyde, Glasgow, G1 1XJ, Scotland, UK

Abstract. A Foucault pendulum is generally considered to swing in a fixed orientation relative to the inertial frame of the fixed stars. However according to general relativity there is a small but finite precession over time of the pendulum swing plane relative to the fixed stars due entirely to the frame-dragging effect predicted by general relativity. This form of frame-dragging is represented physically by the Lense-Thirring precession of a gyroscopic test mass due to the proximity and the rotation of a massive body to the test mass. This precession may be calculated for various astrodynamical scenarios, but can also be modelled and calculated for a small test mass in the vicinity of the rotating planetary mass of the Earth. This manifestation of frame-dragging has already been measured in LEO by the GP-B and LAGEOS missions, but has not, to the authors' knowledge, been measured terrestrially as yet. The work described in this paper is one attempt to make this measurement, using a short, instrumented, Foucault pendulum in the northerly latitude of Glasgow in Scotland. The paper will summarise the work done to date to model the frame-dragging effect using the analogy of gravitoelectromagnetism, and then will focus on the modelling, the design and build of the Foucault pendulum which will be used to attempt the measurement, and will end with a brief summary of the requirements of the measurement itself.

Introduction

An inertial frame is considered not to accelerate in the usual detectable sense. General relativity shows that inertial frames are 'influenced and dragged by the distribution and flow of mass-energy in the universe' [1]. This frame-dragging influences the flow of time around a spinning body. An object on a prograde orbit will take longer to get back to the starting point than a similar object which is travelling retrograde on the same orbit. Twins travelling on exactly the same equatorial orbit but in opposite directions will age differently on meeting up at the starting point by around 10^{-16} s. This is the well-known twins paradox, and a consequence of frame-dragging. Frame-dragging was modelled by Lense and Thirring in 1918 such that inertial frames are dragged around a central rotating mass due to the effect of its gravity on the surrounding spacetime [2]. Rotation of the central mass twists the local spacetime and perturbs the orbits of other masses nearby. This is Lense-Thirring (LT) precession. The Earth's gravitational field is capable of generating frame dragging. We note that LT precession is based on both the presence and the rotation of a massive body in the proximity of a test mass. It is important to note that today, to the authors' knowledge, no terrestrial measurement has been made of LT precession. This is principally because of the extremely high level of accuracy required to discriminate the very small LT precession from other effects and noise, and the fact that this problem is compounded at non-polar locations.

Results and discussion

It is the aim of the research reported here to continue to move a little closer to making a reliable terrestrial measurement. Previous analysis of terrestrial LT measurement [3] obtained a prediction of 219.5 mas/year at the North Pole and 162.6 mas/year in Glasgow, Scotland. The polar value differs by 0.227% from the value of 220 mas/year calculated by Pippard [4] for that location. The work in this paper summarises the measurement of LT from the theoretical perspective of gravitoelectromagnetism, and goes on to propose a measurement algorithm for measurement of the LT precession of the laboratory Foucault pendulum with reference to the azimuth of a guide star. The main features of the Foucault pendulum are described and some of the initialisation tests are stated, specifically that an electromagnetically excited laboratory Foucault pendulum has been installed at the University of Strathclyde in a converted laboratory space and is currently being commissioned. It is 4190 mm in length terminating in a cylindrical copper bob of mass 2.54 kg. The pendulum is suspended from a pivot system designed for accurate and repeatable swing and precession. Bob motion is detected by an optical system, and an algorithm to detect the orientation of the pendulum swing-plane with reference to the azimuthal position of a guide star, and then the LT precession is to be accrued over time.

References

- [1] Chartas G. (2020) Frame Dragging, website <http://chartasg.people.cofc.edu/chartas/Teaching.html>.
- [2] Lense-Thirring Precession, website https://en.wikipedia.org/wiki/Lense%E2%80%93Thirring_precession.
- [3] Cartmell M.P. (2021) On the terrestrial measurement of frame-dragging, 2nd Conference on Nonlinearity, Belgrade, 18-22 October 2021, pp 1-23.
- [4] Pippard A. B. (1988) The parametrically maintained Foucault pendulum and its perturbations. *Proc. Royal Soc. London A*. **420**:81-91.

Nonlinear system identification of a multi-story building with geometrical nonlinearity using a deterministic output-only-data approach

Amirali Sadeqi*, Dario Anastasio** and Stefano Marchesiello**

*Department of Civil and Mechanical Engineering, Technical University of Denmark, Denmark

** Department of Mechanical and Aerospace Engineering, Politecnico di Torino, Italy

Abstract. Nonlinear system identification based on output-only data is challenging since the stochastic approaches require the structure to be excited by random input with a uniform Gaussian distribution. This paper applies a deterministic output-only approach to parameter estimation of a linear multi-story specimen with an amplitude-dependent geometrical nonlinearity. The approach is independent of the input type, value, and number but requires the excitation to be applied away from the nonlinearity. The vibration responses to high-amplitude excitations are taken into a subspace-based identification algorithm that simultaneously yields both nonlinear and underlying linear parameters. The process is verified by comparing the underlying linear parameters with the linear modal parameters of the structure under low-amplitude excitation. The results indicate a superior accuracy of the estimated parameters in the simulation and an acceptable confidence range for the experimental test.

Introduction

The nonlinear system identification is generally an input-output data-driven process since the input (load) and output (response) of nonlinear systems are not proportional. However, there are many real-world nonlinear structures excited by unmeasurable environmental or operational loads. Most recently two multi-test output-only approaches for nonlinear subspace system identification have been introduced based on a mass-change scheme [1] and an input location-change scheme [2]. In this paper, the deterministic subspace identification algorithm recently used for the multi-degree of freedom (MDOF) system [2], [3], is applied to an experimental multi-story building with geometrical nonlinearity (Fig. 1 -a). It was demonstrated when an MDOF is excited, the linear and nonlinear elements attached to DOFs away from the external force can be identified at a time using the response of the whole DOFs. The objective of the present study is to extend the applicability range of the approach to experimental identification of structures with amplitude-dependent nonlinearity type based on vibration response only. Compared to the recent works, the present one is dedicated to simplifying the implementation of the algorithm for the users through the available system identification toolbox in MATLAB and using real vibration measurements.

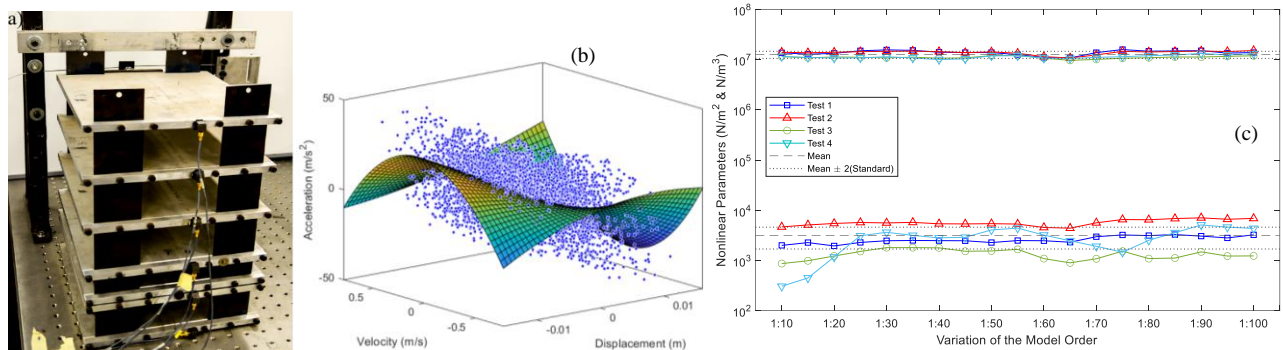


Figure 1: a) Multi-story building test setup with geometrical nonlinearity, b) nonlinear detection, c) nonlinear parameter estimation

Results and discussion

Figure 1-b displays the state-space phase plot of the fifth floor in a typical nonlinear test and corresponding fitted surface indicating the cubic stiffness behavior. Hence polynomial type basis function is used to characterize and estimate the nonlinear dynamics of the specimen. Figure 1-c demonstrates the variation of the nonlinear stiffness parameters estimated in different nonlinear tests. Despite a bias in the natural frequency and damping ratio estimates due to the process error for both integration operation and including the dynamical matrix components of the excited floor in each test, the mode shapes properly match. On the other hand, the stability of the estimated nonlinear parameters verifies the capability of the implemented identification algorithm using output-only measurements.

References

- [1] D. Anastasio and S. Marchesiello, "Free-Decay Nonlinear System Identification via Mass-Change Scheme," *Shock and Vibration*, vol. 2019, 2019.
- [2] A. Sadeqi and S. Moradi, "Nonlinear system identification based on force transmissibility of vibrating structures," *Mech Syst Signal Process*, vol. 172, no. 1, pp. 108978–23, 2021.
- [3] A. Sadeqi, S. Moradi, and K. H. Shirazi, "Nonlinear subspace system identification based on output-only measurements," *J Franklin Inst*, vol. 357, no. 17, pp. 12904–12937, 2020.

An investigation into model extrapolation and stability in nonlinear system identification

D. Anastasio¹, S. Marchesiello¹, G. Gatti², P.J.P. Gonçalves³, A.D. Shaw⁴, M.J. Brennan³

¹Department of Mechanical and Aerospace Engineering, Politecnico di Torino, Torino, Italy

²Department of Mechanical, Energy and Management Engineering, University of Calabria, Rende, Italy

³School of Engineering, State University of São Paulo, Bauru, Brazil

⁴Department of Aerospace Engineering, Swansea University, Swansea, United Kingdom

Abstract. The process of estimating a nonlinear model from experimental measurements of vibrating structures remains a challenging topic, despite the huge progress of recent years. One of the major issues is that the dynamical behaviour of a nonlinear system dramatically depends on the magnitude of the displacement response. Thus, the validity of an identified model structure is generally limited to a certain range of motion. Outside this range the stability of the solutions predicted by the model may not be guaranteed either. This work analyses the extrapolation capabilities of data-driven nonlinear state-space models based a subspace approach. An experimental magnetic beam with a strong geometric nonlinearity is driven through several levels of excitation using broadband random noise. The limitations of the estimated nonlinear state-space models are explored for strong nonlinear behaviour. Model predictions and measurements are compared to assess the accuracy of the identification results.

Introduction

Nonlinear system identification is an essential tool for modelling the dynamics of nonlinear structures, though it represents a challenging task especially for complex nonlinear phenomena [1]. The identification process generally involves three steps: nonlinear detection, characterization, and estimation. The first two steps can be addressed using ad-hoc methods or prior knowledge of the system. The last step involves the estimation of the model parameters from the experimental data, and it is strictly related to the range of motion covered by the data itself. This consideration arises from the fact that the dynamical behaviour of nonlinear systems significantly depends on the motion regimes. Therefore, even in the case of a successful estimation of a model structure, its validity is generally limited to a certain range of motion. This topic is explored in this work by investigating the extrapolation of data-driven nonlinear state-space models estimated using a subspace approach [2,3]. To this end, a magnetic beam with a nonlinear behaviour is driven with several levels of random excitation, and the limitations of the identification process are evaluated by comparing model predictions and measurements. The estimated models are also used to generate the system response under (simulated) harmonic excitation with different amplitudes, to assess the stability of the predicted solutions.

Results and discussions

Eight excitation levels have been considered, covering weak to strong nonlinear phenomena. A nonlinear state-space model was identified for each test level and the models were then used for a dual test: (i) the extrapolation towards stronger nonlinear behaviour and (ii) the stability of the predicted solutions. As an example, Figure 1 shows the measured data from 2 levels (level-2 and level-5) and the corresponding estimated nonlinear restoring force. The extrapolation generates in this case an unstable solution.

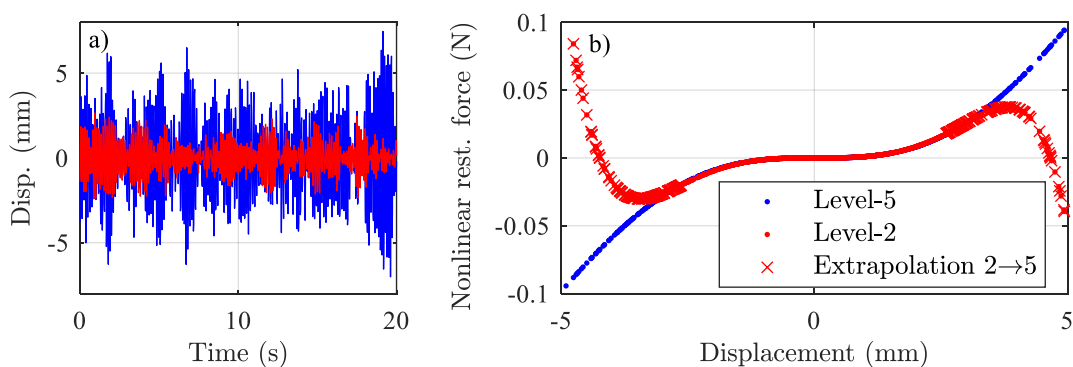


Figure 1: a) Measured data from level-2 (red) and level-5 (blue). b) Estimated nonlinear restoring force.

References

- [1] J.P. Noël, G. Kerschen, Nonlinear system identification in structural dynamics: 10 more years of progress, *Mech. Syst. Sig. Process.* 83 (2017) 2–35. <https://doi.org/10.1016/j.ymssp.2016.07.020>.
- [2] D. Anastasio, S. Marchesiello, G. Kerschen, J.P. Noël, Experimental identification of distributed nonlinearities in the modal domain, *J. Sound Vib.* 458 (2019) 426–444. <https://doi.org/10.1016/j.jsv.2019.07.005>.
- [3] R. Zhu, S. Marchesiello, D. Anastasio, D. Jiang, Q. Fei, Nonlinear system identification of a double-well Duffing oscillator with position-dependent friction, *Nonlinear Dyn.* 108 (2022) 2993–3008. <https://doi.org/10.1007/s11071-022-07346-1>.

Machine learning-based dynamic method of rock characterisation for rotary-percussive drilling

Kenneth Omokhagbo Afebu*, Yang Liu* and Evangelos Papatheou *

*College of Engineering, Mathematics and Physical Sciences, University of Exeter, North Park Rd, Exeter, EX4 4QF, UK.

Abstract. This study presents an unconventional method of rock characterisation at the drill-bit head using drill-bit acceleration signals and machine learning. The signals were processed for features that could be indicative of the stiffness of impacted rock. An impact oscillator mimicking bit-rock impact actions and multilayer perceptron network were used to validate the proposed method numerically and experimentally. Limited experimental data were augmented into RANDEXP and MIXDEXP dataset via random sampling with replacement and mixing with simulation data, respectively. Evaluation of the simulation models showed coefficient of determination (R^2) between 0.982 to 0.999 with normalised mean absolute error (NMAE) values of 0.079 and 0.015, respectively. The best performing experimental model, $R^2=0.86$ and NMAE=0.08 was achieved with RANDEXP data. MIXDEXP models were however more consistent in performance as eight out of the nine models showed R^2 greater than 0.75 compared to RANDEXP data models which were only two.

Introduction

Conventional logging-while-drilling sensors are often housed at a distance ($> 100ft$) from the drill-bit [1], thus yielding lagged information about the drilled rock. Drilling technologies like the vibro-impact drilling [2] requires quantitative rock information at the drill-bit head to function properly. This study presents an unconventional method of rock characterisation at the drill-bit head using drill-bit vibrations and machine learning [4]. Drill-bit acceleration signals were collected and processed for features that could be indicative of the stiffness of impacted rock. An impact oscillator mimicking bit-rock impact actions was employed to theoretically and experimentally validate the proposed method (Fig. 1). Due to its simplicity, low memory usage and ability to model complex nonlinear problems; a supervised multilayer perceptron network [3] was adopted to quantitatively map extracted features to rock stiffness. During experimental validation, the scarce experimental data were augmented into new dataset indexed RANDEXP and MIXDEXP by random sampling with replacement and by mixing with simulation data, respectively.

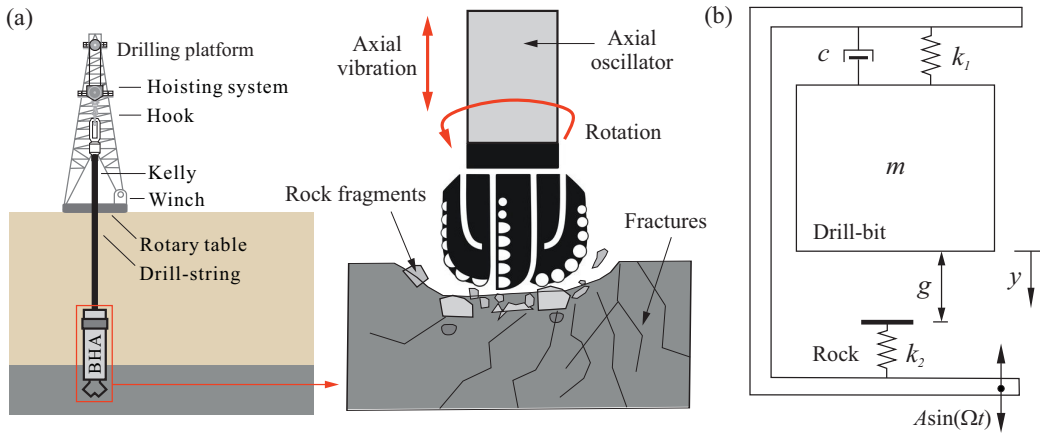


Figure 1: (a) Rock fragmentation in rotary-percussive drilling, and (b) physical model of the impact oscillator.

Results and discussion

Either of the extracted features including average impact duration, statistics of impact durations and statistics of raw signal data were used alongside system parameters as network inputs. Evaluation of simulation data models showed R^2 between 0.982 and 0.999 with NMAE value of 0.079 and 0.015, respectively. The best performing model on experimental data with $R^2=0.86$ and NMAE=0.08 was achieved using the average impact duration of the RANDEXP dataset. MIXDEXP data models however showed better consistency as eight out of the nine models showed R^2 greater than 0.75 unlike the RANDEXP data models which were only two.

Acknowledgement: This work was supported by the Petroleum Technology Development Fund, Nigeria.

References

- [1] Pei J., Dahl T.G., Macpherson J.D., Jogi P.N., Reckmann H. (2019) Synthetic formation evaluation logs based on drilling vibrations. *US Patent* **10,352,158**
- [2] Pavlovskaja E., Hendry D.C., Wiercigroch M. (2015) Modelling of high frequency vibro-impact drilling. *Int. J. Mech. Sci* **91**:110-119.
- [3] Gallinari P., Thiria S., Badran F., Fogelman-Soulie F. (1991) On the relations between discriminant analysis and multilayer perceptrons. *Neural networks* **4(3)**:349-360.
- [4] Afebu, K.O., Liu, Y., Papatheou, E.(2022) Machine learning-based rock characterisation models for rotary-percussive drilling. *Nonlinear Dynamics* **Doi**:10.1007/s11071-022-07565-6, pp.1-21.

An approach to monitor bolt faults in two-dimensional structures without reference

Quankun Li^{*}, Qingzhou Zhao^{*}, Mingfu Liao^{*} and Xiaobo Lei^{**}

^{*}*School of Power and Energy, Northwestern Polytechnical University, Xi'an, Shaanxi, P.R.China*

^{**}*Xi'an Aeronautical Institute, Xi'an, Shaanxi, P.R.China*

Abstract. Monitoring potential bolt faults is very necessary and meaningful to keep structures' healthy operation. For this purpose, an improved approach to monitor bolt faults in two-dimensional structures without reference is proposed. In the new method, nonlinear dynamic behaviours of the structure to be monitored are studied by a general multi-degree-of-freedom (MDOF) mode with nonlinear elements. By exciting the structure many times with the same excitation and the local structural modification method, nonlinear features from the structure to be monitored only are defined. Based on these features, a novel fault index and corresponding improved approach are proposed and explained. With some numerical examples on a two-dimensional structure, the effectiveness and reliability of the method are verified fully.

Introduction

For various two-dimensional engineering structures, bolts are widely applied to clamp different structural components together and to bear external loads. However, bolt connections easily encounter faults since these two-dimensional engineering structures often work with dynamic environments and operations. Bolt faults not only cause decrease of clamping force but also lead to serious slip or separation between structural components [1]. As a result, monitoring potential bolt faults as early as possible is very important and meaningful to keep the normal and smooth operation of these two-dimensional engineering structures. For this objective, a host of output spectrum-based methods have been presented [2]. The fundamental principle of these methods is that output spectrum-based features depend on structural physical properties solely. Thus, any variation in properties caused by bolt faults could be monitored by monitoring changes in output spectrum-based indexes [3-4]. Existing nonlinear output spectrum-based methods provide much more information of two-dimensional structures with potential bolt faults. However, one obvious limitation is that fault data from basement structures are required during the diagnosis of faults. This condition would affect these methods' effectiveness if states of health structures are not known. To overcome this limitation, an improve approach to monitor bolt faults in two-dimensional structures without reference is proposed in this paper. The main contributions and novelties of this paper are, (1) Using nonlinear output spectra of local and damaged two-dimensional engineering structures only and the local structural modification method, local damage features are derived and analysed; (2) With damage features, an improved method with sensitive damage indexes is proposed, and its effectiveness and availability are illustrated through simulation cases on a MDOF model of two-dimensional engineering structures.

Results and discussion

By considering impact of faults as nonlinear forces, two-dimensional discrete MDOF model with nonlinear components could be built for the dynamic analysis of two-dimensional structures.

With the local structural modification method, similar equations from the structure to be monitored could be used to form one matrix, whose rank could be a sensitive index for inspection.

Results from simulation studies on a two-dimensional model with multiple faults show that the proposed method could give precise sates of bolt faults in numerical structures.

References

- [1] Bickford J. (2018) An introduction to the design and behaviour of bolted joints, revised and expanded. Routledge, NY.
- [2] Huang J., Liu J., Gong H., Deng X. (2022) A comprehensive review of loosening detection methods for threaded fasteners. *Mech. Syst. Signal. Rr.* **168**:108652.
- [3] Nikraves S.M.Y., Goudarzi M. (2017) A review paper on looseness detection methods in bolted structures. *Lat. Am. J. Solids Struct.*, **14**:2153-2176.
- [4] Amerini F., Meo M. (2011) Structural health monitoring of bolted joints using linear and nonlinear acoustic/ultrasound methods. *Struct. health monit.* **10**(6):659-672.

Physics-informed sparse identification of a bistable nonlinear energy sink

Qinghua Liu, Junyi Cao

Key Laboratory of Education Ministry for Modern Design and Rotor-Bearing System, Xi'an Jiaotong University, Xi'an, China

Abstract. Bistable nonlinear energy sinks have attracted extensive attention due to their efficient broad-band targeted energy transfer over a wide range of input energy levels. The precise identification of local bistability is of significance to predicting and enhancing the system performance of the vibration energy absorption. However, a multi-degree-of-freedom system with local bistability is difficult to be measured and identified because of snap-through motions. Moreover, the basis functions of many current data-driven identification methods lack physical interpretability. This paper proposed a physics-informed sparse identification method for parameter estimation of bistable nonlinear energy sinks. The restoring force surface is constructed on the local bistable structure and the nonlinear restoring force trajectory is intercepted by assuming two quasi-zero velocity planes. Furthermore, the candidate functions can be physically informed in a sparse identification algorithm by conducting the least-square parameter fitting of the intercepted nonlinear restoring force trajectories.

Introduction

Over the past two decades, passive nonlinear energy sink has been a subject of growing interest due to its wide applications in the fields of vibration mitigation and energy harvesting. Among various nonlinear energy sink devices, it seems that bistable configurations may allow for efficient broad-band targeted energy transfer over a wide range of input energy levels. However, introducing bistability brings a great challenge for nonlinear restoring force identification in practical applications due to the snap-through characteristics in static deformation and cross-well motions in dynamic responses. The traditional restoring force surface method and Hilbert transform-based method may have insufficient accuracy due to noise disturbance. Besides, modern machine learning methods lack physical interpretability in the selection of basis functions.

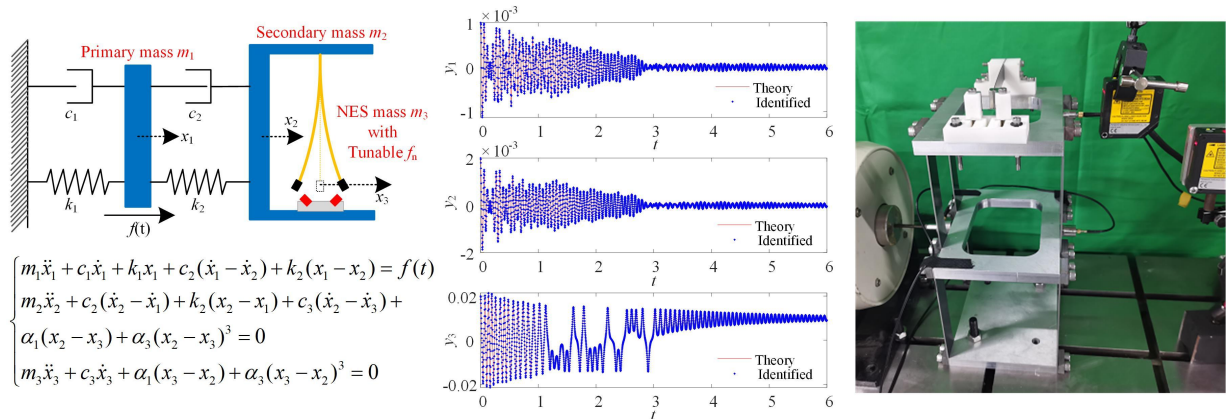


Figure 1: Modeling, Identification and Experimental Validation of A Bistable Nonlinear Energy Sink.

Results and Discussion

This study proposes a physics-informed sparse identification method for the accurate identification of bistable nonlinear energy sinks. The restoring force surface is constructed on a bistable nonlinear energy sink equation and the nonlinear restoring force trajectory is intercepted by assuming two quasi-zero velocity planes. Furthermore, the sparse regression algorithm is conducted based on physics-informed candidate functions and the free vibration response of bistable nonlinear energy sink systems. Numerical simulations are conducted on a three-degree-of-freedom bistable nonlinear energy sink. The results show that the proposed method not only gives sparse identification physics information but also improves the accuracy by 2.64% under the noise level of 30dB. Experimental verifications are performed on a three-story beam-type bistable energy sink structure. Compared to two traditional nonparametric methods: Hilbert transform-based method and restoring force surface method, the superiority has been demonstrated.

References

- [1] Ding H, Chen L. (2020) Designs, Analysis, and Applications of Nonlinear Energy Sinks. *Nonlinear Dynam* **100**:3061–3107.
- [2] Vakakis AF, Gendelman OV, Bergman LA et al. (2022) Nonlinear Targeted Energy Transfer: State of the Art and New Perspectives. *Nonlinear Dynam* **108**:711–741.
- [3] Liu Q, Hou Z, Zhang Y, et al. (2022) Nonlinear Restoring Force Identification of Strongly Nonlinear Structures by Displacement Measurement. *J. Vib. Acoust* **144**:031002.
- [4] Brunton SL, Proctor JL, Kutz JN. (2016) Discovering Governing Equations from Data by Sparse Identification of Nonlinear Dynamical Systems. *P. Natl. Acad. Sci. USA* **113**:3932-3937.

Identification of non-linear model equations based on data-science approaches

Simon Bäuerle*, Timo Baierl* and Hartmut Hetzler*

* Institute for Mechanics, Engineering Dynamics, University of Kassel, Germany

Abstract. This contribution presents two different data-science approaches for identifying non-linear ordinary differential equations from transient system state data. The theory, benefits and pitfalls of a differential approach (called SINDy) and a variational approach are discussed. These are used to identify the DUFFING oscillator equation purely from simulation data.

Introduction

Describing the behavior of dynamical systems with ordinary differential equations $\frac{dx}{dt} = f(x, t)$ is at the core of many disciplines in science. The “classical” approach uses first principles (e.g., momentum balance) to derive a set of governing equations. Data-driven approaches are another way to describe system dynamics: here, a description is achieved purely based on system state data. One possibility is to use neural networks that are trained to replicate the system behavior. If a suitable architecture and hyper-parameters are found, the behavior can be predicted relatively fast. Another way is to identify the (non-linear) model equations directly from the data. This has the advantage that the model equations possibly allow for physical insight into the system and that – in general – less data is needed than for training a neural network. However, some basic understanding of the dynamics present in the system is required. Therefore, this approach tries to combine the two mentioned above. We explore this approach by using two different classes of methods: a differential approach called SINDy (Sparse Identification of Non-linear Dynamics) [1] and a variational approach [2]. Both methods are based on system state data obtained either through experiment or simulation (as done for this contribution). The SINDy approach is described by

$$\dot{X} \stackrel{!}{=} \underbrace{[1 \quad \Phi_1(X) \quad \Phi_2(X) \quad \dots]}_{=\Phi} \underbrace{[\xi_1 \quad \xi_2 \quad \xi_3 \quad \dots]}_{=\xi}, \quad \underset{\xi}{\operatorname{argmin}} \left(\|\Phi\xi - \dot{X}\|_2^2 + \lambda \|\xi\|_1 \right). \quad (1)$$

The matrix X contains the gathered data for each DoF (as column entries). The derivation w.r.t. time \dot{X} is carried out numerically. Then a set of k different possible candidate function terms Φ_k (e.g., monomials, trigonometric functions, ...) is evaluated subject to X . These function terms are weighted with k factors ξ and their sum is required to equal the differentiated data. This represents an over-determined equation system for a first order differential equation. Instead of using a classical least square approach, sparsity of the factors ξ is additionally promoted, since governing equations are mostly sparse in their functional terms. This is achieved by minimizing the Euclidean norm of the residuum *and* the summation norm of the factor vector ξ . The variational approach uses a variational-integral formulation

$$\int_{T_1}^{T_2} \left(\delta U_0(x, \dot{x}) + \sum_k U_k(x, \dot{x}, t) \delta x_k \right) dt = 0. \quad (2)$$

As for SINDy, U_0 and U_k are expressed by k possible candidate function terms Φ , which are evaluated with the gathered data X for arbitrary T_1, T_2 and δx . After (numerical) integration, the coefficients ξ can be calculated.

Results and discussion

We focus on the comparison between the differential and variational methods based on the application to the Duffing oscillator $\ddot{x} + 2D\dot{x} + x + \kappa x^3 = f \cos(\Omega t)$ with an overhanging resonance peak. This is an interesting example since three solutions co-exist. Therefore, we extend the results from [3] and [4] w.r.t. a higher degree of non-linearity. We show that the choice of data is essential for (re-)discovering the governing differential equation: transient data gathered away from attractors led here to better results. Additionally, numerical differentiation as a source of noise has a significant impact. Here, variational methods are less prone to noise, whereby differential methods tend to be more efficient (see also [2]). Finally, we study the influence of numerical parameters and the choice of candidate function terms.

References

- [1] Brunton, S. L., Proctor, J. L., Kutz, J. N. (2016) Discovering governing equations from data by sparse identification of nonlinear dynamical systems *Proc. Natl. Acad. Sci. U.S.A.* **113**(15): 3932–3937.
- [2] Huang, Z., Tian, Y., Li, C., Lin, G., Wu, L., Wang, Y., Jiang, H. (2020) Data-driven automated discovery of variational laws hidden in physical systems *J. Mech. Phys. Solids* **137**: 103871.
- [3] Li, C., Huang, Z., Wang, Y., Jiang, H. (2021). Rapid identification of switched systems: A data-driven method in variational framework. *Sci. China Technol. Sci.* , **64**(1): 148–156.
- [4] Baierl, T. P. (2022) Identification by machine learning of differential equations based on big data (in German). Bachelor Thesis, University of Kassel, Germany.

Neural network hyperparameter tuning for online model parameter updating using inverse mapping models

Bas M. Kessels, Tom M.E. Janssen, Rob H.B. Fey, and Nathan van de Wouw

Dynamics and Control, Department of Mechanical Engineering, Eindhoven University of Technology, The Netherlands

Abstract. To decrease the mismatch between a model and a physical system, physically interpretable model parameter values of nonlinear systems can be updated in real-time by using the Inverse Mapping Parameter Updating (IMPU) method. In this method, an Inverse Mapping Model (IMM), constituted by an Artificial Neural Network (ANN), is trained, offline, using simulated data that consists of features of output responses (ANN inputs) and corresponding parameter values (ANN outputs). In an online phase, the trained ANN can then be used to infer parameter values with high computational efficiency. The (non-trivial) choice of ANN-hyperparameters, e.g., ANN structure and training settings, may significantly influence the accuracy of the trained ANN. Therefore, this work discusses multiple ANN-hyperparameter tuning techniques to increase the accuracy of the IMPU method, of which the Bayesian search technique is the most promising considering accuracy and efficiency as it learns from previously evaluated hyperparameter values.

Introduction

In a digital twin context, model updating is required to ensure that a model accurately represents a physical systems throughout its operational life. In this research, an IMM is employed that enables (near) real-time inference of interpretable parameter values of nonlinear dynamics systems on the basis of a set of features representing measured output response data. This is achieved by training the IMM, which is constituted by an ANN, offline, using simulated training data (pairs of output response functions and corresponding parameter values) should be chosen appropriately. Afterwards, in an online phase, the trained ANN is used to infer parameter values from measured features with little computational cost. For a detailed explanation of this IMPU method, see [1]. To ensure that the ANN accurately estimates parameter values, careful design of the ANN is essential, i.e., its activation functions, its number of layers and neurons, and its training settings (learning rate, number of epochs, and batch size). These hyperparameters should be tuned to minimize the validation loss, i.e., the mean squared error of the inferred parameter values (normalized between 0 and 1), as evaluated on a validation set. In this paper, different tuning strategies are compared: grid, random, and Bayesian searches [2].

Results and discussion

ANN hyperparameter tuning is applied to a closed-loop nonlinear multibody dynamics system consisting of four connected rigid bodies with, in total, 10 Degrees of Freedom (DoFs) of which 3 DoFs are excited and ‘measured’. Using the ‘measured’ output responses, we tune the above-mentioned ANN-hyperparameters such that the values of eight parameters (among which stiffness constants and damping factors) are inferred with high accuracy. In Figure 1, the validation losses obtained using different ANN-hyperparameter searches, as well as one manually tuned ANN (using engineering insight and experience), are ranked in ascending order. Note that, for all search types, the hyperparameter values lie within the same bounded space and the same training and validation data is used. Performing these grid, random, and Bayesian searches takes roughly 78, 15, and 20 hours, respectively and especially the grid search is thus a time consuming (offline) task. In contrast, online inferring of one set of parameter values using the trained ANN only takes approximately 6 ms. From Figure 1, we observe that the Bayesian search finds relatively many ANNs that outperform the manually tuned ANNs, while requiring much less computation time than the grid search. The mean relative (non-normalized) parameter value error (averaged over the eight parameters) for a test data set as obtained using the IMPU method equals 0.26% for the manually tuned ANN and only 0.14% for the best performing ANN of the Bayesian search.

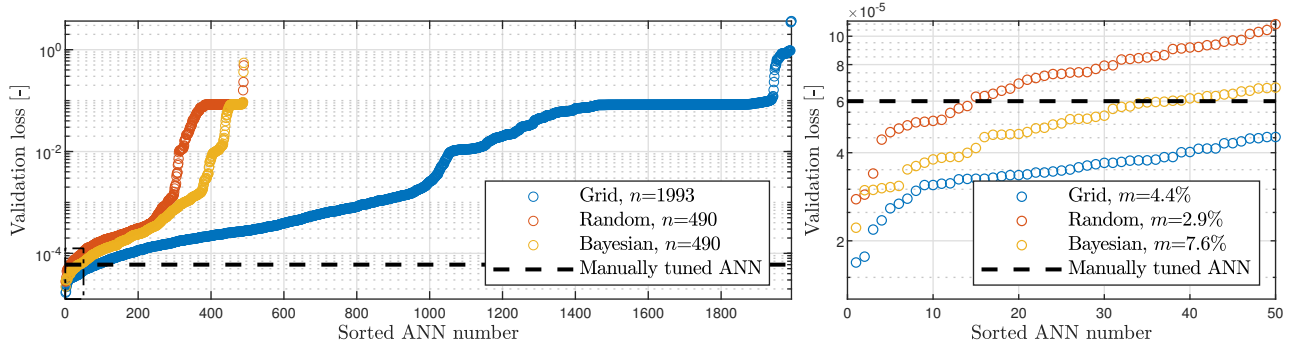


Figure 1: Validation losses as obtained by grid, random, and Bayesian searches. The validation loss of the manually tuned ANN is indicated by the dashed line. The right figure presents a detail of the 50 best performing ANNs per search. The total number of trained ANNs and the relative percentage of ANNs that outperform the manually tuned ANN per search are indicated by n and m , respectively.

References

- [1] Kessels, B.M., Fey, R.H.B., van de Wouw, N. (2022) Real-time parameter updating for nonlinear digital twins using inverse mapping models and transient-based features. *Nonlinear Dynamics* (submitted, preprint available at [researchsquare.com](https://www.researchsquare.com)).
- [2] Zulfiqar, M., Gamage, K.A.A., Kamran, M., Rasheed, M. B. (2022) *Sensors* 22(12):4446.

Reconstructing Nonlinear Backbone Curves from Smooth Coordinate Decomposition of Multivariate Impulse Response

Dalton L. Stein* and David Chelidze*,

*Department of Mechanical, Industrial and Systems Engineering, University of Rhode Island, RI, USA

Abstract. Nonlinear modal coordinate pairs, obtained from the smooth coordinate decomposition of the impulse response trajectories, are used to estimate nonlinear frequency-amplitude backbone curves. This method allows simultaneous estimation of multiple backbone curves for all excited modes.

Introduction

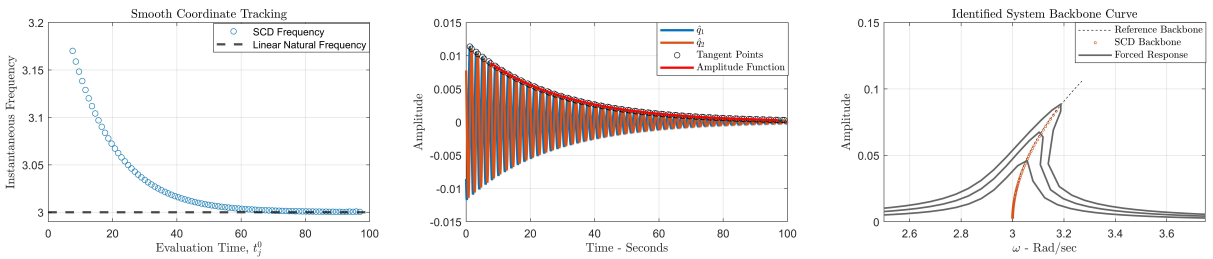
A system's modal parameters' identification is an essential step during the design of engineering structures. Recent advancements in innovative lightweight structures and novel materials require engineers to analyze systems that are inherently nonlinear. Thus, practitioners must find a suitable method to characterize nonlinear phenomena. The backbone curves provide a description of the frequency-amplitude relationship for the undamped and unforced response of the system and are instrumental in the study of the nonlinear system response. Recent experimental nonlinear system identification efforts have focused on obtaining these curves from the output response data [1, 2]. Here, we propose using a state space formulation of the Smooth Coordinate Decomposition (SCD) [3] to estimate the amplitude-frequency-dependent behavior embedded within the smooth orthogonal coordinates.

Results and Discussion

Consider the system response in the form of a trajectory matrix, $Y = [X \ \hat{X}] \in \mathbb{R}^{m \times 2n}$ where \hat{X} is a temporally correlated version of X (e.g., state velocities). The SCD looks for a basis, Φ , that maximizes the variances of the projected field while minimizing their roughness. That is, we are looking for projections of the system response onto the smoothest (i.e., slowest decaying) modes (SMs), Φ . The resulting smooth coordinates (SCs) will have the following structure,

$$Q = Y\Phi^{-T} = \begin{bmatrix} q_1(t_1) & \hat{q}_1(t_1) & q_2(t_1) & \hat{q}_2(t_1) & \cdot & \cdot & q_n(t_1) & \hat{q}_n(t_1) \\ \vdots & \vdots & \vdots & \vdots & \vdots & \vdots & \vdots & \vdots \\ q_1(t_n) & \hat{q}_1(t_n) & q_2(t_n) & \hat{q}_2(t_n) & \cdot & \cdot & q_n(t_n) & \hat{q}_n(t_n) \end{bmatrix}. \quad (1)$$

where the columns of Q will come in distinct pairs, $q_i(t)$ and $\hat{q}_i(t)$, that have the same smoothness but will be 90° phase shifted from each other due to the orthogonality condition. The SC pairs embed the frequency-amplitude relationship for each single-mode response (assuming no internal resonances) of a nonlinear multi-degree-of-freedom arbitrarily excited system. Furthermore, the orthogonality and equivalent oscillation pattern within the pairs allow one to utilize the coordinates in the same way as the analytical signal in the Hilbert Transform-based approach. Hence, the mode separation and construction of a suitable pseudo-analytical signal representation are done within one step. One can then assemble two sequences that pair the frequencies, $\omega_n(t_j)$, and amplitudes, $A(t_j)$, for each evaluation time, t_j , within each mode.



References

- [1] Londono J. M., Cooper J. E., and Neild S. A. "Identification of systems containing nonlinear stiffnesses using backbone curves," *Mechanical Systems and Signal Processing*, vol. 84, pp. 116–135, 2017.
- [2] Feldman M., "Hilbert transform applications in mechanical vibration," John Wiley & Sons, 2011.
- [3] Chelidze D. and Zhou W., "Smooth orthogonal decomposition-based vibration mode identification," *J. of Sound and Vibration*, vol. 292(3), pp. 461–473, 2006.

A Bayesian compressive sampling technique for determining the equations of motion of nonlinear structural systems

G. D. Pasparakis*, V. C. Fragkoulis*, I. A. Kougiumtzoglou** and M. Beer*

*Institute for Risk and Reliability, Leibniz University Hannover, Hannover, Germany

**Department of Civil Engineering and Engineering Mechanics, Columbia University, New York, USA

Abstract. A technique based on Bayesian compressive sampling is developed for determining the governing equations of stochastically excited structural systems exhibiting diverse nonlinear behaviors and/or following a fractional derivative modeling. This is done by relying on measured data and by employing sparsity-promoting optimization algorithms for determining the active coefficients in an expansion basis approximating the system dynamics. A significant advantage of the technique relates to the fact that the uncertainty associated with the model estimate is also quantified.

Introduction

A novel paradigm of data-driven model discovery has emerged in recent years. In this context, it can be argued that the identified model should exhibit sparsity in the sense that the fewest possible terms are considered for the description of the system dynamics. The rationale relates to the fact that the dynamics of most physical systems can be described accurately by considering only very few relevant terms in an appropriate expansion basis; thus, rendering the governing equations sparse in a high-dimensional nonlinear function space. In this regard, several approaches for sparse identification of nonlinear dynamics based on compressive sampling concepts and tools have been proposed recently [1].

Results and discussion

In this paper, a technique based on Bayesian compressive sampling [2] is developed for determining the governing equations of stochastically excited structural systems exhibiting diverse nonlinear behaviors and/or following a fractional derivative modeling. This is done by relying on measured data and by utilizing a state-variable formulation of the system governing equations. Further, considering an expansion basis for approximating the nonlinear system dynamics leads to a non-square system of equations. This is solved based on sparsity-promoting optimization algorithms for determining the active coefficients in the expansion basis. Compared to alternative state-of-the-art schemes that yield deterministic estimates for the expansion coefficient vector, the herein developed technique is capable also of quantifying the uncertainty associated with the model estimate; thus, providing a measurable confidence degree when employing the technique as a predictive tool; see also Fig.1. The reliability of the technique, even in cases of highly limited/incomplete measured data, is demonstrated by considering various numerical examples.

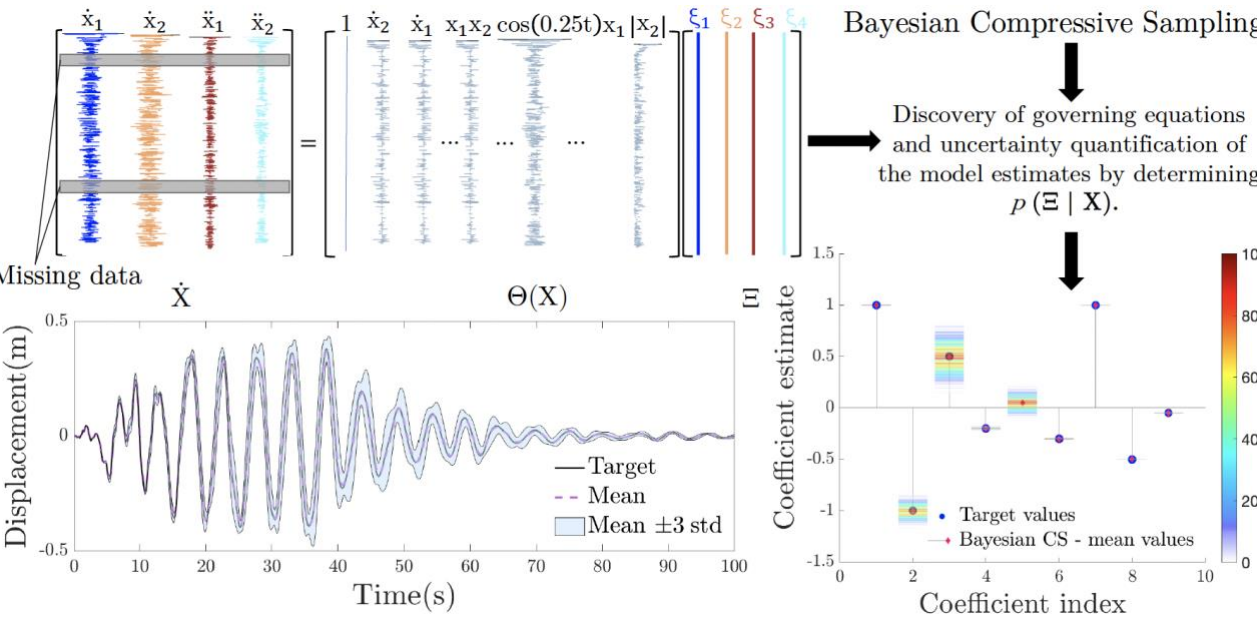


Figure 1: Schematic representation of the Bayesian Compressive Sampling technique for determining governing equations of nonlinear dynamical systems

References

[1] Brunton S., Kutz J. N. Kutz (2022) Data-driven science and engineering: Machine learning, dynamical systems, and control. Cambridge University Press.
 [2] Kougiumtzoglou I. A., Petromichelakis I., Psaros A. F. (2020). Sparse representations and compressive sampling approaches in engineering mechanics: A review of theoretical concepts and diverse applications, *Prob. Eng. Mech.* **61**: 103082.

Physics Enhanced Sparse Identification of Nonlinear Oscillator with Coulomb Friction

Christos Lathourakis* and Alice Cicirello*

*Faculty of Civil Engineering and Geosciences, Delft University of Technology, Netherlands

Abstract. This study investigates the identification of the nonlinear governing equations of a Single-Degree-of-Freedom oscillator under harmonic excitation, including Coulomb friction damping. The approach used for this task is the so-called RK4-SINDy [1], enhanced by incorporating part of the known physics. This simple, yet representative case study, is examined using both artificially generated noisy data, and data obtained from an experimental setup. The obtained results, highlight the potential of this framework in nonlinear system identification, given sparsely collected corrupted data, and the benefits of incorporating already known system information.

Introduction

Frictional joints are present in a plethora of applications and fields, such as the aerospace, automotive, and building industries. Therefore, an ever-important challenge in the analysis of engineering systems is the understanding of friction damping in structural dynamics. Due to its nonlinear and non-smooth nature, the available approaches, including proposing alternative constitutive laws and validating models based on experimental data [2], cannot deal with the identification of friction forces. One way around this is to take advantage of the rapid increase of data availability through measurements for complex engineering systems, and newly developed identification techniques of the underlying differential equations of physical problems based on noisy measurements. A promising framework called Sparse Identification of Nonlinear Dynamics (SINDy) [3] was developed for this purpose, aiming to derive parsimonious solutions of nonlinear systems, which was further improved by combining the principles of dictionary-based learning, which is a key concept in SINDy, with numerical analysis tools, and more specifically the 4th order Runge-Kutta integration scheme [1]. This approach, the so-called RK4-SINDy was proven to be more efficient when dealing with noisy and sparsely collected data, not exploring though the incorporation of physics in discovering nonlinear models.

Results and discussion

The identification of the governing equations of an SDOF oscillator, including harmonic excitation and Coulomb friction damping is investigated (Figure 1a). Part of the system’s equation of motion is assumed known during the identification of the vector field of the global response, incorporating in this way part of the known physics, while regarding the input data, noisy measurements (both artificially generated and experimental) were used.

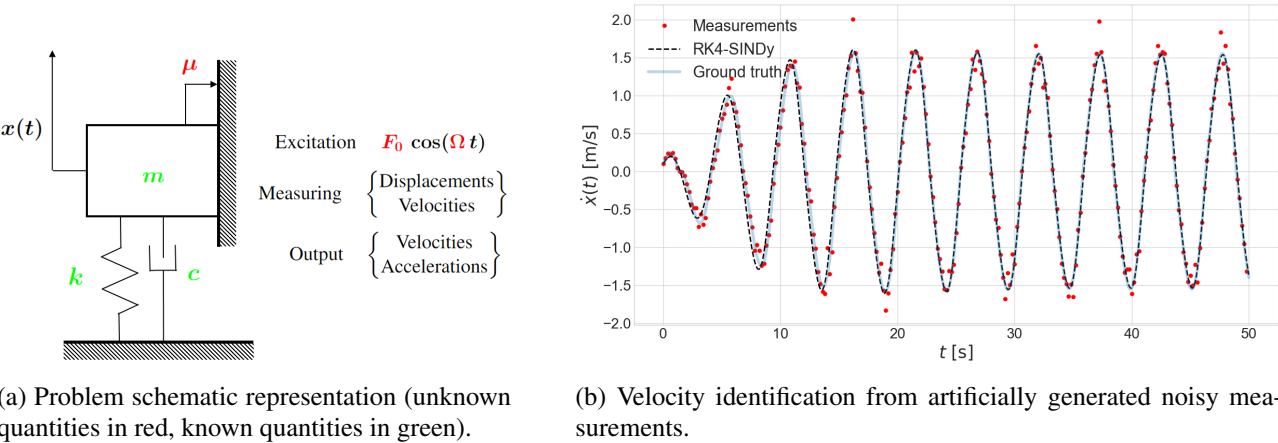


Figure 1: Problem description - Results

It is evident (Figure 1b) that this approach leads to accurate results even for significant noise levels while maintaining a parsimonious solution in order to avoid overfitting the noisy data.

References

- [1] P. Goyal and P. Benner (2022) Discovery of nonlinear dynamical systems using a Runge–Kutta inspired dictionary-based sparse regression approach. *Proceedings of the Royal Society A*, vol. 478, no. 2262, p. 20 210 883.
- [2] A. Cabboi and J. Woodhouse (2018) Validation of a constitutive law for friction-induced vibration under different wear conditions. *Wear*, vol. 396, pp. 107–125.
- [3] S. L. Brunton, J. L. Proctor, and J. N. Kutz (2016) Discovering governing equations from data by sparse identification of nonlinear dynamical systems. *Proceedings of the national academy of sciences*, vol.113, no. 15, pp. 3932–3937.

Experimental Characterization and Identification of the Shear Hysteretic Behavior of a Helical Wire Rope Isolator

Biagio Carboni * and Nicolò Vaiana **

* Department of Structural and Geotechnical Engineering, Sapienza University of Rome, Rome, Italy

** Department of Structures for Engineering and Architecture, University of Naples Federico II, Naples, Italy

Abstract. We experimentally characterize a helical wire rope isolator to study its complex hysteretic behavior along the Shear direction. The asymmetric force-displacement hysteresis loops are simulated by using two different models: a differential one, obtained by a generalization of the Bouc-Wen model, and an exponential one, denominated Vaiana-Rosati model. In particular, their parameters are first identified on the basis of the experimental data; subsequently, the accuracy of the two models is verified by comparing the simulated hysteresis loops with those obtained experimentally.

Introduction

Helical Wire Rope Isolators (HWRI) are metal devices made up of a stainless steel cable and two aluminum alloy or steel retainer bars where the cable is embedded. They can be effectively adopted for the vibration control of museum artifacts, hospital equipment, electrical transformers, supercomputers, and intermodal containers. The main aim of this work is to study the experimental behavior exhibited by a HWRI prototype when it is tested along one of its principal transverse directions, denominated Shear direction. In addition, two recently formulated hysteretic models [1, 2, 3] are proposed to reproduce its complex response and the related parameters are identified on the basis of the experimental data.

Experimental tests

Figure 1a shows the tested HWRI prototype which differs from similar devices, already studied in previous experimental campaigns [4], because of the different way its stainless steel cable is mounted. The experimental tests have been performed at the Department of Structural and Geotechnical Engineering of the Sapienza University of Rome. Figure 1b, or equivalently Figure 1c, illustrates the typical asymmetric restoring force-displacement hysteresis loops (black line) characterizing the device response when a transverse displacement is applied, along the Shear direction, for six different values of amplitude.

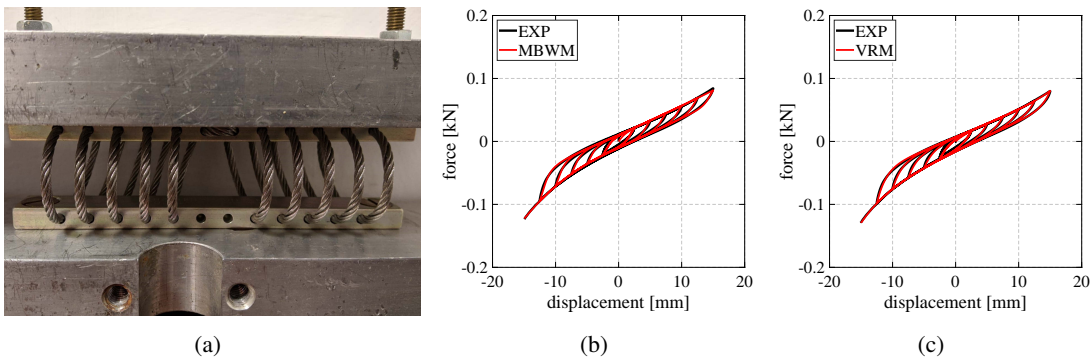


Figure 1: Tested HWRI (a); comparison between experimental responses and those simulated by the MBWM (b) and VRM (c).

Identification and Simulation

In order to simulate the complex device response, two hysteretic models are proposed. The first one represents a Modified Bouc-Wen Model (MBWM), developed by Carboni et al. [1, 2], whereas the second one is the so-called Vaiana-Rosati Model (VRM), recently formulated by Vaiana and Rosati [3]. The MBWM is a differential model that adopts 11 parameters, whereas the VRM represents an exponential model based on two independent sets of 8 parameters that control, respectively, the loading and unloading phases. Figure 1b (Figure 1c) compares the experimental hysteresis loops with those simulated by using the MBWM (VRM). Such comparisons confirm the accuracy of both models.

References

[1] Carboni B., Lacarbonara W., Brewick P. T., Masri S. F. (2018) Dynamical response identification of a class of nonlinear hysteretic systems. *J Intell Mater Syst Struct* **29**(13): 2795-2810.
[2] Salvatore A., Carboni B., Chen L-Q., Lacarbonara W. (2021) Nonlinear Dynamic Response of a Wire Rope Isolator: Experiment, Identification and Validation. *Eng. Struct.* **238**: 112121.
[3] Vaiana N., Rosati L. (2023) Classification and Unified Phenomenological Modeling of Complex Uniaxial Rate-Independent Hysteretic Responses. *Mech. Syst. Signal Pr.* **182**: 109539.
[4] Vaiana N., Spizzuoco M., Serino G. (2017) Wire Rope Isolators for Seismically Base-Isolated Lightweight Structures: Experimental Characterization and Mathematical Modeling. *Eng. Struct.* **140**: 498-514.

A novel vibration response-based approach to monitor faults in bolted complex structures

Quankun Li*, Qingzhou Zhao*, Mingfu Liao* and Xiaobo Lei**

*School of Power and Energy, Northwestern Polytechnical University, Xi'an, Shaanxi, China

**Xi'an Aeronautical Institute, Xi'an, Shaanxi, China

Abstract. Since bolted complex structures are easily subjected to faults like fatigue crack/bolt loosening during their service, monitoring faults is very meaningful and helpful for them. Therefore, a novel vibration response-based approach to monitor faults in bolted complex structures is proposed in this paper. In the new approach, bolted complex structures are simplified as some discrete substructures, whose nonlinear dynamics are studied by a nonlinear multi-degree-of-freedom (MDOF) mode. By stimulating the structure many times with different magnitudes, nonlinear features from the substructure to be monitored only are defined, and a novel fault index and corresponding approach are proposed accordingly. With some experimental studies on a lab bolted complex structure, the effectiveness of the proposed approach is vindicated fully.

Introduction

For complex engineering structures, bolts are widely applied to clamp different elements. However, they are easily subjected to faults like fatigue crack/bolt loosening during their service process since these bolted complex structures often work with dynamic loads like vibration and impact. Bolt faults not only affect structures' safety and reliability, and may cause some catastrophic consequences [1]. Therefore, monitoring bolt faults at an early stage is very meaningful and helpful to keep the healthy operation of bolted complex structures. For this objective, a host of vibration response-based methods have been proposed [2]. Their fundamental principle is that vibration response-based features depend on structural physical properties solely, any change in properties due to bolt faults can thus be monitored by monitoring changes in vibration response-based indexes [3]. Existing nonlinear vibration response-based methods provide much more information of complex structures with bolt faults. However, one obvious limitation is that data from health structures are required during the implementation of methods. This would affect these methods' effectiveness if data of health structures are not known. To consider this issue, a novel vibration response-based approach to monitor faults in bolted complex structures is proposed in this paper. The main novelties of this paper are: i) Stimulating the structure to be monitored only, and using nonlinear vibration responses, local fault features are derived; ii) With fault features, a novel approach with a sensitive fault index is proposed, and its availability is illustrated through experimental cases on a lab bolted complex structure (Figure 1).

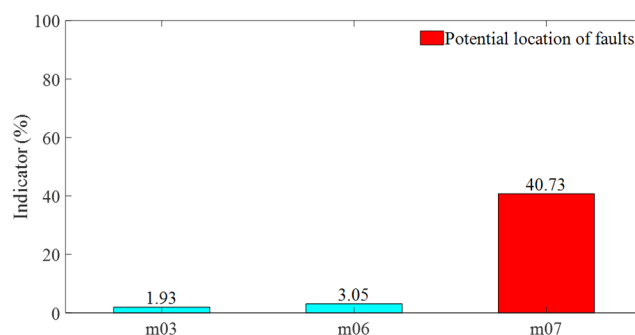


Figure 1: Diagnosis results related masses.

Results and discussion

By considering effect of faults as nonlinear restoring loads, discrete MDOF model with nonlinear elements can be built for the dynamic analysis of bolted complex structures.

Stimulating the structure many times, similar equations from the substructure to be monitored can be applied to form a local and sensitive vibration response-based fault index.

Results from experimental studies on a bolted complex structure with a loosening fault show that the novel approach can give more correct location of faults in the structure.

References

- [1] Bickford J. (2018) An introduction to the design and behaviour of bolted joints, revised and expanded. Routledge, NY.
- [2] Huang J., Liu J., Gong H., Deng X. (2022) A comprehensive review of loosening detection methods for threaded fasteners. *Mech. Syst. Signal. R.* **168**:108652.
- [3] Nikravesh S.M.Y., Goudarzi M. (2017) A review paper on looseness detection methods in bolted structures. *Lat. Am. J. Solids Struct.*, **14**:2153-2176.

Data-driven delay identification with SINDy

Ákos Tamás Köpeczi-Bócz*, Henrik Sykora** and Dénes Takács*

*Department of Applied Mechanics, Budapest University of Technology and Economics, HU

**Institute of Sound and Vibration Research, University of Southampton, UK

Abstract. In this work, we investigate the capabilities of the *Sparse Identification of Nonlinear Dynamics* method for time-delay identification. We test the robustness and effectiveness of the method through data generated using reference systems with known time-delay.

Introduction

Model construction based on data-driven techniques has gained considerable ground over the past years due to the more versatile measurement toolset (such as image recognition, smartphone sensors, etc.) and a large amount of available data. The development of computer sciences, statistical and machine learning tools enable more efficient data processing and model discovery. The appearance of Scientific Machine Learning [1] (SciML) made the model construction more sophisticated by opening a physics-informed toolset for us to discover phenomena described by dynamical systems. Throughout this work, we investigate one of these techniques, the *Sparse Identification of Nonlinear Dynamics* (SINDy) in presence of time delay. The core idea of the method was first presented by Brunton et al. in 2016 [2], that we modify to find the underlying physics of time-delayed systems. We investigate the limits and the prerequisites of this technique through numerical experiments using a dataset constructed by simulating dynamic systems with known parameters and time-delays. We also include a stochastic effect to test out the robustness of the method. We apply the SINDy with the sequentially thresholded least squares algorithm (STLSQ) [3].

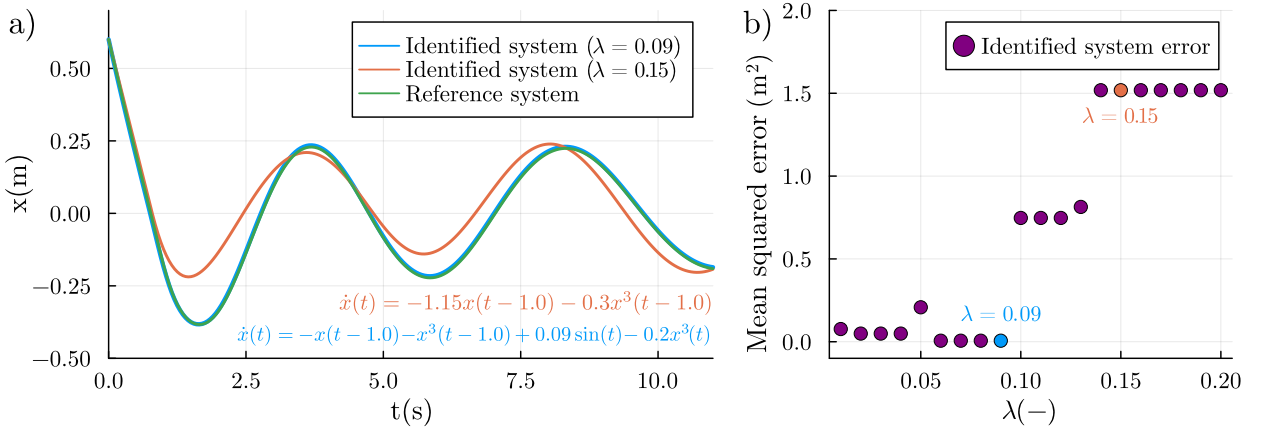


Figure 1: (a) Two identified systems for different λ threshold values of the STLSQ algorithm. The reference system for this case was $\dot{x}(t) = -x^3(t - \tau) - x(t - \tau) + 0.09 \sin(t)$ with $\tau = 1.0$ s. By increasing the value of λ we get a system with increased error on behalf of having less terms to describe it. (b) The errors of the identified systems are shown with respect to the λ values. Identification of the best fitting solution is possible this way. Two cases are highlighted with $\lambda = 0.09$ and $\lambda = 0.15$ thresholds in correspondence with panel a. Note, that even in cases when the error was larger the identified time-delay was correct.

Results and discussion

We have found that on simulated non-linear systems the SINDy algorithm worked well with the proposed method, see example in Fig.1(a). To successfully achieve a sufficient fit we identified the proper threshold value λ for the STLSQ algorithm by sweeping through a range of different values and finding the one with the lowest error as in Fig.1(b). Despite of falsely identified terms, the found time-delay was correct. In our study, the physically meaningful range of delay has to be determined for the algorithm and the candidate terms have to be introduced with a sparse delay distribution. This method was useful in cases when the behavior of the system could be described by expected terms. The developed method is also capable to identify multiple time delays in the same system which is also the subject of our research.

References

- [1] Christopher Rackauckas, Yingbo Ma, Julius Martensen, Collin Warner, Kirill Zubov, Rohit Supekar, Dominic Skinner, Ali Ramadhan, Alan Edelman (2020) Universal Differential Equations for Scientific Machine Learning DOI: 10.48550/ARXIV.2001.04385
- [2] Steven L. Brunton, Joshua L. Proctor, and J. Nathan Kutz. (2016) Discovering governing equations from data by sparse identification of nonlinear dynamical systems. *Proceedings of the National Academy of Sciences* **113**(15): 3932–3937.
- [3] Steven L. Brunton, J. Nathan Kutz (2019) Data-Driven Science and Engineering: Machine Learning, Dynamical Systems, and Control, Cambridge University Press, ISBN: 9781108422093

Model-based Unknown Input Estimation via Partially Observable Markov Decision Processes

Wei Liu^{1,4}, Zhilu Lai^{3,4}, Charikleia D. Stoura², Kiran Bacsá^{2,4} and Eleni Chatzi^{2,4}

¹*Department of Industrial Systems Engineering and Management, National University of Singapore, Singapore*

²*Department of Civil, Environmental and Geomatic Engineering, ETH Zürich, Zürich, Switzerland*

³*Internet of Things Thrust, HKUST(GZ), Guangzhou, China*

⁴*Future Resilient Systems, Singapore-ETH Centre, Singapore*

Abstract. In the context of condition monitoring for structures and industrial assets, the estimation of unknown inputs, usually referring to acting loads, is of salient importance for guaranteeing safe and performant engineered systems. In this work, we propose a novel method for estimating unknown inputs from measured outputs, particularly for the case of dynamical systems with known or learned dynamics. The objective is to search for those system inputs that will reproduce the actual measured outputs. This can be reformulated as a Partially Observable Markov Decision Process (POMDP) problem and solved with well-established planning algorithms for POMDPs. The proposed method is demonstrated using simulated dynamical systems for structures with known dynamics, as well as a real wind turbine with learned dynamics, which is inferred via use of a Neural Extended Kalman Filter (Neural EKF) scheme, a deep learning-based method for learning stochastic dynamics.

Introduction

In the domains of Structural Health Monitoring (SHM) and Prognostics and Health Management (PHM), the assessment of performance or condition, e.g in terms of fatigue accumulation and reliability, can be evaluated more efficiently under adequate estimation of the acting loads. One typical such application is input estimation for vehicles (e.g. via estimation of the road roughness profile); a use case which has found increasing use in recent years, as part of the so called on board monitoring or mobile sensing platforms [1].

In this work, we investigate the input estimation problem from a new perspective. The input estimation problem seeks the inputs that reproduce the measured system responses, which are regarded as the actual reference outputs. With such a consideration, the input estimation problem can be formulated as a Partially Observable Markov Decision Process (POMDP). We choose the cross-entropy method [2] for policy search due to its efficiency and robustness.

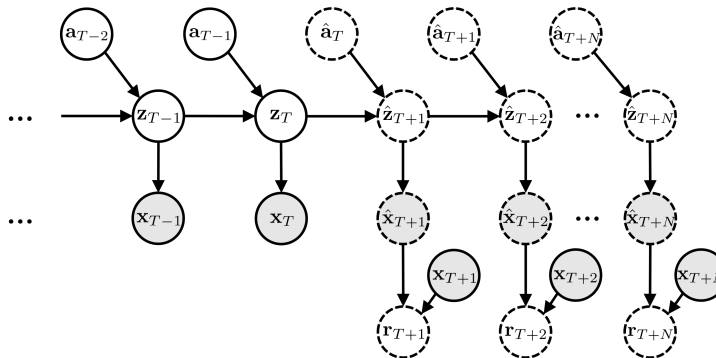


Figure 1: Unknown input estimation problem as a PODMP. The objective is to find a candidate input $\hat{\mathbf{a}}_T$ that can minimize the difference between the observation $\hat{\mathbf{x}}_{T+1}$ that is generated from this candidate input and the true (measured) observation \mathbf{x}_{T+1} .

Results and Discussion

We show the applicability of the proposed methodology in theory and real-world applications. The problem of mobile sensing is examined, where the inputs correspond to road and rail profiles, for the case of road versus railway infrastructure, respectively. These examples demonstrate potential on real-world problems of practical value. Finally, the proposed method is applied on the further problem of input estimation using a real-world dataset obtained from a wind turbine. Here, a deep learning-based dynamics model [3] is first inferred from the available data. Different model-based reinforcement learning frameworks and dynamics modeling methods can be integrated into the proposed methodology. This work aims to set the idea of such a use case for POMDPs in place. The influence of various reinforcement learning methods and a thorough comparison against further input estimation frameworks are left for further work.

References

- [1] Jin N., Dertimanis V. K., Chatzi E. N., Dimitrakopoulos E. G. and Katafygiotis L. S. (2022) Subspace identification of bridge dynamics via traversing vehicle measurements. *J. Sound Vib.* **523**:116690.
- [2] Mannor S., Rubinstein R.Y. and Gat Y. (2003) The cross entropy method for fast policy search. In *Proceedings of the 20th International Conference on Machine Learning (ICML-03)* pp. 512-519.
- [3] Liu W., Lai Z., Bacsá K. and Chatzi E. (2022) Neural Extended Kalman Filters for Learning and Predicting Dynamics of Structural Systems. *arXiv preprint arXiv:2210.04165*.

Uncertainty Quantification in Parameter Estimation Using Physics-integrated Machine Learning

Zihan Liu*, Amirhassan Abbasi*, Prashant N. Kambali* and C. Nataraj*

*Villanova Center for Analytics of Dynamic Systems, Villanova University, Villanova, PA 19085, USA #

Abstract. This paper proposes a hybrid physics-machine learning modeling method to identify unknown parameters of a nonlinear dynamics system and to quantify the uncertainty of parameter predictions. The contribution of this method depends on the introduction of physics-based features to improve the efficiency of data-based modeling and compensate for the inadequacy of data acquisition by generating training data from parameterization. In the physics-based modeling, the perturbation method is applied to obtain the asymptotic solution and frequency response of the nonlinear system. Extracted mathematical relationships provide for the identification of root causes of changes in frequency response. Subsequently, topological changes are quantified to be used as the inputs of the machine learning model. A Gaussian Process Regression (GPR) model is developed which uses physics-based features. After training and testing, the GPR model fed with measured data from real systems is capable of estimating parameters and the confidence interval of the prediction. In this paper, a coupled duffing oscillator system is simulated as a test system. Then a nonlinear pendulum is employed as the experimental setup to verify our method practically. The accurate predictions of damping and stiffness validated by experimental data demonstrate the effectiveness of the proposed method.

Introduction

Operational conditions of system change due to parametric defects, faults, operational environment and so many inevitable reasons compromising the effectiveness of model-based prediction, analysis and control. Therefore, accurate identification of different operational conditions becomes a very practical problem. However, the complexity of traditional physics-based modeling and the insufficiency in the generalization of data-based modeling leave a lot to be desired in state of the art. This paper is focusing on combining physics-based modeling and data-based modeling to reach higher prediction accuracy and to provide quantified uncertainty of this prediction. The method of multiple scales is leveraged to obtain the frequency response for generating physics-based features. The Gaussian Process Regression (GPR) model is able to incorporate these physics-based features to make predictions and measure the uncertainty over these predictions. The flow chart of the proposed method is demonstrated in Fig. 1 (a).

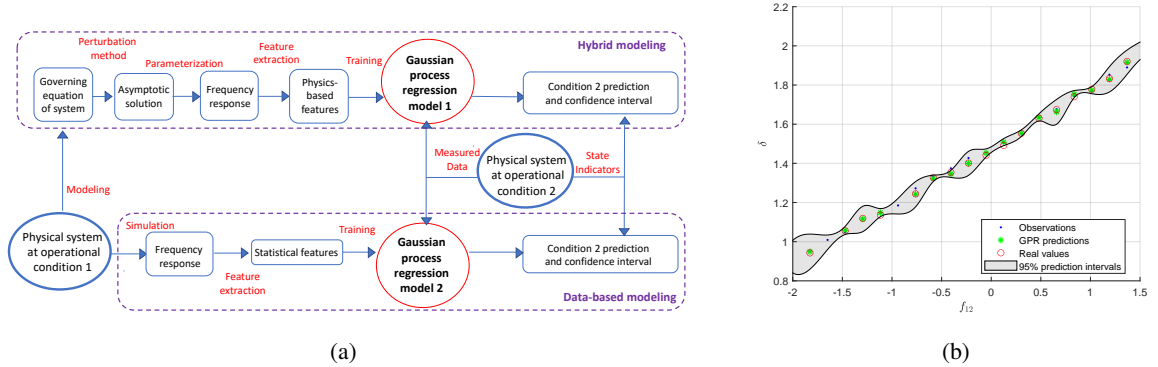


Figure 1: (a) Outline of the proposed method (b) Uncertainty prediction by Gaussian process model

Results and discussion

Gaussian processes (GP) model is a supervised learning method developed by computer science and statistics communities. By integrating prior knowledge as kernel functions, GP provides a probability distribution over possible functions that fit a set of observations. Derived from this, a GPR model can predict the probability distribution of new points, and the corresponding standard deviation can be used to estimate uncertainty over these predictions. Fig. 1 (b) demonstrates the predictions of the coupling coefficient in a system of coupled Duffing oscillators. Trained by four physics-based features (denoted by blue dots), the developed GPR model provides coupling coefficients (denoted by green stars), and 95% confidence intervals (denoted by grey area) with 0.0025 root square error and $6.69e^{-6}$ regression loss, while a data-based GRP model trained by sixteen statistical features including maximum, minimum, median and mean can only reach 0.003 root square error and $8.79e^{-6}$ regression loss. It is clear that the hybrid model outperforms data-based model in accuracy, regression loss and quantity of features. Moreover, these superior results will become more pronounced as the nonlinearity strengthens. The proposed method is also applied to a nonlinear pendulum system for damping and stiffness estimation. The experimental results not only confirm the above conclusions, but also demonstrate the excellent noise resistance ability of the hybrid modeling method.

Bayesian LSTM Neural Networks for Nonlinear System Identification

Thomas Simpson*, Nikolaos Dervilis** and Eleni Chatzi *

*Department of Civil, Environmental and Geomatic Engineering, ETH Zürich, Stefano-Franscini Platz 5, 8093 Zürich, Switzerland

**Dynamics Research Group, Department of Mechanical Engineering, University of Sheffield, S1 3JD Sheffield, UK

Abstract. System identification offers a valuable tool for creating models of systems from experimental or field monitoring data. When dealing with complex systems, characterized by nonlinearity, neural network based methods have proven potent tools in model discovery due to their flexibility and efficient learning algorithms. Long short term memory (LSTM) networks are a type of neural network which shows particular promise for modeling nonlinear structural systems. Previous work on such methods has been focused on deterministic networks. In this work, we adopt a Bayesian implementation of such an LSTM network, which offers the advantage of uncertainty quantification. Such a Bayesian-LSTM is demonstrated in this work applied to an experimental nonlinear structural system.

Introduction

In modern high performance engineering systems the consideration of nonlinearity is inevitable, especially for systems comprising advanced composite materials or subject to extreme environments. Identification of such nonlinear systems is important for many potential applications, such as control or digital twinning, and yet it remains a considerable challenge to create lightweight and accurate nonlinear models for such systems. Recent work has leveraged neural networks for system identification problems, due to their ability to approximate highly complex systems. Recurrent neural networks (RNNs) are a form of neural network which are specifically designed for dealing with sequence data; LSTM networks, a particular type of RNN, have shown particular promise in the domain of nonlinear dynamics [1, 2]. These works have, however, been limited to deterministic LSTM networks. By exploiting a Bayesian framework, a stochastic LSTM network is rendered, able to predict a distribution on possible outputs rather than point estimates. This is particularly valuable within a digital twinning context, where a digital twin forms a necessary element for supporting decisions on operation and m

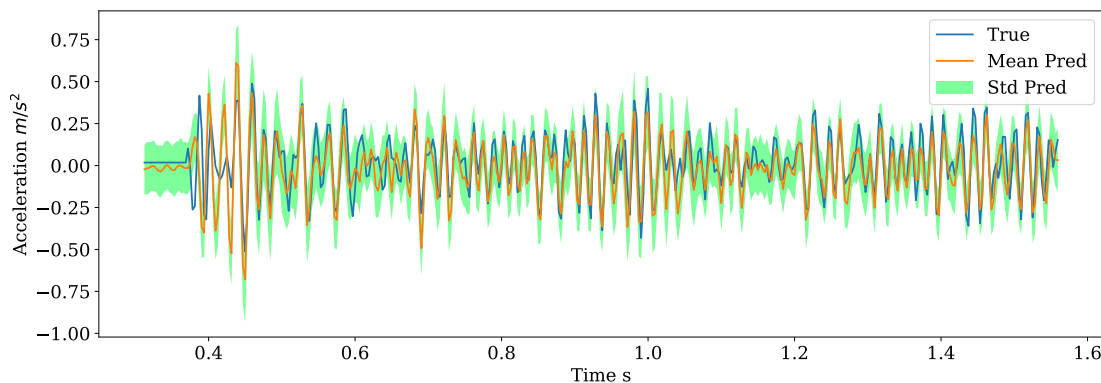


Figure 1: Prediction of acceleration response of 3rd storey to new base excitation input with a Bayesian LSTM, including uncertainty bounds.

Results and Discussion

In this work, we apply a Bayesian implementation of an LSTM neural network for identification of a nonlinear experimental system, namely, a three-storey shear-frame benchmark structure established by the Los Alamos National Laboratory (LANL) [3]. This 3 storey frame structure is excited by random ground motion and nonlinearity is introduced in the form of a rubber bumper acting between the 2nd and 3rd storey, acting as a bi-linear stiffness nonlinearity. We train a Bayesian LSTM to predict the acceleration of the 3 storeys to ground excitation. Some of the experimental runs are used for training the model with others reserved for testing. It is demonstrated that the trained model can successfully approximate the system dynamics by recreating the system response to input time-series not seen in the training set. Simultaneously the Bayesian LSTM can provide estimates of the uncertainty of its response, which are interpretable and useful to the engineer.

References

- [1] Vlachas P.R., Arampatzis G., Uhler C., Koumoutsakos P. (2022) Multiscale simulations of complex systems by learning their effective dynamics *Nature Machine Intelligence* **44**:359-366.
- [2] Simpson T., Dervilis N., Chatzi E. (2021) Machine learning approach to model order reduction of nonlinear systems via autoencoder and lstm networks *Journal of Engineering Mechanics* **147**
- [3] Figueiredo E., Park G., Figueiras J., Farrar C., Worden K. (2009) Structural health monitoring algorithm comparisons using standard data set *Technical Report LA-14393*

Nonparametric identification for time-varying physical parameters and nonlinear restoring force based on UKF and Sage-Husa algorithm

Ye Zhao* and Bin Xu*,**

*College of Civil Engineering, Huaqiao University, Xiamen 361021, China

**Key Laboratory for Intelligent Infrastructures and Monitoring of Fujian Province (Huaqiao University), Xiamen 361021, China

Corresponding author: binxu@hqu.edu.cn

Abstract. With the help of an UKF and Sage-Husa adaptive filter algorithm, a nonparametric NRF and time-varying structural parameters simultaneous identification approach is presented for multi-degree-of-freedom (MDOF) structures under known dynamic loadings using partially available acceleration responses, where the NRF is expressed with a Hermite polynomial model in a nonparametric way. The performance of the proposed approach is studied in the context of a numerical example consisting of a nonlinear MDOF frame structure with a magnetorheological (MR) damper on the fourth story mimicking nonlinear behavior. The MDOF frame is a time-varying parameter model which inter-story stiffness parameter varies with time. Effect of acceleration measurement noise levels on identification results is investigated. Results show that the proposed method can identify the time-varying structural parameters, unknown dynamic responses and NRF exhibiting a strong nonlinear behaviour in a nonparametric way.

Introduction

Structural nonlinearity identification plays key roles in post-event damage detection for engineering structures excited by strong dynamic loadings. Due to high complexity and individuality of structural nonlinearities, it is difficult to provide an exact parametric mathematical model in advance to describe the nonlinear behaviour of a structural member or a substructure under strong dynamic loadings in practice. Identifying the nonlinear restoring force (NRF) of an engineering structure instead of the stiffness in a nonparametric way where no exact parametric mathematical model for NRF is required is more attractive. Additionally, structural physical parameters often vary gradually due to the degradation of material properties or damage initiation and development and engineering structures are usually time-varying systems. Limited studies on the identification approaches for time-varying structural parameters of nonlinear structure have been attempted [1,2]. Traditional unscented Kalman filter (UKF) can only identify time-invariant structural parameters. For time-invariant parameters of nonlinear structures, Zhao et al. [3, 4] proposed nonparametric methods for identifying NRF. Therefore, it is crucial to propose a nonparametric identification method for structural NRF and time-varying structural parameters based on partially measured dynamic responses.

Results and discussion

In this study, time-dependent inter-story stiffness of nonlinear structures is considered. Identified results show that the proposed identification method can effectively identify time-varying structural parameters, unknown dynamic responses and NRF in a nonparametric way. Figs. 1 and 2 show the identification results of the gradually varying stiffness parameters of the 2th floor and the NRF provided the MR damper on the 4th floor.

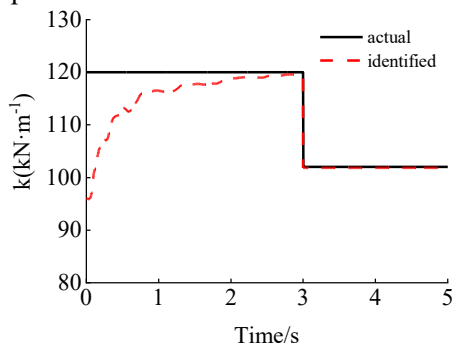


Figure 1: Identification of gradually varying stiffness parameters of the 2th floor

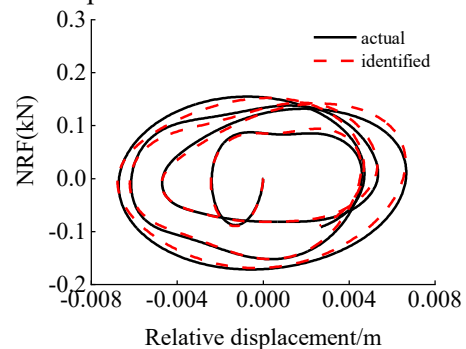


Figure 2: Identified NRF provided MR damper on the 4th floor

References

- [1] Xin Y., Li J., Hao H., et al. (2022) Time-varying system identification of precast segmental columns subjected to seismic excitations. *J. Bridge Eng* **27**(4): 04022013.
- [2] Zhang X., He J., Hua X., et al. (2022) Online identification of time-variant structural parameters under unknown inputs basing on extended Kalman filter. *Nonlinear Dyn.*
- [3] Zhao Y., Xu B., Deng B., et al. (2022) Various damper forces and dynamic excitation nonparametric identification with a double Chebyshev polynomial using limited fused measurements. *Measurement* **193**:110940.
- [4] Zhao Y., Xu B., Deng B., et al. (2022) Hysteresis and dynamic loading nonparametric identification for multi-degree-of-freedom structures using an updated general extended Kalman filter and a Legendre polynomial model. *Struct. Control Health Monit* **29**(11): e3088.

Application of SINDy for the discovery of governing equations of a trapped particle in an acoustic radiation force field

M. Akbarzadeh*, S. Oberst*, S. Sepehriahnama* and B. Halkon*

* Centre for Audio, Acoustics and Vibration, University of Technology Sydney, Sydney, Australia.

Abstract. The contactless technique for trapping, handling, and levitating particles using acoustic radiation forces has many applications in engineering and medicine. Recently, Brunton et al. proposed the Sparse Identification of Nonlinear Dynamics (SINDy) approach to identify governing equations of motion from time series data. We use SINDy to extract the equation of motion of a trapped particle oscillating in an acoustic radiation force field which is related to the family of Duffing oscillators. We simulate the responses of this equation to benchmark SINDy for different dynamical regimes which are then validated for the case of a predicted period-1 limit cycle using experimentally captured data for TinyLev.

Introduction

Although the acoustic radiation force as a nonlinear acoustic phenomenon has been investigated for many years, the interaction of the influence of secondary excitation on the dynamics of a particle in an acoustic force field is yet to be fully studied [1]. By periodically exciting the acoustic force field externally using a shaker with amplitude, A_{ex} , and frequency, ω_{ex} , the particle is also excited with a specific amplitude, $A = f(A_{ex})$, and frequency, $\omega_0 = g(\omega_{ex})$, when f and g being functions relating the external excitation to the particle's oscillation. We explicitly derive that the developed acoustic trap follows the behaviour of a nonlinear Duffing-like oscillator as follows:

$$\ddot{\theta} + a_1|\dot{\theta}| + a_2\theta - \frac{a_2}{6}\theta^3 = F \cos \theta \sin \omega_0 t, \quad (1)$$

where θ is the displacement, ' $\dot{(\cdot)}$ ' is its time derivative, and a_1 and a_2 are coefficients depending on the drag coefficient, the levitated object, and its surrounding fluid properties, and F is a coefficient depending on the A_{ex} . Then, the Sparse Identification of Nonlinear Dynamics (SINDy) algorithm [2,3] is employed (schematic Fig 1a) to extract a set of coefficients representing the particle's equation of motion, see Eq. (1) [4]. Real-life measurements of the oscillations of a Styrofoam bead provide experimental data for a TinyLev [5] system to validate the performance of a period-1 regime using $A_{ex} \leq 0.2$ [mm] and $f_{ex} \leq 100$ [Hz].

Results and discussion

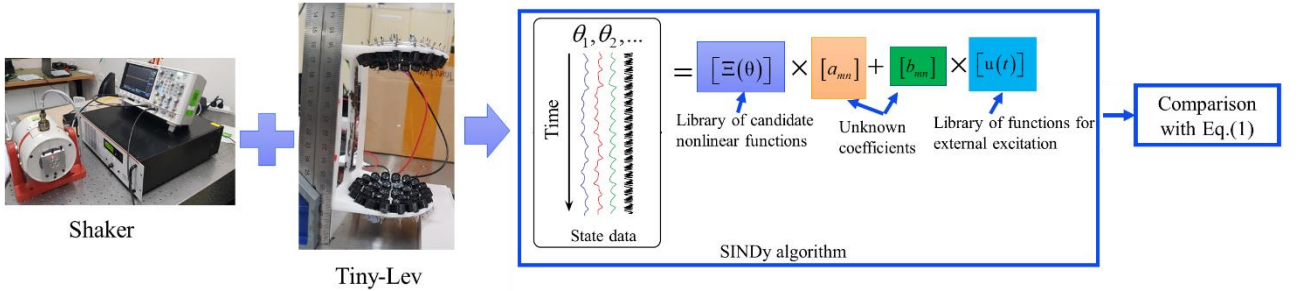


Figure 1: Schematic of SINDy algorithm to identify governing equation from nonlinear time series data. Data are collected from measurements of the system, including a time history of the states θ and derivatives $\dot{\theta}$. $[a_{mn}]$ and $[b_{mn}]$ are unknown coefficients.

It is demonstrated that SINDy is a powerful new technique to identify nonlinear dynamical systems from data without assumptions on the form of the governing equation of motion. Results indicate good correlation with theory, however moving into more complex dynamics at lower excitation amplitudes [4] indicate that higher order nonlinear terms in Eq. (1) might be required.

References

- [1] Andrade Marco A. B., Pérez N., Adamowski J. C. (2017) Review of Progress in Acoustic Levitation. *Braz. J. Phys.* **48**: 190-213.
- [2] Brunton, S. L., Proctor, J. L., Kutz, J. N. (2016) Discovering governing equations from data by sparse identification of nonlinear dynamical systems. *Proc. Natl. Acad. Sci. USA*, **113**, 3932–3937.
- [3] Stender M, Oberst S, Hoffmann (2019) Recovery of differential equations from impulse response time series data for model identification and feature extraction. *Vibration*, **2(1)**, 25-46.
- [4] Akbarzadeh M., Oberst S., Sepehriahnama S., Halkon B. (2022) Sensitivity and Bifurcation Analysis of an Analytical Model of a Trapped Object in an Externally Excited Acoustic Radiation Force Field, NOVEM 2023 Conference, accepted.
- [5] Marzo A., Barnes A., Drinkwater B. W. (2017) TinyLev: A multi-emitter single-axis acoustic levitator. *Rev. Sci. Instrum.* **88(8)**: 085105–085105.

Control of orbital parameters of a dumbbell satellite using moving mass actuators

Valery Pilipchuk*, Steven W. Shaw** and Nabil Chalhoub*

*Mechanical Engineering Department, Wayne State University, Detroit, MI, U.S.A.

**Department of Mechanical and Civil Engineering, Florida Institute of Technology, Melbourne, FL, USA

Abstract. Principles of a moving mass control of the orbital parameters of an artificial satellite are discussed based on the suggested design of the dumbbell shaped satellite. The purpose of the design is to implement a non-jet actuation through the variable geometry of the satellite associated with its internal degrees-of-freedom. Both massive parts of the dumbbell can spin and change their relative distance upon the orbital angle according to the suggested control algorithms. It is shown by analysis and simulations that this is an effective approach to altering orbital parameters.

Introduction

A dumbbell-shaped satellite model enables the two-particle approach to be implemented for representing the dynamics of a rigid-body moving in a central gravitational field. Such modeling eases analytical manipulations with the differential equations of motion; thus, providing a clear way for designing control algorithms. In addition, the dumbbell model captures important dynamic properties of the so-called tethered satellite systems used in experimental investigations of space related exploitation of the Earth's magnetic field [1]. During the past decades, different spinning tethered systems were analyzed in connection with specific space missions, including the Momentum-Exchange/Electrodynamic-Reboost (MXER) project by NASA. The main purpose of the present work is to understand the extent to which orbital parameters of the satellite can be controlled through variations of the satellite geometry, namely, by the satellite length and the relative angles φ of the two massive components with respect to the connecting rod (Fig. 1a).

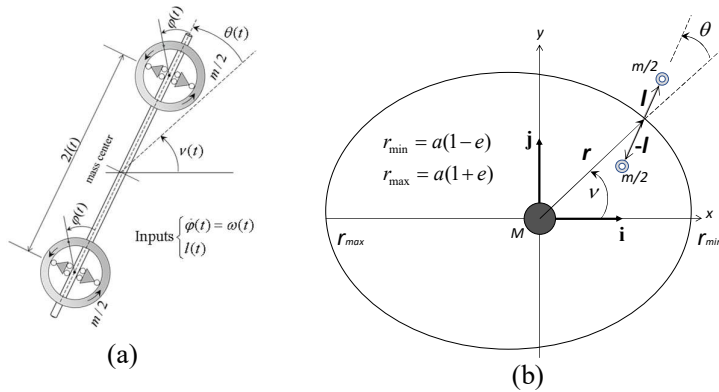


Figure 1: Planar dynamics of the dumbbell satellite with controllable inertial properties: (a) schematic of the satellite, and (b) the model coordinates with mass parameters and elements of the orbit in the inertial Cartesian frame [2].

Results and discussion

It is shown that the total energy of the satellite, $\alpha(v)$, follows the target profile, $\alpha_d(v)$, with both increasing and decreasing intervals, if the satellite angle θ (Fig. 1b) is guided by the prescribed dependence

$$\theta_d(v) = \frac{1}{4} \pi \left(1 + \cos \left[v - \text{sgn}(\alpha_d - \alpha) \frac{\pi}{2} \right] / \sqrt{1 - \beta^2 \sin^2 \left[v - \text{sgn}(\alpha_d - \alpha) \frac{\pi}{2} \right]} \right),$$

where β is a smoothing parameter, such that, for $\beta = 0$, the above equation yields a shifted cosine wave, whereas $\beta \rightarrow 1$ leads to a rectangular pulse train. Both classical PID and robust sliding mode control algorithms assume that the main control input is generated through the rotation of end masses, $\varphi(v)$. The total angular momentum conservation law guarantees the corresponding effect on the angular coordinate $\theta(v)$. The rate of change of the eccentricity per unit orbital cycle is found to be $de/dN = 1.5625 \times 10^{-6}$ for the orbital parameters $a = 13623.58$ km and $e = 0.34456$, and satellite length 10 km, which is reasonable for tether structures. Such relatively minor effects may still be sufficient for long-terms non-jet corrections of orbits since the suggested actuators can use electric energy accumulated from solar panels over the extended operational period.

References

- [1] Beletsky V.V., Levin E.M. (1993) Dynamics of space tether systems. *Advances in the Astronaut. Sci* **83**.
- [2] Pilipchuk V., Shaw S.W., Chalhoub N. (2022) Control of dumbbell satellite orbits using moving mass actuators. *Nonlinear Dynamics* **110**:1373-1391.

Three-dimensional deployment of cable nets for active removal of space debris

Paolo Fisicaro*, Angelo Pasini* and Paolo Sebastiano Valvo *

*Department of Civil and Industrial Engineering, University of Pisa, Pisa, PI, Italy

Abstract. Deployable cable nets are promising capture systems for the active removal of space debris. We propose a finite element model of the cable net with lumped nodal masses and first-order cable elements. The nodal positions are assumed as the main unknowns of the problem. Large displacements and finite deformations are considered through the Green-Lagrange strain tensor. Cable elements are assumed to react only in tension through a hyper-elastic constitutive law. The governing equations are solved numerically by means of the Runge-Kutta method with variable time step. As an example, the three-dimensional deployment of a planar, square-mesh net is simulated. The proposed approach turns out to be computationally effective and accurate.

Introduction

Remediation activities set out for the disposal of massive objects abandoned around the Earth are needed to secure the most valuable orbital regions. For active debris removal (ADR), the development of an effective capturing mechanism is still an open issue. Among several proposals, cable nets are light, easily packable, scalable, and versatile. Nonetheless, guidance, navigation, and control (GNC) aspects are especially critical in both the capture and post-capture phases [1].

Several theoretical models have been proposed to describe the deployment and capture processes. Benvenuto et al. [2] and Botta et al. [3] modelled the net as a system of concentrated masses connected to each others by spring-dampers. In their models, springs react only in tension and infinitesimal strains are considered. Shan et al. [4] compared the simple lumped mass-spring model with a more refined one based on the absolute nodal coordinate formulation (ANCF) proposed by Shabana [5]. They used a third-order cable element, and considered finite strains through the Green-Lagrange strain tensor. The lumped mass-spring and ANCF models predicted similar overall behaviour of the net, but the ANCF model was much more computationally expensive.

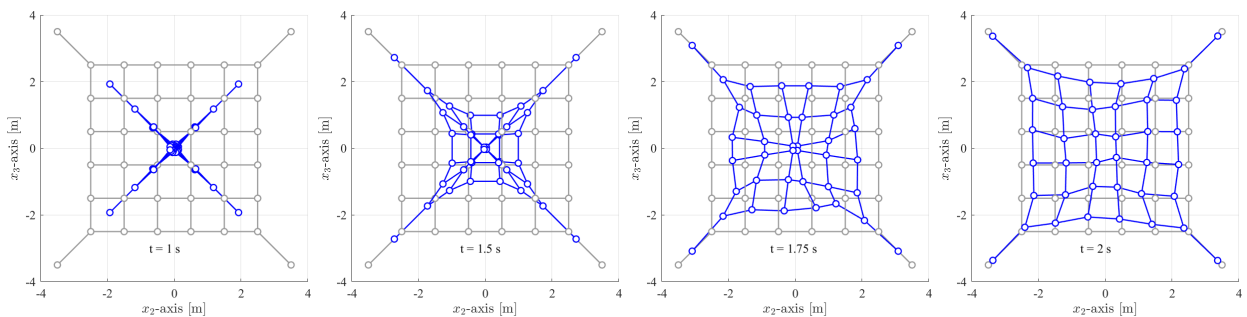


Figure 1: In-plane deployment of the cable net. Grey and blue lines represent the reference and current configurations, respectively.

Results and discussion

We propose a finite element model of the cable net with lumped nodal masses and first-order cable elements. In line with the ANCF, we adopt the nodal positions as the main unknowns of the problem, obtaining a symmetric secant elastic stiffness matrix [6]. Large displacements and finite deformations are considered through the Green-Lagrange strain tensor. Cable elements are assumed to react only in tension according to a hyper-elastic constitutive law [7]. Global damping is introduced into the model according to Rayleigh's hypothesis. The governing equations are solved numerically by means of the Runge-Kutta method with variable time step.

As an illustrative example, we present the simulation of the three-dimensional deployment of a planar, square-mesh net. The proposed approach turns out to be computationally effective and accurate.

References

- [1] Shan M., Guo J., Gill E. (2016) Review and comparison of active space debris capturing and removal methods. *Prog Aerosp Sci* **80**:18-32.
- [2] Benvenuto R., Salvi S., Lavagna M. (2015) Dynamics analysis and GNC design of flexible systems for space debris active removal. *Acta Astronaut* **110**:247-265.
- [3] Botta E.M., Sharf I., Misra A.K. (2017) Energy and momentum analysis of the deployment dynamics of nets in space. *Acta Astronaut* **140**:554-564.
- [4] Shan M., Guo J., Gill E. (2017) Deployment dynamics of tethered-net for space debris removal. *Acta Astronaut* **132**:293-302.
- [5] Shabana A.A. (1998) Computer Implementation of the Absolute Nodal Coordinate Formulation for Flexible Multibody Dynamics. *Nonlin Dyn* **16**:293-306.
- [6] Valvo P.S. (2022) Derivation of symmetric secant stiffness matrices for nonlinear finite element analysis. *Adv Sci Technol Res J* **16**.
- [7] Ogden R.W. (1984) Non-linear Elastic Deformations. Ellis Horwood, Chichester.

Suspension nonlinear analysis and active vibration control of an aerospace structure

Guoliang Ma^{*} and Liquan Chen^{**}

^{*}School of Mechatronic Engineering, Xi'an Technological University, Xi'an, Shaanxi, China

^{**}School of Science, Harbin Institute of Technology, Shenzhen, Guangdong, China

Abstract. Aerospace structure is multi degree of freedom system, which contains complex dynamic characteristics such as time-varying parameters, geometric nonlinearity, gap nonlinearity and so on. According to the law of motion of nonlinear pendulum and considering the influence of geometric nonlinearity of medium swing angle, the relationship between vibration frequency and nonlinear term is obtained by perturbation method, and the influence of parameters on vibration characteristics is studied. Then, the active vibration control system of aerospace structure is established. Variable step size LMS adaptive filtering algorithm or T-S fuzzy control algorithm are used to calculate the control signal, and considering the influence of geometric nonlinearity, the actuator is used to suppress the vibration of the suspended structure. Finally, the amplitude of vibration response decreases by more than 75% under transient excitation and steady-state excitation.

Introduction

Gravity makes the hoop antenna produce serious static deformation, which increases the difficulty of mechanical test and affects the accuracy of vibration control. In order to simulate low gravity environment, suspension method is applied to gravity unloading. Rope suspension has the advantages of large simulation range and no additional inertia^[1]. However, the nonlinearity of the suspension cable interferes with the vibration characteristics. Under the premise that the hoop antenna has complex multi-mode and nonlinear factors^[2], whether it can effectively suppress the vibration is a mechanical problem.

The advantages of hanging the spacecraft by ropes are simple, reliable and small additional stiffness. If the rope length is long enough, low gravity or even zero gravity simulation of the spacecraft can be realized in both active and passive ways. However, the rope used in the suspension device is slender and soft, and the mechanical model is simplified as a string. In order to realize gravity unloading and follow-up movement, the suspension device inevitably produces vibration problems. As the rope (string) vibrates laterally, the nonlinear parameters significantly affect the dynamic characteristics of the rope (string)^[3]. Therefore, according to the law of motion of nonlinear pendulum and considering the influence of geometric nonlinearity of medium swing angle, the oscillation equation with nonlinear term is established.

$$ml\ddot{\theta}(t^*) + mg \sin \theta(t^*) + T \cos \theta(t^*) = 0 \quad (1)$$

Assuming a small swing angle motion, $\sin \theta \approx \theta$, it is simplified to a linear system,

$$\ddot{\theta}(t) + \frac{g}{l} \theta(t) - \frac{g}{6l} \theta^3(t) = 0 \quad (2)$$

If the swing angle is medium, Taylor expansion is used,

$$\ddot{\theta}(t^*) + \frac{g}{l} \theta(t^*) - \frac{T}{2ml} \theta^2(t^*) - \frac{g}{6l} \theta^3(t^*) = -\frac{T}{ml} \quad (3)$$

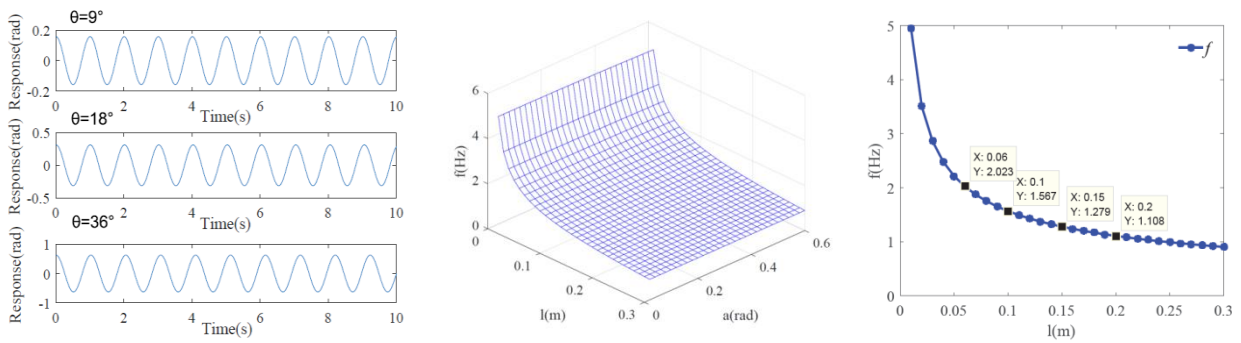


Figure 1: Relationship between vibration frequency, swing angle and rope length

References

- [1] Ma G L, Gao B, Xu M L, Feng B. (2018) Active suspension method and active vibration control of a hoop truss structure. *AIAA J.*, **56**(4): 1689-1695.
- [2] Cao S, Huo M, Qi N, Zhao C, Zhu D F, Sun L J. (2020) Extended continuum model for dynamic analysis of beam-like truss structures with geometrical nonlinearity. *Aero. Sci. and Tech.*, **103**: 105927.
- [3] Ding H, Wang S and Zhang Y W. (2018) Free and forced nonlinear vibration of a transporting belt with pulley support ends. *Nonl. Dyna.*, **92**(4): 2037-2048.

Control of orbital parameters of a dumbbell satellite using moving mass actuators

Valery Pilipchuk*, Steven W. Shaw** and Nabil Chalhoub*

*Mechanical Engineering Department, Wayne State University, Detroit, MI, U.S.A.

**Department of Mechanical and Civil Engineering, Florida Institute of Technology, Melbourne, FL, USA

Abstract. Principles of a moving mass control of the orbital parameters of an artificial satellite are discussed based on the suggested design of the dumbbell shaped satellite. The purpose of the design is to implement a non-jet actuation through the variable geometry of the satellite associated with its internal degrees-of-freedom. Both massive parts of the dumbbell can spin and change their relative distance upon the orbital angle according to the suggested control algorithms. It is shown by analysis and simulations that this is an effective approach to altering orbital parameters.

Introduction

A dumbbell-shaped satellite model enables the two-particle approach to be implemented for representing the dynamics of a rigid-body moving in a central gravitational field. Such modeling eases analytical manipulations with the differential equations of motion; thus, providing a clear way for designing control algorithms. In addition, the dumbbell model captures important dynamic properties of the so-called tethered satellite systems used in experimental investigations of space related exploitation of the Earth's magnetic field [1]. During the past decades, different spinning tethered systems were analyzed in connection with specific space missions, including the Momentum-Exchange/Electrodynamic-Reboost (MXER) project by NASA. The main purpose of the present work is to understand the extent to which orbital parameters of the satellite can be controlled through variations of the satellite geometry, namely, by the satellite length and the relative angles φ of the two massive components with respect to the connecting rod (Fig. 1a).

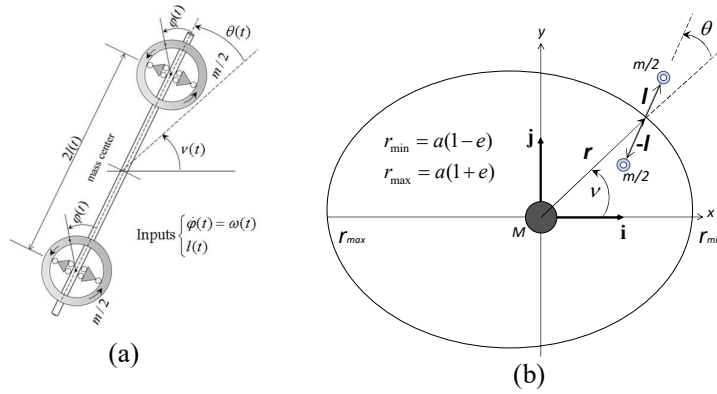


Figure 1: Planar dynamics of the dumbbell satellite with controllable inertial properties: (a) schematic of the satellite, and (b) the model coordinates with mass parameters and elements of the orbit in the inertial Cartesian frame [2].

Results and discussion

It is shown that the total energy of the satellite, $\alpha(v)$, follows the target profile, $\alpha_d(v)$, with both increasing and decreasing intervals, if the satellite angle θ (Fig. 1b) is guided by the prescribed dependence

$$\theta_d(v) = \frac{1}{4}\pi \left(1 + \cos \left[v - \text{sgn}(\alpha_d - \alpha) \frac{\pi}{2} \right] / \sqrt{1 - \beta^2 \sin^2 \left[v - \text{sgn}(\alpha_d - \alpha) \frac{\pi}{2} \right]} \right),$$

where β is a smoothing parameter, such that, for $\beta = 0$, the above equation yields a shifted cosine wave, whereas $\beta \rightarrow 1$ leads to a rectangular pulse train. Both classical PID and robust sliding mode control algorithms assume that the main control input is generated through the rotation of end masses, $\varphi(v)$. The total angular momentum conservation law guarantees the corresponding effect on the angular coordinate $\theta(v)$. The rate of change of the eccentricity per unit orbital cycle is found to be $de/dN = 1.5625 \times 10^{-6}$ for the orbital parameters $a = 13623.58$ km and $e = 0.34456$, and satellite length 10 km, which is reasonable for tether structures. Such relatively minor effects may still be sufficient for long-terms non-jet corrections of orbits since the suggested actuators can use electric energy accumulated from solar panels over the extended operational period.

References

- [1] Beletsky V.V., Levin E.M. (1993) Dynamics of space tether systems. *Advances in the Astronaut. Sci* **83**.
- [2] Pilipchuk V., Shaw S.W., Chalhoub N. (2022) Control of dumbbell satellite orbits using moving mass actuators. *Nonlinear Dynamics* **110**:1373-1391.

Modal Testing of *In Situ* BAE T1A Hawk Wing: Benchmark Dataset

Matthew Bonney*, David Wagg* and Tim Rogers *

*Dynamics Research Group, Department of Mechanical Engineering, The University of Sheffield, Sheffield, UK

Abstract. In the generation of digital twins for existing systems, a BAE T1A Hawk aircraft for this benchmark dataset, required reverse engineering through modelling and experimental testing. This work presents a dataset for the starboard wing that contains vibration test data including multiple repetitions (to test repeatability), excitation types, amplitudes, and configurations (to simulate damage). The dataset is freely available for other researchers to test novel damage detection algorithms, model updating, non-linearity measurements, and other various techniques that can increase the accuracy and usability of a digital twin for managing this and other similar types of systems.

Introduction

Digital twins (DTs) are radically reshaping many aspects of modern engineering systems. One of the major objectives of a DT is the pairing between the virtual and physical systems. For many ageing systems, as is commonplace in aerospace systems, there is a major lack of information regarding the physical asset. Because of this deficiency, the ability to create a DT for such a system requires reverse engineering through data measurements and modelling. However, the actual design did not utilise modern technology such as computer aided drafting and finite element analysis. To progress towards a DT of an aircraft of this age, this work focuses on the development of a benchmark dataset for a BAE T1A Hawk fixed-wing aircraft. This work is part of the main objectives of the Alan Turing Institute funded project *Digital Twins for High-Value Engineering Applications* (DTHIVE) [1].

Dataset

The testing performed to generate this dataset is focused around a dense array of accelerometers applied to the starboard wing that is excited using a single modal shaker at approximately 75% of the wing length on the bottom. There are a total of 55 accelerometers attached at selected locations with a total of six lines of sensors down the length of the wing, four on the top and two on the bottom. The remaining sensors are placed at points of interest such as the root and landing gear. Figure 1 shows a picture taken during the experimental testing showing the accelerometers that are attached to the top of the wing.



Figure 1: Experimental setup for the vibration testing of the Hawk T1A Wing

There are two main excitation types used in this data, a burst random and sine swept. These are performed at varied amplitude levels with multiple repetitions at each excitation level to test for experimental repeatability and non-linearity. In addition to these nominal tests, additional masses were added to the wing at specified locations to mimic wing damage (an increase in mass to mimic a decrease in stiffness). The dataset is freely available to use by other researchers and can be obtained through [2].

References

- [1] <https://www.turing.ac.uk/research/research-projects/digital-twins-high-value-engineering-applications-dthive>
- [2] Bonney, Matthew; Rogers, Tim; Wagg, David (2022): BAE T1A Hawk Starboard Wing Vibration Tests. The University of Sheffield. Collection. <https://doi.org/10.15131/shef.data.c.6269025>

Multi-layers radical morphing: shape transitions and vibration

Ginevra Hausherr* and Giulia Lanzara*

*Department of Civil, Informatics and Aeronautical Technologies, University of Rome, RomaTre, Roma, Italy

Abstract. Shape-shifting materials is entering into many disciplines from engineering to medicine, where passive sensors are needed. The idea of making the material independent of configuring itself on the basis of the surrounding environment thanks to a preliminary training that does not lose its characteristics of the material, is innovative. This study, from an experimental point of view, is aimed at analyzing the morphing capabilities of a multilayer in a fixed temperature range following a preliminary training. A bi-material structure is considered in which one of the two layers is made up of polyethylene (PE) reinforced with polyethylene terephthalate (PET) fibers and the other is made up of a layer of Aluminum Foil. The capacity of this morphing material is to modify its shape configuration and the variation of the dynamic response is compensated by the contribution of the material and geometric variations due to the different configurations.

Introduction

The development of materials with multiple functionalities, as morphing materials, is becoming essential not only in various engineering fields to improve performance of the devices/structures but also to reduce environmental impact. Morphing materials have the intrinsic ability to adapt their shape due to different (even external) stimuli. [2] There are, in particular, some smart materials that can be programmed and transformed using external stimuli such as: the change of temperature, light, water, electricity and magnetic fields. Others that change in which the shape changes are triggered by geometric effects or by exploiting the material's homogeneity or non-homogeneity [7]. Among the existing morphing and smart materials, shape memory polymers (SMPs) are those capable of memorizing a temporary shape and recovering to the permanent shape upon the occurrence of an external stimuli. Although such a basic concept was known for half a century, recent progresses allowed to transfer the usage of such materials, especially in the case of thermo-responsive materials, for practical applications. The fundamental limitation of SMPs is that they are not able to provide cyclic shape changes and that their morphing response can only be achieved under specific and unchangeable inputs. Moreover, in most cases external devices/power are required to provide the relevant stimulus to achieve the desired morphing shape (such as sources of heat, light or humidity). The most intriguing approaches are seeking the spontaneous response of materials when the stimulus is directly provided by the surrounding environment. However, spontaneous cyclability and adaptability to different environmental conditions represents key challenges in the field. With this in mind, here a unique bi-material structure that is able to provide cyclic and indeed radical shape changes at the desired set triggering temperature, is presented together with the vibrational response of the corresponding morphing modes.

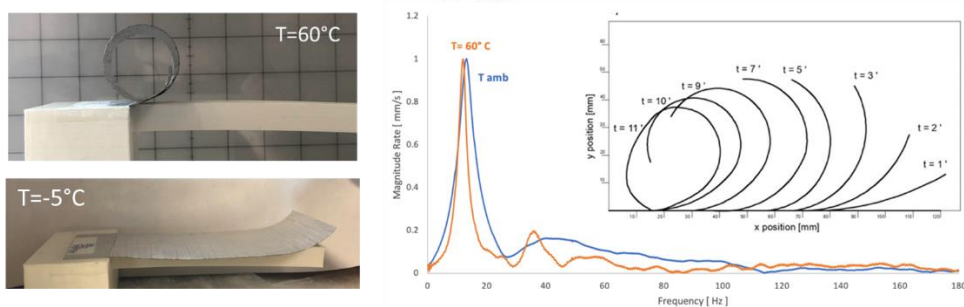


Figure 1: Images showing the designed bi-layer in its two programmed shapes activated by temperature. FFT of the bi-layer in its two configurations (flat and rolled). In the inset the shape changes are plotted at different time intervals.

Bi-layer design and the dynamic response of its morphed shapes

In this work it is shown that a bi-material structure formed by a fiber reinforced composite layer and an aluminum foil, has morphing ability when subjected to both positive and negative thermal gradients. This response can be associated with the opposite coefficients of thermal expansion and glass transition temperature between the forming layers as well as their stiffness variation with temperature and the multi-material plasticization during the “education” step. The vibrational analysis shows that the resonance frequency is just slightly affected by the configuration changes and this is due to the compensation of the loss in stiffness due to temperature with the increase in stiffness due to large-in-scale geometrical changes.

References

- [1] Athanapoulos, N. , Siakavellas J. (2015) Programmable thermal emissivity structures based on bioinspired self-shape materials *Scientific Reports*, 5:17682
- [2] Athanapoulos, N. (2018) Bioinspired Temperature-Responsive Multilayer Films and Their Performance under Thermal Fatigue *Biomimetics*, 3, 3, 20.

Stochastic delay modelling of landslide dynamics

Srdan Kostić* and Nebojša Vasović**

*Jaroslav Černi Water Institute, BGD, SRB, ORCID 0000-0002-3705-3080

**University of Belgrade Faculty of Mining and Geology, BGD, SRB, ORCID 0000-0002-8294-5117

Abstract. In present paper we provide results on qualitative modelling of landslide dynamics under the assumption of delayed failure and the effect of background noise. Results obtained indicate that examined time series, which represent the actual recordings of background noise, belong to a group of stationary linear stochastic processes with Gaussian inputs. Such noise is introduced as the additive term in the system of delay differential equations governing the dynamics of spring-block model composed of n units with delayed failure. Friction law assumed in the model represents the cubic friction force. Results of the performed research, using mean-field approximation and numerical computation, indicates the conditions for occurrence of Andronov-Hopf direct supercritical bifurcation. In particular, it is shown small-amplitude background noise could contribute to the onset of in-stability if the system under study is at the verge of stability.

Introduction

In present paper our analysis is based on the model initially proposed by Davis [1], who assumed that dynamics of accumulation slope could be qualitatively described by the interaction of feeder and accumulation part of the slope. The existence of noise is firstly evaluated using surrogate data testing of the two null hypotheses: that data are independent random numbers, and from a stationary linear stochastic processes with Gaussian inputs. Noise is proposed to be introduced as additive white noise as a part of the system of delay differential equations governing the dynamics of spring-block model composed of n units with delayed failure, which is assumed to qualitatively mimic the landslide motion [1]:

$$\begin{aligned} x_i(t) &= y_i(t)dt \\ dy_i(t) &= - \left[a(V + y_i(t))^3 - b(V + y_i(t))^2 + c(V + y_i(t)) \right] dt + (aV^3 - bV^2 + cV)dt + \\ &+ \sum_{j=1}^N k \left(x_j(t - \tau) - x_i(t) \right) dt + \sqrt{2D}dW_i \end{aligned} \quad (1)$$

where x_i and y_i are displacement and velocity of the i -th block, $V=0.2$ is the constant background velocity of the system, τ is the introduced time delay and k is the spring stiffness. Terms $\sqrt{2D}dW_i$ represent stochastic increments of independent Wiener process, i.e. dW_i satisfy: $E(dW_i) = 0$, $E(dW_i dW_j) = \delta_{ij}dt$, where $E()$ denotes the expectation over many realizations of the stochastic process and D is intensity of additive local noise. Friction law assumed in (1) represents the cubic friction force, with frictional parameters a , b and c as proposed in [2]. As it was shown in previous research [3], noise could represent the main trigger for instability to occur for certain initial conditions or dynamical regime of the system under study.

Results and discussion

In the first phase of the research, surrogate data testing is invoked to examine the recorded background seismic noise [4]. Results obtained indicate that zeroth-order prediction error for the examined time series is smaller than zeroth order prediction error for 20 surrogate time series, which were obtained by random shuffling of the starting data. On the other hand, it seems that the observed time series could be characterized as stochastic linear series with Gaussian inputs, since the results show that distribution of zeroth order prediction error for the starting series with the increase of prediction steps is well within the prediction error for the surrogate tests. In the second part of the research, we examined the dynamics of the proposed model (1). System is analyzed for the following parameter values: $a=3.2$, $b=7.2$ and $c=4.8$, $V=0.2$, and for the following initial conditions: $x_{10}=0.001$, $x_{20}=0.0001$, $y_{10}=0.1$, $y_{20}=0.1$. Results of the performed research, using mean-field approximation and numerical computation, indicates the conditions for occurrence of Andronov-Hopf direct supercritical bifurcation. In particular, it is shown small-amplitude background noise could contribute to the onset of instability if the system under study is at the verge of stability. Moreover, results obtained indicate conditions for which the decrease of friction force and delayed failure leads to onset of instability, as well the conditions for which the increase of friction force leads to stabilization of sliding.

References

- [1] Davis, R.O. (1992) Modelling stability and surging in accumulation slides. *Eng Geol* **33**: 1-9.
- [2] Morales, J. E. M., James, G., Tonnelier, A. (2017) Travelling waves in a spring-block chain sliding down a slope. *Phys Rev E* **96**: 012227.
- [3] Bashkirtseva, I., Ryashko, L., Schurz, H. (2009) Analysis of noise-induced transitions for Hopf system with additive and multiplicative random disturbances. *Chaos Soliton Fract* **39** 72-82.
- [4] Perc, M., Green, A.K., Jane Dixon, C., Marhl, M. (2008) Establishing the stochastic nature of intracellular calcium oscillations from experimental data. *Biophys Chem* **132**: 33-38.

A replacement model for nonlinear dynamics of electro-active liquid crystal coatings

A. Amiri^{* **}, B. Caasenbrood^{*}, D. Liu^{**}, N. van de Wouw^{*}, I. Lopez Arteaga^{*}

^{*}Department of Mechanical Engineering, Eindhoven University of Technology, Eindhoven, Netherlands

^{**}Institute for Complex Molecular Systems, Eindhoven University of Technology, 5600 MB Eindhoven, Netherlands

Abstract. A replacement lumped-parameter model is proposed to simulate the key nonlinear dynamics of electro-responsive liquid crystal polymer networks (LCNs). LCN coatings are responsive material, which have a great potential to be integrated in functional surfaces. However, due to their complex molecular dynamics, low-order dynamic models that can describe and predict their dynamic behavior accurately, are scarce. In light of this research gap, we develop an electric circuit analogy, which in its simplest form, can capture the nonlinear phenomenon of transforming a high frequency input voltage to a relatively slow increase of height in LCN. The comparison of the simulation results and experimental data shows that the nonlinear dynamics of this height increase as a function of input frequency and voltage are captured well by our model. This model allows for the accurate design and prediction of a predefined deformation pattern in LCNs, which is vital for integrating them in application devices.

Introduction

Fabricating responsive surfaces that can generate dynamic deformations in response to remote stimuli is one of the core studies for development of smart surfaces and displays [1]. Electro-responsive LCN coatings are known as one of the great candidates in this field, which have interesting potential for generating various surface patterns [2]. In addition, the feasibility of integrating these smart surfaces in functional devices relies strongly on obtaining an accurate controlled response. However, due to the complex molecular dynamics of the surface deformation in LCN coatings, the low-order dynamic models that can accurately describe their nonlinear responsiveness based on the input parameters (stimuli) are quite scarce. Such low-order models are required for designing controllers, which is a preliminary step for integrating these material in application devices to obtain quantified and precise desired surface deformation.

Results and Discussion

According to the experimental data, when the AC voltage $V(t) = V_0 \sin(2\pi ft)$ is active with frequency f and amplitude V_0 , a dynamic free volume is generated, leading to a nonlinear gradual increase of $h(t)$. Upon turning off the AC voltage, the surface will relax back to its initial state $h(0)$ (Figure 1(a)). Here, we distinguish two nonlinear characteristics of LCN actuation. Firstly, a high-frequency, 900 kHz AC voltage input leads to a relatively slow increase of $h(t)$, in the order of tens of seconds, until a quasi-equilibrium level is reached (Figure 1(b)). Secondly, the quasi-equilibrium level of LCN height increases nonlinearly with an exponential shape, by increasing the input voltage amplitude V_0 (Figure 1(c)). According to these observations, we develop a replacement model in the simplest form of an electric circuit, which is composed of constant and variable resistors (R), capacitors (C), diode (D) and an input signal source ($V(t)$), as shown in Figure 1(d). By incorporating the nonlinear diode component and variable resistors in our model, the frequency-related and amplitude-related nonlinear characteristics of LCN dynamics are captured and simulated, as illustrated in Figure 1(e-f). Our hybrid approach of modelling, which partially connects to the dielectric and physical properties of LCN, suggests an unconventional perspective on the modelling of the macro-scale dynamics of LCN coatings.

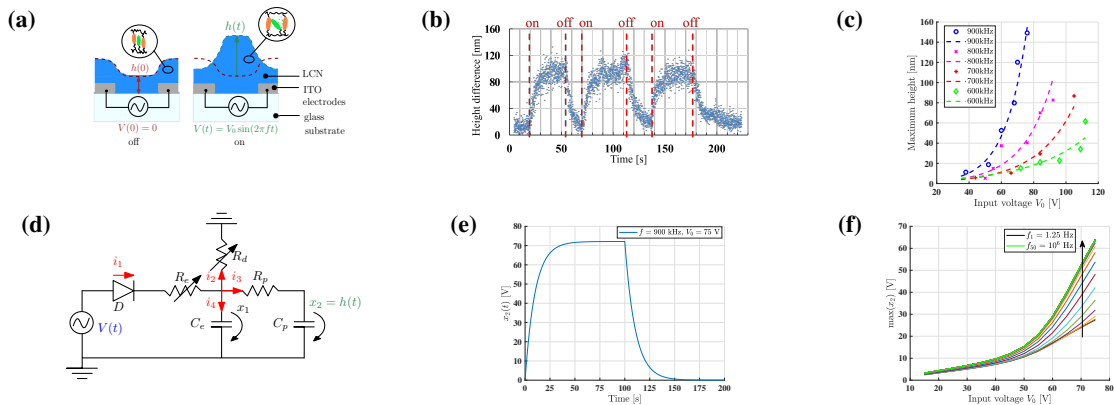


Figure 1: (a) Schematic of LCN actuation. (b) 3 cycles of LCN response at $f = 900$ kHz, $V_0 = 75$ V. (c) Nonlinear response over V_0 . (d) Schematic of the model. (e) and (f) are the simulation results of model in (c).

References

- [1] Liu D., Tito N., Broer D. (2017) Protruding organic surfaces triggered by in-plane electric fields. *Nat. Commun.* **8**:1526.
- [2] Feng W., Broer D., Liu D. (2018) Oscillating Chiral-Nematic Fingerprints Wipe Away Dust. *Adv. Mater.* **30**:1704970.

A new methodology for nonlinear analysis of magneto-rheological elastomers behavior under large amplitude oscillatory axial (LAOA) loadings

Hossein Vatandoost, **Ramin Sedaghati** and Subhash Rakheja

Department of Mechanical, Industrial and Aerospace Engineering, Concordia University, Montreal, QC, CANADA

Abstract. The aim of present paper is to develop a methodology to quantify nonlinear response of magneto-rheological elastomers (MREs) under LAOA loadings using Chebyshev polynomials of the first kind. This permitted determination of the compression and tension elastic moduli at the minimum, zero, and maximum strain, as alternatives to equivalent linear first harmonic moduli extracted using Fourier transform. The proposed local measures can provide the interpretation of inter- and intra-cycles nonlinearities without observing the stress-strain hysteresis response of MREs under LAOA loadings.

Introduction

Composed of magnetically responsive particles embedded within a non-magnetic soft polymeric medium, magneto-rheological (MR) elastomers (MREs) are multifunctional field-responsive smart materials, whose mechanical properties (e.g., stiffness and damping) can be adjusted on-demand via application of external magnetic field [1]. The shear mode characterization of viscoelastic materials, such as MREs under large amplitude oscillatory shear (LAOS) loadings, has been well established [2]. Ewoldt et al. [3] provided a novel framework for quantifying the nonlinear properties of viscoelastic materials under LAOS loadings in a unique manner, in which the inter-cycle (i.e., strain softening) and intra-cycle (i.e., strain-stiffening) measures can be effectively predicted before observing the stress-strain characteristics response. The nonlinear identification of viscoelastic materials under LAOA has been rarely investigated. Particularly no study has been conducted on non-linear identification of MREs under large amplitude oscillatory axial (LAOA) loadings. Hence, in this study, the main objective is to provide a new methodology for identifying nonlinear behavior of smart viscoelastic materials under LAOA loadings.

Results and Discussion

An experimental test setup was designed for the purpose of characterization of MREs under LAOA loadings and wide ranges of magnetic field intensities. The experimental method is comprehensively explained in earlier work [1]. The stress-strain responses were analyzed to extract the elastic and viscous stress using the decomposition method based on Chebyshev polynomial functions. Using the developed approach for MREs under LAOA, the elastic and loss moduli of MREs at zero strain along with at the extreme unloading, and loadings cycles were calculated and compared with those bases on Fourier approximation and experiment. Figure 1 presents results for the stress-strain curve based on the proposed superimposed elastic and viscoelastic via Chebyshev polynomials. The results compare the total stress with a linear stress approximation via Fourier series. It is clear that the first harmonic approximation lacks nonlinear stiffening and softening at the end of loading and unloading cycles. Further development of the current investigation would allow realizing the instantaneous/tangent elastic modulus at extreme loadings as functions of the linear elastic modulus.

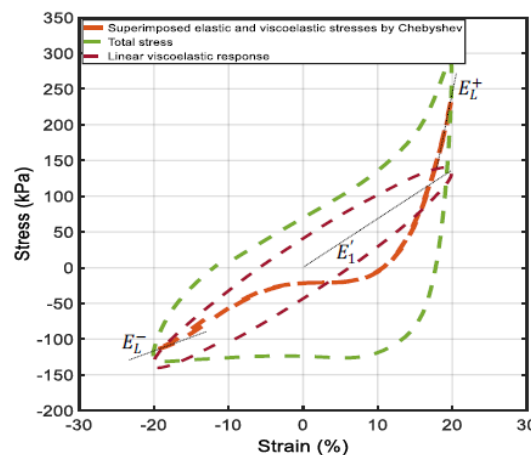


Figure 1: Comparison between linear viscoelastic response by Fourier series (First harmonic mod-uli) and Chebyshev polynomial.

References

- [1] Vatandoost H. et al. (2020) Dynamic characterization of isotropic and anisotropic magnetorheological elastomers in the oscillatory squeeze mode superimposed on large static pre-strain. *Compos B Eng.* 182:107648.
- [2] Hyun K et al. (2011) A review of nonlinear oscillatory shear tests: Analysis and application of large amplitude oscillatory shear (LAOS). *Prog Polym Sci.* 36(12):1697-753.
- [3] Ewoldt RH, Hosoi A, McKinley GH. (2008) New measures for characterizing nonlinear viscoelasticity in large amplitude oscillatory shear. *J. of Rheo.* 52(6):1427-58.

Modeling Asymmetric Hysteresis: Continuous Development using Experimental Data

Jin-Song Pei*, Biagio Carboni** and Walter Lacarbonara***

*University of Oklahoma, Norman OK 73019, USA, ORCID #0000-0002-1042-1859

**Sapienza University of Rome, Rome, Italy, ORCID #0000-0001-6678-8775

***Sapienza University of Rome, Rome, Italy, ORCID #0000-0002-8780-281X

Abstract. Asymmetric hysteresis is tackled using experimental data generated at Sapienza University of Rome. With improved testing apparatus, richer datasets produce more comprehensive views of the asymmetric hysteresis behaviors, making it possible to further advance the proposed Masing model in terms of the Masing rules.

Introduction

The investigated device exhibits asymmetric hysteresis due to coupled geometric nonlinearities and inter-wire frictional dissipation. The testing device comprises two plates connected by two continuous steel wire ropes. The restoring force is acquired by means of a Zwick-Roell testing machine run in displacement control mode. One plate is cyclically moved with displacement histories while the other plate is fixed. A load-cell measures the restoring force provided by the ropes assembly which exhibits an asymmetric response for positive and negative displacements. Sample input and output time histories are given in Fig. 1(a) and (b), respectively.

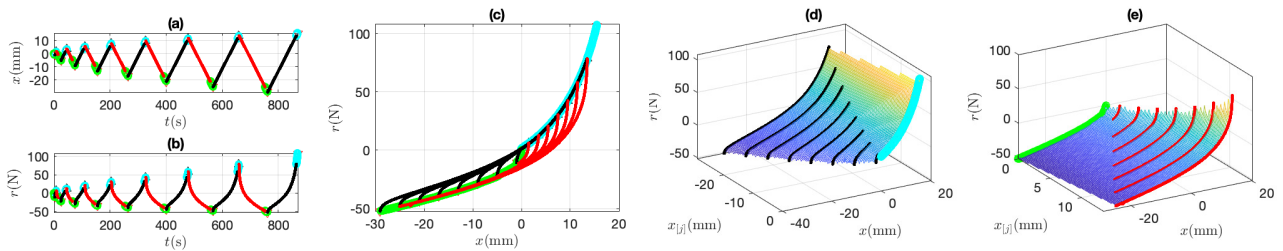


Figure 1: Experimental (a) input and (b) output time histories and (c) corresponding hysteresis loops - using identified reloading and unloading branches in black and red, respectively, and virgin loading and unloading curves in cyan and green, respectively, and (d) and (e) the proposed surfaces regressed from reloading branches and virgin loading curve, and from unloading branches and virgin unloading curve, respectively

The acquired asymmetric hysteretic responses have been studied with various modeling approaches. The number of parameters to be identified can be computationally demanding for the classical Preisach models. The work of [3] shows that the Masing models are Preisach models. As a simpler model than the classical Preisach model, Masing model has been investigated by the authors starting from [5]. In terms of Masing models, an early paper [4] provided the inspiration for later developments of models for softening hysteresis systems, among which the so-called “extended Masing model”, as reviewed in [1], is the starting point for [5] and the current study.

Results and discussion

In the extended Masing model, Masing Rule 1 deals with the relationship between the virgin loading curve and all other reloading and unloading curves, while Masing Rules 2 and 3 address the closure and fate of minor loops relevant to nonlocal memory. Employing Masing Rules 2 and 3, reloading and unloading branches as well as virgin loading curves are identified from experimental data, as illustrated in Fig. 1(a) to (c) using one particular dataset. A direct adoption of Masing Rule 1 is not possible given the asymmetric and hardening features, however the explicit functions as proposed in [5] by extending [2] are further developed in this study; see Fig. 1 (d) and (e) for sample results.

References

- [1] Beck JL, Pei JS (2022) Demonstrating the power of extended masing models for hysteresis through model equivalencies and numerical investigation. *Nonlinear Dynamics* 108(2):827–856
- [2] Jayakumar P (1987) Modeling and identification in structural dynamics. PhD thesis, California Institute of Technology, Pasadena, CA
- [3] Lubarda VA, Sumarac D, Krajcinovic D (1993) Preisach model and hysteretic behaviour of ductile materials. *Eur J Mech A/Solids* 12(4):445–470
- [4] Masing G (1926) Eigenspannungen und verfestigung beim messing. In: *Proceedings of the 2nd International Congress for Applied Mechanics, Zurich, Switzerland*, pp 332–335, in German
- [5] Pei JS, Carboni B, Lacarbonara W (2022) Modeling asymmetric hysteresis inspired and validated by experimental data. In: *Advances in Nonlinear Dynamics*

Preliminary Results on the Simulation of Pressurized Sand Dampers by the Vaiana-Rosati Model

N. Vaiana*, L. Rosati*, X. Palios**, and N. Makris***

* Department of Structures for Engineering and Architecture, University of Naples Federico II, Naples, Italy

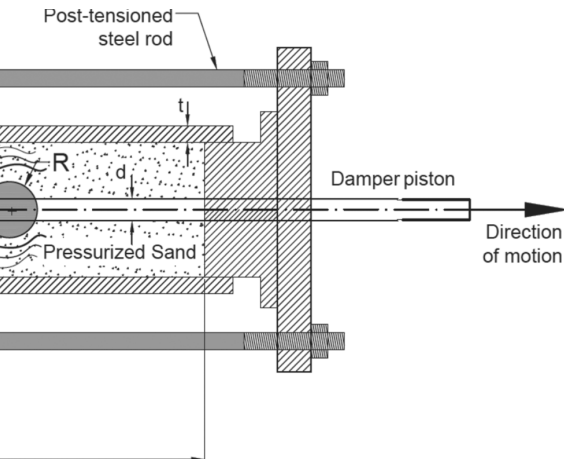
** Department of Civil Engineering, University of Patras, Patras, Greece

*** Department of Civil and Environmental Engineering, Southern Methodist University, Dallas, TX, USA

Abstract. This work briefly illustrates the potentialities of the brand-new Vaiana-Rosati model of hysteresis to reproduce the symmetric and pinched hysteresis loops characterizing the rate-independent hysteretic behavior exhibited by a pressurized sand damper. It represents a novel promising energy dissipation device to be adopted for structural vibration control.

Introduction

Passive energy dissipation devices typically exhibit a complex hysteretic behavior that is referred to as rate-independent (rate-dependent) if the device restoring force depends on the device displacement (velocity). Makris et al. [1] have recently proposed an innovative, low-cost, eco-friendly, long-stroke, fail-safe rate-independent hysteretic device denominated *Pressurized Sand Damper*. The main aim of this work is to show that a recently formulated hysteresis model [2], denominated *Vaiana-Rosati Model*, is sufficiently general to simulate the complex hysteresis loops typically exhibited by such a novel device.



Results and Discussion

Figure 1a shows the device that has been tested at the Structures Laboratory of the University of Naples, consisting of a steel cylinder, having a diameter of 18.9 cm and length of 62 cm, adopting four external post-tensioned steel rods. A sphere with radius of 2 cm, is able to move along the damper axial direction. Figure 1b shows the experimental hysteretic behavior exhibited by the above-described device when subjected to a sinusoidal displacement having amplitude of 40 mm and frequency of 0.1 Hz under the action of a constant pressure. The experimentally derived symmetric and pinched hysteresis loops demonstrate a large amount of mechanical energy dissipation. Figure 1c shows the simulated force-displacement hysteresis loops characterizing the response of the device using the Vaiana-Rosati Model (VRM) [2].

In the literature, the VRM offers some advantages such as: (i) evaluation of the energy dissipated from the hysteresis loops, (ii) simulation of complex hysteresis loop shapes, (iii) modeling of the loading and unloading phases by employing two different sets of parameters; (iv) adoption of parameters having a clear theoretical and/or experimental interpretation, (v) straightforward computer implementation.

Figure 1c illustrates a comparison between the experimental hysteresis loops and those simulated by using the VRM. The very good agreement between such results demonstrates the capability of the VRM to accurately predict the experimental hysteresis loops exhibited by the tested device.

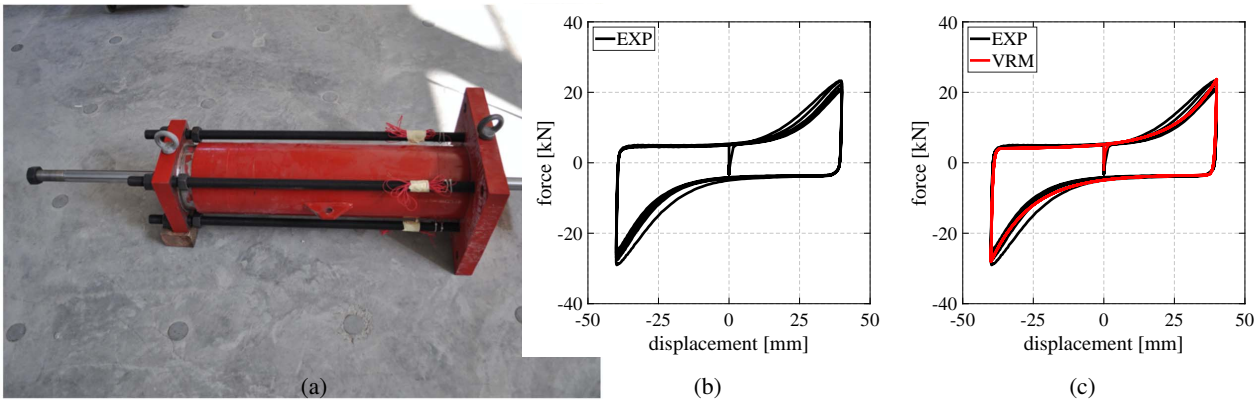


Figure 1: Tested pressured sand damper: picture (a), experimental (b) and simulated (c) force-displacement hysteresis loops.

References

- [1] Makris N., Palios X., Moghimi G., Bousias S. (2021) Pressurized Sand Damper for Earthquake and Wind Engineering: Design, Testing, and Characterization. *J. Eng. Mech.* 147(4):04021014.
- [2] Vaiana N., Rosati L. (2023) Classification and Unified Phenomenological Modeling of Complex Uniaxial Rate-Independent Hysteretic Responses. *Mech. Syst. Signal Pr.* 182:105339.



Differential Formulation of the Vaiana-Rosati Model

Nicolò Vaiana* and Luciano Rosati *

*Department of Structures for Engineering and Architecture, University of Naples Federico II, Napoli, Italy

Abstract. We present a differential formulation of a novel uniaxial rate-independent hysteretic model, denominated Vaiana-Rosati Model, that is capable of simulating complex generalized force-displacement hysteresis loops, ranging from the asymmetric, pinched, S-shaped, flag-shaped ones to those obtained by their arbitrary combination. Such a formulation drastically simplify the model implementation when the nonlinear equilibrium equations of a generic hysteretic mechanical system are expressed in the state-space form.

Introduction

In the field of nonlinear dynamics, the second-order nonlinear Ordinary Differential Equations (ODEs), governing the complex response of hysteretic mechanical systems, are typically reformulated as a set of first-order nonlinear ODEs by introducing the state-space variables [1]. Consequently, hysteretic models are classically expressed in such a way that the output variable is evaluated by solving a differential equation that can be directly added to the set of first-order nonlinear ODEs to be numerically solved.

Conversely, more recent hysteretic models, such as the Vaiana-Rosati Model (VRM)[2], allow for the evaluation of the output variable by means of closed-form expressions having algebraic or transcendental nature.

Vaiana-Rosati Model

The VRM offers a series of advantages over other hysteretic models available in the literature. Indeed, it: i) allows for the evaluation of the generalized force in closed form thus requiring a reduced computational effort, ii) is capable of reproducing different types of complex hysteresis loops, as illustrated in Figure 1, iii) is based on two set of eight parameters that allow one to manage, respectively, the loading and unloading phases, iv) adopts parameters describing specific theoretical and/or experimental properties of the hysteresis loops thus simplifying the identification procedure, and v) can be easily implemented in a computer program.

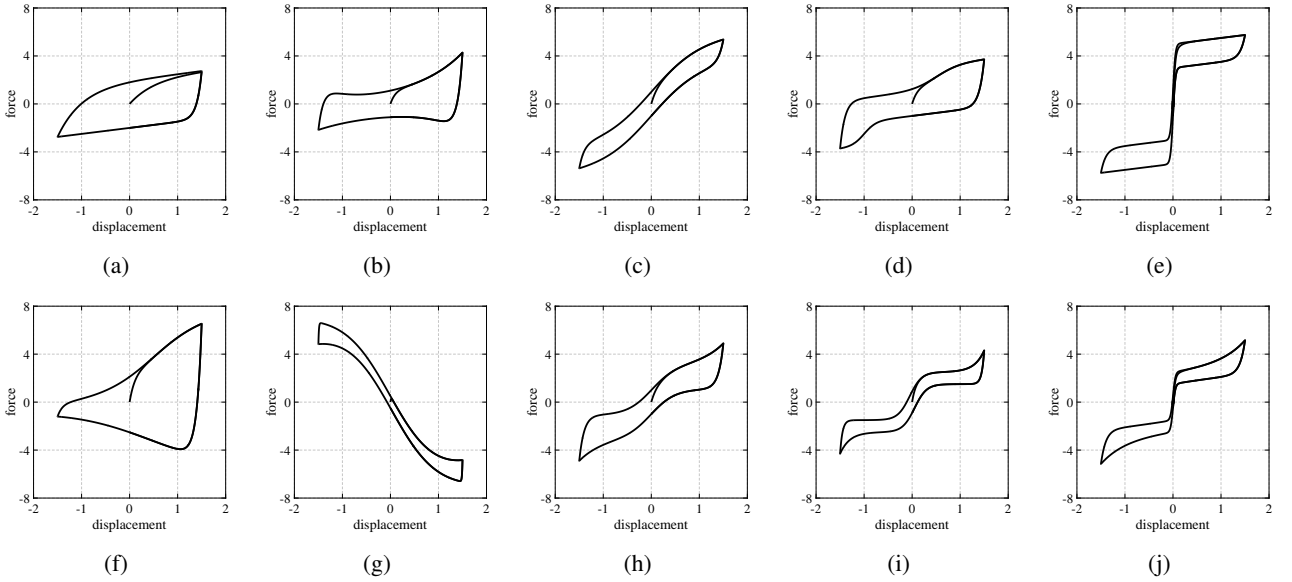


Figure 1: Some types of hysteresis loops simulated by the VRM.

VRM Differential Formulation

In order to foster the use of the VRM in nonlinear dynamics, we present the related differential formulation for which the generalized force f , representing the model output variable, can be evaluated by solving the following first-order ODE:

$$\dot{f}(u, \dot{u}) = [af(u) + b(u)] \dot{u}, \quad (1)$$

where the overdot denotes differentiation with respect to time t , u (\dot{u}) represents the generalized displacement (velocity), a is constant function, whereas $b(u)$ is a nonlinear function of u .

References

- [1] Formica G., Vaiana N., Rosati L., Lacarbonara W. (2021) Pathfollowing of High-Dimensional Hysteretic Systems Under Periodic Forcing. *Nonlinear Dyn.* **103**:3515–3528.
- [2] Vaiana N., Rosati L. (2023) Classification and Unified Phenomenological Modeling of Complex Uniaxial Rate-Independent Hysteretic Responses. *Mech. Syst. Signal Pr.* **182**:109539.

Inverted resonance capture cascade from low to high modal frequency

Kevin Dekemele* and Giuseppe Habib **

*Department of Electromechanical, Systems and Metal Engineering, Ghent University, Ghent, Belgium

**MTA-BME Lendület "Momentum" Global Dynamics Research Group, Department of Applied Mechanics, Budapest University of Technology and Economics, Budapest, Hungary

Abstract. In shock-loaded multi-degree-of-freedom (MDOF) mechanical host systems featuring a nonlinear energy sink (NES), resonance capture cascade (RCC) occurs. This is the sequential transfer and dissipation of modal vibrations from high to low modal frequency from the host system to the NES. The sequence of frequency transfer, from high to low frequency, is caused by the hardening polynomial restoring force that is typically considered in the nonlinear vibration absorber. In this abstract, it is shown that for softening restoring force, the opposite sequence occurs, i.e. from low to high frequency. By applying a multi-dimensional harmonic balancing for all modal vibrations concurrently, slow invariant manifolds are obtained where modal interactions determine the order of modal vibration transfer.

Introduction

Nonlinear vibration absorbers or nonlinear energy sinks (NESs) with a nonlinear restoring force have a variable natural frequency that depends on its amplitude. This property can be exploited to obtain a more broadband absorber under harmonic loading as opposed to linear tuned-mass-dampers (TMD), or to induce resonance capture cascade (RCC) under transient loading to dissipate several frequencies. An MDOF host system, e. g. the 2DOF system in Figure 1a, under shock-loading will vibrate according to its vibration modes. When an NES with a hardening stiffness is attached, the vibrations of the host system transfer and dissipate sequentially from high to low frequency. This phenomenon was first shown in [1], and other the studies existing in literature adopt the hardening stiffness [2, 3]. So far, RCC with other stiffness characteristics such as softening or saturating, see Figure 1b, have not been investigated.

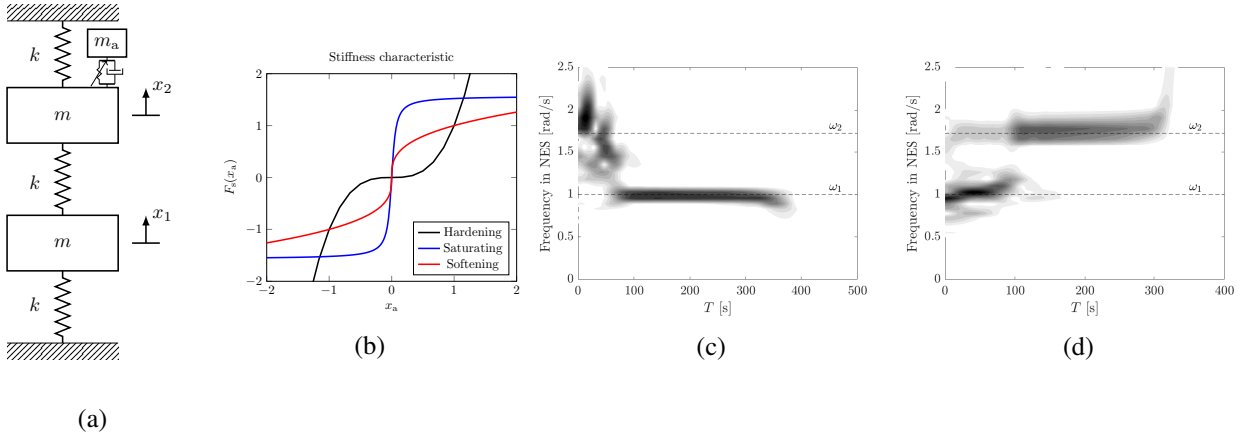


Figure 1: A 2DOF host system with NES on the top mass (a), several nonlinear stiffnesses (b), wavelet transform of NES with hardening stiffness (c) and softening stiffness (d). The RCC and inverted RCC is clearly visible from the wavelet transforms, where the NES sequentially dissipates the modal frequencies ω_1 and ω_2 .

Results and discussion

The 2DOF host system in Figure 1a, with an attached NES, is considered. A classical hardening NES with restoring force x_a^3 , and a softening one with a softening and saturating restoring force $\arctan(20x_a)$ are investigated. In the two cases, wavelet transforms of the NES displacement in free vibrations exhibit opposite behaviors, Figure 1c and Figure 1d for the hardening and softening restoring force, respectively. For a hardening NES, the NES vibrates first with the highest modal frequency (ω_2), and then with the lowest one (ω_1). This corresponds to a typical RCC. The opposite happens for a softening NES, where a so-called inverted RCC takes place. Namely, the NES first interact with the first lower mode, and then higher one.

References

- [1] Vakakis A.F., Manevitch L.I., Gendelman O. and Bergman L. (2003) Dynamics of linear discrete systems connected to local, essentially non-linear attachments. *J. Sound Vib.* **264**(3):559-577.
- [2] Dekemele K., De Keyser R. and Loccufer M. (2018) Performance measures for targeted energy transfer and resonance capture cascading in nonlinear energy sinks. *Nonlinear Dyn.* **93**(2):259-284.
- [3] Habib G. and Romeo P. (2021) Tracking modal interactions in nonlinear energy sink dynamics via high-dimensional invariant manifold. *Nonlinear Dyn.* **103**(4):3187-3208.

Shape Optimization of Curved Mechanical Beams for Internal Resonance Enhancement

Sahar Rosenberg* and Oriel Shoshani*

*Ben-Gurion University of the Negev, Be'er-Sheva 84105, Israel

Abstract. In this study, we develop a genetic algorithm-based optimization procedure for coupling enhancement of nonlinearly interacting modes in curved beams. The coupling enhancement leads to more robust internal resonances (IRs) between the interacting modes and can serve as a means to promote directed or targeted energy transfers between the modes. This study aims to obtain the optimal shape function of a curved beam for a specific IR between a pair of vibrational modes. We consider an initial configuration of a curved beam that yields an approximately rational ratio between two eigenfrequencies of the beam and use an iterative genetic algorithm scheme to perturb the shape of the beam and find the optimal curved configuration of the beam that maximizes the coupling between the corresponding modes.

Introduction

IRs are manifested by nonlinear interactions and energy exchange between vibrational modes that arise when modal frequencies of a given structure are (exactly or nearly) rationally related, e.g., $\omega_1/\omega_2 \approx n/m$, where n and m are integers, is the so-called n -to- m IR [1]. The nonlinear coupling between the modes depends on the structure geometry, material, boundary conditions, and transduction schemes. This study focuses only on the structure geometry and how it can be optimized to enhance nonlinear mode coupling and promote IRs.

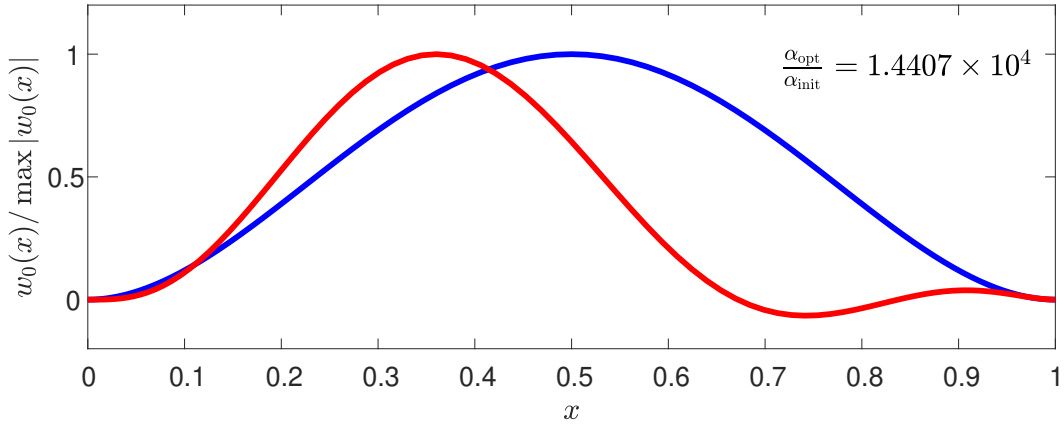


Figure 1: Shape optimization of $w_0(x)$, the initial shape function of the beam, for 1-to-3 IR. Comparison between the normalized initial bell-shaped beam (in blue) and the normalized optimal shape of the beam after 1500 generations of a population of 100 individuals (in red). The 1-to-3 IR stems from a single-term coupling potential of the form $U(x_1, x_2) = \alpha x_1^3 x_2$, where the optimal coupling coefficient α_{opt} is more than three orders of magnitude larger than the initial coupling coefficient α_{init} and the ratio between the eigenfrequencies is $\omega_2/\omega_1 \approx 3.01$.

Results and discussion

We consider IRs that stem from a single-term coupling potential (to leading order) of the form $U(x_1, x_2) = \alpha x_1^m x_2^n$, i.e., the conservative sub-system of the two interacting modes is given by

$$\ddot{x}_1 + \omega_1^2 x_1 + f_1(x_1) = -\partial U / \partial x_1, \quad \ddot{x}_2 + \omega_2^2 x_2 + f_2(x_2) = -\partial U / \partial x_2,$$

where $f_{1,2}$ represent single-mode nonlinearities such as Duffing nonlinearity. We apply a genetic algorithm [2] to find the optimal shape of the curved beam that yields an IR condition with the highest (and lowest) coupling term. The genetic algorithm uses the initial shape of the beam to create a population (group of shape functions) of other solutions in its vicinity. After performing a Galerkin projection onto the first two modes of the initial beam, the algorithm calculates the coupling coefficient α for each individual (certain shape function) of the population (given the constraint $|\omega_1/\omega_2 - n/m| < \epsilon$). The algorithm creates the next generation of the population using the fittest solutions of the last generation by: (i) selection, where the fittest solutions survive for the next generation, (ii) crossover, where every two solutions are being used to create a new solution, and (iii) mutation, where some solutions are changed randomly. The algorithm converged to an optimal shape function for the case of 1-to-3 IR after 1500 generations as shown in Fig. 1. Other ratios of $\alpha_{opt}/\alpha_{int}$, and initial and final beam configurations for the cases of 2-to-1 and 3-to-1 IRs will be given in the presentation.

References

- [1] Nayfeh, Ali Hasan. (2000) Nonlinear interactions: analytical, computational, and experimental methods. New York: Wiley.
- [2] Woon, S., Querin, O. Steven, G. Structural application of a shape optimization method based on a genetic algorithm. *Struct Multidisc Optim* 22:57–64 (2001).

On the non-trivial solutions and their stability in a two-degree-of-freedom Mathieu-Duffing system

Ahmed A. Barakat^{*,**}, Eva M. Weig^{*} and Peter Hagedorn^{**}

^{*}Chair of Nano and Quantum Sensors, Technical University of Munich, Munich, Germany.

^{**}Dynamics and Vibrations Group, Technical University of Darmstadt, Darmstadt, Germany.

Abstract. The Mathieu-Duffing equation represents a basic form for a parametrically excited system with cubic nonlinearities. In multi-degree-of-freedom systems, other interesting instability conditions take place and considered in this work. Accordingly, the non-trivial solutions were obtained, especially when the trivial solution is unstable. At resonant frequencies a bifurcation analysis was carried out using the multiple scales method, followed by investigating the effect of an asynchronous parametric excitation. Since various micro- and nano-systems include cubic non-linearities and subjected to parametric excitation, this work should be of relevant importance.

Introduction

Over the decades, the solutions of the nonlinear Mathieu equation were studied for stability. In a nonlinear system a parametric resonance could lead to stationary non-trivial solutions and limit cycles, in which the amplitudes are governed by the system's nonlinearities [1]. This happens to be of great interest to systems seeking high amplitudes and thereby possible amplification of input signals. Thus, parametric resonances and amplification were automatically exploited to increase the sensitivity of micro- and nano-sensors [2]. Being more common than others in micro- and nano-systems, a special concern is given to cubic nonlinearities. In this case, the equation is referred to as the Mathieu-Duffing equation [1]. However, a lesser effort was given to corresponding multi-degree-of-freedom (M-DoF) systems, in which the added degrees of freedom introduce other resonant frequencies. In addition, controlling the phase of the excitation terms could lead to a broadband parametric amplification, which was found to be useful in microsystems [3].

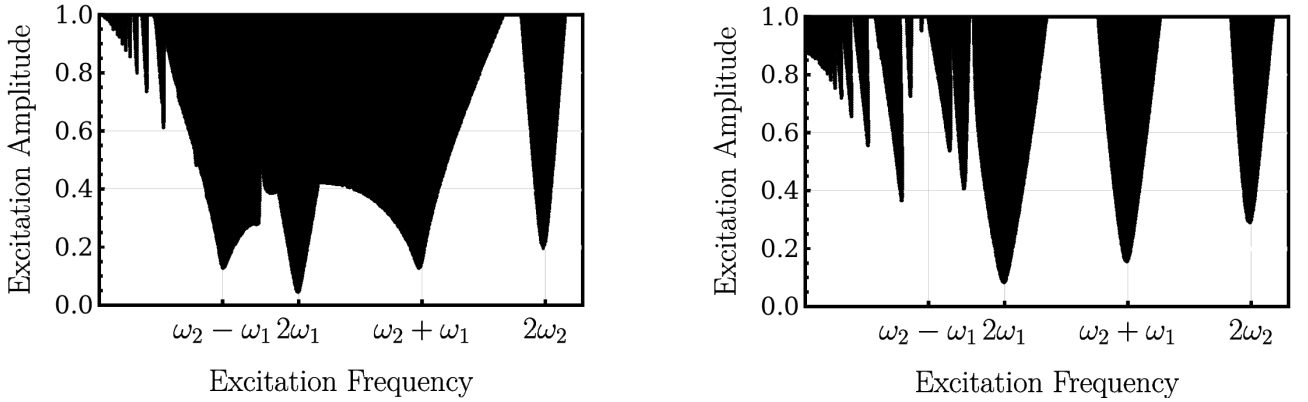


Figure 1: Stability chart: with (left) and without (right) phase-shifted excitation. $\omega_{1,2}$: natural frequencies.

Analysis and results

The trivial solution of the system was studied for stability using Floquet theory and the Lyapunov characteristic exponents were deduced. The resulting stability chart shows the existence of a broadband instability effect under phase-shifted excitation (see Fig. 1, black means unstable). The non-trivial solutions were then obtained in the general excitation case, and especially when the trivial solution turns to be unstable. At resonant frequencies a bifurcation analysis was carried out using the multiple scales method. At the primary resonant frequency the coupling remained ineffective, and a stable limit cycle is detected. However, by controlling the linear damping as a bifurcation parameter, non-trivial stationary solutions were found in a limited domain, exhibiting isolated solutions if the excitation frequency is detuned. By enforcing a one-to-one internal resonance, the energy could be transferred between both degrees of freedom. This transfer of energy occurs also at combination resonant frequencies. Moreover, introducing a phase-shift in the parametric excitation coupling leads to limit cycles at the difference combination frequency. The observed non-linear effects, therefore, show a notable influence on the dynamics, which could be worthwhile for micro and nano-systems using the proposed excitation method.

References

- [1] Kovacic I., Rand R., Sah S.M. (2018) Mathieu's Equation and Its Generalizations: Overview of Stability Charts and Their Features. *Appl Mech Rev* **70**.
- [2] Rugar D., Grütter P. (1991) Mechanical Parametric Amplification and Thermomechanical Noise Squeezing. *Phys Rev Lett* **67**:699.
- [3] Barakat A.A., Hagedorn P. (2021) Broadband Parametric Amplification for Micro-Ring Gyroscopes. *Sens Actuator A Phys* **332**:113130.

Nonlinear interactions of widely spaced modes

Oriel Shoshani* and Steven W. Shaw**

*Department of Mechanical Engineering, Ben-Gurion University of the Negev, Israel

**Department of Mechanical and Civil Engineering, Florida Institute of Technology, FL, USA

Abstract. Nonlinear interactions of modes with vastly different eigenfrequencies (VDE) are ubiquitous and occur in various fields of engineering and physics. We show that the complex dynamics of these interactions can be distilled into a single generic form, namely, the Stuart-Landau oscillator. We use this model to study frequency combs that arise from injection locking and frequency pulling of a driven low-frequency (LF) mode that interacts with a driven blue-detuned high-frequency (HF) mode. Our analysis shows that the frequency combs are tunable around both the high and low carrier frequencies. The novelty of our analysis lies in the minimalistic conceptual view that it offers, including an analogy between these complex interactions and a simple mechanical system model and a connection with the motion of an overdamped particle in a tilted washboard potential. The results are applicable to a wide class of systems and suggest means of generating tunable frequency combs.

Introduction

We consider a model of the form

$$\ddot{q}_0 + 2\Gamma_0\dot{q}_0 + \omega_0^2 q_0 + \alpha q_1^2 = F_0 \cos(\omega_{F_0} t), \quad \ddot{q}_1 + 2\Gamma_1\dot{q}_1 + \omega_1^2 q_1 + 2\alpha q_0 q_1 = F_1 \cos(\omega_{F_1} t), \quad (1)$$

where $\omega_0 \ll \omega_1$. Eq. (1) can be used to model the dynamics of widely spaced modes in mechanical macrostructures [1]; cavity optomechanics and plasmomechanics, where the interactions are between HF optical modes and the LF mechanical modes; interactions between HF nano- and LF micro-mechanical modes; certain classes of aeroelastic instabilities, such as stall flutter and transverse galloping, where these interactions are between HF vortex modes of the turbulent wake (the so-called Kármán vortex street) and the LF modes of the elastic structure; and many other systems.

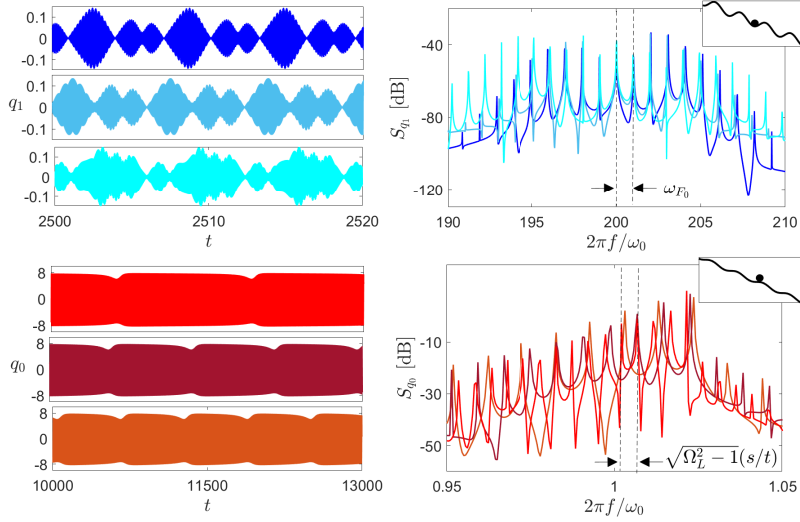


Figure 1: Injection locking (top panel) and pulling (bottom panel) of the LF mode.

Results and Discussion

The HF modes typically decay faster than the LF modes. Thus, we assume that $\Gamma_1 \gg \Gamma_0$, and therefore, q_1 adiabatically tracks q_0 when $t \gg \Gamma_1^{-1}$. In this case, the complex-amplitude equation of the LF mode obeys the Stuart–Landau oscillator $\dot{A}_0 = (\sigma - l|A_0|^2)A_0 - F_0/(4\omega_{F_0})$. Using polar notation for the complex amplitude of the LF mode $A_0 = -a_0^{[\varphi_0 + \arg(\ell)]}/2$, we find that under certain conditions (which will be specified in the presentation), the phase dynamics are governed by the Adler equation $d\varphi_0/ds = \Omega_L - \sin \varphi_0$, where $s = [F_0|\ell|/(4\omega_{F_0}\sqrt{\Re\{\sigma\}\Re\{\ell\}})]t$ is a non-dimensional time and $\Omega_L = 4\omega_{F_0}\Im\{\ell^*\sigma\}\sqrt{\Re\{\sigma\}\Re\{\ell\}}/(F_0|\ell|)$ is the non-dimensional one-sided frequency-locking range (i.e., the overall locking range of the LF mode is $\pm\Omega_L$ around $\omega_0 t/s$). The phase dynamics of φ_0 determines the conditions for injection locking and pulling (Fig. 1). A constant phase $\dot{\varphi}_0 = 0$ (inset of the right top panel) of the injection-locked LF mode generates periodic modulations in the HF mode (top left panel), which corresponds to a frequency comb around ω_1 with a spacing of ω_{F_0} in the power spectral density of q_1 (top right panel). An unlocked phase $\dot{\varphi}_0 \neq 0$ (inset of the right bottom panel) of the injection-pulled LF mode is periodically modulated in a highly non-uniform rate (bottom left panel), which corresponds to a frequency comb around ω_0 with a spacing of $\sqrt{\Omega_L^2 - 1}(s/t)$ in the power spectral density of q_0 (bottom right panel).

References

- [1] A. H. Nayfeh and D. T. Mook, (1995) *Energy Transfer from High-Frequency to Low-Frequency Modes in Structures*, J. Vib. Acoust., 117, 186-195

A hysteretic vibration absorber for the mitigation of a flexible structure response

Paolo Casini* and Fabrizio Vestroni*

*Department of Structural and Geotechnical Engineering, Sapienza University of Rome, Rome, Italy

Abstract. A hysteretic device is proposed to reduce the vibration of a structure. It offers two advantageous aspects: First it naturally increases the dissipative characteristics of the system. Second, more importantly, the strong nonlinearity of hysteresis produces those nonlinear phenomena which give beneficial effects from the transfer of energy from the directly excited mode to other modes of the structure. A real 2DOF structure is used to demonstrate the effectiveness of the proposal.

Introduction

The trend of designing increasingly lean structures emphasizes the importance of dynamic responses and the need to reduce these effects. A standard technique to lower structural vibration is to use elements capable of dissipating energy. The proposal to add a hysteretic element makes it possible to combine the twofold aim of increasing the structure dissipation characteristics and of introducing a nonlinearity which can potentially facilitate the spreading of input energy among the system modes. After the fundamental work by Den Hartog [1] devoted to the vibration mitigation of linear structures, several papers demonstrated the beneficial effects of nonlinear devices connected to structures [2]. Hysteresis characterizes the mechanical behaviour of various materials and elements. With respect to viscoelastic tuned mass damper (TMD), a hysteretic vibration absorber (HVA) has the advantage that the restoring force combines the elastic and dissipation characteristics without the need of a damper. Furthermore, the multivalued constitutive law and the notable dependence of stiffness and damping properties on the oscillation amplitude include this behaviour among those that are strongly nonlinear. This triggers a large variety of nonlinear phenomena: in particular, the modification of frequencies eases the occurring of internal resonance conditions where modal interactions are responsible for the transfer of energy from the directly excited mode towards not directly excited modes. These phenomena are the topic of previous papers [3]; here, focusing on a specific structural application, a hysteretic device described by the Bouc-Wen model is used in vibration reduction of a two degree-of-freedom system.

Results and discussion

The case of internal resonance 1:1 which resembles the Den Hartog proposal is first dealt with. Other than being a simpler solution, its effectiveness is similar to that of viscoelastic TMD, but only in a definite excitation range, due to the dependence of its characteristics on the oscillation amplitude. Moreover, in this case no typical phenomena of nonlinear dynamics are activated. Different is the case of internal resonance conditions $n:1$, with $n > 1$ which promotes the occurrence of a rich variety of nonlinear phenomena. Among them, the occurrence of a novel mode around the first resonance through a bifurcation mechanism involves the second mode in the response, with a beneficial effect on the vibration amplitude of the directly excited first mode. In Fig. 1a around the first resonance, for a certain value of excitation, two peaks appear in the FRC: the reduction of the response due to the addition of the HVA (red curve) with respect to the uncontrolled case (NC) is evident; this advantageous behaviour still remains in a large range of frequency and intensity of excitation (Fig. 1b). Several other internal resonance conditions could be investigated; this application demonstrates the efficiency of introducing a hysteretic element for the passive control of structural vibrations.

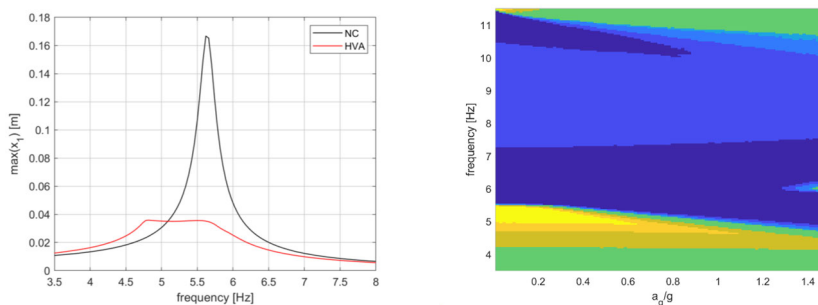


Figure 1: TC4 oscillator close to a (2:1) internal resonance ($\omega_{2A}/\omega_{1A} \approx 2.15$, $\omega_{2B}/\omega_{1B} \approx 1.46$): (a) FRCs of oscillation amplitudes of mass m_1 for non-controlled (NC) and HVA responses at optimal excitation $a_g = 0.83g$ (red curve); (b) Color map comparing the maximum displacements of NC and HVA oscillators (cold colors reveal amplitude reductions)

References

- [1] Den Hartog, J.P. (1934) Mechanical Vibrations; McGraw-Hill: New York, NY, USA.
- [2] Vakakis, A.F. (2017) Intentional utilization of strong nonlinearity in structural dynamics. *Proc. Eng.*, **199**, 70–77.
- [3] Casini, P.; Vestroni, F. (2022) The role of the hysteretic restoring force on modal interactions in nonlinear dynamics. *Int. J. Non-Linear Mech.*, **143**, 104029.

On the role of wave resonances in the nonlinear dynamics of discrete systems

Tiziana Comito*, Miguel D. Bustamante*

* School of Mathematics and Statistics, University College Dublin, Belfield, Dublin 4

Abstract. Nonlinear systems are driven by the interplay between modes, intimately related to whether combinations in wavenumbers and akin in frequency are allowed to interact. Our study investigates the role played by resonances in two selected models: FPUT and Metamaterials, combining dynamical-systems methods with high-accuracy numerical simulations. In each case, we establish a leading order of interactions that dominate the behaviour of the system.

The Fermi-Pasta-Ulam-Tsingou (FPUT) chain was a pioneer work in discrete modellization. The original problem considered a one-dimensional chain made out of N identical masses connected by nonlinear springs with fixed boundary conditions (BCs). Against the expectations, the system seemed not to thermalize: the chain displayed the phenomenon of recurrence, which led to the discovery of solitons and integrable systems. Later it was shown that thermalization does occur over very long times. Our work looks at the $\alpha + \beta$ FPUT system from a fresh viewpoint: allowing for periodic BCs gives rise to several non-trivial resonances, unlike the case of fixed BCs. For our system, it is known that 3-wave resonances do not exist, whereas 4-wave resonances exist but are completely integrable. Thus, one must look at the next interaction orders, namely 5-wave and 6-wave resonances, in order to get energy mixing across modes. A second theme concerns the analytical and numerical treatment of a model of metamaterials based on the elementary FPUT chain coupled with resonators. Metamaterials are artificially engineered geometrical structures that show preference for certain wave excitations, thus encountering the increasing demands for specific features that traditional materials cannot satisfy. The model has a far richer resonant manifold than FPUT. For instance, there is a region of parameter space where 3-wave resonances exist.

Results and discussion

We identified all FPUT resonant quintets and sextuplets analytically [1]. The current work focuses on the dynamical effects of these resonances, using numerical simulations backed with analytical normal-form transformations [2]. Preliminary results (Fig. (a)–(b)) confirm the relevance of quintets, in scenarios ranging from quasi-integrable quintets to hyperchaos due to interacting quintets. We show numerically that these interactions dominate important aspects: the evolution towards thermalization, the distribution of chaotic attractors, and the distinction between fixed and periodic BCs regarding integrability. In the case of metamaterials we show that resonant triads are responsible for the complex dynamics that takes the system beyond integrable quartets, leading eventually to ergodic behaviour and energy equipartition (Fig. (c)–(d)).

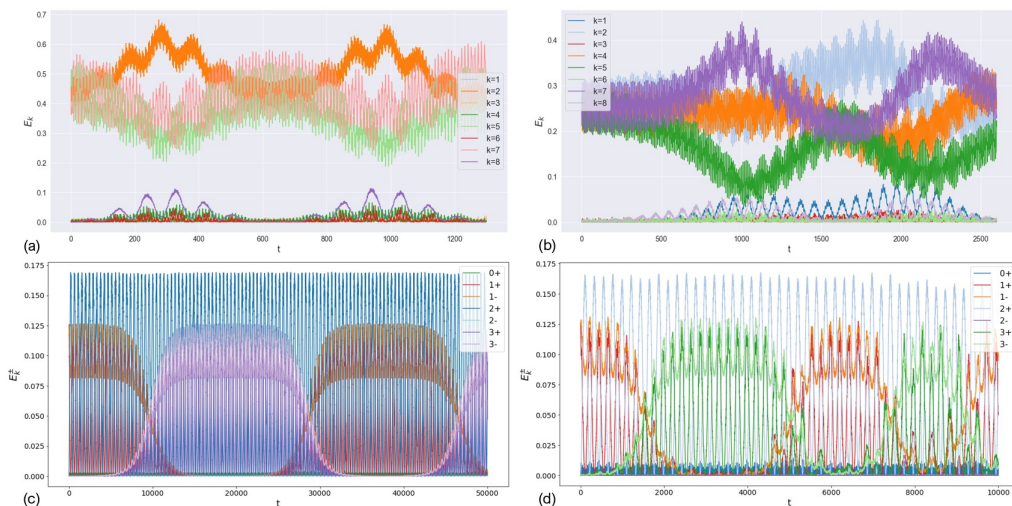


Figure 1: Time evolution of the energy in each normal mode in a series of high-accuracy simulations. FPUT ($N = 9$) shows a quasi-integrable resonant quintet (a) and a chaotic regime of two interacting resonant quintets (b). Metamaterial model ($N = 4$) shows an off-resonance regime (c) versus a chaotic resonant triad regime (d).

References

- [1] Bustamante M. D., Hutchinson K., Lvov Y. V., Onorato M. (2019) Exact discrete resonances in the Fermi–Pasta–Ulam–Tsingou system. *Commun. Nonlinear Sci. Numer. Simul* **73**:437–471.
- [2] Krasitskii V. P. (1994) On reduced equations in the Hamiltonian theory of weakly nonlinear surface waves. *J. Fluid Mech* **272**:1–20.

Nonresonant interactions between a linear system and a light double limit cycle oscillator

D. D. Tandel, Pankaj Wahi and Anindya Chatterjee

Mechanical Engineering, Indian Institute of Technology Kanpur, India

Abstract. We study modal interactions between a primary spring-mass-dashpot system and a light secondary system that can exhibit two limit cycles. The primary system with negative damping can represent a linearly unstable mode of a structure while the secondary system can act as an untuned stabilizer for this unstable mode. The coupled system is then studied using the method of multiple scales. Here, we obtain decoupled amplitude and phase evolution equations. The amplitude evolution equations are further simplified using a parameter-dependent transformation. We find that the system's qualitative dynamics depend only on two non-dimensional parameters. We then identify boundaries in this parameter space between regimes corresponding to different qualitative dynamics. Corresponding amplitude phase portraits allow us to identify system parameters that can offer large basins of attraction for the stabilized primary system.

Introduction

Engineering structures prone to instability, e.g., cables in cross-flow and long boring bars can be modeled as a primary spring-mass oscillator that is negatively damped. Traditional stabilization strategies include active damping which require massive actuators and/or passive tuned linear or nonlinear absorbers which require precise tuning [1]. In contrast, we consider an untuned stabilizer similar to [2] where they showed that an untuned whirling pendulum can stabilize an unstable mode. In the present work, we attach a light, nonresonant, secondary system that can exhibit two limit cycles: one stable and one unstable. We note that the attached system, being nonresonant, does not require precise tuning. Figure 1 (left) shows a schematic of the coupled system for which the final non-dimensional equations of motion are

$$\begin{aligned}\ddot{x} + \mu^2 c \dot{x} + x - \mu m \omega_p^2 z - \mu^2 m \gamma \dot{z} (\nu z^4 - z^2 + 1) &= 0, \\ \ddot{z} + \omega_p^2 z + \mu \gamma \dot{z} (\nu z^4 - z^2 + 1) &= 0,\end{aligned}$$

where μ denotes a small bookkeeping parameter. Details of the nondimensionalization are omitted here. The two uncoupled limit cycles exist for $0 < \nu < 0.125$ with the larger amplitude cycle being stable for $\gamma > 0$.

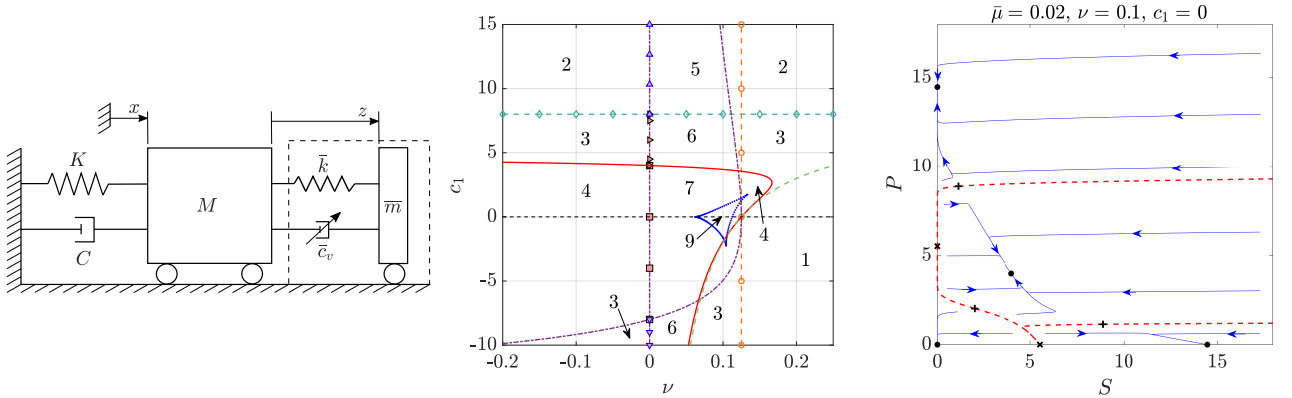


Figure 1: Left: system schematic with usual notations for parameters. Middle: the two parameter plane with number of fixed points in the amplitude plane. Right: the phase portrait corresponding to the c_1 - ν regime with 9 fixed points. $\bar{\mu}$ scales time: S evolves faster.

Results and discussion

The method of multiple scales yields decoupled amplitude and phase evolution equations. That allows us to focus on the amplitude plane only. We transform the amplitude evolution equations into a simple form using a parameter-dependent transformation. The final equations are in terms of the variables P and S denoting squares of the amplitude of the primary and secondary oscillators, respectively. The equations reveal that the qualitative dynamics of the system is governed by two parameters: $c_1 = -\frac{8c(1 - \omega_p^2)^2}{m\gamma}$ representing a measure of the ratio of the damping in the primary and the secondary system and ν , the ratio of the quartic and the quadratic terms in the nonlinear damping of the secondary system. We identify regimes with different number of P - S fixed points in the c_1 - ν plane, see Fig. 1 (middle). The corresponding finite number of phase portraits present the unified system dynamics. Figure 1 (right) shows the one with the highest number of fixed points, clearly showing a stable state with $P = 0$ which represents a stabilized primary system. From this analysis, we can identify c_1 - ν domains that provide large basins of attraction for the stabilized primary oscillator.

References

- [1] Gattulli V., Di Fabio F., Luongo A. (2004) Nonlinear Tuned Mass Damper for self-excited oscillations. *Wind Struct.* **7**(4):251-264.
- [2] Singla S., Chatterjee A. (2020) Nonlinear responses of an SDOF structure with a light, whirling, driven, untuned pendulum. *Int. J. Mech. Sci.* **168**:105305.

Koopman operator based Nonlinear Normal Modes for systems with internal resonance

Rahul Das*, Anil K Bajaj** and Sayan Gupta *.[†]

*Department of Applied Mechanics, Indian Institute of Technology Madras, Chennai 600036, India.

**School of Mechanical Engineering, Purdue University, Indiana 47907, USA.

[†]Complex Systems and Dynamics, Indian Institute of Technology Madras, Chennai 600036, India.

Abstract. This study is focused on the Nonlinear Normal Modes (NNMs) of a 2-dof nonlinear system with an essentially nonlinear substructure. The primary system comprises of an oscillator with cubic stiffness and is coupled with an essentially nonlinear oscillator with cubic stiffness. The energy flow from primary oscillator to the attachment is investigated by quantifying the NNMs of the system, by adapting the Shaw-Piere *invariant manifold technique*. Later the issues regarding the invariant manifold formulation is discussed and solved by introducing *Koopman Operator*.

Introduction

Nonlinear Normal Modes (NNMs) for nonlinear dynamical systems, developed as a generalization of Linear Normal Modes (LNMs), are invariant manifolds in the state space that are tangent to the modal plane of LNM at the equilibrium points. Unlike LNMs, NNMs need not be linearly independent and therefore do not form the basis and can exceed the degrees of freedom of the system in number. Shaw *et. al.* [1] defined NNMs as *invariant manifolds* of dimension 2, embedded in the phase space and extended the idea to non-conservative systems [2]. While there has been significant progress on development of NNMs, the formulation of invariant manifolds for systems with *internal resonating modes*, especially systems with essential nonlinearity appears to be challenging.

This study focuses on formulating the invariant manifold (NNM) by adapting the technique proposed in [1] for a targeted energy transfer problem comprising of a 2-dof nonlinear system with an essentially nonlinear substructure. The primary system is taken to be an oscillator with a cubic stiffness. Identifying the NNMs enable quantifying the unidirectional flow of energy from the primary structure to its attachment. Three different cases, comprising of 3rd order, 5th order and 7th order approximation of the invariant manifold is considered. It is shown that the invariance property is not global on the manifold due to internal resonance. The formulation of invariant manifold is then modified by introducing “*Koopman Operator*” [3], which enables dealing with effects of the complex geometry of folding of the invariant manifolds due to internal resonance.

Results and discussions

Three different order approximations of invariant manifold of a system comprising of a Duffing oscillator attached with a *Nonlinear Energy Sink (NES)*, is shown in Fig. 1. Here, (x_1, y_1) represents the state variables (“master co-ordinates”) of the primary Duffing oscillator, while X_2 represents the displacement of the NES. It is observed that the invariance property holds locally. The deviation of the higher energy trajectories from the invariant manifold is observed to decrease significantly by increasing the order of the approximation.

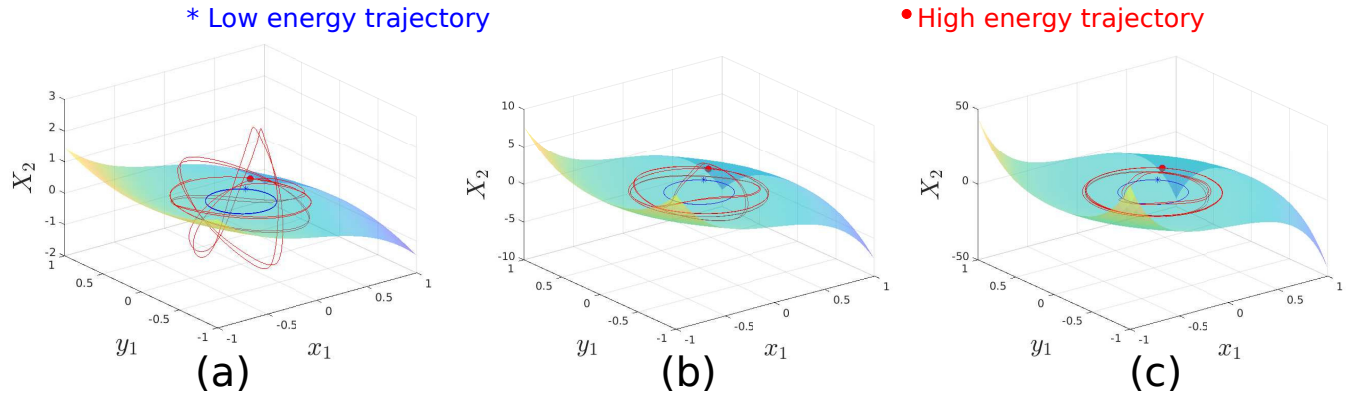


Figure 1: Invariant manifold of Duffing-NES system: (a) 3rd order, (b) 5th order and (c) 7th order approximations.

References

- [1] Steven Shaw and Christophe Pierre. Non-linear normal modes and invariant manifolds. *Journal of sound and Vibration*, 150(1):170–173, 1991.
- [2] Steven W Shaw and Christophe Pierre. Normal modes for non-linear vibratory systems. *Journal of sound and vibration*, 164(1):85–124, 1993.
- [3] Giuseppe Ilario Cirillo, Alexandre Mauroy, Ludovic Renson, Gaëtan Kerschen, and Rodolphe Sepulchre. A spectral characterization of nonlinear normal modes. *Journal of Sound and Vibration*, 377:284–301, 2016.

Unsteady two-temperature heat transport in mass-in-mass chains

Sergei D. Liazhkov^{*,**}, Vitaly A. Kuzkin^{*,**}

^{*}*Peter the Great Saint-Petersburg Polytechnic University, St. Petersburg, Russia*

^{**}*Institute for Problems in Mechanical Engineering of the Russian Academy of Sciences, St. Petersburg, Russia*

Abstract. We investigate the unsteady heat transport in an infinite mass-in-mass chain with a given initial temperature profile. The chain consists of two sublattices: the β -Fermi-Pasta-Ulam-Tsingou (FPUT) chain and oscillators (of a different mass) connected to each FPUT particle. Initial conditions are such that initial kinetic temperatures of the FPUT particles and the oscillators are equal. The harmonic theory predicts that during the heat transfer the temperatures of sublattices are significantly different, while initially and finally (at large times) they are equal. This may look like an artifact of the harmonic approximation, but we show that it is not the case. Two distinct temperatures are also observed in the anharmonic case, even when the heat transport regime is no longer quasi-ballistic. We show that the value of the nonlinearity coefficient required to equalize the temperatures strongly depends on the particle mass ratio. If the oscillators are much lighter than the FPUT particles, a fairly strong nonlinearity is required for the equalization.

Introduction

Far from thermal equilibrium, the concept of temperature as a single scalar parameter, characterizing local thermal state of a system, may be insufficient. Introducing several temperatures for each subsystem is often necessary. For example, in systems subjected to fast laser excitation, the temperatures of the lattice and electronic subsystem are different (see e.g. [1]). In heat conducting lattices, different temperatures can be observed in a nonequilibrium stationary state. For instance, in a one-dimensional diatomic chain limited by thermostats, the kinetic temperatures of sublattices can differ both in the cases of harmonic [2] and anharmonic interactions [3]. Evolution of kinetic temperatures during non-stationary heat transfer remains an open problem, and the current article is devoted to it. We consider an infinite chain of particles of mass interacting with the Fermi-Pasta-Ulam-Tsingou (FPUT) potential. A Duffing oscillator is attached to each particle with a mass (1).

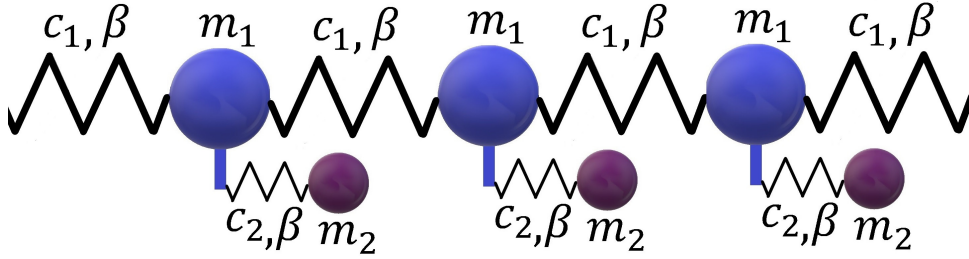


Figure 1: The mass-in-mass chain, consisting of the β -FPUT chain and additional nonlinear oscillators.

In the literature, such a model is referred to as a mass-in-mass chain and is extensively studied as a model of an acoustic metamaterial (see e.g. [4]). Also, the mass-in-mass can be considered as a model of chain of hydrocarbons or a system of phonons interacting with electrons. Results of the investigation may serve for the development of multi-component continuum models with several temperatures, behavior of these can be governed by a coupled system of heat transfer equations. If necessary, the reader can see [5] for details of the study.

Results and discussion

Results of the investigation are next:

1. Closed-form formula for description of evolution of sinusoidal temperature profile in process of ballistic heat transport.
2. Characteristic features of ballistic heat transport in the weakly anharmonic chain are demonstrated.
3. Two different temperatures remain even in the case of strong anharmonicity, causing change of heat transport regimes. Maximum difference of the temperatures significantly depends on the ratio of masses.

References

- [1] Indeitsev D.A., Osipova E.V. (2017) A two-temperature model of optical excitation of acoustic waves in conductors. *Dokl. Phys.* **62**:136–140.
- [2] Kannan V., Dhar A., Lebowitz J.L. (2012) Nonequilibrium stationary state of a harmonic crystal with alternating masses. *Phys. Rev. E* **85**:1–9.
- [3] Shah T.N., Gajjar P.N. (2016) Size dependent heat conduction in one-dimensional diatomic lattices. *Commun. Theor. Phys* **65**:517–522.
- [4] Porubov A.V., Grekova E.F. (2019) On nonlinear modeling of an acoustic metamaterial, *Mech. Res. Commun* **103**:1–4.
- [5] Liazhkov S.D., Kuzkin V.A. (2022) Unsteady two-temperature heat transport in mass-in-mass chains. *Phys. Rev. E* **105**:1–13.

Introducing a Stack of Eccentric Rotors to Semantically Modify Nonlinear Flexible Beam Continua to Considerably Enhance Irreversible Mechanical Energy Flow

Ioannis T. Georgiou*

School of Naval Architecture and Marine Engineering, National Technical University of Athens, Athens, Greece

*Adjunct Faculty, School of Mechanical Engineering, Purdue University, West Lafayette, Indiana, USA

Abstract. A cantilever elastic beam is coupled to a stack of coaxial eccentric rotors to explore experimentally how an embedded multi-stable subsystem creates a nonlinear dynamics environment to support irreversible flow of mechanical energy. Recorded by means of wireless MEMs sensors is the physics fact that the tangential acceleration of the eccentric rotor is strictly positive during phases of irreversible energy flow. Sliding over the surfaces of support stators, the introduced stack of eccentric rotors enhances by speeding up a natural irreversible flow of strain energy from the flexible continuum into the interacting coaxial eccentric rotors. The complicated landscape of products of static equilibria continua speeds up the flow of mechanical energy. This coupled system is a representative of an interesting class of meta-structures: modification of nonlinear elastic continua by embedded multi-stable mechanical subsystems generating contact-induced nonlinear friction forces.

Introduction

In this work explored is the challenging issue of *creating experimental evidence that a specific coexisting static equilibria environment*-formed by a stack of eccentric rotors-embedded in a continuum enables a natural irreversible energy flow. Conceived as a paradigmatic meta-structure, Fig. 1 depicts a modification of nonlinear elastic continuum with a stack of coaxial eccentric rotors to (1) explore the role of a complicated environment of continua of static equilibria in creating irreversible energy flow and (2) explore the role of contact-induced nonlinear frictional forces in shaping this irreversible energy flow phenomena. Previous exploratory work reveals that *the eccentric rotor traps by irreversible flow mechanical energy stored initially in a flexible elastic beam* [1]. We meet the challenge to acquire the right datasets to extract useful information.

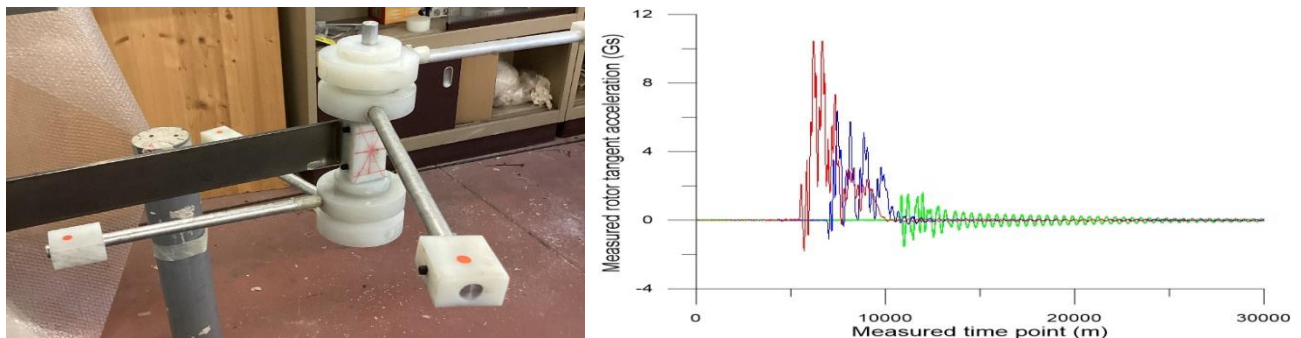


Figure 1: Lab set-up of conceived physical meta-structure (NTUA Nonlinear Dynamics Lab Unit) to explore experimentally dynamics underlined by irreversible energy flow from an elastic beam into an interacting stack of coaxial eccentric rotors in contact with stators. Observation: the tangent acceleration component of the eccentric masses is a strictly positive quantity with pulse-like behavior (right) during energy flow. Interplay of geometric nonlinearities and polygenic nonlinear contact-induced friction.

The methodology followed is acquirement (by state-of-the-art MEMs sensors) of triaxial acceleration datasets followed by systematic reduction analysis with Advanced Proper Orthogonal Decomposition (APOD) tools [2] to gain knowledge on the interplay of geometric nonlinear and friction-induced forces in an environment of coexisting continua of static equilibria. Dynamics phenomena with irreversible energy flow as observed in the specific class of free motions initiated after releasing instantly the beam tip, initially displaced slowly to store strain energy in the elastic continuum. Observed is the physics fact that the four eccentric rotors as a mechanism, initially at a random static equilibrium, start spinning abruptly-and-randomly while the vibration amplitude of the flexible continuum domain decreases quite fast to a small amplitude vibration. The dynamics characteristics of the irreversibly energy flow-energy dissipation phenomenon is imprinted in the local tangential acceleration signal of the eccentric mass in localized and pulse-like pattern, Fig. 1, when energy is flowing. Moreover, energy flows irreversibly when wave motions are created in the elastic continuum domain.

References

- [1] Georgiou, I.T. (2020) Energy Flow Considerations in Nonlinear Systems on the Basis of Interesting Experiments with Three Paradigmatic Physical Systems in Engineering. In: Kovacic, I., Lenci, S. (eds) IUTAM Symposium on Exploiting Nonlinear Dynamics for Engineering Systems. ENOLIDES 2018. IUTAM Bookseries, vol 37. Springer, Cham. https://doi.org/10.1007/978-3-030-23692-2_10.
- [2] Georgiou, I.T. (2015) A single pair-of-sensors technique for geometry consistent sensing of acceleration vector fields in beam structures: damage detection and dissipation estimation by POD modes. *Meccanica* **50**,1303–1330. <https://doi.org/10.1007/s11012-014-0091-y>.

A method for the analysis of the aeroelastic stability of slender wind turbines and its validation

Chao Peng*, Alessandro Tasora** and Pin Lyu***

* Department of Engineering and Architecture, University of Parma, Italy, ORCID 0000-0002-4900-5932

** Department of Engineering and Architecture, University of Parma, Italy, ORCID 0000-0002-2664-7895

*** Xinjiang Goldwind Science and Technology Co., Ltd, Beijing, China, ORCID 0000-0003-2056-3671

Abstract. We present a method for the stability analysis of wind turbines as three-dimensional multi-flexible-body systems. Aerodynamic forces are linearized via numerical perturbation and linear regression fit from multiple points around quasi-static equilibrium status, and a novel coordinate transformation is proposed to convert the basis from the absolute frame of reference to the local frame of reference at the rotating center in a corotational formulation. The modal analysis is performed in the MBC generalised coordinate and damping ratios are extracted to assess the aeroelastic stability of wind turbine. A field validation is performed on two offshore prototype wind turbines, showing a good matching between predictions of unstable wind speed ranges and experimental data.

Introduction

As the blade grows longer and slenderer in the pursuit of lowest levelized cost of electricity (LCOE), the aeroelastic damping ratio of its edgewise mode moves toward zero. The aeroelastic stability has become a major constraint condition for blade design optimization, thus motivating detailed and reliable aeroelastic analyses to rule off the risk of instability.

Modal analysis is commonly used to assess the stability of system. The linearization of the aero-elastic dynamics of wind turbines is widely discussed [1] [2] [3], and custom software tools, for instance, GH Bladed, HAWCStab2, OpenFAST and BHAWC [4] have been developed to this purpose, but no straightforward unstable vibrations in the normal power production mode are measured and compared against their numerical predictions.

Results and discussion

In this work, the linearized dynamics of a wind turbine is established based on a corotational formulation. The analytical expression of the tangent matrices of structural dynamics is derived after transforming from the absolute frame of reference to the local frame of reference at the rotating center. The eigenvalues of the aeroelastic dynamics are computed on two wind turbine prototypes and the damping ratios of the rotor edgewise backward whirling mode are extracted to assess the stability at the determined operational points. A field experiment consisting of three test cases is conducted to validate the prediction. As shown in Figure 1, the scatter diagram of standard deviations of blade root edgewise moment (M_x) in case 1 and 2 indicates that the blade doesn't experience relevant edgewise vibrations: accordingly, the damping ratio in case 1 is positive in the entire wind speed ranges. In case 2 the damping ratio is slightly negative for a sub-interval of the $[W_1, W_2]$ wind speed range, which implies the prediction is conservative. Regarding case 3, the M_x blade root edgewise moment presents a remarkable higher standard deviation. The modal analysis in case 3 predicts a negative damping ratio in the $[W_1, W_2]$ wind speed range and shows a satisfying agreement with experimental data.

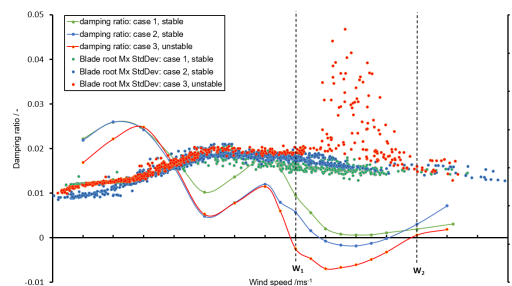


Figure 1: Comparison of measurement and computed damping ratios. Every scatter point represents the standard deviation of blade root edgewise moment (M_x) during a 10 minutes experimental test.

References

- [1] Hansen M.H. (2004) Stability Analysis of Three-Bladed Turbines Using an Eigenvalue Approach. 42nd AIAA Aerospace Sciences Meeting and Exhibit.
- [2] Skjoldan P. (2011) Aeroelastic Modal Dynamics of Wind Turbines Including Anisotropic Effects. Ph.D. thesis, Technical University of Denmark.
- [3] Filsoof O.T., Hansen M.H., Yde A., et al. (2021) A Novel Methodology for Analyzing Modal Dynamics of Multi-rotor Wind Turbines. *J. Sound Vib* **493**:115810.
- [4] Volk D.M., Kallesøe B.S., Johnson S., et al. (2020) Large Wind Turbine Edge Instability Field Validation. TORQUE 2020, website <https://www.torque2020.org>.

Effect of Rub-Impact on Backward Whirl Excitation in a Cracked Rotor System

Mohammad A. AL-Shudeifat*, Rafath Abdul Nasar*

*Aerospace Engineering, Khalifa University of Science and Technology, Abu Dhabi, United Arab Emirates

Abstract. The effect of appearance of multiple faults on backward whirl excitation in a rotor system is investigated here. The breathing crack is one of the common faults which is activated here by the non-synchronous whirl of the shaft in the vicinity of the resonance zone. Therefore, the effect of the breathing crack at the presence of rub-impact on backward whirling in the neighbourhood of resonance speed is investigated in this study for steady-state operation. The Jeffcott rotor model is employed here with both breathing crack and rub impact are incorporated. It is observed that the appearance of breathing crack at the presence of rub-impact has a substantial effect on backward whirl excitation in the resonance zone.

Introduction

The breathing crack model that depends on nonsynchronous whirl in the vicinity of resonance zone in [1] was found to excite the post-resonance backward whirl (Po-BW) in vertical cracked rotor system. This Po-BW phenomena was firstly observed at the transient numerical and experimental whirl response of rotor systems with open crack model in [2] and later in a rotor system with snubbing contact in [3]. Therefore, the current study investigates the effect of appearance of the breathing crack model in [1] at the presence of rub-impact on backward whirl excitation in the vicinity of resonance zone.

Results and discussion

The breathing crack model in [1] is employed here with Jeffcott rotor model of which the physical parameters are given in Table 1. Accordingly, the mathematical equations of motion of the rotor with both crack and rub-impact are numerically solved for the whirl response at steady-state running. Compared with the case of a crack free system with rub-impact in Figure 1a, it is observed in Figure 1b that the propagation of a breathing crack with small crack depth at the presence of rub-impact has strong impact on the whirl response and backward whirl excitation at resonance zone. Alternation between forward and backward whirling at resonance zone is also observed. However, individual appearance of either rub-impact or breathing crack has shown weaker impact on the resonance backward whirl excitation.

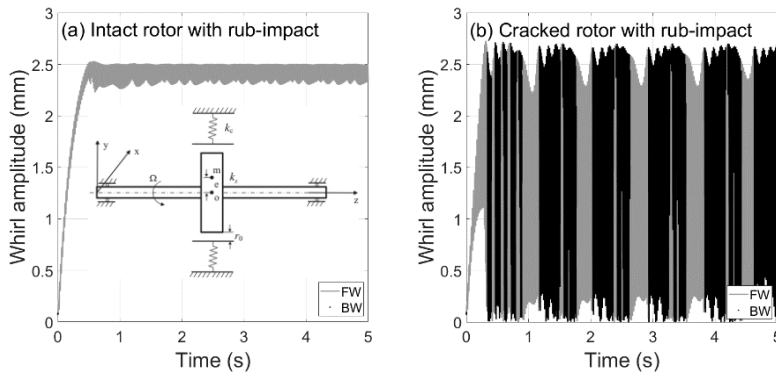


Table 1 System physical parameters

Description	Value
Length of the rotor, L	700 mm
Radius of the rotor, R	9.5 mm
Density of the shaft, ρ_s	7850 kg/m ³
Modulus of elasticity, E	2×10^{11} N/m ²
Mass unbalance, $m \cdot e$	1×10^{-4} kg · m
Disk radius r_d	140 mm

Figure 1 Intact rotor with rub-impact in (a) and with rub-impact and breathing crack in (b) at $\Omega = 55$ rad/s, stiffness ratio $k_c / k_s = 10$, clearance $r_0 = 2.5$ mm and normalized crack depth $\mu = 0.1$.

References

- [1] AL-Shudeifat, M. A. (2022) Impact of Non-Synchronous Whirl on Post-Resonance Backward Whirl in Vertical Cracked Rotors. *J. Sound Vib.* **520**:116605.
- [2] AL-Shudeifat, M. A. (2019) New Backward Whirl Phenomena in Intact and Cracked Rotor Systems. *J. Sound Vib.* **443**: 124–138.
- [3] Al-Shudeifat, M. A., Friswell, M., Shiryayev, O., and Nataraj, C. (2020) On Post-Resonance Backward Whirl in an Overhung Rotor with Snubbing Contact. *Nonlinear Dyn.* **101**: 741–754.

Nonlinear dynamics of an accelerating rotor supported on self-acting air journal bearings

M. R. Pattnayak*, J. K. Dutt* and R. K. Pandey*

*Department of Mechanical Engineering, Indian Institute of Technology Delhi, New Delhi, Delhi-110016, India.

Abstract. Self-acting air bearings are used in several high-speed micro-turbomachines, where frequent acceleration/deceleration of the rotor is common. The whirl amplitude of the rotor must be kept within tolerable limits for safe operations of the system. This research presents, for the very first time, the dynamics of an accelerating rotor supported on self-acting air journal bearings. Due to the rotor unbalance, the dynamics between the translational and spin coordinates get nonlinearly coupled. The work utilizes these coupled equations to plan appropriate acceleration schedules to limit the whirl amplitude and frequency as low as possible. Based on the research, it is found that in the presence of rotor unbalance, the acceleration should be scheduled in at least three regimes: the first with the maximum torque, the second with the minimum torque, and the last with an intermediate torque.

Introduction

With the rise in demand for eco-friendly, high-speed and extreme-temperature micro-turbomachinery, self-acting air bearings are evolving to replace traditional oil/grease-lubricated bearings. The rotors supported on self-acting air journal bearings typically operate at very high rotational speeds in the order of 10^4 to 10^5 rpm. In this process, frequent acceleration to/retardation from such high speeds is prevalent [1,2]. During this phase, the rotors experience high-amplitude whirling, which is undesirable from a safety point of view. The present research presents the non-linear dynamic response of an accelerating rotor supported on self-acting air bearings and proposes suitable acceleration schedules to keep the whirling amplitude and frequency as low as possible. From the point-of-view of mathematical simulations, it is observed that the highly nonlinear rotordynamics of rotors supported on self-acting gas bearings cannot be predicted accurately by considering only the two translational degrees of freedom to build the equations of motions of the rotor. Moreover, the spin direction dynamics are often not considered in this process because it makes the equations of motions highly nonlinear and coupled in all directions. Therefore, the inclusion of spin direction dynamics along with the translational and tilting dynamics to form the equations of motions is essential, particularly for very high-speed rotors, usually supported by self-acting air bearings [2]. Therefore, in the present study, the generic form of equations of motions for a rigid rotor with a non-central disc supported on two self-acting air bearings considering five degrees of freedom (two translations, two tiltings and one rotational degree of freedom) are being proposed. The transient compressible lubrication equation and the equations of motion of the rotor are simultaneously solved to compute the dynamic response of the rotor during the acceleration phase. The mathematical simulations have shown that the driving torque significantly affects the rotordynamic response during the acceleration phase of the rotor. Based on the analysis, the acceleration scheduling is implemented by varying the driving torque at different phases of the acceleration to contain the whirl amplitude and its frequency as low as possible. <TEPUCS: Trace of the Equilibrium Positions Under Constant Speed >

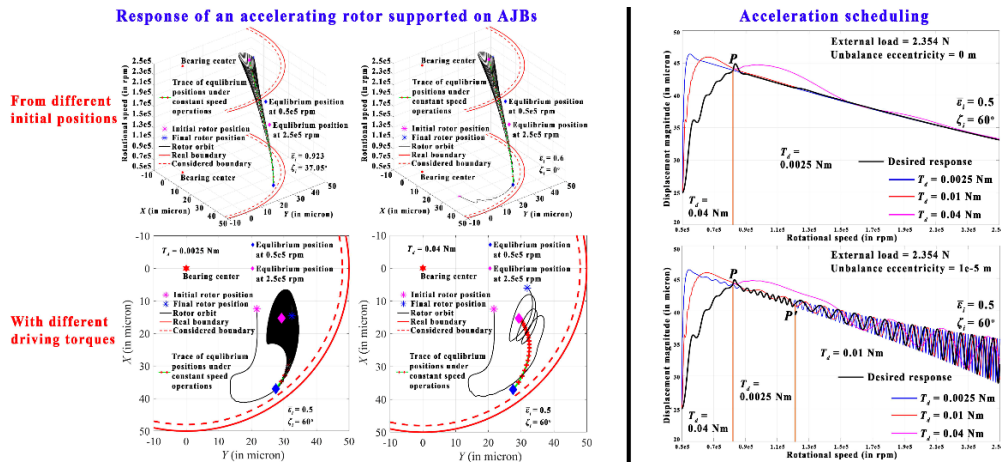


Figure 1: Response of acceleration rotor supported on self-acting air journal bearings and execution of acceleration scheduling

Results and discussion

The core findings are as follows: i) During the initial acceleration, the rotor center moves towards the *TEPUCS* line and later revolves about this line. ii) During the periodic phase, the frequency of whirling reduces with the rise in the external driving torque. iii) During the acceleration, as the rotor approaches the *TEPUCS* line, higher driving torque results in minimum rotor response, whereas the response increases after crossing this line. iv) There should be at least three acceleration schedules to contain whirl response.

References

- [1] Pattnayak M. R., Ganai P., Pandey R. K., Dutt J. K., Fillon M. (2022) An overview and assessment on aerodynamic journal bearings with important findings and scope for explorations. *Tribology International* **174**:107778.
- [2] Pattnayak M. R., Dutt J. K., Pandey R. K. (2022) Rotordynamics of an accelerating rotor supported on aerodynamic journal bearings. *Tribology International* **176**:107883.

On the nonlinear dynamics of rotating hybrid nanocomposite blades with matrix crack

Xu Ouyang^{*}, Krzysztof Kamil Żur^{**} and Hulun Guo^{*}

^{*}Tianjin Key Laboratory of Nonlinear Dynamics and Control, Department of Mechanics, Tianjin University, Tianjin, China

^{**}Faculty of Mechanical Engineering, Bialystok University of Technology, Bialystok, Poland

Abstract. For the first time, nonlinear dynamics of rotating pre-twisted hybrid laminated blades composed of a mixture of matrix cracked graphene platelets reinforced composite (GPLRC) layers and perfect FG carbon nanotube reinforced composite (CNTRC) layers is investigated. The material properties of both nanocomposites are predicted by modified Halpin-Tsai model and the modified rule of mixture. The degraded stiffness of the cracked GPLRC lamina is evaluated within the micromechanical framework of the self-consistent model. Based on the FSDT and the Novozhilov nonlinear shell theory, the discretized nonlinear governing equations are established using the element-free IMLS-Ritz approach and solved employing a direct iterative method. Parametric studies are performed systematically to illustrate the impacts of matrix crack density, CNT distribution configuration, ply angle, and number of layers on the frequency-amplitude relations of rotating matrix cracked hybrid nanocomposite blades.

Introduction

Composite blades are important components in various engineering structures, such as steam turbine, gas turbine, and wind turbine. The laminated FG materials reinforced with GPLs and CNTs possess low weight combined with higher stiffness and strength which are in great demand for rotating machines and their elements [1, 2]. The initial matrix cracks in composite laminates may influence the dynamic properties at a certain extent. Thus the dynamics of rotating hybrid nanocomposite blades with matrix crack should be investigated.

Three coordinate systems in Figure 1 (a) are introduced to describe the geometry properties of the blade with a twisting geometrical shape. As illustrated in Figure 1 (b), it is assumed that the perfect bonded laminated blades are composed of a mixture of GPLRC layers and CNTRC layers. All nanocomposite layers have the same matrix to reduce interlaminar stresses. Number of each lamina increases from the bottom of the multilayer blade to its top. NL is the total number of layers and NL ($NL \geq 3$) is an odd number. Notably, the even-layer and the odd-layer belongs to GPLRC layer and CNTRC layer, respectively. As depicted in Figure 1 (c), the GPLs are evenly distributed in each GPLRC layer and the parallel slit matrix cracks considered to be elliptic cylindrical cavities are dispersed in the matrix of GPLRC layers homogeneously. As an example, three types of five-layer hybrid nanocomposite structures, namely Structure-I, Structure-II, and Structure-III are shown in Figure 1 (d), (e), and (f). The CNTRC layers in Structure-I are considered with CNTs arranged in uniform distributions, while Structure-II and Structure-III are arranged with CNTs FG distributions. Five CNT distribution configurations through the thickness in each CNTRC layer including UD, FG-O, FG-X, FG-V, and FG-A are covered.

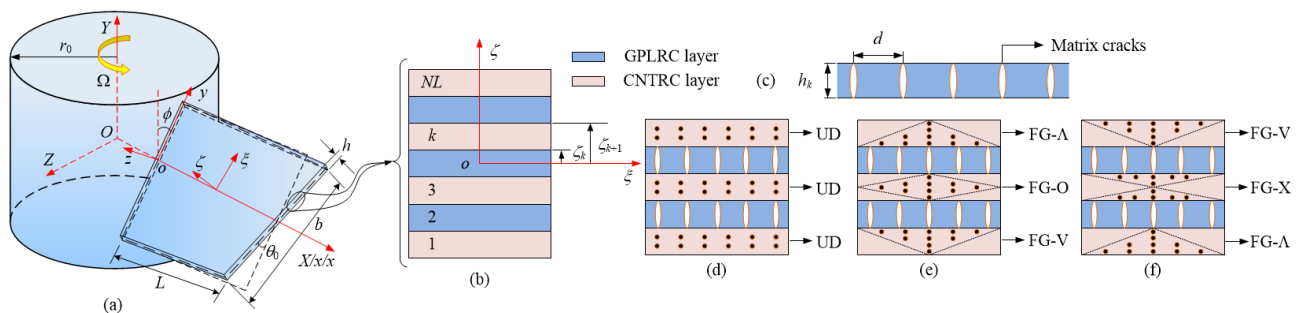


Figure 1: (a) the coordinate system and geometry and (b) the cross-section of rotating pre-twisted perfect bonded laminated hybrid nanocomposite blade; (c) the geometric description of cracks and their distribution in GPLRC layers; the configuration of CNTs in hybrid nanocomposite blade (d) Structure-I, (e) Structure-II, and (f) Structure-III.

Results and discussion

The accuracy and efficiency of the present model are validated in detail by comparing the obtained results with those available in the literature. Parametric studies in the full-length paper are performed systematically to illustrate the impacts of matrix crack density, CNT distribution configuration, GPLs-to-CNTs volume fraction ratio, GPLRC-to-CNTRC layer thickness ratio, ply angle, and a number of layers on nonlinear vibration behaviours of rotating hybrid nanocomposite blades with matrix crack. New insights into the nonlinear dynamics of the considered blades are presented.

References

- [1] Liew K.M., Xiang P., Zhang L.W. (2015) Mechanical properties and characteristics of microtubules: A review. *Compos. Struct* **123**: 98-108.
- [2] Zhao S., Zhao Z., Yang Z., Ke L., Kitipornchai S., Yang J. (2020) Functionally graded graphene reinforced composite structures: A review. *Eng. Struct* **210**: 110339.

Parametric resonances due to torsional oscillations in a multi-degree of freedom driveline coupled by a series of universal joints

Junaid Ali*, Shveta Dhamankar*, Evan Parshall*, Gregory Shaver*, Anil K Bajaj*, Keith Loisel ** and Douglas Hansel **

*Ray W. Herrick Laboratories, School of Mechanical Engineering, Purdue University, West Lafayette, IN, USA

**Allison Transmissions Inc., Indianapolis, IN, USA

Abstract. Here we study the parametric instabilities in a 3-degrees of freedom (DOF) driveline, consisting of a series of two universal joints (U-Joints) phased at 90° . The governing non-linear equations of motion are linearized around a steady rotational motion of the drive shaft in relative coordinates representing rotational dynamics, and for the system with periodic coefficients stability is concluded using Floquet-Lyapunov theory. The existence of harmonic, sub-harmonic and combination-type resonances are identified on the scatter plot or Strutt diagram of the parameter plane. Linear stability analysis results are validated by direct time integration of the full non-linear model for stable and unstable parametric regions using the Runge-Kutta routine.

Introduction

The non-linear kinematical relationship between the input and output angular velocity of a U-Joint varies periodically resulting in a time-periodic behaviour of the dynamic system incorporating the U-Joint. Many studies have been conducted on such dynamic systems though the focus has mostly been on the development of equations of motion and their solutions rather than detailed dynamic behaviour. Bulut and Parlar [1] studied the dynamics of a 2-DOF shaft system interconnected with a U-Joint. The stability of the steady rotational motion of the system was determined using the monodromy matrix method and some parametric resonance regions below and above the fundamental torsional frequency of the system was highlighted. Asokanthan and Meehan [2] obtained conditions for parametric instability of the 2-DOF shaft system using the method of averaging, and determined the quasi-periodic route to chaos for the full nonlinear model utilizing maximal Lyapunov exponent. For the shaft system with a single U-Joint, they arrived at the necessary parametric and combination resonance conditions for chaotic behaviour. For a system with multiple U-Joint drivelines, a variety of challenges arise such as phasing a series of joints in the driveline to cancel the torsional oscillation effects due to the kinematics of U-Joint. Even with proper cancellation, the 2^{nd} Order torsional oscillations are always present in the driveline due to the inertial effects influenced by the inherent non-linearities. Also, in a real-world application, it is very difficult to keep the U-Joint misalignment angles equal for the series of joints in the driveline which invalidates the torsional cancellation effect completely even though joints are properly phased. Under certain operating conditions of the driveline, interesting non-linear resonance phenomena could be observed due to these uncanceled torsional and inertial oscillations present in the driveline. Therefore, it is important to investigate the dynamic stability of a shaft system consisting of multiple U-Joints with equal and unequal misalignment angles. It would be helpful from a design perspective to estimate critical resonance speeds and misalignment angles to prevent parametric or combination-type resonances in the driveline which are a product of the non-linearities of the dynamical system.

Results and Discussion

In this abstract, we have illustrated the parametric instabilities of a two U-Joints shaft system with equal joint misalignment angles $\beta_{1,2}$. Using Floquet theory for linear parametrically excited systems, stable and unstable zones are identified and presented in a strut diagram in $(\Omega, \beta_{1,2})$ plane where red dots represent the unstable region as shown in Figure 1. $(\Omega = 1)$ represents the fundamental torsional resonance and it can be inferred that for a small value of damping ($\zeta = 0.001$). Direct simulations of the fully nonlinear system are also developed.

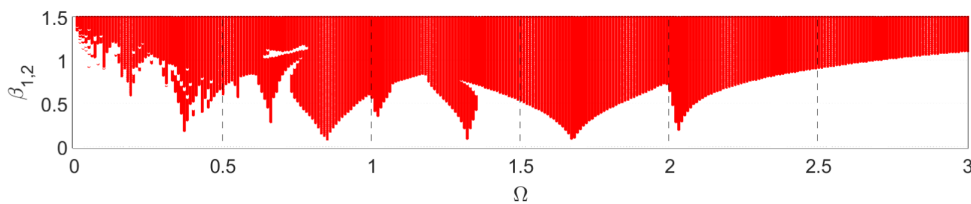


Figure 1: Stability chart - Equal misalignment angle $\beta_1 = \beta_2$

References

- [1] Gökhan Bulut, Zeynep Parlar, Dynamic stability of a shaft system connected through a Hooke's joint, Mechanism and Machine Theory, Volume 46, Issue 11, 2011, Pages 1689-1695.
- [2] S.F. Asokanthan, P.A. Meehan, Non-linear vibration of a torsional system driven by a Hooke's joint, Journal of Sound and Vibration, Volume 233, Issue 2, 2000, Pages 297-310

Transmission of rotation by a geometrically imperfect flexible shaft in a curved channel

Yury Vetyukov

* TU Wien, Institute of Mechanics and Mechatronics, Getreidemarkt 9 / E325, 1060 Vienna, Austria

Abstract. Geometric imperfection of a flexible shaft transmitting rotary motion along a curved path results into a nonlinear relation between the rotation angles at the driving and the driven ends. Even the snap-through instability is possible if the intrinsic curvature of the shaft exceeds a certain threshold. In dynamics, this results into oscillatory response at the driven end when the angular velocity at the driving one is held constant. In the present contribution we analytically consider the case of small imperfection. A closed form expression for the profile of the vibration amplitude along the length coordinate follows after the linearization of the sine-Gordon equation in the vicinity of the stationary rotation regime. A comparison to the numerical finite element solution justifies the analytical result, allows to conclude on its domain of applicability and provides insights regarding the influence of nonlinearity and damping.

Introduction

Flexible shafts are used for delivering rotary motion, torque and power from a motor to a distant point in space in various situations. The particles of the shaft undergo purely rotary motion if the shaft is confined in a borehole or in a stiff housing, such that its axis assumes a shape prescribed by the channel. A geometric imperfection of the shaft in the form of natural (or intrinsic) curvature along with the curvature of the constraining channel may result into highly irregular rotation of the tool even at slow motion and in the absence of friction [1]. A simple explanation is that the configurations, in which the directions of the curvatures coincide are energetically advantageous, and the opposite directions of the curvatures require higher degree of bending of the shaft to fit into the channel. As a result, the rotation angle at the driven end θ_{exit} becomes a nonlinear or even not a single valued function of the rotation angle at the driving end θ_{entry} even in statics, see Fig. 1. The equilibrium paths in the right part of the figure depend on the non-dimensional parameter combination $p\ell$, in which ℓ is the length of the shaft and p^2 is the product of the curvatures of the shaft and of the channel multiplied with the ratio of the bending and the torsional stiffness coefficients of the shaft, see [2].

Analysis

The dynamics of the structure is governed by the boundary value problem for the rotation angle $\theta(s, t)$ as a function of the spatial coordinate s and time t with c being the wave velocity:

$$\theta'' - \frac{1}{c^2} \ddot{\theta} = p^2 \sin \theta, \quad \theta(0, t) = \theta_{\text{entry}}(t), \quad \theta'(\ell, t) = 0. \quad (1)$$

Re-scaling the time and the spatial coordinate, this nonlinear hyperbolic partial differential equation may be transformed to the dimensionless sine-Gordon equation known for its soliton solutions [3]. We are, however, interested in the effect of the nonlinear term on the steady-state dynamics when the driving end of the shaft rotates with a given angular velocity, $\theta_{\text{entry}} = \omega t$, and seek the solution in the form

$$\theta = \omega t + \varphi(s, t), \quad \varphi(0, t) = 0, \quad \varphi'(\ell, t) = 0, \quad \varphi(s, t) = \varphi(s, t + 2\pi/\omega). \quad (2)$$

After the decay of the transient stage, the time period of the perturbation φ coincides with the time needed for a single rotation. At small p , a closed-form solution featuring a simple approximation $\varphi = \tilde{\varphi}(s) \sin \omega t$ becomes possible. A comparison against the results of the transient finite element analysis shows the range of applicability of the obtained analytical expression of the profile of the vibration amplitude $\tilde{\varphi}$.

References

- [1] Alexander Belyaev, Vladimir Eliseev (2018) Flexible rod model for the rotation of a drill string in an arbitrary borehole. *Acta Mechanica* **229**:841–848.
- [2] Yury Vetyukov, Evgenii Oborin (submitted) Snap-through instability during transmission of rotation by a flexible shaft with intrinsic curvature. *International Journal of Nonlinear Mechanics*
- [3] Abdul-Majid Wazwaz (2005) The tanh method: exact solutions of the sine-Gordon and the sinh-Gordon equations. *Applied Mathematics and Computation* **167**(2):1196–1210

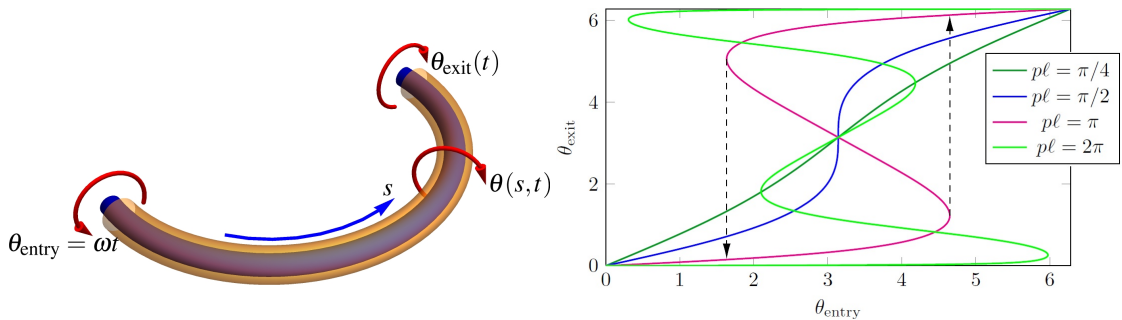


Figure 1: *Left:* Flexible shaft confined in a curved channel. *Right:* Static response of the elastic structure $\theta_{\text{exit}}(\theta_{\text{entry}})$ for various values of non-dimensional parameter combination $p\ell$; snap-through instability is possible at $p\ell > \pi/2$

Nonlinear dynamics of asymmetric rotor subjected to rotor-stator contact

Ali Fasihi*, Grzegorz Kudra* and Jan Awrejcewicz*

* Department of Automation, Biomechanics and Mechatronics, Lodz University of Technology, Lodz, Poland

Abstract. The nonlinear dynamics of an asymmetric rotor subjected to the rotor-stator contact effect were investigated. The rotor was mounted on elastic supports and excited by an unbalanced force arising from the eccentricity of its center of gravity. Equations of motion in the two transverse directions of the rotor were obtained. The obtained governing equations of motion were solved numerically to unveil the system's dynamics, such as the transition among periodic, quasi-periodic, and chaotic motions. In particular, the complex dynamics of the system were studied with the help of bifurcation diagrams, phase plain, time history, and power spectrum.

Introduction

Centripetal forces generated by the imbalance can bring a serious hazard to machines. It is not surprising that studying the effects of imbalance on the dynamics of machines has been in mainstream rotor-dynamic research for decades [1]. This excitation can produce a vibration that causes rotor-stator contact [2]. Asymmetry causes changes in the mode shapes and vibration patterns of the rotor system, therefore, studying the dynamics of asymmetric rotors subjected to rotor-stator contact is significant [3].

The governing equations of motion were derived with the aid of Hamilton principle by employing the Rayleigh beam theory. Impact interaction between the rotor and the stationary outer case was modeled in the form of discontinuous stiffness, and geometrical and inertial nonlinearities due to the inextensibility of the shaft were considered.

Results and discussion

Different tools for dynamical analysis were used to investigate the effects of system parameters on the dynamical characteristics of the rotor. Transition in the dynamical state of the rotor was investigated when the rotating speed, asymmetry, damping coefficient, and impact stiffness coefficient were chosen as control parameters.

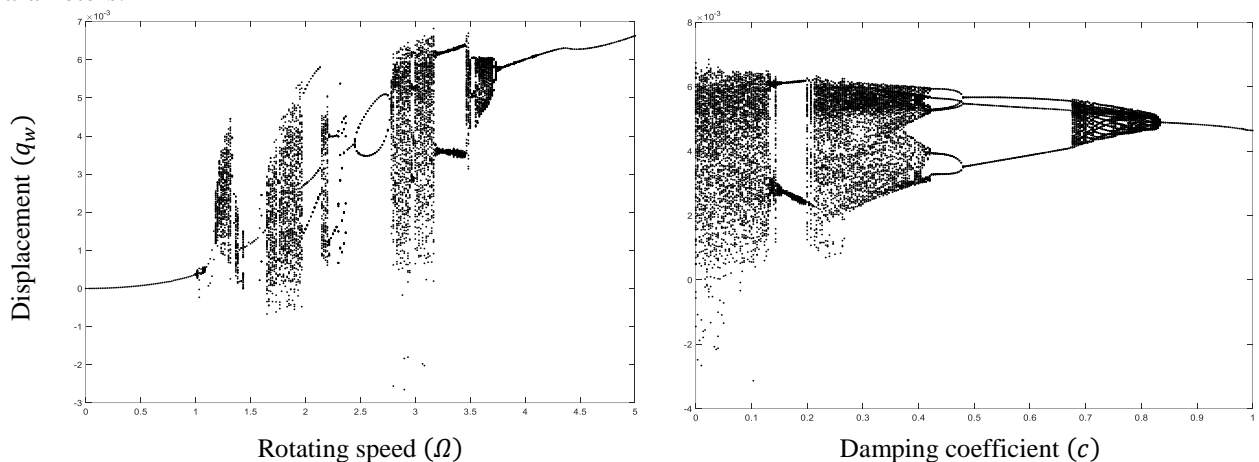


Figure 1: The bifurcation diagram of the maximum displacement of the rotor versus the rotation speed.

When the vibration amplitude of the rotor is smaller than the radial gap, the system vibrates with period-1. By increasing the rotation speed the system experiences quasi-periodic, period-n, and chaotic motion. Moreover, the motion regime changes from chaotic to multi-periodic by increasing the damping coefficient, and the asymmetry and impact stiffness are also of great importance to the dynamical characteristic of the rotor.






Acknowledgments

This abstract was produced as part of the doctoral candidate's participation in a project of the national agency for academic exchange within the framework of "STER" programme as part of the project "Curriculum for advanced doctoral education & training – CADET Academy of Lodz University of Technology".

References

- [1] S. Ahmad, "Rotor Casing Contact Phenomenon in Rotor Dynamics — Literature Survey,," <http://dx.doi.org/10.1177/1077546309341605>, vol. 16, no. 9, pp. 1369–1377, Jun. 2010, doi: 10.1177/1077546309341605.
- [2] E. V. Karpenko, M. Wiercigroch, and M. P. Cartmell, "Regular and chaotic dynamics of a discontinuously nonlinear rotor system," *Chaos, Solitons & Fractals*, vol. 13, no. 6, pp. 1231–1242, May 2002, doi: 10.1016/S0960-0779(01)00126-6.
- [3] M. Shahgholi and S. E. Khadem, "Primary and parametric resonances of asymmetrical rotating shafts with stretching nonlinearity," *Mech. Mach. Theory*, vol. 51, pp. 131–144, May 2012, doi: 10.1016/J.MECHMACHTHEORY.2011.12.012.

Reduced order modeling of rotating structures featuring geometric nonlinearity with the direct parametrisation of invariant manifolds method

Adrien MARTIN¹, Andrea OPRENI², Alessandra VIZZACCARO³,
Loïc SALLES⁴, Olivier THOMAS⁵, Attilio FRANGI² and Cyril TOUZÉ¹
¹IMSIA, ENSTA Paris, CNRS, EDF, CEA, Institut Polytechnique de Paris, Palaiseau, France 
²Department of Civil and Environmental Engineering, Politecnico di Milano, Milano, Italy 
³Department of Engineering Mathematics, University of Bristol, Bristol, England 
⁴Departement of Aerospace & Mechanical Engineering, University of Liège, Liège, Belgium 
⁵Arts et Métiers Institute of Technology, LISPEN, HESAM Université, Lille, France 

Abstract. The direct parametrisation method for invariant manifolds (DPIM) is applied to rotating structures. Reduced-order models of arbitrary order expansion can be derived for non-autonomous systems of nonlinear differential equations stemming from finite element models of continuous structures. The method is applied to a rotating simplified fan blade with comparisons to full order model simulations.

Introduction

Aircraft engine manufacturers are developing larger systems with longer blades where the geometric nonlinearity is enhanced. As a result, the derivation of efficient reduction method to tackle such problems at the design stage is important.

This work addresses the application of the direct parametrisation method for invariant manifolds (DPIM), following the implementation proposed for non-autonomous problems in [2], to rotating structures subjected to large displacements. This method relies on the assumption that the unknowns of the problem, displacement and velocity, as well as the reduced dynamics equation, can be expressed under the form of arbitrary orders polynomials of the new coordinates of the problem, the *normal coordinates*. Examples of such developments are given for the displacement, eq. (1), and the reduced dynamics, eq. (2). More details are given in a dedicated paper [1].

$$\mathbf{u}(t) = \Phi \mathbf{z} + \sum_{p=2}^{o_a} [\psi(\mathbf{z})]_p + \sum_{p=0}^{o_{na}} [\hat{\psi}(\mathbf{z})]_p \quad (1) \quad \dot{\mathbf{z}} = \Lambda \mathbf{z} + \sum_{p=2}^{o_a} [\mathbf{f}(\mathbf{z})]_p + \sum_{p=0}^{o_{na}} [\hat{\mathbf{f}}(\mathbf{z})]_p \quad (2)$$

Results and discussion

The method is applied to a simplified fan blade, shown in fig. 1a, which is 1 m long. The Campbell diagram is given in fig. 1b and shows the classic stiffening of the structure with increasing rotation speed. Finally, comparison between full order simulation and ROM computations using a single master mode, are shown in fig. 1c (blue : 0 rpm; red : 2000 rpm). One can observe the perfect match between the reduced model (dashed line) and the full model (solid line) highlighting the efficiency of the method, coupled to a significant time saving in terms of computation (1 day versus 1 minute).

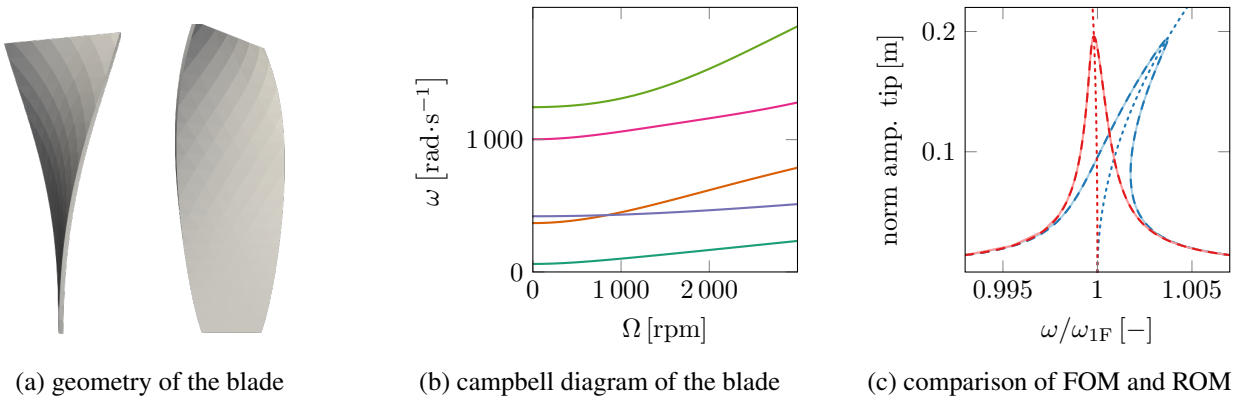


Figure 1: Reduced order model of a simple rotating blade;

(b) : — : 1F; — : 2F; — : 1T; — : 1E; — : 3F; (c) : — : FOM; --- : DPIM $\mathcal{O}(5, 4)$; ----- : DPIM $\mathcal{O}(5)$

References

- [1] A. Martin, A. Opreni, A. Vizzaccaro, L. Salles, A. Frangi, O. Thomas, and C. Touzé. Reduced order modeling of slender structures subjected to centrifugal effects using the direct parametrisation of invariant manifolds. *in preparation*.
- [2] A. Opreni, A. Vizzaccaro, C. Touzé, and A. Frangi. High order direct parametrisation of invariant manifolds for model order reduction of finite element structures: application to generic forcing terms and parametrically excited systems. *Nonlinear Dynamics*, accepted, 2022. doi:10.21203/rs.3.rs-1359763/v1.

Enhanced performance of nonlinear energy sink under harmonic excitation using acoustic black hole effect

Tao Wang* and Qian Ding*

*Department of Mechanics, Tianjin University, Tianjin, China

Abstract. To avoid failure of nonlinear energy sink (NES) under large excitation, a novel design is proposed by attaching ABH beam with damping layer at its tip to the mass block of NES. The introduction of the ABH beam has two main influences: first, it raises the excitation threshold of NES's failure by increasing the energy dissipation pathway. Second, it reduces the main structure's amplitude after NES's failure by utilizing the highly damped modes of ABH structure. This novel NES is called ABH-NES. Its theoretical model is established using the Rayleigh-Ritz method and modal approach. Then the influence of various parameters on the ABH-NES's performance is analyzed. After that, the responses of ABH-NES, NES, and Uniform Beam-NES (UB-NES, using uniform beams to replace ABH beams) are compared. The results show that ABH-NES with the same parameters as the NES has a better and more robust damping effect.

Introduction

Although nonlinear energy sink (NES) solves the frequency dependence of linear tuned-mass-damper (TMD), its damping performance is influenced by the excitation amplitude. Especially for large excitation, the coupled system of the NES may generate an additional high periodic or quasi-periodic solution branch in the frequency band where the excitation frequency is slightly smaller than the main structure's frequency. The high solution branch is also called closed detached response (CDR) [1]. The appearance of CDR means that the damping effect of NES has seriously deteriorated, and continuing to increase the excitation amplitude, the absorber may fail completely. To fix this NES's disadvantage, scholars have done much work [1-5]. References [2, 3] found that nonlinear damping can eliminate CDR while preserving strongly modulated response (SMR). Zang et al. [1] found that increasing the absorber's mass can also improve the performance of the NES under large excitation. Chen et al. [4] utilized piecewise nonlinear stiffness to enhance the performance of the NES under small and large excitations. Zhang et al. [5] found that the increase in the absorber's degrees of freedom can delay the appearance of the CDR.

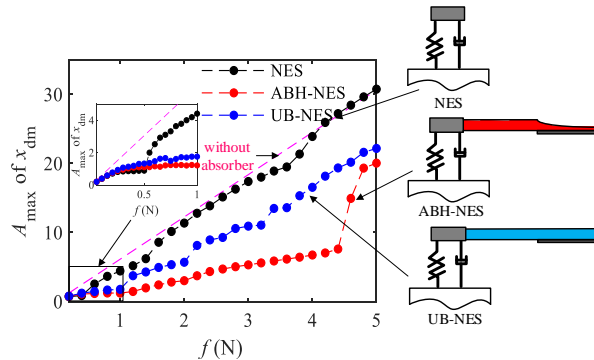


Figure 1: Comparison of NES, ABH-NES, and UB-NES on vibration damping under different excitation amplitude f .

Results and discussion

This research proposes a new NES, ABH-NES, to solve the problem that the conventional NES may fail under large excitation. And through numerical simulation, the following conclusions are obtained: 1. The introduction of the ABH beam has two effects: to delay the CDR's excitation threshold and to reduce the CDR's maximum amplitude. 2. When the second-order frequency of the ABH-NES is close to the main structure frequency, the performance of the ABH-NES may be worse than that of the NES. 3. When the parameters are chosen reasonably, ABH-NES can achieve better and more robust damping performance than NES by using a lighter mass.

References

- [1] Zang J., Yuan T. C., Lu Z. Q., et al. (2018) A lever-type nonlinear energy sink. *J. Sound Vib* **437**: 119-134.
- [2] Starosvetsky Y., Gendelman O.V. (2009) Vibration absorption in systems with a nonlinear energy sink: Nonlinear damping. *J. Sound Vib* **324**:916-939.
- [3] Liu Y., Mojahed A., Bergman L. A., et al. (2019) A new way to introduce geometrically nonlinear stiffness and damping with an application to vibration suppression. *Nonlinear Dynam* **96**:1819-1845.
- [4] Chen J. E., Sun M., Hu W. H., et al. (2020) Performance of non-smooth nonlinear energy sink with descending stiffness. *Nonlinear Dynam* **100**:255-267.
- [5] Zhang Y. F., Kong X. R., Yue C. F., et al. (2021) Dynamic analysis of 1-dof and 2-dof nonlinear energy sink with geometrically nonlinear damping and combined stiffness, *Nonlinear Dynam* **105**:167-190.

Free balls in rotating or non-rotating tracks can mitigate rotor vibration

Michael M. Selwanis*, Mohammed M.Ibrahim*, Mohamed S.Khadr** and Ahmed F. Nemnem ***,*

*Mechanical Engineering Department, Military Technical College (MTC), Cairo, Egypt.

** Mechatronics Department, MTC, Cairo, Egypt. *** Aerospace Engineering Department, MTC, Cairo, Egypt.

* Aerospace and Mechanical Engineering Department, University of Cincinnati, Ohio, USA.

Abstract. Vibration is an undesired response that increases the dynamic loads in rotor systems. The current study demonstrates the effect of a ball moving freely in a circular track on reducing the vibration of an unbalanced rotor, whether due to automatic balancing or energy absorption. We mount the circular track on a ball bearing to prevent its rotation as a part of the primary rotor, proposing a new design for a ball-in-Track Nonlinear Energy Sink (BIT-NES). Thanks to the design that allows fixing the racetrack to the rotor using four screws, we can compare the suppression effect of the new absorber with that of a typical automatic ball balancer (ABB), in which the racetrack rotates as a part of the rotor. For a small radius track, the modified absorber can reduce the rotor vibration at low angular speeds compared to the typical ABB.

Introduction

Rotor vibration resulting from imbalance is a source of uncomfortable operation that reduces the lifetime of rotary machines and possibly damage them. A typical automatic ball balancer (ABB), composed of a ball free to move in a circular track rotating as a part of the primary rotor, can counteract rotor imbalance and mitigates its vibration. The experiments demonstrated that the ABB works effectively at high angular speeds above the rotor critical speed [1], as the ball was located automatically in a proper position to counteract the system imbalance reducing its amplitudes. However, the ABB can result in more vibrations at low angular velocities, because the reaction forces with the track drive the ball away from the desired position. Ball-in-Track Nonlinear energy sink (BIT-NES) is an advanced vibration absorber similar to the ABB in structure but differs in its principle of operation. A recent study [2] has explained how the BIT-NES absorbs the lateral vibration of a prism subjected to airflow in wind tunnel tests. Based on the targeted energy transfer (TET) concept, the ball rotates to absorb energy from the primary system and dissipates it through friction with the NES track walls during rotation. This study proposes a modified design of a BIT-NES, in which the racetrack, integrated on a ball bearing, does not rotate as a part of the rotor shaft. We tested the modified BIT-NES effect in reducing the vibration amplitude of a vertical unbalanced rotor. Moreover, four screws can lock the circular track of the device to resemble a typical ABB. Comparing the suppression effect of the typical ABB to that of the proposed BIT-NES illustrates the impact of the ball track relative rotation with the rotor system.

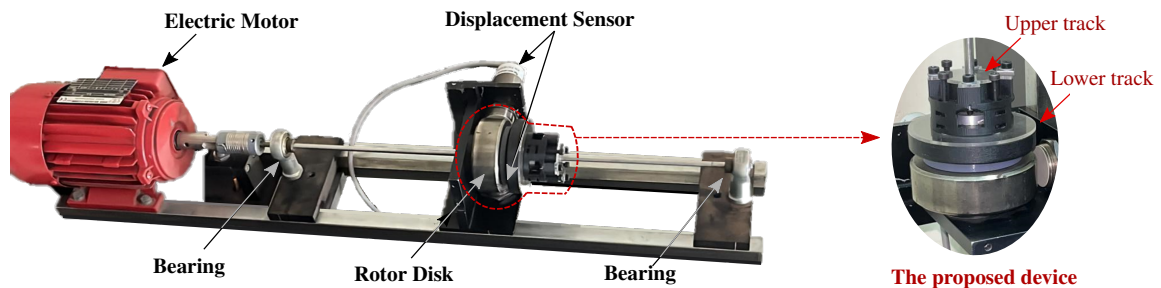


Figure 1: Experimental Setup, simply supported rotor coupled with the proposed BIT-NES.

Results and discussion

The NES main body is coupled with the rotor shaft through a ball bearing in order that we can neglect its rotation. The developed BIT-NES (Fig. 1) has two circular tracks; a racetrack surrounding the ball bearing with a 3 cm mean radius and an upper one with a smaller mean radius of 1 cm. A 2.5 gm ball can occupy one of the two tracks. Besides, the design enables fixing the track with the rotor by four screw bolts to resemble a typical ABB, in which the racetrack rotates as a part of the rotor. The ABB reduces rotor vibration at high angular velocities above the rotor critical speed. However, it increases the amplitudes at lower angular speeds. In the case of a non-rotating track, the BIT-NES of the smaller radius could reduce the rotor amplitudes at low angular speed compared to a typical ABB. While for the larger radius track, the proposed device increases the rotor amplitudes. Furthermore, the ABB is more efficient in mitigating rotor vibrations at higher angular velocities.

References

- [1] Michael Makram et al. (2017) Experimental investigation of ABB effect on unbalanced rotor vibration. JCSMD 7:225-231.
- [2] M. Selwanis, G. R. Franzini, C. Béguin, F. P. Gosselin (2022), How a ball free to orbit in a circular track mitigates the galloping of a square prism. Nonlinear Dyn.

Approximate analytical investigation of the variable inertia rotational mechanism

Nicholas E. Wierschem* and Anika T. Sarkar*

*Department of Civil and Environmental Engineering, University of Tennessee, Knoxville, TN, USA

Abstract. Rotational inertial mechanisms (RIMs) can create large mass effects that can significantly alter the dynamics of the systems they are attached to. While the most commonly considered RIMs are linear devices, other nonlinear RIMs have been proposed. This work considers the variable inertia rotational mechanism (VIRM). Approximate analytical analysis using the harmonic balance method is used to investigate the dynamics of a system with a VIRM attached. The results of this work show that the VIRM introduces an effective softening nonlinearity dependent on input amplitude and VIRM properties.

Introduction

The inerter is a linear rotational inertial mechanism (RIM) that produces a force proportional to the relative acceleration between the mechanism's two terminals. This mechanism is often realized by using a ball-screw or rack and pinion to convert translational motion to the rotational motion of a flywheel with static geometry. Inerters can be advantageous for structural control applications because they typically have relatively small physical mass but can create significant mass effects in structures. The variable inertia rotational mechanism (VIRM) is a nonlinear RIM in which the provided mass effects vary with system response. The VIRM can be realized by modifying the flywheel of a linear RIM such that it includes slider masses that are positioned in connection with springs and guides that allow these sliders to move radially in the flywheel (see Figure 1-Left). With this type of configuration, the mass effects provided by the VIRM to a system increase with increases in the rotational velocity of the flywheel. While numerical analyses have been performed on systems with the VIRM, its fundamental dynamics have not been explored analytically [1]. This work uses the harmonic balance method (HBM) to perform an approximate analytical investigation of the dynamics of this system.

Results and Discussion

The system considered for this analysis is a single-degree-of-freedom (DOF) primary structure with a VIRM attached (see Figure 1-Center). The EOM for this two-DOF combined system with u as the primary system displacement and x as the slider radial displacement are shown in Eq. (1) [2]. In Eq. (1), m_s , c_s , k_s , and $F(t)$ are the primary system's mass, damping, stiffness, and load, respectively; the VIRM properties of I_0 , α , n , m_{sd} , and c_{sd} , are the static rotational inertia, factor relating the linear displacement to number of flywheel rotations, number of sliders, slider mass, and slider damping, respectively, $\dot{\theta}$ is the VIRM rotational velocity, and $F_{bsd}(x)$ is the slider spring force. For this analysis, $F_{bsd}(x)$ includes a main linear stiffness zone and higher stiffness penalty zone to prevent excessive slider displacements. With the HBM, a harmonic force with a given amplitude was used as the load and the response of the system was assumed to be harmonic with unknown amplitude and the same frequency as the load. By plugging in this assumed response into the system EOM and neglecting the higher-order terms, the approximate amplitude of the assumed system response can be solved. An example of the results of the HBM is seen in Figure 1-Right, which shows the response amplitudes resulting from this analysis with different loading frequencies. These results show a softening nonlinearity and bifurcation; however, the stability of each solution would need to be assessed. While softening is still seen, the VIRM properties and load amplitude impact the bending behaviour of the resulting HBM solution.

$$\begin{aligned} m_s \ddot{u} + I_0 \alpha^2 \ddot{u} + 2n m_{sd} x \dot{x} \alpha^2 \dot{u} + n m_{sd} x^2 \alpha^2 \ddot{u} + c_s \dot{u} + k_s u &= F(t) \\ m_{sd} \ddot{x} - m_{sd} x \alpha^2 \dot{u}^2 + F_{bsd}(x) + c_{sd} \dot{x} &= 0 \end{aligned} \quad (1)$$

This research is supported by NSF Grant No. 1944513. All findings and conclusions are the authors' alone.

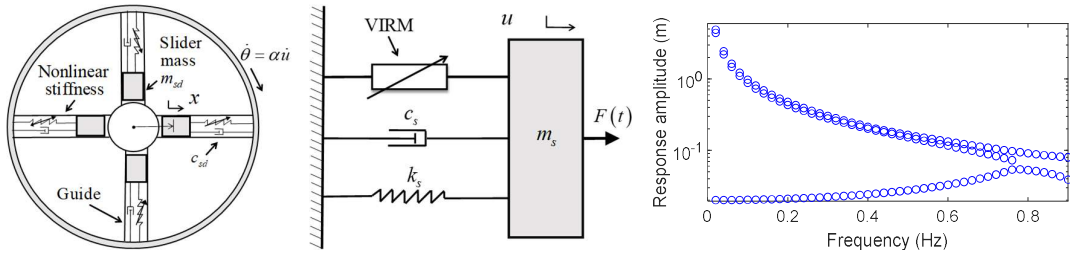


Figure 1: (Left) VIRM flywheel, (Center) Primary system with VIRM, (Right) Example HBM results showing softening behavior

References

- [1] Xu T, Liang M, Li C, Yang S. (2015) Design and analysis of a shock absorber with variable moment of inertia for passive vehicle suspensions. *J Sound Vib*; **355**:66–85. <https://doi.org/10.1016/j.jsv.2015.05.035>.
- [2] Sarkar AT, Wierschem N. (2022) Optimization of the Variable Inertia Rotational Mechanism using Machine Learning. Proceeding 8th World Conf. Struct. Control Monit., Orlando, FL, USA.

The optimum inerter based isolation systems for dynamic response mitigation of multi degree of freedom systems

Sudip Chowdhury*, Arnab Banerjee* and Sondipon Adhikari**

*Civil Engineering Department, Indian Institute of Technology Delhi

**James Watt School of Engineering, The University of Glasgow, Glasgow, Scotland

Abstract. The inerter based isolation systems (Inerter-BI) to control the structural responses of multi-storey buildings, the conceptualized versions of multi degree of freedom systems, are introduced in this paper. H₂ optimization method implements to derive exact closed-form expressions for the optimal design parameters of Inerter-BI. The linear and nonlinear stiffnesses are applied for the superstructural stiffness and the stochastic linearization method applies to linearize each nonlinear element of governing equations of motion. The frequency domain responses are determined through transfer function formation analytically. A numerical study performs with earthquake base excitations to evaluate each isolator's displacement and acceleration reduction capacities using the Newmark-beta method. The dynamic response reduction capacities of Inerter-BI are significantly 71.28 % and 93.61 % superior to dynamic response reduction capacities classical base isolator (CBI) subjected to harmonic and random base excitations.

Introduction

Passive vibration control devices mitigate the structures' dynamic responses to prevent structural damage during natural disasters such as earthquakes and storms. The base isolators [1] are one of the widely applied passive vibration control devices due to their superior vibration reduction capacity. Recently, inerters [2] have been installed inside conventional isolators to increase their vibration reduction capacity without affecting the static mass, stiffness, and damping. However, the inerter and negative stiffness inerters are not applied to the conventional base isolators to mitigate multi-storey building's dynamic responses. The exact closed-form expressions for dynamic responses and optimal closed-form solutions also do not exist in any literature. Therefore, a research scope has been identified from the existing state of the art. To address this research scope, the inerter based isolation systems are introduced in this paper. The governing equations of motion for multi-storey buildings isolated by Inerter-BI are derived using Newton's second law and expressed as

$$m_1 \ddot{y}_1 + (m_1 + m_{nb} + m_{in}) \ddot{y}_{nb} + c_{nb} \dot{y}_{nb} + k_{nb} y_{nb} = -(m_1 + m_{nb}) \ddot{u}_g$$

$$[M] \{\ddot{y}_s\} + [C] \{\dot{y}_s\} + [K] \{y_s\} = -[M] \{1\} (\ddot{u}_g + \ddot{y}_{nb})$$

Results and discussion

From Figure 1, a higher inerter mass ratio recommends to design optimum Inerter-BI.

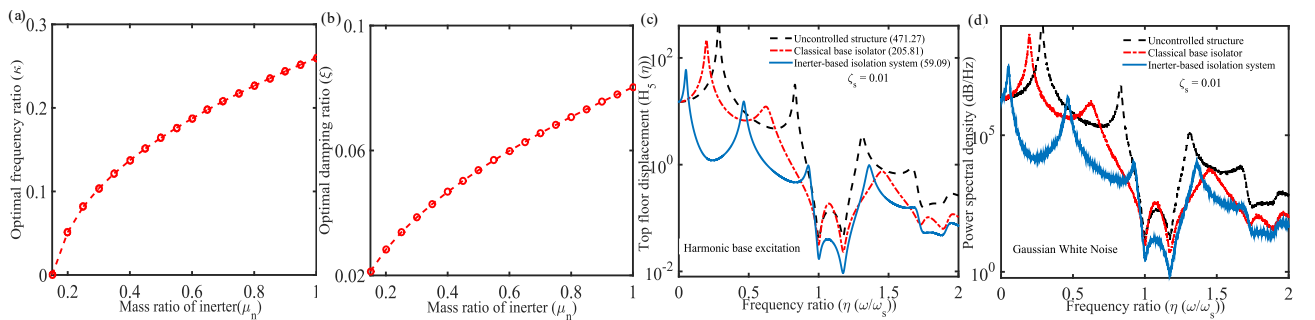


Figure 1: The variation of optimal (a) frequency ratio and (b) damping ratio versus mass ratio of inerter of inerter based isolation system. The variations of displacement responses of multi-storey buildings isolated by classical base isolator and inerter based isolation system subjected to (c) harmonic and (d) random white noise versus frequency ratio.

The variations of CBI and Inerter-BI controlled multi-storey building's dynamic responses have been shown in Figure 1 (c) and Figure 1 (d). The dynamic response reduction capacity of Inerter-BI is significantly 71.28 % superior to CBI. In addition, the maximum dynamic responses of CBI and Inerter-BI controlled structures are determined as 5.53×10^8 dB/Hz and 3.53×10^7 dB/Hz. Accordingly, the dynamic response reduction capacity of Inerter-BI is significantly 93.61 % superior to CBI.

References

- [1] Chowdhury, Sudip, and Arnab Banerjee. (2022) The exact closed-form expressions for optimal design parameters of resonating base isolators. *Int. J. of Mech Sci* 107284.
- [2] Smith, Malcolm C. (2002) Synthesis of mechanical networks: the inerter. *IEEE Trans on automatic cont* 1648-1662.

Vibro-impact NES: Nonlinear mode approximation using the multiple scales method

Balkis Youssef and Remco I. Leine

Institute for Nonlinear Mechanics, University of Stuttgart, Stuttgart, Germany

Abstract. The aim of the paper is to derive a *closed-form* approximation for a nonlinear mode of a system with vibro-impact NES. Hereto, the multiple scales method is used to analyze the dynamical behavior of a linear oscillator coupled with a vibro-impact nonlinear energy sink (VI NES). The steady state response in the vicinity of 1:1 resonance is approximated. The resonance frequency of the examined nonlinear system for different excitation levels is estimated and the corresponding backbone curve is identified. The theoretical findings agree with the simulation results and represent a possible new approach for system identification.

Introduction

A nonlinear energy sink (NES) is a structural element, which is attached to a primary structure to absorb and mitigate the vibration energy, when the structure is excited within a certain frequency range. To assure an optimal design of the NES, many studies (e.g. [4, 3]) have been conducted to understand its working principle, being strongly related to the theory of nonlinear modes (NM). Different numerical approaches, including control-based methods, have been applied to approximate NMs of nonlinear vibrating structures. These methods are mainly based on Rosenberg's definition for nonlinear modes and rely on the invariance property of the NM in the configuration space under the system's flow [1]. In this work, the simplest case of periodic motion of the VI NES is considered, namely 1:1 resonance with 2 symmetric impacts per period. The method of multiple scales is applied to approximate the solutions and to derive a closed-form expression for the backbone curve. In this context, the backbone curve is defined as the curve connecting the maximas of the frequency response functions for different excitation levels [2].

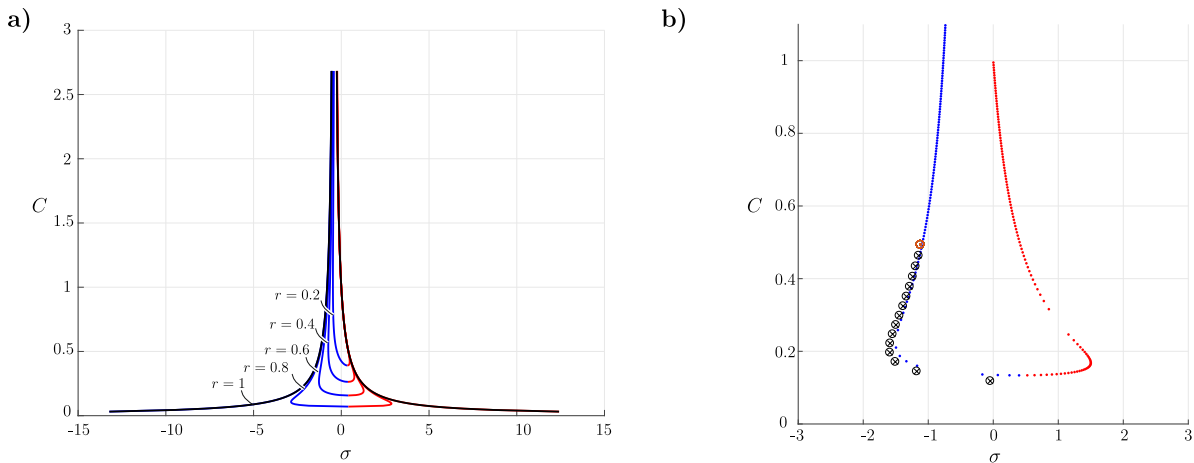


Figure 1: a) Backbone curves for different values of r . b) Backbone curve for $r = 0.65$. The red point on the left branch represents the point attained with PLL. The black crossed circles correspond to the estimated values from the free resonant decay response.

Results and discussion

The developed analytical treatment from [3] is pushed further to extract the modal properties of the studied system. A closed-form description of the system's considered backbone curve is derived and numerically verified. Figure 1 depicts the obtained curves for different values of the coefficient of restitution r .

In a second step, a verification of the obtained modal lines is pursued via a numerical approach. The numerical identification is achieved through the system's resonance decay response combined with a Phase-Locked-Loop (PLL). At this stage, the backbone curve is obtained by means of the decaying free resonant response. The estimated modal line is shown in Figure 1, depicting the numerically identified stable branch of the backbone curve and confirming the analytical results.

References

- [1] G. Kerschen, M. Peeters, J.C. Golinval, A.F. Vakakis (2009) Nonlinear normal modes, Part I: A useful framework for the structural dynamicist. *J. Mechanical Systems and Signal Processing* **23**:170-194.
- [2] S. Peter, R. Riethmüller, R.I. Leine (2016) Tracking of backbone curves of nonlinear systems using phase-locked-loops. *Nonlinear Dynamics* **1**:107-120.
- [3] O.V. Gendelman, A. Alloni, (2015) Dynamics of forced system with vibro-impact energy sink. *J. of Sound and Vibration* **358**:301-314.
- [4] T. Li, S. Seguy, A. Berlioz (2016) Dynamics of cubic and vibro-impact nonlinear energy sink: analytical, numerical, and experimental analysis. *J. Mechanical Systems and Signal Processing* **138**:031010.

Vibration Damping in Fiber-Reinforced Bistable Composites with Magnetic Particles

Alessandro Porrari* and Giulia Lanzara*

*Department of Civil, Informatics and Aerospace Engineering Technologies, University of Rome, RomaTre, Roma, Italy

Abstract. Today one of the greatest engineering challenges in smart materials is on the development of structural morphing materials. Multistable composites have the intrinsic ability to vary their shape but they have some weaknesses that limit their usage in structural applications. For instance, bistable composites lose rigidity while snapping from a configuration to the other and their transition to the new configuration is coupled with undesired vibrations. This paper focuses on solving such criticalities by inserting magnetic particles within the composite matrix. The exposure of such a bistable composite to a magnetic field, allows to dampen these vibrations and increase the overall composite stiffness.

Introduction

Multistable composite laminates have the uniqueness of being characterized by multiple equilibrium configurations, each with a different geometric shape. Shape changes in bistable composites need the actuation of an external force or proper actuation mechanisms [1]. The prediction of the stable shapes and the understanding of the snapping mechanism of asymmetric thin laminates has been carried out by many researchers [e.g. 2] by extending the Classic Laminate Theory while analytical models for predicting the snap-through forces and moments were developed by Dano and Hyer [3,4]. The models were based on Rayleigh–Ritz method also with higher order polynomials [5]. In general, morphing materials should transit smoothly and in a controlled manner from a shape to the other. Unfortunately, bistable composites are affected by undesired vibrations once the material has reached its alternate stable configuration. The most advanced damping approaches in the literature use nanoparticulates to activate exotic stick-slip mechanisms. Such approaches are intrinsically passive. Active solutions instead have the potential to be activated by means of external energy sources.

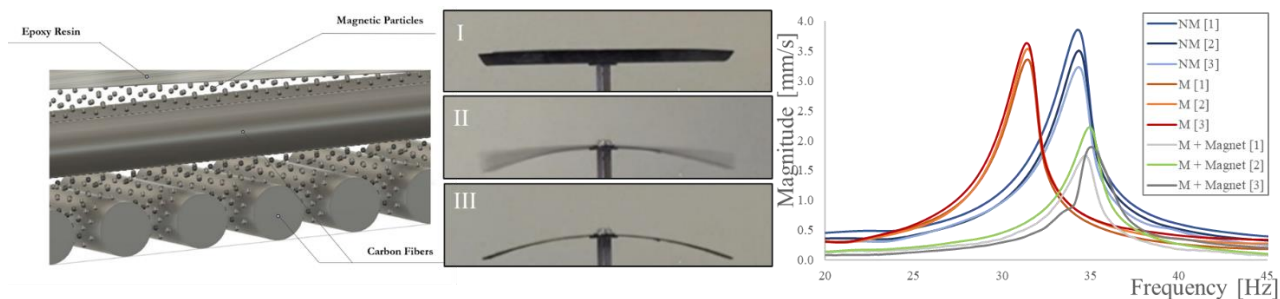


Figure 1: (Left) Schematic of the composite design; (Center) Experimental validation of the vibrations induced in a composite after shapping; (Right) Comparison of the FFT response of a non-magnetic composite (NM), of a micro-composite in its passive state (M) and of a micro-composite exposed to a magnetic field (M+magnet)

A bi-stable magnetic composite and its frequency tunability

This paper aims to investigate a novel bistable composite design in which carbon fibers are embedded in a magnetic micro-composite matrix (schematic in Figure 1). The addition of iron micro-particles allows to enhance the transition from an equilibrium state to the other by damping out vibrations through a passive and active (hybrid) approach. Magnetic particles can in fact work as passive and active fillers, in the latter case thanks to their interaction with an external field.

It is shown that the mass increase can indeed dominate with respect to pure passive stiffening which results in a reduction of resonance frequency, but at the same time the interaction with the magnetic field allows to control finely the material rigidity. It is also demonstrated that such interaction can control the undesired vibrations when a bistable composite snaps from a stable configuration to the other. This work paves the way to composites that can change shape and rigidity in a controlled manner.

References

[1] Schultz M.R. (2008) A concept for airfoil-like active bistable twisting structures. *J Intell Mater Syst Struct*;19(2):157–69.
[2] Hamamoto A, Hyer M.W. (1987) Non-linear temperature-curvature relationships for unsymmetric graphite-epoxy laminates. *Int J Solids Struct*;23:919–35.
[3] Dano M.-L., Hyer M.W. (1996) The response of unsymmetric laminates to simple applied forces. *Mech Compos Mater Struct*;3:65–80.
[4] Dano M.-L, Hyer M.W. (2002) Snap-through of unsymmetric fiber-reinforced composite laminates. *Int J Solids Struct*;39:175 98.
[5] Pirrera A., Avitabile D., Weaver P. (2010) Bistable plates for morphing structures: a refined analytical approach with high-order polynomials. *Int J Solids Struct*; 47:3412–25.

Magnetic Field and Ferrite Particles Interaction for Membranes with Augmented Shock-Absorption Capability

Stefania Fontanella*, Ginevra Hausherr*, Shiela Meryl Cumayas, Antonio Loisi and Giulia Lanzara**
*Engineering Department of Civil, Computer Science and Aeronautics Technologies, University of Rome, RomaTre, Italy

Abstract. Managing vibrations, dynamic responses and damping is one of the challenges of engineering design. The aim of this work is to study the use of damping through nanocomposite materials with a main focus on shock-absorption. The new frontiers of research on multifunctional materials are rapidly moving towards the generation of new nanocomposites based on magnetic nanoparticles that play the role of fillers incorporated in a polymeric matrix. In such materials the interaction between the particles during manufacturing and the interaction of the embedded particles with a surrounding magnetic field is of great importance for the improvement of the performance to obtain small size dampers.

Introduction

One of the main problems in engineered devices and structures is vibration damping. In general shock absorbers, convert the kinetic energy into another form of energy. There are two types of active and passive devices [1]. In the active case, piezoelectric materials generate mechanical forces that oppose the vibrations of the source, instead passive devices, are more complex because they require the sensors feedback and command controls. Generally, piezoelectric elements are integrated with an external shunt circuit, which is heavy and bulky. In recent decades, the interest in the use of composite materials has increased greatly. Recent developments in the field of composites involve the application of nanoscale microparticles in a polymer matrix, which bring numerous improvements in mechanical, thermal, acoustic, flame retardant, and vibration damping properties. Magnetic nanocomposites are among the most innovative materials in recent years because they enable a wide range of functions [2]. In general, the fabrication of nanocomposites is challenging because the material properties and performance are greatly affected by slight variations in the distribution of nanoparticles in the matrix. The fabrication process usually consists of several steps. A nanofiller powder is directly sonicated with a polymer solution, or if such a solution is too viscous, it is first sonicated with solvents. Sonication is also crucial because it affects the final distribution of the nanoparticles, which should be very uniform for optimal material properties. For magnetic particles, this step becomes even more complex because these particles are subject to significant mutual interaction due to their dipole moments. In a fully manufactured nanocomposite, the interaction between particles and the magnetic field is influenced by their relative configuration within the polymer chains.

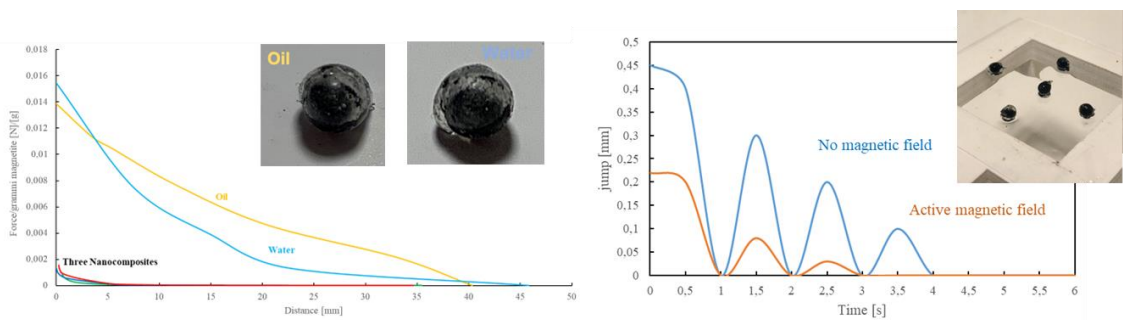


Figure 1: Comparison of the interacting force of various magnetic sphere designs; Damping film with and without a magnetic field.

Objective and results

The goal of this work is a complete understanding of the interaction between individual particles and the interaction of an enclosed group of particles with a magnetic field, combined with the study of shock absorption of ultra-light thin films. This work showed the possibility to improve and modulate, the stiffness and damping coefficient of a silicone membrane, thanks to the inclusion of oil spheres with free magnetite particles. The study, of individual spheres and their interaction with an external magnetic field, allowed to demonstrate that magnetic particles, that are free-to-move inside a shell, have an enhanced interaction with the field than pure nanocomposite spheres. The development of highly performing spheres allowed to create membranes that are greatly able to damp-out vibrations once exposed to a magnetic field also under impulsive actions, leading to the novel concept of an ultra-light membrane that can work as shock absorber.

References

[1] Marshall J. Leitman & Piero Villaggio, The Dynamics of a Membrane Shock-Absorber, <https://doi.org/10.1080/15397730600860895>.
[2] Kim Y., Yuk H., Zhao R., Chester S. A., Zhao X. (2018) Printing ferromagnetic domain for untethered fast-transforming soft materials. Nature 558: 274-279.

Variable Length Control of a Planar Pendulum with Time Averaged Constant Cable Length

H. Joseph*, M. Lanzerotti** and W. Lacarbonara*

*Dipartimento Ingegneria Strutturale e Geotecnica, Sapienza University of Rome, Rome, Italy ORCID #

**Department of Electrical and Computer Engineering, Virginia Polytechnic Institute and State University, Blacksburg, VA. 24061. U.S.A., ORCID # 0000-0001-7802-1117

Abstract. This work proposes the control of oscillations of a pendulum while maintaining a net constant length of the pendulum where the average is taken over several oscillations. As in prior work, the pendulum is shortened at the end of the swing and lengthened in the middle of the swing [1]. In this work, the pendulum is lengthened the same amount as it is shortened so that the net pendulum length remains unchanged as averaged for several oscillations. The shortening and lengthening can be accomplished with uniform shortening and lengthening and also with a hoisting control method with variable cable length [1].

Introduction

We propose a control method to stabilize a payload in medical evacuation rescues [1]-[5]. We consider an operational aspect of medical evacuation (MEDEVAC) rescues with the aim to stabilize the swing angle of an oscillating rescue while maintaining the cable length when averaged over multiple oscillations [1].

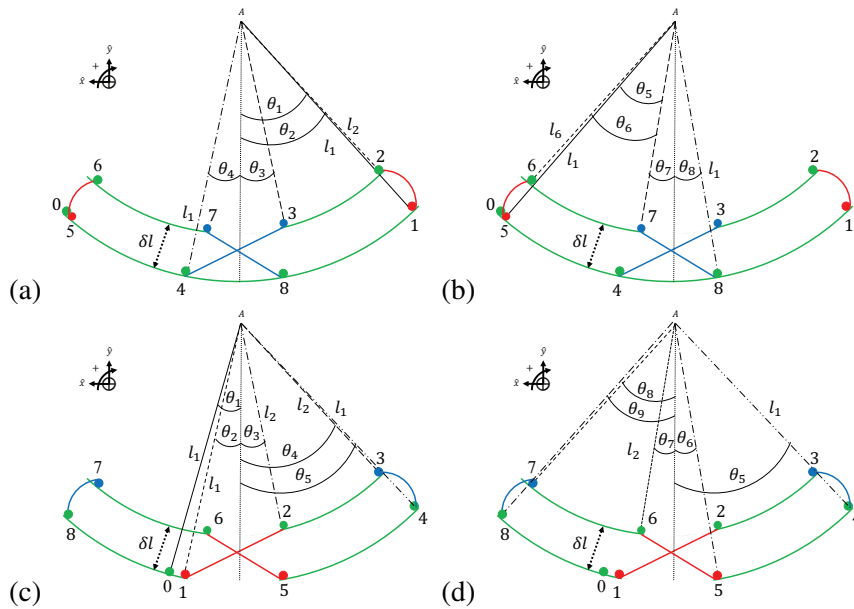


Figure 1: Method to decrease the swing angle of a pendulum while maintaining constant length l_1 in (a) steps 1-4 and (b) steps 5-8; Method to increase swing angle of a pendulum while maintaining constant length l_1 in (c) steps 1-4 and (d) steps 5-8.

Results and Discussion

The proposed method considers the planar pendulum under gravity, g , with the second order nonlinear equation of motion such that $\ddot{\theta} + 2\frac{\dot{l}(t)}{l(t)}\dot{\theta} + \frac{g}{l(t)}\theta = 0$. The length of the cable can be shortened at the ends of the swing (Fig. 1(a)). Some choices of time dependence are: (i) $l(t) = l_0 - v_s t$; (ii) $l(t) = l_a e^{-r(t-t_a)} + l_b - l_b e^{-r(t-t_a)}$ with $l_a > l_b$ (exponential shortening); (iii) $l(t) = l_a + (l_b - l_a) \left[\frac{1}{2} + \frac{1}{2} \tanh(r(t-t_{a,b})) \right]$ with $l_a > l_b$. The cable can also be lengthened at the middle of each swing (Fig. 1(b)). Some choices of time dependence are: (iv) $l(t) = l_0 + v_l t$; (v) $l(t) = l_e e^{-r(t-t_e)} + l_f - l_f e^{-r(t-t_e)}$ with $l_e > l_f$ (exponential lengthening); (vi) $l(t) = l_e + (l_f - l_e) \left[\frac{1}{2} + \frac{1}{2} \tanh(r(t-t_{e,f})) \right]$ with $l_e < l_f$.

References

- [1] Morock, A., Arena, A., Lanzerotti, M., Aldhizer, T., Capps, J., Lacarbonara, W., "Variable length sling load hoisting control method", in Book of Abstracts, *Second Intl. Nonlinear Dynamics Conf. (NODYCON) 2021*, Rome, Feb. 16-19, 2021, pp. 233-242, Nodys Publications.
- [2] Liu, David T., "In-flight stabilization of externally slung helicopter loads". *USAAMRDL Tech. Rep. 73-5*. Northrop Corp., Electr. Div., Hawthorne, CA (1973).
- [3] Cicolani, L.S., Ivler, C., Ott, C., Raz, R., Rosen, A., "Rotational Stabilization of Cargo Container Slung Loads," preprint.
- [4] Arena, A., Lacarbonara, W., Casalotti, A., "Payload oscillations control in harbor cranes via semi-active vibration absorbers: modeling, simulations and experimental results," *Procedia Engineer*, vol. 199, pp. 501-509, 2017.
- [5] Bockstedte, A., Kreuzer, E., "Crane Dynamics with Modulated Hoisting," *Proc Apply Math Mech.* 5, 83-84 (2005).

Hoist Stabilization Design Method

David Reineke*, Duy Nguyen*, Luyi Tang*, M. Lanzerotti* and W. Lacarbonara**

*Department of Electrical and Computer Engineering, Virginia Polytechnic Institute and State University, Blacksburg, VA. 24061. U.S.A., ORCID # 0000-0001-7802-1117

**Dipartimento Ingegneria Strutturale e Geotecnica, Sapienza University of Rome, Rome, Italy ORCID #

Abstract. The goal of this project is to design and model a mechanical stabilization system for low-mass sling loads in medical evacuation (MEDEVAC) helicopter rescues. The additional goal for this project is to create a software simulation of the system. The current project’s final purpose is to test and characterize the model system. There are three target specifications for this project. The first specification outlines the two vertical hoist speeds of the lift at 0.381 m/s and 0.501 m/s. The second specification outlines the stabilization angle from a maximum angle of 15 degrees to less than 5 degrees. Finally, the third specification outlines the two initial cable lengths of 7.9248 meters and 32.3 meters.

Introduction

In a medical evacuation (MEDEVAC) helicopter rescues, the goal of any medical evacuation is to get the patient safely into the helicopter and then to a medical facility as quickly as possible [1]. This project aims to design and model a mechanical stabilization system for low-mass sling loads in medical evacuation (MEDEVAC) helicopter rescues [1]-[5]. The optimal way to achieve this is to have the patient hoisted up into the helicopter while it is moving [4]. This, however, is difficult as the patient is being swung in an oscillating pattern, similar to a pendulum, and would need to be stabilized to not cause further injury or harm. The idea proposed to solve this is to have the sling be hoisted and lowered at various velocities to compensate for the change in angular velocity [5]. This would be achieved by having a device at the helicopter that would measure the rate and angle of oscillation and, using that information, adjust the velocity at which the sling is being hoisted. By having a device that can measure the current angle of the sling as well as control the velocity of hoisting the patient, the swinging motion can be reduced or eliminated. Our model assumes the helicopter is in a steady hover.

Bill of Materials for Design Alternative 1: Encoder and Gyroscope	
Item	Cost (\$)
Encoder and Motor Bundle (None) Bemonoc	\$15.99
Buttons (JF-0020) QTEATAK	\$5.99
Switch (MTS-101-F1) DAIERTEK	\$7.99
Motor Driver (L298N) HiLetgo	\$11.49
Arduino Mega (A000067) Arduino	\$38.93
Boost-Buck Convertor (LM2596) Atmsinc	\$9.29
DC Adapter (12V2A-03081947) DTECH	\$11.88
OLED Module (U602602) UCTRONICS	\$6.99
RUNCL Braided Fishing Line	\$17.99
BWT901 High-Precision Gyroscope	\$45.99
Current Estimated Total	\$172.53

Figure 1: Build of materials.

Results and Discussion

A requirements analysis of the project specifications was performed, and the target specifications were determined. First, a length of 46 feet was determined to be the maximum length a lift would be performed. Second, the maximum weight of the sling was identified at 600 pounds. The lift system has two possible speed settings: slow and fast [4]. The angle takes on a maximum value of 15 degrees with a goal of 5 degrees. The design choice (Fig. 1) was determined to be using the encoder as well as a gyroscope as this allowed for more precise data to be generated and sent to the controller. Building a custom controller was found to be more efficient for the team’s purposes as it allows for more customization.

References

[1] Liu, David T., “In-flight stabilization of externally slung helicopter loads”. *USAAMRDL Tech. Rep.* 73-5. Northrop Corp., Electr. Div., Hawthorne, CA (1973).

[2] Bockstedte, A., Kreuzer, E.: Crane Dynamics with Modulated Hoisting. *Proc Apply Math Mech.* 5, 83-84 (2005).

[3] T. Aldhizer, A. Morock, K. Hughes, M. Lanzerotti, S. Lintelman, S. Christoff, J. Capps, “Suspended Load Swing Stabilization,” *IEEE Int. STEM Educ. Conf. (ISEC)*, Aug. 1, 2020, Princeton, NJ. Virtual.

[4] A. Morock, T. Aldhizer, M. Lanzerotti, A. Arena, W. Lacarbonara, J. Capps, “Stabilization Environment for Swing Stabilization and MEDEVAC hoists,” *AIAA Aviation Forum*, AIAA 2021-2430, August 2-6, 2021. Virtual. <https://doi.org/10.2514/6.2021-2430>.

[5] Morock, A., Arena, A., Lanzerotti, M., Aldhizer, T., Capps, J., Lacarbonara, W., “Variable length sling load hoisting control method”, in *Book of Abstracts, Second Intl. Nonlinear Dynamics Conf. (NODYCON)* 2021, Rome, Feb. 16-19, 2021, pp. 233-242, Nody Publications.

Attenuating nonlinear effects of pendulum tuned mass damper by an isochronous spring

Kai Xu*, Xugang Hua* and Walter Lacarbonara**

*College of Civil Engineering, Hunan University, Changsha, China,

** Department of Structural and Geotechnical Engineering, Sapienza university of Rome, Rome, Italy

Abstract. An isochronous spring is introduced in a pendulum tuned mass damper (PTMD), with the aim of attenuating the detrimental nonlinear effects of PTMDs on vibration control. By letting the third-order term of nonlinear resilience generated by the pendulum and the isochronous spring be opposite, the nonlinear pendulum contribution can be greatly reduced. The frequency response function (FRF) of the primary structure is obtained via the harmonic balance method (HBM) combined with arc-length continuation. The results show that with a proper isochronous spring design, the PTMD response can be tailored to be linear up to 0.85 radians (about 49 degrees), which is much larger than the “linear” oscillation amplitude of the PTMD without the isochronous spring, thus ensuring the PTMD control performance also at large angles.

Introduction

Pendulum tuned mass dampers have been widely used in high-rise buildings to attenuate wind/seismic-induced vibrations^[1]. Usually, PTMDs are treated as linear assuming small oscillation amplitude, while their nonlinear behaviour may have detrimental effects on the control performance when the controlled primary structure is subjected to strong excitations^[2]. Although several studies addressed the PTMD with its nonlinearity^[3], the external excitations are uncertain thus posing a challenge when the design targets a specific excitation intensity. Therefore, in this paper we propose to cope with the nonlinear effects of PTMDs introducing an isochronous spring, referred to as IE-PTMD, which is properly designed to attenuate the PTMD nonlinear effects at large rotation angles.

Problem formulation

A single-degree-of-freedom (SDOF) primary structure is characterized by mass m_1 , stiffness k_1 and damping coefficient c_1 , as shown in Figure1(a). Additionally, a PTMD with tip mass m_θ and damping coefficient c_θ is suspended by a pendulum rod with length l . At the same time, an isochronous spring with original length l_0 and stiffness k_2 is hinged between the pendulum rod and the primary structure, and the distance between the lower hinged and suspended points is denoted by l_2 . In addition, f , ω and t are the excitation amplitude, frequency, and time, respectively. The equations of motion can be obtained using the Lagrangian as:

$$m_1 \ddot{q}_1 + c_1 \dot{q}_1 + k_1 q_1 + m_\theta \ddot{q}_1 + m_\theta l (\ddot{\theta} \cos \theta - \dot{\theta}^2 \sin \theta) = f \cos(\omega t)$$

$$m_\theta l^2 \ddot{\theta} + m_\theta l \cos \theta \ddot{q}_1 + c_\theta l^2 \dot{\theta} + \left[m_\theta g l \sin \theta + k_2 \frac{l_2 \sin \theta (l_0 - \sqrt{[l_0 - l_2(1 - \cos \theta)]^2 + (l_2 \sin \theta)^2}) (l_0 - l_2)}{\sqrt{[l_0 - l_2(1 - \cos \theta)]^2 + (l_2 \sin \theta)^2}} \right] = 0 \quad (1)$$

The squared term in Eq. (1) is expanded in Taylor series, and the third-order term is set to 0, so as to eliminate the main nonlinear term on the system response. The HBM combined with arc-length continuation is utilized to solve Eq. (1) and obtain the FRFs of the primary structure and pendulum, as shown in Figure1(b) and 1(c), respectively. It is found that, with the increase of excitation amplitude, the peak in the FRF of the primary structure with the attached PTMD increases significantly without exhibiting the two equal peaks corresponding to the in- and out-of-phase modes. On the other hand, the IE-PTMD has approximately two equal peaks, indicating much better control performance and nonlinearity attenuation capability. The FRFs of the pendulum have the same trend as that of the primary structure, and the rotation angle can reach 0.85 radians for IE-PTMD while without strong nonlinearities.

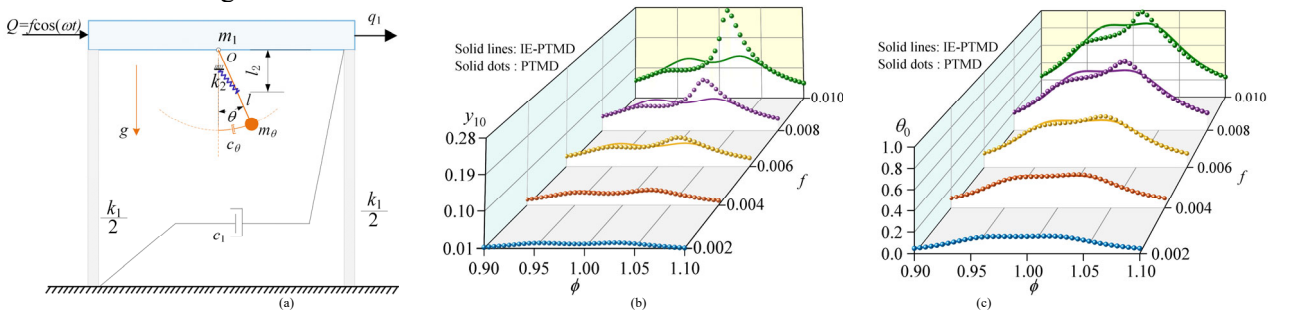


Figure 1: (a) Schematic of IE-PTMD attached to a SDOF primary structure, (b) FRF comparison of primary structure with/without isochronous spring and (c) FRF comparison of pendulum.

References

- [1] Elias, S., and Matsagar V. (2017) Research developments in vibration control of structures using passive tuned mass dampers. *Annu. Rev. Control* 44 (Jan): 129–156
- [2] Xu K., Hua X. G., and Lacarbonara W. et al. (2021) Exploration of the Nonlinear Effect of Pendulum Tuned Mass Dampers on Vibration Control, *J. Eng. Mech* 147(8): 04021047.
- [3] Brzeski, P., Pavlovskaja E., and Kapitaniak T. et al (2015) The application of inerter in tuned mass absorber *Int. J. Non-Linear Mech.* 70 (10): 20–29.

Vibrational Resonance of a Driven Charged Bubble Oscillator

U. E. Vincent^{†*}, O. T. Kolebaje^{†**}, B. E. Benyeogor[†] and P. V. E. McClintock^{*}

[†]Department of Physical Sciences, Redeemer's University, Ede, Nigeria, ORCID 0000-0002-3944-726X

^{*}Department of Physics, Lancaster University, Lancaster, United Kingdom, ORCID 0000-0003-3375-045X

^{**}Department of Physics, Adeyemi College of Education, Ondo, Nigeria, ORCID 0000-0002-7557-0257

Abstract. Vibrational resonance (VR) in a modified Rayleigh-Plesset oscillator for a charged bubble oscillating in a compressible fluid while driven by an amplitude-modulated acoustic force has been investigated. A novel equation of motion for the charged bubble as an oscillator moving in a potential well was obtained. It is shown that the bubble moved in a single-well potential when uncharged, while it can move in varieties of potential wells when charged. In the presence of an amplitude-modulated acoustic wave, an increase in the quantity of charge leads VR, i.e. an increased response of the bubble to the acoustic wave. Furthermore, different patterns of VR can occur with variations of other cavitation properties.

Introduction

The phenomenon of vibrational resonance (VR) [1] was first introduced in 2000 by Landa and McClintock [1]. It is the amplification of a weak signal input by means of high-frequency driving signal, whose frequency $\Omega \gg \omega$, where ω is the frequency of the weak signal. Due to its numerous potential applications, VR has been receiving considerable research attention in the last two decades in many different field, including bubble dynamics [2, 3]. Studies of VR in bubble oscillators are relatively new and were investigated only for uncharged bubble oscillator moving in an incompressible liquid [3]. Research interests in bubble oscillation and cavitation are largely motivated by their applications in fluid engineering (e.g. industrial waste water treatment), sonochemistry and medical diagnostics and therapy. When irradiated by acoustic driving fields, electrostatic charges can be deposited on the bubble surface, thereby negatively charging the bubbles due to the migration of ionic charge from the fluid onto the bubble surface [4, 5]. The effects of charge on bubble dynamics is a longstanding problem, but has not been investigated in relation to VR phenomenon, to best of our knowledge.

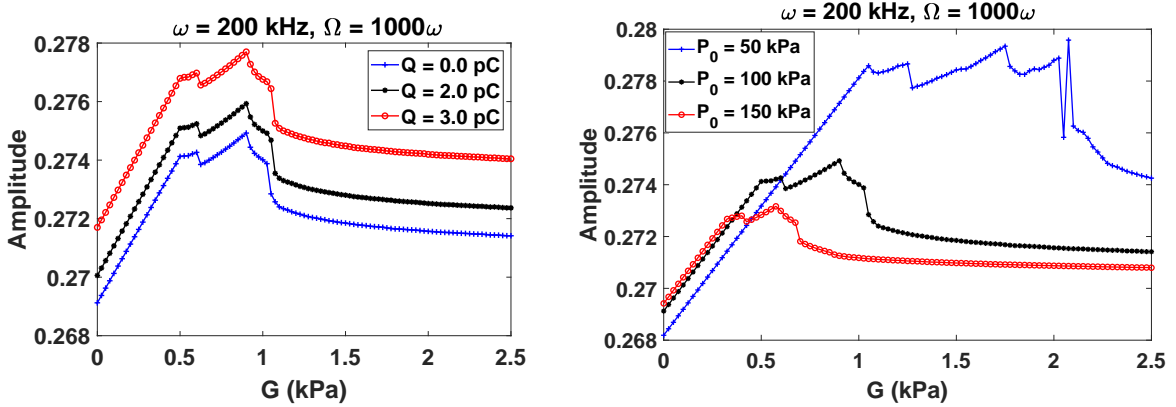


Figure 1: The response amplitude (A) as a function the amplitude of the modulation G for three different quantities of the charge, Q .

Results and discussion

Vibrational Resonance was numerically investigated using Matlab Simulink model of the charged bubble oscillator. The main effect of charge on VR is shown in Figure 1 for different values of the quantity of charge, $Q = 0, 2.0 \text{ pC}$ and 3.0 pC . An increase in Q leads to an increased response of the bubble to the amplitude modulation, namely, enhancement of VR. Furthermore, in the presence of electrostatic charge, variation of other cavitation properties impacts on the occurrence of VR in different pattern, either by enhancing VR or suppressing it - implying that the cavitation properties can be exploited in the presence of charge to control the bubble dynamics for the desired application.

References

- [1] Landa P. S. and McClintock P. V. E. (2000) Vibrational resonance. *J. Phys. A: Math. & Gen.* **33**: L433.
- [2] Vincent U. E., McClintock P. V. E., Khovanov I. A. and Rajasekar S. (2021) Vibrational and stochastic resonance in driven nonlinear systems. *Phil. Trans. R. Soc. A* **379**:20210003.
- [3] Omoteso K. A., Roy-Layinde T. O., Laoye J. A., Vincent U. E. and McClintock P. V. E. (2021) Acoustic vibrational resonance in a Rayleigh-Plesset bubble oscillator. *Ultrason. Sonochem.* **70**:105346.
- [4] Lee Hyang-Bok and Choi Pak-Kon (2020) Electrification of Sonoluminescing Single Bubble. *J. Phys. Chem. B* **124**:3145.
- [5] Hongray T., Ashok B. and Balakrishnan J. (2015) Effect of charge on the dynamics of an acoustically forced bubble. *Nonlinearity* **27**:1157.

Nonlinear control of friction-induced vibrations by using cascade architecture

Lyes Nechak* and Pascal Morin **

* Laboratoire de Tribologie et Dynamique des Systèmes, UMR CNRS 5513, École Centrale de Lyon, 36 avenue Guy de Collongue 69134 Écully Cedex, France.

lyes.nechak@ec-lyon.fr #

** Sorbonne Université, CNRS, UMR 7222, Institut des Systèmes Intelligents et de Robotique ISIR, Paris 75005, France.
morin@isir.upmc.fr #

Abstract. This study proposes a new nonlinear control scheme for friction-induced vibrations (FIV). The approach consists of two stages. The first stage transforms the system into a cascade of independent subsystems and then the second stage focuses on the monitoring of the transient and stationary regimes of the associated dynamics. A comparison between the closed-loop performances of the proposed solution and of an input/output linearization technique has revealed a better efficiency of the present solution, especially for transient tuning in the presence of limited control amplitude. Moreover, the observed performances have shown interesting robustness with respect to the saturation of the corresponding control.

Introduction

Mitigating friction-induced vibrations (VIB) is of central importance in numerous applications [1] in order to avoid their negative effects on the system performances. Numerous methods ranging from classical techniques based on proportional integral and derivative (PID) actions [2] to more sophisticated nonlinear and robust techniques [3, 4], were proposed. Most of these studies have focused on the stability of the steady state at the stationary regime, however, and have neglected transient properties of the controlled FIV. The present work deals with the active control of FIV, and pays particular attention to ensuring good transient properties in terms of damping and settling times. It proposes a new scheme which consists of two control stages. The first stage puts the system into a cascade of independent subsystems the dynamics of which becomes simpler to control. Then, the second stage designs feedback controllers with specified damping characteristics.

Application and results

The Hultèn system given at the left side of Figure (1) and which is widely used in the FIV framework, is considered in the present study in order to assess the efficiency of the proposed control scheme. A comparison between the latter and the nonlinear control based on input/output linearization was carried out. One of the results obtained by both methods is given at the middle and the right side plots in Figure (1). It consists in the time evolution of the vertical displacements X_1 of the mass. The right side plots are zooms on the X_1 transient. Results have revealed that the new architecture yields an asymptotically stabilized dynamics with better transient properties than that obtained by applying an input/output linearizing state feedback. Furthermore, it allowed a better compromise between the damping properties of the transient and the amplitudes of the corresponding controls. Finally, its stabilizing effects have exhibited a better robustness than the input/output linearizing state feedback with respect to the saturation phenomenon occurring when the control amplitudes reach high levels.

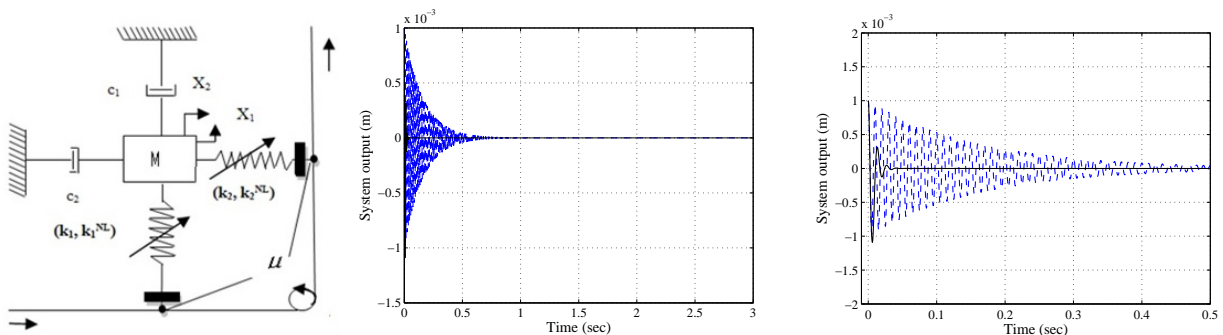


Figure 1: From left to right-Hultèn system - The controlled displacement X_1 -Zoom on the transient of the controlled X_1 . Solid line: Cascade architecture based control, dashed line: Input/output linearizing state feedback control

References

- [1] Armstrong-Helouvry B., Dupont P., Canudas De Wit C. (1994) A survey of models, analysis tools, and compensation methods for the control of machines with friction. *Automatica* **30**:1083-1138.
- [2] Hashemi-Dehkordi S.M., Mailah M., Abu-Bakar A.R. (2010) Suppressing Friction-Induced Vibration due to negative damping and mode coupling effects using active force control. *AJBAS* **4**:3917-3933.
- [3] Zhen C., Jiffri S., Xiang J., Mottershead J.E. (2018) Feedback linearisation of nonlinear vibration problems: A new formulation by the method of receptances. *MSSP* **98**:1058-1068.
- [4] Nechak L. (2022) Robust nonlinear control synthesis by using centre manifold-based reduced models for the mitigating of friction-induced vibration. *Nonlinear Dyn* **108**:1885-1901.

Nonlinear vibration control of a slightly curved beam with distributed piezoelectric patches

Jacek Przybylski

Faculty of Mechanical Engineering and Computer Science, Częstochowa University of Technology, Częstochowa, Poland

Abstract. This paper aims to study the effect of axial forces and bending moment on the static behaviour and natural transversal vibrations of piezoelectrically actuated slightly curved beams subject to prescribed axial end displacement. This is achieved by bonding patches of piezoceramic material at along the top and bottom surfaces of the beam. The governing equations for the system are formulated using Euler-Bernoulli beam theory and on the basis of von Kármán non-linear strain–displacement relations and linear constitutive relations for both the piezoelectric and host beam materials. Due to the nonlinearity of the governing equations, their solutions are attempted by a regular perturbation technique leading to asymptotic expansions of displacements, internal forces and the natural vibration frequency. Numerical examples are presented, including how the geometrical nonlinearity is incorporated in the system's static and dynamic responses as a function of two main variables, the beam initial curvature and the electric field application.

Problem statement

Statics and dynamics of composite structures with geometrical imperfections actuated piezoelectrically or electrostatically have aroused great interest due to their various potential applications [1-3]. In this work a simply supported sandwich piezoelectric beam of length l and width b , composed of two identical external piezoelectric layers (thickness h_p) perfectly bonded to an elastic core of thickness h has been considered. The adhesive layers are neglected. The beam of initial curvature described by function $W_0(x)$ is subjected to a prescribed end displacement δ that changes the distance between the pin supports, as shown in Fig. 1a. The geometry of the beam cross-section is given in Fig. 1b.

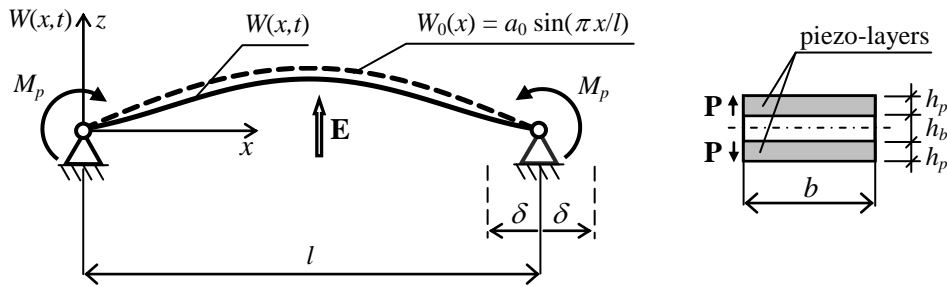


Figure 1: Scheme of a simply supported slightly curved piezoelectric beam and its cross-section.

Since the piezo-layers have an opposite polarization, the application of the electric field of vector \mathbf{E} makes that the upper layer is contracted, whereas the bottom one is expanded and, as a result, the piezoelectric moments of equal values M_p appear at the supports. Moments M_p may be redirected when vector \mathbf{E} will have the opposite direction. As both beam ends are pinned, the beam deflection influences an axial force that is caused by the prescribed displacement. The analysis is based on a nonlinear equation of motion of a shallow beam under both axial and piezoelectric forces. The perturbation method of the solution has been chosen according to which the transversal and axial displacements, the axial forces and the natural vibration frequency are expanded into power series with respect to a small amplitude parameter. Infinite sets of differential equations with associated boundary conditions are obtained for the rising power of the amplitude parameter which are solved sequentially. The first set of equations describes the static response of the system presenting the effect of the axial force and the applied voltage on the static equilibria of the beam. The next set of equations represents the eigenvalue problem for various static equilibrium positions. A large number of results presents the variations of the natural frequencies and mode shapes for equilibrium positions of the beam being stretched or compressed by axial forces resulting from the applied voltage changing from negative to positive magnitudes. The results have also shown the possibility of exploiting electric voltage to tune the stability and natural frequencies of curved beams over a wide range of frequencies.

References

- [1] Faria A.R., Almeida S.F.M. (1999) Enhancement of pre-buckling behavior of composite beams with geometric imperfections using piezoelectric actuators. *Composites Part B: Engineering* **30**(1):43-50.
- [2] Alkharabsheh S.A., Mohammad I.Y. (2013) Statics and Dynamics of MEMS Arches Under Axial Forces. *Journal of Vibration and Acoustics* **135**(2): 021007 (7 pages).
- [3] Chen X, Meguid S.A. (2015) Snap-through buckling of initially curved microbeam subject to an electrostatic force. *Proc. R. Soc. A* **471**:20150072. <http://dx.doi.org/10.1098/rspa.2015.0072>.

Seismic response control of a non-linear structure using magneto-rheological dampers

Mahdi Abdeddaim*, Arnab Anuj Kasar** and Salah Djerouni*

* LARGHYDE Laboratory, Department of Civil engineering and Hydraulics, Faculty of Sciences and Technologies, Biskra University, Biskra, Algeria

** Department of Civil Engineering, Sagar Institute of Science and Technology, Gandhi Nagar, Bhopal, India

Abstract. Structures implemented in high seismicity areas are usually subjected to strong earthquake motion. Hence, high peak ground acceleration values characterize such seismic events. Under such excitations, the structures undergo non-linear behavior, leading to irreversible damage and eventually collapse. To prevent such hazards, seismic dampers are implemented in the structures. This study implements a magneto-rheological (MR) damper in a structure submitted to seismic excitations. The structure is modelled to undergo non-linear behaviour beyond a certain quantity of deformations. The non-linear behaviour of the structure is captured using the Bouc-Wen hysteresis model. The obtained results show a good performance of the magneto-rheological in reducing the response quantities of the structure. The investigated dynamical parameters are the top floor displacement, the inter-story drift and the hysteresis behaviour of the structure.

Introduction

Earthquakes are considered the most destructive natural events. They usually cause damage and loss in lives and materials. Throughout the existence of humankind on the earth, constructing aseismic structures was a relevant and continuously evolving challenge. Nowadays, structures constructed in high seismicity areas are designed and equipped with vibration control devices to reduce seismic-induced motions. It is well established that most structures submitted to seismic excitations will undergo non-linear deformations [1]. However, most of the studies in the literature involving vibration control devices consider that the structures remain in the elastic range leading to an overestimation of the structures and devices' performances. To overcome this lacunas, various models were introduced to represent the non-linear behaviour of structures. One of the most representative models of non-linear hysteresis behaviour is the Bouc-Wen model [2]. This model was used to represent the non-linear behaviour of multi-story buildings, and the results obtained by the approach were correlated using a pushover approach [3]. In this study, a multi-degrees of freedom structure was modelled to undergo non-linear behaviour. The structure is then equipped with four magneto-rheological dampers optimal set to obtain the best response reduction. This study's primary purpose is to investigate the performance of semi-active devices in the non-linear response reduction of structures submitted to earthquakes.

Results and discussion

A multi-degrees of freedom building modelled to express non-linear behaviour is equipped with four magneto-rheological dampers located on the first, second, third and fourth floors, respectively. The structure is submitted to earthquake excitations. The MR damper parameters are optimized using a genetic algorithm (GA) with a single objective function, defined as the reduction of the top floor displacement.

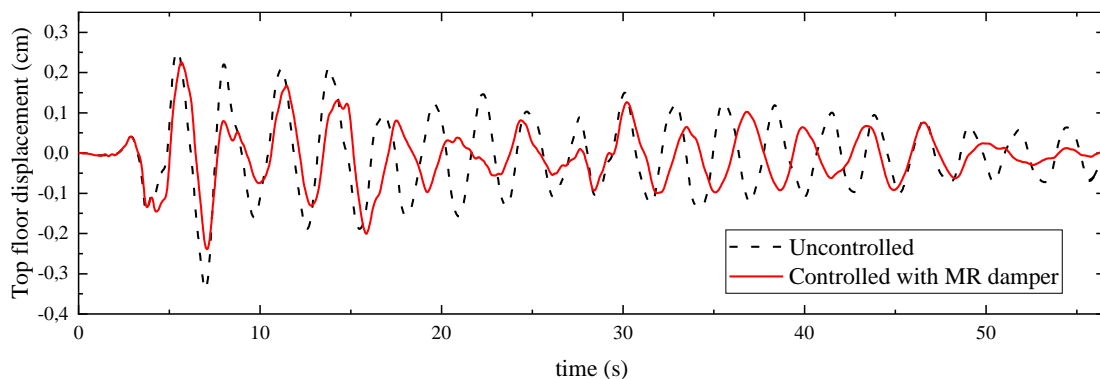


Figure 1: top floor displacement time history of the controlled and uncontrolled structures

The results show a good response reduction using MR dampers, especially in top floor displacement as shown in Figure 1. The MR dampers also reduce the hysteresis behaviour. Hence, reducing the damage induced to the structure by the ground acceleration. It was found that using purely elastic models to calculate the seismic response will lead to an overestimation of the devices' performance. Non-linear models are more accurate and representative of the actual case scenarios.

References

- [1] Lavan O. (2015) A methodology for the integrated seismic design of non-linear buildings with supplemental damping. *Struct Control Health Monit* **22**(3):484-499.
- [2] Wen Y. K. (1976) Method for random vibration of hysteretic systems. *J. Eng Mech* **102**(2):249-263.
- [3] Khansefid A. and M. Ahmadizadeh (2016) An investigation of the effects of structural nonlinearity on the seismic performance degradation of active and passive control systems used for supplemental energy dissipation. *J. Vib Control* **22**(16):3544-3554.

Performance Improvement of Autoparametric Vibration Absorber by Eliminating the Viscous Damping and the Nonlinearity

Chao Zhang*, Hiroshi Yabuno* and Kenji Yasui **

*Mechanical Systems Laboratory, Degree Programs in Systems and Information Engineering, University of Tsukuba, Tsukuba 305-8573, Japan #

**Okumura Corporation, Technical Research Institute, Architecture Research Group, Tsukuba, Ibaraki 300-2612 Japan #

Abstract. Autoparametric vibration absorber attached to a main system is a type of equipment to reduce the resonance amplitude in the main system. In this study, the vibration absorber is primarily composed of a cantilever beam, and we improve the performance of autoparametric vibration absorber by the feedback control. By the position control of the fixed end of the cantilever beam, we decrease the viscous damping and change the natural frequency of the absorber. By performing the nonlinear analysis, we determine the suitable linear velocity feedback gain for reducing the amplitude of the main system. Also, when the amplitude of the absorber is relatively large, due to the nonlinear dependency of the natural frequency on the amplitude, the frequency ratio between the absorber and the main system is deviated from 1:2. We establish a nonlinear feedback control method to compensate for the nonlinearity so that the ratio maintains to be 1:2 regardless of the magnitude of amplitude. Furthermore, we conducted experiments using a simple apparatus. The results demonstrated the validity of the proposed control methods.

Introduction

Harmful vibrations caused by resonances are present in a wide variety of engineering dynamical systems. Dynamic vibration absorber [1] is a type of passive amplitude control system used in many industries such as automotive, construction and aerospace. It reduces the vibration of an object (main system) by vibrating a mass attached as a sub-system when the object is externally excited. Haxton and Barr [2] designed the autoparametric vibration absorber in which a cantilever beam with a mass at the tip is connected to a main system subject to external periodic excitation. Since then, many new devices have been developed to improve the performance of the absorber. An important aspect of this is the widening of the working band of the absorber. Cartmell and Lawson [3] widen the working band range by appropriately moving a lumped mass attached on the absorber. Then, the natural frequency of the abosorber is automatically tuned according to the excitation frequency so that the autoparametric resonance in the absorber is kept and the amplitude of the main system is reduced.

Results and discussion

In this research, in addition to expanding the working band rang like previous researches, we have further enhanced the vibration absorption at resonance point by means of feedback control. We propose an autoparametric vibration absorber in which the viscous damping and the natural frequency of the absorber can be reduced and changed, respectively, as shown in Figure 1(a). Under the absorber with feedback control, the amplitude of main system decrease with 83.5% at resonance point (It is 63.5% without feedback control) as shown in Figure 1(b). Moreover, when the amplitude of the absorber is relatively large, the frequency ratio between the ab-sorber and the main system is deviated from 1:2 due to the cubic nonlinearity of cantilever beam. We propose a nonlinear feedback control method to compensate for the nonlinearity so that the ratio maintains to be 1:2 regardless of the magnitude of amplitude and it is experimentally verified.

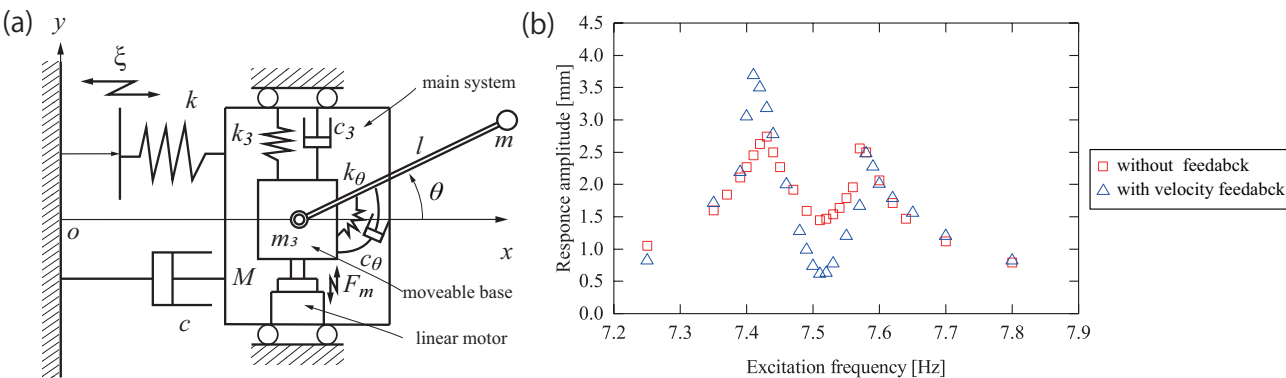


Figure 1: (a) Model of autoparametric dynamic vibration absorber. (b) Frequency response curves of main system.

References

- [1] P. Watts (1883) On a Method of Reducing the Rolling of Ship at Sea. *Transactions of the Institution of Naval Architects* **24**:165-190.
- [2] R.S. Haxton, A.D.S. Barr (1972) The autoparametric vibration absorber. *J. Manuf. Sci. Eng.* **94**(1):119-125.
- [3] M. Cartmell, J.Lawson (1994) Performance enhancement of anautoparametric vibration absorber by means of computer control. *J. Sound Vib* **177**(2):173-195.

Vibration control with a magnetic tristable NES on a cantilever beam

Jun-Dong Fu*, Shui Wan*, Jiwei Shen* and Kevin Dekemele**

*School of Transportation, Southeast University, Nanjing, China

**Department of Electromechanical, Systems and Metal engineering, Ghent University, Ghent, Belgium

Abstract. The vibration suppression effect of novel magnetic tristable nonlinear energy sink (MTNES) on harmonically excited cantilever beam is studied. The performance is investigated through Hamilton's method, assumed mode method and fourth order Runge Kutta method. Taking the amplitude reduction of the end of the cantilever beam as the research objective, the method verified by the experiment is compared with the numerically calculated results. The results show that the MTNES has a good effect on the vibration suppression of cantilever beams and an increased robustness compared to the tuned-mass-damper (TMD).

Introduction

The nonlinear energy sink (NES) captures the vibration frequency of the host structure in a short time after the structure vibrates, and generate 1:1 resonance, realizing the dissipation and transfer of seismic energy. Because its nonlinear restoring force enables a wider frequency bandwidth and robustness than compared to the TMD, it has been studied by many scholars. Magnetic force can be used to obtain a nonlinear restoring force in the magnetic nonlinear energy sink (MNES). Al Shudeifat realized the MNES first by using asymmetric magnets. The MNES significantly improved the impact mitigation performance over broadband energy input compared to the conventional NES with cubic restoring force [1]. Chen proposed a magnetic bistable nonlinear energy sink for seismic control. By applying it to single-DOF and multi-DOF frame structures, he found an improved robustness[2]. Feudo proposed and built an MNES with adjustable restoring force, and used it for the vibration reduction of a three story frame structure[3]. In the current study, a novel tristable magnetical nonlinear energy sink is proposed, which consists of four outer magnets, two inner magnets and a linear spring (see Fig. 1a).

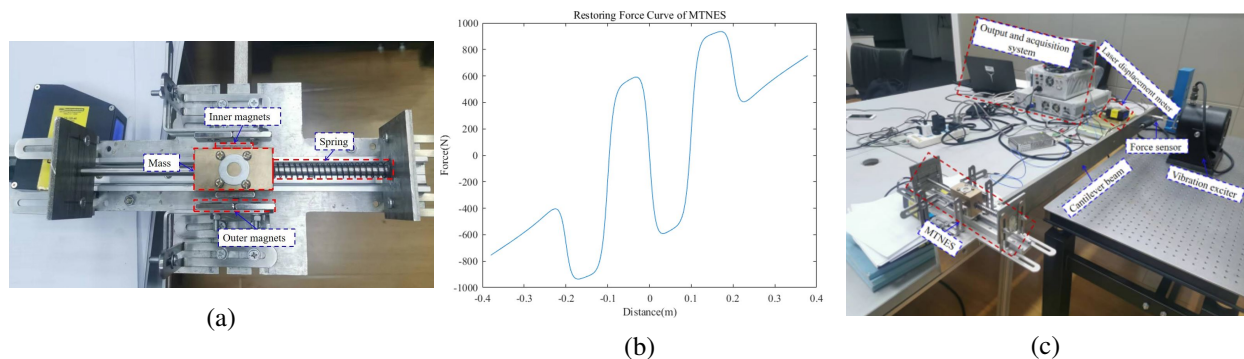


Figure 1: The MTNES (a), restoring force (b) and cantilever beam with MTNES (c).

Results and discussion

This particular configuration of magnets and springs yield the restoring force shown in Fig. 1b. The length, width and thickness of the magnet are 10cm, 10cm and 2cm respectively. The distance between the centers of the outer magnets and inner magnets along the length direction of the spring is 10cm, and the distance perpendicular to the direction of the spring is 3cm. The spring stiffness is 2000N/m. The first resonance frequency of the cantilever beam is 4.32Hz. When the excitation frequency is 4.4Hz, the maximum displacement of the uncontrolled cantilever beam end is 22.4mm, and the maximum displacement of the cantilever beam with MTNES structure is 7.2mm (66.7 % reduction). The setup is shown on Fig. 1c. Furthermore, numerical analysis will be used to study the influence different NES mass, magnetic force and spring stiffness on the performance of MTNES, compared to the MBNES and TMD.

References

- [1] Al-Shudeifat M. (2015) Asymmetric Magnet-Based Nonlinear Energy Sink. *J. Comput. Nonlinear Dyn.* **10**(1):014502.
- [2] Chen Y. Y., Zhao W., Shen C. Y. and Qian Z. C.(2021) Bistable Nonlinear Energy Sink Using Magnets and Linear Springs: Application to Structural Seismic Control. *Shock Vib.* **2021**:9976432
- [3] Feudo S. L., Touzé C., Boisson J. and Cumunel G. (2019) Nonlinear magnetic vibration absorber for passive control of a multi-storey structure. *J. Sound Vib.* **438**:33-43

Nonlinear vibration isolators with spring and inerter configured in linkage

Jian Yang*, Baiyang Shi* and Wei Dai**

*Faculty of Science and Engineering, University of Nottingham Ningbo China, Ningbo 315100, P.R.China

**Huazhong University of Science and Technology, Wuhan 430074, P.R.China

Abstract. This study proposes various nonlinear vibration isolator designs exploiting a hybrid use of the inerter device and diamond-shaped linkage mechanisms. The combined use of the inerter and linkage mechanism is considered to fully exploit inertial properties of the former and the geometric nonlinearity of the latter for performance enhancement of vibration suppression. The steady state responses of the proposed isolators subjected to harmonic force excitations are obtained using analytical harmonic balance (HB) method, alternating frequency time HB and direct numerical integrations, with the results cross-checked and validated. The isolation effectiveness of the proposed isolators is evaluated using the time-averaged vibration energy transmission and force transmissibility as performance indices. Beneficial performance of using inerter and linkage mechanism in the nonlinear isolators is demonstrated, showing great potential for superior vibration attenuation.

Introduction

The inerter is a passive mechanical device with the property that a dynamic force across the two terminals is proportional to their relative accelerations [1]. Such device can be physically realized through a variety of designs using, for example, a ball-screw or a rack-pinion mechanism. Recent developments suggest that semi-active and fluid based inerters can offer a range of benefits and studies have demonstrated benefits of using such devices in automobile shock absorbers, in civil buildings and in aircraft landing gears. Many studies, however, have only considered the use of inerters in linear isolators. Limited studies have been reported with a hybrid use of inerters and the geometric nonlinearity of linkage mechanisms for vibration isolation. Many studies have shown that the introduction of inerter and / or nonlinearity to a vibration suppression device can bring performance benefits [2-4]. For instance, a negative stiffness mechanism can be used together with a linear spring to achieve high-static-low-dynamic stiffness nonlinear vibration isolator, beneficial for low-frequency vibration isolation. The current study explores the embedding of spring, damper and inerter in linkage mechanism for vibration suppression with enhanced performance.

Results and Discussions

Fig. 1(a) shows a configuration of nonlinear vibration isolator using passive spring and inerter connected in diamond-shaped linkage mechanisms with geometric nonlinearity. Fig. 1(b) shows that the natural frequency of the isolator can be reduced, suggesting an enlarged frequency range for effective isolation. The responses are obtained using analytical approximations and numerical integrations. Indices including force/displacement transmissibility and vibration energy flow variables are used to evaluate the performance of the proposed nonlinear isolators. Beneficial performance has been demonstrated by using the inerter devices and geometric nonlinearity of linkage mechanisms to achieve superior vibration suppression.

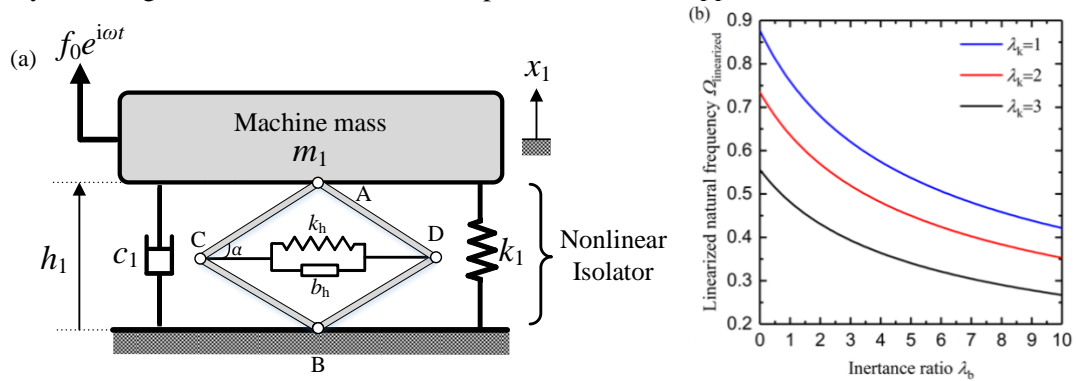


Figure 1: (a) Nonlinear vibration isolators and (b) variation of the linearized natural frequency.

References

- [1] Smith M.C. (2002) Synthesis of mechanical networks: the inerter. *IEEE Trans. Automat. Contr.* **47**: 1648-1662.
- [2] Yang J., Jiang J. Z., Neild. S. A. (2020) Dynamic analysis and performance evaluation of nonlinear inerter-based vibration isolators. *Nonlinear Dyn.* **99**(2):1823-1839.
- [3] Shi B.Y., Yang J., Jiang J. Z. (2022) Tuning methods for tuned inerter dampers coupled to nonlinear primary systems, *Nonlinear Dyn.* **107**(2):1663-1685.
- [4] Shi B.Y., Dai W., Yang J. (2022) Performance analysis of a nonlinear inerter-based vibration isolator with inerter embedded in a linkage mechanism. *Nonlinear Dyn.* **109**(2):1-24.

Numerical and experimental study of a pneumatic Nonlinear Energy Sink

Clément Raimond¹, Thomas Roncen², Thierry Jardin³, Leonardo Sanches¹ and Guilhem Michon¹

¹Department of Mechanics, ICA, CNRS, ISAE-Supaero, Toulouse, France

²Department of Mechanics, Liebherr Aerospace, Toulouse, France

³Department of Aerodynamics, Energetics and Propulsion, ISAE-Supaero, Toulouse, France

Abstract. Aerospace systems can be subjected to severe thermal and vibration environments which may be the limiting factor in the equipment's life. A vibration protection system with adapted damping alleviates the stresses seen by the structures, enhancing their lifetime. One option is an additional device with a relatively small mass, weak dissipation, and nonlinearly coupled to a structure, also known as a nonlinear energy sink (NES). The main problem is the precise adjustment of the damping to prevent detached resonance. The present study proposes a pneumatic nonlinear energy sink which allows for tuning the damping of the NES with the aerodynamic drag. It consists of a circular metallic diaphragm which delimits two air chambers. These chambers are connected by an orifice in the diaphragm and the high-velocity air flowing through this orifice provides nonlinear damping. The theoretical design, experimental realisation and numerical simulations of this pneumatic nonlinear energy sink are developed in this work.

Introduction

Various engineering fields have progressively favoured the use of a nonlinear energy sink as a vibration absorber, mainly due to their low sensitivity to the variation of the main structure properties or the external excitation, contrary to classical linear tuned mass dampers (TMD) [1]. NES is designed to trigger an irreversible energy-pumping phenomenon called targeted energy transfer (TET) from the main structure to the absorber. This phenomenon has been widely studied theoretically and experimentally with different vibration sources. B. Cochelin et al.[2] have studied an absorber with a diaphragm for energy pumping in acoustics which damping is provided by the elastomeric material of the diaphragm. This assembly cannot be operated at high temperatures, reducing the industrial application possibilities. NES promises excellent theoretical performance but they have some shortcomings. The first flaw is the appearance of an undesirable regime called detached resonance, during which the vibration of the main structure is amplified instead of being reduced. NES parameters need to be optimised to suppress the existence of this nonlinear critical phenomenon. This phenomenon is directly linked to the damping of the NES which is very difficult to predict and customise in structures. To overcome this issue, we propose a new concept of a pneumatic nonlinear absorber with controlled damping illustrated in Figure 1. It consists of two air chambers separated by a circular diaphragm with an orifice. The diaphragm and high-velocity flow through the orifice are the key points in the design of the nonlinear elastic force and nonlinear damping, respectively. A metallic diaphragm is chosen to operate at high temperatures. The use of aerodynamic drag helps to determine the global damping of the absorber as the mechanical friction becomes negligible. Analytical treatment of the governing NES equations of motion is performed through an asymptotic approach to model the coupling between structural and fluid components analytically. This will allow the rapid development of an optimised prototype for vibration dissipation. A numerical model is used to verify that the asymptotic approach correctly describes the pumping phenomenon, and finally, experimental tests are used to validate the model and identify its limits.

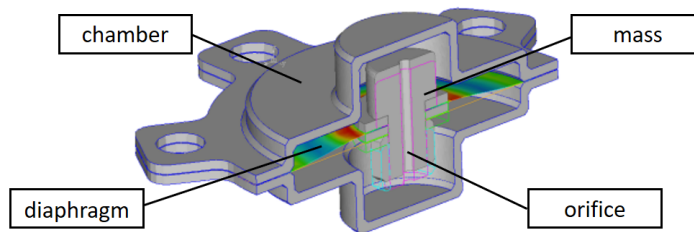


Figure 1: Sectional view of AirNES prototype

Results and discussion

As part of this study, it has been shown that this properly tuned NES achieves effective vibration absorption and outperforms classical TMD. Numerical simulations involving fluid-structure interaction agree with analytical predictions and initial experimental tests. The results will be used to theoretically design a NES which dampens the response of a resonant system while reducing the number of needed iterations in the design process.

References

- [1] Gendelman, O., Manevitch, L. I., Vakakis, A. F., & M'closkey, R. (2001) Energy pumping in nonlinear mechanical oscillators: part I—dynamics of the underlying Hamiltonian systems. *J. Appl. Mech.* **68**(1):34-41.
- [2] Cochelin, B., Herzog, P., & Mattei, P. O. (2006) Experimental evidence of energy pumping in acoustics. *Comptes Rendus Mecanique* **334**(11):639-644.

Exact dynamical solution of the Kuramoto–Sakaguchi Model for finite networks of identical oscillators

Antonio Mihara* and Rene O. Medrano-T.**

*Departamento de Física, Universidade Federal de São Paulo, UNIFESP, Campus Diadema, São Paulo, Brasil

**Departamento de Física, Universidade Federal de São Paulo, UNIFESP, Campus Diadema, São Paulo, Brasil, and
Departamento de Física, Instituto de Geociências e Ciências Exatas, Universidade Estadual Paulista, UNESP, Campus
Rio Claro, São Paulo, Brasil, ORCID 0000-0003-0866-2466

Abstract. We study the Kuramoto–Sakaguchi model composed by any N identical phase oscillators symmetrically coupled. Ranging from local (one-to-one, $R = 1$) to global (all-to-all, $R = N/2$) couplings, we derive the general solution that describes the network dynamics next to an equilibrium. Therewith we build stability diagrams according to N and R bringing to the light a rich scenery of attractors, repellers, saddles, and non-hyperbolic equilibriums.

Introduction

For more than forty years, the paradigmatic system of N one-dimensional coupled phase oscillators, the Kuramoto model [1], has been intensively studied to understand phenomena related to synchronization in biological, chemical, and electronic networks. Despite the simplicity of the dynamics of each oscillator ($\dot{\theta} = \omega$) strong efforts should be dedicated to find analytical solutions for a network of nonlinearly coupled oscillators, due to the high dimensionality of the system. Kuramoto showed a seminal solution giving rise to the prosper application of the mean–field theory where $N \rightarrow \infty$ with oscillators globally coupled. In contrast, accurate results for the finite-size Kuramoto model remains a challenge due to the great number of equations involved, nevertheless, the dynamics is richer. While in the global coupling the full synchronization is the only stable equilibrium, in different topologies of the Kuramoto model multistability is allowed [2]. And, sustained by Lyapunov function argument, the system would reach an equilibrium state as $t \rightarrow \infty$ [3].

Multistability, basin of attractions, and traveling waves are some of fundamental phenomena directly related with equilibriums in variants of the Kuramoto model with both attractive and repulsive phase couplings, where the oscillators do not collapse in a single phase although they synchronize in frequency. These phenomena are also observed in real-world networks [4, 5, 6, 7]. Such manifestations are mostly studied in the continuous thermodynamic limit and keep not yet well understood. Exact solutions for lower number of oscillators in the Kuramoto model are mandatory in this study but they are still a topic of investigation.

Results and discussion

In order to shed some light on those problems we study the Kuramoto–Sakaguchi (KS) model [8], a generalization of the Kuramoto model, explicitly for a finite number of N identical oscillators symmetrically coupled ($G = G^T$, in matrix representation). In opposition of traditional investigations, where the time evolution of the network is followed by the order parameter, we obtain solutions describing precisely the individual trajectories of each oscillator when the system is close to an equilibrium. We present several numerical studies in a great accordance with our theoretical predictions and focus in the role of non-hyperbolic equilibria in the general dynamic behavior. More specifically, we determine the set of eigenvalues associated to each state identifying the complete stability scenario of hyperbolic and non-hyperbolic equilibria for a finite number N of oscillators and calculate the bifurcation these states in the thermodynamic limit.

References

- [1] Y. Kuramoto, Self-entrainment of a population of coupled non-linear oscillators. In: H. Arakai (Ed.), International Symposium on Mathematical Problems in Theoretical Physics, Lecture Notes in Physics, vol. 39, Springer, New York, p. 420, 1975.
- [2] D. A. Wiley and S. H. Strogatz (2006) The size of the sync basin, *Chaos* **16**: 015103.
- [3] J. L. Hemmen and W. F. Wreszinski (1993) Lyapunov function for the kuramoto model of nonlinearly coupled oscillators. *J. of Stat. Phys.* **72**: 145.
- [4] A. H. Cohen, G. B. Ermentrout, T. Kiemel, N. Kopell, K. A. Sigvardte, and T. L. Williams (1992) Modelling of intersegmental coordination in the lamprey central pattern generator for locomotion. *Trends Neurosci.* **15**: 434.
- [5] G. B. Ermentrout and N. Kopell (1994) Inhibition-produced patterning in chains of coupled nonlinear oscillators. *SIAM J. Appl. Math.* **54**: 478.
- [6] M. Tsodyks, T. Kenet, A. Grinvald, and A. Arieli (1999) Linking spontaneous activity of single cortical neurons and the underlying functional architecture. *Science* **286**: 1943.
- [7] J. P. Newman and R. J. Butera (2010) Mechanism, dynamics, and biological existence of multistability in a large class of bursting neurons. *Chaos* **20**: 023118.
- [8] H. Sakaguchi and Y. Kuramoto (1986) A soluble active rotator model showing phase transitions via mutual entrainment. *Prog. Theor. Phys.* **76**: 576.

Frequency-Energy Analysis of Coupled Linear Oscillator with Unsymmetrical Nonlinear Energy Sink

Mohammad A. AL-Shudeifat

Department of Aerospace Engineering, Khalifa University of Science and Technology, Abu Dhabi, United Arab Emirates

Abstract. The underlying nonlinear dynamical behaviour of linear oscillator (LO) attached with a nonlinear energy sink (NES), in which unsymmetrical coupling force is employed, is investigated here on the FEP. The nonlinear force incorporates purely cubic stiffness element on one side of the equilibrium position and linear restoring coupling stiffness on the other side. The obtained FEP of this system reveals different kinds of backbone curves. Accordingly, the FEP shows five new continuous backbones of 1:1 resonance between the LO and the UNES at frequency levels below the LO natural frequency.

Introduction

The frequency energy plot (FEP) analysis has significant impact on revealing the underlying nonlinear dynamical behaviour of LO-NES oscillations. The periodic motion of stiffness-based structure-NES systems has been extensively studied in the literature on the harmonic nonlinear normal modes (NNMs) backbone curves and their associated subharmonic branches [1-5]. The FEPs accompanied with the superimposed wavelet frequency spectrum content have been also employed to confirm the existence of different kinds of resonance captures between the LO and the NES oscillations. The resonance captures on the FEP backbones and their associated subharmonic branches have verified the rapid and passive targeted energy transfer (TET) from the primary system into the NES attachment [1-3]. Accordingly, the FEP analysis is generated here for coupled LO with unsymmetrical nonlinear energy sink (UNES).

The LO-UNES System and the FEP

The considered LO in Figure 1a is coupled with UNES of cubic stiffness on one side and linear stiffness on the other side. The FEP of this LO-UNES system has been obtained at $M = 1$ kg, $m = 0.05$ kg, $k_1 = 1$ N/m, $k_{res} = 0.03$ N/m, $k_{nl} = 1$ N/m³ and zero damping content using the continuation method in [4,5]. The free-response of the Hamiltonian equations of motion of the LO-UNES system is obtained at the given physical parameters for zero velocities and nonzero displacements via numerical simulation. Compared with the NES with purely cubic stiffness force in the literature, the FEP in Figure 1b of the LO-UNES system shows five new continuous backbones named as *a*, *b*, *c*, *d* and *e* at frequency levels below the LO natural frequency. These backbones overlap with the subharmonic branches that appear due to the cubic stiffness effect in the UNES. At these backbones, it is observed that the oscillation is dominated by the linear effect of the UNES below some energy threshold whereas it becomes dominated by the nonlinear effect above that threshold.

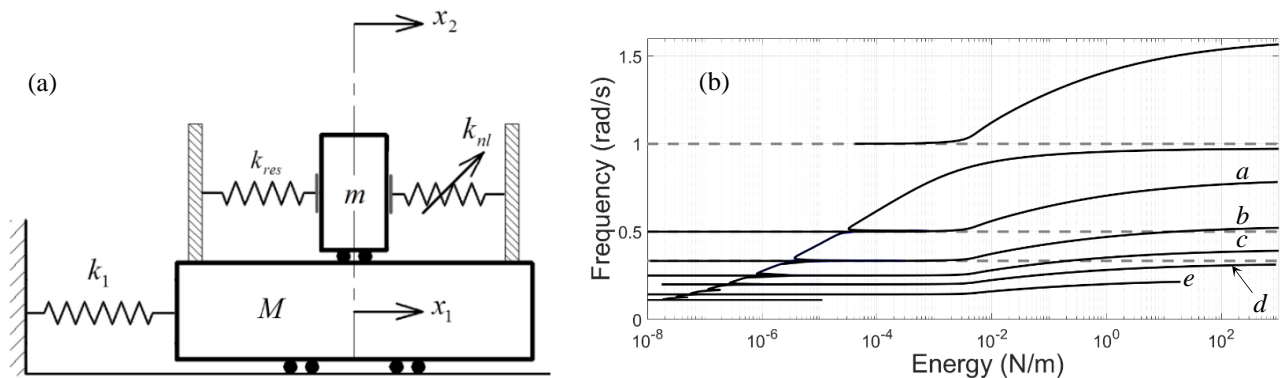


Figure 1: The coupled LO with unsymmetrical NES in (a) and its corresponding FEP in (b)

References

- [1] Vakakis A.F., Gendelman O.V., Bergman L.A., McFarland D.M., Kerschen G., Lee Y.S. (2008) Nonlinear targeted energy transfer in mechanical and structural systems, Springer Science & Business Media,
- [2] Lee Y.S., Kerschen G., Vakakis A.F., Panagopoulos P., Bergman L., McFarland D.M. (2005) Complicated dynamics of a linear oscillator with a light, essentially nonlinear attachment. *Physica D* **204**: 41-69.
- [3] Quinn D.D., Gendelman O., Kerschen G., Sapsis T.P., Bergman L.A., Vakakis A.F. (2008) Efficiency of targeted energy transfers in coupled nonlinear oscillators associated with 1:1 resonance captures: Part I. *J. Sound Vib.* **311**: 1228-1248.
- [4] Kerschen G., Peeters M., Golinval J.-C., Vakakis A.F. (2009) Nonlinear normal modes, Part I: A useful framework for the structural dynamicist. *Mech Syst Signal Process* **23**: 170-194.
- [5] Peeters, Maxime, Vigié, Régis, Sérandour, Guillaume, Kerschen, Gaëtan and Golinval, J.-C. (2009) Nonlinear normal modes, Part II: Toward a practical computation using numerical continuation techniques. *Mech Syst Signal Process* **23**: pp. 195-216.

Time-delay vibration reduction control of tension leg in submerged floating tunnel

Jian Peng*, Xiaowen Chen*, Lianhua Wang** and Stefano Lenzi***

*Hunan Provincial Key Laboratory of Structures for Wind Resistance and Vibration Control, School of Civil Engineering, Hunan University of Science and Technology, Xiangtan, Hunan 411201, PR China

**College of Civil Engineering, Hunan University Changsha, Hunan 410082, PR China

***Department of Civil and Building Engineering and Architecture, Polytechnic University of Marche, Ancona 60131, Italy

Abstract. Based on the Euler-Bernoulli beam theory and the time-delay feedback control strategy, the vibration control equation of the tension leg of the underwater suspension tunnel under parametric excitation is established. The Galerkin method and linear stability analysis are used to obtain the stability boundary conditions of the control system with time delay. The influence of different control parameters on vibration response is analyzed through numerical simulation. The results show that reasonable time delay and gain values can greatly reduce the vibration response to the tension leg of the underwater floating tunnel and improve the structural stability.

Introduction

Submerged Floating Tunnel, also known as SFT, also known as Archimede's Bridge[1], is a potential traffic structure across long waterways and deep straits, mainly relying on the buoyancy and support system of its own structure to ensure that it is in a fixed position, which has its unique advantages over traditional tunnels and bridges, and has a wide range of application prospects. However, due to the complex marine environment, the vibration and stability problems of the suspended tunnel need to be solved urgently [2,3]. In recent years, underwater suspension tunnels and suspension tunnel tension legs have attracted a lot of attention from scholars[4]. In this paper, the vibration control of the suspended tunnel tension leg is studied by using the time-delay vibration damping technology. The tunnel pipe body is assumed to be a mass point, and the Euler-

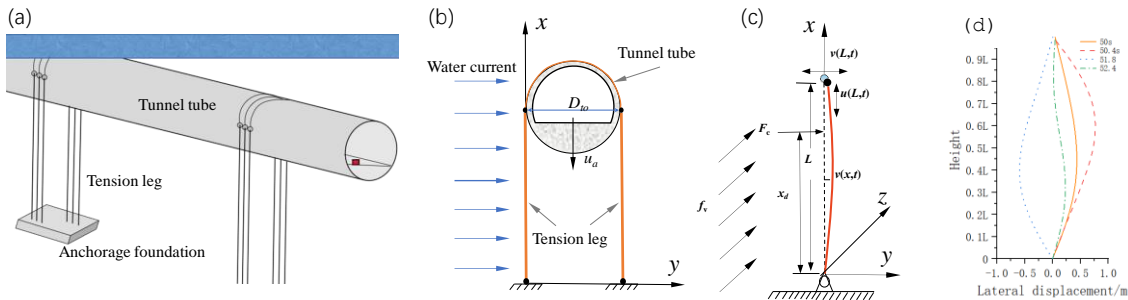


Figure 1: The configurations of the controlled model and displacement deformation diagram. (a) Schematic of the SFT structure. (b) Simplified physical model at the cross-section. (c) Vibration control model of the Tension leg. (d) Displacement deformation diagram of tension leg.

Results and Discussion

The effect of the delay velocity feedback control on the large lateral vibration control of the submerged floating tunnel tension leg is analyzed by using the Euler-Bernoulli beam theory. The results show that the time delayed feedback control can greatly reduce the lateral vibration of the tension leg, improve the structural stability and reduce the fatigue damage. And by determining the stability domain, adjusting the time delay value and gain amount to the appropriate value, the control is set in the middle position of the tension leg, which can make the vibration reduction effect reach the best, and the highest suppression effect can reach more than 90%.

References

[1] Ahrens D. (1997) Chapter 10 Submerged floating tunnels—a concept whose time has arrived. *Tunnelling and Underground Space Technology* 12(2): 317-336.

[2] Jeong K., Min S., Jang M., Kim S. (2022) Feasibility study of submerged floating tunnels with vertical and inclined combined tethers. *Ocean Engineering* 265: 112587.

[3] Xiang Y., Lin H., Bai B., Chen Z., Yang Y. (2021) Numerical simulation and experimental study of submerged floating tunnel subjected to moving vehicle load. *Ocean Engineering* 235: 109431.

[4] Torres-Alves G.A., Hart C.M.P., Morales-Nápoles O., Jonkman S.N. (2022) Structural reliability analysis of a submerged floating tunnel under copula-based traffic load simulations *Engineering Structures* 269: 114752.

An adaptive nonlinear hybrid vibration absorber

L. Mesny, S. Baguet and S. Chesné

Univ Lyon, INSA-Lyon, CNRS UMR5259, LaMCoS, F-69621, France

Abstract. Linear hybrid dampers combining passive and active control are promising devices for vibration mitigation. In this work, we extend this concept to nonlinear vibration absorbers. A nonlinear hybrid vibration absorber is proposed, which combine sensor, actuator, control law and nonlinear dynamics to improve the adaptability and responsiveness of the absorber.

Introduction

Several ways have been explored to improve the classical linear tuned mass damper (TMD). The Nonlinear Energy Sink (NES) is a well known passive absorber device based on the use of an essential nonlinearity to get an irreversible energy transfert, also called Targeted Energy Transfert (TET) [1]. On the other hand, hybrid vibration absorbers [2] combine passive and active control and makes use of sensors, actuators. Besides the increase in performance, it also provides a 'fail-safe' feature since the passive absorber still operates if the active part is shut down. In this paper, the two approaches are combined to create a nonlinear hybrid absorber. The active control is used to make the absorber adaptive by modifying its damping and its nonlinearity when operating conditions are changing.

We consider an academic 2-dof system governed by the adimensionalized following equation :

$$\begin{cases} \ddot{x}_1 + \epsilon\lambda_1\dot{x}_1 + x_1 + \epsilon\lambda_2(\dot{x}_1 - \dot{x}_2) + \epsilon k_2(x_1 - x_2) + \epsilon k_{nl2}(x_1 - x_2)^3 = \epsilon F \sin(\omega t) + \epsilon F_a(x(t), \dot{x}(t)) \\ \ddot{x}_2 + \lambda_2(\dot{x}_2 - \dot{x}_1) + k_2(x_2 - x_1) + k_{nl2}(x_2 - x_1)^3 = -F_a(x(t), \dot{x}(t)) \end{cases} \quad (1)$$

where x_1, x_2 are the mass displacements, F the amplitude of the harmonic external force; $\lambda_1, \lambda_2, k_2$, and k_{nl2} are damping's coefficients, linear and nonlinear coefficients respectively. $\epsilon \ll 1$ the mass ratio. Finally, the nonlinear feedback $F_a(x(t), \dot{x}(t))$ can take different forms : polynomial, non-polynomial. To better understand the energy flows involved in the slow dynamics, the analysis of the system is performed with respect to the Slow Invariant Manifold (SIM) [4].

Results and discussion

In Fig. 1, two numerical results for different active forces are compared : NES with modified singular points (a), NES with polynomial active part (b) and temporal response comparison for a NES with polynomial active part (c). Active control is used to overcome the design flaws of a nonlinear vibration absorber. For example, the nonlinearity of the absorber can be tuned in order to modify the singular points and/or the unstable zone of the SIM, which in turn will change the activation threshold and the appearance of strongly modulated responses, or even create additionnal ones. The robustness of the methodology will be assessed by means of a parametric study [3]. Finally, an experimental validation will complement the proposed numerical model and serve as a proof of concept.

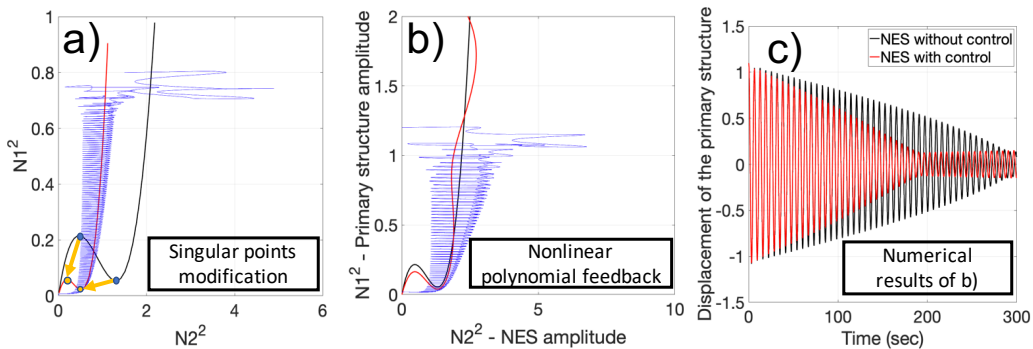


Figure 1: a) & b) SIM : black (no control), red (with control) and transient results in blue. c) Transient comparison of b)

References

- [1] Gendelman O. V. (2011). Targeted energy transfer in systems with external and self-excitation. *Proc. Inst. Mech. Eng., Part C: J. Mech. Eng. Sci.* **225**:9:2007-2043.
- [2] Collette C., Chesne S. (2016) Robust hybrid mass damper. *J. Sound Vib.* **375**:19-27.
- [3] Xie L., Baguet S., Prabel B. and Dufour R. (2017) Bifurcation tracking by Harmonic Balance Method for performance tuning of nonlinear dynamical systems. *Mech. Syst. Sig. Process.* **88**:445-461.
- [4] Manevitch L. (2001) The description of localized normal modes in a chain of nonlinear coupled oscillators using complex variables. *Nonlinear Dyn.* **25**:1: 95-109.

A 3D Structural Model for Nonlinear Dynamic Analyses of Rigid Blocks Supported by Wire Rope Isolators

Stefania Lo Feudo* and Nicolò Vaiana**

* Laboratoire Quartz (EA7393), ISAE-Supméca, St-Ouen-sur-Seine, France

** Department of Structures for Engineering and Architecture, University of Naples Federico II, Naples, Italy

Abstract. In this study we propose a 3D structural model to perform nonlinear dynamic analyses of rigid blocks mounted on Wire Rope Isolators. The complex hysteretic behavior of such devices is simulated by using the recently formulated Vaiana-Rosati model since it is capable of reproducing both symmetric and asymmetric force-displacement hysteresis loops. The dynamic of the base-isolated system under both harmonic and seismic excitation will be addressed.

Introduction

Wire Rope Isolators (WRIs) are metal devices made up of a stainless steel cable and two aluminum alloy or steel retainer bars where the cable is embedded. They can be effectively adopted for the vibration control of museum artifacts, hospital equipment, electrical transformers, supercomputers, and intermodal containers. To allow for an accurate assessment of their performance when they are employed in the above-mentioned applications, we derive the nonlinear equilibrium equations of the three dimensional (3D) structural model shown in Figure 1a. Notably, the rigid block is mounted on a rigid plate supported by four WRIs and is located eccentrically with respect to the center of gravity of the isolation base. To reproduce the typical asymmetric (symmetric) hysteresis loops, as those in Figure 1b (1c), characterizing the WRIs response along their axial direction (transverse directions), we use a recently formulated hysteresis model [1]. The 3D model can be used to perform nonlinear dynamic analyses of the base-isolated system subjected to earthquake excitation.

3D Structural Model

The proposed 3D structural model (Figure 1a) consists of a first rigid body having mass m_1 and a second rigid body of mass m_2 rigidly linked to the first one; it is assumed to have an eccentricity between the two mass centers. Three rate-independent hysteretic elements are attached to each corner of the first rigid body in order to simulate the hysteretic behavior of WRIs along their axial, roll and shear directions.

Vaiana-Rosati Model of Hysteresis

The vertical (horizontal) rate-independent hysteretic elements are adopted to simulate asymmetric (symmetric) restoring force-displacement hysteresis loops. In particular, such responses are reproduced by adopting the Vaiana-Rosati Model (VRM) since it offers a series of advantages with respect to other models available in the literature [2, 3], such as: (i) the evaluation of the output variable in closed form, (ii) the simulation of complex hysteresis loops, (iii) the modeling of the loading and unloading phases by employing two different sets of parameters, (iv) the adoption of parameters having a clear theoretical and/or experimental interpretation, and (v) a straightforward computer implementation.

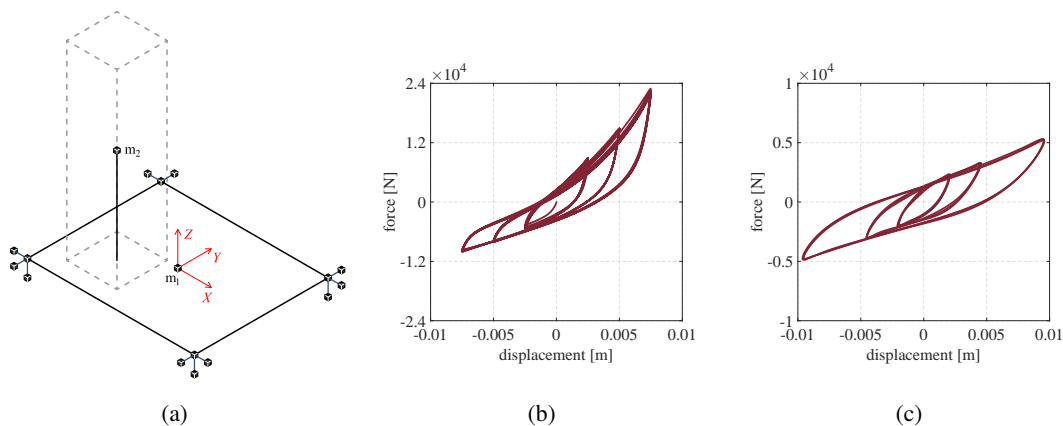


Figure 1: 3D structural model (a) and typical hysteresis loops exhibited by WRIs along their axial (b) and transverse (c) directions.

References

- [1] Vaiana N., Rosati L. (2023) Classification and Unified Phenomenological Modeling of Complex Uniaxial Rate-Independent Hysteretic Responses. *Mech. Syst. Signal Pr.* **182**:109539.
- [2] Demetriades G. F., Constantinou M. C., Reinhorn A. M. (1993) Study of Wire Rope Systems for Seismic Protection of Equipment in Buildings. *Eng. Struct.* **15**:321-334.
- [3] Ni Y. Q., Ko J. M., Wong C. W., Zhan S. (1999) Modelling and Identification of a Wire-Cable Vibration Isolator via a Cyclic Loading Test. Part 1: Experiments and Model Development. *J. Syst. Control. Eng.* **213**:163-171.

The enhanced nonlinear friction bearing isolators using negative stiffness inertial amplifiers

Sudip Chowdhury*, Arnab Banerjee* and Sondipon Adhikari**

*Civil Engineering Department, Indian Institute of Technology Delhi

**James Watt School of Engineering, The University of Glasgow, Glasgow, Scotland

*Corresponding author: sudip.chowdhury@civil.iitd.ac.in

Abstract. The inertial amplifier and negative stiffness inertial amplifier coupled nonlinear friction bearing isolators, such as inertial amplifier resilient friction bearing isolators (IARFBI), negative stiffness inertial amplifier resilient friction bearing isolators (NSIARFBI), inertial amplifier friction pendulum systems (IAFPS), and negative stiffness inertial amplifier friction pendulum systems (NSIAFPS) are introduced in this paper. H₂ optimization method applies to derive the exact mathematical formulation for optimal design parameters for each nonlinear isolator. The stochastic linearization method applies to linearize each element of the highly nonlinear governing equations of motion of the dynamic systems isolated by each nonlinear isolator. The frequency-domain responses are determined analytically through transfer function formation. A numerical study has been performed to assess the vibration reduction capacity of the nonlinear isolators applying the Newmark-beta method. The vibration reduction capacities of IARFBI, NSIARFBI are 36.36 %, 48.48 % and IAFPS, NSIAFPS are 41.76 %, 52.94 %, superior to TRFBI and TFPS.

Introduction

The base isolators [1] are widely applied passive vibration control devices due to their superior vibration reduction capacity. Recently, inerters [2], inertial amplifiers, and negative stiffness devices [3] have been installed inside traditional base isolators to increase their vibration reduction capacity without affecting the static mass. However, the inertial amplifiers and negative stiffness inertial amplifiers are not applied to the traditional nonlinear friction bearing isolators, such as resilient friction bearing isolators and friction pendulum systems. A research scope has been identified from the existing state of the art. Hence, the negative stiffness inertial amplifier nonlinear friction bearing isolators are introduced in this study. Therefore, the nonlinear equations of motion of a single degree of freedom system (SDOF) isolated by the novel isolators are derived as

$$\begin{aligned} m_d \ddot{x}_b + F_{iarfbi,iafps} - c_s \dot{x}_s - k_s x_s &= -m_d \ddot{x}_g \text{ and } m_s \ddot{x}_s + m_s \ddot{x}_b + c_s \dot{x}_s + k_s x_s = -m_s \ddot{x}_g \\ F_{iarfbi} &= c_d \dot{x}_b + k_d x_b + \mu m_d g \operatorname{sgn}(\dot{x}_b) \text{ and } F_{iafps} = k_d x_b + \mu m_d g \operatorname{sgn}(\dot{x}_b) \\ m_d \ddot{x}_b + F_{nsiarfbi,nsiafps} - c_s \dot{x}_s - k_s x_s &= -m_d \ddot{x}_g \text{ and } m_s \ddot{x}_s + m_s \ddot{x}_b + c_s \dot{x}_s + k_s x_s = -m_s \ddot{x}_g \\ F_{nsiarfbi} &= c_d \dot{x}_b + (k_d - k_n) x_b + \mu m_d g \operatorname{sgn}(\dot{x}_b) \text{ and } F_{nsiafps} = (k_d - k_n) x_b + \mu m_d g \operatorname{sgn}(\dot{x}_b) \\ x_{s,b} &= \text{Relative displacement of structure and isolator, } \mu = \text{poisson's ratio, } m_d = m_b + m_a \left(1 + \frac{1}{2 \tan^2 \theta}\right) \end{aligned}$$

Results and discussion

The differences in the dynamic responses of the SDOF systems isolated by TRFBI, IARFBI, NSIARFBI and IAFPS, NSIAFPS, TFPS versus time subjected to the Loma Prieta earthquake have been shown in Figure 1 (a) and Figure 1 (b).

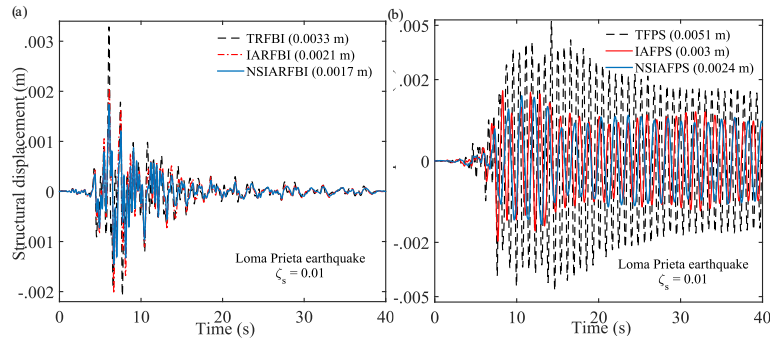


Figure 1: The variations of displacement responses of structures isolated by (a) TRFBI, IARFBI, NSIARFBI and (b) TFPS, IAFPS, NSIAFPS versus time subjected to Loma Prieta earthquake.

Hence, the dynamic response reduction capacities of IARFBI and NSIARFBI are significantly 36.36 % and 48.48 % superior to TRFBI. The dynamic response reduction capacities of IAFPS and NSIAFPS are significantly 41.76 % and 52.94 % superior to TFPS.

References

- [1] Chowdhury, Sudip, and Arnab Banerjee. 2022. "The exact closed-form expressions for optimal design parameters of resonating base isolators." *International Journal of Mechanical Sciences* 107284.
- [2] Smith, Malcolm C. 2002. "Synthesis of mechanical networks: the inerter." *IEEE Transactions on automatic control* 1648-1662.
- [3] Chowdhury, S and Banerjee, A and Adhikari, S. 2022. "Optimal negative stiffness inertial-amplifier-base-isolators: Exact closed-form expressions." *International Journal of Mechanical Sciences* 107044.

Long-stroke hydraulic damping device and verification of its vibration characteristics

Jingchao Guan* and Xilu Zhao*

* Department of Mechanical Engineering, Saitama Institute of Technology, Fukaya, Saitama, Japan

Abstract. This study proposes a new origami-type axially free folding hydraulic damper to improve the structural characteristics of the conventional cylindrical shape with a limited effective stroke relative to the overall length. Firstly, the basic design equations for the proposed paper-folding hydraulic damper are derived by demonstrating that the folding line cylinder on the sidewall always satisfies the foldable condition of the paper-folding hydraulic damper. Next, the fluid flow characteristics inside the origami hydraulic damper and in the flow path were analyzed; it was determined that the actual damping force exerted on the origami damper was proportional to the square of the velocity of motion. Equations of motion were developed considering the derived damping force equation, and a vibration analysis method using the Range–Kutta numerical analysis technique was established. A validation test system with an origami hydraulic damper in a mass-spring vibration system was developed, and vibration tests were performed with actual seismic waves to verify the damping characteristics and effectiveness of the origami hydraulic damper.

Introduction

Hydraulic dampers are primarily used as components for absorbing vibration and shock energy. Nevertheless, the majority of existing hydraulic dampers are of the metal cylinder type, wherein the actual lengths of extension and contraction are limited compared to the total axial length, which limits their applicability when the installation space is limited. New techniques are required for weight reduction by replacing metal cylinders with dampers made of lightweight nonmetallic materials.

Therefore, an experimental setup, shown in Figure 1a, was developed to study the performance of an inverted spiral origami-type hydraulic damper. The experimental setup was composed of an origami damper, elastic spring, mass block, frame, fixed plate, moving plate, and oil tube. As shown in the figure, a validation test system was fabricated to perform practical vibration tests.

Results and discussion

Figure 1b shows the response displacement of the time series when shaking was measured using seismic waves. The solid blue line indicates the measurement results without hydraulic oil, whereas the red dotted line indicates the measurement results with hydraulic oil.

The results in Figure1b indicates that the response displacement of the scenario wherein hydraulic fluid is included are apparently smaller than the response displacement of the scenario in which no hydraulic fluid is included when vibrations are applied using seismic waves. It was evident that the proposed origami hydraulic damper provided a dependable damping effect under complex excitation conditions and could be used as a vibration-damping device.

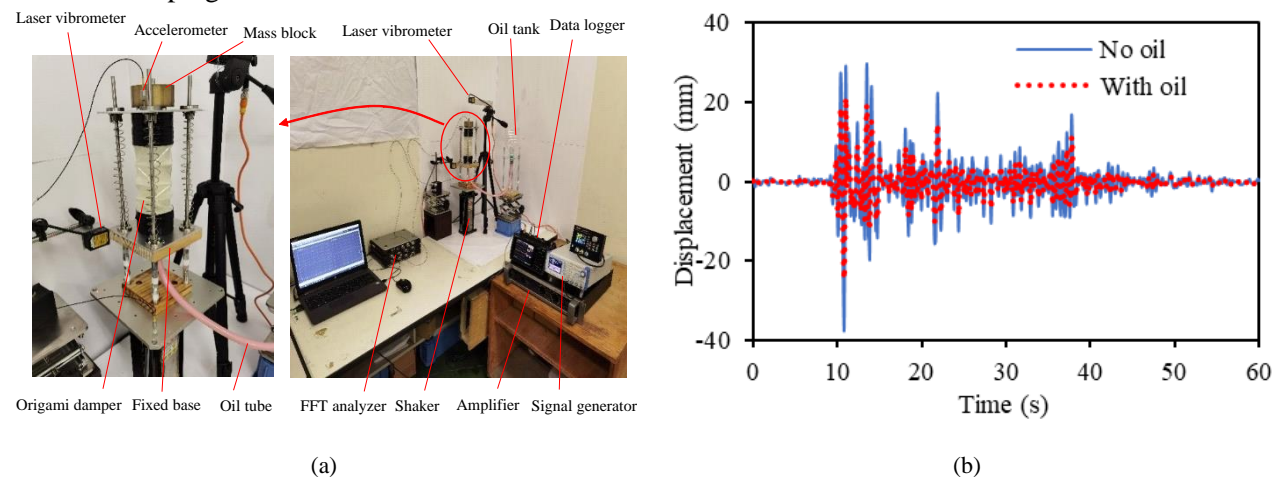


Figure 1: (a) Origami damper device and vibration experiment system. (b) Spectral distribution of displacement.

References

- [1] Wu, Z.; Xu, G.; Yang, H.; Li, M. Analysis of Damping Characteristics of a Hydraulic Shock Absorber. *Shock. Vib.* **2021**, *2021*, 8883024.
- [2] Sun, J.; Jiao, S.; Huang, X.; Hua, H. Investigation into the Impact and Buffering Characteristics of a Non-Newtonian Fluid Damper: Experiment and Simulation. *Shock. Vib.* **2014**, *2014*, 170464.
- [3] Ye, S.; Zhao, P.; Zhao, Y.; Kavousi, F.; Feng, H.; Hao, G. A Novel Radially Closable Tubular Origami Structure (RC-ori) for Valves. *Actuators* **2022**, *11*, 243.

Effect of wear flat length on the global dynamics of rotary drilling

Kapil Kumar and Pankaj Wahi

Department of Mechanical Engineering, Indian Institute of Technology Kanpur, India

Abstract. The regenerative effect developed by the variable thickness of cut in rotary drill system yields self-excited vibrations. These vibrations are the main cause of excessive wear on the tool edge. This cause a wear flat to develop behind the cutting edge. Interaction between the wear flat and rock surface results in a normal force and frictional torque which can effect the overall dynamics of the drill system. We have included a wear flat in the bit-rock interaction model and have considered a lumped parameter model with two degrees of freedom for this analysis. Numerical simulations have been done to analyze the effect of wear flat length which shows the linear stability of the system is not affected by the wear flat length for steady-state conditions. However, the global dynamic behavior of the drilling system varied with the wear-flat length. Here we have studied the effect of various parameters such as coefficient of friction, wear-flat length and damping ratio on the system dynamics.

Introduction

Rotary drilling systems are used to drill deep borewells which are used in exploration and extraction of tract fossil fuels. It consists of a rotary table, a series of hollow pipes (drill-string), a drill collar, and a drill bit. Self-excited vibrations resulting from the regenerative forces are often manifested as bit-bounce and stick-slip vibrations. Gupta and Wahi [1, 2, 3] have studied the effect of various parameters on the stability of the system assuming a sharp edge cutter. A linear stability analysis has been studied by Zhang and Detournay [4] wherein they consider a multi-dimensional model with a wear flat length. However, the global dynamics of drill systems with worn tools have not been studied yet to the best of our knowledge. This model incorporated the various case of normal reaction force acting on the cutter. A simplified rotary drill system with two degrees of freedom is considered; one is in the axial and the other in the torsional direction. The forces and torque between the tool and the rock surface can be considered as reported in [5]. When the normal reaction force is fully mobilized with the surface, the equation of motion in the non-dimensional form of the lumped parameter model is

$$\begin{aligned} \ddot{x}(\tau) + 2\zeta\beta\dot{x}(\tau) + \beta^2x(\tau) = \\ n\psi\delta_0 - n\psi\delta(\tau)H(\omega_0 + \dot{\theta}(\tau))H(\delta(\tau)) + \Lambda_1l(1 - H(v_0 + \dot{x}(\tau))H(\delta(\tau))), \\ \ddot{\theta}(\tau) + 2\kappa\dot{\theta}(\tau) + \theta(\tau) = \\ n\delta_0 - n\delta(\tau)H(\omega_0 + \dot{\theta}(\tau))H(\delta(\tau)) + \Lambda_2l\left(1 - H(v_0 + \dot{x}(\tau))H(\delta(\tau))\text{sgn}(\omega_0 + \dot{\theta}(\tau))\right), \end{aligned} \quad (1)$$

where n is the number of cutters, β is the ratio of axial and torsional frequency, ζ and κ are the axial and torsional damping coefficient, δ_0 is the steady thickness of cut, ω_0 is the non-dimensional angular velocity of the rotary table, τ is the non-dimensional time scale, l is the non-dimensional wear flat length, Λ_1 and Λ_2 are non-dimensional constants. The instantaneous thickness of the cut is modelled as reported in [1] where the cut surface function L is defined between two simultaneous cutters. The function L is governed by the partial differential equation (PDE) reported in [1] with the appropriate boundary condition. These coupled ODE and PDE can be converted into a finite set of first-order system of ODEs with a reduced Galerkin approximation method. Now we have done the numerical analysis to study the effect of parameters on the system.

Results and discussion

We have first considered that the normal reaction force is fully mobilized, i.e., the normal reaction at the wear flat is constant irrespective of the depth of cut and the numerical simulation has been done. It is found that the linear stability analysis of the steady drilling state has not been affected due to the wear-flat on cutters in the non-dimensional parameter space. However, the fully mobilized assumption leads to chattering phenomenon at the inception of the bit-bounce vibrations, i.e., when the cutter is about to leave the rock surface ($\dot{x} + v \leq 0$). Hence, we have incorporated the case when the normal reaction force is linearly varied with the depth of cut before the reaction force is fully mobilized. This leads to a gradual reduction in the normal force when contact is about to be lost and suppresses the chattering behavior. Details of these will be presented at the conference.

References

- [1] Gupta S. K., Wahi P. (2016) Global axial–torsional dynamics during rotary drilling. *J. Sound Vib.* **375**:332-352.
- [2] Gupta S. K., Wahi P. (2018) Bifurcations in the axial–torsional state-dependent delay model of rotary drilling. *Int. J. Non Linear Mech.* **99**:13-30.
- [3] Gupta S. K., Wahi P. (2018) Criticality of bifurcation in the tuned axial–torsional rotary drilling model. *Nonlinear Dyn.* **91**:113-130.
- [4] Zhang H., Detournay E. (2022) A high-dimensional model to study the self-excited oscillations of rotary drilling systems. *Commun. Nonlinear Sci. Numer. Simul.* **112**:106549.
- [5] Detournay E., Richard T., Shepherd M. (2008) Drilling response of drag bits: theory and experiment. *Int. J. Rock Mech. Min. Sci.* **45**:1347-1360.

Control of an acoustic mode by a digitally created Nonlinear Electroacoustic Absorber at low excitation levels: Analytical and Experimental results

Maxime Morell*, Manuel Collet**, Emmanuel Gourdon* and Alireza Ture Savadkoohi*

*Univ Lyon, ENTPE, Ecole Centrale de Lyon, CNRS, LTDS, UMR5513, 69518 Vaulx-en-Velin, France

**Univ Lyon, CNRS, Ecole Centrale de Lyon, ENTPE, LTDS, UMR5513, 69130 Ecully, France

Abstract. In this study, an acoustic mode of a tube is controlled by a digitally created Nonlinear Electroacoustic Absorber (NEA) at low excitation levels, where the nonlinear threshold is usually not reached in the field of acoustics with passive nonlinear energy sink. A comparison is carried out between a linear Electroacoustic Absorber, similar to a Tuned Mass Damper (TMD) in mechanics, and a digital NEA. The innovative method for creating a NEA lies on Real Time Integration of the dynamics of the device. It allows to choose any behavior of the system by digitally programming the corresponding targeted dynamics. Here, a loudspeaker Impedance Control law with a cubic stiffness is considered, as this system is well known in mechanics and provides nonlinear phenomena that are highlighted at low and moderate excitation levels in our study.

Introduction

In the field of acoustics, one can observe nonlinear phenomena when the amplitudes of motion and pressure reached a certain threshold. Nonlinear passives absorbers are usually activated at high amplitudes. Bellet et al. [1] have implemented a visco-elastic membrane behaving as a pure cubic stiffness oscillator above 143 dB Sound Pressure Level (SPL), to control an acoustic mode. Gourdon et al. [4] have implemented a Helmholtz resonator, similar to a TMD in mechanics, in its nonlinear regime and therefore have succeeded to create a nonlinear oscillator above 138 dB SPL. More recently, Guo et al. [3] placed a microphone in the back cavity of a loudspeaker, allowing to add a nonlinear current proportional to the cubic law of the displacement of the membrane to the linear current, modifying the classic Impedance Control around 100 dB. The aim of our study is to create a NEA composed of microphones collocated to a loudspeaker, and monitored by a processor. This processor calculates the current to inject into the loudspeaker coil based on the sensed pressure at each time step to implement any previously digitally defined nonlinear behavior. The first simulations have been realized by De Bono [2]. This innovative method to implement a NEA lies on the evaluation of a target dynamic of the loudspeaker to achieve a desired behavior. The process is based on measured pressure at each time step. Impedance Control is electro-active, but acoustically passive, unlike Active Noise Control, and therefore has to be distinguished. As a result, Impedance Control leads to a low energy consumption, as the electrical current needed is low. In the study, an acoustic mode created with a reduced section of a tube is weakly coupled to the NEA using a coupling box.

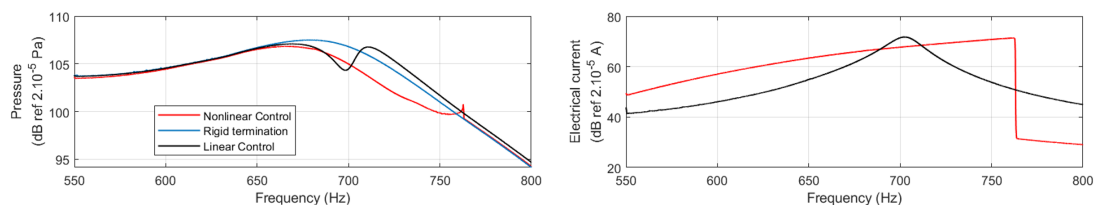


Figure 1: Obtained experimental results in the form of pressure and current for sweeping frequency excitation

Results and discussion

This study highlights the creation of a NEA at low excitation amplitudes. As a result the two peaks usually obtained with a TMD vanish with the NEA. A jump phenomenon in the pressure inside the tube can be seen as the electrical current of the NEA jumps, exposing an unstable zone that can be easily predicted by both analytical and experimental results in the case of a Two Degree Of Freedom system containing a duffing oscillator. A nonlinear behavior of the oscillator is shown.

References

- [1] Bellet R., Cochelin B., Herzog P., Mattei P.-O. (2010) Experimental study of targeted energy transfer from an acoustic system to a nonlinear membrane absorber. *J. Sound Vib.* **329**(14):2768-2791.
- [2] De Bono E., (2021) Electro-active boundary control for noise mitigation : Local and Advective strategies. *PhD thesis*. Ecole Centrale de Lyon.
- [3] Guo X., Lissek H., Fleury R. (2020) Improving Sound Absorption Through Nonlinear Active Electroacoustic Resonators. *Phys. Rev. Appl.* **13**(1):014018.
- [4] Gourdon E., Ture Savadkoohi A., Alamo Vargas V. (2018) Targeted Energy Transfer From One Acoustical Mode to an Helmholtz Resonator With Nonlinear Behavior. *J. Sound Vib.* **140**(6):061005

Vibration control of lossless transmission lines with nonlinear terminators: a simplifying approach

Mohammad Amin Faghihi*, Shabnam Tashakori**,***,****, Ehsan Azadi Yazdi* and Nathan van de Wouw *****

* Department of Mechanical Engineering, Shiraz University, Shiraz, Iran.

**

Centre for Applied Dynamics Research, School of Engineering, University of Aberdeen, United Kingdom *** Department of Mechanical and Aerospace Engineering, Shiraz University of Technology, Shiraz, Iran

**** Rahesh Innovation Center, Iran

***** Department of Mechanical Engineering, Eindhoven University of Technology, 5600 MB Eindhoven, The Netherlands

Abstract. This article proposes mathematical modeling and a simplifying control approach for the nonlinear vibrations of lossless transmission lines. One extremity of the transmission line is under a nonlinear external force while the control force is applied on the other extremity. The model is formulated in terms of Neutral-type Delay Differential Equations (NDDEs). These equations are derived directly by applying D'Alembert's method to the Partial Differential Equation (PDE) governing the lossless transmission line. An approach is developed to simplify the control problem to a simple Retarded Delay Differential Equation (RDDE) with input delay rather than an NDDE. It is shown that a sufficient condition for the NDDE to be stabilized is the existence of a control input which stabilizes the simplified RDDE in the sense of input-to-state stability.

Introduction

In general, a transmission line is a specialized cable or other structure designed to conduct a signal. In electrical engineering, the conducted signal is electromagnetic waves, while in mechanical engineering, it may be mechanical waves such as elastic waves. The governing equation representing a lossless transmission line is given by the following PDE:

$$\frac{\partial^2 f}{\partial t^2}(x, t) = c^2 \frac{\partial^2 f}{\partial x^2}(x, t), \quad (1)$$

where $f(x, t)$ is a function of the variables x and t and c is a constant. The wave equation (1) can be solved by using d'Alembert methods through introducing Riemann variables [1], which ultimately transforms the PDE in (1) to an NDDE. Such mathematical modelling appears in many practical engineering applications such as coaxial cable, chemical engineering reactor applications, ship stabilization, large-scale integration systems, and drilling systems [2]. Generally, three kinds of delays are involved in such NDDE systems, i.e., (i) the state delays, (ii) the delays in the argument of state derivatives (neutral-type delays), and (iii) the input delays. In recent years, there has been a great deal of focus on the control issue of nonlinear systems with input delay [3]. On the other hand, there is no similar study on the control issue of nonlinear neutral-type time delay systems with input delays. In this paper, the control problem of the nonlinear vibrations of a lossless transmission line is addressed. The equations of motion are formulated in terms of NDDEs with constant neutral-type and input delays. For a general case (the general nonlinear load), it is shown that designing a controller for such neutral-type delay dynamics is equivalent to stabilizing a more straightforward dynamics without neutral-type delay terms. In the presence of neutral-type delay terms, there exist vertical eigenvalue asymptotes in the system spectrum, which cannot be changed by any feedback control law. This is the main reason that makes the control design challenging for NDDEs. The proposed approach makes the control design simpler by providing a condition to design a controller for an alternative dynamics (rather than the NDDEs) without neutral-type delay terms, and consequently, in the absence of the vertical eigenvalue asymptotes.

Results and discussion

A novel control approach is presented to simplify the control problem of nonlinear vibrations of a lossless transmission line, formulated in terms of NDDEs. It is shown that by introducing an input transformation, the control problem of the NDDEs is simplified to an alternative control problem for a system without neutral-type delay terms. Indeed, it is proved that showing the input-to-state stability of the simplified system guarantees the asymptotic stability of the original NTD. The proposed approach is applied to a drill-string as a practical example of transmission lines and the stability is obtained by designing a controller for the simplified system.

References

- [1] Tashakori S, Vossoughi G, Zohoor H, Yazdi EA. Modification of the infinite-dimensional neutral-type time-delay dynamic model for the coupled axial-torsional vibrations in drill strings with a drag bit. *Journal of Computational and Nonlinear Dynamics*. 2020.
- [2] Tashakori S, Vossoughi G, Zohoor H, van de Wouw N. Prediction-Based Control for Mitigation of Axial-Torsional Vibrations in a Distributed Drill-String System. *IEEE TCST*. 2021.
- [3] Krstic M. Input delay compensation for forward complete and strict-feedforward nonlinear systems. *IEEE TAC*. 2009.

Preliminary numerical analysis of the Vibro-Impact Isolation systems under seismic excitations

Giuseppe Perna*, Maurizio De Angelis* and Ugo Andreaus*

*Department of Structural and Geotechnical Engineering, Sapienza University of Rome, Via Eudossiana 18, Rome, Italy

Abstract

The problem of large displacements in isolated structures can cause undesirable effects, such as damage to isolation systems or increases in superstructure accelerations. In order to limit these undesirable effects, the authors propose a new integrated design methodology of vibro-impact isolation systems that aims to control large displacements while limiting the increase in accelerations due to the impact phenomenon. Therefore, this paper shows numerical results obtained on single-degree-of-freedom systems isolated at the base subjected to seismic excitations and constrained by two deformable and dissipative devices.

Introduction

Seismic isolation is a widely used passive control methodology for mitigating the dynamic response of structures. However, significant seismic actions can induce considerable displacements in these structures, which in turn can cause damage to the isolation system or impacts against adjacent structures in the case that the seismic gap is insufficient [1]. Vibration-impacted isolation systems (V-IIS) have been studied by the authors through the definition of a single-degree-of-freedom system isolated at the base, whose displacements are limited by deformable and dissipative devices, called bumpers [2-4]. There are three parameters that define V-IIS: the initial seismic gap, the stiffness and the damping of the bumper. In order to mitigate the detrimental effects of large displacements, an optimal design methodology for base action of harmonic type was defined, which produced an optimality relation and an optimal curve, minimizing the maximum accelerations due to impacts. The optimality relation and the optimal curve reduce the design of V-IISs to the initial seismic gap parameter only. The objective of this paper is to apply the proposed methodology in the case of harmonic action for the optimal design of the parameters that characterize V-IISs subjected to seismic actions.

Results and discussion

The numerical response of V-IIS subjected to known seismic actions was studied. The results shown in Figures 1a, 1b and 1c refer to the Irpinia earthquake. Figures 1a and 1b represent, respectively, the maximum relative displacement and maximum absolute acceleration of the system, appropriately normalized, as a function of its natural period and for different initial seismic gaps. In the zone between 1.5 sec and 4 sec, of interest for isolation, there are greater reductions in displacement, compared with the no-impact (FF) case, as the initial gap decreases; from the acceleration point of view, slight increases are obtained for the various gaps investigated except for the null gap case, which even reports reductions, again compared with the FF case. Finally, Figure 1c shows a force-displacement cycle for a particular case. This graph well summarizes the strong displacement reduction and good control of the total system force, compared to the FF case, obtained by the proposed V-IIS optimal design methodology.

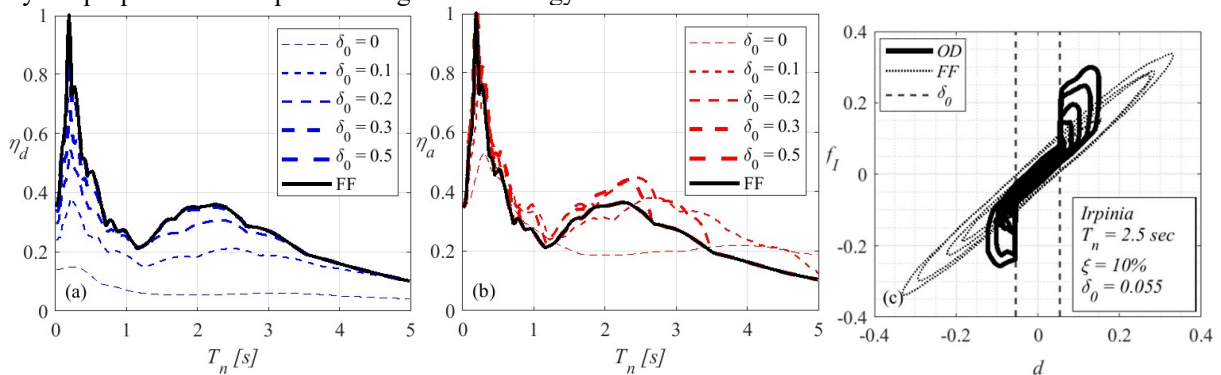


Figure 1: (a) the maximum normalized displacement (η_d) and (b) the maximum normalized acceleration (η_a) of the system as a function of its natural period (T_n), for different initial seismic gap (δ_0); (c) the force-displacement cycle.

References

- [1] Polycarpou, P.C., Komodromos, P., "On poundings of a seismically isolated building with adjacent structures during strong earthquakes", *Earthq Eng Struct Dyn*, 39(8), 2010.
- [2] Andreaus, U., De Angelis, M., "Influence of the characteristics of isolation and mitigation devices on the response of single-degree-of-freedom vibro-impact systems with two-sided bumpers and gaps via shaking table test", *Struct Control Health Monit*, 27(5), 2020.
- [3] Stefani, G., De Angelis, M. Andreaus, U., "Influence of the gap size on the response of a single-degree-of-freedom vibro-impact system with two-sided constraints: Experimental test and numerical modelling", *Int J Mech Sci*, 206, 2021.
- [4] Stefani, G., De Angelis, M. Andreaus, U., "The effect of the presence of obstacles on the dynamic response of single-degree-of-freedom systems: Study of the scenarios aimed at vibration control", *J Sound Vib* 531, 2022.

Nonlinear electroacoustic resonator at low excitation amplitudes: grazing incidence analysis.

Emanuele De Bono*, Maxime Morell**, Manuel Collet***, Emmanuel Gourdon**, Alireza Ture Savadkoohi**, Claude-Henri Lamarque **, Morvan Ouisse*, Gaël Matten*.

*Univ. Bourgogne Franche-Comté, FEMTO-ST Institute, Department of Applied Mechanics, CNRS/UFC/ENSMM/UTBM, 24 Chemin de l'Épitaphe, 25000 Besançon, France.

**Univ. Lyon, Ecole Nationale des Travaux Publics de l'Etat, LTDS – UMR CNRS 5513, 3 rue Maurice Audin, F-69518 Vaulx-en-Velin Cedex, France.

***École Centrale de Lyon, LTDS laboratory, CNRS UMR5513, 36 avenue Guy de Collongue, 69134 Ecully Cedex, France.

Abstract. The electroacoustic resonator is an efficient electro-active device for noise attenuation in enclosed cavities or acoustic waveguides. It is made of a loudspeaker (the actuator) and one or more collocated microphones (the sensors). By driving the electrical current in the speaker coil it is possible to target a desired acoustic impedance on the speaker diaphragm. A novel technique has been recently implemented which allows to target nonlinear operators at low excitation levels. In this contribution, we first expose the concept of such nonlinear control along with its numerical and experimental validation. Then, in the perspective of wave propagation control in an acoustic waveguide, such nonlinear resonator has been analysed in the grazing incidence problem, typical of acoustic liners.

Introduction

In acoustics, the potentialities of nonlinear sound absorption has been explored for designing Helmholtz resonators in the nonlinear regime, or in [2], where Targeted-Energy-Transfer (TET) was achieved from a linear acoustic cavity to a *weakly-coupled* thin visco-elastic membrane which behaves as a Duffing resonator. As the linear ones, passive nonlinear absorbers are not easily tunable for targeting different bandwidths. Moreover, they usually need high-energy threshold in order to trigger the nonlinear behaviour. An electro-active nonlinear absorber might overcome these limitations, by *transforming* the mechano-acoustical dynamics of the loudspeaker from linear to nonlinear, while keeping the same external excitation levels. Here, we expose the model-inversion control problem to transform the acoustical response of the electroacoustic resonator (ER) from LTI to potentially any causal locally-reacting response (nonlinear and/or time-variant). In this contribution, the control algorithm is implemented to achieve a Duffing target acoustical dynamics, with tunable parameters. Then, the nonlinear ER is studied in a grazing-incidence configuration, in order to exploit its potentialities for special scattering phenomena (including solitons) in acoustic waveguides.

Results and discussion

In Figure 1, the *nonlinearly controlled* ER is tested against an external sound source emitting a pure sine at 700 Hz, in a quasi-open field environment. The external sound source is activated after $t = 3$ seconds to assess the control performance also in the transient regime. The time-history of the measured velocity $\dot{u}(t)$ (solid blue) is compared with the target velocity $\dot{u}_d(t)$ in dashed red. Observe that the actual velocity follows the target one with slight difference due to model uncertainties and time delay in the digital control algorithm. Once the nonlinear control is validated in open-field, it can be analysed for modal attenuation in acoustic cavities or in terms of its scattering performances in acoustic waveguides. The latter is the application studied in this contribution, opening the doors toward the design of tunable nonlinear liners at classical excitation levels.

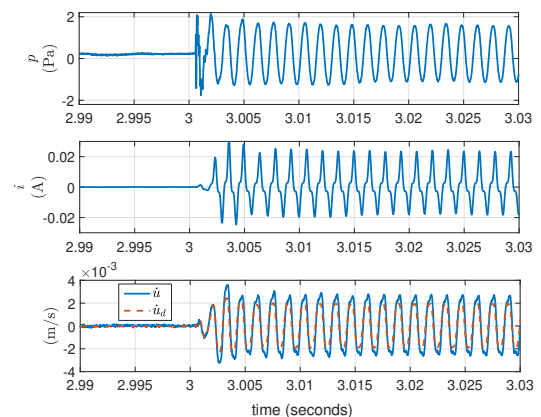


Figure 1: Time histories of pressure $p(t)$, electrical current $i(t)$, target and measured velocities (\dot{u}_d and $\dot{u}(t)$ respectively) on the speaker diaphragm. An external sound source emitting a pure sine at 700 Hz, is activated after $t = 3$ seconds.

References

- [1] Gourdon E., Ture Savadkoohi A., Alamo Vargas V. (2018) Targeted Energy Transfer From One Acoustical Mode to an Helmholtz Resonator With Nonlinear Behavior. *J. Sound Vib.* **140(6)**:061005.
- [2] Cochelin B., Herzog P., Mattei P.-O. (2006), Experimental evidence of energy pumping in acoustics. *Comptes Rendus Mecanique* **334**:639–644.

A Nonlinear Piezoelectric Shunt Absorber with 2:1 Internal Resonance

Zein A. Shami*, Cyril TOUZÉ[‡] and Christophe GIRAUD-AUDINE **, Olivier THOMAS*

*Arts et Métiers Institute of Technology, LISPEN, HESAM Université, Lille, France #

[‡]IMSIA, ENSTA Paris, CNRS, EDF, CEA, Institut Polytechnique de Paris, Palaiseau, France #

** Arts et Mtiers Institute of Technology, L2EP, HESAM Universit, Lille, France#

Abstract. We present a theoretical and experimental analysis of a new nonlinear piezoelectric shunt absorber designed to attenuate the vibration of an elastic structure under external excitation. This absorber is formed by connecting the elastic structure via a piezoelectric patch to an electrical shunt circuit consisting of a resonant shunt combined in series with a nonlinear voltage component, that includes a quadratic and a cubic components, and with its natural frequency tuned to half that of the target mechanical mode. As a consequence, a two to one internal resonance occurs, generating a strong coupling between the mechanical mode and the electrical mode that leads to the creation of a nonlinear antiresonance that replaces the mechanical resonance of the elastic structure. The antiresonance amplitude is also subjected to a saturation, thus becoming independant of the input amplitude and giving this absorber an advantage over the standard linear absorbers. The presentation will describe the shunt circuit and its optimization, its main quadratic voltage component, and the use of the normal form theory to adjust the value of the cubic component, necessary to improve the performance of the absorber.

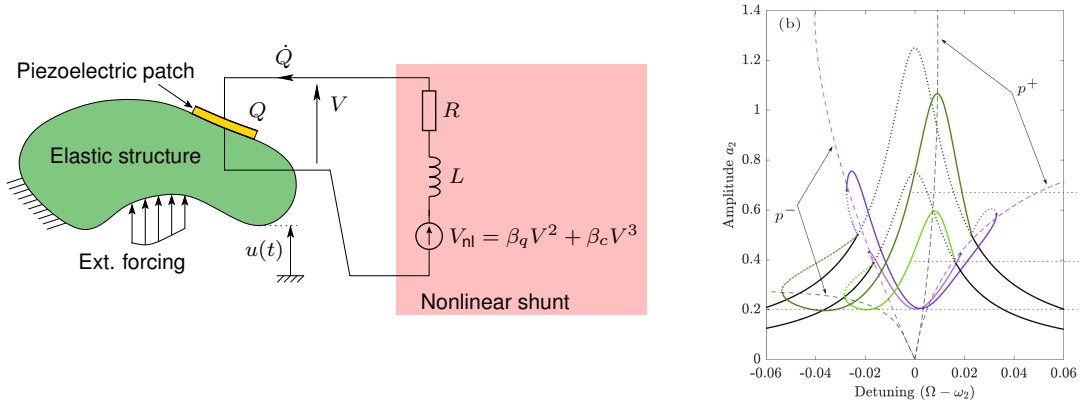


Figure 1: (left) elastic structure coupled to the shunt circuit; (right) Resonance curve of the elastic structure around the target resonance; (black curves): response without the shunt circuit; (green curves): response with the quadratic shunt; (purple curves): response with quadratic and cubic shunt.

We consider an arbitrary elastic structure subjected to an external excitation and connected to a nonlinear shunt circuit via a piezoelectric patch (PE Patch) as shown in Fig. 1. The inductance L in the shunt circuit, together with the capacitance C of the PE patch, create an electrical resonator that is tuned at half a target resonance: $\omega_e = 1/\sqrt{LC} \simeq \omega_m$, where ω_e and ω_m are the natural frequencies of the electrical resonator and the elastic structure. Then, the voltage source $V_{nl} = \beta_q V^2 + \beta_c V^3$ (with V the voltage across the terminals of the PE patch and $\beta_q, \beta_c \in \mathbb{R}$ two gains) creates quadratic and cubic nonlinear terms, in order to activate a 2:1 internal resonance between the elastic mode at ω_m and the electrical mode at ω_e . In practice, a semi-passive circuit made of operational amplifiers is used [1, 3].

A two degree of freedom model of the system in Fig. 1 can be written and solved either by numerical continuation methods and analytical perturbation methods. This enable to first show that the figure of merit of the system is the term $\xi_e/(\kappa\beta_q)$ where ξ_e is the damping ratio of the electrical circuit and κ the piezoelectric coupling factor: thus, increasing the gain β_q improves the performances and can also counterbalance, in a certain extent, a high ξ_e and a low k [2]. However, it can also be shown that a quadratic only shunt (*i.e.* with $\beta_c = 0$) creates the 2:1 internal resonance (which is the desired goal) but also creates some nonresonant terms in the system with a high value, that leads to a detuning of the shunt dependent of the amplitude. Then, properly using the normal form theory and a second order multiple scale analysis, one can compute the nonlinear mode of the coupled system (the backbone curves) and use them to show that the cubic term can be tuned, by adjusting β_c such that $\beta_c = 10\beta_q^2/9$, so as to cancel the effect of the unwanted nonresonant terms and keep the tuning and the saturation phenomenon at high levels of input [4].

References

- [1] Z. A. Shami, C. Giraud-Audine, and O. Thomas. A nonlinear piezoelectric shunt absorber with 2:1 internal resonance: experimental proof of concept. *Smart Materials and Structures*, 31:035006, 2022.
- [2] Z. A. Shami, C. Giraud-Audine, and O. Thomas. A nonlinear piezoelectric shunt absorber with a 2:1 internal resonance: Theory. *Mechanical Systems and Signal Processing*, 170:108768, 2022.
- [3] Z. A. Shami, C. Giraud-Audine, and O. Thomas. Saturation correction for a piezoelectric shunt absorber based on 2:1 internal resonance using a cubic nonlinearity. *Nonlinear Dynamics*, 2023. under review.
- [4] Z. A. Shami, Y. Shen, C. Giraud-Audine, C. Touzé, and O. Thomas. Nonlinear dynamics of coupled oscillators in 1:2 internal resonance: effects of the non-resonant quadratic terms and recovery of the saturation effect. *Meccanica*, 57:2701–2731, 2022.

Damping and negative stiffness characteristics of an electromagnetic mechanism for vibration control

Mehran Shahraeeni*, Vladislav Sorokin*, Brian Mace*, Ashvin Thambyah** and Sinniah Ilanko***

Department of Mechanical and Mechatronics Engineering, University of Auckland, Auckland, New Zealand

*** Department of Chemical and Materials Engineering, The University of Auckland, Auckland, New Zealand*

**** School of Engineering, University of Waikato, Hamilton, New Zealand*

Abstract. Electromagnetic mechanisms are being increasingly used in vibration control and energy harvesting applications due to their controllability and frictionless operation. They can provide negative stiffness to reduce the total dynamic stiffness of the vibrating system and are thus beneficial for low-frequency vibration control. Damping can be generated in an electromagnetic mechanism by eddy currents or by using shunt circuits. In this study, an electromagnetic system including three static coils, a moving magnet, and a conducting chamber is considered. First, the negative stiffness of the system is measured with quasi-static tests. In the next step, the behaviour of the system at higher frequencies is studied experimentally and the effects of electromagnetic-induced damping on the total magnetic force are evaluated. Findings are compared with numerical/analytical results, and a general design of a dual-purpose vibration control mechanism is proposed.

Introduction

Quasi-zero stiffness (QZS) vibration isolators are a class of nonlinear vibration isolators that take advantage of negative stiffness elements. Electromagnetic elements are a common solution to achieve negative stiffness; hence, different electromagnetic QZS isolator designs and configurations can be found in the literature. Furthermore, electromagnetic elements can provide dissipative forces to reduce mechanical vibrations by eddy current damping or electromagnetic shunt damping [1].

This paper concerns the effects of electromagnetic damping in vibration isolators, behaviour that relatively few papers have concerned, e.g. [2,3]. First, a numerical model is developed that considers the negative stiffness, eddy current damping and electromagnetic shunt damping generated by interacting coils and permanent magnets in different configurations. Numerical results are validated by comparison with experimental quasi-static and dynamic measurements.

Results and discussion

Various configurations are considered. It is seen that using coils in attractive-repulsive mode provides a negative stiffness region with tuneable width and magnitude which are functions of the electromagnetic and physical parameters. On the other hand, magnetic damping is frequency dependent and becomes greater at higher frequencies. An example is shown in Fig. 1.

With appropriate values for input current to coils, conductor dimensions and shunt circuit, we can achieve the desired negative stiffness and damping at the working conditions. Therefore, depending on the application, vibration magnitude and frequency, the proposed design can be used as an isolator, as an electromagnetic damper, or as a dual-function vibration isolator-damper. These findings provide a benchmark for designing a tuneable dual-function vibration control mechanism.

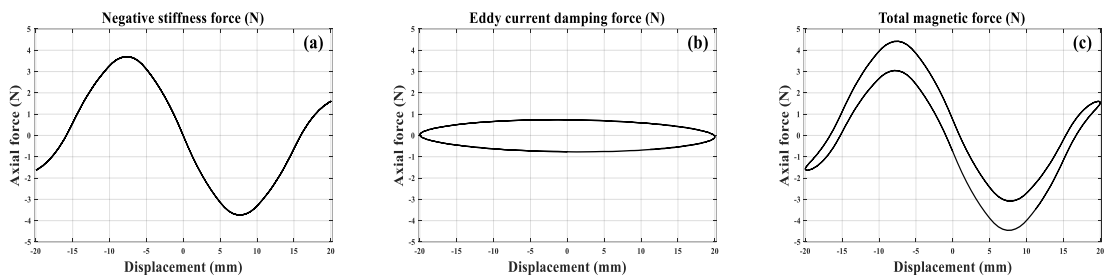


Figure 1: (a) Negative stiffness force, (b) eddy-current damping force, and (c) total magnetic force versus displacement at 10 Hz for three coils and a magnet with the attractive-repulsive arrangement.

References

- [1] E. Diez-Jimenez, R. Rizzo, M.-J. Gómez-García, E. Corral-Abad. (2019) Review of Passive Electromagnetic Devices for Vibration Damping and Isolation. *Shock Vib.*
- [2] S.M.M. Mofidian, H. Bardaweel. (2019) A dual-purpose vibration isolator energy harvester: experiment and model. *Mech. Syst. Signal Process.* **118**: 360–376.
- [3] X. Shi, S. Zhu. (2017) Simulation and optimization of magnetic negative stiffness dampers, *Sensors Actuators, A Phys.* **259**: 14–33.

A method for measuring the mass of multiple substances simultaneously in viscous environments

Zhang Mai*, Hiroshi Yabuno*, Yasuyuki Yamamoto** and Sohei Matsumoto**

* University of Tsukuba, Tsukuba, Ibaraki, JP

** National Institute of Advanced Industrial Science and Technology, Tsukuba, Ibaraki, JP

Abstract. Resonant microsensors have received much attention from researchers because of their low cost, small size, and high sensitivity. Martini et al. proposed a structure for simultaneously measuring the mass of multiple substances. Because of the effect of environmental viscosity, the method based on the frequency response curve under external excitation cannot be used. We propose a method using self-excitation to overcome this difficulty. The feasibility of our proposed method is experimentally verified by using a macro-scale apparatus.

Introduction

Resonant microsensors are widely used to measure the mass of chemical or biological particles because of their low cost, small size, and high sensitivity. In previous researches, resonant microsensors typically consist of a single microcantilever with a functionalized surface. When the target analytes bond to the surface, the mass can be known by observing the resonance frequency shifts of the microcantilever. To measure the mass of multiple substances simultaneously, Martini et al. [1] have proposed a new structure using a shuttle mass coupled with microcantilevers. Under the external excitation to the shuttle mass, the shifts of resonance frequencies of the microcantilevers can be detected from the variations of peaks of the frequency response curve, which is obtained by sensing the displacement of the shuttle mass. However, in high viscous environments, because the peaks are ambiguous [2], the method based on external excitation is not applicable. Based on the characteristics of self-excited vibration, we consider compensating for the viscous damping effect by actuating the shuttle mass based on the feedback control. The feasibility of our proposed method is experimentally verified from the experiments using a macro-scale experimental apparatus.

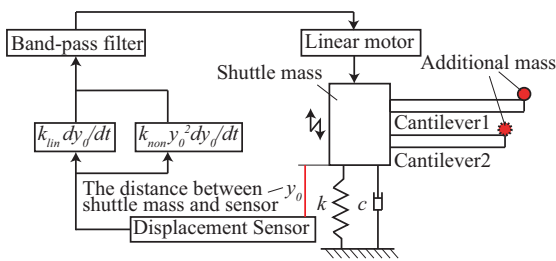


Figure 1: Schematic of the proposed method

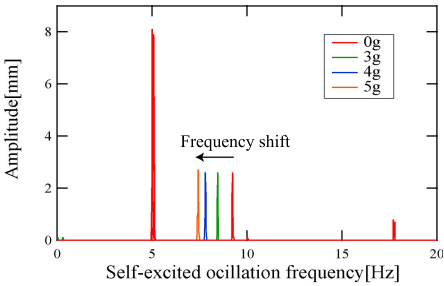


Figure 2: FFT spectrum results when the mass is on cantilever 1

Results and discussion

The schematic of our proposed method is shown in Figure 1. Additional masses can be fixed at the front of cantilevers 1 and 2 coupled with a shuttle mass. In order to produce the self-excited oscillation, the sensor measures the displacement signal of the shuttle mass. Moreover, the linear and nonlinear feedback is established by using this signal. The k_{lin} and k_{non} represent the linear and nonlinear feedback coefficients, respectively. Their functions are compensating for the viscous damping effect in environments and obtaining a steady-state amplitude. A band-pass filter is used to change the self-excited vibration mode and prevents the influence of the phase difference on the experiments. The output signal from the band-pass filter is finally transferred into a linear motor which provides the excitation force to the shuttle mass.

In two sets of preliminary experiments under the self-excited vibration conditions of the shuttle mass, some additional mass is fixed to cantilever 1 or 2, respectively. In Figure 2, the FFT(Fast Fourier Transform) spectrum results indicate that only the resonance peak corresponding to the cantilever with additional mass is significantly shifted. As the magnitude of additional mass increases, the resonance peak shifts become larger. Then the relationship between the self-excited oscillation frequency and the magnitude of additional mass is experimentally examined. As a result, it can be summarized that under self-excited vibration conditions of the shuttle mass, the cantilever on which the mass is fixed (cantilever 1 or cantilever 2) and the magnitude of additional mass can be known simultaneously from the vibration mode and the corresponding response frequency shifts.

References

- [1] B. E. Martini et al. (2008). A single input-single output coupled microresonator array for the detection and identification of multiple analytes. *Appl. Phys. Lett* **93**(5): 054102.
- [2] D. Endo et al. (2018). Mass sensing in a liquid environment using nonlinear self-excited coupled-microcantilevers. *J. Microelectromech. Syst* **27**(5): 774-779.

Evaluating the Shape of a Nonlinear Deformed PVDF Wearable Pressure Sensors by Analyzing the Acoustic Travelling Wave Speed

Masoud Naghdi*, Haifeng Zhang*

*Department of Mechanical Engineering, The University of North Texas, Denton, TX, USA

Abstract. Rolling, folding, and stretching a pressure sensor can change the initial geometry during its performance. This deformation can be nonlinear but is measurable by acoustic methods. For example, the form of a flexible piezoelectric strip can considerably affect the time of flight (ToF) of an acoustic wave traveling alongside a strip. Different ToFs can describe the effect of curvature in the flexible strips, which can predict the geometrical shape of the strips performing as a flexible actuator or sensor.

Introduction

Utilizing flexible piezoelectric pressure sensors has been extensively studied in recent papers. The importance of their application in blood vessels [1, 2], cardiovascular monitoring [3], and biomedical [4] are discussed in many types of research. The shape of a flexible piezoelectric sensor can change due to its performance due to the movement of the parts when they bend, turn, stretch, or roll; thus, the stretchable strips should form and return their original shape during a periodic performance. The effect of the stretches on the final body of the strip is not linear but can be practical on the ToF; consequently, how the geometry has been shaped based on the final measured data is the main idea of this paper. The thickness and depth of the strip are assumed to be constant; thus, the cross-section area is also constant during a vessel's deformation. This sectional area deforms like an ellipse where the area does not change during the deformation.

Results and Discussion

The 2D model geometry is created for numerical simulation. The material is Polyvinylidene Fluoride (PVDF)

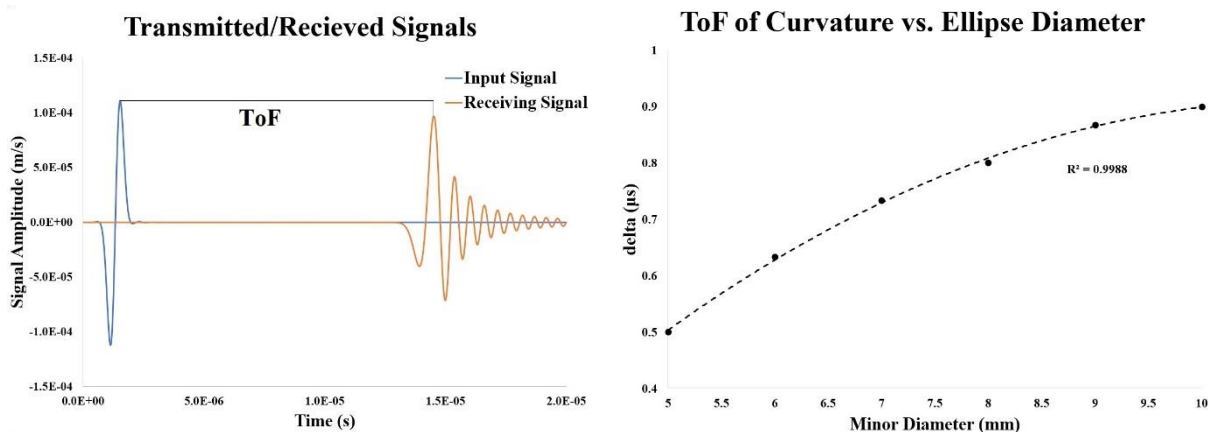


Figure 1. The results show that the effect of the curvature can be measured by ToF

which is anisotropic and has different mechanical characteristics based on the coordinate orientation. The strip thickness is 0.2 mm, and a 2D geometry in COMSOL is utilized. "Elastic Wave" and "Time Explicit" modules are chosen for the simulation. For simplicity, we used the source signal as a bulk acoustic wave. Figure 1 displays the method used to measure the ToF in different cross-sectional areas. In different values of the diameters ("a" in Figure 1), the ToF changes due to the effect of curvature. The trendline is a second-order polynomial with a correlation factor $R^2=0.9988$. Thus, when the ellipse's minimum diameter grows and gets closer to a circular shape ($a=10$ mm), the ToF of the curvature is at the maximum. Thus, the ratio of the ToF of curvature can identify the magnitude of the load on a circular flexible piezoelectric layer around a vessel. The same procedure is practical for other shapes and parameters with different anisotropic materials. The effect of the curvature in ToF can be measured effectively; thus, this idea introduces a new generation of pressure sensors. The following parts of the paper will discuss the experimental prototypes and their results consistent with the final numerical data.

References

- [1] Li, C., Wu, P. M., Lee, S., Gorton, A., Schulz, M. J., & Ahn, C. H. (2008). Flexible dome and bump shape piezoelectric tactile sensors using PVDF-TrFE copolymer. *J. Microelectromechanical Systems* 17(2): 334-341.
- [2] Sharma, T., Aroom, K., Naik, S., Gill, B., & Zhang, J. X. (2013). Flexible thin-film PVDF-TrFE based pressure sensor for smart catheter applications. *Annals of biomedical engineering* 41(4): 744-751.
- [3] Chang, Y. M., Lee, J. S., & Kim, K. J. (2007). Heartbeat monitoring technique based on corona-poled PVDF film sensor for smart apparel application. In *Solid State Phenomena Trans Tech Publications Ltd.* 124: 299-302.
- [4] Johar, M. A., Waseem, A., Hassan, M. A., Bagal, I. V., Abdullah, A., Ha, J. S., & Ryu, S. W. (2020). Highly durable piezoelectric nanogenerator by heteroepitaxy of GaN nanowires on Cu foil for enhanced output using ambient actuation sources. *Advanced Energy Materials* 10(47): 2002608.

Sensing Sound with Electrospun Piezo Materials on a 3D-Printed Structure

Krishna Chytanya Chinnam* and Giulia Lanzara*

*Department of Engineering: Civil, Informatics and Aeronautic Technologies, University of Rome, RomaTre, Roma, Italy

Abstract. The acoustic sensing capability of a non-woven textile made of piezoelectric nanofibers electrospun on a 3D-printed cellular structure, is investigated in this paper. The non-woven textile is made of a complex aggregation of piezoelectric nanofibers that form a porous material. The electro-mechanical response of the textile once exposed to a sound source, is monitored through metallic electrodes that, in a sandwich configuration, let the non-woven textile be directly exposed to sound. The functionality of this unique acoustic sensor was then validated by comparing the sensors response and the response of a commercial microphone when subjected to a 3-minute sweep sound from 10Hz to 10KHz, being the sound source placed at 3cm. The preliminary results confirmed the capability of this textile to greatly monitor acoustic waves with highest performance between 600 and 900 Hz. Such a frequency range makes these devices interesting to be used for micro-damage detection via ultra-light acoustic monitoring.

Introduction

Structural health monitoring systems (SHM) represent a promising solution to deliver structures that can function for an extended lifetime while improving their performance and reliability. Several are the works in the literature showing the capability of piezoelectric sensor/actuator arrays mounted or embedded in structures for structural health monitoring. Despite the extended work in the literature to minimize the impact of such systems in a hosting material or structure [1], there are still challenges to be solved with respect to the material integrity and networks complexity. Recent trends are looking into the development of non-contact approaches, to assess structural integrity. Among those, acoustic waves have been proposed in the literature taking advantage of the fact that such waves are released by a material when damaged [2]. Acoustic monitoring instead is not as established as the PZT technology. The few studies in the literature show the conceptual feasibility in using acoustic waves for structural monitoring with the support of external and large-in-scale microphones. Despite the interesting outcomes of these initial studies, the major limitation is obviously related to the complexity in coupling and isolating such microphones to a structure or material. For this reason, this approach has not been widely explored so far. A great potential to overcome the major limitations in sound monitoring for structural damage, can be found in the usage of novel multifunctional nanostructured materials which could be directly coupled with the structure. With this in mind In this paper an acoustic sensor made of a piezoelectric fiber mat electrospun directly on a 3D-printed cellular structure is explored and characterized in its frequency response.

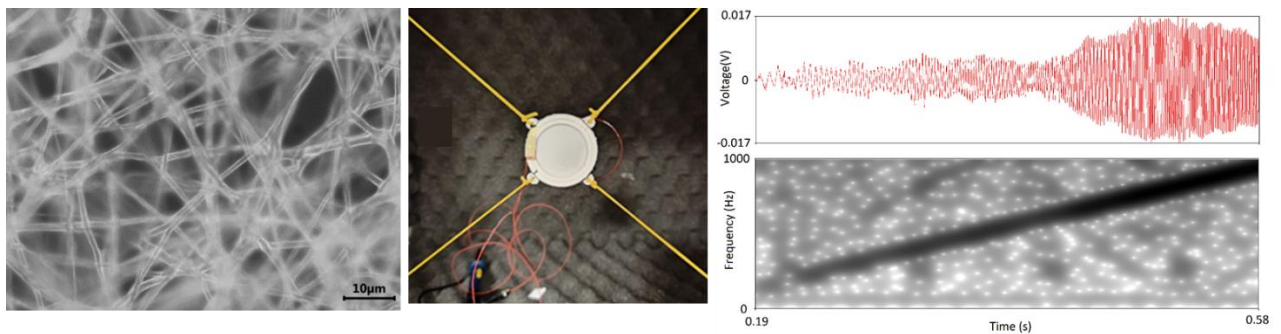


Figure 1: (Left) Electrospun micro-fiber mat; (Center) Suspended hybrid device; (Right) Voltage vs. Time and Spectrogram.

Hybrid cell design and results

A hybrid acoustic sensing device made of a piezoelectric non-woven textile fabricated directly on a 3D-printed, flexible, cell structure, is presented in this paper. This material is fabricated by electrospinning a piezoelectric polymer in the form of nano/microfibers assembled in a random configuration, giving rise to an ultra-light and mechanically flexible porous mat. The electromechanical response of such a mat, when it is exposed to an acoustic wave, is recorded with the support of an oscilloscope. The response of the mat is superior with respect to a commercial microphone because it allows the detection of a pure signal, is lighter, more flexible in its installation and its response frequency can be fine-tuned with that desired for a specific application. Such characteristics make it ideal for the implementation of an unconventional and indeed non-contact monitoring device, as, for instance, for micro-damage detection.

References

- [1] Guo, Z. G., Kim, K., Salowitz, S., Lanzara, G., Wang, Y., Peumans, P., Chan, F.-K. (2017) Functionalization of stretchable networks with sensors and switches for composite materials, *Structural Health Monitoring*, 17, 3.
- [2] Wevers, M., Listening the sound of materials: acoustic emission for the analysis of material behavior. *NDT & International*, 30, 2: 99-106 (1997).

Magneto-Dynamic Characterization of a Silicone Filament Embedded with Magnetic Composite Micro-Spheres

Luis Pedro Vieira Alexandrino^{*}, Alessandro Porrari and Giulia Lanzara^{*}

^{*}Engineering Department of Civil, Computer Science and Aeronautical Technologies, University of Rome, RomaTre, Italy

Abstract. In this paper, a stimuli-responsive silicone filament embedded with a composite micro-sphere of alginate and magnetite is produced and then studied in terms of modal and damping response under the influence of a magnetic field. The interaction of the filament with the magnetic field results in a shift of the resonance frequency and a decrease in the damping ratio especially under the application of increasing loads. The latter behavior is observed to oppose that of the unexposed filament.

Introduction

In the past two decades, there has been a growing interest in the use of smart materials or stimuli-responsive materials in high-tech industries and material science technology. These are a new generation of materials that can be controlled and/or act in a predicted manner.[1] These stimuli-responsive polymers can rapidly change their configuration, dimension, or physical properties with small changes in the appropriate stimuli such as heat, pH, electricity, light, moisture/water, magnetic field, etc. One of the remarkable advantages of this new-generation of materials is their capability to be actuated remotely when exposed to external triggering sources. The use of magnetic fields seems to be promising since it allows accurate control of the deformation modes. It has also been proven to be safe and effective, especially in terms of response time. Magnetic actuation has the potential to lead to very fast response times and is very versatile in terms of the external magnetic field. Stimuli-responsive materials with external magnetic properties can be achieved with a composition of particles of iron oxide, for example. Composites of polymers containing iron oxide were studied, using polymers such as poly(carbonate urethane) (PCU), poly (vinyl chloride) (PVC), PDMS[2], alginate[3], etc.

Alginate is a biopolymer that can be found in the cell of brown algae. It is composed of two residues, a 1,4-linked β -D-Mannuronic acid (M) and 1,4-linked α -L-guluronic acid (G). Alginate properties can be defined with the variation of these sugar residue ratios. Alginate is biocompatible, biodegradable, and easily available. For this reason, is widely used in tissue engineering, drug delivery, wound dressing, food additives, and cell encapsulation. The formation of microspheres of alginate is created by the fast crosslinking of alginate with CaCl_2 . The microspheres can be prepared depending on the application that is intended.

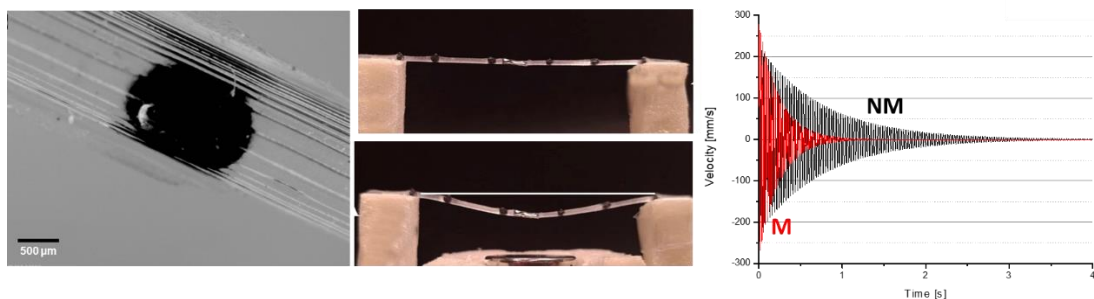


Figure 1: From left to right: Microscope image of a magnetic sphere embedded in a silicone string. Pictures of the filament with and without its exposure to a magnetic field. Time-domain response of the filament with and without the field, acquired with the laser.

Magnetic filament design and results

In this work, a stimuli-responsive material, composed of silicone with embedded alginate micro-spheres with immobilized iron oxide particles, is investigated. The composite is shaped as a filament and its response in terms of frequency and damping ratio is investigated using a laser vibrometer with and without the addition of increasing loads. It is demonstrated that such spheres allow for modification of the filament performance in terms of frequency and damping response when exposed to a magnetic field. In particular, a higher damping factor and a lower resonance frequency are recorded when a magnetic field is applied. Most importantly the study highlights the possibility to fine-tune the material design to reach the desired dynamic response (vibration and damping).

References

- [1] H. Bhanushali, S. Amrutkar, S. Mestry, and S. T. Mhaske, 'Shape memory polymer nanocomposite: a review on structure–property relationship', *Polym. Bull.*, vol. 79, no. 6, pp. 3437–3493, Jun. 2022, doi: 10.1007/s00289-021-03686-x.
- [2] A. A. Paknahad and M. Tahmasebipour, 'An electromagnetic micro-actuator with PDMS- Fe_3O_4 nanocomposite magnetic membrane', *Microelectron. Eng.*, vol. 216, no. May, p. 111031, Aug. 2019, doi: 10.1016/j.mee.2019.111031.
- [3] F. Shen *et al.*, 'Encapsulation of Recombinant Cells with a Novel Magnetized Alginate for Magnetic Resonance Imaging', *Hum. Gene Ther.*, vol. 16, no. 8, pp. 971–984, Aug. 2005, doi: 10.1089/hum.2005.16.971.

Model-based and Model-free Control of a Parallel Manipulator with Flexible Links

Maira Martins da Silva and Fernanda Thaís Colombo

Department of Mechanical Engineering, São Carlos of Engineering, University of São Paulo, Brazil

Abstract. Parallel manipulators may become more energy efficient by reducing their components' inertia. Nevertheless, this reduction might yield vibrations requiring novel joint and task space control strategies. While the former may involve precise models, the latter can be accomplished by adequate computation vision schemes, which impose critical challenges. This work compares two feedback control approaches composed of two control loops. One of these loops is a position-based visual servo that controls rigid-body motion. We implemented the second loop using: (1) a model-based LQG strategy and (2) a model-free strain-based approach. Compared with the position-based visual servo scheme, both strategies attenuate the vibrations and reduce the overshoot response.

Introduction

Designers can improve the parallel manipulators (PMs)' energy efficiency by reducing their moving components' inertia [1]. However, this reduction might yield undesired vibrations due to the components' flexibility, requiring more complex modeling and control strategies.

The literature on modeling and controlling PMs with rigid links is vast. On the other hand, the literature on modeling and controlling PMs with flexible links is scarce, as stated by [2]. Regarding flexible manipulators, the vast majority of the works investigate flexible multi-link serial manipulators. However, controlling the parallel machines may be complex due to their coupled and non-linear dynamics. Moreover, a direct measurement of the manipulator's end-effector pose (position and orientation) may require vision-based measuring techniques. We attenuate the vibration of a parallel planar manipulator with flexible links depicted in Fig. 1(a). This figure shows a 3PRRR with flexible links, which is a kinematic redundant PM since there are two active joints in each kinematic chain. Nevertheless, the prismatic joints are blocked, yielding the non-redundant 3RRR. In this field, R, S, and P stand for revolute, spherical, and prismatic joints. The underlined letters represent the active joints (Motor 1, Motor 2, and Motor 3), while the others are passive.

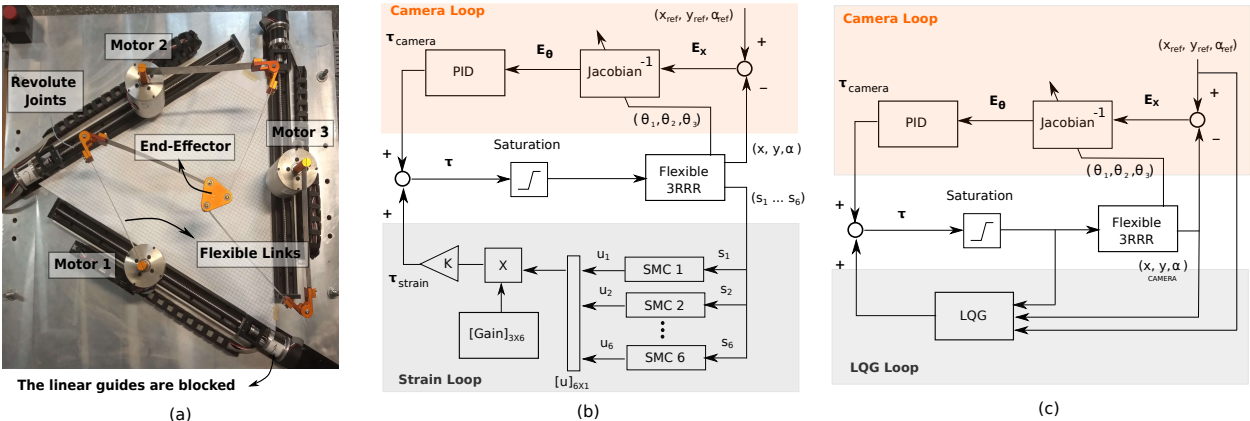


Figure 1: (a) 3RRR with flexible links, (b) Model-free strain-based feedback control strategy, and (c) Model-based LQG control strategy

Results and Discussion

This work compares two feedback control approaches composed of two control loops as illustrated in Fig. 1(b) and (c). One of these loops is a position-based visual servo that controls rigid-body motion (CAMERA Loop). We implemented the second loop using: (1) a model-free strain-based approach (Strain Loop in Fig. 1(b)), and (2) a model-based LQG strategy (LQG Loop in Fig. 1(c)). The model-free strategy requires the use of dedicated instrumentation. In this work, strain gauges measure the deformation of the flexible links. On the other hand, the model-based approach requires a suitable model for deriving the LQG gains. In this work, a reduced model is derived from a multibody finite element model. Compared with the position-based visual servo scheme, both strategies attenuate the vibrations and reduce the overshoot response by 50%.

References

[1] Ruiz A.G., Santos J.C., Croes J., Desmet W., da Silva M.M. (2018) On redundancy resolution and energy consumption of kinematically redundant planar parallel manipulators, *Robotica* **36**(6): 809–821.

[2] Morlock M., Meyer N., Pick M.A., Seifried R. (2021) Real-time trajectory tracking control of a parallel robot with flexible links, *Mech Mach Theory* **158**: 104220.

Super Twisting Sliding Mode Control with Accelerated Gradient Descent Method for Synchronous Reluctance Motor Control System

Jun Moon* and Hyunwoo Kim**

*Department of Electrical Engineering, Hanyang University, Seoul, South Korea, ORCID 0000-0002-8877-9519

**Research Institute of Industrial Science, Hanyang University, Seoul, South Korea, ORCID 0000-0003-4121-1851

Abstract. We propose the new speed and optimal current vector control schemes for synchronous reluctance motors (SynRMs) to achieve fast dynamic response and high efficiency using the super-twisting sliding mode control (STSMC) algorithm and the accelerated gradient descent method (AGDM). Through the experimental testing using the 500W SynRM control system, the proposed STSMC-AGDM scheme shows the better speed control performance and motor efficiency, compared with the conventional proportional-integrator (PI) control with/without AGDM, and STSMC without AGDM.

Introduction

Synchronous reluctance motors (SynRMs) have received a considerable attention in various engineering applications due to its high efficiency, low cost, and fault-tolerant capabilities, compared to other types of motors such as induction motors and PMSMs [1]. The general SynRM control system (see Figure 1) requires the design of speed controller, current vector control algorithm, and current controller. Specifically, the magnitude of current is obtained from the speed controller. Subsequently, the current phase angle is determined by the current vector control algorithm. Based on the magnitude and phase angle of current, the command of dq -axis current is computed. Thereafter, the dq -axis voltage command is obtained using the current controller. The three-phase voltage is applied to SynRM using the voltage source inverter by space vector pulse width modulation. We propose the new speed and optimal current vector control schemes for SynRMs for fast dynamic response and high efficiency using the super-twisting sliding mode control (STSMC) algorithm and the accelerated gradient descent method (AGDM). In current control, PI and first-order SMC are widely used. However, a satisfactory control performance may not be guaranteed due to the presence of nonlinearities, chattering by discontinuity of SMC, and disturbances. To resolve these issues, we propose STSMC, which is continuous and achieves a fast dynamic response under disturbances. For current vector control, there are various approaches such as MTPA, FW, MTPV, MPFC, and MEC, which however may not be reliable when the motor parameters have high non-linear characteristics due to the magnetic saturation [2]. The approach of using Lookup Tables (LUTs) based on FEA has been used widely to cope with such nonlinearities [3]. We apply the AGDM to improve searching the optimal current vector in LUTs. The proposed STSMC-AGDM is implemented in the 500W SynRM system (see Figure 1), where the experiment results show the better speed control performance and motor efficiency, compared with the conventional PI control with/without AGDM, and STSMC without AGDM.

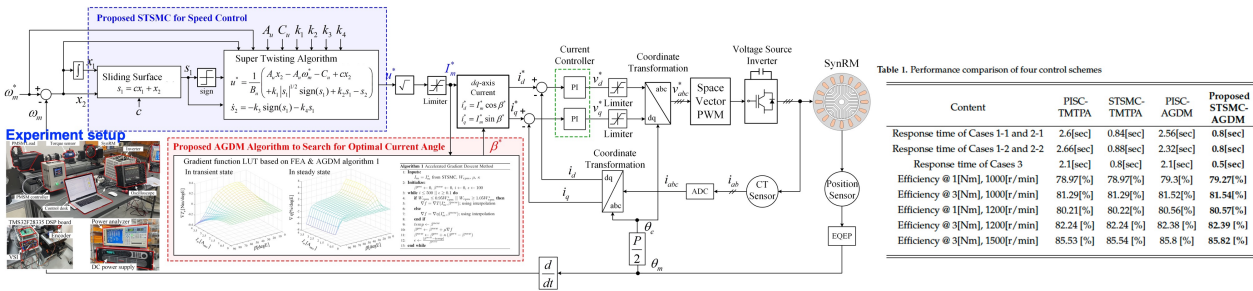


Figure 1: Block diagram, experiment setup, and experiment result of the proposed STSMC-AGDM based SynRM Control System.

Results and Discussion

Figure 1 shows the proposed STSMC-AGDM based SynRM control system, where STSMC is used for speed control and AGDM is applied to optimal current vector control in LUTs. The other blocks in Figure 1, including dq -axis current, PI current controller, limiters, coordinate transformation, ADCs, voltage source inverter, and sensors, are also implemented. The main features of the proposed STSMC-AGDM are as follows: (i) STSMC provides a faster finite-time reachability than the conventional first-order SMC and (ii) AGDM allows to quickly search for the optimal current vector in LUTs to deal with nonlinear motor characteristics.

References

- [1] Stipetic, S. and Zarko, D. Cavar, N. (2020) Adjustment of Rated Current and Power Factor in a Synchronous Reluctance Motor Optimally Designed for Maximum Saliency Ratio. *IEEE Trans. Ind. Appl.* **56**(3):2481-2490.
- [2] Scalcon, F. and Osorio, C., Koch, G., Gabbi, T., Vieira, R., Grundling, H., Oliveira, R. and Montagner, V. (2021) Robust Control of Synchronous Reluctance Motors by Means of Linear Matrix Inequalities. *IEEE Trans. Energy Convers.* **36**(2):779-788.
- [3] Lin, F., Huang, M., Chen, S., Hsu, C. (2019) Intelligent Maximum Torque per Ampere Tracking Control of Synchronous Reluctance Motor Using Recurrent Legendre Fuzzy Neural Network. *IEEE Trans. Power Electron.* **34**(12):12080-12094.

Vibration Control of Time-Varying Nonlinear Systems

Abdullah A. Alshaya*,

*Mechanical Engineering Department, College of Engineering and Petroleum, Kuwait University, PO Box 5969, Safat 13060, Kuwait, ORCID # 0000-0002-9105-5300, email: abdullah.alshaya@ku.edu.kw

Abstract. The induced vibration from a commanded time-varying nonlinear systems is controlled by using a pre-designed shaped input command. The changes of the system parameters during the motion of the system as well as the input and system constraints are accounted when designing the shaped commands. The proposed controlling techniques are tested by suppressing the residual vibration of an overhead crane with simultaneous traveling and hoisting maneuvers. The hoisting and lowering operations when traveling a payload in an overhead crane induce a nonlinear system with time-dependent natural frequency and positive-negative damping-like behavior. The numerical results demonstrate the performance of the proposed shaped commands in suppressing the residual vibration of the suspended payload regardless the hoisting and lowering profiles used during the maneuver.

Introduction

The application of a control input into a time-varying system, e.g., flexible link manipulators [1], crane operation with hoisting/lowering maneuver [2], or pouring and filling operation [3], results in unwanted transient and residual vibrations. The complexity of the dynamical models complicate the controlling procedure of the system's input. The open-loop control, especially the command shaping approach, is commonly used for vibration control with precise and accurate positioning and fast and safe operation. The principle of the command shaping control is to design based on either optimal control approach or input shaper [4] a special input that commands the mechanical system without inducing residual vibration. Unlike the input shaper scheme where the rise time of the generated impulses depends on the system parameters, the optimal control approach has the freedom of selecting the maneuver time to compensate between the move time and required vibration reduction in the transient stage. The objective here is to extend the command shaping approach to control a time-varying nonlinear system while accommodating the changes of the system parameters and satisfying the input and system constraints.

Results and Discussion

The proposed controlling techniques is tested by controlling the induced vibrations of payloads traveled and hoisted by an overhead crane. The input shaped command consists of equidistant steps. The residual pendulum oscillations were suppressed at the end of the command when using linear and quadratic hoisting/lowering profiles, Figure 1. The transient pendulum oscillations can be further reduced by increasing the command time length unlike the classical input shapers that have a fixed command length. Without basing the controlling design on the average system parameters, the time-nature of the system parameters during the motion was considered when designing the shaped command.

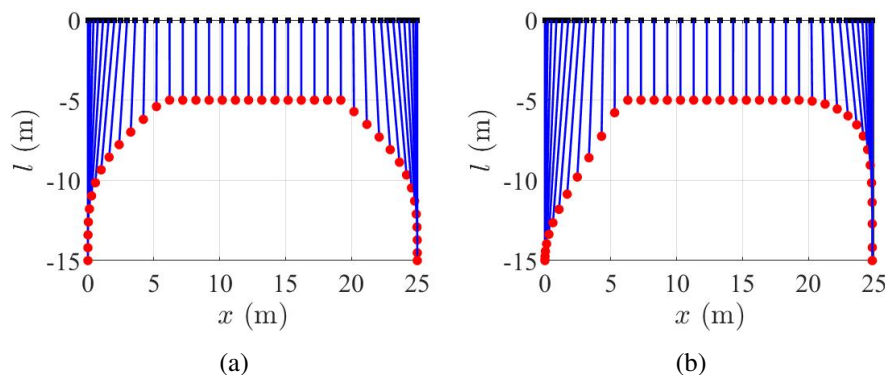


Figure 1: Motion profiles for (a) linear and (b) quadratic hoisting and lowering operations.

References

- [1] Qiu, Z. and Li, C. and Zhang, X. (2019) Experimental study on active vibration control for a kind of two-link flexible manipulator. *Mech. Syst. Signal Pr.* **118**:623-644.
- [2] Abdel-Rahman, E. M., Nayfeh, A. H. and Masoud, Z. N. (2003) Dynamics and control of cranes: A review. *J. Vib. Control.* **9**(7):863-908.
- [3] Pagilla, P. R., Yu, B. and Pau, K. L. (2000) Adaptive control of time-varying mechanical systems: analysis and experiments. *IEEE-ASME T. Mech.* **5**(4):410-418.
- [4] Singer, N. C. and Seering, W. P. (1990) Preshaping command inputs to reduce system vibration. *J. Dyn. Syst.-T. ASME.* **112**(1):76-82.

Assessment of Power Consumption Improvement in Position and Attitude Control of Spacecraft using Electromagnetic Force Assist

Hector Gutierrez*, Oceane Topenot** and Solenne Lamaud**

*Department of Mechanical and Aerospace Engineering, Florida Institute of Technology, Melbourne, FL, USA

** École Nationale Supérieure de Mécanique et des Microtechniques, Besançon, France

Abstract. Electromagnetic Force Assist is proposed as method to reduce power consumption in formation flight maneuvers between spacecraft that use auxiliary coils to generate electromagnetic forces in proximity operations. This paper estimates the potential improvement in power consumption (as indirect metric of potential propellant savings) in spacecraft maneuvers using RINGS (Resonant Inductive Near-field Generation Systems), a prototype system developed to investigate electromagnetic formation flight and wireless power transfer between spacecraft. An assessment of power consumption reduction is based on comparing the control effort required in selected 3-DOF maneuvers. The control effort performance of a linear quadratic Gaussian (LQG) controller for thruster-only maneuvers is used as baseline, and is compared to the control effort when two other controllers (based on sliding mode control and feed-forward control) provide electromagnetic force assist in addition to the baseline thrusters.

Introduction and Motivation

Formation flight requires that the spacecraft involved are able to provide station keeping [1-4]; perturbations such as solar pressure forces consumption of onboard propellant for this purpose [5]. To increase the life expectancy of a formation mission, electromagnetic actuation has been proposed as means to assist the onboard thrusters when compensating disturbances during station keeping. Solar panels provide access to unlimited electric energy that can be used to power actuation coils to generate multi-axial electromagnetic forces. This paper evaluates for the first time the potential propellant savings while using electromagnetic force assist in motion control of formation maneuvers, using the RINGS platform. The paper uses the control effort of a LQG controller (using thrusters only) as baseline, to compare with the control effort of two other controllers that use a combination of thrusters and electromagnetic force assist on a set of proposed maneuvers.

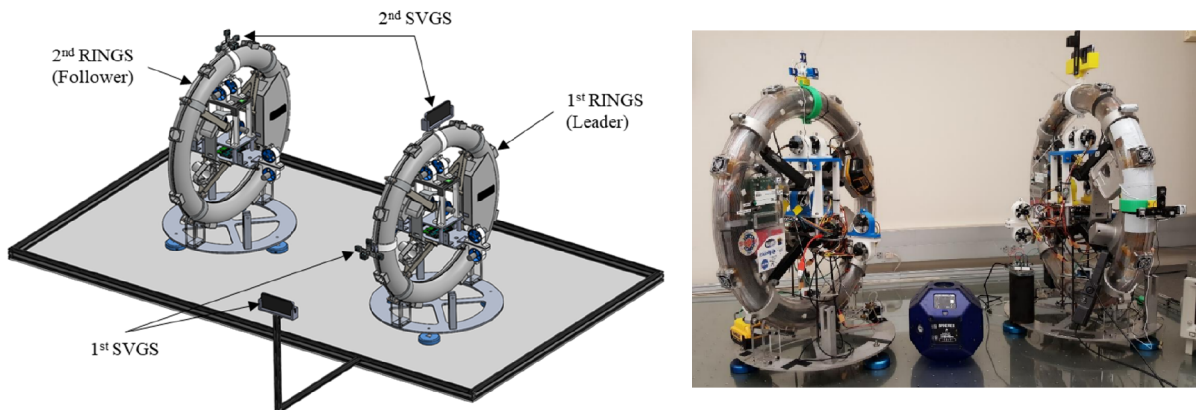


Figure 1. Demonstration of electromagnetic force assist for 3-DOF formation maneuvers using RINGS

Results and Discussion

This paper presents an assessment of power savings in spacecraft formation flight by use of electromagnetic force assist. The assessment was done in simulation using 3-DOF planar motion control platform of the RINGS prototype spacecraft. The results indicate that significant savings in control effort are possible by using electromagnetic force assist, in particular when combining a feedforward controller with sliding mode feedback. The effectiveness of electromagnetic force assist depends on the specific path followed during a maneuver. Optimized path planning is therefore required to maximize the benefits of the proposed method.

References

- [1] Martin, M., Klupar, P., Kilberg, S., Winter, J. (2001) Techsat 21 and revolutionizing space missions using microsatellites. *AIAA*, **SSC01**.
- [2] Sabol, C., Burns, R., McLaughlin, C. (2001) Satellite Formation Flying Design and Evolution. *AIAA J. Spacecraft and Rockets*, **38**: 270-278.
- [3] Hariri, N., Gutierrez, H., Rakoczy, J., Howard, R., Bertaska, I. (2020) Proximity Operations and Three Degree-of-Freedom Maneuvers Using the Smartphone Video Guidance Sensor, *Robotics*, **9(3)** 70: 1-18.
- [4] Miller, D., Sedwick, R. (2002) NIAC Phase I Final Report, 'Electromagnetic Formation Flight', Massachusetts Institute of Technology.
- [5] Kwon, D., Sedwick, R., Lee, S., Ramires-Riberos, J. (2011) Electromagnetic Formation Flight Testbed Using Superconducting Coils, *AIAA J. Spacecraft and Rockets*, **48**: 124-134.

A Reference Governor for Constrained Control of a Multi Degree of Freedom Metamaterial

Rick Schieni*, Mehmet Simsek**, Onur Bilgen* and Laurent Burlion*

*Department of Mechanical and Aerospace Engineering, Rutgers University, NJ, USA

**Koç University, Sariyer, Istanbul, Turkey

Abstract. A reference governor approach is proposed to control a multi degree of freedom metamaterial subject to constraints. The metamaterial consists of an arbitrary number of bistable “segments” which are attached to each other in a serial manner to generate a “distributed” bistable structure. It is shown that each bistable segment may be controlled using its own reference governor in addition to a nominal controller. Effects from attached segments are modelled as disturbances which must be rejected by the control scheme.

Introduction

Morphing structures have become a popular area of research as they show promise for use in aircraft [1] and morphing vehicles [2]. Employing bistable structures in morphing technology is advantageous as they are capable of adopting two stable shapes which do not require energy to be maintained. This work proposes a reference governor control scheme for the constrained control of a metamaterial concept which consists of multiple bistable elements [3]. With single bistable structures commonly being modelled using the Duffing-Holmes oscillator [4, 5], the equation of motion for the n^{th} bistable element in the metamaterial is given by:

$$m_n \ddot{x}_n = F_n - c_n(\dot{x}_n - \dot{x}_{n-1}) + k_n(x_n - x_{n-1}) - k_n^p(x_n - x_{n-1})^3 + c_{n+1}(\dot{x}_{n+1} - \dot{x}_n) - k_{n+1}(x_{n+1} - x_n) + k_{n+1}^p(x_{n+1} - x_n)^3 \quad (1)$$

where x_n is the displacement of the n^{th} structure, F_n is the force from the controlling actuator, m_n is the mass, c_n is the friction coefficient from the mechanical model, k_n is the destabilizing linear spring stiffness, k_n^p is the restorative nonlinear spring stiffness. The proposed work will offer two contributions: a method for controlling the shape change of the metamaterial where the effects of neighboring bistable structures are modelled as disturbances and a demonstration of the efficacy of a reference governor scheme which can address polynomial constraints and disturbances.

Results and discussion

Figure 1 illustrates the efficacy of the reference governor approach to three connected elements of the metamaterial where the constraining bounds are pictured with red dashed lines. Successful shape change of three

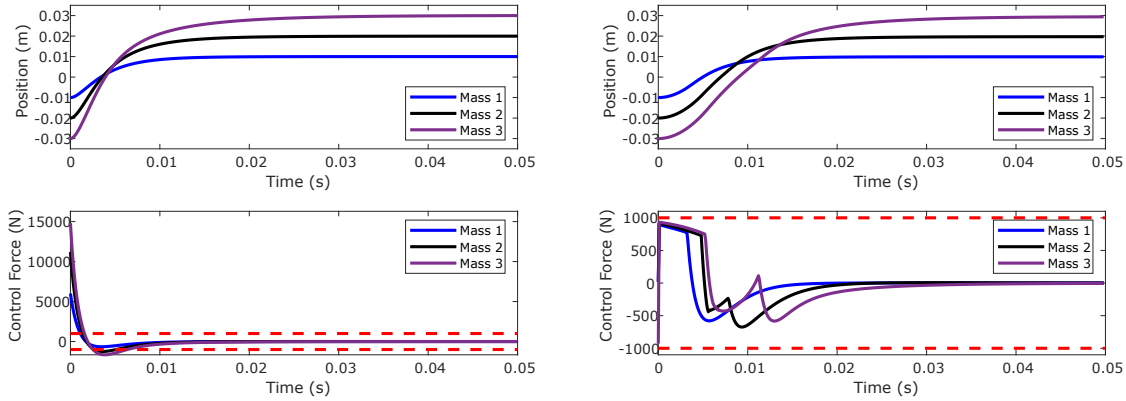


Figure 1: Nominal system response (left) and response with reference governor (right).

series-connected metamaterial elements each initially at a relative displacement of -10 mm and ending at a relative displacement of 10 mm is achieved while satisfying constraints on the control effort which are polynomial in nature.

References

- [1] Barbarino S., Bilgen O., Ajaj R., Friswell M., Inman D. (2011) A review of morphing aircraft. *J. Intell. Mater. Syst. Struct.* **22**:823–877.
- [2] Valasek J. (2012) *Morphing Aerospace Vehicles and Structures*. John Wiley & Sons Ltd, Chichester, United Kingdom.
- [3] Simsek M.R., Schieni R., Burlion L., Bilgen O. (2022) A Hybrid Position Feedback Controlled Bistable Metamaterial Concept. Presented at ENOC 2022 - 10th European Nonlinear Dynamics Conference, Lyon, France, 2022-07-17, 2022.
- [4] Zarepoor M., Bilgen O. (2016) Constrained-energy cross-well actuation of bistable structures. *AIAA J.* **54**:2905–2908.
- [5] Simsek M.R., Bilgen O. (2020) The Duffing-Holmes Oscillator Under Hybrid Position Feedback Controller. *J. Struct. Stab.* **20**(09):2050101.
- [6] Burlion L., Schieni R., Kolmanovsky I. (2022) A Reference Governor for linear systems with polynomial constraints. *Automatica* 110313.

Observer design for semi-linear stochastic partial differential equations

R. Ragul[†], Ju H. Park[‡] and K. Mathiyalagan[†]

[†]Department of Mathematics, Bharathiar University, Coimbatore, 641 046, India.

[‡]Nonlinear Dynamics Group, Department of Electrical Engineering, Yeungnam University, 280 Daehak-Ro, Kyongsan 38541, Republic of Korea.

Abstract. In this work an observer design for semilinear stochastic partial differential equations (SPDEs) involving Lévy type noise is presented. By constructing an appropriate Lyapunov functional, a new set of sufficient conditions are obtained to guarantee the mean square exponential stability (MSES) of the error system.

Introduction

Observers are ingenious tool to estimates the system states which helps to reconstruct the system states for more appropriate performance. In practice random noises are unavoidable, while dealing with such cases SPDEs are most helpful model. Particularly, Lévy process is more interesting because in this, noise splittable as continuous and discontinuous parts. Few results are found in literature on MSES, boundary control for reaction diffusion systems with Brownian motion [1, 2, 3]. With our best knowledge observer based stability analysis of SPDEs not yet investigated. Motivated by above discussions, the main objective of the present work is to design an observer-based boundary control for the considered semilinear SPDE and to derive the sufficient conditions for the MSES of the error system in terms of LMIs with the help of Lyapunov theory.

System description

Consider the following semilinear stochastic parabolic type equation:

$$dy(x, t) = \left\{ A \frac{\partial^2 y}{\partial x^2} + By(x, t) + f(t, y(x, t)) \right\} dt + \sigma(t, y(x, t)) dW(t) + \int_Z \phi(t, y(x, t), z) \tilde{N}(dt, dz),$$

where $y(x, t)$ is the state vector with space variable x and time variable t . Boundary conditions are $\frac{\partial y}{\partial x} \Big|_{x=0} = 0$, $\frac{\partial y}{\partial x} \Big|_{x=1} = u(t)$, output of the system $\bar{y}(x, t) = Cy(x, t)$. $u(t)$ is boundary control input to be design. ‘ A ’ is known constant diagonal matrix and B, C are known constant matrices. $W(t)$ is a one dimensional standard Brownian motion and $\tilde{N}(dt, dz) = N(dt, dz) - \lambda(dz)dt$ is compensated Poisson measure with intensity measure $\lambda(dz)$. $f(\cdot), \sigma(\cdot), \phi(\cdot)$ are semilinear functions satisfies Lipschitz condition. State observer system is considered as

$$d\hat{y}(x, t) = \left\{ A \frac{\partial^2 \hat{y}}{\partial x^2} + B\hat{y}(\cdot) + \hat{f}(\cdot) + L(\bar{y}(\cdot) - \hat{y}(\cdot)) \right\} dt + \hat{\sigma}(\cdot) dW + \int_Z \hat{\phi}(\cdot) \tilde{N}(dt, dz),$$

where $\hat{y}(x, t)$ is estimated state and L is observer gain. Boundary control $u(t) = K\hat{y}(1, t)$, where K is control gain. Let error state be $e(x, t) = y(x, t) - \hat{y}(x, t)$. By constructing Lyapunov functional $V(\cdot) = \int_0^1 (y^T(x, t)P_1y(x, t) + e^T(x, t)P_2e(x, t))dx$, main result is stated below.

Theorem: For given scalar $\alpha > 0$, $c_1, c_2, q_1, q_2, F_1, F_2$, there exist symmetric positive definite diagonal matrices P_1, P_2 , scalars $\bar{\rho}_1, \bar{\rho}_2, \epsilon_1, \epsilon_2$ and appreciate matrices \mathcal{K}, \mathcal{L} the LMIs $[\Xi]_{6 \times 6} < 0$, $P_1 \leq \bar{\rho}_1 I$, $P_2 \leq \bar{\rho}_2 I$ hold with $\Xi = 2P_1B + \bar{\rho}_1c_1I + \bar{\rho}_1q_1I - \frac{2\pi^2}{2}P_1A + 2\alpha P_1 - \epsilon F_1^T F_2$, $\Xi_{12} = \frac{\pi^2}{4}(P_1A)^T$, $\Xi_{13} = P_1^T + \frac{1}{2}\epsilon(F_1 + F_2)I$, $\Xi_{22} = 2AK - \frac{2\pi^2}{4}P_1A$, $\Xi_{25} = (AK)^T$, $\Xi_{33} = \Xi_{66} = -\epsilon I$, $\Xi_{44} = 2P_2B + \bar{\rho}_2c_2I + \bar{\rho}_2q_2I - \frac{2\pi^2}{2}P_2A + 2\mathcal{L}C + 2\alpha P_2 - \epsilon F_1F_2$, $\Xi_{46} = P_2^T + \frac{1}{2}\epsilon(F_1 + F_2)I$, $\Xi_{45} = \frac{\pi^2}{4}(P_2A)^T$, $\Xi_{55} = -\frac{2\pi^2}{4}P_2A$ and other terms are zero. Then, error system is MSES and control & observer gains are $K = P_1^{-1}\mathcal{K}$, $L = P_2^{-1}\mathcal{L}$, respectively.

Numerical example

Letting $f(t, y(x, t)) = y(x, t)(B - y(x, t))$, the considered system represents Fisher’s equation. By fixing $A = \text{diag}\{0.4, 0.7\}$, $B = \begin{bmatrix} -0.51 & 0.065 \\ 0.2 & -0.9 \end{bmatrix}$, $C = \begin{bmatrix} -0.6 & -0.3 \\ 0.01 & -0.2 \end{bmatrix}$, we get the gains $K = \begin{bmatrix} 0.7802 & 0 \\ 0 & 0.5606 \end{bmatrix}$, $L = \begin{bmatrix} 0.2286 & -37.7459 \\ 18.9340 & -26.2291 \end{bmatrix}$, by solving the LMIs in proposed theorem. The sector nonlinearity has bounds $[F_1, F_2] = [-0.002, 0.002]$.

Acknowledgment

This work was supported by the National Research Foundation of Korea (NRF) grant funded by the Korea government (Ministry of Science and ICT) (No. 2019R1A5A8080290).

References

- [1] Li Y., Kao Y. (2012) Stability of stochastic reaction-diffusion systems with Markovian switching and impulsive perturbations. *Math. Probl. Eng.* **2012**:Article ID 429568.
- [2] Pan P.L., Wang J., Wu K.N. (2016) Boundary stabilization and H_∞ Control for Stochastic Reaction-Diffusion Systems. *2016 CCDC*. 2279-2283. **10.1109/CCDC.2016.7531365**.
- [3] Wu K.N., Liu X.Z., Shi P., Lim C.C. (2019) Boundary control of linear stochastic reaction-diffusion systems. *Int.J.Robust Nonl.Contr.* **29**:268-282.

Active Vibration Suppression of Flexible Satellite With Appointed Time Convergence

Danyu Li*, Liang Zhang**, Shijie Xu***, Yuan Li**** and Naigang Cui *****

*School of Aeronautics and Astronautics, Sun Yat-Sen University, Guangzhou, China, 0000-0003-2986-6011 #

**School of Aeronautics and Astronautics, Sun Yat-Sen University, Guangzhou, China, 0000-0002-2652-3884 #

***Beijing Institute of Space Long March Vehicle, Beijing, China, 0000-0002-0788-3446 #

****Nanjing University of Science and Technology, School of Energy and Power Engineering, Nanjing, China, 0000-0003-4421-3000 #

*****Harbin Institute of Technology, School of Astronautics, Harbin, China, 0000-0002-3318-6986 #

Abstract. In this paper, an appointed time active vibration suppression controller is studied for flexible satellite with piezoelectric actuators. Firstly, a piecewise sliding mode controller with the appointed time is designed to guarantee that the attitude error converges at the appointed time. The convergence time of the model can be set with a prior parameter. Secondly, a modal observer is used to estimate the vibration of the flexible elastic modal, and an active vibration suppression controller is designed to converge at a predefined time. The stability of the two controllers is demonstrated by a Lyapunov theory. The Simulink simulation framework is eventually established, and the numerical simulation results of various data demonstrate the appointed time convergence of the proposed controller. Compared with adaptive sliding mode and nonsingular terminal sliding mode, the controller can achieve higher precision control with less energy consumption.

Introduction

Flexible satellite attitude control can be divided into two aspects: maneuvering pointing control and flexible vibration suppression. Maneuvering pointing control is a nonlinear problem with disturbance and uncertainty. The main control methods are robust control, sliding mode control, adaptive control and deep neural network control. Early research in the field of flexible vibration suppression includes passive vibration suppression methods of vibration isolation, energy dissipation, and vibration absorption. However, the control effect of passive vibration suppression is limited and the applicable environment is limited^[1]. Therefore, many scholars have studied active vibration suppression. There are three main active vibration suppression methods applied in the aerospace field: component synthesis vibration suppression(CSVS), input shaping and active vibration control based on intelligent materials^[2].

Results and discussion

We specify that the desired attitude quaternion of the satellite is $\mathbf{q}_d = [1, 0, 0, 0]^T$. The initial value of the attitude quaternion is $\mathbf{q} = [0.8832, 0.3, -0.2, -0.3]^T$. To verify the appointed time convergence performance of the proposed controller, the model parameters and other parameters of the controller are kept constant, the appointed time T_a is set to 100, 200, and 300. The result is shown in Figure 1.

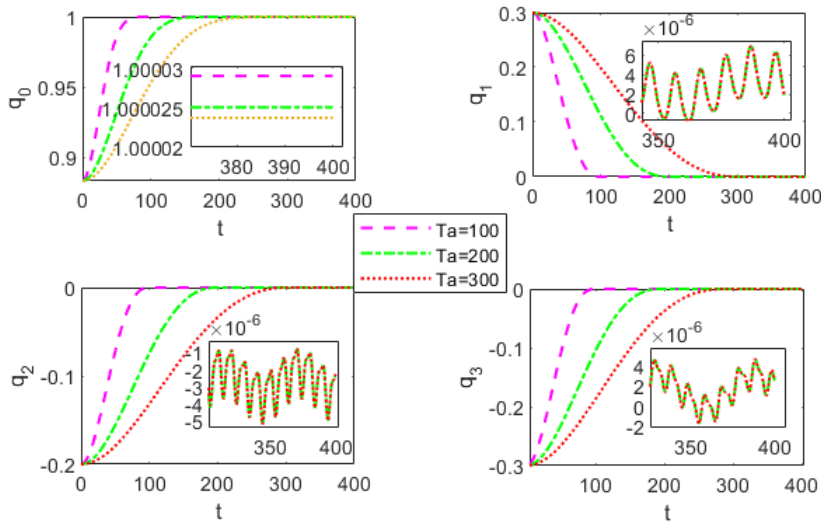


Figure 1: Attitude quaternion at three different convergence times

Even in the presence of external perturbations and model uncertainties, the appointed time sliding mode controller can directly appoint the convergence time of the attitude error, which is independent of the initial conditions of the model.

References

- [1] J. Xu, "Advances of research on vibration control," *Chinese Quarterly of Mechanics*, vol. 36, no. 4, p. 19, 2015.
- [2] S. Xu, "Dynamic modeling and on-orbit vibration control research for flexible spacecraft," Ph.D. dissertation, Harbin Institute of Technology, 2019.

Some comments on Nonlinear Dynamic behaviour and Control of a Duffing 3D oscillator

Jose M. Balthazar^{*,***}, Mauricio A. Ribeiro^{*} and Hilson H. Daum^{**}

^{*}Department of Electronical, UTFPR, Ponta Grossa, Paraná, Brazil

^{**}Industrial Maintenance Department, UTFPR, Guarapuava, Paraná, Brazil

^{***}School of Engineering, UNESP, Bauru, São Paulo, Brasil

Abstract. In this work, the nonlinear dynamic behaviour of a three-dimensional Duffing oscillator was numerically investigated. The oscillator has an additional nonlinear feedback equation of state coupled to the first equation, and therefore has two parameters that determine coupling and control the 3D system. With the non-linear dynamic analysis, it was obtained using the maximum Lyapunov exponent sweeping the coupling parameters of the equations, in this analysis we observed the emergence of shrimp patterns. Bifurcation diagrams, phase maps and Poincaré maps were also used, which corroborated to determine and confirm the chaotic regions of the 3D Duffing oscillator. Once the regions were determined, a control design for chaos suppression was proposed that kept the 3D Duffing oscillator in periodic orbit, using the Optimal Linear Feedback (OLFC) control due to its high computational efficiency and SDRE (State Dependent Riccati Equation).

Introduction

An oscillator that has a lot of prominence is the Duffing oscillator, which is used to describe numerous applications. This paper aims to analyze the nonlinear dynamics of the Duffing oscillator in three dimensions as shown in Eqs. (1):

$$\begin{cases} \dot{x} = y + z \\ \dot{y} = -\gamma y + x - x^3 + f_0 \cos(\omega t) + \rho xz \\ \dot{z} = -xy + \beta z \end{cases} \quad (1)$$

where, x , y and z are the system state variables, γ , f_0 and ω are positive definite constants of the Classical Duffing system. The parameters ρ and β are the additional parameters that couple the equations. The aim work is to analyze the nonlinear dynamics of a 3D Duffing oscillator described by the set of equations [1, 2], and thus propose two control designs to suppress the chaotic behavior that the system presents for a given set of parameters.

Results and discussion

The State Dependent Riccati Equation control (SDRE control) and the Optimal Linear Feedback control (OLFC control) were used, and we compared that the two controllers were efficient for the chaos suppression for coupling to an orbit of the system itself, defined by $(x(t)=-0.8873+0.34 \cos(\omega t)+0.1037 \sin(\omega t)-0.08245 \cos(2\omega t)+0.03784 \sin(2\omega t)+0.01262 \cos(3\omega t)+0.01102 \sin(3\omega t), y(t)=-7.491 \times 10^{-5}+0.09261 \cos(\omega t)-0.3116 \sin(\omega t)-0.0635 \cos(2\omega t)+0.1486 \sin(2\omega t)+0.002646 \cos(3\omega t)+0.03334 \sin(3\omega t)$ and $z(t)=-5.785 \times 10^{-5}+0.0114 \cos(\omega t)-0.02837 \sin(\omega t)-0.01251 \cos(2\omega t)+0.01618 \sin(2\omega t)+0.006706 \cos(3\omega t)-0.004394 \sin(3\omega t))$. To obtain the orbit we consider the time series defined by Eqs. (1) and Fourier Series and the parameters ($\gamma = 0.25$, $f_0 = 0.3$, $\omega = 1.0$. $\beta = -10.4060$ and $\rho = -0.185$). With that we couple the control signals in the three variables of the system (x, y, z) . The very low errors in the application of the control techniques showed that both are efficient for application in the case of the 3D Duffing oscillator. In Figure (1) show the results for SDRE control applied in Eqs.(1) and Figure (2) show the results for OLFC applied in Eqs. 1.

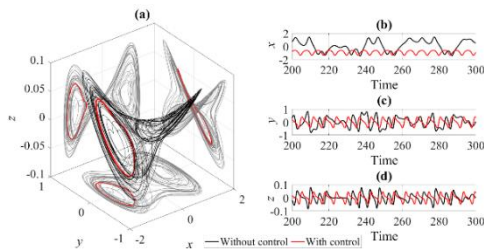


Figure 1: SDRE control applied in Eq. (1) for synchronization with orbit. Chaotic trajectory (Line black) and orbit controlled (red line) (a) Phase Portrait for $\gamma = 0.25$, $f_0 = 0.3$ and $\omega = 1.0$., (b) Time series for x , (c) Time series for y and (d) Time series for z .

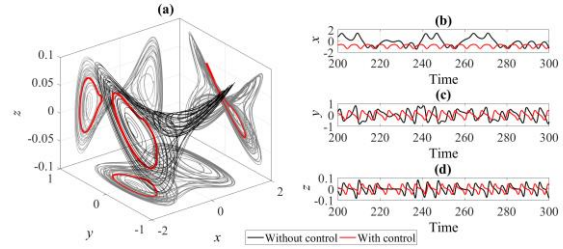


Figure 2: OLEC control applied in Eq. (1) for synchronization with orbit. Chaotic trajectory (Line black) and orbit controlled (red line) (a) Phase Portrait for $\gamma = 0.25$, $f_0 = 0.3$ and $\omega = 1.0$., (b) Time series for x , (c) Time series for y and (d) Time series for z .

References

- [1] Laarem, G., Sohaib, B. (2022) A New Chaotic oscillator generated from the Duffing Analysis and chaos control. *19th Int. Multi. Conf. Syst.*, 1:1504-1511
- [2] Daum, H. H., Tusset, A. M., Ribeiro, M. A., Balthazar, J. M., Bueno, A. M., Litak, G. (2022). *Braz. J. Phys.*. Dynamics and Control of a Vibrating System with Hyperchaotic Behavior Using an Electronic Circuit Implementation. **104**:1-9.

Motion Control of a Pendulum via Magnetic Interaction

Panagiota Atzampou*, Peter Meijers*, Apostolos Tsouvalas*, Andrei Metrikine*

** Delft University of Technology, Faculty of Civil Engineering and Geosciences,
Stevinweg 1, 2628CN Delft, the Netherlands*

Abstract. The present study introduces a modified version of PID Control for the case of a magnetically controlled pendulum. The response was observed in both experimental and numerical simulations taking into consideration the efficiency of the control and the non-linear forces exerted.

Introduction

Offshore wind turbines (OWT) are designed with larger dimensions and get installed by floating vessels in deeper waters due to the ever increasing energy demands. Hence, focus has been recently placed on the development of novel techniques for improving the efficiency of the installation process. Various motion compensation and position control techniques have been employed and tested in situ over the years [1]. All current methods, however, require mechanical equipment in direct contact with the payload as well as some human intervention. This fact, amplified by the delicate nature of positioning OWT components, the small error tolerances and the harsh offshore environment, illuminate a gap for a non-contact position technique for the OWT installation. The concept is based on the magnetic interaction between the component and an electromagnet actuator.

Methodology

In order to develop the contactless technique, a simple magnetically controlled pendulum is investigated (Figure 1a). A Proportional-Derivative (PD) Controller is employed in time domain to impose a desired motion upon a dynamic system with a fixed equilibrium and pivot point. This dynamic system introduces two main sources of non-linear behaviour. These sources are the distance-depended nature of force itself and the saturation of the control system. Thus, a method to improve the overall performance of the control without omitting the non-linearity was tested and compared to a regular linear PD. In order to further validate the control algorithm, a numerical model was developed and compared against experimental measurements to deduce the convergence of the prediction and the overall efficiency of the control.

Results & Discussion

The results, presented in Figure 1b, show that the control of the pendulum was successful at different excitation frequencies. Moreover, there is a satisfactory correspondence between the model predictions and experimental data verifying the predictive capabilities of the numerical model.

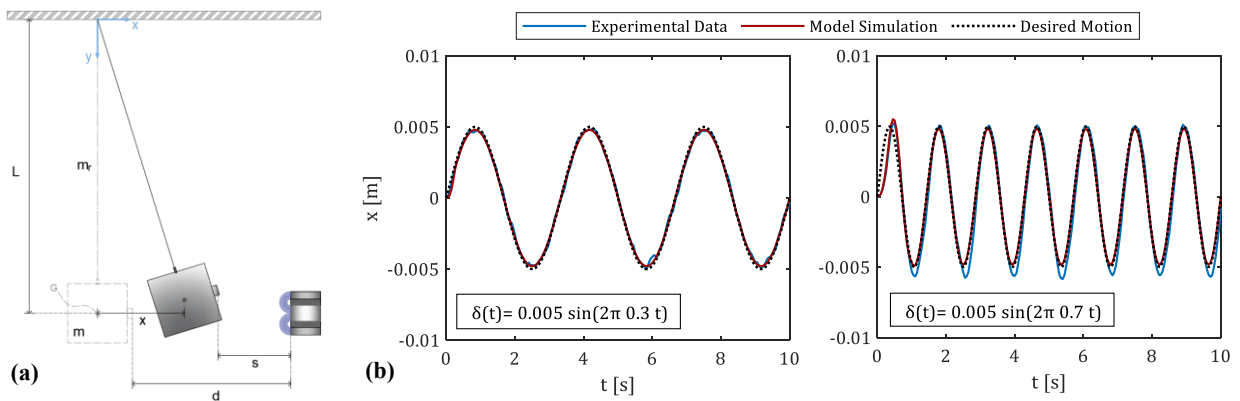


Figure 1: (a) Set-up, (b) Time series of controlled motion for different desired motion patterns.

References

- [1] Sreenivasan, A., & De Kruif, B. (2022). Coupled Control for Motion Compensated Offshore Operations. (<https://doi.org/10.5957/tos-2022-009>)

Koopman-Operator-Based Model Predict Control for Attitude Dynamics on $SO(3)$

Hongyu Chen* and Ti Chen*

*Nanjing University of Aeronautics and Astronautics, Nanjing, Jiangsu, China

Abstract. Attitude dynamics has strong nonlinearity. It is very attractive to use the theory of linear systems to predict, estimate and control strongly nonlinear attitude dynamics by reconstructing nonlinear systems in a linear framework using data-driven methods. In this paper, the nonlinear attitude dynamics on $SO(3)$ are identified and controlled based on Dynamic Mode Decomposition (DMD). Using the manually constructed nonlinear function dictionary as observation, the system approximation is obtained by the Extended Dynamic Mode Decomposition with control (EDMDc) algorithm, and a linear MPC controller is designed based on the EDMDc model. Considering the actual data always contains noise and the sensitivity of the original DMD algorithm to noise, the total least squares DMD (tls-DMD) is used to process the data containing noise. Finally, the effectiveness of MPC control is verified by simulation calculation.

Introduction

The attitude control system is a critical component of a spacecraft. In existing studies, Euler angles, modified Rodrigo parameters or quaternion are usually used to describe spacecraft attitude. However, the singularities of Euler angles and modified Rodrigo parameters exist. Two sets of quaternions correspond to the same attitude, and the continuous attitude control law based on quaternions may have the unwinding phenomenon. Another reason why attitude control on $SO(3)$ still attracts wide attention is the difficulty caused by strong nonlinearity. In 1931, Koopman proved that the behavior of a nonlinear system can be represented by an infinite-dimensional linear operator acting on the observables (or measurement functions) of system states. It is very attractive to use the theory of linear systems to predict, estimate and control strongly nonlinear attitude dynamics by reconstructing nonlinear systems in a linear framework using data-driven methods.

Main result

The extended state is constructed by taking the polynomial of the original state as the nonlinear observation function, and the EDMD algorithm is used to identify the attitude dynamic system from the simulation data. Considering that the global prediction range of EDMD model under extended basis is limited, MPC control is adopted. The sequential quadratic programming (SQP) algorithm is used to optimize the cost function. Stochastic simulation results show that the controller can adjust the attitude to the desired position in a short time. If the data contains noise, tls-DMD is used to eliminate the impact of noise to a certain extent. Although the tls-DMD model has worse accuracy, MPC based on tls-DMD model is still feasible. Some simulation results are shown as follows.

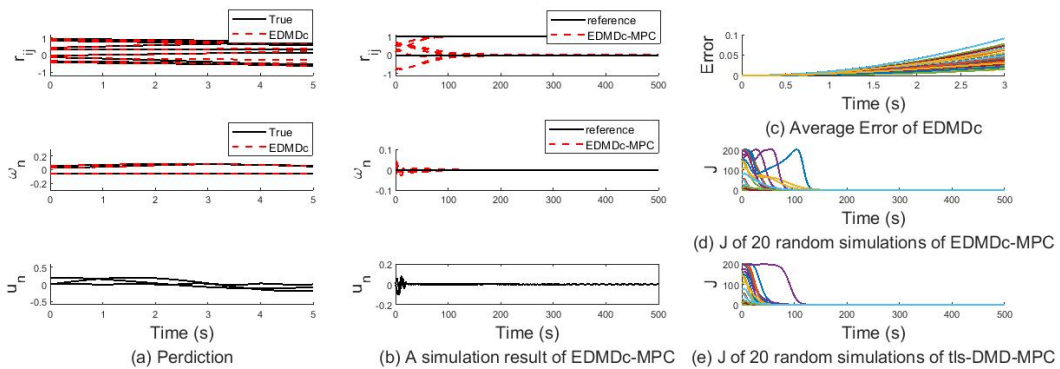


Figure 1: EDMDc model of Attitude dynamics on $SO(3)$

References

- [1] J. N. Kutz, X. Fu, and S. L. Brunton, and J. L. Proctor. *Dynamic Mode Decomposition: Data-Driven Modeling of Complex Systems*. SIAM, 2016.
- [2] Ti Chen, Jinjun Shan, Koopman-Operator-Based Attitude Dynamics and Control on $SO(3)$. *Journal of Guidance, Control, and Dynamics*, 2020. 43(11): p. 2112-2114.
- [3] Milan Korda, Igor Mezić. Linear predictors for nonlinear dynamical systems: Koopman operator meets model predictive control, *Automatica*, Volume 93, 2018, Pages 149-160, ISSN 0005-1098, <https://doi.org/10.1016/j.automatica.2018.03.046>.

On the stability of sampled-data systems with viscous damping and dry friction

Csaba Budai*, Tamás Haba* and Gábor Stépán**

*Department of Mechatronics, Optics and Mechanical Engineering Informatics,
Budapest University of Technology and Economics, Budapest, Hungary

**Department of Applied Mechanics, Budapest University of Technology and Economics, Budapest, Hungary

Abstract. This paper studies the effect of viscous damping and dry friction on the dynamics of sampled-data systems that use discrete-time state feedback in motion control applications. This study aims to present the stabilization effect of Coulomb friction in an otherwise unstable system through the example of a single-degree-of-freedom effective system model. In these systems, unique, so-called concave envelope vibrations occur in cases where the destabilizing effect of sampling can still be compensated to some extent by the presence of dry friction resulting in an unstable limit cycle.

Introduction

One of the fundamental tasks of mechatronics is position control, where the applied controllers aim to drive the system into the desired position. These applications often demand high accuracy and fast operation. However, the necessary performance that can fulfill these requirements may be limited by the presence of physical dissipation and the digital nature of the applied motion controllers.

To illustrate the effect of dissipation, a single-degree-of-freedom mechanical system is considered with viscous damping and dry friction, where discrete-time state feedback with zero-order-hold signal recognition is used to drive the system into the zero reference position. The resulting governing equation of motion is

$$m\ddot{q}(t) + b\dot{q}(t) + f_C \operatorname{sgn}(\dot{q}(t)) = -k_p q(t_j), \quad t \in [t_j, t_j + \tau), \quad t_j = j\tau, \quad j = 0, 1, 2, \dots, \quad (1)$$

where $q(t)$ represents the generalized coordinate as a function of time t , and m denotes the generalized or modal mass. The coefficient of the generalized viscous damping is b and f_C denotes the magnitude of the generalized dry friction force. In addition, the parameter k_p denotes the feedback gain, t_j represents the j th sampling instant and τ is the sampling time.

Results and discussion

When the system is ideal, i.e., no physical dissipation has been taken into account, the system is always unstable [1]. Suppose that the dominant source of dissipation is modeled by viscous damping. In that case, stable control can be achieved using discrete-time state feedback [2], as presented by the yellow region of the stability map shown in the left panel of Fig. 1. Assume that the dominant source of dissipation can be described by the combined model of viscous damping and dry friction. In that case, the stability region is further extended, but at the same time, it also becomes sensitive to the initial position [2]. It is presented by the shaded gray area of the stability map shown in the left panel of Fig. 1. Numerical simulations and experiments verify these results. To reduce the computational cost and the measurement time, the verification process was carried out by the multidimensional bisection method [3]. The measured stability map is presented in the middle panel of Fig. 1, where the green area represents the stable domain, while the blue area the unstable domain. The comparison of the simulated and the measured stability map is presented in the right panel of Fig. 1.

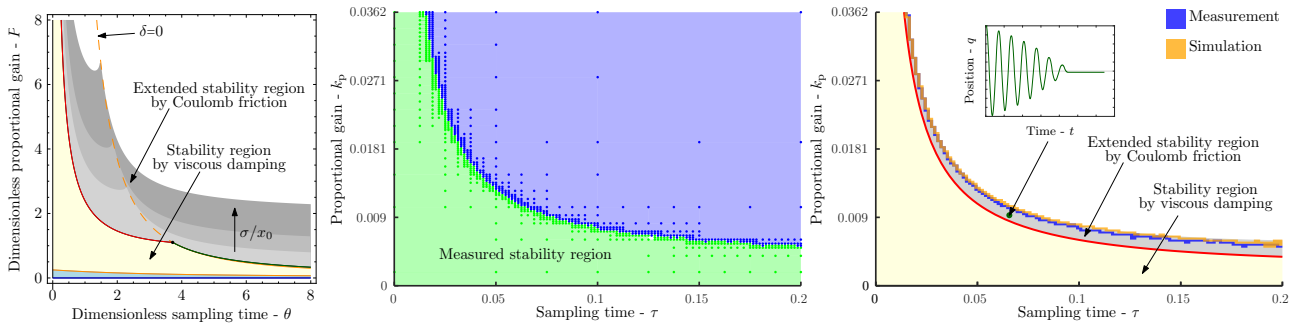


Figure 1: Left panel: Analytical stability chart. Middle panel: Measured stability chart. Right panel: Comparison of the results.

References

- [1] Budai C., Kovacs L.L., Kovacs J., Stepan G. (2017) Effect of dry friction on vibrations of sampled-data mechatronic systems. *Nonlinear Dyn.* **88**:349–361.
- [2] Budai C., Kovacs L.L. (2017) On the Stability of Digital Position Control with Viscous Damping and Coulomb Friction. *Period. Polytech. Mech. Eng.* **61**(4):266–271.
- [3] Bachrathy D., Stepan G. (2012) Bisection method in higher dimensions and the efficiency number. *Period. Polytech. Mech. Eng.* **56**(2):81–86.

The Influence of a Non-Instantaneous Double Support Phase on the Efficiency of a HZD Controlled Bipedal Robot

Yinnan Luo*, Ulrich J. Römer*, Marten Zirkel**, Lena Zentner** and Alexander Fidlin*

*Institute of Engineering Mechanics, Karlsruhe Institute of Technology (KIT), Karlsruhe, Germany

**Compliance Systems Group, Ilmenau University of Technology, Ilmenau, Germany

Abstract. This work introduces the extended hybrid zero dynamics control for periodic gaits containing alternating single and non-instantaneous double support phases of a planar bipedal robot. The model consists of five rigid body segments which are connected by four actuated revolute joints. During both continuous phases, the controller synchronizes the joints to their reference trajectories, which are numerically optimized to minimize the energy consumption of locomotion. The resulting efficiency is compared against gaits with an instantaneous double support phase.

Introduction

Hybrid zero dynamics (HZD) control is a popular control concept to create stable walking gaits for bipedal robots. One of its advantages is that the controller uses the passive dynamics of the system which is suitable for high energy efficiency. The existing HZD control concept is commonly developed for periodic walking gaits that consist of an under-actuated single support phase (SSP) and an instantaneous double support phase (DSP) [1]: during the SSP, the stance leg contacts the ground without slipping and the swing leg moves forward without scuffing. The DSP is described as a discrete transition event, namely an inelastic impact of the swing leg with the ground, immediate lift-off of the former stance leg and swapping the roles of the former swing and stance leg.

Based on a planar five-segment robot model driven by four electric actuators in its joints, our research extends the HZD control strategy to periodic gaits with non-instantaneous DSP. Since both non-slipping stance feet remain on the ground, the legs form a closed kinematic chain that results in one degree of over-actuation (Fig. 1 left). In order to artificially create an under-actuated DSP, two independent virtual actuators are introduced and mapped to the four physical actuators by a projection matrix $\mathbf{P}_{(4 \times 2)}$. In both SSP and DSP, the HZD controller synchronizes the independent joints to their reference trajectories which are parameterized by Bézier curves. For vanishing control errors, the states of the un-actuated absolute orientation are the zero dynamics of the controlled system. Its periodic solution can be obtained by a numerical optimization process, which minimizes the energy consumption of locomotion (evaluated by the cost of transport) while optimizing the Bézier parameters and the projection $\mathbf{P}_{(4 \times 2)}$. The resulting energy efficiency is compared against the original assumption where the DSP is modeled as instantaneous.

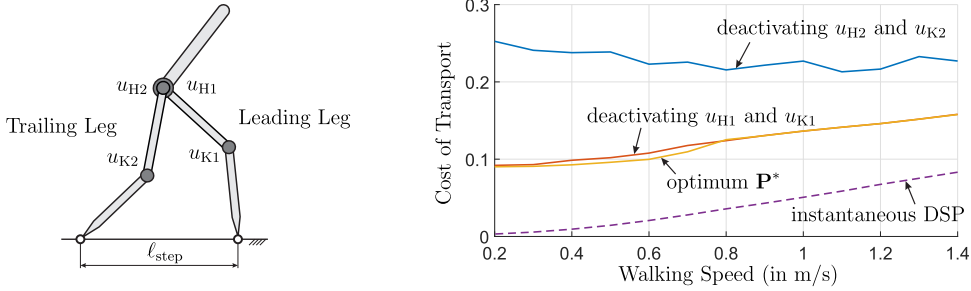


Figure 1: Left: The over-actuated double support phase with the constant step length ℓ_{step} . Right: Optimized cost of transport of different continuous under-actuated DSPs (solid lines) in comparison to the instantaneous DSP (dashed line).

Results and Discussion

As depicted in Fig. 1 (right), the efficiency study is conducted for the speed range $v \in [0.2, \dots, 1.4]$ m/s. The optimum actuator mapping $\mathbf{P}_{(4 \times 2)} = \mathbf{P}^*$ is compared to two other configurations that result in an under-actuated DSP: simply deactivating the actuators of the leading or the trailing leg. According to the optimization results, the actuation in the trailing leg's knee joint should be utilized during DSP to achieve a high efficiency independent of the walking speed. In contrast, the trailing leg's hip actuator is advantageous for high speeds ($v > 0.8$ m/s) and the leading leg's hip actuator for lower speeds. Regarding the DSP as an instantaneous impact event, however, results in the highest efficiency, because its optimum gaits need less negative work (braking) to slow down the movement.

Acknowledgements: This work is financially supported by the German Research Foundation (DFG), grant FI 1761/4-1 | ZE 714/16-1.

References

- [1] E.R. Westervelt, J.W. Grizzle, and D. Koditschek, Hybrid Zero Dynamics of Planar Biped Walkers, *IEEE Transactions on Automatic Control* 48(1), pp. 42–56. (2003).

The migration of a Neural Network Observer training using the Deep Learning approach

Loukil R.* and Gazezi W.**

* RISC Laboratory, Electrical Department, Engineering SCHOOL ENIT, Tunis

** RISC Master ISTIC, Tunis

Abstract. This paper presents the training of a Neural Network Observer using the Deep Learning approach. Then, we suggest a brief comparison between the use of a classic neural observer supervised by the back-propagation algorithm with a Matlab simulation and a new neural observer used the Deep Learning with a Keras, Tensor flow simulation applied to the same example. Deep learning and neural networks may be an intimidating concept, but since it is increasingly popular these days, this topic is most definitely worth your attention. Fortunately, we have deep learning methods by which we can surely circumvent these challenges regarding feature extraction. This study explains the necessity to improve the way of learning for estimation purposes and upgrade the performance of this kind Observer so its migration. According to the results, we propose the migration of the Neural Network Observer for a nonlinear system, which is well trained.

Introduction

Neural networks are increasingly studied in the research due to their ability to predict complex problems and their learning mechanisms based on parallel processing of information. Various architectures and learning techniques have been proposed and discussed in order to solve several problems. Our motivation is to combine two axes of research, which differ totally in term of applications, and to be up to date with the IA, Machine Learning and the Deep Learning as new knowledge. In this section, we present the multilayer networks training algorithms for the neural observer in two cases [2]. The first case refers to a classic Neural Observer and corrects its weights based on the back-propagation algorithm or an Hybrid approach [4].

The second case is based on the new technic of Deep Learning [1] applied to the non-linear observer [3] in order to compare their responses and improve the estimation error for example.

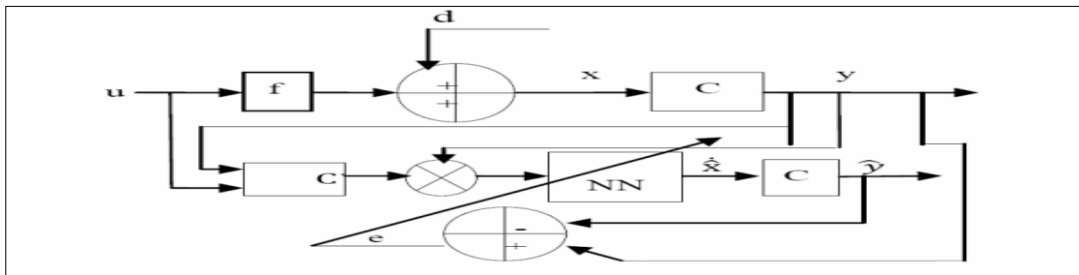


Figure 1: The structure of Neural Observer [2]

Furthermore, the performances of the proposed Neural Observer are tested on a physical nonlinear system. The neural observer assesses the state of the system despite the fact that the nonlinear dynamics of the system is assumed a priori unknown. The comparison will be also between the Matlab language and the Keras as our Python Deep Learning. In addition, we will compare also the efficacy of the two Learning algorithms of the Neural Observer according to their attitudes in estimation purposes.

Results and Discussion

We have trained the proposed Neural Observer tested on a physical nonlinear system named two tanks in cascade which is presented in figure 2; It's is composed of a set of elementary components. Various sensors allow us to measure the height of the product in the tank top (h_1) and the tank bottom (h_2) and the rate of entry of the product (q_{e1}) and (q_{e2}) in the tank top and the pan low respectively [2]. Using the Library Keras added to Python Language, we find that this nonlinear system has different estimation errors for the Neural Observer which has been already decreased and has small value nearly to zero. The rapidity of our algorithm is also detected comparing to the previous simulation. The Deep Larning approach has already improved the performances of our Observer.

References

- [1] Geran A., A. S. (2020) Deep Learning Avec keras and TensorFlow mise en oeuvre et cas concrets , *DUNOD*.
- [2] Loukil R., Chtourou M. and Damak T. "Classic training of a Neural observer for estimation Purposes", International conference on Electrical engineering and Technology, Paris 23-24, 2015.
- [3] Loukil R., Chtourou M. and Damak T. "Observability and Synthesis of Nonlinear Observers", International conference on Sciences and Techniques of Automatic control and computer engineering, Tunisia, Monastir 19- 21 (2010).
- [4] Loukil R., Chtourou M. and Damak T. "Training a Neural Observer using a Hybrid Approach", IEEE conference on Systems, Signals & Devices, Chemnitz, Germany, March 20-23 (2012).

Image-based aerial grasping of a moving target based on model predictive control

M. Moghanipour*, A. Banazadeh*

*Department of Aerospace Engineering, Sharif University of technology, Tehran, Iran

Abstract. This study concentrates on the vision-based aerial grasping of a moving target based on MPC with non-linear prediction and linearization along the trajectory (MPC-NPLT). In this research, using image data MPC-NPLT formulation is developed for aerial grasping of a moving target. The obtained results for moving in the x and y directions suggest that the proposed approach can provide acceptable performance.

Introduction

The aim of visual servoing is to control the pose of the robot's end-effector, relative to the target using the feedback information extracted from the image. One of the most common approaches is the position-based control which uses observed visual features, a calibrated camera, and a known geometric model of the target to estimate the pose of the target, while the image-based control directly uses images 2D data [1] and causes more simplified modelling. In this work, we addressed an image-based grasping modelling of moving targets using features extracted from the image based on MPC-NPLT.

Results and Discussion

As shown in Figure 1-(a), for each point on the target, the vectorial equation can be written as follows:

$$[\mathbf{P}_c^I]^I + [\mathbf{P}_t^C]^I = [\mathbf{P}_t^I]^I \quad (1)$$

By definition $\mathbf{P}_t^C = [X_C \ Y_C \ Z_C]^T = Z_C[x \ y \ 1]^T = Z_C\tilde{\mathbf{P}}$, the non-dimensional form of Eq. (1) will be achieved. Substituting $\mathbf{P}_t^C = Z_C\tilde{\mathbf{P}}$ in Eq. 1, the differential equation can be written as:

$$\begin{bmatrix} \dot{X}_C^I \\ \dot{Y}_C^I \end{bmatrix} + \begin{bmatrix} \dot{Z}_C \mathbf{a}^T \tilde{\mathbf{P}} + Z_C \dot{\mathbf{a}}^T \tilde{\mathbf{P}} + Z_C \mathbf{a}^T \dot{\tilde{\mathbf{P}}} \\ \dot{Z}_C \mathbf{b}^T \tilde{\mathbf{P}} + Z_C \dot{\mathbf{b}}^T \tilde{\mathbf{P}} + Z_C \mathbf{b}^T \dot{\tilde{\mathbf{P}}} \end{bmatrix} = \begin{bmatrix} V_{x_t} \\ V_{y_t} \end{bmatrix} \quad (2)$$

where \mathbf{a} and \mathbf{b} represent the rotational matrix vectors. To use MPC-NPLT, it is needed to linearize Eq. 1. Eventually, by considering $\mathbf{s} = [x \ y]$, $\mathbf{v} = [\mathbf{V}_c^I \ \boldsymbol{\omega}_c^I]$ and $\mathbf{V}_t = [V_{x_t} \ V_{y_t}]$ as image feature points, MPC controller outputs and target velocity, respectively the cost function can be computed as

$$C = \min_{\mathbf{v}} \int_t^{t+T} L(\mathbf{s}, \mathbf{v}) d\tau = \min_{\mathbf{v}} \int_t^{t+T} (|\mathbf{s} - \mathbf{s}_d|^2 + |\mathbf{v}|^2) d\tau \quad (3)$$

Subject to $\dot{\mathbf{s}} = \begin{bmatrix} \dot{x} \\ \dot{y} \end{bmatrix} = L_p \begin{bmatrix} \mathbf{V}_c^I \\ \boldsymbol{\omega}_c^I \end{bmatrix} + L_t \mathbf{V}_t$

$|\mathbf{v}_i| \leq \mathbf{v}_{max}$

The simulation results are summarized in Figure 1-(b) which shows the acceptable performance of the proposed method.

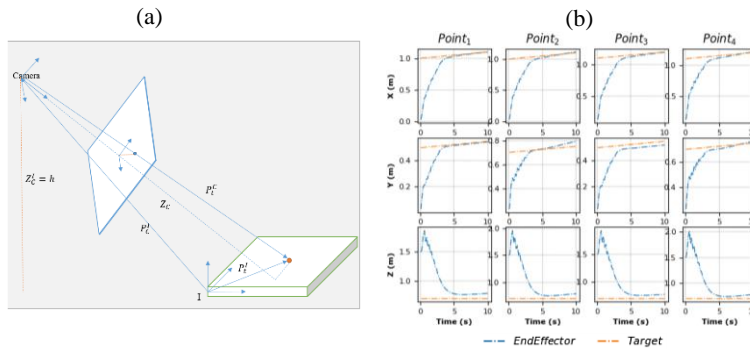


Figure 1: a) Camera and the ground target geometry scheme, b) Simulation results for grasping a moving target.

References

[1] P. Corke, Robotics, vision and control: fundamental algorithms in MATLAB® second, completely revised. Springer, 2017.

Control via Nonlinear Feedback Linearization with Machine Learning

Hector Vargas Alvarez**, Gianluca Fabiani** and Nikolas Kazantzis**, Constantinos Siettos** and Ioannis G. Kevrekidis**

Scuola Superiore Meridionale, Università degli Studi di Napoli Federico II, Naples, Italy

Scuola Superiore Meridionale, Università degli Studi di Napoli Federico II, Naples, Italy

Dept. of Chemical Engineering, Worcester Polytechnic Institute, Massachusetts, USA

Dept. of Mathematics and Applications, Università degli Studi di Napoli Federico II, Naples, Italy

Dept. of Bio and Chem. engineering, Johns Hopkins University, Maryland, USA

Abstract. We use machine learning to implement feedback linearization for the control of nonlinear discrete-time systems. The proposed approach is based on physics-informed neural networks, thus implementing pole-placement and feedback linearization in one step. To demonstrate the efficiency of the scheme we used a nonlinear discrete time model for which the feedback linearization law can be derived analytically.

Introduction

Feedback linearization of nonlinear systems is arguably one of the most used nonlinear control techniques [1, 2]. Building in previous work [1, 2], we propose a Physics-informed machine learning (PIML) scheme that learns a feedback linearizing control law and performs pole placement in one step for discrete time systems of the form:

$$x(t+1) = f(x(t), u(t))$$

Thus we seek for a transformation S such that $z = S(x)$ is coupled with a control law $u = -cz = -cC(x)$ in order to linearize the above system as:

$$z(t+1) = Az(t),$$

where A has the proper set of eigenvalues to ensure stability [1].

Results and discussion

To illustrate the performance of the PIML, we consider the following system of discrete equations [1]:

$$\begin{aligned} x_1(t+1) &= \exp(0.3x_2(t))\sqrt{1+x_1(t)+x_2(t)} - 1 - 0.4x_2(t) + 0.5u(t) \\ x_2(t+1) &= 0.5\ln(1+x_1(t)+x_2(t)) + 0.4x_2(t) \end{aligned} \quad (1)$$

It can be shown [1] that the sought transformation reads:

$$T(x_1, x_2) = [\ln(1+x_1+x_2) \quad x_2] \quad (2)$$

Then $T_1(x_1, x_2) = \ln(1+x_1+x_2)$ in (2) is the desired feedback linearizing control law, where the closed loop poles are governed by the eigenvalues of matrix A here set to $k_1 = 0.8405$ and $k_2 = 0.0595$. Figure (1), shows the approximation of S obtained with the proposed PIML scheme. As it is shown, the scheme is able to learn the transformation in (2) with a numerical approximation accuracy of the order of 10^{-3} .



Figure 1: Numerical approximation accuracy (NAA) between the theoretical sought transformation (2) and the one learned by the PIML scheme. Panel (a) depicts the NAA for the first component $T_1(x_1, x_2)$ and panel (b) refers the same for the second component of $T(x_1, x_2)$.

References

- [1] Zhe and Rincon, David and Christofides, Panagiotis D. (2020) Real-Time Adaptive Machine-Learning-Based Predictive Control of Nonlinear Processes. *Industrial & Engineering Chemistry Research* **59**:2275-2290.
- [2] Siettos, Constantinos I and Kevrekidis, Ioannis G and Kazantzis, Nikolaos (2006) An equation-free approach to nonlinear control: Coarse feedback linearization with pole-placement. *International Journal of Bifurcation and Chaos*, 12029–2041
- [3] Nikolaos Kazantzis (1985) A functional equations approach to nonlinear discrete-time feedback stabilization through pole-placement. *Systems Control Letters*, 361-369

Synchronization of Discrete-Time Fractional Complex Networks with Time Delays via Event-Triggered Strategy

Xiaolin Yuan, Guojian Ren, Yongguang Yu and Wei Chen

School of Mathematics and Statistics, Beijing Jiaotong University, Beijing 100044, People's Republic of China

Abstract. This paper is devoted to the synchronization problem of discrete-time fractional complex networks (DTFCNs) with time delays via an event-triggered strategy. First, based on the nabla-like Riemann-Liouville difference, the DTFCNs are established. And then, the pinning event-triggered controlled networks are given. Furthermore, to reduce the frequency of communications, a novel event-triggered control mechanism that only relies on the information at the trigger time is proposed. Next, some sufficient conditions are proposed for achieving synchronization. By using Lyapunov technology, it is shown that the synchronization of the DTFCNs can be achieved via the proposed event-triggered strategy.

Introduction

In recent years, complex networks exist in various fields such as ecosystems, power grids, telecommunication networks, neural networks, Internet networks, and so on. Generally, according to different principles, complex networks are divided into small-world networks [1] and scale-free networks [2]. In the theory of complex networks, the behaviours of the network dynamics are a hot research topic. Notice that in nature and technical fields, there are a large number of fractional dimensions and self-similarity between whole and part. Therefore, fractional calculus as the basis of fractal geometry and fractional dimension has been applied to many fields, such as oscillation, and random diffusion, etc. In practice applications, the event-triggered control approach was proposed for the purpose of reducing the frequency of controller updates. On the other hand, notice that many of the existing control strategies are designed per discrete-time models in the real world with the adoption of digital computers. However, the synchronization problem of DTFCNs with time delays and event-triggered strategy remains an open problem. This paper aims to fill in the aforementioned gaps.

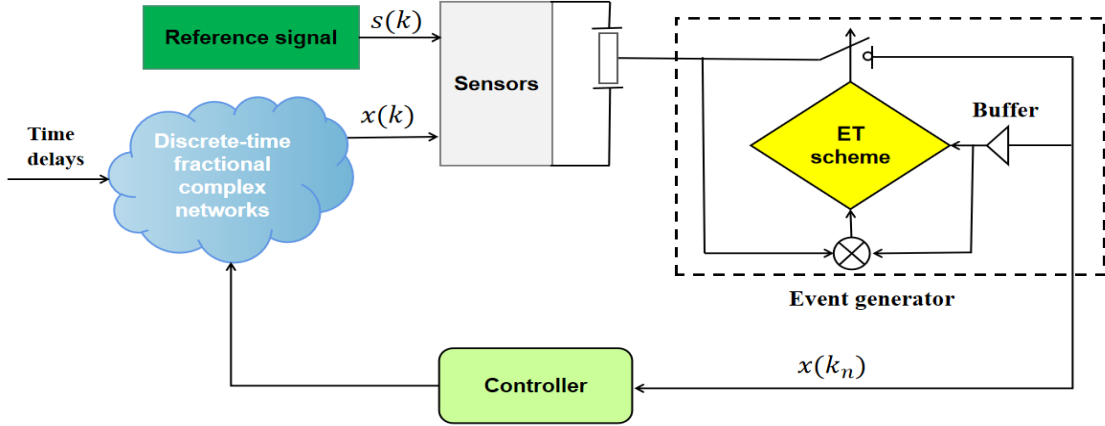


Figure 1: Event-triggered control mechanism.

Results and discussion

In this paper, consider the following DTFCNs with time delays:

$$\nabla_0^\alpha x_i(k) = f(x_i(k), k) + c \sum_{j=1}^N g_{ij} \Gamma x_j(k - \tau_j), \quad i = 1, 2, \dots, N,$$

$$x_i(k) = x_{i0} \in R^n, \quad \underline{\tau} \leq k \leq 0.$$

A novel event-triggered control mechanism of the following form is proposed:

$$\bar{h}_i(z_i(k), \varepsilon_i(k)) = |\varepsilon_i(k)|^2 - 2\xi(\delta_i - 1)\vartheta|z_i(k)|^2, \quad i = 1, 2, \dots, N.$$

Then, some sufficient conditions are given. By using Lyapunov technology, it is shown that the synchronization of the DTFCNs can be achieved via the proposed event-triggered strategy. The event-triggered control mechanism is depicted in Figure 1.

References

- [1] Watts, D.J., Strogatz, S.H. (1998) Collective dynamics of 'small-world' networks. *Nature* **393**, 440-442.
- [2] Barabasi, A.L., Albert, R. (1999) Emergence of scaling in random networks. *Science* **286**, 509-512.

Anti-synchronization of Quaternion Valued Inertial Neural Networks with Unbounded Time Delays: non-reduction, non-separation method

Sunny Singh* and Subir Das*

*Department of Mathematical Sciences, Indian Institute of Technology (BHU), Varanasi (221005), India

Abstract. In this article, Global anti-synchronization for a class of quaternion-valued inertial neural networks (QVINNs) with unbounded delays is considered. Based on the two different types of control strategies (feedback and adaptive controllers) and Lyapunov stability theory, various fruitful criteria are obtained to ensure the global anti-synchronization of QVINNs. Most of the synchronization and anti-synchronization results for QVINNs are based on the variable substitution approach, which reduces the order of the original second-order system into the first-order system; also, quaternion-valued networks are separated into four equivalent real-valued neural networks which are made the analysis process more complicated. However, in the present study, the authors deal with the non-reduction order method and non-separation approach for QVINNs, making the analysis approach more concise and easier to deal with second-order neural networks. Finally, two numerical example are provided to shows the effectiveness of our proposed model

Introduction

Quaternion was first introduced by Hamilton (1853) [7], which is a noncommutative division algebra. Because of the non-commutativity, quaternion research is much more difficult rather than real-valued neural networks (RVNNs) and complex-valued neural networks (CVNNs). This is the major reason for the slow research of the quaternion-valued neural networks (QVNNs). In order to avoid the non-commutativity, some researchers separated the QVNNs into four equivalent RVNNs or two CVNNs to study these problems. However, the separation method increases the dimension of the original systems, which leads to difficulties for mathematical analysis [3]. Luckily, as modern mathematics has advanced and expanded, applications of quaternion for future development have been discovered in recent years. It has good application prospects in three-dimensional and four-dimensional data modeling; also, quaternion has gained increasing attention in various fields, for example, attitude control, computer graphics, etc., [2] etc.

In the last few years, anti-synchronization results have been widely used in many areas, including communication processing and information systems [1]. When using anti-synchronization in communication systems, we can transmit digital signals continuously between anti-synchronization and synchronization to strengthen secrecy. As a result, synchronization or anti-synchronization analysis of nonlinear systems has become more popular. Unfortunately, up to now, the study on exponential anti-synchronization of QVNNs with unbounded delays and a non-separation approach has not been involved.

This article will give multiple new results about the anti-synchronization of QVNNs as follows:

1. This article dealt with the global exponential anti-synchronization of QVNNs with unbounded time-varying delays.
2. This article dealt with the QVNNs with inertial terms by utilizing the non-reduction order and non-separation approach.
3. in this article, authors first time designed the adaptive controller for QVNNs, which are used to study the non-reduction approach for inertial terms in QVNNs.

Results and discussion

Unlike the traditional variable substitution approach for the reduced order method, the article's authors dealt with the global anti-synchronization of QVNNs with unbounded time-varying delays and inertial terms. By constructing the Lyapunov functional and designing a linear quaternion-valued feedback and adaptive controllers, some innovative conditions with less conservative results are obtained in Theorem [1,2] to ensure the global anti-synchronization for QVNNs with the non-separation method. The results of this article are more compact and less calculative due to the non-separation approach [3,4]. Since the time-varying delays are unbounded in this article, the proposed QVNNs are more general and execute wider applicability.

The method adopted in this article is totally new, which motivates the researchers to further study of QVNNs with non-separation and non-reduction methods for finding the fixed time and pre-assigned fixed time stability.

References

- [1] Shi, Jichen, and Zhigang Zeng. "Anti-synchronization of delayed state-based switched inertial neural networks." *IEEE Transactions on Cybernetics* 51.5 (2019): 2540-2549.
- [2] Choe, Su Bang, and Julian J. Faraway. "Modeling head and hand orientation during motion using quaternions." *SAE transactions* (2004): 186-192.
- [3] Singh, Sunny, et al. "Synchronization of Quaternion Valued Neural Networks with Mixed Time Delays Using Lyapunov Function Method." *Neural Processing Letters* 54.2 (2022): 785-801.
- [4] Zhao, Hongyong, and Qi Zhang. "Global impulsive exponential anti-synchronization of delayed chaotic neural networks." *Neurocomputing* 74.4 (2011): 563-567.
- [5] Kumar, Umesh, et al. "Fixed-time synchronization of quaternion-valued neural networks with time-varying delay." *Proceedings of the Royal Society A* 476.2241 (2020): 20200324.
- [6] Babu, N. Ramesh, and P. Balasubramaniam. "Master-slave synchronization of a new fractal-fractional order quaternion-valued neural networks with time-varying delays." *Chaos, Solitons & Fractals* 162 (2022): 112478.
- [7] Hamilton, William Rowan. *Lectures on Quaternions: Containing a Systematic Statement of a New Mathematical Method; of which the Principles Were Communicated in 1843 to the Royal Irish Academy; and which Has Since Formed the Subject of Successive Courses of Lectures, Delivered in 1848 and Subsequent Years in the Halls of Trinity College, Dublin: With Numerous Illustrative Diagrams, and with Some Geometrical and Physical Applications.* Hodges and Smith, 1853.

Explosive death transitions in a complex network of chaotic systems.

Samana Pranesh*, Sayan Gupta**

*Department of Applied Mechanics, Indian Institute of Technology Madras, Chennai-600036, Tamil Nadu, India.

**Complex Systems and Dynamics Group, Indian Institute of Technology Madras, Chennai -600036, Tamil Nadu, India

Abstract. Explosive death transitions in a mean-field coupled network of Rossler system is investigated. The network behaviour is characterised using amplitude order parameter. It is observed that the amplitude order parameter varies smoothly in the forward direction whereas, in the backward direction, it makes an explosive transition. The forward transition point has been derived analytically which matches with the numerical simulations.

Introduction

The route to synchronisation can be abrupt which is termed as explosive synchronization (ES) [1] - are defined as first order transitions and are characterised by hysteretic behaviour. Amplitude death (AD) is a type of oscillation suppression in which the oscillators stabilise to a steady state which is also the steady state of the uncoupled constituents of the network. ES where the network of coupled oscillators transition from the oscillatory state to AD state is termed as explosive death (ED). The focus of this study is on investigating analytically the mechanisms which lead to ED transitions in a mean field coupled complex network of Rossler system. The derivations make no assumption about the topology or the form or order of the oscillator units, apart from that they are assumed to undergo chaotic oscillations. Consider a network of identical chaotic systems, where each node comprises of a Rossler system. The equations of motion for the j -th node, coupled via a mean-field diffusion, is given by

$$\dot{x}_j = -y_j - z_j + \frac{kQ}{d_j} \left[\sum_{s=1}^N g_{js} x_s \right] - kx_j, \dot{y}_j = x_j + ay_j, \dot{z}_j = b + z_j(x_j - c). \quad (1)$$

Here, x_j, y_j, z_j are the three state variables of the j -th node, a, b, c are the system parameters, k is the strength of the coupling, Q is the density of the mean field, g_{js} is a function that represents the coupling weight between the j -th and s -th system in the network and d_j is the degree of node j . The amplitude order parameter [2] is given by $A(k) = \frac{a(k)}{a(0)}$, where, $a(k) = \frac{1}{N} \sum_{i=1}^N ((x_{i,\max})_t - (x_{i,\min})_t)$ and $a(0)$ is the amplitude when all the nodes are uncoupled ($k = 0$).

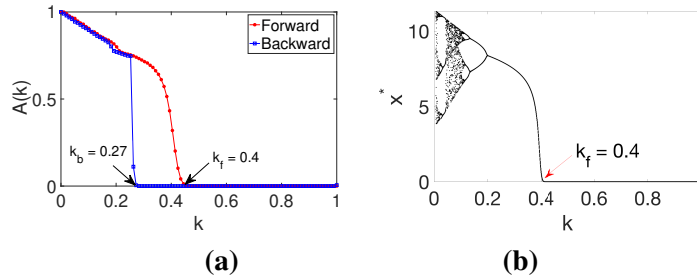


Figure 1: (a) Variation of $A(k)$ with k for Rossler system; $a = b = 0.2$, $c = 5.7$, $Q = 0.5$ and $N = 100$. (b) Bifurcation diagram for Rossler attractor; $a = b = 0.2$, $c = 5.7$, $Q = 0.5$ and $N = 100$

Results and Discussion

From Fig. 1(a), it is seen that in the forward direction, the variation of $A(k)$ with k is smooth and the AD state is attained at $k = 0.4$. As k is decreased adiabatically, $A(k)$ undergoes an explosive transition from the AD state. Since the transition is a second order in the forward direction and first order in the backward direction, it can be said that $A(k)$ exhibits a semi-explosive death behaviour. Fig.1(b) shows the bifurcation diagram for the j -th Rossler attractor with k (varied in the forward direction) as the bifurcation parameter. As k is increased, the system enters into chaotic state. When k is further increased, the system transitions to a period-4 oscillations and subsequently to period-2 oscillations. For $k > 0.2$, the amplitude gradually reduces and reaches the AD state for $k \geq 0.4$.

References

- [1] Zhang, X., Hu, X., Kurths, J., Liu, Z. (2013) Explosive synchronization in a general complex network. *Phys. Rev. E* **88**(1): 010802.
- [2] Verma, U. K., Sharma, A., Kamal, N. K., Kurths, J., Shrimali, M. D. (2017) Explosive death induced by mean-field diffusion in identical oscillators. *Scientific Reports* **7**(1) 1-7.

Anomalies in Synchronization of Globally Coupled Mechanical Metronomes

Omer Livneh*, Oriel Shoshani*

*Ben-Gurion University of the Negev, Be'er-Sheva 84105, Israel

Abstract. Using a combination of theory, experiment, and simulation, we discover and characterize a new kind of asymmetric long-term dynamic state in a fully symmetric system of four globally coupled mechanical metronomes. In this dynamic state that we refer to as the “Runaway,” one of four metronomes settles on an anti-phase relative to the others, and the system randomly “chooses” the identity of the anti-phase metronome. We found that the “Runaway” state can be produced only when the dissipation in the system exceeds a certain threshold. We view this “Runaway” state as a simpler version of a chimera state, in which the symmetry of the oscillator population is broken, but there is no subpopulation with incoherent dynamics.

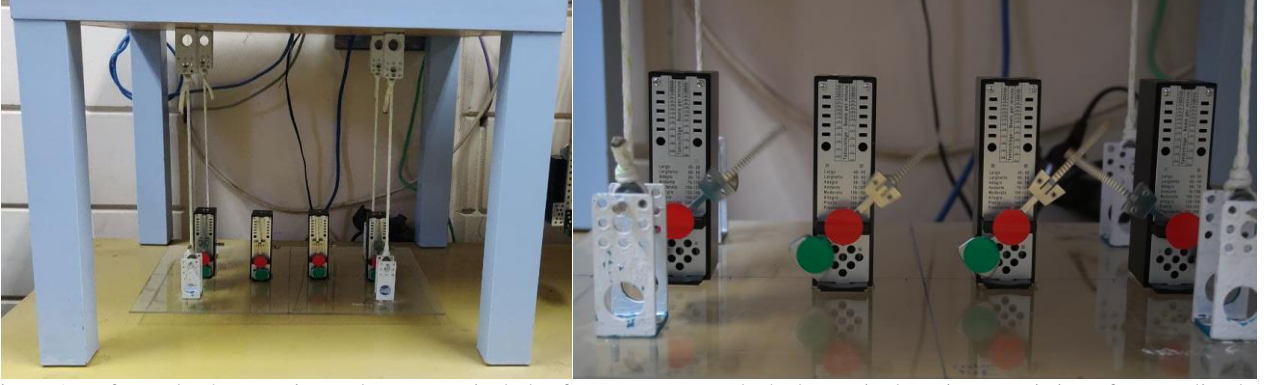


Figure 1: Left panel: The experimental apparatus includes four metronomes docked to a single swing, consisting of an acrylic plate attached to a stationary ceiling via four inextensible ropes and eight pulleys (two pulleys for each rope) to ensure a smooth motion of the swing. The metronomes and the swings are marked with circular colored stickers, and their motion is recorded with a camera. Right panel: Experimental observation of a “Runaway” state. The first metronome from the right is in an anti-phase relative to the other in-phase metronomes.

Introduction

From superconductivity and superfluidity at the subatomic scale to gravitational synchrony at celestial scales, synchronization and collective dynamics pervade all of nature, science, and engineering. In modern technology applications, electronic oscillator networks are frequently used. therefore, their synchronization and collective dynamics are of prime interest, theoretically and practically. Compared to their electronic counterparts, mechanical oscillator networks, such as coupled mechanical metronomes, are considerably simpler to analyse analytically and numerically. Moreover, it has been shown experimentally that mechanical networks of coupled metronomes exhibit a variety of dynamical states, including exotic chimera states [1]. In this study, we explore a simple network of four globally coupled mechanical metronomes (Figure 1, left panel) which obeys the following equations of motion:

$$\ddot{\theta}_i + \sin \theta_i + \dot{\theta}_i [2\Gamma_m - J_m \delta(|\theta_i| - \theta_c) H(\theta_i \dot{\theta}_i)] - \frac{2\alpha}{N} \cos \theta_i \frac{d^2}{d\tau^2} \sum_{j=1}^4 \sin \theta_j = 0, \quad (1)$$

where we used the model in Ref. [2] for the escapement mechanism, $J_m \delta(|\theta_i| - \theta_c) H(\theta_i \dot{\theta}_i)$.

Results and discussion

We note that Eq. (1) possesses a solution in which $\theta_1 = \theta_2 = \theta_3 = -\theta_4$, i.e., a “Runaway” state. Furthermore, due to the simplicity of the dynamical system, we are able to conduct a stability analysis of the “Runaway” state and find the condition and basin of attraction of this state. These analytical results are validated by numerical simulation and experiments (Figure 1, right panel). Although the synergy between analytical, numerical, and experimental analyses gives us a well-rounded picture of the “Runaway” state, we stress that our study is far from exhaustive, and much still remains to be learned about the long-term dynamics of coupled metronomes, despite the fact that it is considered a simple and well-studied.

References

- [1] Martens E. A., Thutupalli S., Fourriere A., and Hallatschek O. (2013) Chimera States in mechanical oscillator networks. *PNAS* **110.26**:10563–10567.
- [2] Goldsztein G. H., Nadeau A. N., and Strogatz S. H. (2021) Synchronization of clocks and metronomes: A perturbation analysis based on multiple timescales. *Chaos* **31.2**: 023109.

Embedding dimension of the dynamical manifold in the phase space as a measure of chimera states

Olesia Dogonasheva*, Boris Gutkin* and Denis Zakharov**

Group of Neural Theory, École Normale Supérieure PSL University, Paris, France

**Centre for Cognition and Decision Making, HSE University, Moscow, Russia

Abstract. The chimera state is a dynamical regime where some elements in a structurally homogeneous network are synchronous while others are asynchronous. Previous studies have shown that even relatively simple networks can have multiple chimera types. Therefore developing methods to identify characteristics of such states has a high potential impact. We propose the embedding dimension as an approach to identify and distinguish chimera states that can be applied to dynamical systems of various natures. The proposed method enables both the accurate identification of chimeras as well as the estimation of the size of their incoherent clusters. To test the new method, we studied a network of type-II Morris-Lecar neurons. with non-local connections. In particular, we considered the evolution of chimera states depending on the parameters of synaptic strength, connectivity, and external current. Using our method, we were able to correctly characterize chimera states and the evolution of their size depending on parameters.

Introduction

Chimera states were first described for a network of phase oscillators [1]. There are now multiple published works that analyze chimeras for a big variety of networks (e.g. see work [2] and refs therein). As a result, several methods have been suggested to determine the characteristics of the chimera states. For example, the Kuramoto order parameter can be used for networks of phase oscillators [1], and the ACM technique can be used for spiking neural networks [3]. In this study, we suggest taking a different angle on this issue based on the idea that network synchronization can be considered as a dimensional reduction of the system dynamics. If all active elements are synchronized, the system activity is effectively equal to the activity of one element. If some of the elements are in an asynchronous regime, then the dimension of the dynamical manifold of the system in phase space has the higher embedding dimension. Moreover, the more there are asynchronous elements in the system, the greater the embedding dimension. Since the chimera states demonstrate partial synchronization, chimera can be identified using the embedding dimension of the dynamical manifold in the phase space.

Results and discussion

We tested a new approach using the same system as in [3]. Examples are shown in Fig. 1.

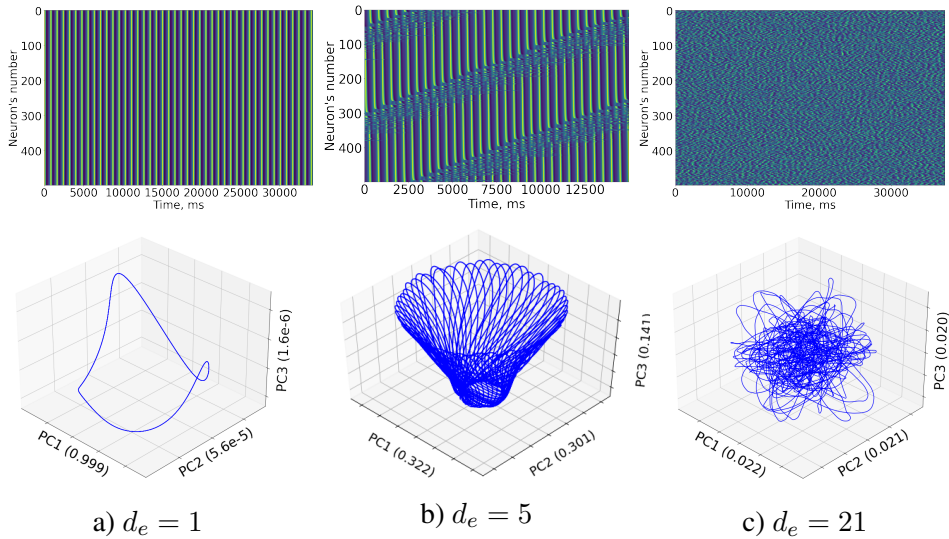


Figure 1: Examples of different dynamical regimes and corresponding embedding dimension d_e . Top panel: rasterplots of the synchronous state (a), a chimera state (b) and an asynchronous regime (c). Bottom: first 3 PCA-components of the corresponding regimes. Explained variance ratio for each component are given in brackets.

The advantage of our approach is that it allows for not only the identification of a chimera but also the determination of the "degree of chimera", that is, how large a synchronization cluster is observed in the system for given parameters and initial conditions. This property allows more flexible control of the dynamic regimes in the system, as well as a deeper understanding of how different modulators affect the network.

References

- [1] Abrams D.M., Strogatz S.H. (2004) Chimera states for coupled oscillators. *Physical review letters*, **93**,17:174102.
- [2] Dogonasheva O.A., Gutkin B., Zakharov D.G. (2021) Calculation of travelling chimera speeds for dynamical systems with ring topologies. *DCNA*:61-64.
- [3] Dogonasheva O.A., Kasatkin D., Gutkin B., Zakharov D.G. (2021) Robust universal approach to identify travelling chimeras and synchronized clusters in spiking networks *Chaos, Solitons & Fractals* **153**:111541.

Bifurcations and Chimera States in Self-Excited Inertia Wheel Pendulum Arrays

Gilad Yakir*, Yuval Levi* and Oded Gottlieb*

**Department of Mechanical Engineering, Technion-Israel institute of Technology, Haifa, Israel*

Abstract. We investigate the bifurcation structure and the onset of chimera states in a coupled pair of self-excited inertia wheel pendula arrays. The dynamical system exhibits asymptotically stable equilibria, periodic limit cycle oscillations, and non-stationary rotations. The analysis reveals that synchronous periodic oscillators are in-phase whereas quasiperiodic oscillators are out-of-phase. Furthermore, non-stationary rotations exhibit combinations of oscillations and rotations of the individual elements which are asynchronous culminating with coexisting synchronous and chimera-like solutions.

Introduction and Problem Formulation

Self-excited synchronous oscillations in multibody dynamical systems have been documented since the middle of the seventeenth century. Huygens made the amazing observation that two pendulum clocks hanging from a common flexible support swung together periodically approaching and receding in opposite motions [1]. During the last two decades there has been a growing interest in the stability and robustness of continuous and intermittent synchronization of periodic and nonstationary oscillations which in addition to neural network populations have been observed in nanomechanical resonator arrays [2] and in experiments of mechanical networks [3]. Of particular interest are the chimera states in which the symmetry of an oscillator population is broken into a synchronous part and an asynchronous part culminating with a novel class of decoherent behaviour [4]. In this research we investigate the emergence of bifurcations and chimera states in a pair of elastically coupled self-excited inertia wheel double pendulum arrays depicted in Figure 1 (left). We derive the equations of motion and examine the complexity of coexisting synchronous and asynchronous self-excited oscillations in the coupled arrays each with three planar pendula augmented with rotating inertia wheels governed by a linear feedback mechanism.

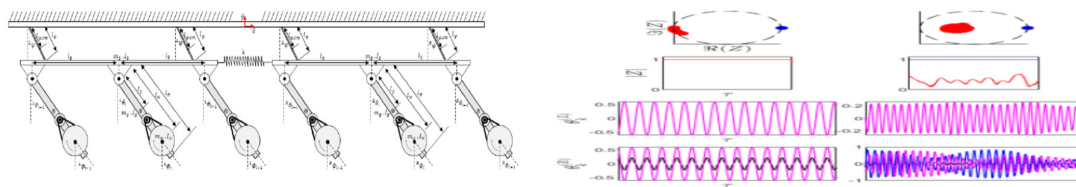


Figure 1: Definition sketch of the coupled pair of inertia wheel pendulum arrays (left) and example in-phase synchronized response and nonstationary decoherent chimera oscillation dynamics (right).

Results and Discussion

We combine an analytical and numerical investigation to determine the bifurcation structure of the self-excited elastically coupled arrays which exhibit periodic limit cycle oscillations and non-stationary rotations. We investigate the synchronous dynamics and the emergence of chimera states within the system and make use of the Kuramoto order parameter [4] which enables identification of synchronized in-phase or anti-phase solutions where the order parameter for both arrays is unity in comparison to chimera state where the order parameter for one of the coupled arrays varies in an irregular manner between zero (describing a decoherent state) and unity (a synchronous state) as shown in Figure 1 (right). The combined analytical and numerical methodologies employed enable construction of a comprehensive bifurcation structure that sheds light on emergence of chimera states, synchronization and decoherence in the elastically coupled arrays in both oscillation and rotation regimes.

References

- [1] Ramirez J.P., Olvera L.A., Nijmeijer H., Alvarez J. (2016). The sympathy of two pendulum clocks: beyond Huygens' observations. *Scientific Reports* **6**: 23580.
- [2] Kambali, P., Torres, F., Barniol, N., Gottlieb, O. (2019). Nonlinear multi-element interactions in an elastically coupled microcantilever array subject to electrodynamic excitation. *Nonlinear Dynamics* **98**: 3067-3094.
- [3] Kapitniak T., Kuzma P., Wojewoda J., Czołczynski K., Maistrenko Y. (2014). Imperfect chimera states for coupled pendula. *Scientific Reports* **4**:1-4.
- [4] Martens E., Thutupallil S., Fourrière A., Hallatschek O. (2013). Chimera states in mechanical oscillator networks. *Proc. National Academy of Sciences*, **110**:10563-10567.

On the self-excited chatter vibration in motorcycles

Alexander Schramm*, Silvio Sorrentino* and Alessandro De Felice*

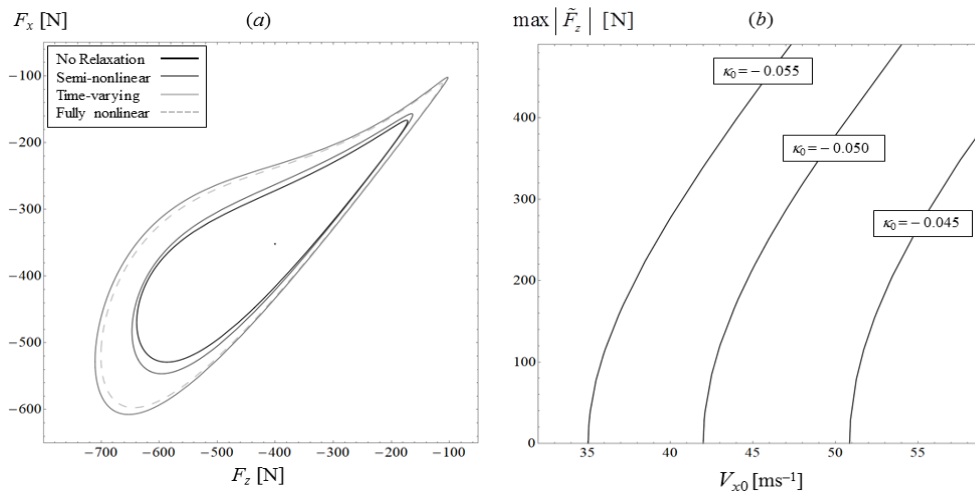
*Department of Engineering Enzo Ferrari, University of Modena and Reggio Emilia, Modena, Italy

Abstract. This study is focused on the understanding of the nonlinear effects of tyre forces and chain geometry on motorcycle chatter, a self-excited oscillation arising at the rear wheel during heavy braking manoeuvres. In particular the post-bifurcation criticality is assessed, whether subcritical or supercritical, with respect to travelling speed.

Introduction

An instability exists in the rear suspension of motorcycles typically called ‘chatter’ that is experienced during heaving braking in the frequency range from 17 to 22 Hz. The causes and mechanisms of this self-excited oscillation have been studied with many focusing on the interaction between rear wheel speed and rear suspension travel, involving the ‘driveline’ mode [2,3]. Previous work has thoroughly investigated the phenomenon using linear methods showing that it is caused by out-of-phase interactions in the normal load and longitudinal tyre forces, with analogy to flutter in aeroelasticity [2]. The gradient of the characteristic function of the tyre force [3] was shown to play a fundamental role in the onset of chatter, and the geometry of the chain transmission in its amplification. It has recently been demonstrated that the roll angle enhances instability in an indirect way, affecting the characteristic function of the tyre force. Stability analyses in the above-mentioned studies were performed on linearized models, either minimal models [2] or large multi-body models [3].

This study looks to assess the post-bifurcation criticality, whether subcritical or supercritical, with respect to travelling speed. This also includes the contribution of tyre relaxation [3], since this aspect has not been investigated in-depth in previous studies. A two-dof minimal model is considered, including the nonlinear terms due to geometry, tyre characteristic function and tyre relaxation. To study the post-bifurcation behaviour and the existence of limit cycles, the harmonic balance method is adopted in combination with Floquet theory, aimed at identifying the most meaningful parameters in limit cycle generation, their amplitude and stability.



Results and Discussion

The nonlinear system without tyre relaxation is found to have a supercritical behaviour within the parameter domain of technological interest, with a single stable limit cycle (figure *a*: limit cycle in terms of longitudinal F_x and vertical F_z tyre forces, and effects of different tyre relaxation models; figure *b*: bifurcation diagram as a function of travelling speed, for different values of tyre slip coefficient κ_0 , showing supercritical behaviour). The growth of the limit cycle soon after the linear stability boundary in any case is strong enough to overcome the limits of what could be acceptable for motorcycle stability. A sensitivity analysis is performed to identify the influence of each of the model parameters on the limit cycle amplitude, with the aid of bifurcation diagrams, confirming that the main driver of nonlinear asymptotic behaviour comes from the tyre force characteristic function. Tyre relaxation produces destabilizing effects both in the linear and nonlinear models, however, adopting realistic values of relaxation length, those effects are found to play a minor role.

References

- [1] Sorrentino S., Leonelli, L. (2017) A. S. (1999) A study on the stability of a motorcycle wheel-swingarm suspension with chain transmission. *Vehicle System Dynamics* **55**(11):1707-1730.
- [2] Leonelli, L., Cattabriga, S., Sorrentino, S. (2018) Driveline instability of racing motorcycles in straight braking manoeuvre. *Journal of Mechanical Engineering Science C* **232**(17):3045-3061.
- [3] Pacejka, H. (2012), Tyre and Vehicle Dynamics. Elsevier Science.

Investigation of the control characteristics for a driver-vehicle system with steering and throttle control

Alois Steindl*, Johannes Edelmann* and Manfred Plöchl*

*Institute for Mechanics and Mechatronics, TU Wien, Getreidemarkt 9, 1060 Vienna, Austria

Abstract. We investigate the control characteristics of a human driver or driving robot of a simple two-wheel vehicle model along a steady-state cornering motion using the “simplified precision model” by McRuer. The aim of this talk is to obtain ranges of driver parameters, that could map human driving behaviour and lead to a stable motion for varied reaction time.

Vehicle and control model

We investigate the stability of a controlled understeer vehicle along a steady-state cornering motion, according to the model described in [1]. To control the trajectory of the vehicle, the human driver is assumed to either adjust the front steering angle δ_F or the driving torque M_R of the rear wheels, according to the deviation of a point P ahead of the vehicle from a reference circle, as displayed in Fig. 1. If we denote the deviation of the point P from the reference circle by Δr_P and the deviation of the control input $u \in \{\delta_F, M_R\}$ from the stationary value by Δu , the “simplified precision model” [2] takes the form

$$T_M \frac{d\Delta u(t)}{dt} + \Delta u(t) = c_P \Delta r_P(t - \tau) + c_D \frac{d\Delta r_P}{dt}(t - \tau), \quad (1)$$

with human reaction time τ , delay time T_M , and control gain parameters c_P and c_D .

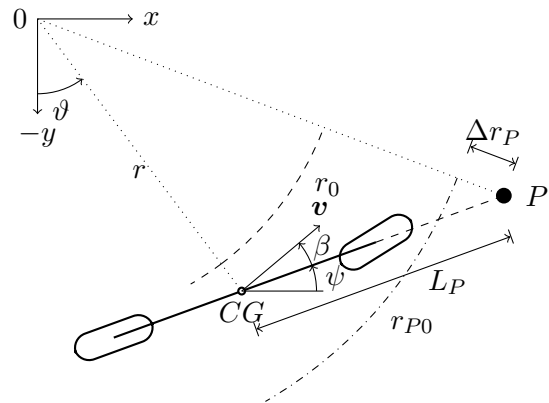


Figure 1: Geometric relations for the driver’s preview model: To follow a circle with radius r_0 , the driver spots a point P at a distance L_P straight ahead of the vehicle, which should move along a circle with radius r_{P0} .

According to [3] it is necessary, that the control loop satisfies cross-over conditions, which guarantee that the driver adapts his/her control inputs to individual vehicles characteristics. We could find boundaries of the (human) controller parameters for stable cornering depending on varied reaction time τ .

References

- [1] Steindl, A., Edelmann, J., Plöchl, M.: Limit cycles at oversteer vehicle. Nonlinear Dynamics (2019). <https://doi.org/10.1007/s11071-019-05081-8>
- [2] McRuer, D.T.; Graham, B.; Krendel, E.S.; Reisner, W.: Human Pilot Dynamics in Compensatory Systems, AFFDL-TR-65-15, 1965.
- [3] Mitschke, M.; Wallentowitz, H.: Dynamik der Kraftfahrzeuge. Springer 2004.

Modelling and Simulation of the Nonlinear Vibrations of Axially Moving Long Slender Continua in Tall Host Structures

Jakob Scheidl*, Yury Vetyukov* and Stefan Kaczmarczyk**

* TU Wien, Institute of Mechanics and Mechatronics, Getreidemarkt 9 / E325, 1060 Vienna, Austria

** University of Northampton, Faculty of Arts, Science and Technology, University Drive, Northampton NN1 5PH, UK

Abstract. Mixed Eulerian-Lagrangian rod finite elements are developed to simulate the transient dynamic behaviour of a suspension rope system of a high-rise elevator subjected to a harmonic sway of the host structure. The suspension cable is modelled as a Kirchhoff rod with full account for inertia, bending stiffness and the geometrically nonlinear coupling of transverse and axial vibrations. The time varying natural frequencies of the suspension system are compared against results available from the literature and primary system parameters are varied to conclude on their impact on the transient elevator operation. The model becomes particularly advantageous for large vibrations at or near the resonance.

Introduction

Lifting systems, such as cranes, mine or elevator hoists, feature axially moving ropes and cables, whose length vary during the operation. These axially moving slender continua with variable length exhibit a rich dynamic behaviour and are susceptible to parametric, self-excited or external excitations. Hence, proper design of such systems with regard to safety and comfort of operation or lifetime estimation requires an accurate mechanical model and a computationally feasible solution thereof.

Benchmark problem, computational model and its validation

We develop and validate a geometrically nonlinear finite element scheme for the transient simulation of a simple elevator model depicted in the figure on the right. It features an elevator cabin of mass M that is suspended by a single rope with time-variable length $L(t)$. The elevator is situated in a tall building structure that is assumed to sway harmonically in a cantilever bending mode $\Psi(\eta)$ due to wind loading, where $\eta = z/Z_0$ denotes the dimensionless vertical coordinate, counted from the ground level. The imposed building motion causes vibrations of the suspension system, whose response changes dynamically as the elevator car is moving in the hoistway.

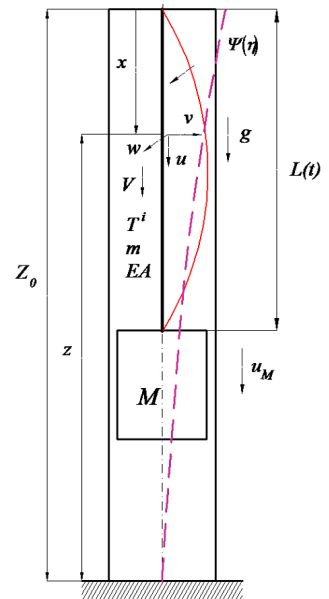
The proposed finite element model of a Kirchhoff rod for the suspension cable features a variant of the Mixed Eulerian-Lagrangian kinematic description established in [1, 2]. The variable length of the suspension rope is taken into account by means of a hybrid (stretched) coordinate $\sigma \in [0, 1]$, with a spatially fixed (Eulerian) node at the entry to the domain and a material (Lagrangian) node at the elevator car. The present scheme numbers among the group of Arbitrary-Lagrangian-Eulerian methods, whose utility for the simulation of reeving systems is well recognised [3].

Traditional methods rely on the semi-analytical treatment of the governing system of partial differential equations by means of the Galerkin procedure using the eigenmodes of the axially moving continua as shape functions. They rely on some simplifying assumptions regarding the amplitude of oscillations or the coupling of transverse and axial vibrations. Specifically, in [4] and [5] different variants of the problem at hand based on the same geometric setup are investigated.

For a range of practical parameters, first, finite element simulations are compared against results available in the literature regarding the system's basic oscillatory response (frequency & amplitude), and, secondly, the influence of selected key parameters on the transient response of the elevator system is established.

References

- [1] Yury Vetyukov (2018) Non-material finite element modelling of large vibrations of axially moving strings and beams. *Journal of Sound and Vibration* **414**:299–317.
- [2] Scheidl Jakob, Yury Vetyukov, Christian Schmidrathner, Klemens Schulmeister and Michael Proschek (2021) Mixed Eulerian–Lagrangian shell model for lateral run-off in a steel belt drive and its experimental validation. *International Journal of Mechanical Sciences* **204**:106572.
- [3] José L. Escalona (2017) An arbitrary Lagrangian–Eulerian discretization method for modeling and simulation of reeving systems in multibody dynamics. *Mechanism and Machine Theory* **112**: 1–21.
- [4] Stefan Kaczmarczyk and Radosław Iwankiewicz (2017) On the nonlinear deterministic and stochastic dynamics of a cable-mass system with time-varying length. *Safety, Reliability, Risk, Resilience and Sustainability of Structures and Infrastructure*, 12th Int. Conf. on Structural Safety and Reliability, Vienna.
- [5] Hanna Weber, Stefan Kaczmarczyk, and Radosław Iwankiewicz (2020) Non-linear stochastic dynamics of a cable-mass system with finite bending stiffness via an equivalent linearization technique. *Journal of Theoretical and Applied Mechanics* **58(2)**:483–497.



Hybrid Autoregressive Neural Networks to predict forced nonlinear Vibrations

Tobias Westmeier*, Daniel Kreuter*, Simon Bäuerle ** and Hartmut Hetzler **

*Corporate Research, Robert Bosch GmbH, Germany

**Institut of Mechanical Engineering, Engineering Dynamics, University of Kassel

Abstract. In this contribution, we propose a hybrid approach for the data-driven prediction of forced oscillations. The combination of a linear transfer function in frequency domain and an Autoregressive Neural Network (ARNN) is used to model the nonlinear transfer behaviour. For validation purposes, the oscillations of the DUFFING equation, experiencing generic functions as excitation and an automotive use-case based on measurement data, are investigated. Finally, we compare our approach to classic non-hybrid approaches and consider different ARNN architectures.

Introduction

The use of Neural Networks (NN) for the identification and prediction of nonlinear vibration behaviour is an exciting field of research, given the vast number of physical and engineering applications. In particular, for time series prediction, several pure Deep Learning (DL) based architectures have been proposed due to the rapid progress in NN research [1, 2]. Once trained, this NN approach enables low-resource, real-time predictions of system responses. While these architectures perform well for many applications, they often lack generalization capability for unseen input data and longer prediction lengths. Furthermore, they may become problematic when depicting the dynamic oscillating behaviour in forced nonlinear systems [3, 4, 5]. We, therefore, explore a hybrid modelling approach to approximate the nonlinear transfer behaviour between the external excitation and the system response. The main building blocks are the linear transfer function in frequency domain to include the linearized oscillating behaviour of our system into the architecture and an Autoregressive Neural Network (hybrid-ARNN) to account for nonlinear influences. In a two-step process, we firstly approximate the linear transfer function to the given data. Afterwards, the ARNN is trained with the nonlinear system response data using the linear solution and the external excitation as input in an autoregressive setting:

$$\hat{y}(t+1) = \mathbf{y}_{\text{lin}}(t+1) + f_{\phi}(\mathbf{x}^s(t+1), \mathbf{y}_{\text{lin}}^s(t+1), \mathbf{y}_{\text{nl}}^s(t)), \quad (1)$$

where $\hat{y}(t+1)$ describes the predicted system state at timestep $t+1$ while $\mathbf{y}_{\text{lin}}(t+1)$ the corresponding linear solution. The external excitation is defined as $\mathbf{x}^s(t)$ where s indicates a sequence (last s time steps). The previous linear and nonlinear system states are defined as $\mathbf{y}_{\text{lin}}^s(t+1)$ and $\mathbf{y}_{\text{nl}}^s(t)$. Lastly, $f(\cdot)$ defines the mapping by the NN with architecture-specific parameters ϕ . We compare Feedforward NN, which are easier to handle and can contain basic properties such as symmetry, to gated recurrent NN, which have internal memory to save information over time. All models are trained using adaptive gradient decent techniques in either closed-loop or open-loop environments.

Results and Discussion

We investigate oscillations of the DUFFING equation $\ddot{x} + 2D\dot{x} + x + \alpha x^3 = f(t)$ and an automotive use case based on measurement data. DUFFING system data is synthesised with generic external excitations $f(t)$ (white noise, sweep signals, sine functions) using a DORMAND-PRINCE integration method. The automotive use case extends this one-dimensional theoretical case towards a multidimensional excitation and response for real-world training and validation data from testing tracks. We investigate multiple regularization techniques and show a clear dependency in accuracy due to specific hyperparameters. Our examples emphasize that the proposed hybrid-ARNN achieves significantly higher prediction accuracy than classical linear methods and converges faster than pure ARNN during training. Feedforward NN train faster and achieve superior accuracy in time and frequency domain, while gated recurrent NN suffer from a recency bias in training. Furthermore, we show that a special penalty formulation applied to the weights significantly reduces the training parameters' sensitivity. We conclude that our novel workflow defines a suitable approach for the prediction of forced vibrations in academic examples as well as for a real-world case based on multidimensional measurement data.

References

- [1] H. Hewamalage et al. (2021), Recurrent Neural Networks for Time Series Forecasting: Current status and future directions, *International Journal of Forecasting*, **37**: 388-427.
- [2] P. Lara-Benitez et al. (2021), An Experimental Review on Deep Learning Architectures for Time Series Forecasting, *International journal of neural systems*, **31(03)**.
- [3] Y. Park et al. (2022). Recurrent Neural Networks for Dynamical Systems: Applications to Ordinary Differential Equations, Collective Motion, and Hydrological Modeling, *arXiv*
- [4] L. Dostal et al. (2020), Predictability of Vibration Loads From Experimental Data by Means of Reduced Vehicle Models and Machine Learning, *IEEE Access*, **8**, pp. 177180-177194.
- [5] E. Diaconescu (2008) The use of NARX neural networks to predict chaotic time series, *WSEAS Transactions on Computer Research*, **3**.

An Initial Bifurcation Analysis of an EV Pickup Truck

Shaun Smith*, Duc Nguyen**, James Knowles*, Mark Lowenberg** and Sean Biggs***

*Loughborough University, Loughborough, UK, ** University of Bristol, Bristol, UK,

*** Jaguar Land Rover, Whitley, UK

Abstract. Vehicles with a beam axle setup, such as trucks, can experience a problem known as “axle tramp”, where the rear axle and wheels undergo a potentially damaging self-sustaining vibration in the vertical, longitudinal and torsional directions. As the automotive industry continues the move towards electrification, it is unknown to what extent adding electric motor(s) to the powertrain changes the problem. The nonlinear nature of the problem make analysis difficult without an efficient method such as bifurcation analysis used in this research. The results characterize an axle tramp region in the electric-drive truck model which is compared to a car with internal combustion engine (ICE). The bifurcation analysis proves to be an efficient way to identify the instability leading to axle tramp, and the harmonically forced bifurcation analysis reveals a further region of tramp not previously observed.

Introduction

Vehicles with a beam axle setup can undergo a problem known as “axle tramp”, in which the rear axle and wheels undergo a potentially dangerous self-sustaining oscillation, with unwanted motion occurring in the vertical, longitudinal and torsional directions. Previous work on the tramp topic is focused on cars, mainly from the 1960s [1] with few studies relating the work to modern vehicles [2]. With the move towards electrification, it is unknown to what extent tramp will be an issue in larger electric vehicles such as trucks. This study aims develop a low order EV truck model and conduct an initial analysis to determine if tramp exists in the system. The authors propose bifurcation methods as a way to study the problem [3], [4] .

Results and Discussion

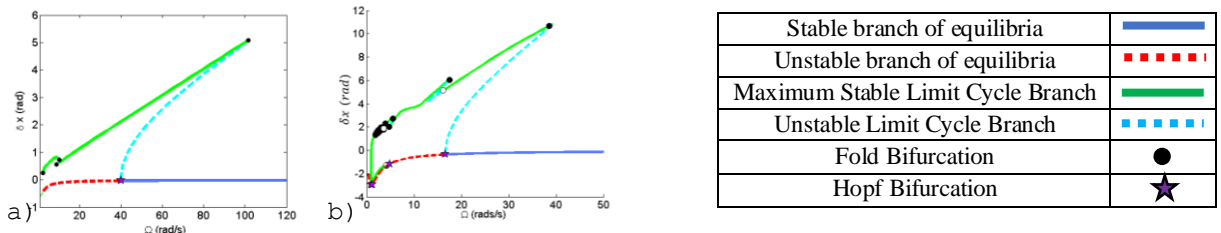


Figure 1. Bifurcation diagrams for: truck (a) and car (b). Angular displacement of the wheel, δx , as a function of engine speed, Ω .

Fig 1 presents an initial bifurcation analysis, showing the electric truck model undergoing tramp (a), with an ICE car for comparison (b). The truck undergoes a Hopf bifurcation at $\Omega=40$ rad/s, with any speed below this threshold causing the system to tramp. A fold bifurcation at $\Omega=102$ rad/s acts an upper limit on where tramp can be observed depending on initial conditions. The torsional vibration, δx , occurs up to a maximum of 5 radians. The torsional vibrations are smaller than the car but occur over a larger speed range.

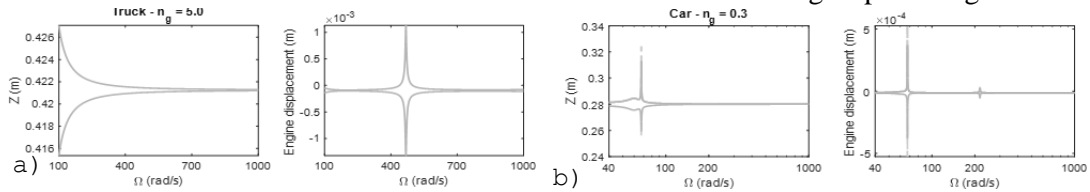


Figure 2. Comparison of the augmented truck (a) and car (b) models. Note that the x-axis starts from the known location of the fold bifurcation in the limit-cycle branch of the unaugmented model. Z is the vertical displacement of axle and wheel.

The models can be extended to include a simple harmonic forcing term. Fig 2b shows an unstable resonance at 67 rad/s in the car model, in addition to the previously observed result, which leads to tramp at a frequency higher than predicted by equilibrium bifurcation analysis as shown in fig 1b. However, the truck does not exhibit unstable oscillations at high frequencies, even at extreme values of forcing amplitudes (Fig. 2a).

References

- [1] R. Sharp, “Nature and Prevention of Axle Tramp,” *Proc. Inst. Mech. Eng. Automob. Div.*, vol. 184, no. 3, pp. 41–54, 1969, doi: 10.1243/pime_auto_1969_184_011_02.
- [2] A. Zargartalebi and K. H. Shirazi, “Dynamic modelling of axle tramp in a sport type car,” *Shock Vib.*, vol. 20, no. 4, pp. 711–723, 2013, doi: 10.3233/SAV-130779.
- [3] S. Smith, J. Knowles, B. Mason, and S. Biggs, “International Journal of Bifurcation and Chaos A bifurcation analysis and sensitivity study of brake creep groan,” *Int. J. Bifurc. & Chaos*.
- [4] D. H. Nguyen, M. H. Lowenberg, and S. A. Neild, “Frequency-domain bifurcation analysis of a nonlinear flight dynamics model,” *J. Guid. Control. Dyn.*, vol. 44, no. 1, pp. 138–150, 2021, doi: 10.2514/1.G005197.

Reversing Along a Curved Path by an Autonomous Truck–Semitrailer Combination

Levente Mihályi*, Dénes Takács*

**Department of Applied Mechanics, Faculty of Mechanical Engineering,
Budapest University of Technology and Economics, Műegyetem rkp. 3.,
H-1111 Budapest, Hungary*

Abstract. In this paper, the stability analysis of the reverse motion along a circular path is presented for the truck–semitrailer combination. The dynamics of the low-speed manoeuvre are investigated with the single track kinematic model, supplemented with the model of the steering system. The time delay emerging in the control loop is also considered. The actuation is achieved by the steering of the truck, for which a linear feedback controller is designed to ensure the stability of the motion, meanwhile, a geometry-based feedforward steering angle is also used to force the system to the desired path. Linear stability charts are calculated in order to properly tune the control gains of the feedback controller with respect to the curvature of the path.

Introduction

The development of self-driving cars is widely known, however, besides passenger cars, such autonomous features are also investigated for various truck-trailer vehicle systems [1, 2]. Advanced driver assistance systems (ADAS) are already available for trucks, which has relevantly reduced the risk of severe road accidents, although several types of trucks in freight transport travel continuously almost every day of the year. These vehicles spent most of their working hours on motorways or in loading bays. Maneuvering in the loading bay is one of the most difficult and time-consuming tasks of a truck driver. Therefore, installing a fully autonomous control system in this area could save time and money for the companies and reduce accidents during loading, too. The purpose of this paper is to introduce a control algorithm for stabilizing the reverse motion of the truck–semitrailer (the most commonly used vehicle system in freight transport) along a circle. The investigation of this manoeuvre could be the basis to realize general path-following control, as it is intended in our future work.

Method and results

The so-called kinematic model of the truck–semitrailer combination is shown in the left panel of Figure 1. The black dashed line represents the desired path followed by the trailer axle (point T). In this work, we assume that the curvature of the path is constant, i.e., a circular track is followed. First, the equations of motion are expressed with nonholonomic constraints, and a coordinate transformation is applied in order to describe path-following motion [3]. Feedforward and linear feedback controller are designed, where the time delay τ emerging of the control loop is considered. Stability charts are computed with semi-discretization method to determine the control gain domains, where the desired motion is stabilized. The effect of the curvature κ on stability is shown in the right panel of Figure 1, where the colored areas belong to stable control gain setups for three different values of curvature. As shown, our results can help the careful selection of the control gains for which stability for any curvatures is ensured.

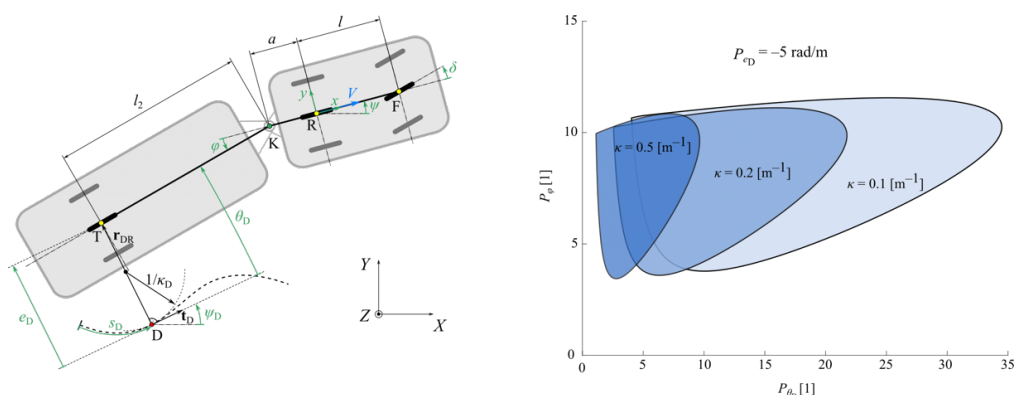


Figure 1: Mechanical model of the truck–semitrailer combination, and a stability chart representing the effect of the path curvature κ on stability ($V = -3$ m/s, $a = -0.8$ m, $l = 3.5$ m, $l_s = 10$ m, $\tau = 0.1$ s)

References

- [1] Werling, Moritz & Reinisch, Philipp & Heidingsfeld, Michael & Gresser, Klaus. (2014). Reversing the General One-Trailer System: Asymptotic Curvature Stabilization and Path Tracking. *Intelligent Transportation Systems*, IEEE Transactions on. 15.627-636. 10.1109/TITS.2013.2285602.
- [2] J. I. Roh & H. Lee & W. Chung. (2011). Control of a car with a trailer using the Driver Assistance System, 2011 IEEE International Conference on Robotics and Biomimetics, 2011, pp. 2890-2895, <https://doi.org/10.1109/ROBIO.2011.6181744>
- [3] Qin, Wubing & Zhang, Yiming & Takács, Dénes & Stépán, Gábor & Orosz, Gábor. (2021). Nonholonomic dynamics and control of road vehicles: moving toward automation. 10.48550/arXiv.2108.02230.

The effects of road curvature on the stability of path-following of automated vehicles

Illés Vörös^{*,**} and Dénes Takács^{*,**}

^{*}Department of Applied Mechanics, Faculty of Mechanical Engineering, Budapest University of Technology and Economics, Műgyetem rkp. 3., H-1111 Budapest, Hungary

^{**}ELKH-BME Dynamics of Machines Research Group, Budapest University of Technology and Economics, Műgyetem rkp. 3., H-1111 Budapest, Hungary

Abstract. The stability analysis of a path-following controller for automated vehicles is presented, with the consideration of path curvature and feedback delay. The analysis is based on a kinematic vehicle model expressed in a path reference frame. The steering controller includes feedforward and feedback terms, and the time delay in the control loop is also considered. The effects of parameters such as the vehicle speed and the path curvature are analyzed using compact analytical expressions and stability charts. The results help the designer select the optimal control gains and the limitations of tuning the controller with the assumption of a straight-line reference path are also shown.

Introduction

Designing stable and safe path following controllers with sufficiently high performance is a crucial step towards vehicle automation and it is also a cornerstone of many advanced driver assistance systems, such as lane-keeping and lane changing control. There are many different approaches to design the corresponding controllers, from simple geometrical considerations to machine learning-based methods [1].

In this study, the analysis of a steering controller for path following is presented, with the consideration of time delay in the control loop and the curvature of the reference path. The calculations are based on a kinematic single-track vehicle model, which allows us to present the results in the form of compact analytical expressions. The lateral constraint forces at the wheels are also calculated to ensure that loss of traction does not occur. Using a coordinate transformation, the vehicle model is transformed from the global coordinate system to a path reference frame (see Fig. 1(a)), so that the vehicle motion is described with respect to the reference path [2].

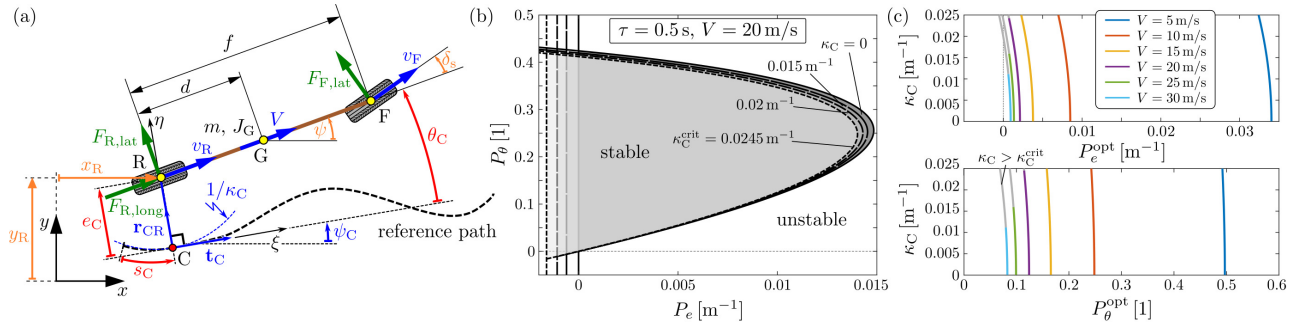


Figure 1: (a) Vehicle model in path reference frame. (b) Stable domains of control gains P_e and P_θ depending on the path curvature κ_C . (c) Optimal control gains in terms of fastest decay for different values of path curvature and vehicle speed.

Results and discussion

In order to achieve stable path following, the steering angle is generated using a combination of feedforward and feedback control. The feedforward term is used to determine the ideal steering angle corresponding to the path curvature based on the kinematics of the vehicle, while the feedback controller ensures the stability of tracking the reference path. The feedback action is based on the lateral deviation e_C and the angle error θ_C of the vehicle with respect to the reference path, and the feedback delay τ in the control loop is also considered. The stability analysis of the controlled vehicle is performed by linearizing the system along the equilibrium of stable path following with zero tracking error. Analytical expressions are then derived for the stability boundaries of the linearized system. This allows us to gain a deeper understanding of how certain parameters affect stability and how the control gains should be adjusted depending on the vehicle speed and the curvature of the reference path (see Fig. 1(b)). The optimal control gains that lead to the fastest decay of the linearized system are also determined and analyzed (Fig. 1(c)). In particular, we show the limitations of tuning the controller with the assumption of a straight-line reference path and the safe ranges of vehicle speed and path curvature for a given controller are also determined.

References

- [1] Paden, B., Čáp, M., Yong, S. Z., Yershov, D., Frazzoli, E. (2016) A survey of motion planning and control techniques for self-driving urban vehicles. *IEEE Transactions on Intelligent Vehicles*, **1**(1):33-55.
- [2] Qin, W. B., Zhang, Y., Takács, D., Stépán, G., Orosz, G. (2022) Nonholonomic dynamics and control of road vehicles: moving toward automation. *Nonlinear Dynamics*, 1-46.

Stability control of two-wheeled trailers

Hanna Zs. Horvath*, Adam Balint Feher* and Denes Takacs**

*Department of Applied Mechanics, Faculty of Mechanical Engineering, Budapest University of Technology and Economics, Budapest, Hungary, ORCID 0000-0002-9427-3565

**ELKH-BME Dynamics of Machines Research Group, Budapest University of Technology and Economics, Budapest, Hungary, ORCID 0000-0003-1226-8613

Abstract. The nonlinear dynamics of towed two-wheeled trailers is investigated. A spatial 4-DoF mechanical model is used, where all the yaw, pitch and roll motions are considered. Geometrical nonlinearities and the non-smooth characteristics of the tire forces are taken into account. A possible control algorithm is analyzed, which actuates by means of braking to one of the wheels of the trailer. Numerical bifurcation analysis is performed in order to investigate the large amplitude vibrations and unsafe (bistable) zones, where the stable rectilinear motion and the stable limit cycle coexist. It is shown, that with appropriately chosen control gains, the size of the bistable region can be decreased.

Introduction

Vehicle handling and stability are critical factors when investigating the so-called snaking motion of trailers. Most of the previous studies are limited to linear stability analysis and/or are based on in-plane models. Here, we investigate the nonlinear dynamics of two-wheeled trailers with a spatial mechanical model. The applied 4-DoF mechanical model is shown in Fig. 1(a), for which the governing equations are summarized in [1].

In order to reduce the unwanted vibrations of the system, stability control is applied, namely, braking forces are driven to the wheels. In [2], the effect of the braking forces is emulated via a control moment. Here, a more reliable model is analyzed, where stability is achieved via braking forces that are proportional to the yaw rate $\dot{\psi}$, see panel (a) of Fig. 1. A deadzone of the controller is also considered, where no braking force is actuated. The non-smooth characteristics of the right and the left braking forces can be formulated as

$$F_R^{\text{brake}} = \begin{cases} D(\dot{\psi} - \dot{\psi}_0), & \text{if } \dot{\psi} > \dot{\psi}_0 \\ 0, & \text{if } \dot{\psi} < \dot{\psi}_0 \end{cases} \quad F_L^{\text{brake}} = \begin{cases} -D(\dot{\psi} + \dot{\psi}_0), & \text{if } \dot{\psi} < \dot{\psi}_0 \\ 0, & \text{if } \dot{\psi} > \dot{\psi}_0 \end{cases}, \quad (1)$$

where D is the control gain for the yaw rate and $\dot{\psi}_0$ is the deadzone of the controller.

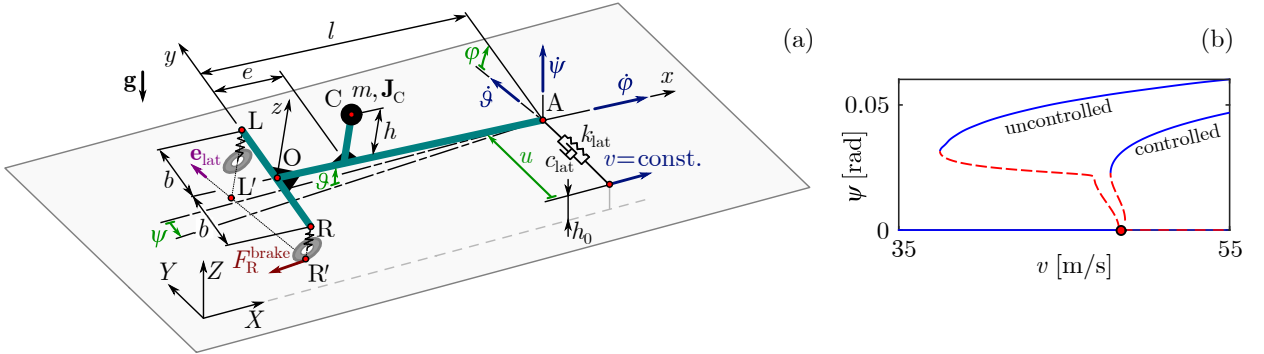


Figure 1: The spatial, 4-DoF mechanical model of towed two-wheeled trailers with the braking force for the right wheel (a), bifurcation diagrams of the uncontrolled and the controlled system for the yaw angle ψ with respect to the towing speed v (b).

Results and discussion

Nonlinear bifurcation analysis of the system is performed with the help of *DDE Biftool* [3], where the non-smooth characteristics of the tire forces and the braking forces are handled by a smoothed version of the Heaviside-function. The bifurcation diagrams of the uncontrolled and the controlled system are depicted in Fig. 1(b) for parameter values described in [1] and for the vertical payload position $h = 0.27$ m. Since the controller has a deadzone, the critical speed of the linear stability boundary (where Hopf bifurcation takes place) does not change due to the stability control. However, the unsafe zone (i.e. the bistable region) is reduced compared to the uncontrolled case.

As a future work, the feedback delay of the controller could be taken into account to tune the control gain with respect to the optimal performance of the controller.

References

- [1] H. Zs. Horvath, D. Takacs (2022) Stability and local bifurcation analyses of two-wheeled trailers considering the nonlinear coupling between lateral and vertical motions. *Nonlinear Dynamics* **107**:2115–2132. DOI 10.1007/s11071-021-07120-9
- [2] H. Zs. Horvath, D. Takacs (2020) The Effect of Time Delay on the Stability Control of Trailers. *Proceedings of the ASME 2020 Dynamic Systems and Control Conference*. DOI 10.1115/DSCC2020-3254
- [3] K. Engelborghs, T. Luzyanina, G. Samaey (2001) DDE-BIFTOOL v. 2.00: a Matlab package for bifurcation analysis of delay differential equations, Department of Computer Science, K.U.Leuven

Analysis of nonlinear tire dynamics in high fidelity nonlinear Finite Element simulation

Lukas Bürger^{*,**} and Frank Naets^{*,**}

^{*} Department of Mechanical Engineering, KU Leuven, Leuven, Belgium
^{**} DMMS Lab, Flanders Make, Belgium

Abstract. The dynamic behavior of tires is of great interest in the tire design process. Due to difficulties in acquiring experimental data (e.g. contact patch measurements) and the time consuming procedure of building prototypes, numerical models are needed. The nonlinear Finite Element Method is employed to accurately model the complex nonlinear structural behavior of tires. While the Arbitrary Lagrangian Eulerian formulation is predominantly used in literature, an alternative newly developed tire model based on the Total Lagrangian formulation is presented. It is shown that both formulations show similar results and that the influence of the excitation caused by the mesh in the Total Lagrangian formulation is limited. Furthermore, the influence of multiple modeling parameters on the dynamic response of the tire is investigated.

Introduction

Tires are a major noise emission source, especially for electric vehicle, and can lead to significant interior and exterior noise. The noise emission originates from the dynamic vibrations of the tire, where the main excitation source of the tire is the tire/road interaction [1]. To properly assess the structural behavior of tires to optimize the design for noise emission, fuel consumption or handling, accurate models are required in the process. The need for numerical models is caused by the inaccessibility of certain measurement quantities such as displacement in the contact patch and the time consuming procedure of prototyping and testing. Due to the present geometric, material and rolling contact nonlinearity accurate, predictive Finite Element (FE) tire modelling poses a challenge. In literature predominantly the Arbitrary Lagrangian Eulerian (ALE) formulation is used [2,3], but the ALE formulation is only applicable to axisymmetric tires. By using a TL formulation for the tire model an arbitrary tire and tread geometry can be assessed. In theory the TL description [4] is more comprehensive, but a direct comparison for tires is missing in literature.

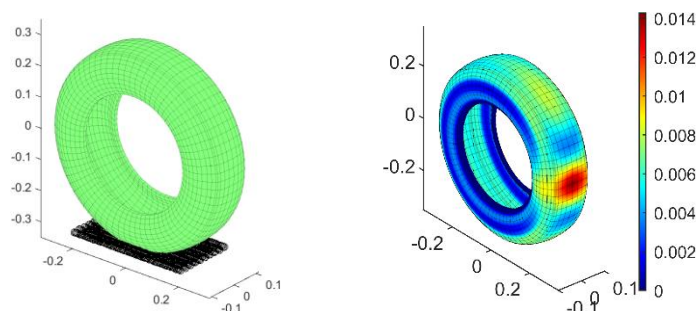


Figure 1: Total Lagrangian tire model mesh and dynamic deformation

Results and Discussion

The main disadvantages of the ALE formulation are limitations in tire geometry (e.g. detailed tread patterns) and difficult treatment of viscoelastic material behavior. While these drawbacks are resolved by the use of the TL formulation, the main challenge is to limit the contamination of the dynamic excitation caused by the spatial discretization of the TL FE model (see Figure 1). This excitation is generated by the actual rotation of the mesh in the TL formulation as opposed to the stationary mesh in the ALE formulation, where the rotation is described in an Eulerian way.

In this work, the tire model is created by the use of 3D volumetric elements in an inhouse FE code including geometric and material nonlinearity. A time domain simulation of the tire model interacting with a rigid road profile is carried out for both formulations. The dynamic behavior of the tire in both cases is compared. It is shown that the TL formulation yields equivalent results as the ALE formulation and the excitation caused by the mesh is limited. Furthermore, the parameter influence of the modelling parameters (e.g. road roughness, material parameters or speed dependence) on the vibrational behavior is analyzed.

References

- [1] U. Sandberg and J. Ejsmont, Tyre/road noise. Reference book, 2002.
- [2] U. Nackenhorst, The ALE-formulation of bodies in rolling contact: Theoretical foundations and finite element approach." Computer methods in applied mechanics and engineering 193.39-41, 2004
- [3] De Gregoriis, Daniel, et al. "Development and validation of a fully predictive high-fidelity simulation approach for predicting coarse road dynamic tire/road rolling contact forces." Journal of Sound and Vibration 452 (2019): 147-168.
- [4] Wriggers, Peter. Nonlinear finite element methods. Springer Science & Business Media, 2008.

Dynamic response of a geometrically nonlinear quarter car model with a MacPherson suspension travelling on a harmonic road profile

Pankaj Wahi and Vaibhav Dhar Dwivedi

**Department of Mechanical Engineering, Indian Institute of Technology Kanpur, Kanpur, India*

Abstract. We perform a detailed study of the geometrically nonlinear quarter car model with a MacPherson suspension system. This study fills the gap in the literature on the influence of the geometric nonlinearity of the MacPherson suspension system on the dynamic response of the car. A kineto-dynamic quarter car model accounting for the kinematics of the MacPherson suspension under dynamic conditions is considered. We have found interesting features like transition from softening to hardening nonlinearity with increase in the suspension stiffness for a given harmonic base amplitude.

Introduction

MacPherson strut shown in Fig.1(a), is a popular passive suspension for passenger cars due to its low cost combined with acceptable performance, easy assembly, and compactness. Most studies [1, 2] on suspension performance consider a simplified reduced-order model of quarter car wherein the strut deformation is aligned with the vibrational direction of the sprung mass resulting in a linear system. Even though this model gives reasonable estimates for the performance; it does not consider the geometric nonlinearity arising due to interconnection between the various members of the suspension assembly. In this paper, we have focused explicitly on the various phenomenon associated with this geometric nonlinearity which has been ignored in most previous studies.

A kineto-dynamic quarter car model accounting for the kinematics of the MacPherson suspension to dynamic responses is considered. Based on existing literature, we have included the wheel hop frequency by considering a linear tyre stiffness along with linear stiffness and damping of the shock absorber in the formulation of a comprehensive quarter car model of MacPherson suspension as shown in Fig.1(b). We derive a two degrees of freedom mathematical model, with respect to ground reference coordinate, using the Lagrangian approach. This model is validated against a similar model assembled in the multibody dynamics simulation software MSC Adams. We review the dynamic features of this linkage suspension in time as well as frequency domain.

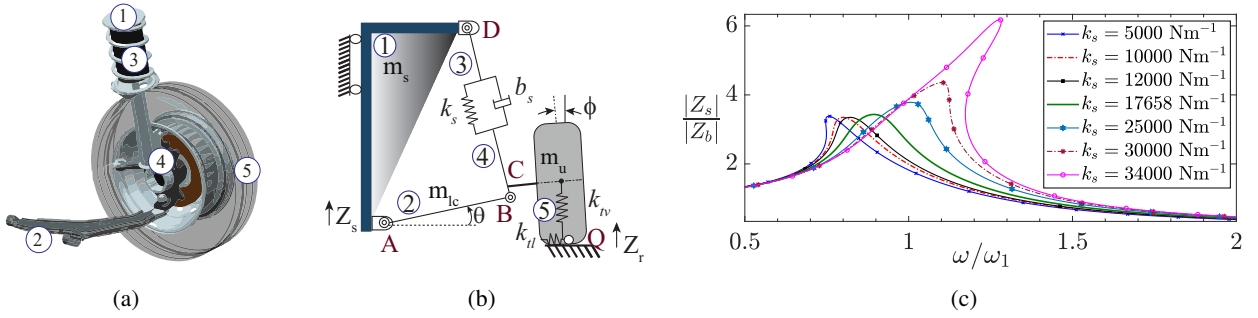


Figure 1: MacPherson suspension assembly (a), Quarter car model of MacPherson suspension assembly (b), and Normalized amplitude response for different suspension stiffness in our quarter car model under harmonic base amplitude of $Z_b = 0.06 \text{ m}$ (c).

Results and discussion

A detailed discussion on the influence of the geometric nonlinearity on the dynamic response is covered in this work which will be presented at the conference. As a sample, we show that the response to harmonic base excitation changes from softening to hardening with an increase in the suspension stiffness, as shown in Fig.1(c). We have ascertained that the geometric nonlinearity associated with the strut deformation is hardening in nature, while that associated with the vertical tyre deformation is largely softening. The geometric nonlinearity due to the lateral tyre deformation is softening for small amplitude response which transitions to hardening even for moderate responses. A combined effect of all of these behavior involves a softening to hardening transition in the response, with the transition amplitude depending on the relative stiffness of the various components.

References

- [1] Fallah, M.S., Bhat, R., and Xie, W.F. (2009) New Model and Simulation of Macpherson Suspension System for Ride Control Applications, *Veh. Syst. Dyn.*, **47**(2): 195-220 .
- [2] Abebe, B.A., Santhosh, J., Ahmed, A.A., Murugan, P., and Ashok, N. (2020) Non-linear Mathematical Modelling for Quarter Car Suspension Model, *Veh. Syst. Dyn.*, **11**: 596-544.

Numerical simulations of energy harvesting in a portal frame coupled with a nonlinear energy sink

A M. Tusset*, Alisson L. Agusti*, Maria E. K. Fuziki** and Giane G. Lenzi**

*Federal University of Technology - Parana, Ponta Grossa, PR, Brazil

**State University of Maringa, Maringa, PR, Brazil

Abstract. The present work presents the investigation of energy harvesting in a portal frame coupled with a non-linear electromagnetic energy sink, excited by an unbalanced DC motor. The energy scavenging is performed by two sources: a piezoelectric material and the energy generated by the electromagnetic energy sink. The coupling of the structure with the piezoelectric material and the electromagnetic energy sink resulted in a non-linear electromechanical coupling model. For dynamics, the analysis of the system considers bifurcation diagrams, phase portraits, power spectral densities, and 0-1 test. Numerical simulations show the existence of chaotic behavior for some regions of the parameter space. Additionally, to control the vibration amplitudes of the structure and improve energy production, an adjustment of the parameters of the non-linear electromagnetic energy sink is proposed.

Introduction

The main advantage of nonlinear energy harvesters is the conversion of energy over a wider range of frequencies of vibrations [1-2]. The Fig. 1a illustrates the portal frame coupled with a non-linear electromagnetic energy sink, excited by an unbalanced DC motor, and Fig. 1b illustrates the displacements for Portal frame and NES for Eq. (1).

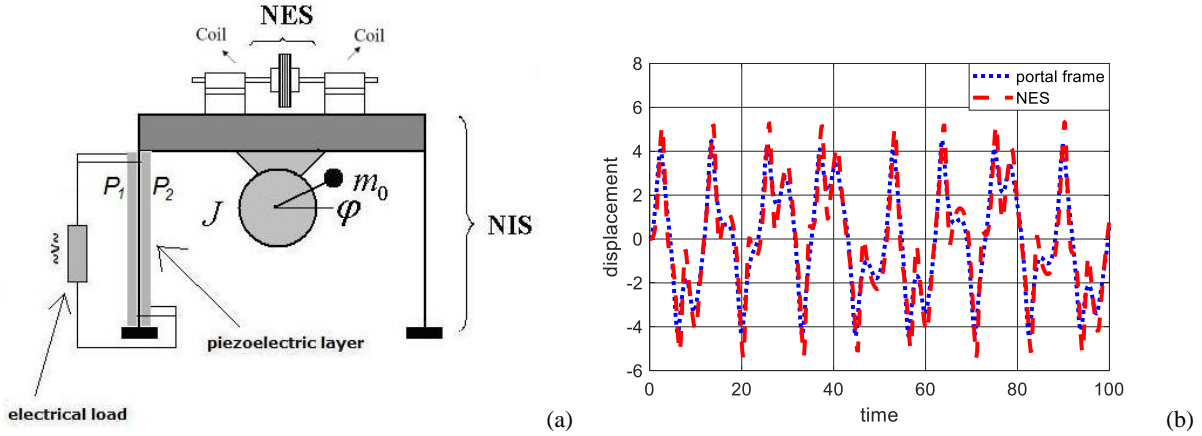


Figure 1: (a) Portal frame energy harvester scheme with nonlinear-energy sink. (b) Portal frame and NES displacements in non-dimensional form.

In Eq. (1) is presented the mathematical model for Fig. 1a in dimensionless form [1-2].

$$\begin{aligned}
 x'' - \beta_1 x + \alpha x' + \alpha_2 (x' - z') + \beta_3 x^3 + \alpha_3 (x - z)^3 - \theta(1 + \Theta/x)v &= \delta_1 \varphi'' \sin \varphi + \delta_1 \varphi'^2 \cos \varphi \\
 z'' - \varepsilon_1 (x' - z') - \varepsilon_2 (x - z)^3 &= 0 \\
 \varphi'' &= \rho_1 \cos \varphi x'' - \rho_3 \varphi' + \rho_2 \\
 \rho v' - \theta(1 + \Theta/x)x + v &= 0 \\
 F_e &= \psi(x' - z')
 \end{aligned} \tag{1}$$

Results and discussion

Numerical simulation results demonstrate a chaotic behavior (test 0-1, $k=0.9$), for parameters: $\alpha_1 = 0.1$, $\beta_1 = 1$, $\beta_3 = 0.2$, $\delta_1 = 8.373$, $\rho_1 = 0.05$, $\rho_2 = 100$, $\rho_3 = 200$, $\alpha_2 = 0.1$, $\alpha_3 = 0.5$, $\varepsilon_1 = 1$, $\varepsilon_2 = 5$, $\theta = 0.20$, $\Theta = 0.60$, $\rho = 1.00$ and $\psi = 1.00$. The numerical results showed a powered generation of the 1.0022 units for using PZT, and 0.1243 units, for using of the non-linear electromagnetic energy sink.

References

- [1] Iliuk, I., Balthazar, J. M., Tusset, A. M., Piqueira, J. R. C., Pontes Jr, B. R., Felix, J. L. P., Bueno, A. M. (2014) Application of passive control to energy harvester efficiency using a non-ideal portal frame structural support system. *J. Intell. Mater. Syst. Struct.*: 417-429.
- [2] Tusset, A. M., Piccirillo, V., Iliuk, I., Lenzi, G. G., Fuziki, M. E. K., Balthazar, J. M., Litak, G., Bernardini, D. (2022) Piezoelectric Energy Harvesting from a Non-ideal Portal Frame System Including Shape Memory Alloy Effect. In *Mechanisms and Machine Science*. Springer: 369-380.

An electromagnetic vibro-impact nonlinear energy sink for effective energy harvesting and vibration reduction of vortex induced vibrations

Haiqin Li*, Mengxin He*, and Qian Ding*

*Department of Mechanics, Tianjin University, Tianjin 300350, China

Abstract. An electromagnetic vibro-impact nonlinear energy sink (EM-VINES) is proposed as a new type of vibration absorber and energy harvester in the application of vortex induced vibration (VIV). The considered system consists of a cylinder-like bluff body subject to an oncoming flow, coupled to a magnet attachment moving in coil of gap enclosure. It is found that EM-VINES can achieve fast targeted energy transfer over the whole lock-in region, thus providing a much more efficient way to absorb and harvest the VIVs than the classical linear and nonlinear ones.

Introduction

Vortex-induced vibration (VIV) is a special fluid-structure coupling phenomenon, that can be widely observed in various engineering fields when a flexible bluff body is subjected to an oncoming flow. Under a certain range of flow velocities, the structure exhibits near-resonant motions, termed as lock-in regime [1]. Suppression of VIVs by active and passive methods represents a significant topic in this field. Among passive methods, the use of a Nonlinear Energy Sink (NES) has gained much attention in recent years [1-3]. Thanks to the irreversible targeted energy transfer (TET) mechanism, an NES can resonate with different modes of vibration of the primary system to localize energy efficiently. On the other hand, prospects of VIV-based energy harvesting techniques could be found in [4,5].

Model description and analysis

In this contribution, we introduce an electromagnetic vibro-impact nonlinear energy sink in the vortex-induced vibrations, for both purposes of vibration suppression and energy harvesting. Such an EM-VINES was first proposed by the present author in [6] by employing a magnet moving inside the clearance of a coil-fixed primary structure. Preliminary numerical and analytical demonstrations of an EM-VINES coupled to a linear oscillator for effective vibration suppression and energy harvesting have been performed in [6,7]. The aim now is thus to introduce EM-VINES to the practical application of VIVs, see in Fig.1(a). The system consists of a cylinder host structure that undergoes an air flow with velocity U in the y direction, be able to activate VIVs in the x direction. A permanent magnet is attached in the coil-fixed clearance 2Δ . Fig.1(b) gives an example of the non-dimensional response amplitude of the cylinder with or without EM-VINES, a good reduction within the lock-in region could be observed. In Fig.1(c), the normalized electric power is reported, confirming the effectiveness of EM-VINES for energy harvesting.

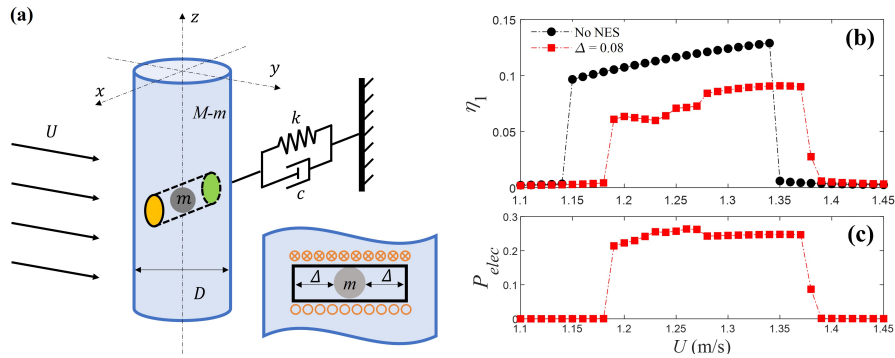


Figure 1: (a) Schematic of the cylinder structure coupled to an EM-VINES, (b) non-dimensional vibration amplitude η_1 of the host cylinder without (black) or with (with) an EM-VINES, (c) electric power P_{elec} harvested by the EM-VINES.

References

- [1] A. Blanchard, L.A. Bergman, A.F. Vakakis, et al. (2019). Vortex-induced vibration of a linearly sprung cylinder with an internal rotational nonlinear energy sink in turbulent flow. *Nonlinear Dynamics*. **99**(1): 593-609.
- [2] H.Ding, L. Chen (2020). Designs, analysis, and applications of nonlinear energy sinks. *Nonlinear Dynamics*. **100**(4): 3061-3107.
- [3] A.T. Chirathalattu, B. Santhosh, C.Bose, et al. (2023). Passive suppression of vortex-induced vibrations using a nonlinear energy sink—Numerical and analytical perspective. *Mechanical Systems and Signal Processing*. **182**: 109556
- [4] R.Naseer, H.Dai, A. Abdelkefi, et al. (2017). Piezomagnetoelastic energy harvesting from vortex-induced vibrations using monostable characteristics. *Applied Energy*. **203**: 142-153.
- [5] Z. Lai, S. Wang, L. Zhu, et al. (2021). A hybrid piezo-dielectric wind energy harvester for high-performance vortex-induced vibration energy harvesting. *Mechanical Systems and Signal Processing*. **150**:107212
- [6] H. Li, A. Li (2021). Potential of a vibro-impact nonlinear energy sink for energy harvesting. *Mechanical Systems and Signal Processing*. **159**: 107827.
- [7] H.Li, A.Li, X.Kong, et al. (2022). Dynamics of an electromagnetic vibro-impact nonlinear energy sink, applications in energy harvesting and vibration absorption. *Nonlinear Dynamics*. **108**(2): 1027-1043.

Leveraging 2:1 Parametric Resonance in a Notional Wave Energy Harvester

Giuseppe Giorgi*

*Marine Offshore Renewable Energy Lab (MOREnergy Lab), Department of Mechanical and Aerospace Engineering (DIMEAS), Politecnico di Torino, Turin, Italy, ORCID 0000-0002-1649-9438

Abstract. In ocean engineering applications, parametric resonance is normally detrimental for both the stability of large structures and energy extraction efficiency, so the vast majority of effort in the literature is towards preventing and reducing it. Conversely, this paper purposely introduces a 2:1 parametric resonance into a pitching wave energy harvester to inherently increase the energy absorption capabilities. Such a change in perspective is enabled by the use of a computationally efficient nonlinear hydrodynamic model, that is able to articulate such a parametric instability in a design-oriented simulation framework. The introduced 2:1 instability is found to be promising, since a significant amplification is obtained in the 2:1 region, where the oscillation amplitude is similar or even higher than in the 1:1 region.

Introduction

Wave energy harvesters (WEHs) are devices that respond to the external wave excitation force, typically with an oscillation motion. WEHs are required to improve their performance to become economically competitive. Efforts to this objective include design optimization and real-time control strategies; however, the underlying linear models, normally used due to computational convenience, are unrepresentative when large motions occur. In addition, the use of linear models causes blindness to instability, which is then discovered only after the preliminary design; consequently, effort is just invested towards after-corrections or live-limitation [1]. However, having a representative and fast numerical model may enable to incorporate such instabilities already at the early stages of design. With this perspective, this paper proposes to embed parametric resonance into WEHs, making it an enabling rather than a detrimental factor: a 2:1 resonance condition is defined by design into a heaving-pitching device, assuming energy extraction in the rotation DoF. Parametric resonance is articulated via a computationally efficient nonlinear Froude-Krylov (NLFK) force model [2]. The claim, herein demonstrated, is that parametric resonance can expand the operational bandwidth of the WEH.

Results and discussion

Figure 1 clearly shows the region of 2:1 parametric resonance (around $T_w = \frac{1}{2}T_5$), where there is a sharp increase of the pitching motion; the amplitude also bends towards larger periods as the wave height increases: such a bending behaviour contributes to enlarge the operational bandwidth of the response. It is also possible to appreciate a nonlinear coupling with heave, which shows a clear decrease as the pitching angle increases; this is usually detrimental for WEH that exploit heaving for the extraction, while is beneficial for WEH working on the pitching DoF. Conversely, in the 1:1 parametric resonance region, the coupling causes a significant increase in the heave motion, which drains energy from the pitching DoF.

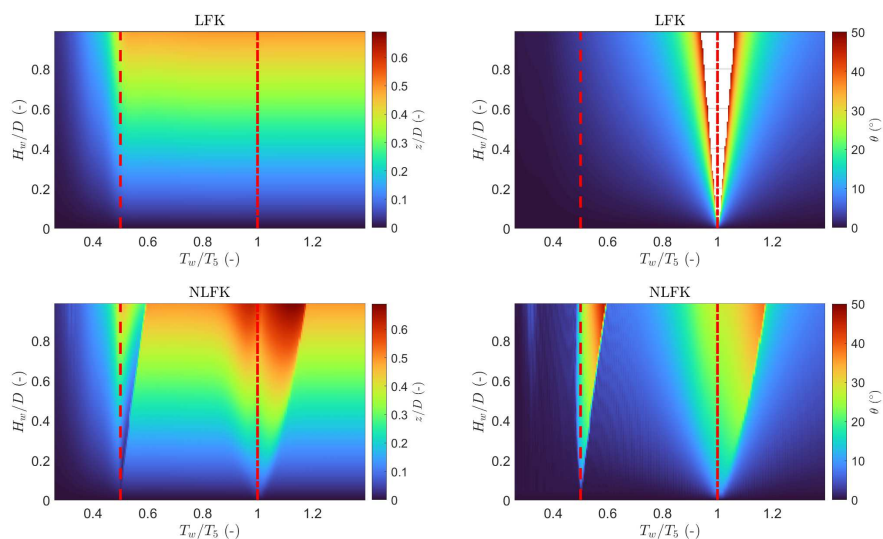


Figure 1: Amplitude of response for heave (left) and pitch (right), according to the linear (top) and nonlinear (bottom) models. The dash-dot and dashed red lines highlight one or half of the pitching natural, respectively. The white region indicates capsizing.

References

- [1] Davidson, J., Kalmár-Nagy, T. A Real-Time Detection System for the Onset of Parametric Resonance in Wave Energy Converters. *J. Marine Sci.* **8**(10), 819 (2020). DOI 10.3390/jmse8100819
- [2] Giorgi, G., Sirigu, S., Bonfanti, M., Bracco, G., Mattiazzo, G.: Fast nonlinear Froude–Krylov force calculation for prismatic floating platforms: a wave energy conversion application case. *J. of Ocean Eng. Marine Energy* **7**(4), 439–457 (2021). DOI 10.1007/S40722-021-00212-Z

A broadband magnet-induced cantilever piezoelectric energy harvester coupled to nonlinear energy sink

Jiwei Shen^{*}, Shui Wan^{*}, Jundong Fu^{*} and Kevin Dekemele^{**}

^{*}School of Transportation, Southeast University, China

^{**}Department of Electromechanical, Systems and Metal engineering, Ghent University, Belgium

Abstract. A broadband magnet-induced cantilever piezoelectric energy harvester (PEH) is designed, realized and coupled to a nonlinear energy sink (NES). The cantilever beam has a magnet attached to the tip and is coupled to the NES through magnetic force. The NES consists of a spring, a slider, and an oscillator mass with a magnet. The magnets generate nonlinear attractive or repulsive force between the cantilever and NES make the structure monostable or bistable. The structure are simulated and tested to observe the energy harvesting performance. Compared with simple piezoelectric cantilever beam, the NES enhanced version has a wider energy frequency band. The distance between magnets is adjusted to observe its effect on the harvested power.

Introduction

The NES has a variable natural vibration frequency, which can produce a series of resonance captures with the primary structure, effectively achieving a wider vibration absorption frequency band compared to linear absorbers. By combing the NES with a vibration energy harvester, it can effectively absorb the vibration energy from the primary structure and convert the vibration energy into electrical energy in a wider frequency band. In 2014, Ahmadabadi and Khadem [1] first proposed the concept of a vibration energy collection system consisting of NES and piezoelectric vibration energy collector, and optimized the system parameters globally, obtaining satisfactory energy harvesting effect. Fauve and Heslot [2] pointed out that stochastic resonance phenomenon can significantly enhance the vibration response of piezoelectric vibrator under low frequency and small amplitude mechanical vibration source, and increase the charge output. Therefore, here we will explore the use of NES to capture small amplitude low-frequency vibration, and then the NES vibrator excited the piezoelectric energy capture device (Figure 1), which generated high-frequency vibration and improved the capture efficiency of vibration energy.

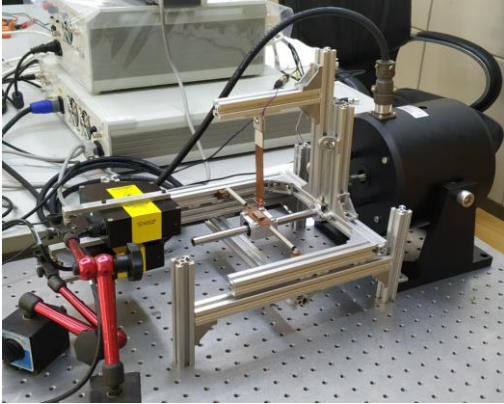


Figure 1: The Experimental Setup.

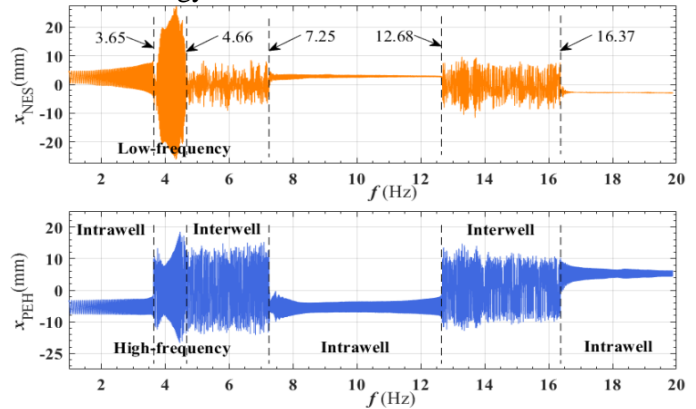


Figure 2: Oscillators Displacement versus Frequency ($a = 0.3g$, $d = 13$ mm)

Results and discussion

Figure 2 shows the displacement of the oscillators when the distance of the magnets d is 13 mm under 0.3g acceleration. Sinusoidal forward sweep is adopted for excitation. In the range of 1~3.65Hz, the displacement of NES oscillator and PEH oscillator stay in one stable state, that is, intrawell vibration. Within 3.65~4.66Hz, the NES oscillator has a large amplitude of low-frequency vibration, while the PEH oscillator is excited to generate high-frequency vibration, meanwhile, the power generated is also the highest. Within 4.66~7.25Hz, the vibration will continuously switching between monostable and bistable states, resulting in interwell vibration. It turns to intrawell vibration within 7.25~12.68 Hz. Due to the PEH resonance, it turns to interwell vibration in the range of 12.68~16.37Hz.

References

- [1] Nili Ahmadabadi Z, Khadem SE. (2014) Nonlinear vibration control and energy harvesting of a beam using a nonlinear energy sink and a piezoelectric device. *Journal of Sound and Vibration*, **333**(19): 4444-4457.
- [2] Fauve S, Heslot F. (1983) Stochastic resonance in a bistable system. *Physics Letters A*, **97**(1-2): 5-7.

Experimental testing of a bi-stable point wave energy absorber under harmonic wave excitations

Mohammad A. Khasawneh*,** and Mohammed F. Daqaq*,**

*Department of Mechanical Engineering, Tandon School of Engineering, New York University, New York, 11201, USA.

**Division of Engineering, NYU Abu Dhabi, Abu Dhabi, UAE.

Abstract. We present in this paper an experimental study dedicated to characterizing the response behaviour of bi-stable Point Wave Energy Absorbers (B-PWAs) under harmonic wave excitations. To this end, we fabricate a small-scale prototype of a B-PWA and analyze its response in an experimental wave flume under different wave frequencies and heights. Using the experimental data, we delineate the complex dynamical features and types of motion (small-amplitude, large-amplitude, periodic, aperiodic) that the B-PWA undergoes, and explore their influence on the power production capabilities of the device. We generate a design map in the frequency–amplitude parameters space that demarcates regions of qualitatively different response behaviors and use it to define an effective bandwidth wherein the B-PWA performs unique periodic large-amplitude oscillations yielding maximum power levels.

Introduction

Traditional point wave energy absorbers (PWAs) operate based on the principle of linear resonance whereby the frequency of the incident wave must match the natural frequency of the absorber to drive the buoy into the large-amplitude motions necessary to generate usable power levels. However, the overlap between the spectrum of the ocean waves and the PWA’s resonance bandwidth is typically difficult to realize for two reasons. First, the natural frequency of the absorber is dictated by the stiffness of the hydrostatic (buoyancy) restoring force, which is typically very high resulting in a natural frequency that is much higher than that associated with naturally occurring waves in energetic marine sites. Second, the frequency of the incident waves is stochastic in nature resulting in a broadband energy spectrum that makes the resonance based approach less than ideal for wave energy absorption.

A large body of literature focused on devising active methods that help maintain the PWA in a proper tuning with the frequency of the incident energetic waves. Including the intentional introduction of a bi-stable nonlinear restoring element to broaden and shift the resonance bandwidth of the PWA towards lower frequencies [1-2].

Results and discussion

In this work, we design and construct a prototype of a B-PWA (Fig. 1 (B)) and test its response behavior under harmonic incident waves. Using the experimental data, we generate design maps in the frequency– amplitude parameters space that demarcate regions of qualitatively different response behaviors of the PWA. A sample of this design map is shown in Fig. 1 (A). Where the region remarked as B_L , delineates the incident wave

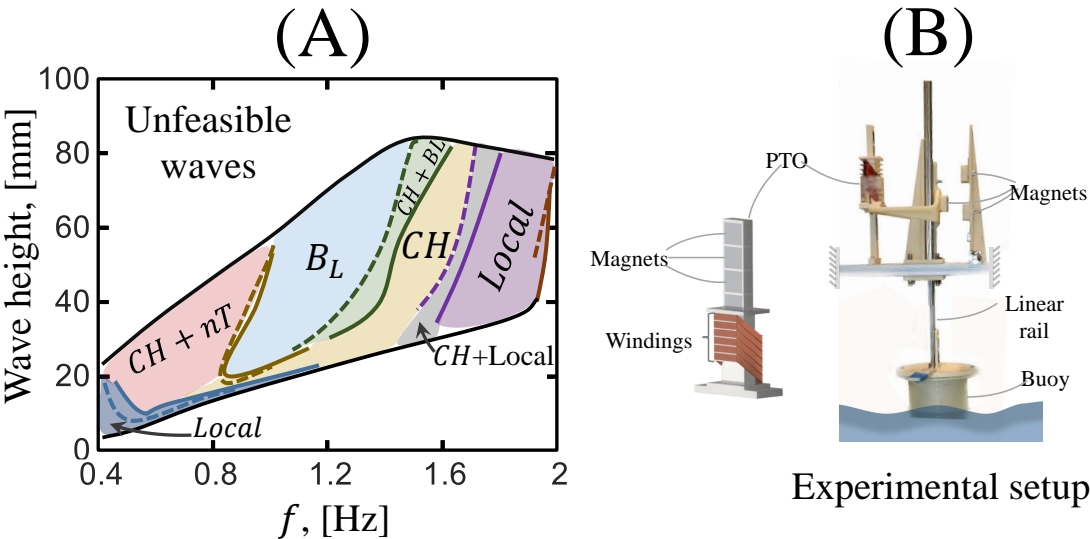


Figure 1: (A): A bifurcation map that demarcates qualitatively-different steady-state motions of the PWA for various combinations of wave heights and frequencies. B_L : large orbits, CH : Chaos, nT : n-period periodic orbits. (B): Overview of the experimental setup.

References

[1] Khasawneh M. A., Daqaq M.F. (2022) Response behavior of bi-stable point wave energy absorbers under harmonic wave excitations. *Nonlinear Dyn.* :1:21.
[2] Khasawneh M. A., Daqaq M.F. (2022) "Performance of bi-stable PWAs under irregular waves. *Nonlinear Dyn.* :1:17.

Self-tuning sliding mass electromagnetic energy harvester for dramatic frequency bandwidth enhancement

Mohammad Bukhari* and Oumar Barry*

*Department of Mechanical Engineering, Virginia Polytechnic Institute and State University, Blacksburg, VA, USA

Abstract. This work investigates a self-adaptive electromagnetic energy harvester using a moving slider mechanism through analytical and experimental methods. The slider moves along a beam with an electromagnetic transducer fixed on its tip, which vibrates within an electromagnetic field. Due to external excitations, nonlinear coupling, because of Coriolis and centrifugal forces, moves the slider along the beam until it settles down on an equilibrium position. This equilibrium position further tunes the harvester to the excitation frequency, and thus increases the harvested power significantly due to resonance. The coupled nonlinear system of equations is analyzed numerically using an adaptive mode shape algorithm based on the instantaneous slider's position. The results demonstrate a dramatic increase in the frequency bandwidth. This further indicates that the current system can be operated over a wide range of frequencies without scarifying any portion of the harvested energy to tune the system.

Introduction

Researchers have recently drawn their attention toward renewable energy sources for clean and sustainable energy conversion and self-powered systems. Vibration energy harvester (VEH) can represent a suitable clean sustainable source that converts environmental vibrations into useful power. These vibrations can be converted into electrical power using electromechanical or electromagnetic VEHs [1]. VEHs are beneficial when tuned to the excitation frequency; however, environmental vibrations have time-variable frequencies, making VEHs effective only at limited frequencies. Increasing the frequency bandwidth can be demonstrated through different passive and active techniques. Although active techniques are effective in tuning VEH, they require scarifying a portion of the harvested energy or external power source. On the contrary, passive self-tuning VEH can be obtained through a sliding mass mechanism [2]. The slider can move along VEH until meeting an equilibrium position, and hence tuning VEH to the excitation frequency. Studies in the literature on self-tuning VEH were limited to electromechanical VEHs, which are beneficial in small scale applications ($\sim \mu\text{W}$). Moreover, the investigations of similar dynamical systems used conventional assumed mode through Galerkin's projection, although system mode shapes are time variable and not constant. In this work, we investigate analytically and experimentally the dynamics of a self-adaptive electromagnetic energy harvester for large-scale energy harvesting applications. Unlike techniques in the literature, we employ an adaptive mode shape algorithm to enhance the current nonlinear system's numerical analyses.

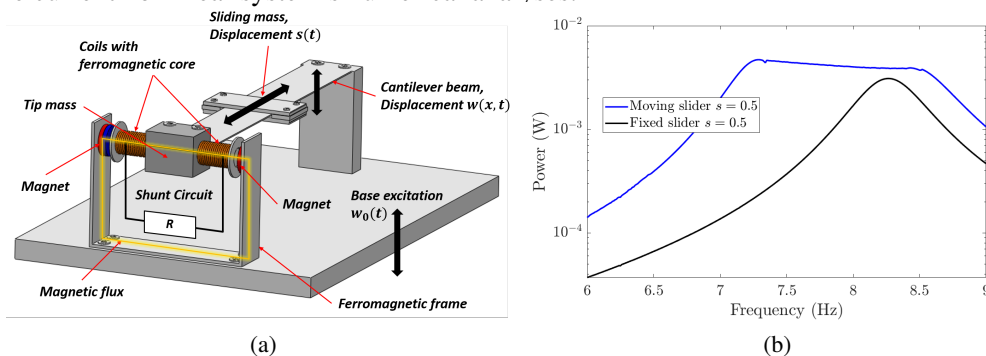


Figure 1: (a): A schematic for the proposed VEH; (b) bandwidth enhancement near the first mode.

Results and discussion

A schematic for the proposed self-tuning VEH is presented in Fig. 1(a). Near each mode, the exact mode shapes and resonance frequencies are determined for each possible instantaneous slider's position. These frequencies range from few hertz to several hundred hertz depending on the mode shape. Next, we continuously feed these frequencies into the numerical simulation to adapt the slider's instantaneous position. The results indicate that the frequency bandwidth of the proposed VEH is significantly wider than that for conventional VEH, as shown in Fig. 1(b) for frequencies near the fundamental mode. This enhancement in the harvested power also holds for higher resonance frequencies and frequency regions in between. Although there is only one equilibrium position near the first mode, several equilibrium positions may exist at higher modes. Therefore, our investigations also reveal that the slider's equilibrium position and the harvested power depend significantly on the initial slider's position and other parameters.

References

- [1] Priya S., Inman D. J. (2009) Energy harvesting technologies. Springer, NY.
- [2] Miller L. M., Pillatsch P., Halvorsen E., Wright P. K., Yeatman E. M., Holmes A. S. (2013) Experimental passive self-tuning behavior of a beam resonator with sliding proof mass.. *J. Sound and Vibration* **332**:7142-7152.

Escape from the potential well of bistable vibration energy harvesters using buckling level modifications

Camille Saint-Martin*, Adrien Morel*, Ludovic Charleux*, Emile Roux*, Aya Benhemou*,
Quentin Demouron* and Adrien Badel*

*Univ Savoie Mont Blanc, SYMME, F-74000, Annecy, France

Abstract. During the last decade, nonlinear vibration energy harvesters (NVEH) have attracted research interests for their broadband characteristics. However, they also exhibit low-power orbits in which they may remain stuck, leading to poor harvesting performances. In this paper, we study an orbit jump strategy that allows to jump from one of these low-power intrawell orbits to high-power interwell orbits. This orbit jump strategy is based on the variation of the buckling level of the bistable vibration energy harvester. We start with a brief presentation of the system dynamics, then we analyze the performances gain with the proposed approach.

Introduction

The availability of vibrations in our environment and the development of wireless sensor networks motivates researchers to develop energy harvesting systems to supply low-power electronic systems [1]. NVEH exhibit broader bandwidths compared to their linear counterpart, making them particularly relevant for harvesting energy from broad and time-varying vibration spectrum [2]. However, NVEH exhibit complex dynamics i.e., there exists multiple orbits of different power for a given vibration frequency. Some orbits are of low power, which may lead to poor harvesting performances. Therefore, to improve the performance of NVEH, researchers worked on the development of orbit jump strategies to shift from low-power orbits to higher power orbits [3]. In this study we use a bistable NVEH based on a buckled beam to which we apply an orbit jump strategy based on the modification of the buckling level.

Results and discussion

Figure 1(a) shows a schematic representation of the Duffing-type piezoelectric vibration energy harvester with two stable equilibrium positions (EP) for $x = \pm x_w$ considered from [3]. This NVEH is composed of a mechanical resonator and an electrical extraction circuit. The NVEH is excited with a sinusoidal acceleration of amplitude A and frequency f_d . The harvested power is the one dissipated in the extraction circuit, which is simply a resistor R . This orbit jump consists in dynamically modifying the buckling level by adjusting the EP x_w of the NVEH. We supposed that the system starts on a low-power orbit. The initial value of the EP $x_w(0)$ is x_w , thereafter we modify the EP with a factor k_w^0 at t_0 : $x_w(t_0) = k_w^0 x_w(0)$. The new value of the EP is maintained for a certain duration Δt . Then, from the instant $t_0 + \Delta t$ the EP is further modified with a factor k_w^1 such as: $x_w(t_0 + \Delta t) = k_w^1 x_w(0)$. Figure 1(a) shows the evolution of the EP. Therefore, the investigated orbit jump strategy depends on four influence parameters $(t_0, \Delta t, k_w^0, k_w^1)$. We used an evolutionary algorithm in order to find optimum parameters combination. The criterion to maximize is the total harvested energy on a duration of $100 T_d$ that takes into account the invested energy to modify the buckling level. Figure 1(b) shows an example of a successful application of such an orbit jump strategy for $f_d = 50$ Hz.

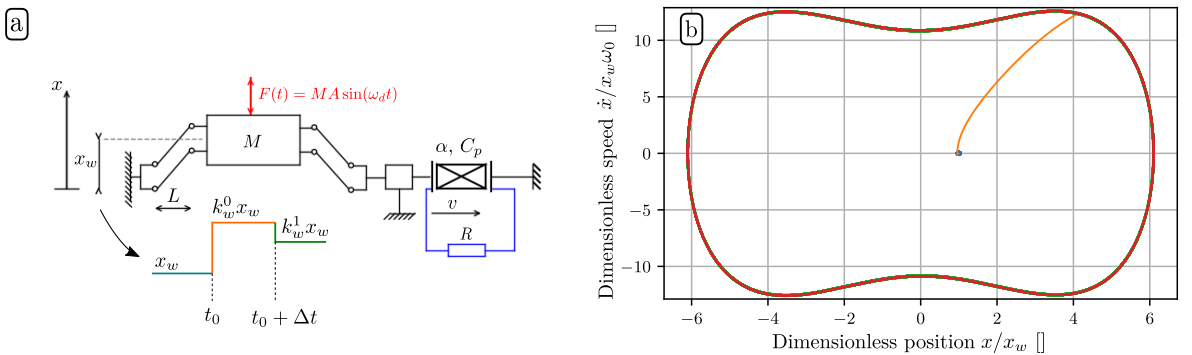


Figure 1: (a) NVEH scheme. (b) Trajectory in the dimensionless phase plane for $f_d = 50$ Hz, $A = 2.5$ m/s² with $(t_0, \Delta t, k_w^0, k_w^1) = (2 \times 10^{-3}, 7 \times 10^{-3}, 5.30, 3.50)$. The system starts on a low power orbit (blue) and converges to a high power orbit (red).

References

- [1] Prajwal K. T. et al. (2022) A review on vibration energy harvesting technologies: analysis and technologies. *The European Physical Journal Special Topics* **231**:1359-1371.
- [2] Sebald G. et al. (2011) Simulation of a Duffing oscillator for broadband piezoelectric energy harvesting. *Smart Materials and Structures* **20**:075022.
- [3] Huguet T. et al. (2019) Orbit jump in bistable energy harvesters through buckling level modification. *Mechanical Systems and Signal Processing* **128**:202-215.

Design and Optimization of Electromechanical Coupling in Electromagnetic Vibrational Harvester

Krzysztof Kecik*, Ewelina Stezycka* and Kateryna Lyubitska **

*Department of Applied Mechanics, Lublin University of Technology, Poland,

**Department of Natural Sciences, Mid Sweden University, Sundsvall, Sweden

Abstract. In this study, electromechanical coupling is used to optimize and change the performance of an electromechanical harvester. The obtained results demonstrated that the electromechanical coupling is inherently nonlinear and can introduce new resonances. The special design of coils and/or magnet allows for the modification of the shape of electromechanical coupling, resulting in an increased energy harvesting. The experimentally determined electromechanical coupling model were compared to finite element analysis results. Finally, the shaker test was performed for different electromechanical transducer configurations.

Introduction

An electromechanical coupling is a measure of the conversion efficiency between electrical and vibration energy. The main disadvantage of electromagnetic harvesters is its low efficiency, which is caused by low vibration levels and weak sensitivity outside the resonance region [1]. The motivation of the paper is maximizing electromagnetic energy harvester effectiveness without increasing harvester's size. The autoparametric vibration absorber, which is extremely sensitive to the system's parameters, uses the proposed harvester as the pendulum tuned mass damper [2].

Results and discussion

The vibrational electromechanical harvester generally consists of the magnet oscillating in the coil. The effectiveness of harvester depends on the interaction between mechanical and electrical systems. This interaction is referred to as the *electromechanical coupling* or *transduction factor*. The modification of the coupling can improve energy harvesting without change in the transducer design. The two methods of the electromechanical coupling shaping is applied here. First method for shaping of the electromechanical coupling based on the modification of the coil. The coil (called modular) consists of four separate independent coils (modules) which can be connected in various ways. Each of the modules can be activated separately or together (for example, modules no. 1 and 4 can be activated). Moreover, the different shape (C, L) of the modular coil are constructed and tested (Fig.1(a)).

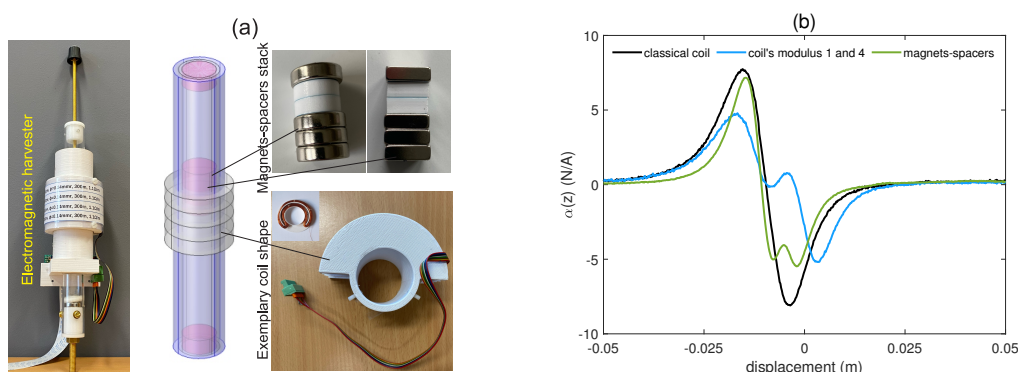


Figure 1: Electromagnetic vibration harvester (a) and exemplary shaped electromechanical coupling functions (b).

The second method is based on an oscillating magnet that has been specially designed. The magnet can have a different shape (circular or rectangle) and/or consists of stacked magnets and spacers (repulsive or attractive orientation).

The electromechanical coupling functions obtained for the coil with the active two modules 1 and 4 (blue line) and for the specially built asymmetric magnet (green line) vs magnet position in the coil are shown in Fig.1(b). As we can see, these functions differ from the typical electromechanical coupling (black line). Therefore, we expected, that the proper configuration of the magnet-coil allows increase effectiveness of energy harvesting.

Acknowledgements

This research was financed in the framework of the project: "Theoretical-experimental analysis possibility of electromechanical coupling shaping in energy harvesting systems" no. DEC-2019/35/B/ST8/01068, funded by the National Science Centre, Poland.

References

- [1] Li X., Meng J., Yang C., Zhang H., Zhang L., Song R.A. (2021) Magnetically coupled electromagnetic energy harvester with low operating frequency for human body kinetic energy. *Micromachines* **12**:1300.
- [2] Kecik K. (2021) Simultaneous vibration mitigation and energy harvesting from a pendulum-type absorber. *Commun Nonlinear Sci Numer Simul.* **92**:105479.

Simultaneous passive suppression and energy harvesting from galloping using a bi-stable piezoelectric nonlinear vibration absorber

Guilherme Rosa Franzini*, Vitor Schwenck Franco Maciel*, Guilherme Jorge Vernizzi* and Daniele Zulli **

*Offshore Mechanics Laboratory (LMO), Escola Politécnica, University of São Paulo, Brazil

**University of L'Aquila, Italy

Abstract. This contributions focuses on numerical studies on the simultaneous passive suppression and energy harvesting from the galloping of a square prism. The suppressor/energy harvester is a bi-stable piezoelectric nonlinear vibration absorber (BS-PNVA). Numerical studies revealed that the investigated device can be employed for the simultaneous passive suppression and energy harvesting.

Introduction

Two topics that have received attention in the last decades are the passive suppression of vibrations using nonlinear vibration absorbers (or, equivalently, nonlinear energy sinks) and the energy harvesting from structural oscillations. As the working mechanism of the nonlinear vibration absorbers involves dynamic responses of the device, some recent works take advantage of this localized motion for energy harvesting purpose. As an example, reference [1] experimentally studied the response of the system composed of a platform to which the suppressor/energy harvester is mounted.

Considering the suppression of the galloping phenomenon (a particular flow-induced vibration problem), the experimental results shown in [2] reveal that a class of nonlinear vibration absorbers effectively mitigates the vibrations of the main structure. The focus of this contribution is to present numerical studies that indicate that BS-PNVA can simultaneously mitigate the galloping response and harvest vibratory energy. At least to the best of the authors knowledge, similar studies are not found in the literature.

Mathematical model and results

The investigated system is composed of a square prism subjected to a uniform free-stream velocity profile. A BS-PNVA, composed of a small mass m_N linked to the main structure by means of a pre-compressed piezoelectric spring and a dashpot of constant c_N , works as the device for simultaneous suppression and energy harvesting; see Fig. 1(a). No impact between the main structure and the BS-PNVA occurs. The nonlinear equations of motion of the solid-fluid-electric oscillator are obtained in the dimensionless form, but not presented here for the sake of brevity of this abstract. The fluid forces are computed by means of the quasi-steady approach; see [3].

Figure 1(b) shows the oscillation amplitude of the prism as a function of the reduced velocity. As can be seen in this plot, the studied BS-PNVA is able to both postpone the critical reduced velocity associated with the Hopf bifurcation and decrease the post-critical responses. The variation of the standard deviation of the electric tension obtained at the energy harvesting circuit $v_{s,t,d}$ with the reduced velocity U_r is presented in Fig. 1(c). From the analysis of Figs. 1(b) and 1(c) one can see that the BS-PNVA is useful for the simultaneous passive suppression and energy harvesting from galloping. In the full paper, different parameters of the BS-PNVA will be considered in the numerical simulations.

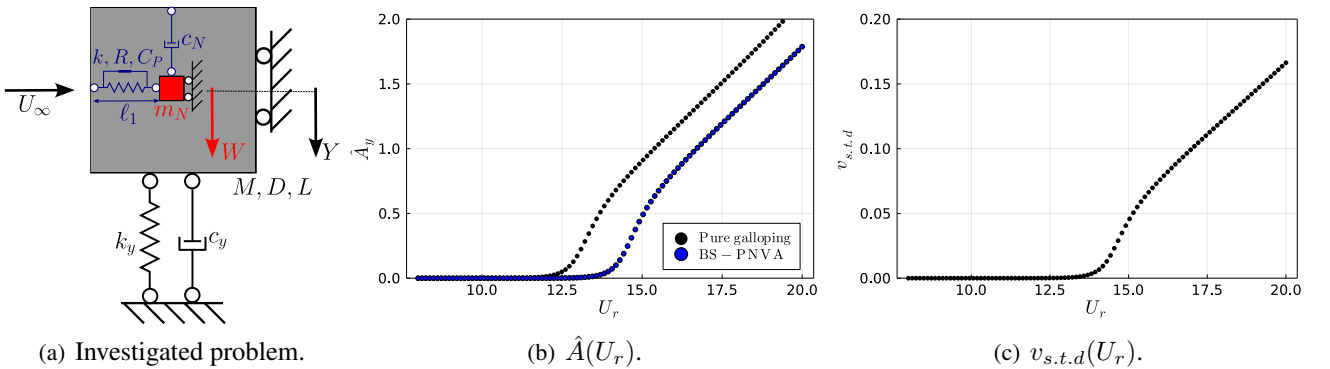


Figure 1: Sketch of the investigated problem and examples of results.

References

- [1] Kremer D., Liu K. (2014) A nonlinear energy sink with an energy harvester: Transient responses. *J. Sound Vib* **333**:4859-4880.
- [2] Selwanis M.M, Franzini G.R., Béguin C., Gosselin F.P. (2021) Wind tunnel demonstration of galloping mitigation with a purely nonlinear energy sink. *J. Fluids Struct* **100**:103169.
- [3] Blevins R.D. (2021) Flow-induced vibration. Krieger Publications.

Probabilistic analysis of an asymmetric bistable energy harvester

João Pedro Norenberg*, Americo Cunha Jr.** , Samuel da Silva*** and Paulo Varoto****

*São Paulo State University, SP, Brazil, ORCID 0000-0003-3558-4053

**Rio de Janeiro State University, RJ, Brazil, ORCID 0000-0002-8342-0363

***São Paulo State University, SP, Brazil, ORCID 0000-0001-6430-3746

****University of São Paulo, SP, Brazil, ORCID 0000-0002-1240-1720

Abstract. A nonlinear bistable vibration energy harvester is an efficient system to convert vibration energy into electricity to power mobile electronic devices, but they present a complex dynamic behavior and sensitivity to slight variations of the parameters. This work aims to show a comprehensive analysis of uncertainties in asymmetric bistable energy harvesters to obtain statistical information about how the variability of each parameter affects the harvesting process.

Introduction

Numerous efforts have been dedicated to nonlinear energy harvesters to convert vibrational energy into electricity using piezoelectric layers. Bistable energy harvesters have been extensively dedicated in the last decade [1]. Even though they are powerful at a broadband frequency, these systems present complex dynamic behaviors due to nonlinearity. In addition, investigating this system can still be a major challenge when introduced into an environment of uncertainty. Therefore, this work studies the effects of uncertainty parameters of the asymmetric bistable energy harvester.

To obtain a sophisticated and reliable model, asymmetries are introduced to take into account the geometry and manufacturing imperfections of the system. The system comprises a clamped-free ferromagnetic elastic beam in a vertical configuration attached to a rigid base, where a pair of magnets is asymmetrically placed on the lower part. The piezoelectric layers are glued on the beam's highest part, responsible for converting the kinetic energy into an electrical signal, which is dissipated in the resistor. An external periodic force excites the rigid base. The harvester is attached to a plane with a sloping angle ϕ , creating an asymmetry force of the gravity of the system. The lumped-parameter equation of motion for this system, presented in [2], are:

$$\ddot{x} + 2\xi\dot{x} - \frac{1}{2}x(1 + 2\delta x - x^2) - \chi v = f \cos(\Omega t) + p \sin \phi \quad \text{and} \quad \dot{v} + \lambda v + \kappa \dot{x} = 0, \quad (1)$$

where x is the amplitude; v is the voltage; ξ is the damping ratio; f is the amplitude of excitation; Ω is the frequency of excitation; λ is a reciprocal time constant; χ and κ represented the piezoelectric coupling terms; δ is a coefficient of the quadratic nonlinearity; p is the equivalent dimensionless constant of gravity.

Results and discussion

Each variable is described by a uniform distribution as defined by [3]. Figure 1 shows the joint-CDF (joint cumulative distribution function) of the mean power conditioned to each parameter of interest under different nominal excitation conditions. This figure shows the correlation of each parameter with the mean power, providing information on how to improve the power recovered.

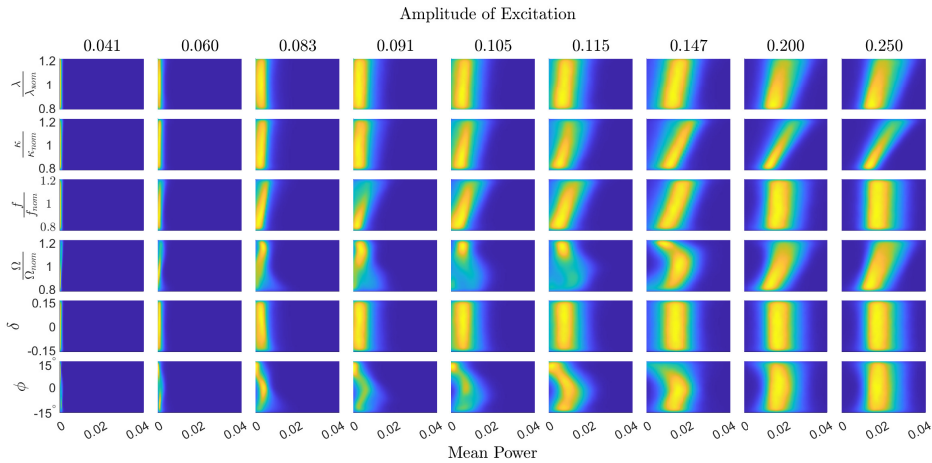


Figure 1: Joint-CDF of mean power conditioned for each parameter of the model for different values of the amplitude of excitation.

References

- [1] Erturk A., Hoffmann J., Inman D.J. (2009) A piezomagnetoelastic structure for broadband vibration energy harvesting, *Appl. Phys. Lett.* **94**:254102.
- [2] Norenberg J.P., et.al. (2022) Nonlinear dynamic analysis of asymmetric bistable energy harvesters. *Preprint: Research Square*.
- [3] Norenberg J.P., et.al. (2022) Global sensitivity analysis of asymmetric energy harvesters, *Nonlinear Dyn.* **109**:443–458.

Effects of energy harvesting from a piezoelectric element attached to a propelling flexible tail

Hossam Alqaleiby*, Mahmoud Ayyad*, Muhammad R. Hajj*, and Lei Zuo **

*Civil, Environmental and Ocean Engineering, Stevens Institute of Technology, Hoboken, NJ 07030, USA.

**Naval Architecture and Marine Engineering, University of Michigan, Ann Arbor, MI 48103, USA.

Abstract. Monitoring fishes migration, which can extend to distances of thousands of kilometers, via autonomous fish tags is important to assess their populations. One constraint of current fish tags is the limited power of their batteries. We propose the development of self-powered tags that generate their own power from a piezoelectric element attached to an oscillating part of the fish body such as its flapping tail. To determine the functionality and potential of this technology, we present simulations that determine the effects of attaching a piezoelectric element to a flexible substrate on performance metrics including thrust generation, propulsive efficiency, and harvested electric power.

Introduction

Fish migration involves relocation of fish groups from one area or body of water to another for duration ranging from one to 365 days. Electronic tagging is currently used for continuous monitoring and assessment of the movement patterns of these groups and fishing levels, which are important to maintain healthy fish stocks. The weight, volume and finite energy of today's batteries that power fish tags limit their operational lifetime. As such, a fish tag that does not fully rely on battery power would support the capability of monitoring fish populations over longer periods. Noting the energy associated with fish body motions, one approach for developing self-powered tags is to mount or implant a piezoelectric element in a moving part of the fish body such as its tail. Still, it is important to evaluate adverse impacts of such attachments on the fish propulsion force, its efficiency, while considering the level of harvested electric power. We address these impacts by assessing energy generated from a piezoelectric element attached to a flexible beam, representing a fish tail and capable of generating propulsion when excited at its root. The basis of our study are the results of Hussein et al. *et al* [1], which showed that there are optimal flexibility and mass ratio parameters for enhancing propulsion. In these simulations, the substrate element, representing the fish tail, is modeled as a thin unimorph cantilever beam using the Euler-Bernoulli beam theory and excited by sinusoidal pitching at its root. The tail's upper surface is covered by a PZT layer connected to an electrical load resistance. The three-dimensional unsteady vortex lattice method is used to calculate the hydrodynamic loads generated by the pitching excitation under constant forward speed. The finite element method is used to solve the coupled time-dependent equations of motion representing the fluid-structure interaction. The implicit finite different method is used to discretize the time-dependent generated voltage equation. The fluid-structure interaction is achieved by passing the hydrodynamic loads to the coupled equations of motion and solving for structural deformation of the tail at each time step where the generated voltage is updated.

Results and discussion

Figure 1 shows plots of generated power and its impact on the propulsive force and efficiency. An optimal value of about $4 \times 10^4 \Omega$ for the electric load resistance for maximum electric power generation is noted. In the low frequency excitation range (Strouhal number, $ST < 0.3$), adding the PZT layer decreases the thrust coefficient and the required power to propel the tail. At higher excitation frequencies ($ST > 0.3$), the generated thrust is increased. However, this requires additional input power as demonstrated by the lower efficiency. The level of harvested electric power is in the range of few mW, which is three orders of magnitude smaller than the level of input or propulsive power, indicating that the piezoelectric energy harvesting should not have a large impact on the power needs by the fish to generate propulsion.

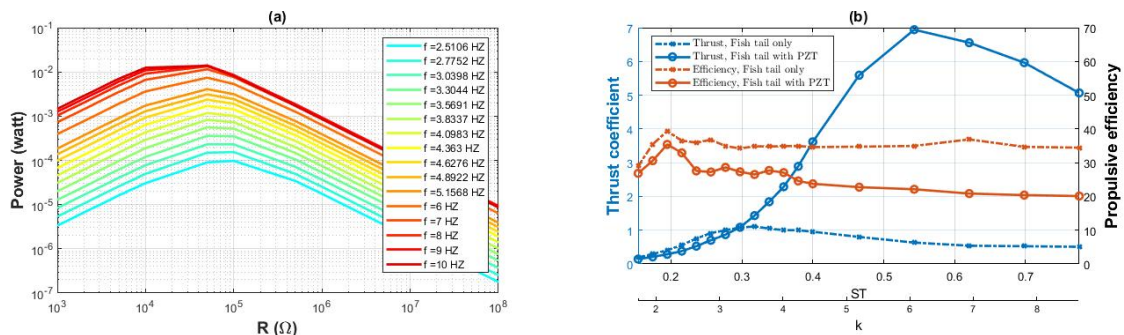


Figure 1: (a) Electric harvested power variation with load resistance at different excitation frequency values. (b) Variation of thrust coefficient and propulsive efficiency with Strouhal number, ST , and reduced frequency, K .

References

- [1] Hussein, A. A., Ragab, S. A., Hajj, M. R., and Patil, M. J. (2021) Material and geometric effects on propulsion of a fish tail. *Bioinspiration & Biomimetics* **16**(6), 066008.

Stochastic analysis of a bistable piezoelectric energy harvester with a matched electrical load

K. Song^{*,**}, M. Bonnin^{*}, F. L. Traversa^{***} and F. Bonani^{**}

^{*}IUSS, University School for Advanced Studies, Pavia, Italy

^{**}Politecnico di Torino, Torino, Italy

^{***}MemComputing Inc., San Diego, CA, USA

Abstract. We present an analysis of a bistable piezoelectric energy harvester subject to random mechanical vibrations and with improved performance thanks to the use of a matching electrical network, that optimizes the energy transfer to the electrical load. The model exploits a stochastic differential equation describing the harvester, matching network and load dynamical system. Analytical methods and different numerical techniques are used for its solutions. Results show that, even for the case of random mechanical vibrations, the application of the matching network improves the performances by a significant amount.

Introduction

One of the main performance limitations for a piezoelectric energy harvester is the sub-optimal energy transfer from the mechanical source to the electrical load, a condition that can be conveniently represented as an impedance mismatch between the electrical equivalent of the entire electro-mechanical system and the load. This suggests to interpose a proper matching network between the harvester and the load to eliminate the mismatch [1,2,3].

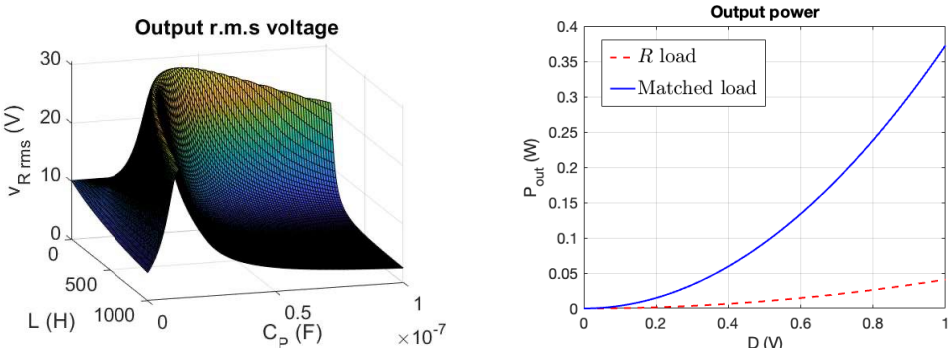
In the simplest case of purely sinusoidal vibrations, i.e. when their energy is concentrated at a single frequency, a relatively straightforward analysis of the harvester is possible [1]. However, a more physically sound description considers the vibration energy spreading on a relatively wide frequency spectrum, thus requiring the use of a stochastic process that, for a negligible noise correlation, can be conveniently modelled with a white Gaussian noise forcing term.

In this contribution, we model a bistable piezoelectric energy harvester subject to random mechanical vibrations, and present novel results through analytical and numerical analysis. The mathematical model is derived from the properties of the mechanical part, from the constitutive equations of linear piezoelectric materials, and from the circuit description of the electrical load. The model includes nonlinearities in the mechanical elastic potential. The equations of motion are stochastic differential equations, here solved using various perturbation methods and different numerical integration schemes. Inspired by our recent work on the application of circuit theory to improve the efficiency of energy harvesting systems, we apply a LC matching network to the load [1,3], and we assess the advantage offered by the modified load in terms of output average voltage, output average power and power efficiency.

Results and discussion

We have performed Monte Carlo simulations for the bistable energy harvester with and without (resistive load) the LC matching network. The SDEs have been solved numerically using different numerical integration schemes, including Euler-Maruyama, strong order 1 stochastic Runge-Kutta, and weak order 2 stochastic Runge-Kutta [4]. The figure below shows on the left, the output voltage rms value for the harvester with matched load, versus the values of the matching

network parameters L and C . Optimal values of the parameters maximizing the harvested voltage are clearly recognizable. The right part shows a comparison of the average harvested power by the harvester with resistive and matched load, versus the noise intensity. Optimum values of parameters of the matching network were chosen. The matched solution offers about nine times more power with respect to the simple resistive load.



Left: Root mean square value for the output voltage vs. the LC matching network parameters. **Right:** Comparison of the average harvested power for the harvester with resistive load and with matched load, versus the noise intensity.

References

- [1] M. Bonnin et al., *Nonlinear Dynamics*, vol. 104, no. 1, pp. 367–382, 2021.
- [2] D. Huang et al., *Nonlinear Dynamics*, vol. 97, no. 1, pp. 663–677, 2019.
- [3] M. Bonnin et al., *Energies*, vol. 15, no. 8, p. 2764, 2022.
- [4] S. Särkkä et al., *Applied stochastic differential equations*. Cambridge University Press, 2019.

Enhancing Aeroelastic Wind Energy Harvesting Using Quasi-Zero Stiffness

Shun Chen*, Liya Zhao*

**School of Mechanical and Manufacturing Engineering, University of New South Wales (UNSW Sydney), Sydney 2052 NSW, Australia*

Corresponding author: liya.zhao2@unsw.edu.au

Abstract. A quasi-zero stiffness (QZS) two degree-of-freedom (DOF) galloping piezoelectric energy harvester (GPEH) is proposed for efficient energy harvesting in the ultra-low wind speed range. At low wind speeds, traditional 1DOF and 2DOF linear harvesters are not capable of generating enough voltage to power microelectronics, while the bistable harvester tends to be trapped in intrawell motion, which is unfavorable for wind energy harvesting. With the feature of a low dynamic frequency, the QZS nonlinear mechanism is applied to remarkably decrease the onset galloping wind speed and boost the power generation. The simulation result shows that the 2DOF QZS-GPEH has the best output performance at low wind speeds, outperforming its 1DOF linear, 2DOF linear and 2DOF bistable counterparts. This work opens new opportunities for efficiently harvesting wind energy at the ultra-low wind speed region.

Introduction

With the development of wireless sensor networks and Internet of Things, vast sensor nodes are deployed in harsh circumstances for monitoring purposes. However, how to provide a reliable and long-term power supply to these sensors is a big challenge. Currently, wind energy harvesting based on galloping become a viable solution due to its large outputs in an infinite wind speed range [1]. Researchers have mainly focused on decreasing the cut-in wind speed, broadening the operational wind speed range, and improving the power output performance [2]. Because the cut-in wind speed is highly related to the oscillation frequency of the structure [2], manipulating the oscillation frequency is essential to decrease the cut-in wind speed and enhance the power performance at low wind speeds for galloping energy harvesting. 2DOF systems provide more flexibility to adjust the galloping frequency for enhanced outputs by modifying the model frequencies [3]. Besides, quasi-zero stiffness (QZS) nonlinearity has been proved to provide a low dynamic resonance frequency at equilibrium [4]. We propose a 2DOF quasi-zero-stiffness galloping piezoelectric energy harvester (QZS-GPEH) for dramatically enhancing the wind power extraction performance at ultra-low wind speeds.

Results and discussion

We design a practical prototype as shown in Fig. 3. The bluff body oscillates horizontally when subjected to the incoming flow. The piezoelectric transducer attached to the primary beam converts the strain energy during oscillation into electricity via piezoelectric transduction. A secondary beam with a tip mass is added at the free end of the primary beam as the second degree-of-freedom. The quasi-zero stiffness is achieved via magnetic interaction between magnets A, B and C to achieve optimal galloping energy harvesting performance.

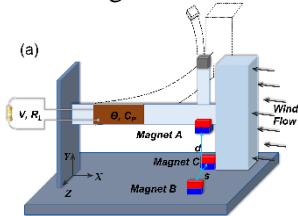


Fig. 1. Configurations of 2DOF QZS-GPEH

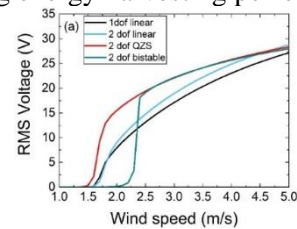


Fig. 2. RMS voltage as a function of wind speed

Figure 2 compares the RMS voltage versus wind speed for the four configurations, including 1DOF linear, 2DOF linear, 2DOF QZS and 2DOF bistable GPEHs based on simulation. Firstly, the cut-in wind speed of the 2DOF QZS-GPEH is reduced to 1.5 m/s, smaller than that of other three configurations. Besides, the output voltage is remarkably larger than that of the other three counterparts, especially at low wind speeds. For instance, the 2DOF QZS-GPEH increases the voltage by 95% and 72% in comparison to the 1DOF linear GPEH, and the 2DOF linear GPEH at 2.0 m/s, respectively. Moreover, below 2.4 m/s, the bistable GPEH is trapped into the intrawell oscillation with very low voltage output. Apparently, the 2DOF QZS-GPEH has the best voltage output performance at low wind speeds, outperforming the other three counterparts.

References

- [1] Yang, Y., Zhao, L., & Tang, L. (2013). Comparative study of tip cross-sections for efficient galloping energy harvesting. *Applied Physics Letters*, 102(6), 064105.
- [2] Zhao, L., & Yang, Y. (2015). Analytical solutions for galloping-based piezoelectric energy harvesters with various interfacing circuits. *Smart Materials and Structures*, 24(7), 075023.
- [3] Zhao, L., Tang, L., & Yang, Y. (2014). Enhanced piezoelectric galloping energy harvesting using 2 degree-of-freedom cut-out cantilever with magnetic interaction. *Japanese Journal of Applied Physics*, 53(6), 060302.
- [4] Gatti, G. (2020). Statics and dynamics of a nonlinear oscillator with quasi-zero stiffness behaviour for large deflections. *Communications in nonlinear science and numerical simulation*, 83, 105143.

Reduced order modelling with Deep Learning methods of the steady-state response in MEMS

Giorgio Gobat*, Alessia Baronchelli* and Attilio Frangi *

*Department of Civil and Environmental Engineering, Politecnico di Milano, Milano, IT

Abstract. Micro-Electro-Mechanical-Systems (MEMS) are nowadays essential components in high-end technology applications e.g., resonators and gyroscopes. The ever-growing demand for increasing performances requires performing nonlinear dynamic simulations that are mostly unaffordable using standard full-order simulation techniques such as the Finite Element Method (FEM). Data-Driven Reduced Order Models (ROMs) provide an appealing alternative starting from data and without acting intrusively in the reduction procedure itself. In this contribution, we propose a technique that, by exploiting deep-learning autoencoders and harmonic decomposition, generates efficient and accurate ROMs for the steady-state regime in resonating MEMS.

Introduction

In order to meet the design requirements related to sensitivity and output signal strength, MEMS are usually actuated at resonance, in near-vacuum conditions with large quality factors. Consequently, these devices experience geometric nonlinearities induced by the large transformations. Predicting the steady-state response of such systems through standard full-order approaches like the FEM creates a computational bottleneck due to the large dimensionality of the resulting nonlinear system and the high-quality factors. Such difficulties can be overcome through dedicated approaches like e.g., the Harmonic Balance (HB) method, as proposed in [1]. Nevertheless, for large systems, non-standard computing facilities are needed. ROMs provide a solution to these problems since, through a dimensionality reduction, the system can be modelled with a limited number of variables i.e., latent variables, that underlie the dynamics. Data-driven, and in particular Deep Learning methods, provide a non-intrusive solution to build ROMs. In this contribution, taking inspiration from many applications in the literature [2, 3, 4], we use a deep-learning autoencoder to build a low-dimensional representation of the dynamics. Furthermore, we enrich these approaches by modelling the steady-state regime through its harmonic components, retained up to the desired order. The latent space, once built, is used to query new unseen solutions through interpolation.

Results and discussion

We consider a MEMS micromirror fabricated by ST Microelectronics, illustrated in Fig.1. The mirror is assumed to be made of isotropic polysilicon, with density $\rho = 2330 \text{ Kg/m}^3$, Young modulus $E = 167 \text{ GPa}$ and Poisson coefficient $\nu = 0.22$. The torsional mode is the third one and has a frequency of 29271 Hz, we assume a quality factor $Q = 1000$. The results from the proposed ROM are compared with Full Order Model (FOM) solutions in Fig. 1 considering different forcing levels. The ROM highlights an excellent accuracy considering that the reduced subspace created with the autoencoder consists of a single latent variable, i.e. equivalent to a one degree of freedom oscillator.

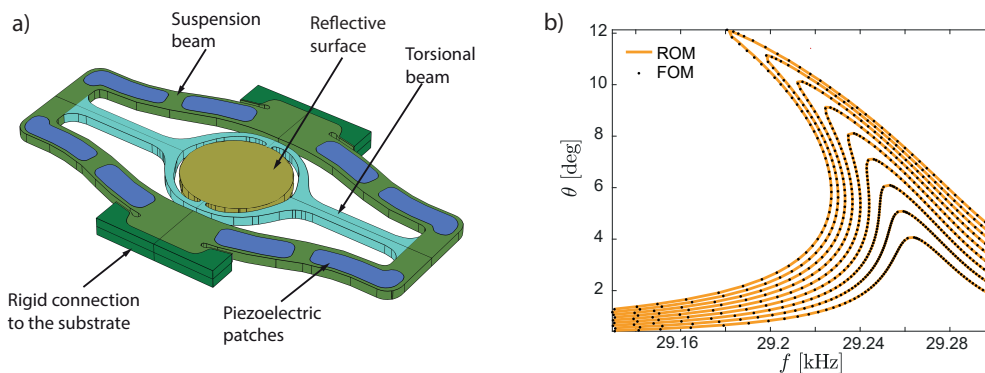


Figure 1: Fig.a) Scheme of the MEMS micromirror. Fig. b) comparison between the FOM solution and the proposed ROM

References

- [1] Opreni, A., et al. (2021) Analysis of the nonlinear response of piezo-micromirrors with the harmonic balance method *Actuators*, **MDPI** **10**:2
- [2] Fresca, S., et al. (2022) POD-DL-ROM: enhancing deep learning-based reduced order models for nonlinear parametrized PDEs by proper orthogonal decomposition *Comp. Meth. in Appl. Mech. and Eng.* **388**:114181
- [3] Champion, K., et al. (2019) Data-driven discovery of coordinates and governing equations *Proc. of the National Academy of Sciences* **116**:45: 22445-22451
- [4] Fresca, S., et al. (2022) Deep learning-based reduced order models for the real-time simulation of the nonlinear dynamics of microstructures *Int. J. for Num. Meth. in Eng.* **123**:20:4749-4777

A MEMS triple sensing scheme based on nonlinear coupled micromachined resonators

Zhengliang Fang*, Stephanos Theodossiades* and Amal Z. Hajjaj*

*School of Mechanical, Electrical, and Manufacturing Engineering, Loughborough University, Loughborough, UK.

Abstract. In the past few decades, advances in micro-electromechanical systems (MEMS) have produced robust, accurate, and high-performance devices. Extensive research has been conducted to improve the selectivity and sensitivity of MEMS sensors by adjusting the device dimensions and adopting nonlinear features. However, the sensing for multiple parameters typically relies on combining several separate MEMS devices. In this work, a new triple sensing scheme via nonlinear weakly coupled resonators is introduced, which could simultaneously detect three different physical stimuli (including vertical acceleration) by monitoring the dynamic response around the first three lowest modes. The Euler-Bernoulli beam model with three-modes Galerkin discretization is used to derive a reduced-order model considering the geometric and electrostatic nonlinearities to characterize the resonator's nonlinear dynamics under the influence of different stimuli. The simulation results show the potential of the nonlinear coupled resonator to perform triple detection.

Introduction

Resonant MEMS sensors rely on the resonance frequencies' variation led by the ambient environment's influence in different ways. The parameters related to the resonance frequencies include the resonator's mass, stiffness, and geometry [1]. Past research on this topic focused on the single parameter sensing and corresponding performance enhancement. This work investigates multi-parameter sensing by introducing different stimuli to different resonators in a single coupled system. To investigate this scheme and its nonlinear dynamics, a theoretical model and simulation are performed.

The triple sensing methodology is demonstrated in three aspects in this sensor design. As shown in the inset of Figure 1(a), the middle bridge resonator W_1 will be heated electrothermally, experiencing convective cooling (or heating) from the target gas. The thermal expansion will change the bridge's stiffness and hence the system resonance frequency [2]. At the same time, the tip of cantilever resonator W_2 will be coated, causing a mass perturbation (as absorbing the target gas) and leading to a frequency shift of the system's resonance frequency. The third bridge resonator W_3 connects to an external mass with springs, used for sensing acceleration in the vertical direction. The variation of resonance frequency is associated with the axial stress of the bridge, which changes with the direction and magnitude of the acceleration [3].

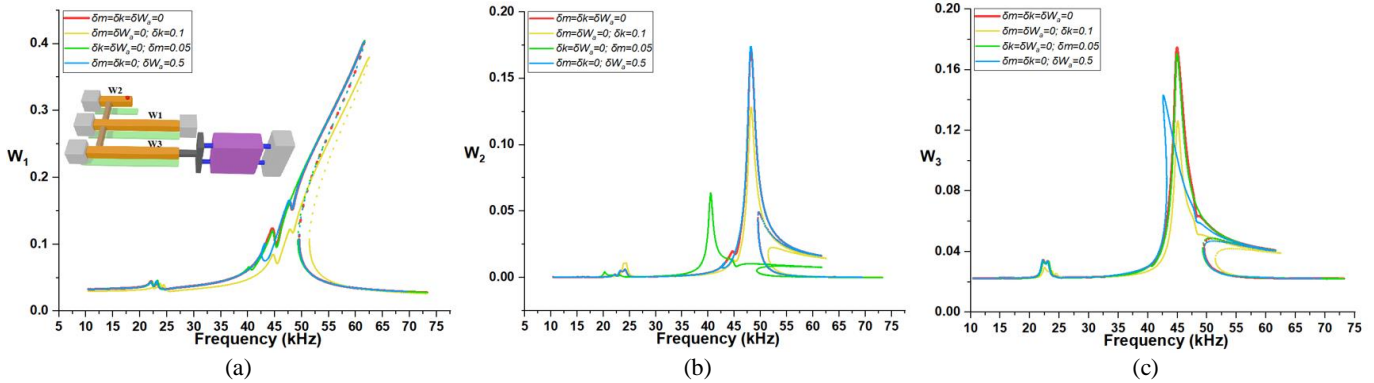


Figure 1: Frequency response under $V_{DC1} = V_{DC3} = 40V$, $V_{DC2} = 10V$, $V_{AC1} = 7.5V$, and different perturbations: (a) Bridge response W_1 . (b) Cantilever resonator W_2 . (c) Bridge response W_3 . Dotted lines denote unstable branches. Amplitudes W_1 , W_2 , and W_3 , mass and stiffness δm and δk are non-dimensional; acceleration δW_a is dimensional (m/s^2). The inset of (a) shows a 3D sketch of the proposed coupled device.

Results and Discussion

The concept of a multi-stimuli sensor has been investigated, as shown in Figure 1, using a novel design comprising multiple resonators, where each resonator's response corresponds to a specific stimulus: (i) the bifurcation jump in bridge response W_1 is influenced by stiffness perturbation δk ; (ii) the peak in cantilever resonator W_2 is influenced by mass perturbation δm and (iii) the peak in bridge response W_3 is influenced by acceleration perturbation δW_a . These preliminary results, developed via long-time integration combined with shooting technique, show the potential of accurately sensing three different parameters through monitoring the first three lowest modes of a single coupled structure as well as the rich dynamic of the proposed device. The full nonlinear response dynamics and the influence of the actuation level, damping, and geometry will be investigated as part of the future work.

References

- [1] Pachkawade, V. (2021) State-of-the-Art in Mode-Localized MEMS Coupled Resonant Sensors: A Comprehensive Review. *IEEE Sens. J* **21**(7): 8751–8779. <https://doi.org/10.1109/JSEN.2021.3051240>
- [2] Hajjaj, A. Z., Jaber, N., Alcheikh, N., & Younis, M. I. (2020) A Resonant Gas Sensor Based on Multimode Excitation of a Buckled Microbeam. *IEEE Sens. J* **20**(4):1778–1785. <https://doi.org/10.1109/JSEN.2019.2950495>
- [3] Morozov, N. F., Indeitsev, D. A., Igumnova, V. S., Lukin, A. v., Popov, I. A., & Shtukin, L. v. (2022) Nonlinear dynamics of mode-localized MEMS accelerometer with two electrostatically coupled microbeam sensing elements. *Int. J. Non-Linear Mech* **138**:103852. <https://doi.org/10.1016/j.ijnonlinmec.2021.103852>

Managing parametric frequency noise using nonlinearity in a High-Q micromechanical torsion pendulum

Jon R. Pratt*, Stephan Schlamminger*, Aman R. Agrawal**, Charles A. Condos**,
Christian M. Pluchar**, and Dalziel J. Wilson**

*National Institute of Standards and Technology, 100 Bureau Drive, Gaithersburg, MD 20899, USA

**Wyant College of Optical Sciences, University of Arizona, Tucson, AZ 85721, USA

Abstract. We derive a nonlinear equation of motion for a micromechanical torsion pendulum and reveal that the dependence of its frequency on amplitude is a conduit for noise in a proposed "clock gravimeter" application. Using the method of multiple scales, we carry out a first order expansion capturing nonlinear effects due to the nanoribbon suspension and pendulation of the mass, express the frequency correction in terms of physical geometry and material properties, and show that the dependence on amplitude can be greatly reduced by judicious selection of device geometry.

Introduction

Gravity can be detected by tracking the frequency of a pendulum. But for microscale pendulums (e.g., Figure 1) to resolve local gravity with relative precision of 10^{-8} in a reasonable time (<1000 seconds), they must be resonantly driven to amplitudes that exceed noise by 3 to 4 orders of magnitude. Such amplitudes exceed the linear range of frequency invariant behaviour, so we must consider the parametric dependence of frequency on amplitude and its consequences.

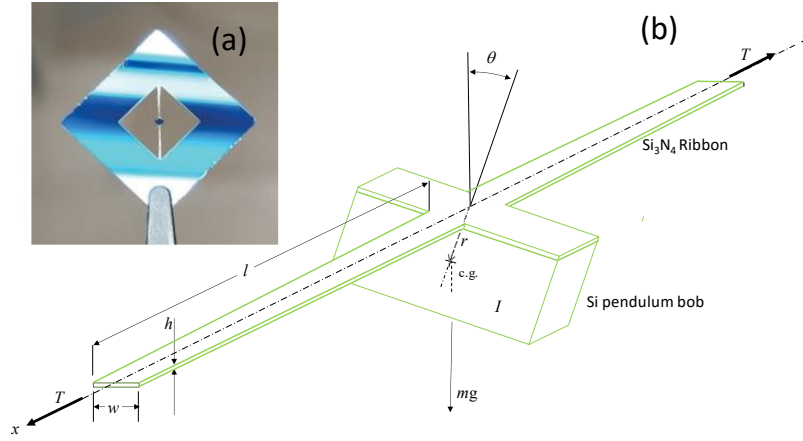


Figure 1: (a) photo of torsion pendulum device (b) schematic of torsion pendulum, formed by suspending a rectangular balance beam of mass m from a ribbon-like torsion fiber under tension, T . Angular displacement of the balance beam θ is measured using an optical lever. The center of gravity (c.g.) of the balance beam is offset a distance r from the rotation axis, resulting in a gravitational restoring torque, $\tau_g = mgr \sin \theta$ that causes the beam to pendulate

Results and discussion

Previously, we found the torsional stiffness of the device of Figure 1 has three components, one dissipative, arising from shear of the ribbon, one nominally conservative, arising from residual stress in the ribbon, and one wholly conservative due to the action of gravity on the suspended mass (e.g., pendulation). The conservative stiffness terms enabled the construction of high-Q devices ($Q > 10^7$) sensitive to gravity yet exceptionally small, with potential as chip-scale relative gravimeters [1]. Here, we extend the previous linear analysis to reveal the projection of amplitude noise onto the pendulum frequency. We include a nonlinear restoring torque arising from mid-plane stretching of the ribbon, finding it is a hardening spring that can be manipulated to counteract the softening character of the gravitational torque. Using the method of multiple scales [2], we carry out a first order expansion including both nonlinear effects, express the frequency correction in terms of physical geometry and material properties, and show that the dependence on amplitude can be greatly reduced by judicious selection of device geometry.

References

- [1] Pratt J.R., Agrawal A.R., Condos C.A., Pluchar C.M., Schlamminger S., Wilson D.J., (2021) Nanoscale torsional dissipation dilution for quantum experiments and precision measurement. arXiv preprint arXiv:2112.08350.
- [2] Nayfeh A.H. (1981) Introduction to Perturbation Techniques. John Wiley & Sons.

Mode Localization of Electrostatically Coupled Shallow MEMS Arches

Hassen M. OUAKAD* and Ayman M. ALNEAMY**

*Department of Mechanical and Industrial Engineering, Sultan Qaboos University, Al-Khoudh, Muscat 123, Oman

**Department of Mechanical Engineering, Jazan University, Jazan 45142, Saudi Arabia

Abstract. This work examines the dynamic behavior of a micro-system design consisting of two electrostatically coupled shallow micro-arches and electrically excited using one stationary electrode. Such coupled arrangement develops nonlinear phenomena such as the multiple snap-through motions, which in turn portray certain mode veering/mode crossing and ultimately mode localization. Essentially, such rich nonlinear dynamics behavior would definitely lead to increasing the design sensitivity if used as a mode-localized micro-sensor. In addition, the use of two different beam configurations in one device offers the possibility of detecting two potential substances at the same time using the two coupled shallow micro-arches resonant peaks.

Introduction

Several research attempts have examined the nonlinear characteristics of single resonator-based micro-sensors in order to depict interesting nonlinear modal interaction behaviors, nevertheless, these structures have shown limitations especially when it comes to being sensitive to detect hazardous substances. Formerly, few groups [1, 2] attempted to design coupled structures to exploit the mode coupling phenomenon and to design extremely sensitive micro-sensors. Consequently, the aim of this research is to suggest and examine a micro-system design consisting of two shallow-arched microbeams coupled and excited electrostatically via one lower in-plane stationary electrode.

Results and Discussions

To examine the dynamic behavior of the coupled resonators, we excited the design using two actuation levels. In the first case, the lower beam actuation voltage is set to zero and the upper beam voltage is varying. Then, we increased the static voltage of the lower beam to 20 (V) and maintain similar actuation conditions for the upper beam. After that, we explore the effect of these excitation signals on the fundamental frequencies of both microbeams. Figure (1)(a) shows the variation in the first resonance frequency of the lower beam (dashed lines) and resonance frequency of the upper beam (solid lines). The veering phenomenon has been noticed for both cases where the lower beam frequency increases and the upper beam frequency decreases.

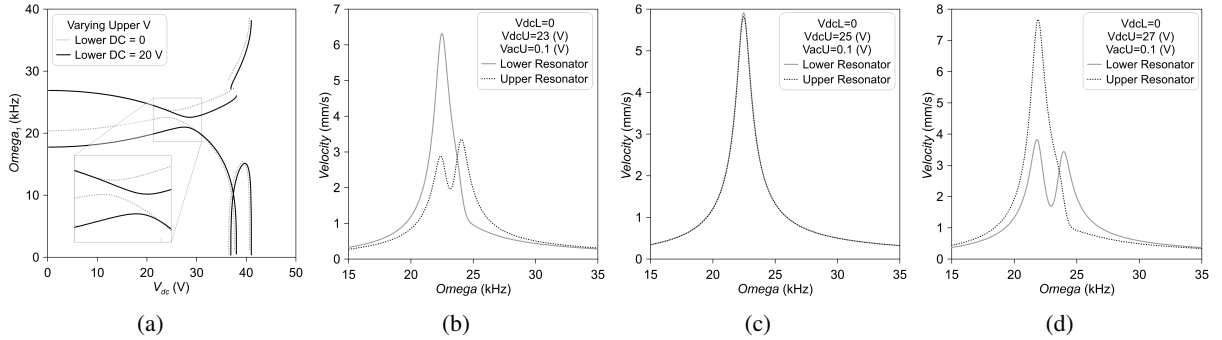


Figure 1: (a) The variation in the first resonance frequency of the lower beam and of the upper beam as a function of the upper static voltage and a lower voltage sets to 0 and 20 (V). Frequency-response curves of the two resonators: (a) before, (c) at and (d) after veering zone.

Furthermore, we examine the frequency-response curves of the first lower and upper resonance frequencies in the vicinity of the veering zone. Employing different excitation voltages will give further insights into the dynamic interaction between the two initially curved-up resonators and how the energy is exchanged among them as the voltage varies. Before entering the veering zone, linear responses have been computed for both resonators with two distinct peaks as shown in Fig. (1)(b). We note that a small peak appears in the vicinity of the fundamental frequency of the lower resonator indicating that an energy channel starts to be activated, however, most of the vibrating energy begins to be more localized at the lower resonator. Increasing the upper voltage leads to a merge between the two frequencies with a single peak as illustrated in Fig. (1)(c). Then, swapping between the two frequencies occurs with a peak dominated by the upper resonator as shown in Fig. (1)(d). This is true because the two frequencies start moving away from each other. Indeed, we carried out an analytical study of the vibration of weakly electrostatically coupled initially curved-up microbeams. Multiple nonlinear behaviors have been obtained which are useful for potential MEMS applications such as mode-localized based inertia sensors.

References

- [1] Morozov, N. F., Indeitsev, D. A., Igumnova, V. S., Lukin, A. V., Popov, I. A., & Shtukin, L. V. (2022). Nonlinear dynamics of mode-localized MEMS accelerometer with two electrostatically coupled microbeam sensing elements. *Int. J. Non-Linear Mech.*, **138**, 103852.
- [2] Song, J., Lyu, M., Kacem, N., Liu, P., Huang, Y., Fan, K., & Zhao, J. (2022). Exploiting bifurcation behaviors in parametrically excited mode-localized resonators for mass sensing. *J. Appl. Mech.*, **89**(11).

Nonlinear modeling of micro-cantilever beams

Ayman Alneamy*, Walter Lacarbonara** and Eihab Abdel-Rahman***

*Department of Mechanical Engineering, Jazan University, Jazan, Saudi Arabia

**Department of Structural and Geotechnical Engineering, Sapienza University of Rome, Rome, Italy

*** Department of Systems Design Engineering, University of Waterloo, Waterloo, ON, Canada

Abstract. In this work, we analytically examine the validity of using a standard nonlinear beam model of an electrostatic micro-cantilever beam compared to a geometrically exact theory that incorporates shear deformability, nonlinear bending curvature, inertia and longitudinal inextensibility. The results show that the geometrically exact model is more suitable to accurately capture the nonlinear behavior of electrostatic MEMS designs.

Introduction and Problem Formulation

The nonlinear characteristics of electrostatically excited micro-cantilever beams play an important role in determining their performance and suitability to design and manufacture useful devices. Here we provide analytical evidence of the importance of a geometrically exact approach when modeling electrostatic cantilever microbeams. The governing equation of motion of the microbeam is a consistent expansion of the geometrically exact equation of motion obtained in [1] and reads:

$$\begin{aligned} (1 - \frac{1}{2}\dot{v}^2)\ddot{v} + \dot{v}' \int_0^{\hat{s}} (\dot{v}'\ddot{v}' + \dot{v}'^2)d\hat{\xi} + \hat{c}\dot{v} + \dot{v}'' \int_{\hat{s}}^1 [\dot{v}'\ddot{v}' - \int_0^{\hat{\xi}} (\dot{v}'\ddot{v}' + (\dot{v}')^2)d\hat{z}]d\hat{\xi} + [\dot{v}'''' + \dot{v}''(\frac{1}{2}\dot{v}''\dot{v}'^2) \\ - \dot{v}'' \int_{\hat{s}}^1 \dot{v}''\dot{v}'''d\hat{\xi}] = \beta f_{es} \end{aligned}$$

where v denotes the transverse motion, the prime and over-dot indicate differentiation with respect to the arc-length and time, respectively, and f_{es} indicates the electrostatic force per unit length.

Results and Discussions

Variation of the tip-section static equilibria with the DC voltage was obtained by eliminating the time derivatives in the equation of motion and employing a ROM with one-, two-, and three-mode projection in the Galerkin expansion. We note that an odd number of mode shapes leads to faster and closer convergence than using an even number, see Fig. 1(a). Henceforth, we adopt the odd-mode ROM approximation in the rest of the static analysis. Then, we compare the results to those obtained using a standard nonlinear beam model [2] with three-modes projection and 2D-FEM models as shown in Fig. 1(b). A good agreement is observed between the proposed model and FEM results, however, the pull-in voltage is slightly higher than FEM model. This, in fact, is expected since the model is stiffer and requires more voltage to pull it down.

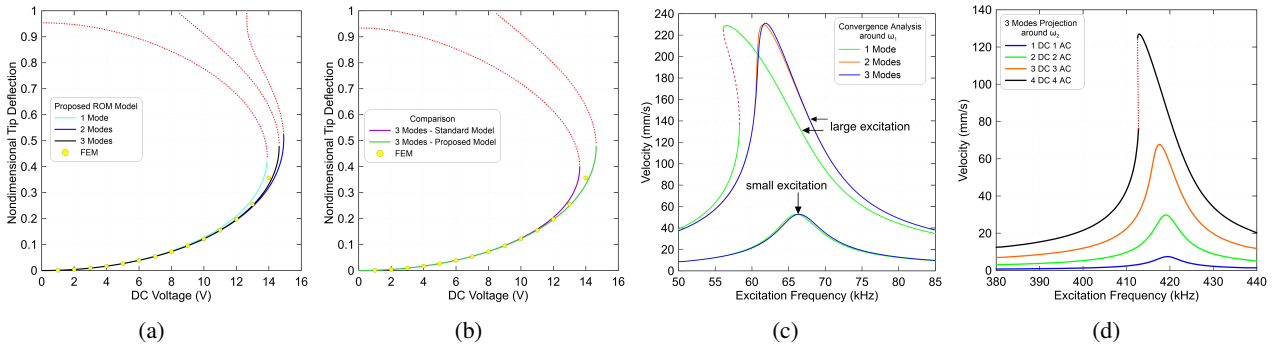


Figure 1: The tip deflection vs. DC voltage obtained considering: (a) 1-, 2- and 3-mode projection and (b) comparison of the standard and geometrically exact models. (c) Dynamic convergence analysis using the proposed model with 1-, 2- and 3-mode projections in the vicinity of the first natural frequency. (d) FRCs around the second natural frequency.

We carried out a dynamic convergence analysis to determine the minimum number of modes required in the expansion. To this end, we obtained the frequency response curves in the vicinity of the first natural frequency with varying actuation waveforms. Figure 1(c) shows that three modes are also required for convergent and robust results. This finding is consistent with that obtained for the static results. We also obtained the frequency-response curves in the vicinity of the second natural frequency under four excitation levels. We note that the response is slightly softening for the second mode. The fully nonlinear model accounts correctly for the inertia and bending curvature nonlinearities as well as the electrostatic nonlinearity.

References

- [1] W Lacarbonara (2013) Nonlinear structural mechanics: theory, dynamical phenomena and modeling. Springer, New York.
- [2] M Younis, E Abdel-Rahman, and A Nayfeh. (2003) A reduced-order model for electrically actuated microbeam-based MEMS. *J. Microelectromechanical Syst* **12.5** : 672-680.

Differential capacitance gas sensors

Fehmi Najar¹, Mehdi Ghommem², Samed Kocer³, Alaaeldin Elhady³, and Eihab Abdel-Rahman³
¹ Applied Mechanics and Systems Research Laboratory (LR03ES06), Tunisia Polytechnic School, University of Carthage, Tunis, Tunisia, ORCID # 0000-0003-3545-809X
² Department of Mechanical Engineering, American University of Sharjah, UAE, , ORCID #0000-0002-8451-8805
³ Systems Design Engineering, University of Waterloo, Waterloo, Ontario, Canada

Abstract. In this work, we investigate the use of modal interactions in asymmetrically actuated electrostatic arch microbeams to realize high sensitivity and high signal-to-noise ratio (SNR) inertial gas sensors. The sensors are made of fixed-fixed microbeams with an actuation electrode extending over half the beam span. We exploit the asymmetry in the beam motions to induce significant rotary motions and realize differential capacitance gas sensors.

Introduction

Given the rich dynamics of electrostatically actuated arch microbeams, several studies have examined their potential use in sensing and actuation. For instance, Najar et al. [1] demonstrated the potential of electrostatic initially-curved microbeams to serve as bifurcation gas sensors in either binary mode, by monitoring for an abrupt transition from regular periodic motions to chaotic motions upon gas detection, or analog mode, by relating the measured RMS of the response amplitude of phase angle to the gas concentration. Arabi et al. [2] reported MEMS static bifurcation sensors for the detection of volatile organic compounds. They demonstrated the capability of their sensors to detect 1 ppm of formaldehyde in a competitive environment including benzene. This work focuses on exploiting the interaction between the symmetric and asymmetric modes of arch beams to enhance the sensitivity of gas detection.

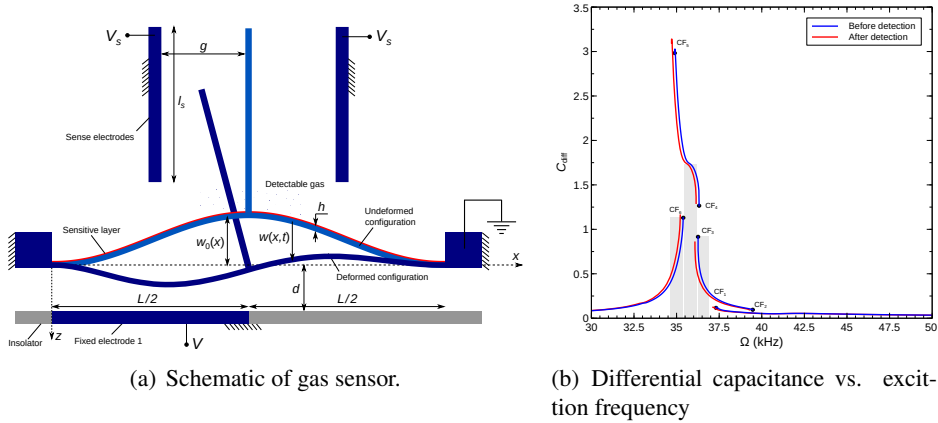


Figure 1: Differential capacitance gas sensor: (a) top view and (b) frequency response before and after detection.

Results and Discussion

The gas sensor under study, Figure 1(a), is made of a clamped-clamped shallow arch. It is electrically actuated by a voltage drop $V(t)$ between the beam and a side electrode. Half-electrode actuation is employed to activate of higher symmetric and anti-symmetric vibration modes. The sensor uses differential capacitive sensing facilitated by a rigid transverse arm connected to the microbeam at its mid-point. The arm is placed at an equal distance from right and left sense electrodes. The sensor is grounded while the sense electrodes are held at a common DC voltage V_s . The detection signal is the difference between the capacitance of a ‘left capacitor’ formed by the rigid arm and the left sense electrode and that of a ‘right capacitor’. In addition to rejecting common mode (parasitic) capacitance, this sensor design amplifies the signal generated by the rotary motions of the rigid arm induced by asymmetry in the sensor response.

A nonlinear dynamic reduced-order model of the sensor is developed and validated experimentally. It is then used to predict the sensor response and identify its bifurcations. The proposed sensor operates across bifurcations that trigger a sudden transition from nearly symmetric to strongly asymmetric beam motions and, therefore, large rotary motions of the rigid arm. The frequency-response curves before and after gas detection are shown in Figure 1(b). Differential capacitance is shown to be an effective sensor measurand when operating across an appropriate cyclic-fold bifurcation.

References

- [1] Najar F. et al. (2021) Arch microbeam bifurcation gas sensors. *Nonlinear Dynamics* **104**:923–940.
- [2] Arabi et al. (2022) Detection of Volatile Organic Compounds by Using MEMS Sensors. *Sensors* **22**:4102.

How to excite anti-symmetric modes in a symmetric MEMS?

Sasan Rahmanian^{1,2}, Ayman Alneamy³, Yasser S. Shama^{1,2,4}, Samed Kocer^{1,2}, Eihab M. Abdel-Rahman^{1,2}, and Mustafa Yavuz^{2,5}

¹Systems Design Engineering, University of Waterloo, Waterloo, ON N2L 3G1, Canada

²Waterloo Institute for Nanotechnology (WIN), University of Waterloo, Waterloo, ON N2L 3G1, Canada

³Department of Mechanical Engineering, Jazan University, Jazan, Saudi Arabia

⁴Mechanical Engineering Department, Benha Faculty of Engineering, Benha University, Benha, Egypt

⁵Mechanical and Mechatronics Engineering Department, University of Waterloo, Waterloo, ON N2L 3G1, Canada

Abstract. This study reports on experimental investigation of modal interaction in a symmetric electrostatically driven micro resonator. The MEMS is made of a clamped-clamped curved-beam electrostatically actuated via a side electrode. A two-to-one ratio exists by design between the second natural frequency (first anti-symmetric in-plane bending mode) and the third natural frequency (second symmetric in-plane bending mode). Because the beam, its boundary conditions, and its actuation force are all symmetric, anti-symmetric modes cannot be directly excited due to the null projection of the excitation force onto the modes. This study shows that those anti-symmetric modes can be indirectly excited by channelling energy from a symmetric mode to the target anti-symmetric mode. The results reveal energy transfer from the directly excited second symmetric mode to the first anti-symmetric mode resulting in an M-shape frequency-response curve with trivial and large-amplitude stable branches.

Introduction

Nonlinear dynamics in Micro-Electro-Mechanical Systems (MEMS) features interesting phenomena that can be employed to improve the performance of MEMS actuators and sensors. In recent years, nonlinear modal interaction has become the focus of attention of many researchers working on the dynamics of MEMS. This phenomenon forms an energy channel between two vibration modes of structures under a special condition, the existence of a commensurate ratio between their natural frequencies. The vibrations of the two modes may occur in one direction [1] or in two perpendicular directions [2]. To the best of our knowledge, modal interactions between symmetric and anti-symmetric modes in electrostatic MEMS resonators are yet to be addressed.

Results and discussion

To excite the first anti-symmetric mode, the MEMS is excited with an electrostatic force whose frequency varies near the third natural frequency to directly excite the second-symmetric mode, thereby indirectly exciting the first anti-symmetric mode ‘from above’. The measured frequency-response curve of the MEMS is M-shaped composed of both trivial and non-trivial stable branches. A Laser Doppler Vibrometer (LDV) was used to measure the velocity of the microbeam optically. To this aim, we put the laser spot on the second-symmetric mode node to measure only the contribution of the first anti-symmetric mode in constructing the MEMS response. As seen in figure 1, while the AC voltage amplitude is set to be 52.5V, below the activation level of modal interaction, no motion is sensed at this degree-of-freedom. However, as the electrostatic force increases further, the energy channel forms between the two engaged modes, causing the first anti-symmetric mode to be excited, interacting with the second-symmetric mode, creating an M-shape steady-state dynamics.

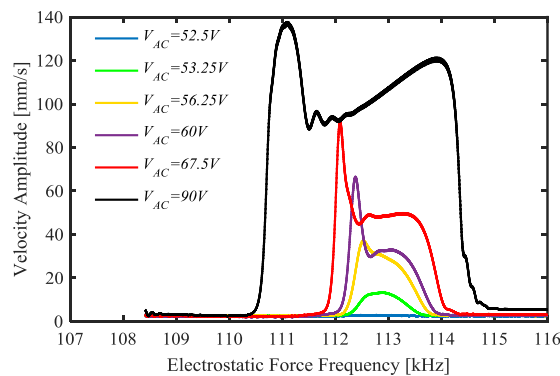


Figure 1: Measured frequency-response behaviour of the MEMS for different values of the AC voltage. The laser spot was focused on the second symmetric mode node, measuring the first anti-symmetric mode contribution.

References

- [1] L. Ruzziconi, N. Jaber, L. Kosuru, M. L. Bellaredj, and M. I. Younis, "Experimental and theoretical investigation of the 2: 1 internal resonance in the higher-order modes of a MEMS microbeam at elevated excitations," *Journal of Sound and Vibration*, vol. 499, p. 115983, 2021.
- [2] R. Wang, C. Xia, D. F. Wang, and T. Ono, "A high-frequency narrow-band filtering mechanism based on auto-parametric internal resonance," in *2021 IEEE 16th International Conference on Nano/Micro Engineered and Molecular Systems (NEMS)*, 2021, pp. 670-675: IEEE.

The response of nonlinear circular viscoelastic panels to electrodynamic excitation

Anish Kumar* and Oded Gottlieb**

*Department of Mechanical Engineering, JK Lakshmipat University, Jaipur, Rajasthan, India

**Department of Mechanical Engineering, Technion-Israel Institute of Technology, Haifa, Israel

Abstract. We investigate the response of nonlinear circular micro- and nano- viscoelastic panels that are subjected to electrodynamic excitation. We make use of a von-Karman strain-displacement relation with a Voigt-Kelvin constitutive law to derive a nonlinear initial-boundary-value problem that consistently incorporates viscoelastic damping in both the field equation and corresponding compatibility condition. A multi-mode dynamical system is then obtained via a Galerkin ansatz which includes coupled linear and nonlinear contributions for both stiffness and damping augmented by combined parametric and external excitation terms. A detailed numerical investigation of the resulting model enables a consistent construction of the dynamical system frequency response culminating with multiple combination and internal resonances which demonstrate the significant contribution of non-negligible nonlinear viscoelastic damping.

Introduction and Problem Formulation

Circular micro and nanopanels are widely used in various applications such as sensors and actuators. Experiments show that damping increases significantly with amplitude increase with both external [1] or self-excited excitation [2]. We thus extend the formulation of Vogl and Nayfeh [3] for a circular nonlinear von-Karman plate [4] by incorporating the contribution of viscoelastic damping based on a Voigt-Kelvin constitutive law in addition to linear viscous damping. A schematic diagram of a clamped circular plate subjected to electrodynamic excitation is depicted in Figure 1(left). A multi-mode dynamical system is then obtained via a Galerkin ansatz which includes coupled linear and nonlinear contributions for both stiffness and damping augmented by combined parametric and external excitation terms derived from a parallel-plate electrodynamic model.

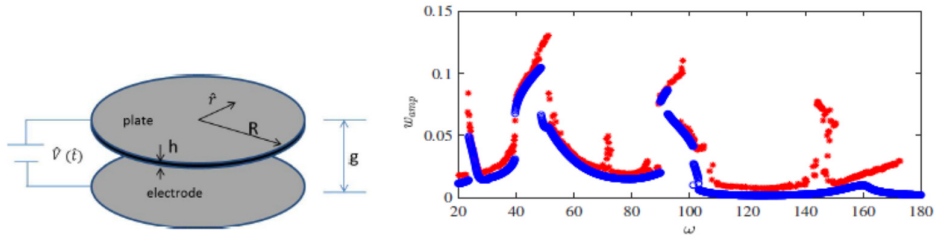


Figure 1: Definition sketch (left) and frequency response curves (right) depicting primary internal resonances and secondary ultra-subharmonic resonances with linear viscous damping (red) and combined linear and nonlinear viscoelastic damping (blue).

Results and Discussion

We investigate the frequency response for three mode interaction and compare the dynamical system frequency response with the linear viscous damping model [3] to a system governed by combined linear and nonlinear viscoelastic damping where the magnitude of the linear viscoelastic damping component is identical to that of the linear viscous damping. We consider combined external and parametric excitation of the first three modes to capture primary, parametric, internal and combination resonances. We present the resulting frequency response curves in Figure 1 (right) where system response to linear viscous damping is portrayed in red and the response to combined linear and nonlinear viscoelastic damping is portrayed in blue. Note that the selected first three natural frequencies associated with the first axi-symmetric modes ($\omega_{1,2,3} = 51.94, 92.29, 155.80$), yield a condition for a 3:2:1 internal resonance demonstrating in Figure 1 (right) that consideration of only linear viscous damping can lead to erroneous conclusion of response magnitude. A detailed numerical investigation of the resulting model thus enables a consistent construction of the dynamical system frequency response culminating with multiple combination and internal resonances which demonstrate the significant contribution of non-negligible nonlinear viscoelastic damping.

References

- [1] Amabili M. (2018). Nonlinear damping in nonlinear vibrations of rectangular plates: Derivation from viscoelasticity and experimental validation. *J. Mechanics and Physics of Solids* **118**: 275-292.
- [2] Hollander E. and Gottlieb O. (2021). Global bifurcations and homoclinic chaos in nonlinear panel optomechanical resonators under combined thermal and radiation stresses. *Nonlinear Dynamics* **103**: 3371-3405.
- [3] Vogl G.W. and Nayfeh A.H. (2005). A reduced model for electrically actuated clamped circular plates. *J. Micromechanics and Microengineering* **315**: 684-690.
- [4] Nayfeh A.H. and Pai, P. F (2004). *Linear and Nonlinear Structural Mechanics*, Wiley, NY.

Multiple internal resonances and impacting dynamics of micromachined arch resonators

Laura Ruzziconi^{*}, Rodrigo T. Rocha^{**}, Wen Zhao^{**}, Amal Z. Hajjaj^{***} and Mohammad I. Younis^{**,****}

^{*}Faculty of Engineering, eCampus University, 22060 Novedrate, Italy

^{**}King Abdullah University of Science and Technology (KAUST), 23955-6900 Thuwal, Saudi Arabia

^{***}School of Mechanical, Electrical, and Manufacturing Engineering, Loughborough University, Loughborough, UK

^{****}Department of Mechanical Engineering, State University of New York at Binghamton, Binghamton, NY 13902, USA

Abstract. The present study investigates the experimental response of an electrically actuated microbeam-based MEMS resonator with arched configuration of concave surface. The resonator is excited using an antisymmetric partial electrode. Forward and backward frequency sweeps are acquired. The device exhibits M-shaped 2:1 internal resonance between the first (first symmetric) and the second (first antisymmetric) mode, showing softening and hardening bending behaviour. We observe the profound coupling induced by the 2:1 internal resonance between these modes. As increasing the oscillations amplitude, the microbeam impacts with the substrate. A specially deposited dielectric layer allows the system to impact with the substrate while preventing electrical shorts. Driven by the impacts, the experimental response shows the activation of additional internal resonances, where the two successive higher-order modes are involved and combined with the main M-shaped 2:1 internal resonance. The experimental dynamics are analysed extensively to investigate the underlying physical phenomena arising in the MEMS response.

Introduction

Specific relationships among the natural frequencies can induce multimode nonlinear interactions [1]. This complexity offers outstanding capabilities for MEMS/NEMS applications [2]. The possibility of activating internal resonances by driving the system into impacts has been recently investigated [3]. Motivated by the increasing interest in operating devices in regime of internal resonance, in the present study we experimentally and theoretically analyse the activation of multiple internal resonances in an arched MEMS device electrically actuated.

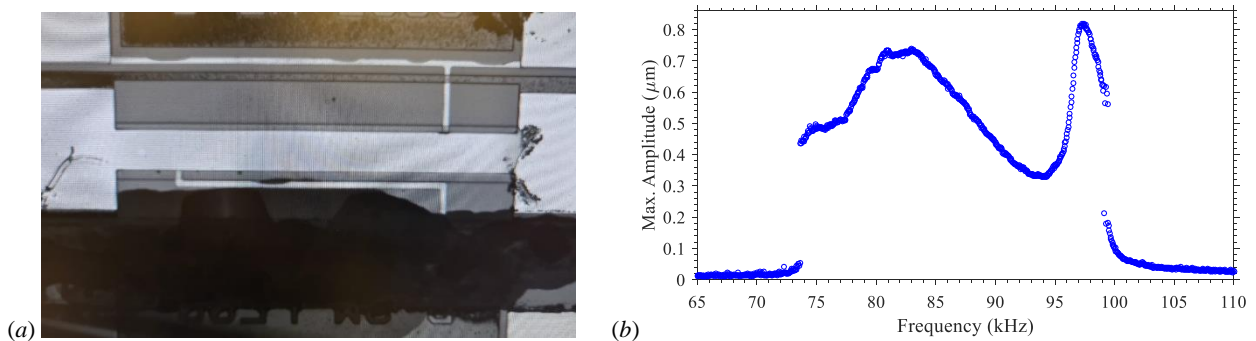


Figure 1: (a) The MEMS device (optical image). (b) Experimental frequency response diagram (amplitude versus drive frequency), at $V_{DC} = 15.0$ V and $V_{AC} = 28.6$ V (backward sweep).

Results and discussion

The MEMS device experimentally tested is shown in Fig. 1(a). It consists of an electrically actuated clamped-clamped microbeam with arched configuration of concave surface. This configuration is a consequence of imperfections due to the fabrication process and residual stress. The device presents a dielectric layer to prevent short-circuiting in case of impact with the substrate. Experimental frequency sweeps are acquired, Fig. 1(b). The experimental response exhibits M-shaped 2:1 internal resonance between the first and second modes. As increasing the oscillations amplitude, the microbeam impacts with the substrate. Due to the impacts, additional resonances related to higher-order modes get activated, which are coupled among each other and with the principal M-shaped 2:1 internal resonance. Simulations are developed based on Galerkin reduced-order model accounting for the modes involved in the multiple internal resonances experimentally observed. To model impacts, the substrate is assumed as a nonlinear elastic foundation, which is described in the framework of the Hertz impact model and Hunt-Crossley damping model [3]. A deep analytical study is developed to capture the characteristics of the MEMS behaviour and to characterise the potential rich and complex dynamics.

References

- [1] Nayfeh A.H. (2000) *Nonlinear Interactions: Analytical, Computational, and Experimental Methods*. Wiley-Interscience.
- [2] Asadi K., Yu J., Cho H. (2018) Nonlinear couplings and energy transfers in micro- and nano-mechanical resonators: Intermodal coupling, internal resonance and synchronization. *Philos. Trans. R. Soc. A Math. Phys. Eng. Sci.* **376**:20170141.
- [3] Ruzziconi L., Jaber N., Kosuru L., Younis M.I. (2022) Activating internal resonance in a microelectromechanical system by inducing impacts. *Nonlinear Dyn.* <https://doi.org/10.1007/s11071-022-07706-x>.

Control of an electrostatically actuated micro portal frame with 2:1 internal resonance subjected to damping disturbances

Wagner B. Lenz^{#,*}, Rodrigo T. Rocha^{#,*}, Fahimullah Khan^{*}, Yousef Algoos^{*} and Mohammad I. Younis^{*,**,**}

^{*}King Abdullah University of Science and Technology, Thuwal 23955, Saudi Arabia

^{**}State University of New York, Binghamton, NY, USA

^{***}Corresponding author

[#]Contributed equally

Abstract. This work aims to electrostatically control a micro portal frame, modeled as a two-degrees-of-freedom (2DOFs) system with 2:1 internal resonance between the second (Y-direction motion) and first (X-direction motion) modes. To avoid the irregular behaviors under the saturation phenomenon within the internal resonance, we propose to use the Linear Quadratic Regulator (LQR) control technique to create an electrostatic force that alleviates the damping effect. A comparison between the efficiency of an ideal control and considering the actuator in the control is highlighted.

Introduction

The dynamics of microelectromechanical systems (MEMS) have been extensively investigated due to the presence of many nonlinear behaviors that arise from excitation and geometric nonlinearities. One of the most intriguing nonlinear phenomena observed in MEMS resonators is internal, or autoparametric, resonance, which occurs when there is a commensurate ratio of the resonance frequencies between two modes of vibration [1,2]. Micro compound resonators have rich dynamics and are very promising to be used in applications, such as the U-shape (portal frame), in which the saturation phenomenon has been shown recently due to 2:1 internal resonance [3]. However, this nonlinear dynamic phenomenon is strongly affected by damping [3], either being suppressed or leading to irregular behaviors due to environmental pressure variations, which compromises the potential practical usage of the device. Therefore, we propose the application of the Linear Quadratic Regulator (LQR) control technique to create an electrostatic counter force that alleviates the pressure effect. The schematic of the utilized micro portal frame is shown in Fig. 1a. The microstructure is subjected to an electrostatic force, by a DC actuation voltage V_{dc} and an AC harmonic voltage V_{ac} , which actuates the 2nd mode, through two electrodes. One electrode is placed on top of the supported beam (Electrode B) and the other is placed on the column (Electrode A), which is used only for control purposes in the 1st mode direction. Control signals V_{cx} and V_{cy} are applied to electrodes A and B to control the 1st and 2nd modes of vibration, respectively. After validating the experimental results, numerical simulations showed that the 2:1 internal resonance is activated and the saturation phenomenon occurs when the structure is actuated with $V_{dc} = 46V$. However, the dynamic behavior can highly change depending on the damping ratio [3]. Fig. 1b shows the Maximum Lyapunov exponent map to the variation of the damping coefficient (ζ) and the AC excitation. Note that at high the AC and the small ζ (lower environmental pressure), chaotic behavior is observed. To control the chaotic behavior, the LQR control technique is implemented to actuate both 1st and 2nd modes. Fig. 1c and 1d show the 1st and 2nd modes phase portraits, respectively, with and without control. Note that applying $V_{cx} = V_{cy} = 15V$ is sufficient to control the chaotic behavior and maintains a stable periodic orbit, which yields a clear signal that improves the readability of the electrical signal for sensing purposes.

Results and discussion

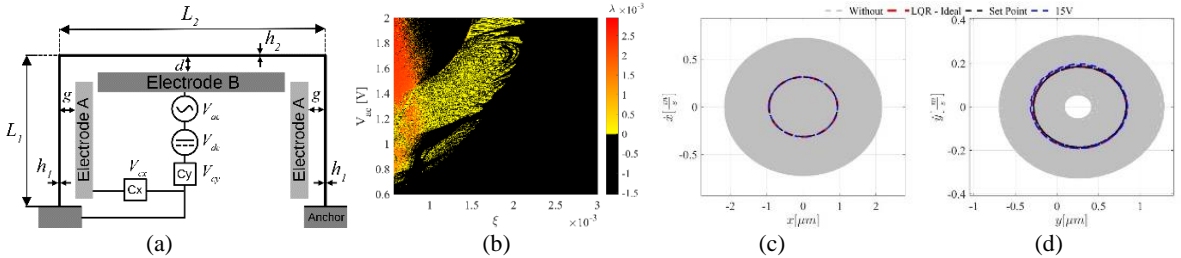


Figure 1: (a) Micro portal frame schematic. (b) Maximum Lyapunov exponent map depending on the damping coefficient and the AC excitation. (c), (d) 1st and 2nd modes phase portraits, respectively, with and without the controls. Red lines show the ideal control applied to the system while the blue dotted lines are the control implemented as an electrostatic force.

This work showed the control of the chaotic behavior when there is 2:1 internal resonance activation. The control shown to be very efficient in converting chaos into a periodic orbit, mainly when the control is implemented as the electrostatic force (V_{cx} and V_{cy}).

References

- [1] Hajjaj, A. Z., Hafiz, M. A., Younis, M. I. (2017). Mode coupling and nonlinear resonances of MEMS arch resonators for bandpass filters. Scientific reports, 7(1):1-7.
- [2] Antonio, D., Zanette, D. H., López, D. (2012). Frequency stabilization in nonlinear micromechanical oscillators. Nature communications, 3(1): 1-6.
- [3] Rocha, R. T., Younis, M. I. (2022). Nonlinear mode saturation in a U-shaped micro-resonator. Scientific reports, 12(1):1-9.

Amplitude-Voltage Response of Superharmonic Resonance of Fourth Order of Electrostatically Actuated MEMS Cantilever Resonators

Dumitru I. Caruntu* and Christopher I. Reyes*

*Department of Mechanical and Aerospace Engineering, University of Texas Rio Grande Valley, Edinburg, TX, USA

Abstract. This paper deals with amplitude-voltage response of electrostatically actuated MEMS cantilever resonator sensors undergoing a superharmonic resonance of fourth order. The system consists of a MEMS cantilever parallel to a ground plate and under an alternating current (AC) producing a hard excitation. The AC frequency is near one eighth of the first natural frequency of the cantilever. This leads to superharmonic resonance of fourth order (or order four). The electrostatic force includes fringe effect and it is modeled using Palmer's formula. The methods used in this work are 1) the method of multiple scales (MMS), 2) homotopy analysis method (HAM), and 3) numerical integration of reduced order model (ROM) using 2 modes (terms) of vibration. The amplitude-voltage response shows a softening effect and two saddle-node bifurcation points. All three methods are in agreement for moderate dimensionless voltage parameter (less than 0.8). The effects of damping, fringe, and detuning frequency on the voltage response are reported. As the damping increases the peak amplitude decreases. As fringe and/or detuning frequency increase the saddle-node bifurcation points shift to lower voltages.

Introduction

This work investigates a MEMS cantilever resonator undergoing superharmonic resonance of order four. This superharmonic resonance case requires hard excitations where the dimensionless voltage applied is greater than 0.5, otherwise the response is too small. MEMS cantilevers have gained in interest over the last couple of decades due to their potential applications in switches, sensors, filters, resonators, energy harvesters, micro probes, and micro pumps. These systems are advantageous in that they have a low fabrication cost, low energy requirement, are light weight, and can be placed in virtually any system due to their micro size. Superharmonic resonances of second order for MEMS devices have been reported in the literature [1].

In this work the MEMS cantilever is modeled as an Euler-Bernoulli beam, Fig. 1. The frequency of the AC voltage applied between the MEMS cantilever and the ground plate is near one eighth of the first natural frequency of the cantilever beam. The electrostatic force actuating the MEMS cantilever includes the fringe effect which is an additional electrostatic force outside of the control volume between the parallel plates, Palmer formula [2].

Results and discussion

Figure 2 shows the amplitude-voltage response using MMS, HAM, and 2T ROM time responses. The MMS, HAM and 2T ROM time responses are in agreement. The two saddle-node bifurcation points *A* and *B* predicted by MMS and HAM, are not contradicted by the time responses. However, time responses predict larger amplitude and lower voltage for the bifurcation point *B*. Also, time responses predict a slightly greater softening effect. As the voltage is sweep up, the system experiences stability and a steady increase in amplitude until the bifurcation point *A* is reached. At this point the system loses stability and jumps to a slightly higher amplitude on the second stable branch. As the voltage is continued to increase the system decreases in amplitude reaching the non-resonant region where in the amplitudes begin to slowly increase. As the voltage is swept down the system experiences stability and an increase in amplitude until reaching the bifurcation point *B* where the system loses stability and jumps to a lower amplitude. As the voltage decreases to zero, the amplitude decreases to zero.

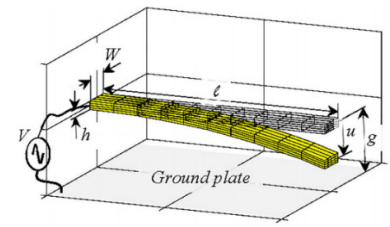


Figure 1: MEMS cantilever

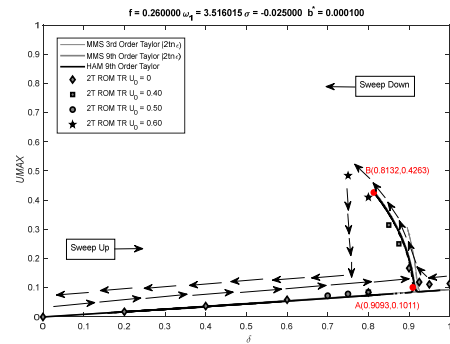


Figure 2: Amplitude (U_{max}) – voltage (δ) response

References

- [1] Caruntu D., Botello M., Reyes C., Beatriz J. (2019) Voltage-Amplitude Response of Superharmonic Resonance of Second Order of Electrostatically Actuated MEMS Cantilever Resonators. *J. Comput. Nonlin. Dyn.* **14**: 031005 (8 pages).
- [2] Batra R.C., Porfiri M., Spinello D. (2006) Electromechanical Model of Electrically Actuated Narrow Microbeams. *J. Microelectromech. Syst.* **15**(5): 1175–1189.

Vibration mitigation by two parametric anti-resonances in high-Q resonators: a preliminary case study

Miguel Ramírez-Barrios* and Fadi Dohnal **

*Professional Interdisciplinary Unit of Biotechnology, National Polytechnic Institute, Mexico, ORCID
#0000-0001-9720-1295

**Research Center for Microtechnology, University of Applied Sciences Vorarlberg, 6850 Dornbirn, Austria, ORCID
#0000-0002-9289-4069

Abstract. The anti-resonance is a well-known phenomenon for two degrees of Freedom (DOF) systems; this contribution presents a potential application of this concept to cancel the transient vibrations. The technique applies two pulses of parametric excitation adequately tuned at the anti-resonance frequencies. A simulation experiment of an array of microelectromechanical systems (MEMS) with three DOF is presented.

Introduction

MEMS with a high-quality factor ($Q = \omega_i/\gamma_i$) have been used in many applications; they have high damping; nevertheless, their transition time to a steady state (t_{ss}) is too long. In [1,2] is presented a technique to reduce t_{ss} using the anti-resonance effect. This contribution describes an improvement and extension of this technique.

Results

The simplified dynamic model of a high-Q MEMS for a beam can be described by $\ddot{x} + \gamma_1 \dot{x} + \omega_1^2 x = 0$; here, the free enveloped response presents a long t_{ss} , as is shown in Fig 1 a). Then, if two beams with a very close natural frequency are added and coupled by a periodic signal, the resulting system can be described by Let the system of equations:

$$\ddot{x} + \Gamma \dot{x} + (\Omega + B_1 \beta_1 \eta(t) + B_2 \beta_2 \nu(t)) x = 0 \quad (1)$$

where $\Gamma = \begin{bmatrix} \gamma_1 & 0 & 0 \\ 0 & \gamma_2 & 0 \\ 0 & 0 & \gamma_3 \end{bmatrix}$, $\Omega = \begin{bmatrix} \omega_1^2 & 0 & 0 \\ 0 & \omega_2^2 & 0 \\ 0 & 0 & \omega_3^2 \end{bmatrix}$, $B_1 = \begin{bmatrix} 0 & b_{12} & 0 \\ b_{21} & 0 & 0 \\ 0 & 0 & 0 \end{bmatrix}$, $B_2 = \begin{bmatrix} 0 & 0 & b_{13} \\ 0 & 0 & 0 \\ b_{31} & 0 & 0 \end{bmatrix}$, $\eta(t) = \cos(\omega_{p1}t)$ and $\nu(t) = \cos(\omega_{p2}t)$. Then, the system (1), is coupled by two parametric excitation signals at frequencies $\omega_{p1} = \omega_2 - \omega_1$ and $\omega_{p2} = \omega_3 - \omega_1$. The parametric excitation signals are applied in a short period t_{pulse} , named pulses. [1] provides a formula to compute t_{pulse} . Simulating the equations for some values of γ_i , ω_i and b_{ij} in the Fig. 1 the results are shown. Fig. a) depicts the free enveloped response of the system in the first mode $x_1(t)$, which can be observed as $t_{ss} = 0.1$ sec. Fig b) presents the response under the pulses of parametric excitation $\eta(t)$ and $\nu(t)$, where the t_{ss} is reduced to 6.6 ms. The excitation pulse's effect is rapidly transferring the vibrations from the first mode to the other two modes acting as dampers once the excitation pulse is over.

References

- [1] Ramírez-Barrios M., Dohnal F., Collado J.(2020). Enhanced vibration decay in high-Q resonators by confined of parametric excitation. *Archive of Applied Mechanics* **90**:1673–1684.
- [2] Ramírez-Barrios, M., Dohnal, F., Collado, J. (2020). Transient Vibrations Suppression in Parametrically Excited Resonators. *LASIRS 2019. Mechanisms and Machine Science*, vol 86. Springer, Cham.

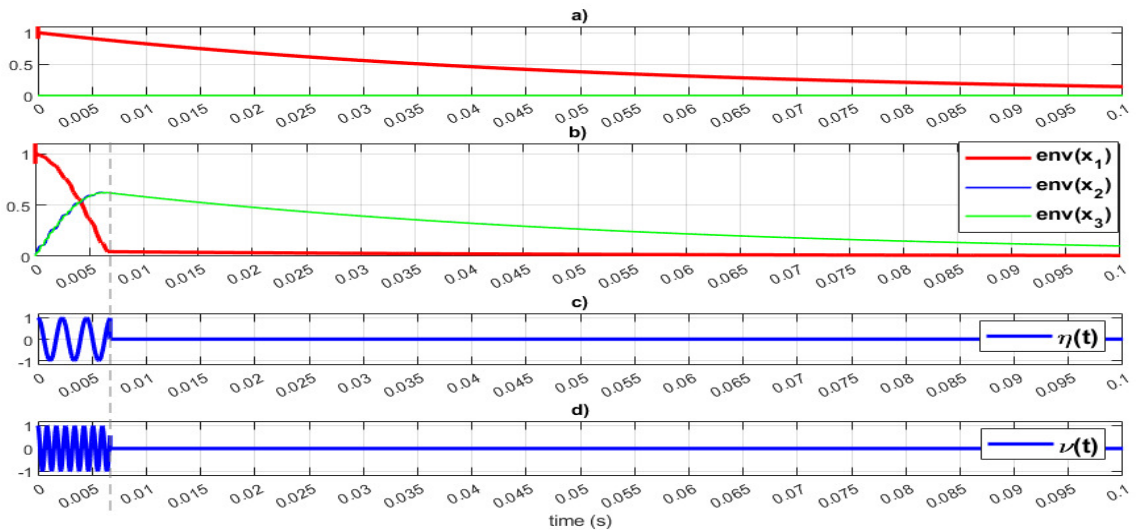


Figure 1:

Detection of pull-in and periodic solutions of magMEMS model using Sturm's theorem

Piotr Skrzypacz*, Bek Kabduali*, and Grant Ellis**,

*Mathematics Department, Nazarbayev University, Astana, Kazakhstan, ORCID 0000-0001-6422-5469

**Independent Researcher, Panang, Malaysia, ORCID 0000-0003-2874-1276

Abstract. An algorithm based on Sturm's theorem is developed to predict and identify periodic and pull-in solutions for a model of magnetic actuator arising from the design of a magnetic Micro-Electro-Mechanical Structure (magMEMS) with current carrying filaments. Numerical simulations are performed to verify the proposed algorithm. The obtained results are useful for understanding the operation of single-degree-of-freedom magMEMS.

Introduction

The operation of magnetic Micro-Electro-Mechanical Structures (MEMS) is affected by a pull-in effect which occurs at certain thresholds. Detection of pull-in in the magnetostatic actuation is necessary for the design and operation of magMEMS devices. Dynamic pull-in phenomena in actuators are effects of certain combination of kinetic and potential energies resulting in the collapse of the moving structure. MEMS with magnetic actuation offer better performance than traditional MEMS with electrostatic actuation due to the generation of much larger force and fields that diminish more slowly with distance. The goal of this work is to present an algorithm that for given system parameters can predict with high accuracy the periodic solution of magMEMS model with current-carrying filaments, see Fig. 1, to avoid the dynamic pull-in.

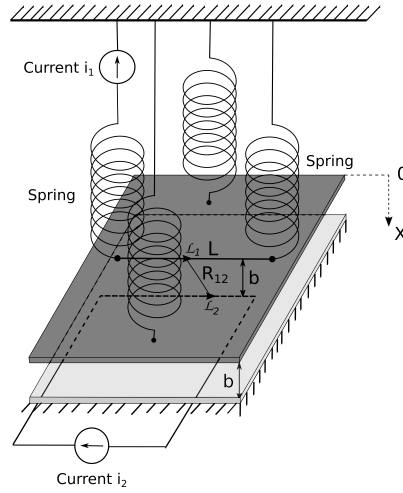


Figure 1: MagMEMS with current-carrying filaments.

Application of Sturm's theorem to detect dynamic pull-in

The motion of the wire can be described as a motion of point mass using a dynamic lumped parameter differential equation and can be derived from the second Newton's law of motion. The resulting zero initial value problem in the dimensionless form reads as follows

$$\ddot{x} + x - K \left[\frac{\xi^2 (1-x)}{\sqrt{\xi^2 (1-x)^2 + 1}} + \frac{1}{(1-x)\sqrt{\xi^2 (1-x)^2 + 1}} - \xi \right] = 0, \quad (1)$$

where the actuation and geometry parameters are given by $K = \frac{\mu_0 i_1 i_2 L}{2\pi k b^2}$, and $\xi = \frac{b}{L}$, respectively, cf. [2]. It is assumed that the currents in both wires are unidirectional, i.e., $K \geq 0$. Notice that for $\xi \rightarrow 0^+$ the motion of the filament is caused by the magnetic field of an infinite current-carrying conductor. In that case solutions are periodic if $K < K_0^*$ whereas the touch-down occurs if $K > K_0^*$ where the dynamic pull-in threshold is given by $K_0^* = 0.203632188 \dots$, cf. [1]. The solution $x(t)$ to zero initial value problem for Eq. (1) is periodic if and only if its phase diagram, x vs. \dot{x} , is a closed curve. In the case of small values of the parameter ξ , the existence of periodic solutions is ensured if $\tilde{f}_{K,\xi}(s) = -s^2 - 2K \log |1-s| - 2Ks\xi - \frac{1}{2}Ks(s-2)\xi^2$ has a root in $(0, 1)$. The existence of roots of the function $\tilde{f}_{K,\xi}(s)$ can be precisely deduced from the Sturm's theorem.

References

- [1] He, J.-H., Nurakhmetov, D., Skrzypacz, P., Wei (2021) D. Dynamic pull-in for microelectromechanical device with a current-carrying conductor. *J Low Freq Noise Vib Active Contr* **2021**; **40**(2): 1059-1066.
- [2] Skrzypacz P., Ellis G., He J.-H., He C.-H.: Dynamic pull-in and oscillations of current-carrying filaments in magnetic micro-electro-mechanical system. *Commun Nonlinear Sci Numer Simul* **109** (2022) 106350

Emergence of nonlinear damping in nanomechanical systems from thermal interactions

Ali Sarafraz*, and Farbod Alijani*

* Department of Precision and Microsystems Engineering, Faculty of Mechanical, Maritime and Materials Engineering, Delft University of Technology, 2628 CD, Delft, The Netherlands.

Abstract. Atomically thin structures exhibit nonlinear damping that is amplitude-dependent. Different sources for this nonlinearity have been hypothesized, but consensus has not been reached. By performing molecular dynamics simulations, we show that nonlinear damping can emerge from coupling to a thermal bath. We perform ring-down with two different configurations. While an isolated crystalline membrane did not show signatures of nonlinear damping, we find that by linking the same system to a heat bath, ring-down measurements show two thermalization time constants. To confirm our observation, we use nonlinear membrane theory, couple it to a Nose-Hoover thermostat, and find that nonlinear damping is mediated through a quadratic coupling to the heat bath. Our simulations highlight the microscopic origins of damping in nanostructures, demonstrating the influence of heat baths in nonlinear dissipation processes experimentally probed in nanomechanical systems.

Introduction

Unlike typical macroscale structures that exhibit linear damping under external harmonic loadings, atomically thin structures tend to display amplitude-dependent nonlinear behaviour. Different physical sources for this behaviour have been enumerated, including coupling between flexural modes and in-plane phonons [1] and internal resonance [2]. Several studies have proposed that energy transfer between a structure and a thermal bath could also result in nonlinear damping [3]. However, it is hypothesized that these secondary resonators (thermal baths) mostly operate at particular resonances. In order to combine statistical thermodynamics and Newtonian mechanics for particles, molecular dynamics simulations have utilized thermostats to simulate thermal bath energy interactions. These thermostats are designed so that the entire system containing the nanostructure and heat bath satisfies the ergodicity criterion. Here we couple continuum mechanics with a Nose-Hoover thermostat to investigate the mechanical damping that can arise from such thermo-elastic interaction.

Results and Discussion

Simulations utilizing the NVE ensemble (a configuration with constant number of atoms, volume, and energy) conserve the entire atom system's energy. However, it has been demonstrated that if a membrane is not properly pre-tensioned or its effective temperature is low, the energy of the first mode will pass to higher modes and cause damping in the resonator due to thermalization [4]. In order to rule out such a damping, we perform our NVE simulation for a sufficiently pre-tensioned membrane at low temperatures and observe that the resonance is not dampened in a ring-down simulation. With the addition of interactions with a heat bath (NVT ensemble), however, the resonances exhibit nonlinear damping. To understand the phenomenon better, we incorporate the Nose-Hoover formalism into a membrane model and observe the same behavior due to the emergence of a nonlinear coupling term. We observe that the nonlinear damping behavior is highly dependent on the bath-to-resonator mass ratio and their thermal energy difference.

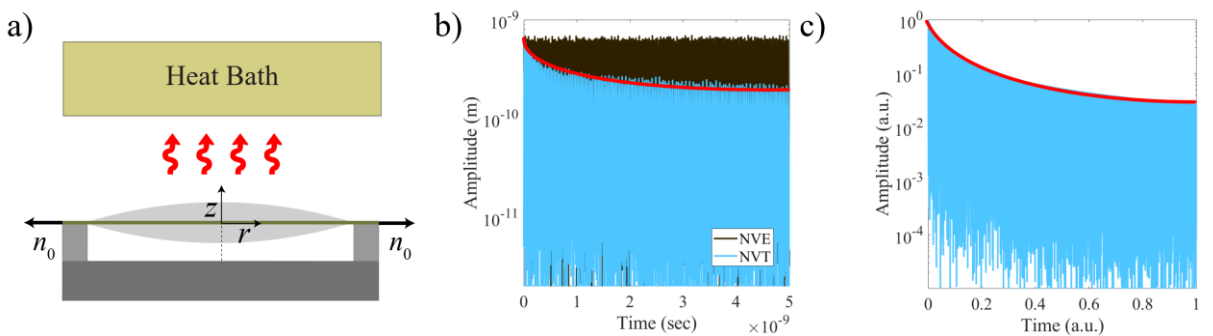


Figure 1: a) Circular membrane interacting thermodynamically with a thermal bath, b) ring-down simulation for a membrane using MD with NVE and NVT ensembles, and c) continuum model incorporating a Nose-Hoover thermostat showing nonlinear damping. Resonances with linear damping should decay linearly due to the logarithmic y-axis; however, the decay is clearly nonlinear.

References

- [1] Croy, A., Midtvedt, D., Isacsson, A., Kinaret, J. M. (2012) Nonlinear damping in graphene resonators. *Phys. Rev. B*, **86**:235435.
- [2] Keşkekler, A., Shoshani, O., Lee, M., van der Zant, H. S., Steeneken, P. G., Alijani, F. (2021) Tuning nonlinear damping in graphene nanoresonators by parametric-direct internal resonance. *Nat. Commun.*, **12**:1-7.
- [3] Shoshani, O., Dykman, M. I., Shaw, S. W. (2020) Tuning linear and nonlinear characteristics of a resonator via nonlinear interaction with a secondary resonator. *Nonlinear Dyn.*, **99**:433-443.
- [4] Midtvedt, D., Croy, A., Isacsson, A., Qi, Z., Park, H. S. (2014) Fermi-pasta-ulam physics with nanomechanical graphene resonators: intrinsic relaxation and thermalization from flexural mode coupling. *Phys. Rev. Lett.*, **112**:145503.

Fractional damping term in the Helmholtz and Duffing nonlinear oscillators.

Mattia Coccolo · Jesús M. Seoane · Miguel Ángel Sanjuán

Nonlinear Dynamics, Chaos and Complex Systems Group, Departamento de Física Universidad Rey Juan Carlos Móstoles Spain

Abstract We present the fractional derivative impact on the dynamics of two systems. In both cases we focus on the cooperation of the damping term, the fractional derivative parameter and the external forcing to study it in the underdamped and the overdamped regime.

Introduction

We analyse the dynamics of the nonlinear Helmholtz and the Duffing oscillator with a fractional order damping. We have investigated the effect of taking the fractional derivative in the dissipative term in function of the parameter α . In both system we have studied the time to reach the asymptotic behaviours, being leave the well or reach an attractor, in function of the fractional parameter. The simulations have been carried for the underdamped and overdamped case.

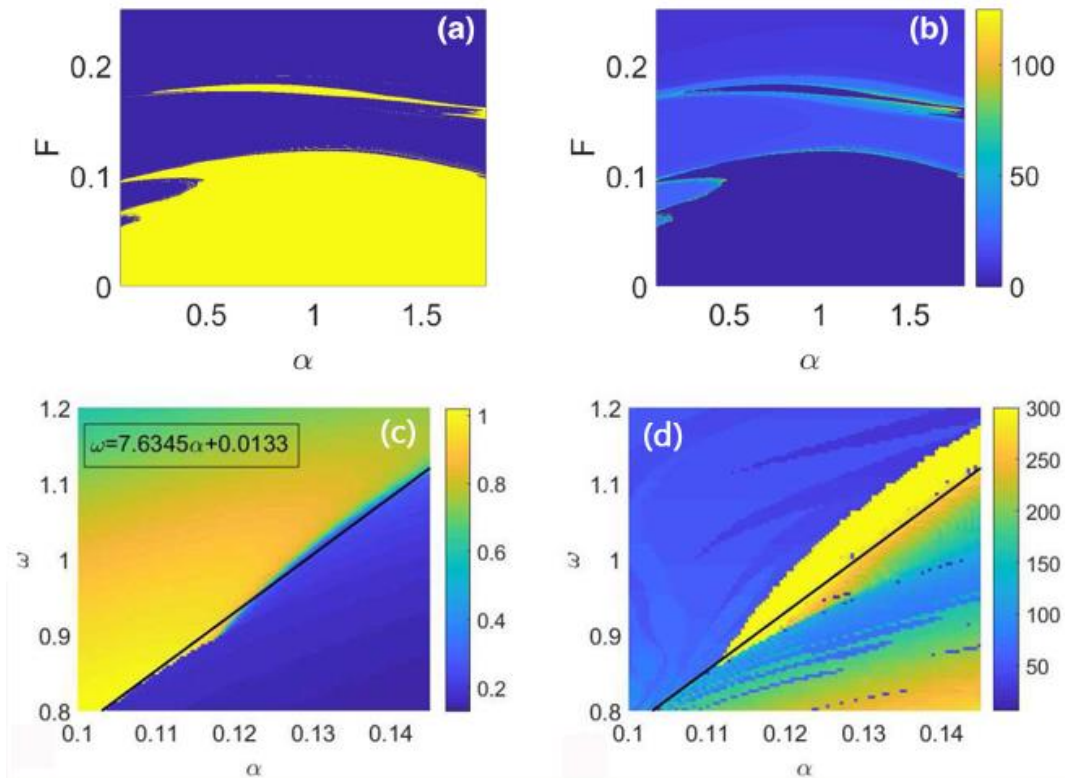


Figure 1: Figures (a) and (c) show the final state for the overdamped regime. Figure (b) and (d) show the time for the system to reach the final state.

Results and discussion

Among other results, we show that in the fractional case, in both systems, the overdamped regime, that in the non-fractional case is easily predictable, becomes more interesting and unpredictable. Moreover, we discuss how some important behaviours of the systems change in function of the fractional parameter, see as an example Figs. 1. The figures show for the overdamped regime the final state of the systems (on the left, figures (a) and (c)) and the times to reach it (on the right, figures (b) and (d)). On the top, for the Helmholtz oscillator, the final state is the escape or not from the well. On the bottom, for the Duffing oscillator, the final state is the amplitude of the oscillations. Moreover, in the Duffing oscillator a resonance-like phenomenon induced by the fractional term can be found. To summarize, the results show that the overdamped case with fractional derivative becomes more interesting than in the classical case.

References

- [1] Ortiz, A., Yang, J., Coccolo, M., Seoane, J. M., & Sanjuán, M. A. (2020). Fractional damping enhances chaos in the nonlinear Helmholtz oscillator. *Nonlinear Dyn.*, 102(4), 2323-2337.
- [2] Syta, A., Litak, G., Lenci, S., & Scheffler, M. (2014). Chaotic vibrations of the duffing system with fractional damping. *Chaos*, 24(1), 013107.

Reliability Problem of a Fractional Stochastic Dynamical System Based on Stochastic Averaging Method and Deep Learning Algorithm

Yu Guan¹, Li Wei^{1*}, Dongmei Huang¹, Natasa Trisovic²

¹*School of Mathematics and Statistics, Xidian University, Xi'an, 710071, China*

²*Department of Mechanics, University of Belgrade, Belgrade, 11000, Serbia*

Abstract. this paper consider a generalized Van der Pol system with fractional derivatives excited by a white Gaussian noise. Firstly, a generalized harmonic transformation is used to get an approximated expression. Applying stochastic averaging methods with energy envelopes to obtain the Ito differential equations and obtaining the Kolmogorov backward equations (KBE) related to the system energy. Then, combining Monte Carlo sampling to perform data-driven and neural network, a new algorithm is obtained to solve the reliability function that satisfies KBE, which is the innovation of this paper. The algorithm does not need boundary conditions and reduces the need for data volume in high-dimensional problems. In addition, the algorithm is applied to obtain the stationary probability density function of the system.

Introduction

Engineering structure with viscoelastic material are generally modelled by a fractional-order system^[1], the reliability problem of relative structural vibration under random excitations is always a hot issue in the field of the stochastic dynamical systems. Since the KBE equation satisfied by the reliability function cannot be solved exactly, in the previous work, methods such as stochastic averaging^[2] and Monte Carlo^[3] are often used to obtain numerical simulation solutions. Based on the fact that deep learning algorithms can show strong accuracy in fitting functions, this paper provides a new algorithm for solving reliability functions.

Results and discussion

this paper uses the deep learning algorithm based on neural network to study the reliability problem of the fractional stochastic dynamical system.

$$\ddot{x} + (\beta_1 - \beta_2 x^2 + \beta_3 x^4) \dot{x} + \omega_0^2 x + \varepsilon D^\alpha x(t) = W(t) \quad (1)$$

The innovation of our deep learning is to use the training sample coming from the combination of Monte Carlo simulation to the system with some certain reference points, which has the advantage of grid-less structure and ability to solve high-dimensional systems. Its loss function is composed by two parts and shown below:

$$L(\theta) = \frac{1}{N_1} \sum_{i=1}^{N_1} (\mathcal{L}\tilde{u}(x_i, \theta))^2 + \frac{1}{N_2} \sum_{j=1}^{N_2} (\tilde{u}(y_j, \theta) - v(y_j))^2 \quad (2)$$

In which the first part is the error caused by the neural network solution fitting the Backward Kolmogorov equation at the training point, the second part is the inaccuracy between the neural network solution at the reference points and the Monte Carlo approximate solutions. It is concluded that the reliability probability is monotonously decreasing with the time increasing, and the results derived from the stochastic averaging method and deep learning algorithm are nearly agreement with the accordant tendency.

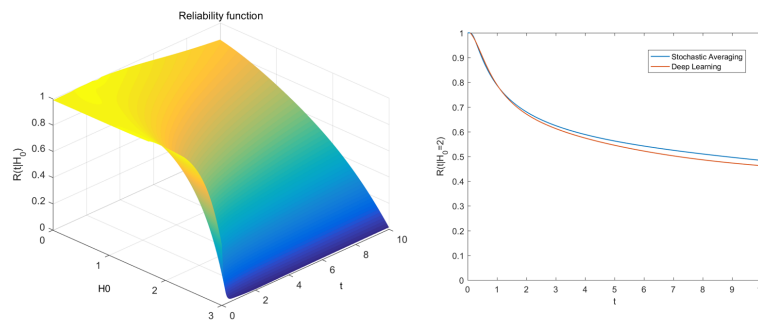


Figure 1: Reliability function derived from stochastic averaging method and deep learning algorithm

References

- [1] Ming.X.(2018).First-passage failure of linear oscillator with non-classical inelastic impact.*Appl Math Model* **54**:284-297.
- [2] Li.W.,Wei.X.,Zhao.J.,& Jin.Y.(2006).First-passage problem for strong nonlinear stochastic dynamical systems.*Chaos Soliton Fract* **28**: 414-421.
- [3] Li.W.,Huang.D.,Zhang.M.,Trisovic.N.,et al.(2019).Bifurcation control of a generalized vdp system driven by color-noise excitation via fopid controller.*Chaos Soliton Fract* **121**:30-38.

Nonlinear vibration of small size beams on fractional visco-elastic foundation

Nikola Nešić^{*}, Milan Cajić^{**}, Danilo Karličić^{**} and Julijana Simonović^{***}

^{*}Faculty of Technical Sciences, University of Priština, Kosovska Mitrovica, Serbia

^{**}Mathematical Institute of Serbian Academy of Science and Arts, Belgrade, Serbia

^{***}Faculty of Mechanical Engineering, University of Niš, Niš, Serbia

Abstract. This paper investigates the dynamic behaviour of a geometrically nonlinear nanobeam resting on the fractional visco-Pasternak foundation and subjected to dynamic axial and transverse loads. The nonlinearity is introduced into the model with the von Karman strain-displacement relation. The equation of motion is derived with Hamilton's principle, discretized with Galerkin's principle, and solved by using three different methods: perturbational multiple scale method, incremental harmonic balance method, and Newmark method. The cases with weak and strong nonlinearity are studied. The influence of different parameters, such as small scale parameters, external excitation, parameters of fractional visco-elastic foundation, etc., on amplitude-frequency diagrams is discussed in detail.

Introduction

Dynamic analysis of nanostructures under different excitation conditions is important for their application in nanoengineering practice. Introducing size and dissipation effects into continuum models of nanoscale structures can lead to more accurate results when compared to experiments and atomistic models. This paper analyses the transversal vibration of nonlocal [1] and nonlocal strain gradient [2] Euler-Bernoulli beam resting on a fractional visco-elastic foundation. The general nonlocal strain gradient constitutive relation is

$$(1 - \mu^2 \nabla^2) t_{xx} = (1 - l^2 \nabla^2) E(z) \varepsilon_{xx}. \quad (1)$$

When $l = 0$, it reduce to nonlocal theory. The nonlinearity is introduced into the model with the von Karman strain-displacement relation. Restitutive force of viscoelastic foundation is defined as:

$$F_m(x) = (k_w + K_w D^\alpha) w - (k_g + K_g D^\alpha) \frac{\partial^2 w}{\partial x^2}, \quad (2)$$

The parameters k_w and k_g are usually set to zero [1], however, we explore their influence with this analysis. Equations of motion are derived with Hamilton's principle, discretized with Galerkin approach, and solved by using three different methods: perturbational multiple scale method, incremental harmonic balance method, and Newmark method. The system dynamics are presented in the form of amplitude-frequency response plots.

Results and discussion

The influence of different parameters, such as small scale parameters, external excitation, parameters of fractional visco-elastic foundation, etc., on amplitude-frequency diagrams is analysed in detail. Results have shown that small parameters coming from stress gradient and strain gradient theory have a minor influence on the amplitude-frequency response. On the other hand, fractional derivative, external excitation, and visco-Pasternak foundation parameters have a significant impact on the response. Additionally, when considering a beam composed of functionally graded material, it has been shown that the power-law index displays a significant effect on the amplitude-frequency response. The system vibration amplitudes are higher for the odd values of the power-law index compared to materials with the even values of this parameter.

References

- [1] Nešić, N., Cajić, M., Karličić, D., Janevski, G. (2021). Nonlinear superharmonic resonance analysis of a nonlocal beam on a fractional visco-Pasternak foundation. *PIME, Part C: J Mech Eng Sci* **235**(20):4594-4611.
- [2] Nešić, N., Cajić, M., Karličić, D., Obradović, A., Simonović, J. (2022). Nonlinear vibration of a nonlocal functionally graded beam on fractional visco-Pasternak foundation. *Nonlin Dyn* **107**(3):2003-2026.

On the Dynamics Analysis of Microresonator System with Fractional-order

Tao Xi *, Jin Xie * and Zhaohui Liu*

*School of Mechanical Engineering, Southwest Jiaotong University, Chengdu, Sichuan, P.R. China

Abstract. It is observed that the fractional derivative model is more accurate in describing the properties of viscoelastic materials, a fractional differential dynamics model of a microresonator is established using Rayleigh-Ritz method, Lagrangian equation and fractional Caputo differential theory, and simulations are carried out to analyse the influence of fractional order and other parameters of the system on the motion of the microresonator.

Introduction

Microresonator is a typical nonlinear dynamic device of micro-electro-mechanical systems (MEMS), in which the viscoelasticity plays a crucial role in its dynamics analysis. It was proved by experiment that the fractional derivative model of viscoelasticity is more accurate than the integer derivative model for soft tissue-like materials [1]. In addition to this, the fractional model has a good agreement with experimental tests on creep and relaxation, which means that fractional model may easily capture both relaxation and creep of materials [2]. And internal thermal damping of fractional model for viscoelastic materials is quite different from that of integer model [3].

In this paper, based on Rayleigh-Ritz method, Lagrangian equation and fractional Caputo differential theory, the fractional differential dynamics model of a microresonator is established with the feature of accurately describing the viscoelastic properties and internal thermal damping of materials. In the model, instead of the terms \ddot{x} and \dot{x} in integer differential equation, the $D^{p_1}x$ and $D^{p_2}x$ represent respectively fractional differentials, $p_1 \in (1, 2)$, $p_2 \in (0, 1)$, which are non-integer. The predictor-corrector method is employed to carry out the simulations to analyse influence of system parameters on the motion of the system.

Results and discussion

Figure 1 depicts the bifurcations of the system with respect to the fractional order p_1 and p_2 . It is shown that the both fractional orders have obvious influence on the motion of the system. The influence of fractional order p_1 is more significant than the fractional order p_2 . This figure also indicates that chaos can be suppressed by changing the viscoelastic and internal damping of the material. In addition to this, the results of this study shows that the amplitude and frequency of excitation voltage also have certain influence on the dynamic characteristics of the system. And with the variation of excitation amplitude and frequency, the system shows more complex dynamics behavior.

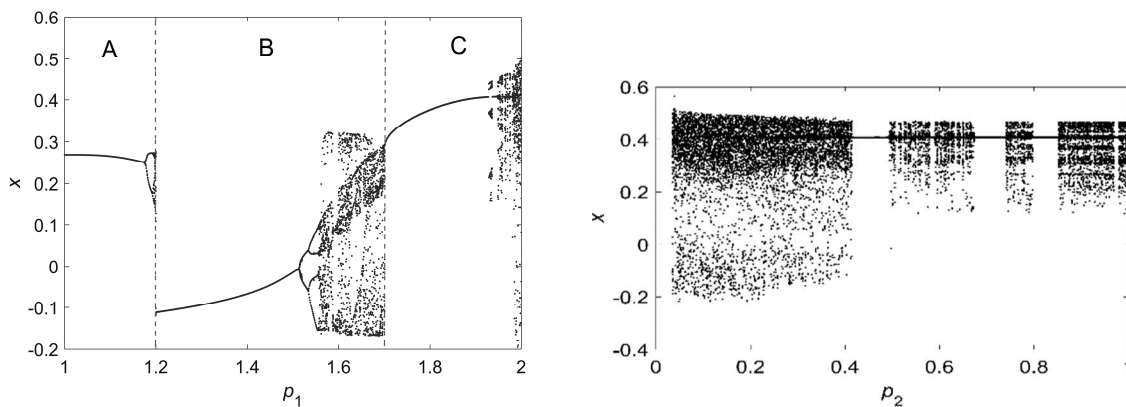


Figure 1: The bifurcation diagram versus p_1 and p_2 .

References

- [1] Meral F. C., Royston T. J., Magin R. (2010) Fractional Calculus in Viscoelasticity: An Experimental Study. *Commun Nonlinear Sci* **15**: 939-945.
- [2] Di Paola M., Pirrotta A., Valenza A. (2011) Visco-elastic Behaviour through Fractional Calculus: An Easier Method for Best Fitting Experimental Results. *Mech Mater* **43**:799-806.
- [3] Zhang W., Shimizu N., Xu H. (2002) Thermal Effects of the Viscoelastic Materials Described by Fractional Calculus Constitutive Law. The First Asian Conference on Multibody Dynamics, website https://www.researchgate.net/publication/317681127_F-5-4-3_Thermal_effects_of_the_viscoelastic_materials_described_by_fractional_calculus_constitutive_law.
- [4] Diethelm K. (1997) An Algorithm for the Numerical Solution of Differential Equations of Fractional Order. *Electron T Numer Ana* **5**:1-6.

State estimation of time-fractional reaction-diffusion SEIR model for COVID-19 with mobile sensors

Fudong Ge* and YangQuan Chen**

*School of Computer Science, China University of Geosciences, Wuhan 430074, PR China

**Department of Mechanical Engineering (MESA-Lab), University of California, Merced, CA 95343, USA

Abstract. To know the state information of the spread of diseases, such as COVID-19 is of great importance as verified by the recent pandemic. In this paper, we aim to investigate the state estimation of the spatial-temporal propagation of COVID-19 based on a time-fractional reaction-diffusion susceptible-exposed-infected-recovered (SEIR) model. For this purpose, we first regard a finite number of static sensors as mobile sensors based on the continuity of the state by traveling between static sensors and supposing that at each given time only one of the static sensors in each line is active. Next, we design an extended Luenberger-type observer that contains a state estimator and the guidance of mobile sensors to ensure the desired state estimation requirements. A numerical example is finally presented to illustrate the accuracy and the promising of our proposed state estimation strategy.

Introduction

To know the state information of epidemic system, which is required for monitoring or designing feedback control is a fundamental issue in epidemiology. However, owing to the economic or physical constraints, this is not easy to be realized. For this problem, based on system's properties and in the spirit of [1], considerable attention has been attracted on using mobile sensors to construct a Luenberger-type observer to estimate the state information of system (see e.g.[2]). This is due to the fact that mobile sensors can contain additional degrees of the freedom hence being more powerful to observing the studied system than that with non-mobile sensors. Then, in this paper, based on our previous work on time-fractional reaction-diffusion SIR epidemic system to model the spatial-temporal propagation of infection [4], we discuss the state estimation problems of the following time-fractional reaction-diffusion SEIR model

$$\begin{cases} {}_0^C D_t^\alpha S(x, t) = d_1 \sum_{i=1}^n \frac{\partial^2 S(x, t)}{\partial x_i^2} - \beta(x, t) I(x, t) \frac{S(x, t)}{N}, \\ {}_0^C D_t^\alpha E(x, t) = d_2 \sum_{i=1}^n \frac{\partial^2 E(x, t)}{\partial x_i^2} + \beta(x, t) I(x, t) \frac{S(x, t)}{N} - \gamma(x, t) E(x, t), \\ {}_0^C D_t^\alpha I(x, t) = d_3 \sum_{i=1}^n \frac{\partial^2 I(x, t)}{\partial x_i^2} + \gamma(x, t) E(x, t) - \kappa(x, t) I(x, t), \\ {}_0^C D_t^\alpha R(x, t) = d_4 \sum_{i=1}^n \frac{\partial^2 R(x, t)}{\partial x_i^2} + \kappa(x, t) I(x, t) \end{cases} \quad (x, t) \in \Omega \times [0, T] \quad (1)$$

under the output function obtained by m -mobile sensors

$$I^*(t) = \begin{pmatrix} I_1^*(t) \\ \vdots \\ I_m^*(t) \end{pmatrix} = \begin{pmatrix} \int_0^L c(x; x_1(t)) I(x, t) dx \\ \vdots \\ \int_0^L c(x; x_m(t)) I(x, t) dx \end{pmatrix}. \quad (2)$$

Here $\Omega \subseteq \mathbf{R}^n$ is a bounded domain with smooth boundary, ${}_0^C D_t^\alpha$, $\alpha \in (0, 1]$ denotes the Caputo fractional derivative and the meanings of rest symbols will be specified in our full-length paper.

In what follows, we aim to propose an approach on using the output (2) to estimate the state of model (1).

Results and discussion

The goal of this paper is to investigate the state estimation problem of system (1) based on the measurements obtained by Eq.(2). For this, we extend our previous results in [2] and design an extended Luenberger-type observer that contains a state estimator and the guidance of mobile sensors to ensure the desired state estimation requirements using rigorous mathematical analysis. To illustrate the effectiveness of our main results, we shall present a numerical illustration by generalizing our previous works in [4] where a numerical example on the control of time-fractional reaction-diffusion SIR epidemic system is presented and in [2] where a finite number of mobile zone sensors is used to estimate the state of semilinear time-fractional diffusion systems.

References

- [1] Luenberger, D. G. (1964) Observing the state of a linear system. *IEEE Trans. Mil. Electron.* **8**(2): 74-80.
- [2] Ge, F., Chen, Y. (2022) Estimation via mobile sensors for semilinear time-fractional diffusion processes. *IEEE Contr. Syst. Lett.* **6**: 2114-2119.
- [3] Khapalov, A. (2001) Mobile point controls versus locally distributed ones for the controllability of the semilinear parabolic equation. *SIAM J. Control Optim.* **40**(1): 231-252.
- [4] Ge, F., Chen, Y. (2021) Optimal vaccination and treatment policies for regional approximate controllability of the time-fractional reaction-diffusion SIR epidemic systems. *ISA Trans.* **115**: 143-152.

Reliability of fractional-order hybrid energy harvesters under random excitations

Ya-Hui Sun^{*}, Yong-Ge Yang^{*} and YangQuan Chen^{**}

^{*}School of Mathematics and Statistics, Guangdong University of Technology, Guangzhou, P.R. China

^{**}School of Engineering, University of California, Merced, CA, USA

Abstract. Reliability of a fractional-order hybrid energy harvester driven by Gaussian white noise is investigated in this paper. Firstly, the approximately equivalent system can be derived with the help of variable transformation and stochastic averaging method. Then the backward Kolmogorov equation governing the conditional reliability function and the generalized Pontryagin equation governing the statistical moments of first-passage time are obtained from the averaged equations. Finally, influences of system parameters on reliability function and first-passage time are presented by numerically solving the corresponding equations.

Introduction

Vibration energy harvester, which can convert the mechanical energy into electrical energy to achieve the self-powered of the micro-electromechanical systems (MEMS), has received extensive attention. To improve the efficiency of vibration energy harvesters, many approaches have been adopted including the combination of two conduction mechanisms, the use of the advanced materials and stochastic loading [1]. Some research results have shown that fractional-order models are suitable to describe the viscoelastic properties of advanced materials [2]. And the response of the fractional-order hybrid energy harvester driven by random excitation has been studied [3]. First-passage problem aims to determine the probability that systems response reaches the boundary of a bounded safe domain of state space within its lifetime. As one branch of reliability in mathematics, it can exactly describe the response feature and fatigue life of structures such as offshore platform, civil construction, etc. To the best of authors' knowledge, there is little work on the reliability analysis of the fractional-order hybrid energy harvester driven by random excitation.

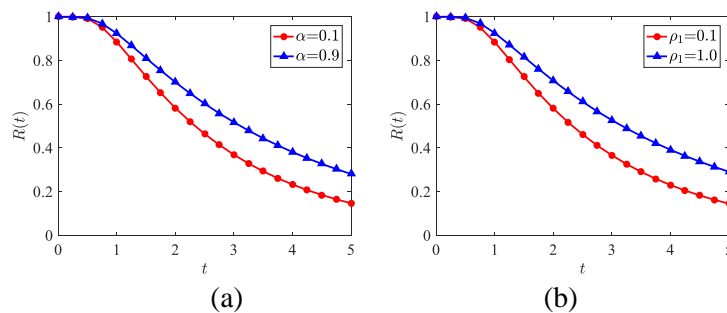


Figure 1: Reliability function for different fractional order (a) and electro-mechanical coupling coefficient (b).

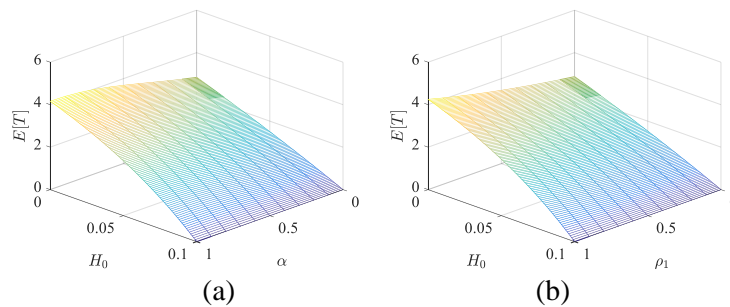


Figure 2: Mean first-passage time for different fractional order (a) and electro-mechanical coupling coefficient (b).

Results and discussion

The reliability analysis of a fractional-order hybrid energy harvester subject to Gaussian white noise has been presented in this paper. As shown in Figs. 1 and 2, the reliability function is monotonically decreasing for time and the mean first-passage time is also monotonically decreasing for initial energy. In addition, the reliability function and the mean first-passage time increase as the fractional order α and the electro-mechanical coupling coefficient ρ_1 increase.

References

- [1] Litak G, Friswell MI, Adhikari S. (2010) Magnetopiezoelectric energy harvesting driven by random excitations. *Appl. Phys. Lett.*, **96**: 214103.
- [2] Chen YQ, Petras I, Xue D. (2009) Fractional order control-a tutorial. *2009 American control conference*, IEEE, **2009**: 1397-1411.
- [3] Yang YG, Sun YH, Xu W. (2021) Stochastic bifurcation analysis of a friction-damped system with impact and fractional derivative damping. *Nonlinear Dyn.*, **105**: 3131-3138.

Bird like trajectories in 6d chaotic system incorporated with fractional order, memristor and encryption

Muhammad Ali Qureshi*

*Department of Physics, University of Karachi, Karachi 75270, Pakistan

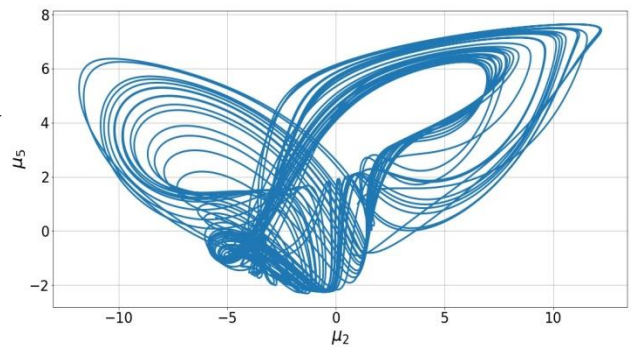
Abstract: This paper reports a novel six dimensional nonlinear dynamical system with the tangent hyperbolic memristor circuit and amalgamated image encryption. The dynamical system is analyzed using standard tools including phase portraits, equilibrium points, Eigenvalues, and Lyapunov exponents. Analysis suggests that the developed system is chaotic in nature and has exiting new 2D trajectories. The system generates two different trajectories of bird like phase portrait. The chaotic system is numerically solved with Caputo fractional order derivative for different values of fractional order (q). The fractional order circuits are designed for $q = 1$ and $q = 0.99$ utilizing the approximation fractional order technique of transfer function, showing great deal of agreement with the numerical results. Lastly, the random number generated from the chaotic system is utilized to scramble the image via the scheme of Amalgamated Image Encryption. The scrambled image is tested using different image security test algorithm to support the idea that the chaotic system and image can together form an advantageous key.

Introduction

The nonlinear dynamics of fractional order system and memristor based circuits have attracted an escalating attention in recent years. Memristor chaotic systems (MCS) have been discussed frequently as a new type of chaotic system. Memristor is the abbreviation of memory resistance, a basic component of a circuit system described by Chua in 1971 [1]. During operation, the memristor's resistance changes with the current flowing through the circuit, but it remains unchanged when switched off. A memristor plays a nonlinear role in voltage-ampere characteristics, allowing chaotic systems to perform better. As a result, chaotic systems have widely adopted it, resulting in MCS. Calculus of fractional order derivatives is now becoming an important aspect in the application of engineering and technology applications [2]. The field deals with integer and non-integer arbitrary order values for derivatives that are then applied to the study of various complex physical systems present in the world. The mathematics of fractional calculus requires great computing skills, as the subject is pretty much dependent on complex numerical solutions, complicated simulations and statistical analysis tools. The advantages of the fractional derivative model over the integer derivative model are its robust results, complex nature solution, its memory effects, and heredity assets for different systems.

This study aims to make development in the field of memristor-based chaotic systems. The main idea is to investigate a novel 6D chaotic system with memristor-based system. Due to the unique nonlinear characteristics of the memristor different pseudo-random numbers are generated which are utilized to do cryptography. A new encryption method is presented, “Amalgamated Image Encryption” in which the chaotic data along with its parameter and initial condition, and a plain image is represented as a key for multimedia (i.e., image and video) [3]. The 6D chaotic equation and one of the phase portraits of the novel system is illustrated below.

$$\begin{aligned}\dot{\mu}_1 &= a(\mu_2 - \mu_1) + \mu_2\mu_3 - h\mu_5\mu_4 - k(\alpha + \beta \tanh(\mu_6)\mu_4 \\ \dot{\mu}_2 &= c\mu_2 - \mu_1\mu_3 \\ \dot{\mu}_3 &= -b\mu_3 + \mu_1\mu_2 \\ \dot{\mu}_4 &= \mu_2\mu_3 - c\mu_5 + \mu_3 - \mu_4^3 \\ \dot{\mu}_5 &= \mu_2\mu_1 + d\mu_4 - \mu_5 - 0.09\exp(\mu_5) \\ \dot{\mu}_6 &= \dot{\mu}_4\end{aligned}$$



Where, $a = 19$, $b = 3$, $c = 10$, $d = 12$, $k = 1$; $\alpha = 1$; $\beta = 0.5$ and $h = 3$

References

- [1] Chua, L.J.I.T.o.c.t., *Memristor-the missing circuit element*. 1971. **18**(5): p. 507-519.
- [2] Hilfer, R., *Applications of fractional calculus in physics*. 2000: World scientific.
- [3] <https://doi.org/10.5281/zenodo.7046557>

Generalized Fractional-Order Complex Logistic Map and Fractals on FPGA

Sara M. Mohamed*, Wafaa S. Sayed**, Lobna A. Said* and A. G. Radwan ***

*Nanoelectronics Integrated Systems Center (NISC), Nile University, Giza, Egypt

**Engineering Mathematics and Physics Dept., Faculty of Engineering, Cairo University, Egypt

***School of Engineering and Applied Sciences, Nile University, Giza, Egypt

Abstract. This paper introduces a generalized fractional-order complex logistic map and the FPGA realization of a corresponding fractal generation application. The chaotic properties of the proposed map are studied through the bifurcation behavior and maximum Lyapunov exponent (MLE). A concise fractal generation process is presented, which results in designing and implementing an optimized hardware architecture. An efficient FPGA implementation of the fractal behavior is validated experimentally on Artix-7 FPGA board. An example of fractal implementation is verified, yielding frequency of 24.34 MHz and throughput of 0.292 Gbit/s. Compared to recent related works, the proposed implementation demonstrates its efficient hardware utilization and suitability for potential applications.

Introduction

Chaos is mentioned in systems that are sensitive to initial conditions such that a small variation cause a significant difference in behavior. Chaotic systems are distinguished by their attractive characteristics like randomness, aperiodicity and fractal identity. Fractals are recognized by their complex geometric structures such as the ones generated from Mandelbrot and Julia maps [1]. Chaotic systems are classified into continuous-time maps and discrete-time maps. The discrete maps are classified into integer-order maps that can be extended to fractional such as logistic and tent maps, and real maps that can be extended to complex such as logistic and Gaussian maps. Several works introduced fractal generation from integer-order complex discrete maps including logistic and Gaussian maps [2, 3, 4]. Realizations in digital hardware have become more practical for industrial use. Fixed-point operations are widely used for hardware realizations to save costs and enhance speed. The generalization of conventional chaotic systems into the fractional-order domain allows more accurate understanding of the map behavior, increases the degree of freedom in design and enhances its performance in applications. Fractional-order discrete chaotic maps are employed in several applications such as encryption, neural networks, synchronization and multi-scroll generation. Among several fractional definitions, EL Raheem definition is simple and suitable for hardware implementation [5]. This paper proposes a generalized fractional-order complex logistic map, fractals and their FPGA realization. The chaotic properties of the proposed map are studied using bifurcation and MLE diagrams. The proposed hardware implementation of the fractals based on the fractional-order complex logistic map utilizes simplified steps. The fractal behaviors are validated experimentally on an Artix-7 FPGA kit. The proposed implementation is compared to recent related works demonstrating its hardware efficiency and suitability for potential applications.

Results and discussion

The proposed design for fractals based on the generalized fractional complex logistic map is written in Verilog HDL with the simulation of Xilinx ISE 14.7 and implemented on Xilinx FPGA Artix-7 XC7A100TCSG324 by using Chip scope. The outputs are wired to a 12-bit Digital to Analog converter, which is connected to a digital oscilloscope to display the fractal behavior. The fractal example is realized and validated experimentally on FPGA. The design achieves frequency of 24.34 MHz and throughput of 0.292 Gbit/s. A summary of FPGA implementation results of this work and other implemented fractal works [2, 3, 4] is presented. The proposed implementation consumes higher resources and lower frequency than [3, 4] due to the excessive arithmetic operations needed for the fractional domain. On the other hand, the proposed implementation achieves efficient hardware utilization and speed than [2] due to the simplicity of operations of the proposed map than Gaussian map. The proposed realization is considered a promising solution to increase the degrees of freedom in the design and enhance the performance in different applications such as encryption schemes and multi-scroll generators.

References

- [1] K. Bouallegue, A. Chaari, and A. Toumi, "Multi-scroll and multi-wing chaotic attractor generated with julia process fractal," *Chaos, solitons & fractals*, vol. 44, no. 1-3, pp. 79–85, 2011.
- [2] B. M. AboAlnaga, L. A. Said, A. H. Madian, and A. G. Radwan, "Analysis and fpga of semi-fractal shapes based on complex gaussian map," *Chaos, Solitons & Fractals*, vol. 142, p. 110493, 2021.
- [3] B.-A. M. Abo-Alnaga, L. A. Said, A. H. Madian, and A. G. Radwan, "Fpga realization of complex logistic map fractal behavior," *Fractals*, vol. 30, no. 01, p. 2250023, 2022.
- [4] S. M. Mohamed, W. S. Sayed, L. A. Said, and A. G. Radwan, "Fpga realization of fractals based on a new generalized complex logistic map," *Chaos, Solitons & Fractals*, vol. 160, p. 112215, 2022.
- [5] Z. El Raheem and S. Salman, "On a discretization process of fractional-order logistic differential equation," *Journal of the Egyptian Mathematical Society*, vol. 22, no. 3, pp. 407–412, 2014.

Fractional control performance assessment of the nonlinear mechanical systems

Patryk Chaber* and Paweł D. Domański**

*Institute of Control and Computation Engineering, Warsaw University of Technology,
ul. Nowowiejska 15/19, 00-665 Warsaw, Poland*

* ORCID #0000-0003-0257-8255 **ORCID #0000-0003-4053-3330

Abstract. There are many approaches to assess control quality, from classical mean-square error or variance, model-based and model-free approaches, to fractal or entropy measures. These indicators can be used for a variety of algorithms. Nonlinear industrial solutions pose new challenges for such solutions. Indicators must be robust, reliable and informative. They must work in the presence of disturbances and uncertainties. The complication of the process, its nonlinearities, mutual correlations, variable delays and outlying anomalies should not limit it. Additionally, human influence must not interfere with its robustness. One of the modern approaches that is gaining popularity is fractional calculus. It allows to consider complex and non-stationary processes. It is shown that Geweke-Porter-Hudak (GPH) fractional order estimator allows to assess control system quality. The method is validated using the laboratory mechanical servomechanism.

Introduction

Industry 4.0 transformation makes production versatile, flexible, sustainable, supporting vertical and horizontal integration. Such plants require stringent control system, which operates close to its technological constraints. Reliable control control performance assessment is a must. There are many approaches for the univariate PID loops [1]. Real non-linear processes exhibit internal correlations with varying delays at different time scales that reflect the long-range dependence or persistence properties. Modeling of such variables with regression models is not enough. Auto-Regressive Fractionally Integrated Moving Average (ARFIMA) models [2] constitute an alternative [3]. Our research follows above assumption. If the fractional model can be considered as the fundamental process behind control data, its coefficients, especially the fractional-order, could be used as its quality measure. This research uses GPH fractional order $-0.5 < d < 0.5$ estimator of the ARFIMA(p, d, q) process [4]. Once $d \in (-0.5, 0)$, the system is anti-persistent and exhibits long-range negative dependence. In case of $d \in (0, 0.5)$, the process is persistent and reflects long memory. Once $d = 0$, it is stationary independent process. Anti-persistent properties indicate aggressive tuning, persistent sluggish and $d = 0$ good control.

Results and discussion

The laboratory nonlinear servomechanism system (Fig. 1) is used to visualize the method. The system allows to measure the speed in two ways: using the tachometer and with the encoders. Each measurement has different characteristics. The first one is very noisy with the noise magnitude that depends on the speed, while the latter one is very smooth. The system is controlled by the PID controller with the anti-windup mechanism. They are tested with stationarity tests and as the results control error data are incremented to remove the non-stationarity.

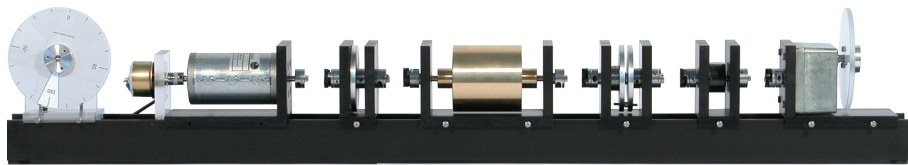


Figure 1: Laboratory servomechanism used during experiments

Table 1 shows sample experimental results that confirm initial assumptions. Fractional order does not depend on the sensor. Similar tuning is reflected by the similar values. The better control is observed close to the $d = 0$ value. Research addresses other issues, like the detailed impact of the PID parameters, the effect of the controller saturation and the anti-windup. The fractional order is compared with other statistical indexes.

Table 1: Fractional order estimates d ; PID parameters: $\{k_p; k_I; k_D; k_H\}$; sensor used for feedback (E) - encoder, (T) - tachometer

	$\{0.1; 0.1; 0.1; 0.0\}$ (E)	$\{2.0; 2.0; 2.0; 10.0\}$ (E)	$\{10.0; 0.001; 0.001; 0.0\}$ (E)	$\{10.0; 0.001; 0.001; 0.0\}$ (T)	$\{10.0; 10.0; 0.0; 10.0\}$ (E)
encoder	-0.3906	-0.4157	-0.1005	-0.0998	-0.1475
tachometer	-0.3700	-0.4056	-0.1031	-0.0959	-0.1535

References

[1] Domański P.D. (2020) Control Performance Assessment: Theoretical Analyses and Industrial Practice. Springer International Publishing, Cham, Switzerland.

[2] Sheng H. Chen YQ and Qiu TS (2012) Fractional Processes and Fractional-Order Signal Processing, Techniques and Applications. Springer-Verlag London Limited, London, UK.

[3] Liu K., Chen YQ and Domański, P.D. (2020) Control Performance Assessment of the Disturbance with Fractional Order Dynamics. In W. Lacarbonara, B. Balachandran, J. Ma, J. A. Tenreiro Machado, and G. Stepan, editors, *Nonlinear Dynamics and Control* 255-264, Springer International Publishing, Cham, Switzerland.

[4] Geweke J. and Porter-Hudak S. (1983) The Estimation and Application of Long Memory Time Series Models. *Journal of Time Series Analysis* 4(4):221–238.

Broadening the operational range of a fractionally damped piezoelectric energy harvester

Stepa Paunović*, Milan Cajić* and Danilo Karličić*

*Department of Mechanics, Mathematical Institute of the Serbian Academy of Sciences and Arts, Serbia, ORCID 0000-0001-9785-4851

Abstract. Bimorph cantilever beams have been widely used for piezoelectric energy harvesting. However, these harvesters are efficient only in very narrow frequency ranges near resonant states. In this contribution a solution is proposed by connecting multiple beams by fractionally viscoelastic coupling layers and adding concentrated masses. The results show that the harvester operational range can be significantly broadened by the presented design procedure.

Introduction

Bimorph cantilever beams have been widely used for energy harvesting [1]. However, their operational frequency range is very narrow, since they are effective only near the resonant state. Electric power output can be improved by connecting beams at their free ends [2], but the operational range is still left narrow. Here, a solution is proposed where N_b bimorph cantilever beams are connected *along their entire length* by coupling layers as shown in Fig.1a, using fractional Kelvin-Voigt viscoelastic model with derivative order β , compliance coefficient κ and retardation time τ . When individual beams' natural frequencies are close but different, the so obtained system enters a near-resonant state more often, effectively broadening the operational range.

Results and discussion

All beams have the same geometry (cross-sectional moment of inertia I and width b , length L and piezo-layer thickness h_p) and material characteristics (mass per unit length m , elasticity modulus Y , piezoelectric constant e_{31} and permittivity ϵ_{33}), while the k -th beam desired dynamic properties are achieved by attaching N_{m_k} concentrated masses $m_{p(k)}$ at positions x_{p_k} , where $k = 1, 2 \dots N_b$, $p = 1, 2 \dots N_{m_k}$. All piezo-layers are connected in parallel to an electric circuit of resistance R . The system is subjected to transverse base motion $w_b(t)$, inducing transverse beam displacements $w_k(x, t)$ and voltage $v(t)$. For elastic Euler-Bernoulli beams, equations of motion, electric circuit and boundary conditions (BCs) are:

$$\left(m + \sum_{p=1}^{N_{m_k}} m_{p(k)} \delta(x - x_{p_k}) \right) \ddot{w}_k + Y I \dot{w}_k'''' - \kappa \left(1 + \tau^\beta D^\beta \right) (w_{k-1} - 2w_k + w_{k+1}) + e_{31} b h_{pc} \dot{v} = 0,$$

$$N_b \frac{\epsilon_{33} b L}{h_p} \dot{v} + \frac{1}{2R} v + e_{31} b h_{pc} \sum_{k=1}^{N_b} \int_0^L \dot{w}_k'' dx = 0, \quad w_k(0, t) = w_b(t), \quad w_k''(L, t) = Y I w_k'''(L, t) = Y I w_k''''(L, t) = 0$$

where D^β is the left Riemann-Liouville fractional derivative and δ is the Dirac δ function. After homogenization of the BCs and applying Galerkin discretisation, fractional derivative is approximated as in [3] and frequency domain solutions for beam displacements and voltage are determined. Fig.1b shows the frequency response function for electric voltage for the case of $N_b = 5$ beams connected by layers with $\tau = 0.2$ and various fractional derivative orders. The results show that by increasing the β , although the maximum voltage amplitude slightly drops, the system operational range broadens significantly, making the harvester more efficient for a wider range of excitation frequencies and proving the effectiveness of the presented procedure.

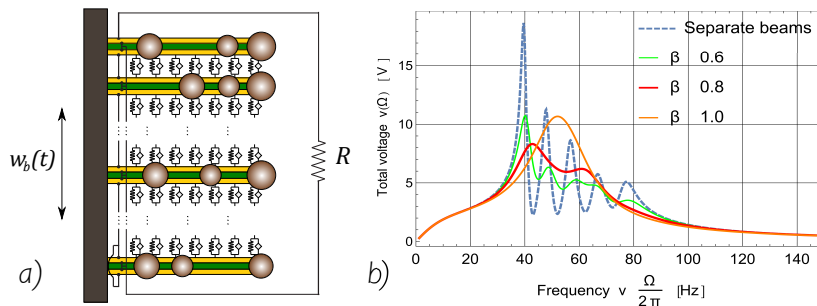


Figure 1: a) The considered system of connected bimorph cantilever beams with attached concentrated masses, b) The electric voltage frequency response function for $N_b = 5$ connected beams and various fractional derivative order for the coupling layer damping

References

- [1] Erturk, A., Inman, D. (2011) Piezoelectric energy harvesting. John Wiley & Sons. West Sussex, UK
- [2] Meruane, V., Pichara, K. (2016) A broadband vibration-based energy harvester using an array of piezoelectric beams connected by springs. *Shock and Vibration* **2016**:1-14.
- [3] Evangelatos, G., Spanos, P. (2011) An Accelerated Newmark Scheme for Integrating the Equation of Motion of Nonlinear Systems Comprising Restoring Elements Governed by Fractional Derivatives. In: Kounadis, A.N., Gdoutos, E.E. (eds) Recent Advances in Mechanics. Springer, Dordrecht.

Fractal Response of a Nonlinear Packaging System

Luis M. Palacios-Pineda*, Óscar Martínez-Romero**, Daniel Olvera-Trejo**, and
Alex Elías-Zúñiga**

*Tecnológico Nacional de México / Instituto Tecnológico de Pachuca, Pachuca, HGO, MÉXICO

** Institute of Advanced Materials for Sustainable Manufacturing, Tecnológico de Monterrey, Monterrey, NL, MÉXICO

Abstract. In this paper the impact curves, obtained from the dropping of a weight over a viscoelastic fractal cushioning packaging system are computed to evaluate the dropping damage of a critical component. To capture high-frequency harmonic components observed during the impact time span, the approximate frequency-amplitude expression of the corresponding equation of motion is obtained via an ancient Chinese algorithm and Jacobi elliptic functions.

Introduction

The equation of motion that capture the fractal cushioning dynamic behavior of anti-vibration fractal materials can be assumed to be of the form [1]:

$$m \frac{d}{dS^\alpha} \left(\frac{dy}{dS^\alpha} \right) + g(y, S) = 0, \quad (1)$$

with initial conditions:

$$y(0) = 0, \quad \dot{y}(0) = v_0. \quad (2)$$

Here α is a fractal parameter related to the cushioning surface porosity. Equation (1) provides information about the shape, duration, and peak magnitudes of the displacement, velocity, and acceleration curves that appear when a weight is dropped over at a certain height over a cushioning surface. Equation (1) can be also written as an ordinary differential equation introducing the fractal derivative definition

$$\frac{dy}{dS^\alpha} (S_0^\alpha) = \Gamma(1 + \alpha) \lim_{\substack{(S-S_0) \\ \Delta S \neq 0}} \frac{y(S) - y(S_0)}{(S - S_0)^\alpha} \quad (3)$$

and the two-scale dimension transform [2] $t = S^\alpha$ to get

$$m \frac{d^2 y}{dt^2} + g(y, t) = 0, \quad y(0) = 0, \quad \frac{dy(0)}{dt^{1/\alpha}} = v_0 \quad (4)$$

Results and discussion

Figure 1a shows the system's acceleration response evolution as the static stress increases. For low static stress values, the dynamic response is less complex when compared with those of higher static stress values. The fractal evolution on the cushioning material energy, as the frequency increases, is shown in Fig. 1b. Also notice from Fig. 1c that for higher cushioning material porosity values of α , the impact traveling wavelength increases, helping to reduce potential damages in the critical component which is consistent with observed practical applications.

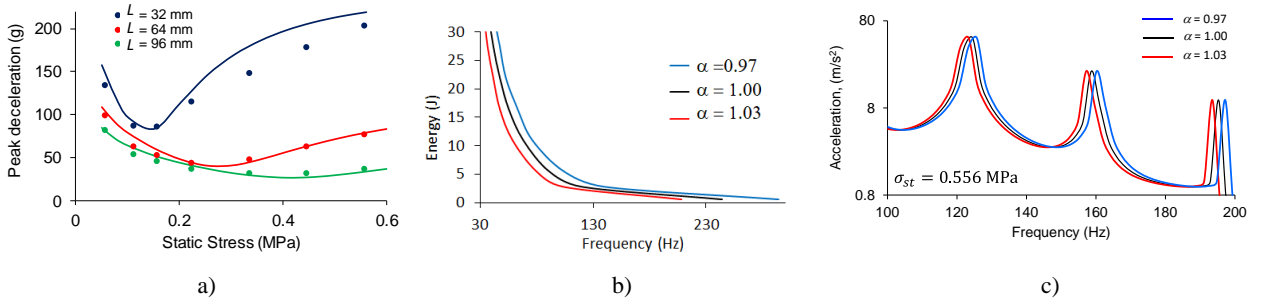


Figure 1: a) Configurational representation of the nonlinear modal amplitudes, b) frequency-amplitude response plot, and c) frequency-energy plot (FEP) that illustrates how the energy is transferred between modes.

This work unveils the advantages of modeling the dynamics of cushion materials considering their molecular fractal structure, adopting a fractal equation of motion, and the two-scale fractal dimension transform as well as the fractal energy-frequency response curves. The fractal dimension parameter values of α elucidates how the energy produced during impact and the acceleration response for different values of static stresses are influenced by the surface porosity of the packaging cushioning system.

Reference

- [1] Elías-Zúñiga A. · Palacios-Pineda L. M., Martínez-Romero O., Olvera-Trejo D. (2022) Dynamic response of a fractal cushioning packaging system. *Fractals* **30** 7: 2250148.

A Metamaterial Concept using the Hybrid Position Feedback Control Method and Bistable Structural Elements

Mehmet Simsek,^{*} Rick Schieni,^{**} Laurent Burlion,^{**} and Onur Bilgen^{**}

^{*}*Koç University, Sariyer, Istanbul, Turkey*

^{**}*Rutgers University, Piscataway, NJ, 08854, USA*

Abstract. A new multi degree of freedom metamaterial concept that utilizes a hybrid position feedback controller is introduced and its characteristics are demonstrated. The concept is based on bistable element and associated controllers that are unstable-then-stable position feedback controllers. An arbitrary number of bistable segments or so-called “material elements” are attached to each other in a serial (or parallel) manner to generate a “distributed” multi-stable structure. This new metamaterial inherits the multiple bistable positions that its building blocks have; hence, the metamaterial becomes multi-stable. It can hold multiple positions without consuming power and has the capability of achieving many shapes. The proposed metamaterial concept can be used in various applications: locomotion in bioinspired systems, undulatory motion, morphing aerodynamic surfaces, wave guiding, and vibration attenuation.

Introduction

A bistable system has two stable configurations and one unstable equilibrium which can be exploited to design a functional metamaterial. The control of bistable structures using piezoelectric actuators has received significant attention recently. Arrieta et al. [1] and Bilgen et al. [2] introduced resonant control with a surface bonded piezoelectric device. Simsek et al. [3, 4] demonstrated an automated method for bidirectional state transfer on a wing-like cross-ply bistable plate using the hybrid control strategy and a piezocomposite actuator. Simsek et al. [5] demonstrated a piezoelectric-material induced monotonic snap-through without possibility of triggering cross-well oscillations or chaotic response. Simsek et al. [6] introduced an HPF controlled bistable metamaterial concept. In this paper, the concept will be extended to multi-DOF model to demonstrate full capacity.

Results and discussion

A parametric analysis is carried out for four different scenarios which are: (1) all forward (from stable state 1 to stable state 2), (2) DOF1 forward while DOF2 backward, (3) DOF1 backward while DOF2 forwards, (4) all backward. Figure 1 demonstrates behavior of a two degrees of freedom (2DOF) system where the elements are in series configuration. The green color indicates the controller parameters that achieve convergence to the desired state for predefined scenarios. The other colors in the figure are undesirable with the number of unsatisfied case(s) indicated in the legend. The results show that the concept is working for a 2DOF system; however, it needs to be extended to multi DOF models to realize the full functionality of metamaterial concept. This will be one of the contributions of the full paper.

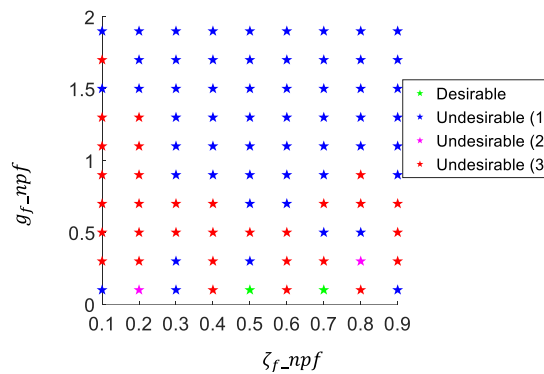


Figure 1: Parametric analysis for the 2DOF bistable Duffing-Holmes system with the hybrid controller in series configuration.

References

- [1] A. F. Arrieta, O. Bilgen, M. I. Friswell, and P. Hagedorn, "Morphing dynamic control for bi-stable composites," in *22nd International Conference on Adaptive Structures and Technologies (ICAST)*, Corfu, Greece, 2011, pp. 10-12.
- [2] O. Bilgen, A. F. Arrieta, M. I. Friswell, and P. Hagedorn, "Dynamic control of a bistable wing under aerodynamic loading," *Smart mat. and struct.*, vol. 22, no. 2, p. 025020, 2013.
- [3] M. R. Simsek and O. Bilgen, "Hybrid position feedback controller for inducing cross-well motion of bistable structures," *AIAA J.*, vol. 54, no. 12, pp. 4011-4021, 2016.
- [4] M. R. Simsek and O. Bilgen, "A Hybrid Position Feedback Controller for Inducing Cross-Well Motion of Bistable Structures," in *24th AIAA/AHS Adaptive Structures Conference*.
- [5] M. R. Simsek and O. Bilgen, "The Duffing-Holmes Oscillator Under Hybrid Position Feedback Controller: Response Type and Basin of Attraction Analyses," *Int. J. of Struct. Stab. and Dyn.*, vol. 20, no. 09, p. 2050101, 2020.
- [6] M. Simsek, R. Schieni, L. Burlion, and O. Bilgen, "A Hybrid Position Feedback Controlled Bistable Metamaterial Concept," presented at the ENOC 2022 - 10th European Nonlinear Dynamics Conference, Lyon, France, 2022-07-17, 2022.

Nonlinear interactions in a nonlinear time-dependent chain

Aur lie Labetoulle*, Alireza Ture Savadkoohi*, Emmanuel Gourdon* and Claude-Henri Lamarque*

*Univ Lyon, ENTPE, Ecole Centrale de Lyon, CNRS, LTDS, UMR5513, 69518 Vaulx-en-Velin, France

Abstract. The energy exchanges in a chain of oscillators is studied. The chain is composed by identical cells which correspond to a two degree-of-freedom (dof) systems composed by a linear oscillators linearly coupled to a grounded nonlinear oscillator with a time-dependent rigidity. The detection of the different dynamics makes it possible to predict the different regimes of the system.

Introduction

We consider a chain of coupled oscillators (see Fig. 1a) which is composed of n identical cells. A unit cell is a two dof system composed of a linear main oscillator (mass M_j) weakly coupled to a grounded nonlinear oscillator (mass m_j) [1] ($j \in [1, n]$). Two adjacent masses M_j are equally spaced at rest position with the distance Δx . We set u_j and v_j the displacements of the mass M_j and m_j , respectively and $\Lambda(v)$ as the nonlinear time-dependent restoring function. We suppose furthermore that $m_j \ll M_j$, each mass M_j is under external excitation ($F_j(t)$) and the chain is periodic.

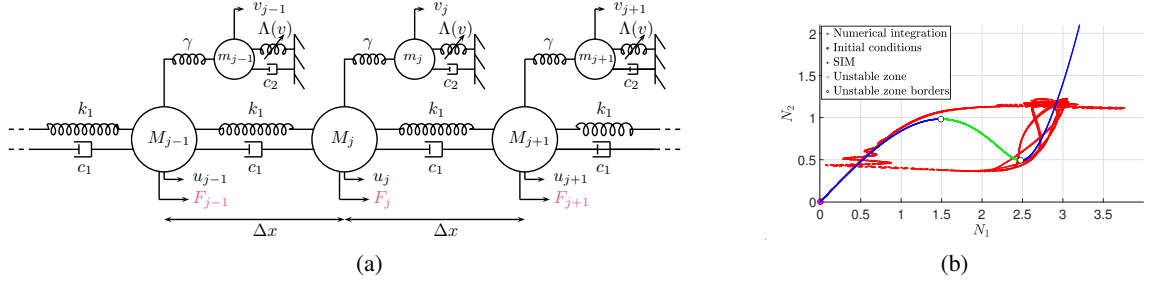


Figure 1: a) Schematic of the studied system: a chain of linearly coupled M_j , $j = 1, 2, \dots, L$ masses which are locally and linearly coupled to m_j masses possessing nonlinear restoring forcing functions. The M_j masses are equally spaced (Δx) at rest positive. b) Slow Invariant Manifold (SIM) (blue line) and numerical integration of governing equations (red line) for the projected chain with a constant nonlinear rigidity.

Results and discussion

We would like to predict responses of the mentioned chain around one of its modes. For this we study the projected equations on an arbitrary mode of the system for a constant and time-dependent nonlinear rigidity. Thus the model of the chain is reduced to a two dof system. The idea is to design the chain for localisation of vibratory energy [2]. For this we will detect the SIM, the fast and slow dynamics of the projected system via introducing the complex variable of Manevitch [3] and using the multiple scale method [4]. This will lead to the determination of characteristics points of the system: equilibrium and singular points corresponding to possible periodic and non-periodic regimes. As an example, Fig. 1b depicts the SIM of the projected system with “constant cubic nonlinearity” (in blue) as function of system amplitudes (N_1 and N_2). This figure is supplemented by numerical results of the forced system (in red). Due to existence of singularities, the system presents modulated response corresponding to repeated bifurcations between stable branches of the SIM. The same study is carried out on the chain with time-dependent nonlinearity which will be presented and commented upon.

To validate and show the relevance of the projection method, the numerical results of the projected chain are compared to those of the discrete chain.

References

- [1] Labetoulle A., Ture Savadkoohi A., Gourdon E. (2021). Detection of different dynamics of two coupled oscillators including a time-dependent cubic nonlinearity. *Acta Mech*, **233**(1): 259-290.
- [2] Charlemagne, S., Ture Savadkoohi, A., Lamarque, C. H. (2018). Dynamics of a linear system coupled to a chain of light nonlinear oscillators analyzed through a continuous approximation. *Phys. D: Nonlinear Phenom*, **374**: 10-20.
- [3] Manevitch L. I. (2001) The description of localized normal modes in a chain of nonlinear coupled oscillators using complex variables. *Nonlinear Dyn*, **25**: 95-109.
- [4] Nayfeh A. H., Mook D. T. (1979) *Nonlinear Oscillations*. Wiley, NY.

Acoustic non-reciprocity in strongly nonlinear locally resonant lattices

Mohammad Bukhari^{1,2}, Oumar Barry¹, and Alexander Vakakis²

¹ Department of Mechanical Engineering, Virginia Polytechnic Institute and State University, Blacksburg, VA, USA

² Department of Mechanical Science and Engineering, University of Illinois Urbana-Champaign, Urbana, IL, USA

Abstract. Due to the impracticality and the need for external bias in dynamic or activated media, the study of passive systems to break acoustic reciprocity have recently gained many researchers' attention. In this work, we aim to passively break acoustic reciprocity using asymmetric strongly nonlinear locally resonant lattices. The asymmetry in the lattice is induced through modulating the stiffness of local resonators embedded within the cells. This allows modifying existing structures without the need to completely replace the structure or conduct major changes. The achieved non-reciprocity is induced by the fact that these structures can support traveling breathers and the presence of different families of breathers depending on the lattice parameters. The stiffness modulation offers tunable passbands (PBs) in the band structure that can overlap and separate at different energy levels. The numerical results demonstrate that the partial overlap between these PBs can lead to strong passive acoustic non-reciprocity.

Introduction

Due to their unique dynamical properties, mechanical metamaterials have recently drawn the attention of many researchers. Beyond the linear regime limit, metamaterials can exhibit interesting nonlinear behavior that can offer additional dynamical properties with no counterpart in linear metamaterials [1]. For instance, nonlinearity can lead to energy-dependent band structures, ultra-low frequency bandgaps, intermodal hopping, and subharmonic bandgaps. In addition, pure strongly nonlinear lattices (i.e., sonic vacua) can support traveling breathers [2]. Breathers are traveling oscillatory wavepackets with spatially localized envelopes and energy-dependent speeds. Strongly nonlinear (sonic vacua) lattices with an asymmetric stiff/soft interface have shown reciprocity breaking induced by breather propagation [3]. The asymmetric stiff/soft interface lattice can be demonstrated through grounding stiffness modulation in sonic vacua lattices. In this work, we consider a strongly nonlinear asymmetric grounded locally resonant lattice waveguide. The lattice's cells are connected by a purely cubic nonlinear stiffness with no linear component (i.e., sonic vacua). The lattice consists of two sub-lattices (i.e., stiff/soft interface). The stiffness modulation is demonstrated through the linear local resonator stiffness.

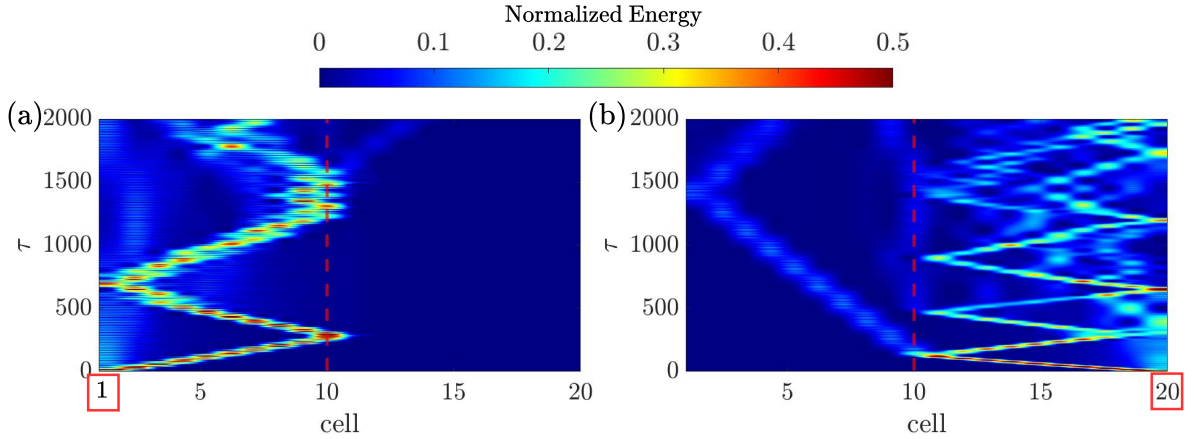


Figure 1: Spatio-temporal plots of the instantaneous total energy in the system excited from the stiff chain (left panels) and from the soft chain (right panels) at different energy levels: (a) Stiff sub-lattice excited, $I_0 = 0.6$. (b) Soft sub-lattice excited, $I_0 = 0.6$.

Results and discussion

Upon exciting the stiff sub-lattice (Fig. 1(a)), breather propagation is also limited to the sub-lattice where breathers are generated and no breathers can penetrate the interface in the stiff/soft direction. However, breathers can penetrate the interface between the sub-lattices and travel through the stiff chain when the soft chain is excited in the soft/stiff direction, as shown in the Fig. 1(b). This indicates that a strong acoustic non-reciprocity at this energy level can be realized passively through the proposed structure. Indeed, the partial overlap between the PBs of both sub-lattices results in breaking the reciprocity at this energy level.

References

- [1] Patil G. Priya S., Matlack K. (2021) Review of exploiting nonlinearity in phononic materials to enable nonlinear wave responses. *Acta Mechanica* **2021**:1-46.
- [2] Bukhari M., Barry O., Vakakis A. (2023) Breather propagation and arrest in a strongly nonlinear locally resonant lattice. *Mechanical Systems and Signal Processing* **183**:109623.
- [3] Mojahed A., Bunyan J., Tawfik S., Vakakis A. (2019) Tunable acoustic nonreciprocity in strongly nonlinear waveguides with asymmetry. *Physical Review Applied* **12**:034033.

Inverse Design of Periodic and Quasi-Periodic Nonlinear Mechanical Metamaterial

Pravinkumar Ghodake

Department of Mechanical Engineering, Indian Institute of Technology Bombay, Mumbai, India

Abstract. In nonlinear ultrasonics, the interaction of a monochromatic wave with nonlinear elastic materials generates higher harmonics ($2f$, $3f$, ...), known as harmonic generation. The sensitivity of higher harmonics amplitudes due to harmonic generation and harmonic scattering towards design parameters of nonlinear metamaterials, such as widths of the nonlinear elastic layers, makes the inverse design of nonlinear metamaterials challenging. Periodic and quasi-periodic linear and nonlinear mechanical metamaterials are designed by solving inverse design problems to control nonlinear elastic waves in solids. The time-dependent inverse design problems include a forward problem implemented using the finite element method. The inverse problem is proposed as a time-dependent optimization problem and solved using the Nelder-Mead algorithm.

Introduction

Nonlinear ultrasonics has shown its effectiveness in quantifying early-stage damages such as micro-cracks, dislocation substructure, micro-voids, etc. Harmonic generation due to the interaction of monochromatic (f) waves with early-stage damages is demonstrated in various theoretical [1], computational [2], and experimental [3] studies. Measuring amplitudes of such higher harmonics is important as they give information about the intensity of early-stage damages. During experiments, system-generated higher harmonics are introduced due to instrumentation, such as a short pulse power amplifier that masks the damaged material's natural harmonic response [4]. Suppression of such system-generated higher harmonics like 2nd ($2f$) and 3rd ($3f$) harmonics can be achieved by designing appropriate metamaterials. The harmonic generation and scattering are highly sensitive to the widths of metallic layers present in metamaterials [1]. The nonlinearity effects of the materials used in the design of metamaterials need to be addressed. This research aims to design robust linear and nonlinear metamaterials for nonlinear ultrasonic applications through the inverse design approach. A shape optimization problem is defined for the design of layered linear, nonlinear, periodic, and quasi-periodic (Figure 1) metamaterials by simulating wave propagation studies using the finite element method.

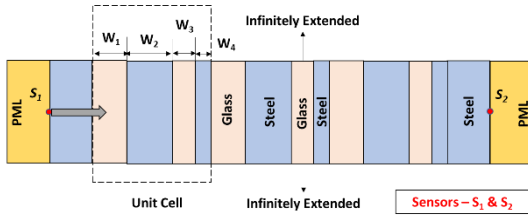


Figure 1: Schematic of quasi-periodic metamaterial.

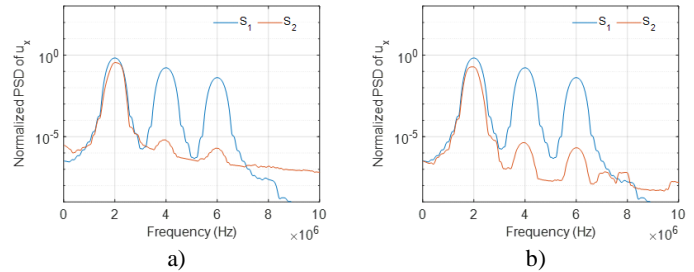


Figure 2: Frequency responses of the waves passing through the inversely designed periodic (a) and quasi-periodic (b) nonlinear metamaterials that suppress 2nd ($2f$) and 3rd ($3f$) harmonics as well as maintaining the amplitude of the 1st (f) harmonics maximum.

Results and Discussion

Capabilities of the inversely designed periodic and quasi-periodic linear and nonlinear metamaterials to control nonlinear waves are demonstrated through this novel, most realistic, and universal inverse design approach (Figure 2). Interestingly, some inversely designed linear metamaterials also show similar responses to nonlinear metamaterials. Harmonically scattered waves are trapped within the metamaterial due to the complex interplay between harmonic generation and scattering of waves between multiple nonlinear elastic layers.

References

- [1] Kube C. M. (2017) Scattering of Harmonic Waves from a Nonlinear Elastic Inclusion. *J. Acoust. Soc. Am.*, **141**(6):4756–4767.
- [2] Ghodake P. (2021) One Dimensional Nonlinear Wave Propagation in a Rate Independent Pinched Hysteretic Material. *Proc. 48th Annu. Rev. Prog. in QNDE*, 1–6.
- [3] Cantrell J. H., Yost W. (2001) Nonlinear Ultrasonic Characterization of Fatigue Microstructures. *Int. J. Fatigue*, **23**:487–490.
- [4] Liu S., Croxford A. J., Neild S. A., Zhou Z. (2011) Effects of Experimental Variables on the Nonlinear Harmonic Generation Technique. *IEEE Trans Ultrason Ferroelectr Freq Control*, **58**(7):1442–1451.

A Nonlinear Metamaterial Induced by Nonlinear Damping Effect with Inertia Amplifiers

Bao Zhao*, Xingbo Pu**, Bart Van Damme***, Andrea Bergamini***, Eleni Chatzi*, and Andrea Colombi*

*Department of Civil, Environmental, and Geomatic Engineering, ETH Zürich, Zürich, Switzerland

**Department of Civil, Chemical, Environmental, and Materials Engineering, University of Bologna, Bologna, Italy

***Laboratory for Acoustics/Noise Control, Empa Materials Science and Technology, Dübendorf, Switzerland

Abstract. In this paper, we studied a nonlinear metamaterial based on the nonlinear damping effect. The proposed design combines a linear host cantilever beam and periodically distributed inertia amplifiers as nonlinear local resonators. Firstly, the geometric nonlinearity induced by the inertia amplifiers is studied to reveal the amplitude-dependent damping effect. Secondly, a modal analysis method is implemented to form a lumped parameter model for the nonlinear metamaterial. This model is further solved by a numerical harmonic balance method under periodic base excitation. Finally, the nonlinear energy transfer inside the proposed design is studied to investigate the nonlinear interaction between local resonators and different vibration modes. The theoretical results show that the bandgap is amplitude-dependent, broadened, and gradually degenerated due to the nonlinear damping effect. It also further leads to an efficient modal dissipation capacity of the host structure, which has significant potential in shock wave mitigation.

Introduction

Recently, locally resonant metamaterials have been proven effective for vibration mitigation. However, their bandgaps decided by the underneath linear structures are usually narrowed when compared with the well-known nonlinear energy sinks [1]. Therefore, the pursuits to introduce nonlinearities into metamaterials have combined the advantages of these two research areas and raised novel concepts in the sense of structural dynamics, such as broadband vibration attenuation, non-reciprocity in periodic lattice, and breather energy localization. Based on this idea, we investigate a nonlinear metamaterial theoretically and experimentally for broadband and shock wave mitigation built on inertia amplifiers [2], which introduces the nonlinear damping effect into the metamaterial.

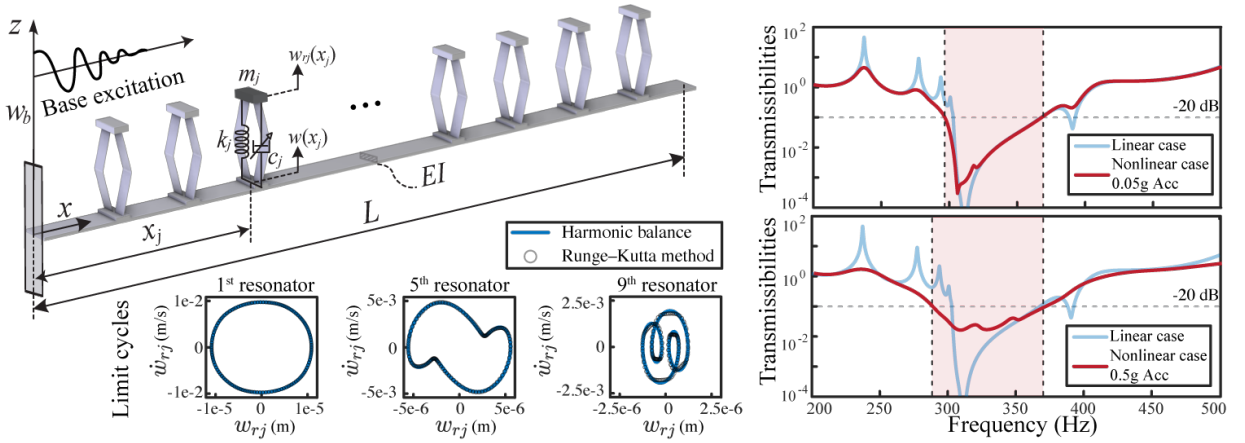


Figure 1: The schematic of the nonlinear metamaterial, the transmissibilities of the host beam, and the limit cycles of nonlinear local resonators.

Results and discussion

The schematic of the nonlinear metamaterials is shown in Fig. 1, which combines a linear host cantilever beam with inertia amplifiers as nonlinear local resonators. A modal analysis, together with a numerical harmonic balance method, is employed to solve the steady-state frequency response of the host beam and local resonators under harmonic excitation. The nonlinear transmissibilities show that the bandgap has been broadened due to the nonlinear damping effect. It also leads to the degeneration of bandgap with the increase of excitation level. In addition to the bandgap range, the modal frequency peaks have also been attenuated due to the nonlinear interactions with local resonators, which is verified by the limit cycles of the local resonators. With the wave propagation from the left to the right side of the host beam, the limit cycles of local resonators indicate more modal frequency interactions. This nonlinear interaction between the host beam and local resonators features an efficient modal dissipation capacity, and could be potentially used in shock wave mitigation.

References

- [1] Rega G. (2022) Nonlinear Dynamics in Mechanics: State of the Art and Expected Future Developments. *J. Comput. Nonlinear Dyn.* **17**:080802
- [2] Van Damme B., Hannema G., Sales Souza L., Weisse B., Tallarico D., & Bergamini A. (2021) Inherent non-linear damping in resonators with inertia amplification. *Appl. Phys. Lett.* **119**:061901

Modal interactions in a non-linear mass-in-mass periodic chain

J. Flosi*, A. Ture Savadkoohi* and C.-H. Lamarque*

*Univ Lyon, ENTPE, Ecole Centrale de Lyon, CNRS, LTDS, UMR5513, 69518 Vaulx-en-Velin, France

Abstract. The multiple scale dynamics of a forced periodic chain composed of cubic mass-in-mass cells is considered. Dispersion equation of the continuous expression of the system permits modal decomposition of response functions. A particular 1 : 3 internal resonance is considered and continuous equations are projected on the two relevant modes. Selection of fast and slow dynamics leads to obtaining the slow invariant manifolds (SIM) and frequency responses of the chain.

Introduction

Firstly introduced in the magnetic field [1], metamaterials are presenting unnatural properties due to their special architecture. Mechanical and vibro-acoustical metamaterials were later designed for control of mechanical energies [2]. Such systems, e.g. mass-in-mass, can be designed to present negative indices. Other variants of this type of metamaterials can be fabricated via multiple inclusions [3] or nonlinearity inclusions [4] leading to multiple tunable bandgaps. In this work, a periodic nonlinear mass-in-mass chain is considered, see Fig.1. In details, it is composed of equally spaced masses m_1 at rest positions which are linearly coupled to each other. Each mass m_1 houses a mass m_2 which possesses a cubic restoring force.

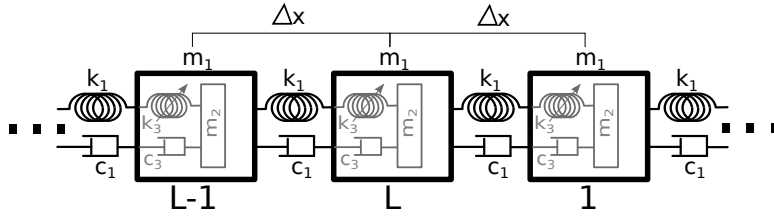


Figure 1: Periodic cubic mass-in-mass chain.



Figure 2: Time histories of modal coordinates of first (p_1) and third (p_2) mode under initial displacement $p_1(0) = 0.75$ and the rest zero

Results and discussion

Inspection of linear part of continuous equations lead to detection of modal characteristics of the system. As an example, a 1 : 3 internal resonance is considered. Response functions are decomposed in well chosen bi-modal form and governing equations are projected on two internally resonant modes. Figure 2 presents time histories of modal coordinates of internally resonant modes (first and third mode) represented by p_1 and p_2 , respectively. Asymptotic responses [5] of the system are considered. Fast dynamics [6] of the projected system leads to detection of two SIMs associated to two internally resonant modes. Slow dynamics [6] provides singular and equilibrium points, which lead to the prediction of periodic and quasi-periodic behaviors.

References

- [1] Veselago V. G. (1968) The electrodynamics of substances with simultaneously negative values of ϵ and μ . *Soviet Physics Uspekhi* **10**:509-514.
- [2] Wu L. et al. (2020) A brief review of dynamic mechanical metamaterials for mechanical energy manipulation. *Materials Today* **44**.
- [3] Rodrigues G.S., Weber H.I. (2017) Elastic Metamaterials Analysis: Simple and Double Resonators. *Research Inventory: International Journal of Engineering And Science* **7**:11-16.
- [4] Cveticanin L. and Zukovic M. (2017) Negative effective mass in acoustic metamaterial with nonlinear mass-in-mass subsystems. *Communications in Nonlinear Science and Numerical Simulation* **51**:89-104.
- [5] Manevitch L. (2001) The Description of Localized Normal Modes in a Chain of Nonlinear Coupled Oscillators Using Complex Variables. *Non Dyn* **25**:95-109.
- [6] Ture Savadkoohi A. et al. (2016) Analysis of the 1:1 resonant energy exchanges between coupled oscillators with rheologies. *Nonlinear Dyn* **86**:2145-2159.

Towards the Robust Optimal Design of Nonlinear Metamaterials

Camila da Silveira Zanin^{*,**}, Samy Missoum^{***}, Alireza Ture Savadkoobi^{*}, Sébastien Baguet^{**} and Régis Dufour^{**}

^{*}Univ Lyon, ENTPE, Ecole Centrale de Lyon, CNRS, LTDS, UMR5513, 69518 Vaulx-en-Velin, France

^{**}Univ Lyon, INSA Lyon, LaMCoS UMR CNRS 5259, 69621 Villeurbanne, France

^{***}Aerospace and Mechanical Engineering Department. University of Arizona. Tucson, USA

Abstract. In the field of metamaterial design, tailoring nonlinearities can markedly expand the realm of wave manipulations. However, the optimal design of metamaterials with nonlinearities is hampered by a dynamic behavior that exhibits discontinuities and is highly sensitive to uncertainties. For this reason, a specific stochastic design optimization approach is introduced. The algorithm tackles discontinuities and accounts for uncertainties. In addition, the approach introduces a formulation based on a field representation of the design variables, thus reducing the dimensionality of the problem. The stochastic optimization algorithm is demonstrated on the vibration mitigation of a chain of nonlinear resonators. It is shown that the combination of the stochastic optimization algorithm and field representation provides more flexibility in tailoring the chain properties.

Introduction

The design and manufacturing of metamaterials has become an intense research field. From simple band gaps, which prevent the propagation of waves within certain frequency ranges, to the creation of invisibility cloaks, metamaterials offer a host of wave manipulation capabilities [1]. It has long been understood that nonlinearities at the unit cell level can substantially increase the range of possible wave manipulations. Nonlinearities of various forms (e.g., stiffness, constitutive law) have been investigated to achieve specific wave characteristics. Among all the possible promising applications, this study focuses on vibration and shock mitigation. The design optimization of metamaterials is tedious for several reasons. First, the presence of nonlinearities can lead to discontinuous responses, representative of the high sensitivity of the system dynamics to uncertainties (e.g., material properties, loading). Another difficulty stems from the very large number of units in a metamaterial, which makes optimizing units individually computationally intractable.

Results and discussion

This work introduces the first step towards a general framework for the robust design of nonlinear metamaterials. Specifically, this research focuses on a stochastic optimization approach which accounts for discontinuities detected through clustering [2]. Clusters correspond to various dynamic behaviors and can be mapped onto different regions of the search space, whose boundaries are identified using a support vector machine classifier. The performance of the metamaterial in each region is approximated using Kriging surrogates, which are efficient to propagate uncertainties. The approach was originally developed for nonlinear energy sinks, which exhibit a discontinuous response in the form of an activation threshold [2]. This work also addresses the difficulty due to the dimensionality of the optimization problem (i.e., large number of unit cells) through the use of a field representation. To reduce the problem dimensionality, properties such as the nonlinear stiffness are represented using a spatial field over the metamaterial domain. The field is governed by a handful of stochastic coefficients, thus substantially reducing the dimensionality of the problem. Among the possible problem formulations, the proposed approach is used to optimize the mean of performance metrics such as the RMS response in the case of vibration mitigation. In this study, the optimization of a one-dimensional chain of resonators is considered for demonstrative purposes (Figure 1). The chain, which follows a “mass-in-mass” configuration, is made of units constituted of a main linear resonator and an internal nonlinear resonator. The nonlinearities considered in this study stem from the stiffness properties of the internal resonators. Uncertainties related to stiffness properties, excitation frequencies and amplitude are included in the optimization problem. It is shown that the stochastic optimization is able to tailor the properties of the chain to, for instance, mitigate vibrations. The results also demonstrate the capability of the field approach to reduce the dimensionality of the stochastic optimization problem while achieving performances not achievable with properties constant over the chain.

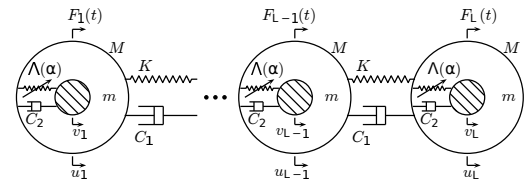


Figure 1: “Mass-in-mass” chain of resonators.

References

- [1] Deymier P.A. (2013). Acoustic Metamaterials and Phononic Crystals. Springer Science & Business Media.
- [2] Boroson, E., Missoum, S., Mattei P.O., Vergez C. (2017). Optimization Under Uncertainty of Parallel Nonlinear Energy Sinks. *J. Sound Vib.* **394**: 451-464.

Topological Indices of Line Graph of Metal Organic Compound

Muhammad Talha Farooq^{1,2} and Pawaton Kaemawichanurat^{1,2}

¹Mathematics and Statistics with Applications (MaSA),

²Department of Mathematics, King Mongkut's University of Technology Thonburi,
Bangkok, Thailand

Abstract:

The transition metal is a planar metallic organic structure, and tetra-cyano-benzene is one of the most studied networks of 3d series of transition metal. Tetra-cyano-benzene behaved as a useful object in the alloy synthesis industry due to its excellency of hardness. Interestingly, the *TM*–*TCNB* systems are metallic in any event in one turn heading and show long-run ferromagnetic coupling on the off chance that for attractive structures, which speak to perfect applicants and a fascinating possibility of uncommon applications in spintronics. To study this, tetra-cyano-benzene structure we use an authentic mathematical tool known as vertex-edge and edge-vertex base topological indicators and shows some physical and chemical properties in numerical form, to understand the structure deeply. The topological indices are the numerical invariants of a molecular graph and are very useful for predicting their physical properties. Here, we calculate the degree based topological indices of line and paraline graph of Transition Metal Tetracyanobenzene $C_{10}H_2N_4[m,n]$ for $(m \times n)$ chain 2D structure like general Randić index R_α for different values of $\alpha = (1, -1, 1/2, -1/2)$, Geometric Arithmetic index, Forgotten topological index, first, second and third Zagreb index, Atom-bond connectivity index, first and second multiplicative Zagreb index, Symmetric division index, Sum-connectivity index, Reduced Reciprocal Randić index, first and second Gourava index, first and second Hyper-gourava index, first, second and third Reduced Zagreb index and Balaban index for transition metal tetra-cyano benzene based on vertex-edge and edge-vertex degree.

Introduction:

The metal-organic networks transition metal of the three-dimensional series: *Ti*, *V*, *Cr*, *Fe*, *Co*, *Ni*, *Cu* or *Zn(TM)* tetracyanobenzene (*TCNB*) has a high melting and boiling point with low band energy which assist the electrical and thermal conductivity. Due to the finer size of *TM*–*TCNB*, it has more physical and mechanical qualities, such as good hardness, as a result, it is mostly employed in the alloy synthesis industry to refine high-temperature stability. Line graphs have been used in chemistry since the very beginning of structural chemistry. Bertz [1] was the first to suggest the use of line graphs of molecular graphs and their invariants for representing organic molecules physicochemical characteristics and also he established the first topological index based on a line graph in 1981, and further the idea of molecular branching and complexity. There are several topological indices based on the molecular graph's line graph. Line graphs were rarely employed in various mutually unrelated disciplines of chemistry.

Topological indices are generally classified into three categories degree-based, distance-based and spectrum-based. Wiener conceived the idea of first topological indices in 1947 while he determined the boiling point of paraffin [2]. After this he named this index "Wiener index". Then came the topological index theory. Now a days there are several topological indexes available like Randić Index, atom bond connectivity index, geometric arithmetic index and Zagreb index. The first Randić index of a chemical graph *G* is introduced by Randić in [3] 1975 this is the first and oldest degree based topological indices. Gutman [4] presented the first and second Zagreb indices in 1972.

References

1. Bertz, S. H. (1981). *The bond graph*. *Journal of the Chemical Society, Chemical Communications*, (16), 818-820
2. Wiener, H. (1947). *Structural determination of paraffin boiling points*. *Journal of the American chemical society*, 69(1), 17-20.
3. Randić, M. (1975). *Characterization of molecular branching*. *Journal of the American Chemical Society*, 97(23), 6609-6615.
4. Gutman, I., & Trinajstić, N. (1972). *Graph theory and molecular orbitals. Total π -electron energy of alternant hydrocarbons*. *Chemical physics letters*, 17(4), 535-538.

Bandgap formation study of a geometrically nonlinear metamaterial

Kyriakos Alexandros Chondrogiannis*, Vasilis Dertimanis* and Eleni Chatzi*

*Department of Civil, Environmental and Geomatic Engineering, ETH Zürich, Zurich, Switzerland

Abstract. The concept of metamaterials can be enhanced with use of nonlinear designs for vibration mitigation purposes. To specify the frequency zones within which wave propagation is prevented, it is necessary to study the corresponding dispersion curves. In this work, a geometrically nonlinear metamaterial inducing a negative stiffness effect is investigated. The bandgap formation is studied with the use of analytical methods and numerical techniques, evaluating their compliance. An energy dependent behaviour is identified, which is attributed to the nonlinear nature of the design.

Introduction

The mitigation and control of mechanical vibrations forms a major challenge in engineering applications. The recently developed concept of metamaterials can be applied for wave manipulation purposes [1]. These are configurations that consist of periodically arranged unit cells and can form specific frequency ranges (bandgaps), where wave propagation is obstructed. The introduction of nonlinearity in such configurations can enhance their vibration mitigation capabilities both in terms of widening the bandgap, as well as shifting this toward lower frequencies. The current study focuses on a geometrically nonlinear metamaterial lattice, inducing negative stiffness behaviour [2]. This is formed by periodic arrangement of repeated unit cells, as depicted in Fig. 1(a). Each cell, of lattice constant a , consists of an external mass m that is connected to an internal mass μ via a nonlinear element and linear viscous damping c_n , while neighboring cells are interconnected with linear stiffness and damping k and c respectively. The adoption of a triangular arch configuration results into geometric nonlinearity under large displacement consideration, while negative stiffness is observed in a specific region of the equilibrium path. This arch is formed by two identical linear springs of stiffness k_n , arranged in a triangular geometry of height H and base $2L$, as shown in Fig. 1(a).

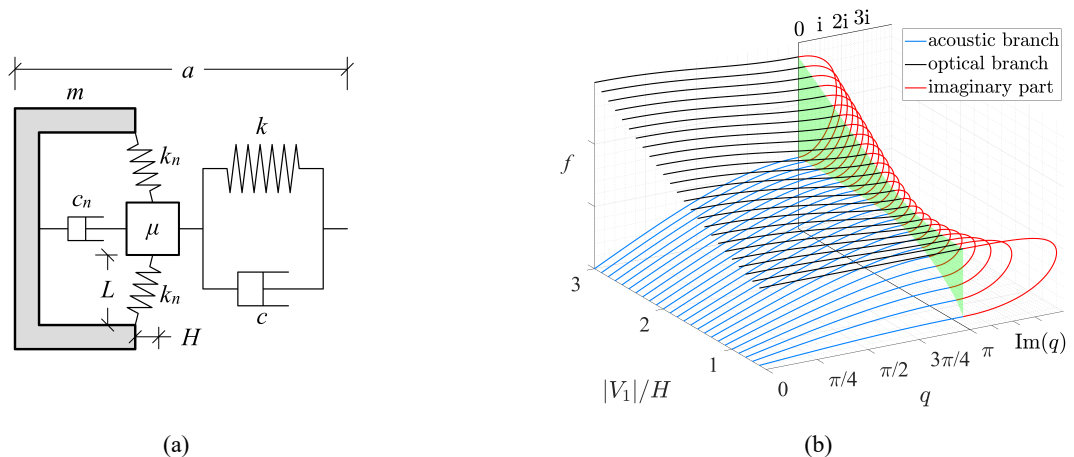


Figure 1: Geometrically nonlinear metamaterial. (a) Unit cell. (b) Dispersion curves (bandgap highlighted in green).

Results and discussion

Determination of the created bandgap requires calculation of the corresponding dispersion curves of an infinite lattice, i.e. the plot of the frequency f versus wave number q , depending on of the response magnitude. This calculation is initially performed via use of the Harmonic Balance Method (HBM), with the results of this process shown in Fig. 1(b). Due to the nonlinear nature of the design, the dispersion relation is dependent on the relative oscillation amplitude $|V_1|$, between the nonlinearly connected masses. The resulting bandgap is defined to be the range, where no real frequency solutions exist. To further study the bandgap characteristics of the system, the Nonlinear Normal Modes of the unit cell are evaluated for varying energy levels. Energy dependent curves are therefore formed for the in-phase and out-of-phase modes, indicating the boundaries of the bandgap [3]. The respective results are compared against the output of the HBM, evaluating the resulting agreement, while estimation of the dispersion curves with numerical techniques validates the analytical calculations.

References

- [1] Craster R.V., Guenneau S. (2013) Acoustic Metamaterials. Springer, Dordrecht.
- [2] Chondrogiannis K. A., et al. (2022) Computational Verification and Experimental Validation of the Vibration-Attenuation Properties of a Geometrically Nonlinear Metamaterial Design. Phys. Rev. Appl., 17(5):054023.
- [3] Mojahed A., et al. (2019) Tunable Acoustic Nonreciprocity in Strongly Nonlinear Waveguides with Asymmetry. Phys. Rev. Appl., 12(3):034033.

Parametric resonance and extreme motions of a cantilever with a tip mass: an experimental-theoretical study

Hamed Farokhi*, Eetu Kohtanen** and Alper Erturk **

*Department of Mechanical and Construction Engineering, Northumbria University, Newcastle upon Tyne NE1 8ST, UK

**George W. Woodruff School of Mechanical Engineering, Georgia Institute of Technology, Atlanta, 30332, USA

Abstract. An experimental-theoretical study is conducted on the extreme parametric resonance response of a cantilever with a tip mass. A state-of-the-art in vacuo base excitation experimental set-up is used, consisting of a vacuum chamber and a feedback-controlled long-stroke shaker, together with a high-speed camera to capture large-amplitude motions. A geometrically exact model based on the centreline rotation is utilised for the theoretical part. Extensive comparisons are conducted between experimental observations and theoretical predictions. It is shown that the geometrically exact model's predictions are in excellent agreement with the precisely conducted experimental measurements.

Introduction

Dynamical characteristics of cantilevers have been the topic of investigation by many researchers over the last few decades, with earlier investigations conducted by Crespo da Silva and Glynn [1], who derived the third-order nonlinear equations of motion of a cantilever using the inextensibility assumption, and utilised the method of multiple scales to solve the equations, and Nayfeh and Pai [2], who investigated the lateral vibrations of a base-excited cantilever using a third-order model and the method of multiple scales. Recently, Farokhi et al. [3] proposed a rotation-based geometrically exact model for examining extreme oscillations of cantilevers, which was followed by an experimental study [4] which validated the accuracy of the proposed rotation-based exact model. This study examines the extreme oscillations of an axially excited cantilever with a tip mass in the parametric resonance region for various base acceleration levels.

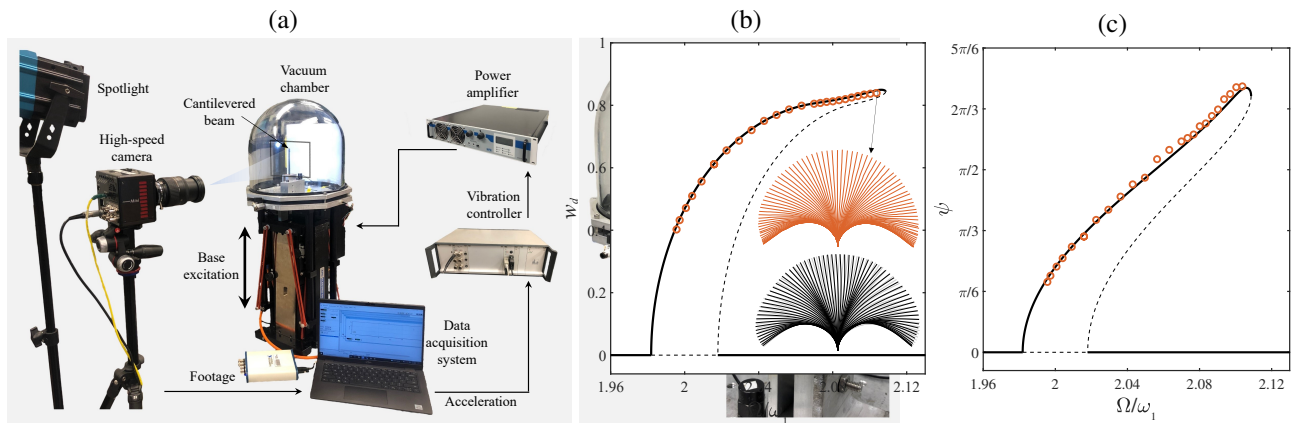


Figure 1: (a) Experimental set-up. (b, c) Parametric resonance responses of the cantilever with the tip mass at 0.25g RMS axial base acceleration for transverse and rotational motions at the tip of the cantilever, respectively. Symbols indicate the experimental results, while solid and dashed lines show the stable and unstable theoretical solutions, respectively.

Results and Discussions

Three sets of experiments are conducted at RMS acceleration levels of 0.15g, 0.20g, and 0.25g using the set-up shown in Fig. 1(a), and detailed comparisons are carried out between the experimental and theoretical results. The results for a representative case are shown here. More specifically, Figs. 1(b) and (c) show the transverse and rotational motion frequency responses for the case of 0.25g RMS base acceleration. As seen, the cantilever displays a hardening-type nonlinear behaviour in the parametric resonance region as predicted theoretically and confirmed via experimental observations. Furthermore, it is seen that the geometrically exact model's predictions are in excellent agreement with the experimental results even at this excitation level for which the cantilever undergoes oscillations of extremely large amplitudes. Hence, these comparisons validate the accuracy of the exact model for moderate to extreme vibration analysis of axially excited cantilevers.

References

- [1] Crespo da Silva MRM, Glynn CC (1978) Nonlinear flexural-flexural-torsional dynamics of inextensional beams. I. Equations of motion. *J. Struct Mech* **6**:437–448.
- [2] Nayfeh, A.H., Pai, P.F. (1989) Non-linear non-planar parametric responses of an inextensional beam. *I. J. Non-Linear Mech* **6**:437–448.
- [3] Farokhi, H., Ghayesh, M.H. (2019) Extremely large oscillations of cantilevers subject to motion constraints. *J. Applied Mech* **86**:031001.
- [4] Farokhi, H., Xia, Y., Erturk, A. (2022) Experimentally validated geometrically exact model for extreme nonlinear motions of cantilevers. *Nonlin Dyn* **107**:457–475.

Nonlinear Reciprocal Dynamics in Systems with Broken Mirror Symmetry

Behrooz Yousefzadeh* and Andrus Giraldo**

*Department of Mechanical, Industrial & Aerospace Engineering, Concordia University, Montreal, QC, Canada

**School of Computational Sciences, Korea Institute for Advanced Study, Seoul, Korea

Abstract. Nonreciprocal devices can provide new functionalities for steering of elastic waves. Breaking the mirror symmetry is a necessary condition for enabling nonreciprocal dynamics in nonlinear devices. But the response of a nonlinear system with broken mirror symmetry is not necessarily nonreciprocal, even near the system resonances. Here, we present methodology for obtaining stable nonlinear reciprocal dynamics in coupled systems with broken mirror symmetry.

Introduction

Reciprocity relations describe invariance properties of elastic wave propagation in materials [1]. In linear, time-invariant materials, reciprocity means that the response of a material to an external load remains invariant with respect to interchanging the locations of the source and receiver. Avoiding this invariance property has posed a challenge in the design of modern devices for wave engineering. Breaking the mirror symmetry is a necessary requirement for nonreciprocal dynamics to exist in nonlinear systems. Such asymmetry is a necessary condition for enabling nonreciprocal dynamics in nonlinear systems, but it is not a sufficient condition.

In this work, we present a methodology for restoring dynamic reciprocity in coupled systems with broken mirror symmetry. We use the archetypal framework of two coupled oscillators for this purpose. The governing equations that we consider are

$$\begin{aligned} \ddot{x}_1 + 2\zeta\dot{x}_1 + x_1 + k_c(x_1 - x_2) + k_N x_1^3 &= F_1 \cos(\omega_f t), \\ \mu\ddot{x}_2 + 2\zeta\dot{x}_2 + r x_2 + k_c(x_2 - x_1) + k_N x_2^3 &= F_2 \cos(\omega_f t) \end{aligned} \quad (1)$$

We develop numerical continuation codes through the software AUTO to compute the steady-state response of Eq. (1) as a family of periodic orbits; see [2] for the further details. We present results corresponding to $\zeta = 0.05$, $k_c = 5$ and $k_N = 1$. Parameters μ and r control the mirror symmetry of the system.

Results and discussion

To test for reciprocity, we need to compare two configurations: (i) *forward*, where $F_1 = P$, $F_2 = 0$ and the monitored output displacement is $x_2^F(t)$, (ii) *backward*, where $F_1 = 0$, $F_2 = P$ and the monitored output displacement is $x_1^B(t)$. Reciprocity holds if and only if $x_2^F(t) = x_1^B(t)$.

Fig. 1(a) shows a special case of nonreciprocal dynamics for $\mu = 1.5$ near the second mode of the system, where nonreciprocity manifests itself as a difference in phase, but not amplitude, of the forward and backward configurations [2]. This state is characterized by a nonreciprocal phase shift, $\Delta\phi$. To achieve reciprocity, we need to simultaneously keep the amplitudes of $x_2^F(t)$ and $x_1^B(t)$ equal and set $\Delta\phi = 0$. This is only possible by using a second symmetry-breaking parameter, r . Fig. 1(b) shows the evolution of the reciprocity norm, $R = (1/T) \int_0^T (x_2^F - x_1^B) dt$, and nonreciprocal phase shift, $\Delta\phi$, as a function of r . Reciprocity is restored, $R = 0 \Leftrightarrow x_2^F(t) = x_1^B(t)$, because the two symmetry-breaking parameters are effectively balancing each other.

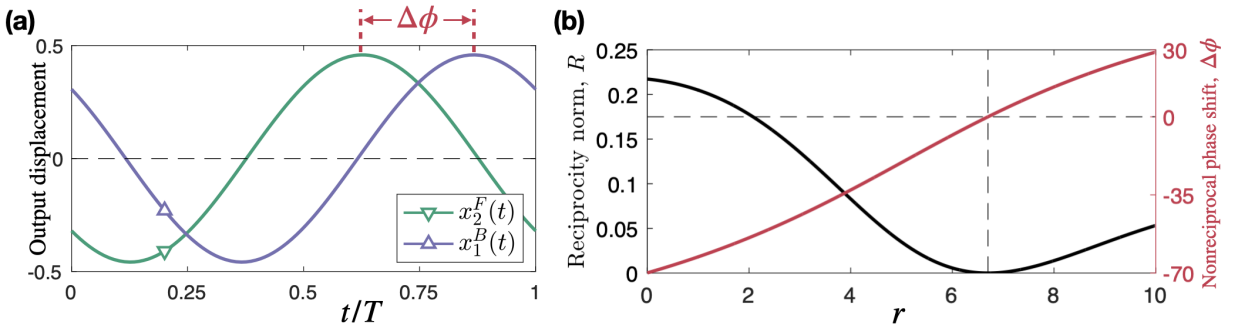


Figure 1: (a) Phase nonreciprocity at $P = 0.5$ with $\mu = 1.5$ as the symmetry-breaking parameter. This is achieved near $\omega_f \approx 3$. (b) A second symmetry-breaking parameter, r , brings nonreciprocal phase shift to zero near $r \approx 6.7$.

In conclusion, we demonstrate the possibility of restoring dynamic reciprocity in coupled nonlinear systems with broken mirror symmetry. This is achieved by simultaneously tuning two symmetry-breaking parameters such that the second symmetry-breaking parameter can counteract the original asymmetry and restore the reciprocity invariance in the system. We interpreted the results in the context of phase nonreciprocity.

References

- [1] Nassar H., et al. (2020) Nonreciprocity in acoustic and elastic materials. *Nat. Rev. Mater.* **5**(9):667-685.
- [2] Yousefzadeh B. (2022) Computation of nonreciprocal dynamics in nonlinear materials. *J. Comp. Dyn.* **9**(3):451-464.

Dispersion properties of metamaterial honeycombs embedding nonlinear resonators

Yichang Shen* and Walter Lacarbonara*

*Department of Structural and Geotechnical Engineering, SAPIENZA University of Rome, Rome, Italy

Abstract. Wave propagation of honeycomb metamaterials hosting nonlinear resonators is studied. The projection method based on the Floquet-Bloch theorem is used to explore the linear and nonlinear dispersion properties. The method of multiple scales is applied to get the closed form expression of the nonlinear manifolds parametrized by the amplitudes, frequency, and wave number. The effects of the nonlinearity on the stop band frequency are thus investigated, furthermore, the optimization issues of the resonators' mass, stiffness, damping and nonlinearity towards certain requirements of the stop band characteristic are addressed.

Introduction

Mechanical metamaterials are attracting a great deal of attention thanks to their potential for suppressing or attenuating the propagation of elastic waves by creating stop bands. In the literature, many works addressing metamaterial focused on the linear dispersion properties or on the nonlinear frequency response, the present work aims to investigate the effects of the local nonlinear resonators parameters on the dispersion relations of the honeycomb (see the schematic view inside Fig. 1(a)), and thus, to ensure stop band behavior and to find the optimal design of the resonators. The analytical prediction of the stop band properties and the comparison between the generated nonlinear stop bands and the linear counterparts are investigated.

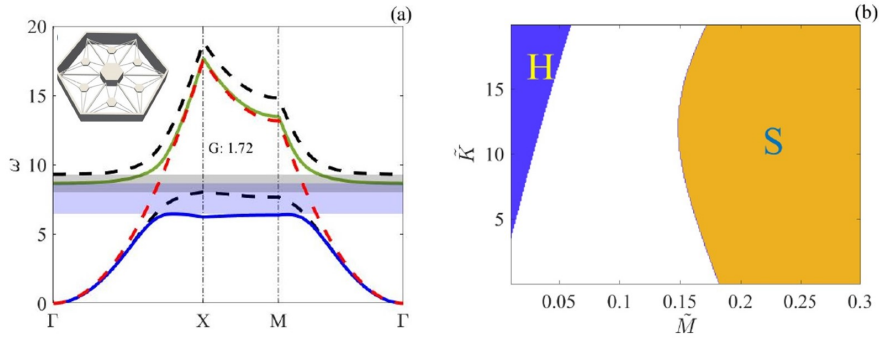


Figure 1: (a) The dispersion curves of the honeycomb with single-dof nonlinear resonators, the red and black dashed curves represent the dispersion properties of the plate without resonators and with linear resonators, respectively. The nonlinear optical and acoustic frequencies are shown by the blue and green curves, respectively. G is the ratio between nonlinear (blue) and linear (grey) stop band width. (b) Design chart with the suggested type of resonator nonlinearity based on the stiffness and mass of resonators.

Results and discussion

The linear dispersion functions ω^- and ω^+ are obtained by the eigenvalue problem of the mechanical system [1], which describe the lower-frequency curve (acoustic branch) and the higher-frequency curve (optical branch) of the linear dispersion spectrum, respectively. By applying the asymptotic approach of multiple scales [2] to the equation of motion in modal coordinates, one can finally obtain the nonlinear frequency of the acoustic mode (ω_{nl}^-) and optical mode (ω_{nl}^+), read as:

$$\omega_{nl}^- = \omega^- + \frac{N_3(3\phi_2^{-4}a^{-2} + 6\phi_2^{-2}\phi_2^{+2}a^{+2})}{8\omega^-}, \quad \omega_{nl}^+ = \omega^+ + \frac{N_3(3\phi_2^{+4}a^{+2} + 6\phi_2^{+2}\phi_2^{-2}a^{-2})}{8\omega^+}, \quad (1)$$

where a^\pm are the modal coordinates and ϕ^\pm are the eigenvectors depend on the resonator's mass and stiffness, N_3 is the resonators nonlinearity. Figure 1(a) shows linear and nonlinear dispersion functions of the honeycomb, it should be noted that the stop band width increases up to 72% when the softening nonlinearity is involved. Figure 1(b) represents a design chart showing the optimal choice of hardening or softening resonators based on the their mass and stiffness to enlarge the stop band width [3]. In summary, an in-depth understanding of the nonlinear metamaterial's dispersion properties and the possibility provided by the exploitation of the resonator nonlinearity to improve the metamaterial's vibration suppression capability can be gained from the numerical sensitivity optimization studies carried out within the analytical computations of the nonlinear wave dispersion properties.

References

- [1] Y. Shen, W. Lacarbonara, (2023) Nonlinear dispersion properties of metamaterial beams hosting nonlinear resonators and stop band optimization. *Mech. Syst. Signal Process* **187**:109920.
- [2] A. H. Nayfeh, D. T. Mook, (1979), *Nonlinear oscillations*, John Wiley & sons, NY.
- [3] Y. Shen, W. Lacarbonara, (2023) Nonlinearity-enhanced wave stop bands in honeycombs embedding spider web-like resonators, *J. Sound Vib.* (Under review).

Multi-objective optimization of a vibro-impact capsule moving in small intestine

Jiapeng Zhu. Maolin Liao *. ZhiQiang Zhu.

*University of Science and Technology Beijing. No.30, Xueyuan Road, Haidian District, Beijing, China

Abstract. In order to promote the controllability of a self-propelled capsule moving in digestive tract and thus improve the detection efficiency of wireless capsule endoscope, a capsule-small intestine coupling model is developed by integrating the dynamic model of a vibro-impact capsule with a small intestinal model. During the optimization, five different target moving speeds (including fast, slow, forward, backward and hovering), the minimal impact force acting on the small intestine, and the minimal energy consumption of the capsule are considered as the optimization objectives. Furthermore, the uncertainty of small intestine environment is considered by varying the radius of small intestine.

Introduction

Under the environment of intestinal peristalsis[1] and radius fluctuation[2], NSGA-II, Monte Carlo, and Six-Sigma algorithms are combined to conduct the multi-objective optimization of capsule both the control and structure parameters[3].as shown in Fig. 1. Based on nonlinear dynamics analysis and sensitivity analysis, the framework of multi-parameter multi-objective optimization algorithm is determined. And the optimization example obtained from the algorithm framework is substituted into the boundary analysis, we can get the relationship between the three optimization objectives and their respective optimization ratio d. Then, by using the response surface (RSM), the relationship between the optimization objective and each optimization parameter is determined. Finally, the neural network algorithm is used to induce the distribution of optimization parameters, and the structure parameter range and control parameter range of capsule design are determined. as shown in Fig. 2. Based on all analysis, we can identify the structural parameter values $e_1 = 1$ mm and $e_2 = 0.5$ mm as suitable choices. In this case, our investigation reveals that all the objective can be achieved optimally.

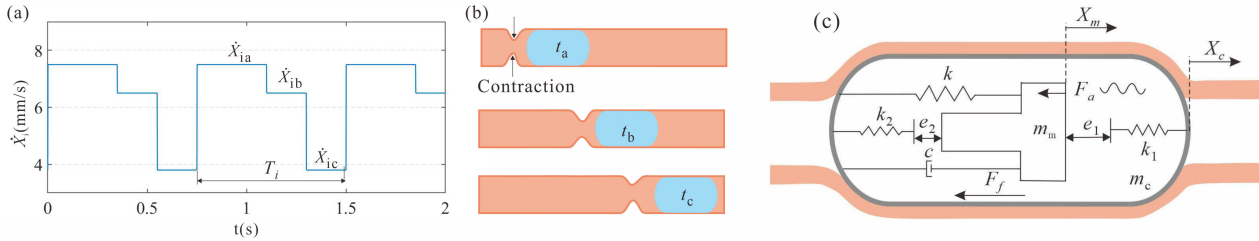


Figure 1: Coupled model (a) Peristalsis velocity profile. (b) Capsule motion under a single peristaltic wave.(c)Coupled dynamic model

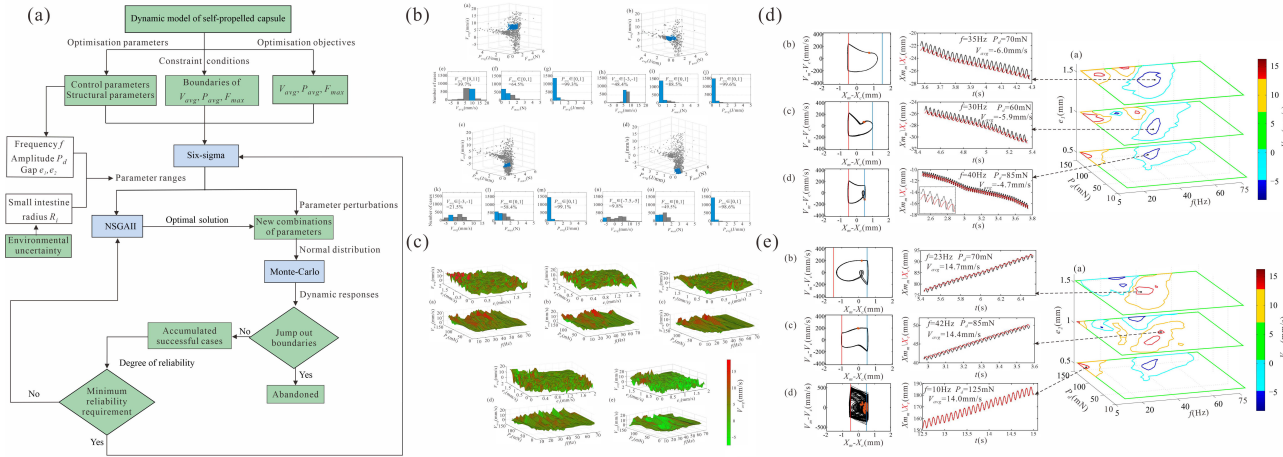


Figure 2: Multi-objective optimization, (a) algorithm framework. (b) Pareto boundary analysis.(c) Response surface (RSM) analysis. (d)-(e) Neural network fitting.

References

- [1] Miftakhov R, Akhmadeev N (2007). Numerical simulations of effects of multiple neurotransmission on intestinal propulsion of a non-deformable bolus. *Comput Math Methods Med* **8**: 11-36.
- [2] Yan Y, Liu Y, Manfredi L, et al. Modelling of a vibro-impact self-propelled capsule in the small intestine. *Nonlinear Dynamics* **96**: 123-144.
- [3] Liu,Y.,Wiercigroch,M., Pavlovskaja, E., et al (2013). Modelling of a vibro-impact capsule system *Int. J. Mech* **66**: 2-11.

AI assisted early bowel cancer detection using a self-propelled capsule robot

Kenneth Omokhagbo Afebu*, Jiyuan Tian*, Evangelos Papatheou*, Yang Liu* and Shyam Prasad**

*College of Engineering, Mathematics and Physical Sciences, University of Exeter, UK

**Endoscopy Department, Royal Devon University Healthcare NHS Foundation Trust, UK

Abstract. In attempt to improve bowel cancer treatment efficiency and patient survival via early detection, the present study proposes a less invasive soft tissue biomechanical characterisation. The method uses dynamic signals from a self-propelled robotic capsule and machine learning techniques to develop AI models capable of biomechanical characterisation. Supervised classification models were developed from selected combinations of extracted features using Multi-layer Perceptron (MLP) and Stacked Ensemble network (SE-Net). Unsupervised classification into benign and malignant lesions was also attempted using k-means clustering. The MLP models showed better performances with average accuracies of 96.4% and 96.5% on simulation and experimental data, respectively. SE-Net was better using raw and unprocessed signal data. K-means clustering achieved accuracies as high as 95.8% and 100% on simulation and experiment data respectively. The results indicate the efficacy of the proposed method to detect hard-to-visualise early bowel cancers.

Introduction

Bowel cancer are lesions in the bowel that have mutated over time to become malignant and it ranks second in the global cancer mortality rating with about 1 million deaths per year [1]. Existing diagnosing methods rely on visual observation of BC post-development features such as numbers, sizes and shapes thus making early detection very difficult. With the onset of BC being characterised with changes in the biomechanical properties of affected tissues [2], the current study investigates a non-conventional and less invasive biomechanical tissue characterisation for early BC detection. The method utilises machine learning and measurable dynamics of a self-propelled robotic capsule travelling in the bowel (See Fig. 1) and encountering lesions of different biomechanical properties to develop AI models capable of biomechanical categorisation. The capsule is propelled by the vibration of an internal magnetic mass under the influence of external magnetic excitation [3]. The proposed approach is based on the fact that resulting capsule dynamics will tend to vary with changes in the biomechanical properties of encountered lesions. Resulting signals were processed to extract features that may be indicative of biomechanical changes. Supervised classification into five classes using MLP and SE-Net, and unsupervised classification into two-classes using k-means clustering was carried out. SE-Net base learners include Support Vector Machine, Decision Tree, Naïve Baye and Randomp Forest.

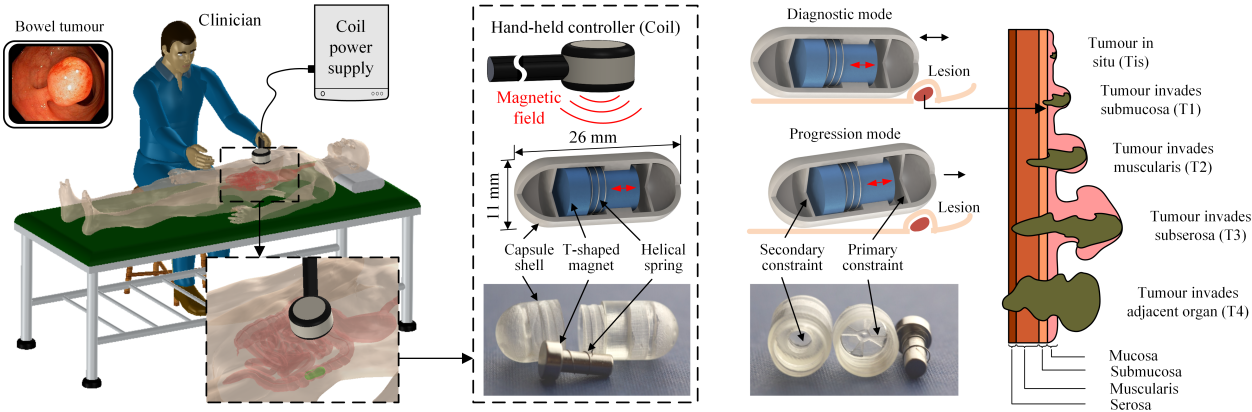


Figure 1: Principle of the proposed early bowel cancer detection and the robotic capsule prototype

Results and discussion

The MLP models showed better performances with average accuracies of 96.4% and 96.5% on simulation and experimental data, respectively. SE-Net, however, had better performance using minimally processed raw signal data. Five class clustering was not possible, however, two class clustering achieved accuracies as high as 95.8% and 100% on simulation and experiment data, respectively. The results indicate that the proposed method has great chances of detecting early stage BC to improve their treatment and survival rate.

Acknowledgements: This work has been supported by EPSRC under Grant No. EP/V047868/1.

References

[1] WHO-IARC (2022) Colorectal Cancer Awareness Month 2022 website <https://www.iarc.who.int>.
[2] Palmieri, V., Lucchetti, D., Maiorana, A., Papi, M., Maulucci, G., Ciasca, G., Svelto, M., De Spirito, M. and Sgambato, A. (2014) Biomechanical investigation of colorectal cancer cells. *Appl. Phys. Lett.* **105**(12): 123701.
[3] Zhang J., Liu Y., Zhu D., Prasad S., Liu C. (2022) Simulation and experimental studies of a vibro-impact capsule system driven by an external magnetic field. *Nonlinear Dyn.* pp. 1-16.

Dynamics of a soft capsule robot self-propelling in the small intestine via finite element analysis

Jiyuan Tian*, Zepeng Wang*, Yang Liu* and Shyam Prasad**

*Engineering Department, University of Exeter, North Park Road, Exeter, UK, EX4 4QF

**Royal Devon University Healthcare NHS Foundation Trust, Barrack Road, Exeter, UK, EX2 5DW

Abstract. This work aims to study the dynamics of a vibro-impact capsule robot interacting with a small intestine via three-dimensional finite element modelling. The capsule was coated with an ultra-soft elastomer to reduce the potential secondary damage to the intestine by its hard shell. It was found that the softer the elastomer coating is, the less contact pressure between the robot and the intestine is, so leading to less potential traumas. Optimum control parameters, such as excitation frequency and duty cycle ratio, were obtained. The findings will be used for prototype fabrication and control system design for the soft capsule robot.

Introduction

Capsule robot, an effective endoscopy technique to diagnose and treat the interior of the gastrointestinal (GI) tract [1], often interacting with the epithelial lining of the digestive tract, potentially induces secondary trauma due to violent vibration and motion of the capsule hard shell or the capsule's external accessories. The small intestine, as the longest portion of the GI tract, with its small diameter combined with peristalsis and segmentation, is considered the strait stage for controlling the movement of self-propelled capsule robots [1]. Previous finite element (FE) studies [2] had primarily investigated the capsule-intestine interactions under different intestinal anatomies by using a rigid capsule made of polyethylene with constant moving speeds, and then, a two-dimensional (2D) FE model have been developed to study the vibro-impact capsule robot developed in the Applied Dynamics and Control Lab at the University of Exeter [3]. In order to reduce the potential trauma to the intestine caused by the hard shell while optimising its progression efficiency and improving the reliability of the FE model, a super-soft elastomer coating was applied to a vibro-impact capsule robot via 3D FE modelling. Since it is a time-dependent dynamic model and due to its structural symmetry, it was simplified as a quarter symmetric FE model as shown in Figure 1(a). In this work, the elastomer coatings with different elastic moduli and thicknesses were conducted to explore the mechanical responses of the vibrating capsule in the lumen of the small intestine. The control parameters of the robot, including the amplitude, frequency and duty cycle of the square-wave excitation, were varied to further investigate the dynamic effect of the coating on the vibro-impact capsule with different excitations.

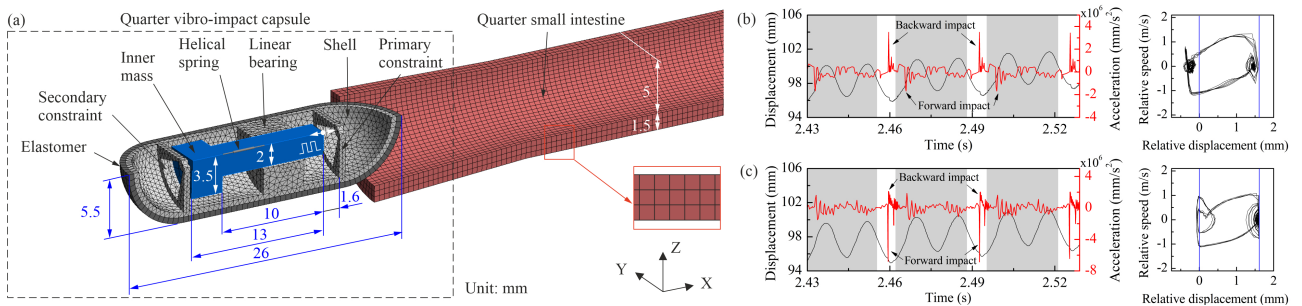


Figure 1: (a) Quarter symmetric view of the FE model, where the coated capsule consists of an inner mass vibrating and impacting with the primary and the secondary constraints under external magnetic excitation and the interaction of a helical spring; FE time histories of inner mass acceleration (red line) and capsule displacement (black line) for (b) the capsule with coating (0.9 mm thickness) and (c) the capsule without coating at the excitation amplitude of 1.2 N, frequency of 30 Hz and duty cycle ratio of 0.8, with their corresponding phase trajectories (right panels), where both vertical blue lines at the relative positions of 0 mm and 1.6 mm on phase portraits represent the secondary (backward) and the primary (forward) constraints of the capsule.

Results and Discussions

Through extensive FE analyses, our proposed FE model can provide quantitative predictions on the contact pressure, resistance force and capsule-intestine dynamics under different elastomer coatings. Figures 1(b) and (c) indicate that soft capsule have fewer forward impact compared with rigid capsule, but with the same capsule moving speed. In addition, it was found that the harder and thinner the elastomer is, the greater the contact pressure between the capsule and intestine, so causing more undesirable tactile sensation to patients.

References

- [1] Barducci, L., Norton, J.C., Sarker, S., Mohammed, S., Jones, R., Valdastrì, P. and Terry, B.S. (2020) Fundamentals of the gut for capsule engineers. *Prog. Biomed. Eng.* **2**:042002.
- [2] Tian, J., Liu, Y., Chen, J., Guo, B. and Prasad, S. (2021) Finite element analysis of a self-propelled capsule robot moving in the small intestine. *Int. J. Mech. Sci.* **206**:106621.
- [3] Yan, Y., Zhang, B., Liu, Y. and Prasad, S. (2022) Dynamics of a vibro-impact self-propelled capsule encountering a circular fold in the small intestine. *Meccanica*.

A nonlinear model for identifying human-exoskeleton coupling parameters in lower extremities

Cheng Huang*, Yao Yan*

*School of Aeronautics and Astronautics, University of Electronic Science and Technology of China, Chengdu 611731, China

Abstract. In this paper, a nonlinear human-exoskeleton coupling dynamics model is proposed for identifying the human-exoskeleton coupling parameters. The accuracy of the new model is verified by the coupling forces predicted by the human-exoskeleton coupling parameters. We recruited 10 adult male and 10 adult female volunteers (Age: 25 ± 4 , Height: 168 ± 14 mm, Weight: 73.85 ± 28.30 kg) to participate in the experiment. In contrast to the linear parameter identification method, the result of experiment has verified that the nonlinear model is more widely applicable in different human-machine coupling situations.

Introduction

In the study of the existing exoskeleton systems, many researches assume that the lower limb exoskeletons can perfectly track human gait[1]. This presumption ignores the human-exoskeleton coupling effect that can affect the comfort of the wearer. The human-exoskeleton coupling effect is very critical for the comfort of wearing exoskeletons. Thus in our previous study, a new human-exoskeleton coupling model is proposed in literature[2] to study the human-exoskeleton coupling effect. This exoskeleton model abandons the user-defined virtual coefficients and replaces them with the damping and stiffness of physical lower limbs as control parameters. Our study[2] has demonstrated the reliability of the linear model. However, further studies reveal that the asymmetry of the coupling force is ignored, and the accuracy of the linear model will decrease significantly in the scenarios of slack coupling in the linear model. To address these issues, we refine the model through adding nonlinear factors into the model.

Results and discussion

Out of the experiments, two typical sets of coupling force predicted by human-exoskeleton coupling model are displayed in Fig. 1. It is seen that both the linear and nonlinear model yield good predictions of the coupling force in Fig. 1(b). However, in Fig. 1(a) which the coupling between human and exoskeleton is very slack the differences in predicted coupling force between the two models emerge. The linear model has poor accuracy, but the nonlinear model is still very reliable in this case. In practical applications, it is a common phenomenon that individual differences in wearers could lead to a different coupling situation. Our further research has found that the human-machine coupling parameters vary in different human-machine coupling situations. Changes in human-machine coupling parameters will result in the changes in human-machine interaction force which is critical for users' feelings. This is why we modified the linear model of human-exoskeleton coupling proposed in our previous study[2].

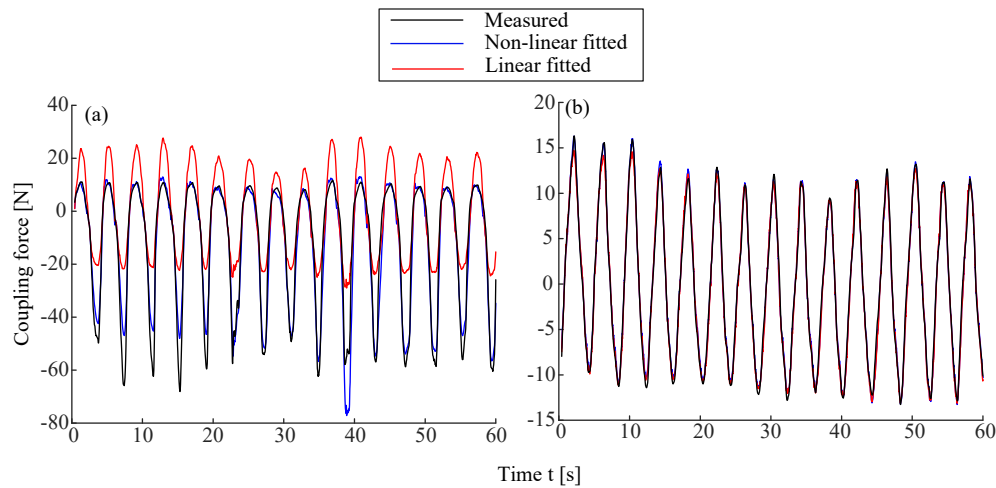


Figure 1: Measured coupling force (black line) and fitted coupling force separately predicted by linear (red line) and nonlinear model (blue line) with different coupling situations: (a) coupling is slack and (b) coupling is tight.

References

- [1] S. Glowinski, T. Krzyzynski, A. Bryndal, and I. Maciejewski (2020) A kinematic model of a humanoid lower limb exoskeleton with hydraulic actuators. *Sensors* **20**:6616.
- [2] Y. Yan, Z. Chen, C. Huang, L. Chen, and Q. Guo (2022) Human-exoskeleton coupling dynamics in the swing of lower limb. *Applied Mathematical Modelling* **104**:439-454.

Dynamics of a vibro-impact self-propelled capsule encountering a bump in the small intestine

Ruifeng Guo*, Yao Yan*

*School of Aeronautics and Astronautics, University of Electronic Science and Technology of China, Chengdu 611731, China

Abstract. Given the anatomy of small-intestine, this paper investigates the kinetic response of a vibro-impact capsule moving through the inner wall of the small intestine, going over single or multiple bumps during its moving, during which the capsule is subjected to resistance from the bumps. In order to make the simulation environment more realistic, two mathematical models of resistance are proposed, simulating a band of annular folds and a cone of cancerous tissue inside the small intestine. Two types of overturning are also designed without considering capsule rotation as well as considering capsule rotation. The resistance analysis of the two kinds of bumps and the two overturning methods has been carried out and found that the conical bump gives less resistance to the capsule under the same conditions, due to the reduced contact surface, while the resistance to the capsule becomes more complex when capsule rotation is taken into account. We will then analyse the kinetic response of the capsule over the bulge under different parameters based on numerical simulations and bifurcation analysis.

Introduction

The main method of examining the inner surface of the small intestine is by using capsule endoscopy, the problem of which is that intermittent peristalsis may lead to a full view of the intestinal surface. Capsule passage times range from 14 to 70 hours [1]. This can be very burdensome for the patient. Prior to the Covid-19 pandemic, endoscopy units in the UK failed to meet demand targets [2]. The average diameter of the adult small bowel is 3.5 cm [3] and therefore the size of the capsule is severely limited. This paper proposes the use of a vibration-driven capsule robot to travel through the small intestine, allowing it to travel over different types of small bowel bulges and then perform kinetic analysis. This will reduce the size of the capsule and speed up the process, while allowing better design parameters to be derived.

Results and discussion

We have completed the derivation of all physical models and equations. Building on previous research, in this paper we will add a conical projection and create a mathematical model of the rotation of the capsule itself. A schematic diagram is shown in Figure 1. In a rotating capsule, the capsule is divided into three parts: head, body and tail. The stress and torque given to it by the intestinal tissues in the vertical direction are integrated separately, and this stress should be balanced with gravity and the torque should be zero, which in the case of the head leads to (1).

$$\begin{cases} F_y = \frac{\rho(x)}{\cos \varphi(x)} \int_{x_2+R \sin \gamma}^{x_2+R} \int_{-0.5\pi}^{0.5\pi} \sigma_y(x, \theta) d\theta dx + \int_{x_2}^{x_2+R \sin \gamma} \int_{-0.5\pi}^{-\beta} \sigma_y(x, \theta) d\theta dx + \int_{x_2+R \sin \gamma}^{x_2+R} \int_{\beta}^{0.5\pi} \sigma_y(x, \theta) d\theta dx = G \\ M = \left(\int_{x_2}^{x_2+R \sin \gamma} \int_{-0.5\pi}^{\beta} \sigma_y + \int_{x_2+R \sin \gamma}^{x_2+R} \int_{-0.5\pi}^{0.5\pi} \sigma_y + \int_{x_2}^{x_2+R \sin \gamma} \int_{\beta}^{0.5\pi} \sigma_y \right) (x - c_x) \frac{\rho d\theta dx}{\cos \varphi} + \left(\int_{x_2+R \sin \gamma}^{x_2+R} \int_{-0.5\pi}^{0.5\pi} \sigma_x + \int_{x_c}^{x_2+R \sin \gamma} \int_{-0.5\pi}^{-\beta} \sigma_x \right) (p - c_y) \frac{\rho d\theta dx}{\cos \varphi} = 0 \end{cases} \quad (1)$$

ρ is the radius of the section, σ is the stress applied, γ is the angle of inclination of the capsule, β is the angle associated with γ and x , and the absolute value of p is the distance from the centre of the tail of the capsule to the y-axis. c_x and c_y are the coordinates of the centre of the capsule.

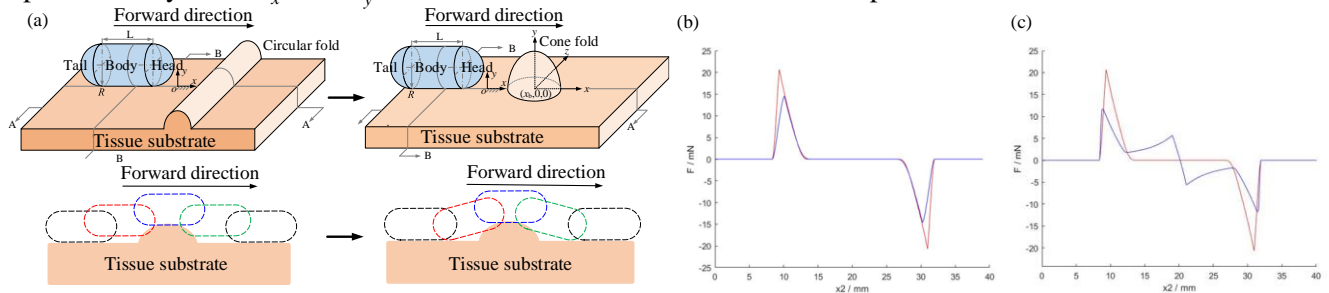


Figure 1: In (a), the capsule will go over two types of bumps, and there are two ways in which the capsule will go over. In (b) the blue line represents a conical projection and the red line represents a ribbon projection. In (c) the blue line represents the rotated way, the red lines represent the non-rotated way.

Solving the equation gives the resistance given to the capsule by the intestinal tissue in the x-direction. The curve of this resistance is shown in Figure 1(b)(c). The next work will investigate the dynamic response of the capsule throughout the process of overturning the bulge based on bifurcation analysis.

References

- [1] M. E. Smith, D. G. Morton. (2010) The Digestive System: Systems of the Body Series, 2nd Edition, Churchill Livingstone, China.
- [2] L. Shenbagaraj, S. Thomas-Gibson (2019) Frontline Gastroenterology, vol. 10, no. 1, pp. 7–15.
- [3] Lee, Y.Y., Erdogan, A. . (2014) J. Neurogastroenterol, Motil. 20(2), 265–270.

A Vibro-Impact Capsule Driven by its Inner GMM Exciter

Zhi Li, Maolin Liao*, Zhipeng Liu, Zexu Wang, Zhihang Feng

School of Mechanical Engineering, University of Science and Technology Beijing, Beijing, China

Abstract. In order to offer a vibro-impact capsule with the self-propelled ability meanwhile getting rid of its dependence on external driving equipment, an exciter made of giant magnetostrictive material (GMM) is applied inside the capsule to provide the vibro-impact driving force. Considering the magnetostrictive properties of GMM, the control mechanisms of both the alternating magnetic field and the preloading force of the exciter are designed. Meanwhile, in order to model the dynamic behaviours of the magnetostrictive exciter, the correlation between the input excitation voltage and the output impact force of the exciter is determined. Comparing the obtained experimental results with the numerical simulations, their consistency is observed. The designed GMM exciter with even a small size can provide the required driving force for the vibro-impact capsule moving in the intestinal environment independently.

Introduction

For design of an electromagnetic exciter, the GMM rod is widely used as the deformation part and the output component, which is characterized by the change of its volume under the action of an alternating magnetic field. Compared with piezoelectric ceramics, the GMM has excellent properties with both the high energy conversion efficiency and the strong output force. Based on existing designs of the GMM exciter [1], its magnetostrictive properties should be calculated precisely, which are mainly determined by the designs of the alternating magnetic field device and preloading force device of the exciter. Furthermore, based on the magnetic-machine coupling schematics of the designed exciter, by establishing the voltage input equation, magnetic flux equation, magnetostrictive force equation and force balance equation, the transfer function expression between the input excitation voltage and the output impact force of the magnetostrictive exciter can be obtained. Finally, the corresponding experiments should be carried out to systematically test all the functions of the exciter [2-3], in particular, the driving force and energy consumption intensity.

Result analysis

During the experimental tests, a self-made miniature acceleration sensor is installed at the front end of the GMM rod of the exciter, see Fig.1(a), and thus the output acceleration signal of the exciter controlled by an input square wave signal is measured, see Fig.1(b). Specifically, an acceleration peak can be observed when the square wave signal is turned on, otherwise the acceleration signal will go back to zero. Moreover, the positive peak indicates the extension of the GMM rod, thereby pushing the capsule to move in the intestinal environment; while the negative peak indicates that the extension of the GMM rod disappears; by this way, the periodic movement of the capsule can be completed.

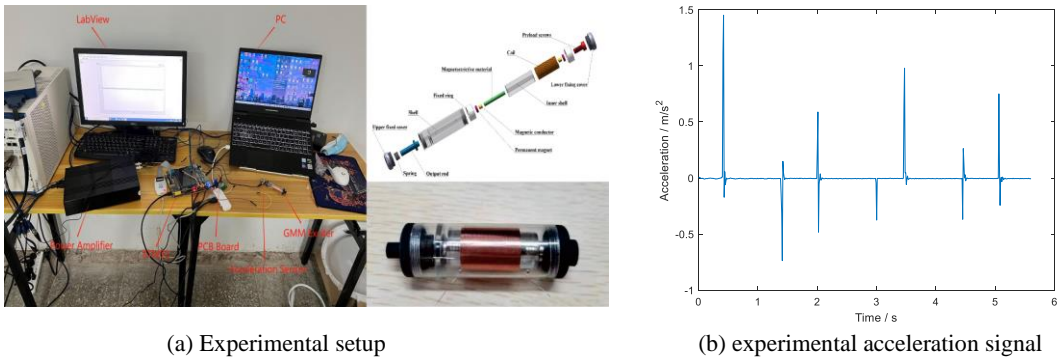


Figure 1: Experimental test, (a) Experimental setup and (b) the measured experimental acceleration signal

References

[1] Bryant, Michael D., and Ning Wang. "Audio range dynamic models and controllability of linear motion terfenol actuators." *Journal of intelligent material systems and structures* 5.3 (1994): 431-436.

[2] Guo, Bingyong, et al. "Self-propelled capsule endoscopy for small-bowel examination: proof-of-concept and model verification." *International Journal of Mechanical Sciences* 174 (2020): 105506.

[3] Zhang, Jiajia, et al. "Simulation and experimental studies of a vibro-impact capsule system driven by an external magnetic field." *Nonlinear Dynamics* (2022): 1-16.

Complex dynamics of a vibro-impacting capsule robot in contact with a circular fold

Shan Yin*, Yao Yan**, Joseph Páez Chávez***, Yang Liu*

*Engineering Department, University of Exeter, North Park Road, Exeter, EX4 4QF, UK

**School of Aeronautics and Astronautics, University of Electronic Sci. and Technology of China, China

***Center for Applied Dynamical Systems and Comput. Methods, Escuela Superior Politécnica del Litoral, Ecuador

Abstract. The circular folds in the lining of the small intestine provide the main source of resistance for the motion of capsule endoscopy. To reveal the capsule-fold dynamics, this paper presents bifurcation analyses for a vibro-impact self-propelled capsule robot contacting with a circular fold. Using the GPU parallel computing and the path-following techniques, one- and two-parameter bifurcation analyses are performed. It is found that the excitation parameters of the capsule robot and the fold's mechanical properties have significant influences on the bifurcation scenario. Performing the basin stability analysis, numerical results indicate that the period-one motion of the capsule-fold interaction and the crossing motion can dominate the global dynamics of the system in the small and large excitation amplitude regions, respectively. The findings of this work will be useful for the locomotion control of the capsule robot in the small intestine when encountering different types of circular folds.

Introduction

Self-propelled locomotion robots have attracted great attention from the research community in recent years, as they can move efficiently in complex environments. In the past decade, various locomotion mechanisms have been developed to provide active propulsive force for driving robots. For example, Guo et al. [1] presented an experimental study on a vibro-impact self-propelled capsule in mesoscale and discussed the feasibility of such a capsule under different frictional environments. The vibro-impact capsule robot is a non-smooth dynamical system driven by its internal vibration and impact in a rectilinear manner in the presence of environmental resistance. However, previous studies only considered capsule dynamics on a flat surface without the consideration of intestinal anatomy. While considering a series of circular folds of different sizes in the lining of the small intestine, the capsule's dynamics and locomotion will be significantly influenced. Thus, the present work will study the capsule's dynamics when encountering various types of circular folds.

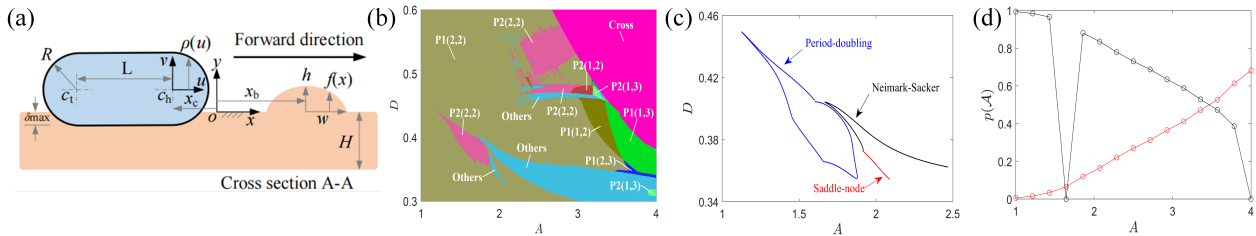


Figure 1: (a) Schematic diagram of the capsule moving on an intestinal substrate with a circular fold. (b) Two-parameter bifurcation diagram. (c) Continuation of bifurcation curves. (d) Occurrence probabilities of the $P1(2, 2)$ (red) and fold crossing (black) motions.

Results and discussion

Modelling the contact force of capsule-fold interaction by a piecewise-smooth nonlinear force [2], the complex dynamics of the capsule robot were presented in Fig. 1(a-d). The two-parameter diagram obtained by GPU calculation in Fig. 1(b) indicated an initial view of the capsule-fold dynamics. Two basic attractors, the $P1(2, 2)$ (a period-one motion with capsule sticking to the fold) and the fold crossing motions, were observed. In practice, the $P1(2, 2)$ motion is one of the desired motions because of its simplicity for locomotion control. Continuation analysis was performed to uncover the bifurcation of the $P1(2, 2)$ motion as shown in Fig. 1(c). Since bifurcation analysis can only provide local information, basin stability analysis was also conducted to characterise the capsule-fold dynamics from a global perspective. Fig. 1(d) showed that the $P1(2, 2)$ motion dominated the global dynamics of the system with a high probability when the excitation amplitude of the robot was small. On the contrast, the fold crossing motion dominated the global dynamics of the system with a high probability when the excitation amplitude was large. Practically, such a high probability for the crossing motion is preferred, as the transit time of the capsule robot in the small intestine should be as short as possible. In summary, such results can provide essential guidance for the locomotion control of the capsule robot.

Acknowledgement: This project has received funding from the European Union's Horizon 2020 research and innovation programme under the Marie Skłodowska-Curie grant agreement No [101018793].

References

- [1] Guo B, Liu Y, Birler R, et al. (2020) Self-propelled capsule endoscopy for small-bowel examination: proof-of-concept and model verification. *Int. J. Mech. Sci* **174**:105506.
- [2] Yan, Y., Zhang, B., Liu, Y. et al. (2022) Dynamics of a vibro-impact self-propelled capsule encountering a circular fold in the small intestine. *Meccanica* <https://doi.org/10.1007/s11012-022-01528-2>.

Parameter identification of a vibro-impact capsule robot through optimisation

Shan Yin*, Jiajia Zhang*, and Yang Liu*

*Engineering Department, University of Exeter, North Park Road, Exeter, EX4 4QF, UK

Abstract. When studying the non-smooth dynamics of a vibro-impact capsule robot, parameter identification of an equivalent theoretical model is of practical significance. However, for such a small-sized robot, the direct measurement of its inner forces, such as the damping force between mass-capsule interaction, will be very difficult, leading to challenges in model parameter identification. Based on the partial information obtained from the robot, this paper presents parameter identification analyses for the vibro-impact capsule robot by defining a trajectory-tracking problem and solving it via optimisation. To ensure the robustness of the identified parameters, three independent cases subjected to different excitation parameters are integrated and solved together. By using the simulated annealing algorithm, the values of damping, spring stiffness, constraint stiffness and intestinal friction coefficient can be identified. Finally, the simulated capsule trajectories in all cases have good agreements with the known data.

Introduction

The strongly nonlinear systems involving impact and friction can be widely found in many engineering applications, e.g., self-propelled locomotion robots, percussive drilling systems and rotor/stator rubbing systems. The nonlinear dynamics of such non-smooth systems, including oscillation patterns and bifurcations, should be thoroughly studied to uncover their underlying instability mechanisms. For example, Guo et al. [1] experimentally studied a vibro-impact self-propelled capsule in mesoscale and revealed some hidden dynamics of the prototype by identifying a theoretical model. The vibro-impact capsule robot, a potential solution for the next-generation active capsule endoscopy shown in Fig. 1(a), is a non-smooth dynamical system driven by its internal vibration and impact in a rectilinear manner in the presence of environmental resistance. From a practical point of view, identifying an equivalent theoretical model of such a robot is vital. However, the direct measurement of its inner forces (e.g., mass-capsule damping force) will be very difficult due to its dimension. Thus, it is very challenging to identify the robot's theoretical model by using only partially known information. This work will study the parameter identification of the vibro-impact capsule robot by defining a trajectory-tracking problem and solving it through optimisation.

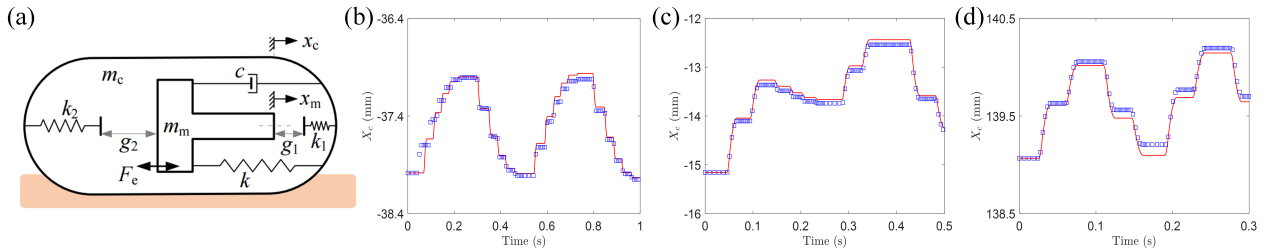


Figure 1: (a) Schematic diagram of the vibro-impact capsule robot self-propelling on an intestinal substrate. (b) Case 1: excitation amplitude 1.5 N and frequency 2 Hz. (c) Case 2: excitation amplitude 1.8 N and frequency 4 Hz. (d) Case 3: excitation amplitude 2 N and frequency 6 Hz. Blue squares indicate the known capsule displacements, and red lines stand for the identified trajectories.

Results and Discussion

To validate the developed parameter identification method, this work adopted the theoretical model shown in Fig. 1(a) to produce the known capsule displacements and velocities, and three independent cases were considered. To identify the model's damping, spring stiffness, constraint stiffness and intestinal friction coefficient, the above three cases were integrated and solved by using the simulated annealing algorithm [2]. After 334 iterations of the algorithm, the defined optimisation problem converged to the neighbourhood of the pre-specified parameter sets. Comparisons between the known data and the identified trajectories of the capsule are shown in Fig. 1(b-d), where good agreements can be observed. Considering the real-world application of the vibro-impact self-propelled capsule robot, it is believed that such a method can provide essential guidance for the identification of capsule-environment interaction, e.g., [3], and will further advance the potential functionality for the capsule robot.

Acknowledgement: This project has received funding from the European Union's Horizon 2020 research and innovation programme under the Marie Skłodowska-Curie grant agreement No [101018793].

References

- [1] Guo B, Liu Y, Birler R, et al. (2020) Self-propelled capsule endoscopy for small-bowel examination: proof-of-concept and model verification. *Int. J. Mech. Sci* **174**:105506.
- [2] Arora J. (2004) Introduction to optimum design (Second Edition). Elsevier.
- [3] Yan, Y., Zhang, B., Liu, Y. et al. (2022) Dynamics of a vibro-impact self-propelled capsule encountering a circular fold in the small intestine. *Meccanica* <https://doi.org/10.1007/s11012-022-01528-2>.

Rectilinear motion of a chain of interacting bodies in a viscous medium

Tatiana Figurina*, Dmitri Knyazkov**

*Ishlinsky Institute for Problems in Mechanics RAS, Russia, ORCID 0000-0003-2068-1993

**Ishlinsky Institute for Problems in Mechanics RAS, Russia, ORCID 0000-0002-2622-8746

Abstract. The rectilinear motion of a chain of identical bodies in a viscous medium is considered. Neighboring bodies interact with each other, there are no restrictions on the magnitude of the interaction forces. The problem of moving the system to a given distance under the condition of coincidence of the configuration of the system and of the velocities of the bodies at the beginning and at the end of the movement is solved. A motion is constructed in which the velocity of each of the bodies is piecewise constant, the velocity of the center of mass is constant. Such motion with the maximum velocity of the center of mass is constructed.

Introduction

The rectilinear motion of a system of N identical bodies A_i , $i = 1, \dots, N$, $N \geq 3$ that moves due to the forces of interaction between the bodies is considered, see Fig. 1. Equations of motion of the system are

$$\dot{x}_i = v_i, \quad m\dot{v}_i = F_i(t) - F_{i-1}(t) + R(v_i), \quad (1)$$

$i = 1, \dots, N$, where m , x_i , and v_i are the mass, the coordinate, and the velocity of body A_i ; $F_i(t)$ is the control force acting from body A_{i+1} on body A_i assuming $F_0 = F_N = 0$; $R(v_i)$ is the resistance force of the medium,

$$R(v_i) = -cv_i|v_i|. \quad (2)$$

There are no restrictions imposed on the control forces $F_i(t)$. Thus, it is possible to instantly change the velocities of bodies v_i , redistributing the total momentum of the system. At the initial time instant:

$$x_i(0) = x_i^0, \quad v_i(0) = v_i^0, \quad i = 1, \dots, N. \quad (3)$$

The described system was studied in [1]–[4] and can model a robotic device moving in viscous media. In [4], the stability of the motion of the system was studied. The current study considers the following problem.

Problem. Move the system of bodies obeying (1)–(3) to a given distance $L > 0$, provided that the configuration of the system and the velocities of each of the bodies are equal at the beginning and at the end of the motion:

$$x_i(T) - x_i^0 = L, \quad v_i(T) = v_i(0), \quad i = 1, \dots, N. \quad (4)$$

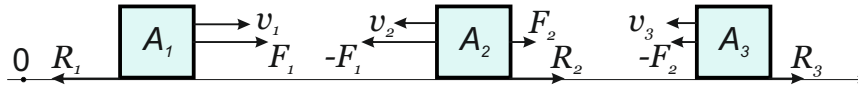


Figure 1: Chain of interacting bodies, $N = 3$.

Results and discussion

The motion that solves Problem is constructed. If at the initial time instant the velocity v of the center of mass of the system is not zero, $v(0) \neq 0$, a motion is constructed in which this velocity is constant, $v(t) \equiv v(0)$, the velocity of each body is piecewise constant and takes values from the set $\{a_i\}$, where these values a_i , $i = 1, \dots, N$ satisfy $\sum_{i=1}^N a_i = Nv(0)$ and $\sum_{i=1}^N a_i|a_i| = 0$. The velocities of bodies change cyclically:

$$v_i(t) \equiv a_{i+k}, \quad i = 1, \dots, N-k, \quad v_i(t) \equiv a_{i-N+k}, \quad i = N-k+1, \dots, N, \quad t \in [t_k, t_{k+1}), \quad k = 0, \dots, N-1.$$

Here, $t_0 = 0$ and $t_N = T$. Additionally, we show how to maximize the velocity of center of mass v under the condition that velocities of all bodies are bounded. It is proved that in optimal motion, part of the bodies moves backward with the maximum allowed velocity, and the other bodies move forward with equal velocities.

If $v(0) = 0$, the motion that solves Problem consists of three stages. At the 1st stage, the bodies are instantly set in motion due to impulse control forces and then they move for a certain time interval with all control forces equal to zero. At the 2nd stage, the motion with a constant velocity of the center of mass is performed. At the last stage, the bodies instantly change velocities, then move freely, and then instantly stop. Thus, in contrary to [1], Problem is also solved for the case, where the initial momentum of the system is zero.

The study is supported by RFBR project 21-51-12004 and by state program № AAAA-A20-120011690138-6.

References

- [1] Chernous'ko F. L. (2017) Translational Motion of a Chain of Bodies in a Resistive Medium. *J Appl Math Mech* **81**:256-261.
- [2] Bolotnik N., Pivovarov M., Zeidis I., Zimmermann K. (2011) The Undulatory Motion of a Chain of Particles in Resistive Medium. *ZAMM* **91**:259-275.
- [3] Steigenberger J., Behn C. (2012) Worm-like Locomotion Systems: an Intermediate Theoretical Approach. Oldenbourg Wissenschaftsverlag, Munich.
- [4] Figurina T., Knyazkov D. (2022) Periodic Gaits of a Locomotion System of Interacting Bodies. *Meccanica* **57**:1463-1476.

The closed-loop controller optimization of a discontinuous capsule drive with the use of neural network in the uncertain frictional environment

Sandra Zarychta*, Marek Balcerzak*, Artur Dąbrowski* and Andrzej Stefański*

*Division of Dynamics, Lodz University of Technology, Lodz, Poland

Abstract. This short paper presents the novel method of designing the closed-loop controller for a nonlinear, discontinuous capsule system. As a foundation of the controller, an optimized open-loop control function is used, based on which the neural network determines the dependencies between the output and the system's state. The robustness of a neural controller is verified in the uncertain frictional environment and compared with the original control function. It is expected that the method can facilitate the design of the systems' closed-loop controllers, especially for non-smooth and discontinuous ones, where typical approaches are not efficient enough.

Introduction

The pendulum capsule drive (Fig. 1a) is an example of a nonlinear, discontinuous system, exhibiting rich and interesting dynamical behaviour. It is not only caused by the pendulum's inherent nonlinearity, but also due to the frictional interactions between the capsule and the underlying surface, resulting in stick-slip discontinuity. Last but not least, the dependence of the contact force on oscillations of the pendulum can be noticed [1]. Control design methods applicable to capsulobots systems with discontinuities such as the pendulum capsule drive considered in this paper, use various approaches, such as the open-loop [2, 3], closed-loop [3], as well as neural networks (NN) [4] and others. However, very little research is dedicated to the NN applications in optimal control drives. One possibility is the use of Reinforcement Learning. Nevertheless, it requires a lot of time and resources [5]. In this case, the authors propose a simpler approach. The open-loop optimal control approximation of a pendulum capsule drive, obtained within the method described in [2], is the base for the NN model created with a specified structure that can determine the dependencies between the open-loop output values and the corresponding states of the capsule system. In such a manner, a closed-loop controller is obtained. The purpose of this study is to test and evaluate the robustness and efficiency of the NN closed-loop controller comparing with the original open-loop one, in an uncertain frictional environment.

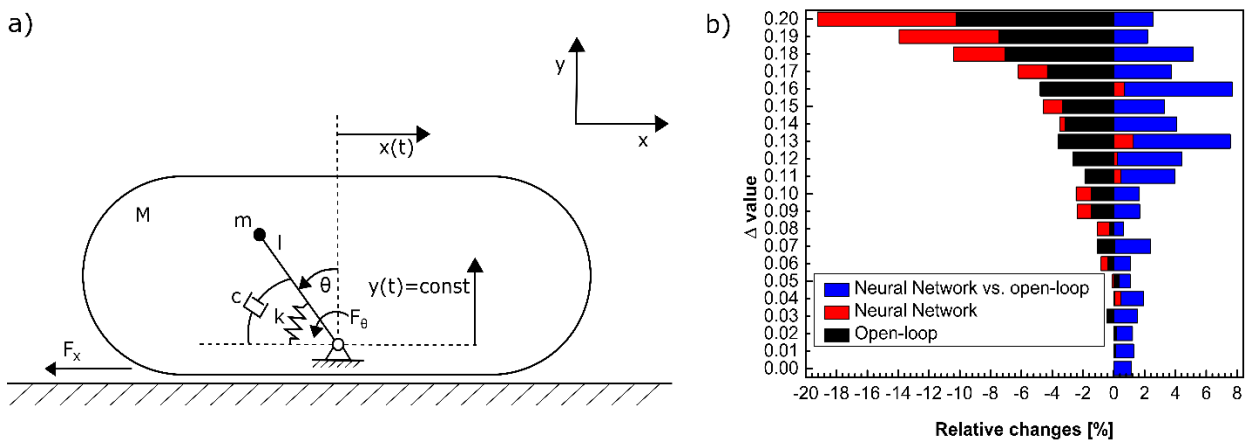


Figure 1: Scheme of the pendulum capsule drive (a) [2] and the robustness comparison of the open-loop and neural controllers (b)

Results and discussion

The controllers' robustness studies revealed a 1.16% higher performance and 7% better resistance of the NN closed-loop controller comparing to the original open-loop, in the constant frictional environment and the uncertain one, respectively (Fig. 1b). Obtained results confirm that the NN controller works more efficiently, offering better robustness against uncertainties appearing in the environment with the varying coefficient of friction, which is one of the main limitations in the open-loop controllers. Moreover, the novel NN closed-loop controller seems to be an interesting option for designing and optimization of the systems controllers, particularly for discontinuous ones, where the open-loop approach is only available.

References

- [1] Liu, P., Yu, H., & Cang, S. (2018). On the dynamics of a vibro-driven capsule system. *Arch. Appl. Mech.* **88**(12):2199–2219.
- [2] Zarychta, S., Sagan, T., Balcerzak, M., Dabrowski, A., Stefanski, A., & Kapitaniak, T. (2022). A novel, Fourier series based method of control optimization and its application to a discontinuous capsule drive model. *Int. J. Mech. Sci.* **219**:107104.
- [3] Liu, Y., Yu, H., & Yang, T. C. (2008). Analysis and control of a capsulobot. *IFAC Proc. Vol.* **41**(2):756–761.
- [4] Liu, P., Yu, H., & Cang, S. (2019). Adaptive neural network tracking control for underactuated systems with matched and mismatched disturbances. *Nonlinear Dyn.* **98**(2):1447–1464.
- [5] Ketkar, N. (2017). *Deep Learning with Python - A Hands-on Introduction*. Apress Berkeley, CA.

Comparison of feed-forward control strategies for hopping model with intrinsic muscle properties of different complexities

Dóra Patkó*, Ambrus Zelei** and Giuseppe Habib*

*MTA-BME Lendület "Momentum" Global Dynamics Research Group, Department of Applied Mechanics, Budapest University of Technology and Economics, Budapest, Hungary,

Patkó ORCID 0000-0001-7594-1882, Habib ORCID 0000-0003-3323-6901

**Department of Whole Vehicle Engineering, Audi Hungaria Faculty of Automotive Engineering, Széchenyi István University, Győr, Hungary, Zelei ORCID 0000-0002-9983-5483

Abstract. In the simplest manner, hopping motion can be modelled by a spring-mass system, resulting in piece-wise smooth dynamics with marginally stable periodic solutions. Let us consider a Hill muscle instead of the spring. This way asymptotically stable periodic motions can occur. The activation level of the muscle is determined by feed-forward control. The physiological background of such control is the central pattern generators found in the spinal cord. The activation level function is chosen in a closed-form such a way that force time-history during periodic motion is symmetrical. In this study, the stability and the dynamical integrity of six different models with various muscle complexities (force-length relations: constant, linear, Hill-type; force-velocity relations: linear, Hill-type) are analysed through the monodromy matrix and the local integrity measure. These models are compared to similar systems with numerically optimised activation level functions found in the literature.

Introduction

Reductionist approach is used to have a better understanding of the core properties of vertical hopping motion. A 1D model is considered with a simplified Hill type muscle, consisting only of the contractile element (CE), as shown in Fig. 1. Haeufle et al. [1] established that, for this model, the intrinsic properties of the CE have stabilizing effect, and for asymptotic stability the force-velocity relation (f_v) has to be at least linear. They optimized the activation level function through genetical algorithm.

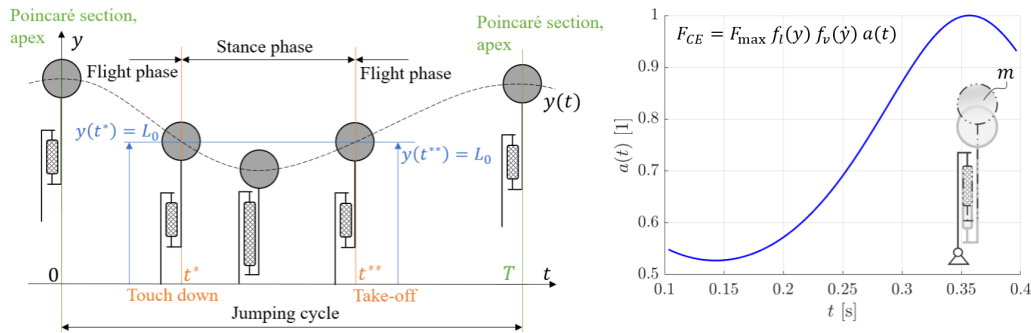


Figure 1: 1D hopping model and the closed form activation level function during the stance phase for linear force-length ($f_l(y)$) and force-velocity ($f_v(\dot{y})$) relations. The force output of the CE depends on the theoretically achievable maximum force value (F_{\max}), the momentary activation level ($a(t)$) and the intrinsic f_l and f_v relation of the muscle.

In this study, the muscle activation is calculated in closed form resulting in symmetric force time-history. The solution is optimized for the same fitness function used in [1]. The stability of the periodic orbits are determined by the eigenvalues of the monodromy matrix, which is calculated as described in [2]. The robustness of stable orbits are characterized by the local integrity measures (LIM), calculated exploiting the DynIn toolbox [3]. The solutions for the six different systems are compared through their multipliers and LIM values to find which muscle intrinsic relation is the most beneficial, and to see whether symmetric motions, occurring from the closed form activation function, has any advantage to asymmetric ones, as found by Haeufle et al [1].

Results and discussion

According to our results, the asymmetric solutions (AS), determined in [1], have better performance than the symmetric solutions (SS), which are calculated with closed form activation function. This means that the AS with approximately 2 Hz jumping frequency have higher jumping heights. In case of the AS, the systems with non-linear f_v have faster convergence than the ones with linear f_v . For the SS, the fastest convergence to the stable periodic orbit is obtained with the linear force-length relation (f_l), while the f_v has no significant effect on the convergence speed. All the AS have oscillatory convergence. Systems with linear f_v have the highest LIM values, and, in general, AS have higher LIM values than SS.

References

- [1] Haeufle D. F. B., Grimmer S., Seyfarth A. (2010) The role of intrinsic muscle properties for stable hopping - Stability is achieved by the force-velocity relation. *Bioinspir Biomim* **5**:016004
- [2] Dankowicz H., Piiroinen P.T. (2002) Exploiting discontinuities for stabilization of recurrent motions. *Dynam Syst* **17**:317-342.
- [3] Habib G. (2021) Dynamical integrity assessment of stable equilibria: a new rapid iterative procedure. *Nonlinear Dyn* **106**:2073-2096.

Time-optimal control approximation for a discontinuous capsule drive

Marek Balcerzak*, Sandra Zarychta*, Artur Dabrowski* and Andrzej Stefanski*

*Division of Dynamics, Lodz University of Technology, Lodz, Poland

Abstract. Research connected with capsule drives seem to attract an increasing attention among scientists. In order to assure efficiency of these devices, it is necessary to investigate optimal control for such systems. In this work, authors test a hypothesis that bang-bang control of the capsule drive can be the time-optimal one. For this purpose, a novel numerical method for bang-bang control parametrization and optimization has been developed. Results of its application are compared with a general-purpose algorithm, which approximates optimal control without any assumptions concerning the shape of the control function. It has been shown that the bang-bang control optimization yields 8% increase of the average speed of the capsule.

Introduction

The optimal control problem (OCP) is to find a way of performing a desired task in a given environment at the lowest possible cost [1]. A particular kind of OCP is the minimum-time problem, in which the target is execution of the expected task in the shortest possible time. In a large subset of such problems, the optimal solution is a so-called “bang-bang” control, i.e. a control function that attains only extreme (maximal or minimal) values from the whole set of allowable controls [1]. Unfortunately, although this fact is proven for a class of smooth systems, is not necessarily true if the controlled object is non-smooth or discontinuous. For instance, one cannot be sure whether the bang-bang control is time-optimal for a capsule drive (Fig. 1a). This system is able to move without external moving parts, solely due to interactions between dry friction on the underlying surface and oscillations of the pendulum located inside the device. However, although the dry friction enables motion of the capsule, it is also the cause of discontinuity in the system and the reason for which the assumption of the bang-bang control optimality cannot be a priori assumed. Nevertheless, the fact that discontinuous dry friction can be well approximated by smooth friction models [2] yields a proposition that the bang-bang control may be optimal for discontinuous capsule drive too. Such hypothesis has been tested numerically. In order to perform the comparison, a novel numerical method for bang-bang control parametrization and optimization has been developed. Results of execution of this algorithm have been compared with effects obtained by means of a more general, Fourier series based numerical method [3], which is able to approximate optimal control of an arbitrary shape.

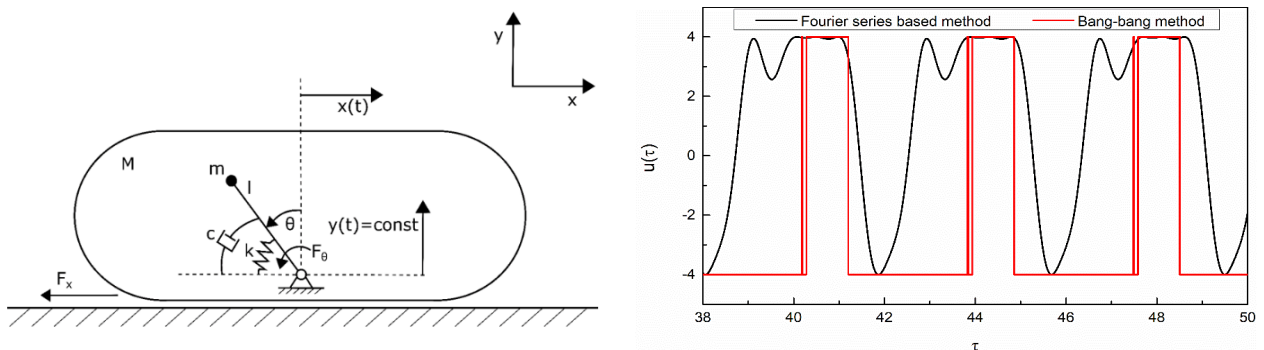


Figure 1: a) Capsule drive scheme (at the left), b) comparison of the optimized control functions (at the right)

Results and discussion

The control function obtained with use of the novel bang-bang optimization method enabled the capsule drive to move with 8% higher mean velocity comparing to the case of optimal control approximation with no restrictions of its shape (Fig. 1b). The obtained results show that restriction of the allowable controls set to bang-bang functions increase efficiency of the system and reduce optimization effort. They can also be regarded as an indication that the bang-bang control may be the optimal one for some discontinuous systems.

Acknowledgements: This study has been supported by the National Science Centre, Poland, PRELUDIUM Programme (Project No. 2020/37/N/ST8/03448). This study has been supported by the National Science Centre, Poland under project No. 2017/27/B/ST8/01619. This paper has been completed while the second author was the Doctoral Candidate in the Interdisciplinary Doctoral School at the Lodz University of Technology, Poland.

References

- [1] Kirk, D. E. (2004). Optimal control theory: an introduction. Courier Corporation.
- [2] Van de Vrande, B. L., Van Campen, D. H., & De Kraker, A. (1999). An approximate analysis of dry-friction-induced stick-slip vibrations by a smoothing procedure. *Nonlinear Dyn.* **19**(2):159-171.
- [3] Zarychta, S., Sagan, T., Balcerzak, M., Dabrowski, A., Stefanski, A., & Kapitaniak, T. (2022). A novel, Fourier series based method of control optimization and its application to a discontinuous capsule drive model. *Int. J. Mech. Sci.* **219**:107104.

Walking on an uneven terrain with a SLIP model based compliant biped

Saptarshi Jana* and Abhishek Gupta*

*Department of Mechanical, Indian Institute of Technology Bombay, Mumbai, India#

Abstract. A spring-loaded inverted pendulum (SLIP) model-based compliant biped is studied to find a method to walk on known irregular terrain. A 2D model with two degrees of freedom (stance leg only) is investigated over the single support phase, followed by an instantaneous double-support phase. Initial leg compression, a new model parameter, is considered in this study. A series of bumps and dips have been considered for preparing an uneven terrain. The impact conditions are modified to determine the following step. This model can walk past obstacles of different magnitudes each step with the various combination of model parameters. The model can walk on surfaces having a height difference of up to 2% of its leg length in each step.

Introduction

Compliant leg biped based on the SLIP model is considered the fundamental template for walking and running. Numerical optimization for planar walking on the flat-ground has found a self-stable periodic gait. In this study, our motivation is to check the ability of a bipedal walking robot to walk over uneven terrain. A device that can walk on an irregular surface becomes even more critical in hazardous areas. Uneven ground is the same as the discrete height change in each walking step. In 2015, Piovan and Byl found it is essential to adjust the net energy of a SLIP model system to walk on uneven terrain. Y. Liu has proposed a method to vary the system energy by changing the rest length of the leg. We prefer to change the initial leg compression (Δl_{td}) in each step according to the height of the bump (or dip). Δl_{td} is defined as the difference in length between the touchdown length (l_{td}) and the equilibrium length. Impact conditions have been derived using the model's configuration, conservation of angular momentum about the impact point, and energy before and after the impact.

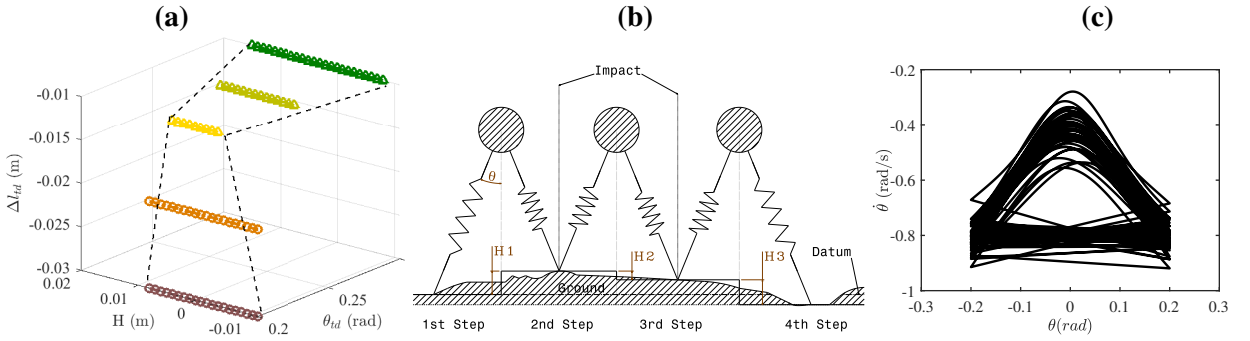


Figure 1: (a) Maximum size of bumps (positive H) and dips (negative H) that the model can overcome for a different combination of initial leg compression (Δl_{td}) and touchdown angle (θ_{td}), Δl_{td} negative indicates more compression from the equilibrium position (b) Kinematic sketch of the model while walking on an irregular surface represented as a series of bumps and dips of heights, H (c) Phase portrait of the configuration variable θ

Result and discussion

For this study, we considered the body mass ($m=80$ kg), leg stiffness ($k=7134$ N/m), and rest length of the leg spring ($l_0=1.13$ m) as constant. Touchdown angle and initial leg compression are varied parameters to obtain the maximum change in surface height (obstacle of the same size present at the impact point) the biped can overcome with that combination (Figure 1 (a)). The model can walk past bigger bumps and dips with greater θ_{td} and Δl_{td} . The impact map determines the initial states of the next step. The impact event gets triggered when the stance leg angle (θ) equals the predefined touchdown angle of the current swing leg (stance leg of next step). The initial leg compression for the next step is adjusted according to the known obstacle height, which eventually decides the l_{td} for the next step. The model can withstand a terrain height variation of 2% of its leg length per step while walking with $\theta_{td}=0.2$ rad and $\Delta l_{td}=-0.03$ m. Figure 1 (c) shows the phase portrait of the variable θ while walking on a randomly generated uneven terrain, and the predefined $\theta_{td}=0.2$ rad. Results show the model's ability to walk at least 40 steps on uneven surfaces.

References

- [1] Geyer H., Seyfarth A., Blickhan R. (2006) Compliant leg behaviour explains basic dynamics of walking and running. *Proc. R. Soc. B.* **273**:2861-2867.
- [2] Piovan G., Byl K. (2015) Reachability-based control for the active SLIP model. *The International Journal of Robotics Research* **34**(3):270-287.
- [3] Liu Y. (2015) A Dual-SLIP Model For Dynamic Walking In A Humanoid Over Uneven Terrain. PhD thesis, The Ohio State University.

Dynamic modelling of a vibro-impact capsule robot self-propelling in the large intestine via finite element method

Zepeng Wang*, Jiyuan Tian*, Yang Liu* and Shyam Prasad**

* Engineering Department, University of Exeter, North Park Road, Exeter, UK, EX4 4QF

** Royal Devon University Healthcare NHS Foundation Trust, Barrack Road, Exeter, UK, EX2 5DW

Abstract. To study the locomotion of a vibro-impact capsule robot self-propelling in the large intestine for colonoscopy, this work concerns the dynamic modelling of capsule-colon interaction by using three-dimensional (3D) finite element (FE) method. The anatomy of the colon, in particular the haustral fold, was considered to test the performance of the robot for self-propulsion. Preliminary results suggest that at sharp turns or when encountering high haustral folds, the capsule may slow down, and different control parameters, e.g., frequency of the external excitation, should be applied.

Introduction

Conventional colonoscopy, a very common procedure for colorectal cancer diagnosis, often results in insertion-related anxiety, pain, and nonadherence, necessitating local anesthesia for patients. Capsule endoscopy, as an alternative technique, provides a wireless, minimally invasive, sedation-free, patient-friendly and safe diagnostic modality [1]. However, due to its passive nature and uncontrollable progression speed by intestinal peristalsis, the procedure of capsule endoscopy is time-consuming and cumbersome for both the patients and clinicians. Our team, the Applied Dynamics and Control Lab at the University of Exeter, has developed a controllable capsule by using the vibro-impact self-propulsion technique [2] to address these difficulties. Our previous FE work [3] mainly focused on the small intestine. In this work, we investigate the locomotion of the self-propelled capsule in the large intestine via FE analysis using Adams. In order to depict the entire large intestine, rectum, sigmoid colon, descending colon, transverse colon, ascending colon and cecum were modelled with haustral folds. The model of the large intestine was assumed to be inflated, which is a key treatment during colonoscopy, so the capsule will only be in contact with the lower surface of the intestine. The model was simplified as a half symmetric FE model with an underneath supporting base as shown in Figure 1(a). The capsule, with a diameter of 19 mm and a length of 47.6 mm, moved in the large intestine with a wall thickness of 3 mm. The capsule was driven by an external square-wave excitation, and its amplitude, frequency and duty cycle were adjustable. By using the proposed FE model, one can obtain the capsule's displacement, moving speed, resistance force and contact pressure between the capsule and the large intestine, which can be used for prototype design and control strategy optimisation.

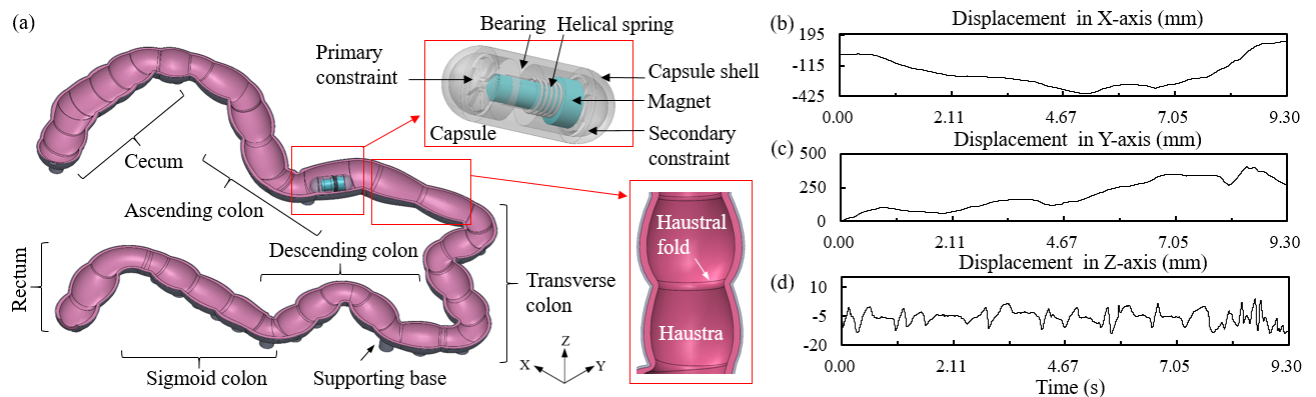


Figure 1: (a) Geometric model of the vibro-impact capsule moving in the large intestine, where the on-board magnet in the capsule interacts with a helical spring and concomitantly impacts with a primary and a secondary constraints under the square-wave excitation from an external magnetic field; FE time histories of the capsule displacement in the direction of (b) X-axis, (c) Y-axis and (d) Z-axis at the excitation amplitude of 0.2 N, frequency of 30 Hz and duty cycle of 0.8.

Results and Discussion

The preliminary results presented in Figures 1(b) and (c) show that the capsule's displacement changed when encountering the curved sections of the large intestine. The capsule fluctuated up and down along the Z-axis as shown in Figure 1(d) due to the haustral effect. The total moving duration of the capsule from the rectum to the cecum was 9.3 s. More studies will be carried out by considering the effect of different dimensions and geometries of the large intestine based on the gender and age of the patients on the locomotion of the capsule.

References

- [1] Dupont, P.E., Nelson, B.J., Goldfarb, M., Hannaford, B., Menciassi, A., O'Malley, M.K., Simaan, N., Valdastrì, P. and Yang, G.Z. (2021) A Decade Retrospective of Medical Robotics Research from 2010 to 2020. *Sci. Robot.* **6**:eabi8017.
- [2] Liu Y., Pérez Chávez J., Zhang J., Tian J., Guo B., Prasad S. (2020) The Vibro-Impact Capsule System in Millimetre Scale: Numerical Optimisation and Experimental Verification. *Meccanica*. **55**:1885–1902.
- [3] Tian, J., Liu, Y., Chen, J., Guo, B. and Prasad, S. (2021) Finite Element Analysis of a Self-Propelled Capsule Robot Moving in the Small Intestine. *Int. J. Mech. Sci.* **206**:106621.

Nonlinear transduction and dynamic buckling of dielectric elastomer actuators

Yi-Husan Hsiao* and Yufeng Chen*

*Department of Electrical Engineering and Computer Science, Massachusetts Institute of Technology, Cambridge, MA, USA

Abstract. Recent advances in the design and fabrication of power-dense dielectric elastomer actuators (DEAs) have enabled agile soft robotic locomotion such as flight. In contrast to most existing DEAs that optimize output energy density, the new DEAs maximize output power density through operating at high frequencies (>200 Hz). Under the dynamic conditions, the DEAs experience nonlinear transduction and dynamic buckling, which reduce DEA performance and lifetime. We characterized these nonlinear dynamic modes and developed mechanical designs to mitigate these effects. Our works resulted in the first soft-actuated aerial robot that can demonstrate controlled hovering flight, acrobatic manoeuvres, as well as in-flight collision-recovery.

Introduction

Dielectric elastomer actuators (DEAs) are soft artificial muscles that have shown promise in a wide range of applications such as haptics, microfluidics, and robotics. Traditionally, researchers aim to maximize DEAs' net energy density through developing soft elastomeric materials of high dielectric strength. Existing DEAs have achieved large deformation ($>1000\%$), and many studies [1] have investigated nonlinear actuation modes and phenomena such as pull-in stability. However, while DEA static nonlinearities have been extensively studied, there lacks accurate models for describing dynamic nonlinearities. In this work [2], we developed DEAs that can operate in the 300 – 500 Hz range. The DEAs drive a flapping-wing robot at system resonance conditions, where they need to overcome large aerodynamic and inertial loads. We identified two unique nonlinear dynamic properties: dynamic buckling and nonlinear transduction. To overcome these effects, we developed mechanical designs and driving strategies to suppress nonlinear modes. For the first time [2], we demonstrated a soft-actuated robot can achieve feedback-controlled hovering flights.

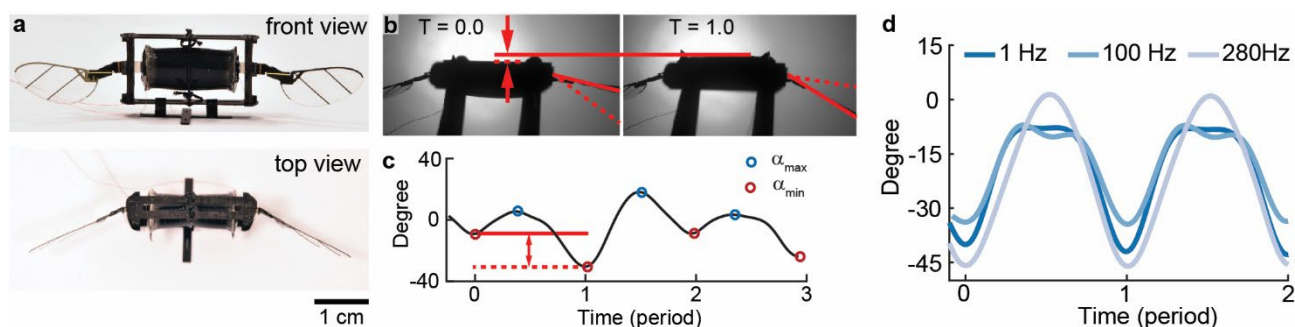


Figure 1: A DEA driven aerial robot and the dynamic nonlinearities associated with the soft actuator. (a) Images of a 155 mg robot. (b) Images that highlight dynamic buckling. (c) Measured wing stroke motion that corresponds to the experiment in (b). The asymmetric peaks illustrate dynamic buckling. (d) Asymmetric wing motion due to nonlinear transduction at different operating frequencies.

Results and discussion

We designed a flapping-wing aerial robot that is driven by a DEA (Figure 1a). When the robot operates at peak conditions (300 Hz and 1400 V), the large aerodynamic load on the DEA causes the actuator to buckle (Figure 1b). We observed period doubling in the corresponding flapping-wing motion (Figure 1c). This period doubling limits the net flapping amplitude, which causes a reduction of system lift force. In addition, buckling leads to large DEA deformation, which causes local dielectric breakdown (self clearing) and reduces actuator performance. This problem can be mitigated by constraining the buckling mode. We constrain the DEA's central plane by tying thread around the DEA. The tension in the thread constrains the DEA from buckling. Furthermore, we measured nonlinear actuation as a function of different operating frequencies. Since a DEA's deformation is proportional to the square of the applied electric field, the robot's output motion does not follow the input waveform. At dynamic conditions, each harmonic component is amplified differently. Consequently, the output wing motion does not resemble sinusoidal driving functions at most operating frequencies (Figure 1d). The asymmetry between upstroke and downstroke motions can cause a 40% reduction of net lift force. To mitigate actuation nonlinearity, we operate the robot near system resonance and remove higher harmonic contributions. Figure 1d shows that at 280 Hz, the robot's flapping-wing motion becomes approximately sinusoidal. Based on these designs, we demonstrated the first controlled flight of an insect-scale soft aerial robot [2], which highlights the potential of applying soft artificial muscles in agile and robust robotic systems.

References

- [1] Goulbourne, N., Eric M., Mary F. (2005) A nonlinear model for dielectric elastomer membranes. 899-906.
- [2] Chen, Y., Zhao, H., Mao, J., Chirarattananon, P., Helbling, E.F., Hyun, N.P., Clarke, D.R., and Wood, R. J. (2019) Controlled flight of a microrobot powered by soft artificial muscles. *Nature* 575., 7782: 324-329.

Numerical investigation of a piezoelectric wrinkled film-based vibration sensor for the vibro-impact capsule robot

Bo Wang*, Haohao Bi*, and Yang Liu**

* Department of Engineering Mechanics, Northwestern Polytechnical University, Xi'an, China

** Engineering Department, University of Exeter, North Park Road, Exeter, UK

Abstract. Monitoring the velocity of the vibro-impact capsule robot [1] during the gastrointestinal endoscopic procedure can enhance diagnosis' controllability and accuracy. To understand the movement of such a robot in the small intestine, a piezoelectric wrinkled film-based vibration sensor is proposed to attach to the outer shell of the capsule. Based on the energy method [2], the mathematical model of this sensor is established. Taking the hoop pressure of the small intestine into account, by utilising the extended Lagrangian principle, the equations of motion of the capsule and the sensor are derived. The effects of the capsule-intestine dynamics on the amplitude of the wrinkled structure are discussed. Findings of this study can be used as the guidelines for sensor fabrication and testing.

Introduction

Pill-sized capsule endoscopes are swallowable for non-invasive diagnosis of the small intestine [3], which is an anatomical site previously considered inaccessible to clinicians due to its small diameter and length. Measuring the physical parameters of the small intestine (e.g., intestine's rigidity) is a key to diagnose potential lesions and determine their locations in the small intestine. Another issue of the capsule endoscopy is the lack of active locomotion [1]. Current endoscopic capsules are passive devices and their locomotion relies on the natural peristalsis of the small intestine, which may lead the risk of missing visualisations at the places of interest of clinicians. To avoid these two problems, a piezoelectric (PZT) wrinkled film-based vibration sensor which can be attached to the outer shell of the vibro-impact capsule robot [1] was studied. A wavy configuration of thin films of PZT on a pre-strained polydimethylsiloxane (PDMS) was conceived, which can make the PZT structure more stretchable by changing its wave amplitudes and wavelengths [2]. A recent study showed that the buckled regions of the structure may enhance the piezoelectric response. Hence, it is essential to investigate the dynamics of this wrinkled structure for predicting the mechanical parameters of the small intestine and the velocity of the capsule robot.

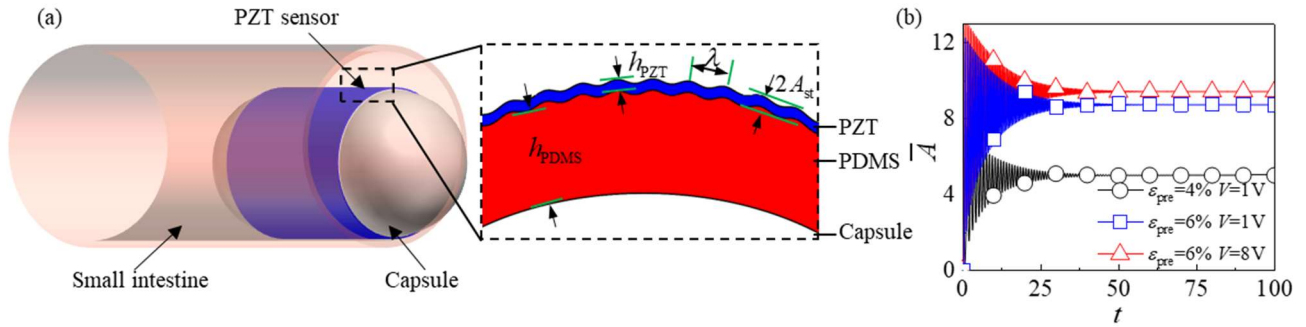


Figure 1: (a) Schematic diagram of the vibro-impact capsule robot in the small intestine; (b) Effects of various pre-strains and applied voltages on the dimensionless time histories of dimensionless displacement \bar{A} of the PZT wrinkled structure. This structure vibrates around the static dimensionless buckling amplitude A_{st} , and the large pre-strain ε_{pre} or applied voltage V enhances the static dimensionless buckling amplitude of this structure.

Results and discussions

Fig. 1(b) illustrates the dimensionless time histories of the PZT wrinkled structure at different pre-strains and applied voltages. The velocity of the capsule robot was set at 4 mm/s. It can be observed that the motion of the wrinkled structure is non-periodic, and the structure vibrates around the static buckling amplitude. As time progresses, the vibration magnitude decreases to the static buckling amplitude. It is also noted that the greater the pre-strain, the greater the amplitude of static buckling. In addition, the applied voltage of the PZT wrinkled structure has a significant influence on the dynamics of this structure. As the applied voltage increases, the static buckling amplitude becomes greater.

References

- [1] Liu Y., Páez Chávez J. (2017) Controlling multistability in a vibro-impact capsule system. *Nonlinear Dynamics*, **88**:1289-1304.
- [2] Wang B., Bi H., Ouyang H., Wang Y., Deng Z. (2020) Dynamic behaviour of piezoelectric nanoribbons with wavy configurations on an elastomeric substrate. *International Journal of Mechanical Sciences*, **182**:105787.
- [3] Ashour S., Dey N., Mohamed S., Tromp G., Sherratt S., Shi F., and Moraru L. (2020) Colored Video Analysis in Wireless Capsule Endoscopy: A Survey of State-of-the-Art. *Current Medical Imaging*, **16**:1074-1084.

Human balance during quiet stance with physiological and exoskeleton time delays

Shahin Sharafi* and Thomas K. Uchida*

*Department of Mechanical Engineering, University of Ottawa, Ottawa, Ontario, Canada

Abstract. Human balance is studied using an inverted pendulum model, considering the effect of time delays in the muscle reflex controller and the controller of an exoskeleton. The model includes two motors at the ankle joint whose torques represent the moments generated by all plantarflexor and dorsiflexor muscles. These “muscle-like” motors obey a proportional–derivative (PD) reflex control law where the states are subject to physiological feedback delays. The exoskeleton applies torques to the ankle joint, also obeying a PD control law but with a different time delay. The stability of this system is analyzed using Galerkin projection to convert the governing neutral delay differential equation (NDDE) into a system of ordinary differential equations (ODEs); the eigenvalues of the ODE system are then computed. Stability charts demonstrate the ability of the exoskeleton to stabilize an inherently unstable biological system.

Introduction

Falling is the leading cause of injury in elderly individuals. A deeper understanding of human balance will enable the development of exoskeletons that can predict and prevent falls. Human balance has been studied using experimental techniques, but experiments are limited by the time and cost of collecting data. Many simulation-based studies of human balance during quiet stance employ a single inverted pendulum model, which has an upright equilibrium point that is inherently unstable. Ahsan et al. [1] studied inverted pendulum models of unassisted human balance, and found that proportional–derivative–acceleration (PDA) feedback generally results in larger stability margins than PD control. In this work, we investigate the stability of human balance during quiet stance when assisted by an exoskeleton at the ankle, where a PD control law is assumed for both the biological reflex controller (gains K_{pb} and K_{db}) and the exoskeleton controller (gains K_{pe} and K_{de}), and they are assumed to have different time delays (200 ms and 100 ms, respectively). Active muscle torque is assumed to depend on the angle and angular velocity of the ankle joint [2]. To study the stability of the governing NDDE, we convert it into a system of partial differential equations, then use the Galerkin approximation method to obtain a system of first-order ODEs whose behaviour approximates that of the original NDDE system. In the Galerkin method, we impose the boundary conditions using the Lagrange multiplier approach [3].

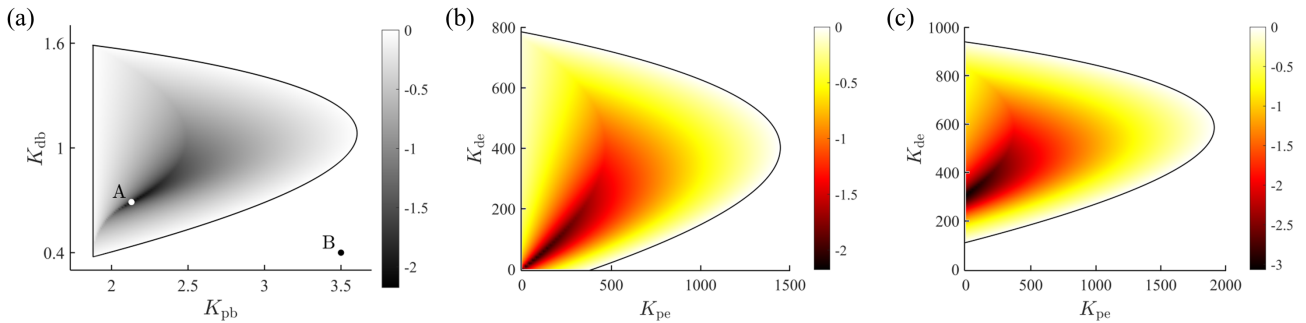


Figure 1: Stability charts of the human stance model (a) without an exoskeleton, (b) with an exoskeleton at point A ($K_{pb} = 2.13$, $K_{db} = 0.69$), and (c) with an exoskeleton at point B ($K_{pb} = 3.5$, $K_{db} = 0.4$). Colour bars indicate the location of the rightmost eigenvalue; black solid lines are the analytical stability boundaries.

Results and Discussion

The stability chart of the unassisted system is shown in Fig. 1(a), obtained using the Galerkin method and validated against the stability boundary computed analytically [4]. Point A denotes the pair of biological controller gains resulting in the most stable system; point B is one example of an inherently unstable biological system. As shown in Fig. 1(b), the stability of the system at point A can be improved by the exoskeleton, though not substantially. Note that the system is inherently stable at point A (i.e., for $K_{pe} = K_{de} = 0$). As shown in Fig. 1(c), the inherently unstable system at point B can be stabilized with the assistance of the exoskeleton. This simulation framework can be used to study the stability of human balance with exoskeleton assistance, considering a range of gains and time delays of the muscle reflex controller and exoskeleton controller.

References

- [1] Ahsan Z., Uchida T.K., Subudhi A., Vyasarayani C.P. (2016) Stability of human balance with reflex delays using Galerkin approximations. *J Comput Nonlinear Dyn* **11**:041009.
- [2] Ashby B.M., Delp S.L. (2006) Optimal control simulations reveal mechanisms by which arm movement improves standing long jump performance. *J Biomech* **39**:1726–1734.
- [3] Vyasarayani C.P. (2013) Galerkin approximations for neutral delay differential equations. *J Comput Nonlinear Dyn* **8**:021014.
- [4] Insperger T., Milton J., Stépán G. (2013) Acceleration feedback improves balancing against reflex delay. *J R Soc Interface* **10**:20120763.

Characterisation of Miniaturised Soft Continuum Robots with Reinforced Chambers

Jialei Shi* Wenlong Gaozhang* and Helge A Wurdemann*

*Department of Mechanical Engineering, University College London, WC1E 6BT London, UK.

Abstract. The chamber fiber-reinforcement of elastomer-based soft continuum robots can limit a large radial expansion, i.e., the ballooning effect. This radial chamber constraint prevents robots from undergoing unexpected deformations and mitigates interference between actuation chambers. A miniaturised dimension of such robots is of paramount importance for space-constrained applications. As such, we design and experimentally characterise the kinematics and tip force generation for four miniaturised robots, with two diameters (10 mm and 15 mm) and two lengths (46 mm and 66 mm).

Introduction

The ballooning effect of elastomer-based soft robots may result in unexpected deformations and concentrated stresses. To mitigate the ballooning, in-extensible fibre reinforcement has been introduced, originally proposed by Suzumori *et al.* [1]. They designed microactuators with three embeded actuation chambers using fiber-reinforced flexible rubber. Moreover, individual chambers can be reinforced, which can further mitigate the interference between actuation chambers, especially when a working channel exists, e.g., the STIFF-FLOP manipulators (with a diameter of 25 mm) devised for minimally invasive surgery [2], or its miniaturised version (with a diameter of 14.5 mm) [3]. However, an investigation of design parameters of such miniaturised soft robots with individually fibre-reinforced chambers remains to be identified. As such, we experimentally evaluate soft robots using two diameters (10 mm and 15 mm) and two lengths (46 mm and 66 mm).

Results and discussion

The fabricated four robots (denoted by R1-R4) and their geometries are shown in Fig. 1(a). The robot has six circular chambers with two adjacent chambers actuated as one chamber pair. As such, the robot can achieve elongation and omni-directional bending motion. The kinematic results are shown in Figs. 1(b)-(d), with the maximum actuation pressure of 1.5 bar. The maximum average bending angles are 178.4° , 116.1° , 211.7° and 154.7° for R1, R2, R3 and R4 robots, with one chamber pair actuation. By contract, the maximum bending angles increase to 249.1° , 149.6° , 413.3° and 295.7° under two chamber pairs actuation. Fig. 1(d) reports the elongation results with all chambers actuated. R1 and R3 robots show a similar elongation response, with the maximum values of 42.3 mm (for the R1 robot) and 41.5 mm (for the R3 robot). In addition, the maximum elongation is 25.1 mm and 28.9 mm for R2 and R4 robots, respectively. In summary, the bending angle is influenced by both the robot diameter and length. Instead, the elongation is mainly determined by the robot length and less influenced by the diameter. Fig. 1(e) reports the tip blocked force when one chamber pair is actuated. The generated forces show a linear relationship with the pressure, and the maximum force values are 0.35 N, 0.39 N, 0.10 N and 0.12 N for the R1, R2, R3 and R4 robots, respectively. The results show that the generated force is less influenced by the length when the cross-sectional dimensions are the same. It is worth mentioning that the reinforced chamber shapes also have influences on the robots' performances [4].

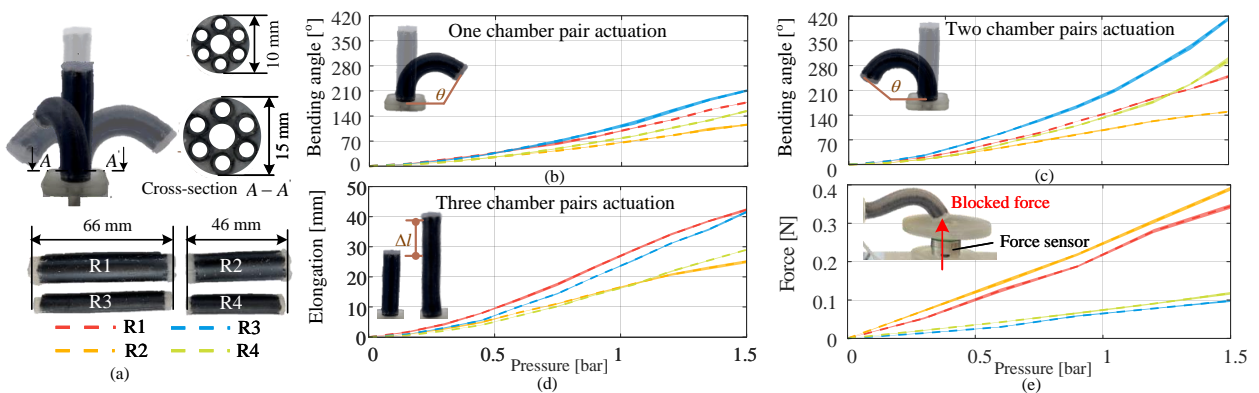


Figure 1: Characterisation results. (a) The designed four robots (R1-R4) and its cross-sectional geometries. The results for (b) one chamber pair actuation (c) two chamber pairs actuation (d) three chamber pairs actuation and (e) tip force generation.

References

- [1] Suzumori K. and et al. (1992) Applying a flexible microactuator to robotic mechanisms. *IEEE Control Sys. Mag.*, 12(1):21-27.
- [2] Fraś J. and et al. (2015) New STIFF-FLOP module construction idea for improved actuation and sensing. In: *Proc. IEEE Int. Conf. Robot. Autom.* pp. 2901-2906.
- [3] Abidi H. and et al. (2018) Highly dexterous 2-module soft robot for intra-organ navigation in minimally invasive surgery. *Int. J. Med. Robot. Comput. Assist. Surg.* 14(1):e1875.
- [4] Shi J. and et al. (2022) Design and characterisation of cross-sectional geometries for soft robotic manipulators with fibre-reinforced chambers. In: *Proc. IEEE Int. Conf. Soft Robot*, pp. 125-131.

Microrobot control from individual to collective

Kiana Abolfathi*, Ali Kafash Hoshlar*

*School of Computer Science and Electronic Engineering, University of Essex, Colchester, UK

Abstract. Microrobots emerged as an ideal tool for minimally invasive medical interventions. In general, microrobots can be categorised into tethered, unthreatened and collective tethered (called microswarm). Initial works were centred on individual microrobot control. However, in many applications (e.g. targeted drug delivery) microrobots should be controlled collectively. This presentation will discuss the required changes to transform the individual to collective control for medical microrobots.

Introduction

Microrobots emerged as powerful yet underdevelopment technology ideal for minimally invasive medical applications. The microrobots size enabled the development of endovascular interventions. Ideally, microrobots are injected into the blood vessels and then guided inside the vascular network to reach the location of interest (e.g. deep brain tumour). Once in the location of interest, the microrobots can perform minimally invasive medical interventions ranging from microsurgery to drug delivery and hyperthermia. Many propulsion systems have been developed to actuate these microrobots, which include chemical, light, acoustic, and magnetic. Magnetic actuation emerged as the favoured approach due to the magnetic field biocompatibility and ease of control. Due to microrobots' small size, the medical imaging systems (MRI, X-Ray and ultrasound) have been investigated to localise them. The control strategy, however, depends on the type of microrobots and the medical interventions. The untethered microrobots are used in closed-loop control schemes, whereas microswarms are designed based on predictive modelling. The microswarms are therapeutic agents which are made of a collection of magnetic nanoparticles (MNPs).

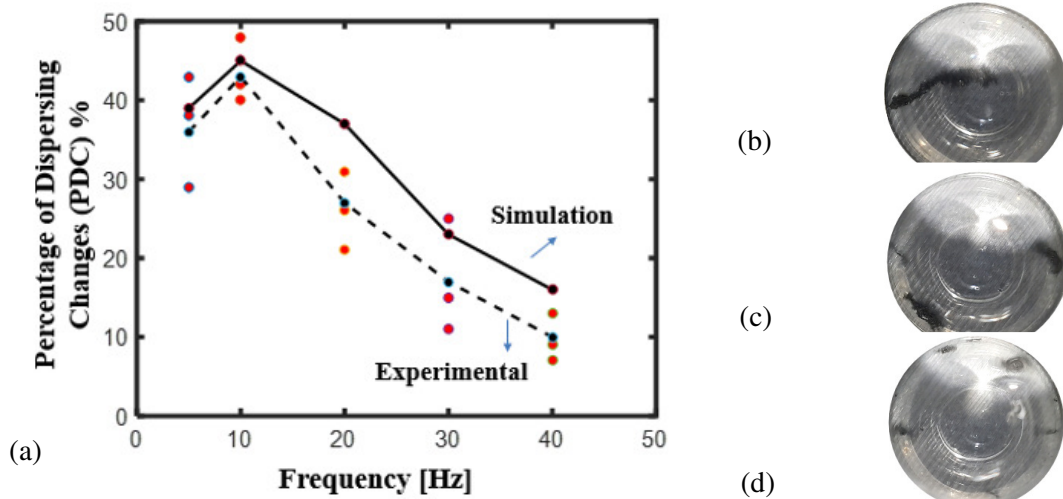


Figure 1(a) shows the comparison between the simulation platform and the experiment results for microswarm creation [1], (b) Rotating magnetic field of 25 mT Fr. 10Hz, (c) Rotating magnetic field of 25 mT Fr. 20Hz, (d) Rotating magnetic field of 25 mT Fr. 30Hz.

Results and discussion

Predictive modelling is used both in collaborative (human-assisted) and feedforward applications. Using mathematical modelling, we have developed a simulation platform (based on discrete element modelling) to predict microswarm shapes and their separation. The platform is validated using experimental data and shows acceptable results [1, 2]. Different parameters have been studied to show their effects on microswarm formation. We showed that in case the initial dispersion is below (<0.12) or above (>0.25), generating the nanoparticle-based microswarm fails. Fig. 1 shows the simulation and experimental result comparison, and Fig. 1 (b-d) shows that the particle disintegrates at a higher frequency (10 to 30 Hz). To guide these microswarms in the vascular network in a dynamic environment, we developed user-in-the-loop interventions [3]. The study on microswarm steering showed that fluid velocity is the most influential parameter. Therefore, we also modified the guidance region for the microswarm to optimise the particles reaching the target.

References

- [1] K. Abolfathi, M. R. H. Yazdi, and A. K. Hoshlar, "Predictable Therapeutic Microswarm Dispersion for Targeted Drug Delivery Application," *EasyChair*, 2516-2314, 2022.
- [2] K. Abolfathi, M. R. H. Yazdi, and A. K. Hoshlar, "Studies of different swarm modes for the MNPs under the rotating magnetic field," *IEEE Transactions on Nanotechnology*, vol. 19, pp. 849-855, 2020.
- [3] B. W. Jarvis, R. Poli, and A. K. Hoshlar, "Online real-time platform for microrobot steering in a multi-bifurcation," in *2022 International Conference on Manipulation, Automation and Robotics at Small Scales (MARSS)*, 2022: IEEE, pp. 1-6.

Shape Forming of a Soft Magnetic Microrobot Using Non-Homogeneous Magnetic Fields

Kiana Abolfathi^{*1}, Jose A. Rosales Medina^{*1}, Hesam Khaksar¹, James H. Chandler², Klaus McDonald- Maier¹, Keyoumars Ashkan³, Pietro Valdastrì², Ali Kafash Hoshier¹

¹*School of Computer Science and Electronic Engineering, University of Essex, Colchester, UK (* equal contributors)*

²*STORM Lab, Institute of Autonomous Systems and Sensing, School of Electronic and Electrical Engineering, University of Leeds, LS2 9JT Leeds, U.K.*

³*Department of Neurosurgery, King's College Hospital, SE5 9RS, London, UK*

Abstract. Microrobotics is an actively growing field with applications in the medical domain. However, miniaturization of robotics presents a challenge in their manipulation and control. Several actuation techniques have offered solutions to this problem, however magnetic actuation has been preferred, due to its remote maneuverability, precise microrobot response and biocompatibility. Soft continuum magnetic microrobots have typically been controlled using homogeneous magnetic fields. In this study, we present the characterization of soft continuum microrobots in a non-homogeneous fields using permanent magnets. Cylindrical permanent magnets were used to apply focused fields across the length of the robot's body, with three different combinations of actuating fields being explored to achieve full body shape control of 600 μm diameter soft continuum magnetic robots. In this approach, one actuating field gives the device a general direction, while a second localized actuation is provided based on the scenario. Using this approach, it is possible to add versatility to the shape forming of microrobots, which we demonstrate using a static 3-point manipulation.

Introduction

Magnetic continuum microrobots have been developed as endovascular interventional tools, where their soft cylindrical structures can be controlled to navigate inside vascular networks [1]. More recently, fully soft continuum robots capable of achieving shape formation have been introduced (Fig. 1 (a)) [2, 3]. The soft continuum microrobots used in the presented work were made of a magnetic responsive elastomer (MRE) material, fabricated by embedding magnetic microparticles in an elastomer matrix. This type of material combines magnetic and elastic properties to allow controlled deformation and manipulation of the devices.

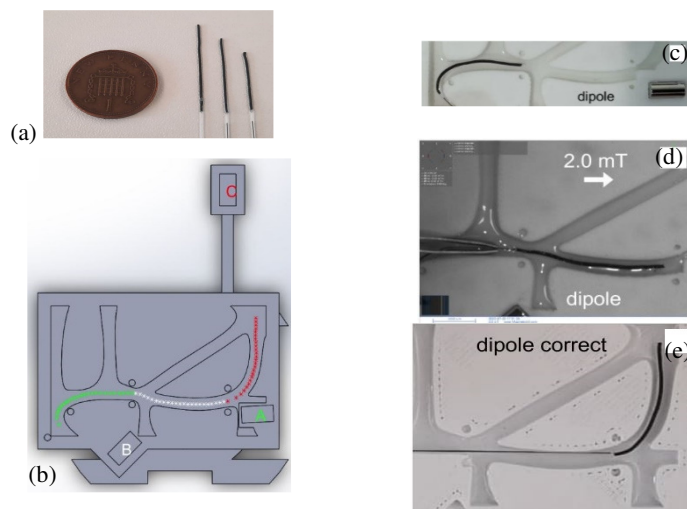


Figure 1. Soft magnetic microrobot shape forming (a) microrobot of with 20mm 25mm 30mm length and (diameter <600 μm), (b) complex path with three shape conditions (c) shape condition with one permanent magnet (d) shape condition with permanent magnet and electromagnet (e) shape condition with two permanent magnets (all conditions are statics)

Results and discussion

The study was divided into three main experiments, all conducted with the microrobot submerged in fluid. This configuration was chosen to reduce friction of between the devices. We first studied the microrobot's behaviour under inhomogeneous fields to identify possible shape-forming primitives. Subsequently, the possibility to achieve more complex, sequential shape forming was simulated (Fig. 1 (b)). Finally, the approach of shape-forming under inhomogeneous fields was tested (Fig. 1 (c), (d) and (e)) which shows the successful proof-of-concept result and five different modes for shape forming was identified.

References

- [1] S. Jeon *et al.*, "A magnetically controlled soft microrobot steering a guidewire in a three-dimensional phantom vascular network," *Soft robotics*, vol. 6, no. 1, pp. 54-68, 2019.
- [2] P. Lloyd *et al.*, "A learnt approach for the design of magnetically actuated shape forming soft tentacle robots," *IEEE Robotics and Automation Letters*, vol. 5, no. 3, pp. 3937-3944, 2020.
- [3] G. Pittiglio *et al.*, "Patient-Specific Magnetic Catheters for Atraumatic Autonomous Endoscopy," *Soft Robotics*, 2022.

Wireless force sensing of a micro-robot penetrating a viscoelastic solid

Moonkwang Jeong^{*,**}, Felix Fischer^{*} and Tian Qiu^{*,**}

^{*}Cyber Valley group – Biomedical Microsystems, Inst. Physical Chemistry, University of Stuttgart, Stuttgart, Germany

^{**}Stuttgart Center for Simulation Science (SC SimTech), University of Stuttgart, Stuttgart, Germany

Abstract. The penetration of biological soft tissues is an essential prerequisite for micro-robots to perform useful biomedical tasks, such as targeted drug delivery and minimally-invasive surgery. However, most wirelessly-driven micro-robots do not exert large enough force to penetrate solid tissues. It is therefore important to understand the fundamental mechanics of tissue fracture at micro-scale to facilitate the optimization of micro-robots. Here, we report the force sensing and modelling of a magnetic micro-robot in a viscoelastic solid. The robot is actuated by a homogeneous magnetic field gradient and its dynamics are analyzed to calculate the resistive forces in a phantom gel. Multiple shapes and surface topology of the micro-robots are compared to identify an optimized design for soft tissue penetration.

Introduction

Micro-robots show great potential for minimally-invasive medicine. Many efforts have been made to power and actuate them, for example, by a magnetic field [1], an ultrasonic field [2], or a light field [3]. The magnetic field is one of the most promising power source for biomedical applications, as the magnetic field is safe for humans and offers a large penetration depth and a higher actuation force comparing to the other fields. As the device gets smaller, the magnetic driving force scales with the volume of the device, but the resistive forces scale with only the surface area. Therefore, it becomes even more difficult for micro-/nano-devices to exert high enough forces to penetrate biological soft tissues. In this work, we report a wireless force sensing system based on magnetic micro-robots. With the new system, the dynamics of the robots moving in viscoelastic phantom gels are measured and modelled.

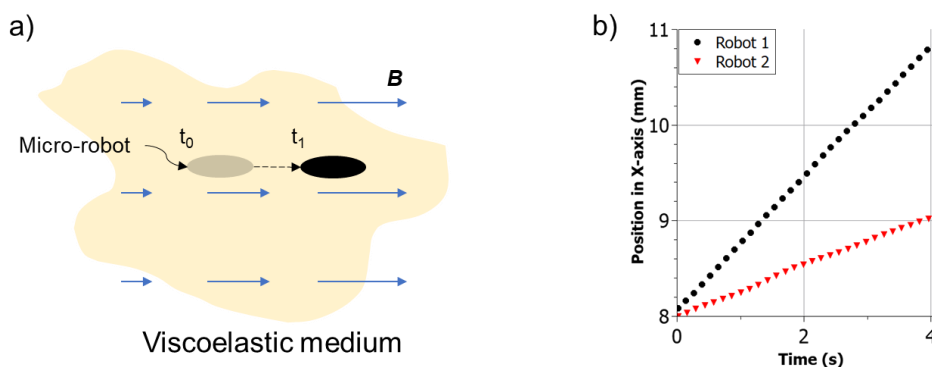


Figure 1: a) Schematic of a micro-robot moving in a viscoelastic medium. The robot's motion is captured while it is actuated by a homogeneous magnetic gradient. b) The displacement curves of two robot designs.

Results and discussion

Experimental results show that the customized system generates a controllable homogeneous magnetic field gradient. A micro-robot moves through a transparent viscoelastic medium actuated by the magnetic gradient, as shown in Figure 1a. The displacement curves of different micro-robots' designs are shown in Figure 1b. The optimization of the robot's shape and surface increases the velocity of 20 %. Moreover, air bubbles were observed that were left on the path of the micro-robot, indicating the fracture of the viscoelastic solid. Future study lies in the modelling of the gel mechanics and optimizing the interaction between the robot and the gel to facilitate an effective penetration with a low actuation force. Furthermore, we expect the experimental results contribute to the understanding of nonlinear fracture mechanisms.

References

- [1] Ghost, A., Fischer, P. (2009) Controlled propulsion of artificial magnetic nanostructured propellers. *Nano Letters* **9.6**: 2243–2245.
- [2] Qiu, T., Palagi, S., Mark, A. G. *et al.* (2017) Active acoustic surfaces enable the propulsion of a wireless robot. *Adv. Mater. Interfaces* **4.21**: 1700933.
- [3] Palagi, S., Mark, A. G., Reigh S. Y. *et al.* (2016) Structured light enables biomimetic swimming and versatile locomotion of photoresponsive soft microrobots. *Nat. Mater.* **15.15.6**: 647–653.

Constrained Green's function for a beam with arbitrary spring and nonlinear spring foundation

X. Zhao*, Q. Wang*, W. D. Zhu**, Y. H. Li***

*School of Civil Engineering and Architecture, Southwest Petroleum University, Chengdu, Sichuan, PR China

**Department of Mechanical Engineering, University of Maryland, Baltimore County, Baltimore, USA

***School of Mechanics and Engineering, Southwest Jiaotong University, Chengdu, Sichuan, PR China

Abstract. As an important structure of micro-robots, micro-beams play an increasingly important role in daily production and life, especially in the biological and medical fields. During the use of micro-beam instruments, vibrations occurs due to the unevenness of the skin, which will affect the accuracy and stability of precision instruments. To analyze this problem, this paper studies the free vibration of beams with spring at arbitrary position and nonlinear spring foundations. Through the Laplace transform and the principle of linear superposition, the constrained Green's function is obtained. Numerical calculations are performed to validate the present solutions and the effects of various important physical parameters are investigated. It was found the mode and deflection of the beam were changed by the spring.

Introduction

The research on the dynamic behavior of beams has been a classic problem, which has attracted many scholars since its inception. As an effective tool, various forced vibration problems are studied through Green's function. In order to study the vibration characteristics of the beam, Li et al.[1] used Green's function to study the deflection and frequency of Timoshenk beam with damping. In order to analyze the interaction of double beam structures, Zhao et al.[2] used Green's function method to study the forced vibration of Timoshenko double beam system under axial compression load. Li et al.[3] proposed a Green's function solution of forced vibration of oil pipelines on the basis of two parameters.

In a word, the previous Green's function method focused on the study of various forced vibration problems, but not on free vibration problems. In this paper, the free vibration of beams with arbitrary springs and nonlinear foundations is studied by applying the Green's function method. The effects of some physical parameters are studied and meaningful conclusions are obtained.

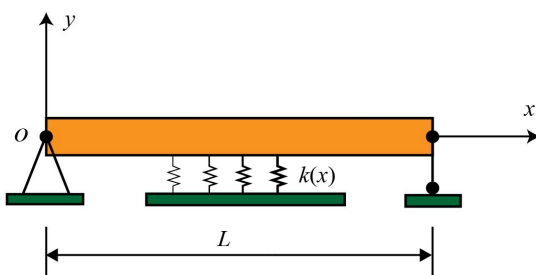


Figure 1: Nonlinear spring foundation.

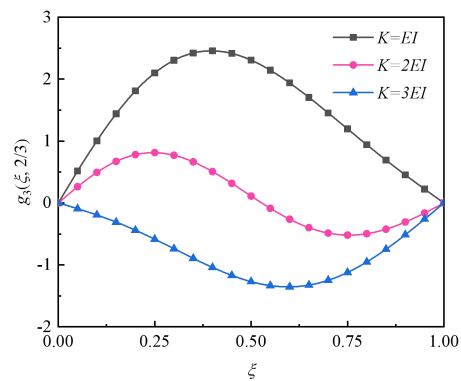


Figure 2: Effect of spring stiffness on the constrained Green's function.

Results and discussion

Figure 1 shows a simply supported beam with springs. There are a series of springs with varying stiffness at the bottom of the beam. In this paper, the free vibration problem is solved by Green's function method.

It can be seen from Figure 2 that the mode is modified by the spring stiffness. As the spring stiffness increases, the mode of the constrained Green's function change accordingly.

References

- [1] Li X.Y., Zhao X., Li Y.H. (2014) Green's Functions of the Forced Vibration of Timoshenko Beams with Damping Effect. *J. Sound Vib* **333**: 1781–1795.
- [2] Zhao X., Chen B., Li Y.H., Zhu W. D., Nkiegaing F. J., Shao Y. B. (2020) Forced Vibration Analysis of Timoshenko Double-Beam System under Compressive Axial Load by Means of Green's Functions. *J. Sound Vib* **464**: 115001.
- [3] Li M., Zhao X., Li X., Chang X.P., Li Y.H. (2020) Stability Analysis of Oil-Conveying Pipes on Two-parameter Foundations with Generalized Boundary Condition by Means of Green's Functions. *Eng. Struct* **173**: 300–312.

Chemical Signalling and Pattern Formation in Schoener's Predator–Prey Model

Purnedu Mishra* and Dariusz Wrzosek**

*Department of Mathematics, Faculty of Science and Technology, Norwegian University of Life Sciences Ås, Norway,

**Faculty of Mathematics, Informatics, and Mechanics, University of Warsaw Poland,

Abstract. This work presents a mathematical model to understand the impact of chemical induced defense mechanism in a special class of predator-prey model. Based on the real world observations [1, 2], we formulate a predator-prey model that considers movement of prey individuals opposite to the gradient of the chemical released by predators. We theoretically able to show existence of solutions in one dimension ($n = 1$) and global-existence of solutions for $n \geq 2$ is still a topic of debate. An onerous linear stability analysis shows that repulsive indirect predator-taxis promotes instability in proposed model and space inhomogeneous Hopf-bifurcation may occur at the critical values of taxis sensitivity parameter χ . We numerically show emergence of spatio-temporal patterning that depicts the tendency to spatio-temporal separation between prey and predators.

Introduction

Let $P(x, t)$, $N(x, t)$ represent the population densities of predator and prey individuals in a domain $\Omega \in \mathbf{R}^n$ with smooth boundary, and $C(x, t)$ is the concentration of chemical released by predators then predator-prey model studied in this paper reads

$$\begin{aligned}\frac{\partial P}{\partial t} &= d_1 \Delta P + \mathcal{F}(N, P), & x \in \Omega, t > 0, \\ \frac{\partial N}{\partial t} &= d_2 \Delta N + \chi \nabla \cdot (N \nabla W) + \mathcal{G}(N, P), & x \in \Omega, t > 0, \\ \frac{\partial C}{\partial t} &= d_3 \Delta C + \sigma P - \mu C, & x \in \Omega, t > 0,\end{aligned}\tag{1}$$

with following non-zero initial condition and homogeneous Neumann boundary condition

$$\begin{aligned}P(x, 0) &= P_0(x), P(x, 0) = N_0(x), C(x, 0) = C_0(x) & x \in \Omega, \\ \partial_\nu P &= \partial_\nu N = \partial_\nu C = 0 & x \in \partial\Omega, t > 0.\end{aligned}\tag{2}$$

In model (1), d_i , $i = 1, 2, 3$ are diffusion coefficients, χ counts repulsive chemo-sensitivity of prey, σ and μ represent chemical production and degradation rate, respectively. We consider Schoener's type [4] kinetic part in (1) with the assumption that both predator and prey exploit competitively a common food resource which is available at some constant rate and shared between the predator and the prey.

Discussion

The mathematical model studied in this paper reveals the defence mechanism by means of chemical signalling. Modeling framework considers a predator-prey model that counts intraguild predation and repulsive taxis opposite to gradient of chemical released by predator. We have proved the existence of global solutions in 1D and by linear stability analysis we show that sufficiently large chemosensitivity gives rise to emergence of inhomogeneous space-time patterns. Numerically we observed beautiful spatio-temporal patterns in 1D indicating that predators and prey have used the same territory at different times in what is called spatio-temporal separation in ecology.

References

- [1] Nolte, D. L., Mason, J. R., Epple, G., Aronov, E., & Campbell, D. L. (1994). Why are predator urines aversive to prey?. *Journal of Chemical Ecology*, **20**(7): 1505-1516.
- [2] Hay, M. E. (2009). Marine chemical ecology: chemical signals and cues structure marine populations, communities, and ecosystems. *Annual review of marine science*, **1**: 193.
- [3] Chivers, D. P., & Smith, R. J. F. (1998). Chemical alarm signalling in aquatic predator-prey systems: a review and prospectus. *Ecoscience*, **5**(3), 338-352.
- [4] Schoener, T. W. (1976). Alternatives to Lotka-Volterra competition: models of intermediate complexity. *Theoretical population biology*, **10**(3), 309-333.

Non-linear dynamics of the temporomandibular joint disc

Jerzy Margielewicz*, Damian Gąska* and Grzegorz Litak**

*Faculty of Transport and Aviation Engineering, Silesian University of Technology, Katowice, Poland

**Faculty of Mechanical Engineering, Lublin University of Technology, Lublin, Poland

Abstract. The paper presents issues related to the identification of a non-linear mathematical model of the temporomandibular joint disc. Laboratory tests consisted in reflecting the mechanical characteristics of the articular disc. Regarding the verified and optimized model, which very well reflects the results of the laboratory experiment, model tests were carried out. Numerical simulations included, among others, plotting a multi-colour map of distribution of the largest Lyapunov exponent, on the basis of which, the areas of occurrence of periodic and chaotic solutions were identified. Bifurcation diagrams of steady states were generated for sample sections of Lyapunov's map and phase flows of periodic and chaotic solutions were presented.

Introduction

The articular disc is an integral element of the temporomandibular joint, which is one of the most complex joints in the human body. These are two points of support, formed by the heads of the condylar processes, performing interconnected complex spatial movements in time, whose heads move on the shape-shifting sockets. The loads acting on the tissues of the articular discs, from a theoretical point of view, can be classified into two types of loads: static and dynamic. Static loads occur when the dental arches are clamped. On the other hand, dynamic loads take place during the act of chewing. The results of experimental studies indicate that, regardless of the deformation zone, the stress in the tissues of the articular disc decreases with each cycle. In addition, with each subsequent load cycle, the hysteresis loop decreases, which results in the loss of dissipation properties [1,2].

Model and experimental research

The results of the model research presented in the paper focused on the formulation of a mathematical model that reliably reproduces the behavior of the articular disc tissues subjected to cyclic loading. The disc model was mapped using a system with two degrees of freedom, consisting of a non-linear elastic element and two non-linear dissipation members. The measurement data were recorded in laboratory conditions, using the Zwick universal testing machine, through which the tissues of the articular disc were cyclically loaded. The conducted numerical experiments indicate that the proposed mathematical model of the articular disc very well reflects the course of experimental research. The compatibility of the simulation results with the measurement data is at the level of approx. 98%.

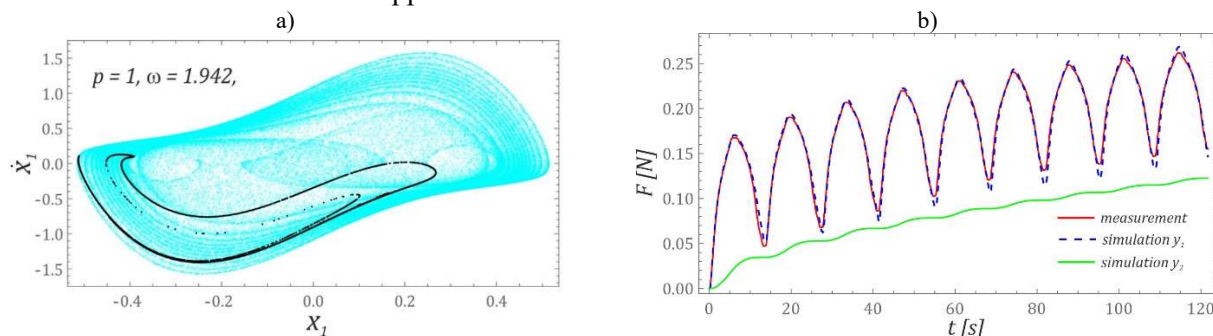


Figure 1: Exemplary results showing a) chaotic solutions, b) verification of mathematical models of temporomandibular joint discs.

At the beginning of the model research, we focused our attention on determining the zones of occurrence of chaotic solutions [3]. Then, for selected values of the amplitude of the external dynamic load acting on the disc tissues, steady-state bifurcation diagrams were plotted. We analyzed the effect of the frequency and the dimensionless amplitude of the external load acting on the tissues of the joint disc. The results of the numerical experiments are presented in the form of stable orbits against which the points of the Poincaré cross-sections are plotted. The last element, which was the subject of model tests included in the paper, was the identification of coexisting solutions. We proved that chaotic system responses and multiple solutions most often occur in the range of low values of the dimensionless amplitude of the external load.

References

- [1] Kijak E., Margielewicz J. and Pihut M.: Identification of Biomechanical Properties of Temporomandibular Discs, Hindawi, Pain Research and Management Volume 2020, Article ID 6032832.
- [2] Aryaei, A., Vapniarsky, N., Hu, J.C. et al. Recent Tissue Engineering Advances for the Treatment of Temporomandibular Joint Disorders. *Curr Osteoporos Rep* 14, 269–279 (2016). <https://doi.org/10.1007/s11914-016-0327-y>.
- [3] Litak G., Borowiec M., Friswell M., Szabelski K.: Chaotic vibration of a quarter-car model excited by the road surface profile. *Communications in Nonlinear Science and Numerical Simulation*. Volume 13, Issue 7, September 2008, Pages 1373-1383

Global dynamical analysis of age-structured population model

Preeti Deolia, Anuraj Singh

Department of Applied Sciences, ABV-Indian Institute of Information Technology and Management, Gwalior, M.P., India.

Abstract. The dynamics of the transmission and spread of infectious diseases are eminently intricate, mainly due to the heterogeneity of the host population. The patterns of interactions among various age groups can be different, which generates a significant degree of heterogeneity. Further, the treatment rate of an infectious disease plays a vital role in decreasing the spread due to the limited treatment facilities. Therefore, it is essential to involve age distribution and saturated treatment rates to model the future disease burden. This paper investigates an age-structured epidemic model incorporating a saturated treatment function. The expression for the basic reproduction number and conditions for the global stability of the system are derived via the graph-theoretic approach. It is observed that the disease-free equilibrium is globally stable if $R_0 \leq 1$ while an endemic equilibrium exists uniquely if $R_0 > 1$. The numerical simulation is demonstrated to illustrate the results.

Results and discussion

In this study, the global dynamics of an SEIR class of epidemic models with discrete age-structure and saturated treatment function is investigated. The expression for the basic reproduction number R_0 is derived using a graph-theoretic form of Gaussian elimination method. It is stated that the basic reproduction number plays the role of a sharp threshold for both the local and global asymptotic stability of each equilibria. More specifically, the disease free equilibrium M_0 is globally asymptotically stable if $R_0 \leq 1$, and if $R_0 > 1$ and the digraph associated to the disease transmission matrix is strongly connected, then the unique endemic equilibrium M^* is globally asymptotically stable under mild condition, which is the main result of this work.

Further, to facilitate the understanding of obtained theoretical results, several numerical simulations are performed vividly. We applied our age-stratified epidemic model incorporating limited treatment facilities to study the response of republic of Italy to the second wave of COVID-19 outbreak. For this purpose, the total population is divided into the following age-groups: (00 – 19)years, (20 – 49)years, (50 – 69)years, (70 – 99)years. The daily new reported cases for the republic of Italy were extracted from WHO situation reports [1] for the period 07th September 2020 to 27th December 2020. The proposed model is fitted to the extracted data and the unknown parameters are estimated. The contact patterns across different age groups have a great degree of heterogeneity. During COVID-19, these mixing patterns are known to be crucial determinants for the model outcome and highly assortative with age. In most mathematical models, the number of people a person contacts per day is assumed to be a constant or follow a particular pattern. In this work, these age-dependent contact rates are estimated via a paper-diary methodology [2], based on a population-prospective survey in European countries. For this purpose, relevant contact data from the POLYMOD (Improving Public Health Policy in Europe through Modelling and Economic Evaluation of Interventions for the Control of Infectious Diseases) study is used. The time profile shows in figure 1 clearly depicts the role of different age-groups in the spread of disease. For the infected individuals lying in the age-group (20-49) years and (50-69) years, the susceptibility to infection is approximately double compared to the exposed population is an important observation of this work. The rapidity of the evolved COVID-19 outbreak in 2020 makes us realize the subverted situation of our world in times of emergency. The results demonstrated in this study helps the policy makers in analyzing the disease severity among different age-groups and therefore in adapting the effective control measures.

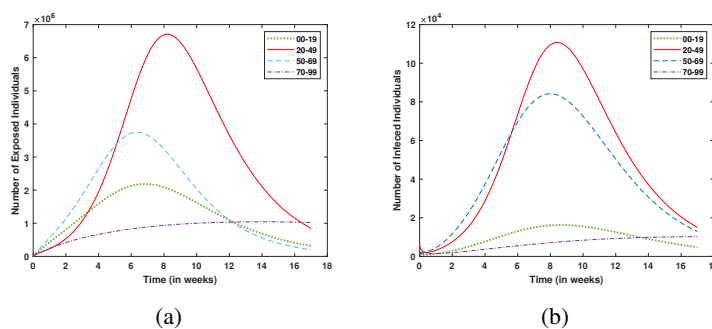


Figure 1: Susceptibility to infection for Exposed and Infected classes varies by age.

References

- [1] World Health Organisation. <https://covid19.who.int/region/euro/country/it>.
- [2] M.I. Meltzer, M. Gambhir, et al. (2015) Standardizing scenarios to assess the need to respond to an influenza pandemic *Clin, Infect. Dis.* **60**:S1-S8.

Synaptic scaling enables extreme selectivity in high-dimensional neurons

Valeri A. Makarov*, Sergey Lobov**, Vasilisa Stepasyuk**, and Julia Makarova***

**Instituto de Matemática Interdisciplinar, Universidad Complutense de Madrid, Madrid, Spain*

***Neurotechnology Dept., Lobachevsky State University, Nizhny Novgorod, Russia*

****Dept of Translational Neuroscience, Cajal Institute, CSIC, Madrid, Spain*

Abstract. A recent discovery of concept cells has revived the longstanding discussions on the role of individual cells in information processing. The theory of a high-dimensional (HD) brain has provided a foundation for their existence in the framework of an oversimplified mathematical model. In this work, we develop a biologically plausible model of concept cells, including spiking neurons, rate information coding, and homeostatic plasticity. Then, we provide analytical and numerical results illustrating the emergence of extreme selectivity in a neuronal aggregate to HD information patterns.

Introduction

In 1890 W. James proposed the hypothesis of a pontifical cell, which started a debate on the role of individual neurons in the brain. A recent discovery of concept cells has revived the longstanding discussion [1]. From the theoretical ground, the encoding of memories and high cognitive abilities require processing high-dimensional representations of the external environment [2]. Then, the recently introduced HD-brain concept has provided a mathematical foundation for these phenomena using formal neurons and an Oja-like learning rule [3, 4]. Its extension to brain neural networks requires biologically relevant models of neurons, information coding, and learning mechanisms. Here, we provide analytical and numerical results pushing further the HD-brain concept. In the long run, developing such models and relating them to electrophysiological data could shed light on the functional principles behind our intelligence.

Results and discussion

To simulate information processing in a neural network, we use the Izhikevich nonlinear model of a single neuron, which faithfully reproduces the spiking behaviors of cortical neurons [5]. We adopt the rate coding of complex information patterns received by HD neurons (with multiple synaptic inputs).

Earlier, on a simplified model, it has been shown that an aggregate of individual neurons can learn an arbitrary high number of unique patterns [6]. We then summarize and discuss the main theorems to develop an adequate nonlinear learning model for spiking neurons with similar properties. On this journey, an essential requisite is local adaptive learning. From one side, it could provide fast learning (by avoiding global optimization) and, from the other side, maintain an optimal spiking frequency.

Most mathematical models simulating learning in brain neural networks use Hebbian plasticity, which postulates an increase in the efficiency of synaptic transmission when the activity of the pre and postsynaptic neurons is correlated [7]. However, in its original form, the Hebbian rule has a severe drawback - it only describes the potentiation of synapses, which can lead to unbounded growth of synaptic weights. This problem can be solved using an ad hoc nonlinear mechanism, the so-called synaptic competition, which suppresses inactive or low-frequency synapses in accordance with experimental findings [8]. Although this approach is mathematically reasonable, its biological relevance remains unclear. We thus propose a nonlinear learning model that exploits homeostatic plasticity, which restores neuronal activity to a specific value after a disturbance. As a result, neurons can compensate for an increased or decreased overall synaptic input.

Using the developed models, we provide rigorous mathematical results and numerical simulations, which confirm that biological neurons can be highly selective to input patterns, as indirectly supported by experimental results [9].

References

- [1] Quiñan Quiroga R. (2019) Akhievitch revisited. *Phys Life Rev* **29**:111-114.
- [2] Makarov V.A., Lobov S.A., Shchanikov S., Mikhaylov A., Kazantsev V.B. (2022) Toward reflective spiking neural networks exploiting memristive devices. *Front Comput Neurosci* **16**:859874.
- [3] Tyukin I., Gorban A.N., Calvo C., Makarova J., Makarov V.A. (2019) High-dimensional brain: A tool for encoding and rapid learning of memories by single neurons. *Bull Math Biol* **81**:4856-4888.
- [4] Gorban A.N., Makarov V.A., Tyukin I.Y. (2020) High-dimensional brain in a high-dimensional world: Blessing of dimensionality. *Entropy* **22**:82.
- [5] Izhikevich E.M. (2003) Simple model of spiking neurons. *IEEE Trans Neur Netw* **14**:1569–1572.
- [6] Calvo Tapia C., Tyukin I., Makarov V.A. (2020) Universal principles justify the existence of concept cells. *Sci. Reports* **10**:7889.
- [7] Pfister J.P., Gerstner W. (2006) Triplets of spikes in a model of spike timing-dependent plasticity. *J. Neurosci* **26**(38):9673-9682.
- [8] Lobov S.A., Chernyshov A.V., Krilova N.P., Shamshin M.O., Kazantsev V. B. (2020) Competitive learning in a spiking neural network: Towards an intelligent pattern classifier. *Sensors* **20**:500.
- [9] Benito N., Martín-Vázquez G., Makarova J., Makarov V.A., Herreras O. (2016) The right hippocampus leads the bilateral integration of gamma-parsed lateralized information. *eLife* **5**:e16658.

Effects of rising sea surface temperature on the dynamics of coral-algal interactions

Sasanka Shekhar Maity*, Joydeb Bhattacharyya** and Samares Pal*

*Department of Mathematics, University of Kalyani, Kalyani – 741235, India

**Department Mathematics, Karimpur Pannadevi College, Nadia, India.

Abstract.

Coral reef ecosystems are most vulnerable to changes in sea surface temperature (SST), a key environmental factor critical to reef-building growth. Elevated SST reduces the ability of corals to produce their calcium carbonate skeletons. Prolonged high SST results in coral bleaching owing to the uncoupling of symbiosis among corals and microalgae. Corals have narrow temperature tolerances. The skeletal growth rate of corals falls sharply to zero even at a slight increase of SST above its temperature tolerance level. Corals are also vulnerable to macroalgal toxicity. Several benthic macroalgae species are known to bring about allelopathic chemical compounds that are very harmful to corals. The toxic-macroalgae produce allelochemicals for which the survivability and settlement of coral larvae are highly affected. Toxic macroalgae species damage coral tissues when in contact by transferring hydrophobic allelochemicals present on macroalgal surfaces, leading to a reduction of corals and even coral mortality. The abundance of toxic macroalgae changes the community structure towards a macroalgae-dominated reef ecosystem. We use a continuous time model to investigate coral-macroalgal phase shifts in the presence of elevated SST and macroalgal toxicity. We have derived the conditions for locally asymptotic stability of steady states. Computer simulations have been carried out to illustrate different analytical results.

Short Introduction:

Coral reefs are the most striking and different marine ecosystems in our globe. Productive and complex, coral reefs host hundreds of thousands of species, but few are described by science. Coral reefs are very well known for their biological diversity, beauty and high productivity [1]. Coral Reefs tend to exist in alternate coral or algae-dominated states. Faster-growing macroalgae always dominate coral reefs by making less available space for the successful settlement of coral larvae [2]. Corals may die due to bleaching, and it takes decades to recover partially or completely. Most of the bleaching events occur when the temperature is at least 1° more than the temperature threshold [3].

In the present paper, the main emphasis will be placed on the dynamic behaviour of coral reefs ecosystem due to increasing sea surface temperature.

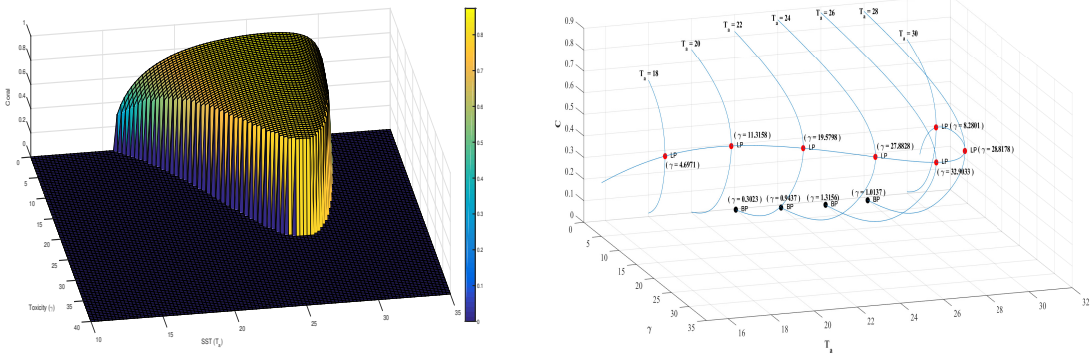


Figure 1: Bifurcation diagram of γ versus the equilibrium value of coral cover for different SST.

Results and discussion

In the tropical zone, we observed that the toxicity in coral increases due to increase of SST upto a threshold value. In case of high SST, the toxicity tolerance in coral reduces extremely and followed by coral-mortality. In the same tropical zone, we observed that higher rate of grazing of the herbivores is required for surviving corals in the system when the SST is either low or high. We observed that the difference of upper and lower SST threshold for surviving corals is maximum when they are in tropical region. The threshold difference is minimum when corals are in temperate zone and it lies between maxima and minima when corals are in subtropical zone.

References

[1] Hoegh-Guldberg Ove (1999) Climate change, coral bleaching and the future of the world's coral reefs. Marine and Freshwater Research **50**, 839-866.
[2] Birrell CL, McCook LJ, Willis BL, Diaz-Pulido GA. Effects of benthic algae on the replenishment of corals and the implications for the resilience of coral reefs. Oceanogr Mar Biol Annu Rev. 2008 Jan 1;**46**:25-63.
[3] Hughes TP, Baird AH, Bellwood DR, Card M, Connolly SR, Folke C, Grosberg R, Hoegh-Guldberg O, Jackson JB, Kleypas J, Lough JM. Climate change, human impacts, and the resilience of coral reefs. science. 2003 Aug 15;**301**(5635):929-33.

Hopf Bifurcation Analysis for a Delayed Nonlinear-SEIR Epidemic Model on Networks

Madhab Barman* and Nachiketa Mishra**

Department of Mathematics, Indian Institute of Information Technology, Design and Manufacturing, Kancheepuram, Chennai-600 127, India

*ORCID: 0000-0002-1233-5305, **ORCID: 0000-0002-4538-8489

Abstract. A delayed SEIR (Susceptible-Exposed-Infected-Removed) epidemic model with a non-linear incidence rate using graph Laplacian diffusion has been considered. The model has a diffusion term that describes population mobility through a network. The local stability analysis for each steady state is demonstrated, and Hopf bifurcation for endemic equilibrium has been examined. Computational experiments are performed to illustrate the theoretical findings on a small-world Watts-Strogatz graph.

Introduction

Population mobility is one of the important key factors for the spatial spread of an epidemic. Many models have been proposed to control an outbreak using a network, but these are based on contact-network between individuals [1]. At the early stage of an outbreak, it is essential to involve a geographical network to understand spatial dynamics. Recently, Tian et al. [2] have investigated delay-driven Hopf bifurcation in a networked Malaria model. Motivated by their work, we investigate Hopf bifurcation in a delayed-SEIR epidemic model on network.

The present model also considers an additional non-linearity called saturated incidence rate [4] of the form $\beta IS/(1 + \alpha I)$, where S and I are the susceptible and infected individuals, respectively. Several studies on dynamical and bifurcation analysis can be found in [3] for which the model have this kind of nonlinear incidence. Since this incidence rate involves the behavioral change and crowding effect of the infective individuals, it appears that this incidence rate is more important than both the bilinear incidence rate and standard bilinear incidence rate [5]. Furthermore, the unboundedness of the contact rate can be prevented by selecting appropriate parameters β and α .

Results and Discussion

The main contributions of this work begin with theoretical results, which include the stability theorems and derivation of the threshold delay time τ_0 for the bifurcations. Then numerical experiments are performed by considering a small-world Watts-Strogatz graph to validate the theoretical findings. One of the important finding is the local behavior of the model, which is governed by basic reproduction number \mathcal{R}_0 . The disease-free equilibrium is asymptotically stable for $\tau \geq 0$ if $\mathcal{R}_0 < 1$. If $\mathcal{R}_0 > 1$, the endemic equilibrium exists uniquely, and under a certain condition on parameters, the model undergoes a Hopf bifurcation when time delay τ surpasses a critical value τ_0 . In Figure.1, the left sub-figure depicts the solutions for all node are stable and converge to the endemic equilibrium simultaneously when $\tau < \tau_0$. The solutions are periodic for the all the nodes when τ greater than the critical value τ_0 . For the shake of clarity, the phase plane for the second node has been displayed in the right sub-figure of Figure.1 when $\tau > \tau_0$.

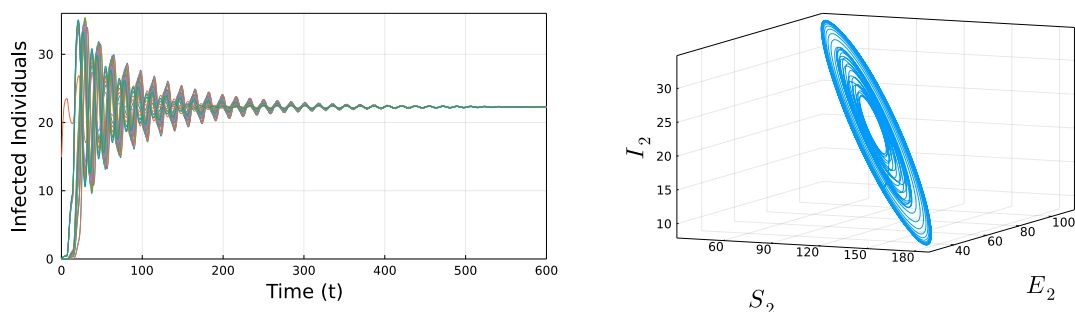


Figure 1: (left) when $\tau < \tau_0$, profile solutions for each infected node, and (right) when $\tau > \tau_0$, phase plane at second node.

References

- [1] R. Pastor-Satorras, C. Castellano, P. V. Mieghem, and A. Vespignani, Epidemic processes in complex networks, *Rev. Mod. Phys.*, 87(925)(2015), 925-979.
- [2] C. Tian, Y. Liu, Delay-driven Hopf bifurcation in a networked Malaria model, *Applied Mathematics Letters*, 132(2022), 108092.
- [3] Z. Hu, W. Ma, S. Ruan, Analysis of SIR epidemic models with nonlinear incidence rate and treatment, *Mathematical Biosciences*, 238(1)(2012), 12-20.
- [4] V. Capasso, G. Serio, A generalization of the Kermack-Mckendrick deterministic epidemic model, *Math. Biosci.* 42(1978),41-61.
- [5] R. Xu, Z. Ma, Global stability of a delayed SEIRS epidemic model with nonlinear incidence rate, *Nonlinear Dyn.*, 61(2010),229-239.

Multiscale Model of Cardiac Muscle Contraction using Langevin Dynamics and Biological Elastic Network Analysis

Yasser Aboelkassem*

*College of Innovation and Technology, University of Michigan-Flint
Michigan Institute for Data Science, University of Michigan, MI, USA

Abstract. In this paper, a multiscale model of cardiac thin filament activation and sarcomere contraction is proposed. The model is derived such that it links atomistic molecular scale data of sarcomere protein-protein interactions to the cellular scale. More specifically, we propose to use (i) an elastic network modeling method to solve for the small scale oscillations of tropomyosin protein dynamics on the surface of actin filament, (ii) Langevin dynamics simulations based on stochastic theory to capture large scale oscillations. These two computational methods provide more accurate modeling of the cardiac contraction biophysics and can be used to predict the effects of point mutations on the cardiac contraction.

Introduction

Cardiac diseases are the leading cause of death worldwide. Many of the inherited cardiac phenotype diseases such as hypertrophic and dilated cardiomyopathies are linked to missense mutations in sarcomeric regulatory (tropomyosin, actin, troponin, myosin) proteins. These mutations and post-translational modifications influence not only the molecular contraction dynamics, but also affect cellular-tissue wall mechanics interactions, which in turn affect heart pumping efficiency. The majority of these mutations has found to be distributed on residues located on the tropomyosin-actin interface and many may modify the interaction energy landscape that regulates the Tm positioning and mobility on the surface of actin filaments. These mutations and post-translational modifications influence not only the Tm dynamics, but affects myofilament Ca^{2+} sensitivity and alter cooperative interactions between actin, Tm, troponin-complex and myosin [1].

Tropomyosin (Tm) is an important protein for regulating cardiac contraction. When Tm gets activated, it oscillates in the azimuthal direction over actin surface. The Tm dynamical motions are believed to play an important role in regulating muscle contraction [2]. Computational models including the Markov Chain Monte Carlo MCMC -based algorithms were proposed in several myofilament mechanistic models [3] in order to understand intrinsic mechanism by which the Tm oscillates between the B-C-M states. Although the MCMC computational models were able to predict with acceptable degrees of accuracy the angular positions events of Tm. Yet, the applicability of MCMC simulations in describing how Tm alternates between angular locations is limited. Most importantly, they cannot be used to time-track the intrinsic Tm dynamic motions between regulatory positions or simulate mutation effects, which is a process that requires molecular and stochastic multiscale high fidelity simulations [4].

Results and discussion

The results using Langevin dynamics stochastic simulations will be used to understand how the Tm molecule fluctuates over the actin filament as a function of the azimuthal angle. The results using protein elastic network model will be used to show the dominant eigen values of these oscillations. Both results will help to better understand the role of Tm dynamics during the cardiac thin filament activation process.

References

- [1] El-Mezgueldi M. (2014) Tropomyosin dynamics. *J. Muscle Res Cell Motil* **35** :203–210. 2014.
- [2] McKillop D. F. and Geeves M. A. (1993) Regulation of the interaction between actin and myosin subfragment 1: Evidence for three states of the thin filament. *Biophys. J.* **65**: 693–701.
- [3] Aboelkassem Y., Bonilla J. A. McCabe K. J. , and Campbell S.(2015) Contributions of Ca^{2+} - independent thin filament activation to cardiac muscle function *Biophys J.* **109**: 2101–2112.
- [4] Aboelkassem Y., McCabe K. J., Huber G., Regnier M., McCammon J. A., and McCulloch A. D. (2019) Stochastic multiscale model of cardiac thin filament activation using Brownian-Langevin dynamics. *Biophys J.* **117**: 2255–2272.

Do strokes affect the brain's critical state? A theoretical perspective.

Jakub Janarek^{1,2}, Zbigniew Drogosz^{1,2}, **Jacek Grela**^{1,2}, Jeremi K. Ochab^{1,2}, Pawel Oswiecimka^{1,2,3},
Maciej A. Nowak^{1,2}, Dante R. Chialvo^{4,5}

¹ *Institute of Theoretical Physics, Jagiellonian University, 30-348 Kraków, Poland*

² *Mark Kac Center for Complex Systems Research, Jagiellonian University, 30-348 Kraków, Poland*

³ *Complex Systems Theory Department, Institute of Nuclear Physics, Polish Academy of Sciences, 31-342 Kraków, Poland*

⁴ *Center for Complex Systems & Brain Sciences (CEMSC³), Escuela de Ciencia y Tecnología, Universidad Nacional de San Martín, Buenos Aires, Argentina*

⁵ *Consejo Nacional de Investigaciones Científicas y Tecnológicas (CONICET), Buenos Aires, Argentina*

Abstract. In recent tests of brain criticality in stroke patients, it was suggested that lesions cause a non-critical state of neural dynamics, and the critical state might subsequently be restored in parallel with a patient's post-stroke behavioral recovery (Rocha et al.). We propose an alternative interpretation in which the brain remains in the critical state at all times; however, as a result of a stroke, it may effectively become divided into two or more weakly connected regions, mimicking the lack of criticality. This interpretation is corroborated by toy simulations of the Ising model and a more realistic Haimovici-Tagliazucchi-Chialvo model based on the Hagmann et al.'s connectome with "artificial strokes" performed by removing connections between two subsystems. In such models, standard indicators of criticality based on cluster size analysis are found to behave similarly to those in models based on real-world MRI scans of stroke patients. Our study suggests that the lack of the peak in the second largest cluster, signaling the loss of criticality, may be an artifact of the division of the original system into weakly connected parts.

Introduction

A canonical example of a complex system is the human brain, whose large numbers of neuronal cells display nontrivial multiscale organization and complex characteristics. The concept of the critical brain suggests that neural networks evolve towards a critical state, where the competition between order and disorder states emerges. Such a system behavior indicates optimization of computational properties related to information processing, such as information transmission and storage or computational power, which is especially appealing in neurosciences [1].

The ideas of critical phenomena have recently been applied to the study of the brain dynamics of stroke patients by Rocha et al. [2]. Their most intriguing result was the fact that the presence and severity of the stroke were related to loss of critical behavior in the brain and possible post-stroke recovery of a patient to the recovery of criticality. Their results were based on the analysis of the sizes of largest clusters of activity. We revisit these findings from a theoretical perspective by studying artificial "strokes" in the toy Ising model and the HTC model.

Results and discussion

In this work, we demonstrate a simple mechanism whereby a critical system consisting of at least two weakly connected parts may appear non-critical to the usual structure-agnostic analysis of the size of the second largest cluster of activity. We replicate this behavior in a set of numerical experiments on real connectomes with a realistic model of brain activity, where artificial "strokes" are introduced by removing some connections between regions of the standard healthy connectome. Furthermore, a finer cluster analysis applied to substructures induced by such strokes reveals the criticality hidden from the structure-agnostic analysis. The results of these experiments bear a close resemblance to the results of simulations based on real-world data from stroke patients. We therefore conclude that by itself the second largest cluster size is not a reliable indicator of criticality when applied to a system with unknown subsystem structure. We further argue that stroke-induced loss of criticality may be only illusory and that the described mechanism is a possible explanation for the previous findings. In light of our work, complementary indicators, such as the autocorrelation coefficient, the eigenvalues of the correlation matrix, or the modularity analysis of the connectome, are needed to make criticality analysis more robust.

References

- [1] Zimmern, V. Why brain criticality is clinically relevant: A scoping review. *Front. Neural Circuits* 14, DOI: 10.3389/fn-cir.2020.00054 (2020).
- [2] Rocha, R. P. et al. Recovery of neural dynamics criticality in personalized whole-brain models of stroke. *Nat. Commun.* 13, 3683, DOI: 10.1038/s41467-022-30892-6 (2022).

A novel alternative formalism of the Wiener path integral technique - circumventing the Markovian assumption for the system response process

Ilias G. Mavromatis*, Apostolos F. Psaros** and Ioannis A. Kougiumtzoglou*

*Department of Civil Engineering and Engineering Mechanics, Columbia University, New York, NY, USA

**Division of Applied Mathematics, Brown University, Providence, RI, USA

Abstract. The formulation of the Wiener path integral (WPI) technique for determining the stochastic response of diverse dynamical systems has been developed to-date in conjunction with the Markovian assumption for the system response process. Herein, a novel WPI formalism is developed to account, in a direct manner, also for systems with non-Markovian response processes. In this regard, nonlinear systems with a history-dependent state, such as hysteretic structures or oscillators endowed with fractional derivative elements, can be treated in a straightforward manner. That is, without resorting to any ad hoc modifications of the WPI technique pertaining, typically, to employing additional auxiliary filter equations and state variables.

Introduction

Various methodologies have been developed over the last six decades in the field of stochastic engineering dynamics for determining response statistics of diverse structural and mechanical systems [1]. Indicatively, relying on the Markovian assumption for the system response process, a wide range of techniques have been developed for solving the Fokker-Planck partial differential equation governing the system response joint transition probability density function (PDF); see [2] for a broad perspective. Nevertheless, for a wide range of systems the convenient Markovian response assumption cannot be reasonably justified. Indicative examples include systems exhibiting hysteresis or subjected to non-white stochastic excitations. This challenge is bypassed, typically, by considering additional auxiliary filter equations and state variables. However, this kind of solution treatment relates usually to increased computational cost due to the increased dimensionality of the problem.

Results and discussion

Kougiumtzoglou and co-workers have developed recently a technique based on the concept of Wiener path integral (WPI) for stochastic response determination of diverse dynamical systems (e.g., [3-5]). Remarkably, the technique exhibits both high accuracy [4] and low computational cost [5]. However, the formulation of the WPI technique has been developed to-date in conjunction with the Markovian assumption for the system response process. In this paper, an alternative novel formalism is developed that circumvents the Markovian response assumption. Specifically, considering the probability of a path corresponding to the Wiener (excitation) process, and employing a functional change of variables in conjunction with the governing stochastic differential equation, yields the probability of a path corresponding to the response process. This leads to representing the system response joint transition PDF as a functional integral over the space of possible paths connecting the initial and final states of the response vector. Overall, the veracity and mathematical legitimacy of the WPI technique to treat also non-Markovian system response processes are demonstrated. Illustrative numerical examples relate to nonlinear oscillators exhibiting hysteresis and endowed with fractional derivative elements. Comparisons with pertinent Monte Carlo simulation (MCS) data demonstrate the accuracy of the developed formalism (Fig.1).

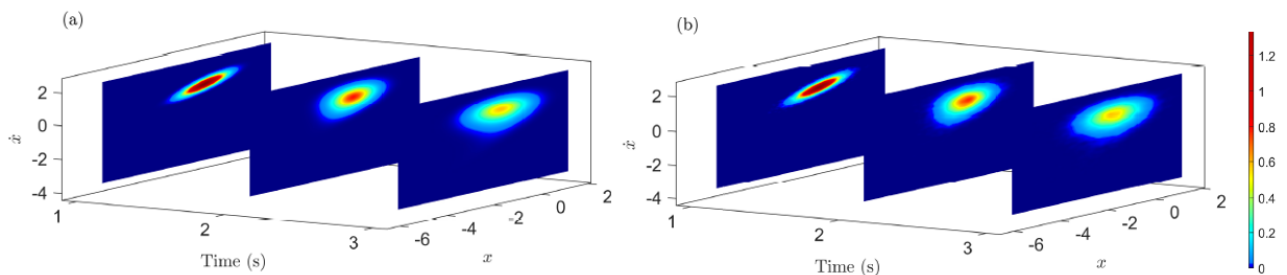


Figure 1: Non-stationary response joint PDF at indicative time instants corresponding to a stochastically excited oscillator with asymmetric nonlinearities and fractional derivative elements:(a) results obtained by the WPI technique; (b) comparison with MCS data.

References

- [1] Li J., Chen J. (2009) Stochastic Dynamics of Structures. John Wiley & Sons, Ltd, Chichester, UK.
- [2] Risken H. (1984) The Fokker-Planck Equation: Methods of Solution and Applications, Springer-Verlag, Berlin, Heidelberg.
- [3] Kougiumtzoglou I. A., Spanos P. D. (2012) An analytical Wiener path integral technique for non-stationary response determination of nonlinear oscillators. *Probabilistic Engineering Mechanics* **28**: 125–131.
- [4] Psaros A. F., Kougiumtzoglou I. A. (2020) Functional series expansions and quadratic approximations for enhancing the accuracy of the Wiener path integral technique. *Journal of Engineering Mechanics*, **146**(7): 04020065
- [5] Petromichelakis I., Kougiumtzoglou I. A. (2020) Addressing the curse of dimensionality in stochastic dynamics: A Wiener path integral variational formulation with free boundaries. *Proc. of the Royal Society A: Mathematical, Physical and Engineering Sciences* **476**:2243.

Diagrammatic perturbation theory for Stochastic nonlinear oscillators

Akshay Pal*, Jayanta kumar Bhattacharjee *

*School of Physical Sciences, Indian Association for the Cultivation of Science, Jadavpur, Kolkata, India

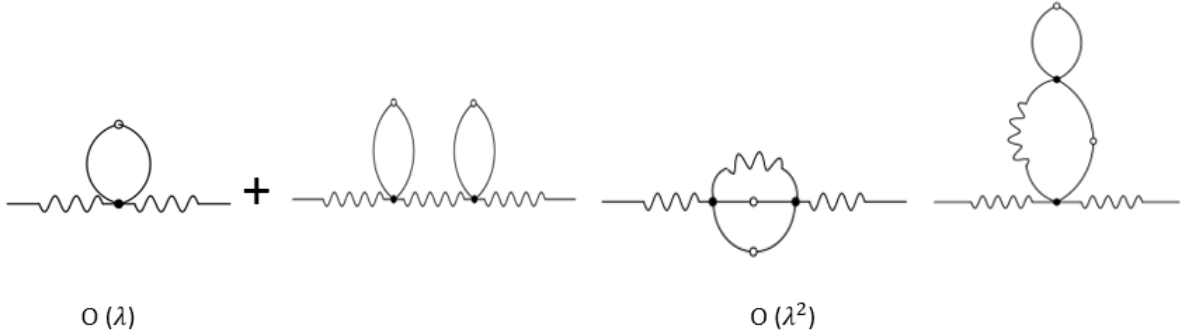
Abstract. In this work we consider stochastic driven damped nonlinear oscillator, characterized by a natural frequency ω_0 and a damping coefficient 2Γ of the linear system. We explore what the time averaged linear response of the nonlinear system will be in the frequency domain. We show that a perturbation theory involving the nonlinear terms is identical to the Feynman diagrams based perturbation theory used in any statistical or quantum field theory. We find that at second order the frequency and the damping coefficient becomes dependent on the frequency ω at which the system is being probed. This is a small but unexpected effect.

Introduction

The noise driven nonlinear oscillator is described by the dynamics:

$$\ddot{x} + 2\Gamma\dot{x} + \omega_0^2 x + \lambda x^3 = f(t) \quad (1)$$

where $f(t)$ is a random Gaussian white noise with the two point correlator given by $\langle f(t_1)f(t_2) \rangle = 2D\delta(t_1 - t_2)$ where D is a constant. For the sinusoidally driven case, we have an additional $A\cos(\Omega t)$ term on the right hand side. The frequency dependent linear response of the system is given by $R(\omega) = \langle \frac{\delta x(\omega)}{\delta f(\omega)} \rangle$ where the angular bracket is a long time average. For $\lambda = 0$, $R(\omega) = R_0(\omega) = (\omega_0^2 - \omega^2 + 2i\Gamma\omega)^{-1}$. At the first order in perturbation theory the addition to ω_0^2 is $\Delta\omega_0^2 = \frac{3\lambda D}{2\omega_0^2}$ which is in agreement with Samanta et al [1,2] and the change $\Delta\Gamma$ in the damping is zero. Our perturbation framework is based on the diagrammatic approach initiated for stochastic dynamics by Kraichnan [3] and Wyld [4]. Our approach is complementary to the recent work of Belousov et al [5]. It allows for a straightforward calculation of the $O(\lambda^2)$ term and we find that the correction to ω_0^2 is frequency dependent and more importantly there is a non-zero $\Delta\Gamma$ which is also frequency dependent. Both corrections vanish at very high frequencies which is physical.



Feynman diagrams of $O(\lambda)$ and $O(\lambda^2)$

Results and discussion

We extend this framework to address the stochastic pendulum with a period forcing $A\cos(\Omega t)$ (an additional contribution to the R.H.S of Eq.(1). The shift in the response function contains joint contribution of the stochastic and deterministic drives i.e AD . Further, if we replace the λx^3 term by μx^2 in Eq.(1), then we have a metastable cubic potential well and our perturbation approach allows us to find the criterion for which the particle can escape from the well. The result we get is analogous to fluctuation dissipation theorem in statistical mechanics. We can also handle the stochastically driven Kapitza pendulum. We find that the stability of the inverted fixed point is possible if we have colored noise, rather than white noise [6].

References

- [1] H.S. Samanta, J.K.Bhattacharjee, A. Bhattacharyay and S. Chakraborty, *Chaos* 24 043122 (2014)
- [2] Prasun Sarkar, Debarshi Banerjee, Shibashis Paul, and Deb Shankar Ray (2022) *Phys. Rev. E* 106, 024203
- [3] R.H. Kraichnan, *J Math. Phys.* 2 124 (1961)
- [4] H W Wyld, *Ann. Phys.* 14 143 (1961)
- [5] R. Belousov, F. Berger and A J Hudspeth, *Phys Rev E* 99 042204 (2019)
- [6] Y.B. Simons and B. Meyerson *Phys Rev E* 80 042120 (2009)

Fuzzy Generalized Cell Mapping with Adaptive Interpolation (FGCM with AI) for Bifurcation Analysis of Nonlinear Systems with Fuzzy Uncertainties

Ling Hong^{*}, Jun Jiang^{*} and Xiao-Ming Liu^{**}

^{*}State Key Laboratory for Strength and Vibration of Mechanical Structures,
Xi'an Jiaotong University, Xi'an, 710049, P. R. China

^{**}State Key Laboratory of Compressor Technology,
Hefei General Machinery Research Institute, Hefei 230031, P. R. China

Abstract. Fuzzy Generalized Cell Mapping (FGCM) method is developed with the help of the Adaptive Interpolation (AI) in the space of fuzzy parameters. The adaptive interpolation on the set-valued fuzzy parameter is introduced in computing the one-step transition membership matrix to enhance the efficiency of the FGCM. For each of initial points in the state space, a coarse database is constructed at first, and then interpolation nodes are inserted into the database iteratively each time errors are examined with the explicit formula of interpolation error until the maximal errors are just under the error bound. With such an adaptively expanded database on hand, interpolating calculations assure the required accuracy with maximum efficiency gains. The new method is termed as Fuzzy Generalized Cell Mapping with Adaptive Interpolation (FGCM-AI), bifurcation analysis shows that the FGCM with AI has a thirtyfold to fiftyfold efficiency over the traditional FGCM to achieve the same analyzing accuracy.

Introduction

Fuzzy Generalized Cell Mapping with Adaptive interpolation (FGCM with AI) is introduced first. The fuzzy master equation is given as follows for the possibility transition of continuous fuzzy process,

$$p(\mathbf{x}, t) = \sup_{\mathbf{x}_0 \in \mathbf{D}} [\min \{p(\mathbf{x}, t | \mathbf{x}_0, t_0), p(\mathbf{x}_0, t_0)\}], \quad \mathbf{x} \in \mathbf{D} \quad (1)$$

where \mathbf{x} is a fuzzy process, $p(\mathbf{x}, t)$ is the membership distribution function of \mathbf{x} at t , and $p(\mathbf{x}, t, \mathbf{x}_0, t_0)$ is the transition possibility function. Equation (1) of the FGCM can be viewed as a discrete representation of fuzzy master equations. A partial differential equation for the fuzzy master equation of continuous time processes, which is analogous to the Fokker-Planck-Kolmogorov equation for the probability density function of stochastic processes. The solution to the equations is in general very difficult to obtain analytically. The FGCM offers a very effective method for solutions to fuzzy master equations, particularly, for fuzzy nonlinear dynamical systems. For the deterministic system $\dot{\mathbf{x}} = \mathbf{f}(\mathbf{x}, t)$, the Interpolated Cell Mapping method is proposed to improve the efficiency of direct numerical simulation. It estimates the solution $\mathbf{x}(T, \mathbf{x}_0)$ by interpolating in the state space. For fuzzy system, since the solution of the equation is continuous with respect to the fuzzy parameter $s \in \text{supp}(S)$, interpolation in the fuzzy parameter space is considered to estimate the solution $\mathbf{x}(T, \mathbf{x}_0, s)$, which is expected to increase the efficiency of the FGCM[1].

Results and discussion

A 3-D jerk system with fuzzy uncertainty is considered here with the help of the FGCM with AI

$$\ddot{x} \in -\dot{x} - \sigma \gamma \dot{x} + \sigma x - \sigma[S]^\alpha x^2 - \sigma x^3$$

where S is a triangular fuzzy number. In the following analyses using the FGCM with AI, the domain $D = [-1.5, 1.5] \times [-3, 3] \times [-0.8, 0.8]$ is discretized into $51 \times 101 \times 27$ cells and $5 \times 5 \times 5$ points are sampled from each cell. $\text{Supp}(S)$ is discretized into 257 equal segments. The duration of one mapping step is $T = 2\pi[2]$.

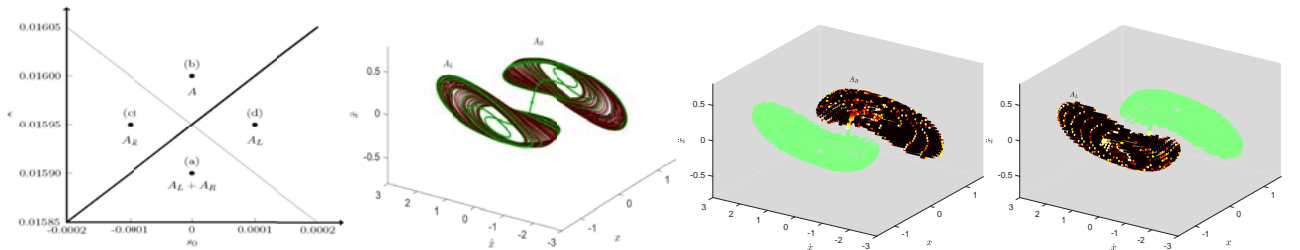


Figure 1: Codimension two bifurcation in the two parameter space of a 3-D Jerk system with fuzzy uncertainty[2]

A codimension two bifurcation of fuzzy chaotic attractors is found at a vertex in a two-parameter plane where catastrophic and explosive bifurcation curves intersect. The dynamics of the fuzzy chaotic systems is extremely rich at the vertex of the codimension two bifurcation. Such a codimension-two bifurcation is fuzzy noise-induced effects which cannot be seen in the deterministic systems.

References

- [1] Liu X. M., Jiang J., Hong L. et al. (2018) Studying the global bifurcation involving Wada boundary metamorphosis by a method of Generalized Cell Mapping with sampling-adaptive interpolation. *Int. J. of Bifurcation and Chaos* **28**(2):1830003.
- [2] Liu X.M., Jiang J., Hong L. et al. (2019) Fuzzy noise induced codimension two bifurcations captured by Fuzzy Generalized Cell Mapping with Adaptive Interpolation. *Int. J. of Bifurcation and Chaos* **29**(11): 1950151.

Response statistics of a conceptual airfoil with consideration of extreme load conditions

Qi Liu*, Yong Xu*,**

*School of Mathematics and Statistics, Northwestern Polytechnical University, Xian, 710072, China

**MIIT Key Laboratory of Dynamics and Control of Complex Systems, Northwestern Polytechnical University, Xian, 710072, China

Abstract. An aircraft sometime serves under extreme flight conditions, which will have a substantial impact on its flight safety. We explore dynamical behaviors of a conceptual airfoil with an extreme random load portrayed by a non-Gaussian Lévy noise. We first theoretically deduce amplitude-frequency equations associated with the deterministic airfoil system. We observe an excellent agreement between the analytical results and the numerical ones, as well as a bistable behavior. Then, the impacts of the extreme random load are numerically examined in depth. Within the bistable regime, the extreme random load can induce stochastic transition and resonance. Interestingly, the Lévy noise is more likely than the Gaussian scenario to cause a highly unexpected stochastic transition. All of the findings would be helpful in ensuring the flight safety and enhancing the structural strength and reliability of aircraft wings operating at extreme flight conditions.

Introduction

The interaction between nonlinearities and stochasticities usually cause sophisticated behaviors than the deterministic systems. Stochastic behaviors of conceptual airfoils with random loads have been extensively investigated [1–5]. In the previous works, we have explored complex dynamics of conceptual airfoil models with Gaussian [1, 2] and narrow-band [3, 4] random excitations via stochastic averaging and multiple-scales methods. But, the previous studies only considered small random fluctuations and effects of extreme load conditions have not been addressed. The idealized Gaussian noise can describe only small fluctuations around the mean value but not large jumps. The non-Gaussian Lévy noise, however, can better model the random loads with both continuous and jumping features [6]. As a result, the purpose of this work is to lead to a better understanding on dynamical behaviors of a conceptual airfoil with extreme random loads modelled as a Lévy noise.

Results and Discussion

The coupled governing equations of the airfoil model with an extreme random load are established as

$$\ddot{h} + \varepsilon^2 x_\theta \ddot{\theta} + \varepsilon^2 \zeta_h \dot{h} + \Omega_h^2 (h + \varepsilon^2 \beta_h h^3) = -\varepsilon^2 2Q\theta/\mu, \quad (1a)$$

$$\varepsilon^2 \frac{x_\theta}{r_\theta^2} \ddot{h} + \ddot{\theta} + \varepsilon^2 \zeta_\theta \dot{\theta} + \Omega_\theta^2 (\theta + \varepsilon^2 \beta_\theta \theta^3) = \varepsilon^2 F \sin(\omega t) + \varepsilon \zeta(t), \quad (1b)$$

here θ and h represent the pitch angle and plunge deflection, $0 < \varepsilon \ll 1$ is a small parameter, $Q = [U/(b\omega_\theta)]^2$ is the generalized flow velocity, F and ω are the amplitude and frequency of external force, and $\zeta(t)$ is the extreme random load as a Lévy noise with the stability index α , skewness parameter β , noise intensity D and mean ν . The other symbols can see Ref. [2]. Response statistics of the airfoil systems (1a) and (1b) are shown in Fig. 1. The system parameters are $\mu = 20.0$, $a = -0.1$, $b = 1.0$, $x_\theta = 0.25$, $r_\theta = \sqrt{0.5}$, $\bar{\omega} = \sqrt{0.2}$, $\zeta_h = 0.1$, $\zeta_\theta = 0.2$, $\beta_h = 0$, $\beta_\theta = 0.1$, $\varepsilon = \sqrt{0.1}$. Bistable behaviors are observed in the airfoil system. The probability $P(\mathcal{A}_{\text{high}})$ gradually decreases as ω increases. Particularly, when $\omega = 1.04$, $P(\mathcal{A}_{\text{high}}) = 0.0191 \ll 1$, thus the undesirable high-amplitude attractor $\mathcal{A}_{\text{high}}$ can be regarded relatively as a rare attractor. The extreme random load can cause a stochastic transition as well as a stochastic resonance. Moreover, a large D or a small α would increase the possibility of stochastic transitions, while the β has basically no effect on them. The Lévy noise is more likely to induce the undesired transitions in comparison with the Gaussian one.

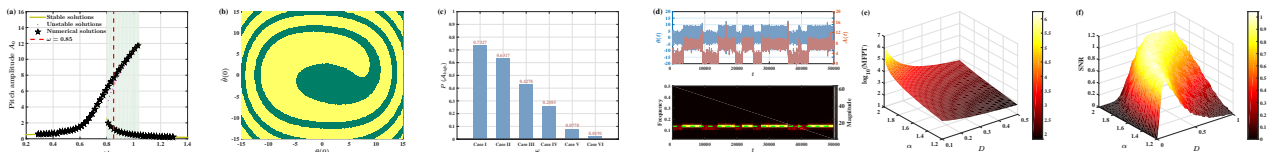


Figure 1: Response statistics of the conceptual airfoil systems (1a) and (1b) with $Q = 6.0$, $F = 2.5$. (a) amplitude-frequency curve; (b) basin of attraction ($\omega = 0.85$), in which the green and yellow regions respectively corresponds to the low-amplitude attractor \mathcal{A}_{low} and the high-amplitude one $\mathcal{A}_{\text{high}}$; (c) probability $P(\mathcal{A}_{\text{high}})$ for $\omega = 0.83$ (Case I), $\omega = 0.85$ (Case II), $\omega = 0.90$ (Case III), $\omega = 0.95$ (Case IV), $\omega = 1.02$ (Case V) and $\omega = 1.04$ (Case VI); (d) time history and time-frequency feature ($\omega = 0.85$, $\alpha = 1.9$, $\beta = 0$, $D = 0.2$); (e) mean first passage time ($\omega = 0.85$, $\beta = 0$); (f) signal-to-noise ratio ($\omega = 0.85$, $\beta = 0$).

References

- [1] Xu Y., Liu Q., Guo G. B., Xu C., Liu D. (2017) Nonlinear Dyn **89**: 1579-1590.
- [2] Liu Q., Xu Y., Xu C. (2018) Appl Math Modell **64**: 249-264.
- [3] Ma J. Z., Liu Q., Xu Y., Kurths J. (2022) Chaos **32**: 033119.
- [4] Liu Q., Xu Y., Kurths J. (2020) Commun Nonlinear Sci Numer Simulat **84**: 105184.
- [5] Liu Q., Xu Y., Kurths J., Liu X. C. (2022) Chaos **32**: 062101.
- [6] Zhang X. Y., Xu Y., Liu Q., Kurths J., Grebogi C. (2021) Chaos **31**: 113115.

Modeling stick balancing with stochastic delay differential equations

Gergő Fodor*, Zoltán Kovács* and Dániel Bachrathy *

*Department of Applied Mechanics, Budapest University of Technology and Economics

Abstract. In this study, we present an extended model for stick balancing. The control parameters in the PD controller are stochastic variables, and we investigate the properties of the corresponding stochastic delay differential equation (SDDE). The noise changes the stability boundaries and reveals important dynamics otherwise hidden in deterministic models. We can mitigate the differences between the popular deterministic models and measurements with this approach.

Introduction

Researchers investigate the neural control of humans through various balancing tasks, for example, postural balance or stick balancing. A popular model of stick balancing is the inverted pendulum and cart system, shown in Fig. 1a), which is unstable. However, we can stabilize it with an appropriately chosen control force. PD control is a common choice [1] because we assume that humans try to measure the angle and the angular velocity. The results of the PD controllers are promising, but we run into significant differences when comparing them to measurement outcomes. Specifically, we are interested in the critical length of the stick, which is the length we can still stabilize with a given reflex delay. There is an analytical formula for the critical length as a function of the delay based on the deterministic model, namely $l_{cr,det} = 3g\tau^2/4$. However, we observe a shift between the measured and analytical curves in Fig. 1b). In reality, the balancing process is more unstable than the deterministic model. There are some extensions to improve the model, for example, sensory deadzones [2] or other controllers [3]. However, we find that handling the parameters of the PD controller as stochastic variables favorably impacts the dynamical behavior. We investigate the second moment, which tells us about the typical deviations of the trajectories from the deterministic solution. Second moment instability means large variances: it translates to uncontrollable angles and angular velocities in our stick-balancing case.

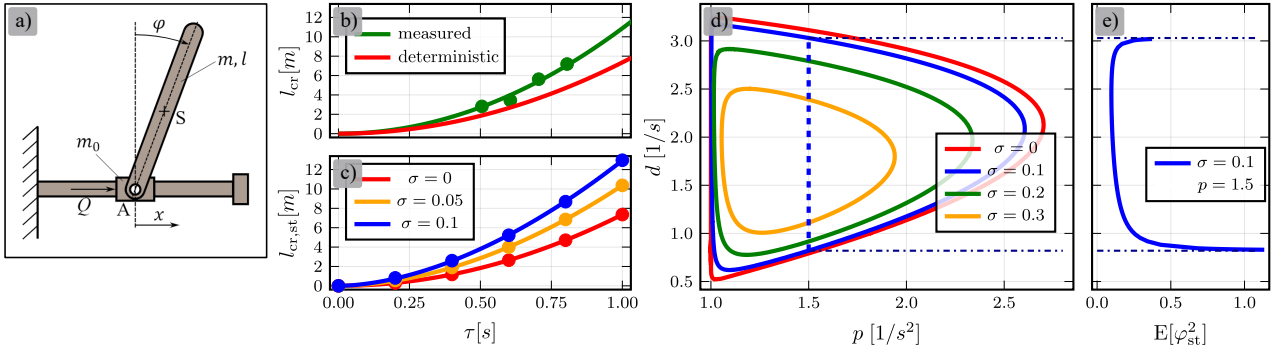


Figure 1: a) Mechanical model. b) Measured critical length l_{cr} as a function of the reaction delay τ . c) Critical length as a function of the delay utilizing the stochastic model with different noise intensities σ . d) Second moment stability boundaries of the stochastic model. e) Stationary second moment dynamics $E[\varphi_{st}^2]$ along $p = 1.5$.

Results and discussion

In Fig. 1d), we present the stability boundaries of the stochastic model in the control parameters' plane. We see the effect of the noise intensity at a given stick length and delay: Larger noise results in smaller stable regions. We determine the critical length at a given delay for different noise intensities by selecting the value where the stable region disappears. Fig. 1c) shows the stochastic critical length curves as a function of the delay. The curves are still second-order polynomials, but their multiplier is a function of the noise intensity, namely $l_{cr,st} = \gamma(\sigma)l_{cr,det}$. Based on this, the estimation of the noise level is around 5% in our measurements. However, in simulations, the highest noise intensity providing stable solutions was 4%. Fig. 1e) shows the stationary second moment dynamics, and we observe high variances even in the stable region. If these variances reach the limit angle of 90° , the probability of losing balance increases significantly. Therefore, we modify our *stable balancing* condition from the disappearance of the stable region to a limit of the stationary second moment. We hope this approach brings the measurements and simulations even more in agreement.

References

- [1] Tamas Insperger, John Milton. (2014). Sensory uncertainty and stick balancing at the fingertip. Biological cybernetics. 108. 10.1007/s00422-013-0582-2.
- [2] Tamas Insperger, John Milton (2017) Stick Balancing with Feedback Delay, Sensory Dead Zone, Acceleration and Jerk Limitation. *Procedia IUTAM* 22:59-66.
- [3] Zhang L, Stepan G, Insperger T. 2018 Saturation limits the contribution of acceleration feedback to balancing against reaction delay. *J. R. Soc. Interface* 15: 20170771.

Effect of an Uncertain Symmetry-Breaking Parameter on the Global Dynamics of the Duffing Oscillator

Kaio C. B. Benedetti*, Paulo B. Gonçalves*, Stefano Lenci** and Giuseppe Rega***

*Department of Civil and Environmental Engineering, Pontifical Catholic University of Rio de Janeiro, Rio de Janeiro, Brazil

**Department of Civil and Building Engineering and Architecture, Polytechnic University of Marche, Ancona, Italy

***Department of Structural and Geotechnical Engineering, Sapienza University of Rome, Rome, Italy

Abstract. An adaptative phase-space discretization, based on an operator approach, is here employed to investigate the influence of a symmetry-breaking parameter on the global dynamics of the symmetric Duffing oscillator, in particular the basins' boundaries, attractors' distributions, and manifolds. The results highlight the importance of uncertainty analysis on the global structures of dynamical systems with competing attractors.

Introduction

The symmetric Duffing oscillator is well studied in literature and may describe a plethora of events in sciences and engineering [1], including systems with one or two potential wells. However, in many applications ranging from quantum physics to engineering, a symmetry-breaking effect described by a quadratic nonlinear term is an important feature, and the magnitude of the quadratic term is often unknown. A well-known example is the nonlinear response of imperfect structures liable to stable or unstable symmetric buckling, such as plates and shells, where the magnitude of the geometric imperfections leading to asymmetry in the potential energy profile is unknown. Similar behavior is observed in the asymmetric Helmholtz-Duffing oscillator [2]. Here the influence of the uncertainty of the quadratic term coefficient, α , on the global dynamics of the following Duffing oscillator is investigated

$$\ddot{x} + 0.1\dot{x} - x - \alpha x^2 + x^3 = \lambda \sin(\omega t).$$

For $\alpha = 0$, the system exhibits a symmetric double-well potential function, whereas for $\alpha \neq 0$, the symmetry is broken.

Results and discussion

An adaptative phase-space discretization [3] is employed in the global analysis of the oscillator. It allows to refine complex basins' boundaries and then observe how the uncertainty in α affects the global dynamics. Depending on the forcing parameters ($\lambda; \omega$), the system can present different numbers of competing solutions. For $\lambda = 0.35$, $\omega = 0.8$ three coexisting solutions are observed for the deterministic system: two in-well and one cross-well solutions. Assuming that α is uniformly distributed ($\alpha \sim U(0; 0.3)$), stochastic global structures, that is, attractors, basins, and manifolds distributions are obtained. The obtained basins are shown in Fig. 1. The left and right in-well attractors are deeply influenced by the symmetry-breaking, indicating a high sensitivity. Particularly the left in-well attractor, with its already small basin, loses stability.

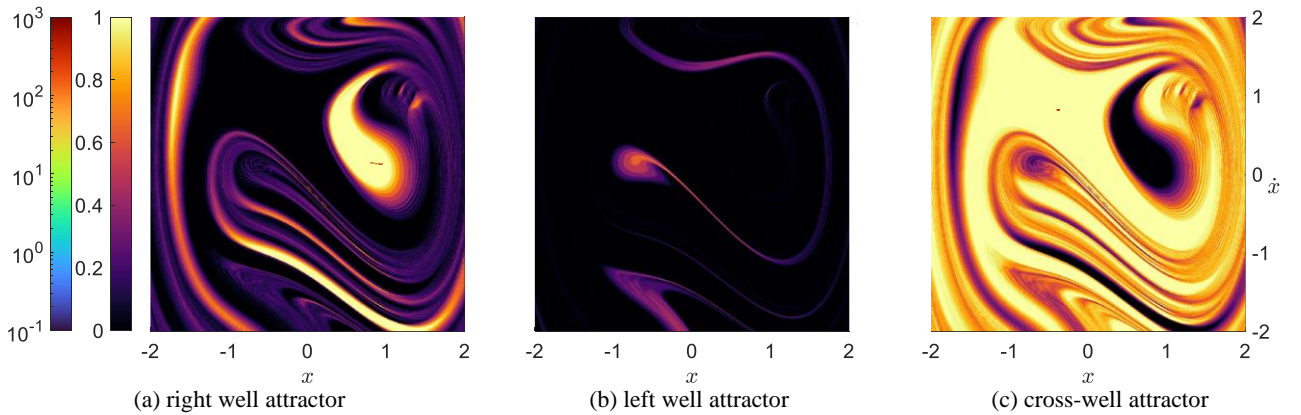


Figure 1: Attractors (left color bar) and basins (right color bar) probability distributions for $\lambda = 0.35$, $\omega = 0.8$, and $\alpha \sim U(0; 0.3)$.

References

- [1] Kovacic, I., & Brennan, M. J. (2011). The Duffing equation: nonlinear oscillators and their behaviour. John Wiley & Sons.
- [2] Lenci, S., & Rega, G. (2004). Global optimal control and system-dependent solutions in the hardening Helmholtz–Duffing oscillator. *Chaos, Solitons & Fractals*, 21(5), 1031-1046.
- [3] Benedetti K C B 2022 Global Analysis of Stochastic Nonlinear Dynamical Systems: an Adaptative Phase-Space Discretization Strategy (Pontifical Catholic University of Rio de Janeiro, PUC-Rio) Rio de Janeiro, Brazil

Control policies for dengue: insights from a mathematical model

Carla M.A. Pinto*, Dumitru Baleanu** and Amin Jajarmi***

*School of Engineering, Polytechnic of Porto, and CMUP, Porto, Portugal, ORCID <https://orcid.org/0000-0002-0729-1133>

** Faculty of Arts and Sciences, Cankaya University, 06530 Ankara, Turkey

Institute of Space Sciences, Magurele-Bucharest, Romania, ORCID <https://orcid.org/0000-0002-0286-7244>

*** Department of Electrical Engineering, University of Bojnord, Iran, ORCID <https://orcid.org/0000-0003-2768-840X>

Abstract. We propose a mathematical model to study the dynamics of dengue fever in a susceptible population. Our main goal is to assess the effect of four different control strategies: existence of sterile male mosquitoes, use of pesticides for larvae, and for adult mosquitoes, and vaccination, in the disease propagation. We discuss the results of numerical simulations from an epidemiological point of view. Inferences on health policy measures are drawn.

Introduction

Dengue is a mosquito-borne viral infection, caused by the dengue virus (DENV) of the *Flaviviridae* family. Dengue incidence has seen a pronounced increase in recent decades. Dengue prevention and control depends on effective vector control measures. These encompass combat mosquito vectors, with the prevention of mosquito breeding, community engagement, reactive vector control, and active mosquito and virus surveillance. Vaccination is also an important prevention strategy.

The proposed model

$$\begin{aligned}
 A'_m &= \phi_1 \left(1 - \frac{A_m}{C}\right) (F_2 + F_4) - (\sigma_A + \mu_A) A_m, \\
 F'_1 &= p\sigma_A A_m - \frac{\beta}{M_1+M_2} F_1 M_1 - \frac{\beta}{M_1+M_2} F_1 M_2 - \mu_m F_1, \\
 F'_2 &= \frac{\beta}{M_1+M_2} F_1 M_1 - \frac{b\beta_m}{H+m} H_i F_2 - \mu_m F_2, \\
 F'_3 &= \frac{\beta}{M_1+M_2} F_1 M_2 - \mu_m F_3, \\
 F'_4 &= \frac{b\beta_m}{H+m} H_i F_2 - \mu_m F_4, \\
 M'_1 &= (1-p)\sigma_A A_m - \mu_m M_1, \\
 M'_2 &= \phi_2 - \mu_m M_2, \\
 H'_s &= \mu_h (H - H_s) - \frac{b\beta_h}{H+m} H_s F_4 + \eta H_r, \\
 H'_e &= \frac{b\beta_h}{H+m} H_s F_4 - (\theta_h + \mu_h) H_e, \\
 H'_i &= \theta_h H_e - (\alpha_h + \mu_h) H_i, \\
 H'_r &= \alpha_h H_i - (\eta + \mu_h) H_r,
 \end{aligned} \tag{1}$$

where A_m -mosquito's aquatic phase, F_1 -uninfected and unmated female mosquito, F_2 - uninfected fertilized female mosquito, F_3 -uninfected mated fertilized female, F_4 -infected mating fertilized female, M_1 -normal male mosquito, M_2 -sterile male mosquito, H_s -susceptible human, H_e -exposed human, H_i -infectious human, H_r -recovered human. Vaccination, $v(t)$, is added as follows. The term $-v(t)H_s(t) + kv(t)H_r(t)$ is added to $H_s(t)$ and subtract from $H_r(t)$. Parameter k represents the waning immunity process.

Results and discussion

In Figure 1, we depict the effect of the four control strategies in the dynamics of dengue spread for the normal male mosquitoes (M_1) and for the infected humans populations (H_i). The results are promising, since they show decrease in the number of normal male mosquitoes and infected humans. Dengue is still a major concern worldwide, with a 70% actual burden in Asia. Epidemiologists can provide substantial advise to policy makers by interpreting the predictions provided by mathematical models.

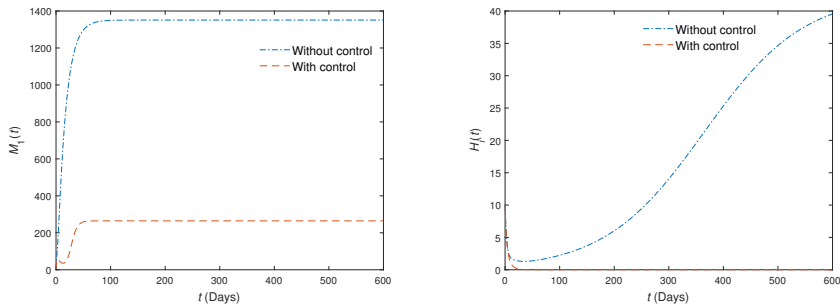


Figure 1: The effect of the four control strategies on the dengue model (1).

References

- [1] Zitzmann, C., Schmid, B., Ruggieri, A., Perelson, A. S., Binder, M., Bartenschlager, R., & Kaderali, L. (2020) A Coupled Mathematical Model of the Intracellular Replication of Dengue Virus and the Host Cell Immune Response to Infection. *Frontiers in microbiology* **11** 725.

A data-driven uncertainty quantification framework for mechanistic epidemic models

Americo Cunha Jr*, David A. W. Barton**, and Thiago G. Ritto***

* Rio de Janeiro State University, Brazil

** University of Bristol, UK

*** Federal University of Rio de Janeiro, Brazil

Abstract. Mechanistic epidemic models are frequently used to predict the evolution of infectious disease outbreaks. However, the uncertain nature of the model parameters (epidemiological parameters, initial conditions, etc.) and the limited horizon of predictability of this dynamic phenomenon make it essential to quantify the underlying uncertainties. In this sense, this work presents a cross-entropy approximate Bayesian computation framework for uncertainty quantification that is particularly interesting for use in epidemic models. The new methodology is tested with actual data from a COVID-19 outbreak, presenting a great capacity to capture the variability and dynamic evolution of the disease records.

Introduction

This work presents a data-driven framework for UQ of mechanistic epidemic models [1, 2] based on the combination of two probabilistic ingredients: (i) cross-entropy method for optimization, used to obtain a baseline calibration of the model parameters; and (ii) approximate Bayesian computation, employed to update the calibration of the parameters and propagate the uncertainties of the parameters through the dynamic model. This framework inherits the good features of the two techniques, gaining meaningful information from the epidemic data. It is tested with the aid of actual data related to the COVID-19 outbreak in Rio de Janeiro (Brazil), using an SEIR(+AHD) compartmental model (Fig. 1 left) as a predictive tool [1, 2].

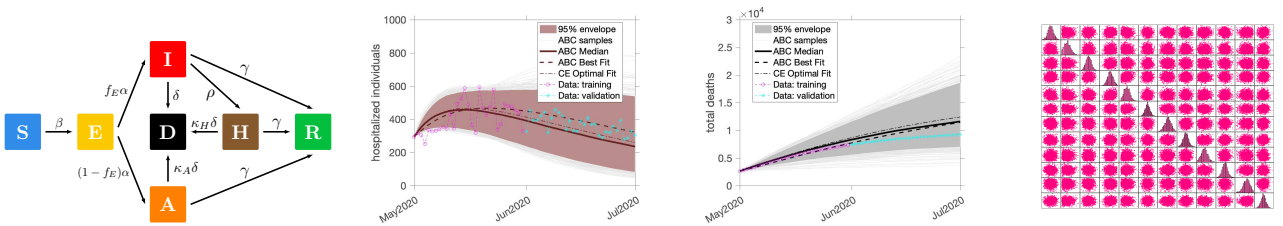


Figure 1: SEIR(+AHD) epidemic model considering susceptible, exposed, infectious, asymptomatic, hospitalized, recovered, and deceased compartments (left); evolution of the number of hospitalized individuals (center left) and total deaths (center right), with the respective 95% credible intervals and actual outbreak data; and the statistical characterization of dynamic model parameters. Further details about these results can be seen in the reference [2].

Results and discussion

The dynamic model is calibrated with epidemiological surveillance data (number of hospitalizations and deaths caused by COVID-19) for one month (1st to 31st of May 2020). Then it is used to extrapolate the behavior of these quantities of interest in a horizon of 30 days ahead, as can be seen in Fig.1 (center), which shows the evolution of these quantities of interest and the corresponding 95% credible intervals. In this effectiveness test of the data-driven UQ methodology, we can note that the quantitative forecasts are excellent in a horizon of up to two weeks, and a good qualitative agreement between data and model response prevails in the 30 days forecast horizon. Fig.1 (right) presents the statistical characterization (marginal histograms and scatter plots) of the parameters of the epidemic model. The unimodal shape of all marginal histograms indicates the effective information gain resulting from the model calibration. These results show the robustness and effectiveness of the proposed framework, which is another tool to assist in modeling epidemic outbreaks when using mechanistic mathematical models (compartmental models).

References

- [1] Ritto, T. G., Cunha, Jr A., Barton, D. A. W., (2021) Parameter calibration and uncertainty quantification in an SEIR-type COVID-19 model using approximate Bayesian computation. In: *42nd Ibero-Latin-American Congress on Computational Methods in Engineering (CILAMCE, 2021)*, Rio de Janeiro.
- [2] Cunha, Jr A., Barton, D. A. W. , Ritto, T. G., (2022) Uncertainty quantification in mechanistic epidemic models via cross-entropy approximate Bayesian computation, *arXiv preprint arXiv:2207.12111* <https://arxiv.org/abs/2207.12111>

Non-stationary dynamics in a complex marine biogeochemical model

Guido Occhipinti^{*,**}, Cosimo Solidoro^{**}, Roberto Grimaudo^{***}, Davide Valenti^{***}, and Paolo Lazzari^{**}

^{*}*Dipartimento di Matematica e Geoscienze, Università degli Studi di Trieste, Via Valerio 12, Trieste, I-34127, Italy #*

^{**}*National Institute of Oceanography and Applied Geophysics - OGS, via Beirut 2, Trieste, I-34014, Italy #*

^{***}*Dipartimento di Fisica e Chimica Emilio Segrè, Università degli Studi di Palermo, Viale delle Scienze, Ed. 18, Palermo, I-90128, Italy #*

Abstract. Although non-stationary dynamics have been observed in nature, it is still unclear if these behaviors are inherent of ecological systems or whether they are the result of external forcings. In order to comprehend how rarely non-stationary dynamics occur in ecosystems, we analyzed a complex biogeochemical model. It was discovered that half of the possible choices of parameter and initial conditions of the model lead to non-stationary dynamics, even if the bulk of such trajectories show relatively tiny oscillations. Such trajectories can resonate with an external noise, making them significant. By altering how the model describes the structure of the food web, we looked for the reasons of its stability. We discovered that traits like omnivory and center of gravity are essential to the stability of the web. Our results support the widely accepted hypothesis that predators that can feed on a variety of prey, potentially at multiple trophic levels, are associated with stable ecosystems.

Introduction

The importance of investigating not stationary dynamics (such as periodic or chaotic behaviours) in ecological systems stems from the abundant evidence of the existence of periodic changes in population densities. However, it is still not clear whether such periodic fluctuations are intrinsic of ecological systems or due to an external forcing. Many studies show that simple models exhibit periodic cycles and chaotic behaviour [1, 2]. Other studies indicate that real natural population systems are unlikely to behave chaotically unless forced by an external factor, such as human actions, even if the seeds of chaos are present [3]. Moreover, it is known that strong oscillations can be induced by stochastic forcing. One of the most important examples of resonance between stochastic noise and internal oscillation modes is reported in [4], where it is demonstrated that glaciation cycles can be described by resonance of stochastic noise with the periodicity of astronomical forcing. In this work, we investigate the presence of internal model oscillations in a complex biogeochemical model to examine the conditions under which resonance with stochastic fluctuations can occur and whether this phenomenon can be considered rare or common.

Results and discussion

We found that half of the possible parameters and initial conditions choices lead to very small fluctuations in the solutions of the model. Such solutions, which we have defined as quasi-stationary, can resonate with stochastic noise and can be the *seeds of chaos* thought to exist in nature. However, only 3% of the perturbed samples has exhibited large fluctuations. This confirms the notion that complex models are stable.

Therefore, we searched for the causes of food web stability. We found that the most important features characterizing food web stability are omnivory and center of gravity. However, omnivory alone is not able to stabilize a web; on the contrary, in long chains it plays a destabilizing role. This can be explained by the fact that predation of top predators at different levels of a food chain enhances the predation at the lowest levels, destabilizing the whole chain. Instead, a low center of gravity, i.e. the presence of alternative prey species, especially at the lowest trophic levels, is a very effective mechanism for reducing unstable dynamics.

References

- [1] Y. Takeuchi, Global Dynamical Properties of Lotka-Volterra Systems, World Scientific, 1996. doi:<https://doi.org/10.1142/2942>.
- [2] G. F. Fussmann, S. P. Ellner, K. W. Shertzer, N. G. H. Jr., Crossing the hopf bifurcation in a live predator-prey system, *Science* 290 (5495) (2000) 1358–1360. doi:[10.1126/science.290.5495.1358](https://doi.org/10.1126/science.290.5495.1358).
- [3] A. Berryman, J. Millstein, Are ecological systems chaotic — and if not, why not?, *Trends in Ecology & Evolution* 4 (1) (1989) 26–28. doi:[10.1016/0169-5347\(89\)90014-1](https://doi.org/10.1016/0169-5347(89)90014-1).
- [4] R. Benzi, G. Parisi, A. Sutera, A. Vulpiani, Stochastic resonance in climatic change, *Tellus* 34 (1) (1982) 10–15. doi:[10.3402/tellusa.v34i1.10782](https://doi.org/10.3402/tellusa.v34i1.10782).

Resonance bifurcations in a discrete-time predator-prey system

Anuraj Singh and Vijay Shankar Sharma

Department of Applied Sciences, ABV-Indian Institute of Information Technology and Management Gwalior, M.P., India
anuraj@iiitm.ac.in, vijays@iiitm.ac.in

Abstract. This paper studies bifurcation analysis and resonances in a discrete-time model analytically and numerically. The local stability conditions of all the fixed points in the system are determined. Here, codim-1 and codim-2 bifurcation, including multiple and generic bifurcations in the discrete model, are explored. The model undergoes fold bifurcation, flip bifurcation, Neimark-Sacker bifurcation and resonances bifurcation of codimension two at different fixed points. Using critical normal form theorem and bifurcation theory, this study obtains the normal form coefficients to confirm the nondegeneracy of codim-1 and codim-2 bifurcations in the model. The numerical simulation gives a wide range of periodic cycles and bifurcation in the system. In the system, NSB signifies that both species can fluctuate near critical parameter values and stable fluctuations seem. The resonance bifurcation in the discrete-time map indicates that both species coincide till order 4 in stable periodic cycles near some critical parametric values.

Introduction

In ecology, the interaction between distinct species causes conflict, cooperation and consumption. The prey-predator system is the most fundamental linkage among them. Almost a century ago, the predator and prey populations had many variations based on their experimental evidence. The Lotka-Volterra model also serves as a general framework for describing other types of nonlinear ecosystem interactions such as competition, scavenging, and mutualism. The study of their dynamical behaviors has drawn the attention of many mathematical biologists [1, 3, 2].

Results and discussion

In this work, we obtained our discretized model by deploying the piecewise constant argument approach in the model, discussed. we explored local stability for all fixed points. The system is explored for different codim-1 and codim-2 bifurcations by using critical normal form coefficient method. The codim-2 bifurcations such as resonance 1:2(R2), resonance 1:3(R3) and resonance 1:4(R4) are occurred under some non-degenerate conditions. An extensive numerical simulation is presented to substantiate the analytical findings. Moreover, the 1:4 resonance bifurcation demonstrates that both species coexist till order 4 in stable periodic cycles near some critical parametric values. Ecologically, the prey-predator species coexist up to the fourth order in the stable high periodic cycle.

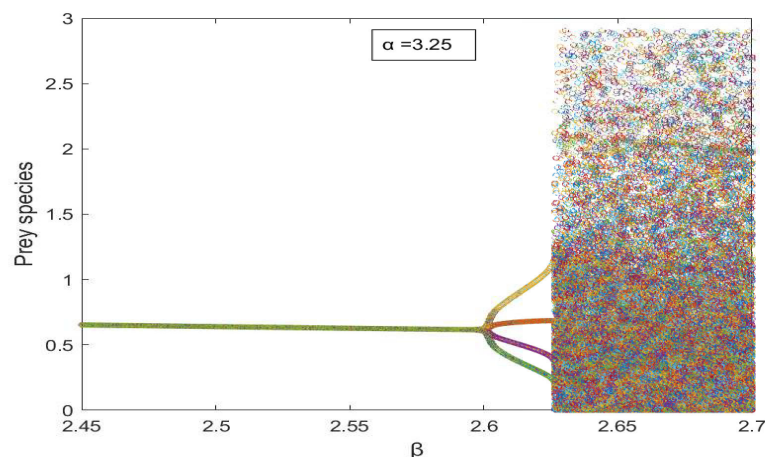


Figure 1: 1;4 (R4) Resonance bifurcation diagram with respect to β when $\alpha = 3.25$

References

- [1] Gakkhar, S., Singh, A.: Control of chaos due to additional predator in the hastings–powell food chain model. *Journal of Mathematical Analysis and Applications* **385**(1), 423–438 (2012)
- [2] He, Z., Lai, X.: Bifurcation and chaotic behavior of a discrete-time predator–prey system. *Nonlinear Analysis: Real World Applications* **12**(1), 403–417 (2011)
- [3] Huang, J.c., Xiao, D.m.: Analyses of bifurcations and stability in a predator-prey system with holling type-iv functional response. *Acta Mathematicae Applicatae Sinica* **20**(1), 167–178 (2004)

An Overview on Time-frequency Effects of ECG Signals Using Synchroextracting Transform

M. Varanis^{*}, S. Hemmati^{**}, M C. Filipus^{***}, F. L. de Abreu^{***}, J. M. Balthazar^{****} and C. Nataraj^{**}

^{*} Physics Institute, Federal University of Mato Grosso do Sul (UFMS), Brazil.

^{**} Villanova Center for Analytics of Dynamic Systems (VCADS), Villanova University, Villanova, PA 19085, USA.

^{***} Faculty of Engineering, Federal University of Grande Dourados, Brazil.

^{****} Department of Electrical Engineering, Federal University of Technology– Parana, Brazil.

Abstract. Cardiac dysfunctions and arrhythmias are nonlinear and complex phenomena and can be monitored using electrocardiogram (ECG) recordings. ECG signals, and their underlying signal generation mechanisms, have strong nonlinear characteristics and in some cases, present rich dynamic responses. In this paper we aim to characterize the abnormalities found in patients with arrhythmias through a novel signal processing procedure applied to ECG signals, and by characterizing them in the time and frequency domains. Specifically, we propose use of the wavelet-based Synchroextracting transform (WSET), an emerging method for time-frequency analysis (TFA). The central idea of WSET is to increase the concentration of energy in the time-frequency representation (TFR), and capture variations of the instantaneous frequency (IF) of the original, weak signal, which enables better characterization of anomalies in the frequency domain. In this study, using a public arrhythmia database, WSET is employed to extract nonlinear and complex features of pathologies present in the ECG signals, thus facilitating characterization and diagnosis of subtle anomalies in the patient's heart.

Introduction

Time-frequency analysis techniques (TFA), such as continuous wavelet transform (CWT), are very efficient in parameter / feature extraction, and solving the fixed window size problem of short time Fourier transform (STFT). Another problem encountered in TFA is the energy dispersion in the TFR which can hide/offset some frequencies, and causing inaccuracy in TFA. Methods based on synchrosqueezing try to mitigate this problem as presented in [1]. Emergent TFA techniques have been proposed in order to concentrate energy in the TFR, including the wavelet-based synchrosqueezing transform (WSST) and wavelet-based synchroextracting transform (WSET). A comprehensive discussion about synchroextracting transform (SET) formulation, with its applications and limitations, is presented in [1]. In this work, WSET will be used, which is one of the emerging methods that has been used in the characterization of signals from mechanical systems [2]. It is important to note that these methods are eminently suitable for characterization of signals with nonstationary, nonlinear and chaotic characteristics. It is well-known that ECG signals are strongly nonlinear: the ECG signal in healthy conditions presents quasi-periodic responses, while a signal containing a pathological condition, in general, presents chaotic or quasi-periodic responses.

Time-frequency analysis using wavelet-based synchrosqueezing transform

Fig.1-a shows a time-domain ECG signal that contains 5 types of abnormalities: Right bundle branch block beat (R), Left bundle branch block beat (L), Premature ventricular contraction (V), Ventricular tachycardia (VT), Ventricular flutter (VFL). WSET scheme is used and are presented in Fig.1-b, it is possible to see how the method characterizes the instantaneous frequencies throughout the signal, allowing better temporal localization of a different clinical condition. We also observe discontinuities in the main frequency. Due to the concentration of energy in the TFR it is possible to observe the strong variation in the frequency spectrum at the instants when the cardiac arrhythmias occur, and this variation is a qualitative indicator of occurrence of period doubling, quasi-periodicity and routes to chaos in nonstationary signals, as described in [3].

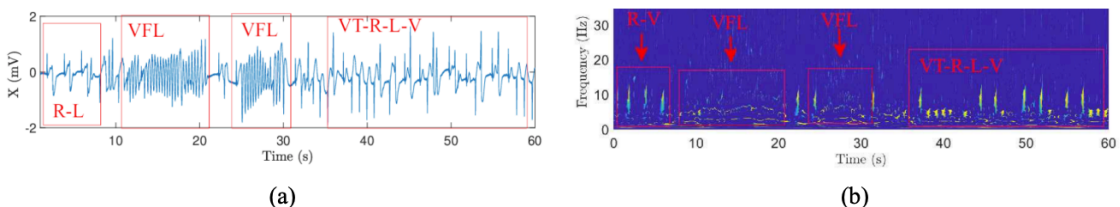


Figure 1: (a) ECG signal with several clinical conditions, and (b) Frequency domain response - WSET scheme.

References

- [1] Yu, Gang and Wang, Zhonghua and Zhao, Ping and Li, Zhen: Local maximum synchrosqueezing transform: An energy-concentrated time-frequency analysis tool. *Mechanical Systems and Signal Processing* 117 (2019): 537–552.
- [2] Shi, Zhenjin, Xu Yang, Yueyang Li, and Gang Yu. Wavelet-based Synchroextracting Transform: An effective TFA tool for machinery fault diagnosis. *Control Engineering Practice* (2021): 114.
- [3] Varanis, Marcus V., Angelo Marcelo Tusset, Jos é Manoel Balthazar, Grzegorz Litak, Clivaldo Oliveira, Rodrigo Tumolin Rocha, Ailton Nabarrete, and Vinicius Piccirillo. "Dynamics and control of periodic and non-periodic behavior of Duffing vibrating system with fractional damping and excited by a non-ideal motor." *Journal of the Franklin Institute* 357.4 (2020): 2067-2082.

Investigation of Parkinsonian tremor signals troughs nonlinear time series analysis

Antonio Zippo*, Francesco Pellicano* and Giovanni Iariccio*

* Department of Engineering "Enzo Ferrari", University of Modena and Reggio Emilia, Modena, Italy.

Abstract. The vibrational phenomena studied in this work regards the arm and forearm vibration with the purpose to detect and recognize the dynamic properties and correlations of onset of pathological tremor in patients affected by Parkinson disease. Experimental data measured by patients will be analyzed using multiscale recursive analysis methodologies through the TISEAN package [1].

Introduction

The characterization and identification of pathological patterns detected through the surface electromyographic (sEMG) and accelerometric signals are an interesting challenge: methodologies for data analysis, time series analysis, and human skills must be combined to detect and extract characteristics for pathological identification. The complexity lies in the very nature of the experimental activity [2] since each patient has slight differences due to the various positions of the electrodes, the different pathologies and the stage of the pathology itself, and the intrinsic complexity of biological systems (high degree of non-linearity, non-stationarity, and signal noise). Pathological tremors can be classified accordingly to their frequency: low (2-4Hz) cerebellar, medium (5-7 Hz) Parkinson's disease (PD), high (>8 Hz) Essential Tremor (ET). The traditional treatment is pharmacological and there are no proven efficacy molecules in cerebellar tremors. Other methods are mechanical, as robotic exoskeletons, or neurosurgical, as deep brain stimulation (DBS), these techniques suffer from various limitations; on the contrary, functional electrostimulation (FES) shows attenuation of 73% in ET, 62% in PD, and 38% in multiple sclerosis (MS). To support the patient affected by Parkinson's disease (PD) or Essential Tremor (ET), physiotherapy and electrostimulation help to reduce the tremor and compensate for the functional loss. From a biomechanical perspective, scientific literature describes the muscular activation and force estimation in several studies and further models allow compensating for errors introduced by measurement and tools. Surface electromyographic signals (EMGs) could be used as inputs for tremor detection[3-4], prediction, and parameter estimation. These could benefit from the implementation, for example, of Active Vibration Control algorithms, where the overall effect of the control loop is to reduce broadband oscillations and mitigate single or multi-vibrated modes without negatively affecting other frequencies (those related to voluntary movements).

Results and discussion

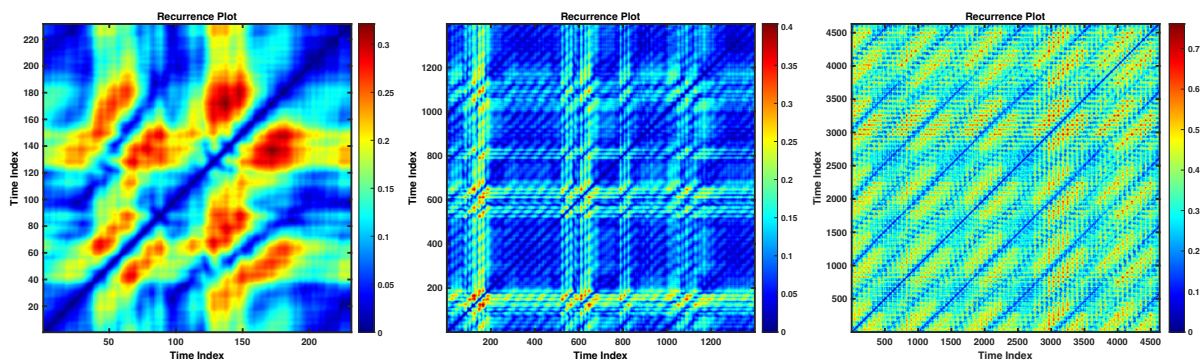


Figure 1: Recurrence plot of sEMG of Parkinsonian tremor at different time span: 0.1 seconds, 0.55second and 1.8 seconds

The showed case, see figure1, presents electrodes location in Arm - Biceps Brachii with posture seated, holding light object (sampling frequency is 2560Hz) and has been analyzed using multiscale recursive analysis methodologies through the TISEAN package; three time span has been considered, showing the complexity of this response in particular, the embedding dimensions is 3 in all cases, but periodicity seems more evident in higher time span related to the 5.153Hz pathological tremor corresponding to the samples distance between the diagonals in the 3rd recurrence plot.

References

- [1] Rainer Hegger, et al. Practical implementation of nonlinear time series methods: The TISEAN package, Chaos: An Interdisciplinary J. of Nonlinear Science June 1999
- [2] Zippo A., Iariccio G., Pellicano F., Synchronicity Phenomena in Circular Cylindrical Shells Under Random Excitation, (2021) Advanced Structured Materials, 157, pp. 127 - 157
- [3] Zippo A., Pellicano F., Iariccio G. (2021). Time series analysis of arm and forearm measurement for functional electrical stimulation control. In: 17th International Conference on Condition Monitoring and Asset Management, CM 2021. British Institute of Non-Destructive Testing, gbr, 2021
- [4] Zippo A., Pellicano F., Iariccio G., Franco V., Francesco C., Identification of dynamic behaviour of forearm for active control of pathological tremor (2019) Proceedings of the 26th International Congress on Sound and Vibration, ICSV 2019.

Novel approaches and “similarity score” for the identification of active sites during patient-specific catheter ablation of atrial fibrillation

Vasanth Ravikumar**, Xiangzhen Kong**, Henri Roukoz***, and Elena G. Tolkacheva*

*Department of Biomedical Engineering, University of Minnesota, Minneapolis, MN, USA

** Department of Electrical and Computer Engineering, University of Minnesota, Minneapolis, MN, USA

*** Division of Cardiology, Department of Medicine, University of Minnesota, Minneapolis, MN, USA

Abstract. Atrial fibrillation (AF) is the most common cardiac arrhythmia and precursor to cardiac diseases. Catheter AF ablation is associated with limited success rates, and existing mapping systems fail to identify target sites for ablation. We evaluated the performance of frequency-, information-, and statistical-based approaches to identify the AF drivers using unipolar and bipolar electrograms (EGMs) obtained from numerical simulations under different clinical scenarios. We also developed a “similarity score” to more accurately identify the spatial location of active sites of arrhythmia in patients with AF. Results from numerical simulations demonstrate that all approaches are able to accurately identify AF drivers from EGMs for clinical catheters. “Similarity score” pinpoints the spatial sites with high values that were observed only in patients with unsuccessful AF termination, suggesting that these active AF sites were missed during the ablation procedure.

Introduction

Atrial fibrillation (AF) is the most common cardiac arrhythmia and precursor to other cardiac diseases. Catheter ablation is associated with limited success rates in patients with persistent AF. Currently, existing mapping systems fail to identify critical target sites for ablation. Recently, we proposed and validated several individual techniques, such as dominant frequency (DF), multiscale frequency (MSF), kurtosis (Kt), and multiscale entropy (MSE), to identify active sites of arrhythmias using simulated intracardiac electrograms (iEGMs). However, the individual performances of these techniques to identify arrhythmogenic substrates are not reliable.

In this study, we aimed to develop a similarity score by combining the various iEGM analysis approaches based on an earth mover’s distance (EMD) method. We further demonstrated that this similarity score can identify active spatial sites of AF in patients with unsuccessful AF termination, while no active sites of AF were present in patients with successful AF termination. Clinical bipolar iEGMs were obtained from patients with AF who underwent either successful ($m = 4$) or unsuccessful ($m = 4$) catheter ablation. A similarity score (0–3) was developed via the EMD approach based on a combination of DF, MSF, MSE, and Kt techniques.

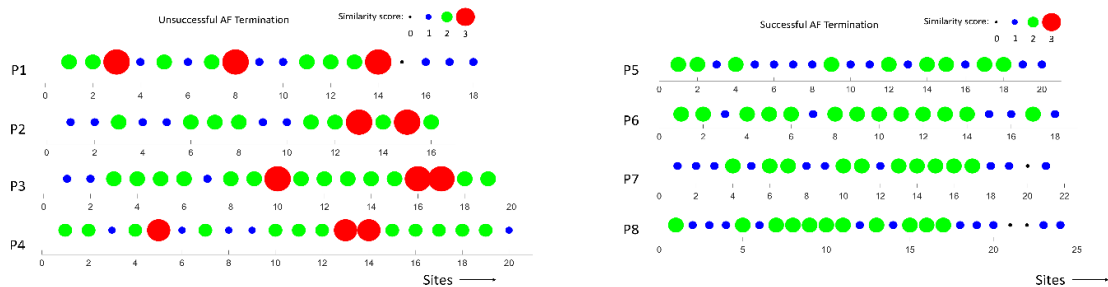


Figure 1: Similarity scores calculated at different spatial sites in patients with unsuccessful (left) and successful (right) AF termination. Note the presence potentially active AF sites with a high similarity score (3, red) in all patients with unsuccessful AF termination.

Results and Discussion

In this retrospective study, we investigated the performance of individual EGM analysis approaches (DF, MSF, Kt, and MSE) and newly developed similarity scores to identify potential, abnormal, electrically active sites in patients with previously unsuccessful AF termination. The major findings of this study are as follows: (1) individual approaches can discriminate between patients with successful and unsuccessful AF termination but fail to robustly identify spatial sites with active AF drivers, (2) a novel EMD-based similarity score was developed and validated to identify the active AF sites in patients with unsuccessful AF termination, and (3) there was no single common region in the atria associated with active AF sites in patients with unsuccessful AF termination, thus indicating the need for patient-specific mapping and ablation therapy.

Generalized Fractional-Order Complex Logistic Map and Fractals on FPGA

Sara M. Mohamed*, Wafaa S. Sayed**, Lobna A. Said* and A. G. Radwan ***

*Nanoelectronics Integrated Systems Center (NISC), Nile University, Giza, Egypt

**Engineering Mathematics and Physics Dept., Faculty of Engineering, Cairo University, Egypt

***School of Engineering and Applied Sciences, Nile University, Giza, Egypt

Abstract. This paper introduces a generalized fractional-order complex logistic map and the FPGA realization of a corresponding fractal generation application. The chaotic properties of the proposed map are studied through the bifurcation behavior and maximum Lyapunov exponent (MLE). A concise fractal generation process is presented, which results in designing and implementing an optimized hardware architecture. An efficient FPGA implementation of the fractal behavior is validated experimentally on Artix-7 FPGA board. An example of fractal implementation is verified, yielding frequency of 24.34 MHz and throughput of 0.292 Gbit/s. Compared to recent related works, the proposed implementation demonstrates its efficient hardware utilization and suitability for potential applications.

Introduction

Chaos is mentioned in systems that are sensitive to initial conditions such that a small variation cause a significant difference in behavior. Chaotic systems are distinguished by their attractive characteristics like randomness, aperiodicity and fractal identity. Fractals are recognized by their complex geometric structures such as the ones generated from Mandelbrot and Julia maps [1]. Chaotic systems are classified into continuous-time maps and discrete-time maps. The discrete maps are classified into integer-order maps that can be extended to fractional such as logistic and tent maps, and real maps that can be extended to complex such as logistic and Gaussian maps. Several works introduced fractal generation from integer-order complex discrete maps including logistic and Gaussian maps [2, 3, 4]. Realizations in digital hardware have become more practical for industrial use. Fixed-point operations are widely used for hardware realizations to save costs and enhance speed. The generalization of conventional chaotic systems into the fractional-order domain allows more accurate understanding of the map behavior, increases the degree of freedom in design and enhances its performance in applications. Fractional-order discrete chaotic maps are employed in several applications such as encryption, neural networks, synchronization and multi-scroll generation. Among several fractional definitions, EL Raheem definition is simple and suitable for hardware implementation [5]. This paper proposes a generalized fractional-order complex logistic map, fractals and their FPGA realization. The chaotic properties of the proposed map are studied using bifurcation and MLE diagrams. The proposed hardware implementation of the fractals based on the fractional-order complex logistic map utilizes simplified steps. The fractal behaviors are validated experimentally on an Artix-7 FPGA kit. The proposed implementation is compared to recent related works demonstrating its hardware efficiency and suitability for potential applications.

Results and discussion

The proposed design for fractals based on the generalized fractional complex logistic map is written in Verilog HDL with the simulation of Xilinx ISE 14.7 and implemented on Xilinx FPGA Artix-7 XC7A100TCSG324 by using Chip scope. The outputs are wired to a 12-bit Digital to Analog converter, which is connected to a digital oscilloscope to display the fractal behavior. The fractal example is realized and validated experimentally on FPGA. The design achieves frequency of 24.34 MHz and throughput of 0.292 Gbit/s. A summary of FPGA implementation results of this work and other implemented fractal works [2, 3, 4] is presented. The proposed implementation consumes higher resources and lower frequency than [3, 4] due to the excessive arithmetic operations needed for the fractional domain. On the other hand, the proposed implementation achieves efficient hardware utilization and speed than [2] due to the simplicity of operations of the proposed map than Gaussian map. The proposed realization is considered a promising solution to increase the degrees of freedom in the design and enhance the performance in different applications such as encryption schemes and multi-scroll generators.

References

- [1] K. Bouallegue, A. Chaari, and A. Toumi, "Multi-scroll and multi-wing chaotic attractor generated with julia process fractal," *Chaos, solitons & fractals*, vol. 44, no. 1-3, pp. 79–85, 2011.
- [2] B. M. AboAlNaga, L. A. Said, A. H. Madian, and A. G. Radwan, "Analysis and fpga of semi-fractal shapes based on complex gaussian map," *Chaos, Solitons & Fractals*, vol. 142, p. 110493, 2021.
- [3] B.-A. M. Abo-Alnaga, L. A. Said, A. H. Madian, and A. G. Radwan, "Fpga realization of complex logistic map fractal behavior," *Fractals*, vol. 30, no. 01, p. 2250023, 2022.
- [4] S. M. Mohamed, W. S. Sayed, L. A. Said, and A. G. Radwan, "Fpga realization of fractals based on a new generalized complex logistic map," *Chaos, Solitons & Fractals*, vol. 160, p. 112215, 2022.
- [5] Z. El Raheem and S. Salman, "On a discretization process of fractional-order logistic differential equation," *Journal of the Egyptian Mathematical Society*, vol. 22, no. 3, pp. 407–412, 2014.

New elemental damping model for nonlinear dynamic response

Chin-Long Lee*

*Department of Civil and Natural Resources Engineering, University of Canterbury, Christchurch, New Zealand,
ORCID # 0000-0003-2885-7113

Abstract. This study proposes a new elemental damping model for incorporating un-modelled energy dissipation in the simulation of seismic response of large-scale structures. It addresses the problems of the existing elemental damping model that result in difficulty in calibrating elemental parameters for desired global structural damping ratio and unintended large coupling effects between modes. The new model maintains the consistency between elemental damping ratio and global structural damping ratio, avoiding unnecessary complex calibration. It also allows the elemental damping ratio to be better correlated with the states of elemental stresses, deformations, damage variables, or any other internal state variables, such that a rational-based update on elemental damping ratio can be used to simulate un-modelled, changing energy dissipation during nonlinear dynamic response. Examples will be used to demonstrate the performance of the new model.

Introduction

Elemental damping models have recently been proposed to address the limitations of Rayleigh damping for incorporating un-modelled energy dissipation in the simulations of seismic response of large-scale structures [1]. In these models, elemental damping coefficient matrices are formulated based on elemental stiffness and mass matrices, and the global damping coefficient matrix is obtained by directly assembling these elemental matrices based on the common nodal degrees of freedom, just like how the global stiffness matrix is obtained from elemental stiffness matrices. This idea is particularly advantageous because it results in a damping coefficient matrix that has the same skyline pattern as the stiffness matrix, so that these models have the same computational efficiency as the Rayleigh model. Unfortunately, the resultant damping coefficient matrix is not proportional, resulting in coupling between modes and the coupling effects could be larger than anticipated. For a decent global damping ratio as low as 2 to 5%, the required elemental damping ratio could also be very large and even larger than 100% [2]. This raises questions on the physical meaning of elemental damping ratio. It is, therefore, warranted to have a new elemental damping model that addresses these problems.

Results and discussions

The new elemental damping model is derived based on the bell-shaped damping model recently proposed [3-6]. It uses a bell-shaped curve as the basis function to generate any user-defined damping ratio curve in the frequency domain, such as a constant, linear, trilinear, or a stepped curve. Although its damping coefficient matrix is fully populated, it can be expanded into a sparse block matrix using the idea of static expansion. The new elemental damping model adopts this sparse block matrix form of the damping matrix on the elemental level, and assemble them to obtain the sparse block matrix form of the global damping coefficient matrix. This big idea maintains a consistent damping ratio on both elemental and global structural level, thereby avoiding complex calibration process. It also allows the elemental damping ratio to be better correlated with the states of elemental stresses, deformations, damage variables, or any other internal state variables, such that a rational-based update on elemental damping ratio can be used to simulate changing un-modelled energy dissipation during nonlinear dynamic response. Examples have demonstrated the excellence performance of the new model.

References

- [1] Puthanpurayil A.M., Lavan O., Carr A.J., Dhakal R.P. (2016) Elemental damping formulation: an alternative modelling of inherent damping in nonlinear dynamic analysis, *Bulletin of Earthquake Engineering* **14**: 2405–2434.
- [2] Ni Y., Zhang Z., MacRae G.A., Carr A.J., Yeow T. (2019) Development of practical method for incorporation of elemental damping in inelastic dynamic time history analysis, in: *Proceedings of the 2019 Pacific Conference on Earthquake Engineering and Annual NZSEE Conference*, Auckland, New Zealand, 4-6 April, p. **4C.11**.
- [3] Lee C.-L. (2020) Proportional viscous damping model for matching damping ratios, *Engineering Structures* **207**:110178.
- [4] Lee C.-L. (2020) Sparse proportional viscous damping model for structures with large number of degrees of freedom, *Journal of Sound and Vibration* **478**:115312.
- [5] Lee C.-L. (2021) Bell-shaped proportional viscous damping models with adjustable frequency bandwidth, *Computers & Structures* **244**:106423.
- [6] Lee C.-L. (2022) Type 4 bell-shaped proportional damping model and energy dissipation for structures with inelastic and softening response, *Computers & Structures* **258**:106663.

Parameter Estimation for Linear Time-Varying (LTV) Uncertain System Using Physics-Informed Machine Learning

Junyeong Kim^{*}, Sejun Park^{*}, Ju H. Park^{**} and Sangmoon Lee^{*}

^{*}Department of Electronic and Electrical Engineering, Kyungpook National University, Daegu, Republic of Korea

^{**}Department of Electrical Engineering, Yeungnam University, Kyungsan, Republic of Korea

Abstract. This paper proposes a Physics-Informed Machine Learning (PIML) based parameter estimation method for Linear Time-Varying (LTV) uncertain systems. The proposed method is first to obtain the training data from the PIML-based Observer and second to estimate the time-varying uncertain parameters. The LTV system can be represented by the polytopic uncertain model, and the model can be accurately estimated from the PIML by finding the parameters for it in the proposed method. It will be applied to the parameter-dependent controller for systems with uncertain parameters.

Introduction

In several decades, many robust control studies have been conducted to design controllers to control systems with polytopic model uncertainty [1]. While the Linear Parameter-Varying (LPV) system is useful to design a controller because a parameter is measurable, the LTV uncertain systems have difficulties in controller synthesis where parameters over time are not available [2]. Therefore, it is very important to find parameters for the analysis and synthesis of systems with time-varying uncertainty and nonlinear dynamics.

Recently, PIML, a neural network structure capable of learning the Ordinary Differential Equation (ODE) or Partial Differential Equation (PDE), has been studied to obtain new physical information in the case of not being measurable with sensors. Therefore, the parameter can be estimated by combining the PIML structure and polytopic state-observer model. When the parameter values are fully estimated, the parameter-dependent control feedback gain can be designed to enhance the system's performance.

The methods of updating the neural network were researched by defining the loss function as an error between the actual state and the estimated state. However, in the PIML, the loss function includes the ODE, the exact solution for training data, and boundary conditions [3]. From the learned PIML, we can find the parameters through the convex combination of the estimated states from the low and upper bound model. After the parameters are computed through the above process, the parameters can be utilized as if they were measured and can be used in the gain scheduling process. Therefore, it is possible to ensure the performance and robustness of the system. The proposed system is described in Figure 1.

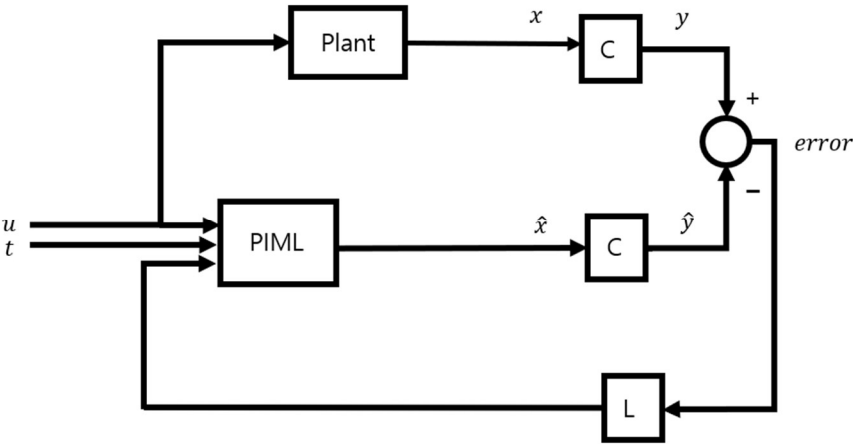


Figure 1: Block Diagram of the proposed method

References

- [1] Nikos Vlassis, Raphaël Jungers, (2014) Polytopic uncertainty for linear systems: New and old complexity results (2014)
- [2] D. Pun, S.L. Lau, and D.Q.Cao, Stability Analysis for Linear Time-Varying Systems With Uncertain Parameters: Application to Steady-State Solutions of Nonlinear Systems (1999)
- [3] M.Raissi, P.Perdikaris, G.E.Karniadakis, Physics-informed neural networks: A deep learning framework for solving forward and inverse problems involving nonlinear partial differential equations (2019)

Stabilization mechanism of limit cycle oscillation using control based continuation and phase locked loop.

Gourc Etienne*, Vergez Christophe* and Cochelin Bruno *

*Aix Marseille Université, CNRS, Centrale Marseille, Laboratoire de Mécanique et d'Acoustique, Marseille, FR

Abstract. This presentation concerns the stabilization of unstable limit cycles using a combination of feedback and phase locked loop control. The proposed control scheme is applied to a Van der Pol oscillator and the stabilization mechanisms are investigated theoretically using the method of multiple scales. Different failure scenarios of the controller are revealed allowing us to express design rules for the controller gains.

Introduction

Control based continuation (CBC) is used to study the bifurcation diagrams of a nonlinear dynamical systems on physical experiments [1]. CBC rely on a feedback controller that is used to stabilize the nonlinear device. The feedback controller must be non-invasive to ensure that a periodic solution of the feedback controlled system is also a solution of the uncontrolled system. CBC has been mostly used to track branches of periodic solutions of non-autonomous (i.e. forced) systems [2]. CBC of autonomous systems presents an additional difficulty since the frequency of the limit cycle (LC) is also an unknown. Numerical continuation algorithms solve this problem by appending the system with a phase condition. In this study, the frequency of the limit cycle is determined in real time by using a phase locked loop controller (PLL). Although CBC has already been tested on various experiments, only few papers deal with the detailed analysis of the underlying stabilization mechanism.

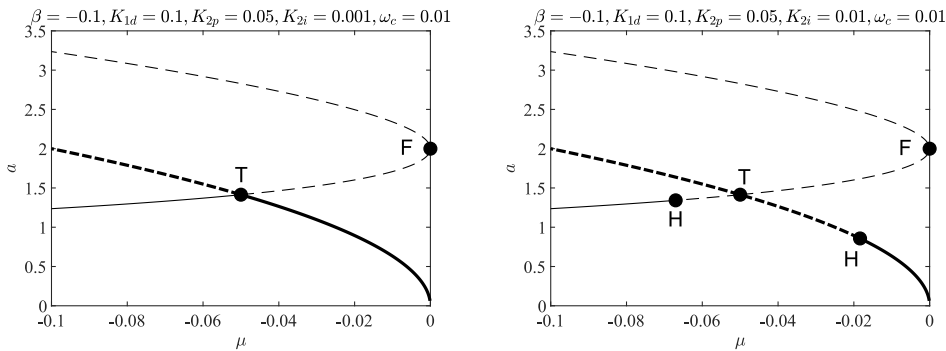


Figure 1: Bifurcation diagram of the controlled VdP

Results and discussion

The proposed control scheme has been applied to a Van der Pol oscillator (VdP). The governing equations of motion are given by

$$\begin{aligned} \ddot{x} + x - (\mu - \beta x^2)\dot{x} &= K_{1d}(\dot{w} - \dot{x}) & \dot{y}_1 &= \omega_c(x \cos \theta - y_1) \\ \dot{y}_2 &= R y_1 & \dot{\theta} &= \omega_0 + K_{2p} y_1 + K_{2i} y_2 \end{aligned} \quad (1)$$

where μ and β are the linear and nonlinear coefficients of the VdP oscillator. K_{1d} is the derivative gain, ω_c the cutoff frequency of the low pass filter of the PLL, R , K_{2p} , K_{2d} are the gains of the PLL and ω_0 the center frequency. $w(t) = W \sin \theta(t)$ is the control target. The uncontrolled VdP oscillator has a Hopf bifurcation at $\mu = 0$, which is subcritical (supercritical) for $\beta < 0$ ($\beta > 0$). The behavior of the controlled VdP has been analyzed by using the method of multiple scales. Since the objective is to stabilize the unstable LC, we considered that the control target amplitude W is equal to the amplitude of the uncontrolled LC, i.e. $W = a_0 \equiv 2\sqrt{\mu/\beta}$. Examples of bifurcation diagram are depicted in fig. 1. Solid (dashed) lines correspond to stable (unstable) solutions. Thick and thin lines correspond to solutions where the controller is non-invasive ($W = a$), or invasive ($W \neq a$), respectively. Multiple scales analysis allows us to express design rules for the controller. Either the controller may fail due to the presence of a transcritical bifurcation at $\mu = -K_{1d}/2$ or due to a Hopf bifurcation if $K_{2p}(K_{1d} + 2\omega_c) < 2RK_{2i}$.

References

- [1] Barton D.A.W, Sieber, J. (2010) Systematic experimental exploration of bifurcations with non-invasive control. *Phys. Rev. E*.
- [2] Abeloos G., Muller F., Ferhatoglu E., Scheel M., Collette C., Kerschen G., Brake M.R.W., Tiso P., Renson L., Krack M. (2022) A consistency analysis of phase-locked-loop testing and control-based continuation for geometrically nonlinear frictional system. *Mech. Syst. Signal Process.*
- [3] Denis V., Jossic M., Giraud-Audine C., Chomette B., Renault A., Thomas O. (2018) Identification of nonlinear modes using phase-locked-loop experimental continuation and normal form. *Mech. Syst. Signal Process.*

Synchronised States and Transients in Minimal Networks of Oscillators

Andrea Elizabeth Biju*, Sneha Srikanth**, Krishna Manoj⁺, Samadhan A. Pawar* and R. I. Sujith *

*Department of Aerospace Engineering, Indian Institute of Technology Madras, Chennai, India

**Department of Mechanical Engineering, Indian Institute of Technology Madras, Chennai, India

⁺Department of Mechanical Engineering, Massachusetts Institute of Technology, Cambridge, MA 02139, USA

Abstract. Several natural and engineering systems can be modelled using minimal networks of oscillators. The oscillatory behaviour in such networks can be altered by factors such as number of oscillators, coupling scheme, coupling strength and time delay in the system. In this study, we investigate the synchronised states and transients exhibited by a minimal ring of Stuart Landau oscillators. For local coupling, we observe in-phase oscillations and splay state of the highest mode at low coupling strengths. For rings with an even number of oscillators having high coupling strengths, we identify a transient modulated 2-cluster state. We also observe that as the coupling becomes non-local, the variety of splay states increases. For global coupling, we observe generalised splay states. We anticipate that the results of this study will help in the characterisation and control of oscillatory behaviour in physical systems including combustors and coupled lasers.

Introduction

Understanding the dynamics of minimal networks of oscillators is crucial to analyse the behaviour of several systems such as coupled lasers and thermo-fluid systems. A few studies have separately considered the effects of different factors such as coupling scheme, coupling parameters, and number of oscillators [1] on the dynamical behaviour of systems consisting of a large number of oscillators (of the order of 100). Unlike systems with such a large number of oscillators [2], a minimal network of oscillators exhibits noticeable changes in its behaviour as the aforementioned factors are varied. In the present study, we formulate a numerical model of a minimal ring of Stuart-Landau oscillators that helps us to understand the effects of the above mentioned factors on the dynamical behaviour of the ring network.

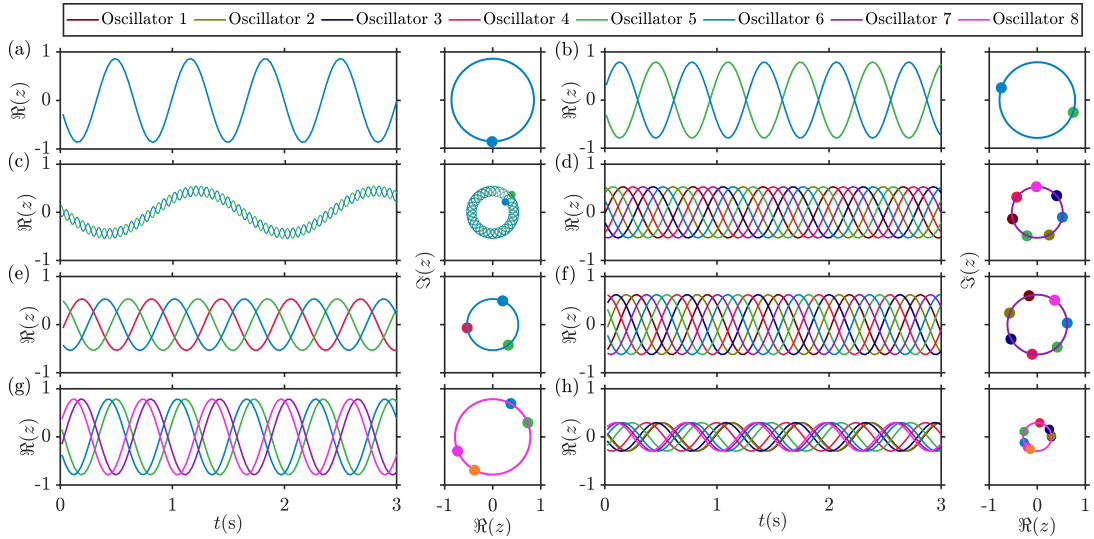


Figure 1: Time series and phase-space representation of various dynamical states (N denotes number of oscillators, K denotes coupling strength, τ denotes time delay). (a) In-phase state ($N = 6$, local coupling, $K = 25$, $\tau = 0.05$), (b) 2-cluster state ($N = 6$, local coupling, $K = 25$, $\tau = 0.30$), (c) Modulated 2-cluster state ($N = 6$, local coupling, $K = 25$, $\tau = 0.15$) (d) Splay state of mode 1 ($N = 7$, non-local coupling, $K = 0.5$, $\tau = 0.15$), (e) 3-cluster state ($N = 6$, non-local coupling, $K = 0.5$, $\tau = 0.25$), (f) Splay state of mode 2 ($N = 7$, non-local coupling, $K = 0.5$, $\tau = 0.25$), (g) Generalised 4-cluster state ($N = 8$, non-local coupling, $K = 0.3$, $\tau = 0.17$), (h) Generalised splay state ($N = 8$, global coupling, $K = 0.5$, $\tau = 0.30$).

Results and discussion

For different combinations of coupling strength, coupling schemes, time delay and number of oscillators, we observe splay states and generalised splay states. In splay states (Fig. 1(a, b, d, e, f, g)), the adjacent pair of oscillators in the ring network exhibit equal phase difference. In a generalised splay state (Fig. 1(h)), the adjacent pair of oscillators exhibit arbitrary phase difference although the order parameter continues to be zero, similar to that observed for a splay state. Additionally, in Fig. 1(c), we observe a transient modulated 2-cluster state characterised by the presence of two dominant frequencies. The lower and higher frequencies correspond to in-phase and 2-cluster states, respectively.

References

- [1] Reddy, D. R., Sen, A. and Johnston, G. L. (1998) Time delay induced death in coupled limit cycle oscillators. *Phys. Rev. Lett.* **80**:5109.
- [2] Zakharova, A. (2020) Chimera Patterns in Networks. Springer, Cham.

Fractional-Order Extension and FPGA Verification of Chaotic Models for Several Diseases

Sara M. Mohamed¹, Wafaa S. Sayed², Mohammad Adm³ Lobna A. Said¹, and A. G. Radwan^{2,4}

¹ Nanoelectronics Integrated Systems Center (NISC), Nile University, Giza, Egypt

² Engineering Mathematics and Physics Dept., Faculty of Engineering, Cairo University, Egypt

³ Department of Applied Mathematics and Physics, College of Applied Sciences, Palestine Polytechnic University

⁴ School of Engineering and Applied Sciences, Nile University, Giza, Egypt

Abstract. Among several definitions and numerical methods for fractional-order derivatives, Grünwald-Letnikov (GL) definition is suitable for numerical calculations and, hence, digital hardware realization. This paper extends several integer-order disease models to the fractional-order domain and verifies their chaotic behavior in software and hardware. The current paper considers Covid and Cancer disease models. All these models are nonlinear, with many terms and parameters. GL implementation adopts simplified steps to calculate the binomial coefficients, summation, and exponentiation of the numerical solution step size raised to the power of the fractional order. For some of the implemented systems, the nonlinear terms include division by the state variable, which is a challenging task in digital implementation. Consequently, the linear approximation method is applied, where the linear binomial coefficients are generated based on MATLAB curve fitting. Fractional-order cancer and Covid-19 models are realized experimentally on Xilinx FPGA Artix-7 XC7A100TCSG324, and the strange attractors are displayed on the Oscilloscope. The two systems operate at maximum frequencies of 33.009 and 2.259 MHz and yield throughputs of 0.396 and 0.267, respectively. The proposed models have more parameters than the corresponding integer models, which improves their modelling capabilities at the expense of slightly higher resource consumption and lower frequencies because of the relatively extensive arithmetic operations needed for the fractional system solution.

Keywords: Chaotic, Diseases Models, FPGA, Fractional Calculus, Grünwald-Letnikov

A vorticity wave packet breaking within a rapidly rotating vortex

Philippe Caillol

Department of Fundamental Sciences, Exact Science Center (CCE),
University of Bio-Bio ORCID # 0000-0002-6548-2595, Chile

Abstract. This study considers the interaction between a free vorticity wave packet and a rapidly rotating vortex in the slowly-evolving regime, a long time after the initial, unsteady, and strong interaction. The interaction starts when the amplitude modulated neutral mode enters resonance with the vortex on a spiraling critical surface, where the phase angular speed is equal to the rotation frequency. The singularity in the modal equation on this asymmetric surface strongly modifies the flow in its neighborhood, the three-dimensional (3D) helical critical layer, the region where the wave/vortex interaction occurs. Through matched asymptotic expansions, we find an analytical solution of the leading-order motion equations inside the 3D critical layer (CL). The system of the coupled evolution equations of the wave amplitude and the low-order CL-induced mean flow on the critical radius has been derived in the quasi-steady regime. The main outcome is that the wave packet/vortex interaction leads to a fast vorticity wave breaking.

Introduction

Though the motion in intense atmospheric vortices such as tropical cyclones can be considered highly axisymmetric above the surface boundary layer, observation often shows asymmetric features. The latter are generated, for instance, by the environmental wind shear, the beta effect, turbulent stress at the sea surface, and moist convection. Through a radiating wave-induced axisymmetric adjustment, these asymmetries are believed to play a significant role in the intensification of these vortices [1]. Latent heat release, for example, creates asymmetric potential vorticity (PV) anomalies that outward propagate in the form of PV waves; their breaking was recently related to the inner spiral rainbands. Observation and numerical simulations indeed show that inner spiral bands mainly exhibit vorticity wave characteristics [2].

Understanding the dynamics of these spiral bands and their contribution to the vortex evolution can greatly help improving the prediction of violently rotating vortex intensity. Wave activity analysis in numerical hurricane-like vortex models shows that vortices only interact with vorticity waves and that the related modes are continuous, that is, admit a CL singularity. This study therefore wishes to improve the understanding of the nonlinear dynamics of continuous vorticity modes embedded in rapidly rotating vortices. In particular, it examines the complex dynamical coupling between a vorticity wave packet and the azimuthally averaged 3D wind through the nonlinear CL theory in the quasi-stationary state assumption. In the previous analytical studies dealing with 2D or 3D, nonlinear and singular wave packets, the induced mean flow was however omitted, which was a stringent mistake.

Results and discussion

This interaction generates a vertically sheared 3D mean flow of higher amplitude than the wave packet. The chosen envelope regime assumes the formation of a mean radial velocity of the same order as the wave packet amplitude, deviating the streamlines in a spiral way with respect to the rotational wind. The critical layer pattern, strongly deformed by the mean radial velocity, loses its symmetries with respect to the azimuthal and radial directions [3]. The knowledge of the wave amplitude, the leading-order mean axial and azimuthal velocity, and axial vorticity evolutions at the critical radius can be simply determined from three first-order differential equations. Numerical simulations of the first-order mean flow truncated system show that the wave packet and vortex kinetic energies slightly grow inside the envelope before the breaking onset in most of the cases, whereas the vortex was intensifying at the expense of the wave packet in the previous and unsteady interaction. The vertical wind shear has the highest effect on the wave/mean flow interaction. When the shear is moderate, it enhances intensification but when it is very large, it prohibits it in both the unsteady and slowly evolving stages [4]. Including the second-order mean flow in this system could, however, avoid the breaking and would permit the interaction to generate an asymptotic constant-speed travelling coherent vortical structure.

References

- [1] Montgomery M. T., Kallenbach R. J. (1997) A theory for vortex Rossby-waves and its application to spiral bands and intensity changes in hurricanes. *Q. J. R. Meteorol. Soc.* **123**:435-465.
- [2] Chen Y., Brunet G., Yau M. K. (2003) Spiral bands in a simulated hurricane. Part II: Wave activity diagnostics. *J. Atmos. Sci.* **60**:1239-1256.
- [3] Caillol P. (2022) A vorticity wave packet breaking within a rapidly rotating vortex. Part I: The critical layer flow. *Stud. Appl. Math.* **148**:825-864.
- [4] Caillol P. (2022) A vorticity wave packet breaking within a rapidly rotating vortex. Part II: Wave/ mean flow interaction. *Stud. Appl. Math.* **148**:865-917.

Chirped optical solitons in fiber Bragg gratings with dispersive reflectivity

Khalil S. Al-Ghafri* and Mani Sankar*

*University of Technology and Applied Sciences, P.O. Box 14, Ibri 516, Oman

Abstract. The present work investigates the chirped optical solitons in a medium of fiber Bragg gratings (BGs) with dispersive reflectivity. BGs is considered here with polynomial law of nonlinear refractive index. The model of coupled nonlinear Schrödinger equations is analyzed and reduced to an integrable form under specific conditions. The results are obtained with the aid of soliton ansatz technique. Different structures of wave solutions including W-shaped, bright, dark, kink and anti-kink solitons are retrieved and their behaviors are presented so as to enhance the applications of fiber BGs.

Introduction

The data transmission through optical fiber for intercontinental distances is based on soliton propagation that arises due to delicate balance between chromatic dispersion (CD) and fiber nonlinearity. However, the CD may have low count that leads to limit the transmission distances. Thus, Bragg gratings (BGs) is found to be one of the effective techniques to tackle this problem by introducing induced dispersion to compensate for low CD and subsequently ensure the existence of soliton transmission. In literatures, many studies have been carried out using the technology of fiber BGs to investigate chirped and chirp-free optical solitons with different forms of nonlinearity, see [1–4]. The current study mainly discusses the dimensionless form of the coupled nonlinear Schrödinger equations in fiber BGs having polynomial law of nonlinearity given by [4]

$$iq_t + a_1 r_{xx} + (b_1 |q|^2 + c_1 |r|^2)q + (d_1 |q|^4 + f_1 |q|^2 |r|^2 + g_1 |r|^4)q + (l_1 |q|^6 + m_1 |q|^4 |r|^2 + n_1 |q|^2 |r|^4 + p_1 |r|^6)q + i h_1 q_x + k_1 r = 0, \quad (1)$$

$$ir_t + a_2 q_{xx} + (b_2 |r|^2 + c_2 |q|^2)r + (d_2 |r|^4 + f_2 |r|^2 |q|^2 + g_2 |q|^4)r + (l_2 |r|^6 + m_2 |r|^4 |q|^2 + n_2 |r|^2 |q|^4 + p_2 |q|^6)r + i h_2 r_x + k_2 q = 0, \quad (2)$$

where the functions $q(x, t)$ and $r(x, t)$ stand for forward and backward propagating waves, respectively, whereas a_j for $j = 1, 2$ represent the coefficients of dispersive reflectivity. In the coupled equations above, b_j indicate the coefficients of self-phase modulation (SPM) and c_j denote the cross-phase modulation (XPM) for cubic nonlinearity portion. For quintic nonlinear part, d_1 are the coefficients of SPM while f_j and g_j are the coefficients of XPM. Regarding septic nonlinearity, l_j are the coefficients of SPM while m_j, n_j and p_j are the coefficients of XPM. Finally, h_j accounts for inter-modal dispersion and k_j define detuning parameters. All of the coefficients are real valued constants and $i = \sqrt{-1}$.

The objective of the present study is to investigate chirped optical solitons in fiber BGs. The system of equations (1) and (2) is handled with the help of traveling wave transformation and then some specific conditions are assumed to ensure an integrable form for the coupled system. The generated traveling wave reduction is effectively solved by means of soliton ansatz method which yields various forms of chirped optical solitons.

Results and discussion

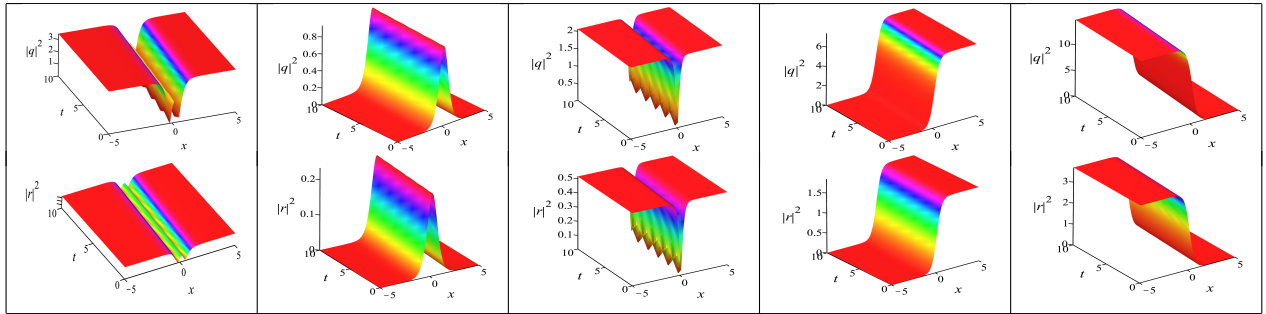


Figure 1: The profile of W-shaped, bright, dark, kink and anti-kink solitons.

The derived wave solutions for the model of the coupled NLSE (1) and (2) describe distinct chirped solitons having nonlinear phase functions in terms of the reciprocal of amplitude function which are entirely different from the previous studies in the literature. The obtained optical solitons include several forms such as W-shaped, bright, dark, kink and anti-kink solitons. These new results obtained here are expected to contribute in improving the experimental studies and engineering applications related to fiber BGs.

References

- [1] Biswas A., Ekici M., Sonmezoglu A., Belic M.R. (2019) *Optik* **185**:50.
- [2] Zayed E., Alngar M., Biswas A., Ekici M., Alzahrani A., Belic M. (2020) *J. Commun. Technol. Electron.* **65**:1267.
- [3] Yildirim Y., Biswas A., Khan S., Guggilla P., Alzahrani A.K., Belic M.R. (2021) *Optik* **237**:166684.
- [4] Zayed E.M., Alngar M.E., Biswas A., Ekici M., Triki H., Alzahrani A.K., Belic M.R. (2020) *Optik* **204**:164096.

Stabilization mechanism of limit cycle oscillation using control based continuation and phase locked loop.

Gourc Etienne*, Vergez Christophe* and Cochelin Bruno *

*Aix Marseille Université, CNRS, Centrale Marseille, Laboratoire de Mécanique et d'Acoustique, Marseille, FR

Abstract. This presentation concerns the stabilization of unstable limit cycles using a combination of feedback and phase locked loop control. The proposed control scheme is applied to a Van der Pol oscillator and the stabilization mechanisms are investigated theoretically using the method of multiple scales. Different failure scenarios of the controller are revealed allowing us to express design rules for the controller gains.

Introduction

Control based continuation (CBC) is used to study the bifurcation diagrams of a nonlinear dynamical systems on physical experiments [1]. CBC rely on a feedback controller that is used to stabilize the nonlinear device. The feedback controller must be non-invasive to ensure that a periodic solution of the feedback controlled system is also a solution of the uncontrolled system. CBC has been mostly used to track branches of periodic solutions of non-autonomous (i.e. forced) systems [2]. CBC of autonomous systems presents an additional difficulty since the frequency of the limit cycle (LC) is also an unknown. Numerical continuation algorithms solve this problem by appending the system with a phase condition. In this study, the frequency of the limit cycle is determined in real time by using a phase locked loop controller (PLL). Although CBC has already been tested on various experiments, only few papers deal with the detailed analysis of the underlying stabilization mechanism.

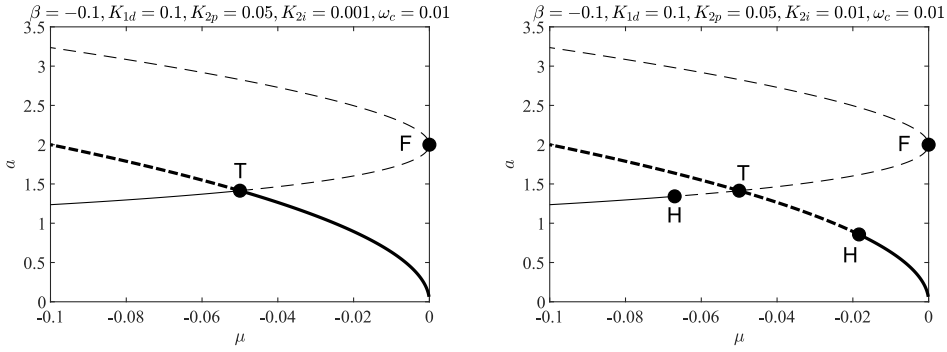


Figure 1: Bifurcation diagram of the controlled VdP

Results and discussion

The proposed control scheme has been applied to a Van der Pol oscillator (VdP). The governing equations of motion are given by

$$\begin{aligned} \ddot{x} + x - (\mu - \beta x^2)\dot{x} &= K_{1d}(\dot{w} - \dot{x}) & \dot{y}_1 &= \omega_c(x \cos \theta - y_1) \\ \dot{y}_2 &= R y_1 & \dot{\theta} &= \omega_0 + K_{2p} y_1 + K_{2i} y_2 \end{aligned} \quad (1)$$

where μ and β are the linear and nonlinear coefficients of the VdP oscillator. K_{1d} is the derivative gain, ω_c the cutoff frequency of the low pass filter of the PLL, R , K_{2p} , K_{2d} are the gains of the PLL and ω_0 the center frequency. $w(t) = W \sin \theta(t)$ is the control target. The uncontrolled VdP oscillator has a Hopf bifurcation at $\mu = 0$, which is subcritical (supercritical) for $\beta < 0$ ($\beta > 0$). The behavior of the controlled VdP has been analyzed by using the method of multiple scales. Since the objective is to stabilize the unstable LC, we considered that the control target amplitude W is equal to the amplitude of the uncontrolled LC, i.e. $W = a_0 \equiv 2\sqrt{\mu/\beta}$. Examples of bifurcation diagram are depicted in fig. 1. Solid (dashed) lines correspond to stable (unstable) solutions. Thick and thin lines correspond to solutions where the controller is non-invasive ($W = a$), or invasive ($W \neq a$), respectively. Multiple scales analysis allows us to express design rules for the controller. Either the controller may fail due to the presence of a transcritical bifurcation at $\mu = -K_{1d}/2$ or due to a Hopf bifurcation if $K_{2p}(K_{1d} + 2\omega_c) < 2RK_{2i}$.

References

- [1] Barton D.A.W, Sieber, J. (2010) Systematic experimental exploration of bifurcations with non-invasive control. *Phys. Rev. E*.
- [2] Abeloos G., Muller F., Ferhatoglu E., Scheel M., Collette C., Kerschen G., Brake M.R.W., Tiso P., Renson L., Krack M. (2022) A consistency analysis of phase-locked-loop testing and control-based continuation for geometrically nonlinear frictional system. *Mech. Syst. Signal Process.*
- [3] Denis V., Jossic M., Giraud-Audine C., Chomette B., Renault A., Thomas O. (2018) Identification of nonlinear modes using phase-locked-loop experimental continuation and normal form. *Mech. Syst. Signal Process.*

Model reduction of a periodically forced slow-fast continuous piecewise linear system

A. Yassine Karoui and Remco I. Leine

*Institute for Nonlinear Mechanics, University of Stuttgart, Germany
ORCID 0000-0003-3350-5200 and ORCID 0000-0001-9859-7519*

Abstract. In this work, singular perturbation theory is exploited to obtain a reduced order model of a slow-fast piecewise linear 2-DOF oscillator subjected to harmonic excitation. The nonsmoothness of piecewise linear nature is studied in the case of bilinear damping as well as with bilinear stiffness characteristics. We propose a continuous matching of the locally invariant slow manifolds obtained in each subregion of the state space, which yields a 1-DOF reduced order model of the same nature as the full dynamics. The frequency response curves obtained from the full system and the reduced models show that the proposed reduction method can capture nonlinear behaviors such as super- and subharmonic resonances.

Introduction

Invariant manifolds play a major role in understanding the behavior of nonlinear dynamical systems. Among their properties, such manifolds can be used to obtain a reduced dynamics capturing the main features of the original system. The existing methods to find these manifolds often require smoothness properties of the system. A typical example is the theory of singular perturbations, where the reduction to a smooth slow manifold yields a reduced order model describing the slow dynamics of the original system. However, this theory cannot be applied on systems containing nonsmooth nonlinearities without suitable extension to take the nonsmoothness into account. A prominent class of nonsmooth systems consists in mechanical models with PWL nonlinearities, which may arise due to several effects such as damage or clearance [1]. In this work, the approach proposed in [2] for the use of singular perturbation theory on slow-fast PWL systems is extended from the autonomous configuration in \mathbb{R}^3 to nonautonomous two degrees of freedom slow-fast oscillators. Motivated by the quarter car model with bilinear damping characteristics [3], two examples of slow-fast PWL oscillators subjected to a harmonic excitation are used to illustrate the reduction in the case of bilinear damping and bilinear stiffness.

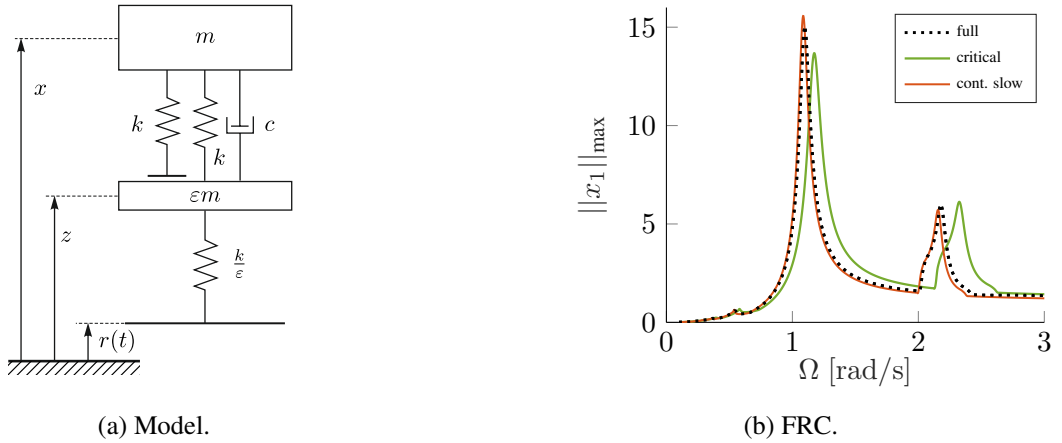


Figure 1: Model and frequency response curve of a 2-DOF slow-fast forced oscillator with PWL stiffness.

Results and discussion

In this contribution, a continuous matching of the locally invariant slow manifolds of a slow-fast forced system with piecewise linear nonlinearities is proposed. It was observed that the resulting reduced dynamics is able to approximate the behavior of the full system with high accuracy for a frequency range around the main harmonic. Due to the convergence property, the PWL system in the case of bilinear damping admits frequency-response curves (FRC) similar to a linear system, which were approximated with high fidelity by the proposed approach. For a similar PWL slow-fast oscillator with bilinear stiffness instead of damping, the system behavior becomes more complex due to the loss of the convergence property and the existence of nonlinear phenomena, such as super- and subharmonic resonances, becomes possible. These nonlinear resonances were accurately captured by the proposed reduction approach for the frequency range around the main resonance.

References

- [1] Butcher, E.: Clearance effects on bilinear normal mode frequencies. *Journal of Sound and Vibration* 224(2), 305–328 (1999)
- [2] Karoui, A.Y., Leine, R.I.: Analysis of a singularly perturbed continuous piecewise linear system. *Proceedings of the 10th European Nonlinear Dynamics Conference - ENOC (2022)*
- [3] Silveira, M., Wahi, P., Fernandes, J.: Effects of asymmetrical damping on a 2 DOF quarter-car model under harmonic excitation. *Communications in Nonlinear Science and Numerical Simulation* 43, 14–24 (2017)

Time-dependent stability margin for autonomous, piece-wise, and discontinuous system

Tomasz Burzyński*, Piotr Brzeski* and Przemysław Perlikowski*

*Division of Dynamics, Lodz University of Technology, Stefanowskiego 1/15, 90-924 Lodz, Poland

Abstract. In recent years, a variety of new metrics to analyze dynamical systems emerged. One of them is a metric called time-dependent stability margin, introduced for the first time in [1]. It is used for systems with coexisting stable attractors. The metric evaluates the stability of the system along the periodic orbit, indicating its reliability and resistance to perturbations. In this paper, the time-dependent stability margin is applied to investigate the real-world, discontinuous, and piece-wise mechanical system with impacts. Numerical results show that the periodic orbit vulnerability to perturbations is increased in close vicinity to the particular impact events. It may induce implications because after time impacts wear the system causing plastic deformation or backlash in the mechanisms. Consequently, it may lead to perturbation sufficient enough to change the attractor.

Introduction

Multi-stable systems are commonly known in mechanical engineering, mathematical biology, fluid dynamics, control engineering, and others. Over the years, a variety of techniques to analyze such systems were developed. Among others, we can distinguish basin stability metrics, basin entropy, survivability, and time-dependent stability margin.

The time-dependent stability margin [1] is a method designed to examine the stability of the system along the periodic orbit. In multi-stable mechanical systems due to coexisting attractors, we can experience a sudden change in dynamical response. The phenomena may be severe for the system as it can trigger undesired behavior. It can also be used to facilitate control over the system. The cost of control can be minimized by applying the impulse at the appropriate time when the stability margin of the current attractor is the smallest. Therefore, such analysis can provide significant advantages when a mechanical system and its control are designed.

In order to test the usefulness of the metric in real-world applications, we perform a time-dependent stability analysis of the novel-yoke-bell clapper system (Figure 1a) with variable geometry. The system is piece-wise due to the nature of excitation and discontinuous due to impacts between the bell and the clapper. The mathematical model of the system was experimentally validated in [2].

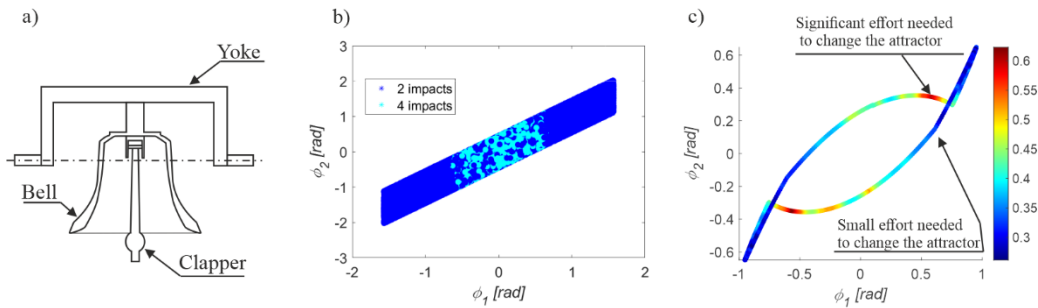


Figure 1: a) Schematic view of the considered system b) Basin of attraction c) Evolution of the stability margin along the attractor with four impacts per period of motion.

Results and discussion

Detailed information considering how the metric is calculated is described in [1]. Figure 1b shows two coexisting attractors (two and four impacts per one period of motion) in phase space, where ϕ_1 is the angular displacement of the bell and ϕ_2 is the angular displacement of the clapper. The stability margin along the attractor with four impacts per period of motion is presented in figure 1c. The metric indicates parts of the orbit that are the most prone to perturbations. In this case, it is in close vicinity to the first and third impact event. On the other hand, the safety margin is the biggest before the second and fourth impact.

After time, impacts wear the structure causing plastic deformation or backlash in the mechanism. As a consequence, the trajectory of the bell or the clapper may be changed and a disturbance may be introduced to the system possibly leading to a sudden change of attractor. This study shows the practical application of the novel tool for the analysis of multi-stable systems. It allows for further investigations considering the control of the system (by means of the desired transition between attractors) or optimization for robustness and safety.

References

- [1] Brzeski, P. et. al. (2018) Time dependent stability margin in multistable systems. *Chaos: An Interdisciplinary Journal of Nonlinear Science*. *Chaos* **28**: 093104.
- [2] Burzyński, T. et. al. (2022) Dynamics loading by swinging bells – Experimental and numerical investigation of the novel yoke-bell-clapper system with variable geometry. *Mechanical Systems and Signal Processing* **180**:109429.

Rolling a heavy ball on a revolving surface

Katica R. (Stevanović) Hedrih^{*,**} [0000-0002-2930-5946]

^{*}Department of Mechanics, Mathematical Institute of Serbian Academy of Science and Arts, Belgrade, Serbia; E-mail: katicah@mi.sanu.ac.rs, khedrih@sbb.rs

^{**}Faculty of Mechanical Engineering at University of Niš, Serbia

Abstract. 5 theorems on the properties of newly constructed orthogonal curvilinear coordinate systems on various revolving surfaces and 10 theorems on the properties of the non-linear dynamics of non-slip rolling of a heavy, homogeneous and isotropic ball on revolving surfaces are defined. For two special cases, when the revolving surfaces were created by the rotation of a parabola, that is, a biquadratic parabola, the corresponding nonlinear differential equations of rolling, without sliding, a heavy homogeneous and isotropic ball, as well as equations of phase trajectories, were derived. It is shown that for such nonlinear rolling dynamics there is a cyclic integral, as well as one cyclic coordinate in all cases of revolving surfaces.

Introduction

The rolling of a ball on curvilinear paths and surfaces has attracted the attention of many researchers since ancient times, both in a scientific-theoretical approach, but also in the interest of application in engineering. There are contemporary authors who claim in their works that the rolling of a ball on a surface is a system with non-holonomic connections, and the author of this paper has shown in her works [1] that the constraints are holonomic and purely geometric and that rolling, without slipping, a heavy homogeneous and isotropic ball on the surface, is a system with two degrees of freedom of rolling and with pure geometric connections. Now let's cite one doctoral dissertation, which deals with a special and interesting complex mechanical system of rolling a ball, which contains a gyroscope [2]. The dissertation was done under the mentorship of Anton Bilimović, and defended, back in 1924, before a commission that included prominent scientists Milutin Milanković, the author of the famous work "The Canon of Sun Insolation", and Mihailo Petrić, the founder of the Serbian School of Mathematics and one of the three Doctoral students of the famous Julius Henri Poincaré.

In this work we present newly constructed orthogonal curvilinear coordinate systems over various revolving surfaces (see Fig.1.b*), as well as the nonlinear dynamics of rolling, without sliding, a heavy, homogeneous and isotropic ball on revolving surfaces (see Fig.1.c* and d*).

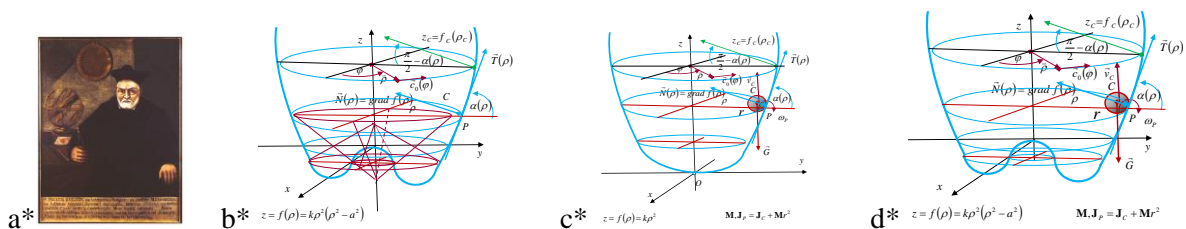


Figure 1. a* Paul Guldin (1577 - 1643); b* Coordinate surfaces and coordinate lines of a curvilinear orthogonal coordinate system constructed over a revolving biquadratic parabolic surface; kinetic parameters of rolling a heavy ball on a revolving parabolic (c*) and biquadratic (d*) parabolic surface.

Main results and discussion

A series of nonlinear differential equations with first integrals and 15 theorems of a rolling ball, without slipping along revolving surface, are derived, and here we state the important theorem 7. The velocity \vec{v}_C of the center of mass of a rolling ball, without slipping, has two components $\vec{v}_{C,m}$ and $\vec{v}_{C,c}$: one $\vec{v}_{C,m}$ in the meridional plane, parallel to the tangent $\vec{T} = \frac{1}{\sqrt{1+4k^2\rho^2}}(\vec{\rho}_0 + 2k\rho\vec{k})$ to the derivative of the revolving parabolic (or general revolving) surface on which the ball rolls, without slipping, and the other component $\vec{v}_{C,c}$ in the circular direction $\vec{c}_0 = -\sin\varphi\vec{i} + \cos\varphi\vec{j}$, which is in the direction tangent to the circle - the curvilinear coordinate line of the parabolic revolving surface.

References

- [1] Hedrih (Stevanović) R. K. (2019) Rolling heavy ball over the sphere in real \mathbb{R}^3 space. *Nonlinear Dyn* **97**:63-82.
- [2] Demčenko V. (1923) Kotrljanje bez klizanja giroskopske lopte po sferi (Rolling without slipping a gyroscopic ball on a sphere). PhD dissertation, University of Belgrade.

NODYCON 2023

THIRD INTERNATIONAL NONLINEAR DYNAMICS CONFERENCE

SPONSORS:

SPRINGER NATURE



UNDER THE AUSPICES OF

